



UNIVERSITY OF
NOVI SAD

FACULTY OF
TECHNICAL SCIENCES

DEPARTMENT OF
PRODUCTION ENGINEERING

13TH INTERNATIONAL
SCIENTIFIC
CONFERENCE

MMA 2018

FLEXIBLE TECHNOLOGIES

PROCEEDINGS

NOVI SAD
SERBIA

SEPTEMBER 28-29, 2018



UNIVERSITY OF NOVI SAD
FACULTY OF TECHNICAL SCIENCES
DEPARTMENT OF PRODUCTION ENGINEERING
NOVI SAD, SERBIA



13th INTERNATIONAL SCIENTIFIC CONFERENCE
MMA 2018 - FLEXIBLE TECHNOLOGIES

MMA 2018
FLEXIBLE TECHNOLOGIES

PROCEEDINGS

Novi Sad, September 28-29, 2018

PROCEEDINGS OF THE 13th INTERNATIONAL SCIENTIFIC CONFERENCE
MMA 2018 - FLEXIBLE TECHNOLOGIES
Novi Sad, 2018

Publisher: **FACULTY OF TECHNICAL SCIENCES
DEPARTMENT OF PRODUCTION ENGINEERING
21000 NOVI SAD, Trg Dositeja Obradovica 6
SERBIA**

*Organization of this Conference was approved by Educational-scientific Council of
Faculty of Technical Sciences in Novi Sad*

Editor: Dr Rade Doroslovački, professor, dean

Technical treatment and design: Dr Mijodrag Milošević, associate professor
Dr Dejan Lukić, associate professor
Dr Aco Antić, associate professor
M.Sc. Miloš Knežev, assistant

Manuscript submitted for publication: September 20, 2018

Printing: 1st

Circulation: 120 copies

CIP classification:

CIP - Каталогизacija y публикацији
Библиотека Матице српске, Нови Сад

621.7/.9(082)

621.9(082)

**INTERNATIONAL Scientific Conference MMA 2018 - Flexible
Technologies (13 ; 2018 ; Novi Sad)**

Proceedings / 13th International Scientific Conference MMA 2018 -
Flexible Technologies, Novi Sad, 28-29 September, 2018 ; [editor Rade
Doroslovački]. - 1st printing. - Novi Sad : Faculty of Technical Sciences,
Department of Production Engineering, 2018 (Novi Sad : FTN, Graphics
Centre GRID). VII, 428 str. : ilustr. ; 30 cm

Tiraž 120. - Bibliografija uz svako rad. - Registar.

ISBN 978-86-6022-094-5

a) Производно машинство - Зборници. b) Метали - Обрада - Зборници
COBISS.SR-ID 325441799

Printing by: FTN, Graphic Centre
GRID, Novi Sad

*Financing of the Proceedings was sponsored by the Ministry of Education, Science and
Technological Development of the Republic of Serbia and supported by the Provincial Secretariat
for Higher Education and Scientific Research of AP Vojvodina.*

CONFERENCE ORGANIZER

University of Novi Sad
Faculty of Technical Sciences
Department of Production Engineering
Novi Sad, Serbia

INTERNATIONAL SCIENTIFIC COMMITTEE

Mijodrag Milošević, FTN Novi Sad, SRB, chairman

Bojan Ačko, FS Maribor, SLO

Sergei Alexandrov, IPM Moskva, RUS

Aco Antić, FTN Novi Sad, SRB

Jan C. Aurich, TU Kaiserslautern, GER

Bojan Babić, MF Beograd, SRB

Sebastian Baloš, FTN Novi Sad, SRB

Konstantinos Bouzakis, AU Thessaloniki, GRE

Erhan Budak, FENS Istanbul, TUR

Igor Budak, FTN Novi Sad, SRB

Ilija Ćosić, FTN Novi Sad, SRB

Predrag Ćosić, FSB Zagreb, CRO

Robert Čep, VŠB Ostrava, CZE

Franc Čuš, FS Maribor, SLO

Livia Dana Beju, US Sibiu, ROU

Goran Devedžić, FIN Kragujevac, SRB

Ljubomir Dimitrov, TU Sofia, BGR

Cristian Doicin, UP Bucharest, ROU

Dragan Domazet, UM Beograd, SRB

Rade Doroslovački, FTN Novi Sad, SRB

Numan M. Durakbasa, TU Vienna, AUT

Kornel Ehmann, NU Illinois, USA

Valentina Gečevska, MF Skopje, MKD

Šefket Goletić, MF Zenica, BIH

Dušan Golubović, MF Istočno Sarajevo, BIH

Marin Gostimirović, FTN Novi Sad, SRB

Miodrag Hadžistević, FTN Novi Sad, SRB

František Holešovský, JEPÚ Usti, CZE

Jerzy Jędrzejewski, UT Wrocław, POL

Janez Kopač, FS Ljubljana, SLO

Pavel Kovač, FTN Novi Sad, SRB

Ivan Kuric, FME Žilina, SVK

Mikolaj Kuzinovski, MF Skopje, MKD

Gordana Lakić Globočki, MF Banja Luka, BIH

Dejan Lukić, FTN Novi Sad, SRB

Ljubomir Lukić, FMG Kraljevo, SRB

Ognjan Lužanin, FTN Novi Sad, SRB

Vidosav Majstorović, MF Beograd, SRB

Miodrag Manić, MF Niš, SRB

Ildiko Mankova, TU Košice, SVK

Dorian Marjanović, FSB Zagreb, CRO

Zoran Miljković, MF Beograd, SRB

Radivoje Mitrović, MF Beograd, SRB

Slobodan Mitrović, FIN Kragujevac, SRB

Bogdan Nedić, FIN Kragujevac, SRB

Duško Pavletić, TF Rijeka, CRO

Darko Petković, MF Zenica, BIH

Petar Petrović, MF Beograd, SRB

Goran Putnik, University of Minho, POR

Radovan Puzović, MF Beograd, SRB

Miroslav Radovanović, MF Niš, SRB

Milenko Sekulić, FTN Novi Sad, SRB

Tomislav Šarić, SF Slavonski Brod, CRO

Mladen Šercer, FSB Zagreb, CRO

Leposava Šiđanin, FTN Novi Sad, SRB

Goran Šimunović, SF Slavonski Brod, CRO

Branko Škorić, FTN Novi Sad, SRB

Ľubomír Šooš, STU Bratislava, SVK

Dušan Šormaz, OH Athens, USA

Tibor Szalay, BUTE Budapest, HUN

Slobodan Tabaković, FTN Novi Sad, SRB

Branko Tadić, FIN, Kragujevac, SRB

Ljubodrag Tanović, MF Beograd, SRB

Radoslav Tomović, MF Podgorica, MNE

Miroslav Trajanović, MF Niš, SRB

Nicolae Ungureanu, FI Baia Mare, ROU

Dragiša Vilotić, FTN Novi Sad, SRB

Mircea Viorel Dragoi, UT Brasov, ROU

Vojo Višekruna, MF Mostar, BIH

Đorđe Vukelić, FTN Novi Sad, SRB

Lihui Wang, KTH Stockholm, SWE

Milan Zeljković, FTN Novi Sad, SRB

HONORARY COMMITTEE

Slavko Arsovski, FIN Kragujevac, SRB

Pavao Bojanić, MF Beograd, SRB

Milenko Jovičić, MF Beograd, SRB

Vid Jovišević, MF Banja Luka, BIH

Milisav Kalajdžić, MF Beograd, SRB

Miodrag Lazić, FIN Kragujevac, SRB

Vučko Mečanin, MF Kraljevo, SRB

Vladimir Milačić, MF Beograd, SRB

Dragoje Milikić, FTN Novi Sad, SRB

Dragan Milutinović, MF Beograd, SRB

Ratko Mitrović, MF Kragujevac, SRB

Sava Sekulić, FTN Novi Sad, SRB

Mirko Soković, FS Ljubljana, SLO

Bogdan Sovilj, FTN Novi Sad, SRB

Jelena Stankov, FTN Novi Sad, SRB

Velimir Todić, FTN Novi Sad, SRB

Dragutin Zelenović, member of SASA, SRB

ORGANIZING COMMITTEE

Dejan Lukić, FTN Novi Sad, SRB, chairman

Aleksandar Živković, FTN Novi Sad, SRB

Boris Agarski, FTN Novi Sad, SRB

Borislav Savković, FTN Novi Sad, SRB

Branko Štrbac, FTN Novi Sad, SRB

Ivan Matin, FTN Novi Sad, SRB

Miloš Knežev, FTN Novi Sad, SRB, secretary

Mario Šokac, FTN Novi Sad, SRB

Željko Santoši, FTN Novi Sad, SRB

Cvijetin Mladenović, FTN Novi Sad, SRB

Milana Ilić Mićunović, FTN Novi Sad, SRB

Dragan Rodić, FTN Novi Sad, SRB

Nenad Kulundžić, FTN Novi Sad, SRB

Zorana Lanc, FTN Novi Sad, SRB

ACKNOWLEDGEMENTS

Organisation of 13th International Scientific Conference MMA 2018 – FLEXIBLE TECHNOLOGIES was made possible with understanding and financial help of following sponsors and donators:

- **MINISTRY OF EDUCATION, SCIENCE AND TECHNOLOGICAL DEVELOPMENT OF THE REPUBLIC OF SERBIA** – Belgrade
- **PROVINCIAL SECRETARIAT FOR HIGHER EDUCATION AND SCIENTIFIC RESEARCH OF AP VOJVODINA** – Novi Sad
- **UNIVERSITY OF NOVI SAD** – Novi Sad
- **FACULTY OF TECHNICAL SCIENCES** – Novi Sad
- **DEPARTMENT OF PRODUCTION ENGINEERING AT THE FACULTY OF TECHNICAL SCIENCES** – Novi Sad
- **FACTORY OF ROLLING BEARINGS AND CARDAN SHAFTS - FKL a.d.** – Temerin
- **FANUC Adria d.o.o.** – Celje, Slovenia
- **ATB SEVER d.o.o.** – Subotica
- **VOS-SYSTEM d.o.o.** – Žabalj
- **STREIT NOVA d.o.o.** – Stara Pazova
- **TEHNOEXPORT** – Inđija
- **HiB - INSTITUT ZA BEZBEDNOST I HUMANIZACIJU RADA** – Novi Sad
- **ČELIK d.o.o.** – Bački Jarak
- **CONTEX ENERGY d.o.o.** – Novi Sad
- **ALEKSANDAR INŽENJERING d.o.o.** – Novi Sad
- **GM-CNC d.o.o.** – Inđija
- **UNIMET d.o.o.** – Kać
- **PRIMAR TEHNO d.o.o.** – Maglić (NS)
- **PRIVREDNA KOMORA VOJVODINE** – Novi Sad
- **ULJARICE BAČKA d.o.o.** – Novi Sad
- **APATINSKA PIVARA d.o.o.** – Apatin
- **LABINPROGRES-TPS d.o.o.** – Novi Kneževac
- **GRUJIĆ & ГРУЈИЋ d.o.o.** – Novi Sad
- **FREZAL d.o.o.** – Ruma
- **VUVES COMMERCE d.o.o.** – Kać
- **POBEDA HOLDING** – Petrovaradin
- **METALFER STEEL MILL d.o.o.** – Sremska Mitrovica
- **FABRIKA REZNOG ALATA a.d.** – Čačak

Continuing a long tradition of more than **40 years**, the **Department of Production Engineering of the Faculty of Technical Sciences** organizes **13th International Scientific Conference MMA 2018 – Flexible Technologies**.

The conference will cover current issues in the field of production engineering as well as multidisciplinary fields of mechanical engineering, information technologies, environmental engineering, bio-medical engineering and other related engineering fields, that play a significant role in successful functioning of manufacturing industry, agriculture, transport, electric power industry, oil industry, military industry, health care and other branches of economy and society.

The scientific-expert conference MMA, with its long tradition and regular organization since 1976, aims to gather and exchange experience of researchers and experts from faculties, institutes and industry, and thus wants to contribute to more intensive scientific and economic development.

The thirteenth International Scientific Conference MMA 2018 - FLEXIBLE TECHNOLOGIES is being held for the tenth time as an international conference. By the number of papers, their quality and participation of domestic and foreign authors achieved so far, the Conference has gained eviable reputation among scientific and professional employees from the faculty and industry. The content of the MMA 2018 – FLEXIBLE TECHNOLOGIES involves the following areas:

- MATERIAL PROCESSING TECHNOLOGIES
- MACHINE TOOLS AND AUTOMATIC FLEXIBLE SYSTEMS, CAX AND CIM PROCEDURES AND SYSTEMS
- METROLOGY, QUALITY, FIXTURES, CUTTING TOOLS AND TRIBOLOGY
- PROCESS PLANNING, OPTIMIZATION, LOGISTICS AND INTERNET TECHNOLOGIES IN PRODUCTION ENGINEERING
- MATERIALS, METAL FORMING, CASTING AND WELDING
- MECHANICAL ENGINEERING AND ENVIRONMENTAL PROTECTION
- BIO-MEDICAL ENGINEERING

With around 90 scientific papers, out of which almost 30% comes from abroad, the 13th International Scientific Conference MMA 2018 - FLEXIBLE TECHNOLOGIES is keeping the pace with the previous conferences. The participation of many domestic and foreign authors, as well as issues covered in the papers, confirm the efforts put in organization of the conference and thus provide contribution to the exchange of knowledge, research results and expert experience from industry, research institutions and universities working in the field of production engineering.

On behalf of the International Scientific and Organizing Committee of the Conference we would like to thank all domestic and foreign authors, reviewers, as well as institutions and individuals who contributed to the realization of high-quality program of the Conference.

Novi Sad, September 2018

Chairman of the International Scientific Committee
Prof. dr Mijodrag Milošević

Chairman of the Organizing Committee
Prof. dr Dejan Lukić

Contents

KEYNOTE PAPERS

Lihui Wang:

COMBINING DIGITAL TWIN AND PROGNOSIS IN FACTORIES OF THE FUTURE1

Dušan Šormaz:

DISTRIBUTED PROCESS PLANNING FOR DIGITAL MANUFACTURING AND INDUSTRY 4.03

Manic, M., Vitkovic, N., Stojkovic, M., Misic, D., Trajanovic, M.:

DESIGN OF CUSTOMIZED ANATOMICALLY ADJUSTED IMPLANTS5

Section A: MATERIAL PROCESSING TECHNOLOGIES

Invited paper

Madić, M., Janković, P., Radovanović, M., Mladenović, S., Petković, D.:

ANALYSIS OF VARIABLE COSTS IN CO₂ LASER CUTTING OF MILD STEEL11

Cerce, L., Borojevic, S., Kramar, D.:

OPTIMIZATION OF THE PROCESS PARAMETERS FOR STABILIZATION AND
IMPROVEMENT OF THE TURNING PROCESS CAPABILITY15

Gostimirovic, M., Pucovsky, V., Rodic, D., Sekulic, M., Kovac, P.:

A NEURAL NETWORK MODEL FOR PREDICTING JET TRAJECTORY
IN THE ABRASIVE WATER JET MACHINING21

Kokotovic, B., Vorkapic, N.:

EVALUATION OF INFED STRATEGIES FOR TURNING OF LARGE THREAD PROFILES25

Mustafic, A., Lovric, S., Nasic, E., Halilovic, J., Osmic, M., Becirovic, D.:

TAGUCHI-BASED GREY RELATIONAL ANALYSIS OF PERFORMANCE CHARACTERISTICS
IN THE MQL TURNING PROCESS OF X5CrNi18-10 STEEL29

Rodic, D., Gostimirovic, M., Kovac, P., Sekulic, M., Savkovic, B.:

PRINCIPLE OF ELECTRICAL DISCHARGE MACHINING OF NON-CONDUCTIVE ZIRCONIA CERAMICS33

Sekulic, M., Gostimirovic, M., Kulundzic, N., Aleksic, A.:

TECHNOLOGICAL CHANGES IN MOLD MAKING INDUSTRY37

Šogorović, D., Vračević, I.:

TESTING OF THE ROUGHNESS PARAMETERS IN THE TURNING PROCESS OF ALUMINUM PARTS41

Žiga, A., Begić-Hajdarević, Đ., Cogo Z.:

MECHANICAL TOYS AND SOUVENIRS OBTAINED BY CO₂ LASER CUTTING OF PLYWOOD45

Section B: MACHINE TOOLS AND AUTOMATIC FLEXIBLE SYSTEMS, CAx AND CIM PROCEDURES AND SYSTEMS

Invited paper

Zivanovic, S., Slavkovic, N.:

APPLICATION OF THE STEP-NC STANDARD ISO 10303 AP238 FOR TURNING OPERATIONS49

Antic, A., Zeljkovic, M., Krstanovic, L., Ungureanu, N.:

A TEXTURE-BASED DESCRIPTORS FOR REAL TIME TOOL CONDITION MONITORING53

Berus, L., Ficko, M., Gotlih, J., Klancnik, S.:

DEVELOPMENT OF A SYSTEM FOR MONITORING TEMPERATURE DISTRIBUTION AND
OPERATING OF HEAT SOURCES INSIDE HEATING DEVICE57

Blanuša, V., Milisavljević, B., Zeljković, M., Živković, A., Savić, B., Sovilj-Nikić, S.:

ANALYSIS OF LOAD DISTRIBUTION IN DOUBLE-ROW CYLINDRICAL
ROLLER BEARING FOR MACHINE TOOLS MAIN SPINDLE ASSEMBLY61

Cerjakovic, E., Topcic, A., Lovric, S., Heric, M.:

DESIGN AND STARTING UP OF AUTOMATED ASSEMBLY LINES IN THE AUTOMOTIVE INDUSTRY65

Crnokić, B., Grubišić, M.:

FUSION OF INFRARED SENSORS AND CAMERA FOR MOBILE
ROBOT NAVIGATION SYSTEM - SIMULATION SCENARIO71

Cica, Dj., Borojevic, S., Sredanovic, B., Tesic, S.:

ARTIFICIAL NEURAL NETWORKS MODEL FOR THE PREDICTION OF
SURFACE ROUGHNESS IN MACHINING THIN WALLED PARTS.....75

Hozdić, E.:

CYBERNETIZATION OF MANUFACTURING SYSTEMS79

Knežev, M., Tabaković, S., Zeljkovic, M., Strbac, B., Mladenovic, C.:

ANALYSIS AND VERIFICATION OF COMPLEX SURFACES
MACHINING BY THREE AXIS MILLING MACHINE CENTER83

Lanc, Z., Zeljkovic, M., Hadzistevec, M., Strbac, B., Zivkovic, A.:

DETERMINATION OF EMISSIVITY OF STEEL ALLOY USING INFRARED THERMOGRAPHIC TECHNIQUE.....87

Matijasevic, L., Milivojevic, M., Petrovic, P.:

MULTIFINGERED UNDER-ACTUATED HANDS IN ROBOTIC ASSEMBLY91

Mladenović, C., Košarac, A., Zeljković, M., Knežev, M.:

EXPERIMENTAL DEFINITION OF MACHINING SYSTEMS STABILITY LOBE DIAGRAM95

Vorkapic, N., Kokotovic, B.:

SYNTHESIS AND ANALYSIS OF THE TOOL DYNAMOMETER FOR TURNING OPERATIONS99

Section C: METROLOGY, QUALITY, FIXTURES, CUTTING TOOLS AND TRIBOLOGY

Invited paper

Majstorovic, D., V., Stojadinovic, M., S., Durakbasa, M., N.:

AN IN - PROCESS MEASUREMENT INSPECTION PLANNING MODEL FOR PRISMATIC PARTS.....103

Invited paper

Sovilj, B., Sovilj-Nikić, S.:

TRIBOLOGICAL RESEARCHES OF GEAR CUTTING PROCESSES OF CYLINDRICAL GEARS107

Ilic, J., Krajsnik, M., Jotic, G., Anic, J.:

FABRICATION OF AUTHENTIC FUNCTIONAL PARTS FOR OLDTIMER USING

INTEGRATION OF REVERSE ENGINEERING AND 3D PRINTING.....117

Janjić, N., Savić, B., Mikić, D., Stanković, N., Petrović, D.:

A PPLICATION OF MODEL OF RELIABILITY ON MACHINE SYSTEMS

BASED ON LOGNORMAL STATISTICAL DISTRIBUTION.....121

Jotić, G., Borojević, S., Hadžistević, M., Štrbac, B., Vukman, J.:

ANALYSIS OF COMPARATIVE MEASUREMENT RESULTS FOR

THIN-WALLED AL 7075 ALLOY STRUCTURES127

Karpe, B., Fercak, Z., Nagode, A., Bavec, B., Kozuh, S.,

Gojic, M., Smolej, S., Sokovic, M., Bizjak, M., Kosec, B.:

THERMAL CHARACTERISTICS OF ENAMELS AND ENAMELLED METAL SHEETS.....131

Klimenko, S., Kopeikina, M., Manokhin, A., Melniychuk, Yu., Naydenko, A., Tanovic, Lj.:

ENHANCED PCBN TOOLS FOR HARD MACHINING137

Knezevic, I., Bojic, S., Lukic, D., Rackov, M. Cavic, M., Pencic, M., Cako, S.:

APPLICATION OF 3D PRINTED FIXTURES FOR WELDING141

Matin, I., Vukelic, D., Hadzistevic, M., Strbac, B., Santosi, Z., Lukic, D.:

AN INTEGRATED DESIGN APPROACH FOR PLASTIC PART DEVELOPMENT145

Palic, N., Sharma, V., Zivic, F., Mitrovic, S., Grujovic, N.:

TRIBOLOGY STUDY OF ALUMINUM-BASED FOAM.....149

Santosi, Z., Sokac, M., Tadic, B., Budak, I., Simunovic, G., Ilic Micunovic, M., Vukelic, D.:

EVALUATION OF KINETIC FRICTION COEFFICIENT FOR WOODEN SPECIMENS.....153

Strbac, B., Bisevac, S., Delic, M., Klobucar, R., Acko, B., Hadzistevic, M.:

COMPETENCE ASSESSMENT OF CMMs FOR DIFFERENT MEASURING TASKS.....157

Velkoska, C., Kuzinovski, M., Tomov, M.:

A REVIEW OF THE QUALITY COST STRUCTURE DEFINITION MODELS – THEORETICAL APPROACH.....161

Velkoska, C., Tomov, M., Kuzinovski, M.:

THEORETICAL ASPECTS RELATED TO THE CREATION OF

ALGORITHM FOR QUALITY COST MEASUREMENT SYSTEM165

Section D: PROCESS PLANNING, OPTIMIZATION, LOGISTICS AND INTERNET TECHNOLOGIES IN PRODUCTION ENGINEERING

Invited paper

Jokanović, S., Pejić, V., Borojević, S.:

STEP MODEL OF MACHINING FEATURES OF SWEEP TYPE169

Invited paper

Petrović, M., Jokić, A., Miljković, Z.:

SINGLE MOBILE ROBOT SCHEDULING: A MATHEMATICAL MODELING OF
THE PROBLEM WITH REAL-WORLD IMPLEMENTATION.....175

Borojević, S., Jovišević, V., Čiča, Đ., Sredanović, B.:

MODELING AND SIMULATION OF PRODUCTION PROCESSES FOR
THE TOOLS OF THE PRESS BRAKE179

Djurdjev, M., Milosevic, M., Lukic, D., Desnica, E., Todić, V., Kuric, I.:

MODIFIED PARTICLE SWARM OPTIMIZATION WITH CHAOTIC
MAPS FOR PROCESS PLANNING OPTIMIZATION183

Fajsi, A., Moraca S., Cvetkovic, N., Vekic, A., Ljubicic, M.:

CLUSTER-BASED PRODUCTION CONCEPT187

Mircheski, I.:

DETERMINATION OF DISASSEMBLY INTERFERENCE MATRIX AND IMPROVED
NONDESTRUCTIVE DISASSEMBLY SEQUENCES FOR THE PRODUCT.....191

Mitrovic, S., Dimic, Z., Jakovljevic, Z.:

DISTRIBUTED CONTROL OF MANUFACTURING RESOURCES – SECURITY RELATED ISSUES195

Moraca, S., Cvetkovic, N., Fajsi, A., Gracanin, D., Suzic, N.:

SCHEDULING IN PROJECT-BASED MANUFACTURING ENVIRONMENT.....199

Petković, D., Jeleč, A.:

CONCEPTUAL SOLUTION FOR FLEXIBILITY IMPROVEMENT OF
PROCESSING SYSTEM IN WOOD PROCESSING SECTOR.....203

Ristić, M., Manić, M., Kosanović, M., Pavlović, M.:

PARAMETRICALLY DESIGNED PRODUCT MANUFACTURABILITY
ANALYSIS USING KNOWLEDGE BASED SYSTEM207

Ristovska, B., Papazoska, E., Gecevska, V.:

IMPROVING MANUFACTURING PROCESS BY OPTIMIZING TIME PARAMETERS211

Skenderovska, T., Gecevska, V., Polenakovik, R.:

INCREASING PRODUCTION CAPACITIES THROUGH THE DEVELOPMENT AND
INTEGRATION OF THE 5 STAGE PROJECT MANAGEMENT METHODOLOGY215

Sormaz, D., Gouveia, R., Sarkar, A.:

RULE BASED PROCESS SELECTION OF MILLING PROCESSES BASED ON GD&T REQUIREMENTS219

Vukman, J., Lukic, D., Borojevic, S., Milosevic, M., Kramar, D.:

EXPERIMENTAL RESEARCH OF THE INFLUENCE OF HIGH-SPEED MACHINING
PARAMETERS ON TIME AND SURFACE ROUGHNESS OF THIN-WALLED PARTS227

Section E: MATERIALS, METAL FORMING, CASTING AND WELDING

Cabrilo, A., Geric, K.:

CHARPY IMPACT PROPERTIES OF A CRACK IN WELD METAL,
HAZ AND BASE METAL OF WELDED ARMOR STEEL233

Flegarić, S., Marjanović, D., Štorga, M., Bojčetić, N.:

SMART SHEET METAL FORMING TOOLS DESIGN237

Ghionea, I. G., Opran, C. G., Ćuković, S., Pleša, M.:

IMPROVEMENTS AND MATERIALS FOR PRODUCTION OF A MAGNETIC
DRIVE MICROPUMP: AN OVERVIEW AND RECOMMENDATIONS241

Kovačević, L., Terek, P., Miletić, A., Kukuruzović, D., Škorić, B.:

INFLUENCE OF COMPUTATIONAL GRID DENSITY ON RESULTS OF CASTING SIMULATION245

Kukuruzović, D., Terek, P., Kovačević, L., Škorić, B., Baloš, S., Panjan, P., Čekada, M., Miletić, A.:

ESTIMATION OF SOLDERING TENDENCY OF AL-ALLOY TOWARD CrAlN
AS A CANDIDATE COATING FOR HPDC TOOLS249

Miletić, A., Panjan, P., Čekada, M., Terek, P., Kovacevic, L., Skoric, B.:

MECHANICAL AND TRIBOLOGICAL PROPERTIES OF INDUSTRIALLY
PREPARED TiAlN HARD CERAMIC COATINGS253

Miletić, O., Todić, M.:

ANALYTICAL-EXPERIMENTAL DETERMINATION OF INSPECTION AT PROFILIZATION OF V-PROFILE257

Milutinović, M., Movrin, D., Skakun, P., Stefanović, Lj., Vilotić, D., Randelović, S.:

SOME REMARKS ON PROCESS OF COMBINED FORWARD - BACKWARD EXTRUSION OF STEEL261

Pecanac, M., Dramicanin, M., Janjatovic, P., Ristic, M., Rajnovic D., Sidjanin, L., Balos, S.:

INFLUENCE OF TOOL GEOMETRY ON FRICTION STIR WELDED JOINTS267

Radman, M., Jovanović, M., Uran, M., Trivković, Lj.:

TRAINING FOR INTERNATIONAL WELDING COORDINATORS271

Randjelović, S., Milutinović, M., Mladenović, S., Blagojević, V.:

FEM ANALYSIS OF DIE PLATE AT PIERCING AND BLANKING TOOL275

Ristic, M., Rajnovic, D., Macas, M., Balos, S., Sidjanin, L., Pecanac, M.:

THE STUDY OF THE CONTAMINATED SURFACE LAYER OF HIP TREATED SUPERALLOY IN100279

Simonović, S.:

ON OPTIMIZATION OF ATOMIC FORCE MICROSCOPE CANTILEVER
DESIGN WITH RESPECT TO ITS MECHANICAL REQUIREMENTS283

Trajanoska, B., Gavriloski, V., Doncheva, E.:

DEVELOPING AND TESTING HYBRID GLASS TO STEEL STRUCTURAL
ELEMENTS – FLEXIBLE DESIGN APPROACH287

Section F: MECHANICAL ENGINEERING AND ENVIRONMENTAL PROTECTION

Ašonja, A., Mikić, D.: FACILITIES WITH RES ON PUBLIC BUILDINGS IN THE CITY OF NOVI SAD	291
Bijelić, Z., Milanović, B., Miletić, D.: DEVELOPMENT OF MATHEMATICAL MODEL FOR OPTIMAL MANAGEMENT OF TECHNOLOGICAL DEVELOPMENT CHANGES.....	297
Cveticanin, L., Zukovic, M.: PROPERTIES OF MASS-IN-MASS UNITS OF THE ELASTIC METAMATERIAL.....	301
Desnica, E., Vulić, M., Pavlović, A., Nikolić, M.: ELV MANAGING THROUGH ANALYSIS OF RESOURCE CAPACITIES OF THE SERBIA: EQUIPMENT, HUMAN RESOURCE AND FINANCIAL SUPPORT	305
Dobrotvorskiy, S., Dobrovolska, L., Aleksenko, B.A.: THE USE OF INTERNAL DISSECTORS IN THE PROCESS OF REGENERATION OF ADSORBENTS BY MEANS OF THE MICROWAVE ENERGY	309
Djordjic, D., Djuric, S., Hadzistevec, M.: ANALYSIS OF FLOWS AND MANAGEMENT OF HAZARDOUS WASTE IN COMPLEX SYSTEMS	313
Ilic, B.: MANUFACTURE OF HEAT AND ELECTRIC ENERGY BY CONSTRUCTION OF MUNICIPAL SOLVENT AND AGRICULTURAL WASTE.....	319
Ilic Micunovic, M., Agarski, B., Hadzistevec, M., Kosec, B., Vukelic, D.: COMPARABILITY OF LIFE CYCLE ASSESSMENT RESULTS IN TYPE III ENVIRONMENTAL DECLARATIONS	323
Karanovic, V., Andric, S., Jocanovic, M., Orosnjak, M., Bugaric, U.: IMPORTANCE OF OFFLINE FILTRATION SYSTEM USE	327
Kecic, V., Prica, M., Kerkez, Đ., Becelic-Tomin, M., Kulic, A., Leovac Macerak, A., Dalmacija, B.: APPLICATION OF A DEFINITIVE SCREENING DESIGN TO MAGENTA DYE DEGRADATION BY HOMOGENEOUS FENTON PROCESS	331
Kovács, R., P.,V., Keszthelyi-Szabó G., Szendrő P.: ENHANCING BIOGAS PRODUCTION KINETIC OF WASTEWATER BY MICROWAVE PRE-TREATMENT	335
Krnjetin, S., Šupić, S.: CONSTRUCTION WITH BALED STRAW - FIRE SAFETY	341
Raspudic, V., Mikulic, Z.: OPTIMUM DESIGN OF I-SHAPED CROSS-SECTION USING NONLINEAR PROGRAMMING	347
Živanić, D., Gajić, A., Zelić, A., Ilanković, N.: FLAT BELT FEEDER REGULATION POSSIBILITIES	351

Section G: BIO-MEDICAL ENGINEERING

Bojanić Šejat, M., Todić, V., Mladjenović, C., Beju, L. D., Grujić, J.: TECHNOLOGICAL PREPARATION OF THE ENDOPROSTHESIS PRODUCTION	355
Kosec, B., Karpe, B., Vodlan, M., Kopac, I., Budak, I., Pavlic, A., Puskar, T., Zupancic, K., Fir, B., Gojic, M., Nagode, A.: THERMAL PROPERTIES OF TITANIUM ALLOYS USED IN DENTAL MEDICINE	359
Puškar, T., Budak I., Jakimov, D., Djurović Koprivica, D., Kojić, V., Ilić Mićunović, M.: TESTING BIOCOMPATIBILITY OF BONE SUBSTITUTE BY FLUORESCENT MICROSCOPY	363
Sekulic, J., Grujic, J., Maric, D., Zeljković, M., Tabakovic, S., Balos, S.: TESTING BIOCOMPATIBILITY OF MATERIAL FOR IMPLANTS	367
Trajanovic, M., Tufegdzic, M.: TRENDS IN PRODUCING PERSONALIZED BONE IMPLANTS USING ADDITIVE MANUFACTURING	371
Zigic, M., Grahovac, N.: ESTIMATION OF HUMAN BODY PARTS ORIENTATION USING DATA FROM IMU SENSORS	375
AUTHOR INDEX	379
INFORMATION ABOUT SPONSORS AND DONATORS	391

MMA 2018

FLEXIBLE TECHNOLOGIES

KEYNOTE PAPERS

Lihui Wang

COMBINING DIGITAL TWIN AND PROGNOSIS IN FACTORIES OF THE FUTURE

Abstract:

Advanced manufacturing depends on the timely acquisition, distribution, and utilisation of information from machines and processes across spatial boundaries. These activities can improve accuracy and reliability in predicting resource needs and allocation, maintenance scheduling, and remaining service life of equipment. As an emerging tool, digital twin provides new opportunities to achieve the goals of advanced manufacturing. This talk will first present the current status and the latest advancement of CPS in manufacturing in general and digital twin in particular. In order to understand CPS and its future potential in manufacturing, definitions and characteristics of CPS will be explained and compared with digital twin concept. This talk will then review the historical development of prognosis theories and techniques, and project their future growth enabled by the emerging CPS and digital twin technologies. Techniques both digital twin and CPS are highlighted, as well as the influence of these techniques on prognosis in smart factories of the future. Research and applications will also be outlined to highlight the latest advancement in the field. While digital twin shows great promise in factories of the future, challenges towards Internet-of-Everything in the areas of future trends remain to be identified in this talk.

Author:

Lihui Wang, Professor and Chair of Sustainable Manufacturing,
Department of Production Engineering, KTH Royal Institute of Technology,
Stockholm, Sweden, Phone: +46(0)8-790 8305
E-mail: lihuiw@kth.se

Dušan Šormaz**DISTRIBUTED PROCESS PLANNING FOR DIGITAL MANUFACTURING AND
INDUSTRY 4.0****Abstract:**

Digitization of manufacturing has been happening for many years, starting with NC machines in 1970's, FMS cells, and extending to CAD/CAM integration and application of computers in manufacturing planning and execution (for example CAPP and MES). An expansion and ubiquitous use of internet in all engineering activities also includes increased connectivity of manufacturing design, planning and execution. There have been several paradigms in recent research: digital manufacturing, smart manufacturing, cloud manufacturing, and, in Germany, Industry 4.0. Fundamental to the current expansion of those technologies is representation of manufacturing planning data in distributed format with covering the data model and semantic marking of the planning and resource data in order to provide an integrative framework for new paradigm of design everywhere - manufacture everywhere.

This presentation will provide an overview of tools and methods for integrative manufacturing planning, which includes distributed (agent-based) applications for product development cycle: design, process planning, setup planning, manufacturing scheduling and FMS simulation. Product development cycle starts with a product design in CAD software and its CAD model transfer to other applications. The first application is feature mapping/feature recognition in order to convert part geometry into valid manufacturing features. Process planning starts with a process selection using rule based tools, proceeds to machine and tool determination, cost and time estimation, and completes with a process network generation and plan optimization through sequencing and clustering for necessary setups. Process plans can be optimized statically (before actual manufacturing) or dynamically (during the manufacturing execution). In the latter case, significant improvements are expected, as process plan network is optimized during execution, and the savings and performance are usually verified by discrete simulation of the manufacturing (FMS) process. We will briefly mention a few extensions of the core model.

In order to accomplish the proposed real time optimization it is necessary that the [proposed] semantic data model interfaces with real time manufacturing control systems and also that the planning model receives real time feedback in terms of machine capabilities, wear and tear, and other data from intelligent sensors. In the second part of the presentation we will discuss methods to integrate digital manufacturing planning with Industry 4.0 tools for real time monitoring of the resources.

We will propose a distributed platform which is built on agent-based framework where various service agents can register and collaborate. Along with the service agents the platform also employs dealer agents (broker agent) to discover service agents for a particular service request. Ontology based agent communication uses semantic message structure to exchange information among different agents. Semantics used in the message structure are in turn referenced by IMPM ontology. In this loosely coupled platform, even AnyLogic simulation software is integrated as a simulation agent, capable of performing real time simulation of job scheduling and machine sequencing on the design data. We will briefly discuss our current work on developing manufacturing planning ontologies as a prerequisite tool to accomplish truly semantically integrative distributed manufacturing planning system.

Key words: *Process Planning, Digital Manufacturing, Industry 4.0*

Author:**Dr. Dušan Šormaz, Professor**

Department of Industrial and Systems Engineering, Russ College of Engineering and Technology,
Ohio University, Athens, OH, USA, Phone: +1 740 593 1545, Fax: +1 740 593 0778

E-mail: sormaz@ohio.edu

Manic, M., Vitkovic, N., Stojkovic, M., Mistic, D., Trajanovic, M.

DESIGN OF CUSTOMIZED ANATOMICALLY ADJUSTED IMPLANTS

Abstract: *Personalization in medicine mainly refers to the use treatments which are adjusted to a specific patient. Design and manufacturing of customized implants is a field that has been developed rapidly during recent years. This paper presents an originally developed method for designing a 3D model of customized anatomically adjusted implants for particular fractures. With this method it is possible to design volumetric implants used to replace a part of the bone or a plate type for fixation of a bone part. It could be used as a guideline for modifying standard implant and / or for creating personalized type of implant. Each of the stages of creation of implant should enable possibility of adequate requirements, knowledge and recommendations of the orthopaedic, and thus, in addition to automation, to provide flexibility to the patient at all stages regarding design and manufacture.*

Key words: *plate implant, 3D model, UDF, personalized medicine*

1. INTRODUCTION

CAOS (Computer Assisted Orthopedic Surgery) is a scientific and technical discipline where computer technology is applied for the treatment of the patients in the field of orthopedic surgery. CAOS brings together various fields of science and technology, like medicine, engineering, mathematics, robotics, computer vision, information systems, and other [1, 2]. The main requirement of CAOS is to provide the best possible medical treatment to the patient in pre-operative, intra-operative and/or post-operative procedures. One of the elements which greatly influence on the outcome of applied CAOS procedures are accurate geometrical models of human bones. The geometrical accuracy, topological similarity, anatomical and morphological correctness of these models are required goals of every procedure applied for their creation. Also, such models enable creation of customized bone implants [3, 4].

For the treatment of bone fractures surgeons apply techniques of internal and external fixation. Both internal and external fixation can be used for the healing of the bone fracture, but internal fixation is preferable, because it provides better functional recovery of the bone [5, 6, 7].

In the case of internal fracture treatment, in some clinical cases, it is of particular importance to utilize internal fixation elements whose geometrical and topological characteristics fully correspond to the shape and size of the patient's bone [4]. This paper focuses on implants which are not of a standardized shape and size, but are adjusted to patient specific needs (customized, personalized implants). The term 'customization' in medicine mainly refers to the use of the treatments which are adjusted to a specific patient. There are not many examples of this kind of approach in the process of implant design.

The geometry and topology of those implants are adjusted to the anatomy and morphology of the bone and fracture of the specific patient. Their application has a positive effect on patients, but on the other hand, requires more time for preoperative planning and manufacturing. Therefore, they are used in areas where

the application of predefined fixators can lead to complications in the surgical interventions or in the process of recovery.

Plate implants are the most used internal fixators. They are made in the various sizes and shapes, in order to be used for different patients [6, 7]. In such cases it is hard to find proper position of the plate, the patient's treatment may be hampered due to inadequate transfer of load during bone healing process. This problem can be reduced by the application of so called Patient Specific Plate Implants (PSPIs). The geometry and shape of PSPIs are adapted to the anatomy and morphology of the bone belonging to the specific patient [9]. Application of PSPIs has a positive effect on patients, but on the other hand requires more time for preoperative planning and their manufacturing [8, 9].

Plate implants are fixed to the bone with screws (Fig. 1). These kinds of implants are placed on the external surface of the fractured part of the bone [4, 7, 8]. In this way, fractured bone fragments are connected into a whole (reduction), and position and direction of the fragments are kept.

There can be found only few described examples of the methods for creating a 3D model of anatomically adjusted internal implants which correspond to the bone contour in the literature. In general, these studies are based on the use of scanned bone 3D model and standard reverse engineering procedures for creating 3D models of plate implants [10-12].

In [13] the description of a method and procedure of designing an internal fixation with plate shape type "medially locking plate" (MLP) is described, which is used for treating fractures of the femur from its lateral side. The position of a plate related to the femur is defined by creating a datum plane. Medial sketch of the MLP was created on the sagittal plane. Sketch was then extruded in both normal directions. The inner side of the fixator are approximated by polygons, and try to follow the bone surface.

In [9] the method which is used for designing an internal plate implant according to Mitkovic type TPL (tibia-plato-lateral) is shown.

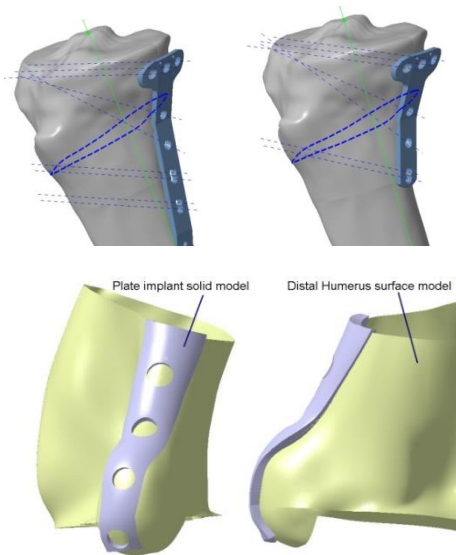


Fig. 1 Insertion of a plate for the upper part of tibia and distal humerus

The suggested method is based on the application of MAF - Method of Anatomical Features and newly developed techniques for designing fixation supporting surfaces, developed by the authors of this research. With this approach it was allowed to change the shape of a fixation in order to adjust it to the patient's bone shape, in this case tibia, based on parameters values (dimensions) read from a suitable X-ray or CT - Computer Tomography – scan.

Many methods for creating customized implants try to create a mirror image 3D model of a sound part of patient's bone.

The case related to reverse engineering of sternum (chest bone) body presented in the paper [14] brings out a method for creating customized implants. The missing part of the sternum, affected by cancer, was redesigned in accordance with the virtual model of the sternum bone that is generated from preceding geometrical analyses of the healthy sternum samples which were geometrically and dimensionally similar to the diseased one..

2. DESIGN PROCESS OF CUSTOMIZED IMPLANTS

The general engineering techniques for design, analysis and manufacturing of customized implants, for specific bones, used in this research, include several tasks [4, 9] (Fig. 2):

1. Creating a 3D parametric model of bones.
2. Creating a 3D parametric model of a fracture using a CT scan of a patient's fractured bones.
3. Selecting the places on the bone where the implant will be placed.
4. Adjusting the geometry of the implant according to the requirements of the surgeon.
5. Creating a customised 3D model of the implant.
6. Simulation of implant placement to bones.
7. Analysis and optimization of the shape and dimensions of implants.
8. Implant manufacturing.

This methodology gives the opportunity to create a

custom implant design adjusted to the patient's bone anatomy. 3D models of implants can then be used for the production of implants, after manufacturability analysis.

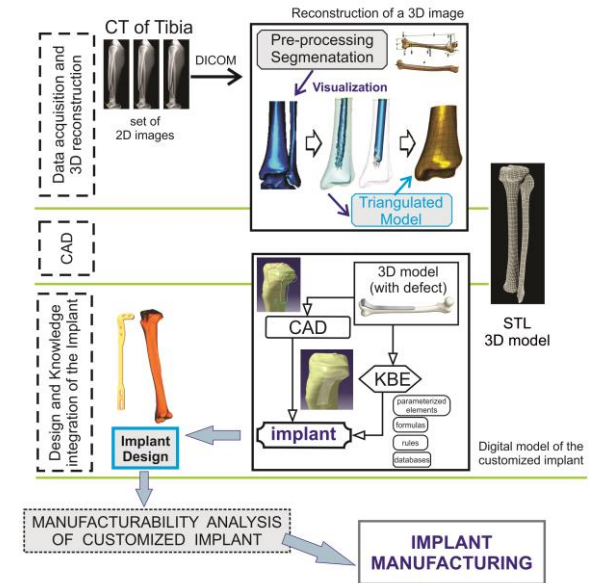


Fig. 2 Phases for designing and manufacturing of customized implants

The creation of 3D models of customized implants are based on the parametric 3D models of the patient bones and 3D model of fracture which is made on the 3D model of the bone.

Design process of anatomical adjusted customized implants, used in this paper, is shown in Fig. 3.

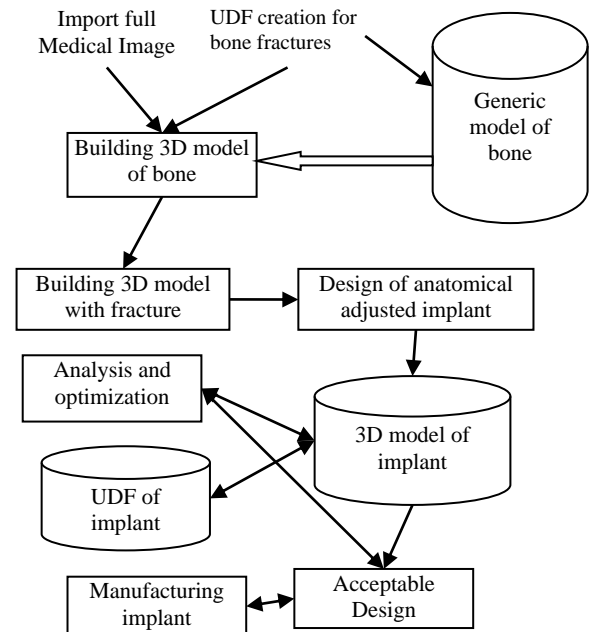


Fig. 3 Typical design process of anatomical adjusted customized implants

For this purpose, the first step is to create a 3D model of a selected bone.

The creation of geometrically accurate 3D models of human bones utilizes a number of different techniques and presents a unique challenge, because their

geometry and form are very complex. These types of shapes can be modelled by using surface patches represented by Bezier or B-spline surfaces, or by using NURBS patches, which are commonly used in traditional CAD applications, e.g. CATIA [2].

The output of CATIA is presented in the STL (Stereolithography) format, which allows it to be directly transferred into an RP (Rapid Prototyping) machine.

Reverse engineering of human bones implies the use of some kind of medical imaging device for the acquisition of medical data (Computer Tomography – CT, Magnetic Resonance Imaging – MRI), then processing the data in medical or CAD software, and at the end, creating a valid geometrical model (surface, volume).

2.1 Reverse modeling of the bone: Human humerus example

The reverse modeling procedure for humerus surface model creation contains several important steps and they are:

- 1 Filtering point cloud model acquired from CT scanning [2]
- 2 Creating polygonal model of the whole bone by the use of technical features implemented
- 3 Definition of the Referential Geometrical Entities (RGEs) [2, 15]
- 4 Creation of spline curves referenced to the RGEs
- 5 Creation of adequate surface models of the anatomical sections

2.2 Definition of the RGEs

The basic prerequisite for successful reverse modeling of a human bone's (humerus in this case) geometry is identification of RGEs. RGEs include characteristic points, directions, planes and views. The Anatomical axis of the proximal part of the humerus (metaphyseal axis) is defined as axis of the cylinder formed in the upper part of the humeral shaft [8].

This is Z axis – axis of the coordinate system. X axis is defined as a projection of the line which goes through tips of the epicondyles of the distal part of humerus on the plane perpendicular to Z axis. Y-axis is the line normal to the plane formed by Z and X axes. Three important planes were defined: Anterior-Posterior plane (X-Z), Lateral-Medial plane (Z-Y), and Axial plane (Y-X). Created RGEs are presented in Fig. 4.

2.3 Surface model of Human humerus

In order to create surface model of the humerus, spline curves were created in cross-sections of planes parallel to axial planes, and polygonal model was created for three anatomical sections: proximal section, shaft section, distal section. The initial cross-section curves were adapted to the geometry and shape of humerus by inserting additional points, or deleting unnecessary points. The positions of the spline curves were adjusted to the anatomical landmarks of the adequate anatomical section of the humerus.

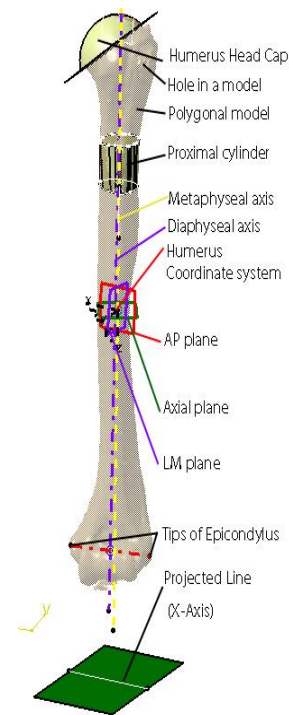


Fig. 4 RGEs defined on humerus bone

The surface models of humeral anatomical sections together with constructed spline curves are presented in Fig. 5. The proximal part and the shaft were created by the use of splines created in the axial planes (Fig. 5a and 5b).

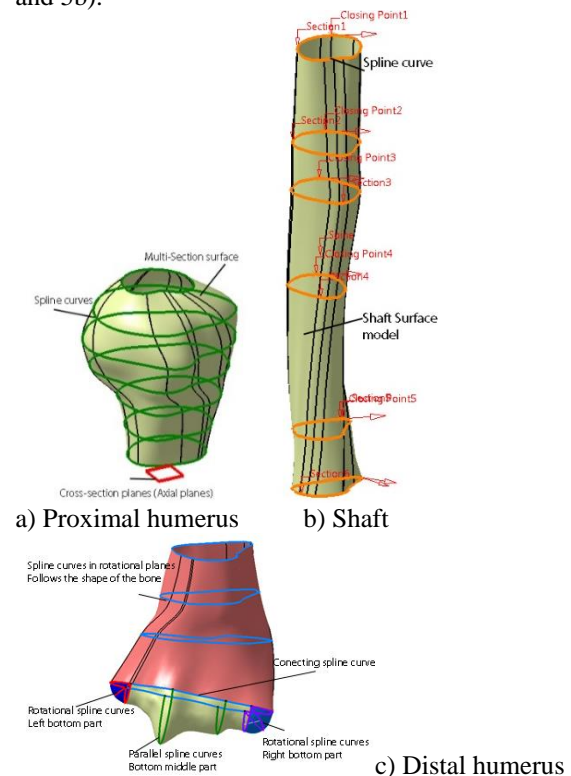


Fig. 5 Geometrical models of the individual parts of the humerus bone

Distal section was created as an assembly of four surface parts. This is done because shape of the distal part is very complex. The upper part was created by the use of spline curves positioned in rotational planes, with the upper ending curve (closer to the shaft) constructed in axial plane. These planes follow the

curvature of the distal part of the humerus. Right and Left bottom parts were created by the rotational curves and middle part was created by the parallel planes normal to the bottom ending plane of the upper part. The surface model of the distal part of the human humerus is presented in Fig. 5c.

2.4 Parametric model of the fracture Creating 3D parametric model of fracture

By using bone a 3D model and spline design techniques in CAD system, according to CT scan of fractured bones, it is possible to create a 3D parametric model of fracture. From a CT scan of the patient's fracture and the surgeon suggestions characteristic points of fracture are measured and transmitted to the 3D bone model.

With connecting them, the outside contour of fracture is obtained. The complete model of fracture is created using adequate engineering techniques for free form surfaces and spline modeling.

For this purpose AO/OTA Fracture and Dislocation Classification [16] is used. Some examples of created 3D model of tibia's fracture are shown in Fig. 6.

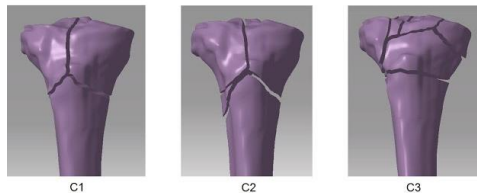


Fig. 6 3D models of a different types of fractures on proximal tibia

3. DESIGN OF AN ANATOMICALLY ADJUSTED IMPLANTS

Our research aim was to develop a design method and technique for creating several types of customized implants (Fig. 7).

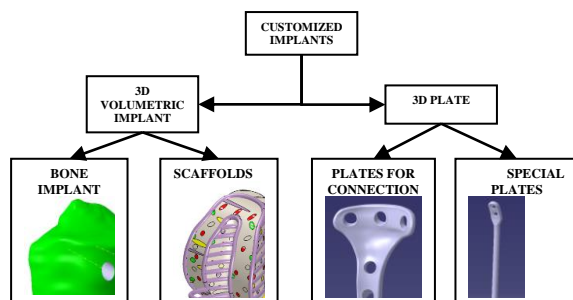


Fig. 7 Different types of customized implants

The principle of anatomical adaptability implies that the internal fixation with its contact surface fully corresponds to the surface of the part of a bone where the fracture is located. In this paper, we present the process of designing anatomically adjusted 3D volumetric implants for long bones, and type plate, by using CATIA V5 software package. For both designs of implant the first step is to create the parametrical 3D geometrical model of bone, or a part of bone, made on the basis of patient's CT scan [2, 8, 14, 15].

3.1 Designing technique of an anatomically adjusted 3D volumetric implants

According to a CT scan of patient's fracture, and the surgeon's suggestions, the model of fracture is created, using adequate engineering techniques for free form surfaces and spline modeling (Fig. 8).

When the fracture is created, and surfaces of the fracture satisfied the needs of surgeons, healthy bone fragments, that do not belong to the implant, are removed (Fig. 8). By removing desired bone fragments a basic 3D model of the implant is created. By using advanced engineering techniques for free form modeling, the initial model of implant can be modified. For instance, bevels, rounding and additional screw holes can be added and everything else that is needed for implant's production and implementation.

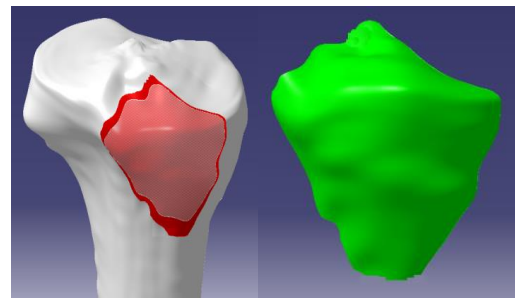


Fig. 8 3D model of fracture & Basic 3D model of volumetric implant

3.2 Designing technique of an anatomically adjusted implants type plate

The first step is creating a model of the fracture (Fig. 9).

Close to the model of the fracture, a datum plane, not far from the lateral surface of bone, is created, which is placed opposite the contour of the fracture (Fig. 9). The surgeon suggest and defines the position and orientation of this plane. Inside it, the contour of the proximal part of the plate is drawn.

Following that, the contour extrusion in the direction of the lateral bone side is performed so as to ensure that extruded contour surface penetrates the bone surface.

The intersected closed contour of the plate's internal side is created in this way. Inside of that contour, curve drawing of the 3D splines that follow the bone contour is performed. After this step, the moment comes when all the surfaces are removed and the only surface left is the one that actually presents the internal side of the plate that is put directly on the bone. Now this surface is extruded to transform it into a full model. With this process completed, we get a full 3D model of a proximal fixation plate that is completely anatomically adjusted to the surface of the proximal part of the bone (Fig. 10).

The the remaining parts of the internal fixator plate type are made with standard technical elements. After the plate has been shaped, the creation of the screw holes on the proximal side of plate part is performed. The process of screw holes creation is based on

projection points and created tangent planes and is performed on the part of the proximal plate surface.

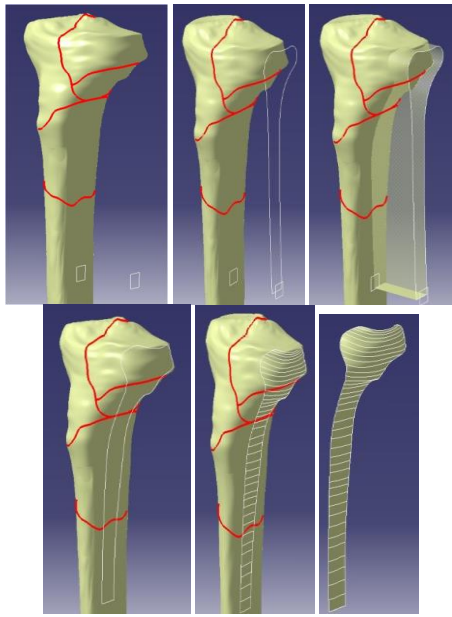


Fig. 9. Plate contact surface creation

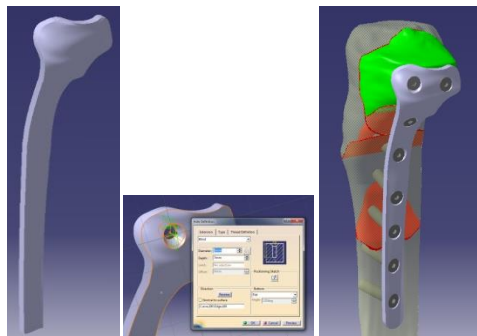


Fig. 10 Plate implant solid model

The assembly module of CAD system can be used to check whether the implant model plate type is appropriate by creating a assembly of a bone part, plate and fixation elements (Fig. 10). In this way, we can check the model, seating, the number of necessary screws, etc..

By combining two previously described techniques a 3D volumetric implant and a plate for its fixation can also be made. Moreover, a set bone-volumetric implant-fixation plate-bonding elements can be designed. The designed set is used for implementation simulation and all the other analyses (FEM etc.).

4. USER DEFINED FEATURE CREATED FOR THE PARAMETRIC FRACTURE

UDF defined for the bone with fracture is created by the use of complex process presented in Fig. 11. Bone fractures in UDFs are defined according to the OTA classification [16].

First element in UDF application is a selection of fracture type, which are presented in Fig. 12.

Next step is to define local coordinate system on the

bone 3D model. In order to create a representation of the fracture, specific points on the bone surface are selected, and spline curve is created. Final UDF is created by slicing the bone model with a fracture line. UDF contains dialog window with defined fracture type and its geometrical components, and type of UDF. UDF can be considered as a template model for the creation of fracture models defined by OTA classification, as presented in Fig 13 and Fig 14.

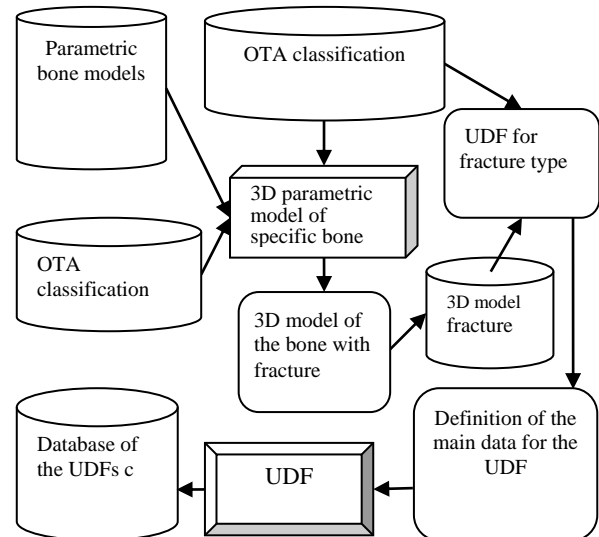


Fig. 11 Definition process for UDF for fracture

4 Tibia/fibula

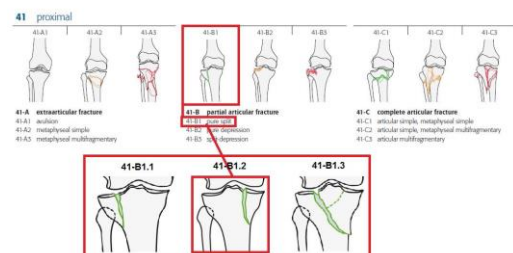


Fig. 12 OTA classification of tibia fractures

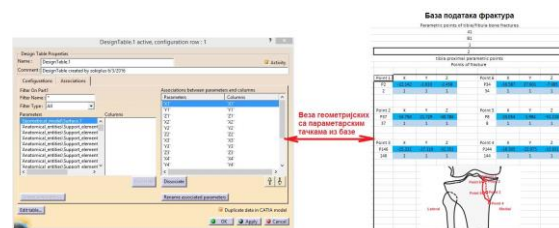


Fig. 13. UDF definition

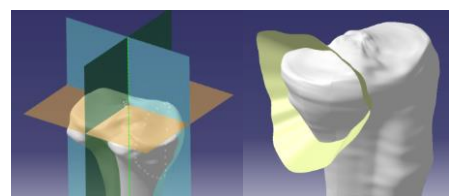


Fig 14. Referential geometry of the tibia fracture

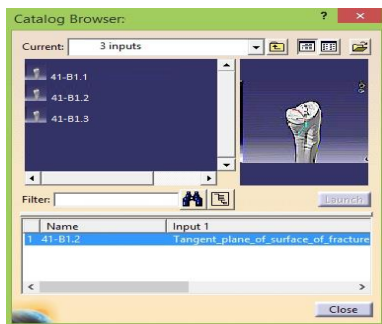


Fig 15. Selection of the UDF type

5. FINAL REMARKS

The presented method is based on designing implants directly on a patient's parametric three-dimensional (3D) bone model.

The created 3D model of plates is ideal for 3D printing or their production using a CNC machine. The method presented in this paper can be used for various kinds of internal fixators, which are directly attached to any bone surface.

6. REFERENCES

- [1] Kanlic, E.M., DeLaRosa, F., Pirela-Cruz, M.: *Computer Assisted Orthopaedic Surgery – CAOS*, Bosnian journal of basic medical sciences, Vol. 6, pp. 7-14, 2006.
- [2] Vitković, N., Milovanović, J., Korunović, N., Trajanović, M., Stojković, M., Mišić, D., Arsić, S.: *Software System for Creation of Human Femur Customized Polygonal Models*, Computer Science and Information Systems, Vol. 10, pp. 1473-1497, 2013.
- [3] Ghysar, R., Subburaj, K., Ravi, B., Agarwal, M.: *Adaptive Probabilistic Approach for Selecting Tumour Knee Prosthesis*, Computer Science and Information Systems, Vol. 10, pp. 1407-1428, 2013.
- [4] Manić, M., Stamenković, Z., Mitković, M., Stojković, M., Shepherd, D.E.T.: *Design of 3D model of customized anatomically adjusted implants*, Facta Universitatis, Series: Mechanical Engineering, Vol. 13, pp. 269-282, 2015.
- [5] Fragomen, A.T., Rozbruch, S.R.: *The Mechanics of External Fixation*, HSS Journal, Vol. 3, pp. 13-29, 2007.
- [6] Chulvi, V., Cabrian-Tarrason, D., Sancho, A., Vidal, R.: *Automated design of customized implants*, Revista Facultad de Ingeniería Universidad de Antioquia, pp. 95-103, 2013.
- [7] Grewal, R., MacDermid, J.C., King, G.J., Faber, K.J.: *Open reduction internal fixation versus percutaneous pinning with external fixation of distal radius fractures: a prospective, randomized clinical trial*, The Journal of Hand Surgery, Vol. 36, pp. 1899-1906, 2011.
- [8] Rashid, M.M., Husain, K.N., Vitković, N., Manić, M., Trajanović, M., Mitković, M., Mitković, M.: *Geometrical Model Creation Methods for Human Humerus Bone and Modified Cloverleaf Plate*, Journal of Scientific & Industrial Research, Vol. 76, pp. 631-639, 2017.
- [9] Vitković, N., Mitković, M.M., Mitković, B.M., Korunović, N., Stevanović, D., Veselinović, M.: *Reverse engineering of the mitkovic type internal fixator for lateral tibial plateau*, Facta Universitatis, Series: Mechanical Engineering, Vol. 13, pp. 259-268, 2015.
- [10] Limin, M., Ye, Z., Ye, Z., Zefeng, L., Lingling, C., Yu, Z., Hong, X., Chuanbin, M.: *3D printed personalized titanium plates improve clinical outcome in microwave ablation of bone tumors around the knee*, Scientific Reports, Vol. 7, Article number: 7626, 2017.
- [11] Cronsar, M.: *On customization of orthopedic implants - from design and additive manufacturing to implementation*, Doctoral thesis, Mid Sweden University, Faculty of Science, Technology and Media, Östersund, 2014.
- [12] Xiaozhong, C., Zhijian, M., Ya, G.: *Rapid development of the fracture implant by combining CAD and CAE technologies based on the patient's information*, Biomedical Research, Vol. 28, pp. 2636-2638, 2017.
- [13] Joshua, A.: *A comprehensive simulation-based methodology for the design and optimization of orthopaedic internal fixation implants*, Doctoral thesis, University of Missouri, Faculty of the Graduate School, Columbia, 2011.
- [14] Stojkovic, M., Milovanovic, J., Vitkovic, N., Trajanovic, M., Grujovic, N., Milivojevic, V., Milisavljevic, S., Mrvic, S.: *Reverse modeling and solid free-form fabrication of sternum implant*, Australasian Physical & Engineering Sciences in Medicine, Vol. 33, pp. 243-250, 2010.
- [15] Majstorovic, V., Trajanovic, M., Vitkovic, N., Stojkovic, M.: *Reverse engineering of human bones by using method of anatomical features*, CIRP Annals – Manufacturing Technology, Vol. 62, pp. 167-170, 2013.
- [16] <https://aotrauma.aofoundation.org>, Last access: 01.09.2018.

Authors: Full Prof. Miodrag Manic, Assist. Prof. Nikola Vitkovic, Full Prof. Miroslav Trajanovic, Assist. Prof. Milos Stojkovic, Assoc Prof. Dragan Mistic, University of Nis, Faculty of Mechanical Engineering, Aleksandra Medvedeva 14, 18000 Nis, Serbia, Phone.: +381 18 500-661.
E-mail: miodrag.manic@masfak.ni.ac.rs, nikola.vitkovic@masfak.ni.ac.rs, miroslav.trajanovic@masfak.ni.ac.rs, milos.stojkovic@masfak.ni.ac.rs, dragan.mistic@masfak.ni.ac.rs,

ACKNOWLEDGMENTS: The paper presents the case that resulted from application of the research project id III 41017 (Virtual Human Osteoarticular System and its Application in Preclinical and Clinical Practice) sponsored by the Ministry of Education, Science and Technological Development of the Republic of Serbia..



Section A:

**MATERIAL PROCESSING
TECHNOLOGIES**

ANALYSIS OF VARIABLE COSTS IN CO₂ LASER CUTTING OF MILD STEEL

Abstract: Selection of the laser cutting conditions for satisfying different dimensional, quality and productivity characteristics while ensuring cutting with the lowest cost is of great importance for companies which use laser cutting technology. Given that laser cutting costs may vary considerable, in this paper an analytical mathematical model for variable cost estimation in CO₂ laser cutting was developed upon proposed influence chart for variable costs. Upon realization of an experimental investigation of CO₂ laser cutting of mild steel, the developed analytical mathematical model for variable costs estimation was translated to an empirical mathematical model. Using the model an analysis of the variable costs in CO₂ laser cutting for different cutting conditions and in relation to the material removal rate was performed.

Key words: CO₂ laser cutting, variable costs, mild steel, material removal rate

1. INTRODUCTION

Trends in small batch manufacturing in the sheet metal industry are a further decrease of batch sizes, shorter delivery times and lower prices [1]. In order to be market leader in sheet metal industry it is necessary to be able to provide high quality products at the lowest price. Therefore determination of the associated costs for a given application is of great importance as the cost calculation is a basis for proposing the final price for a given job to potential customers so that all direct (prime) costs and indirect costs are covered while a certain amount of profit is ensured. In modern industry, use of non-conventional machining processes for contour cutting such as laser cutting is being more implemented every day for its optimal characteristics [2]. In laser cutting cost calculation is complex task considering that one needs to decide which cutting method is to be used for a given workpiece material and its thickness, which performances are to be achieved and finally which set of main factor values, regarding laser power, cutting speed, type and pressure of assist gas, nozzle type and diameter, will be used. In order to consider laser cutting cost in line with other performances like quality criteria, productivity, etc. it is necessary to consider all constitutive aspects of laser cutting costs through development of a mathematical cost model. In such a way, based on the mathematical model, for a given laser cutting application one can simultaneously analyze different performances including cost and make certain trade-offs ensuring that all requirements are satisfied with the least cost [3].

Given that laser cutting costs may vary considerable with respect to selected cutting conditions, the present study aims at proposing an analytical mathematical model for estimation of variable costs in CO₂ laser cutting considering main contributing variable parameters such as laser power, cutting speed, assist gas pressure and nozzle diameter. Upon realization of an experimental investigation of CO₂ laser cutting of mild steel, the developed analytical mathematical model for variable costs estimation was translated to an

empirical mathematical model. Using the model an analysis of the variable costs in CO₂ laser cutting of mild steel was performed considering default and optimized cutting conditions as well as for cutting conditions suggested in literature and by manufacturers. The conducted analysis included joint analysis of variable costs and material removal rate (MRR) through multi-objective optimization.

2. VARIABLE COSTS IN CO₂ LASER CUTTING

Apart from investment cost for buying a laser cutting machine, considerable amount make costs of assist gases and electricity costs, followed by cost of laser gases, maintenance costs (cleaning and replacement of lenses, nozzles, guiding mirrors, etc.), labour costs, etc. All associated costs in laser cutting can be grouped into fixed and variable costs. Investment costs, maintenance costs, labour costs and laser gas (mixture of CO₂, H_e and N₂) costs constitute fixed costs.

Selection of the laser cutting conditions for a given application is predominantly affected by cutting performances which are aimed to achieve (dross absence, perpendicularity of cut, surface roughness, productivity, etc.). As there are no specific recommendations for a given application, process planners and engineers are usually conservative in selecting laser cutting conditions. They are primarily guided by acquired experience and knowledge as well as manufacturers recommendations, often overlooking laser variable costs which are affected by a number of parameters (Figure 1).

According to the basic constitutive cost components (Figure 1) the variable costs in CO₂ laser cutting can be determined as [3]:

$$C_v = C_e + C_{ag} \quad (1)$$

where C_e (EUR/h) is laser electrical power cost and C_{ag} (EUR/h) is assist gas cost.

Laser electrical power cost can be determined as the function of the CO₂ laser cutting machine electrical power, electricity price and maximal and operational

laser power in the following form [4]:

$$C_e = 0.8 \cdot c_e \cdot P_E \cdot \frac{P}{P_{\max}} \quad (2)$$

where 0.8 stands for power factor, c_e (EUR/kWh) is electricity price (0.12 EUR/kWh), P_E (kW) is CO₂ laser cutting machine electrical power, P (kW) is laser power and P_{\max} (kW) is the maximal laser power.

The assist gas cost can be determined as [3]:

$$C_{ag} = c_{ag} \cdot Q_{ag} \quad (3)$$

where c_{ag} (EUR/m³) is the price of the assist gas and Q_{ag} (m³/h) is the consumption of the assist gas.

The general mathematical model for consumption of the assist gas, provided by TRUMPF laser cutting machine manufacturer, is as follows:

$$Q_{ag} = 0.555 \cdot d_n^2 \cdot p \quad (4a)$$

where d_n (mm) is the nozzle diameter and p (bar) is the assist gas pressure.

Also, based on the tabular data provided by Bystronic laser cutting machine manufacturer, one can derive the following mathematical model for consumption of the assist gas, which is valid for low pressure cutting, i.e. laser cutting of mild steel with oxygen:

$$Q_{ag} = 4.554 - 5.775 \cdot d_n - 1.513 \cdot p + 2.036 \cdot d_n^2 + 0.046 \cdot p^2 + 1.725 \cdot d_n \cdot p \quad (4b)$$

The above developed model for the assist gas consumption is valid for nozzle diameters of 0.8, 1, 1.25, 1.5, 2, 2.5 and 3 mm.

The price of the assist gas c_{ag} (EUR/m³) on the Serbian market is variable and is dependent upon the quantity of assist gas ordered as well as assist gas supplier. For smaller quantities the price for oxygen 3.5, provided by one of the leading suppliers of industrial gases, is somewhere around 3.07 EUR/m³. It should be noted that for quantities exceeding 70 tons per year, the price can be ten or more times smaller.

3. RESULTS AND ANALYSIS

3.1 Experimental details

On the basis of previous equations one can estimate variable costs in CO₂ laser cutting for each particular cutting condition, i.e. combination of cutting

parameters (nozzle diameter, assist gas pressure, cutting speed, laser power) as well as cutting method (oxygen or nitrogen cutting). In the present study an analysis of variable costs in CO₂ laser cutting of mild steel is attempted. The previous analytical model for the estimation of variable costs can be transformed into empirical relationship between laser cutting parameters and variable costs for a given experimental hyper-space. In the present investigation an experiment was performed by using full factorial plan 3³ whereby three main laser cutting parameters (cutting speed, laser power and oxygen pressure) were varied at three levels (Table 1). The experimental hyper-space was chosen such that wider region around the manufacturers recommendations is included. The experiment was conducted in real manufacturing environment whereby combination of laser cutting parameters as in trial 14 is used for cutting by default. Apart from estimating variable costs for each particular combination of laser cutting parameters, MRR was also calculated so as to reveal possible relationship between these two laser cutting performance characteristics. MRR was calculated after measuring kerf widths in all trials as the product of kerf width, workpiece material thickness and cutting speed.

In the experiment Bystronic (Switzerland) "ByVention" 3015 CO₂ laser cutting machine with a maximal power of $P_{\max} = 2.2$ kW was used. Electrical power consumption of this machine and its units is $P_E = 35$ kW. In all trials conical nozzle with diameter of $d_n = 1$ mm was used. The nozzle-work piece stand-off distance of 0.7 mm was kept constant during cutting. The Gaussian distribution beam mode (TEM₀₀) was used in trials. Workpiece material was mild steel with thickness of 2 mm. A focusing lens with a focal length of 5 in. (127 mm) was used.

3.2 Analysis of variable costs

As could be observed from Table 1 variable costs in the covered experimental hyper-space range from 7.1 EUR/h to up to 15.96 EUR/h. On the other hand MRR range from 1782 mm³/min to up to 4860 mm³/min. The adopted default cutting conditions in the production practice produce 10.97 EUR/h variable costs and MRR of 3120 mm³/min which represent intermediate values.

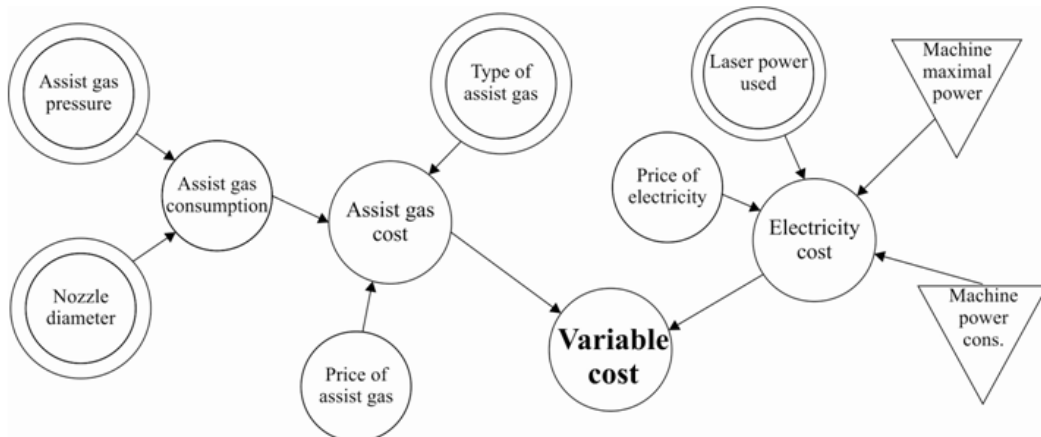


Fig. 1. Influence chart of variable costs in CO₂ laser cutting

Trial	Cutting speed, v (m/min)	Laser power, P (kW)	Oxygen pressure, p (bar)	Variable costs, C_v (EUR/h)	MRR (mm ³ /min)
1	3	0.9	3	7.10	1782
2	3	0.9	5	10.66	2094
3	3	0.9	7	15.35	2136
4	3	1.1	3	7.41	2226
5	3	1.1	5	10.97	2016
6	3	1.1	7	15.66	2805
7	3	1.3	3	7.71	2226
8	3	1.3	5	11.27	2232
9	3	1.3	7	15.96	2556
10	5	0.9	3	7.10	3195
11	5	0.9	5	10.66	2945
12	5	0.9	7	15.35	3125
13	5	1.1	3	7.41	3045
14*	5	1.1	5	10.97	3120
15	5	1.1	7	15.66	3045
16	5	1.3	3	7.71	2965
17	5	1.3	5	11.27	3265
18	5	1.3	7	15.96	3685
19	7	0.9	3	7.10	3710
20	7	0.9	5	10.66	3115
21	7	0.9	7	15.35	4774
22	7	1.1	3	7.41	3535
23	7	1.1	5	10.97	4466
24	7	1.1	7	15.66	4368
25	7	1.3	3	7.71	3710
26	7	1.3	5	11.27	4683
27	7	1.3	7	15.96	4860

* adopted default cutting conditions (currently used in production)

Table 1. Variable costs and MRR in each experimental trial

Based on the provided tabular data one can derive empirical relationships between laser cutting parameters and variable costs and MRR so as to analyse its effects in the covered experimental hyper-space. Using the least square method one can obtain the following models:

$$C_v = 2.502 + 1.527 \cdot P + 0.65 \cdot p + 0.141 \cdot P \cdot p \quad (5)$$

$$\begin{aligned} MRR = & -1456.31 + 425.25 \cdot v + 3833.33 \cdot P - 148.31 \cdot p \\ & - 3.97 \cdot v^2 - 1380.56 \cdot P^2 + 14.94 \cdot p^2 - 30.83 \cdot v \cdot P \\ & + 20.5 \cdot v \cdot p + 10.83 \cdot P \cdot p \end{aligned} \quad (6)$$

The accuracy of developed mathematical models was confirmed with coefficient of determination having high values. Using these models one can estimate variable costs as well as MRR for each particular cutting condition inside the covered experimental hyper-space. Also one can estimate variable costs in laser cutting of mild steel based on manufacturers and handbook recommendations. The comparison of variable costs in EUR/m for different suggested cutting conditions for the adopted laser cutting machine is given in Table 2.

As could be observed from Table 2 there exists a considerable difference in variable costs for given laser cutting conditions and in some cases multiple difference is evident. All afore-given laser cutting recommendations are derived for ensuring stable, dress free cutting conditions. It has to be noted that although optimized cutting conditions produce less variable costs (0.017 EUR/m) than adopted default cutting conditions the problem which arises is dress formation. Given that the mathematical model for MRR was developed an aim was imposed to determine laser cutting conditions so that acceptable trade-off between variable costs and MRR is achieved. Therefore, a set of Pareto optimal solutions was determined using the epsilon constraint method (Figure 2). As could be observed from Figure 2 there exists a perfect linear relationship between variable costs and MRR. All solutions on Pareto front are equally good with respect to trade-off of variable costs and MRR. However, as these optimization solutions correspond to different combinations of cutting speed, laser power and oxygen pressure, one has to consider other criteria.

Cutting conditions	Nozzle diameter, d_n (mm)	Cutting speed, v (m/min)	Laser power, P (kW)	Oxygen pressure, p (bar)	Variable costs, C_v (EUR/m)
Adopted default conditions	1	5	1.1	5	0.037
Optimized conditions	1	7	0.9	3	0.017
[5]	0.8	5	1.2	4.5	0.022
[6]	0.6÷1.2	7	1	2.5÷4	0.01÷0.029
[7]	1.5	4.4	1.2	3	0.055
[8]	0.6÷1.5	5÷6.5	1.5	3÷4	0.012÷0.038

Table 2. Tabular summary of variable costs for different laser cutting conditions

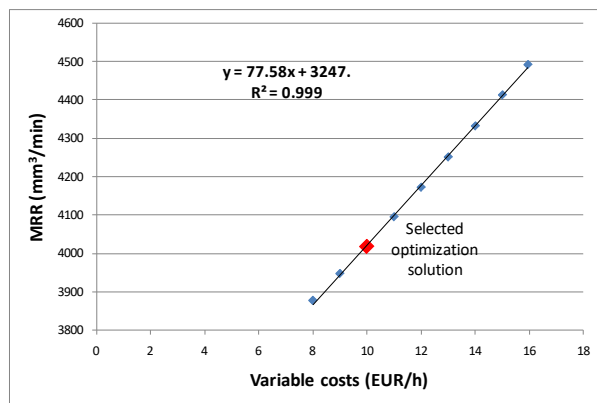


Fig. 2. Pareto front of optimization solutions

Assuming dross formation as one of the most stringent criteria for assessing the quality of laser cuts, a combination of cutting speed of 7 m/min, laser power of 1.3 kW and oxygen pressure of 4.87 bar was selected as the best solution. Namely, in the present experimental investigation it has been revealed that low severance energies (below 5 J/mm²) and intermediate severance energies (between 8 and 12 J/mm²) in combination with high oxygen pressure result in dross formation. This was guiding idea for selecting the final, optimized solution with respect to both variable costs and MRR. The determined laser cutting conditions enable dross free cutting and produces variable costs of 0.026 EUR/m which represents saving of 0.011 EUR/m when considering the adopted default cutting conditions which are currently used in the production. Moreover, the MRR was increased from 3120 mm³/min to 4095 mm³/min which represents about 30% higher productivity.

4. CONCLUSION

Comprehensive analysis of a laser cutting technology involves a number of performance characteristics including quality characteristics, productivity, cutting time as well as cutting costs. The complexity of this non-conventional machining process is reflected through the fact that a number of process parameters differently and to a lesser or greater extent affect all these performance characteristics.

In this paper an analytical mathematical model for CO₂ laser cutting variable cost calculation was developed. The model comprises of electrical power cost and assist gas cost including related parameters which are selected for a given job shop application such as nozzle diameter, assist gas pressure and laser power. Upon realization of an experimental investigation of CO₂ laser cutting of mild steel, the developed analytical mathematical model for variable costs estimation was translated to an empirical mathematical model valid for the covered experimental hyper-space. By using the derived model an analysis of the variable costs in CO₂ laser cutting of mild steel was performed for default and optimized cutting conditions as well as regarding literature and manufacturers recommendations. It has been revealed that variable costs in EUR/m can vary up to five times. Moreover, the conducted analysis included joint analysis of

variable costs and MRR through the development of Pareto front. Perfect linear relationship between these two performance characteristics was observed and as a result cutting conditions for dross free cutting and enhanced MRR and decreased variable costs were determined.

By using the developed model one can calculate variable costs for different possible cutting conditions prior to actual CO₂ laser cutting operation. Also, one can optimize laser cutting process considering variable costs and other performance characteristics which are of prime importance for a given job shop.

5. REFERENCES

- [1] Brinke, E.T.: *Costing support and cost control in manufacturing: a cost estimation tool applied in the sheet metal domain*, PhD Thesis, University of Twente, 2002.
- [2] Nedić, B., Erić, M., Aleksijević, M.: *Calculation of laser cutting costs*, International Journal for Quality Research, 10(3), pp. 487-494, 2016.
- [3] Madić, M., Radovanović, M., Nedić, B., Gostimirović, M.: *CO₂ laser cutting cost estimation: mathematical model and application*, International Journal of Laser Science: Fundamental Theory and Analytical Methods, 1(2), pp. 169-183, 2018.
- [4] Eltawhni, H.A., Hagino, M., Benyounis, K.Y., Inoue, T., Olabi, A.G.: *Effect of CO₂ laser cutting process parameters on edge quality and operating cost of AISI316L*, Optics and Laser Technology, 44(4), pp. 1068-1082, 2012.
- [5] Shulz, W., Hertzler, C.: *Cutting: modeling and data*, In: Poprawe R., Weber H., Herziger G. (eds) Laser Applications. Landolt-Börnstein - Group VIII Advanced Materials and Technologies (Numerical Data and Functional Relationships in Science and Technology), vol 1C. Springer, Berlin, Heidelberg, 2002.
- [6] Berkmanns, C.J., Faerber, U.M.: *Facts about laser technology - laser cutting*. Linde AG. Linde Gas Division. Hollriegelskreuth. Germany.
- [7] <http://www.prclaser.com/calculator.html>
- [8] Schuöcker, D.: *High power lasers in production engineering*, World Scientific Publishing Company, 1999.

Authors: Dr. Miloš Madić, Assoc. Prof. Predrag Janković, Full Prof. Miroslav Radovanović, M.Sc. Srđan Mladenović, Assist. Prof. Dušan Petković, University of Niš, Faculty of Mechanical Engineering in Niš, Aleksandra Medvedeva 14, 18 000 Niš, Serbia, Phone: +381 18 500-687, Fax: +381 18 588-244.
E-mail: madic@masfak.ni.ac.rs; jape@masfak.ni.ac.rs; mirado@masfak.ni.ac.rs; maki@masfak.ni.ac.rs; dulep@masfak.ni.ac.rs

ACKNOWLEDGMENTS: This work was carried out within the project TR 35034 financially supported by the Ministry of Education and Science of the Republic of Serbia.

Cerce, L., Borojevic, S., Kramar, D.

OPTIMIZATION OF THE PROCESS PARAMETERS FOR STABILIZATION AND IMPROVEMENT OF THE TURNING PROCESS CAPABILITY

Abstract: The paper deals with a narrow tolerances turning process. A statistical process control (SPC) on the existent machining process showed that the process was not stable and incapable. Before the machining process analysis a measurement system analysis (MSA) of the applied measuring system has been performed. In order to stabilize the process the machine tool linear axis calibration has been performed. The stability and capability of the machining process increased but the problem of the roundness was still present. The possible process parameters, which could affect the roundness, were examined with the design of the experiment methodology (DOE). The results showed that the clamping force has the largest effect. Therefore a new clamping fixture was suggested to eliminate the roundness problem.

Key words: Roundness; MSA; SPC; DOE

1. INTRODUCTION

In today's highly demanding markets the industrial organizations are under big pressure of competition and can only survive when high-quality products are produced. Manufacturers can achieve higher levels of quality by improving their manufacturing process and/or by product inspection where several different strategies are often available [1]. Each option has its own cost implications that must also be taken into account when the production cost are considered. Juran [2] was one of the first quality leaders who has connected quality control and assurance with costs, and includes all the costs that would appear if defects were produced. These quality-related costs are classified into prevention costs, appraisal costs, and failure costs. In real production these costs are usually not clearly understood. These costs of quality often disappear as the costs of testing, the general developments costs, or the operating expenses, etc. which is misleading. Several studies present and evaluate the impact of quality management activities using cost of quality as a metric [3, 4] or by modeling [5, 6].

In our study cost related to the product inspection would like to be reduced by improving the manufacturing process. The product under consideration is die-casted part of the gearbox housing. Machined surfaces, where bearings are fixed, have narrow tolerances of 20 μm . The production batch is more than 500.000 pieces. 100 % dimensional control of the machined parts is performed at the measurement station, which requires a high level of control over the processing process and, consequently, the loss of time.

1.1 Problem statement - machining process instability

A problem occurs during the machining process in real production, because the machine tool, i.e. CNC lathe does not provide sufficient stability in terms of keeping the produced parts within the tolerance range. When the CNC lathe is in regular operation, the

dimensions are either within the tolerance range or are moved against the tolerance limits. The problem also occurs when the machine tool is stopped (unexpected stop, cleaning, lunch break ...), and consequently cooled down. After the restarting of machine tool, the dimensions deviate considerably; thereby the produced parts are unaccepted. Because of this, 100 % dimensional control and on-line cutting tools offsets correction are necessary. This results in time and cost losses.

The aim of the presented work is to analyse the problem of dimensional deviations of produced parts. With the use of different quality management tools, the stabilization and the capability improvement of turning is expected.

2. MACHINING PROCEDURE AND QUALITY CONTROL

The produced part is bearing housing made of Al alloy with 5 key diameters (Fig. 1). They are manufactured in a tolerance range from 20 to 40 μm . The dimensions of all five holes are 100% controlled at a special measurement station. The other dimensions have a wider tolerance range, so there is no need for 100% control, and they are checked only twice a day.



Fig. 1. Cross section of the bearing housing. [7]

2.1 Machining procedure

The product is manufactured with longitudinal internal and external turning on 4-axis (X, Y, Z and C) CNC lathe with sub-spindle. Poly-crystalline diamond (PCD) cutting inserts are used because their wear is negligible when machining Al alloys. The negligible wear consider as wear, which does not represent an influential factor on the stability of the processes. The used cutting parameters are presented in the table below.

Diameter [mm]	Cutting insert	f_n [mm/rev]	a_p [mm]
64.3	DCMW 11T304	0.08	0.37
65	DCMW 11T304	0.08	0.37
72	DCMW 11T304	0.08	0.37
88e6	CCGW11T308	0.12	0.37
88h6	CCGW11T308	0.12	0.37

Table 1. Cutting parameters.

The clamping of the workpiece is carried out automatically with a robot. The workpiece is placed in a clamping device with three supporting points (Fig. 2), which form a plane perpendicular to the longitudinal (Z) axis of turning.

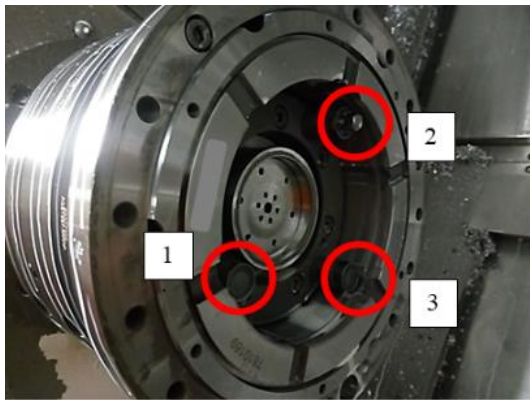


Fig. 2. Three point clamping device. [7]

2.2 Quality control

In the mass production, it is important that the machining process runs smoothly without stops. At the end of the production process the prescribed dimensional tolerances and surface roughness have to be achieved. The stability of the machining process is monitored by measuring the dimensions of the workpiece on the special measuring system (Fig. 3), which is located next to the machining centre.

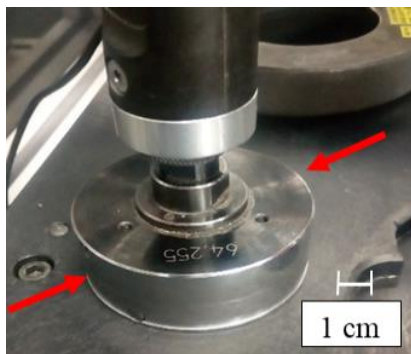


Fig. 3. Measurement system for $\phi 64.3$ mm. [7]

3. OVERVIEW OF THE CURRENT STATE OF THE PRODUCTION PROCESS

An overview of the existing situation is an important step that gives us a feedback on the quality of the production process. In our case the production process consist of the machining and the measuring process. If we realize that the quality of produced parts is not adequate, three characteristic states of the production process occur:

1. The part is acceptable, but the measurement system does not show exact result, thus the product is detected as unacceptable.
2. The machining process is inadequate, which results in an unacceptable product.
3. The measurement process and the machining process are inadequate.

Therefore, the measuring and machining process have to be analysed to establish the current state of the production process.

The measuring process is analysed with the use of Measurement System Analysis (MSA) method, while SPC (Statistical Process Control) and DOE (Design of experiment) methods are used to analyse the machining process.

3.1 Measurement System Analysis (MSA)

MSA is a set tool used to evaluate the statistical properties of the process measurement systems. The purpose of MSA is to statistically verify that current measurement systems provide:

- Representative values of the characteristic being measured,
- Unbiased results,
- Minimal variability.

The following parameters have been used for MSA analyze:

- 3 operators,
- 10 samples,
- 3 measurements for each sample.

The result of MSA method is the calculated percentage of process variation (%GRR). If the %GRR is:

- < 10% - The measurement system is acceptable.
- Between 10% and 30% - The measurement system is acceptable depending on the application, the cost of the measurement device, cost of repair, or other factors.
- > 30% - The measurement system is not acceptable and should be improved [8].

The gage R&R study has been made on all 5 machined diameters, which are 100% measured. The measuring procedure consist of next steps:

- Calibration of the measuring device.
- First operator measures ten samples, which are marked with numbers from one to ten.
- Second operator measures ten samples.
- Third operator measures ten samples.

This steps has been repeated two times. In this way, every operator measured ten samples three times.

Before each operator start with the measurement, the measuring device has been calibrated. Based on the measured results, the percentage of process variation is calculated for each machined diameters. Fig. 4 illustrates the results of Gage R&R study for diameter $\phi 64.3$ mm.

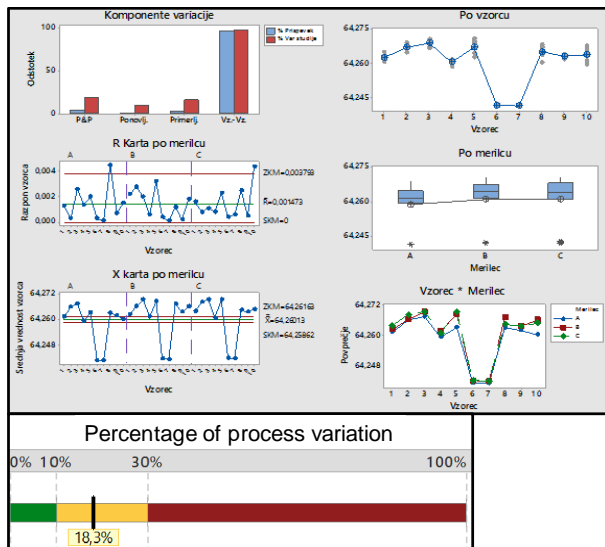


Fig. 4. Results of Gage R&R study for diameter $\phi 64.3$ mm. [7]

The calculated process variation for diameter $\phi 64.3$ mm is 18.3%. The measurement system is conditionally acceptable.

The same procedure has been used to calculate the measurement process variation for all other diameters. Fig. 5 present the overall result of Gage R&R study for all diameters.

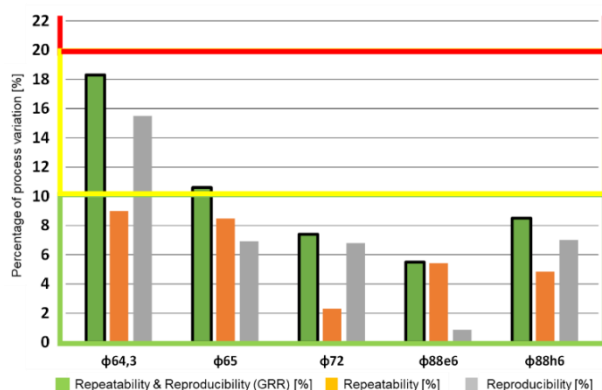


Fig. 5. Results of Gage R&R study for all diameters. [7]

The Gage R&R study showed that the measuring process is acceptable and capable for preforming accurate measurement (Fig. 5, all the results of %GRR are below 30%).

From the results of Gage R&R study it can be concluded, that the causes of the instability of the production process must be found in the machining process. To find the cause of instability, the current state of the machining process should be analysed.

3.2 Analysis of the capability of the machining process

After analysing the measurement system used for the control of machined parts, and found to be appropriate, the ability of the machining process was analyzed. SPC is a method that determines the ability and stability of the machining process based on the obtained data. The method provides feedback on the past and current state of the process. Based on the current state we can predict how the process will behave in the future. In this way we can prevent the destabilisation of the process, which leads to the production of unaccepted products and consequently increased costs.

After the measurements have been taken, the SPC analysis has been carried out with the use of Minitab program. The analysis has been performed on all diameters of the workpiece, which are 100% controlled in a regular production process.

Fig. 6 present the \bar{X} - R chart of measurements for diameter $\phi 64.3$ mm.

The upper graph (Fig. 6) shows the \bar{X} -chart (Average), that present the course of dimensional measurements. The upper and lower control limits are printed on the graph. If the measure is above or below the control limit, the measurement is colored red. From the \bar{X} chart, we can determine whether the product is within tolerance limits or predict when the product will no longer be good.

The lower graph (Fig. 6) shows the R -chart (Range). The R -chart tells you whether the variation of the product's properties has been maintained within acceptable limits. The lower control limit is always zero because the range between two measurements is viewed with an absolute value.

The process was stable up to 40th produced part (Fig. 6, \bar{X} -chart). It was not within the control limits, but it was within tolerance. If the process is stable and is not within the control limits, it means that there was a mistake on the start of the process.

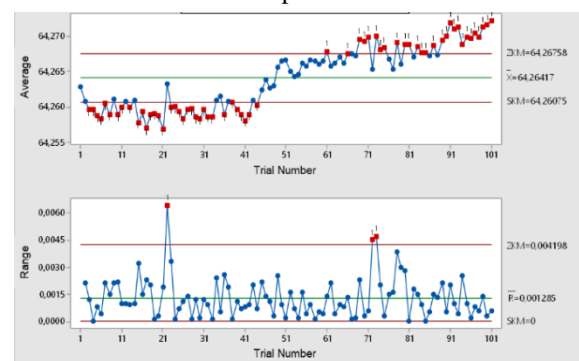


Fig. 6. \bar{X} - R chart of measurements for diameter $\phi 64.3$ mm.

Possible mistakes are:

- the machine tool has not been warmed up to the operating temperature or
- the initially produced parts has not been measured and consequently the cutting tool offsets corrections has not been performed.

From the \bar{X} -chart (Fig. 6 above), it is apparent that a small correction of the cutting tool offset (few micrometres), would have resulted that the measurements would be within the control limits. After 40th part produced, however, it is visible that the measurement has slid to the upper control limit and across.

From the R -chart (Fig. 6 below), it is evident that the measurements did not fluctuate significantly. Just some measurements range are out of the control limits.

The process capability histogram for a diameter of $\phi 64.3$ mm is presented in Fig. 7. A large dispersion of measurements around the mean value is evident.

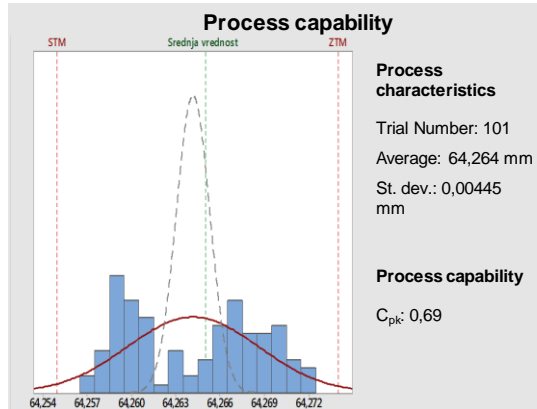


Fig. 7. Process capability analysis for a diameter of $\phi 64.3$ mm.

The average of the measurements does not differ significantly from the desired mean value, but their distribution around the average value is poor, which result in standard deviation of 4.4 μm . The actual process capability index C_{pk} for diameter of $\phi 64.3$ mm is 0.69, is not acceptable (it should be at least 1.3). The same procedure has been used to calculate the C_{pk} of all other diameters. The results are given in Table 2.

Diameter [mm]	Average [mm]	σ [mm]	C_{pk}
$\phi 64.3$	64.264	0.0044	0.69
$\phi 65$	65.018	0.0046	1.33
$\phi 72$	71.95	0.0040	0.73
$\phi 88e6$	87.914	0.0043	0.64
$\phi 88h6$	87.986	0.0049	0.55

Table 2. Results of the SPC analysis for all diameters.

The table 2 shows that the existing situation is unacceptable. The process capability index C_{pk} are in all cases lower than 0.73 except in the case diameter $\phi 65$ mm ($C_{pk} = 1.33$). However, this diameter is not relevant for observing the process's capability due to the width of the tolerance. This means that such manufacturing process would produce more than 35.000 unaccepted pieces in a series of million. The machining process needs to be improved.

3.3 Machine tool positional accuracy measurement and calibration

To increase the accuracy of the machined parts, the positional accuracy and repeatability of the used machine tool has been analysed. The measurements of the linear X-axis has been performed with the Renishaw ML10 Gold laser interferometer system. With a high

accuracy of a single-frequency laser source containing beam stabilization electronics, interpolation and counting of interferential lines, the size of errors can be measured with a nanometer resolution. With the use of EC10 compensation device, the system ensures the linear displacement accuracy of 0.7 $\mu\text{m}/\text{m}$. The compensation device measure and compensate the environmental effects (air and material temperature, relative humidity and air pressure) [7].

For the positional accuracy measurement, the optics were positioned as follows (see Fig. 8):

- The stationary interferometer was placed on the main spindle while the moving reflector on the machine turret.
- The reflector was moved with a certain step along X-axis.

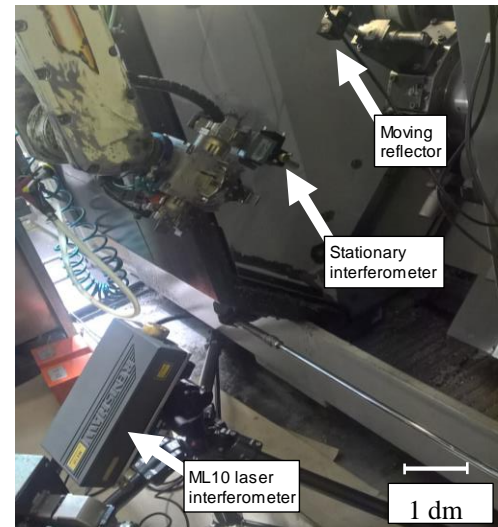


Fig. 8. Positional accuracy measurement setup.

The results of current state of the machine tool positional accuracy measurement are presented in Fig. 9.

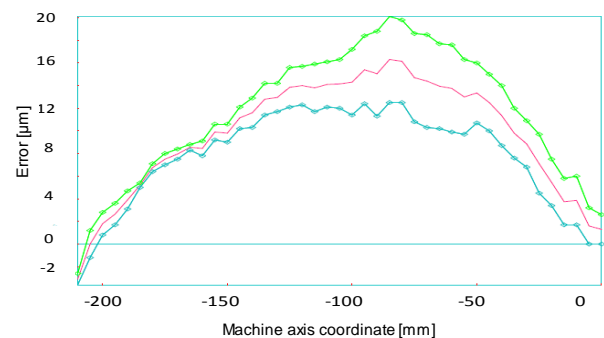


Fig. 9. Current state of X axis positional accuracy and repeatability.

The results illustrated in Fig. 9 are showing a large deviation of approx. 20 μm in the range of -80 mm to -180 mm (X machine coordinate), which is exactly in the range of the maximum error of the machined parts. Based on the measurement results, the compensations are calculated and entered into the machine tool controller. After the calibration of X-axis, the positional accuracy and repeatability significantly increase. The results are presented in Fig. 10.

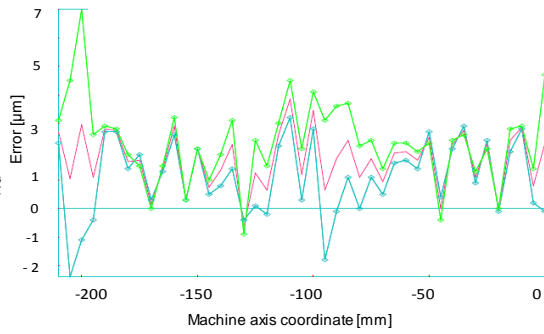


Fig. 10. X axis positional accuracy and repeatability after calibration.

From the presented results shown in Fig. 9 and Fig. 10, it is evident that the position accuracy of the machine tool in the X-axis has been improved from the initial 25 μm to 9 μm . The repeatability was approx. 3 μm .

3.4 Analysis of the capability of the machining process after machine tool calibration

After verifying the accuracy of the machine tool and subsequent calibration of it, the SPC analysis has been performed again. The C_{pk} of the machined process has been calculated from 101 workpiece diameter measurements. Fig. 11 present the $\bar{X} - R$ chart of measurements for diameter of $\phi 64.3$ mm. From the $\bar{X} - R$ chart (Fig. 11) and the process capability histogram (Fig. 12) can be seen, that the stability of the process after the calibration of the machine tool has been improved. Few measurements are still outside the control limits, but the number of it in comparison with the initial state (Fig. 6) is negligible.

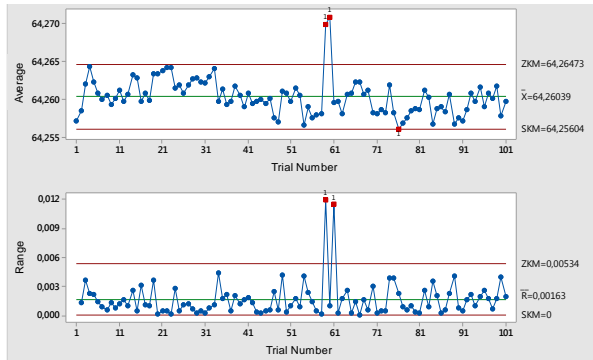


Fig. 11. $\bar{X} - R$ chart of measurements for diameter $\phi 64.3$ mm after machine tool calibration.

From the results, presented in the histogram in Fig. 12 a good dispersion of measurements is evident, but a shift in the mean value is noticed. Also the standard deviation of 2.4 μm is smaller than before the machine tool calibration (Fig. 7).

As a result, the C_{pk} index for diameter of $\phi 64.3$ mm increased to 0.74. From Table 2 and Table 3 it is clear, that the C_{pk} index increased for approx. 20% for all diameters (except for $\phi 88\text{h}6$). The capability of the process significantly improved at $\phi 65$ mm and $\phi 72$ mm ($C_{pk} > 1,3$). For all other diameters, the C_{pk} index has not improved sufficiently ($C_{pk} < 1,3$).

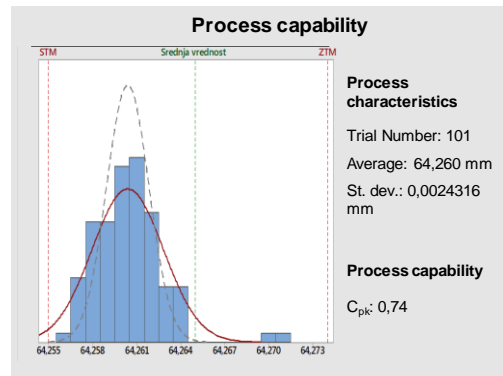


Fig. 12. Process capability analysis for a diameter of $\phi 64.3$ mm after machine tool calibration.

For the diameters $\phi 88\text{h}6$, the C_{pk} index is lower than on the initial state (Table 2). The result is not expected, probably there was an error in performing the measurements.

Diameter [mm]	Average [mm]	σ [mm]	C_{pk}
$\phi 64.3$	64.260	0.0024	0.74
$\phi 65$	65.012	0.0024	1.63
$\phi 72$	71.952	0.0014	2.18
$\phi 88\text{e}6$	87.919	0.0038	0.81
$\phi 88\text{h}6$	87.982	0.0037	0.34

Table 3. Results of the SPC analysis for all diameters after machine tool calibration

As a conclusion, the stability of the machining process after machine tool calibration is more stable, but the problem of some diameter roundness deviation persist. To analyze the influence of machining parameters on the roundness deviation, DOE analyse has been performed and is presented in next chapter.

3.5 DOE - Optimization of process parameters

The aim of DOE analyze is to determine the influence of process parameters on the roundness of machined diameters. Based on the influence of process parameters, the optimization was performed for minimal roundness deviation. The investigated process parameters were:

- Feed rate [f_n],
- Depth of cut [a_p],
- Clamping force [F_{vp}].

Preliminary experiments has been carried out in order to prove the maximum and minimum values of the input parameters (Table 4).

Level	f_n [mm/vrt]	a_p [mm]	F_{vp} [kN]
-1	0.05	0.06	3
0	0.12	0.371	7.5
1	0.19	0.681	12

Table 4. Machining and clamping parameters

The parameters ranges has been determined based on the cutting tool manufacturer and clamping system supplier specifications.

For the design of experiments, the central composite design has been applied. The experiments were carried out and the regression model has been calculated based

on ANOVA. Fig. 13 illustrates the influence of the input (process) parameters on the machining roundness deviation. It can be seen, that the major influential parameter is the clamping force F_{vp} , which affect the roundness deviation proportionally.

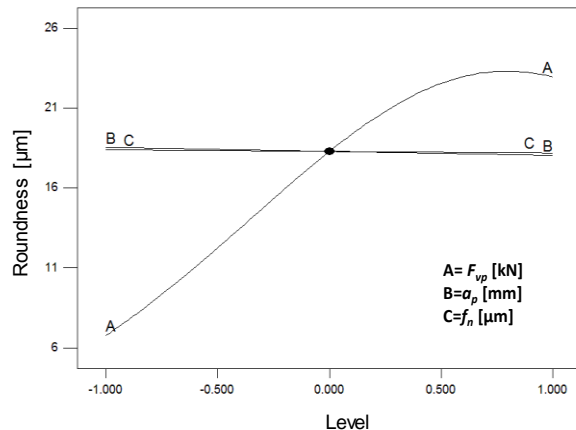


Fig. 13. The influence of the input (process) parameters on the machining roundness.

In the step of the optimization, optimal input parameters for minimal roundness deviation were selected and confirmed with the confirmation test. Optimal setting parameters are:

- $F_{vp} = 3 \text{ kN}$,
- $a_p = 0.06 \text{ mm}$,
- $f_n = 0.12 \text{ mm/rev}$.

The predicted roundness is $6.6 \mu\text{m}$.

For the confirmation test the roundness of ten parts has been measured. The results are presented in the table below.

N	1	2	3	4	5	6	7	8	9	10	Average
Roundness [μm]	6	5	7	6	6	5	8	6	7	8	6.4

Table 5. Confirmation test results.

With the confirmatory test, we have proven that the regression model is appropriate because the proposed value of the response is within the confidence interval $[6 - 6.7 \mu\text{m}]$.

4. CONCLUSIONS

In this paper, an industrial case study of quality improvement of manufacturing process is presented. The problem of dimensional deviations of produced parts has been analysed. With the use of different quality management tools, the stabilization and improvement of the turning capability has been achieved. With the use of DOE, the influence of process parameters on the roundness deviation of machined diameters is analyzed. It was found, that the clamping force F_{vp} has the biggest impact on roundness of the machined parts.

Furthermore, optimal input parameters for minimal roundness deviation have been defined. However, a new clamping device has to be designed to reduce the influence of clamping force on the roundness of the machined parts.

The costs of such quality improvement were not calculated, but the reduction of quality costs and time for inspection is evident. No 100% quality control is needed anymore. Parts are now sampled twice a day and SPC for quality conformation is performed. Even more reductions are expected with the new clamping device.

5. REFERENCES

- [1] Pop, Liviu Dorin, Nagy Elod. 2015. *Improving Product Quality by Implementing ISO / TS 16949*. Procedia Technology. 19: 1004-1011.
- [2] Juran, Joseph M., A. Blanton Godfrey. *Juran's Quality Handbook (5th Edition)*. New York, USA: McGraw-Hill Professional Publishing, 1998.
- [3] Khan, P. M., Sufyan Beg M.M., *Measuring Cost of Quality Measuring Cost of Quality (CoQ) on SDLC Projects is Indispensable for Effective Software Quality Assurance*. International Journal of Soft Computing And Software Engineering, Vol.2, No.9, p. 1-15, 2012.
- [4] Eniko, P., Soković, M., Kramar, D.. *Using quality tools for process development and improvement : case study on cylinder manufacturing*. Advanced quality, ISSN 2217-8155., 2016, vol. 44, 1, p. 27-32.
- [5] Satanova, A., Sedliacikova, M., *Model for Controlling the Total Costs of Quality*. Procedia Economics and Finance, 26, p. 2-4, 2015
- [6] Schifffauerova, A. and V. Thomson, *A Review of Research on Cost of Quality Models and Best Practices*. International Journal of Quality & Reliability Management, 2006. 23(4).
- [7] DaimlerChrysler, Ford Motor Company, and General Motors Corporation. *Measurement Systems Analysis: Reference Manual*, 2010.
- [8] Mlinar, A., *Optimization of the process parameters for stabilization and improvement of the turning capability*, diploma work, 2017.
- [9] Kopač, J., Pušavec, F., Kramar, D.. *How to improve the positional accuracy of hsc machine tools*. V: 7. Congresso Brasileiro de Engenharia de Fabricação, 20-24 de maio de 2013, Penedo, Itatiaia-RJ, Brasil : COBEF, (Congresso Brasileiro de Engenharia de Fabricação, ISSN 2236-0395), 2013, p. 1-10.

Authors:

PhD. Luka Cerce, Assoc. Prof. Davorin Kramar,
University of Ljubljana, Faculty of Mechanical Engineering, Department for Management of Manufacturing Technologies, Askerceva 6, 1000 Ljubljana, Slovenia, Phone.: +386 1 4771-737, Fax: +386 1 477 1 768.

E-mail: luka.cerce@fs.uni-lj.si;

davorin.kramar@fs.uni-lj.si;

Assist. Prof. Stevo Borojevic

University of Banja Luka, Faculty of Mechanical Engineering, Stepe Stepanovića 75, 78000 Banja Luka, Bosnia and Herzegovina, Phone.: +387 51 433 000, Fax: +387 51 465 085.

E-mail: stevoborojevic@hotmail.com

Gostimirovic, M., Pucovsky, V., Rodic, D., Sekulic, M., Kovac, P.

A NEURAL NETWORK MODEL FOR PREDICTING JET TRAJECTORY IN THE ABRASIVE WATER JET MACHINING

Abstract: Abrasive water jet machining (AWJM) is one of the most advanced non-conventional production technologies. However, in order to obtain a product with good surface quality, the AWJM process must be precisely regulated. In this paper, an artificial neural network is used for modeling of trajectory curvature in AWJM process, respectively of the jet lag effect. For this work experiments were conducted and the influence of machining parameters on abrasive water jet trajectory curvature is measured. Steel was used as a workpiece material while water pressure, cutting speed and quantity of abrasive were varied. Based on experimental investigation, the trained neural network establishes nonlinear relationships among the parameters of AWJM process and the jet lag. Consequently the surface quality can be simulated and regulated by adjusting the input parameters of the abrasive water jet machining. The satisfied results were obtained using the neural network model through the check data set.

Key words: AWJM process, jet lag effect, modeling, artificial neural network

1. INTRODUCTION

Abrasive water jet machining (AWJM) is one of the most popular non-traditional machining processes used in manufacturing industry. This process is used to cut different materials or make the holes and kerfs. In AWJM process there is no change in physical and mechanical properties of the workpiece. Therefore, this process is particularly suitable for heat sensitive materials. Theoretically, this type of cutting can be applied on every type of materials such as metal, stone, glass, composites, ceramic etc. AWJM is especially excellent for the cutting of difficult-to-machine materials with complex shapes.

AWJM process works by forcing a large volume of the water mixed with the abrasive through a small orifice in the nozzle d . The set pressure of water p and quantity of abrasive Q travelling through a reduced cross sectional area causes the high energy impact of jet into the workpiece. The extreme pressure of the accelerated water and abrasive contacts a small area of the workpiece material. In this small area the workpiece develops small cracks due to stream impact as a form of micro erosion. The extreme pressure of the water and impact of the abrasive particles in the following stream cause the crack to propagate until the material is cut through. In Fig. 1 is shown the AWJM process mechanism with surface topography.

Mechanism of AWJM cutting is an important process for the machining productivity and quality, especially from the standpoint of the jet velocity and trajectory curvature. Due to loss of kinetic energy the jet changes its shape, so that straight cut is transformed into curved cutting which is reducing speed and quality of processing. Observing the upper and the lower edge of machined material, it is well known that jet traces are visible in the form of lines. If the lines are too straight, AWJM process is underrated sometimes, while arched lines show the need for correction of the machining parameters.

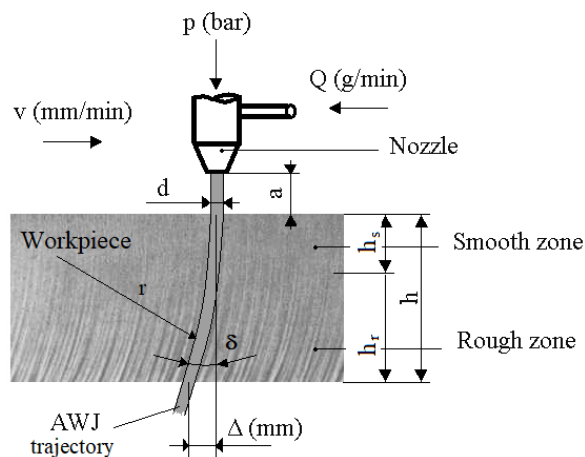


Fig. 1. Model of the AWJM process with the surface topography

In the past, papers regarding the abrasive water jet trajectory curvature have been published. Hashish [1] was among the first to set a theoretical mechanism of the AWJM process. In this model, total cutting depth h consists of two different parts: smooth zone h_s and rough zone h_r . In the smooth zone material removal is striking without angles of attack, while material removal in the rough zone has visible angles of attack. Accordingly, the cutting depth h_s stands for the critical depth where the jet lag effect is not presented.

Following previous model, Zeng and Kim [2] obtained a semi-empirical equation for the calculation of the jet lag Δ , the angle deviation δ and the radius of the trajectory curvature r . Modeling of the abrasive water jet surface topography, simulating the trajectory of jet, is described in work [3]. Analytical correlation for the jet trajectory shape, under different cutting speed, has been developed in papers [4,5]. Evaluation method of the abrasive water jet cutting quality is realized by the experimental research [6].

Although the presence of the abrasive water jet trajectory curvature analysis is recorded, mostly analytical solutions are found. In these days all trends are heading to ever increasing use of computational assistance in solving various tasks. Artificial intelligence, as a tool for analysis and dependence development, is gaining ever more popularity and commercial use. Being aware of this fact and realizing that a smaller number of works cover this subject it is decided to support the scientific community and present an intelligent approach in analysis of the trajectory curvature in AWJM process. Realizing the complexity of presented challenge, only very flexible system could successfully live up to that task. Having previous success with the computational intelligence in other areas [7], in this paper, an artificial neural network is used for modeling of abrasive water jet trajectory curvature, respectively of the jet lag effect between the upper and the lower edge of the machined workpiece.

2. NEURAL NETWORK APPROACH

Artificial intelligence is becoming prevalent technique in solving critical problems of omnipresent advanced manufacturing systems [8,9]. Such Intelligent systems are aimed at exploiting the strong capabilities of the intelligence tools at solving problems that are not amenable for modelling and optimization using traditional methods [10]. This paper discusses the development and application of an artificial neural network methodology for modeling jet lag effect of the abrasive water jet machining.

Artificial neural network possess one trait which separates them from other modeling techniques. It is an ability to derive logical meaning from imprecise or complicated data. They can also be used to extract pattern and detect trends which are way too complex to be noticed by other computer techniques or even human himself. We can perceive trained neural network as a true computer expert in the area for which data was supplied. When properly trained, this intelligence expert can be used to provide simulation of possible "what if" outcomes and also the possible outcomes of unknown situations.

Neural network processes one extraordinary feature and that is an adaptive learning. This means that it has an ability to learn how to perform task based solely on data provided for purpose of training or initial experience. It is also self organized and can create its own organization or interpretation of the information which are received during learning period. Important trait which is characteristic on neural network is fault tolerance via redundant information coding. Translated into common language this means that partial destruction of a network will lead to the corresponding performance degradation. But in special cases some capabilities can be recovered even when major damage happens to neural network.

For neural network model of the abrasive water jet trajectory curvature, main input data set of the experiments are p is the water pressure, v is the cutting speed and Q is the quantity of abrasive, respectively

the jet lag Δ between the upper and the lower edge of the workpiece as output data set, Fig. 2.

The input/output data were divided randomly on training data set, checking data set and validation data set. Training process is accomplished by using Matlab software. In order to determine the optimal network architecture, different training algorithms were used, and the number and type of membership functions, method optimization hybrid or back propagation, and number epoch were changed. For this purpose the feed-forward back propagation network was used with mean square error function as a goal setting path. Two hidden layers are employed with ten neurons inside and whole learning process lasting for one thousand epochs.

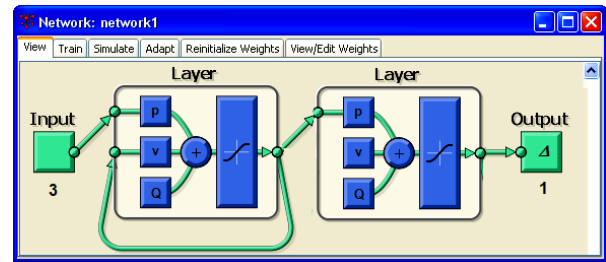


Fig. 2. Architecture of the AWJM neural network model

3. EXPERIMENTS

Experiment investigation was carried out on the abrasive water jet cutting machine, STM from Austria. Cutting was done with sapphire nozzle of the jet diameter $d=0.9$ mm, impact angle $\varphi=90^\circ$ and stand-off distance $z=1$ mm. Sand was used as an abrasive with 0.1 mm grain size. S235JRG2 steel plate was used as the workpiece. Thickness of the steel plate was $h=15$ mm.

During the experiments input parameters, the water pressure p , the cutting speed v and the quantity of abrasive Q were varied at five levels. Water pressure was varied from 160 to 320 MPa at 40 MPa intervals. Cutting speed was varied from 40 to 80 mm/min with 10 mm/min step. Abrasive quantity was 100, 250, 300, 350 and 400 g/min. The reference level was derived using $p=320$ MPa, $v=60$ mm/min and $Q=400$ g/min.

On the machined samples parameters of the AWJM trajectory curvature were measured: the smooth h_s and rough h_r depth of cut, the angle δ , the radius r and the jet lag Δ of the trajectory curvature. Measurements were conducted indirectly by reading the parameters of the trajectory curvature with photos recorded using digital microscope with 200x magnification.

Shown in Fig. 3 are the typical photos of created workpiece surface by AWJM process. The photos are obtained by changing the cutting speed for references level.

Fig. 4 shows the results of experimental research of the abrasive water jet trajectory curvature for the chosen machining conditions. Shown are reference results that illustrate how the input parameters impact on the trend of jet lag.

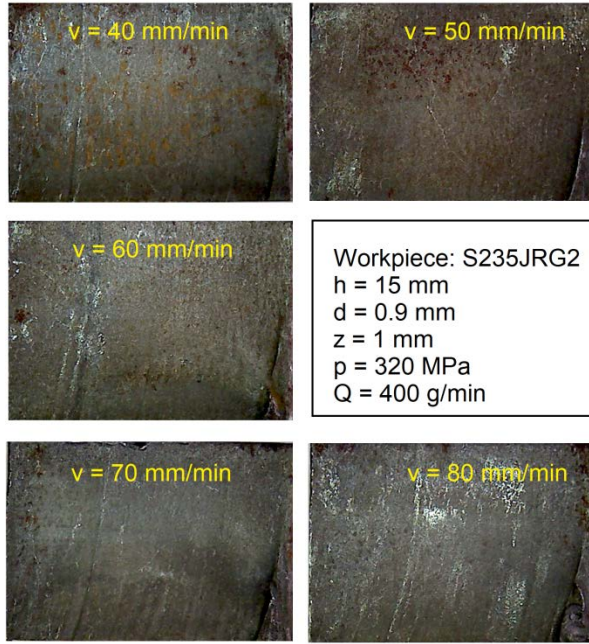


Fig. 3. Typical AWJM workpiece surface topography for different cutting speed

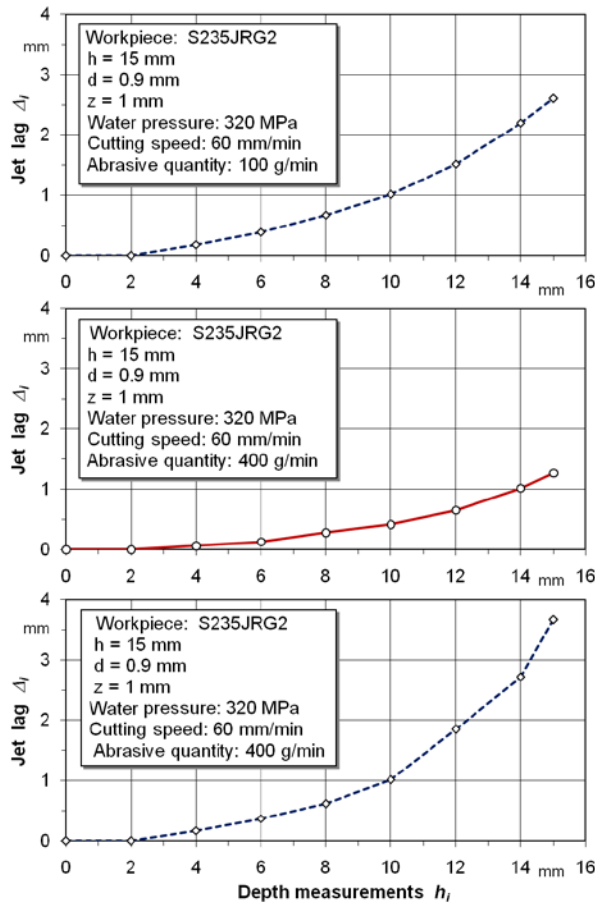


Fig. 4. Influence of the machining parameters on the trajectory curvature

4. RESULTS AND ANALYSIS

The modeling of the abrasive water jet trajectory curvature based on the artificial neural network is

conducted using procedures presented in chapter 2. The main objective was to determine adequate prediction of the trajectory curvature depending on the machining conditions for the AWJM process.

Fig. 5 represents the results of modeling of the jet lag procedure with neural network method. Comparison between the modeled and the measured data is presented for the represent machining conditions. The results for low, medium and high cutting speed are shown beside the water pressure and abrasive quantity, respectively. In order to verify the simulation results was carried out validation of the relative error of the modeled deviation from the measured data.

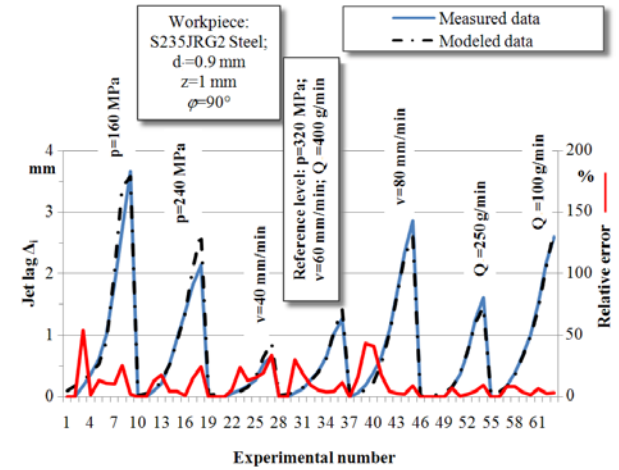


Fig. 5. Representation of the experimental and neural network results of the trajectory curvature

Table 1 shows the results of experimental and modeling investigation for the selected machining conditions. It seems that the neural network and experimental approaches are being close to each other indicating good agreement.

Machining conditions			Jet lag	
Water pressure p (MPa)	Cutting speed v (mm/min)	Abrasive quantity Q (g/min)	EXP Δ_{exp} (mm)	NNM Δ_{nnm} (mm)
160	60	400	3.67	3.5821
200			2.605	2.7224
240			2.145	2.6686
280			1.65	1.871
320			1.272	1.4181
320	40	400	0.653	0.8762
	50		1.157	1.3024
	60		1.272	1.4181
	70		2.612	2.955
	80		2.865	2.6029
320	60	100	2.603	2.6941
		250	1.822	1.7695
		300	1.617	1.46
		350	1.312	1.366
		400	1.272	1.4184
Average error				13,1%

Table 1. The results of experimental and neural network modeling investigation

The average error of the neural network model is checked and is found to be adequate with 13.1 % confidence level. So, this model can be used for predicting the jet lag effect in AWJM.

Analysis of experimental and neural network modeled results revealed that all the input parameters have impact on the abrasive water jet trajectory curvature. Increase of the cutting speed increases the jet lag, while decrease in the water pressure or the abrasive quantity also increases jet lag. Consequently, it is clear that the AWJM machining parameters have inverse effect on the jet lag, which largely complicates analysis of the abrasive water jet trajectory curvature. However, very important is the fact that high water pressure causes with the appropriate abrasive quantity the disappearance of the jet lag. In that context, dominant impact on the abrasive water jet trajectory curvature has the cutting speed.

According to that, regarding artificial neural network model for predicting jet trajectory, results are accurate within expectations. Artificial neural network has once again proven its superb modeling ability of the abrasive water jet trajectory curvature. In the case of reliable experimental results neural network could provide very flexible system for activity process modeling of abrasive water jet trajectory curvature. With the correct database generation the neural network model could generate good output of machining performance, i.e. achieving smooth zone of the AWJM cutting.

5. CONCLUSIONS

Artificial neural network model used in this paper is feasible and could be used to predicting the jet trajectory in the AWJM process. Depending on the machining conditions it is possible to estimate the jet lag in the cutting zone with an acceptable error rate, because values predicted by this model largely agree with the experimental results. Thereby, the stability of neural network method depends on the reliability of the experimental data used in its training. In this respect, the neural network modeling of the abrasive water jet trajectory curvature shows good directions which could be followed by future researches into the optimization of the abrasive water jet machining. The neural network model adequacy can be further improved by considering more variables and ranges of parameters.

6. REFERENCES

- [1] Hashish, M.: *A modeling study of metal cutting with abrasive waterjets*, Journal of Engineering Materials and Technology, Vol. 106, No. 1, pp. 88-100, 1984.
- [2] Zeng, J., Kim, T. J.: *An erosion model of polycrystalline ceramics in abrasive waterjet cutting*, Wear, Vol. 193, No. 2, pp. 207-217, 1996.
- [3] Vikram, G., Ramesh Babu, N.: *Modelling and analysis of abrasive water jet cut surface topography*, International Journal of Machine Tools & Manufacture, Vol. 42, pp. 1345-1354, 2002.
- [4] Deam, R. T., Lemma, E., Ahmed, D. H.: *Modelling of the abrasive water jet cutting process*, Wear, Vol. 257, pp. 877-891, 2004.
- [5] Madic, M., Radovanovic, M., Gostimirovic, M.: *ANN modeling of kerf taper angle in CO2 laser cutting and optimization of cutting parameters using Monte Carlo method*, International Journal of Industrial Engineering Computations, Vol. 6, pp. 33-42, 2015.
- [6] Hlavac, L. M., Hlavacova, I. M., Gembalova, L., Kalicinsky, J., Fabian, S., Mestaneek, J., Kmec, J., Madr, V.: *Experimental method for the investigation of the abrasive water jet cutting quality*, Journal of Materials Processing Technology, Vol. 209, pp. 6190-6195, 2009.
- [7] Rodic, D., Gostimirovic, M., Kovac, P., Radovanovic, M., Savkovic, B.: *Comparison of fuzzy logic and neural network for modelling surface roughness in EDM*, International Journal of Recent advances in Mechanical Engineering, Vol. 3, No. 3, pp. 69-78, 2014.
- [8] Kovac, P., Rodic, D., Pucovski, V., Mankova, I., Savkovic, B., Gostimirovic, M.: *A review of artificial intelligence approaches applied in intelligent processes*, Journal of Production Engineering, Vol. 15, No. 1, pp. 1-6, 2012.
- [9] Park, K. S., Kim, S. H.: *Artificial intelligence approaches to determination of CNC machining parameters in manufacturing: a review*, Artificial Intelligence in Engineering, Vol. 12, No. 1-2, pp. 127-134, 1998.
- [10] Rao, R. V.: *Advanced modeling and optimization of manufacturing processes*, Springer-Verlag, London, 2011.

Authors: Full Prof. Marin Gostimirovic, M.Sc. Vladimir Pucovsky, M.Sc. Dragan Rodic, Full Prof. Milenko Sekulic, Full Prof. Pavel Kovac, University of Novi Sad, Faculty of Technical Sciences, Department of Production Engineering, Trg Dositeja Obradovica 6, 21000 Novi Sad, Serbia, Phone.: +381 21 450-366, Fax: +381 21 454-495.
E-mail: maring@uns.ac.rs; pucovski@uns.ac.rs; rodicdr@uns.ac.rs; milenkos@uns.ac.rs; pkovac@uns.ac.rs

ACKNOWLEDGMENTS: The paper is the result of the research within the project TR 35015 financed by the Ministry of Education, Science and Technological Development of the Republic of Serbia.

Kokotovic, B., Vorkapic, N.

EVALUATION OF INFEEED STRATEGIES FOR TURNING OF LARGE THREAD PROFILES

Abstract: Several infeed strategies for multipass threading operations on CNC lathes are well known and they are implemented in form of appropriate canned cycles in system software of CNCs. These strategies are especially suitable for triangular profiles of thread. Paper presents method developed for analysing of infeed strategy in threading operations for arbitrary geometry of thread profile and geometry of tool profile, including trapezoidal threads and worm wheels. Proposed method uses two criteria for evaluation of specific infeed strategy in multipass turning of threads. The first one is the measure of balance of uncut chip area in subsequent passes (implemented application in Matlab is described). Calculation of chip area is based on numerical integration. The second criterion is referred to prediction of cutting forces and their distribution in subsequent passes.. Cutting force estimation is based on specific cutting forces and engaged chip area acting on discretized lengths of cutting edges.

Key words: CNC lathe, threading, infeed strategy, turning operations

1. INTRODUCTION

CNC lathes enable very efficient machining of the helix surfaces on rotating parts. It is possible, in mode of strong kinematic connection (G32 function) between main spindle and X and Z servo axis, to machine of various internal and external threads, lead screws, worm wheels and spiral slots on face of the workpiece. In cases of small thread profile (small pitch and depth) programming of machining of thread is very simple, and it is reduced on one or two program blocks, with call of specific canned cycle, and with specification of input parameters (thread geometry, thread profile and technology parameters) of this cycle. In such case (small profile) critical element of whole system is the cutting tool and its vulnerable nose.

In some cases, especially in machining of larger thread profiles, these cycles may exhibit some limitations. In these situations tool design is more complex, larger length of cutting edges are engaged, power consumption and required spindle torque are not negligible. There is also higher tendency to vibrations especially in machining of thin-walled parts.

Comparing to other machining methods, turning of threads is treated in very small number of scientific papers [1, 2]. This paper presents results of research aimed to develop procedures for better insight in this process, with focus on prediction of cutting forces.

2. TYPICAL INFEEED STRATEGIES IN CANNED CYCLES FOR THREAD TURNING

Different infeed strategies [5] implemented in canned cycles for thread turning assume infeed with constant radial increment, or with constant cross section of uncut chip for subsequent machining passes (strategy with decreasing increment). Also (Fig.1a) infeed can be performed in radial direction (R), along flank (F) of profile or with alternating infeed (incremental infeed- I).

One of the most popular formula for calculation of radial infeed amount for particular pass is derived, according to Fig.1b, assuming zero radius of tool nose (H_r denotes profile depth reduced for finishing allowance, p -number of passes):

$$dA_{c,i} = u_i^2 \tan\left(\frac{\alpha}{2}\right), dA_{c,i} = \tan\left(\frac{\alpha}{2}\right)(u_i^2 - u_{i-1}^2)$$

$$(u_i^2 - u_{i-1}^2) = K, Ap = H_r^2 \tan\left(\frac{\alpha}{2}\right)$$

$$Ap = \sum_{i=1}^p dA_c(i) = pK, K = H_r / \sqrt{p}$$

$$u_1 = H_r / \sqrt{p}, u_i = \sqrt{(H_r^2 / p) + u_{i-1}^2}. \quad (1)$$

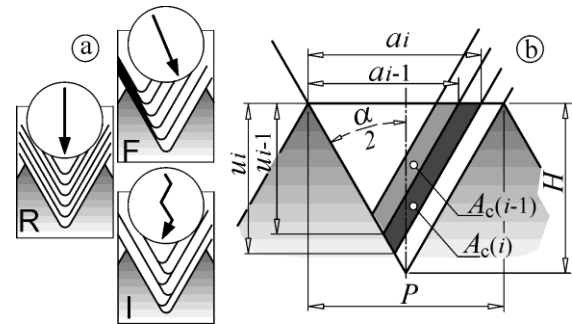


Fig1. Different infeed strategies (a) and model for infeed strategy with constant chip area (b)

This strategy, simple but effective, is implemented in many CNCs of lathes. Another, empirical, formula is recommended from [3]:

$$u_i = H_r \sqrt{\frac{\varphi_i}{p-1}}, \varphi_1 = 0.3, \varphi_2 = 1, \varphi_i = p-1 \quad (2)$$

$$\varphi_i = i-1, \text{ for } i = 3, \dots, p.$$

Finally, recommended number of passes and quantity of infeeds, for particular standard thread and its nominal pitch can be found in form of tables [3].

3. EVALUATION OF INFEEED STRATEGIES FOR TURNING OF THREADS

Among the other criteria, evaluation of quality of infeed strategy for turning of particular thread can be performed through analysis in two levels in order to achieve:

1. Limited and balanced cross sections of uncut chip area in subsequent passes.

This criterion is based on premise that cutting forces, among other factors, are strongly influenced with area of engaged uncut chip section. This dependence is not quiet linear, but without some other criteria, balanced chip area in all passes are indicator for well planned process. Exception is the last pass, with intentionally small chip area, needed for finishing of thread flanks and root.

2. Limited and balanced cutting force component s in subsequent passes.

Prediction of cutting forces is one of the most reliable tool for evaluating of planned machining process. As a rule this approach assumes more complex input data structure, as well as more complex procedures implemented in computer programs.

In chapter 3 of this paper, procedure and implemented Matlab application for prediction of chip area during passes of thread turning, is presented. In chapter 4, mechanistic approach of cutting force predicting is discussed and one procedure for identification of chip thickness, for arbitrary element of discretized cutting edge, is presented.

4. ESTIMATION OF UNCUT CHIP AREA

Calculation of chip cross section in particular passes of thread turning process, based on specific cutting tool geometry and infeed strategy, has not trivial solution. Some authors [2] developed algorithms of analytical obtaining of this area, but only for few kinds of standard thread profile (API-Buttress). Different approach, using discretization of workpiece longitudinal section, and specific description of cutting tool geometry, in our research was applied. Calculation of chip cross section area is based on numerical integration, and it is found that this approach is more flexible and sufficiently accurate.

Developed Matlab application requires three input data files: *ThreadProfile*, *ToolProfile* and *InfeedStrat*. The last one is two column matrix with subsequent infeeds, for all passes, in Z and X (radius) direction. *ThreadProfile* matrix has rows with attributes of linear segments and arcs of thread profile in form of:

$$[1, Z_{start}, X_{start}, Z_{end}, X_{end}, 0, 0, 0, 0, 0]$$

for linear segments, and:

$$[2(3), Z_{start}, X_{start}, Z_{end}, X_{end}, R, X_c, Z_c, A_{start}, A_{end}]$$

for arcs on cutting edge (constant 2 or 3 indicates if arc is convex or concave, view from X+). Matrix *ToolProfile* has *ToolSeg* rows with almost the same structure as rows of *ThreadProfile*. Additional attribute in description of tool segment is indicator that shows if the particular line or arc is part of cutting edge or noncutting geometry of the tool. This noncutting segments are useful in checking of possible collision

during machining of thread.

Additional two input variables are radial allowance (*TopStockR*) for full profile machining, as well as resolution (R_f) of rays (fringes) parallel to Xaxis, needed for discretization of the workpiece. In area of workpiece with length of one thread pitch N_{ray} fringes parallel to Xaxis will be generated, according to *FrgRes*, from raw material axis to its diameter. This is the way for discretization of longitudinal cross section of the workpiece. Default value for R_f is $P/100$, for achieving of high accuracy of numerical integration of particular areas. For certain threading pass ($i=1:np$) several steps will be performed:

Step 1. Translation of each segment ($j=1:tseg$) of the tool profile according to infeed parameters (*InfStrat*($i,:$)).

Step 2. For fringe ($k=1:nf$) check if $Z_f(k)$ is between Z limits of particular j translated segment of the cutting edge (Case1).

If the Case1 is satisfied, find intersection of fringe k with *ToolSeg*(j). In case of $X_f(k) > X_t(T(Z_f))$ of intersection, Calculate $dAc(i)=X_f-X_{int}$, as the contribution of this fringe to the total chip area. Update local radius of the workpiece $X_f(k)=X_f(k)-dAc(i)$. Proceed to next fringe ($k=k+1$)

If the Case 1 is not satisfied proceed with checking of next segment of the tool edge ($j=j+1$)

Step 3. Go back to step 2

Step 4. Calculate chip area for current pass

$$A_c(i)=dA_c * R_f$$

Step 5. Return to step 1.

Results of this developed Matlab application in (ThreadSimArea.m) are supported with diagrams of workpiece/tool engagement for each threading pass and with diagram of change of chip area for each pass. One illustrative example of these results, for turning of ISO Tr6 thread in extremely low number of passes (6 passes are practically impossible) are shown in Fig.2.

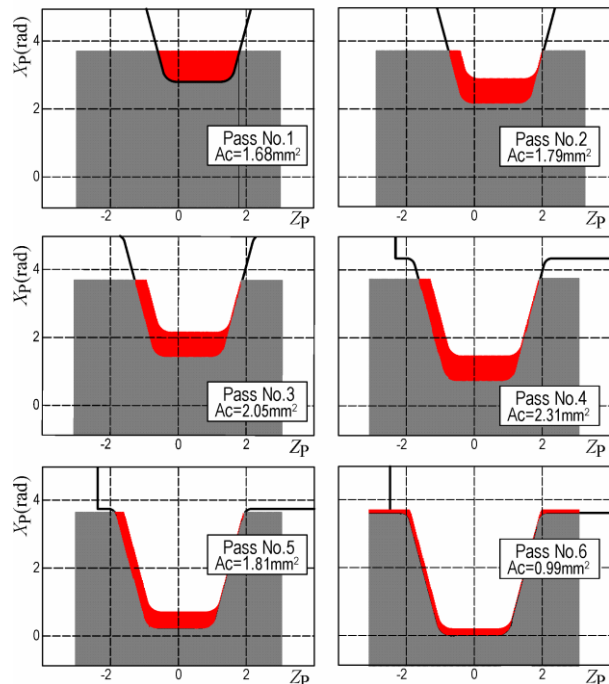


Fig 2 One example of calculation of uncut chip area in subsequent passes of thread turning

Accuracy of calculated chip areas were checked through CAD program in number of examples, and it was found that with error was not greater than 0.5% with chosen resolution $R_f=P/100$.

Fig.3 shows comparison of calculated uncut chip area for the same example, and another example with 16 passes according with recommendations [3]. Uncut chip area is the same for the last pass in both cases (both with same finish allowance).

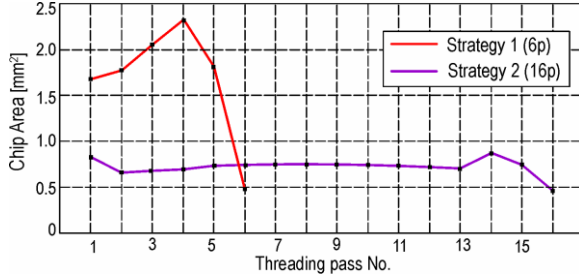


Fig 3 Comparison of two infeed strategies for ISO Tr6

One of practical problem in using of this Matlab application is generation of required data for tool profile description in proposed format. From this reason, one program module is developed to complete matrix *ToolProfile*, using generic geometry of several thread profiles and data from tables in standards for various threads (ISO-MM, ISO-Tr, DIN-Tr, Worms 20°). Creating of *ToolProfile* matrix, need just few additional parameters (in dialog) for specification details of cutting edge responsible for generating the top of the profile (full profile machining).

5. PREDICTION OF CUTTING FORCES IN TURNING OF THREADS

During recent decades, very good results in modeling of cutting forces using mechanistic models, were achieved, for different machining methods. Basic idea is very simple. It assumes discretization of cutting edge(s) in small increment of length dL . Three cutting force components ($dF_t(l)$, $dF_r(l)$ and $dF_a(l)$), acting on particular increment of cutting edge are functions of: area of uncut chip corresponding to this increment, orientation of incremental edge to cutting speed and feed vectors and of specific cutting forces (K_v , K_f) obtained from tests with orthogonal cutting. After completion of calculation of $dF_t(l)$, $dF_r(l)$ and $dF_a(l)$, for all $l=1:ne$, they should be integrated and project onto three orthogonal directions (y, z and x) for obtaining three corresponding principal cutting force components (F_1 , F_2 and F_3) [2]:

$$\begin{bmatrix} dF_t(l) \\ dF_r(l) \\ dF_a(l) \end{bmatrix} = \begin{bmatrix} K_{tc}(l) \\ K_{rc}(l) \\ K_{ac}(l) \end{bmatrix} dL(l)h(l) \quad (3)$$

With $h(l)$ the local uncut chip thickness is denoted. Specific cutting forces in oblique cutting can be obtained from orthogonal cutting data and angles of orientation of cutting edge $dL(l)$:

$$\begin{bmatrix} K_{tc}(l) \\ K_{rc}(l) \\ K_{ac}(l) \end{bmatrix} = T_{ob}(l) \begin{bmatrix} K_v(l) \\ K_f(l) \end{bmatrix} \quad (4)$$

Supposing that chip flow angle $\eta(l)$ is equal to the local inclination angle $\lambda(l)$, elements of T_{ob} can be calculated from sine and cosine functions of $\lambda(l)$ and local rake angle $\chi(l)$ [2].

In order to build program application for predicting of cutting force components in particular pass of thread turning it is obvious that functions for calculation of local chip depth are required. Further text of this paper deals with this issue.

5.1 Uncut chip area on finite length of cutting edge

It should be noted that previous application (ThreadSimArea.m) creates Matlab workspace with all of its input matrices, and results in form of vectors of x coordinates of all updated fringes for all machining passes. Procedure for calculating of chip area corresponding to particular finite length of cutting edge starts with discretization of its length. Increment for discretization (ΔL on fig.4) need not to be too small, as (R_f) for procedure for estimating chip area for entire tool.

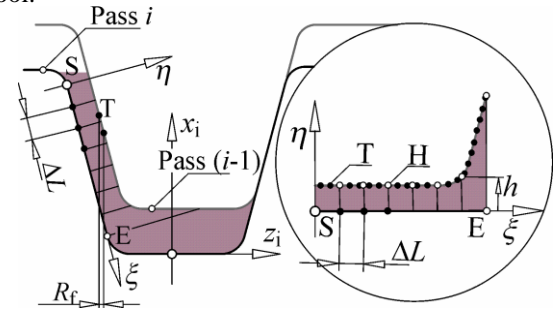


Fig4.

Points of discretized edge can be found from description of tool geometry (*ToolProfile* matrix), and from offsets of tool coordinate system, according to elements of *InfeedStrat* for current machining pass. Establishing of local coordinate system $S\xi\eta$ for particular segment of cutting edge is required. For all points on profile of previous pass (T points) their ξ and η coordinate need to be calculated (only points with $|\xi_T| < \xi_E$). All pairs (ξ_T , η_T) of one segment of cutting edge can be used for interpolation in calculating of η_H (local depth h of the chip) for particular ξ_H (obtain through discretization of edge segment). Local chip area can be obtained as $\xi_H \Delta L$.

This approach has two problems, illustrated on Fig.5. The first one is the fact that, in general case, particular points on contour, made in previous pass, have their orthogonal projections (E' , E'' , on Fig.5) on more than one segment of cutting edge. As a consequence, a part of chip area (A_i) contributes to chip load corresponding to more than one edge segment, and this situation should be avoided. Another problem is obtaining the part (A_R) of uncut chip area corresponding to arc segments of the cutting edge

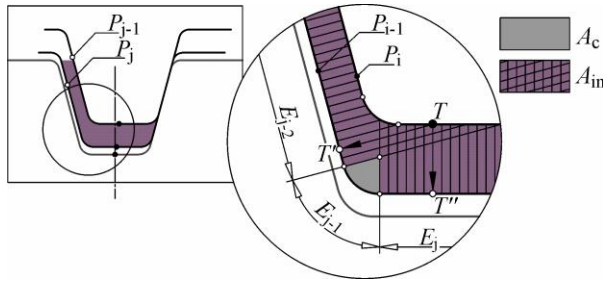


Fig.5 Initial solution for chip thickness for finite length of edge

In order to overcome these problems specific algorithm was presented in [2]. It uses rediscretization of workpiece contours in previous and current pass. This rediscretization assumes that both contours for analyzing have the same number of points, with limitation of angles between connecting lines of corresponding points and edge segment in previous and current pass.

In this paper an alternative approach is presented. Procedure of correction of η_H -coordinates (chip thickness, h , Fig.5) corresponding to finite length of the cutting edge assumes following steps:

For current linear segment of cutting edge (Fig. 6):

1. Find η_H coordinates of all T points from contour P_{i-1} in local coordinate $\xi\eta$ system of current linear segment E_j .
2. Find angle between actual E_j and first previous linear segment E_{pr} .
3. If this angle is greater than 180° keep η_H coordinates obtained through the step1. If this angle is less than 180° reduce η_H until to intersection with symmetry line of E_j and E_{pr} .
4. Find angle between current E_j and first next linear edge segment E_{nx} .
5. If this angle is greater than 180° keep η_H coordinates obtained through the step 1. If this angle is less than 180° reduce η_H until to intersection with symmetry line of E_j and E_{nx} .

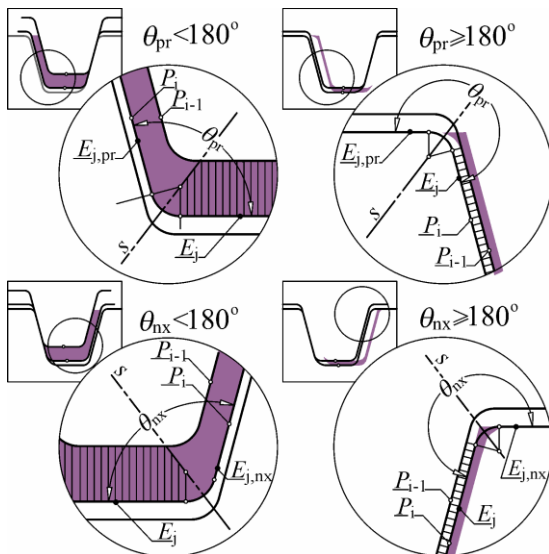


Fig.6 Examples of corrections of chip thickness on finite length of discretized cutting edge

For current arc segment of cutting edge points for discretization are obtained keeping the same increment of discretization as for linear segments. Obtaining of local chip thickness, $\rho(l)$, and area, on finite length of such edge segment is performing through scanning of contour of previous pass with lines, each of them connecting point on arc edge and its center:

$$d\theta = dL / R_n, \quad \bar{\rho}(l) = 0.5(\rho(l-1) + \rho(l)) \quad (5)$$

$$dA_c(l) = \frac{dL + (R_n - \bar{\rho}(l))d\theta}{2} \bar{\rho}(l) \cos\left(\frac{d\theta}{2}\right) \quad (6)$$

6. CONCLUSION

Two procedures for evaluating of process of thread turning are discussed in this paper. The first one is based on calculation of engaged chip area in subsequent machining passes, according to specified infeed strategy. Developed Matlab application performs these calculations, using very limited set of input data. It is flexible and it can be use for arbitrary tool geometry and infeed strategy. The second procedure for evaluating of the process is based on mechanistic approach in modeling of cutting forces. That model requires relatively small experimental base and more complex algorithm. In that sense, this paper presents algorithm for computing of chip area on arbitrary finite lengths of discretized cutting edge. Further work on this problem assumes Matlab implementation of this algorithm and its experimental verification.

7. REFERENCES

- [1] Nalbant,M., Gunay,M., Yildiz, Y., *Modeling of the Effect of Deferent Infeed Angles and Cutting Areas on the Cutting Forces in External Threading*, Turkish J. Eng. Env. Sci., Vol.32 (2008), pp. 153 – 161.
- [2] Khoshdarregi,M.R., Altintas,Y., *Generalized modeling of chip geometry and cutting forces in multi-point thread turning*, Int.J.of Mach.Tool & Manufacture, Vol. 98 (2015), pp.21-32.
- [3] SANDVIK Coromant, *Threading applications Guide*,<https://www.sandvik.coromant.com/sitecollectiondocuments/downloads/global/technical%20guides/en-gb/c-2920-031.pdf> (2018)
- [4] DIN 103 Teil 1, *Metrisches ISO Trapezgewinde, Gewindeprofile*, Beuth Verlag, April 1977.
- [5] SIEMENS, *Sinumerik 808D, Programming and Operating Procedures for Turning*, (2013)

Authors: Assist. Prof. Branko Kokotovic, Nikola Vorkapic Ph.D. student, University of Belgrade, Mechanical Engineering Faculty, Department of Production Engineering, Kraljice Marije 16, 11000 Belgrade, Serbia, Phone.: +381 11 3302-375, Fax: +381 11 3370-364.

E-mail: bkokotovic@mas.bg.ac.rs;
nikola.vorkapic92@gmail.com

ACKNOWLEDGMENTS: The authors would like to thank the Ministry of Education, Science and Technological Development of Serbia for providing financial support that made this work possible.

Mustafic, A., Lovric, S., Nasic, E., Halilovic, J., Osmic, M., Becirovic, D.

TAGUCHI-BASED GREY RELATIONAL ANALYSIS OF PERFORMANCE CHARACTERISTICS IN THE MQL TURNING PROCESS OF X5CrNi18-10 STEEL

Abstract: This study focuses on experimental investigation and effective approach to optimize the MQL performance characteristics in the turning process of X5CrNi18-10 stainless steel. In order to achieve minimum surface roughness, minimum cutting forces and maximum material removal rate with a minimum number of trials, a standard $L_9 (3^4)$ Taguchi orthogonal array is selected. The effect of process parameters such as cutting speed, feed rate, depth of cut and volumetric concentration of the aerosol were simultaneously optimized using the Taguchi-based grey relational analysis. According to the optimization results, which were obtained from the largest signal-to-noise ratio of the grey relational grade, it was observed that cutting depth was the most dominant parameter in the optimization of all measured output variables, followed by cutting speed, volumetric concentration and the feed rate.

Key words: Multi-response optimization, Taguchi method, Grey Relational Analysis, MQL machining

1. INTRODUCTION

Reducing the production costs and improving the product quality are the effective ways to strengthen the competitiveness of enterprises. This need gave birth to a new technology called the minimum quantity lubrication (MQL). MQL machining refers to the use of a small amount of cutting fluid, and has achieved noticeable attention in academic and industry research area. This is because the usage of minimal quantities of fluid in MQL machining can definitely reduce the cost of using cutting fluids and the auxiliary equipment [1].

The determination of optimal machining parameters is a continuous task which goals are to reduce the production costs and to achieve desired product quality. In turning process, one of the main performance indicators are surface roughness. Achieving the desired surface quality is of great importance for the functional behavior of a part. At the same time, higher material removal rate and lower cutting forces are considered as factors that directly affect the production costs and the machining hour rate. Therefore, a multi-response optimization method based on a combination of Taguchi and the grey relational analysis (GRA) was applied to evaluate the optimal values of machining parameters (e.g. cutting speed, feed rate and depth of cut), as well as the volumetric concentration of the pulverized oil-on-water aerosol are investigated in order to obtain better surface quality, minimum cutting forces and increased material removal rate [2].

2. EXPERIMENTAL SETUP

2.1 Material, experimental conditions and measurements

The experimental studies were performed on a conventional lathe machine *Potisje PA 501A*. This machine meets all the necessary requirements for research objectives, ensuring sufficient rigidity, accuracy and precision of turned parts. All tests were

conducted under different settings of cutting speed, feed rate and depth of cut, by using an advanced MQL system as the cooling/lubrication technique, produced by *Daido Metal - Japan*. This MQL system has the ability to independently adjust oil and water delivery rates which are in the range of 10-50 ml/h and 300-1800 ml/h, respectively. Thus, there is a possibility of delivering atomized aerosols of variable volumetric concentrations. According to that, the atomized MQL mist in this study was delivered to the interface of workpiece-cutting tool at different oil-to-water mixture ratios using a vegetable based cutting oil. The summary of experimental conditions are listed in Table 1. Commercial WSM20 grade with Al_2O_3 coated carbide insert of *Walter Tiger Tec* CNMG120408-NF and PCLNR 2020K-12 tool holder were selected for the turning tests. In order to minimize the influence of cutting tool wear on the investigated quantities, each set of turning experiments was conducted using a new insert edge.

A quenched and tempered X5CrNi18-10 austenitic stainless steel was used as the workpiece material. All machining tests were carried out on a bar of 70 mm diameter with separated 15 mm long segments for each cutting test. The cutting forces were measured using a *Kistler 5070* dynamometer connected to an amplifier and a computer equipped with manufacturer's *DynoWare* software. Measurements of the surface roughness parameter R_a (arithmetic average deviation of the profile) were performed on a *Mitutoyo Surftest SJ-301* profilometer at three different locations to minimize the deviation. The average values of R_a were considered for the analysis. The material removal rate (MRR) was calculated for each experimental run according to Eq. (1):

$$MRR = v_c \cdot f \cdot a \quad (1)$$

Fig. 1 shows the experimental setup for the turning experiments.

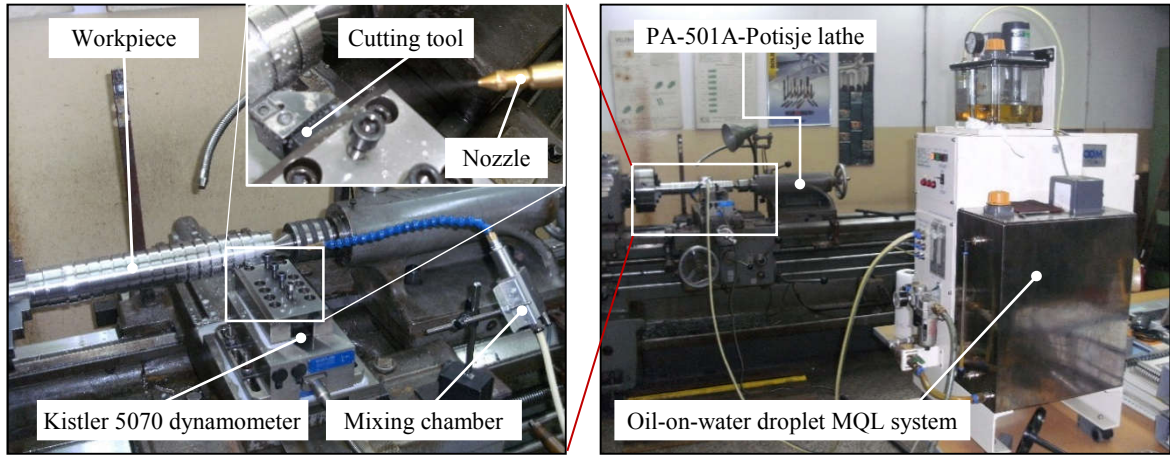


Fig. 1. Experimental setup for turning tests

2.2 Design of experiment

A specially designed experimental procedure is required to evaluate the effect of machining and MQL parameters on the performance characteristics [4]. In the present study a full-factorial design would require 81 experimental runs. However, the experimental cost for such selected design would be prohibitive and unrealistic. Therefore, the Taguchi method – a powerful and frequently used design of experiments was used. According to the Taguchi quality concept, a $L_9 (3^4)$ orthogonal array with nine rows was used for the experiments as shown in Table 2.

preprocessed into quantitative indices for normalizing raw data for further analysis [3]. Preprocessing the raw data is a process of converting an original sequence in decimal sequences between 0-1. For data preprocessing in the grey theory, the lower surface roughness and cutting forces and higher material removal rate are indication of better performance in the turning process. For the calculation of normalized values of the surface roughness parameter and the resultant cutting force, the corresponding characteristic is “smaller-is-better”, which can be expressed as [4]:

Symbol	Parameters	Notation	Unit	Level values		
				1	2	3
A	Cutting speed	v_c	m/min	55,41	108,33	160,32
B	Feed rate	f	mm/rev	0,04	0,196	0,357
C	Depth of cut	a	mm	0,2	1	1,8
D	Oil-to-water ratio	$OilW-ratio$	%	0,55	2,85	16,66

Table 1. Machining parameters and their levels

No.	Levels of cutting parameters				Measured data of responses						Normalized values of responses		
	A	B	C	D	F_X (N)	F_Y (N)	F_Z (N)	F_R (N)	R_a (μm)	MRR (cm^3/min)	Norm F_R	Norm R_a	Norm MRR
1	1	1	1	1	55,02	91,7	83,9	135,9	0,416	0,459	1	1	0
2	1	2	2	2	349,7	296,6	673,1	814,4	0,750	11,252	0,670	0,489	0,190
3	1	3	3	3	871,6	604,6	1920	2193,5	1	36,891	0	0,107	0,641
4	2	1	2	3	189,2	125,1	203,4	304,6	0,950	4,333	0,918	0,183	0,068
5	2	2	3	1	526,2	319	1044	1211,8	1,023	38,218	0,477	0,071	0,665
6	2	3	1	2	104,3	272,7	359,6	463,2	0,763	7,734	0,841	0,469	0,128
7	3	1	3	2	313,8	133,2	321,3	468,4	0,753	11,543	0,838	0,484	0,195
8	3	2	1	3	95,54	205,8	228,4	321,9	0,463	6,284	0,909	0,928	0,102
9	3	3	2	1	349,6	399,1	961,3	1097,9	1,070	57,234	0,532	0	1

Table 2. Machining parameters and their levels

3. GREY RELATIONAL ANALYSIS (GRA)

Grey relational analysis is used to determine the optimum condition of various parameters to obtain the best quality characteristics [3]. This method is widely applied in complex and multivariable systems, where the relationship among various parameters is usually unclear. Grey relational analysis is an impacting measurement method in so called “grey system theory”, which analyzes uncertain relations between one main factor and all other factors in an investigated system [4]. In this regard, the data to be used in GRA must be

$$x_i^*(k) = \frac{\max x_i^o(k) - x_i^o(k)}{\max x_i^o(k) - \min x_i^o(k)} \quad (2)$$

The normalized values for the material removal rate are obtained for the “larger-is-better” characteristic using the Eq. (3) [4]:

$$x_i^*(k) = \frac{x_i^o(k) - \min x_i^o(k)}{\max x_i^o(k) - \min x_i^o(k)} \quad (3)$$

where $i=1, \dots, m$; $k=1, \dots, n$. m is the number of experimental data items and n is the number of

parameters. $x_i^o(k)$ denotes the original sequence, $x_i^*(k)$ denotes the sequence after the data preprocessing, $\max x_i^o(k)$ denotes the largest value of $x_i^o(k)$, $\min x_i^o(k)$ denotes the smallest value of $x_i^o(k)$. After the process of normalization is carried out, the grey relation coefficient is calculated using the following equation [4]:

$$\xi_i(k) = \frac{\Delta_{\min} + \zeta \Delta_{\max}}{\Delta_{oi}(k) + \zeta \Delta_{\max}} \quad (4)$$

Where $\Delta_{oi}(k)$ is the absolute value of the difference between targeted sequence and the comparative sequence and where Δ_{\max} and Δ_{\min} take maximum and minimum obtained values. ζ is the distinguishing coefficient and its value lies between 0 and 1. Then, grey relational coefficient expresses the level of correlation between the reference and comparability sequences. Grey relational grade is a weighted sum of the grey relational coefficients and is calculated as follows: [3,4]:

$$\gamma_i = \frac{1}{n} \sum_{k=1}^n \xi_i(k) \quad (5)$$

where n is the number of performance characteristics.

No.	Grey relational coefficient (GRC)			Grey relational grade (GRG)		
	F_R	R_a	MRR	Grade	S/N ratio	Rank
1	1	1	0,333	0,777	-2,182	1
2	0,603	0,494	0,381	0,493	-6,141	7
3	0,333	0,358	0,582	0,424	-7,433	9
4	0,859	0,379	0,349	0,529	-5,524	6
5	0,489	0,350	0,598	0,479	-6,389	8
6	0,758	0,485	0,364	0,536	-5,415	5
7	0,755	0,492	0,383	0,543	-5,291	4
8	0,846	0,875	0,357	0,693	-3,182	2
9	0,516	0,333	1	0,616	-4,198	3

Table 3. GRA coefficients and GRA grade for each experimental setting

Levels	Grey relational grade			
	Cutting speed	Feed rate	Depth of cut	Oil-to-Water ratio
1	0,5653	0,6170*	0,6690*	0,6246*
2	0,5149	0,5552	0,5464	0,5243
3	0,6179*	0,5259	0,4827	0,5492
Delta	0,1030	0,0911	0,1864	0,1002
Rank	2	4	1	3

Table 4. Response table for the mean GRG

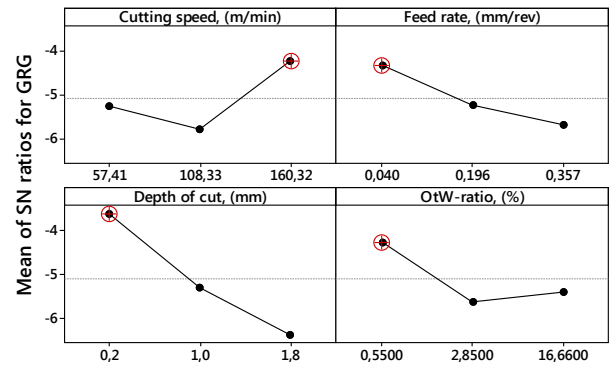
4. ANALYSIS OF EXPERIMENTAL RESULTS

In the present research, the surface roughness, cutting forces and material removal rate for different turning and MQL parameters are given in Table 2. A lower surface roughness, resultant cutting force and higher material removal rate are the main indicators of

better process performance. Thus, for data pre-processing in the grey relational process, surface roughness and resultant cutting force are taken as the “smaller-is-better” and material removal rate as the “larger-is-better” characteristic using Eq. (2) and (3). Results of the performed data normalization are listed in Table 2. After the calculation of deviation sequences for all nine experiments, the distinguishing coefficient can be substituted into Eq. (4) to produce the grey relational coefficient. In this particular case, the value of ζ is taken as 0,5 since it provides a balanced effect on the grey relational coefficient. The grey relational coefficient and grade values for each of the L_9 orthogonal array were calculated by applying Eq. (4) and (5), and are given in Table 3. According to the performed experiment design, it can be observed from Table 3 that the MQL and turning parameters, setting of experiment no.1 has the highest value of grey relational grade. Thus, the first experiment gives the best multi-performance characteristics among the nine experiments. In addition, the “larger-is-better” S/N quality characteristic was used to obtain the optimal combination for multiple response optimization because higher grade was desirable. Quality characteristic of the larger-is-better is defined as follows [4]:

$$S/N = -10 \log_{10} \left[\frac{1}{n} \left(\sum_{i=1}^n \frac{1}{y_i^2} \right) \right] \quad (6)$$

The S/N ratios of multiple quality characteristic calculated by applying Eq. (6) are given in Table 3.



Signal-to-noise: Larger is better

Fig. 2. Main effects plot of S/N ratios for GRG

Since the highest S/N ratio gives the best result (Fig. 2), the optimum cutting conditions were cutting speed of 160,32 (m/min), feed rate of 0,04 (mm/rev), depth of cut of 0,2 (mm) and minimum oil-to-water mixture of 0,55% and were obtained for multiple quality characteristics. The optimum process parameter levels can be shortly given as A3-B1-C1-D1. In addition, according to the Taguchi methodology, the GRG response table for means was used for the analysis of control parameters on the multiple characteristic value. This results are given in Table 4. The most effective parameter affecting the performance characteristics is determined by comparing the difference between the maximum and the minimum value of the grey relational grade. Therefore, depth of cut was the most important parameter affecting

the overall grey relational grade. The order of importance of the controllable parameters to the multi-performance characteristics in the MQL assisted turning process of X5CrNi18-10 stainless steel can be listed as: parameter (C) depth of cut, cutting speed (A), oil-to-water concentration (D) and feed rate (B). This illustrates that the turning performance was strongly influenced by the depth of cut. As listed in Table 5, ANOVA analysis was carried out to see the effects of the experimental parameters on the result of multiple-performance characteristics. The results of ANOVA indicated that cutting speed, feed rate, depth of cut and the oil-to-water mixture ratio influenced the grey relation grade values by 16,07%, 13,09%, 54,32% and 16,50%, respectively. According to this, depth of cut had the most percentile contribution on the multiple performance characteristic. Unlike the response table for the grey relational grade, ANOVA analysis showed that oil-to-water mixture ratio of the pulverized aerosol had a higher contribution in the multiple-characteristic performance compared to the cutting speed and feed rate. Another interesting finding from the ANOVA analysis is that none of the investigated parameters had statistically significance at the confidence level of 95%.

Source	Deg. of freedom (DF)	Sum of Squares (SS)	Mean square (MS)	F-Value F	Contribution PC (%)
A	2	0,01592	0,0079	1,23	16,07
B	2	0,0129*	-	-	-
C	2	0,05384	0,0269	4,15	54,34
D	2	0,01635	0,0081	1,26	16,50
Pooled Error	2	0,01297	0,0064		13,09
Total	8	0,09908			100

Table 5. Results of ANOVA for GRG (*Pooled factor)

5. CONCLUSIONS

In this study, the Taguchi-based grey relational analysis (GRA) was used to determine the optimal turning parameters in turning of X5CrNi18-10 stainless steel under near dry cooling and lubrication conditions. Since the used MQL system with oil-on-water droplet mist has the ability to independently adjust water and oil flow rate, one of the control factors in the experimental investigation besides the machining parameters was the volumetric concentration of the atomized mist. The minimum surface roughness and cutting forces, and the maximum material removal rate were selected as the quality targets. All experimental results were evaluated using the S/N quality characteristics and ANOVA. The following conclusions can be drawn as follows:

- The application of the Taguchi-based grey relational analysis, directly combines the multiple quality responses (R_a , F_R and MRR) into a single performance indicator through the grey relational grade. Based on the results, which were obtained from the largest grey relational grade (GRG), it was demonstrated that the optimum cutting and lubrication conditions were cutting speed of 160,32 (m/min), feed rate of 0,04 (mm/rev), depth of cut of 0,2 (mm) and minimum oil-to-water mixture of

0,55%. The optimum process parameter levels can be shortly given as A3-B1-C1-D1.

- According to the response table for the mean GRG it was found that the depth of cut has the strongest effect on the multiple-performance characteristic among other parameters.
- The order of importance of the controllable factors to the multi-performance characteristics in MQL assisted turning process of X5CrNi18-10 steel is depth of cut, cutting speed, oil-to-water concentration and feed rate.
- Based on the results of ANOVA, the main parameter affecting the multi-performance characteristics was depth of cut with a percentage contribution of 54,32%. The contributions rates of cutting speed, feed rate and volumetric concentration were, 16,07%, 13,09% and 16,50%, respectively.
- Using a vegetable-based cutting oil with a flow rate of 10 ml/h in combination of water flow of 1800 ml/h, a volumetric concentration of 0,55% showed to be the best option in simultaneous optimization of all measured response variables. Therefore, the cooling effect is more effective than the lubrication effect, and gives overall best process performance in the simultaneous optimization. On the other hand, this may be caused by better chip breakage, which reduces cutting forces and provides lower surface roughness.

6. REFERENCES

- [1] Ji, X., Li, B., Zhang X, Liang S.Y.: *The effects of Minimum Quantity Lubrication (MQL) on machining force, temperature and residual stress*, International Journal of Precision Engineering and Manufacturing Vol. 15. No.11, pp.2443-2451, 2014.
- [2] Puh, F., Brezocnik, M., Jurkovic, Z., Cukor, G., Peric, Mladen, Sekulic M.: *Multi response optimization of turning parameters using the grey-based Taguchi method*, Journal of Trends in the Development of Machinery and Associated Technology, Vol.19, No.1, pp.13-16, 2015.
- [3] Sentilkumar, N, Tamizharasan, T., Anandakrishnan, V.: *Experimental investigation and performance analysis of cemented carbide inserts of different geometries using Taguchi based grey relation analysis*, Measurement Vol. 58, pp.520-536, 2014.
- [4] Tosun, N., Pihtili, H.: *Gray relational analysis of performance characteristics in MQL milling of 7075 Al alloy*, Int. J. Adv. Manuf. Technol. Vol. 46, pp.509-515, 2010.

Authors: Assist. Prof. Adnan Mustafic, Assist. Prof. Sladjan Lovric, M.Sc. Edis Nasic, M.Sc. Jasmin Halilovic, Assist. Prof. Midhat Osmic, B.Sc. Denis Becirovic, University of Tuzla, Faculty of Mechanical Engineering, Univerzitetska 4, 75000 Tuzla, Bosnia and Herzegovina,
Phone.: +387 35 320-920, Fax: +387 35 320-921.
E-mail:
adnan.mustafic@untz.ba; sladjan.lovric@untz.ba;
edis.nasic@untz.ba; jasmin.halilovic@untz.ba;
midhat.osmic@untz.ba; denis.becirovic.mf@untz.ba

Rodic, D., Gostimirovic, M., Kovac, P., Sekulic, M., Savkovic, B.

PRINCIPLE OF ELECTRICAL DISCHARGE MACHINING OF NON-CONDUCTIVE ZIRCONIA CERAMICS

Abstract: The electrical discharge machining (EDM) is a nonconventional machining process for precision machining of hard and electrically conductive materials. Previously known that non-conductive materials could not be machined by the EDM method. The new technology for electrical discharge machining non-conductive materials was named as the assisting electrode method. In this method, an electrically conductive thin layer is placed on the upper surface of the workpiece, in order to establish discharge process. As the purpose of this paper is to present the new machining method for the non-conductive ceramics by conventional EDM machine. The machining procedures and characteristics were explained and the machining mechanism were discussed.

Key words: Electrical discharge machining, assisting electrode, zirconia ceramics.

1. INTRODUCTION

Die sinking electrical discharge machining (EDM) is non-conventional machining process widely applied to generate three-dimensional complex shapes in many different classes of materials [1]. It is capable of machining heat treated steels, heat resistant steels, composites, super alloys, ceramics, carbides, etc., used in various industry. The only condition is that the materials must be electro-conductive [2].

EDM is an electro-thermal machining process used to machining conductive materials. By applying an assisting electrode (conductive layer on top of the non-conductive material) the EDM process can also be used to machining non-conductive ceramics [3].

Insulating ceramic such as zirconium ZrO_2 has been widely used in die making and other industrial applications [4]. Due to their high hardness and brittleness properties zirconium ceramic is very hard to machine by traditional machining method such as grinding and diamond cutting processes [5]. Various unconventional methods are also applied to the processing of non-conductive ceramics like laser machining, ultrasonic machining and water jet machining. The efficient processing of non-conductive ceramics is poor and shape parts are still difficult to machine. Therefore, there is a need new possibilities for machining these materials.

In this paper, the machining properties of ZrO_2 is evaluated on sinking EDM. The machining procedures and characteristics were explained and the machining mechanism were discussed. The theory of assisting electrode machining method is explained and the effects of different electrical parameters on the machining process are presented.

2. ASSISTING ELECTRODE METHOD (AEM)

The assisting electrode can be made up of electrical conductive material that can be applied on top of insulating ceramic, fig 1. Some techniques have been developed over the years to apply conductive material

on insulating ceramic. One way of applying a metal film on top of the non-conductive ceramic is chemical vapor deposition (CVD). However for stable machining process, the conductive layer need to be more than 10 μm . To obtain a layer over this limit by method PVD is very expensive and unprofitable. The conductive layer on top surface insulating ceramic could also be deposited by physical vapor deposition (PVD). Mohri et. al. have used a conductive layer of titanium-nitride produced by PVD process as an assisting electrode to machining non-conductive silicon nitride ceramic [6]. They concluded that this method has the same disadvantage as the CVD process.

Second way of applying conductive layer on top of the non-conductive ceramic is baked carbon based lacquer. Hosel et al. studied a new lacquer based assisting electrode. They are eroded bars in zirconia samples [7]. The assisting electrode made by baked carbon has brittle. When EDM is performed with higher energies leads to the removal of the layer in undesired places.

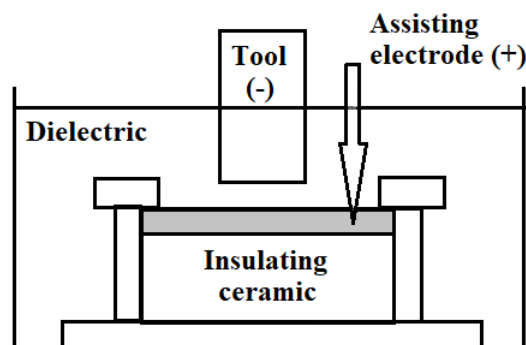


Fig. 1. Assisting electrode method

Third and one of simple way would be to attach an metal layer on top of the non-conductive ceramic [8]. The major disadvantage of this methods is drawback of a direct contact between the metal and the non-conductive ceramic. This disadvantage can be compensated using combination of metal foil and carbon lacquer as hybrid assisting electrode or self-adhesive

metal foil with electrical conductive glue. The carbon lacquer would provide conductive adhesive between the metal foil and the non-conductive ceramic.

This paper presents the EDM machining of insulating ZrO₂ ceramics with copper self-adhesive foil as an assisting electrode on top surface. The major advantage of this methods is its simplicity.

3. MATERIAL REMOVAL MECHANISM

The removal mechanism of non-conductive ceramic is a different that for metals [9, 10]. The EDM of non-conductive ceramics consists of two stages. First, the material needs to be removed. Second a conductive adhered layer needs to be formed. Without formation of conductive adhered layer, the EDM process will not proceed further.

Compared to metals ceramics have a higher melting point and lower thermal conductivity [11]. The material removal mechanisms such as thermal spalling and chemical decomposition takes place [12].

4. EXPERIMENTAL SETUP

Experiments were performed on an Agie Charmilles EDM machine (model SP1-U). The work piece material was ZrO₂ alloy with the dimension of 15×15×8 mm. A Toyo Tanso TTK-50 graphite electrode cross section of 10×10 mm and the height of 100 mm was used as electrode in this study. In addition, Castrol oil Ilocut EDM 180 was employed as a dielectric fluid in this investigation.

Self adhesive electrically conductive copper tape (3M grade 1181) thickness 0.066 mm is used as assisting electrode. Figure 2 shows an insulating ZrO₂ ceramic without and with assisting electrode.

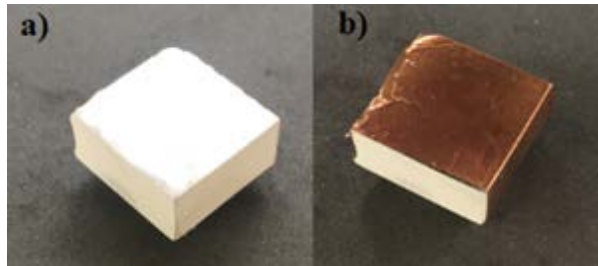


Fig. 2. Insulating ZrO₂ ceramic: a) without and b) with assisting electrode

The machining characteristics of material removal rate MRR (mm³/min), end wear ER (%), and surface roughness SR (Ra, μm) were adopted to the effects of machining parameters on the EDM characteristics of ZrO₂ ceramic.

Material removal rate, which is the volume of metal removed from a workpiece in a specified period of time, is often expressed as cubic millimeters per minute (mm³/min), equation 1. The erosion depth was read directly from the machine.

$$MMR = \frac{\text{Electrode area (mm}^2\text{)} * \text{Depth of cut (mm)}}{\text{Time of cut (min)}} \quad (1)$$

End wear was measured with an Abbe Length measuring device. Before and after cut, the electrode was measured to determine its overall length, equation 2.

$$EW = \frac{\text{Start lenght (mm)} - \text{Final lenght (mm)}}{\text{Depth of cut (mm)}} * 100 \quad (2)$$

Surface roughness average measured in μm was chosen as the standard method for defining surface finish. Measurements were made using a Mahr MarSurf PS1 instrument.

The electrical machining contitions was selected based on previously examined results from litarture, for various insulating ceramic [13, 14]. The detailed machining conditions are given in Table 1.

Working condition	Description
Tool	Graphite TTK-50
Workpiece	ZrO ₂
Polarity	(-) negative
Adhesive foil	Copper 3M grade 1181
Discharge current	2 A
Pulse duration	75 μs
Duty factor	50%
High-tension current	0.5 A
No-load voltage	300 V
Dielectric	Castrol Ilocut EDM 180
Electrode jumping interval	2 s
Electrode jumping height	1.5 mm
Working time	60 min

Table 1. Table Experimental conditions in EDM

5. RESULTS AND DISCUSSION

Non-conductive ceramic can be machined with the EDM process by using a conductive layer marked as assisting electrode. The assisting electrode is applied on top of the non-conductive ceramic. This is provided electric contact for the non-conductive ceramic and is responsible for the initial discharges.

The insulating ceramic ZrO₂ is covered with a self-adhesive copper foil (electrically conductive material). The machining process is performed using only working oil. The erosion start from electrically conductive material, figure 3.

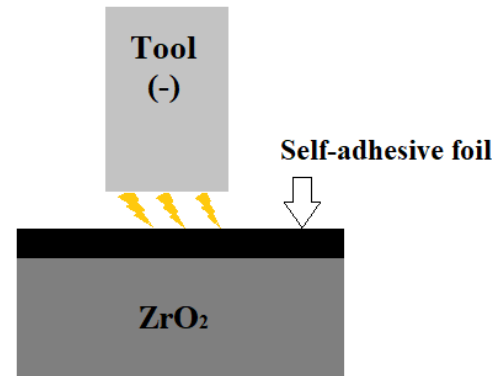


Fig. 3. Schematic illustration of EDM for ZrO₂ with a self adhesive foil, initial stage

After removing the assisted electrode layer, discharge occurs continuously throughout the self-adhesive foil and into the insulating ceramic area, figure 4.

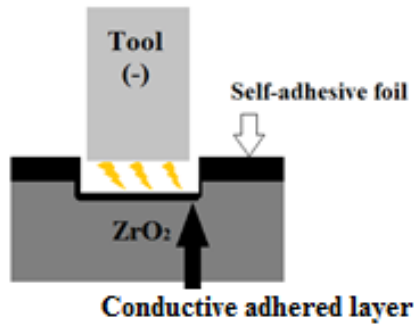


Fig. 4. Removing assisted electrode and forming conductive adhered layer

During the erosion process, a carbonized conductive layer (figure 5) is generated on the non-conductive ceramic from the dielectric oil and graphite electrode. The continuous erosion indicates that electrically conductive products (carbon from working oil and graphite electrode) became adhered to the ceramic during machining.

The conductive adhered layer maintains electrical conductivity after the self-adhesive foil is removed. Adhesion of conductive layer degrades the surface properties and has harmful influence on erosion accuracy. Machined workpiece of ZrO_2 using EDM with self-adhesive copper foil is showed on figure 5.

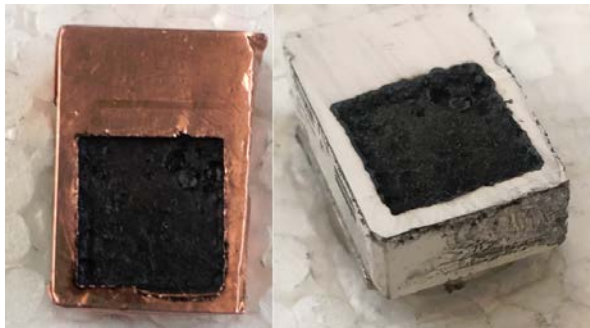


Fig. 5. Machined workpiece of ZrO_2 using EDM with self-adhesive copper foil

Table 2 shows result of machining ZrO_2 ceramic by die-sinking EDM. As a result, very high surface roughness, small material removal rate and high end wear are obtained by this process.

Surface roughness	μm	12.06
Material removal rate	mm^3/min	2.51
End wear	%	56.52%
Depth erosion (60 min)	mm	1.5

Table 2. Result of experiment

The machined surface with conditions from Table 1 is shown on figure 6. There was many pores and cracks that arise during resolidifying and shrinking process in surface layer after melting arised by the discharges. The

surface of tool after machining is shown on figure 7. Also, as with the machined surface of workpiece, there are pores and cracks. Tool wear is more pronounced because of the use of negative polarity during machining.

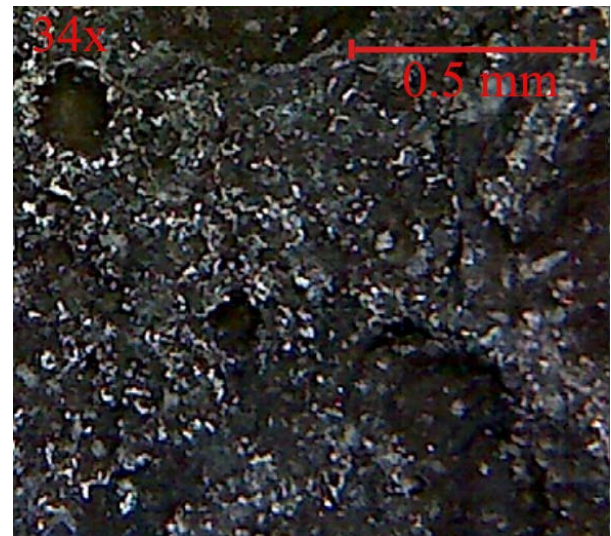


Fig. 6. Machined surface with condition from Table 2



Fig.7. Surface tool after machining ZrO_2 (9x)

The typical curve of movement electrode is shown in figure 8.

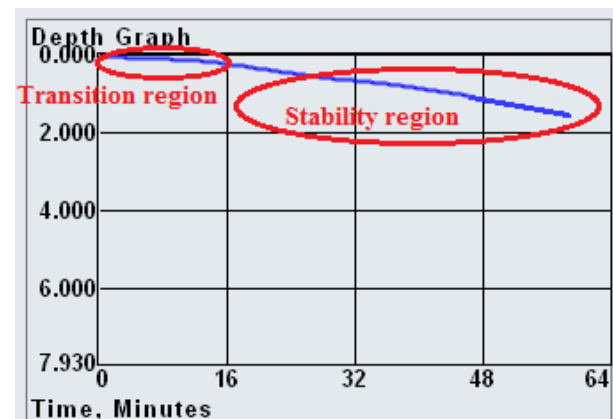


Fig.8. Depth graph from machine display

The typical curve can be divided into two stages. The first stage corresponds to machining assisting electrode and after that curve maintains constant value. In this stage carbonized conductive layer is formed. The name of this stage is transition region. The length of this stage depended from assisting electrode material.

In the second stage, named stability region, the curve has a steep slope. In this stage, constant discharge generation occurs for a long period.

6. CONCLUSIONS

EDM requires both tool and workpiece to be conductive. Insulating ceramic can be machined with the EDM process using assisting electrode. In this investigation, the process assisting electrode method in electrical discharge machining of insulating ceramics ZrO₂ is presented.

The removal mechanism of non-conductive ceramic are thermal spalling and chemical decomposition.

The EDM of insulating ceramic can be divided into three sub processes. The first is removing assisting electrode. The second is generation of conductive adhered layer. Conductive adhered layer generated from the dielectric and graphite electrode during erosion process ensures maintained electric contact after assisting electrode has been removed. And the third is removal process with discharge generated under stable conditions.

The paper describes principle of electrical discharge machining of non-conductive zirconia ceramics. Further experimental studies especially influence machining parameter and analysis can be carried out in order to better understand the process.

7. REFERENCES

- [1] Gostimirovic, M., P. Kovac, B. Skoric and M. Sekulic. "Effect of electrical pulse parameters on the machining performance in EDM." *Indian Journal of Engineering & Materials Sciences* Vol. **18**, pp. 411-415, 2012.
- [2] Fukuzawa, Y., T. Tani, E. Iwane and N. MOHRI. "Some Machining Methods of Insulating Materials by an Electrical Discharge Machine." *Journal of the JAPAN Society of electrical machining engineers* Vol. **29** (60), pp. 11-21, 1995.
- [3] Fukuzawa, Y., T. Tani, E. Iwane and N. Mohri. "A new machining method for insulating ceramics with an electrical discharge phenomenon." *Journal of the Ceramic Society of Japan* Vol. **103** (1202), pp. 1000-1005, 1995.
- [4] Tani, T., Y. Fukuzawa, N. Mohri, N. Saito and M. Okada. "Machining phenomena in WEDM of insulating ceramics." *Journal of materials processing technology* Vol. **149** (1-3), pp. 124-128, 2004.
- [5] Guo, Y. F., G. Q. Deng, J. C. Bai and Z. S. Lu (2008). *Electrical discharge machining (EDM) phenomena of insulating ZrO₂ ceramics with assisting electrode*. Key Engineering Materials, Trans Tech Publ.
- [6] Mohri, N., Y. Fukusima, Y. Fukuzawa, T. Tani and N. Saito. "Layer generation process on work-piece in electrical discharge machining." *CIRP Annals-Manufacturing Technology* Vol. **52** (1), pp. 157-160, 2003.
- [7] Hösel, T., C. Müller and H. Reinecke. "Spark erosive structuring of electrically nonconductive zirconia with an assisting electrode." *CIRP Journal of Manufacturing Science and Technology* Vol. **4** (4), pp. 357-361, 2011.
- [8] Ojha, N., C. Mueller and H. Reinecke. "Parametric Analysis of μ -Electric Discharge Machining of non-conductive Si₃N₄." *Applied Mechanics & Materials* Vol. (564), 2014.
- [9] Trueman, C. and J. Huddleston. "Material removal by spalling during EDM of ceramics." *Journal of the European Ceramic Society* Vol. **20** (10), pp. 1629-1635, 2000.
- [10] Zhang, J., T. Lee and W. Lau. "Study on the electro-discharge machining of a hot pressed aluminum oxide based ceramic." *Journal of materials processing technology* Vol. **63** (1-3), pp. 908-912, 1997.
- [11] Ojha, N., T. Hösel, F. Zeller, C. Müller and H. Reinecke (2013). *Major parameters affecting the electric discharge machining of non-conductive SiC*. Proceedings of the 10th International Conference on Multi-Material Micro Manufacture, S. Azcárate and S. Dimov, eds., Research Publishing.
- [12] Hu, C., Y. Zhou and Y. Bao. "Material removal and surface damage in EDM of Ti₃SiC₂ ceramic." *Ceramics International* Vol. **34** (3), pp. 537-541, 2008.
- [13] Put, S., J. Vleugels, O. Van der Biest, C. Trueman and J. Huddleston. "Die sink electrodischarge machining of zirconia based composites." *British ceramic transactions* Vol. **100** (5), pp. 207-213, 2001.
- [14] Banu, A., M. Y. Ali and M. A. Rahman. "Micro-electro discharge machining of non-conductive zirconia ceramic: investigation of MRR and recast layer hardness." *The International Journal of Advanced Manufacturing Technology* Vol. **75** (1-4), pp. 257-267, 2014.

Authors: MSc Dragan Rodic, Full Prof. Marin Gostimirovic, Full Prof. Pavel Kovac, Full Prof. Milenko Sekulic, Assist. Prof. Borislav Savkovic. University of Novi Sad, Faculty of Technical Sciences, Department of Production Engineering, Trg Dositeja Obradovica 6, 21000 Novi Sad, Serbia, Phone.: +381 21 450-2324, Fax: +381 21 454-495.

E-mail: rodicdr@uns.ac.rs; maring@uns.ac.rs; pkovac@uns.ac.rs; milenkos@uns.ac.rs; savkovic@uns.ac.rs

ACKNOWLEDGMENTS: This paper is the result of the research within the project TR35015 financed by the Ministry of Science and Technological Development of the Republic of Serbia.

Sekulic, M., Gostimirovic, M., Kulundzic, N., Aleksic, A.

TECHNOLOGICAL CHANGES IN MOLD MAKING INDUSTRY

Abstract: A tool is a component that can be used to make other products. In most cases, the tool is used to fabricate a large number of identical components before it is destroyed due to wear, corrosion, and mechanical failure. Tools (molds) are essential in replication processes such as injection molding. Injection molding is by far the most popular process used for the production of plastic parts for all kinds of applications. The available technologies for tooling are changed, since traditional mold making technologies such as copy milling, die-sinking electro discharge machining (EDM), wire EDM, grinding, polishing, etc... have lower limits as to the obtainable geometries, complexity, surface roughness, costs, production time. New tooling technologies for mold making have emerged which enable reduced costs and lead time. Mold delivery time can be reduced by 50% or more. This paper presents recent technological changes in mold making industry which offers new possibilities to the customers.

Key words: mold making industry, technological, changes

1. INTRODUCTION

The mold making industry faces a number of key challenges. The cost of manufacturing is on the rise, and there are products demand across a number of industries, including automotive, aerospace and consumer goods. Product complexity continues to be on the rise as new technologies are introduced and consumer preferences evolve. For mold manufacturers, increased product complexity results in an increased demand for tools, which, of course, is positive for the industry. However, with manufacturing costs on the

rise, companies must look for ways to decrease cost of the manufacturing process, especially at the tooling level. Mold makers can no longer afford to make molds the same way they were done in the past. They have to face an increasing pressure to improve quality, reduced costs, and to meet stricter delivery times.

A process chain consists of all of the process steps necessary to produce the mold. Mold production process begins with a mold quotation request, and finishes with the adjustment/change and pre-injection stages, Fig. 1.

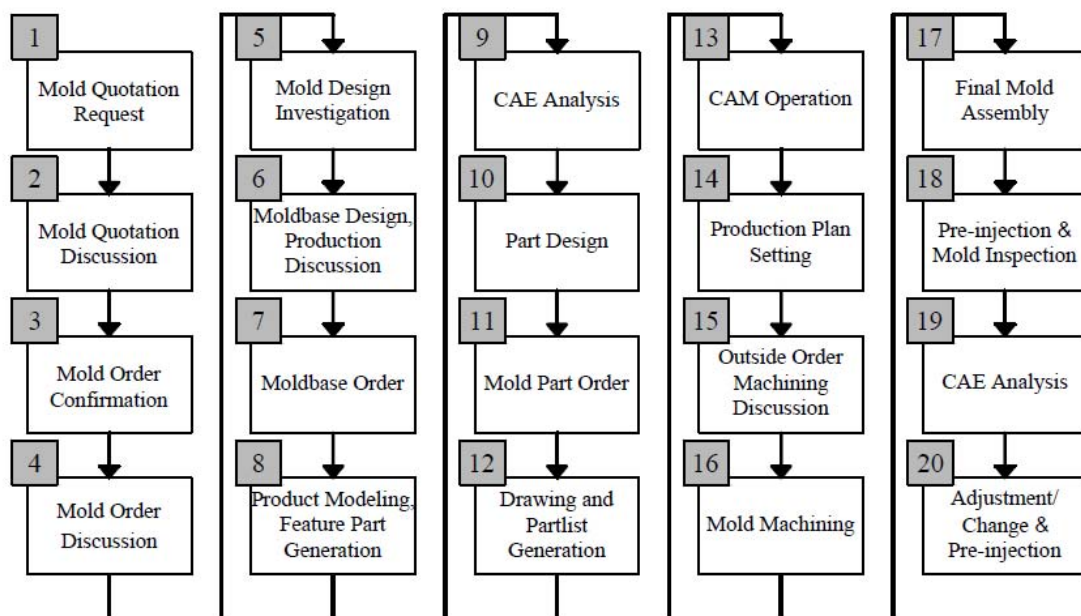


Fig. 1. A process chain in mold making industry [1]

The processes is shown in Fig. 1 can be classified into business processes [1–3], design processes [4–12], production processes [13–16], and assembly and try out processes [17–20]. Driving down manufacturing costs is only possible by redesigning and enhancing the

entire process chain. In production processes only tool maker is responsible for time-to-market. Technological process chain has a huge indirect influence on lead time and costs. Optimization of machining time and costs can be carried out through development of new

production concepts. Mould making companies must have a clear technology strategy, based on the most modern generation of processing machines. It's a major challenge for the mold making industry, because the molds have to be manufactured to a high standard of quality without driving up costs.

2. EVOLUTION OF PRODUCTION CONCEPTS IN MOLD MANUFACTURING TECHNOLOGIES

Actual state and time evolution of most relevant molds manufacturing technologies are shown in Fig. 2. In current practice, the process chain in mold making involves milling, hardening, surface treatment by spark erosion, and often final finishing by hand. After the 90's, most of the introduced manufacturing technologies are deeply based on microprocessors or digital technologies able to support the programming and control tasks [2]. Digital based technologies can be found from the design to the manufacturing processes, where five-axis machining, coordinate measuring or rapid tooling are only some examples.

Digital technologies was improved EDM process, too (the electrode orbital movement, the improvement of the discharging process through more sophisticated electronic circuits based on transistor and capacitors and the piloting of the spark generator, CNC machining, inserting the electrodes in the tool changer to a finished polished cavity or cavities, complete integration with CAD/CAM systems, the tool changer device).

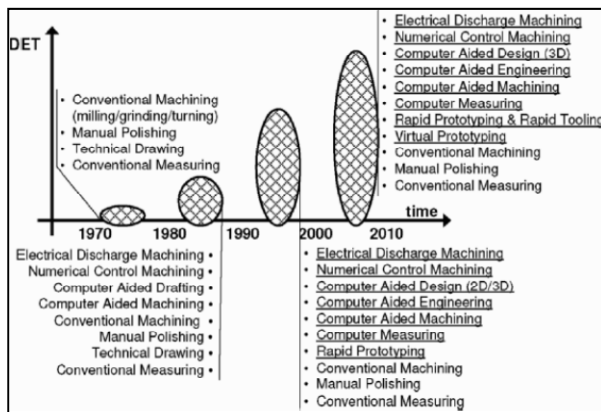


Fig. 2. Time evolution of most relevant molds manufacturing technologies [2]

Compared to 20 years ago, molds have become much more demanding from a technical standpoint as well as from customer requirements. Successful mold making businesses today not only offer their customers the most modern equipment and well-trained staff, but additional services as well. These services can include all aspects of process support, including part development and design, FEM calculations, mold and molding simulation, bench tests and prototyping. The actual creation of the mold often does not occur until the very end of the process.

Mold engineers depend on CAD/CAE/CAM software applications for drafting, design and manufacturing their molds. Importance of the CAX-

process chain in mold making is very huge. Programming of NC programs often has small share of the whole process chain (estimation: 5-10%) but only few mold makers perceive the potentials of optimisation in NC-programming.

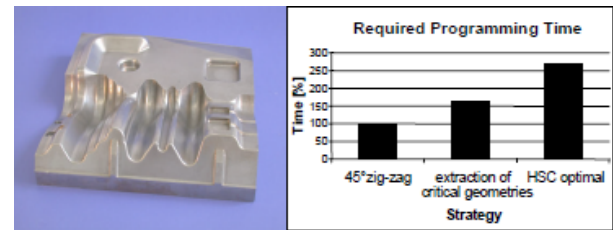


Fig. 3. Programming time for different machining strategies [3]

Possible steps to generate NC-programs are shown in Fig. 4.

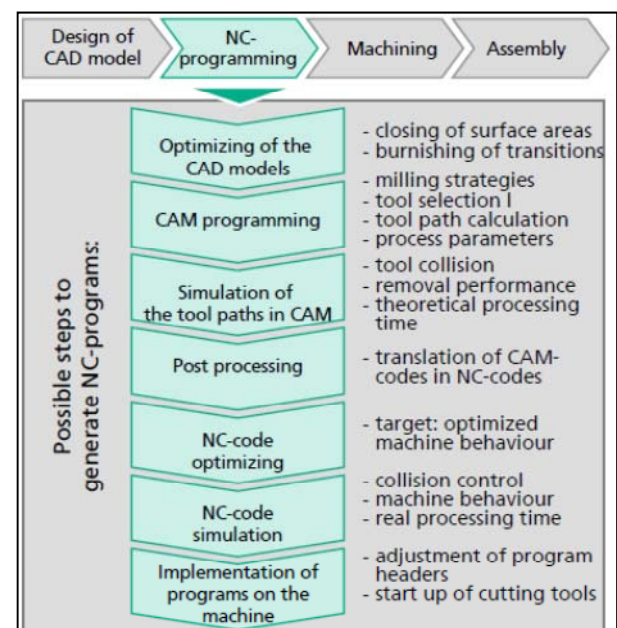


Fig. 4. Substantial steps for mold making [4]

2.1 Full 5-axis and 3+2 machining

The amount of machining effort and time required for manufacturing free-form surfaces in mold manufacture is very high so that it is necessary to find alternatives to conventional 3-axis milling machining for fast and economical tool production. Logical step in evolution of production concepts is the step up to 3 + 2 or full 5-axis machining. 3 + 2 machining allows the use of a shorter, more rigid cutting tool that can be angled toward the workpiece surface for faster feeds and speeds. The tool axis is changed when the tool is not cutting, and then remains fixed while the tool is engaged with the material in a given area. Common applications for 3 + 2 operations include roughing and other aggressive high-speed machining techniques. The shorter tool length also enables undercuts in cavities and steep walls, a capability well suited for mold making and other workpiece applications involving curves or angled tubular shapes.

Using efficient 5-axis chip removal technologies enables us to substantially scale back machining times.

The use of simultaneous five axis hard milling offers significant optimization potential. In simultaneous 5-axis machining, the machine tool's three linear axes (X, Y and Z) and two rotational axes (A and B) all engage at the same time to perform complex contour surface machining. There are many advantages of full 5-axis machining, all of which significantly impact productivity and profitability, a few of the more common ones are:

1. *Use fewer setups.* 5-axis machining allows for milling complex shapes with one setup, versus using multiple setup to accommodate the machine, spindle and tooling.
2. *Finish with shorter cutters.* This allows you to tilt the tool axis around the part, allowing for the use of shorter cutters and smaller L/D (length/diameter) ratios.
3. *Mill deeper areas.* Often deep areas of a part that are difficult to reach from straight in the Z-axis can be milled by rotating the tool axis, and performing a 3+2 or simultaneous 5-axis operation.

4. *Reduce EDM processes.* 5-axis milling of deep areas and ribs can reduce the need for slower EDM operations, reducing time to ship.

5. *Save time and money.* Using shorter cutters often allows for faster feed rates, due to deflection and vibration. Reducing EDM processes saves time.

Some obstacles for the more application of simultaneous 5-axis machining in mold making industry are: HSC machining provides capable approaches for most of the machining tasks, high effort during of CAM programming, limited availability of capable CAM modules, complex NC-process chain impairs process stability. Simultaneous five-axis programming requires a significantly higher level of programming expertise. Recent field tests indicate that with a 10-percent increase in programming effort, five-axis machines can improve machining productivity up to 30 percent. Molds with deep cavities and small, vertical corners are the primary targets. Influence of technological changes in mold making industry on productivity/economic efficiency is shown in Fig. 5.

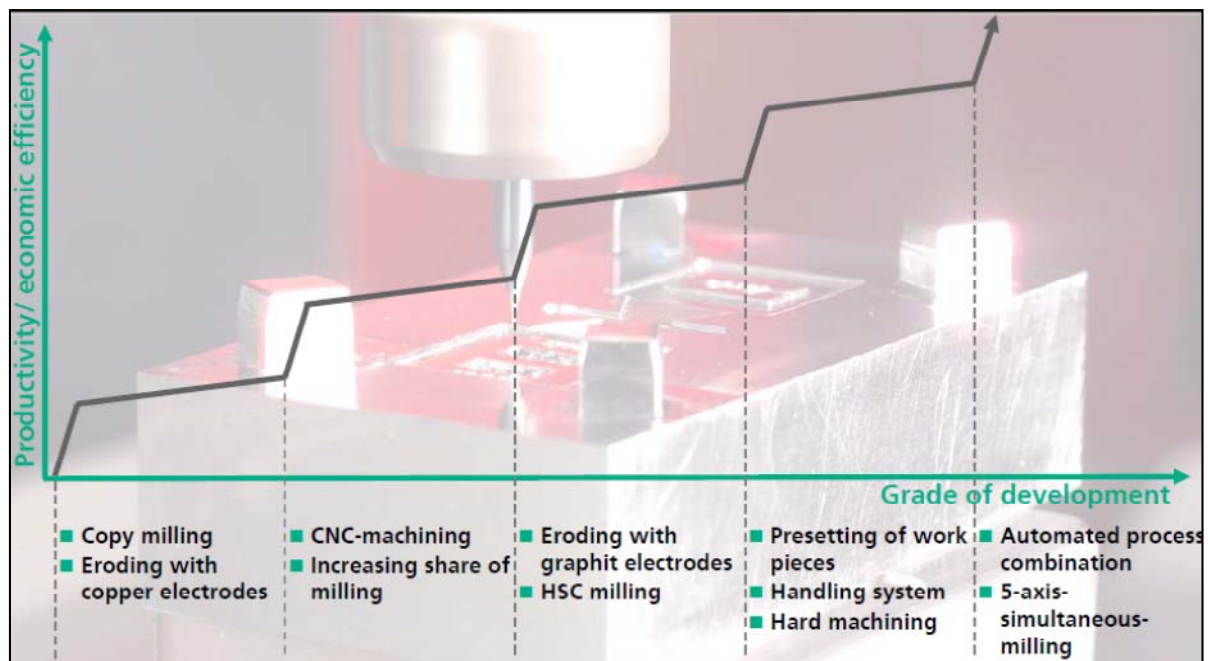


Fig. 5. Influence of technological changes on productivity/economic efficiency [4]

2.2 Rapid tooling

Molds are composed of functional (cavity, core insert, punch) and support components (guide pins, holder, die plate). Often support components and a number of holes need only 2D or 2½ D machining, but may require 50 to 60% of the total manufacturing time. This fact is often neglected but must be considered in effective planning of the machining operations. Conventional mold making practice that depends on machining operations to generate the desired mold cavity is not found to be competitive any longer. This has led to a significant growth in rapid prototyping (RP) based tooling, referred to as rapid tooling [5]. Rapid tooling (RT) is the process of production of fast tooling through the prototypes made by RP. Technologists involved in RT development aims to reduce lead-times and development costs through

manufacturing additively production tooling via RP.

There are a variety of rapid tooling techniques and materials. These processes can be classified as patterns for casting (the fabrication of patterns to produce the sand molds), direct rapid tooling (layer-by-layer build up of mold), in which molds are fabricated in a rapid prototyping system-RP, or indirect rapid tooling (shaping of mold from RP-made master pattern), in which a rapid prototype master is converted into a mold using a secondary process [6]. These processes can also be classified based on their expected mold life (number of parts that can be produced in the mold), as soft (a few injected parts), bridge (several thousand injected parts) and hard tooling (above one hundred thousand injected parts).

The soft and bridge tooling methods can produce either nonmetallic or softer metal (compared to

conventional tool steels) molds and usually cannot withstand the pressures and temperatures involved in conventional injection molding. The hard tooling methods enable fabricating metal tooling that can be used in injection molding machines, and result in better quality and larger quantity of parts (compared to soft and bridge tooling) [5]. Classification of rapid tooling processes is shown in Fig. 6.

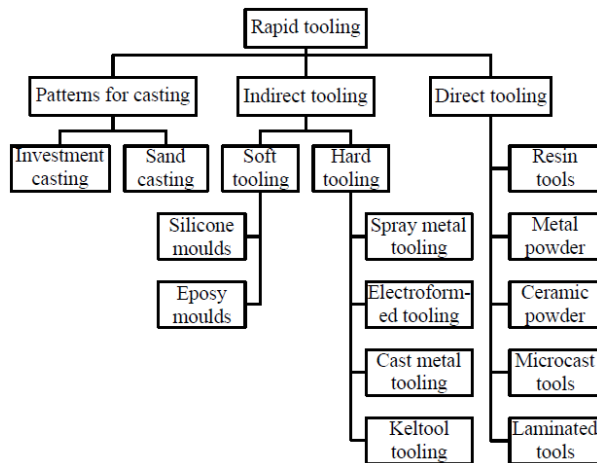


Fig. 6. Classification of rapid tooling processes [6]

Rapid tooling has got numerous advantages. The major advantages of RT are as follows:

- shorten the tooling lead time (reducing tooling development time by 50% or more),
- low cost (the traditional production tooling method takes about five times longer than RT),
- allows functional test of parts on initial design stage,
- data CAD direct transfer (many imperfections due to drawings misinterpretation can be avoided using the original CAD model all through the RP process and then along to RT process),
- the high cost of labor can be overcome, the use of CAD technologies allows the use of modular dies with base-mold tooling (match plates) and specially fabricated inserts,
- chill- and cooling-channel placement in molds can be optimized more easily, leading to reduced cycle times.

The major disadvantages and limitations of RT are as follows:

- still very expensive equipments, materials and services,
- a limited number of available materials (permanently on the rise),
- a limited durability of mold inserts,
- the part produced by the rapid tooling still need to be machined as the surface finish is not so good which is a limitation over the conventional process which can produce part to the required surface finish tolerance,
- in the event of a sharper measurement tolerance, most procedures unsatisfactory (requiring subsequent processing).

3. CONCLUSION

Modern information and communication technologies and their application in mold making industry enable ensure operative excellence (decreasing of life cycle costs and time-to-market, increasing of quality and productivity). These technologies offer new possibilities to decrease development and production times of molds. According to industrial analysis today mainly subtractive machining processes like high speed milling-HSM, EDM, grinding and polishing play a major role in mold making. In order to shorten manufacturing time for new products and their moulds, the use and the development of modern techniques are critical.

Some of such new technologies are simultaneous 5-axis machining and the rapid tooling methods. These technologies enable to reduce lead-times and decrease development costs. Advances in technology does not replace the necessity for training, knowledge, and experience in creating a sophisticated plastic injection mold. In fact, our reliance on today's modern technology necessitates a higher level skill set than the outmoded technology of yesterday.

4. REFERENCES

- [1] Cho, Y., Leem, C., Shin, K.: *An assessment of the level of informatization in the Korea mold industry as a prerequisite for e-collaboration: an exploratory empirical investigation*, Int. J. Adv. Manuf. Technol, Vol. 29, pp 897 – 911, 2006.
- [2] Henriques, E., Peças, P., Cunha, P.: *Perspectives of mould making industry for digital global manufacturing*, Digital Enterprise Technologies – Perspectives and Future Challenges, Springer, 2007.
- [3] Schützer, K., Abele, E., Stroh, C., Gyldenfeldt, C.: *Using Advanced CAM-Systems for Optimized HSC-Machining of Complex Free Form Surfaces*, J. of the Braz. Soc. of Mech. Sci. & Eng., Vol. XXIX, No. 3, pp. 313-316, 2007.
- [4] Arntz, K.: *Technologies for tool, die and mould making – Today and Tomorrow*, Uddeholm Automotive Tooling Seminar 2008, Sunne, Sweden, 2008.
- [5] Nagahnumaiah, K., Subburaj, B. Ravi: *Computer aided rapid tooling process selection and manufacturability evaluation for injection mold development*, Computers in Industry, Vol. 59, pp. 262–276, 2008.
- [6] Altan, T., Lilly, B., Yen, Y.C.: *Manufacturing of Dies and Molds*, CIRP Annals, Vol. 50 (2), pp. 404-422, 2001.

Authors: Full Prof. Milenko Sekulic, Full Prof. Marin Gostimirovic, PhD student Nenad Kulundzic, MSc student Andjelko Aleksic, University of Novi Sad, Faculty of Technical Sciences, Department of Production Engineering, Trg Dositeja Obradovica 6, 21000 Novi Sad, Serbia, Phone: +381 21 450-366, Fax: +381 21 454-495.
E-mail: milenkos@uns.ac.rs; maring@uns.ac.rs; kulundzic@uns.ac.rs; andjelkoa94@uns.ac.rs

Šogorović, D., Vračević, I.

TESTING OF THE ROUGHNESS PARAMETERS IN THE TURNING PROCESS OF ALUMINUM PARTS

Abstract: This paper examines the influence of technological parameters (elements of the cutting process) on the roughness of the surface in the turning process of a part of aluminium (more than 98% of aluminium alloy). The aim of the paper is to analyse the impact of cutting speed, feed and depth of cut on the roughness parameter R_a . The machine tool, tool used, the material and the device for measuring the roughness parameters are shown. An adequate mathematical model was developed by statistical analysis, which describes the effect of technological parameters on roughness. The results of the experiments are presented in table and graphic and are suitable only for observed cutting conditions, used tools and material.

Key words: technological parameters, roughness parameters, turning process, experiment.

1. INTRODUCTION

Most manufacturing companies determine the technological parameters of machining based on an experience of workers or recommendations from various manuals. The modernization of production is constantly increasing over the past decades, so it is essential to focus on economic analysis in combination with technological knowledge in order to make investments in production more logical and no random. This paper examines the influence of technological parameters on the surface roughness in turning process.

2. ELEMENTS OF THE CUTTING PROCESS

The production process is enabled by the certain elements of the cutting process i.e. technological parameters. There are specific technological parameters for machining with cutting whose value derive from the ability of the technical system in order to solve the requirements of production. For the each process it is necessary to specify the technological parameters because they directly affect at the efficiency of the turning process. The efficiency of the process cannot be increased in any case, because there is a functional relation between the elements of the cutting process which results in individual value.

The elements of the cutting process are:

- The depth of cut a_p [mm] is the layer of material removed in the cut [1]. It is a thickness of the layer in a direction perpendicular to the machined surface. It is half the difference between the work diameter and the diameter of machined surface.

$$a_p = \frac{D-d}{2} \quad (1)$$

Where are:

a_p – depth of cut,

D – work diameter,

d – diameter of machined surface.

- The cutting speed v_c [m/min] is the travel of a point on the cutting edge relative to the

surface of the cut in unit time in the process of accomplishing the primary cutting motion. In the machine tool with rotary as primary cutting motion, the cutting speed is equal to peripheral speed with maximum diameter of workpiece.

$$v_c = \frac{D\pi n}{1000} \quad (2)$$

Where are:

D – maximum diameter of workpiece [mm]

π – Ludolph's number

n – rotational speed [min^{-1}]

- The feed (more precisely, the rate of feed) f [mm/o] is the travel of the cutting edge in the direction of the feed motion during one revolution of the workpiece. For the various work conditions, the feed is being chosen as maximal as possible. The feed depends on material of workpiece, dimension of the workpiece, the depth of cut, tool life and the cutting edge resistance. Direction of feed is perpendicular on direction of cutting speed v_c [2]

3. THE DEFINITIONS OF ROUGHNESS AND PARAMETERS OF ROUGHNESS

The roughness of a machined surface is the whole complex of microirregularities (relatively finely spaced ridges and valleys), the height, width and direction of which establish the predominant surface pattern. Those microirregularities is caused by machining or by others influences. [3]

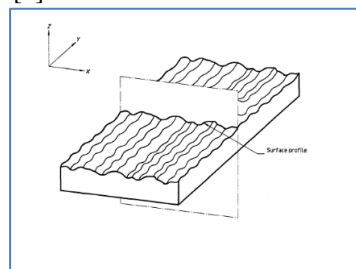


Fig 1. Surface profile [4]

3.1 The parameters of roughness

There are different parameters in order to define the surface roughness:

- Arithmetic average roughness (R_a)

It is arithmetic average value of filtered roughness profile determined from deviations about the centre line within the evaluation (sampling) length L . This parameter is most widely used one-dimension roughness parameter. [5]

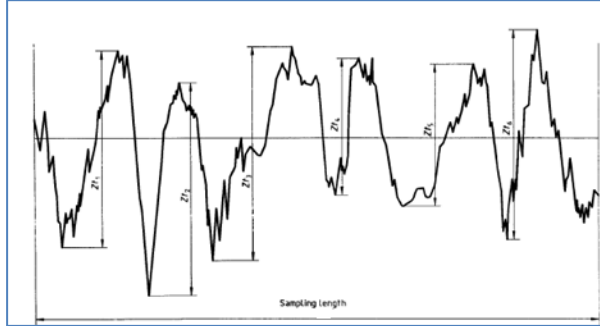


Fig 2. Arithmetic average roughness [4]

Formula for arithmetic average roughness is.

$$R_a = \frac{1}{n} \sum_{i=1}^n |z_i| = \frac{1}{l} \int_0^l |z| dx \quad (3)$$

Where are:

R_a [μm] – arithmetic average roughness,

l [μm] – the evaluation line,

$z(x)$, z_i [μm] – value of the roughness profile determined from the centre line,

n – number of the measured points. [4]

- Maximum height of the profile R_{max}

It is the vertical distance between the highest and lowest points of the profile within the evaluation length.

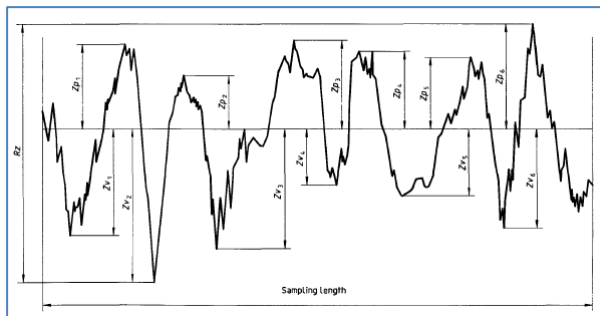


Fig 3. Maximum height of the profile [4]

- Ten point height of irregularities (R_z)

It is the average value of the absolute values of the heights of five highest profile peaks and the depths of the five deepest valleys within the evaluation length. [6]

$$R_z = \frac{(R_1 + R_3 + \dots + R_9) - (R_2 + R_4 + \dots + R_{10})}{5} \approx 4R_a \quad (4)$$

Value of the ten point height of irregularities is approximately equal to $4R_a$

The basic criteria is arithmetic average roughness while the others two and many of unmentioned parameters are additional criteria.

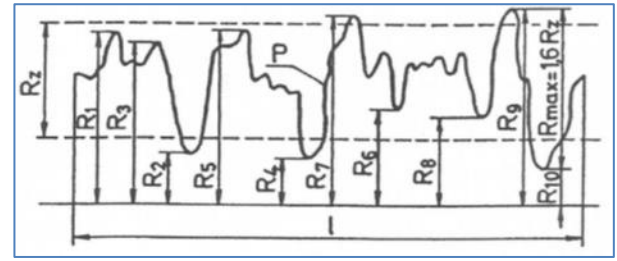


Fig 4. Ten point height of irregularities [7]

Roughness value, R_a [μm]	Roughness value, R_z [μm]	Roughness N ISO grade number
50	200	N12
25	100	N11
12,5	50	N10
6,3	25	N9
3,2	12,5	N8
1,6	6,3	N7
0,8	3,2	N6
0,4	1,6	N5
0,2	0,8	N4
0,1	0,4	N3
0,05	0,2	N2
0,025	0,1	N1

Table 1. Roughness N ISO grade number (DIN 1302)

3.2 Relation between surface roughness and machining with cutting

Quality of machined surfaces in the turning process depends on various factors and the basic are:

- technology parameters,
- material of workpiece and tool,
- tool geometry (tool angles),
- dynamic behaviour of operation system,
- uses of cutting fluids,
- tool wear etc.

These factors affect at the depth of the defect layer (D) and its value is 15 to 80 μm . Due to large number of factors, it is difficult to establish the interconnection between various machining processes and the quality of machined surface. [8]

4. TESTING OF THE ROUGHNESS PARAMETERS

An analyse of influence of technological parameters (cutting speed, depth of cut and feed) on arithmetic average roughness R_a in longitudinal turning is performed in this experimental testing. It is necessary to determine the adequate mathematical model which describes the real process.

The input (independent) sizes are:

- cutting speed (v_c)
- feed (f)
- depth of cut (a_p)

The output size is arithmetic average roughness R_a and function of machinability:

$$R_a = f(v_c, f, a_p) \quad (5)$$

For determination of surface roughness in relation with input sizes the fractional experimental design 2^3 is being chosen. It has 3 factors and each factor has two level and there are 8 experimental conditions in this design. This composition of experimental conditions is being added a number of experiments ($n_0 = 4$) in the central point of the plan. So, the total number of experiments is:

$$N = 2^3 + 4 = 12 \quad (6)$$

4.1 Equipment for the experiments

The machine tool is lathe machine made in Russia (former SU) which is placed in laboratory at University of Mostar. This machine has the transmission reduction for main spindle with 32 rotational speeds and transmission reduction for feed motion with 48 rates of feed. The ranges of rotational speed and rate of feed are good and they fully satisfied the values of input sizes of experiments.



Fig 5. Lathe machine used in the experiments

For longitudinal turning operation, tool produced in Serbia (Corun, RS71.5-2525M 16).



Fig 6. Tool used in the experiments

Workpiece is pipe made from aluminium alloy (more than 98% Al).



Fig 7. Workpieces before machining

For the testing of the surface roughness, following device is used:

- Device name: Hommel-Etamic W5,
- Producer: Hommel-Etamic GmbH, Alte Tuttlinger Str. 20, D- 78056 Villingen – Schwenningen
- Version: 1.0
- Number of device: 10050286

This device is only used in testing of surface roughness in accordance with standards. The device may only be operated in perfect technical condition and not in heavily dust-contaminated, chemically aggressive, explosive or radioactive environment.

Hommel-Etamic W5 is used for simply wireless measurement of roughness:

- flat surfaces,
- shafts,
- bore holes,
- concave and convex surfaces.



Fig 8. Device for measurement of roughness

4.2 Performing of experiments

Before the performing of the experiments it is necessary to make the table of level of factors and table of experimental conditions.

Factors	Fi,min	Fi,sr	Fi,max
v_c [m/min]	120	155	200
a_p [mm]	0,5	1,22	3
s [mm/o]	0,08	0,14	0,25
Cod	-1	0	1

Table 2. Level of factors

No	No. of measuring	Input factors			Output factor
		v_c	a_p	s	R_a
1	3	200	3	0,25	18,112
2	7	200	3	0,08	0,675
3	11	200	0,5	0,25	14,055
4	5	200	0,5	0,08	0,811
5	10	120	3	0,25	4,357
6	1	120	3	0,08	1,066
7	4	120	0,5	0,25	4,72
8	9	120	0,5	0,08	0,629
9	12	155	1,22	0,14	1,621
10	2	155	1,22	0,14	1,652
11	8	155	1,22	0,14	1,662
12	6	155	1,22	0,14	1,691

Table 3. Experimental conditions

Experimental conditions and the choice of experimental design plan is performed by using of software programme Design – Expert 11. After the input of values of surface roughness (obtained from the experiments) in programme Design – Expert 11, the results are shown in Figure 9.

Source	Sum of Squares	df	Mean Square	F-value	p-value	
Model	279,97	3	93,32	8,96	0,0062	significant
A-A	69,18	1	69,18	6,64	0,0328	
B-B	4,74	1	4,74	0,4552	0,5189	
C-C	199,76	1	199,76	19,18	0,0024	
Residual	83,32	8	10,42			
Lack of Fit	83,32	5	16,66	19989,21	< 0.0001	significant
Pure Error	0,0025	3	0,0008			
Cor Total	363,29	11				

Std. Dev.	3,23		R²	0,7706
Mean	4,25		Adjusted R²	0,6846
C.V. %	75,86		Predicted R²	0,2438
			Adeq Precision	9,2446

Fig 9. The analyse of the results of the experiments

The statistical significance of mathematical model is depends on value of empiric F-value and p-value in table ANOVA. The F-value is 8,96 and it shows that chosen model is significant i.e. the model which describes the arithmetic average roughness is adequate and reliable. The p-value less than 0,500 shows a significance of two factors in model. In this case, the cutting speed and fees are significant.

Coded model of roughness is:

$$Ra = 4,79 + 2,93A + 0,7485B + 4,93C \quad (7)$$

De-coded model of roughness is:

$$Ra = -17,38769 + 0,073339*v_c + 0,598768*a_p + 58,00774*s \quad (8)$$

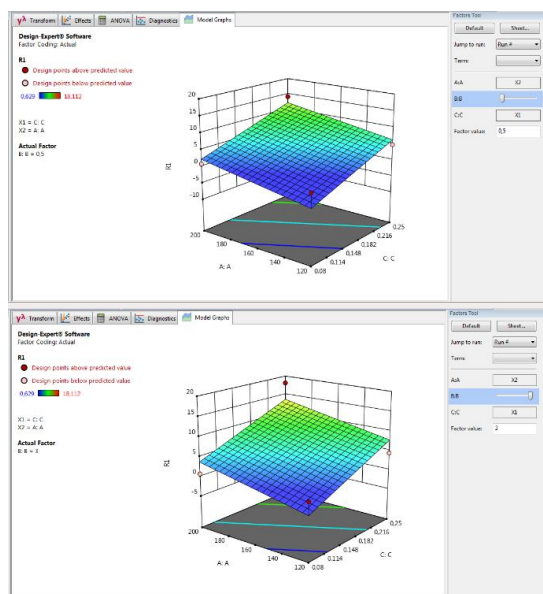


Fig. 10. Diagram of relation $Ra=f(v_c, f)$ with maximal and minimal influence of factor a_p

5. CONCLUSION

There are many factors which influence on roughness of machined surface but one of the most important are technology parameters. The performed experiments shows that the depth of cut has no significant influence on the roughness of machined surface. The other two elements of the cutting process, cutting speed and feed have significant influence on roughness. This conclusion are reliable only for this material of workpiece, used tool and the other testing conditions and equipment which were being used in these testing.

As is already known from the theory, this testing proves that the less roughness means minor feed rate and moderately small cutting speed. But this is not economic efficient in the real manufacturing conditions because the machining time is multiple increases. Future research will be focused on the other materials of workpieces as well as on the other operation of machining with cutting, i.e. drilling, milling, grinding, etc. and this paper is one small step in the future study of influence of technology parameters on surface roughness.

6. REFERENCES

- [1] <http://www.fsb.hr/kas> Oblikovanje deformiranjem i obrada odvajanjem, 5.02.2018.
- [2] Šime Šavar, *Obrada metala odvajanjem čestica*, svezak 2, Školska knjiga, Zagreb, 1990.
- [3] <https://www.fsb.unizg.hr/elementroj/pdf/design/2007/hrapavost-tehnickih-povrsina.pdf> 5.02.2018.
- [4] DIN EN ISO 1302
- [5] <https://www.scribd.com/document/244271124/mjer-enje-i-kontrola-kvalitete>, 16.04.2018.
- [6] Damir Jelaska, *Elementi strojeva – skripta za studente Industrijskog inženjerstva*, Split 2005.
- [7] <https://www.scribd.com/doc/52265660/tehnologija-obrade-materijala-tokarenjem>, 10.02.2018.
- [8] Zvonko Herold, *Računalna i inženjerska grafika*. Zagreb; Fakultet strojarstva i brodogradnje, Zagreb, 2003.

Authors: Assist. Prof. Danijel Šogorović, Isabella Vračević, M.Sc. student, University of Mostar, Faculty of Mechanical Engineering, Computing and Electrical Engineering, Department of Production Engineering, Matice hrvatske bb, 88000 Mostar, Bosnia-Herzegovina, Phone.: +387 36 337-001, Fax: +387 36 337-012.

E-mail: danijel.sogorovic@fsre.sum.ba; isabella.vracevic@student.fsr.ba

ACKNOWLEDGMENTS: Authors wishing to thank the Federal ministry of education and science of Federation of Bosnia and Herzegovina for financial support in purchasing of the device Hommel-Etamic W5 for testing of surface roughness.

This support helps student author to perform the experiments in master thesis in order to finish her master degree study.

Žiga, A., Begić-Hajdarević, Đ., Cogo Z.

MECHANICAL TOYS AND SOUVENIRS OBTAINED BY CO₂ LASER CUTTING OF PLYWOOD

Abstract: Design and production of mechanical toys and souvenirs can be very attractive process for students of technical faculties. They have opportunity to learn about mechanical principles on a fun way, opportunity to express their creativity and to be innovative. 3D modeling software was used for product design and simulation of motion and software for 2D drawing was used to prepare parts for laser cutting. CO₂ process of laser cutting of plywood is cheap, simple and the most importantly it is safe for students.

Key words: Mechanical toys and souvenirs, plywood, CO₂ laser cutting

1. INTRODUCTION

Students of technical faculties learn about various mechanical parts separately. The knowledge about machine elements and mechanisms is very important in their education. They see pictures, illustrations of motions, production process in factories, but they have rare opportunity to design these parts, produce them and make experiments. New technologies like 3D printing and laser-cutting are there to fulfill these gaps and allow students to bring their ideas to life. There are some limitations like the cost of these production units and that they are used to produce small parts and to obtain the prototypes. Used materials are usually plastics, wood, plywood and cardboard. Best side of these technologies is that they are safe for students.

Firmani, Kadhum and Wild (2015), [1], have started a project that complements the theoretical content of Theory of Mechanisms course and exposes students to an engineering design problem. The project consisted of designing and building an automaton for young children – a mechanical toy operated by a hand crank. They have reported that the project was a success and that the students enjoyed designing and building the automata, but they had recommendations about safety. It has been noticed that students could be somewhat careless with the use of powered tools.

Odlin and Fleming (2014), [2], concluded that the design and construction of automata in the classroom appeals to a wide range of students and contributes significantly to students' understanding of mechanisms and their engagement with technology. "Learning in technology is further enhanced when it is integrated into the other curriculum areas. Students learning about mechanisms in science while making an automaton in the workshop would learn to understand each subject more deeply, and not experience technology as an isolated subject."

Blauvelt (2006), [3, 4], highlights the advantages of precise design and construction made possible by the combination of design software and a laser cutter for fabrication. He emphasizes a surprising number of books and videos that are available describing the art of

the automaton maker ([5], [6] for excellent examples). The process is similar in most respects to the design and construction of any mechanical object:

1. An initial idea is conceived.
2. A design is created.
3. Prototypes are iteratively built and tested.
4. A final object is fabricated and assembled.

2. MECHANICAL TOYS AND SOUVENIRS

Mechanical faculty in Sarajevo and Mechanical faculty in Zenica have started project to design mechanical toys and souvenirs during student's diploma works (graduate theses). Students are encouraged to realize their own ideas. Material for models is poplar plywood, 4 mm thick, purchased as sheet with dimensions 400x400 mm. Fabrication of models is done by CO₂ laser cutter. When choosing idea, students should have in mind that toys (or souvenirs) must have a size for office desk. Models have to be fun and appealing for office workers or tourists, simple and cheap for production. Idea that distinguishes these souvenirs from others found in the region is the presence of movable parts. Students are suggested to use some of these:

- linkages,
- slider cranks,
- cams,
- gears,
- Geneva wheels,
- Scotch Yoke mechanism,
- Iris mechanism, etc.

All these components have to be operated by manually turning a crank.

Project goals are:

- learning about mechanism and machines in a fun way,
- learning to be creative and innovative,
- learning how to commercialize the idea.

From the beginning of academic 2017/18 year, three models have been made by the students: the swinging dove (Figure 1), simple marble machine (Figure 2) and

box with Iris mechanism (Figure 3 and 4).



Fig. 1. The swinging dove

Idea for swinging dove has been taken from web site: Maschinenbau: einfache Maschinen für den Technik- und Werkunterricht [7]. The swinging dove is operated with the crank. Pair of gears has ratio 1:2. It takes two full rotations of the small gear for one rotation of the big gear. The shaft with big gear has a cam on which there is a ring follower with lever connected to the dove. The lever, in the middle, has an axle on which another pair of levers is attached, which are connected on one side to the rear axle and have wing wires attached to them on the other side. During cam rotations, these levers operate like scissor which allows dove to swing and to wave with wings.

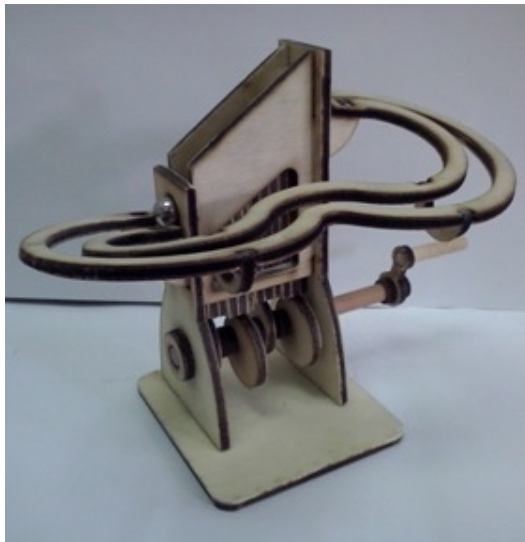


Fig. 2 Simple marble machine

Simple marble machine (SMM) is made of poplar plywood, 4 mm thick, unlike the original seen on the site [8] Simple Marble Machine - Busted Bricks which has been made of MDF board (medium density fiber). The main concern during design was the ability of that material to bend. So analysis of stress has been made which is published in paper [9] by Žiga, Cogo,

Kačmarčík (2018). Basic mechanism in SMM is made of four cams operated with the crank. During each turn, the pair of stairs is in the same level so metal balls roll from one stair to another, which produces lifting effect.



Fig. 3 Box with Iris

Third model is a box with Iris mechanism. Iris mechanism is seen on numerous internet videos like on the site: Making a mechanical Iris [10]. It has five petals like spring flower. During ring rotation these petals open, revealing mirror hidden inside. The box has been designed with living hinges. The number of required vertical bars in living hinges had to be calculated due to allowable torsion stress.



Fig. 4 Box with Iris-petals opened

3. PROCESS OF DESIGN

The process of design starts with an idea, most commonly seen on the Internet. After some paper sketches and initial dimensions selections, 3D models can be made. Software for 3D modeling allows students to create their designs, to match dimensions, to see functionality, to check interferences and to see parts in motion. On the other side the obtaining of physical model of virtual part has numerous advantages: the first is a real size of object, its ability to match with other parts in mechanism, its strength or ability to be bent,

twisted, pulled or compressed. Another concern in the real model is how to compensate friction during the motion of parts.

Figure 5 shows motion analysis of SMM in software for 3D analysis. The rotation of the shaft moves the stairs. Each of the four stairs consists of three layers of plywood with different lengths to achieve the slope of the surface on which the balls roll. Cams are actually circular discs with eccentrically positioned holes for the shaft. The two adjacent holes are positioned so that their tips (end positions) close a 180° angle. This ensures that one stair is lowered when the one next to it is being lifted up. When one stair is raised to the uppermost top position, the adjacent one is in the lowest position so that its level is slightly lower, allowing the ball to roll from one onto the other. The action is repeated so that the balls are lifted in a very simple way to the track where they descend again to the beginning of the stairs.

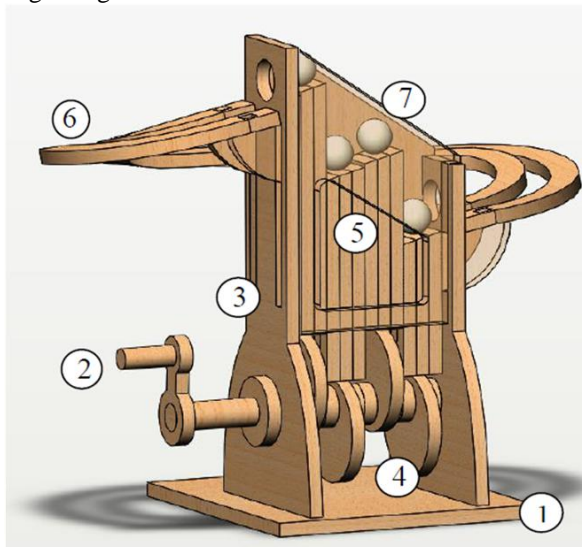


Fig. 5. Parts of SMM assembly: 1-stand, 2- crank, 3- housing, 4-cams, 5-stairs, 6-track, 7-balls

4. PROCESS OF CUTTING

When mechanical principles of 3D model, dimensions and assembly have been tested, the technical documentation can be made by using SOLIDWORKS Drawings. This allows direct transmission of parts of the model (in different views) to the paper drawings. The resulting drawing is saved in .dwg format so that it can be opened with AutoCAD. After that, in AutoCAD 2015, the boundaries of purchased plywood (400x400) are drawn, and all parts were set within these limits (Figure 6). Some boundaries of the parts have to be corrected. During this process, a designer has to know functions of all parts. Some parts need gaps for motion but others need press-fit connection. Initial dimensions have to be corrected including the width of the laser cut, called "kerf". The openings need to be cut before the outer contours, so they are painted in different colors so the software that manages the laser cutter (Figure 7) can recognize the cutting order.

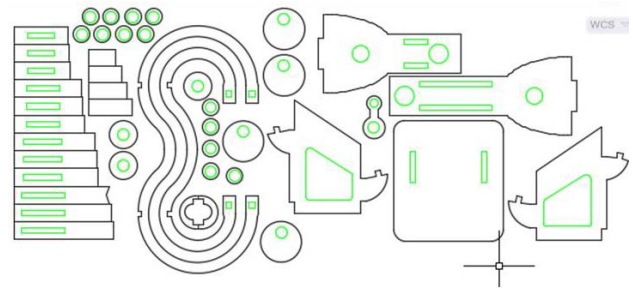


Fig. 6. AutoCAD drawing of parts for SMM, prepared for laser cutting

This laser cutter has a number of advantages: it is compact, highly precise, fast in operation, compatible with commercially available drawing software, and capable of cutting and etching a wide variety of materials including wood, plastic, cardboard, paper and fabric. The laser cutter is an excellent alternative to traditional cutting tools like knives and saws. Disadvantage is the initial investment; the capital costs of laser cutting machine purchase are large, but the cost of cutting process is generally very small.



Fig. 7. The 80 watt CO2 laser cutter in lab of MF in Sarajevo

5. PROCESS OF ASSEMBLY

The assembly process has revealed some of conceptual flaws and problems. These problems couldn't be identified in the conceptualization phase or even in the preliminary design phase where the simulations of the CAD models worked as expected. However, once the prototype was built, the transmission of motion failed in different places. Common causes were: frictional force, lack of press-fit connections, breakage of parts due to stress concentrations, misalignment of parts. But good side of working with plywood is its ability to compensate small mistakes. Student can use wax to reduce friction, add extra glue, or use additional ring to make press-fit connection, increase moisture content to make parts more flexible and reduce stress concentrations etc. One student (constructor of SMM) concluded his project with remark: "Unlike other technical materials, wood is made up of the remains of once-living cells,

and in the same way it behaves like a living being, every part in its manners, with unpredictable errors and unexpected advantages.

When designing prototypes, there are always imperfections and areas to improve design. No matter how much time was spent in the preparatory stages, some things remain unnoticed. After the entire design and fabrication process completion, there are some things that need to be changed, although in the software they look good and work well. It can be said that the situation in reality is always a little different from the one assumed with the help of software and analytical tools, and that production sometimes requires improvisation in order to overcome the unforeseen circumstances''

6. FINAL REMARKS

This project provides a complete experience in engineering design and complements the theoretical content of the courses: Mechanics, Theory of mechanism, Strength of material and Unconventional processing technology.

Obtained models display a variety of levers, cranks, and cams in their construction. Students have enjoyed during the design and model building. Prototypes have exposed some of conceptual flaws and helped students to gain better insight in mechanisms motion.

7. REFERENCES

- [1] Firmani, F., Kadhum, S., & Wild, P. (2015, August). Expanding Engineering Design with mini projects–Theory of Mechanisms a pilot course. In *Proc. CEEA Canadian Engineering Education Association Conference* (pp. 8-11).
- [2] Odlin, S., & Fleming, J. S. (2014). Using Automata to Teach Science Concepts in Technology Education. *International Journal of Science in Society*, 5(3).
- [3] Blauvelt, G., & Eisenberg, M. (2006). Computer aided design of mechanical automata: Engineering education for children. In *Proceedings of International Conference on Education and Technology* (pp. 61-66).
- [4] Blauvelt, G., Eisenberg, M., & Wensch, T. (2001, July). Creating Mechanical Toys: Steps Toward a CAD Tool for Educational Automata. In *WCCE2001, The World Conference on Computers in Education*, Copenhagen, Denmark.
- [5] Newstead, K. How to Make Automata: Mechanisms and Methods, Retrieved July 20, 2018, from <https://cabaret.co.uk/store/video/how-to-make-automata>
- [6] Peppé, R. (2002). *Automata and mechanical toys*. Crowood.
- [7] Maschinenbau: einfache Maschinen für den Technik- und Werkunterricht , Retrieved July 20, 2018, from <http://www.werken-technik.de/2014/2014papagei.html>
- [8] Simple Marble Machine - Busted Bricks. Retrieved May 15, 2018, from <http://www.bustedbricks.com/simple-marble-machine-4-p.asp>
- [9] Žiga, A., Cogo, Z., Kačmarčik, J. (2018). *Out-of-plane deflection of J-shaped beam*. In The 21th International Research/Expert Conference TMT 2018.
- [10] Making a mechanical Iris. Retrieved July 20, 2018, from <http://lepton.com/blog/2011/07/11/making-a-mechanical-iris/>

Authors:

Assoc. Prof. Žiga Alma,

University of Zenica, Faculty of Mechanical Engineering, Mechanical Department, Fakultetska 1, Zenica, e-mail: aziga@mf.unze.ba

Assoc. Prof. Đerzija Begić-Hajdarević

University of Sarajevo, Faculty of Mechanical Engineering, Department of Production Engineering, Vilsonovo šetalište 9, Sarajevo, e-mail: begic@mef.unsa.ba

Zlatan Cogo,

Graduate student of Faculty of Mechanical Engineering in Zenica, e-mail: zlatan.cogo@gmail.com



Section B:

**MACHINE TOOLS AND AUTOMATIC
FLEXIBLE TECHNOLOGICAL SYSTEMS,
CAx AND CIM PROCEDURES AND
SYSTEMS**

APPLICATION OF THE STEP-NC STANDARD ISO 10303 AP238 FOR TURNING OPERATIONS

Abstract: The paper considers the possibility of applying a new programming method according to the STEP-NC standard for turning operations. The programming method in this paper is based on the STEP-NC standard ISO 10303 AP238. In order to verify the programming method, a virtual CNC lathe is configured that can interpret STEP-NC programs. Virtual lathe is integrated with software STEP-NC Machine. The method for obtaining the STEP-NC program is proposed, as well as the possibility for the current application of such programs, on the current machine tool control unit that interpret G-code, using the export option of STEP-NC Machine.

Key words: STEP-NC, programming, simulation, turning operations, CNC lathe

1. INTRODUCTION

For more than half a century, programming of CNC machine tools is based on G-code, according to ISO 6983 standard. This standard, commonly known as G and M codes, focuses on programming the path of the cutter centre location with respect to the machine axes, rather than the machining task with respect to a part [1].

Programs in G code address directly the individual axes of the machine, so it is necessary to use postprocessors for each control unit and the kinematics of the machine in particular. It is necessary to prepare the tool path for each type of CNC machine tools individually using appropriate postprocessor. It requires large number of different postprocessor for each type of machine tool. Therefore, programs for CNC machine tools in G-code do not include any useful information about the product, such as data about the geometric primitives of the model, tolerances, material properties, setting up fixture, and other information created during the design and planning of manufacturing technology. All of this information will disappear when postprocessing tool path into G code [2]. In this case, information flow is one-way, from CAD/CAM to a CNC machine tool, Figure 1a.

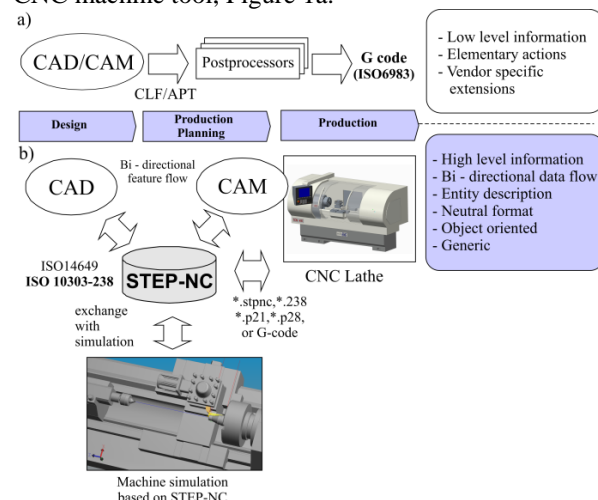


Fig. 1. Current ISO 6983 and new STEP-NC interface for programming CNC lathes

Today a new standard, informally known as STEP-NC (Standard for Product Model Data Exchange for Numerical Control), is being used as the basis for development of the next generation of CNC controller [3-6]. This new standard is ISO 14649 and ISO 10303 AP 238. STEP-NC is a new interface that has been developed for exchange of information between CAD/CAM systems and CNC controllers. Its object oriented design and the use of data elements of the widely disseminated STEP standard support comprehensive bi-directional data exchange whilst using common databases [7], Figure 1b.

Benefits of using STEP-NC are: (i) providing new opportunities to support high level information from design to CNC controller; (ii) the STEP-NC data interface is a neutral data description; (iii) bi-directional information flow; (iv) STEP-NC is independent from the machine tool vendor; (v) higher quality of information on the shop floor; (vi) STEP-NC programs in XML formats can be used for information transfer and enable Web based manufacturing or e-manufacturing.

However, classical programming in the G code is still current and dominant, while the object programming using STEP-NC standards has not been introduced to the full extent so far, and both of these programming methods exist parallel, as illustrated in Figure 1.

There are plenty of results for the application of STEP-NC standards for turning operations [1,8-10] and all are generally based on ISO14649 standard. This paper aims to explore the application of new STEP-NC standard ISO10303-AP238 for programming CNC lathes i.e. for CNC machining of turned parts to enable data exchange of manufacturing rich information from CAD/CAM to CNC.

2. STEP-NC FOR PROGRAMMING CNC LATHES

This section provides a literature review of the STEP-NC compliant research focused on turning operations.

One of the first systems based on the STEP standard related to the machining of rotational parts by turning is the STEPTurn system [1,8]. The STEPTurn has been developed by researchers from the Institute for Control Engineering of Machine Tools and Manufacturing Units at the University of Stuttgart (ISW), Germany. This system is a CAPP system bridging the gap between CAD and CAM and it reads geometry data firstly from a STEP AP203 Part 21 file and displays the part geometry and performs normal process-planning tasks such as feature recognition and Workingstep sequencing in order to generate a STEP-NC physical file [1].

The other such system, TurnSTEP is developed by a mutual participation of researchers from the national research laboratory for STEP-NC technologies POSTECH (Korea) and from ISW University in Stuttgart. The TurnSTEP is to be fully compliant with ISO 14649 and suitable for e-manufacturing. In terms of turning machining, TurnSTEP is one of the earliest systems to have been developed for compliance with STEP-NC and supported by XML schema [1].

The G2STEP system has been designed based on design and functional considerations developed by researchers from the National Research Laboratory for STEP-NC, POSTECH, South Korea together with a researcher from the EPFL, Switzerland and is based on the ISO 14649 data model, the ARM model and instruction schema on G-code based on the FANUC0 series. The main proposal for G2STEP is to generate a STEP-NC part program from a G-code program with additional information related to real machining that is easily generated by skilled operators [1].

If we focus on turning operations, only three proposed systems are available, STEPTurn, TurnSTEP and G2STEP. For e-manufacturing, STEPTurn leads in this aspect due to the capability of internet file transfer. The TurnSTEP clearly defines the number of set-ups as either one set-up or two set-ups dependent on the independent machine format. The output of this system can be in text and XML file formats. As reported TurnSTEP is at a prototype stage and the implementation of another part, which is intelligent and autonomous is still under development [1].

3. TURNING MACHINE SIMULATION BASED ON STEP-NC

Today, a small number of machines can directly interpret the STEP-NC program. In this regard, for the direct verification of the STEP-NC program, it is advantageous to use virtual machines that can work in the STEP-NC Machine environment.

This section demonstrates how to configure a virtual CNC lathe, with a possibility of machining simulations when the machine working using the STEP-NC program according to ISO 10303 AP238.

Configured virtual CNC Lathe is able to interpret the STEP-NC program in the software STEP-NC Machine environment. To load the configured machine in the STEP-NC Machine, it is necessary to follow the next procedure:

- 1) Prepare a CAD model of the CNC lathe in available CAD/CAM system [11];
- 2) Store the prepared model of CNC lathe in STEP format (AP203, AP214 or AP224);
- 3) Prepare XML file, with description basic information about machine;
- 4) Save XML and STEP file in folder ... / Machine;
- 5) Run the STEP-NC Machine and load the configured CNC Lathe from the drop down menu Machine Tool.

Basic information for machine in XML file includes: (i) machine name, (ii) control algorithm, (iii) name of the STEP file machine, (iv) description of the machine base structure, which is stationary, (v) description of tool side structure, (vi) defining placement location for tool, (vii) description of workpiece side structure, (viii) defining placement location for workpiece, (ix) description of NC axes and their feeds.

An example of the XML file fragment for configured 2-axis CNC lathe (TCN410), with comments and illustrations is given in Fig. 2.

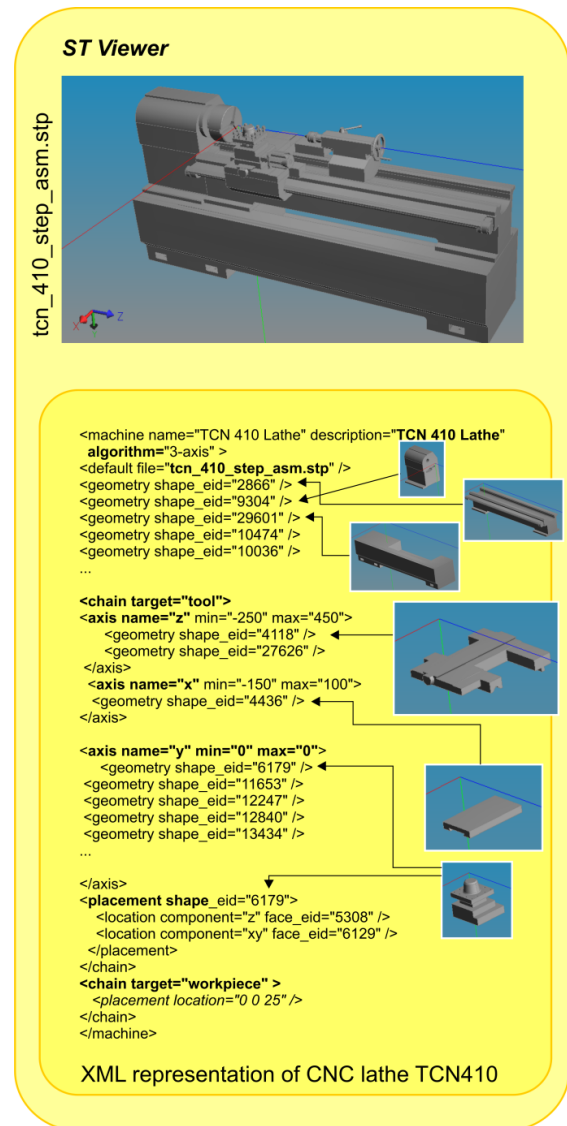


Fig. 2. STEP and *.XML representation of CNC Lathe TCN410 for machining simulation in STEP-NC Machine environment

In order to correctly create the XML file structure and the description of the assembly components that are loaded in the CNC lathe machine model for the needs of simulation, the software ST Viewer is also used to define geometry *shape_eid* for each part and *face_eid* for corresponding surfaces. Three elementary entities can be distinguished in a structure: machine stationary components, chain target-tool and chain target –workpiece. Movable sliders are placed here on the side of the tool for moving along X and Z axes. The third axis must be also defined since the algorithm for 3-axis serial kinematics is used. Moving along the third Y axis does not exist, because it is the CNC lathe with two control axes, and consequently Y axis define with movement min=0, max=0.

Placement location for the workpiece is defined with respect to a specific coordinate system of the CNC lathe from the *tcn_410_step_asm.stp* file, Fig.2. This coordinate system is a zero point, and it can be moved along the Z axis.

Virtual CNC lathe does not need to include all existing components of the original model, so the

virtual model is simpler and it is more easily and quickly loaded. For the case of the CNC lathe TCN410, because of the better visibility of working area and simpler model, the cabin of the machine was not include in model of virtual machine.

Thus prepared virtual CNC lathe is loaded in the STEP-NC Machine environment, where it will appear as a new machine in a dropdown menu of *Machine Tool*, Fig. 3. In the STEP-NC Machine environment, there have not been any CNC lathes up to now.

Upon selecting the machine from the menu, it is loaded in the STEP-NC Machine environment and can execute STEP-NC programs. This is of importance for training in a new method of programming, because it is now possible to check STEP-NC programs by simulating work on a virtual machine.

Virtual simulation allows off-line programming with verification and testing on a remote site without machine engagement. Working in the virtual environment is also suitable for training and education in programming especially if you do not have CNC lathe which has interpret STEP-NC programs directly.

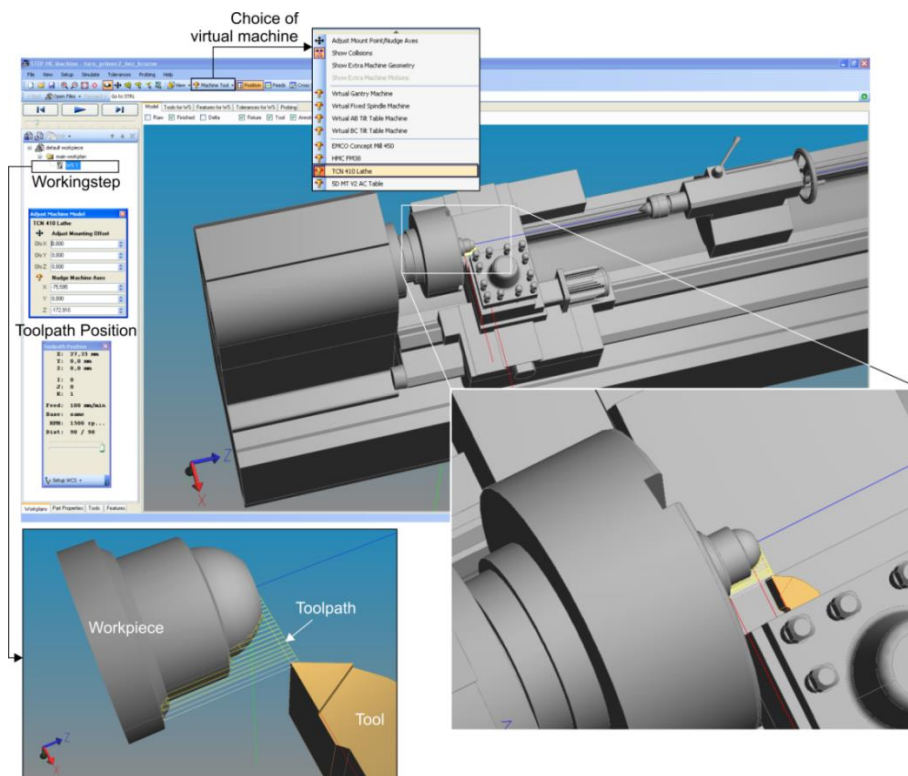


Fig. 3. Virtual CNC Lathe TCN410 in STEP-NC Machine

4. PROPOSED STEP-NC PROGRAMMING METHOD FOR TURNING OPERATIONS

To practice a new programming method in the case of turning operations, it is currently not possible to load the machine from the STEP-NC Machine software because CNC lathe does not exist, but it is therefore possible to configure and integrate own virtual CNC lathe machine into the software, as shown in Chapter 3. This chapter proposes the method by which to prepare its own STEP-NC program for turning operations, based on ISO 10303 AP238, using the manufacturing technology in the available CAD/CAM system. For the selected machining process, it is necessary to prepare

technology.

Preparation of the STEP-NC program for turning operations involves the first preparation of the necessary geometric information about the workpiece and tool, in the STEP format. It is then necessary to prepare the tool path in the available CAD/CAM system in CLF/APT format. For this approach of programming, the PTC Creo environment was used.

Figure 4 shows the procedure with the basic order of events for the preparation of the STEP-NC program. Procedure starts in the CAD/CAM system and ends in the STEP-NC Machine software. For the considered case of turning operation, the machining technology was prepared in the CAD/CAM system. Model of

workpiece and tool in STEP format and toolpath in CLF/APT format were exported from CAD/CAM system and loaded into the STEP-NC Machine software, where all this information is integrated into a single STEP-NC program.

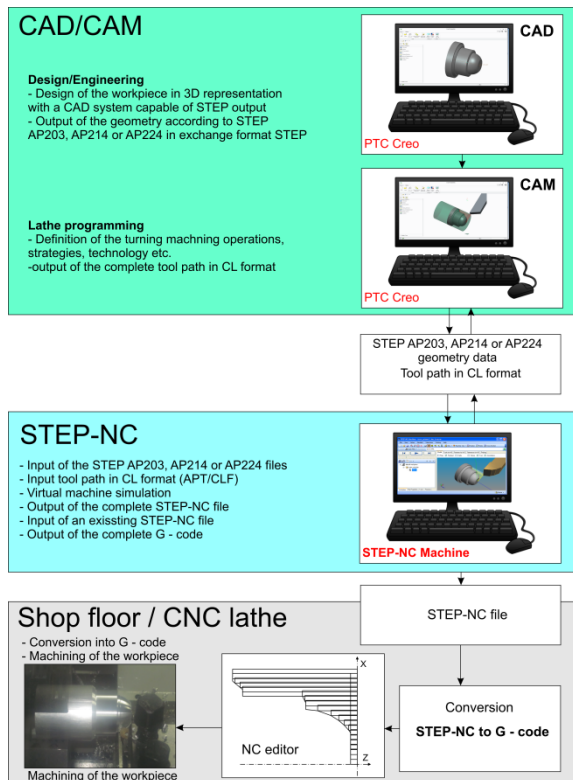


Fig. 4. Turning process chain based on STEP-NC

The generated STEP-NC program can be simulated in the STEP-NC Machine environment on the configured virtual CNC lathe (TCN410), Figure 3. In order to enable the workpiece to be machined on most of the available CNC lathes that are controlled using the G-code, the STEP-NC program so obtained can be converted into G-code using the Exoprt option of the STEP-NC Machine software, or using own program translator. For now, this is just a preparation for a new programming method, with a lot of constraints, but which can be applied to existing CNC lathes.

5. CONCLUSION

Promotion and dissemination of a new programming method are usually performed on hybrid machining systems. These machines are typically programmed with the G code, but also have the ability to convert, in some way, a program prepared by programming using STEP-NC standard. In this paper the STEP-NC Machine software is used for converting the STEP-NC program directly into the G code.

The method proposed in this paper is one of the possible ways of preparation for the new method of programming using the STEP-NC standard ISO 10303 AP238. Configured and integrated virtual CNC lathe, which running by the STEP-NC program in the STEP-NC Machine environment, is aimed at practicing for the future implementation of a new programming method.

6. REFERENCES

- [1] Yusof, Y.: *Review of STEP-compliant Manufacturing for Turning operation*, Asian Journal of Industrial Engineering, Vol.2, No.3, pp.77-88, 2010.
- [2] Zivanovic, S., Vasilic, G.: *A New CNC Programming Method using STEP-NC Protocol*, FME Transactions, Vol. 45, No. 1, pp. 149-158, 2017.
- [3] Step Tools, Inc., <https://www.steptools.com/>
- [4] Glavonjic, M., Zivanovic, S.: *A new cnc programming method using STEP-NC*, Proceedings of the 38th JUPITER Conference, 34th Symposium "NC-ROBOTS-FMS", (in Serbian), pp.3.112-3.117, Faculty of Mechanical Engineering, Belgrade, Serbia, May 2012.
- [5] Živanović, S., Glavonjić, M.: *Methodology for implementation scenarios for applying protocol STEP-NC*, Journal of Production Engineering. Vol.17, No.1, pp 71-74, 2014.
- [6] Glavonjic, M., Zivanovic, S.: *STEP-NC protocol for programming CNC machine tools*, TEHNIKA (TECHNICS), (in Serbian), Vol.6, pp.937-942, 2012.
- [7] Weck, M., Wolf, J., Kiritsis, D.: *The STEP compliant NC programming interface evaluation and improvements on the modern interface*, In: IMS Project Forum, Verita/Ascona, Switzerland, 2001.
- [8] Heusinger, S.: *ISO 14649 STEP-NC; Data model and implementation for turning in Germany*, 2002.
- [9] Yusof Y., Case, K.: *Design of a STEP compliant system for turning operations*, Journal of Robotics and Computer-Integrated Manufacturing, Vol. 26, No.6, pp.753-758, 2010.
- [10] Shin, S. J. , Suh, S. H., Stroud, I.: *Reincarnation of G-code based part programs into STEP-NC for turning applications*, Computer Aided Design, Vol. 39, No. 1, pp.1-16, 2007.
- [11] Živanović, S., Kokotović, B., Jakovljević, Ž.: *Turning machine simulation for program verification*, Proceedings of the 12th International Scientific Conference mma 2015, pp. 157-160, University of Novi Sad, Faculty of Technical Sciences, Novi Sad, septembar 2015.

Authors: Assoc. Prof. Sasa Zivanovic, Assist. Prof. Nikola Slavkovic, University of Belgrade, Faculty of Mechanical Engineering, Production Engineering Department, Kraljice Marije 16, 11120 Belgrade, Serbia, Phone.: +381 11 33-02-423, Fax: +381 11 33-70-364.

E-mail: szivanovic@mas.bg.ac.rs ;
nslavkovic@mas.bg.ac.rs ;

ACKNOWLEDGMENTS: The authors would like to thank the Ministry of Education, Science and Technological Development of Serbia for providing financial support that made this work possible.

Antic, A., Zeljkovic, M., Krstanovic, L., Ungureanu, N.

A TEXTURE-BASED DESCRIPTORS FOR REAL TIME TOOL CONDITION MONITORING

Abstract: All state-of-the-art TCM systems, especially those that use vibration sensors, in the tool wear recognition task, heavily depend on the choice of descriptors that contain information concerning the tool wear state, which are extracted from the particular sensor signals. We consider the module of the Short Term Discrete Furrier Transform (STDFT) spectra obtained from the particular vibration sensors signal utterance, as the 2D textured image. This is done by identifying the time scale of STDFT as the first dimension, and the frequency scale as the second dimension of the particular textured image. The obtained textured image is then divided into particular 2D texture patches, covering part of the frequency range of interest.

Key words: tool wear, texture descriptors, signal processing

1. INTRODUCTION

Real time Tool Condition Monitoring (TCM) in a turning process is very important in manufacturing processes and has been of great interest to many academic and practical researches. In order to prevent possible damages to the work-piece or the machine tool, reliable monitoring techniques are required to provide fast response to the unexpected tool failure [1]. Signal processing and information technology has resulted in the use of multiple sensors for the effective monitoring of tool wear conditions, which is the most crucial feedback information to the process control and tool wear prediction [2]. The tool failure can be prevented by efficiently monitoring conditional changes in the tool. Cho et al, in their basic work, divided tool conditions into following categories: tool breakage, tool chipping, and tool wear [3]. A key issue for an unattended and automated machining system is the development of reliable and robust TCM systems. There are many different ways to gather information about the tool failure, by the usage of adequate sensors, and thus corresponding signals used in TCMs.

All Intelligent TCM systems, and especially those that use vibration sensors, heavily depends on the choice of descriptors, i.e., features extracted from the particular sensor signals. This is due to the fact that if the descriptors do not describe the signal adequately, other techniques, such as feature extraction or feature selection, as well as recognition methodology, fail to be efficient as well. Bahr et al in [4], the first to apply the descriptors obtained from vibration signals in the TCM tasks. Actually, they used RMS and/or the mean of the vibration sensor signal, in order to detect an increase in vibration magnitude, which corresponds to the increase in cutting energy generated due to flank wear. Also in [5], the mean and peak values of vibration sensor signals are used in the TCM task. In [6], Dimila analyzed the correlation of vibration signal features to cutting-tool wear, in both the time and the frequency domains, during turning operations. Time domain features were deemed to be more sensitive to the

cutting condition than tool wear, whereas certain peak values in the frequency domain correlated well with the measured wear values.

In this work, we propose tool wear monitoring strategy which includes novel texture based descriptors, to be applied in the TCM problems utilizing vibration sensor signals. Actually, the texture based approach to the descriptor construction is, to the knowledge of authors, completely novel in the field of TCM. The proposed descriptors obtained from vibration sensor signals are spectral domain based. They rely on considering the module of the Short Term Discrete Furrier Transform (STDFT) spectra obtained from the particular sensor signal, as the 2D textured "image". We identify the time scale as the first dimension, and the frequency scale as the second dimension of module of the STDFT of the particular sensor signal of interest. The 2D textured image obtained in such way is then divided into particular disjoint narrow 2D texture patches, covering part of the frequency range of interest. Further, by applying appropriate filter bank, for each predefined frequency band (where those bands form the partition of the whole frequency range), we extract 2D textons (see [7]), i.e., low dimensional feature vectors in filter response space. The goal is to increase the discriminativity of the obtained descriptors in the task of tool wear classification. The reason for that is that, discriminativity between texture patches belonging to different tool wear condition classes is contained in vertical lines spread across entire frequency range, and many of the used techniques in texture analysis could not take that into account. In this paper, we apply the particular filter bank, proposed in [7], used in the problems of texture recognition, which has the mentioned capability. We apply it on 2D texture patches, obtained from the STDFT of the vibration sensor signal, in order to efficiently extract the information concerning the mentioned lines, in the form of textons, i.e. features in filter response space.

We additional model probability distributions, for each frequency band, which describe every particular utterance in filter response space, and use them as the

low dimensional, robust descriptors. This is obtained by using first four moments (averaging process is in time), and obtain final descriptors that represent the particular utterance to be used in the training or recognition process.

2. APPARATUS USED IN EXPERIMENTS

Machining experiments were performed on CNC GU 600 lathe manufactured by INDEX and installed in a laboratory of the Faculty of Technical Sciences in Novi Sad. Investigation of tool wear process encompassed the monitoring of the dominant wear mechanism through following parameters: wear band, crater wear and tool life. In the course of the turning process, vibration signal were registered at the tool shank. For each tool pass the generated chip segments were sampled. The setup of tool sensors, as well as the dimension of workpiece used in this experiment is shown in Fig. 1.

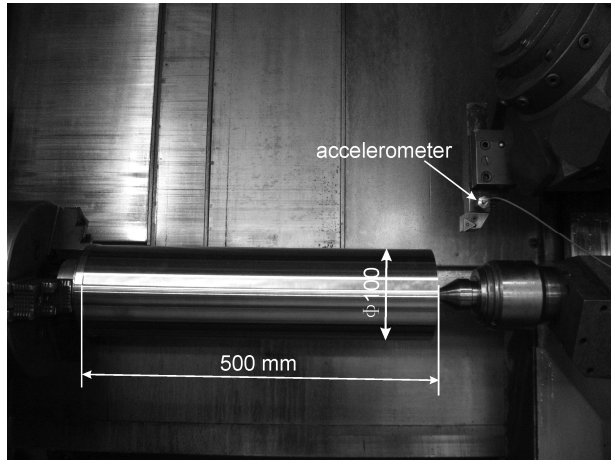


Fig. 1. Experimental setup

During the experiment two cutting speeds were employed, 180 to 250m/min, in conjunction with 0.15 and 0.3mm/rev feed rates. Cross section of the tool shank used in the experiment was 20x20mm. The machining was performed with P25 tool inserts designated TNMM 110408. Accelerometer Kistler 8002 was fixed onto the tool holder, and used to measure acceleration of vibrations. This signal was sampled at 625 kHz, using A/D converter NI 625 USB, National Instruments. Workpiece material was 42CrMo4, 310 HB hardness and 950MPa respectively with guaranteed mechanical and chemical properties given in Table 1.

C%	Si%	Mn%	S%	P%	Cr%	Mo%	Ni%	Cu%	V%
0,4	0,43	0,6	0,3	0,35	0,8	0,15	0,3	0,2	-

Table 1 Chemical composition of work material

3. TEXTURE BASED FEATURES

The utterance u from which we extract descriptors and consequently the features that we use in the training as well as in the recognition phase of the classifier is the

signal, of various lengths, obtained from the vibration sensor. In this work, we view the problem of tool wear state classification from the texture recognition perspective. The most challenging difficulties present in real texture recognition problem with 3D variations, come from the variability of those textures, i.e., the fact that the classical texture is primarily a function of the following variables: the texture surface, its albedo (i.e., the reflection factor of the corresponding surface), the illumination, the camera and its viewing position. We note, that the texture that corresponds to the STDFT spectrogram of the vibration sensor signal that we consider is viewed as 2D texture. Nevertheless, the presence of vertical lines in the STDFT (viewed as the texture) of interest and our goal to efficiently extract them, and/or to obtain the reliable information of their presence, imposes the necessity for texture feature extraction that utilizes appropriate and specific filter bank, capable to capture those.

3.1 Forming the texton based descriptors

Actually, we identify the discrete time frame k of the STDFT spectrogram of the utterance of interest, as the discrete x -axis of the textured image, and the discrete frequency ω , as the discrete y -axis of the corresponding textured image. The idea, that we later confirm as a hypothesis in our experiments, is that considering the STDFT spectrogram, discriminatively between different tool wear states is in the great sense contained in the characteristics (number, position, structure) of (approximately) vertical lines that appears on the corresponding textured images (see Figure 2). Actually, the condition of the tool wear states is strongly correlated with the characteristics of those lines. The lines actually present sudden jumps in frequency of the signal obtained from particular sensors, on various frequency scales, induced by the underlying tool cutting process.

We invoke novel texture based descriptors in the task of TCM and call them the Texture Based Tool Condition Descriptors (TBTCD). The TBTCD descriptors are obtained by considering the STDFT spectrogram of the windowed time frames delivered from the previously mentioned utterance, as the 2D textured image.

We proceed as follows: As it is common for most texture recognition approaches, we divide the STDFT textured image into texture patches spread across different filter bands. The crucial is to select appropriate filter bank that is able to efficiently extract the information on the presence of mentioned lines, for each frequency bend. Let $F(x, y)$ be the textured image that corresponds, i.e., is identified with the STDFT spectrogram of the vibration sensor signal of the particular utterance s . The STDFT spectrogram is defined as the square module of the spectral density, i.e., $|S(k, \omega)|^2$, where

$$F(x, y) = |S(k, \omega)|^2 \quad (2)$$

$$x = 0, \dots, x_{\max}, y = 0, \dots, y_{\max}$$

$$k = 0, \dots, k_{\max}, \omega = 0, \dots, \omega_{\max}$$

We further do all our analysis on textured image $F(x, y)$ obtained as it is explained previously, where for the easier modeling, without loss of generalization, we consider the continuous case $x \in [0, x_{\max}]$ and $y \in [0, y_{\max}]$.

We briefly describe the filter that we use: Let

$$G(\sigma_x, \sigma_y, \theta, x, y) = \frac{1}{2\pi\sigma_x\sigma_y} e^{(A(\theta)^T [x \ y]) \begin{bmatrix} \sigma_x^2 & 0 \\ 0 & \sigma_y^2 \end{bmatrix} (A(\theta) \begin{bmatrix} x \\ y \end{bmatrix})} \quad (3)$$

be the directed anisotropic Gaussian kernel. The fixed terms $\sigma_1 > 0$ and $\sigma_2 > 0$ denote scales in $x \in [0, x_{\max}]$, $y \in [0, y_{\max}]$ direction, respectively, while θ and $A(\theta) = \begin{bmatrix} \cos\theta & -\sin\theta \\ \sin\theta & \cos\theta \end{bmatrix}$, for $\theta \in [0, 2\pi]$, denote the orientation of the kernel (3) and its 2D rotational matrix, respectively. The MR8 filter bank that we use in our application consist of 38 Gaussian filters of the form (3), at 6 different orientations $\theta_j \in \{j\pi/6 \mid j = 0, \dots, 5\}$, and 3 different scales

$$(\sigma_x, \sigma_y) \in \{(1,3), (2,6), (4,12)\},$$

and also 6 Laplacians of Gaussians, defined as $\Delta G(\sigma_x, \sigma_y, \theta, x, y)$, where $\Delta = \partial_x^2 + \partial_y^2$ is the Laplace operator of differentiation, evaluated at the same orientations and scales (for more details see [13, 18]). The filter outputs are collapsed, by taking only the maximum values, across all orientations, obtaining 6 different filter responses. Additional two responses are isotropic, thus unable to extract characteristic lines in the textured image F , so we do not use them in application.

Further we proceed with the procedure of texton extraction. We divide the interval $[0, y_{\max}]$ where texture image F have its values into M sub-intervals $\{[y_{q-1}, y_q] \mid q = 1, \dots, M\}$, $y_0 = 0$, $y_M = y_{\max}$ where for every index $x = 0, \dots, x_{\max}$, the sub-patch of $F(x, y)$, is defined as matrix of pixels bounded by $[y_{q-1}, y_q]$ on yaccess and by $[x, x + T]$ on xaccess. Here, T is predefined width of the patch. We denote such described textured patch as $P_{x,q}$, $q = 1, \dots, M$. The texton in the form of filter response are then formed for every interval $[y_{q-1}, y_q]$ and discrete coordinates. We note, that the interval $[y_{q-1}, y_q]$ of the textured image F , corresponds to the frequency band $[\omega_{q-1}, \omega_q]$ of the STDFT spectrogram of particular utterance.

Actually, for each x and each different band q , texton $v_{x,q}$ is composed of $Q = 6$ components of the MR8 filter bank. Thus, we have:

$$v_{x,q}^l = [v_{x,q}^{l(1)} \mid v_{x,q}^{l(2)}] \mid l \in L \quad (4)$$

where

$$v_{x,q}^{l(1)} = \max_{\theta} G(\sigma_x, \sigma_y, \theta, x, y) * P_{x,q}$$

$$v_{x,q}^{l(2)} = \max_{\theta} \Delta G(\sigma_x, \sigma_y, \theta, x, y) * P_{x,q}$$

$$\theta \in \{j\pi/6 \mid j = 0, \dots, 5\}$$

and

$$L = \{(\sigma_x, \sigma_y) \mid (1,3), (2,6), (4,12)\}.$$

4. EXPERIMENTAL SETUP

Tool wear state classification is conducted indirectly by monitoring vibration signals during the cutting process. The experiments have been conducted over 150 vibration signals, classified into 3 states (50 signals per each state), based on the level of abrasion (new plate, i.e., no wear, small wear, i.e., up to 0.25 mm, and a large wear, i.e. above 0.5 mm). Bearing in mind that the tool wears condition changes continually, the borders between classes could not be ideally sharp. The analyses of the results are provided by using 5-fold cross validation, i.e., 120 vibration signals used for the training of the classifier, and another 30 vibration signals used for the test, while each 3 categories have been equally represented in both sets). 5 results from the folds have been averaged to produce final estimation.

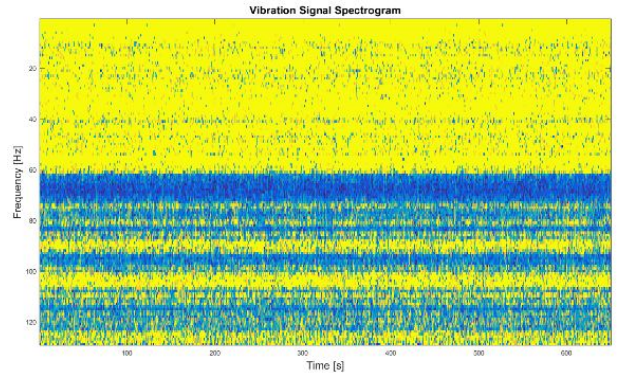


Fig. 2. Vibration signal spectrogram

Signal transformation for both sets begins by computing the spectrum of vibration signals, using a discrete-time Short-Time Fourier Transform (STFT) for $M = 256$ frequency points and the Hamming window of equal length, with $M/4$ overlap between the segments (example is given in Fig. 2). The signals are 125000 samples long, with the sampling frequency of 10 kHz. The result is a matrix containing 129 frequencies ($M/2 + 1$ for real signals and even number of frequency points, although we used a limited frequency range for subsequent transformations) and 650 time bins (the number of segments). Each segment represents the estimation of a short-time, time-localized frequency content of input vibration signals. The convolution is conducted between the spectrum and the appropriate filter from the MR8 filter bank described in 3.1. Thus, the robust features, i.e., descriptors are obtained as it is described in section 3.1 where we treated one simple band case, $M = 1$. We used $P = 3$ moments: variance, skewness and kurtosis, while the first moment, i.e., mean is excluded from our consideration, since we treated only centralized spectrograms, i.e., corresponding centralized textured

image, Resulting total of 9 coefficients per each signal are obtained.

The recognition is performed by using fuzzy classifier over the selected set of features. The classifier generates a Fuzzy Inference System (FIS) structure of the Mamdani type from input coefficients, using Fuzzy C-Means (FCM) clustering algorithm, by extracting a set of rules that models the data behavior. Each input signal is represented by a vector of 3 (per scale) or 9 coefficients and classified into one of the 3 output states, marked by numerical values 1, 2 and 3, depending on the wear state (the level of abrasion) of a steel plate. Rather than being attached to only one cluster, each vector has a degree of belonging to the clusters, depending on the distance from the center of a cluster.

5. EXPERIMENTAL RESULTS

In Table 2, the average classification accuracy for 5 folds (F1 to F5) is presented for fuzzy classification conducted per each scale separately (3 moments per scale). The output values are averaged for all 3 scales in order to obtain the final result. These values are classified in the following way: less than 1.5 - class 1, 1.5 to 2.5 - class 2, more than 2.5 - class 3.

Tool Wear	new plate (class 1)	0.25 mm (class 1)	0.5 mm or more (class 3)
scale 1	96 %	100 %	98 %
scale 2	98 %	100 %	100 %
scale 3	96 %	98 %	100 %
final classification	98 %	100 %	100 %

Table 1. The average fuzzy classification accuracy (separate scales)

The classification accuracy obtained by using 9 coefficients (3 moments per 3 scales) for 5 folds is given in Table 2. The results are presented for 5 folds, using 100 clusters. The optimal number of clusters was smaller in this case, having in mind the fact that we had the same amount of data (number of signals) in higher dimensional space. Better results were obtained in the case of sum of the output values for separate scales pondered by 1/3, than in the case of classification for all 3 scales together.

6. CONCLUSION

In this work, we propose Toll Wear Monitoring Strategy, which relies on the novel texture based descriptors. We use the module of the STDFT spectra obtained from the particular vibration sensors signal utterance and consider it as a 2D textured image, by identifying the time scale of STDFT as the x dimension, and the frequency scale as the y dimension of the image. Then, we extract 2D texture patches, covering part of the frequency range of interest. By applying the appropriate filter bank, for each predefined frequency band 2D textons are extracted. For each band of interest, we extract information

regarding the PDF. Of those textons in the form of lower-order moments, where the averaging was done in x dimension of the 2D textured image. Thus, we obtain discriminative and robust tool wear state descriptors. The experiments conducted on the real TCM system, show that the proposed descriptors, together with the fuzzy classifiers provide very high recognition accuracy in the tool wear state recognition task, making it suitable for application in efficient TCM systems.

7. REFERENCES

- [1] Siddhpura, A. Paurobally, R.: *A review of flank wear prediction methods for tool condition monitoring in a turning process*, International Journal of Advanced Manufacturing Technology, 65, 371–393, 2013.
- [2] Abellan-Nebot, J.V., Subirón, F.R.: *A review of machining monitoring systems based on artificial intelligence process models*, International Journal of Advanced Manufacturing Technology, 47, 237–257, 2010.
- [3] Cho, S. Binsaeid, S. Asfour, S.: *Design of multisensor fusion-based tool condition monitoring system in end milling*, International Journal of Advanced Manufacturing Technology, 46, 681–694, 2010.
- [4] Bahr, B, Motavalli, S, Arfi, T.: *Sensor fusion for monitoring machine tool conditions*, International Journal Comput Integr Manuf, 10, 314–323. 1997.
- [5] Haber RE, Jimenez, J.E., Peres, C.R., Alique, J.R.: *An investigation of tool-wear monitoring in a high-speed machining process*, Sensors and Actuators A-Phys, 116, 539–545, 2004.
- [6] Dimla, D.E.: *The correlation of vibration signal features to cutting tool wear in a metal turning operation*, International Journal of Advanced Manufacturing Technology, 19, 705–713, 2002.
- [7] Varma, M., Zisserman, A.: *A Statistical Approach to Material Classification Using Image Patch Exemplars*, IEEE Transactions on Pattern Analysis and Machine Intelligence, (31)11, 2032 - 2047, 2009.

Authors: Assoc. Prof. Aco Antic, Professor Milan Zeljkovic, Department of Production Engineering, Assist. Prof. Lidija Krstanovic, Department of fundamental sciences, Faculty of Technical Sciences, Trg D. Obradovica 6, University of Novi Sad, 21000 Novi Sad Serbia; Full Prof. Nicolae Ungureanu, Technical University of Cluj-Napoca, Department of Engineering and Technologic Management, Dr. V. Babes 62/A, 430083 Baia Mare, Romania.
E-mail: antica@uns.ac.rs; milanz@uns.ac.rs; lidijakrstanovic@uns.ac.rs; unicu@ubm.ro

ACKNOWLEDGMENTS: This paper presents a segment of the research on the project "Contemporary approaches in the development of special solutions bearing in mechanical engineering and medical prosthetics", project number TR 35025, financed by the Ministry of Education and Science of the Republic of Serbia.

Berus, L., Ficko, M., Gotlih, J., Klancnik, S.

DEVELOPMENT OF A SYSTEM FOR MONITORING TEMPERATURE DISTRIBUTION AND OPERATING OF HEAT SOURCES INSIDE HEATING DEVICE

Abstract: *This study focuses on designing a system for monitoring temperature distributions and managing heat sources inside an oven. Proposed protocol can be translated to different heating devices. The system displays monitored temperatures gathered with temperature sensors. Thermocouple J-type sensors are distributed on horizontal plane inside an oven, representing the baking load (for example baking tray). Heaters are operated with relay module switch, which enables the splitting-off of electrical circuits. Relay module settings are altered by pulse-width modulation (PWM) signal. Monitoring and operating of the system components is enabled by data acquisition (DAQ) device. DAQ device sends information to heaters and records temperatures inside heating device. Designed graphical interface offers visual and numerical information about temperature field during operating time. Included safety protocol serves as an off-switch if temperature inside the oven reaches critical level. In the future the system could be adopted for optimization of temperature inside heating devices aiming to achieve better temperature control and homogenous temperature distribution.*

Key words: *heating devices, oven, graphical interface, temperature monitoring, temperature distribution*

1. INTRODUCTION

In cooking, the conventional oven is a kitchen device, used by many households for heating and roasting. Foods normally cooked in this manner include meat, bread, cake and other desserts. Outside the culinary world, heating devices are used also for melting (furnace for steel manufacture) and drying (kilns for ceramics, wood and cement manufacturing). For controlling the conditions inside these kind of heating devices companies have adopted different techniques. Some have resolved oven issues with supervisory control and data acquisition systems, both on premise and even remotely. Other manufactures have adopted other kind of computer software, such as line cameras to monitor and provide remote assistance or even fix problems around the world [1, 2].

Food industry in recent years gained on quality and restrictions needed for the production of good and acceptable products. The quality of food is influenced by heating device properties, such as distribution of heaters, fan properties, outside conditions, materials used and many more. Baking operation efficiency is determined by the oven properties and operating conditions [3]. Baking is a simultaneous heat and mass transfer phenomena (heat is transferred with conduction, convection and radiation) [4], it's a non-reversible process, thus any unsatisfactory product has to be discharged. Baking is a very complex process, during which products are exposed to numerous physical, chemical and biochemical changes, such as water and fat phase transition, denaturation of protein, crust formation, water evaporation, volume expansion, browning reaction, generation of porous structure etc. Temperature and water content are responsible for all physiochemical processes associated with baking process and variations in the product can potentially be minimized by optimizing the processing conditions

[5]. There are few parameters that has to be monitored inside a heating device; heat flux, humidity, air velocity and temperature.

This study concentrates on designing a system, that operates the heaters in an oven and simultaneously depicts temperature field inside an oven. Research aim is to design user friendly procedure to control the air temperature parameters inside the oven. System of this sort will in future enable the optimization of temperature field variations and will be able to translate into other kind of heating or cooling processes.

2. MATERIALS AND METHODS

2.1 Sensors

Sensor is a device, whose purpose is the detection of events or changes in the environment. Information about environment is then sent and processed by computer or other type of electronics. Sensors, also called transducers, converts inputs representing to physical phenomena in environment into measurable signal output, that is readable to a human. Temperature sensors monitor free stream air temperature associated with convection. Mathematical models and computer software are used to create temperature graphs. By measuring the temperature one can analyze the precise baking process and use that information to control product quality. Thermocouple temperature sensors work by producing a small electrical current, that is proportional to temperature difference between two ends, named hot and cold junction.

For this study J-type thermocouple sensors were used. J-type sensor is made of iron and constantan alloy combination and has a temperature range from 0 to 400 °C. Sixteen J-type thermocouple sensors are connected to sixteen analog input ports of DAQ. Temperature difference between cold and hot junction is calculated with following formula:

$$\Delta T = T_0 + \frac{(v-v_0)(p_1+(v-v_0)(p_2+(v-v_0)(p_3+p_4(v-v_0))))}{1+(v-v_0)(q_1+(v-v_0)(q_2+q_3(v-v_0)))}, \quad (1)$$

where v is the voltage difference between junctions. T_0 , p_1 , p_2 , p_3 , p_4 , q_1 , q_2 , q_3 and v_0 represent specific J-Type coefficients stated in Table 1. Real temperature in the oven chamber is calculated with summation of ambient temperature $T_{ambient}$ and temperature difference ΔT .

Coefficients	
T_0	2.5066947E+02
p_1	1.8014787E+01
p_2	-6.5218881E-02
p_3	-1.2179108E-02
p_4	2.0061707E-04
q_1	-3.9494552E-03
q_2	-7.3728206E-04
q_3	1.6679731E-05
v_0	1.3592329E+01

Table 1: J-type thermocouple sensor coefficients

Fig. 1 shows the placement of sixteen sensors inside an oven chamber. For this study single plane arrangement was used. Temperatures were sampled with **1000** Hz samplint rate.

Oven's back side

13	14	15	16
9	10	11	12
5	6	7	8
1	2	3	4

Oven's front side



Fig. 1: Sensors numbers and plane arrangement

2.2 Relays

Relay is an electrically operated switch that separates electrical currents. Relays are used where it is necessary to control circuits by a separate low-power signal, or where several circuits must be controlled by one signal. Many relays use an electromagnet to mechanically operate a switch, but there are also other operating principles, such as solid-state relays.

For this study 4 channel 5V relay module was used. Pulse-width modulation (PWM) signal parameters for operating a relay are period, duty cycle and delay (Fig. 2). On the basis of a proposal of oven manufacturer we decided that we will fixate a period parameter on minimum 45 seconds value, because if the period value was lower, the disturbances on an electric grid would become too significant.

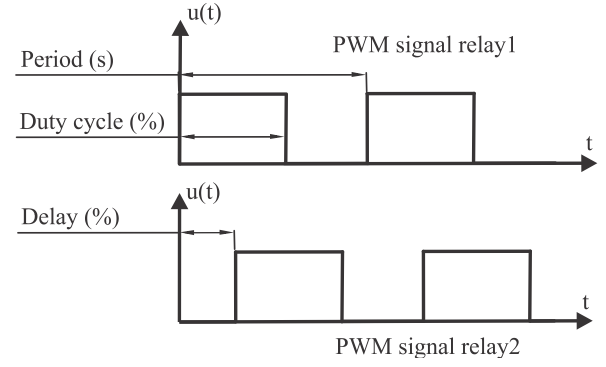


Fig. 2: PWM signal adjustable heater parameters

Relays are operated with three digital outputs of DAQ device, one relay channel serve as safety switch (if T_{limit} is reached it cuts down electrical current of other two channels that operate heaters). Fig. 3 shows the circuit connection between heaters and relays.

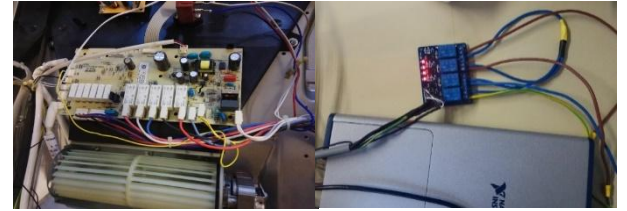
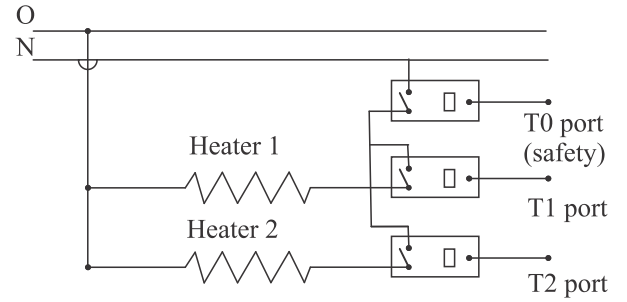


Fig. 3: Circuit connection between heaters and relays

2.3 Data acquisition system

Data acquisition (DAQ) is the process of measuring real world physical phenomena and converting the resulting samples into digital numeric values, that can be manipulated with computer. DAQ systems exploit the processing power, display, connectivity and productivity capabilities of industry standard computers. A DAQ system consists of sensors and actuators, DAQ device, and a computer with programmable software.

For this study NI USB-6343 DAQ device was used. DAG device is connected to PC and manipulated it with software. Sixteen thermocouple sensors were plugged into analog ports v_0 to v_7 and v_{17} to v_{24} . Relay switches were controlled with 3 digital ports T_0 to T_2 .



Fig. 4: Whole system; sensors, ASKO OCS8487S oven, DAQ device and PC

3. RESULTS AND DISCUSION

Fig. 5 presents a flowchart of proposed system for monitoring temperature distributions and operating heat sources inside heating device. System enables real time monitoring and altering of the conditions inside an oven chamber.

First the user specifies a desired PWM cycle for heaters (program), working temperature $T_{working}$ (warm-up), limit temperature T_{limit} and working time. During warm-up procedure heaters are working with full percentage duty cycle (and minimum delay), until the desired $T_{working}$ is reached. $T_{working}$ is read from desired temperature sensor, in our case we used a sensor no. 4. Then the program (with specified PWM signal) starts operating the heaters and simutaniously gather the temperature field and display it in real-time to the user. Temperature field is shown in a 3D graph and in an ordinary 2D graph that offer a countinuous user control of temperature field inside heating device. T_{limit} is a part of a safety protocol, that stops the oven if the limiting temperature is surpassed and informs the user. At the end of working time the temperature field results are exported.

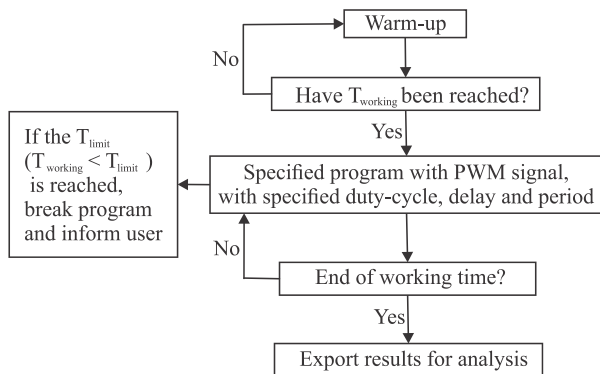


Fig. 5: Workflow of the proposed system

Fig. 6 shows a 2D temperature graph of temperatures inside oven chamber. Fig. 6 and 7 show a temperature field of PWM signal with properties:

- duty cycle heater1 = 20%,
- duty cycle heater2 = 35%,
- delay heater1 = 50%,
- delay heater2 = 0%,
- period heater1 = 45s and
- period heater2 = 45s.

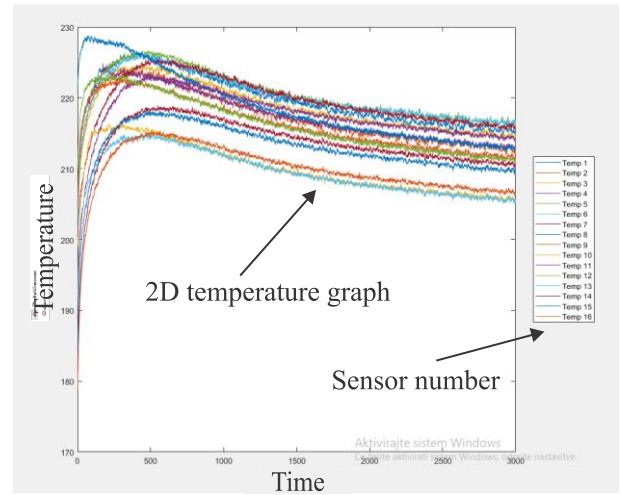


Fig. 6: 2D graph of temperatures inside oven chamber

Fig. 7 shows a 3D temperature graph field inside oven chamber. With slider the user can visualize a temperature field through time. Sensors are located in the positions as stated in Fig. 1. Sensor no. 1 has position (1,1), sensor no. 2 position (2,1) and so on up to sensor no. 16 located at position (4,4). User can also monitor current temperature of all sixteen sensors on the right side of Fig. 7.

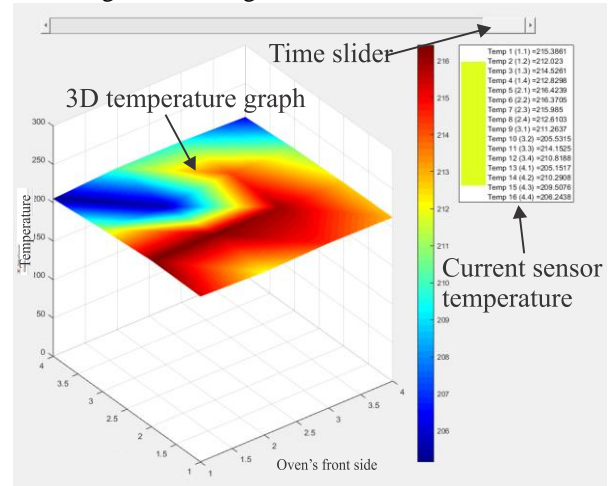


Fig. 7: 3D graph of temperature field inside oven chamber

4. CONCLUSION

Proposed system is able to accurately depict temperature field inside an oven in real-time. Whole procedure of defining the program with specified PWM signals can be separated into desired number of sub-procedures for more efficient baking operation, offering better products to consumer.

In the future we plan to optimize the temperature field differences inside oven by finding the right sequence of ON/OFF turning the heaters (appropriate PWM signal), in order to achieve uniform temperature distributions. The optimization can potentially be tackled with any heuristic optimization algorithm (PSO; ABC, GA etc.), where fitness value function is defined as difference between minimal and maximal averaged temperatures, when temperatures in the oven

chamber settle (start fluctuate around fixed values). We also plan to include a fan to manipulate airflow velocity in an oven chamber, that would increase heat flux to the product and possibly increase temperature uniformity.

5. REFERENCES

- [1] Malovany, D.: *Proceedings of the 87th Annual Technical Conference*, The Journal of American Baking, Chicago, 2011.
- [2] Popa, B., Popescu, I., M., Popescu, D., Bobașu, E.: *Real-time monitoring system of a closed oven*, pp. 27-32, 19th Internacional Carpathian Control Conference (ICCC), Szilvasvarad, 2018.
- [3] Kokolj, U., Škerget, L., Ravnik, J.: *The validation of numerical methodology for oven design optimization using numerical simulations and baking experiments*, Journal of Mechanical Engineering, vol. 63, pp. 215-224, 2017
- [4] Marcotte, M: *Heat and mass transfer during baking*, WIT transactions on state-of-art in science and engineering, 2007.
- [5] Chhanwal, N., Tank, A., Raghavarao, K., Anandharamakrishnan, C.: *Computational Fluid Dynamics (CFD) modeling for bread baking proces-A review*, Food and Bioprocess Technology, vol. 4, pp. 1157-1172, 2012.

Authors: Lucijano Berus, mag. inž. str., izr. prof. dr. Mirko Ficko, asist. Janez Gotlih, doc. dr. Simon Klancnik, University of Maribor, Faculty of Mechanical Engineering, Smetanova ul. 17, 2000 Maribor, Slovenia, Phone: +386 (0)2/220-7500, Fax: 02 220 79 90.

E-mail: lucijano.berus@um.si; mirko.ficko@um.si; janez.gotlih@um.si; simon.klancnik@um.si

Blanuša, V., Milisavljević, B., Zeljković, M., Živković, A., Savić, B., Sovilj-Nikić, S.

ANALYSIS OF LOAD DISTRIBUTION IN DOUBLE-ROW CYLINDRICAL ROLLER BEARING FOR MACHINE TOOLS MAIN SPINDLE ASSEMBLY

Abstract: *The internal bearing geometry (clearance, zero clearance and positive clearance) has the significant effect on the load distribution in bearing. Cylindrical roller bearings for machine tools main spindles are mounted with radial positive clearance due to necessary stiffness of assembly. The paper shows the application of Sheval load distribution theory when the bearing is mounted with positive clearance. The effect of load distribution factor on the static behaviour of the bearing has been considered. By the application of programmable system of general use on the basis of finite element method the displacements and Von Mises stresses in bearing have been determined in dependence on the load distribution per rolling elements.*

Key words: *Main spindle assembly, double-row cylindrical roller bearing, load distribution, static behaviour*

1. INTRODUCTION

A large number of researchers have been involved in and are concerned with the problems of load distribution in the bearing over a long period of time. Distribution of outer load in bearing mainly depends on internal bearing geometry, i.e. on the mounting procedure (clearance, zero clearance and positive clearance). In addition, load distribution has the significant effect on the static and thermal behaviour of assembly into which the bearing is mounted [1].

Stribeck, R. [2] was the first one who considered the problems of load distribution per rolling bodies of inclined contact ball bearing. These problems are still actual for research. The paper [2] shows the expressions determined on the basis of Hertz contact theory for computing of axial and radial load distribution per rolling bodies – balls. Mathematical model was defined for the load of bearing mounted with clearance $\varepsilon \leq 0.5$, i.e. for the case when the total radial load is transferred only to rolling bodies accommodated under meridian plane. Experimental testings of balls deformation were made under the action of load transferred to the ball by the pressure of flat surface or other balls accommodated into the cage. Additionally, the values of contact surface deformation were determined in dependence on ball diameter and load.

Sjoväll, H. [3] is considering load distribution in radial and axial direction in roller bearings to and above meridian plane. He also shows the distribution of axial load per rolling bodies and concludes that the axial load distribution in roller bearings is linear, while the axial load distribution in inclined ball bearings is non-linear. The author introduces the complete elliptic integrals of the first and the second kind for computing of radial and axial integral in order to determine the load distribution on the rolling bodies above meridian plane. He also defines the expressions for determination of radial and axial load on certain rolling bodies.

Russian scientist Makushin, in the field of Theory of Elasticity is the author of a chapter included into the Manual for the calculation of strength in mechanical engineering, relating to stress theory, evaluation of stiffness, as well as the statically undetermined systems [4]. Here is also a chapter dedicated to Hertz contact theory and its application to the load distribution in roller bearings. After the clearly exhibited Hertz contact theory for two elastic bodies Makushin exhibits the theory of load distribution in rolling ball bearings according to Stribeck.

Kovaljev, M. and Narodecki, M. [5] exhibited the various technical solutions and theoretical reviews relating to reliances in machines and devices as well as the analysis of contact stresses and deformations occurred in contact of elastic bodies. Previously there was a basis for consideration of load distribution in radial bearings. Load distribution in radial bearings was considered with radial load and zero clearance, as well as with radial load and clearance. Stiffness of radial bearing has been also considered. The analysis covered the cases of static and dynamic load of bearing. Stribeck theory was exhibited in details. Then, Sheval theory was shown, in which radial and axial integrals figured out, expressed without application of elliptic integrals, thus simplifying the estimate itself. The application of software packages even more facilitate the estimate procedure of load distribution.

Koshelj, M. V. [6] considers the types of roller bearings at first and then in the second chapter analyzes the kinematics, stresses and forces acting in bearings. After the analysis of friction and its characteristics in roller bearings he shows the analysis of stress and deformation. The consideration is given to load distribution in roller bearings and that for single-row ball bearings under radial and combined load. The application of Stribeck theory is shown in details. By using Sheval theory the author determines the radial and axial component of load and defines the approximate expressions for computing of these components containing the radial and axial integral. Also, the tables shown contain the values of these

integrals in the wide diapason of load distribution factor.

Harris, A. and Kotzalas, M. [7] systematized the equation for determination of load distribution in axial and radial direction for roller bearings (inclined ball bearings and cylindrical roller bearings). The values of radial and axial integral for point and line contact are shown numerically in the form of tables. The value of exponent for point contact amounts to $n=3/2$, and for line contact $n=10/9$. The shown are the numerical values of load distribution factor ϵ for point and line contact under bearing radial load.

Ricci, C. M. [8] uses iterative method for calculation to determine the static load distribution in single-row inclined ball bearings. The paper shows the numerical aspects of iterative method. The numerical results are classified according to the results of the other authors. The total axial load of inclined ball bearing of 17.800 N, amounts to 1.676 N for each bearing ball according to Harris, and as shown in the paper 1.681 N. The deviation of this method from Harris method is -0,34 %. Shown is the dependence of ball angular contact on the size of axial load as well as axial displacement of rings. The results of Harris and Ricci are lined up.

2. BEARING MOUNTING

Comprehensive analysis of cylindrical roller bearings for special applications includes complex testing of a large number of parameters influencing the behaviour of bearing in exploitation. One of the most important parameters in the analysis of behaviour is the load distribution per rolling bodies in dependence on load distribution factor, the method of bearing mounting respectively.

Load distribution to rolling bodies depends directly on the bearing internal geometry and the bearing mounting is possible to be done in three ways:

- with clearance,
- with zero clearance,
- with positive clearense.

When the bearing is mounted with clearance, the total radial load is transferred only to those rolling bodies which are accommodated under meridian plane (under the bearing central axis) $\epsilon < 0,5$. When the bearing is mounted with zero clearance $\epsilon = 0,5$ the distribution of radial load is done up to meridian plane where the rolling bodies at the level of meridian plane are unloaded. Load of rolling bodies from meridian plane up to the rolling body accommodated under the bearing central axis is increasing according to certain regularity so that the rolling body accommodated exactly under the central axis transfers the highest load. When the bearing is mounted with positive clearense $\epsilon > 1$ all rolling bodies are radially loaded.

When the bearing is mounted with positive clearense, preloading appears in the bearing. Preloading represents the force acting between rolling elements and bearing rings not resulting from the action of outer active load. Preloading may be considered the negative clearance (positive clearense). The reasons for preloading are:

- higher stiffness,
- higher guiding accuracy,
- lower noise level,
- longer bearing lifetime.

Figure 1 shows the view of cylindrical roller bearing mounted with clearance, zero clearance and positive clearense as well as load distribution.

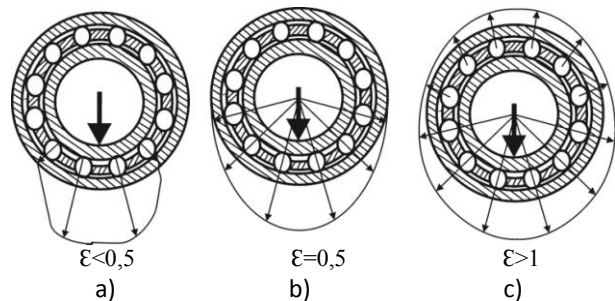


Fig. 1. Load distribution to rolling bodies of the bearing mounted with clearance (a), zero clearance (b) and positive clearense (c)

3. MATHEMATICAL MODEL FOR DETERMINATION OF LOAD DISTRIBUTION

Cylindrical roller bearings for machine tools main spindles are mounted with positive clearense and transfer high active radial loads in exploitation.

Being observed is the radial roller bearing exposed to the action of combined load consisting of radial and axial force. The action of axial force causes the uniform elastic deformation in all rolling bodies due to which the transversal straight lines of outer and inner rings, normal to the bearing axis, remain parallel. Due to this fact the load distribution in axial direction for roller bearings must be linear, while the load distribution in radial direction is non-linear. Distribution of axial and radial load of roller bearing is shown in figure 2.

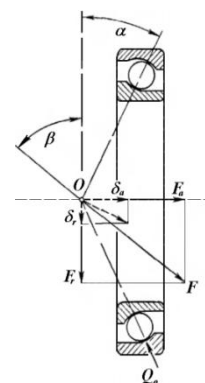


Fig.2. Axial and radial load of roller bearing

Force F acting on the bearing has two components:

$$F_r = F \cdot \cos \beta \quad (1)$$

$$F_a = F \cdot \sin \beta \quad (2)$$

Force F_r produces radial deformation δ_r , which is changeable in radial direction depending on angle ψ ,

which describes the position of rolling body in relation to bearing axis (Figure 3).

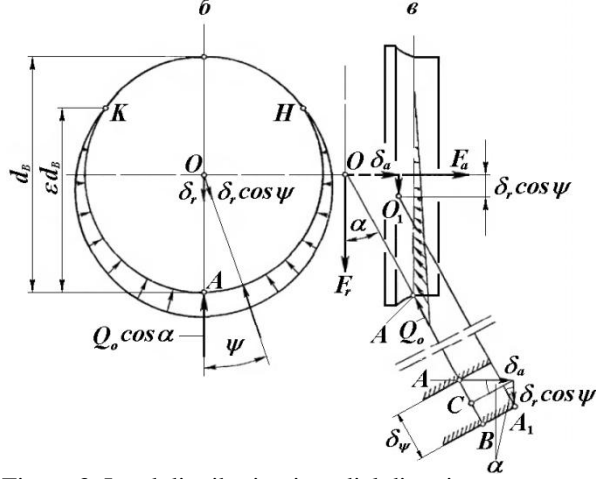


Figure 3. Load distribution in radial direction

$$\psi = \max \left(1 - \frac{1}{2\varepsilon} (1 - \cos \psi) \right)^n \quad (3)$$

where $n=3/2$ is taken for point contact and $n=\frac{1}{0.925}=1.081081$ for line contact. This value of coefficient n was determined by Kunert (Karl-Heinz Kunert). Harris and Kotzalas [7] determined the value of coefficient n for line contact $n=10/9$. Coefficient ε represents the load distribution factor and depends on the type of bearing and preloading value.

The radial force can be calculated by applying the following equation:

$$F_r = \max \left[\frac{z}{2\pi} \int_{-\varphi}^{\varphi} \left(1 - \frac{1}{2\varepsilon} (1 - \cos \psi) \right)^n \cos \psi \, d\psi \right] \cos \alpha, \quad (4)$$

i.e.

$$F_r = z Q_{\max} \left[\frac{1}{2\pi} \int_{-\varphi}^{\varphi} \left(1 - \frac{1}{2\varepsilon} (1 - \cos \psi) \right)^n \cos \psi \, d\psi \right] \cos \alpha, \quad (5)$$

or:

$$F_r = z Q_{\max} J_r(\varepsilon) \cos \alpha. \quad (6)$$

The calculation of radial integral $J_r(\varepsilon)$ will be explained in continuation.

The procedure similar to radial force is applied to axial force:

$$F_a = Q_{\max} \left[\frac{z}{2\pi} \int_{-\varphi}^{\varphi} \left(1 - \frac{1}{2\varepsilon} (1 - \cos \psi) \right)^n d\psi \right] \sin \alpha, \quad (7)$$

i.e.:

$$F_a = z \max \left[\frac{1}{2\pi} \int_{-\varphi}^{\varphi} \left(1 - \frac{1}{2\varepsilon} (1 - \cos \psi) \right)^n d\psi \right] \sin \alpha, \quad (8)$$

or:

$$F_a = z Q_{\max} J_a(\varepsilon) \sin \alpha. \quad (9)$$

Finally, the equations for determination of maximum force in radial and axial direction can be written down. Load distribution in axial direction in roller bearings is linear and the total axial force is shared between a number of rolling elements in a bearing.

$$\max = \frac{F_r}{z J_r(\varepsilon) \cos \alpha}, \quad (10)$$

$$\max = \frac{F_a}{z J_a(\varepsilon) \sin \alpha}. \quad (11)$$

Sheval (Sjöval Harald) was the first one who introduced the radial and axial integral and its calculation.

Radial J_r and axial integral J_a are the values which are in the function of parameter ε (load distribution factor) and the units for determination of these integrals are:

$$J_r(\varepsilon) = \frac{1}{2\pi} \int_{-\varphi}^{\varphi} \left(1 - \frac{1}{2\varepsilon} (1 - \cos \psi) \right)^n \cos \psi \, d\psi, \quad (12)$$

i

$$J_a(\varepsilon) = \frac{1}{2\pi} \int_{-\varphi}^{\varphi} \left(1 - \frac{1}{2\varepsilon} (1 - \cos \psi) \right)^n d\psi. \quad (13)$$

Value of radial integral J_r is in the function of load distribution factor ε and its values for line contact are shown in table 1.

J_r	Line contact			
ε	Harris and Kotzalas	Koshelj	Paper [9] $n=10/9$	Paper [9] $n=1/0.925$
0	1/z	1/z	1/z	1/z
0.1	0.1268	0.1274	0.126406	0.127376
0.2	0.1737	0.1744	0.173175	0.174432
0.3	0.2055	0.2063	0.204958	0.206351
0.4	0.2286	0.2295	0.228038	0.213746
0.5	0.2462	0.2453	0.244799	0.246173
0.6	0.2576	0.2568	0.256362	0.257602
0.7	0.2642	0.2636	0.263236	0.264256
0.8	0.2662	0.2658	0.265492	0.266188
0.9	0.2629	0.2628	0.262664	0.262890
1	0.2519	0.2523	0.252530	0.251962
2.5	0.1061	0.1075	0.108305	0.106107
5	0.0536	0.0544	0.054901	0.053588
∞	0	0	0	0

Table 1. Values of radial integral for line contact

4. LOAD DISTRIBUTION IN CYLINDRICAL ROLLER BEARING AND RESULTS

Figure 4. shows the algorithm for determination of load distribution to each roller.

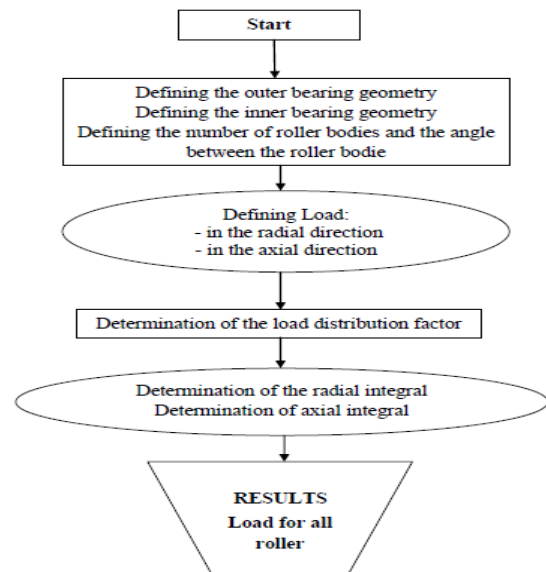


Figure 4. Load distribution for each roller

The view of double-row cylindrical roller bearing for machine tools main spindle assembly, designated as: **SKF 3011 NN TN/SP** with numerical rolling elements is shown in figure 5.

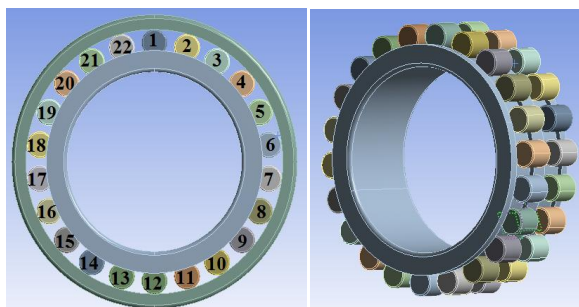


Figure 5. View of double-row cylindrical roller bearing

Load distribution per bearing rolling elements was made for load distribution factor $\varepsilon=1$ and radial load of 2000 N, what is 2/3 of the total radial load of the spindle. Cylindrical roller bearing belongs to the group of radial bearings and it is usually accommodated in pair with ball bearings when it is necessary to obtain high radial stiffness and this is the basic reason for the mathematical model to include the fact that 2/3 of load is transferred via it. Figure 6 shows the load distribution per rolling elements depending on their position.

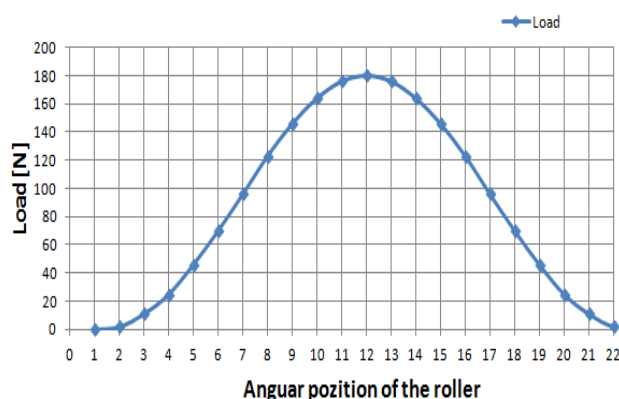


Figure 6. Distribution of radial load per rolling elements depending on their position.

5. CONCLUSION

The paper shows the mathematical model for determination of load distribution per rolling elements of roller bearing for machine tools main spindles. Based on the results it may be concluded that the load distribution factor plays an important role in the load distribution, what is in the function of bearing preloading. The load appearing on rolling bodies above meridian plane has an opposite direction in relation to those being under the meridian plane. It can be also concluded that the load on rolling bodies above meridian plane is dropping down up to the roller which is the furthest from meridian plane.

6. REFERENCES

- [1] Blanuša, V.: *Analiza ponašanja cilindrično valjkastih ležaja za specijalne namene*, Doktorska disertacija, Fakultet tehničkih nauka-Noví Sad, 2017.
- [2] Stribeck, R.: *Ball bearings for various loads*, Trans. ASME 29, pp. 420-463, 1907.
- [3] Sjövall, H.: *The Load Distribution within Ball and Roller Bearings under Given External Radial and Axial Load*, Teknisk Tidskrift, Mekanik, Hefte. 9, Pages: 1-6, 1933.
- [4] Макушин, М. В.: *Упругие перемещения и напряженное состояние в местах силового контакта деталей*, Расчеты на прочность в машиностроении II, Москва, 1959.
- [5] Ковалев, П. М., Народецки, З. М.: *Расчет высокоточных шарикоподшипников*, Машиностроение, Москва, 1975.
- [6] Кошелёв, В. М.: *Подшипники качения*, Наука и техника, ISBN: 5-343-00926-3, Минск, 1993.
- [7] Harris, A. T., Kotzalas M.: *Rolling bearing analysis: Essential Concepts of Bearing Technology*, Fifth edition, Taylor&Francis Group, USA, ISBN: 0-8493-7183-X, 2007.
- [8] Ricci, C. M.: *Internal Loading distribution in statically loaded ball bearings subjected to a centric thrust load: Numerical aspect*, International Journal of Mechanical, Aerospace, Industrial, Mechatronic and Manufacturing Engineering, Vol. 4, No. 3, Pages: 322-330, 2010.
- [9] Milisavljević, B.: *Hercova teorija kontakta i analiza raspodele opterećenja*, Nepublikovani materijal, Novi Sad, 2017.

Authors: DSc Vladimir Blanuša, DSc Branko Milisavljević prof. professional studies, DSc Branko Savić prof. professional studies, High technical school of professional studies, Školska 1, 21000 Novi Sad, Serbia, Phone.: +381 21 4892 511, Fax: +381 21 4892 515.
E-mail: blanusa@vtsns.edu.rs; savic@vtsns.edu.rs

DSc Milan Zeljković full prof., DSc. Aleksandar Živković assoc.prof., University of Novi Sad, Faculty of Technical Sciences, Department of Production Engineering, Trg Dositeja Obradovica 6, 21000 Novi Sad, Serbia, Phone.: +381 21 450-366, Fax: +381 21 454-495.
E-mail: milanz@uns.ac.rs; acozy@uns.ac.rs

DSc Sandra Sovilj-Nikić, scientific associate, Iritel a.d. Beograd, Batajnički put 23, 11080 Belgrade, Serbia, Phone.: +381 64 2302938, Fax: +381 21 454-495.
E-mail: sandrasn@eunet.rs

ACKNOWLEDGMENTS: In this research, part of the research results for the project, "Modern approaches in the development of special bearing solutions in mechanical engineering and medical prosthetics" TR 35025, which was financed by the Ministry of Education, Science, and Technological Development for the Republic of Serbia.

Cerjakovic, E., Topcic, A., Lovric, S., Heric, M.

DESIGN AND STARTING UP OF AUTOMATED ASSEMBLY LINES IN THE AUTOMOTIVE INDUSTRY

Abstract: *In order to maintain and improve the competitiveness of its products, the production companies strives to minimize the total production costs. In some industrial branches, this requirement is particularly pronounced. Due to global business, a large number of competing manufacturers, constant product improvement requirements, limited costs, etc., the automotive industry is the one of the most demanding and the most turbulent industry sectors. Automation of all manufacturing processes in the automotive industry is a long-term trend that, in spite of high investments, ultimately ensures a reduction in total production costs respecting the requirements set versus the products quality level. However, implementation of this approach is associated with a number of problems, where designing and starting up of such complex systems is a special challenge. One of the approaches that provides an adequate solution to above mentioned problems is based on the application of parallel design, on the development and the optimisation of the control codes and algorithms at an early designing stages of the of the production process. In this way, in the earliest phases of the development and implementation of the project, with certain degree of accuracy, the relevant characteristics of the production are established, which allows preventive action and elimination of any defects and unwanted characteristics. This systematically conceived methodology is known under the pseudonym of "digital factory", and comprehensively presentation of its characteristics and the specific ways of its implementation in automotive industry is presented in this paper.*

Key words: *competitiveness, automotive industry, production/assembly lines, starting up, digital factory*

1. INTRODUCTION

The contemporary consumer society with permanent radical demands has shaped the global economy for the last three decades, and thus directly influences the processes of production of physical products. Manufacturers acting on the local, and especially on, the global market are forced to offer innovative, complex, multifunctional and individualized products to the modern customer, which, in addition, must possess the characteristics of a market competitively product, i.e. product need to be: high-quality, cheap, reliable, secure and desirable. According to [1], with a view to achieving, maintaining or improving existing company positions in relation to competition, companies are forced to continuously systematically upgrade existing or develop new products, taking in to account to finding a compromise between three essential aspects: price - quality - time, with preconditions to achieve a certain degree of adaptability, i.e., readiness to respond quickly to the market demands.

Thanks to the specific demands placed to all members in the production chain, the automotive industry is surely positioned as one of the leading industries in global industrial production that generates and applies new specific strategies and methods to increase the efficiency of all segments of direct production as well as related activities. In this way, by upgrading the existing ones and application the new strategies and methods, it is possible to efficiently and economically fulfil the specific goals of this type of production: large quantities of products, production without stock, forced tact, production without mistakes,

forced trend of reducing the costs of the components over time, etc. The fulfilment of the aforementioned requirements has resulted in a wide application of dedicated production equipment in the automotive manufacturing facilities, and the obvious representative of that trend are the automated assembly lines, Figure 1. It is necessary to emphasize that in this case the total connection of a few assembly cells synchronized that are working in a forced manner into a single production system is implied, and that detection only one fault requires the halt of total production. Such automated assembly lines are conceived as flexible manufacturing structures due to the production and assembly of different product variants with a slight influence of replacement of tools on the production process, [2].

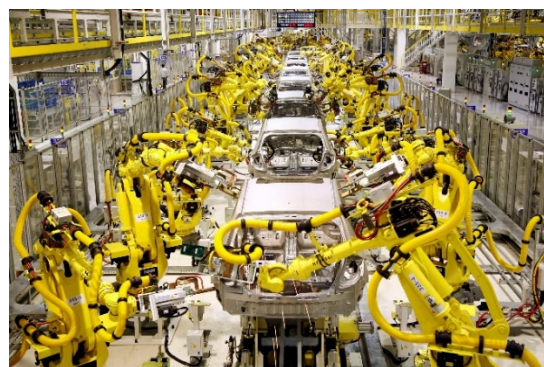


Fig. 1. Example of automated assembly lines in the automotive industry

Due to its function, the importance and complexity of development, design and adaptation to the new demands of such complex production lines is a long-

lasting and complex task. Namely, the necessity of applying a tool which has the possibility to enable development and analysis of an intelligent, lean and efficient production system at the preliminary design phase of project has emerged. One of the potential solutions to this task was to apply the concept of a digital factory.

2. DIGITAL FACTORY

By constantly advancing of the science and technology, the idea of Computer Integrated Manufacturing (CIM) has been improved daily and experienced various transformations and mutations. One such transformation of the CIM concept two decades ago became known as the concept of a digital factory, which according to VDI 4499 is defined as: „ a general

name for a global network of digital models and methods, including simulation and 3D visualization, whose purpose is to fully plan, realize, manage, and continuously improvement all essential processes and resources that are in interaction with the product“.

In essence, the technology of a digital factory is based on the application of a virtual factory that integrates models of products and devices that are simulated based on the planned production process so that the ultimate output of this activities is a developed process whose results need to be utilised by "real" production. Conceptual realization the digital factory model is presented on the Figure 2. In addition to the aerospace industry, the concept of a digital factory in the last two decades has the highest practical application within the automotive industry.

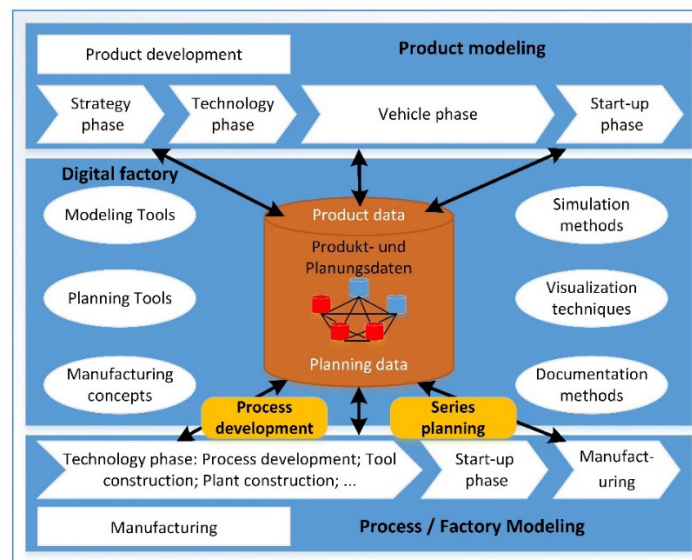


Fig. 2. Digital factory integrator of product and process development, [4]

3. AUTOMATED ASSEMBLY LINES WITH DIGITAL FACTORY

Given the numerous advantages and opportunities offered by automated assembly lines, they have become a concept on which is based a modern manufacturing in the automotive industry. However, the application of a forced tact, as well as the synchronization of all manufacturing/assembly processes is very complicated to accomplish and requires a complicated designing procedures that will be presented below.

3.1 Digital factory in automotive industry

The level of information that can be generated using the concept of a digital factory in the earliest stages of products development (e.g., the stage of development of conceptual design), allows "with a little delay" the design of the production processes for developed products. Thanks to the above mentioned, the integration of various *CAX* systems into the concept of a digital factory has been significantly applied to a series of developmental and accompanying processes in the automotive industry. The mentioned integration of all developmental and accompanying processes into

one entity is the main adute that the concept of the digital factory fully replaced the principle of "insular" product development and manufacturing process that was applied during the 1990s, [4].

By applying the new concept is enabled continual adjustment-updating of real and digital models, related strategies and solutions during the process of product development, as well as, the planning of the technological processes and realization of the production of the developed product. According to [5], within the automotive industry, the concept of a digital factory is applied in the following areas:

- Design of factory layout;
- Implementation of Factory-DMpU (Digital Mock-Up) compiling of all data, formal examining, joint alignment, CAD realization, delivery of new status;
- Logistical processes (planning and management of warehouses, planning and simulation of material flows (macro level), simulation of material flow (micro level), planning and development of resources for work;
- Planning of technological processes based on deformation of metals (product analysis, feasibility analysis of technological process, simulation of technological process, development of tool

kinematics, tool construction);

- Car body production planning (product analysis, technology process planning, layout development, quantity determination, capacity availability simulation, robot moving simulation and offline programming);
- Planning of car painting (product analysis, testing of painting possibilities, simulation, planning of 3D Layout and painting plants);
- Planning of the production of sub-assemblies (product analysis, planning of technological process and plant planning, simulation of material flow on a micro level, NC-simulation);
- Planning of final assembly of the car (product analysis, plan of implementation of technological processes, solution presentation, development, planning and analysis of Layout, of working tools, of ergonomics, planning of material needs by default production cycle).

In view of the characteristic process structure that is necessary to realize, in the following text, will be presented the issues of the planning of the car bodywork production (Figure 3) by implementation of different production technologies. At the same time car bodywork is conceived for assembly on the automatic assembly line.



Fig. 2. Car bodywork

3.2 Design of automated assembly lines

Considering to the large-scale and massive character of production in the automotive industry, timely planning of production is of utmost importance because relatively small savings per unit of product with regard to the number of pieces produced are profitable and justified. Consequently, the process of optimization must be carried out at an early stage of the preliminary design of production concept, which is extremely complex because of:

- usage of production equipment that often does not even exist physically,
- application of concentration of procedures during realization of the production,
- manufacturing with a forced tact,
- automatic stoppage of the entire production line, which are often consist from several dozen of manufacturing cells, if a fault is detected in the production,
- application of internal standards that strictly define certain parameters, procedures, mode of realization,

etc.

Considering all of the above mentioned issues, the designing process of assembly lines can be summarized on:

1. management of 3D CAx models;
2. Planning of investment realization costs and production costs;
3. Planning of manufacturing processes (planning of processes and products through the application of rules, integration of calibration and collision analysis, tact);
4. Virtual Start -Up / Start-Up.

3.2.1. Management of 3D CAD models

Given that projects related to the production of the same type of car are carried out at different production locations and have many working projects derived from main project, it is extremely important to apply a clear way of managing of 3D CAx models in order to realize and follow the course of the project without any problems.

As the first important prerequisite for the identical creation of 3D CAx models is to set the model in space according to the characteristic coordinate system:

- *HallZero* – in each 3d CAx model it is necessary to set the zero position of the industrial hall (the mark where the plant is located in order to correctly know hls_hallzero) the position of the assembly line in the space, Figure 3;
- *FacilitieZero* – it is necessary to set the Word Frame cells to indicate the zero Point (FacilitieZero) that is used for orientation of all 3D CAx models within assembly line, Figure 3;
- *AutomobilZero* – For models in which any segment of the car is used, all models are set to the zero point of the car (according to DIN 70000) as shown in Figure 4. This parameter is extremely important for assembly lines. Namely, due to the constant delivery of new products which request manipulation within assembly line and for which a car zero coordinate system is defined, it is necessary to precisely define their positions that are used in accordance with the given tolerances for calculating of the compensation parameters for all manufacturing equipment within the assembly line which most often has a fixed position. In this way, the positioning error decreases to the smallest value.

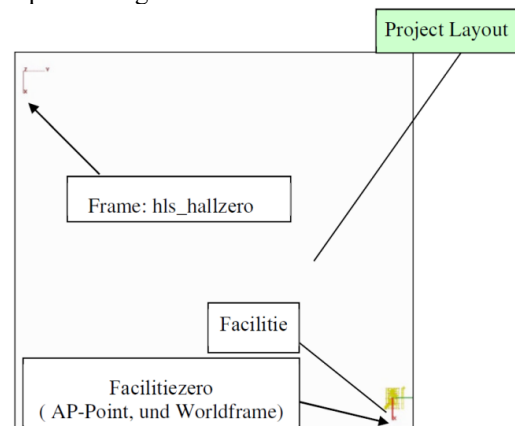


Fig. 3. General coordinate system of the plant

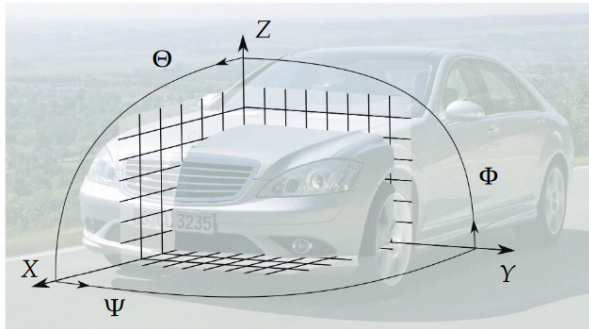


Fig. 4. Basic coordinate system of the car

It is necessary to state that the all available data necessary for designing the production process in its entirety are used simultaneously by both direct car makers and all subcontractors that are integrated into the process of development, planning, and production realization. The general model of the data structure is given on the Figure 5.

All the aforementioned parties that participating in the realization of a concrete project of a digital factory, with the aim to fulfil the project requirements, simultaneously generate a number of alternative solutions from their field of activity that send on to the superior level to be updated and to generate the current state of the project. This state of the project is adopted by the main project management at given time and it becomes the approved state of the project, Figure 6.

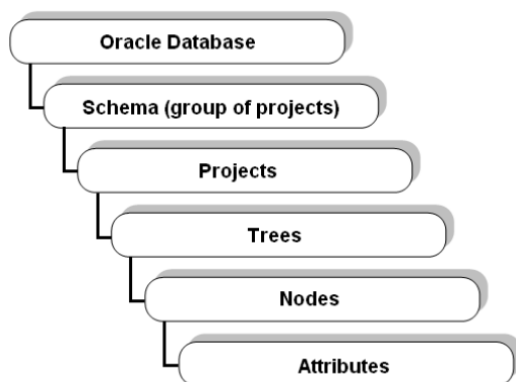


Fig. 5. General data structure of project of a digital factory

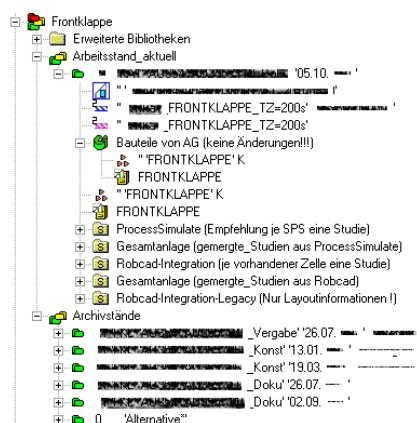


Fig. 6. Data structure in Tecnomatix/Process Design (Siemens)

For this reason, internal rules have been created that regulate the way of marking, storing, exchanging and using of a 3D CAX models for the application of the concept of a digital factory.

3.2.2. Planning of investment realization costs and production costs

Since the complete production structure is based on 3D data management, the way of determining costs is done by integrating already defined unit costs and procurement costs for each component of the assembly line. Costs are divided into:

- Costs of work equipment (expressed through costs with / without costs of construction),
- Costs for non-cell elements (protective fence, PLC, etc.),
- "The superior" costs (transport, production management, etc.),
- Plant-specific costs.

Most of these data are only available to a direct automaker and are the basis for negotiating with suppliers.

3.2.3 Planning of manufacturing processes

The designing of production processes according to the previous presentation is complex and it can be divided into subprojects i.e. 4 phases:

- 1st phase – the feasibility study based on the coarse planning and concept creation;
- 2nd phase - fine planning / simulation;
- 3rd phase – simulation / Offline - programming;
- 4th phase – delivery, final status.

Phase I – the feasibility study based on the coarse planning and concept creation is the process of generating of 3D CAX models where all the models of products and elements necessary for the realization of the manufacturing process are integrated into a single entity, positioned on their places, kinematic functionality of individual elements is established, specific points and coordinated systems are inserted and defined, as well as the analysis of possibility of realization of the production process is carried out. After the realization of afore mentioned procedures it is necessary to generate a checklist and transfer it to the next phase.

Phase II – fine planning / simulation is a process based on generating of production process simulation with special emphasis on process analysis within the assembly line. At this stage, all the rules and order of the assembly process are established, as well as the trajectories of the movement of individual elements are created. Here it is necessary to state that due to its flexible application the most commonly used manipulative element with production as well as manipulative tool is the industrial robot. Therefore, at this stage, as a first step, two different types of calibration values are introducing with the aim to minimize the differences in the positioning of the model in reality and on the 3D CAX model:

- Calibration of the plant – determining of the actual position of the model on the spot and its correction

in the 3D CAX model. Two specific cases may appear in this step:

- Calibration of industrial robots when the same tool is used by several industrial robots;
- Calibration of tools when one industrial robots use several different tools;
- Calibration of the industrial robot – by usage of mathematical alignment due to the presence of tolerances (lengths and angles) between individual axes of an industrial robot that occur when parts are being fabricated.

The next stage of the production process planning is based on the definition of real movement of industrial robot, which requires the usage of a RCS-Module (Real Controller Simulation), which is essentially an auxiliary module that has the task to correct the movement i.e. the trajectory of the executive member (end effector) of industrial robot in accordance to required load, speed and acceleration.

Solving the calibration problem using the RCS-Module provided all preconditions for collision-free movement analysis. Given that each car manufacturer has its own internal rules for setting conditions for collision-free movement analysis, in the Table 2 are given the parameters used for mentioned simulations within the VW group.

Parameter	Values
Time Raster for detection	0,2 [s]
Tolerance area	5 [mm]
Collapsing tool spacing	20 [mm]
Secondary cable	50 [mm]
Protective fence	100 [mm]
The body of a robot	100 [mm]

Table 1. Parameters for detection of collision of the general elements of a digital factory

Furthermore, it is necessary to conduct an analysis of the movement of industrial robots and to establish safety zones on the places where possibility of disruption of the safety collision space exist during realization of production processes. Therefore, it is necessary to define clear procedures that do not allow presence and/or movement of more than one industrial robot within certain security zone at the same time.

The next step at this stage of the production process planning is to determine the load on an industrial robot by determining of the centre of gravity, weights and orientation of loads of industrial robot.

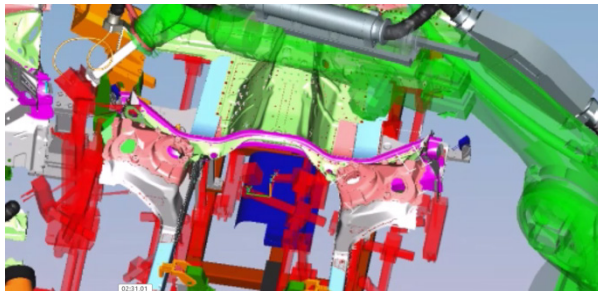


Fig. 7. Detection of collision of parts

By applying all the above elements, all preconditions

for determining of the tact of assembly line are met. Presentation of the final concept of solving a specific task and the delivery of the same to the superior level signifies the completion of this phase.

Phase III – The simulation / offline programming represents the final stage of the production process planning in which all current 3D CAX models are integrated within assembly line and the errors detected during second phase of realization are eliminated. Realizing of these activities often means correcting of 3D CAX models of individual components.

For purposes of simulation, to the obtained 3D CAX model are:

- added instructions for communication with the superior PLC;
- defined program structures required for control of industrial robot;
- defined the correction values for: TollFrame, BaseFrame and Load Definition;
- generated driver for industrial robots located in the assembly line in such a way that the BaseFrame of robot is zero-coordinate system of the car, Figure 8.

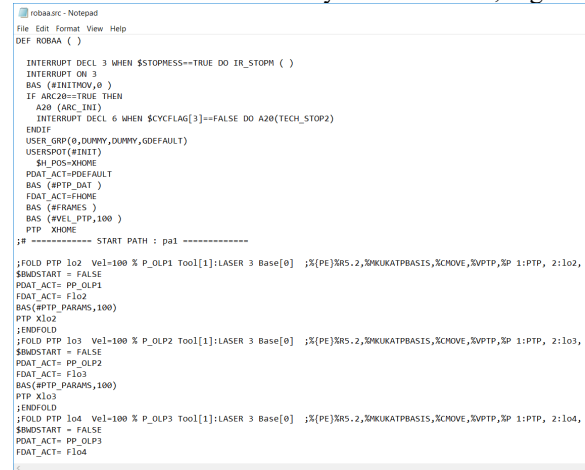


Fig. 8. Results of Off-line programming

Phase IV – Delivery, Final Status - represents the final act where are the generated documents and drivers integrated into the real production / assembly cells and are then released into operation. At this stage, it is necessary to make certain corrections of mistakes or deficiencies that are appear due to the difference between the 3D CAX models and the real state. Those corrections should be made on the spot if it is possible, and if it is not possible then corrections should be made in the simulation model.

3.2.4 Virtual launching of production

Lately, the application of the digital factory concept is expanding to the virtual launching of production processes, where the existing simulation model is extended by communication with real or virtual control elements (PLC, electronics, and the like). In this way it is possible to solve the possible errors caused by the complex interaction of a multitude of elements that make up the model of a certain digital factory. Currently it is a trend that the process of virtual launching of production is left as an auxiliary element

to the real manufacturing due to the possibility of storing the entire conditions and parameters that have led to a certain event and its presentation in the 3D environment. In this way, the detection and diagnosis of the system states greatly accelerates, in comparison to the approaches based on the storage of the process parameters themselves in a database and which are subsequently analysed to determine the causes that led to a particular event.

3.3 Features of simulation tools

The following simulation tools are used to design automated assembly lines in the automotive industry:

- *Tecnomatix* (Process Designer and Process Simulate) producer: Siemens,
- *RobotExpert*, producer: Siemens
- *Delmia*, producer: Desault System,
- *Robcad*, producer: Siemens.

Functions of simulation tools	Tecnomatix	RobotExpert	Delmia	Robcad
Database	+	-	+/-	-
Work out of database	+	/	+	/
Modelling	+/-	+/-	+	+
Modelling of kinematics movement	+	+	+	+
Static and dynamic collision detection	+	+	+	+
Human tasks simulation	+	-	+	+
Sequencing of operation	+	+	+	+
RCS Module and Robot Controller integration	+	+	+	+
Assembly and robotic path planning	+	+	+	+
Spot Welding	+	-	+	+
Costs planning	+	-	-	-
Virtual Commissioning	+	-	-	-
Compatibility with requirements of modern automotive industry	+	-	+	-
User friendly	+	+	+	-

Table 2. Characteristics of simulation tools for the concept of a digital factory

In accordance with its capabilities, the simulation tools can be used: with integrated databases (Connect), outside of integrated databases (Disconnect) and without any database (Independently). The aforementioned feature of integrating with/without databases is the main limit of further spreading of the application of these simulation tools to both large and small production systems. Namely, it is only worthwhile for large systems to have a simulation tool integrated with the database, since from the aspect of the administration it requires a considerable amount of data administration, but also the significant investment. Therefore, for clients with limited resources and the smaller scope of usage of the concept of a digital factory in this segment are developed simulation tools (such as: RobotExpert and Robcad) that are not integrated into the database.

4. CONCLUSION

The modern mode of manufacturing based on efficiency and low production costs generated a specific, complex and demanding generation of automatic assembly lines. The application of this concept of production in terms of production planning has completely marginalized partial production planning methods, and in the last two decades, the integral concept of production planning based on the application of the generated 3D production environment known under the name of a digital factory is increasingly being applied and developed.

Given that the integral concept is based on the parallel development and improvement of the CAX model from the conceptual project up to the end of the exploitation of production / assembly equipment, as well as on the cooperation of multiple development teams, the process of applying the concept of a digital factory within the automotive industry is fully defined by the application of internal standards. By this way any form of incompatibility between development teams are eliminated, and the same components required for assembly/production are in usage by different teams in parallel for practical application and/or for development/improvement of components.

A key factor for the successful application of the concept of a digital factory is the characteristic of the applied simulation tools. Namely, the possibility or inability to integrate the used simulation tools with the database as well as the extent of the technologies that can be stimulated are the most important factors to be taken into account when implementing the concept of digital factory in a concrete situation.

5. REFERENCES

- [1] Topčić, A., Tufekčić, Dz., Cerjakovic, E.: *Razvoj proizvoda*, Off-set Stamparija Tuzla, Tuzla, 2012.
- [2] Tang, Q., Li, J., Floudas, A. C., Deng, M., Yan, Y., Xi, Z., Chen, P., Kong, J.: *Optimization framework for process scheduling of operation-dependent automobile assembly lines*, Optimization Letters, Volume 6, Issue 4, pp. 797–824, April 2012.
- [3] Bracht, U.: *Ansätze und Methoden der Digitalen Fabrik*, pp. 1-11, Simulation und Visualisierung 2002 (SimVis 2002), Magdeburg, 2002.
- [4] Klauke, S.: *Methoden und Datenmodell der "Offenen Virtuellen Fabrik" zur Optimierung simultaner Produktionsprozesse*, VDI Verlag, Düsseldorf, 2002.
- [5] Kühn W.: *Digitale Fabrik: Fabriksimulation für Produktionsplaner*, Carl Hanser Verlag, München, 2006.

Authors: Assoc. Prof. Edin Cerjaković, Full Prof. Alan Topčić, Assist. Prof. Sladan Lovrić, M.Sc. Muhamed Herić, University of Tuzla, Faculty of Mechanical Engineering Tuzla, Univerzitetska 4, 75000 Tuzla, Bosnia and Herzegovina, Phone.: +387 35 320-920, Fax: +387 35 320-921.

E-mail: edin.cerjakovic@untz.ba; alan.topcic@untz.ba; sladjan.lovric@untz.ba; muhamed.heric@untz.ba

Crnokić, B., Grubišić, M.

FUSION OF INFRARED SENSORS AND CAMERA FOR MOBILE ROBOT NAVIGATION SYSTEM - SIMULATION SCENARIO

Abstract: *This paper presents a simulation scenario of a mobile robot navigation system. Navigation system is based on data collecting from three infrared sensors and camera, on which basis the fusion process of detection and avoidance of obstacles is realized. Information from camera was used to detect edges of the obstacles in the environment, while infrared sensors were used to measure the distance from the obstacles. Multilayer perceptron network, trained with backpropagation algorithm, was used for classification of detected obstacles. Experiment was realized through simulation in the simulation environment "Robotino SIM". The control algorithm was implemented in MATLAB. Sensor fusion has proven to be a much better solution than using infrared sensors or cameras separately. This experiment showed that the developed algorithm gives very good results (accuracy: 89.61%), and the navigation system itself performs required tasks of detecting and avoiding most of the obstacles on which it was tested.*

Key words: *Mobile robot navigation, Sensor fusion, Infrared sensors, Camera, Artificial neural networks*

1. INTRODUCTION

Navigation is one of the main problems in the design and development of intelligent mobile robots. Different navigation systems, based on one or more types of sensors, have been developed. Common problems of all these systems are robot self-location, route planning and environmental map construction. To solve this problems, accurate and reliable information are needed to determine the status of the environment in which mobile robot is located. [1] Navigation system of a mobile robot which is based on environmental data obtained from only one type of sensor is a major problem due to the disadvantages of each type of sensor individually. Solution of this problem is in combining multiple different types of sensors, or fusion of data (measurements) from multiple sensor.

There are many methods for fusion of data obtained from sensors used in a mobile robot, such as: Bayes' theory, Dempster-Shafer's (DS) evidence theory, weight factor model method, Kalman filter method, fuzzy fusion, artificial neural networks fusion method, etc.[2] Conventional numerical methods require quite a lot of computing time and large memory capacity, which creates difficulties and limitations in time-limited applications and functions. Artificial neural networks, including Support vector machines (SVM), Principal component analysis (PCA), etc., and their applications, in recent decades have an important place in many fields such as information processing and control systems.[3] In the paper [4] a multilayer model of neural network was introduced for avoidance of obstacles through increased learning. The MONODA system was implemented on the mobile robot NOMAD, where fusion of infrared and ultrasonic sensors was used to detect and avoid obstacles.[5] In paper [6] it is shown that the mobile robot NOMAD can categorize (note and classify) information from the environment obtained from different sensors (camera,

infrared sensors, microphone, contact sensors, ...), and link those categories to the values of the loaded signal patterns, and then take the appropriate action. Fusion of infrared sensors and sonar, based on preconfigured neural networks, is presented in the paper [7]. The use of computer vision, image processing and distance measurement using infrared sensors was used in [8] for detecting different shapes and colours. In the mobile navigation system NEURO-NAV feedforward neural network was also used to determine the approximate angular values between the robot motion direction and the corridor orientation to keep the robot on the path in the middle of the corridor. [9], [10] In the paper [11], neural units with higher-order synaptic operations have been used for image processing applications, i.e. for edge detection and for processing of edge detection data with Hough's transformation. Kohonen type of neural networks have been used to identify and provide coordinates of landmarks with use of laser sensing measurements. [12]

This paper presents a simulation scenario of a mobile robot navigation system based on artificial neural networks.

2. HARDWARE AND SOFTWARE USED

Hardware used in this paper includes mobile robot Robotino 2 (Figure 1.a)) and mobile PC (laptop), while the navigation system algorithm is implemented in programming environment MATLAB/Simulink and through software package RobotinoView2. Robotino SIM simulating environment was used for the simulation of navigation system based on artificial neural networks, implemented on Robotino in the environment cluttered with obstacles. Mobile mechatronic system Robotino 2 is manufactured by the German company "Festo Didactic". Robotino possesses various types of sensors, actuators and software interfaces which are at the highest level in the field of

mobile robotics. [13]

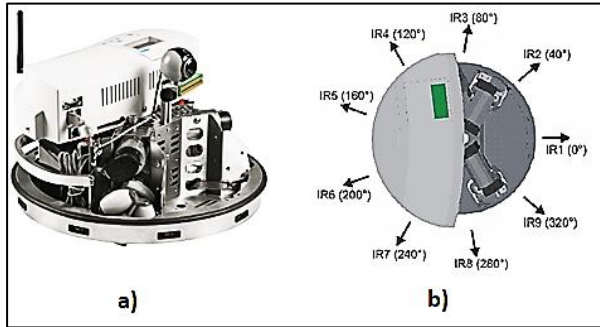


Fig. 1. a) Robotino®2, b) Arrangement of 9 IR sensors on Robotino [14]

Robotino moves with three independent, omnidirectional drive units, mounted at an angle of 120° relative to another drive. This drive system enables movement in all directions: forward, backward, sideways and rotation. The system can work independently as well as linked to the external computer via Wi-Fi connection. Robotino has various types of sensors. Some of these sensors come as standard equipment, such as: 9 infrared sensors (IR sensors - Figure 1.b)), VGA camera, incremental encoder and anti-collision sensor. Infrared sensors have the ability to detect objects at a distance from 3 to 40 cm, and 9 infrared sensors (IR1 - IR9) on robot are arranged on a chassis at an angle of 40° . Robotino is equipped with a camera Logitech C250 whose height and inclination can be regulated. Resolution can be set in Robotino View by selecting Camera (Block Camera) in the Program dialog box.

MATLAB (MATrix LABoratory) is a multifunctional numerical computational environment that allows manipulation of matrices, drawing of the functions, creating user interfaces and interfaces of programs written in other programming languages. [15] RobotinoView2 is an intuitive graphical programming environment designed specifically for the creation and implementation of control algorithms for mobile robot Robotino. [16] Robotino SIM is a Windows program for 3D simulation of Robotino in predefined virtual experimental environment. This program allows control of Robotino with the use of RobotinoView2 or MATLAB programming interface. [16]

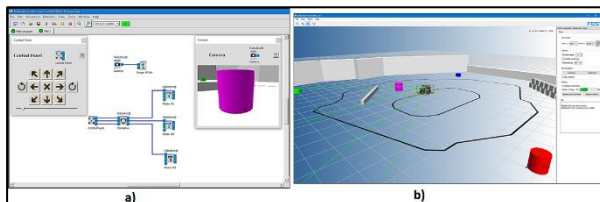


Fig 2. a) RobotinoView2 programming interface, b) Robotino SIM simulation environment

3. STRUCUTRE OF THE PROPOSED NAVIGATION SYSTEM

Infrared sensors (IR1 - IR9) and cameras installed on Robotino are used to provide information about robot's environment. In order to simplify the system

and to reduce the computational complexity of the control algorithm, in the experiment only three front IR sensors are used, labelled as IR1, IR2 and IR9 in Figure 1.b). Using only these three sensor proved to be sufficient to detect obstacles in front Robotino, or left and right of the Robotino.

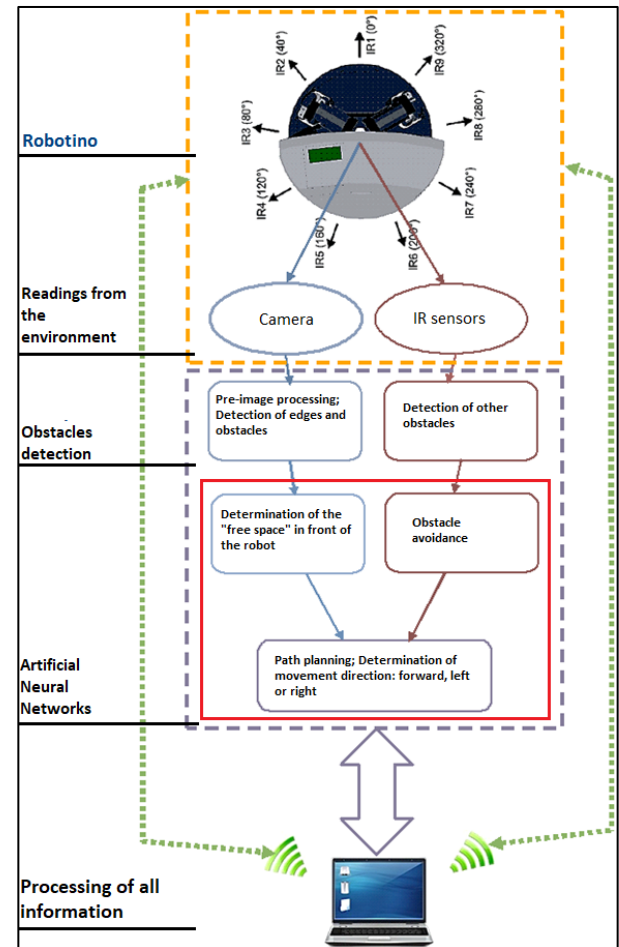


Fig. 3. Structure of the proposed mobile robot navigation system [16]

Obstacles detection is separated in two parts, for readings from the cameras and from IR sensors. The camera serves to detect landmarks and for localization, i.e. to detect edges, overhangs, and free space for unobstructed locomotion of the robot. IR sensors are used to measure distance from obstacles and to detect additional obstacles in free space in real time. For image pre-processing, i.e. for detection of edges and extraction of features Canny method is used combined with LPQ descriptor. Artificial neural network performs the task of learning the system to detect obstacles in the environment using the information obtained from the camera. After training the network, the system is able to decide whether the robot should continue to move forward, if no trace of obstacles is detected, or to avoid an obstacle if any of them is detected. Additional information on detected obstacles are coming from 3 IR sensors. These data sets merge with the previous information gathered from the camera to give the final confirmation to the robot which direction of motion should be selected. Computer (laptop) is used to process all information

(sensor information, pre-image processing, and all processes in neural networks), which is connected over Wi-Fi network with control unit of Robotino.

4. PROPOSED APPROACH AND RESEARCH METHODS

4.1. Collecting of information from the sensors

Robotino View program was used to collect images for training of the neural network and also to set image resolution. It is possible to lead Robotino to any position in the environment using the block "Control Panel". This block is connected to the omni-directional module "Omnidrive" which controls the three motors (Motor #1, Motor #2, Motor #3), and thus allows movement of the robot in any direction. The camera module is activated via the "Camera" block and the image is saved using the "Image Writer" block. In this module it is possible to select two image resolution, 320x240 and 640x480, and the resolution of the collected images for training of the neural network in the displayed navigation system is 320x240. Obtaining information from three infrared sensors is done in MATLAB. Where the three infrared sensors are marked in sequence as DistanceSensor0, DistanceSensor1 and DistanceSensor8. A voltage of 0.7 V or a distance of about 17 cm is taken as the reference distance at which the obstacle will be detected.

4.2. Avoidance of obstacles detected by IR sensors

Depending on whether one of the three IR sensors has detected the obstacle, an obstacle avoidance vector is defined, i.e., the velocities v_x and v_y are set in the direction of robot movement along x axis or y axis. The velocity values are expressed in mm/s . Depending on the direction of the obstacle avoidance, the speed values are 0, 100 or -100 mm/s . By combining different speed values, and considering the position of the obstacle, the robot can move in the following directions:

- forward, for $v_x = 100$, $v_y = 0$ (if there is no detected obstacle in front of the robot),
- right, for $v_x = 0$, $v_y = 100$ (if obstacle is detected on the left side of the robot),
- left, for $v_x = 0$, $v_y = -100$ (if obstacle is detected on the right side of the robot).

4.3. Artificial neural network

After data collection, two steps must be taken before using the training data:

- perform image pre-processing (Canny + LPQ),
- the data needs to be divided into different sub-groups.

To train the neural network in this experiment, 36 images were taken, and 9 more images of the same obstacles were taken for testing. Obstacles are divided into three image classes. The first class consists of cylinders (red, blue, yellow and pink). These obstacles should simulate obstacles of a similar shape in a real environment, such as furniture parts or a particular bulkhead. The second class of obstacles is formed by the images of obstacles that represent all types of walls.

This class should simulate obstacles in a real

environment such as walls, corridors, or furniture parts of a similar shape, such as cabinets. The third class are lines on the floor. This class should simulate negative obstacles, such as stairs edges.

The artificial neural network used in this experiment is a multilayer perceptron feedforward network for pattern detection with one input, one output and one hidden layer:

- Input layer consists of 256 input units (nodes) representing the image obtained after pre-processing. Since 36 pictures were taken for training, the network input is a 256x36 matrix.
- Hidden layer has 10 nodes.
- Output layer has 3 nodes. Nodes represent outputs that determine one of the three input image classes, and finally determine the direction of movement of the robot (forward, right or left).

5. ANALYSIS AND IMPLEMENTATION OF THE RESULTS

Table 1. shows the classification of obstacle detection by the type of obstacles, by the type of sensor that has detected an obstacle and by accuracy of detecting a certain obstacle.





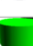

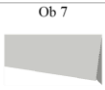


Type of obstacle	Detection			Sensor		Sensor (%)		Accuracy (%)
	YES	NO	Σ	Cam	IR	Cam	IR	
Ob 1 	19	1	20	5	14	26,32	73,68	95,00
Ob 2 	19	1	20	6	13	31,58	68,42	95,00
Ob 3 	19	1	20	5	14	26,32	73,68	95,00
Ob 4 	18	2	20	7	11	38,89	61,11	90,00
Ob 5 	20	0	20	4	16	20,00	80,00	100,00
Ob 6 	20	0	20	10	10	50,00	50,00	100,00
Ob 7 	19	1	20	11	8	57,89	42,11	95,00
Ob 8 	20	0	20	8	12	40,00	60,00	100,00
Ob 9 	0	20	20	0	0	0	0	0
Σ	154	26	180	56	98	36,36	63,64	85,56

Table 1. Classification of obstacles detection accuracy

This section shows simulation results of control algorithm tested in the simulation environment Robotino SIM. Since this is a demo version of this program, it is not possible to make an arbitrary environment. However, although the simulation environment is limited, the results have shown that this simulation environment is very suitable to simulate proposed control algorithm. The table was formed in a way that 20 attempts were made to detect each of the obstacles. Robotino approached obstacles from different sides, at different angles of approach and from

different distances. Successful detection of a certain obstacle is marked with "YES", while unsuccessful obstacle detection is marked with "NO". Successful detection is further classified according to the type of sensor (camera - "Cam", infrared sensors - "IR") that has detected an obstacle.

6. CONCLUSIONS AND RECOMMENDATIONS

The total number of attempts to detect all obstacles was 180. In 154 attempts obstacles were detected successfully, while 26 attempts were unsuccessfully (obstacles were not detected). Such a number of detected and undetected obstacles resulted in 85.56% accuracy of obstacle detection. Since the system is based on camera and infrared sensor fusion, it is also interesting to see the ratio of detected obstacles for each sensor. Three infrared sensors detected 98 times some of the obstacles (63.64%) while the camera detected 56 times some of the obstacles (36.36%). IC sensors had better efficiency when detecting the cylinders and the camera had better efficiency when detecting the walls. In the Robotino SIM environment it is not possible to manipulate obstacles by using certain commands, however, with the robot movements some of the obstacles could be "knocked down". These "knocked down" obstacles have become a good test for the proposed system since the neural network is not trained for such a "new" obstacles. In the case of detecting these and similar obstacles, the system proved to be the same accurate as in case of detecting obstacles that were represented to the neural network through the learning process. The sensor fusion has proven to be a much better solution than using only infrared sensors or cameras separately. The advantage of the IC sensor is expressed through a faster response, i.e. through a higher detection rate.

Disadvantages of the proposed algorithm are first of all the ability to move the robot only left, right and forward, without rotation, backward motion and combined motions. The most important upgrade to improve the system is the use of a greater number of IC sensors and omnidirectional camera that will have the ability to rotate and thus to cover a larger area around the robot. Future work can be focused on the application of other methods and sensors, which can be incorporated into the existing algorithm. Also, the use of other edge detection methods should be considered in the future work.

7. REFERENCES

- [1] B. Crnokić and S. Rezić, "Robots as an Important Factor in Development of Science and New Technologies," in *1th Internacionalna konferencija „NOVE TEHNOLOGIJE“ razvoj i primjena „NT-2014“*, 2014, vol. 1, no. 1, pp. 123–133.
- [2] Y. Qingmei and S. Jianmin, "A data fusion method applied in an autonomous robot," *2008 27th Chinese Control Conf.*, pp. 361–364, Jul. 2008.
- [3] Z.-G. H. Z.-G. Hou, M. T. M. Tan, M. M. Gupta, P. N. Nikiforuk, and N. Homma, "Neural network methods for the localization and navigation of mobile robots," *Can. Conf. Electr. Comput. Eng.* 2005., no. May, pp. 1057–1060, 2005.
- [4] I. E. T. Fujii, Y. Arai, H. Asama, "Multilayered reinforcement learning for complicated collision avoidance problems," *Robot. Autom.* 1998. *Proceedings. 1998 IEEE Int. Conf.*, pp. 2186–2191, 1998.
- [5] C. Silva and M. Cris, "MONODA: A Neural Modular Architecture for Obstacle Avoidance Without Knowledge of the Environment," *Proc. IEEE-INNS-ENNS Int. Jt. Conf. Neural Networks. IJCNN 2000. Neural Comput. New Challenges Perspect. New Millenn.*, vol. 6, pp. 334–339, 2000.
- [6] J. L. Krichmar, J. A. Snook, J. Jay, and H. Drive, "A Neural Approach to Adaptive Behavior and Multi-Sensor Action Selection in a Mobile Device," *Robot. Autom.* 2002. *Proceedings. ICRA '02. IEEE Int. Conf.*, vol. 4, no. May, pp. 3864–3869, 2002.
- [7] H. M. Barberá, A. G. Skarmeta, and M. Z. Izquierdo, "Neural Networks for Sonar and Infrared Sensors Fusion," *Proc. Third Int. Conf. Inf. Fusion*, vol. 2, p. 18–25., 2000.
- [8] J. Eduardo and C. Ortiz, "Visual Servoing for an Omnidirectional Mobile Robot Using the Neural network - Multilayer Perceptron," *Eng. Appl. (WEA), 2012 Work.*, pp. 1–6, 2012.
- [9] A. C. Meng, M., Kak, "Fast Vision-Guided Mobile Robot Navigation Using Neural Networks," *Proc. IEEE Int. Conf. Syst. Man Cybern.*, vol. 1, pp. 111–116, 1992.
- [10] A. C. Meng, M., Kak, "Mobile robot navigation using neural networks and nonmetrical environment models," *Control Syst. IEEE*, vol. 13, no. 5, pp. 30–39, 1993.
- [11] Z.-G. Hou, K.-Y. Song, M. M. Gupta, and M. Tan, "Neural Units with Higher-Order Synaptic Operations for Robotic Image Processing Applications," *Soft Comput.*, vol. 11, no. 3, pp. 221–228, Mar. 2006.
- [12] H. Hu and D. Gu, "Landmark-based navigation of industrial mobile robots," *Ind. Robot An Int. J.*, vol. 27, no. 6, pp. 458–467, 2000.
- [13] B. Crnokić, M. Grubisic, and T. Volaric, "Different Applications of Mobile Robots in Education," *Int. J. Integr. Technol. Educ.*, vol. 6, no. 3, pp. 15–28, Sep. 2017.
- [14] Festo Didactic, "Robotino-Workbook With CD-ROM Festo Didactic 544307 en," Denkendorf, 2012.
- [15] P.H. Pawar R.P. Patil, "Image Edge Detection Techniques using MATLAB Simulink," *Int. J. Eng. Res. Technol.*, vol. 3, no. 6, pp. 2149–2153, 2014.
- [16] B. Crnokić, "Development of the algorithm for control of mobile robot navigation with application of artificial neural networks," University of Mostar, 2016.

Authors: Assist. Prof. Boris Crnokić, Assist. Prof. Miroslav Grubišić, Matice hrvatske bb, 88000, Mostar Bosnia and Herzegovina, Phone.: +387 36 337-001, Fax: +387 36 337-012.
E-mail: boris.crnokic@fsre.sum.ba, miroslav.grubisic@fsre.sum.ba.

Cica, Dj., Borojevic, S., Sredanovic, B., Tesic, S.

ARTIFICIAL NEURAL NETWORKS MODEL FOR THE PREDICTION OF SURFACE ROUGHNESS IN MACHINING THIN WALLED PARTS

Abstract: Surface roughness is one of the most important factors which determines the quality and functional properties of machined products. In this study, artificial neural networks model was used to predict the workpiece surface roughness after the end milling process of thin-walled components. Three machining parameters, namely machining strategy, thickness of the rib and feed, were selected as input parameters, while surface roughness was output parameter. Furthermore, effects of same machining parameters were analyzed on machining time and predictive model was developed. The proposed prediction models were validated with the experimental data and it is observed that the present methodology is able to make accurate prediction of surface roughness and machining time by utilizing relatively small sized training and testing datasets.

Key words: neural networks, surface roughness, thin-walled parts

1. INTRODUCTION

In order to reduce the self-weight, improve the structure strength and replace large number of assembled component, many parts used in the aerospace industry are usually monolithic components. Machining of these monolithic structural components involves several thin-wall rib and flange sections which are dictated by design consideration to meet required strength and weight constraints. Although, thin-walled parts can be forged or cast to the approximate final shape and then finished by end milling process, nowadays they are machined from a raw block of material by end milling with roughing and finishing cuts and removing up to 95% of the weight of the initial block [1]. During milling process of this component, a high productivity can only be achieved by increasing the material removal rate (MRR) as much as possible. However, at high MRR conditions static and dynamic problems often occur due to the low rigidity of the thin-walled structures. As a consequence, unacceptable surface roughness, large deviations in dimensional accuracy of the machined part or even part damage may occur.

Because of their poor stiffness, the machining of thin walled work pieces is complicated, where periodically varying cutting forces excite the flexible plate structures both statically and dynamically and leading to significant deformations [2]. Budak [3] presented models for the peripheral milling of very flexible, cantilevered plates with slender end mills. Aijun and Zhanqiang [4] proposed an analytical deformation model suitable for static deformations prediction of thin-walled plate with low rigidity. Ning et al. [5] applies the finite element method (FEM) to the quantitative analysis and calculation of the deformations of a typical thin-walled structure in the process of machining. Ratchev et al. [6] presented machining error compensation approach focused on force-induced errors in machining of thin-wall structures. The prediction algorithm takes into account the deflection of the part in different points of the tool path. Liu [7] proposed the three-dimensional

finite element models of a helical tool and a thin-walled part with a cantilever in order to predict the cutting deformation of a thin-walled part in milling process. Wan et al. [8] develop efficient strategies for controlling the force-induced surface dimensional errors in peripheral milling of thin-walled structures.

The end milling of thin-walled components is complicated, and major concerns that should be taken into consideration are the minimization of the machining time, while maintaining the accuracy and quality within acceptable limits. The tool path strategies and machining parameters are one of the most important parameters which strongly influences the surface roughness, as well as the machining time. Based on this information, in order to assure the best possible performances, in terms of productivity and quality, improvements on selecting the best tool path strategy and cutting parameters in end milling of thin-walled components can be observed. The objective of this paper is to study effects of tool path strategy as well as cutting parameters on surface roughness and machining time of thin-walled aluminum alloys. Afterwards, a predictive model for surface roughness and machining time using artificial neural networks (ANN) was proposed and validated with experimental results.

2. EXPERIMENTAL DESIGN AND SETUP

The experiments were performed on machining aluminium alloy 7075-T6. Due to its a relatively low cost high strength and density, thermal properties, etc. these aluminium alloy is widely used in aerospace industry. The tensile strength of this alloy is $\sigma = 560$ MPa, the modulus of elasticity is $E = 72$ GPa, the hardness is 150 HBW and its chemical composition is shown in Table 1. All experimental works were performed on a vertical 3-axis CNC milling machine fitted with a maximum spindle power of 11 kW, which has a maximum speed of 12 000 rpm. Prior to milling process, aluminum blocks were prepared by dimensions of 40×40×70 mm. The cutting tools used was solid

carbide square shoulder end mill SANDVIK CoroMill Plura R216.32-10025-AK32A H10F. The cutter has a diameter of 10 mm, flute helix angle of 25° and an axial rake angle of 13.5°.

In this study, three levels of tool path strategies (zig-zag, parallel spiral and true spiral) five levels of the feed (150, 179, 250, 321 and 350 mm/min) and five levels of thickness of the rib (0.50, 0.65, 1.00, 1.35 and 1.50 mm)

were used as the variables for surface roughness modeling. An orthogonal array L_{33} has been used for design of experiments (DOE). The surface roughness was measured with a stylus type instrument Innovatest R130. The surface roughness response is the average reading of three consecutive measurements. The experimental setup is shown in Fig. 1, and the DOE and measured results are provided in Table 2.

Al	Zn	Mg	Cu	Fe	Cr	Si	Mn	Zr	Ti
86.9-91.4	5.1-6.1	2.1-2.9	1.2-2.0	0-0.5	0.18-0.28	0-0.4	0-0.3	0-0.25	0-0.25

Table 1. Chemical composition of 7075-T6 alloy (in % weight)

No.	Tool path strategy <i>S</i>	Thickness of the rib <i>a</i> (mm)	Feed <i>f</i> (mm/min)	Surface roughness <i>R_a</i> (μm)	Machining time <i>t</i> (min)
Training data set					
1.	Zig-zag	1.35	179	1.17	42.65
2.	Zig-zag	0.65	321	0.55	24.85
3.	Zig-zag	0.50	250	0.49	30.91
4.	Zig-zag	1.50	250	1.41	31.11
5.	Zig-zag	1.00	350	1.06	23.00
6.	Zig-zag	1.00	250	1.12	31.21
7.	Parallel spiral	1.00	250	1.37	31.21
8.	Parallel spiral	0.65	179	1.98	31.75
9.	Parallel spiral	0.65	321	2.96	18.90
10.	Parallel spiral	1.35	321	2.07	18.65
11.	Parallel spiral	1.50	250	2.03	22.76
12.	Parallel spiral	1.00	150	2.37	36.96
13.	Parallel spiral	1.00	250	2.35	23.46
14.	Parallel spiral	1.00	250	2.17	23.46
15.	True spiral	0.65	179	0.38	68.80
16.	True spiral	1.35	179	0.83	67.73
17.	True spiral	1.35	321	0.69	37.86
18.	True spiral	0.50	250	0.5	49.58
19.	True spiral	1.00	150	0.71	80.51
20.	True spiral	1.00	350	0.56	35.46
21.	True spiral	1.00	250	0.67	49.38
22.	True spiral	1.00	250	0.68	49.38
Testing data set					
1.	Zig-zag	0.65	179	0.49	42.66
2.	Zig-zag	1.35	321	1.16	24.78
3.	Zig-zag	1.00	150	0.97	50.35
4.	Zig-zag	1.00	250	1.35	31.21
5.	Parallel spiral	1.35	179	2.21	31.33
6.	Parallel spiral	0.50	250	2.18	23.60
7.	Parallel spiral	1.00	350	2.08	16.71
8.	Parallel spiral	1.00	250	2.53	23.46
9.	True spiral	0.65	321	0.40	38.21
10.	True spiral	1.50	250	0.83	48.28
11.	True spiral	1.00	250	0.71	49.38

Table 2. Experimental conditions and results

3. ARTIFICIAL NEURAL NETWORKS MODEL

The artificial neural networks (ANN) are a representation of the computational architecture and work of the human brain. ANN is a complex structure of highly interconnected processing elements called neurons which have several distinguishing features such as number of input signals, weight factor that is applied

to each input signal, activation function, transformation function, output signal and learning algorithm. Although various types of ANN models have been developed, the multilayer feed-forward ANN is the most popular and this model has been used in the present study. As can be seen from Fig. 2. feed-forward ANN has three types of layers: an input layer, one or more hidden layers and an output layer, consisting of nodes which processes the

input information and produces an output. Nodes are fully interconnected to each other, except that there are no connections between the neurons in the same layer. The input layer consists of the systems inputs and neurons in these layer transmit the information to the next layer as a value. A feed-forward neural network consists of one or more number of hidden layers, placed between input and output layers. Hidden layers represent the core of the ANN and consists of many neurons and the values associated with each neuron are estimated from the sum of the multiplications between input neuron values and weights of the links connected to that neuron. The output layer is the layer where the final output from the network are generated.

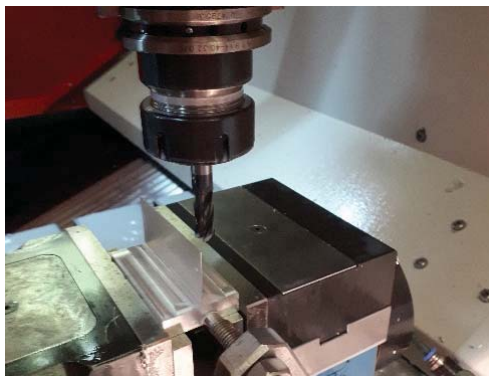


Fig. 1. Experimental setup

In order to obtain desired results, it is necessary to develop learning strategy for neural networks. There are many learning methods utilized in ANN and in this study back-propagation (BP) learning algorithm was used as the most popular technique for training feed-forward neural networks. BP algorithm is based on the principle on the error-correction learning rule where errors are minimized in a ANN output and modification of network values were performed according to the minimized values.

In this study ANN were used as an alternative way to estimate the surface quality and machining time in machining of thin-walled components. As shown in Fig. 2, neural network architecture consists of three different layers: an input layer, a hidden layer and an output layer. The number of neurons in the input and output layers is based on the geometry of the problem. So the input layer which receives the input variables thickness of the rib, feed and tool path strategy has three neurons. The number of neurons in the output layer is the same as the number of output parameters. In our case that is the corresponding surface roughness and machining time. This layer has one neuron because surface roughness and machining time have been evaluated individually. Several researchers have proposed different approaches for determining an optimal number of hidden layers for any application. However, there is no general rule for selection of the number of hidden layers and the number of neurons in this layer. Hence, the number of layers and the number of neurons present in the hidden layers have been determined by on a trial-and-error basis to obtain the best result.

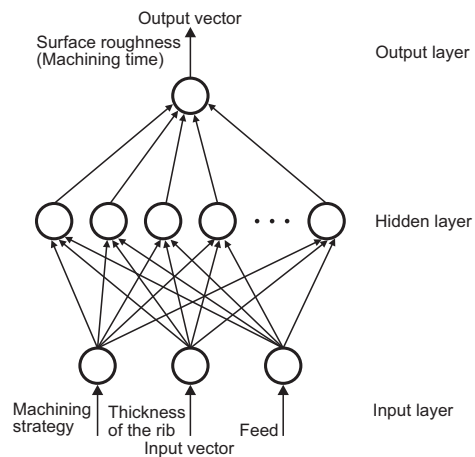


Fig. 2. Structure of feed-forward artificial neural networks

The experimental results data set was divided randomly in two groups from a total of 33 values: 22 training samples and 11 data testing samples. Data normalization is usually performed before the training and testing process begins, so input and output parameters were normalized within the range of ± 1 . For training the network, due its robustness the Levenberg-Marquardt algorithm (LMA) was used. Transfer function for neurons in hidden layer was hyperbolic tangent sigmoid function, whereas for output neurons it was pure linear. The stopping criterion for training was obtained when generalization stopped improving.

In order to estimate the prediction capability of the developed structures of the ANN models, errors were analyzed using three criteria: normalized root mean square error (NRMSE), absolute fraction of variance (R^2), mean absolute percent error (MAPE), and maximum absolute percent errors (MaxAPE). Optimization of ANN models were performed over the number of neurons in the hidden layer and numbers of hidden layers. The result showed that the network structure with one hidden layer with six neurons is more accurate and reliable for the prediction of the surface roughness and machining time performance measure, respectively.

4. RESULTS AND DISCUSSION

The predictions obtained from the ANN model described in the previous section are compared with the experimental data set that has not been used in training neural network. As can be seen from Fig. 3 the ANN predictions of surface quality are very close to the experimental results. The mean absolute percent error and normalized root mean square error were 5.7% and 0.151, respectively. Maximum absolute percent error was 13.3%. Absolute fraction of variance for surface roughness model was 0.98848 which indicate a very good fit between the ANN outputs and the target (measured) values.

Referring to Fig. 4, indicates the comparison of errors in prediction of machining time obtained using developed ANN model. The mean absolute percent error and

maximum absolute percent error were 2.1 and 5.6%, respectively. Normalized root mean square error was 0.0863 and absolute fraction of variance was 0.9982.

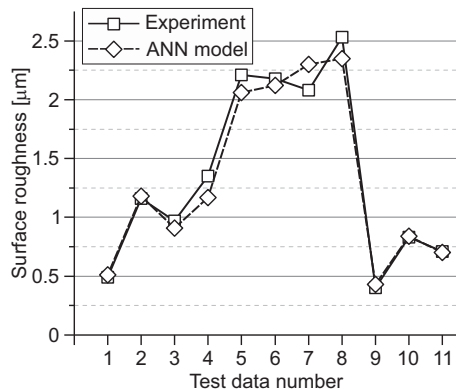


Fig. 3. Comparison of measured and estimated surface roughness

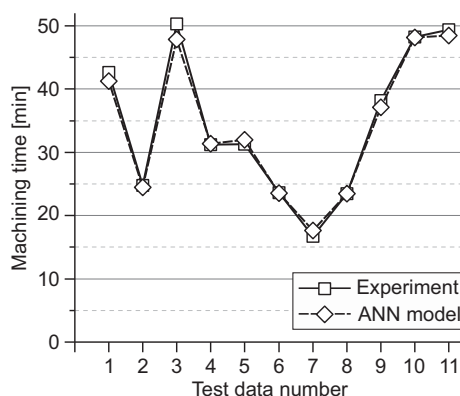


Fig. 4. Comparison of measured and estimated machining time

Hence, it is evident that predicted values from developed ANN models and experimental data are fairly close which indicates that the artificial neural networks are a good alternative for prediction of the surface quality and machining time in machining thin-walled components under the given set of machining conditions.

5. CONCLUSION

In this study, artificial neural network approach was used to predict the surface roughness and machining time of thin-walled aluminum alloys. The parameters such as tool path strategies, feed and thickness of the rib were used to develop the artificial neural networks based models. For this purpose, Taguchi's design of experiments was carried out in order to collect surface roughness and machining time values. For selected 3-6-1 architecture of feed forward neural network based on back-propagation algorithm a good agreement has been found between predictions and experimental data for the 11 cutting conditions used as a test data set. The statistical results namely, normalized root mean square error, absolute fraction of variance and mean absolute percent error were within an acceptable range and meet

the integrity of the ANN learning and testing stages. Thus, a very good agreement between the predicted and experimental data indicate supports the reliability of the developed ANN models. Future work should involve extending the predictive force model to include the large experimental data and considering the additional machining parameters.

6. REFERENCES

- [1] Seguy, S., Campa, F.J., López de Lacalle, L.N., Arnaud, L., Dessein, G., Aramendi, G.: *Toolpath dependent stability lobes for the milling of thin-walled parts*, International Journal of Machining and Machinability of Materials, Vol. 4, No. 4, pp. 377-392, 2008.
- [2] Ratchev, S., Liu, S., Becker, A.A.: *Error compensation strategy in milling flexible thin-wall parts*, Journal of Material Processing Technology, Vol. 162-163, pp. 673-681, 2005.
- [3] Budak, E.: *Analytical models for high performance milling. Part I. Cutting forces, structural deformations and tolerance integrity*, International Journal of Machine Tools and Manufacture, Vol. 46, No. 12-13, pp. 1478-1488, 2006.
- [4] Aijun, T., Zhanqiang, L.: *Deformations of thin-walled plate due to static end milling force*, Journal of materials processing technology, Vol. 206, No. 1-3, pp. 345-351, 2008.
- [5] Ning, H., Zhigang, W., Chengyu, J., Bing, Z.: *Finite element method analysis and control stratagem for machining deformation of thin-walled components*, Journal of Materials Processing Technology, Vol. 139, No. 1-3, pp. 332-336, 2003.
- [6] Ratchev, S., Liu, S., Huang, W., Becker, A.A.: *An advanced FEA based force induced error compensation strategy in milling*, International Journal of Machine Tools and Manufacture, Vol. 46, No 5, pp. 542-551, 2006.
- [7] Liu, G.: *Study on deformation of titanium thin-walled part in milling process*, Journal of Materials Processing Technology, Vol. 206, No. 6, pp. 2788-2793, 2009.
- [8] Wan, M., Zhang, W.H., Qin, G.H., Wang, Z.P.: *Strategies for error prediction and error control in peripheral milling of thin-walled workpiece*, International Journal of Machine Tools and Manufacture, Vol. 48, No. 12-13, pp. 1366-1374, 2008.

Authors: ¹Assoc. Prof. Djordje Cica, ¹Assist. Prof. Stevo Borojevic, ¹M.Sc. Branislav Sredanovic, ¹M.Sc. Sasa Tesic.

¹University of Banja Luka, Faculty of Mechanical Engineering, Vojvode Stepe Stepanovica 71, 78 000 Banja Luka, BiH, Phone: +387 51 433 000,

²University of Novi Sad, Faculty of Technical Sciences, Trg Dositeja Obradovica 6, 21000 Novi Sad, Serbia.

E-mail: djordje.cica@mf.unibl.org;

stevo.borojevic@mf.unibl.org;

branislav.sredanovic@mf.unibl.org;

sasa.tesic@mf.unibl.org

Hozdić, E.

CYBERNETIZATION OF MANUFACTURING SYSTEMS

Abstract: *Under the influence of globalization which brings many changes in all spheres of life and in the sphere of industrial production, manufacturing enterprises are forced to adapt their manufacturing structure these challenges in order to promptly and effectively respond to the complex demands of today's market, which is global and less national. Over time, it's developed different concepts of manufacturing systems. They were intended to respond to market demands in a time in which existed. Today, thanks to the developed information-communication technologies, manufacturing enterprises tend to structure their systems in a spirit of cyber-physical systems.*

This work presents a new concept for the restructuring of systemic and organization manufacturing structures in manufacturing enterprises. In the proposed concept is the role of man improved and the role of manager will be given to man, in real time. It is developed the basic concept of socio-cyber-physical systems of work that represents a building blocks for the new conception of an advanced manufacturing systems in a spirit of socio-cyber-physical systems (SCPS).

Key words: *Cybernetics, cyber-physical systems, digitalization, manufacturing systems, Subject*

1. INTRODUCTION

The term cybernetization refers to the application of scientific-theoretical knowledge of cybernetics and methodological concepts of system engineering. Cybernetics as a science directs production systems towards more efficient functioning and management of the development of the production system as a complex, dynamic, network and distributed system.

The concept of cybernetics derives from the Greek word *kybernáo*, which at the same time means managing, controlling, steering. In contemporary scientific terminology, the term cybernetics is introduced by Norbert Wiener in 1948 [1] through his book *Cybernetics or Control and Communication in the Animal and the Machine*. Wiener explains that under the term "organism" is also meant a combination of man-machine, and it follows that cybernetics is a science of management in living beings, machines and their combinations.

However, in today's literature there are different definitions that point to the diversity of the concept of cybernetics.

According to Bertalanffy's opinion, cybernetics is a management theory as part of a general system theory. Basically, such a concept of cybernetics is the use of feedback and information principles. In 1954, in his book *The Human Use of Human Beings, Cybernetics and Society*, Norbert Wiener approached the cybernetics of a wider circle of readers. Founded on these Wiener works, the cyberspace has become a major science of cybernetic management, regardless of their physical form. Cybernetics has been raised to a very high degree of abstraction where general principles and governance are defined and set. Peklenik defines cybernetics from the point of view of system control in real-time [2]. Under the term "control", Peklenik means the process we are organizing to operate on a "management object" with the effort to reach the object or the goals.

Product Cybernetics is oriented towards studying the principles and the legality of the management of technical-technological production systems. Today, its focus on the field of development and management in complex, distributed, complex and advanced production systems is very strong, based on real physical and cybernetic elements.

With globalization, the competitiveness of production systems undoubtedly increases, and the rapid development of science and information-communication technologies (ICT) open up new opportunities and challenges to successfully manage complex, distributed, network and advanced production systems. The global market demands greater efficiency of the above-mentioned production systems and better service support for such production systems. Global advances in the ICT and the Internet, as well as global market demands, at the same time create new momentum for the development of cybernetics itself, and its applications in the domain of modern production systems, their concepts and models [3].

The aim of this paper is cybernetization of manufacturing systems, definition of socio-cyber-physical manufacturing systems, definition of its building blocks and characterization of its relations to production, service, and social network, as well as smart environments. In this context, special focus is put on the role of human resources.

2. CYBER-PHYSICAL SYSTEMS

In the last two or three decades, several influencing attempts to reshaping industrial production have been published, which can be recognized as cornerstones of Industry 4.0 [4]. A review of the listed approaches and concepts of manufacturing systems are presented in the paper [5].

Recently, a new approach is emerging in terms of a cyber-physical production system (CPPS) [6], which upgrades in a way the mentioned attempts. It originates from the concept of cyber-physical systems (CPS) [7], and links physical and virtual components of a manufacturing system into a coherent whole.

Cyber-physical systems are a new generation of systems that integrate computer and physical capabilities [8].

Using the appropriate sensor and actuator technologies, these systems are able to receive direct physical signals and convert them into digital data and, on the basis of such information, enable management of systems in real time. They can share collected data in the form of information and make them available through digital networks, making in that way the Internet of Things [9].

CPPSs partly break with the traditional automation pyramid. The typical control and field levels, which include common PLCs (programmable logic controllers) close to the technical processes providing the highest performance for critical control loops still exist, while in the other, higher levels of the hierarchy a more decentralized way of functioning is characteristic in CPPS [6].

Contemporary manufacturing systems or factories are composed of a social and technological part. When designing factory, beside the technological system, which includes processes, machinery, tools, logistic means, etc., various social aspect must be considered, such as organizational forms, management structures, roles of employees, recruitment, education and training, knowledge and specific know-how, work instructions, human factors and ergonomics, safety, innovation management, etc.

Therefore, manufacturing systems can be characterized as socio-technological systems with three main types of relations: between people, between machines and between people and machines.

The social system and the technological system follow different laws: the first one follows the laws of social sciences, while the second one is subjected to the laws of natural sciences. Yet, the systems are correlated as the process of manufacturing requires the interaction of both. Thus, improving either of the systems independently cannot advance the system as a whole. Only by jointly developing both systems can the best match be achieved.

In this respect the socio-technological perspective is not only important while designing a system, but equally important in system's operations, learning and improvement.

Cyber-physical systems will introduce a cyber system into manufacturing systems. Thus, a transformation of manufacturing systems from a traditional socio-technological system into a new kind of socio-cyber-physical manufacturing system is anticipated. It will result in significantly changed roles of people or, better to say, human subjects in the next generation manufacturing systems.

3. SOCIO-CYBER-PHYSICAL MANUFACTURING SYSTEMS

The transition to new manufacturing structures, which will be based on the concept of cyber-physical systems, requires the development of new reference models of manufacturing systems. These models must enable: (1) the appropriate position of man in the manufacturing system, because his role in cyber-physical systems significantly changes, (2) digitization and cybernetization of existing (traditional) work processes, (3) development and realization of new "smart" functionality that enables digitization and cybernetization of work, (4) connectivity to "smart environments", (5) vertical linkage to integrated work structures, and (6) horizontal linkage to networks at different levels of action.

The role of people, or Subject [2], will change significantly in the future generation of manufacturing systems. Due to automation and digitization, in some processes the immediate influences of people are almost excluded. There is a question as to what will be the role of Subject in future manufacturing systems? It should be borne in mind that it is only the Subject that has the motive and the benefit of operating the manufacturing systems. Based on that I have to be very careful about the role of Subject in modeling and structuring the future generation of manufacturing systems, which will become socio-cyber-physical systems. Such an approach opens up a new space, cyber space, through which the Subject, as a social element and physical work systems (PWS), will be linked as a physical element. Such space can be enriched with new digitized and cybernetised functions such as real-time management, self-organization, self-diagnosis, prognostication, self-adaptation, etc. and (2) "unconnectively" connect to different network environments, such as Industrial Internet of Things (IIoT), service networks, production networks, etc., which open up new opportunities for action in the horizontal integration of manufacturing systems.

To understand the new concept of manufacturing systems, which is based on linking the social, cyber and physical environments of the manufacturing system, it is necessary to define the basic systemic manufacturing structures that are present in traditional production-business systems. Such system structures are: elementary work system (EWS) [2], autonomous work system (AWS) [10] and production system (PS). Peklenik defined the manufacturing system or the factory as a complexity adaptive manufacturing system (CAMS) [11]. The concept of CAMS envisages three organizational levels within the manufacturing enterprise (1) the operation level in which the basic EWS element exists, (2) coordination level (the AWS and service unit (SU) exist), and (3) the business level in which the key component is the manufacturing system. Such a structure is shown in Fig 1.

The EWS is horizontally integrated into a traditional organizational structure such as the Flexible Manufacturing System (FMS) and Dedicated Manufacturing Line (DML), and is horizontal connectivity to the online manufacturing structures (internet of things).

The vertical connecting of the operation and cyber level of the traditional manufacturing enterprise is ensured through the communication connectivity of the systemic manufacturing structures (AWS and EWS). Vertical integration of organizational manufacturing structure of the operation level into more organizational forms of co-ordination level is facilitated through the integration of FMS and DML into manufacturing departments and manufacturing plants.

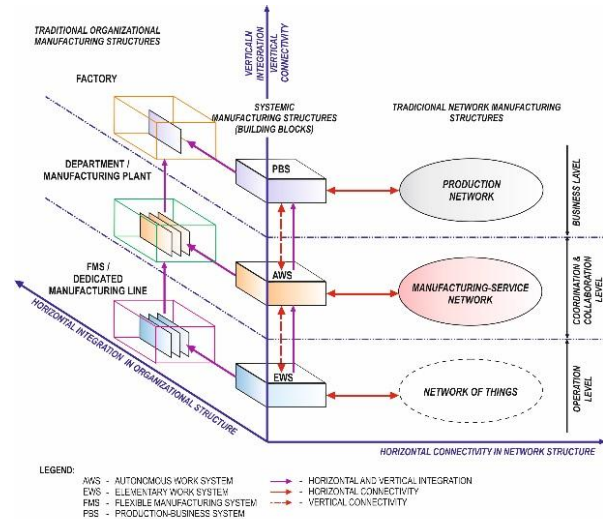


Fig. 1. Horizontal and vertical connectivity of traditional systemic manufacturing structures

AWS represents the systematic manufacturing structure of the middle part of the production company or its co-ordination level. Enable vertical connectivity of EWS to multiple system manufacturing structures (e.g. manufacturing system) or network manufacturing structures such as a manufacturing-oriented service network. AWS is horizontally integrated into the production plant/division and is horizontally connected to the network structure.

The system production structure of a traditional enterprise that represents the superior structure of AWS (and their EWS) is a production-business system (PBS). PBS as a basic element of the business enterprise level of traditional manufacturing enterprises enables horizontal integration into the organizational manufacturing structure of the appointed factory and horizontal connectivity of the enterprise to the network manufacturing structure of the named production network (PN).

Exceptional thinking about creating new concepts of manufacturing systems based on the integration of social, cyber and physical manufacturing environment is Fig 2.

Figure 2 illustrates a reference model for connectivity social, cyber and physical spaces and their systems to a cyber functional system manufacturing structure called socio-cyber-physical systems (SCPS). Thus structured system manufacturing structure is composed of three levels or spaces: social, physical and cyber space.

Physical space of SCPS contains systemic structures such as: physical system of elementary work system, physical system of logistics system (LS), physical system of service system (SS) etc.

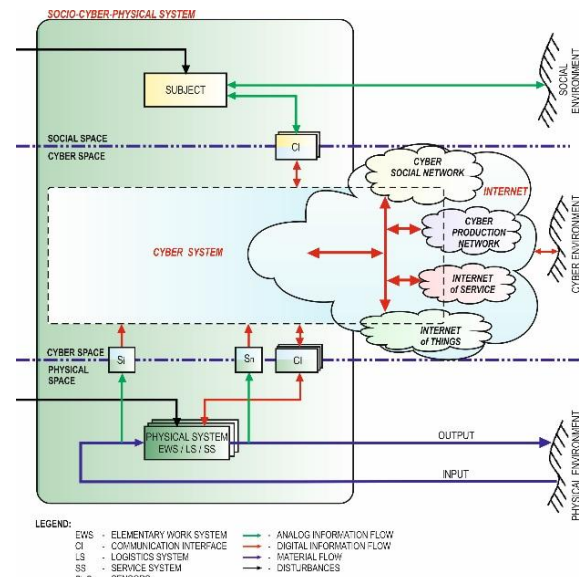


Fig. 2. Concept socio-cyber-physical manufacturing systems (SCPMS)

The cyber space, shown in Fig 2, is on one side connected to the physical space, on the other side with the social space. The systemic basis for the vertical connectivity of system manufacturing structures as well as their horizontal connectivity to different cyber network structures enables the establishment of a cyber system within the cyber space.

The cyber system of a manufacturing company can be defined as a three-tier structure with three levels: (1) operation level, (2) coordination & collaboration level, and (3) business level of cyber system.

The operation cyber level of cyber system contains cyber system structures in the form of a cyber system of EWS, cyber system of LS, cyber system of SS etc. These structures are horizontally connectivity to the Internet of Things network, which is part of the global Internet of Things network.

The coordination & collaboration level of cyber system is the interface between the operation and business level of the cyber system. Enables the existence of a cyber manufacturing structure of AWS and SU as well as their inclusion in the global Internet of Service.

The business level of cyber system is a part of a cyber system that enables the establishment of a cyber manufacturing structure in the form of a cyber manufacturing and business system (PBS). Horizontal connection of such a cyber system structure in the cyber system enables the production company to be included in the production network (PN) and the establishment of different virtual enterprises (VEs) within such a network structure.

The introduction of cyber elements, cyber system structures, and their horizontal and vertical connection, enables a significant change in role of Subject in socio-cyber-physical manufacturing systems. This change is realized through the cyber-physical manufacturing system cybernetization of work in cyber space. Cybernetization of work contributes to improving the management, guidance and control of the future generation of manufacturing and work systems.

In the developed concept of socio-cyber-physical

manufacturing systems (SCPMS), a new role of Subject has been defined. The Subject is placed in a separate space or social space and is connected to other social systems as well as cyber system. The connectivity with the cyber system is enabled through different communication interfaces. The horizontal and vertical communication of the Subject with the elements of the cyber system is shown in Fig 3.

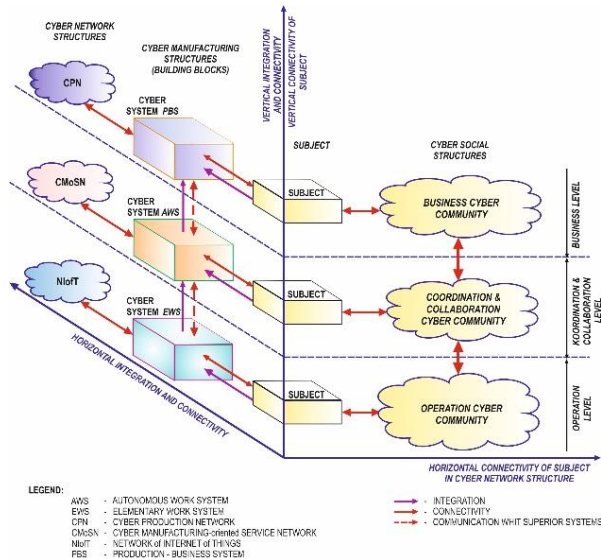


Fig. 3. Connectivity of Subject in the concept of socio-cyber-physical manufacturing systems

The development of new concepts of socio-cyber-physical systems in the manufacturing domain represents a major step in the evolution of organizational and systemic forms of manufacturing structures and their transition from socio-technical to socio-cyber-physical manufacturing systems. Newly structured SCPMS become systems with a certain degree of intelligence, is become so called "smart systems", which will significantly enable greater agility and adaptivity of manufacturing enterprises to the needs of the modern market and society. With these SCPMS are systems based on the principles of the forthcoming Industrial Revolution of Industry 4.0. Such systems will in the future make it possible to enable the business operations and operations of a manufacturing company on a global market under competitive conditions. It is expected that the changed role of a man, capable of managing the manufacturing system in real time, will affect the responsiveness, robustness and efficiency of CSPS-structured manufacturing systems.

4. CONCLUSION

The paper presents an overview of the part of the research work on the theme of cybernetization of production structures and the structuring of the model of cyber-physical production systems. The proposed paper presents part of the concept of cyber-physical manufacturing systems with an accent on the social element as an indispensable component of all manufacturing systems.

Based on the developed concept, the integration of physical and cyber and social elements of the manufacturing system, as well as the transformation of

traditional manufacturing structures into new advanced manufacturing structures based on cybernetization, is enabled.

Future work needs to be directed to the description of digitized and cybernetised functionalities of system manufacturing structures within the developed concept and their realization.

5. REFERENCES

- [1] N. Wiener, *CYBERNETICS or control and communication in the animal and the machine*. The Massachusetts Institute of Technology, 1948.
- [2] J. Peklenik, *Fertigungs kybernetik, eine neue wissenschaftliche Disziplin für die Produktionstechnik*. Berlin: Festvortrag anlässlich der Verleihung des Georg - Schlesinger Preises 1988 des Landes Berlin, 1988.
- [3] E. Hozdić and Z. Jurković, "Cybernetization of Industrial Product-Service Systems in Network Environment," in *New Technologies, Development and Application*, Springer, 2019, pp. 262–270.
- [4] E. Hozdić, "Smart factory for Industry 4.0: A Review," *Int. J. Modern Manuf. Technol.*, vol. VII, no. 1, 2015.
- [5] L. Monostori *et al.*, "Cyber-physical systems in manufacturing," *CIRP Ann. - Manuf. Technol.*, vol. 65, no. 2, pp. 621–641, 2016.
- [6] L. Monostori, "Cyber-physical production systems: Roots, expectations and R&D challenges," in *Procedia CIRP*, 2014, vol. 17, pp. 9–13.
- [7] H. Gill, "NSF perspective and status on cyber-physical systems. In National Workshop on Cyber-physical Systems," Austin, TX., 2006.
- [8] E. A. Lee, "Cyber Physical Systems: Design Challenges," in *International Symposium on Object/Component/Service-Oriented Real-Time Distributed Computing (ISORC)*, 2008, pp. 363–369.
- [9] B. Vogel-Heuser, G. Bayrak, and U. Frank, "Agenda CPS - scenario Smart Factory (Agenda CPS - Szenario smart factory), in 'Increased Availability and Transparent Production,'" Kassel, 2011.
- [10] P. Butala and A. Sluga, "Autonomous work systems in manufacturing networks," *CIRP Ann. - Manuf. Technol.*, vol. 55, no. 1, pp. 521–524, Jan. 2006.
- [11] A. Sluga, P. Butala, and J. Peklenik, "A Conceptual Framework for Collaborative Design and Operations of Manufacturing Work Systems," *CIRP Ann. - Manuf. Technol.*, vol. 54, no. 1, pp. 437–440, Jan. 2005.

Author: PhD student **Elvis Hozdić**, University of Ljubljana, Faculty of Mechanical Engineering, Aškarčeva ul. 6, SI-1000 Ljubljana, Slovenia
E-mail: ehozdic@yahoo.com

ACKNOWLEDGEMENT: This work was partially supported by the Public Scholarship, Development, Disability and Maintenance Fund of the Republic of Slovenia, Grant No. 11011-79/2013.

Knežev, M., Tabaković, S., Zeljkovic, M., Strbac, B., Mladenovic, C.

ANALYSIS AND VERIFICATION OF COMPLEX SURFACES MACHINING BY THREE AXIS MILLING MACHINE CENTER

Abstract: Machine tool accuracy is one of the most important performance properties which affect the part quality. Manufacturing on machining centers with three numerical axes nowadays very often includes machining the complex surfaces, which topology influences on the occurrence of different problems in the machine kinematics. According to mentioned, inaccurate surfaces are given, caused by complex surface geometry which is machined and increment of movement along the axis during the whole tool path. This paper proposes an efficient method based on computer numerical control (CNC) program simulation analysis with aim to determinate inaccuracies on complex surfaces during the design process. An inaccuracies analysis are conducted in two phases: by special software, which allows comparison between computer aided design (CAD) model and model given by machining simulation. Second phase was comparing point cloud given by contact method physical scanning of produced part by and comparing with CAD model.

Key words: complex surface, process errors, tool path verification, contact scanning

1. INTRODUCTION

The parts commonly used in mechanical systems, industrial structures and the functional products in the mold, automobile and aerospace industries have number of complex shapes. These forms are generally obtained by multi-axis milling and specifically by 5-axis milling. [1] However, in some cases, three axis milling machine tools should do the job instead five axis machine tool, of course within the reasonable limitations. Through those limitations occurs inaccuracy.

Accuracy of machining process on numerical machine tools represents complex issue, which includes all factors in process. These include machine tool characteristics (stiffness, movement accuracy, measuring system accuracy...), tool system, fixture stiffness, inaccuracies which are occurs during the tool path approximation, etc. [2]

Modern machining centers efficient exploitation, on nowadays level of automatization, cannot be imagined without using computer and CAD/CAE/CAM software systems. This especially can be noticed, while machining the part with complex configuration.

Virtual manufacturing is the addition of simulation to control models and actual processes, allowing for seamless simulation for optimization during the actual production cycle. The modeling as an approach in which the complete machining process can be simulated and optimized before resorting to costly and time consuming physical trials on the real production environment. Using computer models and simulation of manufacturing processes in virtual environments have provided key tools for presenting products with high level of efficiency and accuracy. [3] Nowadays, machining simulation plays an important role in manufacturing. Machine simulation is the safest and the most cost-effective way to verify tool paths. There are

many benefits of machine simulation. One of the most important is safe and time unlimited testing of machining program. Crashing machine on the computer screen is not a big problem, whereas crashing a real machine is catastrophic [4].

One of the important segments of product design using a computer includes process planning with aim to define production technology and design CNC program using CAM software systems. Using them give a lot of benefits, meaning for production, as productivity, collision prediction, tool load, machine load, etc. According to these results, multiple solutions can be analyzed, and obtained the optimal. Previously could be achieved by varying, strategies, cutting conditions, tools, fixtures as well as tool path defining method, until an optimal solution is obtained.

Observing the total error which occurs in complex shape machining process, on numerical machine tools, tool path approximation presents a very significant factor. That is caused by converting a complex tool path with linear, circular and polynomial segments.

The first part of research presented in this paper, show analysis errors caused by approximation. While the second one includes total error analysis, of characteristic geometrical shapes, on the part. This phase is conducted by physical scanning on CMM (*Coordinate Measuring Machine*) where the result is point cloud, comparing with CAD model which is used for CNC program design. This comparison gives the total deviation of nominal CAD model.

2. TOOL PATH APPROXIMATION ISSUE

CAM software can produce commands for CNC machines. Integral parts of these commands are descriptions of desired motions of the cutting tool relative to the workpiece. Such descriptions are commonly referred to as tool paths. In general, tool

paths are discretized and presented to a machine's controller as a locus of poses. A single pose defines a tool's position and orientation. Tool path can also be considered as a locus of positions when a desired motion does not require changes in orientation. A controller attempts to interpolate discretized tool paths by coordinating motion of independent translational and/or rotational axes. [5]

In addition to the fact that CAM software is present for many years, tool path approximation error analyses are neglected in that area. [6] These errors are result by processing a toolpath, as well as post processing.

The basic reason for neglecting these inaccuracies is that in most cases parts which are represented in industry are not very complex. Their configurations are consist of rectilinear and circular shapes, which are basic geometric shapes, and machine control unit according on installed interpolation function realize them with very high accuracy, and approximation errors are basically absent. This can be seen also on fact that the work piece for testing the working accuracy of machine tools (NCG recommendations, manufacturers), consists exclusively of forms that are in group of basic geometrical shapes. Development of a complex product which consisting a surfaces which not belong to the previous group, as a new technological challenge came mainly from the automotive, aerospace, plastic mold industry, etc. dramatically speeded up the upgrading of CAM software. In these cases, the curvilinear tool path is most often approximated with: lines, circles, or in a latest control systems with spline segments (which is still rare in the industry). Figure 1 shows an example of an elliptical segment approximation a) with circle b) with lines, which inevitably leads to the appearance of errors shown in red.

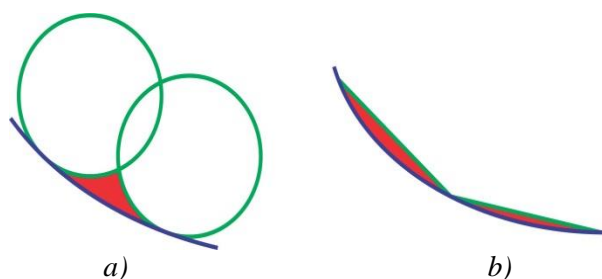


Fig. 1. Approximation of the elliptical segment
a) circles b) lines

Analysis of the mathematical algorithms implemented in software systems for CAM programming of numerically controlled machine tools, with the aim of approximating the curvilinear paths, enable users to gain insight into the accuracy and capabilities of the CAM software and by correcting the individual parameters with the path of the "optimal accuracy" path, the function of the optimization goal allowed deviation from the shape of the treated surface. Application of CAD/CAM program systems is considered as the most effective solution for implementation in the technological preparation of the manufacturing for products with complex geometry. [7]

2.1 Approximation error analysis

Design of computer numerical control program could be realized on few ways, manually or by using the various CAM software systems. If the answer is CAM software system, then is not easy to determinate whether designed. Toolpath accurately describes given geometry. Designed program can be checked by specialized software for verification. Approximation errors occur while processing the toolpath as well as during the translation program for specific CNC machine. They are particularly pronounced when the tool path is formed by linear interpolation segments.

Toolpath verification and approximation error analysis means that tool path generated by CAM software, should be loaded in specialized verification software. According to given program, tools, workpiece, software simulates machining process, and remove material, at the end software gives a workpiece. After that given model and original designed CAD model can be compared. For that purpose various software could be used. In this research was chosen Vericut and his verification functions, AutoDiff shown on Figure 2.

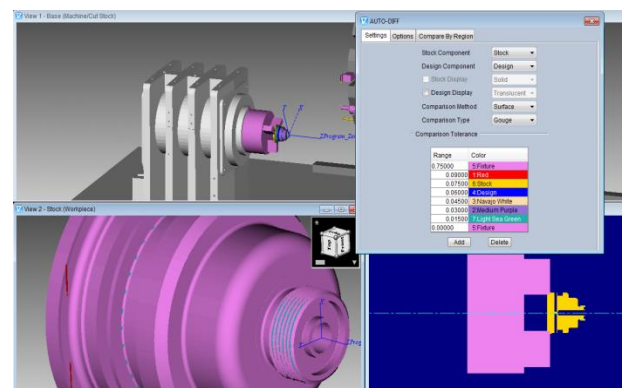


Fig 2 AutoDiff in Vericut

Vericut as well as most of these software, allows direct communication with most of CAD/CAM software, with aim to distribute CAD model, and if it's not possible direct, then communication will be realized by any of neutral format (STEP, IGES, etc.). Analysis in Vericut after comparing models provide report which provide nature of appeared errors, tolerance value, exactly the sentence in program where error occur, errors by machining zones.

3. PHYSICAL TOOL PATH VERIFICATION

To verify program and postprocessor, special complex workpiece have been machined. Physical analysis of toolpath was realized on CNC milling/drilling machining center Haidenraich & Harback FM38 with Sinumerik840d control unit, Sinumerik Operate 4.5 software and machining process have been done on. Horizontal Machining Center H&H FM38 belongs to a group of numerically controlled machine tools conventional kinematic structure, with 3 numerically controlled linear axis and the indexed CNC rotary table i.e. rotational axis (B axis), Fig. 5. This experiment should show that the proposed

methodology for program verification which includes all kinds of simulation can be directly used by CNC programmers and operators.

3.1 Approximation error analysis

In order to analyze toolpath in computer numerical control program, which is generated for special test workpiece, machining was realized for the piece of aluminum 7075, with two tools. Test workpiece has prismatic shape, with multiple characteristic basic and complex shapes Fig. 3:

1. cone
2. calotte (concave and convex)
3. three sided pyramid
4. convex torus
5. coaxial cylinders (three)
6. prismatic slot
7. prismatic spigot (straight and at an angle)



Fig. 3. Machined workpiece

The rough machining were made with milling cutter diameter 5 [mm], and flat surfaces as well with the same tool but with different cutting conditions. The finishing machining of the characteristic shapes (cone, both calotte, three sided pyramid, convex torus) was performed with a ball mill diameter 8 [mm]. Machining center and tools are shown on fig. 4.

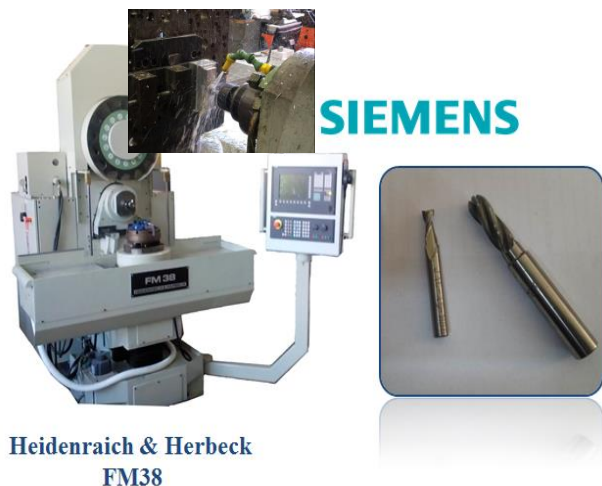


Fig. 4. Machining center and tools

4. RESULTS AND DISCUSSION

4.1 Verification using software

Model generated by verification software, after processing the simulation, based on computer numerical program, was compared with the workpiece CAD model, and deviations are illustrated on figure 5.

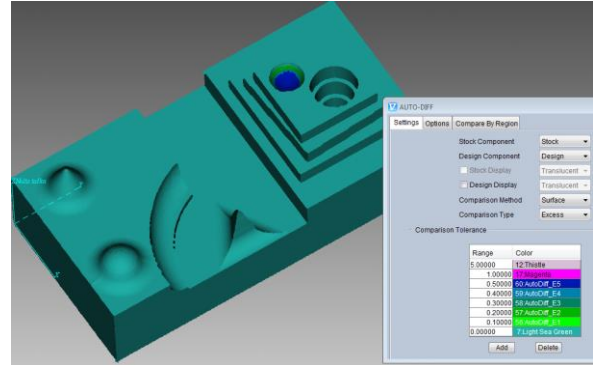


Fig. 5 Processing errors after simulation

According to illustration could be concluded that on the flat surfaces, does not occur errors as is assumed. In this case, errors doesn't occur neither on complex shapes actually at the crossings i.e. radius between flat surfaces and some shapes (cone, three sided pyramid, torus, concave calotte) where were expected. Report shows that approximation error was 0 [mm] and it is shown by *Light Sea Green* color. It could be explained with CAM software setup, where was defined tight toolpath tolerance, and very small stopover between passes, while tool was machining the characteristic complex shapes. Only one zone where from this point of view, occurs huge error, 0.5 [mm] is at convex calotte. The reason of such errors, could be explained with fact that diameter of convex calotte was the same amount as tool diameter 8 [mm], tool nose radius 4 [mm]. According to strategy which was spiral, could be told that in button zone of calotte tool couldn't make a spiral, and as well couldn't machine calotte. Amount of approximation errors at convex calotte vary from 0 [mm] at the upper zone to 0.5 linear along the depth of calotte, as is shown of Fig 6.

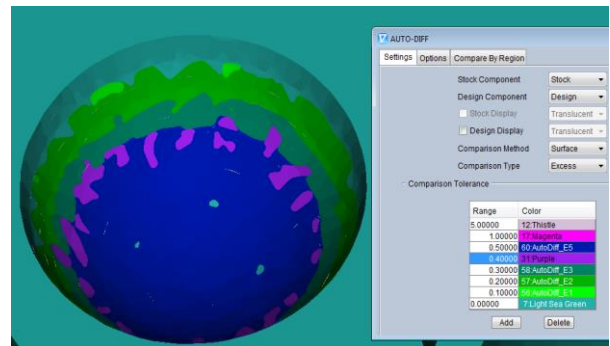


Fig 6 Approximation errors at convex callote

4.1 Physical verification

After processing the workpiece, with aim to analyze machining error, three axes CMM has been used for digitalization, using tactile method. Zeiss Contura G2, as shown on figure 7.



Fig 7. Tactile scanning on CMM Contura G2

The principle of operation of all tactile methods is based on mechanical contact with the object of measurement and probe. Then the signals are derived for further processing. Contact method has been characterized as mostly used with, high accuracy and very good results in repeatability which are as well some of the significant advantages of these systems.

Result of tactile scanning is the point cloud, but scanned were only characteristic shapes, horizontal flat was not considered. Point cloud was imported in software Autodesk PowerInspect 2018 Ultimate, and reconstruction of surfaces has been done according to point cloud. After that reconstructed surfaces were used to compare with original workpiece CAD model, in order to determine the value of deviations from the nominal size. Given errors represents total errors i.e. and they are combination of toolpath approximation error, machine, fixture, cutting tool errors, as well as, CMM errors. After the comparison results are as shown on figure 8.

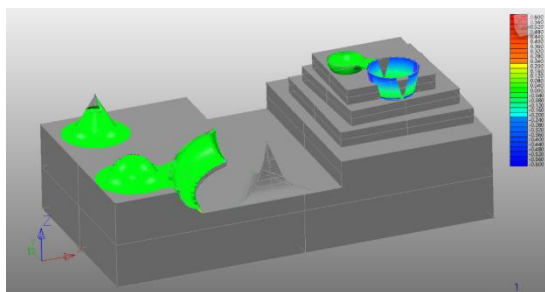


Fig. 8. Errors processing at the workpiece

Results obtained by physical verification indicates bigger amount of errors, than those obtained by software simulation. Basis on these results, can be concluded that errors by toolpath approximation have lesser impact on the errors which occurs during the machining process, could be told that it was expected according the complexity of machining process.

5. FINAL REMARKS

In the present paper, the errors of a 3 axis machine center are enforced on G-codes of parts in virtual environment in order to imitate the real machining environment. The virtual verification machining software was used for toolpath approximation errors analysis, i.e. comparison with original workpiece CAD. Next step was physical machine realization, conducted on machine, and produced part was digitalized with

CMM by tactile method, and given point cloud have been compared with original CAD model of workpiece, and results shows bigger amount of errors in range from 0.040[mm] to -0.280[mm], it was caused by many influencing factors of the process, mentioned above.

6. REFERENCES

- [1] Lofti, S., Rami, B., Maher, B., Gilles, D., Wassila, B.: *An approach to modeling the chip thickness and cutter workpiece engagement region in 3 and 5 axis ball end milling*, Journal of manufacturing Processes, pp. 7-17, 2018, ISSN 1526 6125
- [2] Tabakovic, S., Knezev, M., Zeljkovic, M., Zivanovic, S., Strbac, B.: *Aanaliza i verifikacija obrade slozenih geometrijskih površina operacijom troosnog glodanja na nu mašinama alatkama*, 41. JUPITER KONFERENCIJA, Beograd, Masinski fakultet Beograd, Beograd, 05-06th june 2018.
- [3] Zivanovic, S., Kokotovic, B., Jakovljevic, Z.: *Turning machine simulation for program verification*, 12. International Scientific Conference - Flexible Technologies-MMA 2015, Novi Sad, Fakultet tehničkih nauka, pp. 43-46, 2015, ISBN 978-86-7892-722-5
- [4] Apro, K.: *Secrets of 5-axis machining*. Industrial Press Inc., New York, Printed by Thomson Press India Limited, 2008.
- [5] Chanda, L., Cripps, J., R.: *Characterising the effects of shape on tool path motion*, International Journal of Machine Tools and Manufacture, pp. 17-35, 2018, ISSN 0890 6955
- [6] Tabaković, S., Gatalo, R., Zeljković, M.: *Analiza tačnosti aproksimacije profila pri generisanju upravljačkog programa za CNC mašine primenom programskog sistema ProEngineer*, VIII Međunarodna konferencija fleksibilne tehnologije, Novi Sad, Srbija i Crna Gora, 26-27. jun, 2003.
- [7] Majerik, J., Jambor, J.: *Computer Aided Design and Manufacturing Evaluation of Milling Cutter when High Speed Machining of Hardened Steels*, 25th DAAAM International Symposium on Intelligent Manufacturing and Automation, DAAAM 2014, Vienna, Austria, pp. 450-459.

Authors: M.Sc. Milos Knezev, Assoc. Prof. Slobodan Tabakovic, Full. Prof. Milan Zeljkovic, Assist. Prof. Branko Strbac, M.Sc. Cvijetin Mladenović, University of Novi Sad, Faculty of Technical Sciences, Department of Production Engineering, Trg Dositeja Obradovica 6, 21000 Novi Sad, Serbia, Phone.: +381 21 450-366, Fax: +381 21 454-495.

E-mail: knezev@uns.ac.rs; tabak@uns.ac.rs; milanz@uns.ac.rs; strbacb@uns.ac.rs; mladja@uns.ac.rs

ACKNOWLEDGMENTS: The work is part of research project on "Modern approaches in the development of special bearings in mechanical engineering and medical prosthetics," TR 35025, supported by the Ministry of Education, Science and Technological Development, Republic of Serbia.

Lanc, Z., Zeljkovic, M., Hadzistevic, M., Strbac, B., Zivkovic, A.

DETERMINATION OF EMISSIVITY OF STEEL ALLOY USING INFRARED THERMOGRAPHIC TECHNIQUE

Abstract: *This paper presents experimental determination of the emissivity of steel depending on surface roughness and temperature. The investigation was conducted on steel alloy EN 42CrMo4 workpieces with different degrees of surface roughness during the continuous cooling process and using the infrared thermographic technique (ITT). The results obtained showed that the emissivity of the chosen steel alloy increases with greater surface roughness and decreases during the cooling process, its value ranging from 0.15 to 0.7. It was concluded that surface roughness has a greater influence on the increase of the emissivity at higher temperatures. Multiple regression analysis confirmed a strong correlation between the examined parameters and the emissivity, and an original multiple regression model was determined.*

Key words: *emissivity, steel, infrared thermographic technique (ITT), multiple regression analysis*

1. INTRODUCTION

Infrared thermographic technique (ITT) is a non-contact and non-destructive temperature measurement technique suitable for preventive and predictive maintenance [1,2]. ITT works on the principle of transformation of spatial variations in the emitted infrared radiation from the surface of the observed object into a two-dimensional infrared (IR) image, where the differences in temperature distribution are presented as a range of colours or tones [3]. The key material parameter for the practical use of ITT is emissivity. Emissivity is a function of surface state or atmospheric chemical reactions, temperature, and wavelengths. Because of these non-linearities, it is very complicated to evaluate such a real problem by numerical simulation, and experimental work seems to be the most reliable evaluation procedure [4]. The emissivity of metal is usually experimentally determined because of its tendency to change depending on the different chemical and physical conditions of surface [5]. Many authors investigated the effect of the type of material, surface roughness, microstructure, temperature, wavelength, etc. on the metal emissivity characteristics, especially steel because of its wide range of use.

Kobayashi et al. measured normal spectral emissivity and its time variation for a total of thirty kinds of pure metals and alloys at temperatures between 780 and 1200°C. The spectral data were obtained at about 100 wavelengths from 0.55 to 5.3 μm under different environmental conditions including oxidation. It is shown that the emissivity variations were monotonic for cold-rolled steel, and steel alloy SUS310S. Additionally, authors made a database to facilitate the dissemination to researchers and engineers interested in the emissivity of metals. Indexes to the emissivity data are metal name, wavelength, temperature, time, and degree of oxidation represented by an effective thickness of oxide film on the specimen surface [6].

Wen applied several emissivity models to examine Multispectral Radiation Thermometry (MRT) on inferring surface temperature in order to investigate steel emissivity behaviors. The data show that emissivity decreases with increasing wavelength. For steel containing high chromium, emissivity is usually lower than others because of the chromium oxide protection layer. Two emissivity models provide the best overall compensation for different alloys, number of wavelengths, and temperatures. The results reveal that if the emissivity model can well represent the real emissivity behaviors, the more accurate inferred temperature can be achieved [7]. A year later, author conducted new experiments to measure the emissivity values of a variety of steel samples at 427, 527, and 627 °C. The effects of wavelength, temperature, alloy composition, and heating time on emissivity were investigated. Multispectral radiation thermometry (MRT) with linear emissivity models (LEMs) and log-linear emissivity models (LLEs) were then applied to predict surface temperature. Results show that the spectral emissivity decreases with increasing wavelength and increases with increasing temperature. Steel with higher chromium content has lower emissivity value because of the chromium oxide protection layer. The spectral emissivity reaches steady state after the third hour heating due to the surface oxidation becoming fully developed [8]. Shi et. al measured the variations in spectral emissivity of Usibor® 1500P steel during a two-step austenitization and in two different heating atmospheres, argon and air, using a near infrared spectrometer and a Fourier transform infrared reflectometer. Phase transformations of the Al-Si coating and surface oxidation lead to the changes in surface phase composition and surface roughness, which in turn influence the spectral emissivity [9]. Xing et. al measured the normal spectral emissivity during the growth of oxide layer on the surface of steel 430 at a wavelength of 1.5 μm over a temperature range 527 - 827°C using thermocouples,

which were symmetrically welded onto the front surface of specimens [10].

Previous studies showed that the emissivity of metals increases with the increase in temperature and surface roughness during heating. This paper includes an investigation into the emissivity behavior of the steel alloy EN 42CrMo4 during the continuous cooling process using ITT. The reason for this is similar heating and cooling rate of metals. This study considered the possibility of use of multiple regression analysis for theoretical determination of the emissivity, on the base of experimentally obtained data. The aim of the study was investigated whether ITT can be used for reliable temperature measurement of heated steel surfaces on the work equipment, and by implication, for the assessment of risk of burn injuries.

2. MATERIALS AND METHODS

The experimental determination of the emissivity was conducted on the steel alloy EN 42CrMo4. EN 42CrMo4 alloy steel is widely used for engineering steel purpose, such as: making various kinds of machinery, automobile, mining spare part, the gearwheel of the engine, the driving gear of supercharger, the connecting rod, parts for power train applications, cold formed fastener components, shafts, gears, drill collars for the oil exploration, etc. Chemical characteristics of the chosen steel alloy are given in Table 1.

C	0.38 – 0.45
Mn	0.60 – 0.90
Si	0.40 max
P	0.035 max
S	0.035 max
Cr	0.90 – 1.20
Mo	0.15 – 0.30

Table 1. Chemical characteristics of the EN 42CrMo4 steel alloy

For the purpose of the experimental work, two workpieces were made with dimensions of (150 × 150 × 10) mm. The first workpiece was ground, whereas the other one was milled. The roughness of the workpieces was measured with a contact method using a MarSurf PS1 device. The mean roughness (roughness average, R_a) was measured in 30 points uniformly distributed on the surface of the workpiece. The average value of the measured roughness (\bar{R}_a) was taken as the surface roughness of the workpiece (Table 2). Roughness profile of S_1 and S_2 workpiece are given on Fig. 1 and Fig. 2, respectively.

Type of machining	\bar{R}_a [μm]	Labels
grinding	0.262	S_1
milling	1.385	S_2

Table 1. Surface roughness of the workpieces

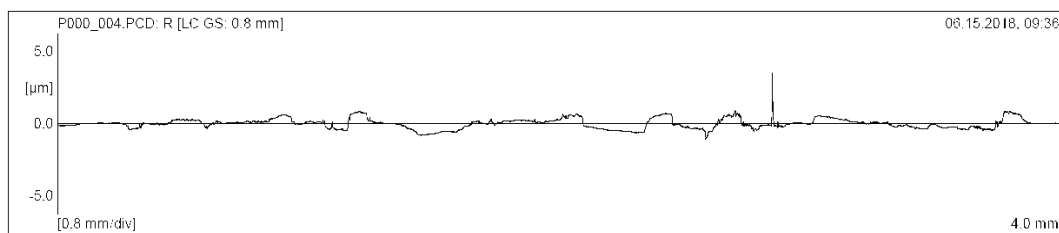


Fig. 1. Roughness profile of S_1 workpiece

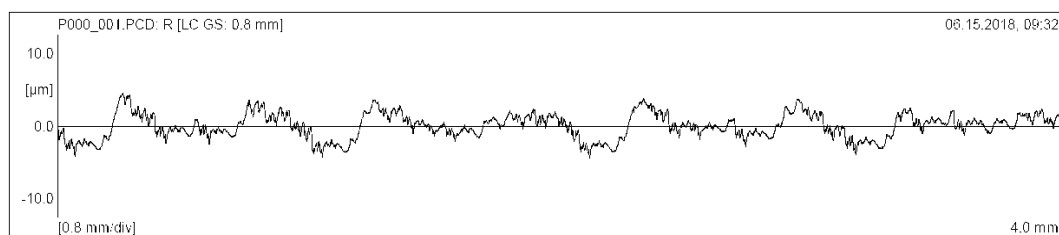


Fig. 2. Roughness profile of S_2 workpiece

The emissivity of steel workpieces was determined using experimental setup shown in Fig. 3. Methodology is based on simultaneous heating of a single workpiece, measuring the temperature by means of an IR camera and measuring the reference temperature on the analyzed surface. The reference temperature was measured using type-K thermocouples. Two thermocouples were placed on the back surface of the workpiece, whereas the third thermocouple was attached to the front surface of the workpiece using black rubber. For the purpose of this paper a heat-treat furnace was used for heating the workpieces. For achieving a uniform temperature distribution on the

target area of the sample, every workpiece was placed upright in the center of the furnace and tested separately. The radiation emitted from the heat furnace can affect the thermography test to a large extent. Thus, prior to the measurement, a 2-mm black tin box was placed into the furnace in order to eliminate the effect of the furnace walls on the measurement results. The infrared camera used for thermal imaging was camera IR ThermoPro TP8S with a spectral range of 8–14 μm and temperature accuracy of ± 1 °C.

After installing the thermocouples and setting the IR camera, a workpiece was heated up to 200 °C. Having reached this temperature, the workpiece was being

cooled down to the ambient temperature of 25 °C. At the same time, the camera took an IR image of the workpiece at 50, 100, 150 and 200 °C. The described procedure was repeated for both workpiece. The obtained IR images were processed using the Guide Ir Analyser program where the average emissivity of a workpiece was adjusted to a value from 0 to 1 until the temperature became equal to the reference temperature. During the IR-image processing, the temperature used as the reference temperature was the average of the temperature values obtained with the thermocouples.

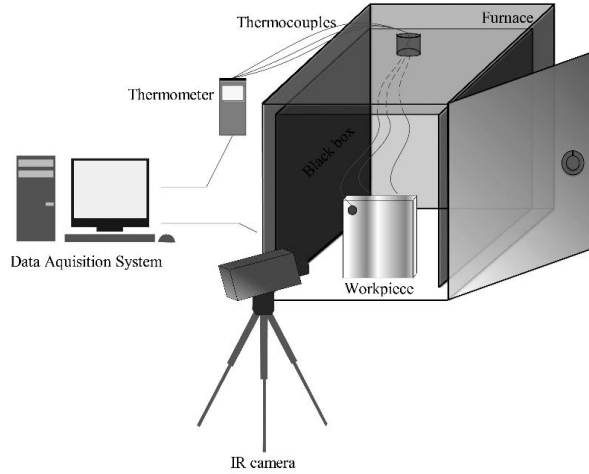


Fig. 3. Experimental setup

3. RESULTS AND DISCUSSION

The experimental data show that the average emissivity of steel alloy EN 42CrMo4 in the spectral range of 8–14 μm decreases during the cooling and increases with an increase in the surface roughness. The emissivity ranges from 0.15 to 0.7. At temperatures from 50 to 200 °C, the emissivity values of the workpieces are rising, and their mutual differences are only the results of the surface roughness (Figure 4).

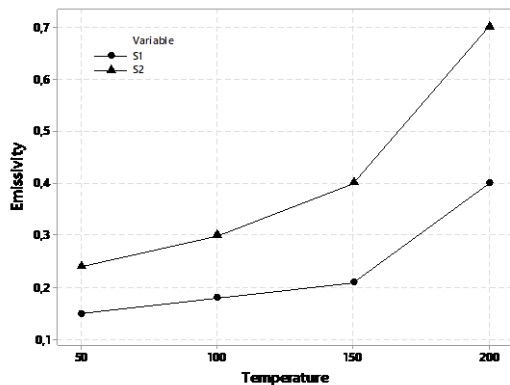


Fig. 4. Emissivity of steel alloy EN 42CrMo4

3.1 Multiple-linear-regression analysis

Multiple regression analysis makes it possible to examine the effect of several independent variables on the dependent output variable. The result of this approach is a multiple regression model which, in the form of a mathematical formula, connects the effect of two independent variables on the dependent variable

[14]. In this concrete case, the dependent variable - the emissivity (ε) is related to two independent variables - temperature (T) and surface roughness (R_a) using the following model (equation 1):

$$\varepsilon = \beta_0 + \beta_1 \cdot T + \beta_2 \cdot R_a + r \quad (1)$$

where $\beta_0, \beta_1, \beta_2$ represent regression coefficients and r is the component of random error. For the assessment of the model for $n = 8$ observations and the number of independent variables $k = 2$, the matrix form of the equation 1 is given by matrix equation 2:

$$Y = \begin{bmatrix} e_1 \\ e_2 \\ \vdots \\ e_8 \end{bmatrix}; X = \begin{bmatrix} 1 & x_{11} & x_{12} \\ 1 & x_{21} & x_{22} \\ \vdots & \vdots & \vdots \\ 1 & x_{(8)1} & x_{(8)2} \end{bmatrix}; \quad (2)$$

$$\beta = \begin{bmatrix} \beta_0 \\ \beta_1 \\ \beta_2 \end{bmatrix}; r = \begin{bmatrix} r_1 \\ r_2 \\ \vdots \\ r_8 \end{bmatrix}$$

Solving the matrix equation (2) according to results in the following multiple linear regression model (equation 3):

$$\varepsilon = 0.00226 T + 0.1558 R_a - 0.0883 \quad (3)$$

The presented model can be used for temperatures range from 50 to 200 °C and surface roughness from 0.262 to 1.385 μm . In this case, the multiple coefficient of determination R^2 shows that 84.14 % of variation in the emissivity comes from variation in temperature and surface roughness, whereas the remaining 15.86 % is the consequence of the effect other parameters such as humidity, permeability of the atmosphere, temperature of the environment, etc. The model can be used for prediction of the value of the emissivity at temperatures and surface roughness values which are beyond the mentioned ranges, with a somewhat lower coefficient of determination R^2_{pred} of 53.17 %. Multiple regression was used to determine the strength of dependence between the emissivity and the observed parameters based on the correlation coefficient r . The correlation coefficient was 0.8 which points to the fact that there is a strong (direct) linear dependence between temperature and surface roughness and the emissivity. The scatter plot (Figure 4) shows a small degree of data deviation around the established regression line, indicated by the value of the standard error S of 0.08.

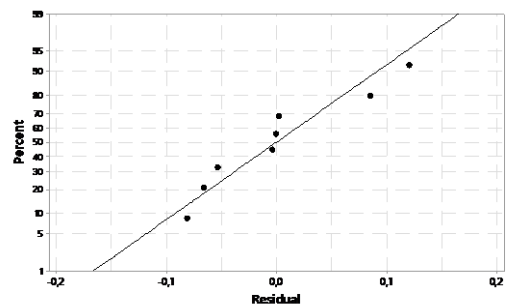


Fig. 5. Scatter plot

4. CONCLUSION

The emissivity of steel alloy EN 42CrMo4 in the cooling process from 200 to 50 °C was experimental determinate using infrared thermographic technique. The investigation showed that the emissivity of the chosen alloy ranges from 0.15 to 0.7 and that it decreases with the decrease in temperature and increases with the increase in surface roughness. At higher temperatures, the differences between the emissivity of the workpieces are bigger. The analysis of IR images showed that this phenomenon is a consequence of a more significant effect of surface roughness on the emissivity at higher temperatures.

Although ITT is not recommendable for precise determination of the emissivity of metals, in the post processing of IR images the authors managed to determine the emissivity. Multiple regression analysis confirmed a strong correlation between the investigated parameters and the emissivity and a multiple regression model was determined.

Presented model can only be applied with low and medium temperatures since at higher temperatures there is a somewhat greater deviation of the experimental data from the regression line. The reason for this is uneven distribution of temperature on the surface of a workpiece due to defects which occurred during its machining.

5. REFERENCES

- [1] Krešák J., Peterka P., Kropuch S., Novák L. (2014): *Measurement of tight in steel ropes by a mean of thermovision*, Measurement, Vol. 50, pp. 93-98, 2014.
- [2] Kosec B., Karpe B., Budak I., Ličen M., Đorđević M., Nagode A., Kosec G.: *Efficiency and quality of inductive heating and quenching of planetary shafts*, Metallurgy, Vol. 51, pp. 71-74, 2012.
- [3] Glavaš H., Jozsa L., Barić T.: *Infrared thermography in energy audit of electrical installations*, Tehnički vjesnik, Vol. 23, pp. 1533-1539, 2016.
- [4] Švantner, M., Honnerová, P., Veselý, Z.: *The influence of furnace wall emissivity on steel charge heating*, Infrared Physics and Technology, Vol. 74, pp. 63-71, 2016.
- [5] Lanc, Z., Štrbac, B., Zeljković, M., Živković, A., Hadžistević, M.: *Emissivity of Aluminium Alloy Using Infrared Thermography Technique*, Materiali in Tehnologije, Vol. 52(3), pp. 232-237, 2018.
- [6] Kobayashi, M., Ono, A., Otsuki, M., Sakate, H., Sakuma, F.: *A Database of Normal Spectral Emissivities of Metals at High Temperatures*, International Journal of Thermophysics, Vol. 20, pp. 299-308, 1999.
- [7] Wen, CD.: *Investigation of steel emissivity behaviors: Examination of Multispectral Radiation Thermometry (MRT) emissivity models*, International Journal of Heat and Mass Transfer, Vol. 53, pp. 2035-2043, 2010.
- [8] Wen, CD.: *Study of Steel Emissivity Characteristics and Application of Multispectral Radiation Thermometry (MRT)*, Journal of Materials Engineering and Performance, Vol. 20, pp. 289-297, 2011.
- [9] Shi, C., Daun, K., Wells, M.: *Spectral emissivity characteristics of the Usibor® 1500P steel during austenitization in argon and air atmospheres*, International Journal of Heat and Mass Transfer, Vol. 91, pp. 818-828, 2015.
- [10] Xing, W., Shi, D., Sun, J., Zhu, Z.: *Emissivity model of steel 430 during the growth of oxide layer at 800–1100 K and 1.5 μm*, Infrared Physics and Technology, Vol. 88, pp. 23-31, 2018.

Authors: M.Sc. Zorana Lanc, Full Prof. Milan Zeljković, Full Prof. Miodrag Hadžistević, Assist. Prof. Branko Štrbac, Assoc. Prof. Aleksandar Živković, University of Novi Sad, Faculty of Technical Sciences, Department of Production Engineering, Trg Dositeja Obradovica 6, 21000 Novi Sad, Serbia, Phone.: +381 21 450-366, Fax: +381 21 454-495. E-mail: zoranalanc@uns.ac.rs; milanz@uns.ac.rs; miodrags@uns.ac.rs; strbacb@uns.ac.rs; acoz@uns.ac.rs;

Matijasevic, L., Milivojevic, M., Petrovic, P.

MULTIFINGERED UNDER-ACTUATED HANDS IN ROBOTIC ASSEMBLY

Abstract: New production paradigm of mass customization imposes the development of flexible gripping systems with exceptional dexterity, capable of mimicking grasping behavior of human hands. In this context, the most demanding technical challenges are: motoric capabilities and related design aspects, overall weight and size, and tactile and other perceptual capabilities. Also, to make the gripper industry acceptable, it should be in affordable price range. Having all that in mind, concept of the multifingered under-actuated hand appears as good candidate to be an optimal, general purpose solution. This paper presents the general conceptual framework for development of multifingered hands which are based on under-actuation principle.

Key words: Robotic assembly, Grasping, Multifingered hands.

1. INTRODUCTION

Modern industrial robotic arms and hands excel over human's in most aspects. They are capable of lifting heavier loads, they are more repeatable and on top of that they are faster. With that said when it comes to gripping objects the situation is different.

Grippers used at assembly and manufacturing lines are typically simple mechanisms and are used for gripping and manipulation of fairly simple parts and part families. New production paradigm of mass customization requires flexible grippers that are capable of in hand manipulation for task of manipulating complex object of different sizes and shapes.

This paper there will focus on robot grasping foundations and on human and robot dexterous manipulation. Paper concludes with multifingered under-actuated hands for dexterous and cognitive grasping and manipulation of objects in industrial setting.

2. ROBOTIC GRASPING FOUNDATIONS

End-effectors on a robot arm, that is used to grasp and manipulate object is a gripper. Based on their morphology they are separated into two main groups, regular grippers and robotic hands, as shown on Fig. 1.

Dexterity or, as described in [3], easy in-hand manipulation of object, after it was grasped, is main difference between these two groups. Grippers are fairly simple mechanisms that work on simple principles and can't perform in hand manipulation. Example of those grippers range from magnetic and pneumatic grippers or three finger adaptive grippers. Robotic hands are divided into three groups. There are under-actuated hands (where number of DOF of finger, n , is larger than number of actuators, m), fully-actuated hands ($n=m$) and humanoid hands. Humanoid hands are made to, more or less, recreate human hand's grasping capabilities and morphology. In industrial setting, however, usage of humanoid hands is scarce. Reason for that is found in robustness and overall cost of used

grippers. Functionality of regular grippers satisfies needs of industry because of their simpler mechanisms that makes them robust and they cost less than multifingered humanoid hands. On the other hand they are less flexible than robotic hands and mass customization imposes flexibility as main ability that gripping systems must have. Robotic hands can perform in hand manipulation regardless of shape of object they manipulate. Three and more fingers grippers are flexible enough to manipulate objects of different sizes and weights and also different stiffness.

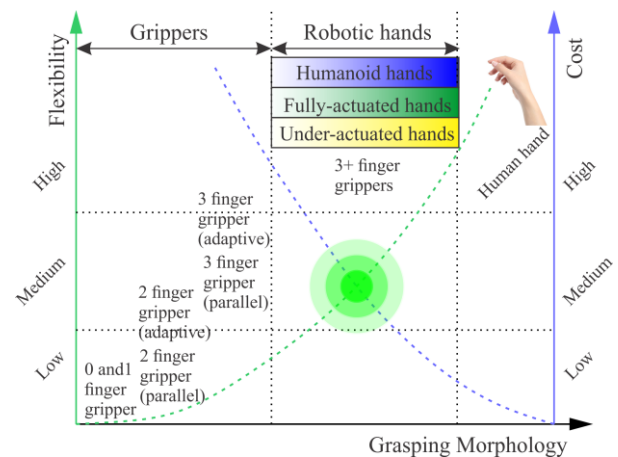


Fig. 1 Classification of grippers, from zero finger grippers (e.g. magnet gripper) to a human hand, based on their morphology, flexibility and overall cost.

So to make optimal solution, from mechanical standpoint, compromise of cost and flexibility must be found, and that area is illustrated in Fig. 1, with green circles. Another aspect of robotic hand systems is cognitive aspect. Just like with humans, grasping system needs to be able to define optimal solution for grasping different objects and by implementing this aspect robotic system becomes more flexible.

Notice that robotic grasping occupies multidimensional space that spans from mechanical over control complexity to cognition, so Fig. 1. does not illustrate that whole space.

2.1 Grasping theory

Determining conditions for grasping and manipulation of certain object requires fundamental definitions to be described first. There are several definitions in grasping, [2].

Definition 1: A grasp is commonly defined as a set of contacts on the surface of the object, which purpose is to constrain the potential movements of the object in the event of external disturbances. To be able to determine forces and torques that are required for manipulator to exert on the contact area a proper contact model should be defined. There are two main approaches in robotic grasping: analysis and synthesis.

Definition 2: Grasp analysis consists on finding whether the grasp is stable using common closure properties, given an object and a set of contacts. Then, quality measures can be evaluated in order to enable the robot to select the best grasp to execute.

Definition 3: Grasp synthesis is the problem of finding a suitable set of contacts given an object and some constraints on the allowable contacts.

A contact can be defined as a joint between the finger and the object. The shape of the contacting surface and the stiffness and frictional characteristics of the contacting bodies define the nature of this joint. Contact models maps the forces that can be transmitted through the contact on object. There are three contact models: point contact without friction, point contact with friction and soft finger contact model.

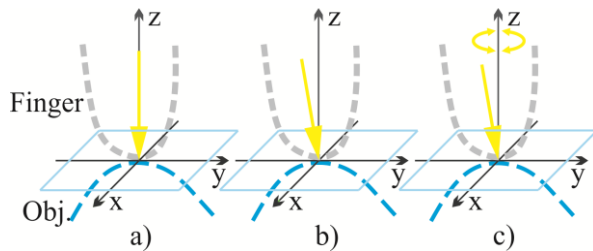


Fig. 2 Contact types: a) point contact without friction, b) point contact with friction and c) soft finger contact.

Point contact without friction, shown in Fig. 2 a), can only transmit forces along the normal to the object surface at the contact point. It does not represent the real contact that appear in robotic manufacturing operations. Point contact with friction, shown in Fig. 2 b), is used when there is significant contact friction, but the contact patch is so small so that no usable friction moment exists. It can transmit forces in the normal and tangential directions to the surface at the contact point but can't transmit moment components. Soft finger contact model, shown in Fig. 2 c), is used when the surface friction and the contact patch are large enough to generate significant friction forces and a friction moment about the contact normal. This model also correlates to usage of palm in grasping. In human case, palm is used extensively in grasping tasks, so in robot grasping it needs to be taken into account.

When discussing the ability of gripper to constrain movement of manipulated object, there are two closure properties that describes stable grasp of an object. Those are form and force closure.

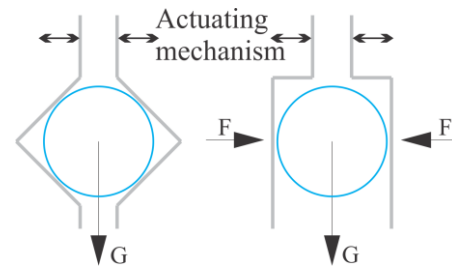


Fig. 3 Form and force closure interpretation

A grasp is in form closure, if the location of the contact points on the object ensures its immobility and grasp is in force closure, if the fingers can apply, through the set of contacts, enough force and torque on the object, which means that any motion of the object is resisted by the contact forces. Form closure is a stronger condition. Force closure is used when performing precision grasping, but it requires control of internal forces, [2].

Besides achieving proper closure property, for hand to be dexterous it requires grasp synthesis to provide suitable hand configuration for grasping, which is explained in [2].

3. DEXTEROUS MANIPULATION

The concept of dexterous manipulation is most important aspect in making of more flexible gripping systems (mechanical hands, both robotic and prosthetic) that can mimic functionality of the human hand. To be able to accurately define dexterity it is important to consider decomposing manipulative tasks first. Manipulative tasks can be observed from object or environment-centric and hand-centric point of view, [3]. Consider opening a bottle of water. Object-centric view of the task would be: there needs to be rotational movement about axis of cap of bottle and axial movement along that axis to remove the cap. When considering hand-centric views this can be done multiple ways. It can be done within hand motions of thumb and forefinger or for example with power grasp of the cap and motion of entire arm to do the same job. There are multiple options to choose from when considering hand-centric point of view, and due to so many possible ways to do the task, object-centric view of manipulation task does not directly correlate with hand ability. So, given the circumstances, artificial grasping system should be able to distinguish different object properties and compute optimal approach to the given task. And mechanically, artificial hand needs to be dexterous enough to be able to perform computed grasping of an object.

Dexterity, in broad meaning, can be described as skill to use hands, [1]. It is often referred to as in-hand manipulation. So, the most dexterous hand, would be the one that could serve as a general-purpose manipulator, capable of performing the most diverse set of operations in a manufacturing environment. This definition would be valid if dexterity would come only from mechanical capabilities of hand mechanisms. When we take human grasping capabilities in consideration, dexterity could be defined as task of

finding optimal kinematical solution for any situation and in any condition. This definition focuses not only on mechanical capabilities of hand to allow the versatility of dexterous movements, but on motor control systems to adapt movements to challenging environmental conditions.

Dexterity of human grasping is highly dependable on synergy of torso, arms and hands [4]. Most tasks of grasping are performed not only with hands but with arms and torso also. This ability is crucial to implement in artificial grasping system. In bimanual assembly systems, for instance, using multifingered hands on both arms of robotic assembly station leads to optimal assembly of objects where one hand can be used as fixture and other as tool used for assembly. This ability is essential when task is manipulation of larger objects, but when it comes to precision work, in-hand manipulation is crucial. When observing human grasping, for instance in precision soldering, we tend to decouple some joints by, for example, resting elbow joint or forearm on the working table. This makes that precision task dependable solely on in-hand manipulation.

So, with all mentioned in above sections, concept of the multifingered under-actuated hand appears as good candidate to be an optimal, general purpose solution for solving both mechanical and control part of complex tasks of grasping.

4. MULTIFINGERED UNDERACTUATED HAND

Complexity of the control and complexity of mechanisms incorporated in multifingered hands dictates actuation systems that are expensive, heavy, and hard to put in one, decent size, user friendly package. Because of these disadvantages, efforts are made in order to develop under-actuated fingers for multifingered hands.

4.1 Under-actuated robotic hands

Under-actuated robotic hands have become quite popular in industry and research applications, for a number of reasons. Hands such as these occupy a niche among the wide spectrum of robotic hands that lie between simple 2-fingered industrial grippers and complex 5-fingered anthropomorphic hands. Utilizing usually one actuator or less to operate a single finger, these hands allow a much more simplified control compared to traditional fully actuated multi-finger hands. Low cost, simple design, and the potential for mass application all make under-actuating hands quite promising for current and future development in artificial prosthetics and humanoid robotics, [5]. The concept of underactuation in robotic fingers, with fewer actuators than degrees of freedom through the use of springs and mechanical limits, allows the hand to adjust itself to an irregularly shaped object without complex control strategy and numerous sensors.

Process of grasping, when closing on an object, can be divided into three essential stages: the initial stage, the pre-shaping stage, and the closing stage as described in [6]. In the initial stage, shown in Fig. 4. (a), the finger is straightened and only first segment is

touching the object. The pre-shaping stage can be described as the interval beginning when actuation is applied and ending when any segment touches the object. During this time, the finger acquires a pre-shaped configuration. As shown in Fig. 4. (b), once the actuator moves down and applies a tensile force on the tendon, the finger will start closing. All the joints will be rotating simultaneously in a coupled relationship.

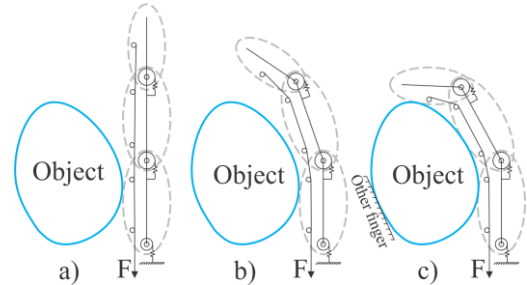


Fig. 4. Under-actuated finger with (a) initial stage, following (b) pre-shaping stage and (c) closing stage.

The closing stage will describe the interval beginning with the moment of object contact and ending when no segment can continue to move (when the grasp is completed). As shown in Fig. 4. (c), when the middle segment is blocked and the tendon is continuously pulled down, the distal segment can continue to bend because the two joint angles have been decoupled by the object. That is main advantage of under-actuated hands over fully actuated hands.

Two most popular and widely used concepts for under-actuated multifingered robot hands are tendon and linkage based mechanisms, [7], shown in Fig.5.

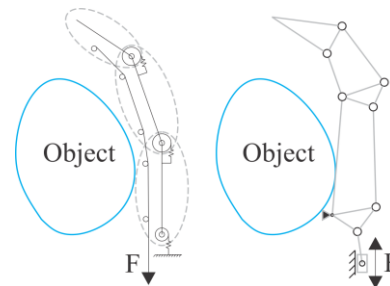


Fig. 5. Types of mechanisms, tendon and linkage based, used in under-actuated multifingered hands.

Pulley-Tendon/Cable driving of the under-actuated mechanical structures enables relatively simple and very compact designs, as well as remote location of the actuators. As described in [7] control of motion is problematic. Rigid linkage drive is more predictable, more accurate and more controllable. Rigid linkage drive is more appropriate for industrial use, and because this paper focuses on industrial application of these grippers, rigid linkage drive configurations will be used in following examples.

When observing their ability to grasp, known and unknown objects, it is important to state that stability of such grasp isn't always same. Grasping with under-actuated multifingered hands can lead to two possible outcomes, stable or unstable grasp. As mentioned in section 2, form grasp is usually more stable than force

grasp because in form grasping fingers are enveloping object contact points. Examples of the discrete states of stable grasp performed by the three phalanx finger driven by the two four bars mechanism (the object to be grasped is assumed fixed in space) is shown in Fig. 6.

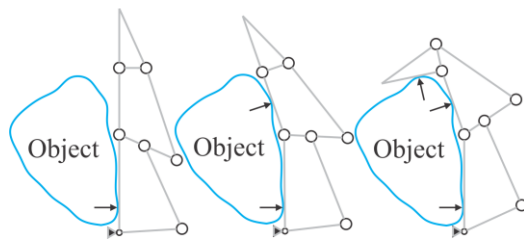


Fig. 6. Stable grasp of object.

In some configurations, the force distribution in an under-actuated finger can degenerate. The finger can no longer apply forces on the object, leading to, in some cases, the ejection of the latter from the hand, despite a continuous closing motion from the actuator. Discrete states of unstable grasp which is generated from initially stable grasp due to appearance of negative contact forces on some phalanx are shown on Fig. 7.

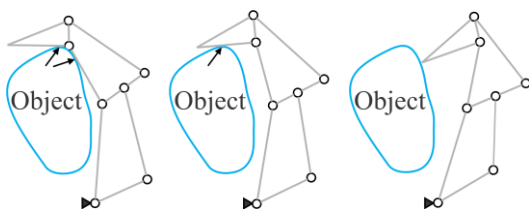


Fig. 7. Unstable grasp of object.

4.2 Multifingered human-like robot hands

Capabilities of dexterous grasping, mentioned in above sections, are easily achievable by human hand. So, it is only natural that many researchers are looking at human hands for inspiration. Human hand complexity makes it really hard to achieve anthropomorphic robotic hand that can do all the tasks human hand can. In the same time, being robust and sensitive, gives human hand abilities to do tasks in virtually any environment and the ability to do precise and some not so precise tasks like heavy lifting and similar tasks.

Multifingered flexible anthropomorphic grippers are rarely used in industrial setting. As mentioned, they are still in research stage and are primarily used in space exploration, military application and similar. One used in industry is shown on Fig. 8.



Fig. 8 The Robotiq 3-Finger adaptive gripper that's used in industry.

Grasping of an object does not rely exclusively on mechanical capabilities of hand but on sensing and cognitive aspects also. Sensing technologies have improved over the years, so equipping fingers of robot hands with it, allows better force control and better motor control of grasping system. By implementing tactile sensors on fingers and give fingers the ability of object gaiting as described in [8]. System can use of tactile information from fingers and make proper grasp plan to grab an object.

5. FUTURE WORK AND CONCLUSION

There are several interesting topics which will be considered in future research. Kinematic properties of under-actuated finger will be studied in order to develop stable grasping system from kinematics standpoint. A proper grasp planning algorithm should be developed using 3D vision based systems working in conjunction with tactile sensors that can give information about grasping quality as well as object properties. Finally development of under-actuated multifingered hand system for use in industrial setting for small-batch assembly is a ultimate goal of this research.

6. REFERENCES

- [1] Sturges, H.: *A Quantification of Machine Dexterity Applied to an Assembly Task*, Int'l J. Robotic Research, vol. 9, pp. 49-62, June 1990.
- [2] Beatriz, L., et al.: *From Robot to Human Grasping Simulation*, Springer, London, 2014.
- [3] Bullock, M., Ma, R., Dollar, A.: *A Hand-Centric Classification of Human and Robot Dexterous Manipulation*, IEEE Transactions on Haptics, vol. 6, pp. 129-144, April-June 2013.
- [4] Pettinato, J., Stephanou, H.: *Manipulability and Stability of a Tentacle Based Robot Manipulator*, Int'l Conf. Robotics and Automation, pp. 458-463, USA, IEEE, Scottsdale, May 1989.
- [5] Liarokapis, M., Dollar, A.: *Deriving dexterous, in-hand manipulation primitives for adaptive robot hands*, Intelligent Robots and Systems, pp. 25-27, Canada, IEEE, Vancouver, 24-28 September 2017.
- [6] Long, W., et al.: *A highly-under-actuated robotic hand with force and joint angle sensors*, Intelligent Robots and Systems, pp. 25-27, California, IEEE, San Francisco, 25-30 September 2011.
- [7] Birglen, L., et al.: *Under-actuated Robotic Hands*, Springer, Berlin, 2008.
- [8] Ma, R., Dollar, A.: *An under-actuated hand for efficient finger-gaiting-based dexterous manipulation*, Robotics and Biomimetics, pp. 2214-2219, Indonesia, IEEE, Bali, 05-10 December 2014.

Authors: Lazar Matijasevic, Milos Milivojevic, Full Prof. Petar B. Petrovic, University of Belgrade, Faculty of Mechanical Engineering, Department of Production Engineering, Cyber-Manufacturing Systems Laboratory

E-mail: pbpetrovic@mas.bg.ac.rs;
lmaticjasevic@mas.bg.ac.rs;
mmilivojevic@mas.bg.ac.rs;

Mladenović, C., Košarac, A., Zeljković, M., Knežev, M.

EXPERIMENTAL DEFINITION OF MACHINING SYSTEMS STABILITY LOBE DIAGRAM

Abstract: *The occurrence of self-excited vibrations in machining can cause a number of problems, such as. tool wear or breakage, poor surface quality, increase energy consumption, increase of noise, etc. In order to avoid the consequences of self-excited vibration it is necessary to define those cutting regimes which can not cause the occurrence of these vibrations. For this purpose, it is necessary to define a stability lobe diagram of the observed machining system, which shows the boundary between stable and unstable zone of machining operations, depending on the number of revolutions of the spindle and cutting depth.*

This paper, presents experimental method for defining of stability lobe diagram, in case of a milling machining center EMCO Concept Mill 450.

Key words: *dynamic behavior of the machining system; self-excited vibrations; frequency response function; stability lobe diagram*

1. INTRODUCTION

When the machine tool works, it may cause the emergence of various types of vibration which have a significant impact on the machining process. These types of vibration are free, forced and self-excited vibrations.

The most unfavorable vibrations that occur in machining processes, are self-excited vibration, which draw the energy necessary for their creation and growth of amplitude from the cutting process itself. These vibrations can occur due to friction in the tool-workpiece system, due to thermo-mechanical effects, or as a result of the regenerative effect, i.e. variation of cutting depth during machining. Self-excited vibrations often lead to unstable operation of machine tools, and also reduce the quality of the machined surface, causing the appearance of noise, leads to rapid wear of the cutting tools and elements of machine tools, etc. [12].

In order to avoid the consequences of self-excited vibrations, it is often not possible to use certain cutting regimes, because they cause unstable operation of the machine tool. Diagrams which show the stable and unstable area of machine tools operation, are called stability lobe diagrams (SLD), and they are defined according to the number of revolutions of the main spindle and the cutting depth. Stability lobe diagrams are usually defined analytically based on the modal parameters of a machining system and the parameters of the cutting process.

The first research on mathematical modeling of self-excited vibrations are conducted by Tobias [15] and Tlustý [14], which identified a regenerative mechanism of self-excited vibration, and developed a mathematical model in the form of delay differential equations (DDE). The zeroth order approximation, ZOA, method of Altintas and Budak [1] suggest making stability predictions using the zeroth order Fourier term to approximate the cutting force variation and achieve

reasonably accurate stability lobe diagrams predictions for processes, where the cutting force varies relatively little, i.e. considerable radial immersions and large number of teeth.

Besides the above mentioned, a number of researchers is also applied complicated mathematical expressions for modeling self-excited vibrations in order to define stability lobe diagrams, and so Insperger and Stephan [5, 6] apply semi-discretization method (SD) to reduce a complicated DDE method to series of ordinary differential equations (ODE) with a known solution. Gradišek [4] compared the stability limit of milling process obtained by methods ZOA and SD, and concluded that the two methods yield very similar stability lobe diagrams for machining with relatively large values of radial immersions, while for small values of the radial immersions these two methods provides stability lobe diagrams with significant differences.

As an alternative to SLD definition by mathematical modeling of systems dynamic behavior, there is also a method which is based on experimental tests. This approach, in comparison with analytical methods, defines a more precise stability lobe diagram because no approximation is taken into account, as is the case in modeling of systems dynamic behavior. The disadvantage of this approach is that it is limited to only observed machining system.

Among the first researchers who examine self-excited vibrations in order to define the stability lobe diagram for turning process were Koenigsberger and Tlustý who in [7] recommended three variants for testing the universal lathe:

- A. workpiece is clamped only in the chuck and cutting is done only at free end in variants of longitudinal and transverse machining,
- B. workpiece is clamped into the chuck and supported by a spike, and cutting is performed on his entire length,

C. workpiece is clamped between centres, and cutting is performed near main spindle.

For the adopted feed in each tool passage the depth of the cutting is increased until the appearance of self-excited vibrations is noticed. Cutting depth at which the self-excited vibrations have occurred is considered to be the limit for the applied RPMs, and based on these data it is easy to draw SLD

In addition to these authors, one of the pioneers in this field was V.A. Kudinov, who showed in [8] the dimensions and shape of workpiece, as well as method of its clamping, to investigate the dynamic behavior of lathes.

More recently, with the development of computer technologies, researchers have more sophisticated methods for testing and analyzing self-excited vibrations, and thus simpler methods for experimental definition of stability lobe diagram. Thus, Quintana with authors [12] proposed a method for defining a SLD using a sound mapping technique. For the purpose of defining the SLD, authors carried out 600 experiments, varying 30 different RPMs and 20 cutting depths. For each of these experiments, the noise level is measured and entered in the 3D soundmap. Based on this map and FFT analysis of the sound signal, the authors defined stability lobe diagram, which showed a satisfactory accuracy in comparison with SLD created by the analytical method.

The occurrence of self-excited vibrations are also analyzed by Milisavljević and Zeljković [9,10,11], who developed the two-dimensional model for prediction of self-excited vibration, based on the Sokolovski oscillator.

This paper discusses the method of identifying stability lobe diagram for milling process, based on a series of experimental tests. The method is based on experiments where the workpiece shape permits a gradual increase of the axial depth of cut in the feed direction until self-excited vibrations arises. The spindle speed is increased between passes in order to obtain combinations of a spindle speed and an axial depth of cut in the stability frontier and describe the SLD. Once the SLD is identified, the workshop operator can select the proper process parameters to perform operations without self-excited vibration.

In order to implement the calculation needed to define SLD and in order to collect experimental data, the MATLAB and LabVIEW program environment was used, respectively.

2. METHODOLOGY FOR EXPERIMENTAL DEFINITION OF MACHINING SYSTEM STABILITY LOBE DIAGRAM

As already mentioned, the stability lobe diagram shows the boundary between the stable and the unstable cutting zone, in function of the axial depth of cut (b_{lim}) and main machine spindles RPMs (Fig. 1).

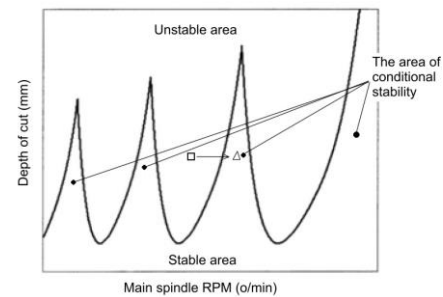


Fig. 1. Example of a stability lobe diagram

The experimental definition of the stability chart is carried out on a specific machining system. This method is based on a series of experiments, with varying the depth of cutting and main spindles RPMs, whereby the cutting tool amplitude of oscillation is monitored.

In order to define the experimental stability lobe diagramby, axial depth of cut increases, thanks to the inclined plane presented by the workpiece. When the cutting tool reaches the stability frontier, chatter occurs suddenly and the machine is stopped, and test procedure is repeated for the next spindle speed. According to Dornfeld [2], with a continuous increase in cutting depth, at one time, (at critical cut depth) forced vibrations from cutting process turn to self-excited, and the cutting process becomes unstable, figure 2.

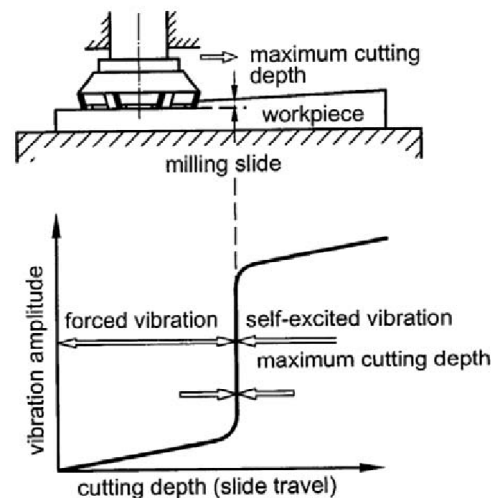


Fig. 2. Illustration of forced and self-excited vibration sensitivity to machining conditions [2]

Detecting the moment of self-excited vibrations occurrence is performed by monitoring oscillation of cutting tool with sensor (accelerometer) or by monitoring the noise level in the work area of the machine tool. At the moment of a sudden increase in tool oscillation amplitude, or a sudden increase in the noise level, the emergence of self-excited vibrations is detected and the machine tool is stopped. The axial depth at which the tool is located at the time of self-excited vibrations appear, is the critical depth of cut for observed RPM. The combination of these values (the depth of cut - RPM) is plotted in the diagram, and by repeating the experiment with a gradual increase of the main spindle rotational speed, a stability card is obtained.

3. EXPERIMENTAL STABILITY LOBE DIAGRAM OF MACHINING CENTER EMCO CONCEPT MILL 450

Experimental definition of the stability lobe diagram was done on the example of EMCO Concept Mill 450 machining center (Figure 3).



Fig. 3. Machining center EMCO Concept Mill 450

The cutting tool used was a HSS flat end mill, with 10mm diameter and 4 cutting edges. The workpiece material was aluminium AL 7075 (Figure 3).

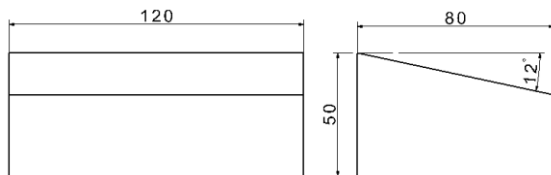


Fig. 4. Workpiece made of Al7075

Eight experiments were carried out, in which the cutting speed ranged from 80 m/min to 150 m/min, maintaining a constant feed per tooth of 0.02 mm/tooth. Detailed cutting regimes for each experiment are shown in Table 1.

Experiment No.	Cutting speed [m/min]	Main spindle RPM [rev/min]	Feed [mm/min]
1.	80	2550	200
2.	90	2866	230
3.	100	3185	254
4.	110	3503	280
5.	120	3822	305
6.	130	4140	331
7.	140	4459	356
8.	150	4777	381

Table 1. Cutting regimes for the experimental definition of SLD

The definition of SLD by experimental method was done as axial depth of cut increases, thanks to the inclined plane presented by the workpiece. This allows the tool to move along the Y coordinate of the SLD. When the cutting tool reaches the stability frontier, self-excited vibrations occurs suddenly and the machine is stopped. Afterwards, the spindle speed is increased to carry out another pass moving along the SLD X coordinate. The procedure was repeated until the SLD is physically machined onto the workpiece. During the experiment, the main spindle vibration was measured using a diagnostic instrumentation, consisting of an accelerometer *PCB Model: 352C33* and A/D card *National Instruments USB 4432*.

Although the moment of self-excited vibrations was determined subjectively based on sound, the analysis of the acceleration sensor signal shows that in each of the eight performed experiments, self-vibration vibrations occurred. Figure 5 shows the accelerometer signal after analysis in the case of experiment no. 4.

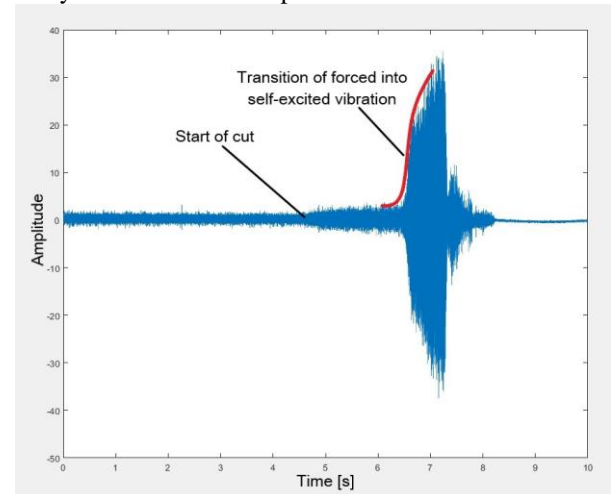


Fig. 5. An accelerometer signal for experiment no. 4.

By this methodology, a SLD is defined which is physically machined onto the workpiece, and it is possible to physically measure cutting depths for the individual RPMs of main spindle, i.e. for individual cutting speeds. Figure 6 shows the stability lobe diagram plotted on workpiece, obtained by previously explained experimental testing.

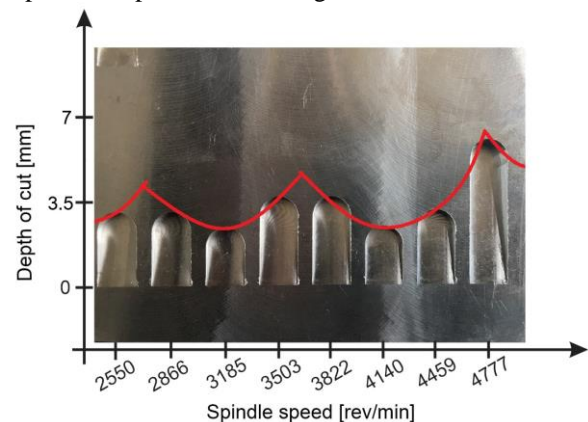


Fig. 6. Expertly defined SLD of EMCO Concept Mill 450 machining center

The values of the limit depth of cut for each cutting speed (RPMs), measured directly from the workpiece, are shown in Table 2.

Experiment No.	Main spindle RPM [rev/min]	Limit depth of cut [mm]
1.	2550	3
2.	2866	3.1
3.	3185	2.45
4.	3503	3.6
5.	3822	3.65
6.	4140	2.4
7.	4459	3.2
8.	4777	6.25

Table 2. Measured limit depths of cut

4. CONCLUSION

The relative oscillation between the tool and the workpiece, which occurs during the cutting process, can lead to a loss of process stability and self-excited vibrations.

Compared to the stable cutting process, the appearance of self-excited vibrations is characterized by a sudden increase in cutting tool oscillation amplitude, reduction in the quality of machined surface, appearance of noise, etc.

This paper discusses the method of identifying stability lobe diagram for milling process, based on a series of experimental tests. The method is based on experiments where the workpiece shape permits a gradual increase of the axial depth of cut in the feed direction until self-excited vibrations arises. The spindle speed is increased between passes in order to obtain combinations of a spindle speed and an axial depth of cut in the stability frontier and describe the SLD.

This method of defining the SLD was applied on EMCO Concept Mill 450 machining center.

In order for the methodology to define SLD of machining system, which was carried out in this paper, was complete, it is necessary to define analytical SLD of the EMCO Concept Mill 450 machining center, and then compare results with the experimentally obtained data. Also, in order to eliminate the subjective influence on determining the moment of self-excited vibrations, it is necessary to analyze in detail signals collected by the diagnostic equipment.

5. REFERENCES

- [1] Altintas, Y., Budak, E.: *Analytical Prediction of Stability Lobes in Milling*, Annals of the CIRP, Vol. 44/1, pp. 357-362, 1995.
- [2] Dornfeld, D.: *Precision Manufacturing*, first ed., Springer, New York, NY, 2007.
- [3] Duncan, S. G.: *Milling Dynamics Prediction and Uncertainty Analysis Using Receptance Coupling Substructure Analysis*, Doctoral Thesis, University of Florida, 2006.
- [4] Gradisek, J., Kalveram, M., Insperger, T., Weinert, K., Stepan, G., Govekar, E.: *On stability prediction for milling*, International Journal of Machine Tools and Manufacture, Vol. 45, Issues 7-8, pp. 769-781, 2005/06.
- [5] Insperger, T., Stepan, G.: *Semi-discretization method for delayed systems*, International Journal for Numerical Methods in Engineering, Vol. 55, Issues 5, pp. 503-518, 2002.
- [6] Insperger, T., Stepan, G.: *Updated semi-discretization method for periodic delay-differential equations with discrete delay*, International Journal for Numerical Methods in Engineering, Vol. 61, Issue 1, pp. 117-141, 2004.
- [7] Koenigsberger, F., Tlustý, J.: *Machine Tool Structures*, Volume 1, Pergamon Press, 1970.
- [8] Кудинов, В.А.: *Динамика станков*, Машиностроение, Москва, 1967.
- [9] Milisavljević, B., Zeljković, M.: *Bifurkacije i samopobudne vibracije pri obradi rezanjem - dvodimenzionalni model*, Zbornik radova, VI međunarodna naučno-stručna konferencija MMA '97 - Fleksibilne tehnologije, Novi Sad, 1997, str.103-108
- [10] Milisavljević, B., Zeljković, M., Gatalo, R.: *The nonlinear model of a chatter and bifurcation*, Proceedings of the 5th engineering systems design and analysis conference - ESDA - ASME 2000, PD. Vol. 82, New York, 2000, pp 391 - 398
- [11] Milisavljević, B., Zeljković, M.: *Bifurkacija ravnotežnog stanja pri obradi rezanjem: oscilator Sokolovskog*, Zbornik radova, 27. JUPITER konferencija - 23. simpozijum NU-ROBOTI-FTS, Beograd, 2001, str. 3.37 - 3.40
- [12] Quintana, G., Ciurana, J., Teixidor, D.: *A new experimental methodology for identification of stability lobes diagram in milling operations*, International Journal of Machine Tools and Manufacture, Vol. 48, Issue 15, pp. 1637-1645, 2008.
- [13] Quintana, G., Ciurana, J.: *Chatter in machining processes: A review*, International Journal of Machine Tools and Manufacture, Vol. 51, pp. 363-376, 2011.
- [14] Tlustý, J. Polacek, M.: *The stability of machine tools against self-excited vibrations in machining*, Proceedings of the ASME Production Engineering Research Conference, pp. 465-474, 1963.
- [15] Tobias, S.A.; Fishwick, W.: *Theory of regenerative machine tool chatter*, The engineer 1958, 258.

Authors: MSc. Cvijetin Mladenović, Dr Milan Zeljković, MSc Milos Knezev, University of Novi Sad, Faculty of Technical Sciences, Department for Production Engineering, Trg Dositeja Obradovica 6, 21000 Novi Sad, Serbia, Phone: +381 21 450-366, Fax: +381 21 454-495. E-mail: mladja@uns.ac.rs, milanz@uns.ac.rs, knezev@uns.ac.rs Dr Aleksandar Košarac, Faculty of Mechanical Engineering East Sarajevo, East Sarajevo, Bosina and Hercegovina, Phone: +387 57 340 847, E-mail: aleksandar.kosarac@ues.rs.ba

ACKNOWLEDGMENTS: This paper presents a part of the research results on the project "Contemporary Approaches in the Development of Special Solutions Bearing in Mechanical Engineering and Medical Prosthetics", TR 35025, financed by the Ministry of Education and Science of the Republic of Serbia.

Vorkapic, N., Kokotovic, B.

SYNTHESIS AND ANALYSIS OF THE TOOL DYNAMOMETER FOR TURNING OPERATIONS

Abstract: Virtual manufacturing has predicting of cutting forces in prepared program for CNC machine tool as one of the most important functional block. Development of reliable models of cutting forces requires appropriate sensor technique. It's application is needed in building of data base with specific cutting forces, as well as for evaluation of developed models of cutting forces. Wide use of superior piezo-electric tool dynamometers is significantly reduced because its very high price. Paper presents development of the three- component tool dynamometer with strain gauges. Basic shape of this dynamometer is well known double extended octagonal ring (DEOR). Geometric parameters of the dynamometer body is optimised through FEA analysis. Designed dynamometer achieves partial decomposition of force components. Completing of such force decomposition is realized through decomposition matrix, created using FEA environment.

Key words: Cutting forces, Dynamometer, FEA analysis

1. INTRODUCTION

There are several reasons for applying of sensors for cutting force measurements. One of them is the need for identification of specific cutting forces in orthogonal cutting, which are necessary for developing of various procedures for predicting of cutting forces and off line optimization of machining process for certain parts. For this purpose it is enough to have two-component dynamometer. Verification of such procedures and testing of specific tools and machining data also requires dynamometers for cutting forces, but with ability for measuring more than two components. Developing of procedures for monitoring and on-line adaptive control (AC) of machining processes also need acquisition of cutting force components. The first and the second field of application of dynamometers assume laboratory environment. This paper describes some results in developing of three-component dynamometer intended for measuring of cutting forces in turning operations. Sensor elements are with resistance strain gauges (RSG).

2. CUTTING FORCE DYNAMOMETERS

Different physical principles for transformation of cutting force in some electrical quantity were used in developing of cutting force dynamometers (CtFD). Among them there are two approaches which were widely used in recent decades. These are piezoelectric sensors and sensors with resistance strain gauges (RSG). RSG force sensors have: simple construction, high and adjustable resolution, and high reliability [1]. At the same time they have following disadvantages: higher power consumption, lacking reproducibility and, as the most significant, lower stiffness and lower dynamic range.

2.1 Dynamometers with strain gauges

Many of applications of RSG dynamometers are not

too demanding: all what is needed is max permissible load. Linearity, in general case, is sufficient. These are (single component) load cells and weighing devices, sometimes extremely low cost, intended for measuring of static force.

Most of research projects dealing with CtFD use one of three typical design of sensitive elements of dynamometer (Fig.1): specific arrangement of several octagonal rings (OR) [2,3,5,6], extended octagonal ring (EOR) and double extended octagonal ring (DEOR) [4]. Each of these designs, shown on Fig.1, assumes the areas in which the strain is concentrated.

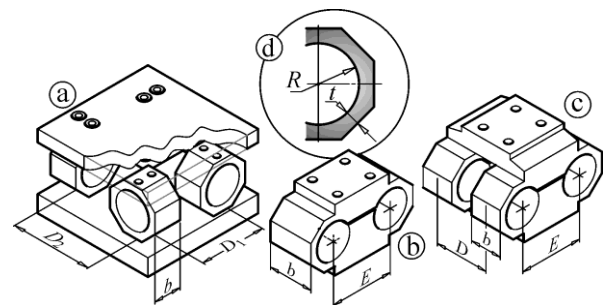


Fig. 1 Typical Sensitive elements of RSG-CtFD and their design parameters

. These are places where RSG should be applied, in such manner that, connected in Wheatston bridge, they enable sufficient level of signal of force component which induces this strain.

Octagonal ring has property of decoupling of two orthogonal force components (directions n and t) acting opposite from its base. Such design is inspired with theory of thin circular rings [2,6], which also have this ability. This theory shows limitations especially in cases where ratios t/R increase.

In design of the CtFD, presented in this paper, a DEOR type of sensitive element was used. Reason for such choice was in intention to avoid possible nonlinearities of dynamometer with ORs, caused by nonlinear nature of contact between base, ORs and platform.

3. DESIGN OF TOOL DYNAMOMETER FOR TURNING

In design of tool dynamometer for turning operations, presented in this paper, intention was to satisfy typical functional requirements: (i) Design of sensitive element which enables measuring of three orthogonal forces in turning up to max values (max $F_1, F_2, F_3 = 5\text{ kN}, 3\text{ kN}, 3\text{ kN}$) with permitted overload approx. 20%, (ii) First modal frequency (with cutting tool) greater than 1000 Hz. (iii) Displacement of the tip of CtFD lower than 0.15 mm in all coordinate direction in case of simultaneous acting of $F_1, F_2, F_3 = 3\text{ kN}$, (iv) Easy exchange and fixing of the turning tool into dynamometer body, (v) CtFD for right hand and left hand tools, allowing operation in M3/M4 direction of spindle rotation, (vi) Reliable protection from damage (hot chip, coolant) of RSG, their leads and cable to signal conditioning devices.

Design of dynamometer assembly is shown on Fig. 2. Basic part is sensitive (dynamometer body) element (1) DEOR type, symmetric, made of steel, quenched and tempered ($R_m \approx 950\text{ N/mm}^2$). Its base is in form of square flange. Its platform is in form of rigid block with square hole intended for placing of 20x20 mm tool shank. Platform (block) is partially separated from base (flange) with thin cut made with wire EDM. Central hole in the flange is 22x22 mm, for free displacement of the rear end of longer tool shank. Concept of this CtFD assumes different adapters for mounting on different tool holders. One example of adapter (3) is shown, with details (4) on flange for its aligning to adapter. Two vertical M8 screws (6) and one screw (5) on side is for fixing of the tool shank in the body.

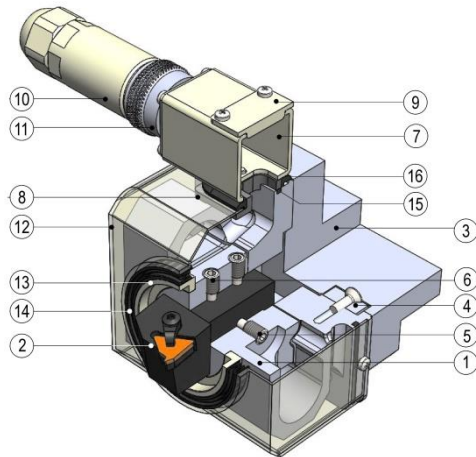


Fig. 2 Assembly of proposed 3-component tool dynamometer for turning

On the top of the body is one terminal box (7) (closed square inox tube) mounted via angular element (8) to the flange of the body. Purpose of terminal box is to offer enough protected space needed for collecting leads from RSG to the connector (11) of the box. Appropriate 12-pin sealed circular cable connector is with modified extension. Such modification was made for reliable fixing of three cables (LiYCY 4x0.34) for housing of the connector in corrugated protection steel

tube (StaPa 3''/8). For better approach to numerous RSG leads, there is removable sealed steel cup (9). Protection of RSGs and their leads is realized using shield (12). Its rear end has square contour for positioning on the flange. Fixing of shield to flange is using 4 screws. Front end of the platform (block) has pressed ring (13) with small overhang. Radial seal (14) is mounted between this ring and hole in the shield. For sealing between shield and flange of dynamometer body an O-ring (15) was used, placed in the slot on the flange contour. Specific rubber seal (16) is mounted under the terminal box ensuring the sealing between several components (1, 7, 8, 12).

4. DESIGN OF ELASTIC SENSITIVE ELEMENT

Role of cut between tool block and flange is to direct load from tool on half rings (4 rings) making concentrate strain in this part of volume. These 4 rings build DEOR composition. Following parameters of DEOR were selected: $R = 12.5\text{ mm}$, $t_1 = 5\text{ mm}$ (horizontal), $t_2 = 6.3\text{ mm}$ (inclined), $b = 24\text{ mm}$, $E = 40\text{ mm}$ and $D = 54\text{ mm}$ (designation acc. Fig 1). Choice of these parameters assumes compromise between intention to achieve high sensitivity (high level of strain) with low level of displacement (high stiffness is required) at the same time. Generally speaking, these functions for OR [1,6] are in form:

$$\varepsilon_i = \frac{K_{i,\varepsilon} F_i R}{E b t^2}, \quad \delta_i = \frac{K_{i,\delta} F_i R^3}{E b t^3} \quad (1)$$

In choice of parameters R and t , for CtFD, presented here, high stiffness was a priority. Ratio t/R is significantly high (0.504 and 0.4). That implies great stiffness but also lower level of sensitivity and need of higher amplification in devices for signal conditioning.

Significant part of volume of the tool block is removed in order to reduce mass of moving platform without significant decrease of its stiffness. That is very important for keeping modal frequencies of the CtFD sufficiently high.

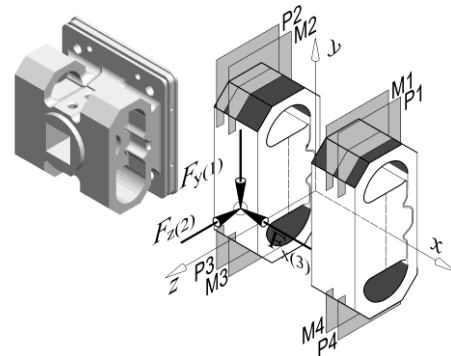


Fig. 3 Sensitive element of proposed dynamometer and cross sections for applying of RSGs

Figure 3 shows solid model of the sensitive element of the CtFD and particular sections of its half-rings. Planes are designated with P (Peripheral) and M (Mid in x dir.) and with number of quadrant of xy plane. These planes are referred as candidate cross sections for applying of RSGs.

Analysis of stresses, strains and displacement of the sensitive elements of the CtFD body were performed through FEM simulation (SolidWorks Student Edition). For more precise insight in distribution of strain specific application in Matlab were made. This application uses output files with strain data, from FEM simulation and calculate strain in tangent direction, which is important because RSG is sensitive to deformation in this direction

4.1 FEM analysis

Figure 4 shows, as part of results, distribution of strain ε_{zz} in case of F_2 (a) and F_3 (b) applied on the tool tip. As the representative tool MTJNR-2020K16 standad holder for turning inserts was chosen (simplified geometry for FEA purposes is shown).

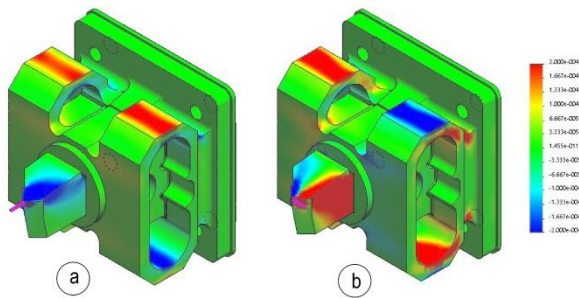


Fig.4 Strain ε_{zz} of the CtFD body
Load $F_2=3\text{kN}$ (a), Load $F_3=3\text{kN}$ (b)

FEM simulation of displacements was separately performed for forces F_1 , F_2 and F_3 , applied on the tool tip. For this analysis 2 representative points were chosen: tool tip (TT) and center (BC) of the face of dynamometer body. Based on results of displacement analysis elements $C_{ij}[\text{mm/N}]$ of compliance matrices were obtained for these points.

$$C_{TT} = 1E^{-6} * \begin{bmatrix} -78.9 & 4.67 & 6.95 \\ 2.22 & -70.3 & 11.47 \\ 7.27 & 14.56 & -14.55 \end{bmatrix} \quad (2)$$

$$C_{BC} = 1E^{-6} * \begin{bmatrix} -16.05 & -0.23 & 0.95 \\ -0.74 & -25.6 & 1.40 \\ -2.88 & -2.67 & -4.89 \end{bmatrix} \quad (3)$$

Rapid rise of displacements from BC to TT should be treated with some reserve. It can be referred to the great overhanging section of the tool, but it also can be the consequence of the modelling of specific kind of contact between tool and dynamometer body.

	1 st Mode [Hz]	2 nd Mode[Hz]
CtFDBody + Tool	1395	2135
CtFDBody w/o Tool	1633	2567

Table 1: Frequencies of dominant modes

Dynamic analysis were performed for (i) assembly of dynamometer body with fixed tool and (ii) for dynamometer body without tool. Figure 5 shows mode shapes of the first and second mode obtained through dynamic FEM analysis. Mode shapes are similar for

both cases (Shear in plane YZ for mode 1, and tilting around Y axis for mode 2). Obtained modal frequencies are shown in Table 1.

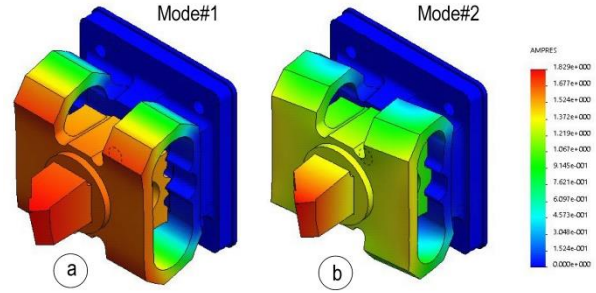


Fig.5 Mode shapes for mode 1 and mode 2.

4.2 Strain analysis in local tangential direction

For correct design of number, arrangement of DMS and its connection in Wheatston bridges for each force component, strain in places of applying RSG, align with its sensitive direction is required. In design of sensor, described in this paper, direction of main sensitivity for each RSGs is assumed to belong one of the planes $x=\text{const}$. Strain FEM analysis in SolidWorks does not offer such kind of results. From this reason, output files with strain analysis ε_x , ε_z and γ_{yz} for simulation of strain for each particular load (F_1 , F_2 , F_3) were exported for use in specific Matlab application, made for this purpose. In this program for each point of model (in sensitive zones) transformations of strains is performed in order to calculate strain in direction applying of possible RSG. Calculation of angle θ_N from $y+$ axis to normal vector of local surface need to be calculated for each point, according to geometry of dynamometer body (Fig .6).

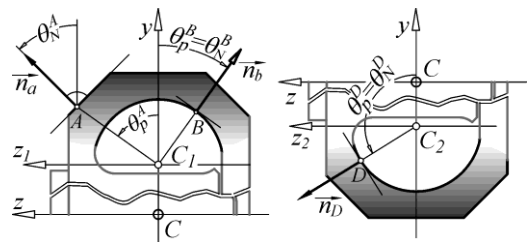


Fig.6 Examples of obtaining angular position of point (θ_p) and angle of local normal vector (θ_N)

Transformation of strains on direction t is calculated according to:

$$\varepsilon_t = \varepsilon_{yy} \sin^2 \theta_N + \varepsilon_{zz} \cos^2 \theta_N - \gamma_{yz} \sin \theta_N \cdot \cos \theta_N \quad (4)$$

For better presentation of distribution of ε_t , transformation of yz -coordinates of points, on rings, to angular coordinate θ_p was performed. Origin of this polar diagram is either C_1 or C_2 (axis through centres of inner rings) as shown on Fig 6. FEM analysis of strain and described postprocessing in Matlab of these results were performed for internal (I) and external (E) half-rings of sensor in 4 different cross sections (middle sections: x_{M1} , x_{M2} and peripheral sections: x_{P1} , x_{P2}) according to Fig.3. Results of for mid sections are shown in Figure 7 (I-internal surfaces) and Fig.8 (for E-external surfaces). Results for peripheral planes are not

shown here.

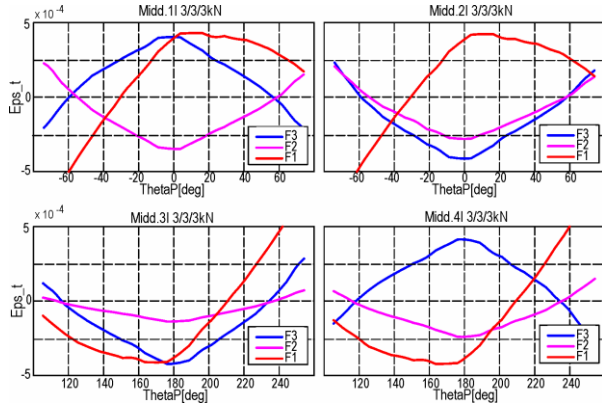


Fig.7 Distribution of ε_i for internal half-rings

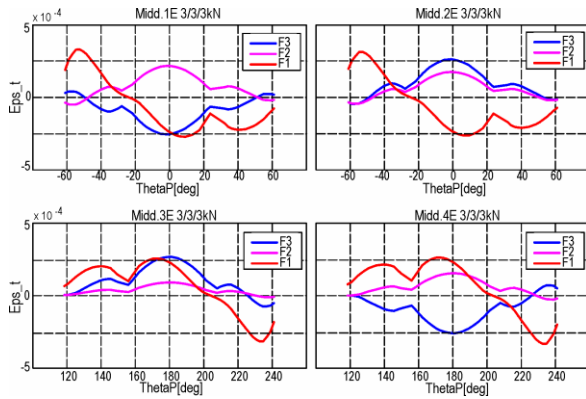


Fig.8 Distribution of ε_i for external half-rings

4.3 Sensitivity and cross-sensitivity

One of the most important performances of multi component CtFD is its ability to achieve reliable decoupling of components of force acting on its sensitive element. Maximum of sensitivities (S_{ii}) and minimum of cross sensitivities (S_{ij}) is required.

$$S_{ii} = \frac{\varepsilon_i}{F_i} \left[\frac{\text{mV}}{\text{V} \cdot \text{N}} \right], S_{ij} = \frac{\varepsilon_i}{F_j} \left[\frac{\text{mV}}{\text{V} \cdot \text{N}} \right] \quad (5)$$

Several important conclusions, needed for design of RSGs arrangement and its connection in bridges, can be made based on diagrams on Fig.7 and 8. Strain ε_i induced by F_1 (Fig.8) has an asymmetric distribution. Decoupling of F_1 from measured strains seems very simple. Figure 8 shows nodes of deformation ε_i induced by F_2 and F_3 (for values θ_p close to $-60^\circ/60^\circ$ and $117^\circ/227^\circ$. Angular positions for RSGs for F_1 , near $-50^\circ/50^\circ$ for upper rings, and near $135^\circ/225^\circ$ are good candidates.

Candidate RSGs for F_2 and F_3 should be placed near $\theta_p=0^\circ$ (upper zone) or $\theta_p=180^\circ$ (lower zone), on internal and external surfaces of the half-rings. These locations include huge problem of decoupling of force components. Nodes of $\varepsilon_i(F_1)$ are too far from this location. Additional problem is the fact that both F_2 and F_3 have their extreme values around these locations. Possible solution is specific connection of RSGs in branches of the bridge. That means 2 RSGs (with same sign of strain) in series in each branch.

Analysis based on results shown on Fig.7 and 8, with specific connection of RSGs, for each component

enables calculation of elements of sensitivity matrix:

$$S = \begin{bmatrix} S_{11} & S_{12} & S_{13} \\ S_{21} & S_{22} & S_{23} \\ S_{31} & S_{32} & S_{33} \end{bmatrix} = 10^{-9} \begin{bmatrix} 183 & 0 & 0 \\ 6.25 & 139 & 4.16 \\ 2.08 & 22.6 & 159 \end{bmatrix} \quad (6)$$

Max absolute value of ratio S_{ii}/S_{ij} is 14%. Such result implies good decoupling performances of designed dynamometer, but also implies need for software decoupling using inverse of S . Relatively lower level of direct sensitivities is consequence of intention to keep high stiffness of dynamometer body.

5. CONCLUSION

Very good performances (strain, stiffness, sensitivity) in analysis of presented design of 3 component RSG tool dynamometer for turning, were shown. It is expected that prototype of this dynamometer will be useful in experimental activities referred to cutting force measurements. Final estimation of its performances needs to be obtained through experiments. One of the future tasks is obtaining of maps of these performances for different tools, regarding eccentricity of their tips.

6. REFERENCES

- [1] Soliman, E., *Performance analysis of octal rings as mechanical force transducers*, Alexandria Engineering Journal, 2015, Vol.54, pp.155–162.
- [2] Yaldiz, S., *Development and Testing of a Cutting Force Dynamometer for Milling*, Journal of Polytechnic, 2005, Vol. 8, No. 1, pp. 61-68.
- [3] Yaldiz, S., Unsacar, F., *A dynamometer design for measurement the cutting forces on turning*, Measurement, Vol. 39, pp. 80-89, 2006.
- [4] McLaughlin, N.B., Tessier, S., Guilbert, A., *Improved double extended octagonal ring drawbar transducer for 3-D force measurement*, Canadian Agricultural Engineering, 1998, Vol. 40, No.4, pp.257-264.
- [5] Zhao, Y., S. Liang, S., Zhou, G., *A High Performance Sensor for Triaxial Cutting Force Measurement in Turning*, Sensors, 2015, Vol.15, 7969-7984.
- [6] Uddin, M.S., Songyi, D., *On the design and analysis of an octagonal–ellipse ring based cutting force measuring transducer*, Measurement, 2016, Vol. 90, pp. 168–177..

Authors: Nikola Vorkapic Ph.D. student, Assist. Prof. Branko Kokotovic, University of Belgrade, Mechanical Engineering Faculty, Department of Production Engineering, Kraljice Marije 16, 11000 Belgrade, Serbia, Phone.: +381 11 3302-375, Fax: +381 11 3370-364.
E-mail: nikola.vorkapic92@gmail.com
bkokotovic@mas.bg.ac.rs;

ACKNOWLEDGMENTS: The authors would like to thank the Ministry of Education, Science and Technological Development of Serbia for providing financial support that made this work possible.



Section C:

**METROLOGY, QUALITY, FIXTURES,
CUTTING TOOLS AND TRIBOLOGY**

Majstorovic, D., V., Stojadinovic, M., S., Durakbasa, M., N.

AN IN - PROCESS MEASUREMENT INSPECTION PLANNING MODEL FOR PRISMATIC PARTS

Abstract: *In this paper is presented modeling and simulation of measurement path in – process inspection in the case of measurement prismatic parts on CMM. The path modeling consist from the developing mathematical model for distribution of measurement points and nodal points, the defining of optimal probe path by ants colony and simulation of the measurement path.. The purpose simulation of inspection is visually check from standpoint collision and generate the measuring protocol and program code at the output, which among other things, contains data about the coordinates of the measuring points and the nodal points. The advantage of this approach is reduction of the total measurement time by reducing the time required to the prepare measurements in in-process inspection of metrological complex prismatic parts.*

Key words: *measuring path, simulation, prismatic parts, CMM*

1. INTRODUCTION

The path planning of the measuring sensor in the process inspection (in-process measurement) depends on the geometric and metrological complexity of the measurement parts. Geometric complexity refers to the distribution, size and type of the measuring surfaces, their accessibility for measuring probe, etc. The metrological complexity is primarily refers to the forms and quality of tolerances, which appear on one measurement part, as well as their number. In coordinate metrology these types of complexity cannot be separately observed, but integrated. A common element in that integration is an object of touch or a measure feature. Its position and orientation are geometric characteristics, and the type of the tolerance zone, the values that limit the zone, the reference element, etc., are tolerance characteristics.

An improved approach to modeling the measurement path in-process measurement is presented in this paper by defining the objects of contact (measurements) from a geometric - tolerance point of view. The geometric information of object contact is extracted from the IGES file. The basis for them is the 3D CAD model of measurement part. The integration of geometric and tolerance information takes place in the knowledge base given in [1]. With the help of this integration, relations between objects of measurement and tolerance of measuring parts are defined.

Based on the defined relationship of tolerance and geometry of the parts, this path model as the output gives the coordinates of the points with their exact order. In addition to the given measuring points, the points of the node are also given, through which the

measuring probe passes in order to avoid collision. In this way, the initial measurement paths are obtained by defining the measurement and node points. The initial path is further used to obtain an optimal measurement path using ants colony technique.

The purpose of inspection simulation is visual check the measurement path from the standpoint of the collision avoidance and generating measurement protocol, and as well the control data list for the process of the measurement execution.

2. A MODEL IN - PROCES MEASUREMENT INSPECTION PLANNING

The model of the existing measuring system presented in [2] can be used as the starting base for the measurement path model presented in this chapter. In this case, by modifying such a system is coming to the in-process measurement model shows in Figure 1. The model provides a complete flow of information for planning in-the process of measurement and inspection for two types of final measuring devices and it measures the head and measuring probe

2.1 Inspection features

The modeling of the measuring path encompasses the definition of features for inspection, which is based on the basic geometric features and their parameters. The geometric features encompassed by this modeling are the point, plane, circle, hemisphere, cylinder, cone, truncated cone, truncated hemisphere [2-5]. Parameters of the features are uniquely determined for each of them. The definition of the feature parameters is done so that their geometry is fully described and whether the feature is full or hollow. Defining a full and hollow feature is done on the basis of a feature fullness vector

as parameter, which provides information whether the inspection of a given feature is done inside or out. The defined inspection features and their parameters are the basis for the development of algorithms such as the algorithm for distributing measurement points, collision

avoidance and planning the path where, addition to them, ontologically defined connections of primitives and specified tolerances [4,5] also are used. The flow or procedure for extracting the feature parameters on the base IGES file is given in Figure 2.

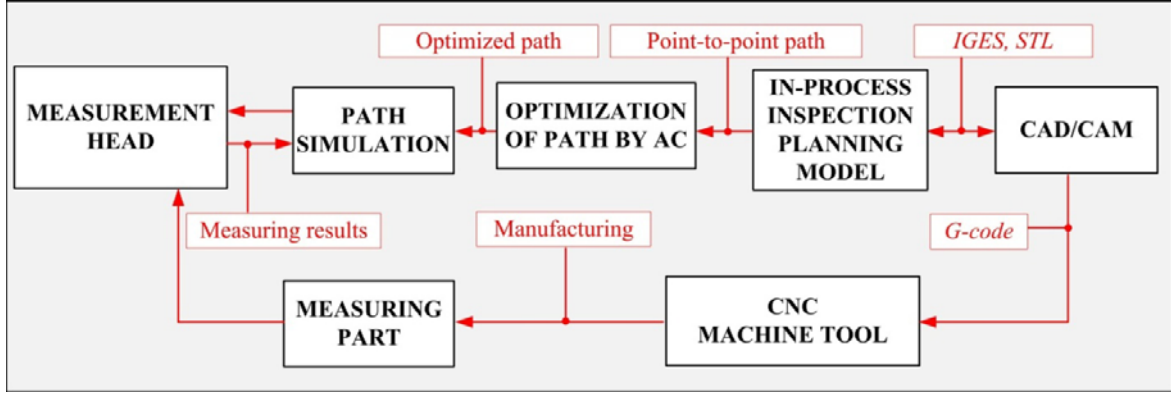


Fig. 1. Principle distribution measuring points (a) plane and b) cylinder), simulation (d) plane and e) cylinder) and optimized measuring path (e))

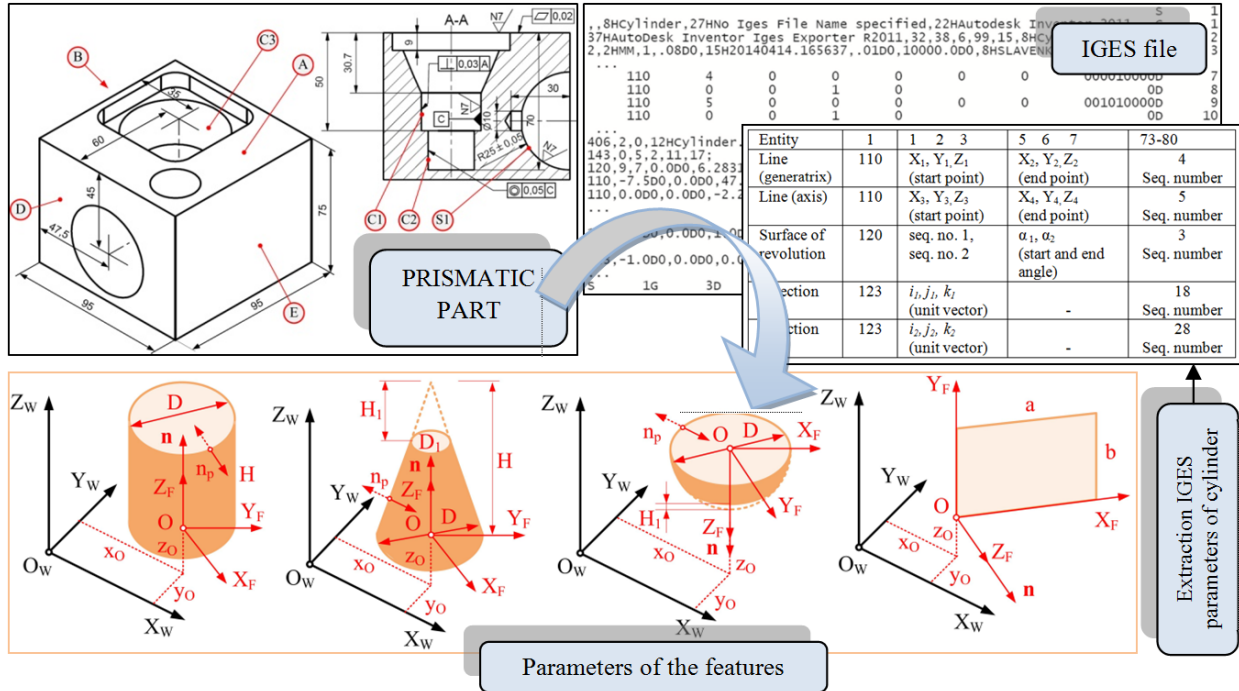


Fig. 2. Extraction parameters of metrological features (cylinder, transcendent cone, transcendent sphere and plane)

2.2 Generating initial measurement path

Generating point-to-point measurement path or initial path defines distribution of two sets of points: (i) set of measuring points, and (ii) set of nodes which is composed of two sub-sets. Distribution of measuring point for different geometric features such as plane, circle, hemisphere, cylinder, etc. is obtained by modifying Hemmersly [6] sequences. Coordinates of measuring points are presented in Cartesian coordinate system and designated as $P_i(s_i, t_i, w_i)$. An example of formulas for calculation of measuring points coordinates for a hemisphere is given as follows:

$$s_i = \sqrt{R^2 - \left(\left(\sum_{j=0}^{k-1} \left(\left[\frac{i}{2^j} \right] \text{Mod} 2 \right) \cdot 2^{-(j+1)} \right) \cdot R \right)^2} \cdot \cos \left(\frac{i}{N} \cdot 360^\circ \right)$$

$$t_i = \sqrt{R^2 - \left(\left(\sum_{j=0}^{k-1} \left(\left[\frac{i}{2^j} \right] \text{Mod} 2 \right) \cdot 2^{-(j+1)} \right) \cdot R \right)^2} \cdot \sin \left(\frac{i}{N} \cdot 360^\circ \right)$$

$$w_i = \left(\sum_{j=0}^{k-1} \left(\left[\frac{i}{2^j} \right] \text{Mod} 2 \right) \cdot 2^{-(j+1)} \right) \cdot R$$

where R [mm] is radius of a hemisphere.

As it has been already mentioned, set of node points implies two sub-sets $P_{i1}(s_{i1}, t_{i1}, w_{i1})$ and $P_{i2}(s_{i2}, t_{i2}, w_{i2})$,

where $i = 0, 1, 2, \dots, (N-1)$. Sub-set $P_{i1}(x_{i1}, y_{i1}, z_{i1})$ presents points for the transition from fast to slow feed. The distance that measuring probe crosses between points $P_{i1}(x_{i1}, y_{i1}, z_{i1})$ and $P_i(x_i, y_i, z_i)$ is presented by d_1 - slow feed path, and the distance between points $P_{i2}(x_{i2}, y_{i2}, z_{i2})$ and $P_{i1}(x_{i1}, y_{i1}, z_{i1})$ is d_2 - rapid feed path.

3. PATH OPTIMIZATION BY ANTS COLONY

Application of ants colony optimization (ACO) in a coordinate metrology is based on the solution of travelling salesmen problem (TSP), where the set of cities that the salesman should pass through with the shortest possible path corresponds to the set of points of a minimal measuring path length. The model is based on equation (4) for calculation of the measuring probe path during the measurement on N measuring points:

$$\min\{D_{tot}\} = K + \left\{ \sum_{i=0}^{N-1} \left(\min\left\{ \left| \overline{P_{i1}P_{(i+1)2}} \right| \right\} \vee \min\left\{ \left| \overline{P_{i1}P_{(i+1)1}} \right| \right\} \vee \min\left\{ \left| \overline{P_{i(i+1)}P_{(i+1)2}} \right| \right\} \vee \min\left\{ \left| \overline{P_{i2}P_{(i+1)1}} \right| \right\} \right) \right\}$$

where $K = N \cdot (2 \cdot d_1 + d_2)$, $d_2 = \left| \overline{P_{i2}P_{i1}} \right|$ and $d_1 = \left| \overline{P_{i1}P_i} \right|$ as shows at fig. 3.

According to [7,8] TSP can be represented by a complete weighted graph $G = (N, A)$ (fig. 3) with N being the set of nodes representing the cities, and A being the set of arcs. Each arc $(i, j) \in A$ is assigned a value (length) d_{ij} , which is the distance between cities i and j , with $i, j \in N$. The goal in TSP is to find a minimum length Hamiltonian circuit of the graph where a Hamiltonian circuit is a closed path visiting each of the $n = |N|$ nodes of G exactly once [7], so that an optimal solution to the TSP is a permutation π of the node indices $\{1, 2, \dots, n\}$ such that the length $f(\pi)$ is minimal where $f(\pi)$ is given by:

$$f(\pi) = \sum_{i=1}^{n-1} d_{\pi(i)\pi(i+1)} + d_{\pi(n)\pi(1)}$$

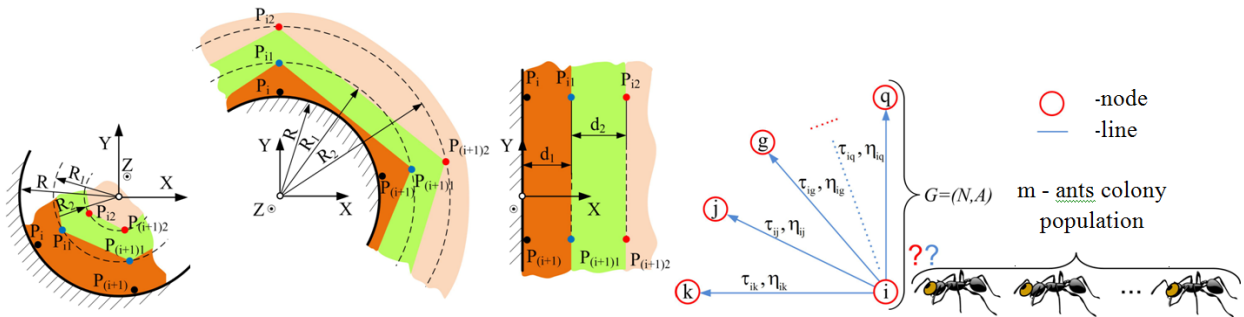


Fig. 3. Collision zones (green – optimal free collision zone; brown – collision zone; other - free collision zone) for three types of surfaces and graph of potential ants moving in optimal free collision zone

4. SIMULATION OF PATH AND RESULTS

The purpose of inspection simulation is visual check the measurement path from the standpoint of the collision for the given workpiece and its specified tolerance. Simulation is based on the previously mentioned inspection planning model and provides a measurement protocol and a list of control data as the output. Simulation of the path is performed in the Pro/Engineer software version Wildfire 4.0 (PTC Creo) and software MatLab. For the simulation of the path in the software, the Manufacturing module was used within the CMM submodule as well. Figure 4 shows the path of inspecting the diameter of the hemisphere as well as the introductory part of the generated CL file. The CL file generates the software as an output report that contains data about the motion of a measuring sensor. Figure 5 shows the measuring path lengths obtained by three methods (d_m , d_s and d_o), as well as the result of comparison, i.e. improvements (values I_s i I_m). For the features as it hemisphere, ratios of the measuring path lengths d_o/d_s are less than 86,61 %, which presents reduction of the measuring path

obtained by ACO at least for 13,39%. Ratios of the measuring path lengths d_o/d_m are less than 64,97 %, presenting reduction of the measuring path at least for 35,03%.

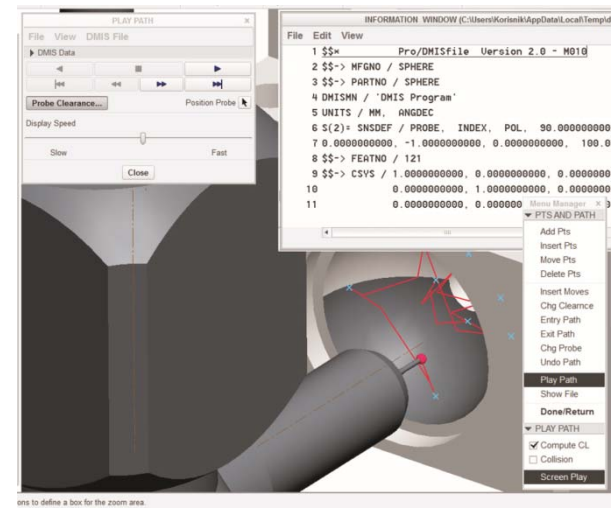


Fig. 4 Path simulation in PTC Creo (Pro/Engineer)

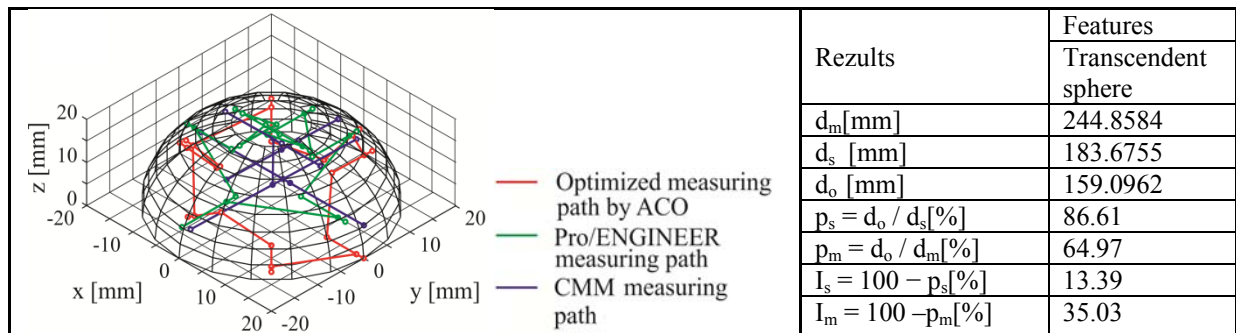


Fig. 5 Path simulation in software MatLab and results of comparison three type of path

5. CONCLUSION

Inspection on the CMM is based on a complex of software, which supports a variety of metrological tasks (tolerances). Implementation of a uniform plan of inspection represents the special problem, which depend from the metrological complexity of the prismatic parts, intuition and experiential knowledge of the inspection planer.

The purpose of inspection simulation is visual check the measurement path from the standpoint of the collision avoidance and generating measurement protocol, and as well the control data list for the process of the measurement execution. The advantage of this approach is to reduce the measurement time by optimization of the measurement path for measurement of complex prismatic parts.

Conducted research in this paper is an answer to the industry's requirement as it maintenance of the constant - required level of inspection by modeling and simulation of the part of activity witch perform inspection planer.

The limitation of the developed approach of modeling is application only for prismatic parts, but not for parts with free surfaces for inspection, because the model was developed only for the basic geometric features from which the prismatic parts consist.

6. REFERENCE

- [1] Majstorovic, D. V., Stojadinovic, M. S., *Research and Development of Knowledge Base for Inspection Planning Prismatic Parts on CMM*, 11th International Symposium on Measurement and Quality Control, Cracow-Kielce, Poland, September 11-13, 2013.
- [2] Stojadinovic, S., Majstorovic, V., Durakbasa, N., Sibalija, T., *Towards an intelligent approach for CMM inspection planning of prismatic parts*, Measurement, 92: 326-339, 2016,
- [3] Stojadinovic, S., Majstorovic, V., Durakbasa, N., Sibalija, T., *Ants Colony Optimization of the Measuring Path of Prismatic Parts on a CMM*, Metrology and Measurement Systems, 23/1:119-132, 2016.
- [4] Stojadinovic S., Majstorović V., *Towards the Development of Feature – Based Ontology for Inspection Planning System on CMM*, Journal of Machine Engineering, Editorial Institution of the Wroclaw Board of Scientific Technical Societies Federation NOT, Wroclaw, Poland, 12/1:89-98, 2012.
- [5] Stojadinovic S., Majstorović, V., *Metrological primitives in production metrology–ontological approach*, Proceedings of the 34th International Conference on Production Engineering, pp. 29-30, Nis, Serbia, 28– 30th September, 2011.
- [6] Lee G., Mou J., Shen Y., *Sampling strategy design for dimensional measurement of geometric features using coordinate measuring machine*, Int. J. Mach. Tools Manufact., Great Britain, 37/7:917-934, 1997.
- [7] Dorigo, M., Stützle, T., (2004). *Ant Colony Optimization*, The MIT Press Cambridge, Massachusetts London.
- [8] Dorigo, M., Blum, C., (2005). Ant colony optimization theory: A survey, *Theoretical Computer Science*, 344, 243 – 278.

Authors: Full Prof. Vidosav Majstorovic, Asist. Prof. Slavenko Stojadinovic, Full Prof. Numan Durakbasa, University of Belgrade, Faculty of Mechanical Engineering, Department of Production Engineering, Kraljice Marije 16, 11000 Beograd, Serbia, Phone.: +381 3370-341, Fax: +381 3370-364. Vienna University of Technology, Department for Interchangeable Manufacturing and Industrial Metrology, High Precision Measurement Room – Nanometrology Laboratory.
E-mail: vmajstorovic@mas.bg.ac.rs; sstojadinovic@mas.bg.ac.rs; durakbasa@ift.tuwien.ac.at;

ACKNOWLEDGMENTS: The presented research was supported by the Ministry of Education, Science and Technological Development of the Republic of Serbia.

Sovilj, B., Sovilj-Nikić, S.

TRIBOLOGICAL RESEARCHES OF GEAR CUTTING PROCESSES OF CYLINDRICAL GEARS

Abstract: *Abstract: The availability, adaptability, reliability and productivity of modern industrial complexes, maintenance costs, energy costs and industrial production costs depend also on the intensity of wear of the elements of tribo-mechanical systems. Gear cutting operations are usually a bottleneck of production, especially in higher types of production. The complexity of the procedure of determining tribological properties of tribo-mechanical system elements from an economic aspect is provoked by the presence of possibility to choose numerous parameters for monitoring the process development of their wear as well as selection of wear criteria.*

Key words: *tribological processes, wear, tool life, cutting geometry, construction*

1. INTRODUCTION

In industrialized countries, as well as in Serbia today through wear and corrosion resulting losses are expressed in billions. Lack of scientific knowledge in the field of hob milling as well as the present economic situation require further research of this process.

Contemporary production implies a market-oriented production, does not accept independent relations between production and the market, it emphasizes the inseparable connection of their whole, pointing to the need to establish a circular flow. Providing production preconditions for meeting the existing needs and creating the necessary conditions for continuing research for new products is a priority task in modern production.

The structure and individual components of modern industrial complexes represent superior range and the most complex products in the respective fields of science. Consequently, the greatest technological achievements of various industrial branches are merged at the constructors of modern industrial complexes and they are integrated into their products.

Due to the previous data, a significant contribution was made to the development of new types of work-piece materials, tool materials, machines, cutting tools, deforming tools, fixtures, measuring devices, cutting fluids and a better understanding of the nature of the cutting process in different machining conditions [1]. Improvement of machining technology is very important, taking into account the fact that productivity and techno-economic effects reached in the manufacturing process depend on the level of machining technology.

The contemporary characteristics of the society and the desire for continuous improvement of the quality of life require continuous improvement of the quality of production. The product is the most characteristic parameter of the technical development of a country. Analyzing the century-long coupling and mutual relations between man and the industrial product, at each stage of their life cycle, it can be concluded that the industrial product is material creation which is

consciously developed and realized in industrial conditions of production. By directing the process of production development to the development of various systems, it is especially important to find ways to improve the quality of products.

In tribological processes, the very small mass of the tool material and the large mass of the material of the work-piece are involved in the gear cutting. Scheme of tribological system and four different types of boundary between the base and coating are given in Figure 1 [2].

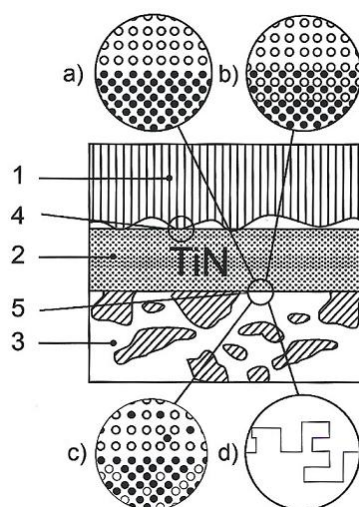


Fig. 1. Scheme of tribological system: 1-work-piece, 2-hard coating, 3-base, 4-tribological contact (lubricant), 5-adhesive joint between the coating and base: a)keen boundary, b)connected boundary, c)diffusion boundary, d)mechanical boundary

The consequences of the development of tribological processes in the zones of contact are the friction and wear of the cutting elements of hob milling tools. In the Figure 2 [3] examples of tribo-mechanical systems are given, and with the number one the critical element of each tribo-mechanical system is marked, that is, the element which is worn at the most in the process of achieving contact.

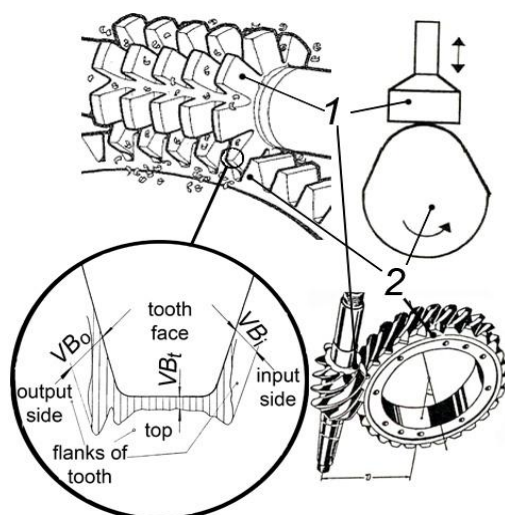


Fig. 2. Example of tribo-mechanical systems with basic elements 1 and 2 and details with wear parameters of hob milling tool

2. GEAR CUTTING AND WEAR PROCESS OF HOB MILLING TOOLS

The problem of the production of gears is analyzed in science and practice in various ways, identifying it once as an element of the machine and another time as a part of the production, that is, a final product. Designed and properly manufactured gears are key components in most complex systems. Gears with involute teeth are among the most important components of efficient modern transmission techniques, in accordance with relevant legislation on pollution and energy saving.

In the hob milling process, the teeth and hollows between teeth are formed by removing the material from the work-piece. Problems that arise in the process of material removal are due to the presence of tribological processes on the contact surfaces of the elements of tribo-mechanical system.

A fundamental knowledge of the process of producing transmission gears is crucial to oppose the demands for continuous improvement in a globalized market. Related development is continually involved in the development and production of machine tools and tools for gear cutting.

Manufacturers of involute cylindrical gears during their production process, regardless of their size, from a few millimeters to several meters, face common technological problems. The predictability of machining parameters, such as geometry and chip flow, tool wear, etc., with regard to work-piece, tool and machining data is of great interest for research and industry. The changeable chip formation during the manufacturing process of serration of cylindrical gears causes different wear laws.

Production operations and methods in mass production depend on various parameters such as the cost of machining, production philosophy, practical experience, etc. A common strategy is to achieve the highest possible accuracy during roughing and to perform thermal treatment with the necessary tolerance to completely avoid finishing [1].

Hob milling process is a complex process with a very wide range of factors and process parameters which are important for finding the optimum machining conditions. Insufficient state of scientific knowledge in the field of hob milling requires further development and research of this kind of machining. Lack of information is increased by applying a variety of tools and materials of hob milling in the machining of gears teeth which are made of various materials.

Economy of gear cutting depends primarily on the character of teeth wear of hob milling tool. Numerous factors and their alternating effects make the research of wear process of hob milling tool very difficult (Figure 3) [3].

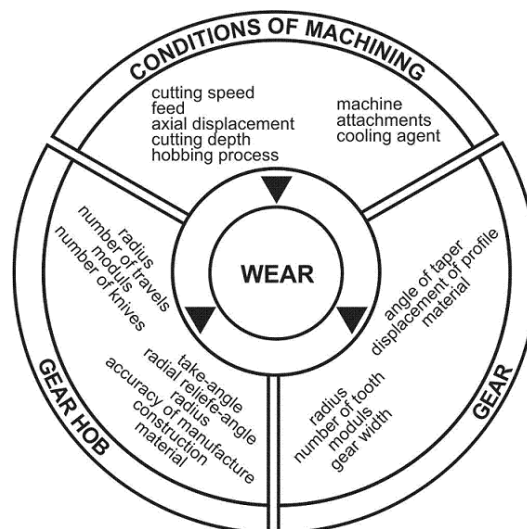


Fig. 3. Influential parameters on wear process of hob milling tool

Detailed analysis of the most influential factors and parameters can serve as a basis for understanding the ways of increasing economy of gear cutting by hob milling. Wear is one of the ending negative phenomena in the machining process. It is believed that the relatively high pressures and high temperatures on contact surfaces of coupled pairs, and the high relative velocity of coupled pairs are the basic conditions for the occurrence and intensive development of tool wear process. Wear of cutting elements of hob milling tools takes place continuously in all moments of contact, and also in all technological conditions and machining regimes [4,5,6].

The development of wear process on the teeth of hob milling tool depends on the combination of tool and work-piece materials [1], machine and applied coolant and lubrication, and also depends on the treatment conditions and machining parameters. Geometry of hob milling tool, gear geometry and hob milling procedures also affect the process of hob milling. The problem of identifying a machining process or mathematical dependencies by which they are characterized is very complex.

Hob milling, as one of the most complex machining processes, has the widest application in the gear cutting of cylindrical gears due to the high productivity of the process. In Figure 4 [7], the principle of hob milling and kinematics are shown.

The complicated kinematics and geometric relations between the hob milling tool and the work-piece create a series of difficulties and problems that prevent the optimal use of tool and machine.

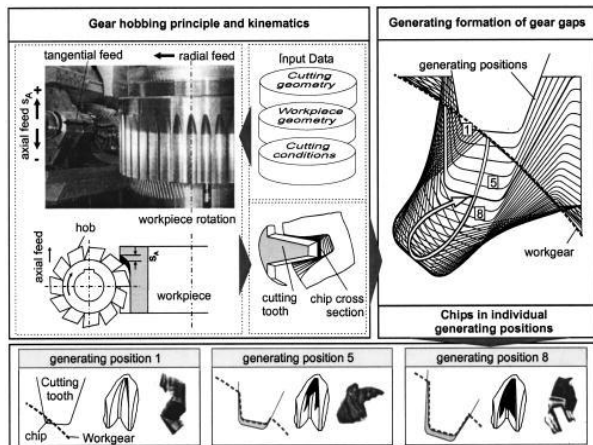


Fig. 4. Hob milling principle and kinematics

Hob milling is a multi parametric and complex method for gear cutting of cylindrical gears. Hob milling is an efficient machining process for the production of serration of high quality cylindrical gears. This process is related to complicated kinematics, the formation and the flow of chip, as well as to the hard-to-describe tool wear mechanisms.

The hob milling process is one of the most important links in the chain of gear cutting, having in mind that the productivity, the final geometric accuracy and the quality of the serration depend to a great extent on the hob milling process. Gear cutting operations most often represent a bottleneck in the production of cylindrical gears, especially in higher types of production. Therefore, the necessity of research and development of optimal tool constructions, as well as research of the optimal conditions of these processes, especially hob milling, is obvious.

The optimization of the production conditions for the gear cutting of the cylindrical gears depends to a large extent on the correctness of the selection and maintenance of the hob milling tool, as well as on the selection of the appropriate cutting regimes.

The modern technical development of the production of cylindrical gears is directed in two basic directions: increase the productivity of the appropriate process and gear cutting while improving the quality of the machined serration. Achieving these, mostly opposite, demands is a very complex task.

The productivity and cost-effectiveness of the hob milling is determined by: the characteristics of the hob milling machine, the construction characteristics of the hob milling tool and the material of the cutting edge [8]. The enhancement of the hob milling of serration of cylindrical gears can be achieved by increasing the productivity and increasing the quality of the serration ([1,8]).

Production operations and methods of gear cutting in mass production depend on various parameters such as the cost of gear cutting, production philosophy, practical experience, etc. A common strategy is to

achieve the highest possible accuracy during rough machining of gear serration and to carry out thermal treatment with the necessary tolerance to completely avoid finishing of the gear serration [1].

Hob milling is also significantly improved and the limits of its development are not yet visible. On the basis of the previous one, the following are being developed: work-piece materials, hob milling tool materials, hob milling tools, fixtures, hob milling machines and automation of the gear cutting process.

The design of hob milling tools, that will provide minimal losses, is of great importance expressed through the construction and cutting geometry of the hob milling tool, and also through the selection of the optimal tool material.

Improving and finding more perfect materials has played the most important role in the development of gear cutting tools of cylindrical gears by hob milling [1,9,10]. Hob milling tools are made of high-speed steel, cemented-carbide, sintered alloys, etc. The development of new and improvement of the existing materials for the production of hob milling tools in order to minimize the total cost of gear cutting and retain the same quality of gear cutting is of great importance in view of the current economic situation. The steadily growing demands placed on the hob milling tools require the continuous development and finding of new methods for making combined materials. Significant progress has been made in that field in the last fifteen years. A large number of hard materials coating methods have been developed in order to protect against the wear of the hob milling tools, but due to insufficient knowledge and experience, they slowly find application in the industry.

The process of the gear cutting by hob milling is characterized by different thicknesses and lengths of the chips, and the materials from which the cutting edge of hob milling tools are made should have significant tenacity and hardness. Based on the previous significant attention is paid to the strengthening of the hob milling tool by applying a permanent layer to the working surfaces of the hob milling tool. The application of coated hob milling tools is conditioned by their high efficiency. Until now there is no correlation between the strength of the hob milling tool and the properties of the coating layer, and the issues of optimizing the properties of the complex layer and the tool base remain open. There are also difficulties in the industrial application of progressive surface reinforcement technology and the rational application of a reinforced hob milling tool.

Today, high-speed steel hob milling tools continue to be used primarily for gear cutting in the automotive industry, especially in the production of truck changers. The further evolution of metallurgy of powdered high-speed steel in combination with the application of PVD layers has contributed to this application and the development of high-speed steel. Coated hob milling tools made of high-speed steels are also used for dry gear cutting of cylindrical gears.

Most of the hob milling tools can be classified into three groups according to their design (Figure 5a [1,8,11,12]). Integrated hob milling tools can be

manufactured from conventional high-speed steel, high-speed steels produced by sintering and for smaller modules made of cemented-carbide. All of the aforementioned hob milling tools can be coated. The hob milling tools with changeable teeth or strips from high speed steel, cemented-carbide or sintered alloy consist of a basic body made of cheaper material and are particularly suitable for larger diameters and larger modules. The hob milling tools with changeable teeth beside that they allow larger constructive back angles, they also have a relatively large, usable cutting length (Figure 5 a [1,8,11,12]). Various variants of hob milling tools that combine different processes such as roughing and finishing and machining of chamfers for removing irregularities (Figure 5 b [1,8,11,12]) have also been developed.

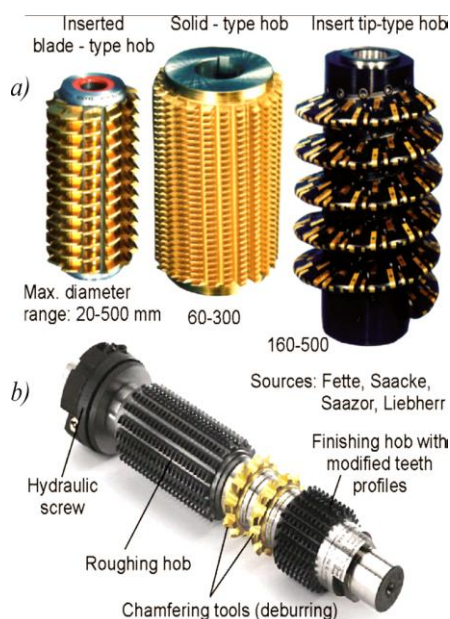


Fig. 5. Modern hob milling tools

In order to increase the productivity of the hob milling, gear cutting process is very close to the limit of the technological capabilities of the machine tools and the hob milling machines. Therefore, the optimal choice of the hob milling tool material is important in achieving this goal. The tendency of the material development for the hob milling tools and the technology of their surface reinforcement are conditioned by the need directed towards improving the physical and mechanical properties of the material for the hob milling tools, among which strength, thermostability, resistance and brittleness have long been considered to be important, while other properties are considered to be less important. Ignoring the importance of certain properties of the hob milling tool materials is one of the main reasons for the lack of understanding of the main functions of the layer's stability on the hob milling tool. There are more than one hundred different methods of surface coating of metals and alloys, by which it is possible to increase the efficiency of the tool to a certain extent.

The fields of application of the knowledge of the chip formation are widespread according to the direction of the evaluation of the cutting properties of

the tools for gear cutting and materials of the hob milling tools, the machining economy, the conditions in the gear cutting on modern hob milling machines, the use of cutting fluids in the gear cutting, etc. The production of toothed tools requires a preliminary basic study, calculation and construction for each specific case. In this field, there are great opportunities for improving production as a whole.

The influencing factors in the process of designing of gear cutting tools are given in Figure 6 [1,12]

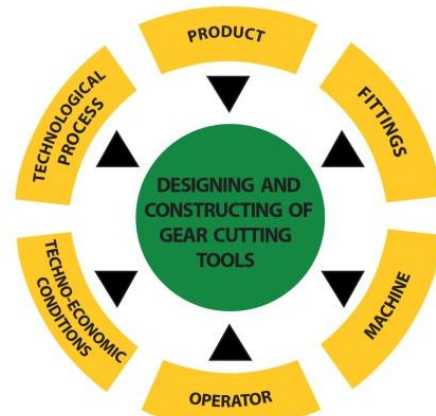


Fig.6. Influencing factors on designing of gear cutting tools

The design quality is one of the essential factors of product quality and one of the most important conditions in product development. The gear cutting tools is a product of a certain branch of production. During production, tribological processes occur. It is indisputable that tribological processes are very complex processes and also depend on a large number of factors. Because of this, there are many possibilities that the designer, or constructor, can develop a tribologically correct construction in the design process. As in a wider sense, at this time the construction is organized and regulated in the correct tribological behavior, the available possibilities are divided into three groups of regulators: structural, technological and exploitation (Figure 7) [13].

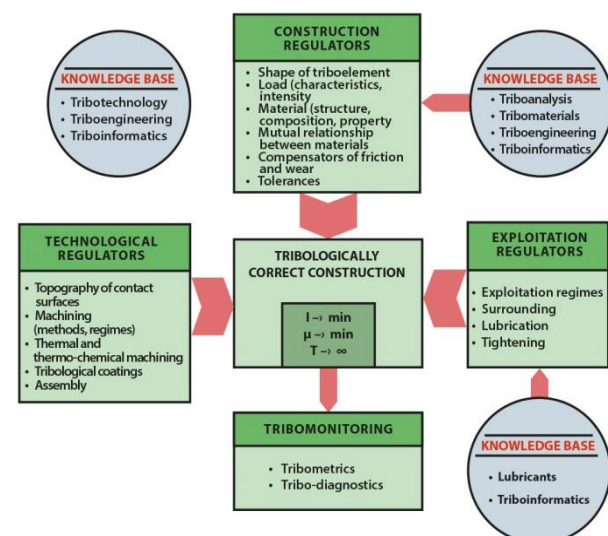


Fig.7. Regulators of tribologically correct construction

In the process of tribological design and construction, it is necessary to have a large number of precisely defined tribological information, because tribology has an interdisciplinary character and a wide range of possible aspects of study. The scientific world today cannot boast of a significant amount of tribological information, in particular the amount of systematized information applied in practical design and construction. In that sense, the development of triboinformatics in recent years encourages as a necessity for the systematization of information and the need for a more efficient exchange between scientific institutions and other potential users of tribological knowledge [13].

The tribological aspect of construction and tribology in construction are necessary conditions for correct construction. They are important in every stage of the construction process, and their application raises the quality and extends the life of the product. The connection between construction and tribology is direct despite the problems that exist in insufficient communication between constructors and tribologists. Contemporary methods of designing and constructing increasingly include consideration of the constructive tribological aspect. This is understandable if we have in mind the requirements for their high reliability and economy.

3. RESULTS OF TRIBOLOGICAL RESEARCHES OF THE HOB MILLING PROCESS OF SERRATION OF CYLINDRICAL GEARS

Starting from the analysis of the basic legalities of the gear cutting of cylindrical gears by hob milling at the Department of Production Engineering of the Faculty of Technical Sciences, the research took place in two basic directions:

- investigation of the influence of geometric parameters and constructions of the hob milling tools on tribological processes
- investigation of the influence of the parameters of the cutting regime on tribological processes.

This paper presents an overview of the research results related to the influence of geometric parameters and the constructions of the hob milling tools on tribological processes.

3.1 Investigation of the influence of geometric parameters and the construction of hob milling tools on tribological processes of gear cutting

The hob milling tool has a large number of geometric parameters. Constructive geometry, and especially cutting geometry, is very important for the process of hob milling of the serration of cylindrical gears. The construction of the hob milling tool, tool materials and coating affect on the tribological processes of the gear cutting of the cylindrical gears.

3.1.1 The influence of cutting geometry on tribological processes of gear cutting

The influence of the cutting geometry of the teeth of hob milling tool on the shape and intensity of wear is

not sufficiently tested, therefore the data in the literature are often very scarce. The tool life of the hob milling tool depends on geometric parameters. The cutting parameters are the most important of all geometric parameters. The rake-angle, radial relief-angle and radius of the top are significant elements of cutting geometry. In the papers [14,15], a part of the results of the study of the influence of the cutting geometry of the hob milling tool on the tool life function in the gear cutting of cylindrical gears by the hob milling was given. When optimizing the geometrical parameters of the hob milling tool, the tool life is usually adopted as a goal function. The reason for this is the fact that a significant portion in the total cost of the gear cutting operation has the cost of exploitation of the tools (about 30%), and within which 86-94% are the costs of amortization of the hob milling tool. In the concrete case, the determination of a reliable state function in laboratory conditions was carried out using the methods of model testing and modern methods of mathematical statistics based on a multifactorial experiment. As a criterion for the wear of the hob milling tool, the width of the wear belt $VB_0=0,6\text{mm}$, determined based on the curves of wear (Figure 8) has been adopted. Cutting regimes, i.e. process parameters were $v_c=98,125\text{m/min}$, $f_a=2\text{mm/r}$, work-piece material 20 CrMo 5, $z_2=50$, $m_n=3\text{mm}$, $b=54\text{mm}$, $\alpha_n=20^\circ$, $\beta=0^\circ$, $d_{ht}=125\text{mm}$, $z_1=1$, $n_t=15$, tool material HS 6-5-2-5, (up) conventional milling, $\gamma=6^\circ$, $\alpha=14^\circ$, $r=0,65\text{mm}$.

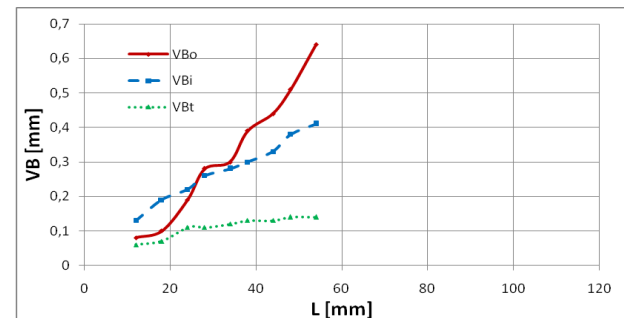


Fig. 8. The development of the wear process on model hob milling tool for tenth point of three-factor experiment

Based on the statistical processing of the obtained results, a reliable function of the tool life of the hob milling tool was determined in the form of:

$$L = -5.33 + 6.75\gamma + 1.896\alpha + 40r - 0.5\gamma\alpha - 10.556\gamma r + 1.25\alpha r + 0.903\gamma\alpha r \quad (1)$$

On the basis of the obtained results of the study [14,15] of the given complex machining process, it can be concluded that by increasing the analyzed geometric parameters of the teeth of the hob milling tool (γ, α, r) the increase of the tool life of the hob milling tool is achieved. The investigated model of tool life function (1) expresses a certain legality and contains certain information about the nature of the investigated process. The results of statistical analysis of model adequacy [1] show that the mathematical model adequately describes the machining process within the

boundaries of the multifactor space, and the significance of the model parameters indicates that all the parameters except the zero are insignificant. For the above reasons, additional experiments were carried out for an extended form of tool life function [15,16]. The tests were performed on the basis of the application of the three-factor central composite experimental plan. In determining the tool life of the hob milling tool $VB_o=0,6\text{mm}$, determined on the basis of the wear curves (Figure 9), was adopted as a wear criterion.

Based on the statistical processing of the obtained results, a reliable function of the tool life of the hob milling tool was determined in the form of:

$$L = -444.03 + 2.84\gamma + 5.54\alpha + 1336.17r - 0.37\gamma^2 - 0.27\alpha^2 - 1089.41r^2 + 0.08\gamma\alpha + 2.08\gamma r + 6.37\alpha r \quad (2)$$

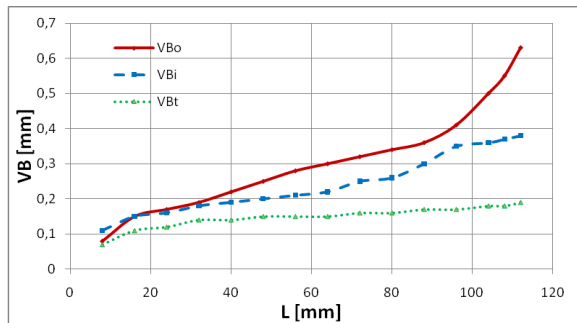


Fig.9. The development of the wear process on model hob milling tool for 19-th point of three-factor central experimental plan

Based on the analysis of the new form of the tool life function (2), it can be concluded that the model is adequate and that the model parameters are significant. Based on the model, local extremes were determined within the geometric parameters surveyed area. Optimum tool life $L = 98.149 \text{ mm}$ is achieved by optimum teeth geometry of the hob milling tool $\gamma=7^\circ 50'$, $\alpha=20^\circ 5' 24''$, $r=0,696\text{mm}$. With this cutting geometry of the teeth of hob milling tool, the increase of tool life in comparison to the standard tool by 44.9% is achieved. This enables a significant increase in productivity.

3.1.2 Application of genetic algorithm in optimization of geometric parameters of hob milling tool

An analysis of the parameters influencing the wear process of the hob milling tool was performed. Also, determining the functional dependence of tool resistance on geometric parameters using a genetic algorithm was performed. Special emphasis has been placed on the interaction between determination of optimal geometric parameters and determination of optimal regime parameters.

Obtained experimental results are shown in [10]. For each experimental point, values of characteristic wears are obtained by measuring. On the basis of analysis, the adoption criterion of a single tooth tool was adopted. It is the width of the wear zone on the output flank $VB_o=0,6\text{mm}$. For each experimental point, the curves of wear process development are drawn (Figure 10). Experimental conditions are the same as in

experiments shown in Figures 8 and 9. The parameters of cutting geometry are $\gamma=12^\circ$, $\alpha=20^\circ$, $r=0,75\text{mm}$.

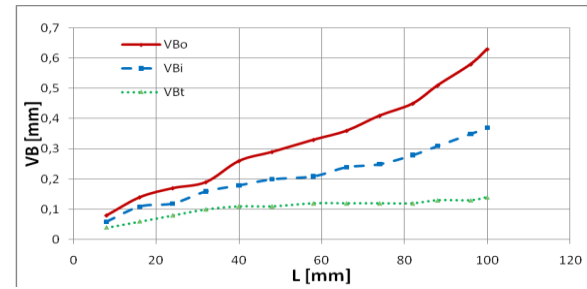


Fig. 10. The development of the wear process on model hob milling tool for fourth point of experiment

Using genetic algorithm some possible models satisfying the selection criterion were obtained. Therefore, they represent a potential solution of the problem. Characteristics of one of these models of tool life function are:

$$L = 3.47514 + 4.84292\gamma + 0.00449625\alpha + 23.1512r - 0.195747\gamma\alpha - 5.9446\gamma r + 0.36683\alpha r + 0.323794\gamma\alpha r - 0.0495238\gamma^2 + 0.0859158\alpha^2 + 18.7778r^2 \quad (3)$$

- Total absolute difference of the best individual: 40.977
- Deviation of the best individual in percentages: 2.7318
- Generation with the best individual: 18885

In the Figure 11 the diagram showing the tendency of organism improvement through the generations is given. On the diagram one can see that the successfulness of the best organism increases rapidly at the beginning, in other words the values of successfulness measure decrease rapidly. After 1500 generations this trend starts to decrease more and more, and it exceeds into stagnation. Finally, it achieves the largest successfulness in the 18885-th generation in which the organism with average deviation $\Delta(i, t) = 2.7318 \%$ was obtained. After achievement of the largest successfulness it decreases. Identical value of the largest successfulness will appear in later generations again, but the number of its appearance is almost insignificant with constant tendency to successfulness reduction, i.e. increasing of $\Delta(i)$.

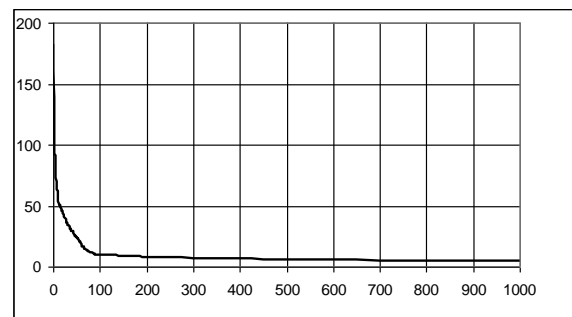


Fig. 11. Average percentage deviation of the best models

Variety of individuals in the population was very large with permanent oscillating in all generations (Figure 12). Dependence of tool life on geometrical parameters of hob milling tool is shown in Figure 13.

On the basis of the best model the determination of maximum tool life and optimal geometric parameters was performed.

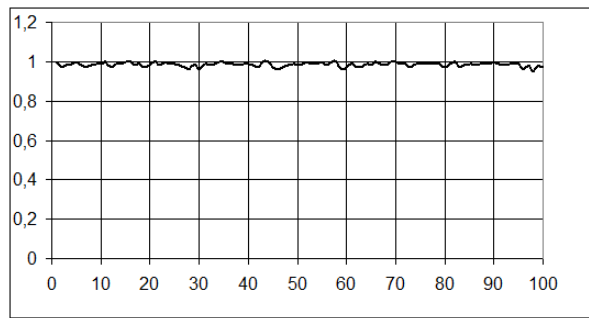


Fig. 12. Variety curve of the population

Using mathematical methods maximal tool life $L=105.836$ mm was determined. Geometric parameters which provide global maximum for the given model are $r=0.818$ mm, $\alpha=24.092^\circ$, $\gamma=16.092^\circ$.

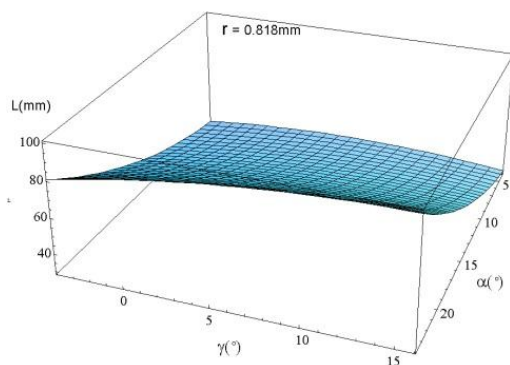


Fig. 13. Dependence of tool life on geometrical parameters of hob milling tool

Optimization of fitness function using genetic algorithm requires much less information about fitness function and it does not need satisfying of some conditions like classical methods for instance function differentiability and continuity.

3.2 Investigation of the impact of constructive geometry, material and the coating on tribological processes of gear cutting

The structural characteristics of the hob milling tool and the material of its cutting edge determine, above all, the productivity and cost-effectiveness of the hob milling of serration of the cylindrical gears. In the field of improvement and increase of the tool life of the milling cutters for the cutting of the gears of cylindrical gears, there is a tendency to improve their constructive parameters, the application of new materials for the cutting elements of the tools and the application of certain coatings on the cutting elements of the tools.

3.2.1 The influence of the constructive geometry of the hob milling tools on the tribological processes of the gear cutting

In the paper [17], on the basis of the analysis of the complex process of the gear cutting of the cylindrical gears, by hob milling in real conditions, comparative

experimental tests of the tool life of certain types and the constructive geometry of the hob milling tools were performed. Experimental examinations of integral hob milling tools and hob milling tools with inserted cutting elements were carried out in several positions. The development of the wear process for one tooth of the integral hob milling tool is shown in the Figure 14. The wear of the output lateral flank $VB_0 = 0.7$ mm has been adopted as a wear criterion. At speed $v_c = 47.1$ m/min and axial feed $f_a = 2$ mm/r, work-piece material 14 CrNi 6, $z_2 = 24$, $m_n = 9$ mm, $b = 62$ mm, $\alpha_n = 26^\circ$, $\beta = 0^\circ$, $d_{ht} = 150$ mm, $z_1 = 1$, $n_i = 14$, tool material HS 18-1-2-5, (up) conventional milling. The integral hob milling tool has a tool life of $T_i = 420$ min. The development of the wear process of one tooth of the hob milling tool with inserted cutting elements from HS 6-5-2 (Figure 15) at speed $v_c = 47.1$ m/min and axial feed $f_a = 2$ mm/r was $T_c = 420$ min. The wear criterion was also $VB_0 = 0.7$ mm. The experimental conditions are the same as in the experiment shown in Figure 14.

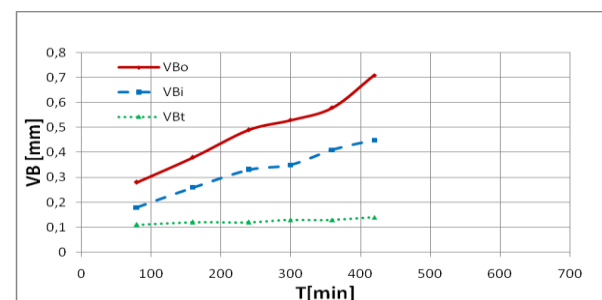


Fig. 14. The development of the wear process on integral hob milling tool

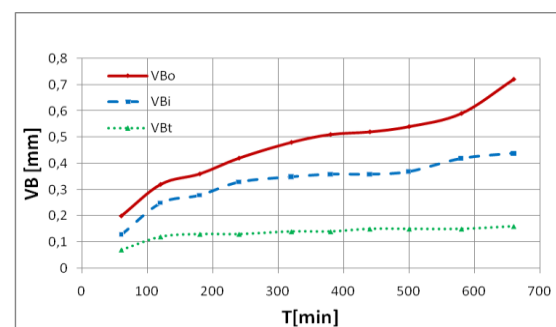


Fig. 15. The development of the wear process on hob milling tool with inserted combs

Experimental researches have shown that hob milling tools with inserted cutting edges have a higher tool life of 63.3% in comparison to integral hob milling tools. Within these tests, a detailed analysis of the costs of the operation of the gear cutting with integral hob milling tools and hob milling tools with the inserted cutting elements was carried out. This analysis has shown that the costs of the gear cutting operation with integral hob milling tool is higher by 25.5% in comparison to the work with the hob milling tools with the inserted cutting elements from HS 6-5-2.

3.2.2 Investigation of the influence of material and coating of cutting elements on tribological processes of gear cutting

In the last 30 years, a great deal of progress has been made in the development of new materials for hob milling tools, and also the coating for cutting elements of tools. In science and practice, the question, which will need to be answered in the future technological development, is constantly raised. That question is how the new technical materials will influence the production processes and in what direction research have to be directed in order to adopt the technological processes of machining these materials in the next period. It's a good fact that we cannot even use materials that we cannot process. The enhancement of the hob milling of serration of cylindrical gears can be achieved by increasing the productivity and increasing the quality of the serration [1,8,9].

In the paper [18], comparative investigations of the tribological processes of hob milling tools with inserted cutting elements from HS 6-5-2-5 made with powder metallurgy and hob milling tools with inserted cutting elements from HS 6-5-2-5 made with powder metallurgy and coated with TiN are given.

The primary processes of wear are the most important. In the experiments shown in this paper, the flank wear of the hob milling tool teeth is the primary wear zone. The flank of the teeth of hob milling tools wears on the input lateral flank, the tip flank and the output lateral flank.

The development of the wear process on one tooth of the hob milling tool is given in the Figure 16. The Figure shows the wear on all three back surfaces. The wear of the output lateral flank $VB_o = 0.7 \text{ mm}$ in roughing has been adopted as a wear criterion. At the cutting speed of $v_c = 101.94 \text{ m/min}$, $n = 224 \text{ r/min}$, axial feed $f_a = 2 \text{ mm/r}$, work-piece material 20 MnCr 5, $z_2 = 39$, $m_n = 4.75 \text{ mm}$, $b = 66 \text{ mm}$, $\alpha_n = 20^\circ$, $\beta = 0^\circ$, $d_{ht} = 145 \text{ mm}$, $z_1 = 1$, $n_i = 12$, tool material HS 6-5-2-5, (up) conventional milling. The hob milling tool with inserted uncoated combs made of HS 6-5-2-5 manufactured by powder metallurgy had a tool life $L = 1584 \text{ mm}$ on machined serration of straight cylindrical gear (Figure 16).

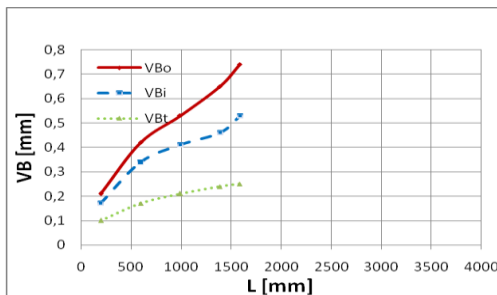


Fig. 16. The development of the wear process on uncoated hob milling tool

The development of the wear process on one tooth of the hob milling tool with inserted combs of high

speed steel manufactured by powder metallurgy and combs coated with TiN is shown in the Figure 17. The experimental conditions are the same as in the experiment shown in Figure 16. The tool life of this tool with the same cutting regimes and the same wear criterion was $L = 2178 \text{ mm}$ on machined serration of straight cylindrical gears.

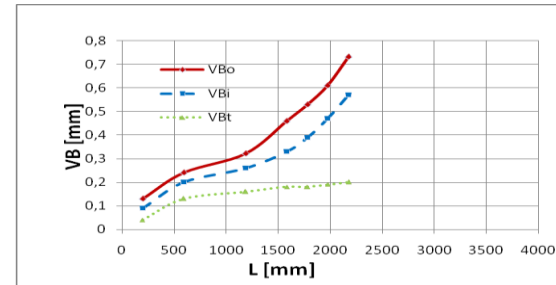


Fig.17. The development of the wear process on hob milling tool coated with TiN

In the paper [19], comparative studies of the tribological processes of the hob milling tools with inserted cutting elements from HS 6-5-2-5 made with powder metallurgy are shown, whereby they are coated with TiN as in the paper [18] and coated with TiAlN. The process parameters in [19] are the same as in [18].

The development of the wear process on one tooth of the hob milling tool with inserted combs of high speed steel manufactured by powder metallurgy and combs coated with TiAlN is shown in the Figure 18. The experimental conditions are the same as in the experiment shown in Figure 17. The tool life of this tool with the same cutting regimes and the same wear criterion was $L = 3498 \text{ mm}$ of machined serration of straight cylindrical gears.

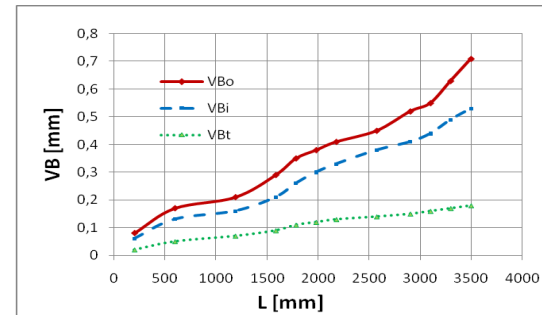


Fig. 18. The development of the wear process on hob milling tool coated with TiAlN

Comparative studies of hob milling tools with inserted uncoated combs made of high speed steel, manufactured by powder metallurgy and hob milling tools with inserted combs of the same material and coated with TiN were performed in real production conditions.

The experimental researches have shown that the hob milling tools with inserted coated combs have a higher tool life of 27.28% in comparison to the hob milling tools with inserted uncoated combs. The experimental researches have shown that the hob milling tools with inserted TiAlN coated combs have a higher tool life of 60.6% in comparison to the hob milling tools with inserted TiN coated combs.

These experimental researches once again confirmed that there is a concentrated wear on the cutting elements of the hob milling tools when gear cutting of straight cylindrical gears. The morphology of the flank wear is characterized by the appearance of most commonly two grooves on the output lateral flank and one groove at the input lateral flank. The grooves in the cutting elements of the hob milling tool are located in the transition areas of the tip flank into the output and input lateral flanks.

Previous and these studies have shown that the design, that is, the construction of the hob milling tools and the coating with TiAlN, have great significance for increasing the tool life of the hob milling tools and the quality of the machined serration. It is important to note that the operating modes were the same for all the hob milling tools used in experimental research. Based on the knowledge in the available literature and own research with tools coated with TiAlN, it is possible to apply larger cutting regimes and thus achieve even more techno-economic effects. In further research, comparative testing and application of hob milling tools coated with three or more layers of different manufacturers should be carried out as well as their more rational application. It is necessary to research the technological and economical characteristics of hob milling tools with several beginnings and a new construction of hob milling tools.

4. CONCLUSION

On the basis of theoretical and experimental research, the need for exploring the hob milling process of serration of straight cylindrical gear is obvious. In this research, the optimal geometry of the blade was researched. The obtained results enable construction, production and application of gear hobs which give better techno-economic effects.

Experimental researches have shown that assembly hob milling tools with inserted cutting elements have a higher tool life of 63.3% and a reduction in the cost of gear cutting operation by 25.5% in comparison to the integral hob milling tools.

The hob milling tools with inserted combs made of high-speed steel manufactured by powder metallurgy are very suitable for gear cutting of straight cylindrical gears. It should be noted that these hob milling tools require higher propulsion power of the hob milling machine and greater static and dynamic rigidity of the entire machining system.

Experimental researches have shown that hob milling tools with inserted coated combs with TiN have a higher tool life of 27.28% compared to hob milling tools with inserted uncoated combs.

Experimental researches have shown that hob milling tools with inserted coated combs with TiAlN have a higher tool life of 60.6% compared to hob milling tools with inserted coated combs with TiN. Tribological researches at the Faculty of Technical Sciences, the Department of Production Engineering have yielded significant results in the field of gear cutting of cylindrical gears by hob milling.

5. REFERENCES

- [1] Sovilj-Nikić, I.: *Modelovanje i optimizacija procesa odvalnog glodanja*, Fakultet tehničkih nauka, Novi Sad, Serbia, Doctoral Thesis (unpublished)
- [2] Sovilj, B., Sovilj-Nikić, I., Ješić, D.: *Measurement methodology of characteristics and election of materials of elements of tribomechanical systems*, Metalurgija / Metallurgy, Vol. 50 No. 2, pp. 107-112, 2011.
- [3] Sovilj-Nikić I., Sovilj, B., Kandevara, M., Gajić, V., Sovilj-Nikić, S., Legutko, S., Kovač, P.: *Tribological characteristics of hob milling tools from economic aspect*, Journal of the Balkan Tribological Association, Vol. 18 No.4, pp. 577-585, 2012.
- [4] Bouzakis, K.D., Skoridatis, G., Michalidis, M.: *Innovative methods for characterizing coatings mechanical properties*, in Proceedings of International Conference 'The Coatings 2008', Kallithea, Greece, 2008.
- [5] Sovilj-Nikić, I., Sovilj, B., Brezocnik, M.: Application of genetic algorithm in analysis of influence of gear hob geometric parameters on the tool life, in Proceedings of International Conference 'ICMEN 2008', Kallithea, Greece, 2008.
- [6] Sovilj, B.: Identifikacija tribolo[kih procesa pri odvalnom glodanju, Fakultet tehničkih nauka, Novi Sad, Serbia, Doctoral Thesis, 1988.
- [7] Antoniadis, A., Vidakis, N., Bilalis, N.: *Fatigue fracture investigation of cemented carbide tools in gear hobbing*, Journal of Manufacturing Science and Engineering, Vol. 124, No. 4, pp. 784-791, 2002.
- [8] Bouzakis, K. D., Lili, E., Michalidis, N., Friderikos, O.: *Manufacturing of cylindrical gears by generating cutting processes: A critical synthesis of analysis methods*, CIRP Annals-Manufacturing Technology, Vol. 57 pp. 676-696, 2008.
- [9] Sovilj-Nikić, S., Sovilj, B., Ješić, D., Blanuša, V., Tonkonoggy, V. M., Bovnegra, L.: *Development of the method of direct temperature measurement for gear cutting of cylindrical gears by hob milling*, Annual Session of Scientific Papers IMT ORADEA 2018, Vol. 184, p.6, 2018.
- [10] Sovilj-Nikić, I.: *Primena genetskog algoritma u optimizaciji geometrijskih parametara odvalnog glodala*, Fakultet tehničkih nauka, Novi Sad, Serbia, Master Thesis, 2007.
- [11] Abler, J., Felten, K., Kobialka, C., Lierse, T., Mundt, A., Pomp, J., Sulzer, G.: *Gear Cutting Technology, Practice Hand Book*, Liebherr GmbH, Kempten, 2004.
- [12] Sovilj-Nikić, I., Sovilj-Nikić, S., Sovilj, B., Đokić, R.: *Analysis of roughness parameters of the tooth-face of model hob milling tool*, Machine design, Vol. 9 No. 3, pp. 99-106, 2017.
- [13] Tanasijević, S.: *Tribološki ispravno konstruisanje*, Mašinski fakultet u Kragujevcu, Kragujevac, 2004.

- [14] Banjac, D., Sovilj, B., Vasić, S.: *Uticaj rezne geometrije odvalnog glodala na funkciju postojanosti pri ozubljenju cilindričnih zupčanika*, XIV Savetovanje proizvodnog mašinstva Jugoslavije, 13-22, Čačak, 1980.
- [15] Sovilj, B.: Optimizacija geometrijskih parametara odvalnog glodala, Fakultet tehničkih nauka, Novi Sad, Serbia, Master Thesis, 1980.
- [16] Sovilj, B., Banjac, D.: *Određivanje optimalnih geometrijskih parametara odvalnog glodala*, III. Naučno-stručni skup MMA'83, pp. 487-498, Novi Sad, 1983.
- [17] Sovilj, B., Popov, A., Ješić, D., Kolev, I., Sovilj-Nikić, I.: *Treatment in tribological processes of spur gear in modern agricultural engineering*, Savremena poljoprivredna tehnika/Contemporary Agricultural Engineering, Vol. 37 No. 3, pp. 305-314, 2011.
- [18] Sovilj, B., Sovilj-Nikić, S., Varga, Gy., Ungueranu, N., Blanuša, V.: *Analysis of the possibility of improving the characteristics of hob milling tools for gear cutting of cylindrical gears*, Machine design, Vol.10, No. 2, pp. 63-68, 2018.
- [19] Sovilj-Nikić, S., Sovilj, B., Varga, Gy., Ungueranu, N., Blanuša, V.: *Analysis of the tool life of coated hob milling tools for gear cutting of cylindrical gears*, Annual Session of Scientific Papers IMT ORADEA 2018, Vol. 184, p.6, 2018.

Authors: Full Prof. Bogdan Sovilj, University of Novi Sad, Faculty of Technical Sciences, Department of Production Engineering, Trg Dositeja Obradovića 6, 21000 Novi Sad, Serbia, Phone: +381 21 4852343.

E-mail: bsovilj@uns.ac.rs

DSc Sandra Sovilj-Nikić, scientific associate, Iritel a.d. Beograd, Batajnički put 23, 11080 Belgrade, Serbia, Phone.: +381 64 2302938.

E-mail: sandrasn@eunet.rs

ACKNOWLEDGMENTS: The research was funded by the Ministry of Education, Science and Technological Development of the Republic of Serbia within the project III 43008, and it is also the result of the cooperation within CEEPUS projects CIII- RO-0058-07-1718 and CIII-RS-0304-10-1718.

Ilic, J., Krajsnik, M., Jotic, G., Anic, J.

FABRICATION OF AUTHENTIC FUNCTIONAL PARTS FOR OLDTIMER USING INTEGRATION OF REVERSE ENGINEERING AND 3D PRINTING

Abstract: This paper presents and emphasizes the advantages of advanced technologies such as rapid prototyping and reverse engineering. Particularly prominent advantages of the integration of these two techniques are the ability to obtain a CAD model based on a real model using reverse engineering and then its precise replica using 3D printing technology. On the example of fabrication functional part for oldtimer emphasized the great importance of these technologies, especially if it is a one piece or small batches.

Key words: Reverse Engineering, Additive Manufacturing, Functional parts

1. INTRODUCTION

In times of globalization, manufacturers are constantly exposed to the challenges of finding new technology solutions that will enable the shortening of time needed to launch a new product on the market. In addition, they have to respond to customer requirements related to the functionality of the part and they must also reduce production costs to have an acceptable selling price. If it is a small batch of parts of a complex geometric configuration, or a complex part, its production using conventional technologies would be very expensive and in some cases it would not be possible. Additional difficulties arise when downloading geometric shapes or detailed dimensions from a real model whose copy needs to be created. It is clear that the use of traditional manufacturing, based on conventional technology for small batches or individual parts, was very complex and supremely economically unacceptable for both, and the manufacturer and the customer.

The solution to the concrete problem is the possibility of using advanced technologies such as reverse engineering, enabling a CAD model to be obtained quickly and relatively easy from a real model. The further approach implies the use of 3D printer by which one a real 3D model, i.e. a functional part, is obtained based on the generated CAD model, eliminating the application of expensive tools and accessories. A special aspect of reverse engineering and 3D printing technology is the production of authentic parts in the automotive industry. Namely, the owners and the collectors of oldtimers are constantly faced with the problem of purchasing and fabrication of spare parts, since it is very difficult or almost impossible to find them on the market [1]. This paper presents the example of fabrication of a functional part based on the damaged part, the significance of the integration of these advanced technologies and the advantages they have when developing individual or small batches of complex parts. The basic principle of integration of reversible engineering and 3D printing is shown in Figure 1.

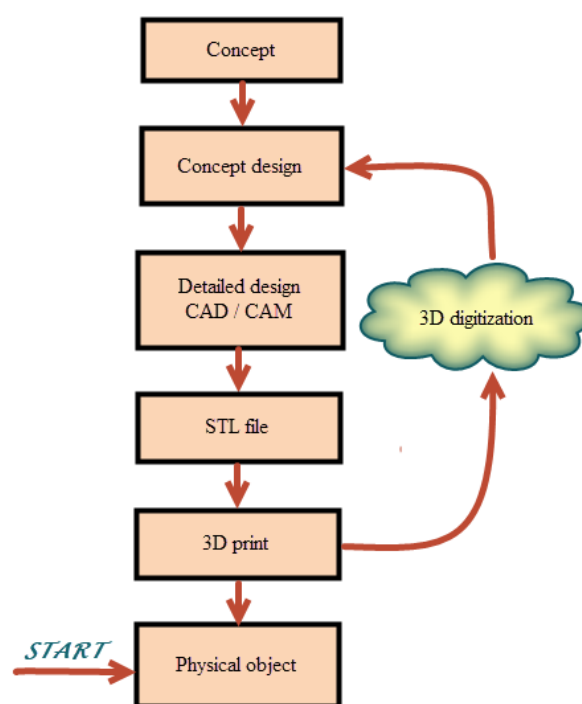


Fig. 1. Integration of reverse engineering and 3D printing [2]

2. CASE STUDIES

2.1 Preparation of the damaged original part

In the particular case, at the request of the owner of the oldtimer, it is necessary to make a impeller of the water pump in relation to the already damaged original part, which is shown in Figure 2. Due to the fact that several vanes were broken, the preparation of the damaged part for 3D scanning was done, which included detailed cleaning of the impeller, gluing the damaged vanes (Fig. 3) and grinding the glued joint in order to obtain the best quality of the joint, i.e., in order to minimize defects reproduced on the model during 3D scanning [3]. The prepared part for 3D scanning is shown in Figure 4.



Fig. 2. Damaged original part



Fig. 3. Preparation and gluing of damaged wings on impeller

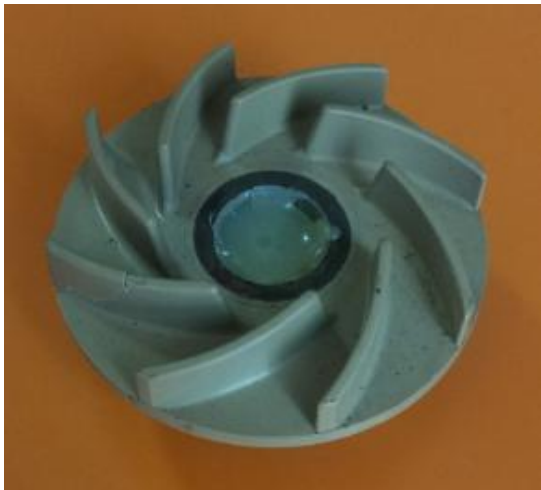


Fig. 4. Original part prepared for 3D scanning

2.2 3D scanning impeller of water pump for oldtimer and scan processing

The prepared impeller (Fig. 5) which represents a physical object with complex geometry and surfaces is relatively advantageous for scanning since there is no reflection on the surface and there are no areas that are inaccessible to the scanner. Nikon MCx20+

measuring arm and 3D Nikon MMDx100 scanner were used for scanning with the basic characteristics shown in Table 1. After the preparation of the model and performing a calibration of the proper geometric forms by the contact method (flat, cylinder ...) and then the model scanning, i.e., generating the cloud of points (Fig. 6). After 3D digitization of the model, follows the process of generating a 3D model based on the cloud of points [4]. For this purpose was used software package Solid Works, module Scan to 3D. The methodology of polygonal models was used, in which the 3D surface model is obtained by converting the clouds into the polygonal network from which is then generated the surface model. Then follows the segmentation of the surface and at the end the creation of the CAD model. The result of this procedure is a solid CAD model that completely looks like a generated cloud of points, i.e., credible original part (Fig. 7).

Specifications of measuring arm Nikon MCx20+ with handheld laser scanner Nikon MMDx100	
Measuring range	2000 mm
Point repeatability	0.023 mm
Volume length accuracy	± 0.033 mm
Arm weight	8.2 kg
Laser scanning system accuracy	0.048 mm
Working temperature	0 – 50 °C
Shock & Impact	6ms

Table 1. Specification of measuring arm and handheld laser scanner



Fig. 5. Scan of the prepared model

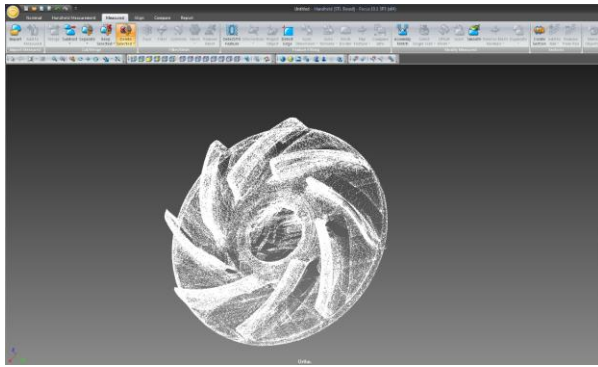


Fig. 6. Generated cloud of points in the software package Focus for scan processing

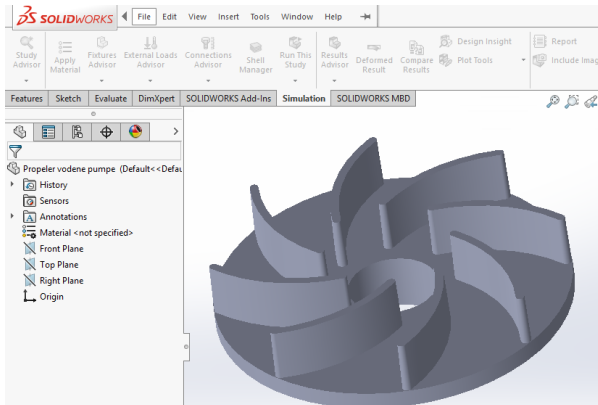


Fig. 7. CAD model of water pump impeller

2.3 Processing and production of water pump impeller on 3D printer

The development of the water pump impeller was carried out on a 3D printer based on the material extrusion technology (Stratasys - Dimension Elite), whose basic characteristics are given in Table 2. The ABSplus material was used for the impeller construction, whose mechanical and physical characteristics can meet the requirements and conditions of the part exploitation. The CAD model obtained by reverse engineering on the basis of the damaged original part is converted into a SolidWorks software package in a format that a 3D printer recognizes, which represents a triangular representation of a 3D surface geometry [5] (Fig. 8).

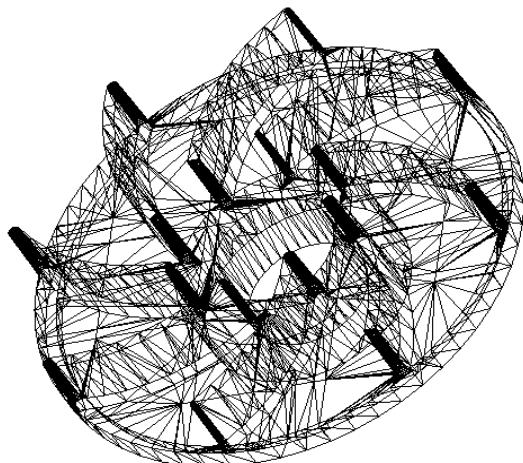


Fig. 8. Model of water pump impeller in STL format

Dimension Elite 3D printer specifications:	
Model material:	ABSplus
Support material:	Soluble Support Technology
Build size:	203 x 203 x 305 mm
Layer thickness:	0.178 or 0.254 mm
Size and weight:	686 x 914 x 1041 mm and 127 kg

Table 2. 3D printer specifications

In the processing phase, special attention should be paid to the positioning and orientation of the model on the 3D printer platform. The procedure that has been necessary to obtain a master model or impeller of water pump is as follows [6]:

- Product design in some of the CAD software packages (Fig. 7),
- Conversion of CAD models in STL format that is recognized by a 3D printer (Fig. 8.),
- Transfer of STL files to the computer that controls the three-dimensional printer,
- Processing of STL files within the CatalystEX program in which all the parameters are set and adjusted according to the required model (Fig. 9 and Fig. 10),
- Creating a three-dimensional model using additive technology and
- Further processing of created part.

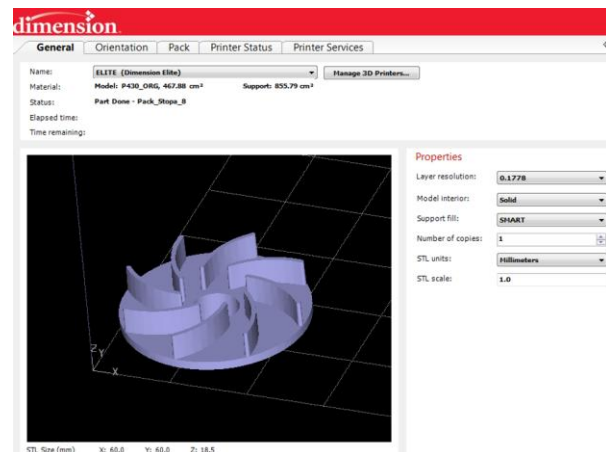


Fig. 9. Setting the resolution and orientation of the model in the software package CatalystEX

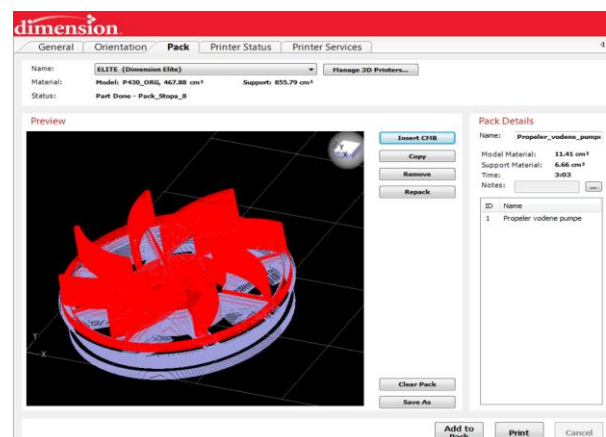


Fig. 10. The generated printer head trajectory and support structure in the CatalystEX software package

After fabrication of the model on a 3D printer follows a postprocessing of the model which involves removal of support, polishing and varnishing. The final functional part is shown in Figure 11.



Fig. 11 New functional part

All experimental researches were carried out at the Laboratory for CAD and PLM systems and Laboratory for Plasticity and Processing Systems at the Faculty of Mechanical Engineering in Banja Luka.

3. CONCLUSION

This paper presents a complete procedure and all the necessary steps to get a new functional part based on the damaged original part. Also, in the case of fabrication a part for oldtimer are prominent all the possibilities and advantages of advanced technologies such as additive technology and reverse engineering. It is particularly emphasized the importance of this approach for the fabrication of individual parts, i.e. small batches, where functional part is obtained with relatively short time and with low costs.

4. REFERENCES

- [1] Beldiman, D., Blanke-Roeser, C.: Future Outlook: The Spare Parts Debate in the Era of 3D Printing, An International Perspective on Design Protection of Visible Spare Parts, pp.115-130, Springer, 2017
- [2] Budak, I., Hodolic, J., Besic, I., Vukelic Dj., Osanna, H.P., Durakbasa, M.N.: Coordinate Measuring Machines and CAD-Inspection, Faculty of Technical Sciences, Novi Sad, 2009
- [3] Sokol, K., Cekus, D.: Reverse engineering as a solution in parts restoration process, XXI International Polish-Slovak Conference „Machine Modeling and Simulations 2016“, Procedia Engineering 177, pp. 210-217, Elsevier, 2017
- [4] Zhang, J., Yu, Z.: Overview of 3D Printing Technologies for Reverse Engineering Product Design, Automatic Control and Computer Sciences, Volume 50, pp.91-97, Springer, 2016
- [5] Paulic, M., Irgolic, T., Balic, J., Cus, F., Cupar, A., Brajliah, T., Drstvensek, I.: Reverse Engineering of Parts with Optical Scanning and Additive Manufacturing, 24th DAAAM International Symposium on Intelligent Manufacturing and Automation, Procedia Engineering 69, pp.795-803, Elsevier, 2014
- [6] Kraisnik, M., Šljivic, M., Ilic, J., Anic, J.: Fabrication of small batches of functional and authentic parts for oldtimers using integration of material extrusion and vacuum casting technologies, 6th International Conference on Manufacturing Engineering, Thessaloniki, 2017

Authors: **Teaching Assistant, Jovica Ilic**, University of Banja Luka, Faculty of Mechanical Engineering, Stepe Stepanovica 71, 78000 Banja Luka, Phone: +387 51 433 000, **Assistant Professor, Milija Kraisnik**, University of East Sarajevo, Faculty of Mechanical Engineering, Department of Production Engineering, Vuka Karadzica 30, 71123 East Sarajevo, Phone: +387 57 340847, **Teaching Assistant, Goran Jotic**, University of Banja Luka, Faculty of Mechanical Engineering, Stepe Stepanovica 71, 78000 Banja Luka, Phone: +387 51 433 000, **Senior Assistant Jelica Anic**, University of East Sarajevo, Faculty of Mechanical Engineering, Department of Production Engineering Vuka Karadzica 30, 71123 East Sarajevo, Phone: +387 57 340847

E-mail: jovica.ilic@mf.unibl.org
milija.kraisnik@ues.rs.ba
goran.jotic@mf.unibl.org
jelicaanic91@gmail.com

Janjić, N., Savić, B., Mikić, D., Stanković, N., Petrović, D.

APPLICATION OF MODEL OF RELIABILITY ON MACHINE SYSTEMS BASED ON LOGNORMAL STATISTICAL DISTRIBUTION

Abstract: Lognormal distribution, and its modifications, in reliability on motor vehicles have a significant application in science and technology. The lognormal distribution is closely related to the probability calculation that can be used for standardized machine elements in systems. The largest number of components of the motor vehicle has a continuous change of the state parameters in the function of the operating time, which is a condition for the implementation of the concept and preventive maintenance model with parameter checking by lognormal distribution. Modern level of the machine industry, characterized by the necessity of gradual analysis of large mass of data and information and requirements for reliable, that is, scientifically based inputs of the system. The work represents a novelty for the analysis of the system and the effects of the proposed measures to improve the condition of the quality and reliability of the motor vehicle.

Key words: Log-normal distribution, system state, maintenance, reliability, quality.

1. INTRODUCTION

In this paper we shall present a part of probability examples and show some of the results on the basic distribution of random variables. Apart from these, there is still a certain number of distributions that are of an exceptional importance in statistics and here we shall give the review of some of them, primarily the determination of parameters based on the samples (lognormal distribution).

The basic objective in this paper is surely the modelling of the specified phenomenon and finding of an adequate model that describes the contemplated phenomenon on the basis of available results. In the context of operational risk modelling it is primarily indispensable to find an adequate model that describes the occurrences causing the operational loss, as well as the quantity of operational loss caused by the phenomenon of denoted occurrence. Therefore, some basic models describing the phenomenon and the quantity of loss are specified and used in practice when modelling this type of distribution, i.e. losses. Along with finding of the relevant model it is essential to make good estimation of parameters that define the model features and then to test whether the obtained model sufficiently describes the permissible group of data related to the contemplated phenomenon. For this reason, in this paper are listed the methods for the estimation of parameters and the tests of compliance.

2. PROBLEM OF DEVELOPING A QUALITY IMPROVEMENT SYSTEM AND RELIABILITY OF MECHANICAL SYSTEMS

A special emphasis in the world is dominated by the market philosophy that forces all participants in the market game to keep improving their products and services and to reduce the costs and in this improvement the functionality and the quality are favoured as the most important features of a product. When it comes to the products of the mechanical

systems especially of car industry, the improvements are, besides the quality and competitiveness, directed to their safety/security in use. The improvement of these car features is undertaken by all participants in their production - by supply chains, what requires very close cooperation between them. The dominant criterion in mechanical practice and in the practice of car industry in the world is to engage more suppliers and to fulfill the quality and price requirements [2], [3], [4]. It means that car industry should simultaneously prepare itself for globalization and for the fulfilment of the customers requirements. Such requirements mostly refer to the prices and the quality i.e. the application of standards/technical specifications ISO/TS 16949- The special requirements for the application of ISO 9001:2000 in car industry [5].

3. MEASURES FOR IMPROVING A QUALITY SYSTEM STATE AND RELIABILITY OF MECHANICAL SYSTEMS

The fact is that the most organizations of car industry are not currently competitive at global level and are losing the positions in the domestic market. For that reason it is obvious that car industry should be globalized. To attain this objective it is necessary for the companies as of the domestic car industry to show the ability of permanent provision of the required quality in car industry and to fulfill the specific requirements of those foreign companies.

Quality Management System according to ISO/TS 16949 is currently in the possession of 5 domestic manufactureres only, what means that the inclusion of the most other suppliers into the world distribution of labour is now hardly feasible unless they comply with the requirements of the standard (table 1). Normally, they will, besides privatization, be supported by the government. A specific form of support could be co-financing of activities for the establishment and certification of quality management system in car industry according to ISO/TS 16949, [6], [7].

3.1. Commitment of individual manufacturers to ISO/TS 16949

Basic postulates of ISO/TS 16949 are:

- basic methodological procedures (plan, do, test and react),
- basic quality management principles (8 principles),
- process approach to quality management.

Commitment of manufacturer to ISO/TS 16949	
BMW	ISO/TS 16 949
Daimler Chrysler	VDA 6.1 or QS 9000 pr ISO/TS 16 949→ 2004 only ISO/TS 16 949
Fiat	ISO/TS 16 949
GM	QS 9000 or ISO/TS 16 949
PSA	EAQF ili ISO/TS 16 949→ 2004 only ISO/TS 16 949
VW	VDA 6.1 or ISO/TS 16 949
Ford	QS 9000 or ISO/TS 16 949
Renault	EAQF or ISO/TS 16 949
Nissan	ISO/TS 16 949 –possible VDA 6.1 or QS 9000 or EAQF or AVSQ

Table 1. Manufacturers applying ISO/TS 16949

4. SOLVING OF PROBLEMS BY APPLYING THE SPECIFIED PARAMETERS TO THE MODEL OF MECHANICAL SYSTEM STATE DIAGNOSTICS

The state of motor vehicles with all their components and accompanied with the application of each specific parametar determines the operational ability i.e. the correct functioning of motor vehicle assemblies. During the operational exploitation of motor vehicles, the maintenance of their components as the most complicated task, takes the place of priority. The operational parameters determine the technical state of motor vehicle assembly components and are distinctive and should comply with the target value design under the specified conditions and within the specified time interval. The changes of parameters mostly result in the reduced functionality with constantly increasing and suddenly acting influences on the state of motor vehicles assemblies.

Based on the dependence of the state parameters and functional ability of motor vehicle components , the state parameters can be sorted to the selection of component state parameters with their permanent influence, selection of component state parameters with their gradual influence and selection of component state parameters with their instant influence. The first group of parameters is applied within the period of motor vehicle operation where any change causes the component of motor vehicle to function differently. The second group refers to the time of motor vehicle component functioning where the ascertainment of the state is made and obtained after reaching one of the defined parameter values. The third group of parameters registers the change of one defined value and instantly prevents the possibility of further use.

If we select the state parameters of motor vehicle

assemblies containing the values of inlet, process and outlet working parameters within the limits of permissible deviations from the target value design. When applying U_n indication – measuring values of component n of the inlet variables $U_1, U_2, ..., U_n$, which characterize the motor vehicle assemblies exploitation conditions, R is the measuring internal variable $R_1, R_2, ..., R_n$, which represents the mode indicators, I is the measuring outlet function $I_1, I_2, ..., I_m$, which represents the influence of component state parameters change, D is the measuring risk $D_1, D_2, ..., D_r$, which in addition to all exploitation characteristics comprise the reliability indicators of motor vehicle components.

4.1. Application of reliability model obtained on the basis of statistical lognormal distribution of reliability function

Although this model lost its importance due to nonmatching with the usual technical characteristics, it is still presently used due to its simple application in calculation estimates.

In other words, this model is possible to be applied in the description of distribution with minimum or maximum limit. The usual examples of its application are the shape and position measurements, examples for the purpose of flatness, in some cases, coating thickness and hardness.

Normal distribution belongs to the probability distribution with absolutely continuous random variables. Considering that this distribution approximates a large number of natural phenomena very well , it has a wide application and represents one of the most important distributions. Normal distribution depends on two parameters, $m \in \mathbb{R}$ $\sigma > 0$. Parameter m represents the expectations of this distribution and all density curves of distribution are symmetric in relation to the straight line $x = m$. Normal distribution is bell shaped where the increase of σ parameter increases the density curve flatness i.e. it comes to the higher dissipation around point $x = m$.

In the course of presenting the reliability equation which represents the total influence of individual state parameters on the mode of motor vehicle components, the presented quotation is [8, 9]:

$$K_a(t) = \varphi_i(U, R, D, I).$$

Knowing the fact that the motor vehicle consists of a large number of components, for the inlet parameters we shall have the indicators of their mode $R_1, R_2, ..., R_r$, and for the outlet parameters the indicators of their state $M_1, M_2, ..., M_n$, [8, 9]:

$$\begin{aligned} K_{U, M_1}(t) &= U(U_1, U_2, ..., U_n) = \\ &= f_t(M_1, M_2, ..., M_n, R_1, R_2, ..., R_n) \end{aligned}$$

The previous state shows that the conditions for exploitation process and mode diagnostics of motor vehicle components make the influence on their state to change, as well as on the reliability indicators. Therefore, the functional dependence is established between the change of motor vehicles state parameters [8, 9].

$$K_p(t) = I(I_1, I_2, ..., I_n) = f_t(M_1, M_2, ..., M_n).$$

5. OVERVIEW OF RESULTS OBTAINED BY THE SELECTED STATISTICAL RELIABILITY DISTRIBUTION

The results of component assembly functioning comprise the correction of reliability values in case of the selected statistical reliability distribution out of which follows that the corrective value σ is obtained from the datasets [8, 9]:

$$\sigma = \frac{K(r)}{s \cdot \tau_z(t)} \approx \frac{0,955}{800000 \cdot 1.537 \cdot 10^{-6}} \approx 4,020$$

Where:

$\tau_r(t) = 1,537 \cdot 10^{-6}$ – is the failure density function,

$s = 800000 \text{ km}$ – is travel distance before failure,

$K(r)$ – is corrective reliability value obtained from

empirical datasets: $K_{F_i}(t) \approx 0,955$

$r = 0,95$ – is parameter of component in operation.

The shown values of statistical data distribution method of the specified parameters taken from the exploitation of the shown component characteristics at the measuring points are:

$$k(r) = 0,955 \Rightarrow R_{M_1}(t) = K(r)0,955 \Rightarrow \sigma = 4,020 [10].$$

Based on already obtained values of standard normal statistical reliability distribution of the component assembly, the following parameter values are adopted:

$$\varphi = \ln s - r \cdot \sigma = \ln 800000 - 0,95 \cdot 4,020 = 1,390.$$

From such values of statistical distribution method result all parameter values since they represent the beginning of component failure states of motor vehicle components assembly [10].

Graph of transmission function $K_a(t)$, is defined by statistical reliability distribution of the component

on the basis of which further corrections of reliability dependence of analyzed motor vehicle assembly components will be carried out. Also, the relative reliability values as shown in figure 1 will be obtained from the operating time.

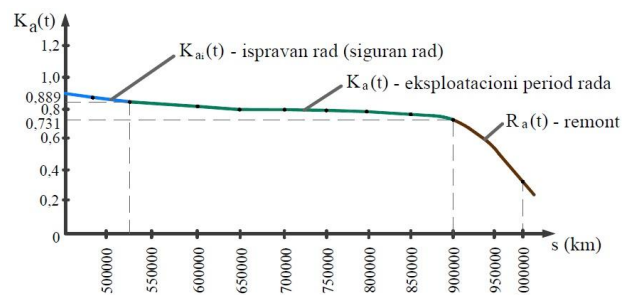


Fig. 1. Graph of the shown reliability value of component travel distance in the exploitation area at the measuring point M1 of motor vehicles – Volvo – D7C 275, JGSP – Novi Sad [9, 10]

For more precise determination of reliability results for the safe work of the analyzed motor vehicle assembly components, the corrective reliability values obtained on the basis of statistical lognormal reliability distribution as the selected distribution will be taken. The calculated corrective reliability values will be tabulated (table 2) and the results are the applications of the selected statistical longnormal reliability distribution in form 8]:

$$K_i(t) = 1 - K(t) = 1 - \int_0^t \frac{1}{\sigma \cdot t \cdot \sqrt{2\pi}} \cdot e^{\frac{1}{2} \left(\frac{\ln t - \mu}{\sigma} \right)^2} dt$$

No.	Time interval of component before failure	Travel distance of components	Name of components of motor vehicles	$g_{n_i}(t)$	z	φ	σ	$K_{a_i}(t) = \varphi(z)$	$R_{a_i}(t)$
1.	31.12.2010 ÷ 31.12.2011	500000-1200000	Crank shaft (main) bearing M ₁	$1,291 \cdot 10^{-5}$	0,12	1,390	4,020	0,889	0,731
2.	31.12.2011 ÷ 31.12.2012	500000-1200000	Crank shaft (big end) bearing M ₂	$1,103 \cdot 10^{-6}$	0,11	1,171	3,361	0,912	0,782
3.	31.12.2012 ÷ 31.12.2013	500000-1200000	Cam shaft M ₃	$1,047 \cdot 10^{-5}$	0,08	1,094	2,403	0,957	0,815

Table 2. Results of parameters $g(t)$, z , μ , σ , K_a in case of reliability lognormal distribution of motor vehicles components (M1, M2 i M3) Volvo – D9B 340, JGSP – Novi Sad [9, 10]

$$\text{By interchanging we get: } z = \frac{x - \mu}{\sigma} = \frac{\ln t - \mu}{\sigma};$$

and differentiate $p_0(t)$,

$$z = \left(\frac{\ln t - \mu}{\sigma} \right)' = \frac{(\ln t - \mu)\sigma - (\ln t - \mu)\sigma}{\sigma^2} \Rightarrow$$

$$\Rightarrow \frac{dz}{dt} = \frac{1}{t} \cdot \frac{\sigma}{\sigma^2} = \frac{1}{t \cdot \sigma} \Rightarrow z = \frac{dt}{t \cdot \sigma}$$

For the reason of $K(t) = 1 - \int_{-\infty}^z \varphi(z) dz$ and

$\varphi(z) = t \cdot \sigma \cdot f(t)$ follows the final expression for the calculation of reliability function of the analyzed assembly components [8], [9]:

$$K_a(t) = \frac{f(t)}{\lambda_0(t)} = \frac{\varphi(z)}{\lambda_0(t) \cdot t \cdot \sigma}$$

where:

$\lambda_0(t)$ - is failure intensity,

σ - is standard deviation.

The obtained safety areas can be the basis for the prediction of safe operating time, operating time with the permissible risk and operating areas pointing to the necessity of general repair of components and the whole assembly [11, 12, 13, 14]. The analysis will be used during the determination of correlation between the influences of reliability dependence, changes of temperature and wear of the bearings at the measuring points of the analyzed assemblies (figures 1, 2 i 3). Diagrams on which the reliabilities are shown, exactly display the reliability points of inflection into the state of general repair per measuring point (overview in figures 1, 2 i 3) and determination of dependence of the correct functioning of motor vehicles assembly components [11, 12, 13, 14].

For possible prediction of the moment when the basic characteristics of motor vehicle components will deviate from the permissible values is very important that the selected state parameters completely define the state of the motor vehicle components. The base for the selection of parameters is most frequently taken condition relating to the lowest number of them. In addition to these, there is very large number of inlet parameters which characterize the optimum state and exploitation conditions of motor vehicle components (anticorrosive environment, kinematic factors, thermal elasticity, etc.) [11, 12, 13, 14].

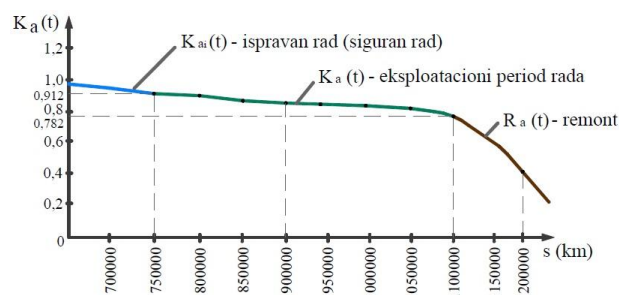


Fig. 2. Graph of the reliability values, travel distance of components in the exploitation area at the measuring point M2 of motor vehicle – Volvo – D7C 275, JGSP – Novi Sad [9]

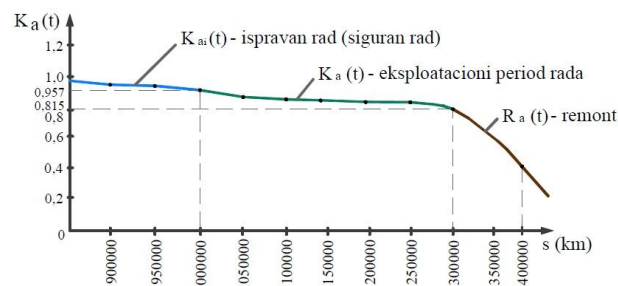


Fig. 3. Graph of the reliability values, travel distance of components in the exploitation area at the measuring point M3 of motor vehicle – Volvo – D7C 275, JGSP – Novi Sad [9]

6. CONCLUSION

For the description of distribution on mechanical technical systems and the obtained results, the proposed measures can contribute to the improvement of state both in our and world mechanical industry particularly in car industry. The selection of the most favourable conception and the model of diagnostic state shown in car industry in terms of time scheduled preventive maintenance application is conditioned by a series of influences of technical and economic character. The precise methodology imposes the necessity for the special systematic approach which is being considered in this research. The basic characteristic of systematic approach methodology is its orientation towards the target value design, which should resolve the researched problem, so that the selection of the most favourable conception and the model for certain components of the system in whole is to be done from the standpoint of the influence of the defined criteria and the defined target. Therefore, by the application of this approach is possible to reach the optimum solution of the problem for specified conditions. Algorithm is developed for monitoring of exploitation system of diagnostification and the selection of the model for state diagnosis for the application at the level of the vehicle components and based on computer simulation model.

The model shown precisely describes all more important properties of the components for the successful resolving of the problem in state diagnosis and their influence to the reliability of motor vehicles. Also, it is based on the methodology comprising the determination of safety during the functioning of analyzed vehicle components. By this application is possible to realize the significant effects, to sustain the required level of reliability of motor vehicles simultaneously reducing the costs of maintenance, particularly as a result of lifetime extension of motor vehicle components.

7. REFERENCES

- [1] Andre P., Đekić I.: "Preporuke kako ocenjivati QMS prema zahtevima QS 9000", Savetovanje Standardi sistema kvaliteta svetske automobilske industrije i njihova kompatibilnost sa JUS ISO 9001:2001, Kragujevac 14 - 15. mart 2002. godine - Zbornik na CD.

- [2] Karaklajić, D., Vuković, M.: *Problemi kvaliteta i konkurentnosti u auto-industriji Srbije, uzroci i mogućnosti poboljšavanja stanja*, Festival kvaliteta 2008, 35. Nacionalna konferencija o kvalitetu, Kragujevac, 2008.
- [3] Pešić, R., Đokić D., Petković S., Veinović S.: *Zaštita okoline-Ključni cilj automobilske industrije*, Festival kvaliteta 2006, 1. Nacionalna konferencija o kvalitetu života, Kragujevac, 2006.
- [4] Mikić, D., Alihodžić, A.: *Problematika automatizacije upravljanja kvalitetom na nivou preduzeća*, 33. JUPITER KONFERENCIJA, 13. Simpozijum, Menadžment kvalitetom sa međunarodnim učešćem, Zbornik radova, Univerzitet u Beogradu-Mašinski fakultet, Zlatibor, maja 2007, str. 534-538.
- [5] ISO/TS 16949 - pripremili i izdali *Međunarodna automobilska radna grupa - IATF i Japansko udruženje proizvođača automobila - JAMA*, uz pomoć ISO Komiteta za menadžment kvalitetom - ISO/TC 176.
- [6] IATF-DaimlerChrysler, Ford, General Motors and Plexus ISO/TS 16949 Training System, Plexus Corporation, DaimlerChrysler, Ford Motor Company, General Motors Corporation, 2003.
- [7] Ašonja, A., Mikić, D., Gligorić, R.: *Opravdanost upotrebe automatskih podmazivača*, Traktori i pogonske mašine, Poljoprivredni fakultet Novi Sad - Departman za poljoprivrednu tehniku, Naučno društvo za pogonske mašine, traktore i održavanje JUMTO, XVII Naučni skup, Razvoj traktora i mobilnih sistema, Vol.15, No.5,42-46, Novi Sad, 03.12.2010.
- [8] Vujanović N.: *Teorija pouzdanosti tehničkih sistema*, Vojno izdavački novinski centar, Beograd, 1990.
- [9] Janjić N.: *Doktorska disertacija, Modeli dijagnostike stanja i njihov uticaj na pouzdanost motornih vozila*, Zrenjanin, 2015.
- [10] Janjić, N., Adamović, Ž., Nikolić, D., Janjić, Z.: *Istraživanje ekstremnih vrednosti pouzdanosti na ležajevima motornih vozila*, Časopis „Održavanja mašina“ godina X, broj 3-4, ISSN 1452-9688 UDK 005, Smederevo, 2014.
- [11] Nezirić, E., Isić, S., Džih, E.: *Vibration analysis and repair process for the ventilation system for smoke drain in the thermal power plant*, Applied Engineering Letters, Vol.3, No.1, pp.40-45, 2018.
- [12] Ašonja, A., Desnica, E., Palinkaš, I.: *Analysis of the static behavior of the shaft based on finite element method under effect of different variants of load*, Applied Engineering Letters, Vol. 1, No. 1, pp. 8-15, 2016.
- [13] Miladinović, S., Radosavljević, S., Veličković, S., Atyat, R., Skulić, A., Šljivić, V.: *Optimization of efficiency of worm gear reducer by using taguchi-grey method*, Applied Engineering Letters, Vol. 2, No. 2, pp. 69-75, 2017.
- [14] Pastukhov, A., Timashov, Evgen, Parnikova, T.: *System approach to assessment of thermal stress of units of transmissions*, Applied Engineering Letters, Vol. 2, No. 2, pp. 65-68, 2017.

Authors: Assoc. prof. **Nenad Janjić**, Assoc. prof. **Branko Savić**, m.sc **Nenad Stanković**, Higher Education Technical School of Professional Studies in Novi Sad,

E-mail: janjic@vtsns.edu.rs; savic@vtsns.edu.rs; stankovic@vtsns.edu.rs

Assoc. prof. Danilo Mikić, Higher Education Technical School of Professional Studies Zvečan, Kosovska Mitrovica,

E-mail: mikicdanilo@gmail.com

m.sc Petrović Dragan, Technical school “Jovan Žujović” Gornji Milanovac,

E-mail: gago.petrovic@yahoo.com

Jotić, G., Borojević, S., Hadžistević, M., Štrbac, B., Vukman, J.

ANALYSIS OF COMPARATIVE MEASUREMENT RESULTS FOR THIN-WALLED AL 7075 ALLOY STRUCTURES

Abstract: Comparative measurements can serve as the basis for the analysis of accuracy and reliability of measurement results, that is, measurement systems being used. In this paper three measurement devices/ systems were used: micrometre, the Nikon Manual Coordinate Measuring Arm and Coordinate Measuring Machine Axiom. The measurements were carried out on aluminium honeycomb structures machined by cutting. Given the complicated machining process and poor rigidity of thin-walled plates, deformation and surface errors are apparent in workpieces. The processing of measurement results involves the analysis of the wall thickness values obtained by applying different measurement systems. The aim of the paper is to analyse the accuracy, reliability and validity of the measurement systems used in specific production conditions.

Key words: CMM, honeycomb thin-walled structures, comparative measurements

1. INTRODUCTION

It is known that the production of any machine parts is not possible without the implementation of a production control carried out by appropriate measurement methods. The development of measurement techniques and the use of new technologies in this area led to the introduction of new methods of measurement and control in the process of manufacturing parts. In addition to the contact principle of measurement, using conventional measuring devices, new methods involving the use of coordinate measurement systems are increasingly being used. The accuracy in detecting the position of the measuring points depends primarily on the type of coordinate measuring system (hardware structure), the sampling system (measuring sensor), the way of sampling points, etc. The Coordinate Measurement Systems (CMS) can be divided into two groups: systems that sample points in a discreet way and systems that collect points in the form of a scan [1]. The first group includes machines with serial kinematics, i.e. conventional coordinate measuring machines (CMM) and measuring arms. Scanning systems include: point scanners, line laser scanners, edge projection systems, and computer tomography [1]. Observing all the above methods of measurement, the question arises in regards to the accuracy and reliability of the obtained measurement results, as well as justification of the use of certain measurement methods in concrete production conditions, which is also the subject of research of this paper.

In this paper the objects of measurement are parts belonging to thin-walled structures made of aluminium alloys by machining methods, which are described in more detail in chapter 2 of this paper. The experiment

plan, the measuring devices used in the measurement, the measurement methodology and the measurement sizes are presented in chapter 3. The results of the measurements and their analysis are presented in chapter 4, while the final considerations are presented in chapter 5 of this paper.

2. THIN-WALLED STRUCTURES

Thin-walled parts are important structural parts in the cars and aircraft industry. These parts have the advantages of low weight, low design requirement, and corrosion resistance and are typically composed of titanium/ aluminium alloy to reduce their weight and enhance their strength. Two common problems in milling are workpiece deformation (cutter back-off, overcut, and bending) and tool wear, which are due to the inherent low rigidity and poor machinability of thin-walled geometries. The identification and control of machining errors due to workpiece deformation and tool wear are crucial to achieving high machining accuracy [2].

As an example of these components, the following forms can be indicated: longitudinal ribs, transverse ribs, cantilevers, bulkheads and others. The production of thin-walled structures is most often done by machining methods, that is, by removing material from full raw material up to 95% of the mass of the raw material [2]. Constructive solutions of thin-walled structures have changed over time. At the beginning of the design and application of thin-walled structures, simple linear and rectangular shapes were used, and as such, they had significant advantages over the previous construction solutions of the product (Figure 1).

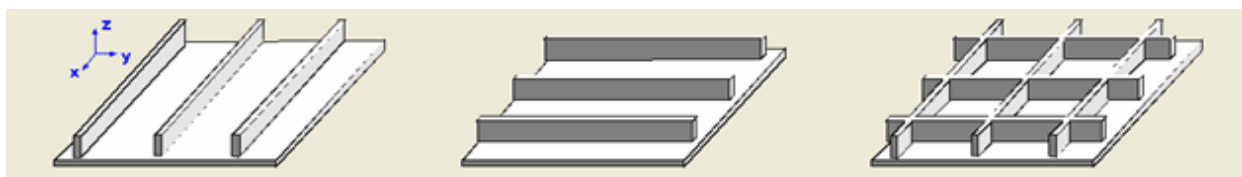


Figure 1. Simple constructional forms of thin-walled structures [2]

With the increasing industrial demands and complexity of products, more complex forms of thin-walled structures followed: honeycomb (hexagonal), pocket form, combined (Figure 2). The machining process of complex thin-walled structures is technologically and

timely demanding. Due to the large amount of material to be removed by machining, the geometry and small stiffness of the structure's walls, machining errors occur, which is important in identifying the use of appropriate measurement methods.

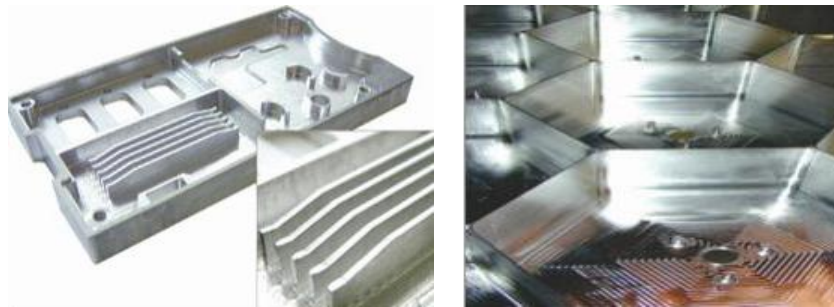


Figure 2. Complex constructive forms of thin-walled aluminium structures [2]

Figure 3 shows the analysed objects, i.e. thin-walled structures. The samples are made of aluminium alloy Al 7075 (AlZnMgCu1.5), characterized by high mechanical properties, as well as very high fatigue and corrosion resistance, which makes it suitable for

making thin-walled structures. Mechanical characteristics: tensile strength (560 MPa), $R_{p0.2}$ (500 MPa), elongation-stretch before ultimate failure (7%) and hardness (150 HBW) [3].

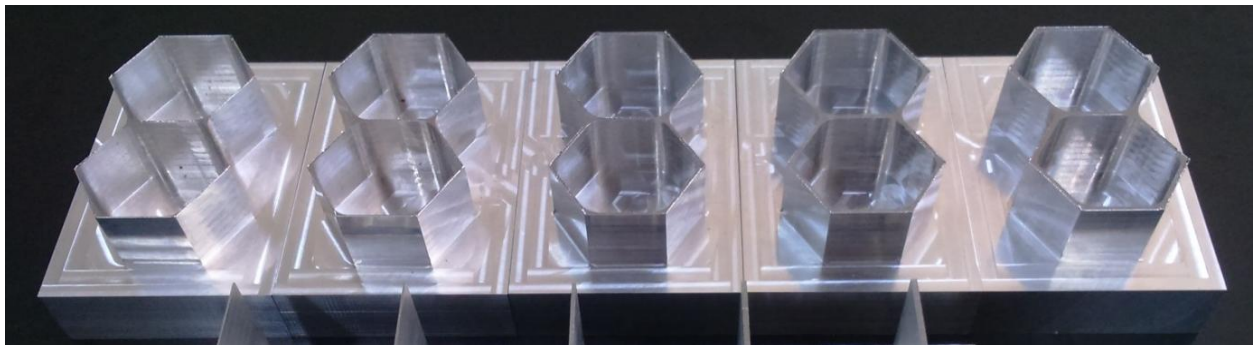


Figure 3. The analysed honeycomb aluminium structures

All samples were made by the machining (milling) method, following the same conditions and machining parameters. The spiral machining strategy was generated in SolidCAM, while tool Hoffman Garant®, code 202480. The samples were created at the EMCO Concept Mill 450 machining centre. Machining parameters of the thin-walled structures are constant, that is, a feed rate of 250 mm/min and a spindle speed of 4000 rpm.

3. EXPERIMENT

The corresponding parameters were measured on the illustrated aluminium thin-walled structures using different measurement systems (Figure 3). Five samples, identified with numbers 3, 4, 5, 6 and 11, with different wall thickness were analysed (Table 1). Constant dimensions of the structures are the distances of the opposing outer walls surfaces ($d=34.64$ mm), while the variable dimension refers to the wall thickness (h). The wall thickness marked with numbers 1 to 11 was measured (Figure 4). Three measuring devices/ systems were used to measure these parameters: a micrometre, coordinate measuring machine (CMM) with a touch point sensor and a

measuring arm with a rigid contact sensor.

No. model	5	3	11	4	6
Wall thickness (h)	0.5	0.65	1	1.35	1.5

Table 1. Parameters of analysed thin-walled structures

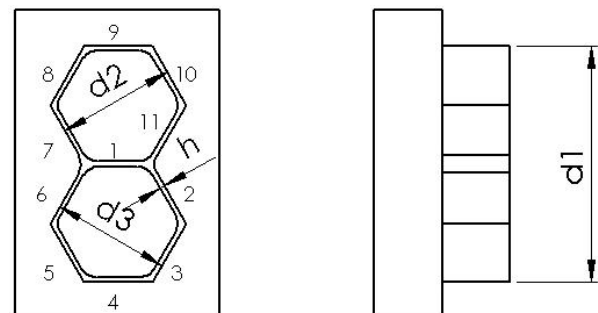


Figure 4. Parameters of analysed thin-walled structures

The characteristics of the used measuring devices are given in Table 2.



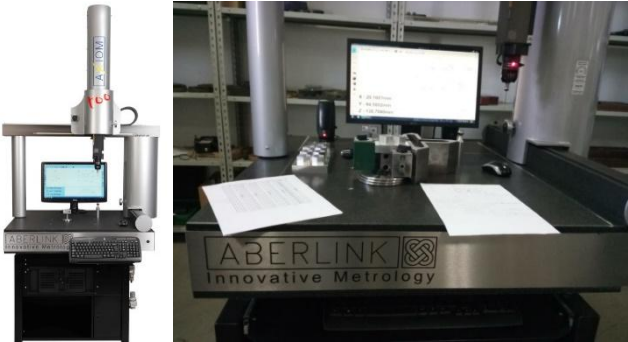
<p>Micrometre Digitmaster, Tesa</p>  <p>Accuracy 0.002 mm</p>	<p>MCAx Nikon arm, model MCAx 20+</p>  <p>Accuracy ± 0.033 mm</p>
<p>CMM Axiom too, ABERLINK</p>  <p>$MPE_E = 2.4 + 0.4L/100 \mu m$ (L in mm)</p>	

Table 2. Measuring devices and characteristics

According to the specification, the micrometre has the highest accuracy. On the other hand, the coordinate measurement systems used have considerably greater possibilities in terms of the complexity of the measurement tasks (Figure 4). Considering the possibilities of the used measuring devices/ systems, the micrometre was used only to measure the wall thickness. The wall thickness marked with number 1 cannot be measured by the micrometre.

Due to its technology, MCAx is only operated manually. The user brings a mobile probe to the object to touch a set of points on its surface. This is an important difference from CMMs, which are typically controlled by CNC. CMMs software makes it possible to create routines to automatically perform the same measurements on identical objects [4].

Differences in the way in which the coordinate system measurement sensors are guided results in the inability to equally sample points on the structure walls.

4. RESULTS OF EXPERIMENT

The wall thickness, marked with numbers 1 to 11, was measured in all samples (Figure 4). Figure 5 shows a diagram of the deviation of measured wall thickness values from the nominal values defined by the CAD model (Δh). One of the tasks was to analyse the accuracy and justification of the application of the said measurement systems. A different approach in the process of sampling points on the walls of the structure shows that, in addition to accuracy, there are other causes of the displayed deviations.

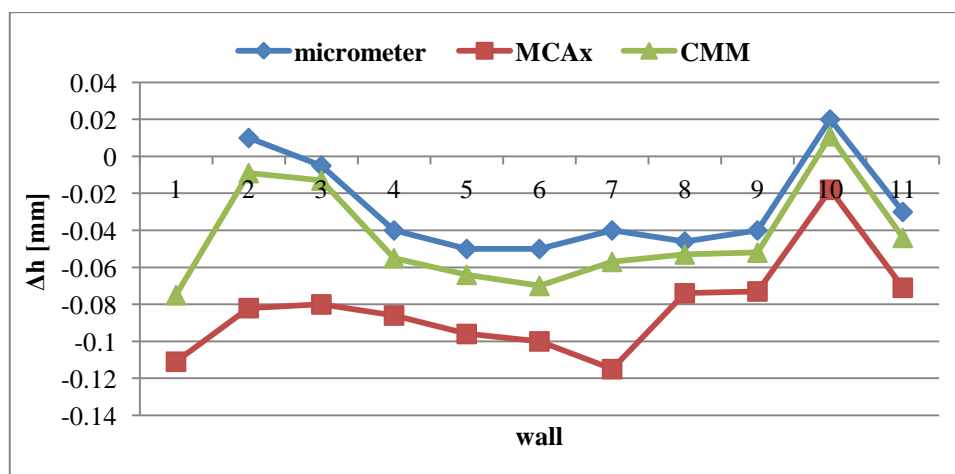


Figure 5. Deviation Δh , sample number 5

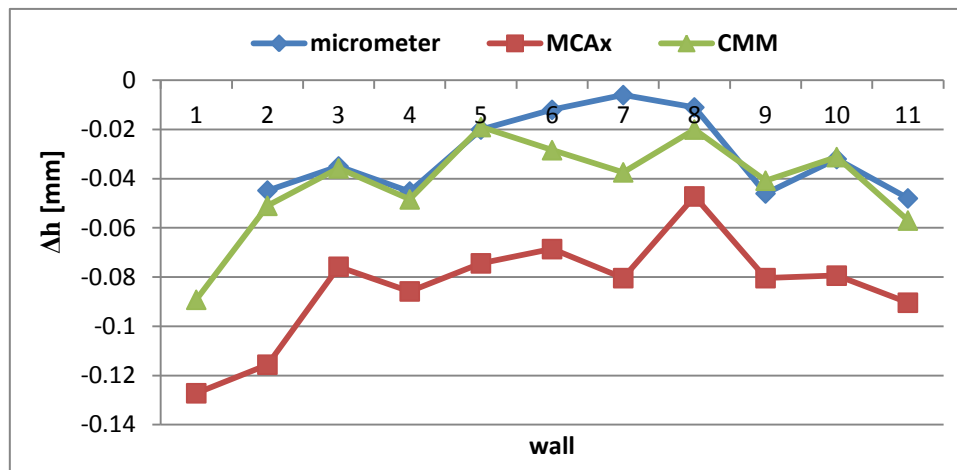


Figure 6. Deviation mean Δh , all samples

The approximately equidistant position of the deviation diagram for all three measuring devices has confirmed the good repeatability of the measurement results of the used devices (Figure 5). Figure 6 shows the values of wall thickness variance Δh from the nominal values obtained on all five samples. The order in terms of deviation value (Micrometre-CMM-MCAx) remained the same as in individual cases of all five structures, which confirms the absence of random and huge measurement errors.

5. CONCLUSION

Based on the comparisons shown above, it can be concluded that the smallest deviations of wall thickness from the nominal value are the values measured by the micrometre, then CMM, while the greatest deviations are given by the MCAx measuring arm. The executed comparisons shown are not a valid indicator of the accuracy of the used measuring devices. In order to compare the measuring devices/ systems in terms of accuracy, it is necessary to perform calibration of the samples in order to obtain the reference values.

Cutting force, tool wear, and selection of cutting parameters are the main factors that determine machining errors due to low stiffness and poor machinability of thin-walled parts. However, it is difficult to accurately predict workpiece-tool deflection because the evolution of cutting force and heat, tool wear, and workpiece deformation are comparatively nonlinear. The monitoring of cutting force and tool wear will inevitably increase the cost of online monitoring. By selecting an adequate measurement system and permanent control throughout the machining process, the compensation method for improving the machining accuracy of thin-walled parts could be proposed. This method is mainly based on online measuring experiments to compensate for processing errors. This method is simple and economical to carry out and does not require complex machining dynamics modelling. More importantly, this method does not require expensive sensors to monitor the cutting force, power, and torque online. Furthermore, the method does not require many trial-

cutting data or artificial participation and can save time and money in milling thin-walled parts with new structures. Therefore, this method is easier to apply in engineering applications.

6. REFERENCES

- [1] Weckenmann, A., Estler, T., Peggs, G., McMurtry, D.: *Probing systems in dimensional metrology*, CIRP Annals- Manufacturing Technology, 53 (2), 657-684, 2004.
- [2] Gang, W., Wen-long, L., Gang, T., Chang-tao, P.: *Improving the machining accuracy of thin-walled parts by online measuring and allowance compensation*, Int. J. of Advances Manufacturing Technology, 92 (5-8), 2755-2763, 2017.
- [3] Qiong, W., Da-Peng, L., Lei, R., Shuai, M.: *Detecting milling deformation in 7075 aluminum alloy thin-walled plates using finite difference method*, Int. J. of Advances Manufacturing Technology, 85 (5-8), 1291-1302, 2016.
- [4] Fiorenzo, F., Domenico, M., Luca, M.: *Mobile spatial coordinate measuring system (MScMS) and CMMs: a structured comparison*, Int. J. of Advances Manufacturing Technology, 42 (11-12), 1089-1102, 2009.

Authors: M.Sc. Goran Jotić, Assist. Prof. Stevo Borojević, University of Banja Luka, Faculty of Mechanical Engineering, vojvode Stepe Stepanovića 71, 78 000 Banja Luka. Phone.: +387 51 430-000, Fax: +387 21 465-085. **Full Prof. Miodrag Hadžistević, Assist. Prof. Branko Štrbac, M.Sc. Jovan Vukman**, University of Novi Sad, Faculty of Technical Sciences, Department of Production Engineering, Trg Dositeja Obradovica 6, 21000 Novi Sad, Serbia, Phone.: +381 21 450-366, Fax: +381 21 454-495.

E-mail: goran.jotic@mf.unibl.org;
stevo.borojevic@mf.unibl.org;
miodrags@uns.ac.rs;
strbacb@uns.ac.rs;
vukman@uns.ac.rs

Karpe, B., Fercak, Z., Nagode, A., Bavec, B., Kozuh, S., Gojic, M., Smolej, S., Sokovic, M., Bizjak, M., Kosec, B.

THERMAL CHARACTERISTICS OF ENAMELS AND ENAMELLED METAL SHEETS

Abstract: *The main task of the research was to find out why sometimes cracking of the enamelled layer occur and to what extent enamel layer affects the heat transfer in the cooking oven. The samples of the enamelled steel sheet were metallographically analysed by scanning electron microscopy (SEM-EDX) and optical microscopy (OM). Measurements of the thermal properties of two types of enamels, which are used for oven interior enamelling was carried out in accordance with the standard ISO 22007-2 by transient planar heat source method (TPS Hot Disk 2200). To ensure proper measurement conditions, the samples of the enamels were prepared in the form of thick layers. The results show that enamel density has significant influence on its thermal properties. An assessment of the influence of the thermal conductivity of the enamel layer on the heat transfer in the oven is also given.*

Key words: *Thermal properties, Enamels, Enamelled steel sheet, TPS method, Measurement*

1. INTRODUCTION

Porcelain enamel is a glassy coating over the metal substrate, intended to improve its corrosion resistance, abrasion resistance, antibacterial characteristic or aesthetic appearance. Enamelling is a technological process in which a fine enamel powder is applied to the metallic substrate and heated to the melting temperature of the enamel (750-850°C), whereby the melt adhesively binds to the metal substrate and a solid, continuous glass coating is formed on the surface of the metal surface.

The enamels can be classified in several ways: depending on the substrate on which the enamel is applied, depending on the function they perform or according to the enamelling methods [1].

According to the metal substrate they can be classified as:

- Enamels for steel sheet
- Enamels for cast iron
- Enamels for aluminium
- Enamels for stainless steel and high-temperature resistant alloys
- Enamels for electronic applications
- Enamels for jewellery (precious metals, copper alloys)

According to the function they are designed for:

- Ground enamels that improve adherence between cover coats and substrate
- Cover coat enamels, which are further divided by the colour or by the certain physical and/or chemical property
- Direct enamels, which have the function of both ground and cover enamel

According to the enamelling technology:

- Dry electrostatic enamels
- Wet electrostatic enamels

Recently, the most commonly used industrial enamelling technology employs direct enamels, with

one coat and one firing process or for some application ground and cover coat enamels with one unified firing process.

When selecting a steel for enamelling, it is important to consider the following factors: Basic ability for enamelling (enamelability), absence of surface defects, and resistance to sagging at enamelling temperatures, while other characteristic such as formability, weldability, strength, etc. are of primary concern of product manufacturing technology before enamelling or mechanical property requirements of the final product.

By the term enamelability of steel we mean the absence of excessive formation of gas bubbles that cause the boiling of the enamel. Evolution of gas, which can originate from steel and enamel as well, is caused by various reactions at the steel/enamel interface. With spectrographic analysis, it was found out that gases evolving when enamelling steel are carbon monoxide, carbon dioxide, hydrogen, water vapour, and nitrogen. The most detrimental gas evolving reaction is the oxidation of carbon in the steel surface and the formation of carbon monoxide. Therefore, steel with low carbon (usually below 0.08 wt.%) or carbon stabilized (with Ti or Nb) chemical compositions should be primarily selected. If high-carbon steel cannot be avoided, special surface preparation techniques must be applied before enamelling.

2. THERMAL CONDUCTIVITY MEASUREMENT

Transient planar heat source method (TPS, Hot disk AB®) was used for the measurement of the thermal properties of enamels. With this method, the thermal conductivity can be measured with an accuracy of $\pm 2\%$ and specific thermal capacity and temperature diffusivity with accuracy of $\pm 5\%$ in accordance with ISO 22007-2 standard [2]. Thermal conductivity can be measured in the range from 0.01 to 500 Wm⁻¹K⁻¹, specific thermal capacity up to 5 MJm⁻³K⁻¹ and

temperature diffusivity from 0.1 to 300 mm²s⁻¹. The device is also equipped with a laboratory muffle furnace and allows the measurement of thermal properties up to 700°C in an inert atmosphere (Figure 1).



Fig 1. TPS 2200 Hot disk AB ® analyser.

The thermal analyser utilises a sensor element in the shape of double spiral (Figure 2), which acts both as heating element for increasing the temperature of the sample and as an electric resistance thermometer. The spiral is made by selective etching from 10 µm thick nickel foil, supported and electrically insulated on both sides with insulating foil. In the temperature range from sub-zero up to 300°C polyimide foil (Kapton® Du Pont) is used as insulating material, while above 300°C mica foil is used as insulating material. Before the measurement the sensor is sandwiched between two halves of the sample (solids) or embedded in the sample (liquids, powders). The main principle of the measurement system is that the sensor is first supplied with a constant electrical power which creates a dynamic temperature field in its surroundings, and then 200 x in succession measures the change in sensor electrical resistance at a selected time interval. Parameters like heating power, measurement time for electrical resistivity measurement and sensor radius are used to optimize the settings for the experiment.

Since we are not equipped with a module for measuring the thermal properties of thin insulating films, enamel samples were prepared in the form of an approximately 1 cm thick layer. To make such samples, first dies (9 x 6 x 1.5 cm) from low carbon ferritic steel were made. Dies were filled with enamel powder and gradually heated to 850°C and 900°C for 10 minutes and then slowly cooled in the furnace [3].



Fig 2. Thick enamel layer (left), sensor position (right).

Since enamel melts wet the steel surface well it is very difficult to make two identical samples with parallel free surfaces (non-concave), which would enable the insertion of the sensor between them without an air gap. Therefore, the measurements were carried out using a single-side method, where the sensor is “sandwiched” between the investigating sample and insulation material of known thermal conductivity (Styrofoam). Several measurements were performed on various areas of the individual sample.

Table 1. Thermal properties of enamel 1

Pos.	λ [Wm ⁻¹ K ⁻¹]	a [mm ² s ⁻¹]	C_p [MJm ⁻³ K ⁻¹]
1	0.6821	0.4286	1.591
1	0.6845	0.4335	1.579
1	0.6852	0.4390	1.579
1	0.6840	0.4385	1.560
2	0.6667	0.4239	1.573
2	0.6678	0.4273	1.563
2	0.6683	0.4251	1.572

Table 2. Thermal properties of enamel 2

Pos.	λ [Wm ⁻¹ K ⁻¹]	a [mm ² s ⁻¹]	C_p [MJm ⁻³ K ⁻¹]
1	0.8786	0.4410	1.992
1	0.8879	0.4626	1.919
1	0.8867	0.4588	1.932
1	0.8866	0.4588	1.932
2	0.8641	0.4267	2.025
2	0.8621	0.4311	2.000
2	0.8626	0.4309	2.002

Several samples prepared from the same enamel, but with different densities (due to firing temperature variation) were measured. Results show significant influence of density on the thermal conductivity of enamel. Tables 6 and 7 show results of thermal conductivity of individual enamel as a function of its density.

Table 3. Thermal conductivity as a function of enamel layer density (enamel 1)

ρ [g/cm ³]	λ [Wm ⁻¹ K ⁻¹]
1.88 – 1.89	0.66 – 0.69
1.77 – 1.78	0.65 – 0.67
1.73 – 1.75	0.60 – 0.61

Table 4. Thermal conductivity as a function of enamel layer density (enamel 2)

ρ [g/cm ³]	λ [Wm ⁻¹ K ⁻¹]
2.20 – 2.22	0.94 – 0.95
2.06 – 2.13	0.83 – 0.84

3. MICROSTRUCTURE INVESTIGATION

The microstructure of the enamel is shown in the figure 3. The results of micro-chemical analyses (EDX) of the areas marked in the figure 3 by squares are presented in the table 2.

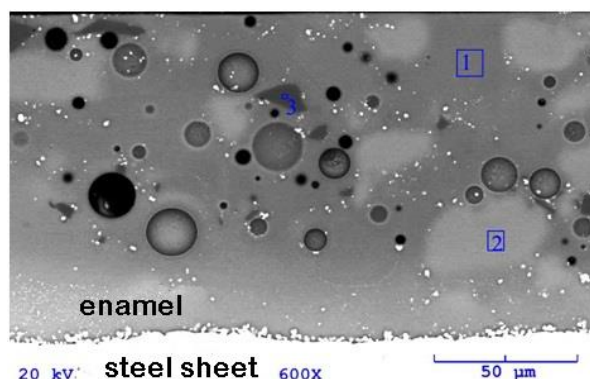


Fig 3. Microstructure of enamel layer (SEM).

Table 3. Microchemical analysis (EDX) of areas marked in Figure 3

Element	M. 1 wt. [%]	M. 2 wt. [%]	M. 3 wt. [%]
O	15.237	13.091	15.020
Na	5.298	4.471	-
Al	0.716	0.880	-
Si	47.904	45.043	84.980
K	5.923	6.181	-
Ca	4.852	2.717	-
Ti	6.638	2.961	-
Mn	3.749	1.328	-
Fe	6.038	8.537	-
Co	1.588	0.923	-
Cu	0.744	0.353	-
Zr	1.313	13.515	-

From the figure 3 can be seen that enamel layer is not homogenous, but consist of various crystal phases, pores, and amorphous areas with different chemical compositions. Brighter contrasted areas have much higher Zr content (added as ZrO), while darker contrasted areas contain a higher percentage of Ti and Mn (added as TiO₂ and MnO). Sharp dark phases are SiO₂ crystals, and spheres porosity. In addition, small bright particles located near the steel-enamel interface and in areas rich with titanium and manganese are also visible. Although the quantitative evaluation of the chemical composition with EDX microchemical analysis of such small analytical volumes is not accurate, it nevertheless points out the differences in chemical composition of the bright particles located near the steel/enamel interface and bright particles in the bulk enamel layer. Namely, particles in the enamel contain chromium while particles at the interface contain cobalt. The chromium was not detected in particles at the steel/enamel interface except for location 2 (Figure 4), which shows a different, more

sharp morphology, so that the possibility of interaction between the particle already in the enamel and steel surface cannot be excluded. In addition, the particles in the enamel do not contain cobalt, which is present in all particles at the interface. Since the presence of chromium in enamels is not common [4], we analysed the enamel powders before the enamelling process.

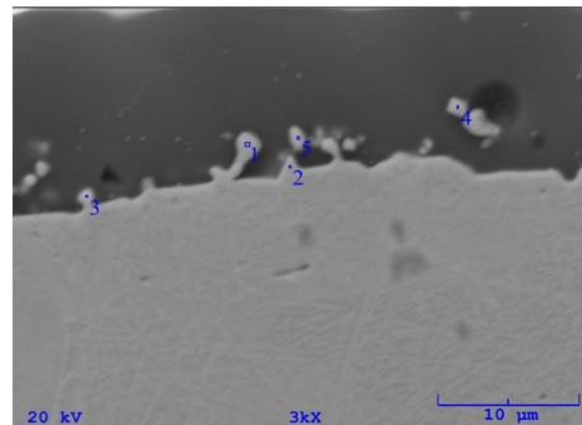


Fig 4. Steel/enamel interface (SEM).

Table 4. Microchemical analysis (EDX) of areas marked in Figure 4

El.	M. 1 wt. [%]	M. 2 wt. [%]	M. 3 wt. [%]	M. 4 wt. [%]	M. 5 wt. [%]
O	4.230	4.921	7.821	12.682	8.779
Na	3.159	2.642	5.300	4.532	4.919
Al	0.534	0.436	0.971	1.095	0.803
Si	15.438	11.630	25.410	35.872	27.692
K	1.079	0.805	1.943	3.215	2.191
Ca	1.278	0.869	2.202	3.409	2.701
Ti	1.346	1.624	2.472	3.847	2.817
Cr	-	4.615	-	-	-
Mn	0.636	0.867	1.328	2.358	1.677
Fe	63.106	65.821	48.264	28.678	43.851
Co	6.716	3.494	2.827	1.620	3.510
Cu	2.048	1.848	0.794	-	-
Zr	0.430	0.427	0.666	2.693	1.060

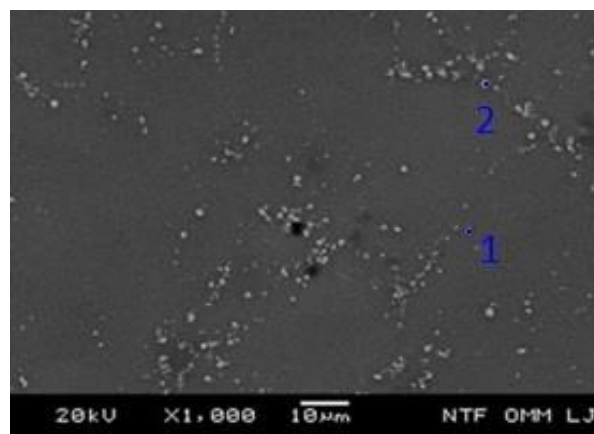


Fig 5. Bright particles on the enamel surface (SEM).

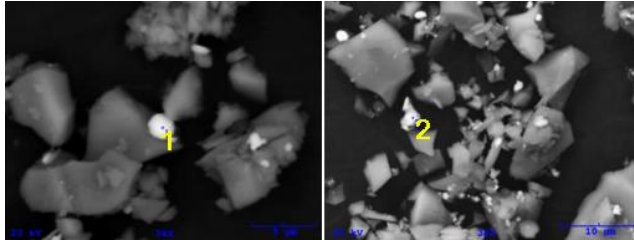


Fig 6. Bright particles in the enamel powder (SEM).

Table 5. Microchemical analysis of bright particles in enamel layer after firing (Figure 5) and in enamel powder before firing (Figure 6)

Element	M. 1 Fig. 5 wt. [%]	M. 2 Fig. 5 wt. [%]	M. 1 Fig. 6 wt. [%]	M. 2 Fig. 6 wt. [%]
O	6.025	5.319	0.484	11.61
Na	2.232	1.307	0.455	1.49
Al	1.163	0.253	0.45	0.997
Si	17.889	8.226	3.81	7.603
K	1.509	0.659	0.71	0.314
Ca	0.805	0.571	1.247	0.259
Ti	1.104	2.416	0.614	0.228
Cr	27.364	19.629	26.18	14.521
Cu	0.469	1.507	1.285	0.702
Fe	39.536	59.735	64.604	61.823
Zr	1.904	0.376	0.145	0.45

Figure 6 shows the enamel powder after final grinding, ready for application to the metal substrate. As we can see, in the powder is a noticeable number of shiny particles of similar size (most of which less than 1 μm) as detected in the enamel layer after firing. By microchemical analysis (EDX) was determined that these particles also contain higher concentrations of chromium and iron (Table 5). This is a proof that the particles found in the enamel layer after firing originate from the previous preparation of enamel powder and are not the result of chemical reactions during firing of the enamel.

4. HEAT TRANSFER THROUGH ENAMELLED STEEL SHEET

Heat transfer rate through enamelled steel sheet per unit of area can be calculated by equation:

$$U = \frac{\Delta T}{\frac{1}{\alpha_{out}} + \frac{\delta_{steel}}{\lambda_{steel}} + \frac{\delta_{en}}{\lambda_{en}} + \frac{1}{\alpha_{in}}} \left[\frac{W}{m^2} \right]$$

Where δ_{steel} and δ_{en} represents thickness of steel sheet and enamel layer, λ_{steel} and λ_{en} thermal conductivities of the steel sheet and enamel, α_{out} in α_{in} heat transfer coefficients (radiation + convection) on

both sides of enamelled steel sheet, and ΔT temperature difference. For heat transfer coefficients in kitchen ovens values between 15 - 40 $\text{Wm}^{-2}\text{K}^{-1}$ can be found in the literature [5]. In the case of one side enamelled steel sheet (200 μm thick enamel layer + 1 mm thick steel sheet), individual thermal resistances can be evaluated.

Thermal resistances:

$$\frac{\delta_{steel}}{\lambda_{steel}} = \frac{0,001}{54} = 1,85 \cdot 10^{-5} \text{ m}^2\text{K/W}$$

$$\frac{\delta_{en}}{\lambda_{en}} = \frac{200 \cdot 10^{-6}}{0,3 \div 1,3} = 6,6 \cdot 10^{-4} \div 1,5 \cdot 10^{-4} \text{ m}^2\text{K/W}$$

$$\frac{1}{\alpha_{in/out}} = \frac{1}{15 \div 40} = 6,6 \cdot 10^{-2} \div 2,5 \cdot 10^{-2} \text{ m}^2\text{K/W}$$

We can quickly figure out that conduction thermal resistance of enamelled steel sheet is negligible factor compared to convective resistance if heat transfer coefficient at only one side is below 100 $\text{Wm}^{-2}\text{K}^{-1}$. Even if we consider extreme values of heat transfer coefficients (500 $\text{Wm}^{-2}\text{K}^{-1}$) on both sides of enamelled steel sheet and calculate the heat transfer rate with limited values of enamel thermal conductivity (0,3 or 1,3 $\text{Wm}^{-1}\text{K}^{-1}$) the difference in heat transfer rate will be less than 13%. However, in the case of kitchen ovens, such values of heat transfer coefficients will never be achieved.

5. CONCLUSIONS

The thermal properties of the enamel are mostly affected by the density of the enamel. The greater the density, the higher will be thermal conductivity and the specific volume heat capacity, which is in accordance with the theory. Namely, gases exhibit at least an order of magnitude lower thermal conductivity than solids. The density of the enameled layer depends on the chemical composition of the enamel and the process parameters of the enameling which influence the amount of porosity.

Enamel layer has a multiphase structure composed of amorphous areas with different chemical composition, crystal phases (SiO_2 , metal particles) and pores. Certain crystalline phases (metal inclusions) found in the enamel layer after firing originate from the process of preparing the powder (grinding, sieving) or are intentionally added. In all analyzed enamel powders, the metallic inclusions were detected, which have a similar chemical composition and size as metal inclusions located in the enamel layer after firing. If these particles agglomerate during firing they will cause cracking of the enamel layer.

Microstructural observations enable precise monitoring of the changes in the material at any technological stage and allow faster detection of the defect origin.

6. REFERENCES

- [1] I. A. Andrews, S. Pagliuca, D. W. Faust, Porcelain (vitreous) enamels and industrial enamelling processes. The preparation, application and properties of enamels, Mantova: Typografia commerciale, 2011, 900.
- [2] Slovenski standard SIST EN ISO 22007-2:2012. (2012). Polimerni materiali – Ugotavljanje toplotne prevodnosti in toplotne razprševalnosti – 2.del: Metoda s tranzientnim ploskovnim toplotnim virom (vroči disk) (ISO 22007-2:2008), Ljubljana: Slovenski inštitut za standardizacijo.
- [3] B. Kosec, B. Karpe, Instrument for thermal properties analysis Hot Disk TPS 2200, IRT3000, 70 (2017), 67.
- [4] M. Bodaghi, A. Davarpanah: The influence of cobalt on the microstructure and adherence characteristics of enamel on steel sheet, Processing and Application of Ceramics, 2011, vol. 5, 215-222.

Authors: Ass. Prof. Dr. Blaž Karpe, Žan Ferčak, Samo Smolej, Prof. Dr. Milan Bizjak, Assoc. Prof. Dr. Aleš Nagode, Prof. Dr. Borut Kosec, University of Ljubljana, Faculty of Natural Sciences and Engineering, Aškerčeva 12, 1000 Ljubljana, Slovenia, Phone: +386 1 2000413, Fax: +386 1 4704560. E-mail: blaz.karpe@omm.ntf.uni-lj.si; zanf@gmail.com; samo.smolej@omm.ntf.uni-lj.si; milan.bizjak@omm.ntf.uni-lj.si; ales.nagode@omm.ntf.uni-lj.si; borut.kosec@omm.ntf.uni-lj.si;

Boštjan Bavec, Gorenje d.d., Partizanska cesta 12, 3320 Velenje, Slovenia, Phone: +386 3 8991000, Fax: +386 3 8991001. E-mail: bostjan.bavec@gorenje.com

Prof. Dr. Mirko Gojić, Assoc. Prof. Dr. Stjepan Kožuh, University of Zagreb, Faculty of Metallurgy, Aškerčeva 6, 1000 Sisak, Croatia, Phone: +385 43 533 381, Fax: +385 43 533 381. E-mail: gojic@simet.hr; kozuh@simet.hr

Prof. Dr. Mirko Soković, University of Novo mesto, Faculty of Mechanical Engineering, Na Loko 2, 8000 Novo mesto, Slovenia, Phone: +386 7 3930019, Fax: +386 7 3930013. E-mail: mirko.sokovic@gmail.com;

Klimenko, S., Kopeikina, M., Manokhin, A., Melniychuk, Yu., Naydenko, A., Tanovic, Lj.

ENHANCED PCBN TOOLS FOR HARD MACHINING

Abstract. The different approaches of enhancement of PCBN cutting tools and its application have been described. Technology which implies application of oblique cutting tools substantially increases feed rates while roughness of machined surfaces stays comparatively low. Efficiency of machining can also be increased by adding components to a composite or protective coating, which would provide an increased partial nitrogen pressure in the cutting zone. This leads to suppression of wear mechanism of PCBN composites caused by contact-reactive melting under conditions of hard turning.

Key words: PCBN, hardened steels, contact interaction, efficiency of tool, protective coating

1. INTRODUCTION

To increase the efficiency of the application of cutting tools from superhard materials in machining hardened steels, several alternative ways may be suggested. One of the ways is the improvement of cutting tools design and optimization of cutting conditions in order to remove larger material volume per unit time (wiper tools, inserts with big nose-radius, etc.). The other way is to change the tool-workpiece interaction characteristics in the cutting zone by developing new composites with high physical and mechanical properties, optimization of binder and superhard phase relation in the composite, application of protective coatings, etc. The tool improvement in the framework of the second way is aimed at increasing maximum cutting velocity. The point is that in any case an increase in the productivity is reached by development of cutting tools, optimized under specific technological conditions.

2. SPECIAL TOOLS

To realize the first of these ways we have proposed special oblique cutting tools for hardened steel turning: single-edged tools and tools with cylindrical rake face. The use of these tools is characterized by high feed and cutting speed and high machined surface quality [1, 2]. Design of such tools implies the use of special toolholders equipped with standard indexable inserts (SNUN 120408, RNMN 070300F, RNMN 09T300F).

Because of the process peculiarities, the determination of the undeformed chip cross section in turning with such tools is of particular interest. These tools geometrical parameters makes it possible to form a wide and thin undeformed chip cross section and thus to avoid the loads on the cutting edge, which can destroy the tool even at high feed. For comparison Fig. 1 shows the shapes of undeformed chip cross sections calculated for a conventional

cutting tool (1) and a tool with cylindrical rake face (2). Cutting conditions were equal (feed $S = 0.5$ mm/rev; depth of cut $t = 0.1$ mm; workpiece diameter $\varnothing = 50$ mm), both these tools were equipped with indexable cutting inserts RNMN 070300F.

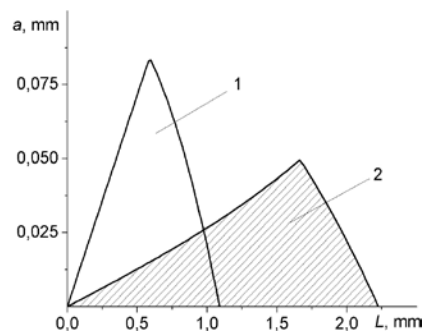


Fig. 1. Shape of undeformed chip cross section.

The use of the tool with cylindrical rake face allows the feed rates $S = 0.2-0.7$ mm/rev, which is 2–5 times as high as that of the conventional tool feed in hardened steel finishing. In spite of this, the surface quality is very high (Ra 0.20–0.80; Rz 1.25–2.5, Fig. 2, a).

The curvature of the cutting edge projection of a tool with cylindrical rake face on the reference plane is essentially smaller than that of the conventional tool. These tools significantly decrease the roughness of the surface machined. In our opinion, the regularities of plastic deformation in the cutting zone are one more reason, responsible for high quality of the machined surfaces in the case that oblique cutting tools are used.

It is known, that there is a correlation between the peak-to-valley height and degree of strain in the shear zone. This phenomenon is due to the formation of the strain wave in front of descending chip, which is caused by a collision of removed material flows generated by principal and auxiliary cutting edges. At the point before rake face, which corresponds to maximum tangential stresses, a separation of the

material removed takes place onto the cut-off and extruded parts. The last one moves in the direction of a peak of the microirregularity being formed and thus leads to an increase of the surface roughness [3].

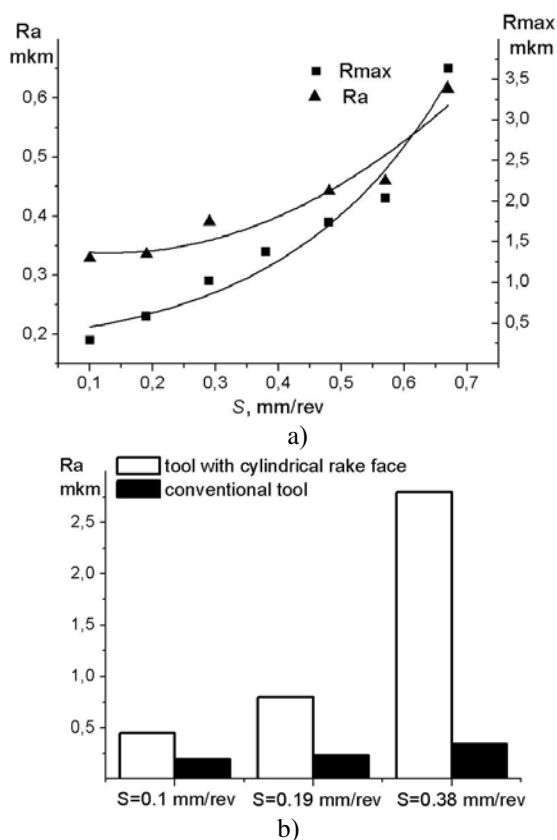


Fig. 2. Feed influence on the machined surface roughness (a), comparison of technological possibilities of conventional and cylindrical rake face cutting tools (b)

In using the oblique tools the machining conditions are close to a free cutting and the influence of the above effect is reduced, which allows one to achieve a much more higher quality of machined surfaces as compared to those achieved by other turning methods (Fig. 2 b). It should be noted that the roughness of a workpiece surface layer is characterized by specific microirregularities: similar peaks are repeated with the feed pitch (Fig. 3).

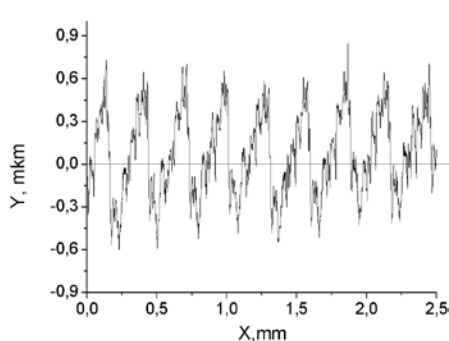


Fig. 3. Profilogram of the surface machined by a tool with cylindrical rake face.

The tool life of a tool with cylindrical rake face equipped with PSHM while cutting hardened ShKh-15 steel (60–62 HRC) is from 30 to 80 minutes depending on the feed rate. We recommend the following cutting conditions: depth of cut $t = 0.005–0.2$ mm, cutting speed 1.0–2.0 m/s.

Due to the extension of feed range the turning with single-edged and cylindrical rake face cutting tools allows us to increase productivity of hardened steel finish tuning by a factor of 2–5.

3. CHEMICAL INTERACTION IN THE CUTTING ZONE

As has been mentioned, in the framework of the second way, it is advisable to optimize the conditions for chemical interaction in the cutting zone. It is known that high efficiency cutting of hardened steels with PCBN (polycrystalline cubic boron nitride) cutting tools is characterized by high thermobaric loads: contact pressures of 3–5 GPa and temperatures of about 1100 °C. Our previous research has shown, that in the tool-workpiece contact zone the contact-reactive melting mechanism is realized, which is one of the main reasons for intensive tool wear [4].

This interaction is accompanied by the formation of metal borides and free nitrogen release. Taking this into account, we propose to control chemical interaction between the materials of a tool and workpiece by arranging such conditions in the cutting zone, which would shift the chemical interaction to form Fe and/or Ni borides into higher temperature range. This can be achieved by doping nitrogen into cutting zone. The thermodynamic analysis confirms an increase of the borides formation temperature by 150–300 °C in the presence of an increased nitrogen partial pressure in the system (Fig. 4).

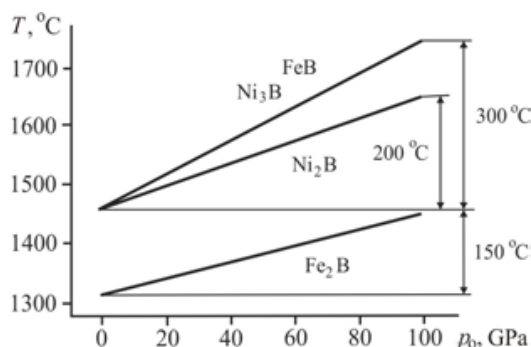


Fig. 4. Nitrogen pressure influence on the increase of the Fe and Ni borides formation temperature.

In addition to the function of inhibitor, nitrogen reduces the intensity of the tool material oxidation in the cutting zone. This causes changes in the tool wear mechanism and reduces its intensity, especially in high-speed machining.

Thus, to increase the performance of cutting tools equipped with PCBN, one should add components to a composite or protective coating, which would provide

an increased partial nitrogen pressure in the cutting zone under thermobaric conditions of the machining process. In this case the interaction between these components and elements of the material machined that is accompanied by a free nitrogen release begins at temperatures, which are not high enough to start an interaction between cBN and metals. As a consequence, the mechanism of a cBN tool wear by contact-reactive melting is suppressed. The analysis of physical and mechanical properties of different nitrides allows us to propose silicon nitride (Si_3N_4) or niobium nitride (NbN) as an additive. Silicon nitride can be added to the PCBN composition, while niobium nitride as a component of tool protective coating. The tool wear is of a complicated and integral character. The wearing process includes mechanical, adhesion, chemical, and other phenomena on the tool contact surfaces. In the case of PCBN tools, an increase of the temperature of borides and oxiborides formation in the cutting zone (because of the doping with the Si_3N_4 and NbN nitrides) and then the formation of eutectics and their contact melting in the (cBN- Si_3N_4)-(Cr,Fe,Ni) system plays an important role for increasing the PCBN tool life.

4. EXPERIMENTAL TEST

For substantiation of the above proposals and to confirm the results of the model experiments a set of indexable cutting inserts from cBN- Si_3N_4 composite containing up to 10 % Si_3N_4 was made. The PCBN tool from 2 to 5 % Si_3N_4 -doped tested in turning Ni-based alloys exhibited the maximum tool life.

The investigation have demonstrated that the application of cBN- Si_3N_4 composites helps to increase the performance of cutting tools in cutting difficult-to-machine materials (Fig. 5) by reducing their wear intensity due to the decrease of chemical and adhesion interactions between the tool and workpiece in the cutting zone.

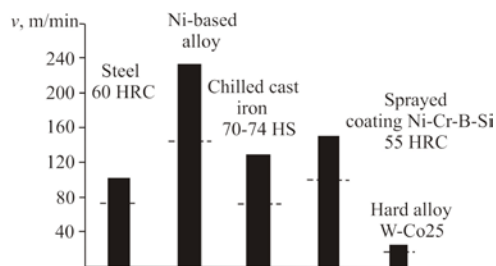


Fig. 5. Increase of cutting speed (over the dash line) while using cBN- Si_3N_4 composite.

5. CONCLUSIONS

Based on the investigation results the ways of cBN cutting tools improvement have been proposed

to increase the efficiency of cutting of difficult-to-machine materials.

When using special oblique cutting tools the specialties of their geometry allow us to increase feed rate by a factor of 2–5 without a decrease in quality of machined surfaces. In finishing, when the productivity is determined mainly by the surface area machined per time unit, the enhancement in the productivity is proportional to the increase of feed.

As our study has shown, an increase in the productivity can also be achieved by doping cBN composites with Si_3N_4 . This is due to the increase of the onset temperature of the chemical interaction and wear. Thus, one can apply a higher cutting speed without decreasing the tool life.

6. REFERENCES

- [1] Klimenko, S.A., Manokhin, A.S.: *Hard "Skiving" Turning*, J. of Superhard Mat., vol. 31 2009, № 1, pp. 42–55.
- [2] Melniychuk, Yu.A., Klimenko, S.A., and Manokhin, A.S., *Surface Roughness of hardened steel workpieces in turning with a tool having a cylindrical rake face: Porodorazrushayushchii i metalloobrabatyvayushchii instrument – tekhnika i tehnologiya ego izgotovleniya i primeneniya* (Rock Destruction and Metal-Working Tools – Techniques and Technology of the Tool Production and Applications), Collect. Sci. Papers, Kiev: Bakul' ISM, 2010, issue 13, pp. 484–491.
- [3] Klimenko, S.A.: *On the mechanism of the surface microgeometry generation in cutting*, J. of Superhard Mat., vol. 19 1997, № 5 pp. 43–53.
- [4] Klimenko, S.A., Kopeikina, M.Yu., Melniychuk, Yu.A., Kulik, O.G., Petrusha, I.A., Mukovoz, Yu.A.: *Increase in the efficiency of cutting tools with application of CBN-based polycrystalline superhard materials*, J. of Superhard Mat., vol. 25 2003, № 5, pp. 69–73.

Authors: Full Prof. Sergii Klimenko, Assoc. Prof. Marina Kopeykina, Ph. D. Andry Manokhin, Ph. D. Yrii Mel'niychuk, Ph. D. Artem Naydenko

V.Bakul Institute for Superhard materials of the National Academy of Sciences of Ukraine, 2, Avtozavodskaya Str., 04074, Kiev, Ukraine.

Phone: +38 044 468-86-32, fax: +38 044 468-86-32

E-mail: atm@meta.ua; atm1@meta.ua;

the.manokhin@gmail.com

Full Prof. Ljubodrag Tanovic

University of Belgrade, Kraljice Marije, 16, Belgrade, Serbia

E-mail: ltanovic@mas.bg.ac.rs

Knezevic, I., Bojic, S., Lukic, D., Rackov, M. Cavic, M., Pencic, M., Cako, S.

APPLICATION OF 3D PRINTED FIXTURES FOR WELDING

Abstract: 3D printing is also known as additive manufacturing (AM). Additive Manufacturing is the manufacturing of products by the addition of layers of material. Additive Manufacturing, in comparison with conventional production processes where the material is taken from workpiece, enables the manufacturing of parts with a minimum quantity of material. 3D printing is often used for rapid prototyping. This paper presents the application of 3D printing for the manufacturing of fixture for welding, in case of welding two parts that form a spatial angle whose accuracy affects the quality of the product's work. The fixture is used for welding the disc support on the agricultural machine, stubble cultivator. This paper presents the procedure of 3D modeling of fixture, preparing for 3D printing and setting the printing parameters. The fixture is printed using the 3D printer Makerbot Replicator 2X from ABS plastic. ABS plastic was selected due to better mechanical properties at higher temperature in relation to PLA material.

Key words: 3D printing, fixtures, welding, ABS plastic.

1. INTRODUCTION

The process of rational production requires the connection of the process of designing products with the technological processes necessary for its production. In practice, a number of DfX methods are used that help the successful cooperation between constructors and technologists. In the literature there are two interpretations of the meaning of "X" within the term DfX. First, the design for "X", where "X" represents a variable that can relate to: M-manufacturing, A-assembling, C-cost, etc. Second, design for excellence where "X" represents the application of all "Design for" methods, in order to achieve "excellence" of the product [1].

Design for Manufacturing (DfM) represents the connection between design and technology, as a measure of the benefits of the product for manufacturing. During product design, if consideration is not given to the construction of a product from the aspect of the convenience of its manufacture and assembly, we can get a product that is difficult to manufacture, or too expensive. Production costs affect the price of the final product, and thus to the size of the profit, and on the sustainability of products on the market. For this reason, when designing a product, it is trying to create a product that fulfills the project tasks, while having low production costs. By applying the DfM method, a reduction in product manufacturing costs is achieved, productivity increases are achieved by increasing the number of produced products in a unit of time.

At the design stage we strive to, designed parts are being manufactured on computer numerically controlled machines (CNC), which are easily accessible today and financially acceptable. By manufacturing parts on CNC machines the possibility of employee error is minimal. Parts made in this way are ready to be fitted into assemblies so that the worker's job in the production is assembling and/or welding. In this way,

the manufacturing time of the product is significantly reduced.

Using fixtures for the positioning of parts in the assembly process, the possibility of error is further reduced as well as the time of assembling. Fixtures can be made using conventional or non-conventional methods, such as 3D printing. This paper presents the application of 3D printing for the production of fixture for the positioning of parts when welding the sub-assembly of the disc support of the agricultural machine stubble cultivator. In this example, the successful application of the DfM method is shown, where designers and technologists work on the development of product that meets the conditions defined by the project task, while being constructive and technologically feasible, as well as financially justified.

2. STATE OF THE ART

Additive Manufacturing (AM) is a technology that has been developing intensively for more than 30 years, and the basic principle of working is the addition of layers of materials in the manufacturing process. According to [2] the contribution of Additive Manufacturing has grown significantly over the past 30 years. At first, AM technology was used primarily for prototyping Rapid Prototyping/RP. With the development of technology, the scope of AM application development is being expanded at tool production, Rapid Tooling/RT. Today it is possible to manufacture products that are ready to be used, and that technology has name Rapid Manufacturing /RM [3].

3D printing is often used as the name for Additive Manufacturing and it is widely used in all areas of human activity such as industry, medicine, education, art, and others. Like any technology in development and 3D printing, it has disadvantages such as low precision, low speed of production and in some cases high price. Stereo-Lithography (SLA), Selective Laser

Sintering (SLS), Fused Deposition Modeling (FDM) and Laminated Object Manufacturing (LOM) are the most advanced technologies [4]. Among them, the most common is FDM, a technology used by the 3D printer Makerbot Replicator 2X of the American manufacturer Makerbot, which was used to manufacture the fixture analyzed in this paper. Fixtures made with 3D printing technology are easy to manufacture and use, the cost of manufacturing is not high, and the accuracy of the geometry of the parts is sufficient and they have a low mass. Changes to the fixtures are carried out by additional printing of new fixtures or if it is modular, printing only those modules that are being changed. A wide range of materials that are used today in Additive Manufacturing has led to it finding a place in almost all industries and areas of human society. Standard ISO 17296 provides basic terminology, materials, test methods and data format in the field of Additive Manufacturing.

The tools and fixtures made by FDM technology take a significant place in large systems. Paper [5] gives an overview of the most frequently applied materials in FDM technology and their applications with basic characteristics. Because of its good mechanical properties, acrylonitrile butadiene styrene (ABS) material is the most used in the field automotive, aerospace and medical-device. According to [6], tools and fixtures made by FDM technology make significant savings in money and time. In the case of BMW, manufacturing fixture from ABS plastic, a reduction in the weight of fixture by 1.3 kg was achieved, compared to the same fixture made by conventional methods. Mass reduction significantly affects the efficiency of the workers who use the fixtures many times in the shift. Significant savings in the manufacturing of fixture are also realized in the fact that it is not necessary to produce technical documentation, but the 3D model can be directly converted into a file suitable for making on a 3D printer.

[7] gives an overview of the results of the effect of setting the parameters of the 3D printing on the mechanical characteristics of the part printed from ABS plastic, while [8] shows the influence of layering and wire laying on the mechanical characteristics of the ABS plastic specimen.

3. DESIGN AND PRINTING OF FIXTURE

3.1 Description of the problem of construction and technology of fixture manufacturing

Disc support with discs of the stubble cultivator, which is analyzed in this paper, is given in Figure 1. The role of discs is that the soil is smashed and prevents the outflow of the soil outside from the workplace.

Figure 2 shows a subassembly of the disk support which is obtained by welding certain parts. The subassembly consists of a vertical plate (1) for which the plates for disc hub (2) are welded. The main problem with welding plates for disc hub is their placement into the correct position at a certain spatial

angle, which is difficult to achieve without use of fixture. If it is known that the position of the discs affects the quality of the operation of the machine, it was necessary to construct and manufacture the fixture for placement and welding, as shown below.

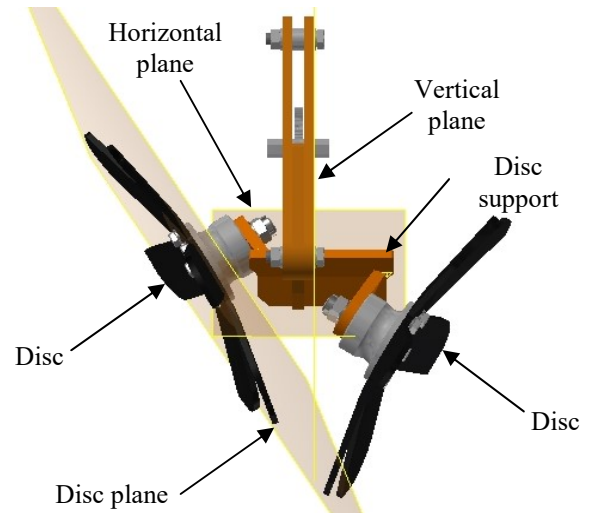


Fig. 1. Disc support with discs

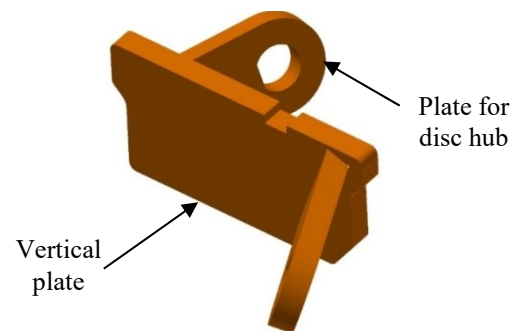


Fig. 2. Subassembly of disc support 1- (vertical plate), 2- (plate for disk hub)

3.2 3D modelling and setting of 3D printing of fixture

The basic construction condition is to satisfy the required angles of 20° that the plane of the disc builds with the horizontal and vertical plane, Figure 1. The components of the disc support are made of steel sheet. The shape of these parts is made so that it is suitable for assembling, and the requirements for quality and accuracy of parts manufacture are not large and it can be realized on a laser plasma or cutting machine. In this way, the manufactured parts can be mounted without finishing, thus reducing the time and cost of production.

In order for the manufacture fixture by 3D printing, it is necessary to create its 3D model. The development of the 3D model of fixture starts with subtracting the subassembly of the disk support from the initial shape of the square and in this way remains a negative, Figure 3. After that, the excess material is removed and gets the final shape of the fixture. During 3D printing there is a slight shrinkage of the material, so it is necessary to increase the dimensions of the holes and grooves in order to get the desired dimensions after printing. The

fixture consists of two parts that are assembled using a groove and provided with a shaft through the tool holes, Figure 4.

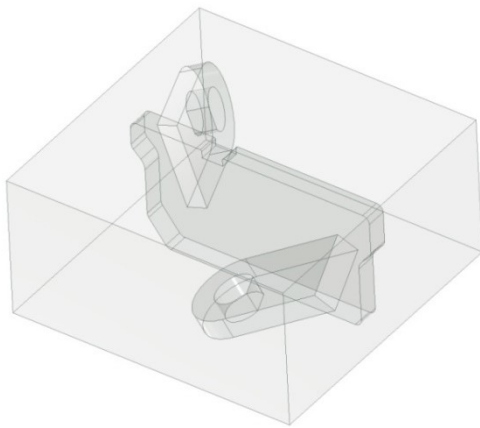


Fig.3. Initial shape of fixture

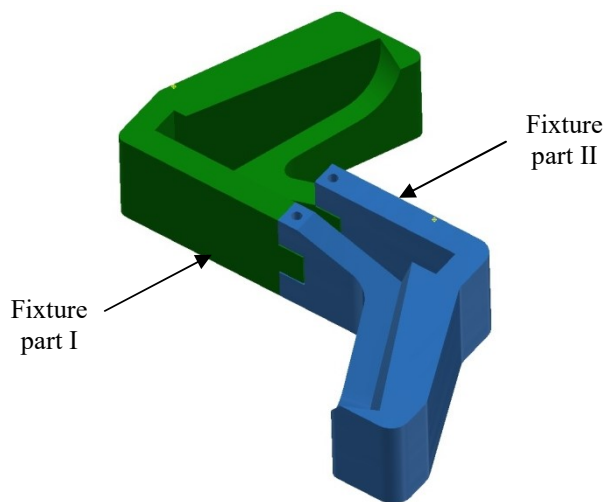


Fig.4. Fixtures for welding of disc support

In order to obtain a quality product, it is necessary to make good preparation and adjustment of parameters of the 3D printing process. The originally 3D model is converted into STL (Stereo-lithographic) format in order to be suitable for further processing in the appropriate software. The model in the STL format consists of a mesh of triangular planes and represents an approximation of the 3D model. Correctly adjusted mesh density allow satisfactory print quality. The STL file that is being prepared for printing is imported into the Makerbot Desktop software. There are a number of settings that affect the result of the printed fixture, which are displayed on Figure 5. and 6.

First, the layer height is set, that is, how the model will be sliced in the Z axis. For the part that should be done precisely, the height of the layer is from 0.1 to 0.2 mm. In our case, high precision is not required, so the height of the layer is 0.4 mm. By reducing the height of the layers it significantly affects the increase in the printing time and vice versa.

The next setting to be implemented is the infill. If the infill is 100%, the part will be made entirely of plastic. If the percentage of infill is lower, then the software will, depending on the settings, define the way to infill of part volume, e.g. hexagonal, linear, etc. In this case, a percentage of infill of 10% is sufficient and

a hexagonal fill is selected, which significantly affects the reduction in the amount of material used and the time of the printing. In addition, the number of shells must be set. The most common in use are 2, 3 or 4 number of shells. In this case 6 shells are adopted in order to improve the rigidity and durability of the fixture. By increasing the number of shells, a larger thickness of the outer shell of the fixture is obtained, and in this way the surfaces in contact with the parts are more durable and the fixture is able to withstand a higher number of use cycles.

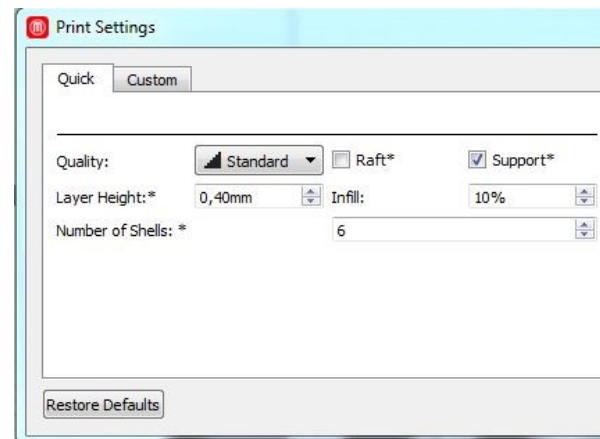


Fig. 5. Print settings part I

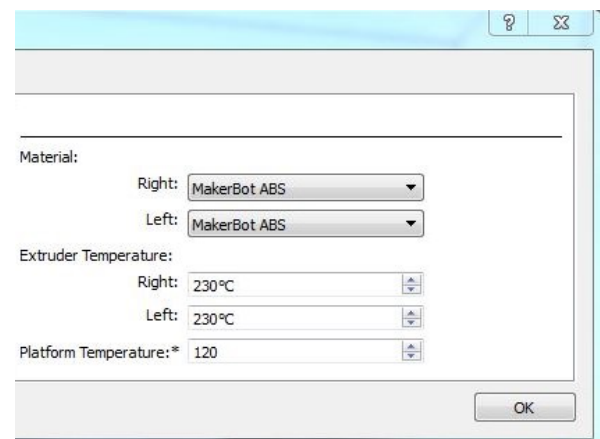


Fig. 6. Print settings part II

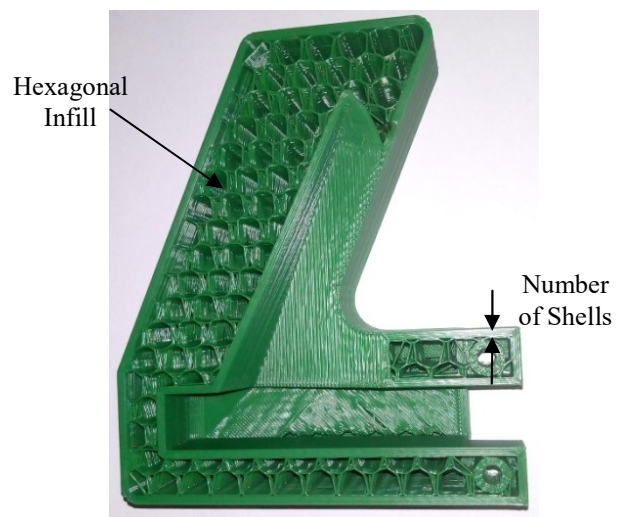


Fig. 7. Cross section of fuxture

By adjusting the parameters of the 3D printing in this way the fast manufacturing fixture is obtained. Amount of used material is minimal, and the surfaces in contact with the parts are robust and durable. The hexagonal infill allows a significant reduction in the weight of the fixtures, while providing sufficient rigidity and dimensional stability of the fixture. A cross section of the fixture is given in Figure 7. The fixture analyzed in this paper is printed from ABS plastic because it has better mechanical properties, especially at higher temperature, compared to PLA plastic. Figure 8 shows the fixture and parts of the disc support in the welding position.

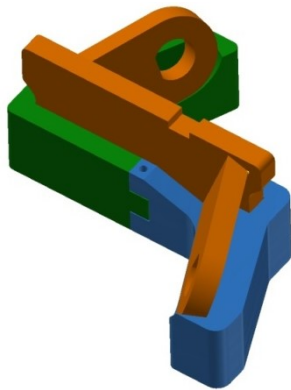


Fig. 8. Fixture and parts before welding

4. RESULTS

The result of the work is simultaneously designed and printed fixture (Figure 9) which can be immediately exploited. Changes that may be necessary may be done by changing the 3D model and then printing a new fixture or part of it. Technical documentation is not necessary, which affects the reduction of the cost of manufacturing the fixture. The material for manufacturing is very cheap today, and the entire fixture has a weight of only 300 g, which significantly reduces the costs in individual and small-sized production. The only drawback of this method of production is the printing time that is about 9 hours for these two-component fixture.

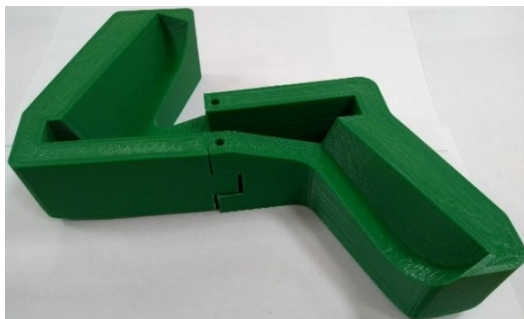


Fig. 9. Printed fixture

5. CONCLUSION

Today, tools and fixtures can be made with different manufacturing methods, among which AM technologies are increasingly in use. This way of manufacturing opens the possibility of creating new shapes and purposes of tools and fixtures that were not

possible or difficult to produce by conventional manufacturing processes, and in addition they have high production costs. Further research directions may be aimed at analyzing other structural and technoeconomic characteristics of fixtures, such as the accuracy of assembling assemblies, determining the durability of fixtures, etc.

6. REFERENCES

- [1] Tarr, M., The DFX concept, URL: http://www.ami.ac.uk/courses/topics/0248_dfx/index.html.
- [2] Eysers D., Potter A.: *Industrial Additive Manufacturing: A manufacturing systems perspective*, Computers in Industry, 92-93, pp. 208-218, 2017.
- [3] Levy G., Schindel R., Kruth P.: *Rapid Manufacturing and Rapid Tooling with Layer Manufacturing (LM) Technologies, State of the Art and Future Perspectives*, CIRP Annals Manufacturing Technology, 52, pp 483-695, 2003.
- [4] Mitrovic R., Miskovic Z.: *Investigation on Influence of 3D Printing Direction on Mechanical Properties of ABS Plastic Prototypes*, COMETA 3rd International Scientific Conference: Conference on Mechanical Engineering Technologies and Applications, pp. 293-300, Jahorina, B&H, Faculty of Mechanical Engineering in East Sarajevo, Jahorina, Dec. 7 – 9. 2016.
- [5] Jian-Yuan L., Jia A., and Chee Kai C.: *Fundamentals and applications of 3D printing for novel materials*, Applied Materials Today, 7, pp. 121-132, 2017.
- [6] Stratasys, *Direct Digital Manufacturing at BMW, Manufacturing Jigs and Fixtures with FDM*, http://www.stratasys.com/~media/CaseStudies/Automotive/CS_FDM_AU_BMW_EN_0916.pdf?la=en, (accessed on March 2018)
- [7] Cantrell J., Rohde S., Damiani D.: *Experimental characterization of the mechanical properties of 3D-printed ABS and polycarbonate parts*, Rapid Prototyping Journal, 23, pp. 811-824, 2017.
- [8] Cole D., Riddick J., Jaim I., Strawhecker K., Zander E.: *Interfacial mechanical behavior of 3D printed ABS*, Applied Polymer Science, 133, 2016.

Authors: M.Sc. Ivan Knezevic, Assoc. Prof. Savo Bojic, Assoc. Prof. Dejan Lukic, Assist. Prof. Milan Rackov, Assist. Prof. MajaCavic, M.Sc. Marko Pencic, M.Sc. Sabole Cako, University of Novi Sad, Faculty of Technical Sciences, Trg Dositeja Obradovica 6, 21000 Novi Sad, Serbia.

E-mail: ivanknezevic@uns.ac.rs; bojicsavo@uns.ac.rs; lukicd@uns.ac.rs; racmil@uns.ac.rs; scomaja@uns.ac.rs; mpencic@uns.ac.rs; szabolcsako@uns.ac.rs

ACKNOWLEDGMENTS:

This paper is a result of the TR35036 project. The project is titled "Application of information technologies in the ports of Serbia - from the monitoring of machines to the networked system with the EU environment".

Matin, I., Vukelic, D., Hadzistevic, M., Strbac, B., Santosi, Z., Lukic, D.

AN INTEGRATED DESIGN APPROACH FOR PLASTIC PART DEVELOPMENT

Abstract: *The objective of this paper is to present an integrated design approach for plastic part development. Reverse engineering (RE), re-engineering (ReE) and mold design systems have been incorporated to infuse agile characteristics in the proposed design and development process. Integration of RE and ReE presented in this paper reduced lead times for development of plastic cover.*

Key words: *Reverse engineering, Re-engineering, mold design*

1. INTRODUCTION

Reverse engineering (RE) is a kind of engineering, which takes advantage of an already created object. The reconstruction of digital geometric models of physical objects, usually indicated as RE in the CAD field, has been extensively studied in recent years, due to the development and spreading of 3D scanning technologies and the increase in number of potential applications [1-9]. RE in fact, exploit 3D data acquired on the physical object and describing its surfaces as starting point for the reconstruction framework [2,3,10-11]. Paulic et al. [1] and Brajlili et al. [12] presented method for data acquisition from the object. This RE method is very popular in industry. It consists of getting the virtual 3D CAD model of an existing object with the help of developed software. The virtual model has to be obtained with optical scanner. In addition, with different software the authors could repair the mesh, orientate it and define the position of the mesh. Due to the complex form of the part, the authors presented general procedure for solid part creation using SolidWorks software. Mostly, RE requires design modification in order to enhance product performance by improving material properties and optimize the part geometry. Many researches have contributed to the re-engineering (ReE) area demonstrating its usefulness to leverage the product design and development process. Chang et al. [13,14] proposed an integrated test bed approach for development of aging systems and components. The authors performed topology combined with boundary smoothing and geometry reconstruction operations in order to improve material characteristics in the product design process. Garcia et al. [15] examined a FEM analyses together with algorithms for shape design to minimize stress and weight of designed parts. The other authors have used CAD and CAE to correct the design. The created CAD model is then modified further to get an optimal product design. This process is defined as systematic evaluation of a product with the purpose of replication, which involves either direct copies when no design and manufacturing documentation exists, or improvement of an existing design. In addition, RE subject area has been widely recognized as being a substantial step in

the product development process. Other applications of RE include recovery of damaged or broken part, design of a new component and inspection of a simulation model [3,10,11,16].

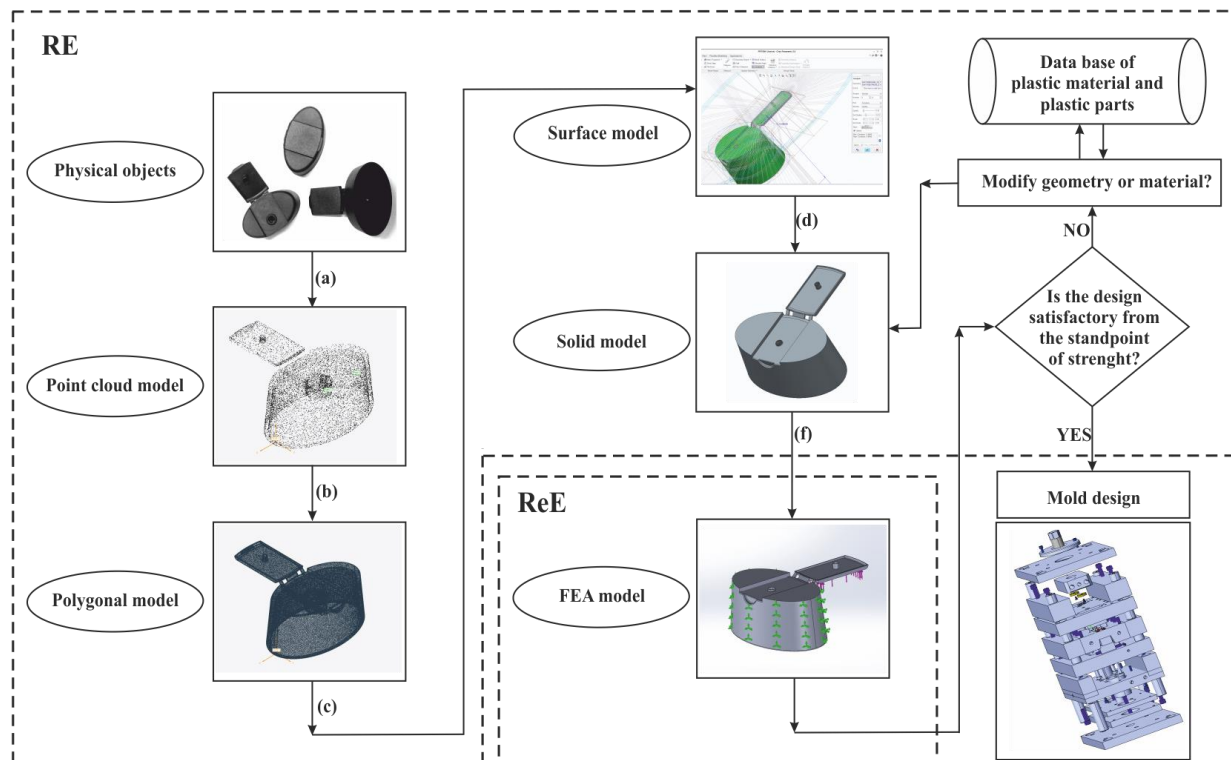
Many research studies are indicating that by integrating RE, ReE and rapid manufacture principles in the contemporary product design process, companies can achieve high rate in manufacturing [3-6, 9-22]. Having this in mind, it can be concluded that it is essential to build integrated design for revised plastic parts. The segment of this approach is to combine RE, ReE and moldesign options for model reconstruction using PTC Creo Parametric and Pro/Mechanica software. The purpose is to create new object geometrically similar to the existing object. The new object must have better mechanical properties. The next segment is to prepare correct CAD/CAE model of the reconstructed part that is necessary for mold design and injection molding. The RE workflow involves the sequential development of discrete model for data acquisition, data capture, data editing and data fitting phases. These include physical object, point cloud model, mesh model, surface model, and digitized parametric CAD model. The ReE workflow also involves development of a discrete model to detect high stressed regions.

2. METHODOLOGY

The physical object selected for demonstration of the proposed RE and ReE workflow is forced for retrieval from design and manufacturing process. In addition, the damaged part geometry needs to be recovered in order to improve the part functionality and to overcome the design flaws in the existing design. Physical object, which is used in this study, is a broken shower gel cover, where some of its mechanical properties do not meet acceptable values. The compact class 3D scanner ATOS converts the physical object into point cloud using triple scan method. The ATOS systems return full-field data about deviations between the actual 3D coordinates and the CAD data. As this measuring data contains the information, in addition to the surface deviations from the CAD, the software also derives detailed information such as geometric

dimensions and tolerances and, trimming or hole positions. The accuracy of optical measuring systems is based on state-of-the-art optoelectronics, precise image processing and algorithms, ensured by precision

standards and an automated calibration procedure. Integrated design flow for plastic part development is indicated in Fig.1.



Notes: (a) Data acquisition; (b) wrap and merge point cloud; (c) patch design; (d) solidify process using automatic option; (f) mesh digitized parametric CAD model

Fig.1. Integrated design flow for plastic part development

After scanning, data acquisition, surface modeling and conventional solid modeling, object was ready for meshing using Finite element method (FEM) in Pro/Mechanica software. Studying or analyzing a phenomenon with FEM is referred to as a finite element analysis (FEA). Authors modified some geometry specification and changed plastic material of the model, and then made satisfactory ReE design of the model ready for injection molding process simulation and mold design. RE and ReE activities are data acquisition, point cloud creation, model reconstruction and patch design, solidify procedure using automatic options and stress simulation (Fig.1). The FEM model can be directly imported into injection molding simulation software such as Pro/Plastic Advisor, MoldFlow or Moldex 3D without loss of the semantics and topological information inherent in feature-based or mesh representations. Injection molding parameters such as flow length, location of gate, mold temperature, melt temperature, injection pressure, maximal injection molding machine pressure determinate using injection molding simulation in Pro/Plastic Advisor. PTC Creo is used for core and cavity desing and final mold design. Cross section of the designed mold assembly is indicated in Fig.2.

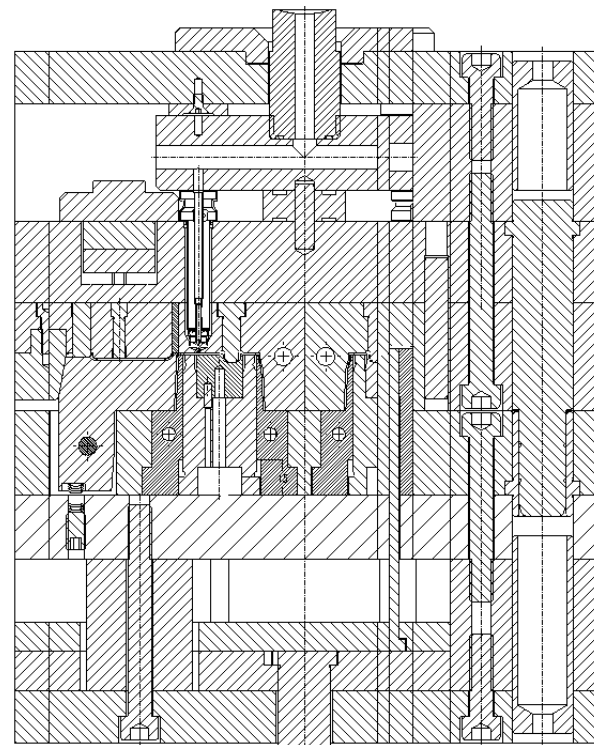


Fig. 2. Cross section of the mold

CAD model of the designed final mold assembly for injection molding of the shower gel cover is indicated in Fig.3.

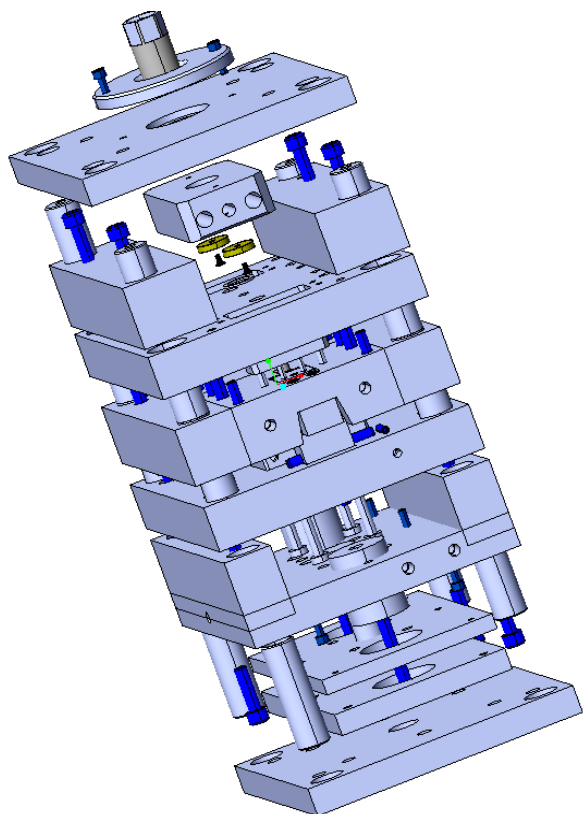


Fig. 3. 3D model of the final mold assembly

3. CONCLUSIONS

The methodology indicates that complete RE and ReE works have satisfactory performance, which can improve quality of a part. The objective of this research was to develop and manufacture a correct part with acceptable material and geometry. The described working modeling process is feature-based, object-oriented and parametric. An integration of RE, ReE and mold design tools display a good affinity in achieving agile characteristics in the contemporary product design and development process of shower gel cover. RE and CAD systems were instrumental in the development of parametric CAD model, which was then carried iteratively to testing in a CAE environment for simulation of stress regions in order to enhance geometrical modification.

Future research is currently being pursued in the area of ReE for further mechanical properties optimization in order to reduce the weight of part. Finally, through this research study, agility in manufacturing was achieved by integration of RE, ReE tools and techniques for mold and part product development. Future improvements may include the CAD inspection of the part using GOM Inspect software. Finally, other scanning procedures, such as close range photogrammetry method with application specialized software for image processing are also a field of potential interest.

ACKNOWLEDGMENTS: Results of the investigation presented in this paper are a part of the research realized in the framework of the project “Research and Development of Modeling Methods and Approaches in the Manufacturing of Dental Recoveries with the Application of Modern Technologies and Computer Aided Systems“, TR-035020, financed by the Ministry of Education and Science of the Republic of Serbia.

4. REFERENCES

- [1] Paulic, M., Irgolic, T., Balic, J., Cus, F., Cupar, A., Brajliah, T., Drstvensek, I.: *Reverse Engineering of Parts with Optical Scanning and Additive Manufacturing*, 24th DAAAM International Symposium on Intelligent Manufacturing and Automation, Procedia Engineering, Vol. 69, pp. 795-803, 2014.
- [2] Matin, I., Hadzisteivić, M., Hodolic, J., Vukelic, D., Markovic, D., Potran, M., Puskar, T.: *Reconstruction of the dental CAD model*, Proceeding of 11th International scientific conference on flexible technologies - MMA, pp. 501-504, Novi Sad, 20-21 September 2012.
- [3] Fahraz, A., Chowdary, B.V., Gonzales, L.: *An integrated design approach for rapid product development: A case study through application of reverse engineering, re-engineering and fast prototyping tools*, Journal of Engineering, Design and Technology, Vol. 11, Issue: 2, pp. 178-189, 2013.
- [4] Buonomici, F., Carfagni, M., Furferi, R., Governi, L., Lapini, A., Volpe, F.: *Reverse engineering of mechanical parts: A template-based approach*, Journal of Computational Design and Engineering, Vol. 5, pp. 145-159, 2018.
- [5] Solaberrieta, E., Minguez, R., Barrenetxea, L., Sierra, E., Etxaniz, O.: *Computer-aided dental prostheses construction using reverse engineering*, Computer Methods in Biomechanics and Biomedical Engineering, Vol. 17, pp. 1335-1346, 2014.
- [6] Varady, T., Martin, R., Cox, J.: *Reverse engineering of geometric models - an introduction*. Computer-Aided Design, Vol. 29, pp. 255-268, 2007.
- [7] Voicu, A., Gheorghe, I.G., Badita, L.L., Cirstoiu, A.: *3D Measuring of complex automotive parts by multiple laser scanning*, Applied Mechanics and Materials, Vol. 371, pp. 519-523, 2013.
- [8] Wang, J., Gu, D., Gao, Z., Yu, Z., Tan, C., Zhou, L.: *Feature-based solid model reconstruction*, Journal of Computing and Information Science in Engineering, Vol. 13, pp. 211-223, 2013.
- [9] Wang, J., Gu, D., Yu, Z., Tan, C., Zhou, L.: *A framework for 3D model reconstruction in reverse engineering*, Computers and Industrial Engineering, Vol. 63, pp. 1189-1200, 2012.
- [10] Chowdary, B.V., De Noon, A., Ali, F., Imbert, C.: *An investigation for improvement of the 3D-digitization process: a reverse engineering*

- approach*, Journal of Manufacturing Technology Management, Vol. 22, Issue: 1, pp. 131-147, 2011.
- [11] Afeez, A., Sanjay., Kumar, A.: *Application of CAD and reverse engineering methodology for development of complex assemblies*, Journal of Engineering Design and Technology, Vol. 11, Issue: 3, pp. 375-390, 2013.
- [12] Brajlili, T., Tasic, T., Drstvensek I., Valentan B., Pogacar, V., Balic, J., Acko, B.: *Possibilities of using three-dimensional optical scanning in complex geometrical inspection*, Strojniski vestnik - Journal of Mechanical Engineering, Vol. 57, pp. 826-833, 2011.
- [13] Chang, K.H., Chen, C.: *3D shape engineering and design parameterization*, Computer-Aided Design and Applications, Vol. 8, pp. 681-692, 2011.
- [14] Chang, K.H., Siddique, Z., Edke, M. and Chen, Z.: *An integrated testbed for reverse engineering of aging systems and components*, Computer-Aided Design and Applications, Vol. 3, pp. 21-30, 2006.
- [15] Garcia, M.J., Boulanger, P., Henau, M.: *Structural optimization of as-built parts using reverse engineering and evolution strategies*, Structural and Multidisciplinary Optimization, Vol. 35, pp. 541-550, 2008.
- [16] Chintala, G., Gudimetla, P.: *Optimum material evaluation for gas turbine blade using Reverse Engineering (RE) and FEA*, Procedia Engineering, Vol. 97, pp. 1332-1340, 2014.
- [17] Beniere, R., Subsol, G., Gesquiere, G., Le Breton, F., Puech, W.: *A comprehensive process of reverse engineering from 3D meshes to CAD models*, Computer-Aided Design, Vol. 45, pp. 1382-1393, 2015.
- [18] Li, L., Li, C., Tang, Y., Du, Y.: *An integrated approach of reverse engineering aided remanufacturing process for worn components*, Robotics and Computer-Integrated Manufacturing, Vol. 48, pp. 39-50, 2017.
- [19] Ferreira, J.C., Alves, N.F.: *Integration of reverse engineering and rapid tooling in foundry technology*, Journal of Materials Processing Technology, Vol. 142, pp. 374-382, 2003.
- [20] Geren, N., Akcali, O.O., Bayramoglu, M.: *Parametric design of automotive ball joint based on variable design methodology using knowledge and feature-based computer assisted 3D modelling*, Engineering Applications of Artificial Intelligence, Vol. 66, pp. 87-103, 2017.
- [21] Seno, T., Ohtake, Y., Kikuchi, Y., Saito, N., Suzuki, H., Nagai, Y.: *3D scanning based mold correction for planar and cylindrical parts in aluminum die casting*, Journal of Computational Design and Engineering, Vol. 2, pp. 96-104, 2015.
- [22] Zhou, J., Li, J., Hu, Y., Yang, J., Cheng, K.: *Plastic mold design of top-cover of out-shell of mouse based on CAE*, Advanced in Control Engineering and Information Science, Procedia Engineering, Vol. 15, pp. 4441-4445, 2011.

Authors: Dr Ivan Matin, Dr Djordje Vukelic, Dr Miodrag Hadzistevic, Dr Branko Strbac, M.Sc. Zeljko Santosi, Dr Dejan Lukic, University of Novi Sad, Faculty of Technical Sciences, Department of Production Engineering, Trg Dositeja Obradovica 6, 21000 Novi Sad, Serbia, Phone.: +381 21 4850-2332, Fax: +381 21 454-495.
E-mail: matini@uns.ac.rs
vukelic@uns.ac.rs
miodrags@uns.ac.rs
strbacb@uns.ac.rs
zeljkos@uns.ac.rs
lukicd@uns.ac.rs

Palic, N., Sharma, V., Zivic, F., Mitrovic, S., Grujovic, N.

TRIBOLOGY STUDY OF ALUMINUM-BASED FOAM

Abstract: *Closed cell metallic foam prepared from ALUHAB technology has been studied using tribological methodology. The main goal of the study was tribological properties of closed cell porous structure made of aluminium alloy. Tribological testing of the porous Al-based alloy were realised under different low loads: 10 mN, 25 mN, 50 mN, 75 mN, and 100 mN using CSM nanotribometer, with linear reciprocating mode. Ball-on-disc contact geometry was used and dynamic friction coefficient was observed. Results revealed that, friction coefficient exhibited large fluctuations in values under different loads, from moderate friction coefficient (0.2 at 100 mN load) up to the very high values (1.4 at 25 mN load). Under very small loads (10 mN) it was hard to get reliable results due to porosity influence and extremely high friction coefficient values were obtained.*

Key words: *Porous structures, Closed – cell Al-based foam, Dynamic Friction coefficient*

1. INTRODUCTION

Wear is generally defined as damage to a solid surface which involves loss of material due to relative motion between two surfaces in contact [1]. This motion can be both intentional and unintentional. The frictional force is defined as a tangential force experienced by the resisting interface which is associated with rolling or sliding motion. The nature of relative motion between the bodies and physical mechanism by which material is removed or displaced, categorizes wear into different types such as two body, three body, abrasive or adhesive wear. Quantification of wear is done in terms of volume, mass of material removed or change in linear dimension. Amount of wear is also assessed in terms of wear rate which is defined as rate of material removed per unit of time. According to Archard model of wear quantification constant “K” has important role in determining severity of wear process wherein higher values of K are associated with severe abrasions between surfaces in contact. These values of K find their importance for practical engineering purposes in tribological design [2]. There are some steps which are taken into considerations as described below.

Selection of wear and friction tests. In order to ensure good tribological performance friction and wear testing is done at various stages of the lifecycle of a product.

Selection of approach for testing. Various approaches have been implemented by researchers to assess wear and friction which primarily depends on scale and complexity of elements that are being tested. During the final stage of product abstraction usually, cost-effective laboratory testing is done for better understanding of tribological systems. There are two main situations during which laboratory testing is applied: firstly, when the product is in development stage and is to be selected for the general field of application; Secondly, when a specific application is required which need defined conditions for tribological contact. The selection of parameters is of prime importance for generation of a valid test which can help tribological evaluation of process parameters.

Test parameters. Control parameters and conditions of tribological contact influence wear and friction coefficient. These parameters refer to normal speed, sliding speed, materials of triboelements, temperature [5], contact geometry and environment [3-4], which can be defined by using specific control methods or using same test systems for the whole program.

Interaction with other degradation mechanisms. Chemical reactions and fatigue can also contribute to wear rate. Triboelements exposed to the aqueous environment can experience a positive or negative synergy which increases or reduces wear rate respectively. Similarly, temperature [4] and other stresses such as rolling contact fatigue can also influence degradation mechanism.

Experimental planning and presentation of results. Planning of the tribological testing includes definition of controlling mechanical test conditions and sample parameters. Mapping techniques can also be used where two or more factors are changed in a controlled way and results are plotted as individual points or contours. This mapping technique is an efficient way of determining overall behaviour which provides detailed knowledge of wear and friction.

Tribological testing parameters for standard metallic materials are rather well defined, as well as approach to testing under macro loads. However, porous structures which have emerged during the last years imposed certain problems in tribological investigations. The major issue is to provide continuous contact between the surfaces in relative motion where one of the surfaces exhibit porosity, meaning discontinued contact during tribological tests within the zones of the pores. There are some ways to overcome this problem, but in general, more study is needed.

In general, metallic foams have wide range of applications in the aerospace, automotive, and biomedical industries. A large number of researches have performed studies on deformation, fracture, plasticity, dynamic response and energy absorption of cellular foams experimentally and numerically [6]. Open cell aluminium foam has been used for heat transfer enhancement at cryogenic temperature. Such aluminium foam was tested for cryogenic energy storage with a phase change of nitrogen [7]. The properties of Al-based foam are closely related to its pore structure, including pore size, pore distribution and porosity levels [8]. The kinetics of aluminium reaction is manipulated to increase the porosity of geopolymers without adding extra foaming agent, and the impact on porosity development and the characteristics of binding skeleton has been investigated. It is shown that by adjusting the ratio of alkali activators, the oxidation rate of aluminium powder can be regulated, which further impacts the extent of foaming [9].

In this paper, porous aluminium (Al) based alloys have been investigated in relation to application of new structural forms such as open or semi-closed cell foams in different areas, due to their properties such as light weight and ductility. Al-based foams have practical applications as structural materials in many fields (automotive industries, heat transfer systems, anti-vibration systems, and construction industries). Al-based alloys exhibit good corrosion resistance, due to formation of protective layer which prevents further oxidation. However, there are still different issues related to the influence of porous structure, variable temperature, and corrosive environment effects, especially on

tribological and mechanical behaviour. Porous structures have significant influence on mechanical properties and further on its tribocorrosive behaviour, in comparison to solid materials. Tribological behaviour of Al-based foams has not been largely investigated. Determination of the wear mechanisms and its development, and friction coefficient behaviour will indicate further improvement in design of these advanced materials. With this aim, this paper investigated tribological properties of closed cell porous structure made of aluminium.

2. MATERIAL AND METHODS

Material used during the testing was closed cell porous structure, as shown in Fig. 1. It was prepared from base material aluminium, with proprietary ALUHAB technology used for the generation and preparation of closed cell porous structure and properties are shown in Table 1. This technology was applied due to its flexibility in terms of uniform, controlled pore size distribution and pore thickness. Minimum cell size that can be achieved using this method was 1 mm.

Density	0.6g/cm ³
Cell size	0.5-5.0 mm
Pore size	1.0 mm.
Average cell size	1.0 mm.

Table 1. Physical specifications of ALUHAB based closed cell pore

Tribological testing of the porous Al foam were realised under different low loads: 10 mN, 25 mN, 50 mN, 75 mN, 100 mN. The tests were performed at CSM nanotribometer, with linear reciprocating mode. Purpose of using linear motion is due to its real-world mechanism. It enables calculation of the friction coefficient during the forward and backward movement.



Fig. 1. Front view of the closed cell metallic foam with aluminum as a based material prepared by using ALUHAB Technology

Ball-on-disc contact geometry was used, whereas alumina ball was in sliding contact with Al-based foam and dynamic friction coefficient was observed, as shown in Fig. 2. Tribology tests for sliding contact are distinctly categorized into two distinct types depending on the extent of relative movement.

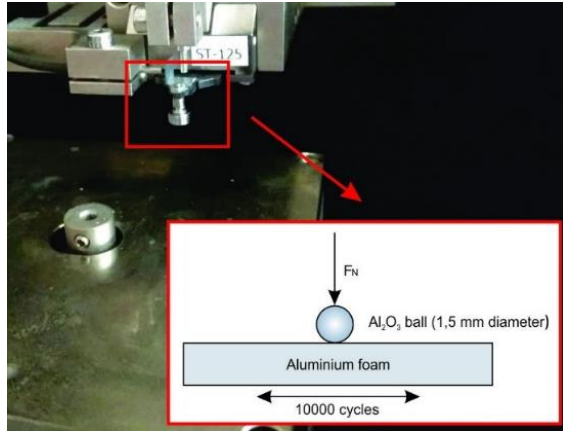


Fig. 2. Represent principle of the nanotribometer, including the module (ball on disc)

In the first case, relative movement is sufficiently large (typically greater than $300\mu\text{m}$) so that all contact points on at least one of the bodies are out of contact for some of the test period. Contrastingly, the second is a case of fretting, where at least part of the contact area on both samples is always in contact. Ball-on-disc and reciprocating geometries are the most often used tribological test geometries since many applications involve reciprocating motion.

3. EXPERIMENTAL PROCEDURES

Porous samples of Al-based alloys were prepared by cutting them from the originally prepared Al-based foam for structural applications. Afterwards the samples were cleaned thoroughly by the flow of dry air. Then the samples were positioned within the two-component epoxy, in order to provide appropriate flat surface for the nanotribological contact. Adequate positioning was important to enable stability of the contact force during the sliding. Table 2. shows the conditions employed during the testing.

Acquisition	Linear Mode
1/2 amplitude	0.25 mm
Max linear speed	2.00 mm/s
Number of cycles	10000 cycles
Acquisition rate	20.0 Hz

Table 2. Tribological Test set up conditions used during the testing.

4. RESULTS AND DISCUSSION

For friction force measurement, most common methods employed are force transducers which are further connected to elastic elements that can sense deflection when force is applied [1].

Frictional coefficients have been identified to be of two types. First is the static friction coefficient which represents friction opposing onset of relative motion. The second type is the kinetic friction coefficient which represents the friction opposing the continuance of relative motion once that motion has started.

Our results showed that porous structure influenced large fluctuations of the friction coefficient. Friction coefficient exhibited large fluctuations in values at different loads, from moderate friction coefficient (0.2 at 100 mN load) up to the very high values (1.4 at 25 mN load). Under very small loads (10 mN) it was hard to get repeatability due to porosity influence and the friction coefficient values in this domain needs further studies since in some repeated tests, under this lowest load extremely high friction coefficient values were obtained.

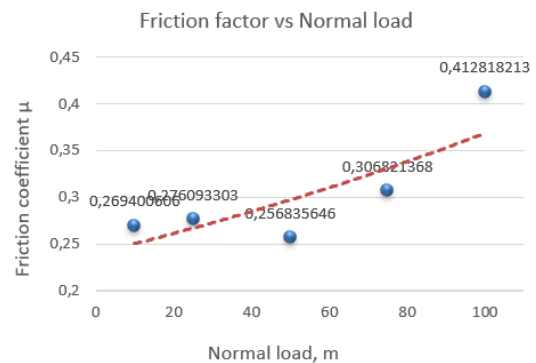


Fig. 3. Friction coefficient versus Normal load during the different loading conditions

It can be concluded from Fig. 3, as the normal force of the ball on the surface of the sample increases, the friction coefficient increases. In an area where the normal force approaches 100mN, a large increase in the friction coefficient was observed. This is caused by the high roughness of the aluminium foam surface.

Figure 4. shows penetration depth versus sliding distance during the different loading conditions. Based on Fig. 4., it can be concluded that with the increase in normal force, penetration depth started to increase. However, it can be noticed that in the case of load of 75mN, penetration depth is less than for a 50mN load. This phenomenon probably occurred due to the inhomogeneity of the surface of the porous material.

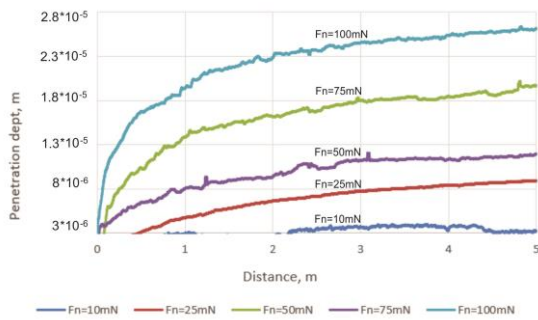


Fig. 5. Penetration depth versus distance during the different loading conditions

This variation in the results is due to the influence of the structure geometry and differences in contact imposed by the differences exhibited by the porous structure properties (high change of surface roughness). Also, topological inhomogeneity has significant influence on the results.

4. CONCLUSIONS

This paper deals with the tribological study of closed-cell aluminium-based foam using nanotribo-meter. Results indicated that due to zig-zag arrangement of pores it is hard to establish the reliable setup for experiments, especially under very low loads. Different low loads were applied, (10 mN, 25 mN, 50 mN, 75 mN, 100 mN) and rather large fluctuations of the dynamic friction coefficient were exhibited.

Porosity (size and shape of voids, as well as their distribution) greatly influenced the results due to introduction of non-uniform surface properties, from both aspects of contact area and roughness changes over the surface. Topological inhomogeneity caused deviation in results. Further testing of contact conditions and influences, are needed especially for very low loads (below 10 mN).

5. REFERENCES

- [1] Standard G40: *Standard terminology relating to wear and erosion* American Society for Testing and Materials (ASTM International, West Conshohocken 2005)
- [2] M. B. Peterson, W. O. Winer (Eds.): *Glossary of terms and definitions in the field of friction, wear and lubrication*, Tribology, republished in: *Wear Control Handbook* (Am. Soc. Mechanical Engineers, New York, 1980) pp. 1143–1303
- [3] M. Hutchings: *Tribology: Friction and Wear of Engineering Materials*, Arnold, London 1992
- [4] M. J. Neale, M. G. Gee: *Guide to Wear Problems and Testing for Industry* (William Andrew, Norwich 2001)
- [5] V. V. Dunaevsky: *Friction temperatures*, Tribology Data Handbook, ed. by E. R. Booser (CRC, Boca Raton 1997) pp. 462–473
- [6] Y. Hua, Q. Fanga, B. Shab, M. Zhaoc: *Effect of the large cells on the fatigue properties of closed-cell aluminum alloy foam*, Composite Structures, 200 (2018) 59–68
- [7] K. Chunhui, C. Liubiao, W. Xianlin, Z. Yuan, W. Junjie: *Thermal Conductivity of Open Cell Aluminum Foam and Its Application as Advanced Thermal Storage Unit at Low Temperature*, Rare Metal Materials and Engineering, Volume 47, Issue 4, April 2018, Online English edition of the Chinese language journal
- [8] Y. Ma, X. Yang, C. He, K. Yang, J. Xu, J. Sha, C. Shi, J. Li, N. Zhao, *Fabrication of insitu grown carbon nanotubes reinforced aluminum alloy matrix composite foams based on powder metallurgy method*, Materials Letters (2018)
- [9] A. Hajimohammadi, T. Ng, P. Mendis, J. Sanjayan: *Regulating the chemical foaming reaction to control the porosity of geopolymer foams*, Materials and Design, 120 (2017) 255–265

Authors: Nikola Palic, Varun Sharma, Fatima Zivic, Slobodan Mitrovic, Nenad Grujovic, University of Kragujevac, Faculty of Engineering, Kragujevac, Sestre Janjic 6, 34000 Kragujevac, Serbia

Phone.: +381 34 335 990

E-mail: nikpa2112@gmail.com;
varun.eu@gmail.com; zivic@kg.ac.rs;
boban@kg.ac.rs; gruja@kg.ac.rs

ACKNOWLEDGMENTS: This work has been supported by the research grant SELECTA H2020-MSCA-ITN-2014 No. 642642 and Ministry of Science and Technological Development, Serbia, projects no. III41017 and no. TR35021.

Santosi, Z., Sokac, M., Tadic, B., Budak, I., Simunovic, G., Ilic Micunovic, M., Vukelic, D.

EVALUATION OF KINETIC FRICTION COEFFICIENT FOR WOODEN SPECIMENS

Abstract: The paper presents research results of the kinetic friction coefficient on the specimens fabricated from different wood types – ash and walnut. The measurements of the kinetic friction coefficient were performed for different values of the rpm and normal load on a specially designed tribometer. The kinetic friction coefficient of the ash samples has higher values for smaller normal load values and higher speed, and vice versa. In the case of walnut samples, the kinetic friction coefficient has a higher value for higher normal loads, while increasing the speed. The obtained results for both types of samples indicate that the values of the kinetic friction coefficient are very close. The paper ends with appropriate conclusions and directions of future research.

Key words: kinetic friction, friction coefficient, wood

1. INTRODUCTION

Friction is a very complex phenomenon arising at the contact of surfaces. Experiments indicate a functional dependence upon a large variety of parameters, including sliding speed, acceleration, critical sliding distance, temperature, normal load, humidity, surface preparation, material combination, etc. [1]. Friction can be quantified through friction coefficient. Two types of friction coefficients can be distinguished: one that represents the friction opposing the onset of relative motion (impending motion), and one that represents the friction opposing the continuance of relative motion once that motion has started. The former is called the static friction coefficient (μ_s), and the latter, the kinetic friction coefficient (μ_k). In the case of solid-on-solid friction (with or without lubricants), these two types of friction coefficients are conventionally defined as follows [2]:

$$\mu_s = F_s / F_n \quad (1)$$

$$\mu_k = F_k / F_n \quad (2)$$

where F_s is the force just sufficient to prevent the relative motion between two bodies, F_k is the force needed to maintain relative motion between two bodies, and F_n is the force normal to the interface between the sliding bodies.

In previous years a large number of researches have been performed in the field of quantification, modelling and measurement of friction parameters. Fujii (2008) developed a method for measuring the coefficient of friction between sliding solid. In the proposed method, both frictional and normal forces were measured as inertial forces acting on masses [3]. Al-Bender and De Moerloose [4] dedicated to the investigation of the relation between the normal load and the friction force in the pre-sliding regime up to gross sliding. A Maxwell–Slip model strategy was supplied with model parameters, determined by an existing physics-based model. The coefficient of friction was little affected by the elasticity, the hardness and the distribution of the asperity heights, but decreases with increasing normal

load, surface roughness and plasticity index. Hwang and Zum Gahra [5] studied the frictional behaviour both static and sliding friction under unlubricated or oil lubricated conditions. Coefficient of static friction and transition from static to kinetic friction was determined. Results showed a significant effect of surface finish on both the static and kinetic coefficients of friction as well as on the transition behaviour, which was strongly dependent on the materials mated. Sedlacek et al. [6] investigated the influence of surface preparation on roughness parameters and correlation between roughness parameters and friction. Dry and lubricated pin-on-disc tests were carried out using different contact conditions. Coefficient of friction was monitored as a function of time and wear of contact surface determined after the test by means of topography analysis. Cho and Bhushan [7] (2016, TI) investigated friction of various polymer pairs used for labels and wipers in labelling machines. Friction tests were carried with various parameters such as load, speed, and existence of varnish coating. Effects of load and speed were elucidated from frictional heating and formation of tribofilm. Persson et al. discussed the nature of the static and kinetic frictions [8]. An analytical model that differs from the classical block-on-belt one is presented by Tang et al., and the influence of the difference between the static and the kinetic ones on the occurrence of stick–slip vibration and the performance of the drilling equipment is investigated [9]. Tribological tests were conducted on different pairs of the bearing steel and a commercial alumina. The self-mated steel pairs showed greater values of kinetic than static coefficient of friction while no significant difference of both friction values was measured on self-mated alumina pairs with ground plate specimens [10]. Also researchers are focussed on investigation of friction coefficient on different types of polymer [11,12], rubber [13] and composites [14]. Xie et al. [15] investigated the effects of surface roughness on the kinetic friction between SiC nanowires and SiN substrates by use of experimental testing and numerical modelling. Roy et al. [16] presented measurements of the kinetic friction between ZnO nanowires and

substrate by using the optical nanomanipulation technique. The collisional friction between particles and solid boundaries was investigated based on the kinetic theory for granular flows and analyses show that the collisional friction is significantly affected by the shear of bounded granular flows [17]. The simulations of the kinetic friction due to a layer of adsorbed molecules between two crystalline surfaces are presented in [18]. The kinetic friction and stiction properties of the dilute solution of palmitic acid (PA, friction modifier additive) in poly (α -olefin) (PAO) confined between molecularly smooth mica surfaces were investigated using the surface forces apparatus (SFA). The SFA results for smooth surfaces obtained here seem inconsistent with the observations in macroscopic tribology [19]. Cho et al. [20] explored effects of various speed, load, and dwell time conditions on static and kinetic friction of polymeric materials. Static and kinetic friction exhibits dependence on surface roughness which affects mechanical interaction of asperities and real contact area.

Unlike in the previous literature, the aim of this research is to define the kinetic friction coefficient from two wooden samples, and those are ash and walnut.

2. METHODOLOGY

For the purposes of this research, the measurement of the kinetic friction coefficient on wooden specimens under the "block on cylinder" system was observed. This can be observed in correlation with the standard ASTM test method [21] when testing the kinetic friction coefficient for metals. In Fig. 1, the theoretical experimental setup is presented.

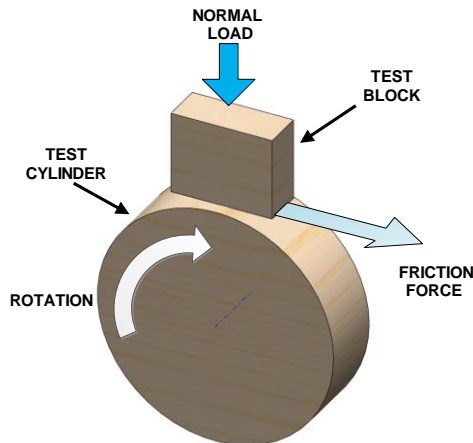


Fig. 1. "Block on cylinder" test used for wooden specimens

The kinetic friction coefficient was determined on a specially designed tribometer (Fig. 2). Tribomechanical characteristics of the tested samples from different materials and in different working conditions, with or without the use of lubricants for the lubrication, can be performed on this tribometer. It also serves for the research of finishing processes that work on basis of constant penetration force of tools into the workpiece.



Fig. 2. Specially designed tribometer for evaluation of kinetic friction coefficient

The physical and measuring range of the normal load for the friction coefficient measurement ranges from 0 to 140 N. The measurement range of the friction force ranges from 0 to 100 N, and the measurement error is less than 1%. The normal contact load is achieved through weights. Weights are positioned on a rod which at the same time represents the contact carrier. On the rod, a sleeve with a damping element made of fibroflex is placed on the short side, which is in contact with the friction force sensor during measurement. The measuring system of the device consists of signal conditioning devices, tensometric sensors of normal load and friction force, as well as corresponding structural elements on which these sensors are located. The measuring system and tribometer have the appropriate software support that enables recording of measurement results and presentation of measurement results in the form of appropriate diagrams and histograms.

Wood specimens were previously prepared and processed. The cylinders are made with dimensions $\varnothing 35 \pm 0.2 \times 30$ mm with a clamping attachment of $\varnothing 25 \times 25$ mm, and the dimensions of the block are $15 \times 12 \times 6$ mm (Fig. 3). A cylindrical wooden sample is placed inside the clamping head of the tribometer, while a block is placed in the weight carrier. To determine the kinetic friction coefficient, it is necessary to achieve the desired speed, then load the cylinder through the contact carrier pair with the corresponding normal force.

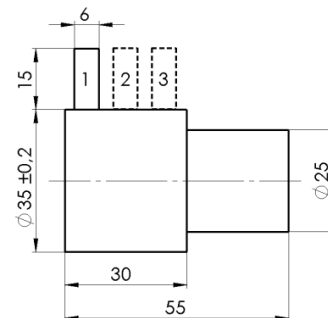


Fig. 3. Dimensions of specimens used in experiment

The reading of the friction coefficient was performed after the normal load sensor constantly recorded the given normal force. According to the experiment plan, the speed and normal load values were varied. Each new regime setting and the measurement of the kinetic friction coefficient required the use of a new block made out of the same type of wood and a test site on the cylinder. The cylinder size allows three measurements to be made (Fig. 3).

3. RESULTS

Experimental research was conducted for two types of wood, ash and walnut. These two types of wood have similar mechanical properties (Table 1).

Properties	Ash	Walnut
Hardness HB (N/mm ²)	74	70
Elastic Modulus E (GPa)	13.4	12.5
Bending strength Rms (N/mm ²)	122	137
Crushing Strength (N/mm ²)	58	72
Tensile strength Rm (N/mm ²)	165	167

Table 1. Mechanical properties of wooden specimens

Prior to performing experimental research, the mean arithmetic roughness for samples was measured on 10 different sites. The obtained values are shown in Table 2. The results of kinetic friction coefficient for different values of normal loads and different values of the speed of wooden samples are shown in Figs. 4 and 5.

Surface roughness	Ash	Walnut
Ra ₁ (μm)	4.56	4.46
Ra ₂ (μm)	4.66	4.52
Ra ₃ (μm)	4.64	4.54
Ra ₄ (μm)	4.32	4.61
Ra ₅ (μm)	4.44	4.49
Ra ₆ (μm)	4.56	4.54
Ra ₇ (μm)	4.44	4.48
Ra ₈ (μm)	4.53	3.62
Ra ₉ (μm)	4.54	4.52
Ra ₁₀ (μm)	4.57	4.69
Ra _{mean} (μm)	4.53	4.45

Table 2. Mean arithmetic value of roughness of specimens

By analysing Figs. 4 and 5 it can be concluded that the values of the kinetic friction coefficient do not have a pronounced trend of growth or decrease for both types of wood. For the ash specimen with lower values of normal loads, the kinetic friction coefficient increases with the increase of the speed. For higher values of normal load, with increasing speed, the kinetic friction coefficient decreases.

When it comes to walnut specimens for smaller values of normal loads, the kinetic friction coefficient first decreases and then grows with the increased speed. For higher values of normal load, with increasing speed, the kinetic friction coefficient first grows and then decreases.

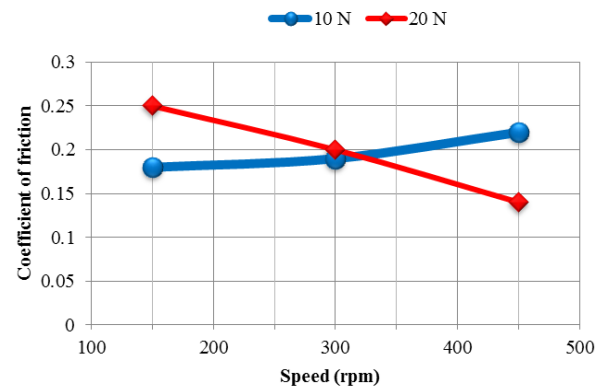


Fig. 4. Dependence of kinetic friction coefficient of normal load and speed for ash specimens

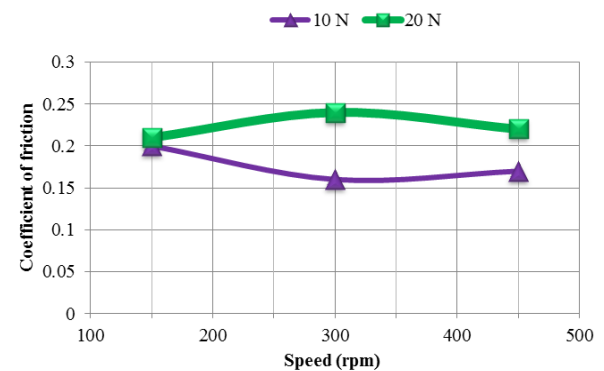


Fig. 5. Dependence of kinetic friction coefficient of normal load and speed for walnut specimens

4. CONCLUSION

For the defined values of the normal load of 10 and 20 N, as well as for the speed values of 150, 300 and 450 rpm, the values of the kinetic friction coefficient range within the following limits:

- for ash samples
 - and lower normal loads 0.18 - 0.22,
 - and higher normal loads 0.14 - 0.25,
- for walnut samples
 - and lower normal loads 0.16 - 0.2
 - and higher normal loads 0.21 - 0.24

The kinetic friction coefficient of the ash samples has higher values for smaller normal load values and higher speed, and vice versa. In the case of walnut samples, the kinetic friction coefficient has a higher value for higher normal loads, while increasing speed.

A comparative analysis of the obtained results for both types of samples indicates that the values of the kinetic friction coefficient are very close. The dispersion of the obtained results of the kinetic friction coefficient is due to the large variability of the wood properties. Namely, wood is a natural material whose characteristics are very different in the same species, even within the same individual, i.e., tree. Wood is a material that has unique and independent properties in the direction of the longitudinal, radial and tangential axes. Non-homogeneity, anisotropy and hygroscopicity are characteristics of each type of wood. Prepared samples for performing experimental research are

characterized by non-homogeneity of structure, anisotropy and the presence of various defects. Porosity, microwaves, leakiness, fiber defects, the content of chemical elements, deformation of wood due to shrinkage and swelling are just some of the factors that influence the results obtained. Also, the size, shape and arrangement of fibers, tubes and pores are not identical in the structure of the samples.

Future research will focus on determining the friction coefficient on a wider range of samples that are made of different types of wood, with different mechanical and physical properties, under different normal load, and at different speeds.

5. REERENCES

- [1] Berger, E.J.: *Friction modeling for dynamic system simulation*, Applied Mechanics Reviews, Vol. 55, pp. 535-577, 2002.
- [2] Blau, J.P.: *The significance and use of the friction coefficient*, Tribology International, Vol. 34, pp. 585-91, 2001.
- [3] Fujii Y.: *Method for measuring transient friction coefficients for rubber wiper blades on glass surface*, Tribology International, Vol. 41, pp. 17-23, 2008.
- [4] Al-Bender, F., De Moerlooze, K.: *On the relationship between normal load and friction force in pre-sliding frictional contacts. Part 1: Theoretical analysis*, Wear, Vol. 269, pp. 174-182, 2010.
- [5] Hwang, H.D., Zum Gahra, H.K.: *Transition from static to kinetic friction of unlubricated or oil lubricated steel/steel, steel/ceramic and ceramic/ceramic pairs*, Wear, Vol. 255, pp. 365-375, 2003.
- [6] Sedlacek, M., Podgornik, B., Vizintin, J.: *Influence of surface preparation on roughness parameters, friction and wear*, Wear, Vol. 266, pp. 482-487, 2009.
- [7] Cho, D.H., Bhushan, B.: *Friction and wear of various polymer pairs used for label and wiper in labeling machine*, Tribology International, Vol. 98, pp. 10-19, 2016.
- [8] Persson, B.N.J., Albohr, O., Mancosu, F., Peveri, V., Samoilov, V.N., Sivebaek, I.M.: *On the nature of the static friction, kinetic friction and creep*, Wear, Vol. 254, pp. 835-851, 2003.
- [9] Tang, L., Zhu, X., Arab, J.: *Effects of the Difference Between the Static and the Kinetic Friction Coefficients on a Drill String Vibration Linear Approach*, Arabian Journal for Science and Engineering, Vol. 40, pp. 3723-3729, 2015.
- [10] Hwang, D.-H., Zum Gahr, K.H.: *Transition from static to kinetic friction of unlubricated or oil lubricated steel/steel, steel/ceramic and ceramic/ceramic pairs*, Wear, Vol. 255, pp. 365-375, 2003.
- [11] Haugstad, G.: *Contrasting static-to-kinetic friction transitions on layers of an autophobically dewetted polymer film using Fourier-analyzed shear modulation force microscopy*, Tribology Letters, Vol. 19, pp. 49-57, 2005.
- [12] Momozono, S., Akeuchi, H., Iguchi, Y., Nakamura, K., Kyogoku, K.: *Dissipation characteristics of adhesive kinetic friction on amorphous polymer surfaces*, Tribology International, Vol. 48, pp. 122-127, 2012.
- [13] Ke, Y., Yao, X., Yang, H., Liu, X.: *Kinetic friction characterizations of the tubular rubber seals*, Tribology International, Vol. 72, pp. 35-41, 2014.
- [14] Li, H., Yin, Z., Jiang, D., Jin, L., Cao, Q., Qu, Y.: *A Study of the Static/Kinetic Friction Behavior of PTFE-Based Fabric Composites*, Tribology Transactions, Vol. 61, pp. 122-132, 2018.
- [15] Xie, H., Wang, S., Huang, H.: *Effects of Surface Roughness on the Kinetic Friction of SiC Nanowires on SiN Substrates*, Tribology Letters, Vol. 66, pp. 1-9, 2018.
- [16] Roy, A., Xie, H., Wang, S., Huang, H.: *The kinetic friction of ZnO nanowires on amorphous SiO₂ and SiN substrates*, Applied Surface Science, Vol. 389, pp. 797-801, 2016.
- [17] Zhang, L., Zhong, D., Sun, Q., Wu, B.: *A kinetic description of collisional frictions between particles and solid boundary in simple sheared granular flows*, Powder Technology, Vol. 276, pp. 204-213, 2015.
- [18] He, G., Robbins, M.O.: *Simulations of the kinetic friction due to adsorbed surface layers*, Tribology Letters, Vol. 10, pp. 7-14, 2001.
- [19] Yamada, S., Inomata, K.A., Kobayashi, E. Tanabe, T., Kurihara, K.: *Effect of a Fatty Acid Additive on the Kinetic Friction and Stiction of Confined Liquid Lubricants*, Tribology Letters, Vol. 64, pp. 1-11, 2016.
- [20] Cho, D.H., Bhushan, B., Dyess, J.: *Mechanisms of static and kinetic friction of polypropylene, polyethylene terephthalate, and high-density polyethylene pairs during sliding*, Tribology International, Vol. 94, pp. 165-175, 2016.
- [21] ASTM G77-17: *Standard Test Method for Ranking Resistance of Materials to Sliding Wear Using Block-on-Ring Wear Test*, ASTM International, 2017.

Authors:

M.Sc. Zeljko Santosi, M.Sc. Mario Sokac, Dr.Sc. Igor Budak, M.Sc. Milana Ilic Micunovic, Dr.Sc. Djordje Vukelic, University of Novi Sad, Faculty of Technical Sciences, Trg Dositeja Obradovica 6, 21000 Novi Sad, Serbia.
E-mail: zeljkos@uns.ac.rs; marios@uns.ac.rs, budaki@uns.ac.rs; milanai@uns.ac.rs, vukelic@uns.ac.rs

Dr.Sc. Branko Tadic, University of Kragujevac, Faculty of Engineering, Sestre Janjic 6, 34000 Kragujevac, Serbia.
E-mail: btadic@kg.ac.rs

Dr.Sc. Goran Simunovic, Josip Juraj Strossmayer University of Osijek, Mechanical Engineering Faculty, Trg Ivane Brlic Mazuranic 2, 35000, Slavonski Brod, Croatia.
E-mail: goran.simunovic@sfsb.hr

Strbac, B., Bisevac, S., Delic, M., Klobucar, R., Acko, B., Hadzistevic, M.

COMPETENCE ASSESSMENT OF CMMs FOR DIFFERENT MEASURING TASKS

Abstract: In order to check the competence of measurement laboratories, there is a need for laboratories to participate in interlaboratory comparisons. Competence of a laboratory is expressed through En number which compares measurement results and measurement uncertainty of the examined laboratory with measurement results and measurement uncertainty of the reference laboratory. In this research, the design of experiments (DoE) was used for the assessment of measurement uncertainty. Two characteristics of a ring gauge were measured using a coordinate measuring machine (CMM) - diameter and roundness. Experimental investigations were carried out in the Laboratory for Metrology in Novi Sad and the Laboratory for Dimensional Metrology in Maribor, which is the holder of the national standard of the Republic of Slovenia.

Key words: interlaboratory comparison, measurement uncertainty, DoE, CMM.

1. INTRODUCTION

Systemic solutions which are acceptable to quality management and the possibility of their certification in compliance with a series of ISO 9000 standards means that numerous metrological laboratories have to face measurement uncertainty, calibration, and metrological traceability. For that purpose, a large number of recommendations and metrological standards are needed. In the field of dimensional metrology coordinate measuring machines (CMMs) have a leading role in verification operations. All macro tolerances stated in the standard of the geometrical product specifications (GPS) can be inspected using CMMs. To guarantee the adequacy of inspection, measurement results have to be validated through a rigorous system of traceability. Every measurement result obtained by means of a CMM has to be stated along with measurement uncertainty, with the aim of providing a satisfactory basis for deciding about compliance with the specification. However, due to the complexity of CMMs and the widespread use of these in different measurements, traceability maintenance and the assessment of measurement uncertainty are quite complicated. Results obtained by means of a CMM can be documented by participating in interlaboratory comparison. In order to assess the performance of different metrological laboratories, from national metrological institutes to market-oriented laboratories, a metrological tool – interlaboratory comparison is used. Interlaboratory comparisons are also very important in proving the quality of measurement when measurement uncertainty is hard to determine [1, 2]. According to ISO/IEC 17043:2010, interlaboratory comparison includes organization, conduction and evaluation of measurements or tests on the same or similar objects performed by two or more laboratories or inspection institutes in accordance with previously defined conditions [3]. In this paper, experimental investigations were carried out according to a defined design of experiments in two metrological

laboratories by means of CMMs. Measurement results enabled conducting a study of interlaboratory comparison.

2. THEORETICAL FRAMEWORK AND SUBJECT OF RESEARCH

In order to determine the effectiveness of participants in interlaboratory comparison, measurement data are taken from all the participants and assessed by means of the agreed upon statistical approach. Unique measured values reported by participants are compared with the agreed upon reference value, taking into account the reported measurement uncertainties and the uncertainty of the reference value. En number represents the factor of agreement between results and is calculated with the aim of assessing the compatibility of measurement results of laboratories taking part in the comparison with the reference result. En number is used in comparisons in which participating laboratories report measurement uncertainty in accordance with the Guide to the expression of uncertainty in measurement (GUM). When uncertainty is assessed in accordance with GUM, En number expresses the validity of the assessment of expanded uncertainty which accompanies every measurement result. The condition $|En| < 1$ shows that measurements conducted in the examined laboratory are compatible with the reference laboratory, i.e. the more the value of En approaches zero, the higher the compatibility of the result. En number is calculated using the expression (1):

$$En = \frac{x_{lab} - x_{ref}}{\sqrt{U_{lab}^2 - U_{ref}^2}} \quad (1)$$

x_{lab} – measurement result of participating laboratory, x_{ref} – measurement result of reference laboratory, U_{lab} – expanded uncertainty of participating laboratory, U_{ref} – expanded uncertainty of reference laboratory.

It is clear from the expression (1) that it is necessary to determine the expanded uncertainty of CMM

measurements in order to perform successful interlaboratory comparison. In assessing measurement uncertainty of CMM measurements, various factors affecting measurement uncertainty need to be considered. Factors affecting measurement uncertainty can be classified into five categories: CMM hardware, work environment, workpiece, sampling strategy and evaluation strategy. It is not possible to include all influential factors in the assessment of measurement uncertainty in the currently used assessment methods [4]. The Guide to the expression of uncertainty in measurement (GUM) can be used although it is limited to a great extent. Over the past two decades a lot of effort has been made in the field of assessing measurement uncertainty in CMMs. What is more, every measuring task has a different measurement uncertainty with the same CMM. Therefore, the concept of “task specific uncertainty” has been introduced into literature. The result of continuous research in this field over many years is the introduction of standard methods within ISO 15530:2008, implying the use of calibrated workpieces - ISO 15530 - 3 and computer simulation ISO 15530 - 4. The use of the design of experiments (DoE) makes it possible to include a number of factors and determine the effect of every factor and their interactions on measurement uncertainty [5, 6]. By means of repeated measurements, standard deviation is expressed for each observation, representing the basis for expressing measurement uncertainty which is calculated using the expression (2) [7]:

$$U = k \times \sqrt{u_{cal}^2 + u_{proc}^2 + u_{AT}^2} \quad (2)$$

U – expanded measurement uncertainty, k – coverage factor, u_{cal} – standard calibration uncertainty of the measured object, u_{proc} – standard uncertainty of measurement procedure, u_{AT} – standard uncertainty of the effect of temperature.

2.1 Design of experiments

The design of experiments is used in numerous applications to help understand a certain process or variable. In order to include the most influential factors which affect measurement uncertainty in measuring the characteristics of holes by means of CMMs, the following factors and their corresponding levels were considered (Table 1).

Factor	Level				Code
Position of workpiece on CMM table	1	2	3	4	A
Alignment	CMM		Workpiece		B
Stylus tip diameter	5mm		15mm		C
Sampling size	15		150		D

Table1. Analyzed factors and levels

The factor “position of workpiece on CMM table” includes the effect of hardware errors on measurement uncertainty: random and systematic errors of the probe and geometric errors of the CMM. This factor is present on four levels, i.e. the workpiece was positioned in the corners of the table (Fig.1). The

“alignment” factor considers the assessment of the workpiece features if the coordinate system for the sampled points is positioned in a different way. This way evaluation strategy was taken into account. Fig. 1 also shows that on the first level of this factor, coordinates of points are expressed using the machine coordinate system (MCS), whereas on the second level the coordinates of points are expressed using the coordinate system of the workpiece (PCS). The factor “stylus tip diameter” introduces mechanical filtration for sampling deviations from the workpiece. This factor is particularly important when measuring roundness because it filters out the effect of roughness and waviness on the form error (Fig.2). The factor “sampling size” refers to the number of points which describe real geometry (Fig. 3). Interacting with form deviation of a workpiece and the applied evaluation algorithm, it can affect the measurement result to a great extent (measurement uncertainty) when assessing form deviation [8].

3. EXPERIMENTAL INVESTIGATIONS

With the aim of making interlaboratory comparisons, a ring gauge with the diameter of $D=60\text{mm}$ was measured according to the previously described design of experiments in the Laboratory for Metrology, Novi Sad (CMM Carl Zeiss Contura g2 RDS, $MPE_E=1.9+L/330\text{ }\mu\text{m}$) and in the Laboratory for Dimensional Metrology, Maribor (CMM Carl Zeiss UMS 850, $MPE_E=2.1+L/300\text{ }\mu\text{m}$). Two features of the ring gauge were analyzed: diameter and roundness. Each observation had five replicates so that the total number of experiments in one laboratory was 160. The experiment was completely randomized. As the Laboratory for Dimensional Metrology is the holder of the national standard in Slovenia, reference values for the diameter, roundness were determined in this laboratory, as well as the values of standard uncertainty of calibration of the measured object u_{cal} . Measurements were taken in temperature controlled laboratories.

3.1 Results of the experiments and uncertainty assessment

Statistical analysis of the measured results was performed using Minitab 17 software. Based on the variance analysis (ANOVA) with the significance level of $\alpha=0.05$, it was determined which factors and factor interactions were significant for the diameter and roundness of the ring gauge in the experiments conducted in the two laboratories (Table 2). Additionally, Table 2 presents the levels of factors where the deviation of values of the observed characteristics from the reference value is the smallest and the largest. Standard deviation is used as a measure of measurement uncertainty (type A uncertainty) and is calculated for each combination of factors based on five replicates. The combinations of factors with the smallest and the largest standard deviation for the observed characteristics are given in Table 3. It can be seen in Table 3 that the values of standard deviations vary enormously with different values of levels of factors.

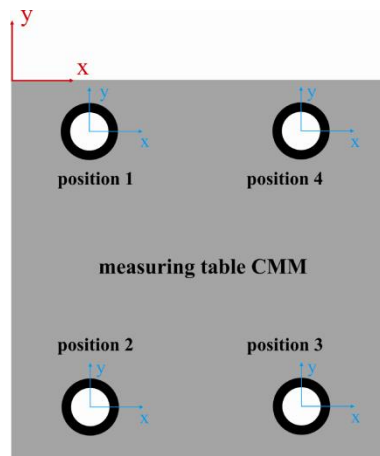


Fig. 1. Factors „position workpiece on CMM table“ and „alignment“ and their levels

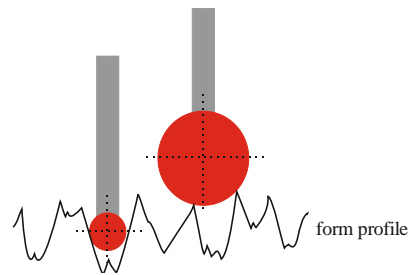


Fig. 2. Factor „stylus tip diameter“

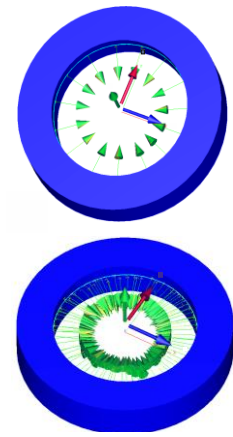


Fig. 3. Factor „sampling size“

	Diameter_Maribor		Roundness_Maribor		Diameter_Novi Sad		Roundness_Novi Sad	
Statistically significant parameters	A, C, D, A*B, A*C, A*D, A*B*C, A*C*D		A, D, A*D,		A, C, D, A*B, A*C, A*D, B*C,		A, C, D, A*C, A*D, B*D, C*D, A*B*C, A*C*D	
Levels of factors with smallest deviation from reference value	Variable	Setting	Variable	Setting	Variable	Setting	Variable	Setting
	A	4	A	3	A	1	A	3
	B	Workpiece	B	Workpiece	B	Workpiece	B	CMM
	C	5	C	5	C	15	C	15
Levels of factors with greatest deviation from reference value	D	15	D	15	D	15	D	15
	Variable	Setting	Variable	Setting	Variable	Setting	Variable	Setting
	A	3	A	1	A	1	A	1
	B	Workpiece	B	Workpiece	B	CMM	B	CMM
	C	5	C	5	C	5	C	5
	D	150	D	150	D	15	D	15

Table 2. Significance of factors and levels of factors with largest and smallest deviation

Characteristic	Standard deviation	Levels of factors			
		A	B	C	D
Dia_Maribor	max=0.9094μm	4	CMM	5	150
	min=0.0002 μm	2	Workpiece	5	150
Round_Maribor	max=0.6955μm	4	CMM	5	150
	min=0.0102	3	CMM	15	150
Dia_Novi Sad	max=0.5273μm	3	CMM	5	150
	min=0.001 μm	1	CMM	5	15
Round_Novi Sad	max=3.668μm	2	Workpiece	5	15
	min=0.0001 μm	4	Workpiece	15	150

Table 3. Combinations of factors with the smallest and the largest standard deviation for the observed characteristics

Comparing the levels of factors from Table 2 and Table 3, it can be concluded that the levels of factors which give the smallest deviation from the reference value (measurement error) are not the same levels which show the smallest standard deviation as a measure of measurement uncertainty. Likewise, the considered factors are not on the same level if we observe the smallest measurement error or the smallest standard deviation for different characteristics, such as diameter and roundness in this case. This confirms that the assessment of measurement uncertainty in coordinate measuring is very complex and that every measuring task has different measurement uncertainty which is the result of a number of factors all of which cannot be analyzed. Expanded measurement uncertainty is calculated using the expression (2), whereas the

standard uncertainty of measurement procedure is calculated using the expression (3):

$$u_{proc} = \sqrt{\frac{MPE_E^2}{a} + u_{rep}^2}, \quad (3)$$

where MPE_E/a is the maximum permissible error with the applied adequate distribution function (e.g. rectangular) and u_{rep} denotes reproducibility of measurement obtained through repeated measurements. As presented in Table 3, the value of u_{rep} varies from the smallest to the greatest value. However, it was the average value of all standard deviations for all experiments that was taken to calculate the expanded measurement uncertainty U . The values of the expanded uncertainties are presented in Table 4.

	Expanded uncertainty U [μm]
Dia_Maribor	0,272
Round_Maribor	0,263
Dia_Novi Sad	0,351
Round_Novi Sad	0,989

Table 4. Values of expanded uncertainties

4. INTERLABORATORY COMPARISON

Compatibility of the participating laboratory with the reference laboratory was determined using the expression (1) and the results were the following:

$$E_{n(Dia)} = \frac{x_{lab} - x_{ref}}{\sqrt{U_{lab}^2 - U_{ref}^2}} = \frac{60,0017 - 60,0012}{\sqrt{0,000351^2 - 0,000272^2}} = 2.25$$

$$E_{n(Round)} = \frac{x_{lab} - x_{ref}}{\sqrt{U_{lab}^2 - U_{ref}^2}} = \frac{0,002072 - 0,001372}{\sqrt{0,00098^2 - 0,000263^2}} = 0.74$$

The results show that the examined laboratory is compatible in the case of measuring roundness, whereas it is incompatible in the case of measuring diameter. This statement is somewhat surprising because the CMM in Novi Sad has a smaller specified maximum permissible error. The reason for this lies in the increase in geometric errors of the CMM in question. Likewise, measurement error and the error of the assessed measurement uncertainty for both metrological tasks were greater in Novi Sad laboratory. Fig. 4 is a graphical representation of comparison of measurement error and measurement uncertainty when measuring diameter.

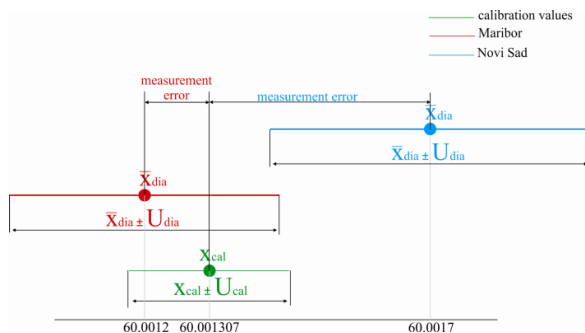


Fig. 1. Graphical representation of interlaboratory comparison

5. CONCLUSION

This paper presents interlaboratory comparison between two metrological laboratories with the aim of determining the capability of CMMs to perform different tasks of measurement and control. It was necessary to assess measurement uncertainty of a specific measuring task in order to make the comparison. The use of the design of experiments was thoroughly described. The conducted study, focusing on two characteristics of a ring gauge (diameter and roundness), showed different scenarios of the effect of factors on measurement error and measurement uncertainty, both for different characteristics and different CMMs. Future studies will incorporate temperature into the design of experiments since this

factor has a significant effect on measurement error and measurement uncertainty.

6. REFERENCES

- [1] Cox, M.G.: *The evaluation of key comparison data: determining the largest consistent subset*, Metrologia, Vol. 44(3), pp.187–200, 2007.
- [2] Acko, B., Brezovnik, S., Crepinsek Lipus, L., Klobucar, R: *Verification of statistical calculations in interlaboratory comparisons by simulating input datasets*, International journal of Simulation Modeling, Vol. 14 (2), pp. 227-237, 2015.
- [3] ISO/IEC Guide 43-1:2008: *Proficiency testing by Interlaboratory comparison, Part 1: Development and operation of proficiency testing schemes*“ ISO/CASCO Committee on conformity assessment, 2008.
- [4] Štrbac, B., Radlovački, V., Spasić – Jokić, V., Delić, M. Hadžistević, M.: *The difference between GUM and ISO/TC 15530-3 method to evaluate the measurement uncertainty of flatness by a CMM*, Journal of Metrology Society of India, Vol. 32(4), pp. 251-257, 2017.
- [5] Vrba, I., Palenčar, R., Hadžistević, M., Štrbac, B., Spasić – Jokić, V., Hodolič, J.: *Different Approaches in Uncertainty Evaluation for Measurement of Complex Surfaces Using Coordinate Measuring Machine*, Measurement Science Review, Vol. 15(3), pp. 111-118, 2015.
- [6] Feng, C.-X.J., Saal, A.L., Salsbury, J.G., Ness, A.R., Lin, G.C.S.: *Design and analysis of experiments in CMM measurement uncertainty study*, Precision Engineering, Vol. 31(2), pp. 94-101, 2007.
- [7] Barini, E.M., Tosello, G., De Chiffre, L.: *Uncertainty analysis of point-by-point sampling complex surfaces using touch probe CMMs: DOE for complex surfaces verification with CMM*, Precision Engineering, Vol. 34(1), pp. 16-21, 2010.
- [8] Hadžistević, M., Štrbac, B., Spasić Jokić, V., Delić, M. Sekulić, M., Hodolič, J.: *Fastors of estimating flatness error as a surface requirement of exploitation*, Metallurgy, Vol. 54(1), pp. 239-242, 2015.

Assist. Prof Branko Štrbac, MSc Sonja Bisevac, Full Prof. Miodrag Hadzistevic, University of Novi Sad, Faculty of Technical Sciences, Department of Production Engineering, Trg Dositeja Obradovica 6, 21000 Novi Sad, Serbia.

e-mail: strbacb@uns.ac.rs,

sonja.bisevac@hotmail.com, miodrags@uns.ac.rs.

Assist. Prof Milan Delic, University of Novi Sad, Faculty of Technical Sciences, Department of Industrial Engineering and Engineering Management, Trg Dositeja Obradovica 6, 21000 Novi Sad, Serbia.

e-mail: delic@uns.ac.rs.

Full Prof. Bojan Acko, PhD Rok Klobucar, University of Maribor, Faculty of Mechanical Engineering, Chair of Production Engineering, Smetanova ul. 17, 2000 Maribor.

E-mail: bojan.acko@um.si, rok.klobucar@um.si.

Velkoska, C., Kuzinovski, M., Tomov, M.

A REVIEW OF THE QUALITY COST STRUCTURE DEFINITION MODELS – THEORETICAL APPROACH

Abstract: The paper presents a review with an analysis of the achievements in the understanding and the various approaches to defining and categorizing the structure of the quality cost models. It explains the Cost of Quality (CoQ) concept as a comprehensive system of the organizations dedicated to continuous improvement of quality with a view of reducing the total quality costs. The paper analyzes four groups of quality cost models: Quality cost structure definition models developed by authors, models formalized in national and international standards, models officialized in documents of quality organizations and models with the so called model approach to the quality cost classification created by companies and deriving from their goals, needs and expectations.

Key words: *quality, cost of quality, quality cost models,*

1. INTRODUCTION

“Quality initiatives” represent one of the most important developments in the second half of the 20th century [1], when the continuous quality improvement principle became a crucial factor in achieving customer satisfaction and market competitiveness [2]. In an environment of invasive economic liberalization, intensive communication, and technological progress, the quality initiative refer to: development, implementation and evaluation of quality management programs [3], certification of quality management systems, promotions of quality award models (Malcolm Baldrige National Quality Award (MBNQA), European Quality Award (EFQM), Turkish National Quality Award (KALDER), etc.), application of quality management principles, quality characteristics design methods and quality assurance tools [1], in order to maximize the quality of the product and minimize the quality assurance costs [2, 4, 5].

The quality costs concept, as one of the most efficient tools for quality management programs performance evaluation [6, 7], should be embraces not only at the company level [2, 7], but also at the level of industry and the national economy as well [7]. The determination of the costs of quality using quality costs models represents an important task in the modern TQM philosophical paradigm for attainment of greater productivity [6], contributes to the benefits of the company as a response to quality related issues [8], which is especially important for the strategic corporate planning by management, also known as managerial accounting [9], with a view of building a strategy for the survival and development of the company [10].

2. QUALITY COSTS CONCEPT KNOWLEDGE

The quality costs concept still waves the scientific and the professional community with its controversy, nature, the variety of aspects and the approaches to its understanding, as well as the constructive critical overview and the debates on the significance and

usefulness of application of this concept [11]. The costs of quality are also known as “costs of non-quality”, “costs of poor quality”, “inequality costs” or “quality related costs” [11]. In the most general context, quality costs encompass all of the costs for prevention of poor quality and the costs arising from poor quality [2, 7, 12], or the difference between the actual and the ideal costs for achieving quality [13].

Criterion	Classical approach to quality costs	Modern approach to quality costs
Concept	<i>Economics of quality</i>	<i>Zero defects</i>
Standard for quality	<i>Economical quality</i>	<i>Perfect quality</i>
Nature of approach	<i>Statical</i>	<i>Dynamical</i>
Focus	<i>Reduction of quality costs</i>	<i>Continual improvement</i>
Matrix of thinking	<i>Failure mind-set</i>	<i>Prevention mind-set</i>
Behavior of total cost of quality	<i>Higher level of quality, higher costs</i>	<i>Higher level of quality, lower costs</i>
Maturity of quality	<i>Low level of quality maturity</i>	<i>High level of quality maturity</i>
Investments in costs of prevention and appraisal	<i>Unjustified</i>	<i>Justified</i>
Behavior costs of prevention and appraisal to perfectly level	<i>Asymptotic behavior towards infinity</i>	<i>Exponential behavior to finite cost</i>
Time perception	<i>Short time</i>	<i>Long time</i>
Responsibility	<i>Quality control Department</i>	<i>Corporate Department</i>

Table 1. Comparison between the classical and the modern approach to quality costs, conceptualized according to [2, 6, 7, 10, 11, 16, 17].

Generic model	Cost/Activity categories	Focus in model	Authors of publications describing the concept of quality costs, analyzing or developing cost quality models
P-A-F model	Prevention + Appraisal + Failure	Focus on activities (operations-oriented)	Juran (1951), Feigenbaum (1956), Masser (1957), Morse (1983), Merino (1988), Dawes (1989), Israilii Fisher (1991), Dale and Plunkett (1991), Sumanth and Arora (1992), Purgslove and Dale (1995), Gupta and Campbell (1995), Chang <i>et al.</i> (1996), Burgess (1996), Tatikonda and Tatikonda (1996), Bottorff (1997), Sorqvist (1997), Weheba and Elshennawy (2004), Bamford and Land (2006), Tannock and Saelem (2007), Freeman (2008), Kim and Nakhai (2008), Chopra and Garg (2011), Junior (2016), Plewa <i>et al.</i> (2016), Malk <i>et al.</i> (2016).
Crosby's model	Price of conformance + Price of non-conformance	Focus on activities (effect-oriented)	Crosby (1979), Denton and Kowalski (1988), Suminsky (1994)
Opportunity models	Prevention + Appraisal + Failure + Opportunity	Focus on opportunity costs	Modaress and Ansari (1987), Sandoval-Chavez and Beruvides (1998)
	Conformance + non-conformance + Opportunity		Carr (1992), Malchi and McGurk (2001), Ramudhin <i>et al.</i> (2008), Alzaman <i>et al.</i> (2010),
	P-A-F (failure cost includes opportunity cost)		Heagy (1991), Chiadamrong (2003)
Intangible cost models	Tangibles + Intangibles	Focus on Intangible costs	Juran <i>et al.</i> (1975), Juran (1989), Guinotet <i>et al.</i> (2016).
Process cost models	Conformance to process + Non-conformance to process	Focus on process	Ross (1977), Marsh (1989), Crossfield and Dale (1990), Goulden and Rawlins (1995), Briffaut and Saccone (2002), Sharma <i>et al.</i> (2007), Doomun and Jungum (2008), Machuca <i>et al.</i> (2009).
Taguchi loss function model	Loss of sales revenue due to poor quality + process inefficiencies + losses when a quality characteristic deviates from a target	Focus on loss function due to deviation from target	Soumaya Jacqueline (1998), Chin-C <i>et al.</i> (1998), Jia (2007), Johannes (2008), Naidu (2008).
Integrated models	P-A-F model and ABC technique	Focus on activities	Tsai (1998)
	P-A-F model, Crosby's model (opportunity) and process cost model	Focus on activities and processes	Czajkowski (2017)
ABC (Activity based costing) models - technique	Value-added + Non-value-added	Focus on process and activities (value-based)	Cooper (1988), Cooper and Kaplan (1988), Jorgenson and Enkerlin (1992), Creeseet <i>et al.</i> (1992), Cooper <i>et al.</i> (1992), Dawes and Siff (1993), Hester (1993), Park and Kim (1995), Lewis (1995), Ong (1995), Feng <i>et al.</i> (1996), Quyang and Lin (1997), Aderoba (1997), Zhang and Fuh (1998), Tsai (1998), Tseng and Jiang (2000), Tornberg <i>et al.</i> (2002), Ben-Arieh and Qian (2003), Ozbayrak <i>et al.</i> (2004), Park and Simpson (2005), H'Mida <i>et al.</i> (2006), Niazi <i>et al.</i> (2006), Chen and Wang (2007), Qian and Ben-Arieh (2008), Khataie and Bulgak (2013).

Table 2. Generic models of quality costs, conceptualized according to [2, 6, 8, 9, 10,12,13,14].

According to Dale B. and Plunkett J. (1995) the costs of quality are a sum of the “quality management system costs, the costs of all the efforts for continuous improvement, the costs of system and product failures, as well as costs of the activities that do not add value, but are seen as “essential” for achieving the required product quality” [12].

Different authors, industries and nations use different definitions of the costs of quality [14]. Some of them stick strictly to the technical aspect [11], while the definitions of Crosby (1979), Deming (1986), Drucker (1993) incorporate the “user satisfaction

principle” [13]. Nevertheless, the understanding of quality costs comprises four main aspects: quality assurance, quality standards, zero defects and the social aspect [14].

The concept of the costs of quality emerged from the scientific work of the quality costs pioneers such as J.M. Juran (1951), Feigenbaum (1956) [7, 15], Masser (1957) [11]. They divided the costs of quality into three categories: prevention costs, evaluation costs and failure costs, known in the literature as “the classical quality costs concept” [11], i.e. the PAF (Prevention, Appraisal, Failure) model [10]. This concept essentially

relies on the existence of a cost-effective quality level (economics of quality), which strikes a balance between the prevention costs and evaluation costs on one hand and the failure costs on the other [10], while the attainment of a 100% compliance is possible only with infinite total quality costs [16]. It also reflects the prevailing operational circumstances in the 20th century [7, 16]. This approach can be modified into a learning based approach [7], where the identification and the ability to correct the defects and the errors enhance the knowledge and the potential of the employees through experiences with good practices [13] which ultimately leads to the reduction of the total costs of quality under the level expected from the classical approach [7].

Authors Crosby P. (1979) [9, 13], Wildemann H. (1992), introduced the expressions “costs of compliance” and “costs of non-compliance” together with the requirements reflecting the dichotomy of the modern quality costs concept [11], also known as the zero defects concept [10] or, the more attractive expression “quality is free” [6], or as “the par value model” [16], which is representative of the end of the 20th century [7]. The modern concept promotes a trend of achieving a perfect quality level (100% compliance with the requirements) at the lowest total quality costs [16].

Table 1 shows the comparison between the classical and the modern approach to quality costs. Both approaches feature serious relevancy constraints [8, 16]. Authors Dale B. and Plunkett J., primarily emphasize that both approaches presume a perfect quality design, indicated by the reduction of the failure costs to zero in an environment of 100% compliance [16]. The latter could be expected for the internal errors, but not for the external ones [8, 16]. Secondly, both approaches feature levels of compliance where the quality costs (or the prevention costs and the appraisal costs) exceed the non-compliance costs (or the costs for internal and external failures) [8, 16], which tells management that errors are cheaper than prevention, which, on the other hand, repudiates the continuous improvement philosophy [16].

Authors Gamal S. Weheba and Ahmad K. Elshennawy (2004) propose a new approach to the understanding of the quality costs concept, focusing on the value of continuous process improvement, expressed through two cost functions [16]. One function refers to the reactive costs of sustaining a stable level of the process and the other function reflects the proactive costs for attaining an enhanced level of compliance [16].

The new trends of the 21st century shift towards a holistic approach to quality cost management and understanding, which should integrate the technical aspect, the environmental aspect and the innovation aspect [6]. The development of a robust quality costs model requires a hybrid approach based on the integration of the already proven approaches and models, as well as the complementarity (accumulation) of the benefits [13].

3. QUALITY COSTS MODELS

The analysis of the available literature suggests that many stakeholders contributed to the continuous development of the quality costs structure definition models, including:

- Author developed models, represented by seven generic models: PAF model, Crosby model, Lost opportunities model, Model of intangible costs, Process costs model, Model of the Taguchi Loss Function, Integrated model and ABC model (Table 2).

Institute for Standardization	Standard	Recommendation/ Cost of quality model/approach
British Standards Institution	BS 4891:1972 Economics of quality assurance	The optimal level of quality should correspond the lowest quality costs.
British Standards Institution	BS 6143: 1981 Guide to the Determination and Use of Quality Related Costs	Guidance on the operation of a quality costs system.
Standards Association of Australia	AS 2561-1982: Guide to the Determination and Use of Quality Costs AS 2561-2010	Determination and Use of Quality Costs - PAF model.
Indian Standards	IS: 10708-1985 Guide for analysis of quality cost	PAF model
British Standards Institution	BSI 6143-2: 1990 Guide to the economics of quality: Prevention, appraisal, failure model	PAF model
British Standards Institution	BS 4778: 1991	The cost of quality incurred by the producer, customer and community.
British Standards Institution	BSI 6143-1: 1992 Guide to the economics of quality: The process cost model	Process cost model
German Institute for Standardization - DIN	1992	Modern approach to quality costs
	DIN 55350-11:2008	PAF model
International Organization for Standardization	ISO 9004-3:1993 Quality management and quality system elements.	PAF model
	ISO 9004-1:1994 Quality management and quality system elements.	PAF model and Process cost model.

Table 3. Models formalized in national and international standards conceptualized according to [5, 6, 9, 11, 13, 14, 15, 17, 18, 19].

- Models formalized in national and international standards (Table 3):

- Models officialized in quality organization documents: the American Society of Quality ASQ (1971) [5, 14], and the Australian Organization for Quality Control (AOQC) adopted the PAF model [15], The European Organization for Quality Control (EOQC) defines quality costs as the costs of implementing and controlling the standards of quality [14], while the German Quality Association (DGO) in 1985 adopted in the classical approach and in 2000 it adopted the modern approach to quality costs [11].

- Models from the so called model approach to the classification of the costs of quality have been created by the individual companies and derive from their goals, needs and expectations [20], quality police, purpose of quality costing, history, culture, size of company, processes, products [14], and can be based on knowledge developed and promoted by some of the previous three groups of models.

4. CONCLUSION

The costs of quality can be determined only by having deep knowledge of the various approaches and models for defining the structure of the quality costs. The conducted research presented in this paper suggests that the quality costs concept represents a current concept subject to continuous development. The descriptive interpretation of the models arises from the current trends in understanding quality, quality systems, quality standards, quality initiatives, quality associations policies, as well as the needs and the requirements of the companies themselves.

5. REFERENCES

- [1] Uyar, A.: *An Empirical Investigation of the Relationship between Quality Initiatives and Financial Performance*, Eurasian Journal of Business and Economics, 1 (1), 25-36, 2008.
- [2] Schiffauerova, A., Thomson, V.: *A Review of Research on Cost of Quality Models and Best Practices*, International Journal of Quality and Reliability Management, 23 (6), 647-669, 2006.
- [3] Campanella, J.: *Principles of Quality Costs: principles, implementation and use*, third edition, 1999.
- [4] Rasamanie Murugan, Kanapathy Kanagi, *The Implementation of Cost of Quality (COQ) Reporting System in Malaysian Manufacturing Companies: Difficulties Encountered and Benefits Acquired*, International Journal of Business and Social Science Vol. 2 No. 6; April 2011.
- [5] Snieska, V., Daunoriene, A., Zekeviciene, A.: *Hidden Costs in the Evaluation of Quality Failure Costs*, Inzinerine Ekonomika - Engineering Economics, 24(3), 176-186, 2013.
- [6] Jaju, S.B., Mohanty, R.P., Lakhe, R.R.: *Towards managing quality cost: A case study*, Total Quality Management, 20 (10), 1075-1094, 2009.
- [7] Omurgonulsen, M.: *A research on the measurement of quality costs in the Turkish food manufacturing industry*, Total Quality Management, 20 (5), 547-562, 2009.
- [8] Omar, M.K., Murgan, S.: *An improved model for the cost of quality*, International Journal of Quality&Reliability Management, 31 (4), 395-418, 2014.
- [9] Rabfeld, C., Behmer, F., Durlich, M., Jochem, R.: *Do quality costs still matter?*, Total Quality Management, 26 (10), 1071-1082, 2015.
- [10] Cheah, S-J., Shah, Md.S.A., Taib, F.Md.: *Tracking hidden quality costs in a manufacturing company: an action research*, International Journal of Quality&Reliability Management, 28 (4), 405-425, 2011.
- [11] Cebeci, C.: *Analysis and evaluation of different approaches to determine quality costs*, Yonetim vkonomi Arasturmalan Dergisi, 21, 281-298, 2013.
- [12] Tsai, W-H., Hsu, W.: *A novel hybrid model based on DEMATEL and ANP for selecting cost of quality model development*, Total Quality Management, 21 (4), 439-456, 2010.
- [13] Czajkowski, M.: *Managing SME with an innovative hybrid cost of quality model*, Measuring Business Excellence, 21 (4), 351-376, 2017.
- [14] Hwang, G.H., Aspinwall, E.M.: *Quality cost models and their application: a review*, Total Quality Management, 7 (3), 267-281, 1996.
- [15] Williams, A.R.T., Van der Wiele, A., Dale, B.G.: *Quality costing: a management review*, International Journal of Management Review, 1 (4), 441-460, 1999.
- [16] Weheba, G.S., Elshennawy, A.K.: *A revised model for the cost of quality*, International Journal of Quality&Reliability Management, 21 (3), 291-308, 2004.
- [17] Banasik, M.A., Beruvides, M.G.: *A Case Study of the Costs of Quality: Water Utilities*, Engineering Management Journal, 24 (2), 3-14, 2012.
- [18] Plewa, M., Kaiser, G., Hartmann, E.: *Is quality still free?* International Journal of Quality&Reliability Management, 33 (9), 1270-1285, 2016.
- [19] Velkoska, C.: *Analysis of the methods for determining the quality costs in the product development stages*, "Ss. Cyril and Methodius" University in Skopje, Faculty of Mechanical Engineering, Master thesis, 2014.
- [20] Szczepanska, K.: *Koszty jakosci dla inzenierow*, Wydawnictwo Placet, Warszawa, 2009.

Authors: PhD student Cvetanka Velkoska, Full Prof. Mikolaj Kuzinovski, Assoc. Prof. Mite Tomov, "Ss. Cyril and Methodius" University in Skopje Faculty of Mechanical Engineering, 1000 Skopje, Macedonia, Phone.: +389 02 30 99 298
E-mail: cvelkoska@yahoo.com;
mikolaj.kuzinovski@mf.edu.mk;
mite.tomov@mf.edu.mk;

Velkoska, C., Tomov, M., Kuzinovski, M.

THEORETICAL ASPECTS RELATED TO THE CREATION OF ALGORITHM FOR QUALITY COST MEASUREMENT SYSTEM

Abstract: This paper presents the theoretical aspects taken into account when creating an algorithm for a quality cost measurement system, developed using a descriptive-analytical method. The methodological approach relies on the systemic thinking about management of success, including the elements of integration, innovation and agility, taken into account when developing the scope, rules, criteria, possibilities and alternatives. The proposed algorithm provides a structured approach and systematic measurement of the quality costs, which, in turn provides for better understanding, detection and correction of the errors on the spot where they actually occurred and not where they appeared. This ensures the timeliness, accuracy and reliability of the data and information about the costs of quality, opens possibilities not only for diagnostic analytics but also for predictive and prescriptive analytics, which increases the efficiency of the company.

Key words: *algorithm, system, measurement, quality costs*

1. INTRODUCTION

The need for sustainability of the modern business and products in an environment entailing complex technical and technological, information and societal and economical systems, contributes to increasing the influence of the quality costs, as an economic category indicating the quality of the operations [1]. In addition to being a measure of the effectiveness and efficiency of the activities, processes and systems, as well as the realization of the quality objectives [1], the quality costs also represent a tool in the rational process making strategic management decisions, used to identify quality related issues and the weaknesses of companies, justify the undertaking of preventive and corrective measures, as well as evaluate the productivity of the company [2, 3].

It has become exceptionally important that quality costs related data and information to feature the properties of so called “enhanced information”, i.e. be “as relevant as possible” and presented in an “as suitable as possible” form for the users [4]. The fulfillment of these requirements entails the design and implementation of a methodologically harmonized process in the quality costs measuring system.

This paper presents a quality costs measurement system algorithm, the methodological approach and explains the phases and the stages of the system, makes note of specific properties and importance, as well as affirmation for efficient implementation and functioning of the quality costs measurement system.

2. METHODOLOGICAL APPROACH FOR THE QUALITY COSTS MEASUREMENT SYSTEM ALGORITHM

The creation of the quality costs measurement system algorithm employed a descriptive and analytical methodological approach, including systematic management of the interrelated phases, stages and units in the system with the necessary number of iterations.

The algorithm incorporates the following affirmations that provide for the functionality of the quality costs measurement system:

1. Acceptance of the “management of success” teaching based on the elaboration of the scope, rules, criteria, alternatives and the opportunities of a certain subject matter, featuring a proactive character [5],
2. Adoption of the ecology of quality assurance, including integration of company resources (human, material and methodological), product and process innovation and the agility related to the fulfillment of the requirements [6],
3. Reviewing the quality costs measurement system using the four functional units: input unit (human resources, material, equipment, knowledge, procedures), processing unit (activities and functions which transform the inputs into outputs), output unit (notifications, reports, publications, recommendations) and recipient unit (internal and external users) [2],
4. Introduction of the principle of integration and cooperativeness of the quality and accountancy experts [1, 2].

3. DESCRIPTION OF THE QUALITY COSTS MEASUREMENT SYSTEM

The quality costs measurement system should be able to identify all quality costs elements, show the true value of the quality costs (by categories and by quality costs elements), track the quality costs to their primary sources and measure the occurrence of the quality costs in real time [3]. Indeed, there exist obvious difficulties to designing a quality costs measurement system, which will systemically identify, record, measure, register, calculate, compare and analyze all quality costs elements in real time [3]. With a view to overcoming the evident difficulties in designing such a system, the proposed algorithm employs the approach of the author Sorqvist L. [3], who suggests five levels of quality costs measurements: first level–traditional quality costs according to the categorization of the PAF

(Prevention-Appraisal-Failure) model, second level–hidden quality costs, third level –lost revenues, fourth level–user costs and fifth level–social and economic costs. In the most general context, the quality costs measurement system entails three interrelated phases [4] (figure 1.):

Phase 1 refers to a complex understanding of the quality costs measurement system framework, which contains and describes the competitive position of the company, the stakeholders – users, owners and employees, the organizational goals, policies and strategies, the available resources, methodologies and procedures, followed-up and defined from the point of view and acceptable directives, risks, behaviors and policies of all of the elements of the quality costs measurements system. This framework should also contain an understanding of the quality costs beyond the functional limits of the quality departments [2], i.e. within the overall company management [7]. Furthermore, quality costs should be looked at as a comprehensive system and not just a quality management tool [7]

Phase 2 refers to the quality costs measurement process, which comprises three steps: measurement

process design, quality costs data collection and recording and analysis – synthesis – recommendation – results and final recommendations. The measurement process design involves the creation and development of a measurement process protocol comprising a design for: data collection; data recording and archiving; access to the data and the realization of the analysis, synthesis and the results.

Phase 3 refers to decision making and taking action, exceptionally important in the field of quality cost measurement system, because it refers to issues related to strategic, tactical and operational objectives and interests of the organization. Therefore the presentation of the results and recommendations should present the output data exhaustively and comprehensively, in the most appropriate, clear and understandable form, impartially, and completely intended for specific users.

The systematic phases require the setup of the entire quality cost measurement system on a level of standpoint or a culture of quality in the company, taking into account the top 10 principles of the quality costs measurement system, proposed by J. Juran [4].

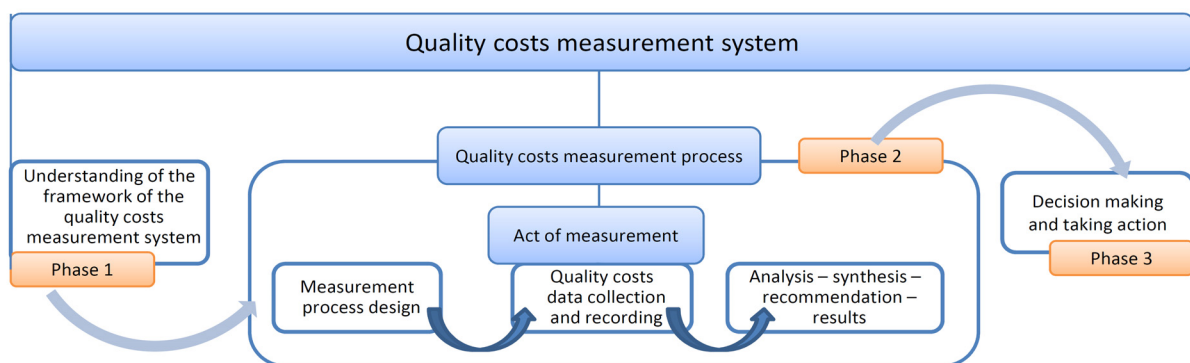


Figure 1. Quality costs measurement system

The quality costs measurement system should 1.) be managed, 2.) provide for a sufficient packet of measurements, 3.) determine who makes the decisions and how, 4.) the decisions as close as possible to the activities, 5.) have prepared measurement process plans, 6.) facilitate the measurements, analyses and the presentation of results, 7.) ensure the implementation of measurement protocols and data quality programs, 8.) be continuously improved, 9.) help the decision makers manage their processes and responsibilities, 10.) and acknowledge that it functions within limiting circumstances.

4. QUALITY COSTS MEASUREMENT SYSTEM

Figure 2 shows the quality costs measurement system algorithm [1, 2, 3, 4, 8, 9, 10, 11, 12], i.e. a structured, integrated and systematic approach to understanding planning, implementation, maintenance and management of the quality costs measurement system.

The algorithm, by nature, functions interactively,

starting from the first iteration which refers to known elements, followed by subsequent iterations which incorporate less known elements in order to “softly” include the employees and avoid the occurrence of the learning anxiety phenomenon [13].

The algorithm design relies on the principle stipulating the planning, designing and incorporation of quality, rather than controlling the quality [3, 10]. This means that it is always more cost effective to do things well from first time [3]. Hence, each and every stage of product creation and utilization should plan, identify, track, measure, calculate, rank, sort, analyze and synthesize the costs of quality. Most of the quality costs can be only estimated due to the difficulties or the impossibility to measure them [3]. For example, the quality costs in the group of non-measurable external error costs can be estimated using the Taguchi loss function [3]. From a broader perspective, quality cost measurement represents a joint effort of the entire company and therefore the proposed algorithm involves the organizational practice, the technical and technological aspect, the knowledge related to the modern calculation systems [7] and the knowledge in

the field of quality. Ultimately, this aims at changing the mentality in the organizational culture and the acceptable level of error [2], and replaces it with a zero defects philosophy [3].

The quality costs measurement protocol (phase 2, stage 1) is of especial importance for the measurement of the costs of quality. It should ensure the relevance,

simplicity accuracy and cost-effectiveness of the quality cost data [10]. The collection and recording of the quality costs entails the creation of an environment (“absolutely mandatory”) for the company experts responsible for quality and the experts responsible for accounting will work in synergy [2, 1].

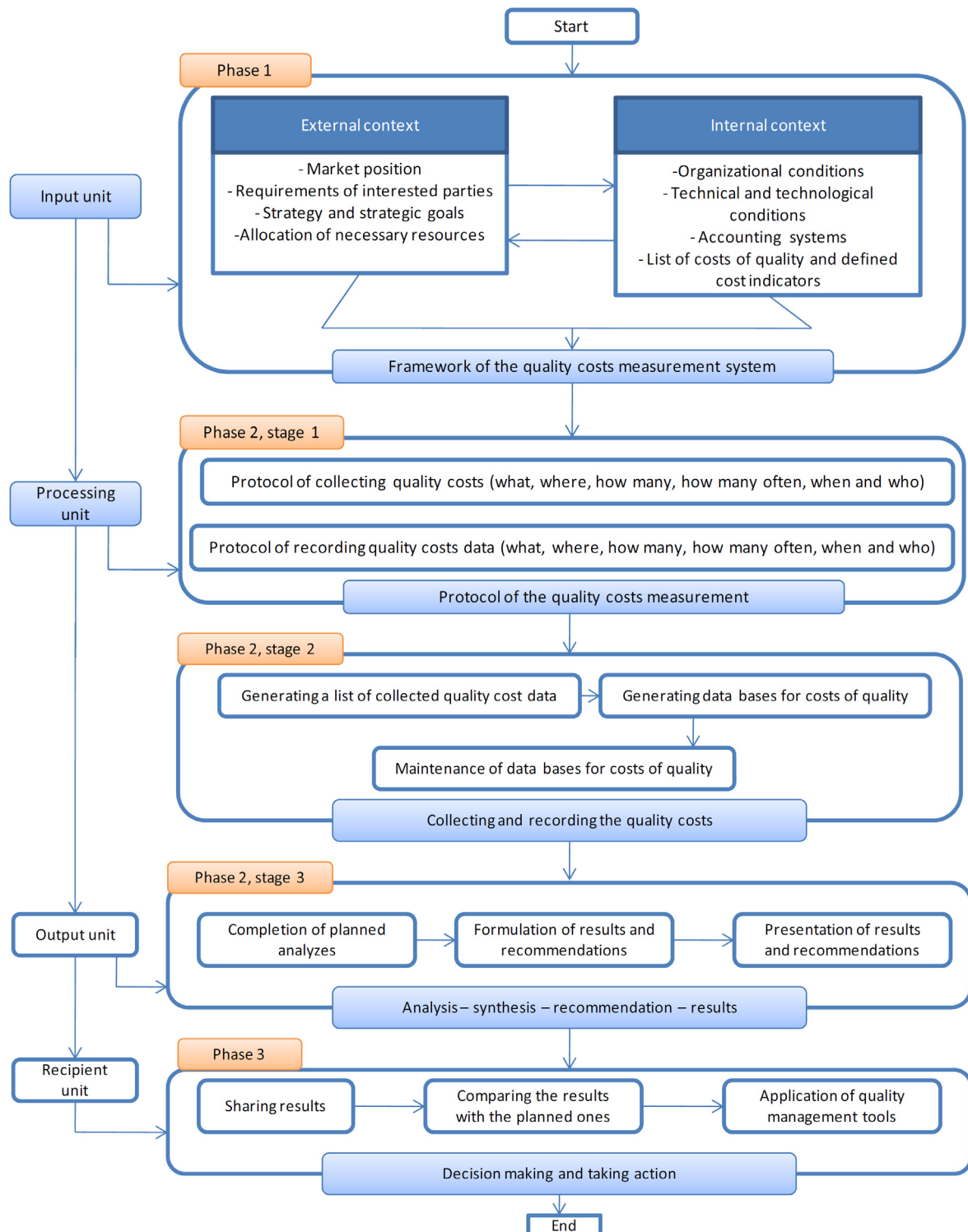


Figure 2. Quality costs measurement system algorithm

The most frequently presented methods for collecting quality costs include: collection from the accounting records, by persons involved in a given activity, by working hours, by error types, using the personal logs of the employees [2], by time [12], by the elements and the categories of the costs of quality, by organizational units and by processes [10]. The analysis of the quality costs data (phase 2, stage 3) can cover a long term and can apply to the process of strategic planning and monitoring of the entire progress; short term and apply to the process of promoting and attainment of the objectives specified for the organizational units; and short term and useful for tracking quality costs data in order to identify and eliminate the reasons for non-compliance and errors [10].

The unit of recipients (phase 3) is the final unit of the quality costs measurement system in the presented algorithm. Phase 3 involves activities such as results sharing, comparisons between actual and planned results and application of quality management tools. The results of the integration of the activities in phase 3 are recognized in the existence of three types of main responsible centers: 1.) Cost center which analyses the company performance by monitoring the costs and the responsibility for the costs, 2.) Profit center which analyses both the costs and the profits of the company and 3.) Investment center which tracks the costs, the revenues and the investments of the company [11].

5. CONCLUSION

The quality costs measurement system represents one of the ways to measure the effect of the programs and initiatives for company quality improvement. The proposed algorithm clearly shows the sequential activities in the quality costs measurement process, adapted to the real needs and capabilities of the companies in an environment of limited knowledge and limited resources. The stage and the systemic structure of the quality costs measurement system algorithm facilitate identification and tracking of the quality costs at the places where they actually occur and not at the places where they appear. This ensures the timeliness, accuracy and reliability of the data and information about the costs of quality, opens possibilities not only for diagnostic analytics but also for predictive and prescriptive Analytics of the costs of quality. Using this approach, companies that have introduced adequate, proper and acceptable quality costs measurement systems, where all components function as planned with the assistance of a program for provision of quality data and measurements also have the highest efficiency.

6. REFERENCES

- [1] Rehacek, P.: *Quality Costs as an Instrument of verifying the Effectiveness of Quality Management System*, Quality access to success, Vol. 18 No. 161, pp. 109-112, December 2017.
- [2] Johnson, M. A.: *The development of measures of the cost of quality for an engineering unit*, International Journal of Quality & Reliability Management, Vol. 12 No. 2, pp. 86-100, 1995.
- [3] Sippola, K.: *Two case studies on real time quality cost measurement in software business*, Dissertation, Faculty of Economics, Department of Accounting and Finance, University of Oulu, Finland, 2008.
- [4] Juran, J. M., Godfrey, A.B.: *JURAN'S QUALITY HANDBOOK* (Fifth edition), McGraw-Hill Companies, New York, 1998.
- [5] Mihail, L-A.: *The ISO quality management principles and the EFQM model*, Academic Journal of Manufacturing Engineering, 10(3) 6-11, 2012.
- [6] Wong, V. Y-Y.: *An alternative view of quality assurance and enhancement*, Management in education, 26(1) 38-42, 2012.
- [7] Chopra, A., Garg, D.: *Introducing models for implementing cost of quality system*, The TQM Journal, Vol. 24, No. 6, pp: 498-504, 2012.
- [8] Szczepanska, K.: *Koszty jakosci dla inzenierow*, Wydawnictwo Placet, Warszawa, 2009.
- [9] Pacana, A., Stadnicka, D.: *Systemy zarzadzania jakosci a zgodne z ISO 9001*, Wdrazanie, auditowanie i doskonalenie, Oficyna Wydawnictwa Politechniki Rzeszowskiej, Rzeszow, 2009.
- [10] Stanciuc, A-M, Branzas, B.V.: *Controversy and aspects of quality costs models*, Proceedings of the 8th International Management Conference "Management challenges for sustainable development", November 6th-7th, Bucharest, Romania 780-789, 2014.
- [11] Mrsa, J., Smoljan, B.: *Measuring quality related costs*, Advanced Manufacturing Systems and Technology, CISM Courses and Lectures No. 372, Springer Verlag, Wien New York, 801-806, 1996.
- [12] Zimak, G.: *Cost of quality (COQ): Which collection system should be used?*, ASQ's 54th Annual Quality Congress Proceedings, pp: 18-24, California, American Society for Quality, 2000.
- [13] Cheah, S-J., Shabbudin, A. S. Md., Taib, F. Md.: *Tracking hidden quality costs in a manufacturing company: an action research*, International Journal of Quality & Reliability Management, Vol. 28, No. 4, pp. 405-425, 2011.

Authors: PhD student Cvetanka Velkoska, Assoc. Prof. Mite Tomov, Full Prof. Micolaj Kuzinovski, "Ss. Cyril and Methodius" University in Skopje, Faculty of Mechanical Engineering, 1000 Skopje, Macedonia.
 Phone.: +389 02 30 99 298
 E-mail: cvelkoska@yahoo.com;
mite.tomov@mf.edu.mk;
micolaj.kuzinovski@mf.edu.mk;



Section D:

**PROCESS PLANNING,
OPTIMIZATION, LOGISTICS AND
INTERNET TECHNOLOGIES IN
PRODUCTION ENGINEERING**

Jokanović, S., Pejić, V., Borojević, S.

STEP MODEL OF MACHINING FEATURES OF SWEEP TYPE

Abstract: ISO 10303 or STEP standard is composed of parts such as: Description methodes, Integrated Resources (IR), Application Protocols (AP), Application Interpreted Constructs (AIC), Implementation methods, and Conformance Testing Methods. The whole structure is too voluminous and complex that hinder the application of STEP in industry. This paper is focused on STEP AP 224 – machining features. There is very little about this AP in the literature and at STEP implementation bodies. Specially, while there are recommended practices and instruments for conformance testing of other application protocols there are neither of the things for AP 224 in the world temporarily. This paper gives detailed definition of machining features of sweep type. This is a subset of machining features given by sweeping a two dimensional profile along a 3D path. Enlightening data model of sweep feature is of great importance since the largest number of machining features in STEP are defined as sweep feature, like boss, pocket, slot, round hole, step, planar face etc. In the paper precise definition, ready for implementation, given in EXPRESS language is exposed. Implementation of the given model is also carried out. Implementation is done using ST-Developer software of STEP Tools Inc. Testing of the solution is performed in available testing instruments. Possible usage of the model are application like automation of process planning, OpenCNC as well as conventional CNC machining.

Key words: STEP standard, Application Protocol, Machining feature, Computer Numerical Control

1. INTRODUCTION TO STEP

To CAD/CAM community STEP is the best known as a standard format for exchanging CAD models between different CAD systems, but STEP is intended to be much more. STEP objective is to provide the computer-interpretable representation and the exchange of product data throughout entire life cycle of a product. The main parts of STEP architecture are integrated resources and application protocols.

Integrated resources is a library of pre-defined information constructs (data types, entities, relationships and constraints) that can be used in different application contexts. They avoid duplication and assure a single concept is represented only once within the STEP (Fig. 1).

Particular application experts can be interested in and be able to deal with the part of STEP information model addressing their field. Such, application fitted information models are called Application Protocols (AP) [1]. Application protocol describes what integrated resources are used and how they are interpreted to satisfy the information requirements of a

specific application. This interpretation results in an application interpreted model (AIM) that is the basis for implementations of STEP. Only the AIM is allowed to be implemented in a STEP standard [2].

The information constructs used in Integrated Resources, as well as in Application Protocols, are defined using EXPRESS information modeling language. The language was formalized in Part 11 of STEP (ISO 10303-11) [3], [4]. Even though to someone it can look like a programming language EXPRESS cannot be used for development of executable programs. Instead, it is used to define the data types, entities, relationships and constraints on which programs operate.

Studying an AP carefully one will find the Application Interpreted Model is preceded with the Application Reference Model (ARM). ARM describes relevant information in an application specific language and terminology. It enables application specialists to express required information more easily and understand its meaning clearly. AIM is basis for implementation and it assures consistency of information across the STEP. There is a mapping between these two tiers. The Application Reference Model, the Application Interpreted Model, and the Integrated Resources are related and cross referenced through the Mapping Tables [5].

2. INTRODUCTION TO STEP AP 224

STEP AP 224 (ISO 10303 – 224) is the application protocol that specifies the use of the integrated resources necessary for the representation and exchange of information needed for manufacturing mechanical parts or assemblies [5]. This application

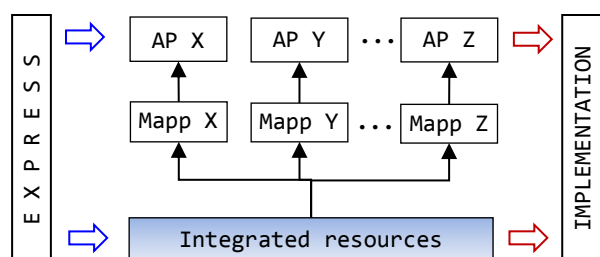


Fig.1 STEP structure at the highest level

protocol identifies specific characteristics of part shape used in manufacturing and uses them for defining machining features.

AP 224 defines a set of 21 machining features among them being hole, pocket, slot, boss, fillet, chamfer, draft, etc. Double definition of features is provided a) by a set of defining parameters and b) by explicit bounding geometry. Definition in terms of boundary representation is less feasible. It is given by a collection of faces that first must be reordered into the meaningful sequence which machining operations can be deduced from [7]. This, so called feature recognition process is not yet successfully solved task. In this work we are focused on implicit feature definition by a set parameters.

The key integrated resource entities used in AP224 are:

- `characterised_object`,
- `property_definition`,
- `property_definition_representation`,
- `representation` and
- `shape_aspect`

All these entities are root or base STEP entities. A simplified representation of these entities and their derived entities most relevant for this work is shown in Fig. 2. Thin, dot-ended lines show attributes, and thick lines show inheritance hierarchy. Only main attributes are shown. Some entities have more attributes. Root entities always have name and description attributes.

In third edition of AP 224 large part of AIM is moved to “Application Interpreted Construct (AIC): Machining features (ISO 10303-522)”. An AIC specifies a piece of an AIM that may be used in two or more APs. It enables cooperative use of multiple APs in an enterprise.

Implementation ready machining features are defined is that part of STEP, shortly AIC 522.

2.1 Definition of machining features in AP 224 (AIC 522)

IR provides two entities that are basis for definition of machining features: `feature_definition` and

`instanced_feature`. Machining features are subtypes of `feature_definition` defined in AIC522 part of STEP. Entity `feature_definition` is a subtype of `characterized_object` (Fig. 3.) It is defined in STEP part 47 (IR: Shape variation tolerances) since it is not only basis for machining features but serves other purposes too, like the features in GD&T system. AIC 522 defines a set of 21 subtypes of `feature_definition`: `boss`, `pocket`, `slot`, etc. The set is named `machining_feature_definition`. It is realized as an EXPRESS SELECT type [3]. The type is undergone further constraints and rules the most important being:

- Shall be either a `boss`, `pocket`, `round_hole`, `slot`, etc.
- Shall have just one implicit representation of type `shape_representation_with_parameters`;
- Exactly one of their representation items shall be of type `placement` with a name of 'orientation'. It defines location and orientation of a feature.

There is another important characteristic of feature that had to be considered here. Conceptually, feature is a shape aspect of part's shape. Entity `instanced_feature` realizes that concept. It is a subtype of `feature_definition` and of `shape_aspect` (Fig. 4). It is about the mechanism of multiple inheritance, taken from object-oriented languages, that joins `shape_aspect` to `feature_definition`.

Through multiple inheritance feature inherits twofold behaving: being `characterized_object` feature may have properties attached to it; being `shape_aspect` it can be attached to the product shape (through its `of_shape` attribute, see Fig. 2).

Each machining feature is given its own definition in AP224. Detail explanation will be given in the text that follows. The focus is on sweep feature types.

3. SWEEP FEATURE DEFINITION

In AP224 sweep features are defined as sweep bodies, i.e. by sweeping 2 dimensional profile along a 3D path.

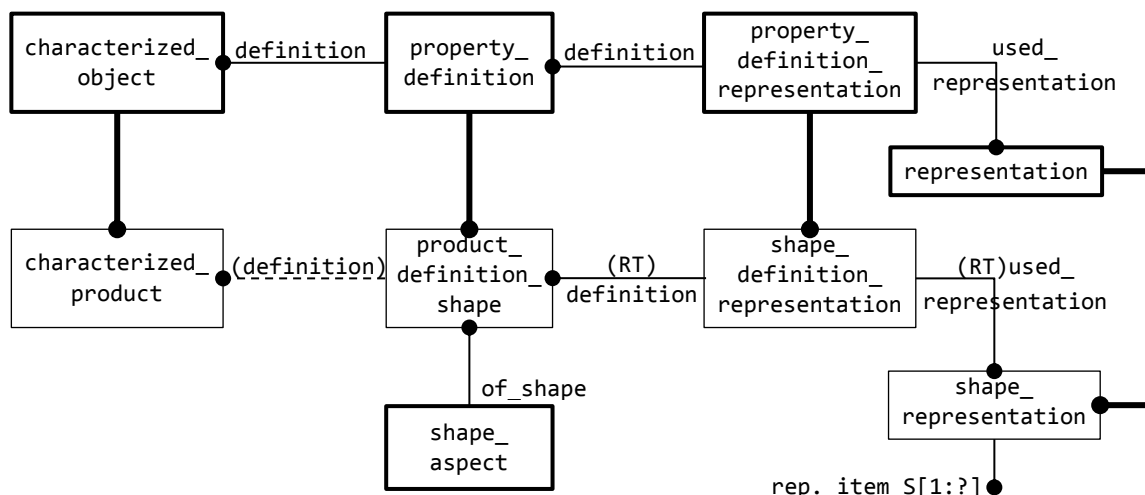


Fig. 2 Basis IR entities used in AP224

```

ENTITY feature_definition
  SUBTYPE OF (characterized_object);
END_ENTITY;

ENTITY step
  SUBTYPE OF (feature_definition);
WHERE
  WR1: ... ;
  WR2: ... ;
  WR3: ... ;
  WR4: ... ;
  WR5: ... ;
END_ENTITY;

```

Fig. 3 EXPRESS definition of entities feature_definition and step feature.

```

ENTITY instanced_feature
  SUBTYPE OF (feature_definition, shape-
    _aspect);
WHERE
  wr1: ...; -- shall be an aspect of the
    shape of a product
  wr2: ...; -- shall lie on the boundary
    of the part
END_ENTITY;

```

Fig. 4 EXPRESS definition of instanced_feature

Examples are: boss, flat_face, outer_round, outside_profile, pocket, revolved_profile, round_hole, rounded_end, step, and slot. A few examples are presented in Fig. 8 and 9.

It is easy to evident four components of a sweep feature:

1. placement (position and orientation),
2. profile,
3. path and
4. end conditions.

The basic geometry is defined by profile and path. The placement is necessary for definition of position and orientation of the feature on the part. End conditions define shape at feature ends.

What is surprising is that for definition of these elements no new attributes are added to machining feature entities. All data needed for a particular feature definition are added through the rules and constraints given in EXPRESS language. Step feature encompasses 5 rules (see Fig. 3).

3.1 Defining feature's placement

STEP integrated resources provides placement entity for objects positioning. It is defined in STEP geometry scheme (ISO 10303-42) of IR. It enables specification of the position by its only attribute named location that is of cartesian_point STEP type. However, its subtypes enable specification of orientation, too. For 3D work axis2_placement_3d is used. It defines the position and orientation in 3D space of 2 mutually perpendicular axes. One of two axes is Z axis (axis attribute) and the other is an approximation to the X axis direction (ref_direction attribute). Two examples of feature placement are shown in Fig. 9.

```

ENTITY placement
  SUPERTYPE OF (ONEOF (axis1_placement,
    axis2_placement_2d,
    axis2_placement_3d))

  SUBTYPE OF
    (geometric_representation_item);
  location : cartesian_point;
END_ENTITY;

ENTITY axis2_placement_3d
  SUBTYPE OF (placement);
  axis : OPTIONAL direction;
  ref_direction : OPTIONAL direction;
WHERE
  ...
END_ENTITY;

```

Fig. 5. EXPRESS definition of placement

3.2 Defining profile of a feature

Profile, as well as other feature components can also be considered as aspect of a feature shape. As such, they are also specified as subtypes of the shape_aspect entity.

There are eleven shape_aspect subtypes that are intended to designate feature profiles. They are:

1. linear_profile,
2. circular_closed_profile,
3. partial_circular_profile,
4. rectangular_closed_profile,
5. square_u_profile,
6. rounded_u_profile,
7. tee_profile,
8. vee_profile,
9. n_gon_closed_profile,
10. open_path_profile,
11. closed_path_profile.

First nine profiles allow for implicit representation by a couple of parameters. As type of shape_aspect profiles inherits two attributes: name and description, but they are not used in the definition of a profile. Definition is done by EXPRESS rules introduced in each profile.

Parameters of a profile are defined just at the representation stage of the profile. Representation item's name and description attributes play that role. One parameter is represented by one item. Implicit representation of a profile is done by IR entity shape_representation_with_parameters, that is a specialization of shape_representation.

For example, in the case of circular_closed_profile rules prescribe that the profile is to be represented with only two representation items, one of type placement, with the name 'orientation' and the other of type measure_representation_item and length_measure_with_unit with the name of 'diameter'. Hence, in the definition of circular closed profile the only data needed are a) placement (position and orientation) and b) diameter of the circle.

Each profile needs placement type representation item with the name 'orientation'. Some profiles require two or more numeric parameters. However, the approach for parameter specifications is the same. Each parameter is represented by individual representation item with the given name and the value.

In the case of `square_u_profile`, the parameter names are: 'depth', 'width', 'first angle', 'second angle', 'first radius', and 'second radius'.

The last two profiles support definition of arbitrary shapes by a set of connected (not intersecting) curves. Definition of such set of curves is supported by path entity available in geometry schema of STEP integrated resources (ISO 10303 – 42).

3.3 Binding profile to its feature

The profile is an aspect of the shape of a feature. However, there must be kept in mind that a profile is, in first order, aspect of the part's shape. That's why it cannot be linked to feature shape only. The solution is to establish relationship of a profile to its feature. The relation is done by `shape_defining_relationship` entity that is a specialization of the `shape_aspect_relationship` that relates two shape aspects of the part [5]. Precise provision is given in each feature that needs a profile. Graphical illustration of the rule WR2 of AIM 522 clause 4.4.51 that assigns a profile to the slot feature is given in Fig. 6.

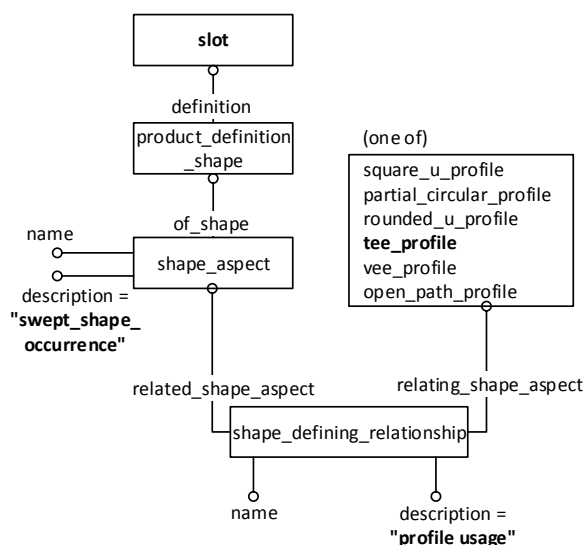


Fig. 6. Binding a profile to the slot feature

3.4 Defining path of a feature

Unlike the profile case, there is only one `shape_aspect` subtype for description of the path of a sweep feature. It is the `path_feature_component` subtype. There are four types of path as it is shown in Fig. 7. Type of the path is designated by the description attribute of `path_feature_component` entity. Parameters of a profile are designated through representation items of `path_feature_component` which is also represented by `shape_representation_with_parameters`. One representation item is to define path orientation. The other items vary from profile to profile and may be of vector, scalar or general path type.

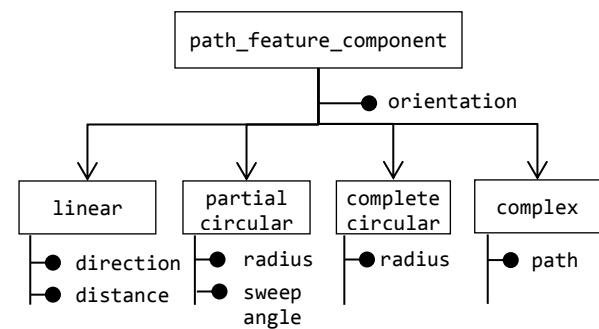


Fig. 7. Types of path with parameters assigned

3.5 Binding a path and a feature

Binding a feature to its path is done by propositions similar to that binding it to the profile. For example, in the case of pocket feature the next constraints are to be fulfilled:

- Shape aspect that references the pocket (related shape aspect) has its attribute: `description = 'pocket depth occurrence'`
- `shape_defining_relationship` attributes are: `name = 'pocket depth'` and `description = 'path feature component usage'`
- Relating shape aspect references a `path_feature_component` with `description = 'linear'`.

Presentation of STEP data relating a profile and a path to their feature, in the case of the boss and the pocket feature, is given in Fig. 8. Even though the structure looks complex one can soon realize that data pattern repeats in a large ratio.

3.6 Positioning feature and its components

In their representations feature, profile and path all have one, usually first item of type `axis2_placement_3d` with the name of 'orientation'. It defines positioning and orientation of coordinate systems of a feature and its components. AP 224 rules force these coordinate to be coincident. Example is linear slot in Fig. 9. When this approach makes no sense, like it is in the case of circular slot in Fig. 9, the special solution is given by explicit EXPRESS rule.

3.7 Auxiliary items of feature definition

AIC 522 encompasses a number of additional items that may be needed to complete feature definition. The most of them are about feature end conditions like: `hole_bottom`, `boss_top`, `pocket_bottom`, `slot_end`, `thread_runout`, etc.

There are also other elements not related exclusively to the feature ends but are spread out the whole feature like `taper`, `chamfer_offset`, `transition_feature`, etc. Like profile and path all these additional items are subtypes of `shape_aspect` entity. The type of a feature that an end condition is related to can be induced from the name of a particular `shape_aspect` subtype. Thus, the `hole_bottom` is related to the `round_hole` feature.

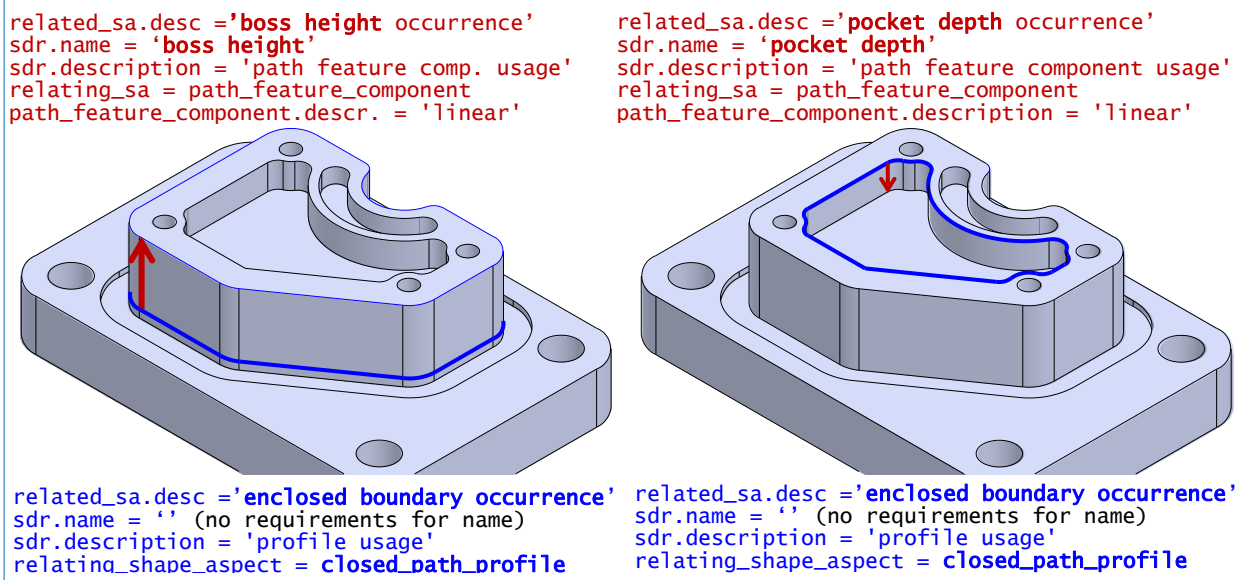


Fig. 8. Profile and path definitional elements in the case of boss and pocket feature.

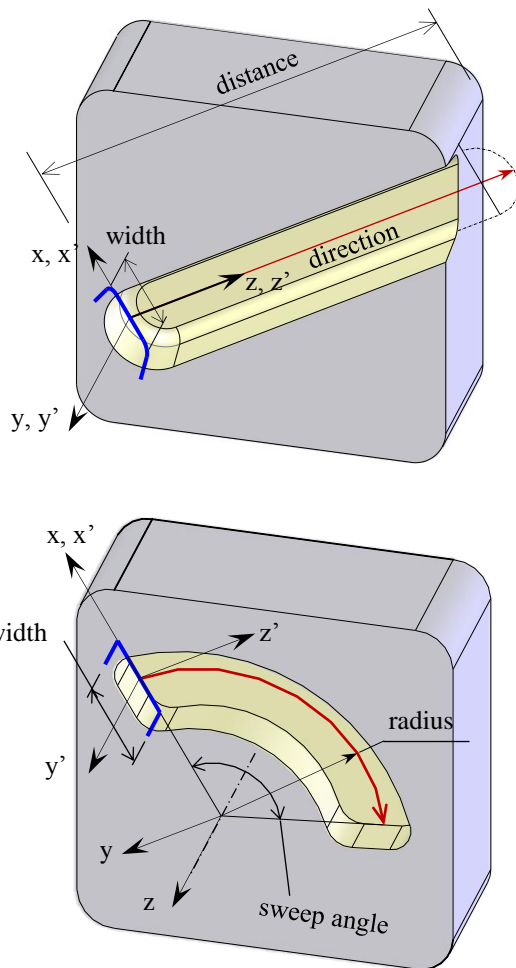


Fig. 9. Slot feature: placement of coordinate system depends on type of path; $x'y'z'$ – profile CS, xyz – feature CS and path CS

The type of the bottom of the hole is defined in the description attribute of hole_bottom shape_aspect subtype, which is to be either 'through', 'flat', 'flat with radius', 'flat with taper', 'spherical' or 'conical'.

Precise definition end condition and other auxiliary items for each feature is given

4. IMPLEMENTATION

STEP implementation methods are defined in Part 21 to Part 29 of the standard. The most widespread implementation is STEP translator – physical file format for exchanging CAD models between different CAx systems. The syntax of the exchange structure, together with the mapping from EXPRESS information constructs onto that syntax, is defined in Part 21 of STEP (ISO 10303-21).

For applications aiming to manipulate STEP data (defined by EXPRESS) an other implementation method "Standard Data Access Interface (SDAI)" is defined in Part 22. Bindings of the SDAI specification to C++, C, IML and Java programming language are defined in Parts 23, 24, 26 and 27.

An implementation of STEP requires translation of EXPRESS entities and rules into a programming language constructs, for example C++ classes, that can be used in application programs. Fortunately, there are some implementation tools available for free use. The most remarkable seem to be the solutions made by US National Institute of Standards and Technology (NIST) and STEP Tools, Inc. [9].

STEP Tools' ST-Developer was used for implementation of models developed in this paper. ST-Developer is an application development environment based on STEP Class Library generated from EXPRESS schema by ST-Developer's EXPRESS compiler. C++ Class Library was used in this work but the libraries for Java and Visual Basic are also available. In addition to the classes that correspond to EXPRESS entities, ST-Developer provides classes and functions that support query of data structure, reading and writing data to storage and other useful functions.

ST-Developer classes that hold EXPRESS-defined data keep the same name as STEP entities prepended with stp_ prefix. Attributes are prefixed with PARAM_ string

(Fig. 10). Each class provides constructors as well as access and update functions for its attributes. The function without argument read an attribute, and function with argument update an attribute.

```

stp_axis2_placement_3d(
    const char* name,
    stp_cartesian_point * location,
    stp_direction * axis,
    stp_direction * ref_direction
);

stp_axis2_placement_3d->name(); //access name
stp_axis2_placement_3d->name(const char*);
                                //update name

```

Fig. 10. C++ class `stp_axis2_placement_3d` mapping `axis2_placement3D` EXPRESS entity: a constructor, an access, and an update function.

5. MODEL TESTING

Alongside standardizing product information and representation and implementation methods STEP also standardizes methods for testing applications which implement Application Protocols. Based on this standardization some tools were developed to help ensure that the data in a STEP file are valid. Checkers for AP 203 and AP214 are widely available and almost all CAD systems have STEP 203 and 214 translators. Checking instrument for application protocol dealing with PMI information, AP242, is developed at NIST [10]. However, there are no instruments for conformance testing of AP224 as it is known to the authors. Authors of [11] reported about STEP interpreters for GibbsCAM and Master CAM but practical solutions couldn't be found.

Nevertheless, a kind of checking validity of model developed in the work was done. First, STEP file containing feature definitions was imported to a few CAD systems: SolidWorks, CATIA and Inventor. CAD systems didn't report any errors, they recognized geometry but filtered out machining data as they don't support AP224 protocol. Little bit better testing were possible by NIST's Step file Analyzer (SFA) tool. Even though in SFA AP224 doesn't explicitly cite it checks the common structure, rules and relationships among entities and attributes.

In the last test we used STEP-NC machine application [12].



Fig. 11. STEP-NC recognises and lists AP 224 features

STEP file with our AP224 machining features was open in STEP-NC machine which correctly recognized features contained in the file. Unfortunately, STEP-NC doesn't list any features data: profile, path, parameters, etc. That's why we cannot assert the features fully agree with STEP standard. But exclamation icon (Fig. 11) in a case of omission or wrong definition proves that features are checked thoroughly. Right defined features can be processes with any application working with AP 224 STEP features.

6. REFERENCES

- [1] ISO 10303-1:1994, Product data representation and exchange – Part 1: Overview and Fundamental Principles.
- [2] Loffredo, D.: *Fundamentals of STEP Implementation*, Sep. 9, 1999, STEP Tools, Inc., pp. 1-12
- [3] ISO 10303-11 Description Methods: The EXPRESS Language Reference Manual.
- [4] Schuler, R. W. , *The Application of ISO 10303-11* (the EXPRESS Language), http://www.reocities.com/collegepark/library/6460/express/EXPRESS_data_modeling.pdf
- [5] ISO 10303-224:2006 Product data representation and exchange: Application protocol: *Mechanical product definition for process planning using machining features*.
- [6] Fowler, J.: *STEP for Data Management, Exchange and Sharing*, Technology Appraisals (ISBN 1-871802-36-9) (1995)
- [7] Proctor, F. M., Kramer, T. R.: *A Feature-based Machining System using STEP*, Proceedings of SPIE – The International Society for Optical Engineering, Vol. 35, No. 18, pp.156–163 (1998)
- [8] Feeney, A.: *The STEP Modular Architecture*, ASME. J. Comput. Inf. Sci. Eng. 2002;2(2):132-135. doi:10.1115/1.1511520.
- [9] <http://www.steptools.com>, last accessed 11.8.2016.
- [10] Lipman, R., Lubell, J.: *Conformance checking of PMI representation in CAD model STEP data exchange files*, Computer-Aided Design, Volume 66, pp 14-23, ISSN 0010-4485, 2015
- [11] Feeney, A. B., Frechette, S.: *Testing STEP-NC implementations*, Proceedings of the 5th Biannual World Automation Congress, Orlando, FL, 2002, pp. 39-44.
- [12] Hardwick, M., *Manufacturing Integration using the STEP-NC DLL*, STEP Tools, Inc., 2006.

Authors: Assoc. Prof. Simo Jakanović, Assist. Prof. Stevo Borojević, University of Banja Luka, Faculty of Mechanical Engineering, Department of Production Engineering, Stepe Stepanovića 75, 78000 Banja Luka, BiH/Republic of Srpska;

E-mail: simo.jakanovic@mf.unibl.org;
stevo.borojevic@mf.unibl.org

Assist. Prof. Vlastimir Pejić, College of business and technical education, Ozrenskih srpskih brigada 5A, 74000 Dobo, BiH/Republic of Srpska,
E-mail: vlastimirpejic@gmail.com

Petrović, M., Jokić, A., Miljković, Z.

SINGLE MOBILE ROBOT SCHEDULING: A MATHEMATICAL MODELING OF THE PROBLEM WITH REAL-WORLD IMPLEMENTATION

Abstract: *In this paper, the authors focus on the mathematical formulation of the single mobile robot scheduling problem concerning an intelligent manufacturing system (IMS) with n parts, m machine tools and one mobile robot used to transport parts between machines. Furthermore, the following five flexibility types of the scheduling plans are analyzed: (i) process, (ii) sequence, (iii) machine tool, (iv) tool and (v) tool access direction (TAD) flexibility. Since there are numerous ways to schedule the manufacturing resources in an IMS, this problem is considered to be NP-hard in terms of combinatorial optimization. In order to solve this type of optimization problem, the authors propose three metaheuristic algorithms: Whale Optimization Algorithm (WOA), Particle Swarm Optimization (PSO) algorithm and Genetic Algorithm (GA). All the algorithms are implemented in MATLAB software package and tested on real-world problem. The experimental results show that the optimal solution obtained by the WOA is superior to the optimal solutions obtained by two other algorithms.*

Key words: *single mobile robot scheduling, mathematical modeling, optimization, whale optimization algorithm, particle swarm optimization algorithm*

1. INTRODUCTION

Intelligent mobile robots are among various advanced material handling systems that are finding increasing applications in modern manufacturing environments. Features such as intelligence, capability to learn and ability to adapt to dynamically changing environments, allow mobile robots to work efficiently and effectively in different environments and to be widely used in large number of industrial applications, including transportation, inspection, exploration, or manipulation tasks. On the other hand, operating on the shop floor as a component of material transport system, intelligent mobile robot tasks need to be optimally scheduled due to its impact on the efficiency of the overall manufacturing system. Having these facts in mind, this paper analyses integration of single mobile robot and its scheduling in intelligent manufacturing system.

Mobile robot scheduling problem belongs to the class of NP-hard problems, which has attracted interest of researchers in recent years. In reference [1], Chen and Tseng proposed GA-based methodology for solving a path and location planning problem of the workpiece with objective to minimize time required for a robot to transport a workpiece. Maimon et al. [2] proposed a neural network-based approach to schedule one material-handling robot for tasks of loading and unloading of parts into and from the machines. The aim of this research was to minimize a weighted objective of the total robot travel time and the tardiness of the sequenced tasks. In reference [3], the authors presented tabu search and probabilistic tabu search to solve the single vehicle pickup and delivery problem with time windows. The aim was to minimize the total distance traveled by the vehicle. Experiments showed the superiority of tabu over probabilistic tabu search in both time aspect and quality of obtained solutions.

Hurink and Knust [4] considered a single-machine scheduling problem in a job-shop environment where the jobs have to be transported between the machines by a single transport robot. They used a local tabu search algorithm to solve the problem, with objective to minimize the sum of all traveling and waiting times. The problem of finding optimal feeding sequence in a manufacturing cell with feeders fed by a mobile robot with manipulation arm was analyzed in reference [5]. A genetic algorithm-based heuristic was developed to find the near optimal solution for scheduling of autonomous mobile robot called „Little Helper“ in a real-world industrial application.

In this paper, a methodology for intelligent material transport in manufacturing environment by using single mobile robot is presented. Mathematical modeling of the problem is defined and the implementation procedure based on biologically inspired Whale Optimization Algorithm (WOA) is described. Scheduling plans obtained by the proposed methodology are tested by Khepera II mobile robot in a laboratory model of manufacturing environment.

The structure of the paper is as follows. In Section 2 we briefly describe the single mobile robot scheduling problem. Mathematical modeling of the problem and three optimization objectives are formulated in Section 3. Implementation of the proposed WOA is outlined in Section 4. The proposed algorithm is experimentally tested and comparative results are presented in Section 5. Finally, concluding remarks and references are stated in Section 6 and Section 7, respectively.

2. PROBLEM DEFINITION

In this paper, we analyze integrated process planning and scheduling (IPPS) problem where parts (jobs) manufactured in production environment have to be transported between machine tools by using single

mobile robot. IPPS problem with single robot used to satisfy transportation requests may be formulated as follows: We are given m machine tools and n parts, where each part can be machined by using p cutting tools orientated in 6 possible TADs (+x, -x, +y, -y, +z, -z). Each scheduling plan has five flexibility types [6]. It consists of sequence of operations which have to be processed in order defined by flexible process plan network and information about manufacturing resources (machine tools, cutting tools, and TADs). For each operation only one machine tool, one cutting tool, and one TAD can be selected. Furthermore, each machine can process at most one operation at a time and at time zero all the jobs are on machines where their first operation is manufactured. Additionally, transportation times for loaded and empty robot trip between machine tools are considered. We also assume that loaded transport tasks have to be done by single mobile robot which can handle at most one part at a time.

3. MATHEMATICAL MODELING

Definition of the mathematical model for single mobile robot scheduling problem is presented in following section. The three fitness functions, regarding mobile robot scheduling, are utilized: (i) transport time, (ii) level of robot utilization as well as (iii) total robot and job waiting time. In intelligent manufacturing systems, transport time can be a major constraint due to the restricted battery life of the mobile robot. To minimize transport time and extend the time robot is active, the authors propose the first fitness function represented by equation (1):

$$f_1 = \min \left(\sum_{i=1}^N \sum_{j=2}^{P_{il}} \Theta_{ijl} \cdot \left(T_{i(j-1)l}^{k''} + R_{ijlk_r} \cdot T_{ijli(j-1)l}^{k,k''} \right) \right) \quad (1)$$

where:

- Θ_{ijl} is a decision variable that has value 1 if machine k of operation O_{ijl}^k is different than machine k'' of operation $O_{i(j-1)l}^{k''}$, and 0 otherwise,
- O_{ijl}^k is the j -th operation in alternative process plan l of job i , manufactured on machine k ,
- R_{ijlk_r} is equal to 1 if machine k'' of operation $O_{i(j-1)l}^{k''}$ is different from machine k_r where robot is currently, and 0 otherwise,
- $T_{i(j-1)l}^{k''}$ is transport time between machines k'' (machine for previous operation of the job i) and k (machine for current operation),
- $T_{ijli(j-1)l}^{k,k''}$ is transport time between machine k_r (machine where robot was on the start of current operation) and machine k'' ,
- N is number of jobs, and P_{il} is number of operations of the j -th job and the l -th process plan.

Level of robot utilization (equation 2) is the balance between the robot utilization and total processing time. This fitness function guarantees that

robot is properly utilized while processing time stays reasonable.

$$f_2 = \min \left(\frac{f_1}{\max(c_{ijl}^k)} \cdot 100 + \max(c_{ijl}^k) \right) \quad (2)$$

Parameter c_{ijl}^k is completion time of the j -th operation in alternative process plan l of the i -th job that is manufactured on the k -th machine.

The third fitness function (equation 3) can be applied to the Just-In-Time manufacturing system. In this kind of system, the aim is to minimize all the wastes, e.g. robot waiting time and job waiting time.

$$f_3 = \min \left(\sum_{i=1}^N \sum_{j=1}^{P_{il}} Jwt_{ijl} + Rwt_{ijl} \right) \quad (3)$$

Rwt_{ijl} is robot waiting time during the j -th operation in alternative process plan l of the i -th job. Jwt_{ijl} is job waiting time during the j -th operation in alternative process plan l of the i -th job. After operation is completed, job waiting time is a period job waited for the robot to transport it to the next machine.

4. WHALE OPTIMIZATION ALGORITHM

The Whale Optimization Algorithm [7] is one of the newly developed biologically inspired optimization algorithms. Its working principle is inspired by hunting mechanism of the humpbacks whale. This hunting method is unique in the animal kingdom and it consists of two phases. The first phase refers to exploring waters for the prey. The second one (exploitation phase) begins when whales find their prey and continues when they start making spiral movements while releasing the bubbles. They make a net of bubbles to disorientate the prey and to catch it. The algorithm is modelled in the same two phases and whales are called agents.

The first phase in this algorithm is exploration phase. In this phase, the agents search state space by changing their locations while attempting to find global minima. Every agent can change its location in regards to any other randomly chosen agent. The mathematical equations that represent this phase are (4) and (5):

$$\vec{D} = \left| \vec{C} \cdot \vec{X}_{\text{rand}} - \vec{X} \right| \quad (4)$$

$$\vec{X}(t+1) = \vec{X}_{\text{rand}} - \vec{A} \vec{D} \quad (5)$$

$$\vec{A} = 2\vec{a} \cdot \vec{r} - \vec{a} \quad (6)$$

$$\vec{C} = 2 \cdot \vec{r} \quad (7)$$

where:

- t represents the current iteration of the algorithm,
- $\vec{r} \in [0,1]$ is vector of random numbers,
- \vec{X} and \vec{X}_{rand} are vectors of the current and random agent, respectively,
- a has initial value of 2 and it linearly decreases to 0 during the iterations of the algorithm,
- \cdot is elementwise multiplication.

In exploration phase, the agents change their location in regards to the leader. The leader is the agent

$$\overrightarrow{D} = \left| \overrightarrow{C} \cdot \overrightarrow{X}^*(t) - \overrightarrow{X}(t) \right| \quad (8)$$

$$\overrightarrow{X}(t+1) = \overrightarrow{X}^*(t) - \overrightarrow{AD} \quad (9)$$

$$\overrightarrow{D}' = \left| \overrightarrow{X}^*(t) - \overrightarrow{X}(t) \right| \quad (10)$$

$$\overrightarrow{X}(t+1) = \overrightarrow{D}' \cdot e^{bl} \cdot \cos(2\pi l) + \overrightarrow{X}^*(t) \quad (11)$$

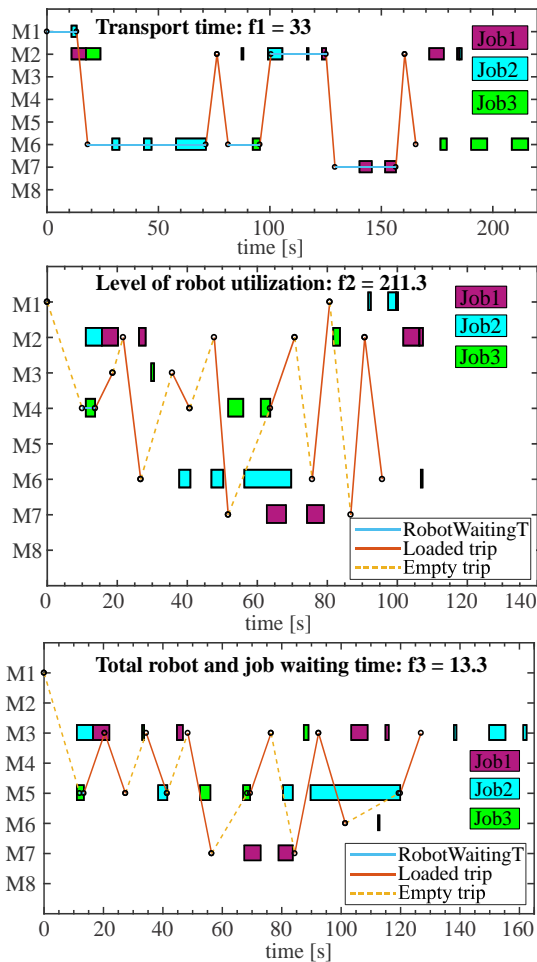


Fig. 3. Gantt charts of the mobile robot and machine tools schedule under fitness functions f_1 , f_2 and f_3

Fig. 4 demonstrates a few scheduling sequences in an IMS: a) unloading part#3 from M3, b) robot moving part#3 to M5, c) loading part#3 into M5, d) empty trip, unloading part#2 from M4 and loading part#2 into M7.

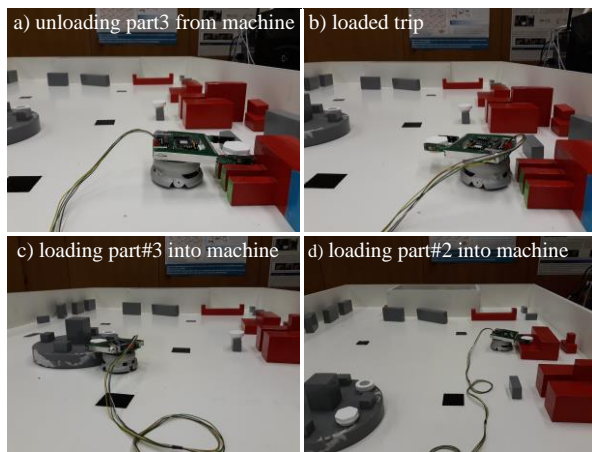


Fig. 4. Khepera II mobile robot scheduling in IMS

6. CONCLUSION

In recent years, the application of biologically inspired methods has been gaining popularity in research related to engineering optimization problems. In this paper, a new approach based on Whale Optimization Algorithm (WOA) is proposed to

optimize combinatorial NP-hard single mobile robot scheduling problem. Solutions of the scheduling problem are encoded into WOA agents in order to intelligently search for the optimal sequence of mobile robot transportation tasks. Optimal schedule sequence is found in accordance with three fitness functions (transport time, level of robot utilization, and robot and job waiting time), which are introduced and mathematically defined. The performance of the proposed WOA algorithm is evaluated in comparison with the results obtained with PSO and GA. All the algorithms are coded in the MATLAB environment and implemented on the Khepera II mobile robot. Experimental results indicate that the proposed algorithm performs better in comparison with other bio-inspired optimization algorithms.

7. REFERENCES

- [1] Chen, C. J., Tseng, C. S.: *The path and location planning of workpieces by genetic algorithms*, Journal of Intelligent Manufacturing, 7(1), pp. 69-76, 1996.
- [2] Maimon, O., Braha, D., Seth, V.: *A neural network approach for a robot task sequencing problem*, Artificial intelligence in engineering, 14(2), pp. 175-189, 2000.
- [3] Landrieu, A., Mati, Y., Binder, Z.: *A tabu search heuristic for the single vehicle pickup and delivery problem with time windows*, Journal of Intelligent Manufacturing, 12(5-6), pp. 497-508, 2001.
- [4] Hurink J., Knust S.: *A tabu search algorithm for scheduling a single robot in a job-shop environment*, Discrete Applied Mathematics, 119 (1), pp. 181-203, 2002.
- [5] Dang, Q. V., Nielsen, I., Steger-Jensen, K., Madsen, O.: *Scheduling a single mobile robot for part-feeding tasks of production lines*, Journal of Intelligent Manufacturing, 25(6), pp. 1271-1287, 2014.
- [6] Petrović, M., Vuković, N., Mitić, M., Miljković, Z.: *Integration of process planning and scheduling using chaotic particle swarm optimization algorithm*, Expert Systems with Applications, 64, pp. 569-588, 2016.
- [7] Mirjalili, S., Lewis, A.: *The whale optimization algorithm*, Advances in Engineering Software, 95, pp. 51-67, 2016.

Authors: Assist. Prof. Dr. Milica Petrović, M.Sc. Aleksandar Jokić, Full Prof. Dr. Zoran Miljković, University of Belgrade, Faculty of Mechanical Engineering, Department of Production Engineering, Kraljice Marije 16, 11120 Belgrade 35, Serbia, Phone: +381 11 3302-264, Fax: +381 11 3370364. E-mail: mmpetrovic@mas.bg.ac.rs; jokic1.aleksandar@gmail.com; zmiljkovic@mas.bg.ac.rs;

ACKNOWLEDGMENTS: This research is supported by the Serbian Government – the Ministry of Education, Science and Technological Development under Grant TR35004 (2011–2018).

Borojević, S., Jovišević, V., Čiča, Đ., Sredanović, B.

MODELING AND SIMULATION OF PRODUCTION PROCESSES FOR THE TOOLS OF THE PRESS BRAKE

Abstract: This paper presents a methodology for modeling and simulation of production processes using the software Tecnomatix Plant Simulation®. A simulation model was created within the aforementioned software, by which the analysis of production processes, within the production system for the production of the press brake tools, was executed. The analysis of production processes was carried out with the aim of achieving minimal costs of production equipment and maximum utilization of machines in relation to the quantity of products on an annual basis. As a result of this analysis, the maximum quantities of the press brake tools on an annual basis, the number of machines, the number and position of the buffers, as well as the layout proposal of production equipment for the production of the press brake tools are generated.

Key words: process planning modeling and simulation, press brake tools, virtual production

1. INTRODUCTION

In order to constantly improve the production process and increase the efficiency and effectiveness of production systems, there has been a need for computer applications that have the ability to model, display and simulate virtual production systems. These applications have the ability to manage the production environment, collect data from material flows from the production process and enable the optimization of the production of the observed products. Simulation of the complete material flow in the production, including all relevant production, storage and transportation activities, is a key part of the virtual factories that are often used in the process of production process planning. By reducing inventory and shortening the time cycles from 20% to 60%, it is possible to increase the productivity of real processes by 15% to 20% [1]. The need and execution of the simulation depends on the strategic and technological goals, and can be based on the capacities, number and utilization of machines, time cycles, size and number of buffers, logistics, work states, spatial capacities, etc. From the strategic point of view, the simulation covers a longer period of time, and the user of the simulation gets answers to the questions: where is the best location for the new production system, what size are the optimal areas for the production system, as well as the answers to other logistical questions, labor issues, production costs, storage, etc. From a technological point of view, the simulation covers a shorter period of time, and it is done for the purpose of analyzing existing or new resources, optimizing the operations sequence, as also processing times, etc [2].

2. SIMULATION OF PRODUCTION PROCESS WITH TECNOMATIX PLANT SIMULATION

One of the applications that enable the realization of the above mentioned tasks from the domain of simulation and optimization of production processes is

Tecnomatix Plant Simulation® (TPS) [3], whose working environment is shown in Figure 1. TPS provides a wide range of tools for analyzing production simulation models using stochastic algorithms for calculating and managing experiments, and also for determining the target parameters and realization of optimization of production processes. The results of the simulation depend on the quality of the input data and the degree of similarity between simulation model and process in the real environment. Compared to other applications, TPS provides a very flexible way of managing with the model and thus quickly adapts to the conditions in the real environment of the production system.

Simulation of production processes using TPS is carried out using the following steps [4]:

- estimating and collecting data from real production processes that are necessary for designing of the simulation model;
- determining the goal of the simulation study and creating a simulation model in accordance with the defined goals;
- running a experiments within a simulation model;
- interpretation of the results of the performed simulated experiments.

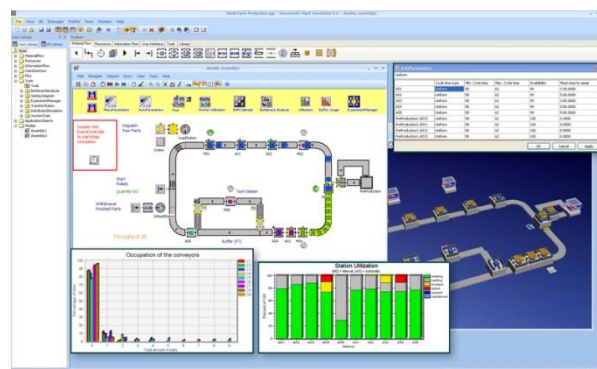


Fig. 1. Working environment of *Tecnomatix Plant Simulation®*

Modeling and development of the simulation model with TPS is a cycle and evaluation process. The simulation study is performed based on the initial simulation model. On the basis of the obtained results, the initial simulation model is corrected and improved. This process is repeated until the goal of the simulation study is achieved.

The simulation study is most often applied in the following cases [5]:

- When the new production system is planned - in this case the simulation is used to: determine and optimize the times (processing, delay, restart, failure), as well as the capacity of production systems, determine the efficiency of machines and production plants as a whole, identification of the required number of workers and machines for the designed capacities, acquire knowledge of the behavior of the production plant, reduce the investment costs for the production lines without compromising the required output sizes, etc.
- When the existing production system is improved - in this case the simulation is used to: improve the performance of existing production systems, optimize control strategies, and test the execution of everyday processes in order to ensure the smooth running of the production process.
- When the introduces a new products in existing production system - in this cases the simulation is used for the purpose of: forming patterns for creating control strategies, testing different scenarios during the test phase of the production, training of the operators on machines in different environments in which machines and equipment are located, etc.

3. CASE STUDY

3.1 Problem definition

This paper presents the development of a simulation model that has a goal to simulate the actual production system for the production of one type of product. Products were defined by technological process plans and detailed drawings. The requirements which were set for the simulation study are as follows:

- develop a simulation model for defined technological process plans, as well as in accordance with the defined processing times and set-up times;
- the result of the simulation study should ensure optimum cost of production equipment in relation to the quantity of products on an annual basis; and
- it was necessary to strive for the uniform and higher is possible utilization rate of production equipment.

3.2 Input data

Design of the simulation model for the observed production system was based on existing technology for a given group of products, i.e. for the group of the upper tools for press brake. The forms of the press brake tools were defined by the detail drawings, which are developed according to customer requirements and the characteristics of the brake press on which the

product will be used. Based on the given group of tools for the press brake, analysis of products using group technology was performed and a complex part was designed. By analyzing the complex part, it was observed that one of the given (real) products from the group of products - actually represents the real complex part. The real complex part is shown in Figure 2. Then, the reduction of products quantities was carried out, and an amount of 8260 pieces per year was obtained as a reduced quantity. In addition, a group process plan has been developed for the real complex part, and it is shown in Table 1. Within the developed group process plan, the following parameters were identified:

- the operations sequence;
- processing times for operations (T_i);
- types of machines; and
- set-up times for operations (T_s).

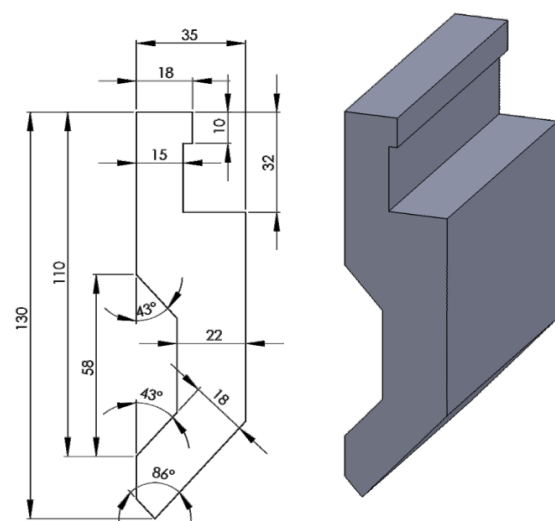


Fig. 2. Real complex part - upper tool for press brake

No.	Operation	Machine	T_s [min]	T_i [min]
10	Cutting	Sawing machine	10	10
20	Milling	Portal milling machine	30	90
30	Vibrating	Device for vibrating	15	20
40	Planing	Planer	30	42
50	Quenching	Device for quenching	15	9
60	Vibrating	Device for vibrating	15	20
70	Plane grinding	Grinding plane machine	10	52
80	Cutting on length	Sawing machine	5	10
90	Face milling	Horizontal milling machine	15	10
100	Face grinding	Grinding face machine	60	36
110	Washing	Device for washing	5	5

Table 1. Group process plan for press brake tools

3.3 Modeling of production system

The purpose of this simulation study is to present three different conceptually designed production

processes, with the same technological process plan, and choosing the optimal production process in accordance with the requirements of this study.

MODEL No.1

Model 1 (Fig. 3) use nine machines and four buffers in purpose to prevent bottleneck during the production process. On machines RM_1001 and RM_1003 were used inverse operations. The input of the material into the production process was carried out continuously with an interval of 56 minutes. Labels and machine types correspond to the technological process plan.

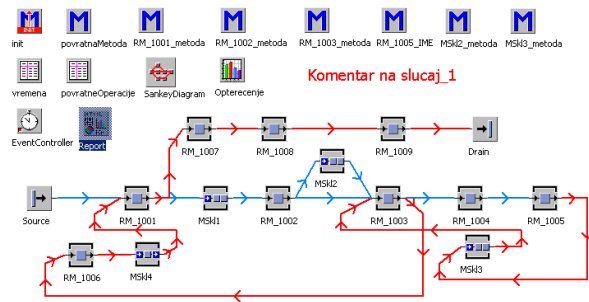


Fig. 3. Model No.1 of production system

MODEL No.2

By simulating the production in Model 1, a bottleneck was identified at operation 20. In order to eliminate it, and thereby increase the productivity of the entire production facility, another machine for the observed operation was added. The enhanced Model 2 is shown in Fig. 4.

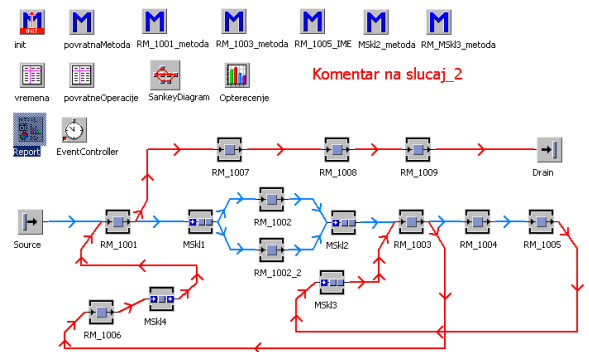


Fig. 4. Model No.2 of production system

In Model 2, as in Model 1, it was used similar methods for managing of time and material flows. The *SankeyDiagram* tool was used in all models as an indicator of the material flow path.

MODEL No.3

By simulating Model 2 we came to the conclusion that processing on the machine RM_1003 represents a problem for production process. The problem arises because the workpieces were individually processed on the first operation 30 and in the inverse material flow at operation 60, too. In the simulation model each time when operation was changed, it was necessary to execute a machine set-up for processing of the next operation, leading to a major slowdown of the machine RM_1003, and therefore the whole production. As a

solution to this problem in Model 3 (Figure 5) a group input of workpieces was introduced into the observed machine, in groups of 10 pieces. Firstly, group 10 workpieces are processed on operation 30, and then group of 10 workpieces at operation 60, on same machine.

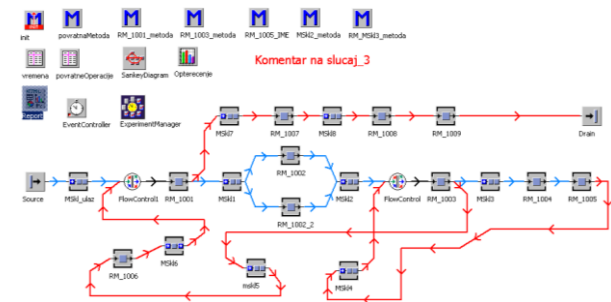


Fig. 5. Model No.3 of production system

The *FlowControl* tool was used to distribute groups of workpieces. In the simulation model there was another *FlowControl* tool that regulates the input of workpieces on the machine RM_1001. The machine RM_1001 processes the operations 10 and 80 in groups of three or less, depending on the state of the MSkl6 buffer. In Model 3, the *ExperimentManager* tool was used to determine the optimum size of the MSkl1, MSkl2, and MSkl6 buffers, which were important to this study in terms of material flow.

4. RESULTS

Testing the simulation model begin after creating the Model 1. The simulation of the all models was monitored annually. With computer simulation, it was able to obtain the results (outputs) from production system without the cost of probation period of production in production plant. Figure 6 shows a low degree of utilization for almost all machines, but also that the machine RM_1001 was in a blocking state of over 70% of the time. Also, the simulation results show that the annual quantity of manufactured products (4957 pc/yr) was far below the required quantity (8260 pc/yr).

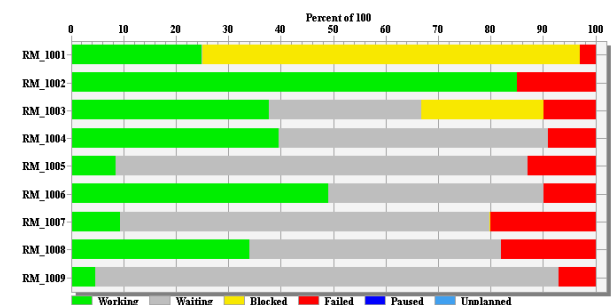


Fig. 6. Graph of machine utilization in Model 1

After the correction of Model 1, in terms of adding the new machine to operation 20, a simulation of the new Model 2 was performed. As a result of Model 2, an annual product increase of 26% was obtained, which gives a total of 6733 pieces per year. By comparing the

data in Figure 6 and Figure 7, it can be concluded that this intervention produce an increase of productivity on almost all machines. It was also evident that the RM_1003 increased the working time by 13%, but also increased the blocking time of the machine by 15%.

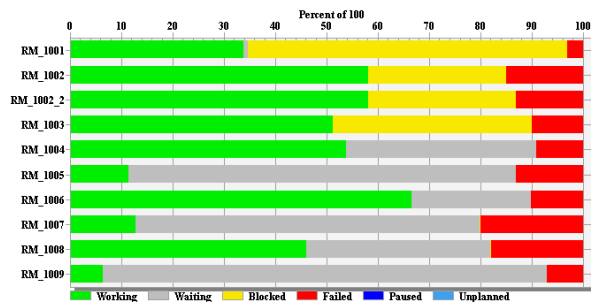


Fig. 7. Graph of machine utilization in Model 2

With further modification of Model 2, described in the previous chapter, it was generated a Model 3. The results of simulation for the Model 3 (Figure 8) show a significant increase in the utilization of all machines, and especially for the machine RM_1003 by 17%. The amount of product that Model 3 can produce now reaches 9069 pieces per year, which is 25% higher productivity than Model 2, or 45% higher productivity than Model 1. The achieved productivity in this case meets the previously set requirements.

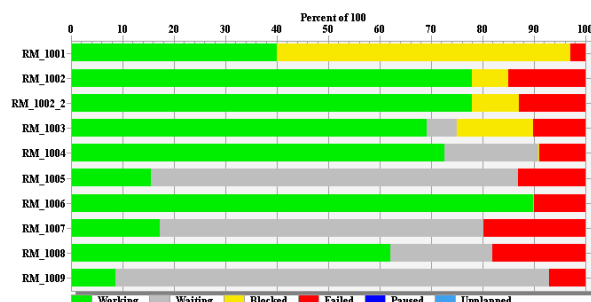


Fig. 8. Graph of machine utilization in Model 3

In order to meet the last requirement, in terms of defining the optimal size of the buffers, *ExperimentManager* tool was used. Optimization of the size of the buffers was performed for the buffers MSK11, MSK12 and MSK16. The results of these optimization studies are shown in Figure 9. Most of the output results (products) were obtained at 10th experiment, which define the size of the buffer MSK11, MSK12 and MSK16, as follows: 1, 4, and 5, respectively.

Input values (Model parameter)				Output values (Results of the simulator)	
Control value	root.MSK11.Capacity	root.MSK12.Capacity	root.MSK16.Capacity	Target value	root.Drain.statDeleted
Exp 01	1	1	1	Exp 01	14
Exp 02	1	1	2	Exp 02	26
Exp 03	1	1	3	Exp 03	2102
Exp 04	1	1	4	Exp 04	2102
Exp 05	1	1	5	Exp 05	2102
Exp 06	1	4	1	Exp 06	17
Exp 07	1	4	2	Exp 07	55
Exp 08	1	4	3	Exp 08	85
Exp 09	1	4	4	Exp 09	594
Exp 10	1	4	5	Exp 10	2473
Exp 11	1	7	1	Exp 11	25
Exp 12	1	7	2	Exp 12	85
Exp 13	1	7	3	Exp 13	85
Exp 14	1	7	4	Exp 14	594

Fig 9. Input and output data from optimization of buffer size

5. CONCLUSION

As conclusion, we can state that Model 3 meets all the requirements of the simulation study. As a result of the addition of one machine, several buffers and product grouping on the machines RM_1003 and RM_1001, production was increased in relation to Model 1 by 45%, or 25% compared to Model 2. Table 2 shows comparative data related to simulation models.

Model	Quantity of products	No. machines	No. buffers	Increasing of productivity related to Model 1
Model 1	4957	9	4	--
Model 2	6733	10	4	25 %
Model 3	9069	10	8	45 %

Table 2. Comparative data related to simulation models

This paper shows that planning and simulation of production processes is an important task in launching a new production or in upgrading the existing one. To avoid running costs and various problems that may arise when starting new or upgrading existing production, it is possible to use *Tecnomatix Plant Simulation* to create a number of simulation models of the production processes and choose the one that generates the best results. Thus virtual simulation models contain all the characteristics of real production systems. Also, there is the possibility of displaying a 3D simulation model, based on a 2D simulation.

6. REFERENCES

- [1] Zelenović, D.: *Projektovanje proizvodnih sistema*, Fakultet tehničkih nauka, Novi Sad, 2003.
- [2] Jovišević, V.: *Projektovanje tehnoloških procesa*, Mašinski fakultet Banjaluka, Banjaluka, 2005.
- [3] Programski sistem *Tecnomatix Plant Simulation* – UGS Corporation - Siemens Product Lifecycle Management Software Inc., 2009.
- [4] Bangsow, S.: *Tecnomatix Plant Simulation: Modeling and Programming by Means of Examples*, Springer International Publishing, 2015.
- [5] Borojević, S., Jovišević, V., Jokanović, S. *Modelling, simulation and optimization of technological process plans*, MMA Novi Sad, 2009.

Authors: Assist. Prof. Stevo Borojević, Full Prof. Vid Jovišević, Assoc. Prof. Đorđe Čiča, Assist. Prof. Branislav Sredanović,, University of Banjaluka, Faculty of Mechanical Engineering, Department of Production and Computer Aided Technologies, Stepe Stepanovića 71, 78000 Banjaluka, Republic of Srpska, Bosnia and Herzegovina, Phone.: +387 51 433-000, Fax: +387 51 465-085.

E-mail: stevoborojevic@hotmail.com;
vid.jovisevic@blic.net;
djordjecica@gmail.com;
sredanovic@gmail.com

Djurdjev, M., Milosevic, M., Lukic, D., Desnica, E., Todoc, V., Kuric, I.

MODIFIED PARTICLE SWARM OPTIMIZATION WITH CHAOTIC MAPS FOR PROCESS PLANNING OPTIMIZATION

Abstract: *Process planning optimization is known to be a popular optimization problem in the literature. Its goal is to find optimal operations sequence and assign appropriate machines, tools and tool approach directions. In addition, constraints in a form of precedence relationships among operations must not be violated. This paper represents the modified particle swarm optimization algorithm (mPSO) employed to solve the process planning problem. Main strategies of genetic algorithm, such as crossover and two mutation strategies have been included in order to improve the performance of the mPSO. Also, due to its large and successful application, chaotic maps are used to add diversity and increase search space. A simulation experiment from the literature has been carried out to verify the validity of the algorithm and the results show that the mPSO performs significantly better than existing algorithms for a given problem instance.*

Key words: *process planning, optimization, precedence relationships, modified PSO, chaotic maps*

1. INTRODUCTION

Computer-aided process planning (CAPP) represents an essential component between computer-aided design and computer-aided manufacturing. The goal of CAPP system is to transform product design into a set of manufacturing instructions. Process planning includes activities such as selection and sequencing of machining operations, selection of available machines, cutting tools and tool approach directions, determination of setup plans, choice of fixtures and calculation of manufacturing time and cost [1]. Assuming the fact that a number of available alternatives of manufacturing resources as well as operations sequences are very large in most cases, an efficient approach in dealing with this issue is highly recommended. The process planning optimization problem belongs to the class of non-deterministic polynomial (NP) hard problems which are based on the fact that number of solutions affect the time and memory required by computer to find the solution. Classic, conventional methods that solve this problem using step-by-step procedure are not efficient enough which boils options down to metaheuristic algorithms and their probabilistic approach to these problems.

Many different methods in the last decade deriving from the field of swarm intelligence are widely implemented for various engineering problems including process planning optimization. Wen et. al. [2] proposed an algorithm based on the mating process between honey bees with the inclusion of precedence relationships among operations. Precedence relationships that form constraints in process planning optimization are involved in order to affect the quality, cost or efficiency of a process plan. They are divided into “hard” constraints a process plan must be consistent with and “soft” constraints that can be violated at some points. Precedence constraints are given in more detail in [3]. Huang et al. [1] developed a genetic algorithm approach which is highly improved

by adding additional techniques for adjusting infeasible process plans to a feasible domain. Apart from standard GA components, crossover and mutation, emphasizing precedence relationships and operation precedence graph, this method proved to be very efficient at the time. Similar approach with a slight changes of techniques for adjustment can be found in [4]. An algorithm that largely influenced this work was proposed by Petrovic et. al [5]. Here, the particle swarm optimization algorithm is enhanced using chaos theory with the emphasis on chaotic maps. This combination has shown to be one of the most effective for process planning optimization so far and the many experiments conducted for its purpose prove it to be true.

This paper is focused on similar approach, introduction of modified particle swarm optimization that involves crossover and two mutation strategies from the GA represented in [1] as well as chaotic maps which were used mostly for increasing search space and improving diversity of the algorithm.

The paper is divided into these sections. Section 2 is concerned with the representation of process plan. Section 3 briefly represents the mathematical model of process planning optimization problem. Section 4 and 5 are focused on the proposed modified PSO approach and the results of simulation experiment, respectively. Concluding remarks are stated in Section 6.

2. REPRESENTATION OF PROCESS PLANNING PROBLEM

Taking into account that, when approaching the process planning problem, one can use two different representation methods. The first, and more frequent in literature, is the one based on AND/OR networks, which can be found in [5]. The other method is based on precedence relationships (PRs) among operations as aforementioned. These representations are proposed by authors in [1, 3, 4].

So called knowledge-based representation of a process plan, this procedure provides a detailed information about numbers of machining operations and their associated machines, tools and tool approach directions (TADs) that are randomly selected from the set of available candidates. Since the mPSO is coded in Matlab programming environment, the following steps of representing process plans slightly differ from the ones given in [1, 3, 4] due to the fact these algorithms were coded in object-oriented programming languages. In a form of a structure array, position of a particle in a swarm is consisted of four string arrays, sequence of operations, machines, tools and TADs, respectively, Fig.1.

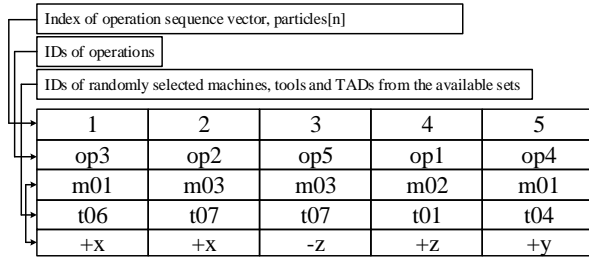


Fig. 1. Representation of a process plan [1, 4]

The number of bits in a string matches the number of operations. The topmost string stands for the indices used for manipulating the data during the search process. As far as PRs are concerned, the best way to formulate them is using matrices, whereas graphs are well suited for providing adequate illustration of precedences among operations. The adjacency matrix is used for showing precedence constraints in which a number 1 means that an operation number in an observed row precedes operation in an observed column, Fig.2. More detailed explanation of knowledge-based representation of process plans can be found in [1, 3, 4].

	op1	op2	op3	op4	op5
op1	0	0	1	0	0
op2	0	0	1	0	0
op3	0	0	0	1	1
op4	0	0	0	0	0
op5	0	0	0	0	0

Fig. 2. Example of the adjacency matrix

3. MATHEMATICAL MODEL OF PROCESS PLANNING OPTIMIZATION

According to the authors [6], the mathematical model is formed on the basis of machining cost criteria of process plans. The total machining cost (PC) of a process plan consists of the following components that are briefly expressed below.

- Total machine cost (MC):

$$MC = \sum_{i=1}^n MCI_i \quad (1)$$

- Total tool cost (TC):

$$TC = \sum_{i=1}^n TCI_i \quad (2)$$

- Machine change cost (MCC):

$$MCC = MCCI \times \sum_{i=1}^n \Omega (M_{i+1} - M_i) \quad (3)$$

- Tool change cost (TCC):

$$TCC = TCCI \times \sum_{i=1}^{n-1} \Omega_2 (\Omega_1 (M_i - M_{i+1}) - \Omega_1 (T_i - T_{i+1})) \quad (4)$$

$$\Omega_1 (X - Y) = \begin{cases} 1, & \text{if } X \neq Y \\ 0, & \text{if } X = Y \end{cases}$$

$$\Omega_2 (X - Y) = \begin{cases} 0, & \text{if } X = Y = 0 \\ 1, & \text{otherwise} \end{cases}$$

- Setup change cost (SCC):

$$SCC = SCCI \times \sum_{i=1}^{n-1} \Omega_2 (\Omega_1 (M_i - M_{i+1}) - \Omega_1 (TAD_i - TAD_{i+1})) \quad (5)$$

- where n stands for the number of operations while MCI_i, TCI_i, MCC_i, TCC_i and SCC_i represent cost indices for used resources and their changes. Total machining cost is calculated as the sum of these cost components. Weight coefficients are excluded from this study.

4. MODIFIED PARTICLE SWARM OPTIMIZATION WITH CHAOTIC MAPS

PSO is one of the most widely applied population-based metaheuristic algorithm belonging to the area of swarm intelligence. It proved to be very effective for various types of combinatorial problems. The natural process that the PSO imitates is social foraging behavior of organisms in "swarms" (flocks, schools etc.) such as birds or fish. The population of particles evolves through generations while recording their positions in each generation as well as their velocities which are important features for achieving balance between exploitation and exploration of search space.

Considering the complexity of the process planning problem, the PSO such as other methods as well, require additional modification in order to achieve efficiency and rapidness in the search process. For that purpose, the standard components of genetic algorithm, crossover and mutation, are employed to diversify the search. Classic swap mutation was implemented as the first mutation strategy in which two genes of a randomly selected particle swap their positions. The second mutation strategy is adopted from the [1, 4] and it refers to machine, tool and TAD mutation of a randomly chosen operation.

Additional improvement of the traditional PSO algorithm within this study is achieved by adding chaotic behavior. Chaotic maps in the literature prove to possess the properties of certainty, stochasticity and ergodicity [5]. Chaos is unpredictable and random which perfectly adapts to the nature of metaheuristics such as the PSO. Ten standard chaotic maps are employed to improve the performance of the PSO, such as Chebyshev, Circle, Gauss/Mouse, Iterative, Logistic, Piecewise, Sine, Singer, Sinusoidal and Tent,

identically as in [5]. The steps of the proposed approach are shortly described in the following subsection.

Steps of mPSO with chaotic maps

Main steps of the modified PSO algorithm with the use of chaotic maps are shortly presented here:

- 1) Initializing swarm – This step creates a population of individuals, so called swarm of particles, using the aforementioned knowledge-based representation of a process plan. Each particle's position represents an array consisted of randomly generated sequence of operations and randomly chosen machines, tools and TADs from the available sets.
- 2) Adjusting infeasible particles – After generating random swarm of particles, some particles are not feasible because of the violation of precedence constraints defined in the adjacency matrix. Namely, the specific heuristic algorithm proposed by [1] has been introduced to adjust infeasible particles to a feasible domain. Due to its complexity and a larger number of steps, this heuristic is described in more detail in [1].
- 3) Fitness evaluation – Fitness of each particle is evaluated after the completion of their adjustment. The objective function is based on total machining cost described in the section 3.
- 4) Global and local best – Initialize global best position values of particles (the best position of all particles so far) and local best position values (the best position of current particle so far).
- 5) Update positions and velocities - Update particle's positions and velocities using standard formulas in which one slight change was made, random numbers are replaced with chaos numbers generated from chaotic maps previously mentioned. Example of machine vector of a particle update :

$$\begin{aligned}
 & \text{part}(i). \text{VelVectors. Machines} = \\
 & w \cdot \text{part}(i). \text{VelVectors. Machines} + c_1 \cdot \text{chaos}(it) \cdot \\
 & \left(\text{part}(i). \text{LocalBest. Machines} - \text{part}(i). \text{PosVectors. Machines} \right) + c_2 \cdot \text{chaos}(it) \cdot \\
 & \left(\text{part}(i). \text{GlobalBest. Machines} - \text{part}(i). \text{PosVectors. Machines} \right) \quad (6) \\
 & \text{part}(i). \text{PosVectors. Machines} \\
 & = \text{part}(i). \text{PosVectors. Machines} \quad (7) \\
 & + \text{part}(i). \text{VelVectors. Machines}
 \end{aligned}$$

where w stands for inertia coefficient and c_1 and c_2 are acceleration coefficients.

- 6) Crossover – With adequate crossover probability p_c , some particles are randomly picked out for crossover. The standard crossover strategy with one point crossover is adopted. Two particles are selected as parents, they are crossed with randomly chosen point, and the first part of parent 1 goes to offspring 1 and the second to offspring 2. The same procedure, but opposite, stands for parent 2 and offspring 2.

- 7) Swap mutation – The first mutation strategy, using p_{m1} mutation probability, works by picking a random particle from a swarm and then randomly selecting two of its genes (using operation indices) where a gene

represents an operation with associated machine, tool and TAD. Positions of these genes are then exchanged. However, the heuristic algorithm from the step 2 is required again, in order to adjust infeasible particles because of the possibility of violating precedence constraints after swapping two genes of a particle.

- 8) Mutation 2 – The second mutation strategy is partially adopted from [1]. Here, after randomly choosing a particle and later one of its genes for mutation with mutation probability p_{m2} , algorithm is programmed to check if there is another available machine for the selected operation (gene) in the set of machine candidates other than the one which is current. If there are no available machines, the current one stays. The same is for tools and TADs within this strategy.

- 9) Repeat over generations – Next, after evaluating updated particles, steps from 4 to 8 are repeated over the defined number of generations.

5. EXPERIMENTAL RESULTS

For the purpose of obtaining optimal process plans, the simulation experiment has been proposed. As already mentioned, the mPSO with chaotic maps is coded in Matlab software using the PC with satisfying configurations: Intel i3 2,1 GHz processor with 3 GB RAM with Windows 7 operating system. The experiment used for testing the algorithm is the prismatic part adopted from authors in [6]. The problem instance consists of 20 operations that need to be sequenced, then 4 machines, 10 tools and 7 different TADs in total. This model is most frequently used prismatic part in the literature.

As far as parameters of the mPSO are concerned, mention the following information is worth mentioning: number of generations is 200, number of particles in a swarm is 80, inertia coefficient starts from 0.5 and linearly decreases to 0.2, both acceleration constants C_1 and C_2 are 1. For the GA strategies: crossover probability p_c is 0.6, and both mutation probabilities p_{m1} and p_{m2} are 0.4.

The optimization objective is to find optimal process plan that has minimal total machining cost previously described in the section 3. Computational results obtained by the modified PSO with chaotic maps clearly expresses its superiority comparing to not only classical PSO but also to the efficient GA approach given in [1]. The results cannot be compared to those obtained from the GA in [3] due to the fact this approach includes additional penalty cost component which is not considered in this study.

The mPSO with chaotic maps proved to be very effective in escaping local optima and its high performances resulted in economical and feasible process plans which may confidently qualify to be new optimal solutions for this problem sample.

Table 1 shows experimental results obtained by the mPSO with chaotic maps for prismatic model from [6] and all available resources. The algorithm was tested for all chaotic maps and 12 runs were made using each of them. Excellent results were obtained with all the maps which proved that chaos has a huge influence on

metaheuristic's performance. Piecewise and Sinusoidal map were the ones that generated process plans with the lowest total machining cost with 2350 and 2360 respectively. The mPSO with the assistance of each chaotic map individually gave at least one result that

was 2500 or below in total machining cost. Apart from only Piecewise and Sinusoidal map, Gauss/Mouse map gave the result which is below 2400. The best result achieved by traditional PSO is greater than 2800.

Operation	1	6	2	11	12	13	14	5	18	7	8	9	15	16	17	4	3	19	20	10
Machine	2	2	2	2	2	2	2	2	2	2	2	2	2	2	2	2	2	3	3	3
Tool	8	2	7	7	3	9	10	7	6	7	4	9	1	5	7	2	7	9	10	10
TAD	+z	-z	-z	-z	-z	-z	-z	-z	-z	a	a	a	-z	-z	-z	-z	+x	+z	+z	a
MC = 980; TC = 270; MCC = 160; TCC = 340; SC = 600; PC = 2350; fitness = 0,00042553																				

Table 1. One optimal process plan for prismatic part [6] using modified PSO and Piecewise chaotic map

Figure 3 shows the convergence curve which provides information about how algorithm advances in finding the optimum during iteration process. This curve matches the run in which mPSO was combined with Piecewise map that resulted in the best process plan so far, so long as the minimal total machining time is concerned. Piecewise and Sinusoidal map are represented in Figure 4.

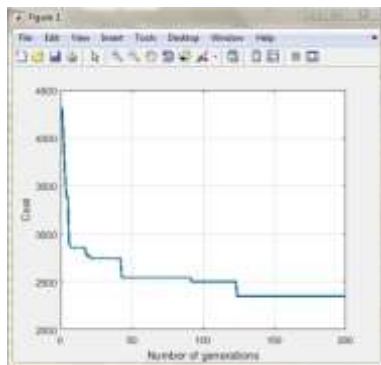


Fig. 3. Convergence curve of the mPSO with chaotic maps

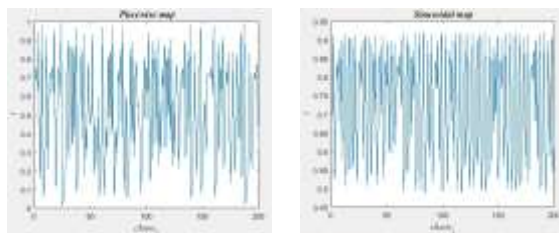


Fig. 4. Piecewise (a) and Sinusoidal (b) chaotic map

6. CONCLUDING REMARKS

Modified particle swarm optimization algorithm with chaotic maps was presented in small detail in this paper. It was proposed for solving process planning optimization problem that has shown to be among the hardest combinatorial optimization problems so far. The algorithm was tested on the sample part model from the literature in order to prove its efficiency. With the emphasis on precedence relationships among operations, the mPSO with chaotic maps gave far better results than expected. With genetic strategies such as crossover and mutation on one side and chaotic maps for improving diversity on the other side, this algorithm found optimal solutions for a problem instance in a reasonable time and appropriate number of generations.

7. REFERENCES

- [1] Huang, W., Hu, Y., Cai, L.: *An effective hybrid graph and genetic algorithm approach to process planning optimization for prismatic parts*, International Journal of Advanced Manufacturing Technologies, Vol. 62, pp. 1219-1232, December 2011.
- [2] Wen, X., Li, X., Gao, L., Sang, H.: *Honey bees mating optimization algorithm for process planning problem*, Journal of Intelligent Manufacturing, Vol.25, pp. 459-472, 2012.
- [3] Li, W. D., Ong, S. K., Nee, A.Y.C.: *Integrated and Collaborative Product Development Environment – Technologies and Implementations*, Series on Manufacturing Systems and Technology Vol.2, World Scientific Publishing Co. Pte. Ltd., Singapore, 2006.
- [4] Borojevic, S.: *Razvoj sistema za simultano projektovanje proizvoda i tehnoloških procesa* – in serbian, Phd thesis, Faculty of Technical Sciences, Novi Sad, Serbia, pp. 157-178, 2015.
- [5] Petrovic, M., Mitic, M., Vukovic, N., Miljkovic, Z.: *Chaotic particle swarm optimization algorithm for flexible process planning*, International Journal of Advanced Manufacturing Technologies, Vol. 85, pp. 2535-2555, November 2015.
- [6] Guo, Y.W., Mileham, A.R., Owen, G.W., Li, W.D.: *Operation sequencing optimization using a particle swarm optimization approach*, Proceedings of the Institution of Mechanical Engineers, Part B: Journal of Engineering Manufacture, Vol. 220, pp. 1945-1958, December 2006.

Authors: MSc Mića Đurđev, Assoc. Prof. Eleonora Desnica, University of Novi Sad, Technical Faculty “Mihajlo Pupin”, Zrenjanin, Đure Đakovića bb, 23000, Zrenjanin, Serbia, Phone.: + 381 23 550 515, E-mail: mica.djurdjev@tfzr.rs ; desnica@tfzr.uns.ac.rs

Assoc. Prof. Mijodrag Milošević, Assoc. Prof. Dejan Lukić, Full Prof. Velimir Todić, University of Novi Sad, Faculty of Technical Sciences, Trg Dositeja Obradovića 6, 21000 Novi Sad, Serbia, Phone.:+381 21 458-2346, E-mail: mido@uns.ac.rs; lukicd@uns.ac.rs; todvel@uns.ac.rs

Full Prof. Ivan Kuric, University of Zilina, Faculty of Mechanical Engineering, Univerzitná 8215/1, 010 26 Žilina, Slovakia, Phone: 041 513 28 07, E-mail: ivan.kuric@fstroj.uniza.sk

Fajsi, A., Moraca S., Cvetkovic, N., Vekic, A., Ljubicic, M.

CLUSTER-BASED PRODUCTION CONCEPT

Abstract: *The development of technology enable manufacturing becomes global affair, not only local activity. Nowadays, companies can relocate their business activities to any part of the world, creating global value chains or becoming member of existing ones. All stakeholders have interdependence in the economic infrastructure but on the other hand, they need to cooperate together in order to achieve desired results. Manufacturing need to be agile and designed to respond effectively to uncertain situations. Small companies are faced with number of problems related to absence of resources, financing sources, expertise, access to technology and software, etc., and today, be agile means adopting approach to solving these problems Most of SMEs are organized within cluster which have a significant role in agile manufacturing achievement. The aim of this paper is to show that agile manufacturing concept is applicable in cluster environment by using Fog computing technology. Cluster-based advanced manufacturing algorithm is shown and described in this paper.*

Key words: *Agility, Agile Manufacturing, Cluster, SMEs*

1. INTRODUCTION

Implementation of agile production concept increases competitiveness and enable companies to have cost efficiently production. This concept supports cooperation with other stakeholders - universities, research and innovation centers, institutes, laboratories, other companies, which is based on open access to the latest knowledge and technologies in all sectors. In the beginning, such kind of concept had use in learning process, theoretical process and knowledge sharing, but over time, it has found its use in industry.

Agile production concept is applicable in both large corporations and small companies, both issues are covered in the literature. The aim of this paper is to show that agile production concept is applicable in cluster environment. Rapid development of ICT technology enables application of this concept and for this purpose, this paper highlights advantages of using Fog computing paradigm.

2. AGILITY AND SMEs

2.1. Agile production concept

The production has several transitions over the years, from the craft industry, to mass production, and the latest stage is agility. The main characteristic of agile production concept is fast adoption to change. Change tends to bring uncertainty to production process and entire business, therefore agility helps companies to overcome these risks and challenges in order to become competitive on the domestic and foreign market. The agile production company is seen as successful organization of the future which is characterized by its ability to respond to unpredictable changes. [1].

Youssef [2] stated that agility goes beyond speed of adjusting of changes; it requires structural and infrastructural changes around company.

Agile production can be considered as the integration of organization, highly skilled and knowledgeable

people, and advanced technologies, to achieve co-operation and innovation in response to the need to supply our customers with high quality customized products [3], [4].

Dimensions of agility of the company are oriented towards competition, changes, customers and people and information. The company needs to utilize resources regardless of type of business and location. As changes in the environment occur, agile production concept enables producers and customers to overcome these barriers. A key competitive advantage of this concept is to promote cooperation within the company and among companies. [1]

The most valued resources in the agile enterprise are people and information. Agility can be achieved by integration of the people, information and technology in order to overcome uncertainty and become flexible and agile company. Gunasekaran (1999) stated that flexibility was the basis for agility [5].

2.2. Agile SMEs and clusters

Basic assumptions for the implementation of Agile production concept in the cluster environment lies in the fact that SMEs, especially ones located in less developed countries have not enough resources for integration of new technologies/resources [6], creating new knowledge, or opportunities to gather information about other organizations. Therefore, it can be said that their success depends mostly on the networking with other stakeholders to provide necessary knowledge, resources and technologies. Agile production concept integrates:

- research and scientific potential of institutions (universities, institutes, and laboratories),
- innovative solutions and flexibility of SMEs, and
- power and potential of clusters, business networks and inter-cluster cooperation will be designed.

Networking should be directed towards: promotion and

boost of technological knowledge and its production personnel to share a common database of parts and products, to share data on production capacities and problems [7].

The agility concept aims to encourage businesses to be forward thinking or proactive in their approach to the marketplace [8]. Dynamic business environment push SMEs to constantly searching for new ways to create and to add value to their products/services/processes in order to increase competitiveness on the international market..

It is also important for SMEs to exchange information constantly and jointly participate in product development. Implementation of agile production concept allows the producers, stakeholders and designers to work together to achieve optimal production with cost-reduction.

The agility of a business depends on many enablers, factors and variables.

Figure 2 highlights some of the key factors that enable business agility.

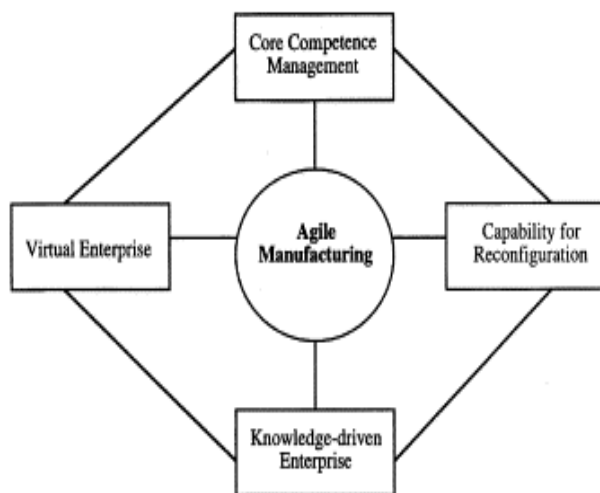


Fig 1. Drivers of agility[2]

Cao (2005) studied the impact of the virtual and knowledge-based enterprises on business performance in an AM environment. The study showed positive links between these categories, virtual and knowledge-based enterprises enable agility in business processes [9]. The essences of both kinds of companies are cooperation and networking with stakeholders

Goldman (1995) states several benefits that companies achieve through cooperation [10]:

- Reduce product development costs, time to market, and business risks,
- Ethic of trust is built and maintained ,
- Acceleration of technology transfer as well as an increase in resource availability,
- Better focus on the human and technological resources.

One of the most important services that cluster provide is certainly possibility of using common equipment and software for common design of products.

This kind of cooperation enable the exchange of

information, assistance in developing and establishing business partnerships, access to modern production technologies and knowledge (Agile technology, Key Enabling Technologies (KET), Lean Manufacturing, Total Quality Management), support in the creation of innovative solutions, projects, products as well as support in establishing the Value Network.

Due to dynamic changes and more stricter customer requirements, clusters tend to become more international and tend to grow from their original form to global value network. Value network can be defined as "any set of roles and interactions in which people engage in both tangible and intangible exchanges to achieve economic or social good" [11].

Agile production concept is focused on meeting the needs of customers while maintaining high standards of quality and controlling the overall costs involved in the production of a particular product on the local and international level.

Clusters have an important role in implementing agile production concept among SMEs by enhancing collaboration, flexibility and knowledge /resources/technology sharing.

In the next chapter will be proposed model which indicating position of cluster and the company in the agile production process and relations between them.

3. APPLICATION OF AGILE PRODUCTION IN THE CLUSTER ENVIRONMENT

3.1. Cluster-based agile production

The key element of proposed model is cluster-based advanced production algorithm which is launched for each product. The aim of this algorithm is using of advanced technologies (nano technology, automatization, new materials, rapid prototyping, rapid tooling..) in the early phases in order to create compatible parts for development common products.

In this model focus is put on the higher level of networking. Each member of network doing business and develop things they know the best based on the principle of flexible specialization .

The main idea of this model is application of the Agile production concept as a concept of optimization of planning and programming production processes in complex organizational structures like cluster. Implementing this approach on the cluster level presents new concept where working cells are actually companies or their division within cluster.

Based on flexible specialization concept they will be elected by criteria such as the best experience, the best knowledge they have and adequate technology. Each of them has a own role in creating of new or improved products.

Adoption of agile production is not a trivial task with barriers existing throughout its entire life cycle, from development and implementation to its maintenance and improvement phases.

Figure 3 represents proposed model of implementing Agile production concept in the cluster environment.

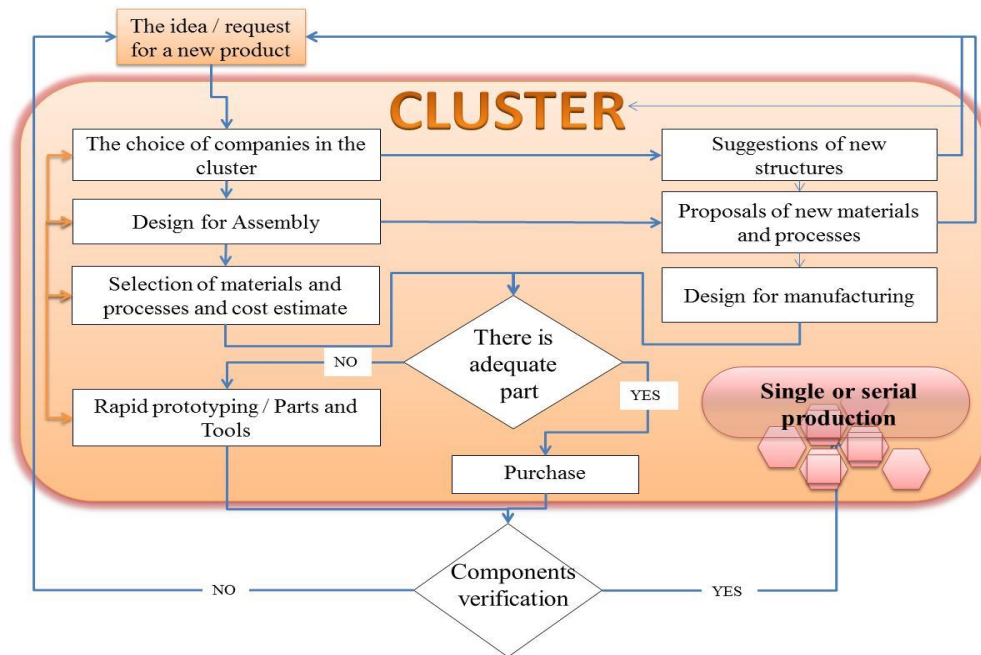


Fig. 2. Cluster-based advanced manufacturing model

However, this model has limitations, agile production is affected by number of factors from environment. Hasan (2007) proposed the most usual barriers to agile manufacturing: Poor design-manufacture interface, Lack of customers feedback, Insufficient training, education and reward system, Resistance to organizational change, Poor partnership (or supply chain) formation, Unavailability of appropriate technology Lack of top management support and commitment, There is no assessment technique to justify high investment in advanced manufacturing technology, Poor incorporation of flexibility measures into management, Inappropriate measurement approaches for qualitative benefits and agility, Lack of methodologies to enhance agility[13].

Cluster provides clear defined rules, standards and procedures, consistency in the work for overcoming these barriers, and the most important it provides communication among low organizational levels.

It is necessary to organize a geographically distributed production that needs to be controlled and built according to some principles and rules. It can be achieved by application of Fog computing paradigm.

3.2. Fog computing

The emerging paradigm of agile production systems has revolutionized the building of intelligent and decentralized structures in cluster environment.

In the paper agile production concept is introduced through special emphasis is laid on methodological issues and deployed decentralized industrial systems.

For the effective functioning of the agile production concept in the cluster environment it is necessary to organize a geographically distributed production that should provide lower costs of production and shorter delivery time. All this should be enabled by using of Fog computing ICT infrastructure

Two modern ICT technologies that enable the integration of the cluster based production systems and facilitate the realization of the concept of agile production are: cloud computing and fog computing.

Fog Computing extends the Cloud Computing paradigm to the edge of the network [13]. This paradigm provides improved quality of services, low latency and location awareness to nodes.

Fog computing is defined “as a distributed computing paradigm that fundamentally extends the services provided by the cloud to the edge of the network”. [14] Figure 4 presents graphical explanation of Fog computing paradigm.

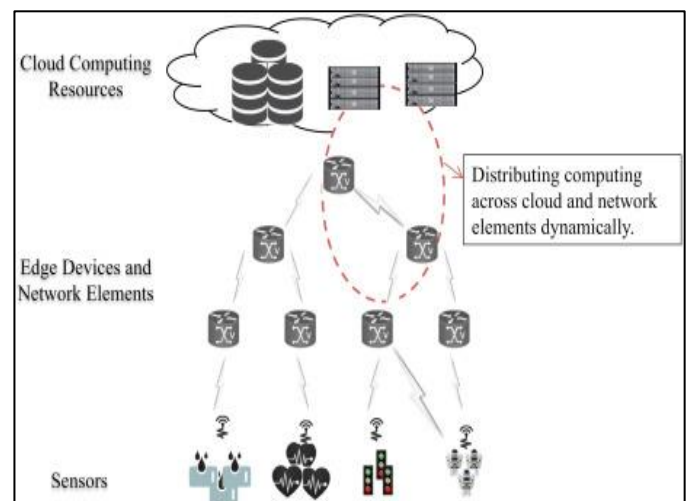


Fig.3 Fog Computing Paradigm [14]

Very similar to Cloud, Fog computing provides data, compute, storage, and application services to customers and brings a lot of advantages to production system such as: reduction of network traffic, suitable for

Internet of Things tasks: low-latency requirement, scalability [15].

One important effect of cluster based agile production is the fact that due to using control automation many work pieces can be produced cost-effectively not just in large quantities, but also in much smaller lots. Fog computing provide better quality of service in terms of delay, power consumption, reduced data traffic over the Internet, then supports applications that require low latency, and mobility [16].

4. FINAL REMARKS

Understanding application of Agile manufacturing concept in the cluster environment is based on the understanding concepts of cooperation and networking. The aim of this model is using of advanced technologies such as nano technology, automatization, new materials, rapid prototyping, rapid tooling, in the early research and production phases in order to create compatible parts for development common products. Companies within the network are in the most cases incompatible and much time goes making them compatible. By using advanced ICT paradigms, such as Fog computing, production from geographically distributed locations becomes integrated and cost-efficient.

Creating an innovative environment allows the development and the production of highly customized joint products that are in accordance with specific customer requirements, produced in the shortest possible time and with the lowest cost.

The main advantage of proposed concept is its functioning for a longer period and possibility to help SMEs to find their place in the production cycle that will make them better positioned on the international market.

5. REFERENCES

- [1] Meade, L. & Sarkis, J. *Analyzing organizational project alternatives for agile manufacturing processes: an analytical network approach*, 37(2), 241-26, International Journal of Production Research, 1999
- [2] Yusuf, Y., Sarhadi, M., & Gunasekaran, A. *Agile manufacturing: The drivers, concepts and attributes*, 62(1-2), 33-43., International Journal of production economics, 1999
- [3] Jackson, M., & Johansson, C.. *An agility analysis from a production system perspective*. 14(6), 482-488. Integrated Manufacturing Systems, 2003
- [4] Goldman, S. L., Nagel, R. N. a&nd Preiss, K., *Agile Competitors and Virtual Organizations*, Van Nostrand Reinhold, New York, 1995
- [5] Gunasekaran, A. *Agile manufacturing: a framework for research and development*. 62(1-2), 87-105, International journal of production economics, 1999
- [6] Van de Vrande, V., De Jong, J. P., Vanhaverbeke, W., & De Rochemont, M. *Open innovation in SMEs: Trends, motives and management challenges*. 29(6-7), 423-437, Technovation, 2009
- [7] Kumar, Babu, Saravanan, & Murugan, *Agile manufacturing in small and medium scale enterprises*, Second National Conference on Trends in Automotive Parts Systems and Applications (TAPSA-2014), India, 2014
- [8] Ismail, H. S., Poolton, J., & Sharifi, H. *The role of agile strategic capabilities in achieving resilience in manufacturing-based small companies*. 49(18), 5469-5487 International Journal of Production Research, , 2011
- [9] Cao, Q., & Dowlatshahi, S. *The impact of alignment between virtual enterprise and information technology on business performance in an agile manufacturing environment*. 23(5), 531-550, Journal of Operations Management , 2005
- [10] Goldman, S. L. & Nagel, R. N., *Management, technology, and agility: the emergence of a new era in manufacturing*. 8, 18- 38, International Journal of Technology Management, 1993,
- [11] Allee, V. *Value network analysis and value conversion of tangible and intangible assets*. 9(1), 5-24, Journal of intellectual capital, 2008
- [12] Hasan, M. A., Shankar, R., & Sarkis, J. *A study of barriers to agile manufacturing*. 2(1), 1-22, International Journal of Agile Systems and Management, 2007
- [13] Osanaiye, O., Chen, S., Yan, Z., Lu, R., Choo, K. K. R., & Dlodlo, M. *From cloud to fog computing: A review and a conceptual live VM migration framework*. 5, 8284-8300 IEEE, 2017
- [14] Dastjerdi, A. V., Gupta, H., Calheiros, R. N., Ghosh, S. K., & Buyya, R. *Fog computing: Principles, architectures, and applications*. pp. 61-75, In Internet of Things, 2016
- [15] Stojmenovic, I., & Wen, S. *The fog computing paradigm: Scenarios and security issues*. In Computer Science and Information Systems (FedCSIS), pp. 1-8, Federated Conference IEEE, 2014
- [16] Firdhous, M., Ghazali, O., & Hassan, S. *Fog computing: Will it be the future of cloud computing?*. The Third International Conference on Informatics & Applications, 2014

¹M.Sc Angela Fajsi, ²Assoc. Prof. Slobodan Moraca, ³M.Sc Nela Cvetkovic, ⁴M.Sc Aleksandar Vekic, ⁵Marko Ljubičić

¹²³⁴University of Novi Sad, Faculty of Technical Sciences, Department of Industrial Engineering and Management, Trg Dositeja Obradovica 6, 21000 Novi Sad, Serbia, Phone.: +381 21 485 2188;

⁵Donghua University of China

E-mail: angela.fajsi@uns.ac.rs; moraca@uns.ac.rs; nelacvetkovic@uns.ac.rs; vekic@uns.ac.rs; mr.ljubicic@gmail.com

ACKNOWLEDGMENTS:

This work was partially supported by the Ministry of Education, Science and Technology Development of the Republic Serbia under Grant number TR-35050, for the period 2011-2018.

Mircheski, I.

DETERMINATION OF DISASSEMBLY INTERFERENCE MATRIX AND IMPROVED NONDESTRUCTIVE DISASSEMBLY SEQUENCES FOR THE PRODUCT

Abstract: *This paper presents improved method for determination of disassembly interference matrix and improved nondestructive disassembly sequences during the product evaluation stage. The main objective of the improved method for nondestructive disassembly is increasing of recycling, recovery or reuse of the components. The determination of disassembly interference matrix is based on information obtained from 3d CAD model of product and developed software package. The goal of this research is to support and help product designer to create product with improved performance in order to nondestructive disassembly and predict, evaluate and define nondestructive disassembly sequences with low costs for disassembly, minimizing of reorientation of tools in the design stage when the 3d CAD model of product is available. Verification of the improved method for determination of disassembly interference matrix and improved nondestructive disassembly sequences is presented through an illustrative example.*

Key words: *disassembly interference matrix, nondestructive disassembly sequences, product*

1. INTRODUCTION

Nondestructive disassembly is the process of removing the connectivity of components in the product and separate components in order to improved process of recycling, recovery or reuse. At the end of their useful life, products become waste [1]. The waste from end-of-life products can be defined as unnecessary goods or residues that do not have value for the owner [2]. During the last few decades, the rapid development of automobiles, electric and electronic equipment, resulted in creation of billions tones of waste. For instance, “around 3 billion tonnes of waste are generated in the EU each year - over 6 tonnes for every European citizen [3].” Current legal regulations clearly indicate that technical products should be designed considering the recovery of the product at its end-of-life stage. In Europe, designers have to follow European directives for environment protection and are obliged to incorporate these directives into the product design in order to preserve the environment or minimize the impact of pollution.

Design for Disassembly – DfD is a design tool for optimization of product structure and other design parameters in order to simplify and improve the disassembly of components for service, replacement or reuse [4]. DfD improves the disassembly of components by selecting proper fasteners, grouping the materials for recycling, and optimizing the product architecture and characteristics of the components in the product assembly to limit the costs of disassembly. The benefits of the design for disassembly are resulting in: increasing the percentage of reuse of components and material recycling; reduction of their adverse impact on the environment; easier servicing and maintenance of products, and greater total return from the end-of-life products.

2. RELATED WORK

Product disassembly is required both during the product life cycle and after the end of the product useful life. The disassembly process can be destructive and non-destructive. Destructive disassembly represents a process where the stream of end-of-life products is shredded in small fragments which are later separated according to their material composition using special separation techniques [5]. Non-destructive disassembly process is applied during the exploitation of the product and at product end-of-life. During the product exploitation, maintenance, service or replacement of some non-functional components is needed. For end-of-life products, the nondestructive disassembly process is needed for: the recovering of functional components; the removal of hazardous materials from the product that can have negative influence on the recycling process and can pollute the environment; the extraction of precious materials from the product; remanufacturing, etc [6]. In general the disassembly process requires two main processes which are the disjoining process and removal of the components from the product structure [7].

Many authors have developed different methods for determining of the improved disassembly sequence and for planning of the disassembly process. Lambert and Gupta in series of papers [8-10] propose a linear programming method for determination of optimal disassembly sequences for end-of-life products. The method of linear programming contributes to the optimization of the disassembly process. F. Cappelli et al. [11] presents a theoretical basis for creation of computer-aided design tool for optimization of the disassembly sequences of mechanical systems for improving maintenance and recycling activities. In the first step, the physical constraints that oppose the movement of mechanical elements are investigated, starting from the three-dimensional computer-aided design representation and an AND/OR graph of

mechanical disassembly are generated. The second step is the representation of binary trees that allow automatic exploration of the set of all possible disassembly sequences. F. Giudice et al. in the papers [12,13] proposed a structured methodology for analysis and reconfiguration of disassembly depth distribution of components in the product assembly with aim for obtaining a generalised improvement in disassemblability in relation with requirements for servicing.

Computer-aided design (CAD) today is an inseparable part of the design process. In the paper [14] is presented an integrated approach of disassembly constraint generation, based on object-oriented prototype which is designed and developed. With this approach is obtained CAD model information necessary for designers for implementation of information in further application for disassembly planning. Huang et al. presents [15] disassembly matrix in a binary system for solving of disassembly processes of product. By using a Boolean operation or arithmetic operator with depth-first-search method is developed algorithm for generating of possible disassembly sequences together with directions of components removing. Disadvantage of proposed algorithm is the inability to obtain parallel disassembly sequences. This algorithm can be used only for obtaining of sequential disassembly sequences.

3. DETERMINATION OF DISASSEMBLY INTERFERENCE MATRIX

3.1 Product representation

The product assembly consists of a number of discrete components, such as, parts, fasteners, etc. Components can be grouped in subassemblies. A subassembly is a connected set of components and fasteners. If components are physically linked, such link is called a connection.

Connections restrict the freedom of motion of the components involved. In many cases, specialized components such as fasteners are used for connections. Fasteners can be discrete components such as screws, which are obtained with developed CAD macro module for reading from the CAD assembly model or non-discrete virtual objects such as snap fits, press fits, etc, which are defined manually in the developed software module between connection of components. The set of components can be given by the following expression:

$$C = \{C_1, C_2, \dots, C_n\} \quad (1)$$

The set of fasteners can be given by the following expression:

$$F = \{F_1, F_2, \dots, F_m\} \quad (2)$$

where n is the number of components in the product assembly and m is the number of fasteners in the product. The assembly is composed of all components and fasteners and can be represented mathematically with the expression $A = C_1 C_2 \dots C_n F_1 F_2 \dots F_m$.

In order to demonstrate the proposed 3D CAD integrated method for improving of the design for nondestructive disassembly process, the shaft with gears assembly shown in the Figure 1 is used as an

example.

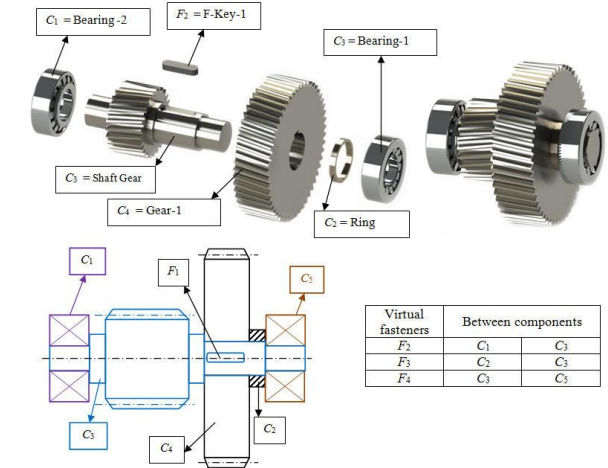


Fig. 1. Exploded view, assembly and cross-section view of subassembly shaft with gears.

3.2 Contact matrix

The relationships between components and fasteners in an assembly are required in order to determine all subassemblies in the assembly. For this reason, a contact matrix and contact diagram between components and fasteners and components are defined. The contact diagram represents a visualization tool for analysis of the subassemblies in the product assembly. If the component is in contact with some fastener in the assembly the element $F_j C_i$ in contact matrix will be equal of 1, in otherwise 0. If the component is in contact with other component in the assembly the element C_{ij} in contact matrix will be equal of 1, or otherwise 0. The contact matrix between components can be represented with the follow equation [16]:

$$CC = [C_{ij}]_{i=1,2,\dots,n}^{j=1,2,\dots,n} \quad (3)$$

The contact matrix between components and fasteners can be represented with the following equation [16]:

$$FC = [F_j C_i]_{i=1,2,\dots,n}^{j=1,2,\dots,m} \quad (4)$$

In the Figure 2a) is represented contact matrix and diagram between components, and 2b) contact matrix and diagram between components and fasteners for example which is shown in the Figure 1.

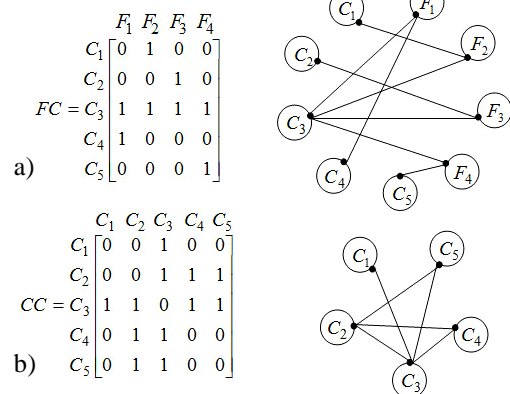


Fig. 2. Contact matrix and diagram for a) contacts between components, and b) contacts between components and fasteners in the product assembly.

3.3 Subassemblies

The total number of subassemblies generated for the example assembly is 14.

$$SA = \{ C_1C_2C_3C_4F_1F_2F_3, C_1C_3C_4C_5F_1F_2F_4, C_2C_3C_4C_5F_1F_3F_4, C_1C_2C_3C_5F_2F_3F_4, C_1C_3C_4F_1F_2, C_2C_3C_4F_1F_3, C_3C_4C_5F_1F_4, C_1C_2C_3F_2F_3, C_1C_3C_5F_2F_4, C_2C_3C_5F_3F_4, C_3C_5F_4, C_2C_3F_3, C_1C_3F_2, C_3C_4F_1 \}.$$

3.4 Disassembly operation

The total number of disassembly operations for this example is 38. The disassembly operations are shown in Figure 3.

0;C1,C2,C3,C4,C5,F1,F2,F3,F4;	19;C2,C3,C5,F3,F4;C4,F1
1;C1,C2,C3,C4,F1,F2,F3;C5,F4	20;C1,C2,C3,F2,F3;C5,F4
2;C1,C3,C4,C5,F1,F2,F4;C2,F3	21;C1,C3,C5,F2,F4;C2,F3
3;C2,C3,C4,C5,F1,F3,F4;C1,F2	22;C2,C3,C5,F3,F4;C1,F2
4;C1,C2,C3,C5,F2,F3,F4;C4,F1	23;C1,C3,F2;C4,F1
5;C1,C3,C4,F1,F2;C2,C5,F3,F4	24;C3,C4,F1;C1,F2
6;C2,C3,C5,F3,F4;C1,C4,F1,F2	25;C2,C3,F3;C4,F1
7;C2,C3,C4,F1,F3;C1,C5,F2,F4	26;C3,C4,F1;C2,F3
8;C1,C3,C5,F2,F4;C2,C4,F1,F3	27;C3,C5,F4;C4,F1
9;C3,C4,C5,F1,F4;C1,C2,F2,F3	28;C3,C4,F1;C5,F4
10;C1,C2,C3,F2,F3;C4,C5,F1,F4	29;C2,C3,F3;C1,F2
11;C1,C3,C4,F1,F2;C2,F3	30;C1,C3,F2;C2,F3
12;C2,C3,C4,F1,F3;C1,F2	31;C3,C5,F4;C1,F2
13;C1,C2,C3,F2,F3;C4,F1	32;C1,C3,F2;C5,F4
14;C1,C3,C4,F1,F2;C5,F4	33;C3,C5,F4;C2,F3
15;C3,C4,C5,F1,F4;C1,F2	34;C2,C3,F3;C5,F4
16;C1,C3,C5,F2,F4;C4,F1	35;C3,C5,F4
17;C2,C3,C4,F1,F3;C5,F4	36;C2,C3,F3
18;C3,C4,C5,F1,F4;C2,F3	37;C1,C3,F2
	38;C3,C4,F1

Fig. 3. List of disassembly operations

3.5 Nondestructive disassembly sequences

The total number of nondestructive disassembly sequences is shown in Figure 4.

0;1;11;23;37	0;3;17;25;36	0;5;23;37
0;1;11;24;38	0;3;17;26;38	0;5;24;38
0;1;12;25;36	0;3;18;27;35	0;6;33;35
0;1;12;26;38	0;3;18;28;38	0;6;34;36
0;1;13;29;36	0;3;19;33;35	0;7;25;36
0;1;13;30;37	0;3;19;34;36	0;7;26;38
0;2;14;23;37	0;4;20;29;36	0;8;31;35
0;2;14;24;38	0;4;20;30;37	0;8;32;37
0;2;15;27;35	0;4;21;31;35	0;9;27;35
0;2;15;28;38	0;4;21;32;37	0;9;28;38
0;2;16;31;35	0;4;22;33;35	0;10;29;36
0;2;16;32;37	0;4;22;34;36	0;10;30;37

Fig. 4. List of the total number of nondestructive disassembly operations

3.6 Disassembly interference matrix

Disassembly interference matrix is obtained from 3D CAD assembly model of product based on the directions of $\pm x$, $\pm y$ and $\pm z$ axis, respectively. The matrix is with dimension $n+m \times n+m$ which depends on the number of components n and fasteners m in the product. The elements in the matrix are binary pairs of numbers $x_i y_i z_i$ where $i = 1, \dots, n+m$. If interference exists between components or fasteners C_i or F_i and C_j or F_j , where $j = 1, \dots, n+m$ and $i < j$, in direction of the $+x$ -axis, then the element $x_{i,j}$ in the matrix (5) is equal to 1. In the opposite, the element $x_{i,j}$ in the

matrix (5) is 0. If $i=j$ the element $x_{i,j}$ is equal to 0, because no component or fastener can have interference with itself [17].

With the disassembly interference matrix, the priority for detachment of components and fasteners in directions of $\pm x$, $\pm y$ and $\pm z$ axis is defined. The disassembly priority is required in the process of the generation of disassembly sequences with a goal to keep only the feasible disassembly operations. The disassembly interference matrix for the product assembly example is given with equation (5).

$$I_{\pm x \pm y \pm z} = \begin{matrix} & C_2 & C_1 & C_4 & F_1 & C_3 & C_5 & F_2 & F_3 & F_4 \\ \begin{matrix} C_2 \\ C_1 \\ C_4 \\ F_1 \\ C_3 \\ F_2 \\ F_3 \\ F_4 \end{matrix} & \begin{bmatrix} 000000 & 001000 & 001000 & 001000 & 111110 & 000001 & 000000 & 000000 & 000000 \\ 000001 & 000000 & 000001 & 000001 & 110111 & 000001 & 000000 & 000000 & 000000 \\ 000001 & 001000 & 000000 & 110110 & 111110 & 000001 & 000000 & 000000 & 000000 \\ 000001 & 001000 & 110110 & 000000 & 111101 & 000001 & 000000 & 000000 & 000000 \\ 110111 & 111110 & 110111 & 101111 & 000000 & 110111 & 000000 & 000000 & 000000 \\ 001000 & 001000 & 001000 & 001000 & 111110 & 000000 & 000000 & 000000 & 000000 \\ 000000 & 000000 & 000000 & 000000 & 000000 & 000000 & 000000 & 000000 & 000000 \\ 000000 & 000000 & 000000 & 000000 & 000000 & 000000 & 000000 & 000000 & 000000 \end{bmatrix} \end{matrix} \quad (5)$$

4. DETERMINATION OF IMPROVED NONDESTRUCTIVE DISASSEMBLY SEQUENCES

After determining the priority of detaching of components and fasteners in the product and after definition of the lists for all disassembly direction, all disassembly sequences are checked and impossible disassembly operations are deleted.

The generated possible disassembly sequences are shown in Figure 5. The total number of disassembly sequences is this case is 8.

0;1 (C5 F4);11 (C2 F3);23 (C4 F1);37 (C1 C3 F2);
0;1 (C5 F4);11 (C2 F3);24 (C1 F2);38 (C3 C4 F1);
0;1 (C5 F4);12 (C1 F2);26 (C2 F3);38 (C3 C4 F1);
0;3 (C1 F2);17 (C5 F4);26 (C2 F3);38 (C3 C4 F1);
0;5 (C2 C5 F3 F4);23 (C4 F1);37 (C1 C3 F2); parallel
33 (C2 F3);35 (C5 F4);
0;5 (C2 C5 F3 F4);23 (C4 F1);37 (C1 C3 F2); parallel
34 (C5 F4);36 (C2 F3);
0;5 (C2 C5 F3 F4);24 (C1 F2);38 (C3 C4 F1); parallel
33 (C2 F3);35 (C5 F4);
0;5 (C2 C5 F3 F4);24 (C1 F2);38 (C3 C4 F1); parallel
34 (C5 F4);36 (C2 F3);

Fig. 5. The list from all possible disassembly sequences

5. CONCLUSION

The goal of the paper is to provide an improved method for DfD analysis of the product in the early phase of the product development, through generation of the improved disassembly sequence, fastener analysis and product structure examination. Such method should help the designers during of virtual design phase in order to satisfy the European waste directives, and to improve further the suitability of the new products from the aspect of disassembly and recycling.

3D CAD integrated methodology for product design for nondestructive disassembly process for determination of the improved disassembly sequence is presented. The proposed methodology is applied in solving a realistic problem in the product design phase. With the developed method and software, all possible subassemblies and disassembly operations for the

product can be determined, based on the priority for detachment in different disassembly directions. Also, the improved disassembly sequence can be estimated based on the disassembly times, revenue and costs of disassembly. The input of geometric data in the system is performed automatically by analysis of the CAD model of the product.

The developed method and integrated software package will assist designers in creating better technical products that will be improved for nondestructive disassembly. However, as the efficiency of the disassembly sequence is strongly governed by the relationship between the cost of the envisioned disassembly operations and the respectively generated potential revenues, the excellence of the designer in selecting the most desirable fasteners in terms of nondestructive disassembly of the final product remains to be of crucial importance.

6. REFERENCES

- [1] Gungor, A., and Gupta, S.M.: *Issues in environmentally conscious manufacturing and product recovery: a survey*, Computers & Industrial Engineering, 36, pp. 811-853, Elsevier Science Ltd., 1999.
- [2] Hentschel, C.: *The greening of products and production. A new challenge for engineers*, In: Pappas IA, Tatsiopoulou IP, editors. *Advances in production management systems B-13*. Amsterdam, The Netherlands: Elsevier Science Publishers, pp. 39-46, 1993.
- [3] Life Cycle Thinking and Assessment for Waste Management, http://ec.europa.eu/environment/waste/publication/s/pdf/Making_Sust_Consumption.pdf
- [4] Lambert, A.J.D., Gupta S.M.: *Disassembly Modeling for Assembly, Maintenance, Reuse, and Recycling*, CRC PRESS, New York, pp. 287-336, 2005.
- [5] Giudice, F., Guido, L.R., Risitano, A.: *Product Design for the Environment – A Life Cycle Approach*, Taylor & Francis Ltd., London, pp. 375-404, 2006.
- [6] Xanthopoulos, A., Iakovou E.: *On the optimal design of the disassembly and recovery processes*, Waste Management 29, Elsevier Ltd., pp. 1702–1711, 2009.
- [7] Sodhi, R., Sonnenberg, M., Das, S.: *Evaluating the unfastening effort in design for disassembly and serviceability*, J. Eng. Design, Vol. 15, No. 1, Taylor & Francis Ltd., pp. 69–90, 2004.
- [8] Lambert, A.J.D.: *Optimal disassembly of complex products*, Int. J. Prod. Res., vol. 35, no. 9, Taylor & Francis Ltd., pp. 2509-2523, 1997.
- [9] Lambert, A.J.D.: *Determining optimum disassembly sequences in electronic equipment*, Computers & Industrial Engineering 43, Pergamon, pp. 553–575, 2002.
- [10] Lambert, A. J. D., Gupta, S.M.: *Methods for optimum and near optimum disassembly sequencing*, International Journal of Production Research, Taylor & Francis Ltd., Vol. 46, No. 11, pp. 2845–2865, 2008.
- [11] Cappelli, F., Delogu, M., Pierini, M., Schiavone, F.: *Design for disassembly a methodology for identifying the optimal disassembly sequence*, Journal of Engineering Design, Vol. 18, No. 6, Taylor & Francis Ltd., pp. 563–575, 2007.
- [12] Giudice, F., Fargione, G.: *Disassembly planning of mechanical systems for service and recovery a genetic algorithms based approach*, J. Intell. Manuf. 18, Springer Science+Business Media, pp. 313–329, 2007.
- [13] Giudice, F.: *Disassembly depth distribution for ease of service: a rule-based approach*, Journal of Engineering Design, Vol. 21, No. 4, Taylor & Francis Ltd., pp. 375–411, 2010.
- [14] Rong L.J., Wang Q., Hui Huang P.: *An integrated disassembly constraint generation approach for product design evaluation*, International Journal of Computer Integrated, Vol. 25, No. 7, Taylor & Francis Ltd., pp. 565–577, 2012.
- [15] Huang, Y.M., Chun, T.H.: *Disassembly matrix for disassembly processes of products*, Int. J. Prod. Res., vol. 40, no. 2, Taylor & Francis Ltd., pp. 255-273, 2002.
- [16] Mircheski, I., Kandikjan, T.: *Design for disassembly methodology for determination of optimal disassembly sequence based on contact relations between components and fasteners in the product assembly*, Proceedings of the 11th International Scientific Conference MMA 2012 – Advanced production technologies, Faculty of technical sciences Novi Sad, Serbia, pp. 263-268, 2012.
- [17] Mircheski, I., Kandikjan, T., Prangoski, B.: *A mathematical model of non-destructive disassembly process*, International Journal of Mechanical and Production Engineering Research and Development, Vol. 2-4, TJPRC, pp. 61-72, 2012.

Author: Assist. Prof. Ile Mircheski, University Ss. Cyril and Methodius, Faculty of Mechanical Engineering - Skopje, Karposh 2 bb, 1000 Skopje, Republic of Macedonia, Phone.: +389 70 271185.
E-mail: ile.mircheski@mf.edu.mk

Mitrovic, S., Dimic, Z., Jakovljevic, Z.

DISTRIBUTED CONTROL OF MANUFACTURING RESOURCES – SECURITY RELATED ISSUES

Abstract: Industry 4.0 paradigm dictates highly efficient and flexible production through introduction of reconfigurable manufacturing systems and resources characterized by modularity, interoperability, scalability and communication capabilities. Various approaches are currently researched worldwide in an effort to achieve the next level of production technologies without compromising the production itself. Considered approaches imply implementation of Cyber Physical Systems, Internet of Things and generation of manufacturing systems Digital Twins. Complex industrial control systems, which were traditionally wired and considered safe, are now becoming distributed, internet-connected, usually based on wireless communication and wide open for all kinds of malicious exploits with potentially fatal consequences. This paper presents a review of security related issues that are crucial in developing safer wireless distributed control of manufacturing resources, adept for challenges in coming times.

Key words: Industry 4.0, distributed control systems, manufacturing cyber security, Internet of Things.

1. INTRODUCTION

Rapid advancement and broad deployment of information and communication technologies (ICT) is radically changing the world of today. Miniaturized, multipurpose, high performance electronic networked devices are becoming ubiquitous and indispensable in all segments of modern society, including the industry. Under the influence of ever growing market demands, in an attempt to further boost quality of the goods and shorten response time, production companies are evolving, maintaining competitiveness by steadily embracing new production paradigms based on coming technologies – Internet of Things (IoT) [1] and Cyber-Physical Systems (CPS) [2].

Introduction of the IoT and services into the manufacturing environment represents a base for fourth industrial revolution – Industry 4.0 [3]. It is expected that smart factories will be able to meet requirements of each individual customer, including one-off items. IoT and, consequently, CPS are perceived as innovative, disruptive technologies, with horizontal and vertical digital integration possibilities based on pervasive deployment and networking of smart objects [4]. Such a vast and complex network poses many challenges, among which security and reliability are of the highest priority. Cyber threats are already formidable for every mission-critical system (power and water distribution, production, waste management etc.).

This paper aims to review several security related issues, in particular cyberattacks whose modeling is of high priority for generation of secure wireless distributed control of manufacturing resources. Due to the difference in system's control and modeling approaches, we will consider possible attacks in continuous time and discrete event systems separately. The remainder of the paper is structured as follows. In Section 2, distributed control systems and potential attack variants are discussed. Section 3 presents

deception attacks in continuous time systems while Section 4 deals with attacks in discrete event systems. Finally, in Section 5, we give some concluding remarks along with guidelines regarding future work.

2. DISTRIBUTED CONTROL SYSTEMS AND ATTACKS

IoT and CPS implementation, through utilization of smart devices with integrated computation and communication capabilities, bring about significant changes in manufacturing systems and resources control. Although all functional elements of five-level automation hierarchy will remain, strict automation pyramid gives the way to distributed control systems. In distributed control, instead of controlling manufacturing system or resources centrally, the control is carried out through communication and interoperation of different smart devices (Fig. 1). As CPS based and communication intensive, distributed control systems are inherently prone to different kinds of cyberattacks. In addition, since, as expected [3], a significant part of communication will be wireless, security issues become even more severe.

Although all components of the system (sensors, actuators, etc.) may be subject of an attack in a cyber or physical domain, targeting them individually or in a combined manner, in this paper we will focus on the attacks carried out through communication channels.

During communication between different agents in distributed control system, confidentiality, integrity and availability of the data must be preserved at all times.

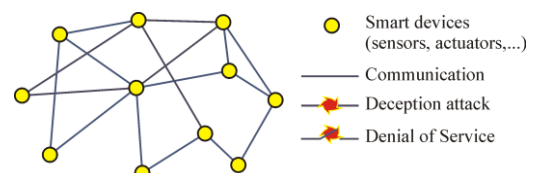


Fig. 1. Distributed control system and types of attack.

Confidentiality allows only the party with proper access rights to read the data, while integrity guarantees that the received data is genuine and no unauthorized changes were made. Availability enables access to data and system resources within the required time frame. Depending on the type of attack, adversaries aim to change some or all of the listed data properties.

In general, malicious cyberattacks can be split into two basic groups – Denial of Service (DoS) and deception attacks. DoS attacks compromise the availability of data, making the data or the requested resource permanently or temporarily inaccessible causing data loss or data delay. DoS attacks are disruptive, do not require knowledge about the attacked system and are not stealthy, but can be misdiagnosed, typically as network connection issues [5].

Deception attacks compromise data integrity and send corrupted data to the system components, thus altering behavior of the system. Deception attacks are more sophisticated than DoS attacks, require more resources and can be carried out in a number of ways.

Depending on the attack scenario, resources required for the successful attack vary. In order to compromise a control system, the adversary may need *a priori* system model, disclosure resources and/or disruption resources [6]. *A priori* system model represents an indispensable weapon for generation of stealthy attack; once the adversary gets the correct *a priori* system model, it is able to generate sophisticated attacks that security system cannot easily recognize. Nevertheless, if *a priori* system model is not available, disclosure resources can be utilized to violate data confidentiality and enable the adversary to obtain sensitive information about the targeted system, e.g. sensor readings and control signals. Data gathering and unauthorized system identification represents an attack *per se*, called Cyber Physical Intelligence attack [7]. Identified system model alone or in combination with *a priori* model represents a basis for generation of attacks. Finally, disruption resources work online, affect the communication operation and carry out active component of the attack.

3. DECEPTION ATTACKS IN CONTINUOUS TIME SYSTEMS

Application of smart sensors and actuators in continuous time systems can be regarded as networked control system (NCS) in which the loop between physical plant and controller is closed over communication network (Fig. 2) [7]. Physical plant can be described using linear stationary continuous time system [8]:

$$\begin{aligned}\dot{\mathbf{x}}(t) &= \mathbf{A}\mathbf{x}(t) + \mathbf{B}\mathbf{u}(t) \\ \mathbf{y}(t) &= \mathbf{C}\mathbf{x}(t) + \mathbf{D}\mathbf{u}(t)\end{aligned}\quad (1)$$

where $\mathbf{x} \in \mathbf{R}^n$ represents the state vector, $\mathbf{u} \in \mathbf{R}^m$ the control input vector, $\mathbf{y} \in \mathbf{R}^p$ the vector of measured output signal (Fig. 2) and \mathbf{A} , \mathbf{B} , \mathbf{C} , and \mathbf{D} are matrices with appropriate dimensions. In NCS, using feedback and forward communication lines, $\mathbf{y}(t)$ and $\mathbf{u}(t)$ are transmitted between plant and controller as complete time series. In deception attack, adversaries change $\mathbf{y}(t)$

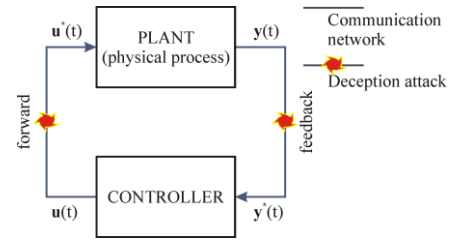


Fig. 2. Model of a continuous time system.

and $\mathbf{u}(t)$ by injecting false data $\mathbf{y}^*(t)$ and $\mathbf{u}^*(t)$ based on available Cyber Physical Intelligence. Depending on the applied procedures for ensuring the stealthiness of $\mathbf{y}^*(t)$ and $\mathbf{u}^*(t)$ injection, there exist different types of deception attacks, and some of them will be shortly explained in the sequel.

Replay attack [9] is a type of deception attack that records $\mathbf{y}(t)$ and $\mathbf{u}(t)$ time series for a certain time period and replays them in another period as $\mathbf{y}^*(t)$ and $\mathbf{u}^*(t)$ to attack the system. Evidently, preceding the actual replay attack, there is a Cyber Physical Intelligence attack, which is used to record as much relevant data from the system as possible. After some time, recorded data is replayed and presented to the system.

Attacks that are even more malicious eavesdrop data on communication lines and change them online according to the desired effect. For example, bias attack [6] adds the following signal to the communicated data

$$a_{k+1} = \beta a_k + (1 - \beta) a_\infty \quad (2)$$

where $a_0=0$, a_∞ and β are coefficients that can be optimized [6] to get the desired effect and ensure stealthiness. An example of the effect of bias attack on insertion force signal during Peg-in-Hole part making is presented in Fig. 3.

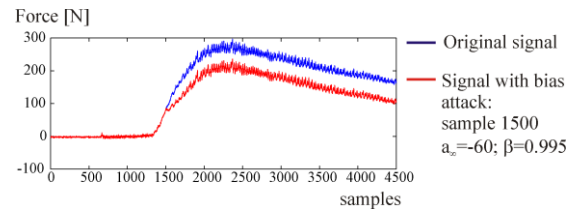


Fig. 3. Bias attack on insertion force signal during Peg-in-Hole part making.

Zero-dynamics attack [6, 10] is a very sophisticated deception attack requiring perfect knowledge of the plant dynamics represented through its *a priori* model. It is based on the open-loop predictions of the output changes due to the attack and it does not necessitate system identification through Cyber Physical Intelligence attack. Zero-dynamics attack targets global or local unstable zeros of control system transfer functions, aiming to shift the system into unsafe state, causing geometrical growth of the attack and great damage to the physical process. However, if the zeros of the system are stable, the attack will asymptotically decay to zero with little effect on the physical process.

Covert attacks [7, 11] are one of the most complex and sophisticated deception attacks that can covertly appropriate the control of the physical process to the adversary, while remaining undetected by the original

controller and the security system. Complete knowledge of the system model is necessary and it is assumed that the adversary can eavesdrop and modify both, the sensing and actuation signals [11]. The adversary, in this case covert agent, connects between forward and feedback lines in parallel with the controller. Based on eavesdropped $\mathbf{y}(t)$ and $\mathbf{u}(t)$ signals, and utilizing plant model, it generates $\mathbf{y}^*(t)$ and $\mathbf{u}^*(t)$ in such a way to get desired performance of the plant.

4. ATTACKS IN DISCRETE EVENT SYSTEMS

Discrete event systems (DES) represent dynamic systems that change their state in discrete time instants, with typically irregular intervals according to the occurrence of instantaneous events. In DES, instead of communicating sensory signals change in time, the nodes in control network communicate the information about certain events represented by symbols defined by upper levels of communication protocols.

Supervisory control theory (SCT) [12, 13], that is based on logical DES model generated using formal languages and its formalisms, can be readily employed for modeling cyberattacks in DES [14]. Within SCT [12], the finite set of events' labels that cause state transitions in DES, represents an alphabet Σ , while Σ^* (where $*$ denotes Kleene star) represents a set of all strings on Σ including empty string ε . Within Σ^* , a language L ($L \subseteq \Sigma^*$) that contains all admissible, i.e., physically possible, event strings in DES can be identified. The behavior of DES is modeled as a prefix closed language $L = \bar{L}$ where [12]:

$$\bar{L} = \{u \in \Sigma^* \mid u \leq v \text{ for some } v \in L\} \quad (3)$$

and $u \leq v$ denotes that u represents a prefix of v , i.e., $v = uw$ for some $w \in \Sigma^*$. The events alphabet Σ can be partitioned into two subsets ($\Sigma = \Sigma_c \cup \Sigma_u$) representing (i) Σ_c – set of controllable events that can be disabled at any time, and (ii) Σ_u – set of uncontrollable events that the agent cannot influence.

In the case of distributed control systems, each node in control network can observe only a part of events that occur within the system as a whole; these events represent an observation alphabet Σ_o , defined by [12]:

$$P(\sigma) = \begin{cases} \sigma, & \text{if } \sigma \in \Sigma_o \\ \varepsilon, & \text{if } \sigma \notin \Sigma_o \end{cases} \quad (4)$$

Projection from (4) represents a natural projection (mask) that can be extended to the strings as follows:

$$P(s\sigma) = P(s)P(\sigma), \text{ for } s \in \Sigma^*, \sigma \in \Sigma \quad (5)$$

In DES, attacks can be introduced by removing, inserting or replacing symbols in observation strings. As shown in [14], the attack can be modeled as $A: \Sigma_o^* \rightarrow 2^{\Sigma_o^*}$ that maps original string $w \in \Sigma_o^*$ into a set of corrupted strings. Since, in general, attack is neither unique nor deterministic, the mapping A represents a set valued function, i.e., $A(w)$ is a set of corrupted strings [14]; eventually, the node will receive only one string $y \in A(w)$, for which it also holds that $y \in \Sigma_o^*$. Note that $y \notin \Sigma_o^*$ represents an attack that can be easily detected and it is not covered by mapping A .

It should be emphasized that the attack that represents a removal of a symbol represents a natural projection given in (4) and (5). The masks that model symbol insertion and replacement do not represent natural projection, but in these cases, relation (5) holds.

Example: In this example, we will consider 2 DoF pneumatic “pick and place” manipulator that is made of three intelligent pneumatic cylinders (C1, C2 and C3); C1 and C2 realize linear DoF while C3 represents a gripper. Each cylinder represents a CPS by itself and it has integrated microcontroller with computation and communication capabilities, employed for cylinder control. In addition, each cylinder is equipped with 5/2 monostable dual control valve and two limit switches for detection of final advanced and retracted position. Cylinder microcontrollers represent network nodes and manipulator control system is distributed over them [14]. Manipulator moves a part between two positions, (Fig. 4) performing the following sequence:

$$C2 + C3 + C2 - C1 + C2 + C3 - C2 - C1 - \quad (6)$$

During manipulator's regular operation, the events presented in Table 1 occur and can be detected by cylinder nodes as rising and falling edges of corresponding limit switches' signals; controllable events are denoted by capital, and uncontrollable by lower letters. The sequence from relation (6) can be represented as the following sequence of events:

$$CdEfDcAbCdFeDcBa \quad (7)$$

For proper functioning of the manipulator, in addition to the events locally detected by nodes (Table 1), it is necessary to communicate certain events between them [14]. In this way, each node i , $i = 1, 2, 3$ has its own observation alphabet Σ_{oi} : $\Sigma_{o1} = \{a, A, b, B, c\}$, $\Sigma_{o2} = \{c, C, d, D, a, b, e, f\}$, $\Sigma_{o3} = \{e, E, f, F, d\}$ obtained from the whole system observation alphabet $\Sigma_o = \{a, A, b, B, c, C, d, D, e, E, f, F\}$ by applying natural projections P_i as defined in relation (4).

Note that the events communicated between nodes are obtained during control system generation, considering that C1 changes position always after C2 reaches retracted position, C3 changes position after C2 reaches advanced position, while the control of C2 is

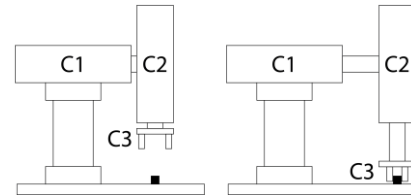


Fig. 4. Pneumatic manipulator – left: position I, right: position II.

Description of event per cylinder	C1 symbol	C2 symbol	C3 symbol
Reaches retracted position	a	c	e
Starts advancing	A	C	E
Reaches advanced position	b	d	f
Starts retracting	B	D	F

Table 1. Events during manipulator's regular operation.

more complex and requires signals from both, C1 and C3 [15], as can be observed from (6).

As an example, we will consider two attacks on communication between C2 and C3. Attack A_1 represents an occasional removal of symbol d from the sequence of symbols observed by C3, represented by the following mask:

$$A_1(\sigma) = \begin{cases} \sigma, & \text{if } \sigma \in \Sigma_{o3} \setminus \{d\} \\ \{\varepsilon, d\}, & \text{if } \sigma = d \end{cases} \quad (8)$$

Attack A_2 , on the other hand, represents insertion of symbols $\{e, f\}$ in communication of events from C3 to C2 and it affects symbols observed by C2 as follows:

$$A_2(\sigma) = \begin{cases} \sigma, & \text{if } \sigma \in \Sigma_{o3} \setminus \{d\} \\ \{e, f\}, & \text{if } \sigma = \varepsilon \end{cases} \quad (9)$$

Attack A_1 would affect the functioning of gripper as the occurrence of this attack would prevent start of gripping or releasing operation. Nevertheless, the consequences of this attack alone would not be catastrophic since, after this attack, the system would stop functioning, waiting for the events e or f from C3. However, the consequences of attack A_2 can be far more serious. If this attack occurs after cylinder C2 reaches advanced position and before C3 performs gripping/releasing, it can lead: (i) to an inappropriate gripping of the part; (ii) to the movement of manipulator from position I to position II without part in the gripper; (iii) to the release of part in an arbitrary position during motion of manipulator from position II to position I. Which of the considered scenarios would emerge depends on the moment of attack occurrence and the time necessary for gripping/releasing and retracting of C2. The combination of attacks A_1 and A_2 can give even worse consequences represented through completely stochastic motion of cylinders.

5. CONCLUSION

Implementation of IoT and CPS in manufacturing systems leads to the distribution of control tasks and high level reliance on communication network. This inevitably brings about increased vulnerability of the control systems to cyberattacks. In this paper, we have reviewed several attack scenarios and potential hazards that they pose against distributed control systems in continuous time and discrete event control. In an attempt to illustrate negative effects that a real attack can have unless properly neutralized, an example was given, where a combination of DoS and deception attacks were targeting discrete event system. Future work will consider methods that are suitable for securing CPS-based distributed discrete event systems.

6. REFERENCES

- [1] Atzori, L., Iera, A., Morabito, G.: *The Internet of Things: A survey*, Computer Networks, vol. 54, no. 15, pp. 2787-2805, 2010.
- [2] Lee, G. M., Crespi, N., Choi, J. K., Boussard, M.: *Internet of Things*, Evolution of Telecommunication Services, pp. 257-282, Springer, Berlin, Heidelberg, 2013.
- [3] ACATECH: *Recommendations for implementing the strategic initiative INDUSTRIE 4.0*, April 2013.
- [4] Kopetz, H.: *Internet of Things*, Real-Time Systems, Springer, Boston, MA, pp. 307-323, 2011. DOI: 10.1007/978-1-4419-8237-7_13
- [5] Amin S., Cárdenas A.A., Sastry S.S.: *Safe and Secure Networked Control Systems under Denial-of-Service Attacks*, *Hybrid Systems: Computation and Control*, Lecture Notes in Computer Science, vol. 5469, pp. 31-45, Springer, Berlin, 2009.
- [6] Teixeira, A., Shames, I., Sandberg, H., Johansson, K.H.: *A Secure Control Framework for Resource-Limited Adversaries*, Automatica, vol. 51, pp. 135-148, 2015.
- [7] De Sá, A.O., Carmo, L.F.R.d.C., Machado, R.C.S.: *Covert Attacks in Cyber-Physical Control Systems*, IEEE Transactions on Industrial Informatics, vol. 13, no. 4, pp. 1641-1651, Aug. 2017.
- [8] Pasqualetti, F., Dorfler, F., Bullo, F.: *Attack detection and identification in cyber-physical systems*, IEEE Transactions on Automatic Control, vol. 58, no. 11, pp. 2715-2729, Nov. 2013.
- [9] Mo, Y., Sinopoli, B.: *Secure control against replay attacks*, 47th Annual Allerton Conference on Communication, Control, and Computing, pp. 911-918, 2009.
- [10] Hoehn, A., Zhang, P.: *Detection of Covert Attacks and Zero Dynamics Attacks in Cyber-Physical Systems*, Proceedings of the American Control Conference, pp. 302-307, 2016.
- [11] Smith, R.S.: *Covert Misappropriation of Networked Control Systems: Presenting a Feedback Structure*, IEEE Control Systems, vol. 35, no. 1, pp. 82-92, Feb. 2015.
- [12] Ramadge, P.J.G., Wonham, W.M.: *The Control of Discrete Event Systems*, Proceedings of the IEEE, vol. 77, no. 1, pp. 81-98, Jan. 1989.
- [13] Thistle, J.G.: *Supervisory control of discrete event systems*, Mathematical and Computer Modelling, vol. 23 (11-12), pp. 25-53, 1996.
- [14] Wakaiki, M., Tabuada, P., Hespanha, J. P.: *Supervisory Control of Discrete-event Systems under Attacks*, arXiv:1701.00881v1, 2017.
- [15] Mitrović, S., Jakovljević, Ž.: *The application of distributed control system based on IEC 61499 and 802.15.4 standards*, Proceedings of ETIKUM Conference, pp. 37-40, Dec. 2017. (In Serbian)

Authors: Research Assistant **Stefan Mitrovic**, Research Associate **Dr. Zoran Dimic**, Lola Institute, Kneza Visaslava 70a, 11000 Belgrade, Serbia;
Dr. Zivana Jakovljevic, associate professor, University of Belgrade, Faculty of Mechanical Engineering, Kraljice Marije 16, 11000 Belgrade, Serbia.
 E-mail: stefan.mitrovic@li.rs, zoran.dimic@li.rs, zjakovljevic@mas.bg.ac.rs

ACKNOWLEDGMENTS: This paper is supported by Ministry of Education, Science and Technological Development of the Republic of Serbia under grants TR35004, TR35020 and TR35023.

Moraca, S., Cvetkovic, N., Fajsi, A., Gracanin, D., Suzic, N.

SCHEDULING IN PROJECT-BASED MANUFACTURING ENVIRONMENT

Abstract: *A trend in the manufacturing industry towards made-to-order products, constant redesigning of products, system reconfiguration and its global distribution, led to viewing manufacturing of each item as a project. Thus, manufacturing companies started organizing themselves as project-based. Project-based production implies frequent changes of customers and engineers' requirements, involvement of various stakeholders and cooperative supply chain. As a result, traditional, front-end scheduling became inadequate for such a production environment. This paper discusses the nature of project-based production and relevant scheduling approaches in project-based environment.*

Key words: *project-based production; scheduling; manufacturing;*

1. INTRODUCTION

Global competition and rapidly changing customer requirements are demanding increasing changes in manufacturing environments. Enterprises are required to constantly redesign their products and continuously reconfigure their manufacturing systems. They tend to offer more features and facilities in its product and to be more flexible while dealing with its customers. A company can remain different from its competitors with many strategies [1], [2].

A trend in the manufacturing industry towards made-to-order products and its global distribution, led to viewing manufacturing of each item as a project [3], i.e. to the project-based production systems.

In traditional production strategy literature, project-based production is described in general terms as only one type of production systems. Nowadays we can say that project-based production is not only one type of production systems, but new approach that from organizational and technical point of view represents significant direction for further development of production systems and industry 4.0 concept.

Project-based productions include certain challenges due to the dynamic requirements characteristic for these approach, such as: need for fast responsiveness to the frequent engineer changes, decision making in distributed system in a timely manner, effective use of resources and similar. These challenges are especially emphasized if we take into consideration time and cost requirements of each project [3], which are the constraints each company tends to resolve. Thus, in this paper we discuss the nature of project-based production and relevant scheduling approaches in project-based environment.

2. PROJECT-BASED PRODUCTION SYSTEMS

Project-based production system is seen as a temporary infrastructure of resources and value-generating processes strategically arranged for new product development. It can be explained as the

production management and technology-based approach in which "the project is structured and managed as a value generating process" [4].

Project-based production focuses on new value generation and knowledge embeddedness into the product. The idea is to offer knowledge and intangible value, not only work or embedded material.

Other characteristic of project-based production is possible involvement of large number of stakeholders in order to fit the final product to the demands of particular customers. Additionally, it implies the cooperative supply chains. Each stakeholder has a certain role in the project with clearly defined outcomes and generated values it has to realize. In such a case, since processing is performed in different companies, it is necessary to ensure that all the elements are adjusted for the assembly of the final product taking into the consideration all the specific demands by designers, clients etc. which may occur during the project implementation.

During the 90's, Production and Supply Chain Systems have switched from the traditional mass production to the mass customization with aim to confront the increase of the global market competition [5]. High competition between enterprises and market volatility led then enterprises to be more project oriented.

Project oriented production, from the control perspective, is seen as suitable to operate with a high level of coordination and proactivity throughout the supply-chain, and at the same time to react efficiently to impediments on the shop floor [5].

In their classification of production system types [6], Schmenner (1993) places projects on one extreme (figure 1), where products are unique and flows are "very jumbled" [7].

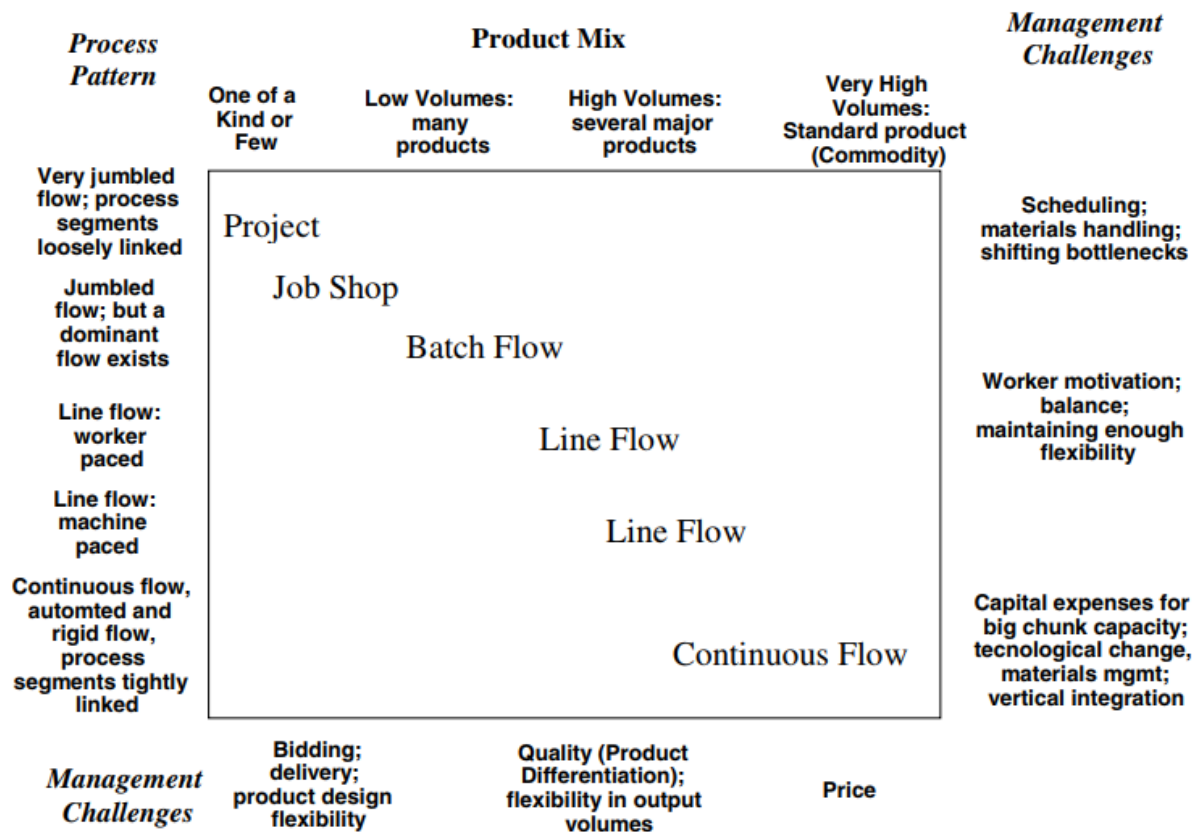


Figure 1. Product/Process Matrix [7]

3. TOWARDS LEAN PROJECT-BASED MANUFACTURING

Within the development of mass customization trend, many manufacturing firms became matrix or project-based organization. In such a way, new dynamics and challenges occur in this environment. Koch described how this dynamics possibly lead to pressures on few levels [8]:

- *Pressure to deliver on organizational level:* projects are seen as composition and balancing of resources and tasks related to the product demands [9];
- *Pressure on individual level:* knowledge workers such as engineers and technicians are subject to demands relating to cross-disciplinary approaches that require competencies related to extensive communication, problem-solving and coordination [10].

While mass production has a goal to solely accomplish acceptable number of defects, maximum acceptable level of inventories, and a narrow range of standardized products, which would not exceed inherent human capabilities or cost, Lean production philosophy strives for more [1],[11]. Lean strives towards perfection and constant improvement: decrease of costs, elimination of defects and inventories and high variety of products [1]. In this sense, excellence in manufacturing tends to enhance the activities contributing to the customer's satisfaction that are usually unappreciated in traditional mass production [12].

Requests for more individuality and customer-specific product variants demand new paradigms of production [13]. Small, more agile and scalable distributed

manufacturing units are capable of ensuring what modern operating systems demand for – just in time delivery, adjustability of production capacity and functionality in accordance with clients requirements, and sustainable production and supply chains [14].

However, although Lean project-based manufacturing has various benefits, its implementation in project organization instead of assembly lines and worker-paced flow lines demands different approach, including planning and scheduling processes.

4. SCHEDULING IN LEAN PROJECT-BASED PRODUCTION SYSTEMS

Basic traditional centralized and hierarchical production systems provide certain optimal solutions for some kind of mass production, planning and scheduling, and system control. However, the monolithic, centrally located planning and control systems cannot scale economically to meet the demands imposed by project-based productions in a distributed manufacturing environment existing today [3]. The solution is to design and develop an effective management, planning and scheduling system matched to the distributed, multi-participants, and dynamic nature of the distributed manufacturing.

In centralized approaches, decision making is “hierarchically broadcasted from the higher decisional levels down to the operational units” [7]. What makes this approach successful is the ability to ensure long term optimization of production planning and scheduling [5].

However, with the modern market challenges other decision making philosophies and strategies have emerged. Requirements for more and more reactivity and flexibility have led to the implementation of distributed approaches. Unfortunately, these new ways to pilot and control the material flows have led to “black boxes” in management systems, and have highlighted the need for more and more real-time closed-loop information systems” [15].

In project-based organizations project execution has a direct impact on firm performances wherefore project planning, including scheduling, has significant role. In

the project planning phase, baseline and predictive schedule are developed according to the assumed resource availability, current requirements and uncertainties [16]. However, in the project implementation phase, projects are affected by various disruptions such as requirements changes, unpredicted events and similar, resulting in disrupted project schedules. In the literature there have been distinguished few approaches to production scheduling intended to overcome these disruptions. The approaches and their characteristics are presented in the table 1.

Production scheduling approaches	Description
<i>Stochastic project scheduling</i>	Scheduling is seen as multi-stage decision process. Schedule-related decisions are made dynamically at stochastic decision points corresponding to the start of the project and the completion of activities. Decisions are based on the observed past and priori knowledge about the activity processing time distributions [17]. This method is especially useful in areas where variations are high [16].
<i>Rolling Horizon, Decomposition and Hierarchy</i>	This approach presents method suitable for production scheduling dealing with different time scales. According to the rolling horizon only a subset of planning periods includes the detailed scheduling decisions with shorter time increments [16]. This is important for the production industry where parameters interact in real time and have a severe effect on the production schedule. In this approach, the first planning period is usually detailed scheduling model while the future planning periods include only planning decisions [16].
<i>Knowledge Based Systems</i>	Production scheduling within developed knowledge based systems or expert systems relies on logical thinking and experts’ knowledge and embedded series of parameters used to evaluate different scheduling scenarios [18]. However, what constraints this method is the amount and quality of the rules embedded in the experts system required at the outset, which ultimately limits the speed at which the system can learn [16].
<i>Sensitivity Analysis</i>	Sensitivity analysis approach tends to answer “What if” type of questions, such as: “Which are the parameters that affect the schedule the most? What is the limit for a given parameter while still ensuring schedule feasibility?” [16]. Thus, Thiele & Kurth (2014) used sensitivity analysis to determine the best possible parameter combination to ensure optimal solutions for the production scheduling problem [19].
<i>Proactive-Reactive Scheduling</i>	The reactive schedule implies revising the baseline schedules in the case of disruptions. This way it includes possibility to rely also on parameters that were not exactly known during the planning phase but do have effect on disruptions. Such proactive-reactive scheduling method are: fuzz numbers, robust optimization and robust scheduling or reactive scheduling [16].

Table 1. Production scheduling approaches and their characteristics

Independent of scheduling approach, a typical scheduling problem in smart factories requires substantial computing resources each time the factory needs reconfiguration [20]. Thus, as addition to any of the above described methods, authors [20], proposed cloud-based optimization. Additionally, considering the high probability of disruptions in production

environment, Hsiang-Ling Chen et. Al. (2014) developed an integrative scheduling framework that includes these uncertainties and possible disruptions from the very beginning using the experience and methodologies developed in the production scheduling environment [16].

5. CONCLUSION

This paper represents an overview on characteristics and need for project-based production in today's dynamic market environment where made-to-order products and mass customization become a global trend. It may be concluded that project-based production focuses not only on providing labour and final tangible product, but to generate new value for the customer and other stakeholders and to embed the knowledge into the final product.

Additionally, production scheduling approaches in such an environment are presented. Project-based production demands for more agile and flexible scheduling method than traditional, front-end scheduling. Project-based scheduling approaches, such as stochastic scheduling, proactive scheduling, experts system and other methods enable far more effective planning and scheduling system that matches to the distributed, multi-participants, and dynamic nature of the distributed manufacturing characteristic for project-based environment.

6. REFERENCES

- [1] Junior, J.: *Achieving breakthrough on manufacturing floor through project-based manufacturing*, SAE Technical Paper Series, 18. Congresso e Expocisao Internacionais da tecnologia da Mobilidade, Sociedade de Engenheiros Mobilidade, Sao Paolo, 2009.
- [2] Hill, A., Hill, T.: *Manufacturing operations strategy-3rd edition*, Palgrave Macmillan, UK, 2009.
- [3] Wu, S., Kotak, D.: *Agent-based collaborative project management system for distributed manufacturing*, SMC'03 Conference Proceedings, IEEE International Conference on Systems, Man and Cybernetics. Conference Theme - System Security and Assurance, 2003.
- [4] Ballard, G.: *The Last Planner system of Production control*, University of Birmingham, 2000.
- [5] Thomas, A., Trentesaux, D., Valckenaers, P.: *Intelligent distributed production control*, 2012.
- [6] Schmenner Roger, W.: *Production/Operations Management 5th edition*, Prentice Hall, Englewood Cliffs, NJ. 1993.
- [7] Brink, T., Ballard, G.: *Slam- a case study in applying lean to job shops*, Proceedings of the 2005 ASCE Construction Research Congress, San Diego, April 5-7, 2005.
- [8] Koch, C.: *Operations strategy development in project based production – a political process perspective*, Journal of manufacturing technology management, Vol. 26, pp. 501-514, 2015.
- [9] Newel, S., Robertson, M., Scarbrough, H., Swan, J.: *Managing knowledge work*, Palgrave Macmillan, London, 2002.
- [10] Garrick, J., Clegg, S.: *Knowledge work and the new demands of learning*, Journal of Knowledge Management, Vol. 4, pp. 279-286. 2000.
- [11] Womack, J.P., Roos, D.: *Project management and business development: integrating strategy, structure, process and projects*. International Journal of Project Management, p.401-411, Elsevier Science, 2002.
- [12] Hall, R.: *Attaining manufacturing excellence*. McGraw-Hill, New York, 1987.
- [13] Matt, D.T., Rauch, E., Dallasega, P.: *Trends towards Distributed Manufacturing Systems and Modern Forms for their Design*. Procedia CIRP, 33, 185-190., 2015.
- [14] Kohtala, C.: *Addressing sustainability in research on distributed production: an integrated literature review*. Journal of Cleaner Production, 106, 654–668, 2015.
- [15] Klein, T.: *Le Kanban actif pour assurer l'interopérabilité décisionnelle centra- lise/distribue. Application a un industriel del' ameublement*, PhD thesis, Université Henri Poincaré, Nancy I, 2008.
- [16] Hsiang-Ling Chen, A., Liang, Y., Padilla, J.: *An Experimental Reactive Scheduling Framework for the Multi-Mode Resource Constrained Project Scheduling Problem*, Proceedings of the International Multi Conference of Engineers and Computer Scientists, Hong Kong, 2014.
- [17] Herroelen, W., R. Leus.: *Project scheduling under uncertainty—survey and research potentials*. European Journal of Operational Research, 165(2): p. 289–306, 2005.
- [18] O'Kane, J.F.: *A knowledge-based system for reactive scheduling decision-making in FMS*. Journal of Intelligent Manufacturing, 11(5): p. 461–474, 2000.
- [19] Thiele, J.C., Kurth, W., Grimm, V.: *Facilitating Parameter Estimation and Sensitivity Analysis of Agent-Based Models: A Cookbook Using NetLogo and 'R'*. Journal of Artificial Societies and Social Simulation, 17(3): p. 11. 2014.
- [20] Dziuranski, P., Swan, J., Indrusiak, L.: *Value-Based Manufacturing Optimisation in Serverless Clouds for Industry 4.0*, ACM, New York, NY, 2018.

Authors: Assoc. Prof. Slobodan Moraca¹, M.Sc. Nela Cvetkovic¹, M.Sc. Angela Fajsi¹, Assist. Prof. Danijela Gracanin¹, Nikola Suzic²

¹ University of Novi Sad, Faculty of Technical Sciences, Department of Industrial Engineering and Engineering management, Trg Dositeja Obradovica 6, 21000 Novi Sad, Serbia, Phone.: +381 21 485-2188, Fax: +381 21 454-495.

² University of Padova | UNIPD · Department of Management and Engineering, Padova, Italy
E-mail: moraca@uns.ac.rs; nelacvetkovic@uns.ac.rs; angela.fajsi@uns.ac.rs; gracanin@uns.ac.rs; suzic@gest.unipd.it

Petković, D., Jeleč, A.

CONCEPTUAL SOLUTION FOR FLEXIBILITY IMPROVEMENT OF PROCESSING SYSTEM IN WOOD PROCESSING SECTOR

Abstract: Flexibility as characteristic of modern production systems defines need for multidisciplinary access in automation improvement of the processing system. Processing system as a segment of production process in wood processing sector can be characterized as basis for different systems implementation in field of processing objects transportation, storage and manipulation. These areas in accordance with the flexibility of the processing process represent the basis for implementation of technologies characterised as CIM technology.

Key words: Processing systems, flexibility, CIM technology, manipulation, transportation, storage.

1. INTRODUCTION

Flexibility as a characteristic of modern manufacturing systems includes a wide range of production process segments such as processing, transport and assembly. Taking into account the basics of modern production systems such as automation, it is possible to characterize this system as the basis for production systems flexibility achievement. Achieving an appropriate degree of automation defines the need for a multidisciplinary approach in field of integrating different CIM system characteristic. This implies the application of numerically controlled machines with integrated automated transport system.

Although numerically controlled machining centers represent automation of processing process, however, they can be characterized as basis for different systems integration, required for machining process realization. In addition to the transport system, automation refers to the storage system and management system such as an computer integrated system. Implementation of these systems enables flexibility degree improvement of existing machining systems in different industrial branches such as the wood processing sector. The need of flexibility increase primarily of manufacturing process as a segment of entire production process is associated with shortening of processing operation, resulting in increased efficiency. Increasing the efficiency level in addition to profitability of manufacturing process enables manufacturing process improvement in the production assortment segment.

2. FLEXIBILITY IN WOOD PROCESSING SECTOR

Flexibility of complex production systems such as wood processing production systems can be presented through:

- possibility of producing different products on a single processing system
- production of similar products on different processing systems
- production of improved products and new products on the same processing systems and

- equipment of the machine in terms of adaptation to the changes of visual and technical characteristics.

From this it can be seen that the base of production system is machining center characterized as a multiple machining center controlled by a computer system.

Taking into account the characteristics of machining centers present in mentioned production sector, the degree of flexibility is increased by use of multiple processing tables. Application of these principles enables shortening of workpiece positioning time covered by the preparatory time of manufacturing process. Although these principles increase the degree of automation, they still prevent the elimination of human factor's influence on the processing process.

The mentioned influence is characterized as negative in terms of manufacturing process automation degree and ultimately the flexibility degree. By CIM system application it is possible to significantly increase the flexibility of machining systems in wood processing sector while eliminating significant limiting factors.

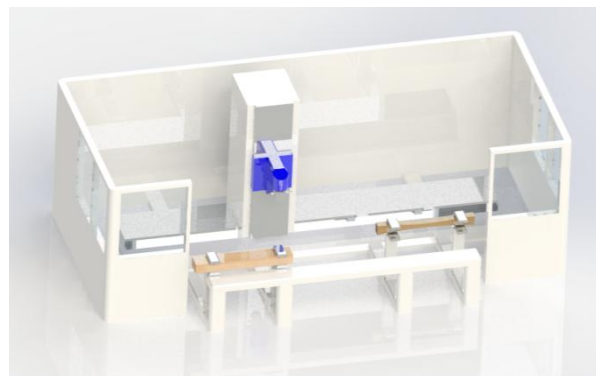


Fig. 1. Increasing the flexibility using double processing table

3. AUTOMATION LEVEL IMPROVEMENT IN MACHINING SYSTEM

The presence of human factor in workpiece positioning can be presented as an influence on workpiece desired geometry positioning and machining

process precision.

Inadequate workpiece positioning as result of human factor influence disables achievement in high degree of geometry repeatability of final products. Inability to achieve repeatability also affects precision of the processing itself. Above mentioned provides the basis for the CIM system implementation which enables achievement of high degree of repeatability in workpiece positioning - robotic manipulator. By implementing a robotic manipulator in the machining system it is possible to alternately position the workpiece on the work table. In addition to workpiece manipulation in the working area, the robot manipulator's handling capabilities have been expanded to take over the workpiece from a specially designed platform and restore the workpiece after machining process realization. From this, it is visible to create the basis for automated storage space by implementation of a robot manipulator.

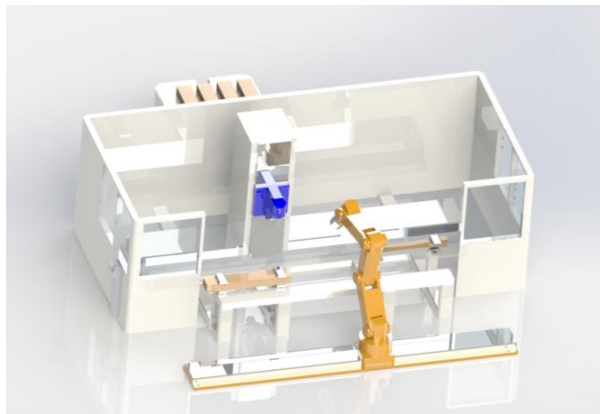


Fig. 2. Robot manipulator implementation in a machining system

The PLC controller as an integral component of the robot manipulator represents an inescapable segment in flexibility improvement of machining system through adapting robot manipulator movement to different processing objects. PLC controller implementation in interaction with the optical or laser sensors system enables automated positioning of robot manipulator in accordance with database stored in the PLC controller.

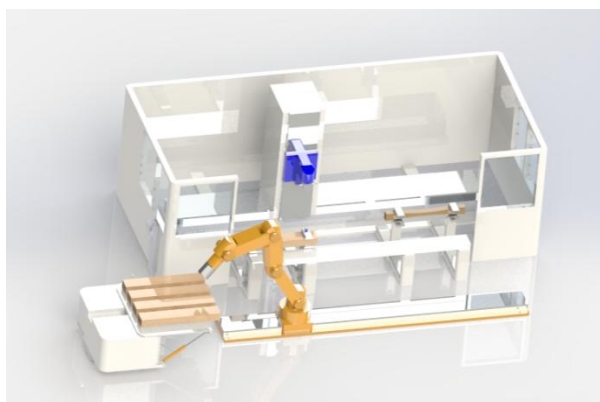


Fig. 3. Movement of a robot manipulator according to different processing objects

The previously mentioned implementation of robot manipulator creates the necessity for development of an automated transport system that will enable cyclicity of machining process to be achieved with processing time shortening of different processing objects.

CIM system suitable for this application is a system based on the automated guided vehicles -AGV. Implementation of the AGV system implies advantage transfer of of this system such as precision in motion and positioning as well as automated movement in accordance with previously defined conditions and parameters, on the entire machining system. Integration of AGV system based on fixed travel route enables simultaneous delivery and refinement of processing objects with high degree of automation. Cyclicity as a segment of flexibility in accordance with the need for continuous servicing of a robot manipulator, defines necessity for the application of at least three AGV vehicles. It is necessary to state that the application of fixed path AGV vehicle movement is associated with the aim of creating an autonomous machining station which by its operation will not directly affect other subsystems present in the production process.

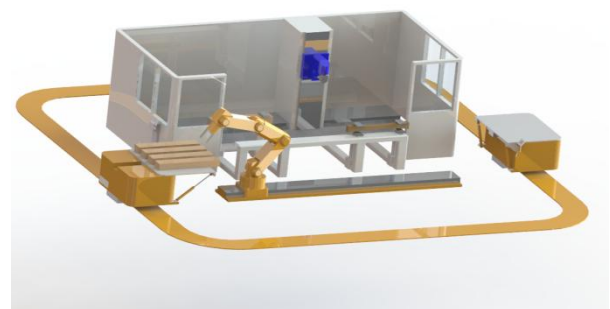


Fig. 4. Implementation of AGV vehicle in the process of machining system servicing.

The number of AGV vehicles applied is directly dependent on the complexity of machining process and the need to serve the input storage space, processing system and output storage space. In accordance with the basic characteristics of processing systems present in woodworking sector it is possible to define a minimum number of 3 AGV vehicles.

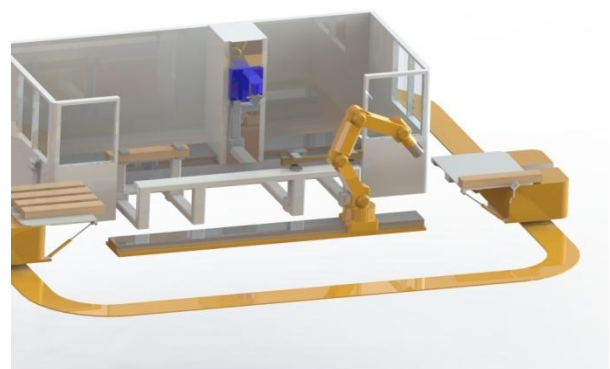


Fig. 5. Achieving the cyclicity by integrating two AGV vehicles

By analyzing the basic specificities in the implementation of the above-mentioned systems, elimination of the human factor's influence on the machining process is evident. Eliminating the human factor's impact can be shown by eliminating the deficiencies of existing machining systems. Processing systems dominant in the woodworking sector are often based on manual positioning of processing objects in the processing system. By means of the aforementioned method, the preparation time of manufacturing process is in full dependence on the skill and expertise of workers. In addition to placing processing objects in the working area, the delivery and dispatch of processing objects is most commonly realized using conventional manipulation tools.

The above significantly affect the level of automation of the entire machining system with the creation of limitations for achieving flexibility of the overall system. It is necessary to state that by implementing this system, it is possible to achieve the autonomy of the processing system and to create the basis for application of group technology principles.

Implementing group technology principles in this system significantly increases flexibility in the wide range production of different products.

In addition to the above-mentioned application of group technology principles, it is possible to adapt the whole system by using similarities in operations and movements of the manipulator and the machining center itself. Realizing the processing and transportation of the workpiece creates the basis for automation degree increase of extremely important segment such as workpiece and final product storage. Storage systems are primarily intended to keep the movement of processing objects for a certain period of time with the aim of balancing the production system cycle. In addition to balancing the storage system is used to synchronize production processes, ie individual production processes.

In addition to the above, storage systems are also used to realize the production process with least amount of delay. Depending on the characteristics of the production system and depending on the processing subject, different forms of storage systems are applied in practice. In addition to the above, when selecting warehouse systems, it is necessary to consider the required degree of automation, which is directly related to the storage system's flexibility. Warehouses currently dominant in use are regal warehouses based on the storage of unified palletized systems in selective regal.

It is necessary to state that regal storage systems are based on high storage racks for storing palletised storage items. In addition to the high storage systems with the needs of production system, it is possible to use various regal warehouses that can include an automated system for individual loading and unloading of processing objects.

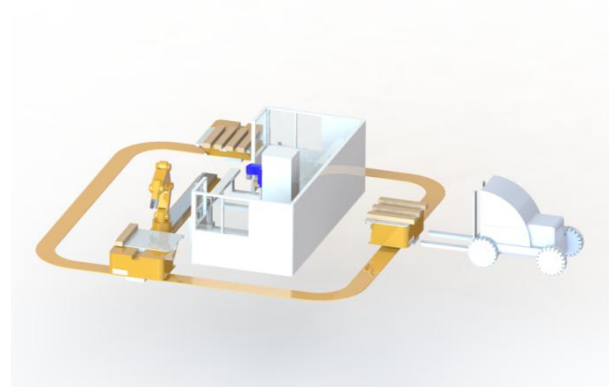


Fig. 6. Conventional way of serving the automated system

With the aim of improving the flexibility of processing system, the possibility of implementing a horizontal regal warehouse with mobile platforms, which enables temporary processing of workpieces, is considered. It is necessary to state that when designing the project solution, consideration was given to the possibility of using a regal warehouse for physically separate loading and unloading of processing objects.

The conventional mode of service shown in fig. 6 is based on application of conventional forklifts which, at the time of entering a blank AGV vehicle, must place processing objects on the same for the purpose of preventing the occurrence of stoppages. The basic disadvantage of this mode of service is that the worker in the production plant must continuously monitor the movement of the AGV, which can be a limiting factor for achieving flexibility.

In order to eliminate this limitation, an automated warehouse is implemented in the presented system.

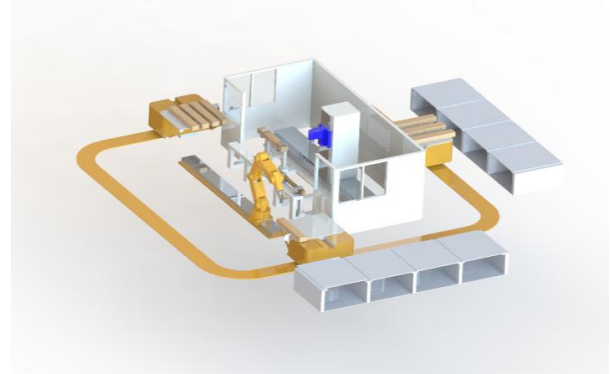


Fig. 7. Storage warehouse implemented in the processing system

Fig. 7. shows that the storage system includes two regal warehouses for loading and unloading of processing objects on AGV vehicle. By applying the present storage system can be seen that eight stations for loading and unloading can eliminate the need for the constant presence of workers served by a conventional forklift. The used storage system enables continuous realization of four processing operation, which provides enough time for setting the workpiece necessary to start the next operation processing.

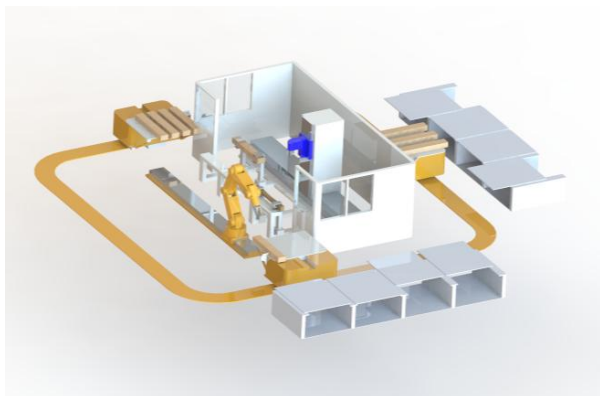


Fig. 8. Automatic service of the AGV vehicle by the regal warehouse

After finishing the machining process, the AGV continues to move through the defined route to a regal warehouse, which by the automated platform takes over the objects on which the machining process is completed. It is necessary to state that filling up the storage space is done in a precisely defined order.

3. CONCLUSION

Flexibility as a characteristic of contemporary production systems requires the application of various automated systems, which enable the improvement of existing production systems in terms of adapting to the different production process requirements.

Different requirements may be in terms of geometry of processing objects, production capacities, processing speeds, etc.

Although the automated processing system, however, increasing the degree of flexibility requires the implementation of various automated systems such as AGV vehicles, sensor systems of automated regal warehouses.

By implementing these systems, it is possible to overcome the various limiting factors such as, the presence of a human factor, the occurrence of a delay, the empty walkway of machine. By applying the AGV vehicle, it is possible to achieve the cyclicity of the machining process, which is the basis for the application of robot manipulator used for servicing the CNC machining center.

Further improvement of the processing system is the application of an automated regal warehouse, which reduces the need for the permanent presence of AGV servicing workers. By implementing these systems, it is possible to increase the degree of flexibility of the machining center with respect to the time of production preparation, the geometry of the processing and the diversity of the production assortment.

6. REFERENCES

- [1] Danijel K.: "Završni rad", Zagreb, 2013
- [2] Josip. S.: "Analiza i optimizacija skladišnog procesa u tvrtki V.B.Z d.o.o., Zagreb, 2016
- [3] Robert. G.: "Skladišni sustav kao logistički podsustav poduzeća, Požega, 2017
- [4] Tomislav. N.: "Završni rad", Zagreb, 2010
- [5] Nikola. K.: "Prikaz i analiza skladišnog sustava poduzeća Feroterm", Zagreb, 2014.

Authors: Full Prof. Darko Petkovic, Ajdin Jelec, dipl.pr.ing. University of Zenica, Polytechnic Faculty in Zenica

E-mail: darko.petkovic@mail.com;
a.jelec@hotmail.com

Ristić, M., Manić, M., Kosanović, M., Pavlović, M.

PARAMETRICALLY DESIGNED PRODUCT MANUFACTURABILITY ANALYSIS USING KNOWLEDGE BASED SYSTEM

Abstract: *The greatest savings in product development are achieved in the product design and construction phase, by involving multidisciplinary teams of experts. Manufacturability analysis is an approach based on the concept of design for manufacturing and aims at reducing the number of iterations in design, so that the price of the product becomes lower as well. Decision makers very often have to shape the numerous data in the desired form in order to make a decision. The basis for decision-making in the process of manufacturability analysis is the parametrically designed CAD model of products using features. Product model knowledge is added to the virtual product model using attributes and characteristics. On the other hand, rules and checks are defined with the aim of ensuring the implementation of all technological limitations. In this paper, a parametrically design model of the gearbox housing will be presented and an assessment of the manufacturing possibilities will be made.*

Key words: *Design for Manufacturing, Manufacturability analysis, Gearbox housing, Knowledge-based systems*

1. INTRODUCTION

Contemporary product development [1] is an activity in which a multidisciplinary approach is required. Unlike sequential design, where the process phases take place one after another, simultaneous (concurrent) engineering provides simultaneous execution of certain activities [2]. Such an approach is possible thanks to powerful CAx tools, within a strong information system, which are important support to decision-making processes. The greatest savings in product development are achieved in the initial stages of designing and constructing products. Each modification in any of the following stages implies a redesign and, at the very least, a revision of the designed product. Integrated product development and simultaneous (concurrent) engineering ensures that multidisciplinary teams of experts work in parallel with product development [3]. In this way, the product is perceived from all Design for X (DFX) aspects of the product life cycle.

The aim of the companies is to reduce production costs and production time (including the time of product distribution to the market), while increasing the quality. On the other hand, the demands of the market and customers emphasize individual requirements, so it is a big challenge for companies to create a small series product with the effectiveness of equivalent mass or serial production.

Design for Manufacturability DFM [4] presents a methodology that examines the product manufacturing possibility, meaning that what is emphasize is the adjusting the design to manufacturing capacities. In this way, the designer and the production engineer are not on opposite sides, on the contrary, together they develop a product looking for an optimal solution. All of this is aimed at early analysis of products and processes, in order to make all decisions in the product design stages, not during its manufacturing.

The virtual product development at this stage has a significant contribution. It is the basis for the

development of a modern product. Collaboration of all participants in the process, including the customer itself or customer market, provides the basis for integrated product development. In this sense, the digital factory, which represents the integration of a virtual and real factory, is gaining importance. The digital factory is a universal term for the entire network of digital models, methods and tools, including simulation and 3D visualization, integrated with a continuous data management system [5]. Within the virtual factory, products, processes and resources are modeled on the basis of real data. Planned products as well as their production processes are intensely verified and enhanced using virtual models until they are fully developed [6].

Information technologies enabled team members not only to communicate with each other more efficiently and work with shared documents, but they, through the Internet and web applications, have included end-users indirectly in the product design process. In such a process, decision-makers must not only be adequately informed, but they also seek support in decision-making processes. For such needs, decision support systems based on artificial intelligence methods have been created.

By developing the method of artificial intelligence, the decision-making process receives strong support [7]. Knowledge-based systems are one of the methods of artificial intelligence that can provide adequate support to designers, but also to managers, depending on the need. They can be developed as independent systems for manufacturability analysis that work using the application. On the other hand, the expertise of these systems can be integrated directly into the CAD system, through a certain module [8]

In this paper we will show the manufacturability analysis of the mechanical power transmission housing. The housing is parametrically designed using the CATIA V5 software package, and expert product knowledge is incorporated into the Knowledge-Based

System using rules, which provides an automated process of manufacturability analysis.

2. SIMULTANEOUS PRODUCT DESIGNING

Product development is a very complex task because it needs to meet the market criteria and achieve the expected profit in as short time as possible and with as little use of resources as possible. Simultaneous engineering integrated a numerous activities, as well as the collaboration of experts in various fields, thanks primarily to a strong information system. Such a concept is called Simultaneous engineering or Concurrent engineering, and it emphasizes the computer integration of all development and product development activities, and in recent years it has been called Integrated product and process development.

In the field of product design, modern CAD systems have special modules for different analyzes and simulations. The purpose of these modules is to facilitate the design decision-maker, and the basis for their work is a product model knowledge. Knowledge actually presents the facts that are selected according to the appropriate rules.

The knowledge necessary for the product design and its manufacturability is most often represented by objects and rules. The object is considered a model entity that is described by the attributes and associated with the environment by procedures. The rules are relational dependencies that represent a list of actions to be performed under certain conditions, and checks are certain expressions or relationships that can be verified immediately or on request to inform the user in case the conditional part of the check has been violated. Generally, both the rules and the checks ensure that the design that is being designed complies with the defined limitations.

3. MANUFACTURABILITY ANALYSIS

Each production process has its advantages and disadvantages, which makes it impossible to choose a universal method of manufacturing for all products, but by manufacturability analysis, we come to an optimal method or manufacturing process. In order to select the appropriate production process for a particular product, it is necessary to compare the necessary characteristics of this product with the capacities of the process.

Product manufacturability analysis is a specific activity, which aims at familiarizing with the product's manufacturing characteristics and the level of problems that can arise during its manufacturing [9]. In a typical CAD environment, the designer creates a product model and uses analysis software to examine various aspects of the proposed construction functionality.

Manufacturability analysis systems are, in fact, knowledge-based systems (KBs) that use existing knowledge to solve problems in a particular field. Certain CAD programs integrate KB systems, so CATIA has a "Knowledgware" module that is one type of expert system. Manufacturability process analysis actually evaluates the application of manufacturing technology to a particular product model. The process

takes place automatically by comparing the available techniques according to available resources and technological constraints.

4. MANUFACTURABILITY ANALYSIS AT THE EXAMPLE OF THE MECHANICAL POWER TRANSMISSION HOUSING

Housings are an important stationary element of mechanical power transmitters. The basic forms of the housing depend on the type of gear unit, the type of bearing and the mode of manufacturing (Is the housing cast or welded?).

The choice whether the housing will be made by casting or welding is mostly influenced by the volume of the series. In the case of a cast housing, the so-called. constant costs are greater (model, core molds), but are therefore smaller variable costs, i.e. costs are in proportion to the number of pieces manufactured.

Basically, cast housing is only cost-effective when a larger number of pieces (min 3) is made, while in individual production welded housings are used, since they are easier and less rigid [10]. Whether the manufacturer will opt for cast or welded housing, or combined housing (welded and casted), depends also on the availability of materials and tools in the factory, that is, on all the elements that define the manufacturing technology and the final price of the product in detail.

4.1 Recommendations and manufacturability limitations for housing manufacturing

The shape of the casting should be such as to ensure the smallest possible difference in the cooling speed of its parts, thereby reducing the defects during the casting process. The uniformity of the cooling speed is achieved by the uniformity of the thickness of the external walls (if possible, the difference in the thickness of adjacent walls should not exceed 50%). The change in thickness should be gradual, and the transition from one plane to another must have a round. The inner walls, which are cooler due to their position, should be thinner than the external ones by 20% to 40% [8].

The sharp edges at the transition between two walls or too small radius of the transient round lead to strong internal stresses and to the crack. This location should not have too great curvature, because in this case the material is accumulated, and at the center of such a transition, melted material is still accumulated due to hardening and cooling, while the adjacent walls have already solidified, thus breaking the possibility of passing new material to this spot, and therefore an internal cavity appears [8].

The smallest thickness of the walls that are successfully cast is limited because too thin a wall can lead to hardening of the material throughout the cross section until the entire mold is still not filled with casting, so that some parts of the mold remain unfilled. In case of casting parts made of gray cast, constructive recommendations do not allow the wall thickness to be below 6 mm, thus ensuring the functionality of the product [8].

4.2 Power Transmitter Housing Manufacturability Assessment

Manufacturing limitations are entered in software in the form of rules. The rules are in fact a set of commands that are grouped into databases, using the programming language. In the case of CATIA V5, a VB Script was used in which the user defines rules using the if / then relations [9]. By creating special tables that link to Excel databases, certain values that become the basis for later validation or check are entered.

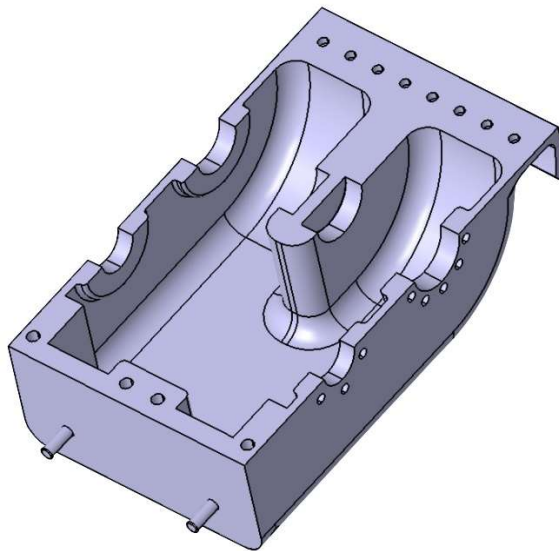


Fig. 1. Parametrically designed gearbox housing

The rules may sometimes have side effects, so it is important to incorporate mechanisms into the model that provide control and verification. This is achieved by special user-defined elements of knowledge, so-called checks (Figure 2). If the check shows that certain parameters are not in accordance with the defined rules, the user gets information about the impossibility of functioning in the form of notifications or advice. In this way, continuous control of any modification over the parametric model of the product is ensured, according to the established rules (restrictions).

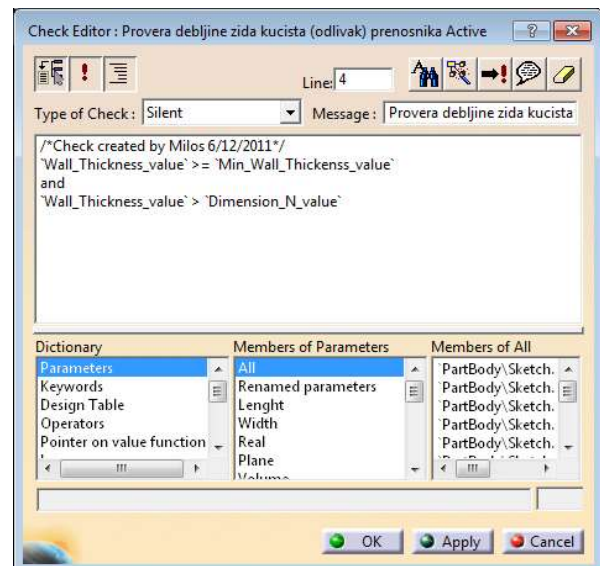


Fig. 2. Rule editor

5. EXAMPLE OF THE TECHNOLOGICAL ADVISOR FOR THE CREATED SCENARIO

The process of designing a product from the aspect of manufacturability is checked on the example of gearbox power transmission housing. The power transmission housing shown in Fig. 1 is parametrically modeled and then further described by attributes (spatial orientation, tolerance, materials, etc.). Such a knowledge model is integrated with the bases of available tools, available materials, and other numerous geometrical and technological limitations of. The integration of the module within the software package ensured that the software works as a virtual technology advisor.

If the designer wants to alter the wall thickness value (Figure 3), such as, for example, a thickness of 2.5 mm, a virtual technology advisor needs to examine the action and react to it as needed.

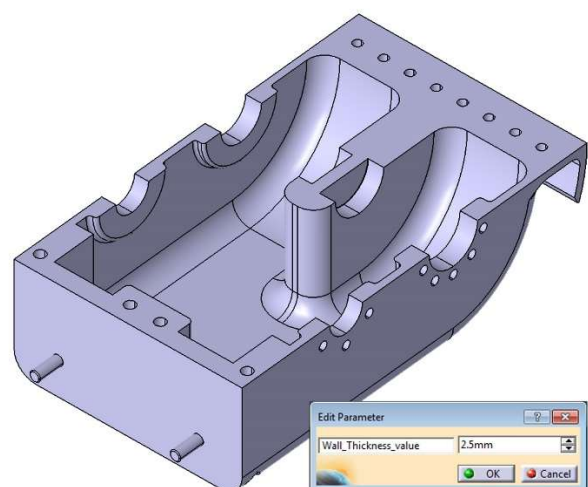


Fig 3. The designer enters the parameter change

As the previous steps defined a housing knowledge model and therefore the defined minimum thickness of

the housing wall, a virtual technological advisor with CATIA Knowledgeware, with previously defined relative dependencies in the form of rules, first announces the reason why it is not possible to make this change and gives notice in the form of a message:

"The minimum thickness of the casting can not be less than 4mm!"

After that, according to the maximum possible length of the housing, it determines the thickness of the wall. As this parameter (maximum possible length) is influenced by the total height, width and length of the housing, and based on the dimensions entered, Knowledgeware will make a change to 8 mm according to these parameters and give the following notice shown in Fig. 4:

"The thickness of the wall of the casting (depending on the maximum length produced) will be 8 mm."

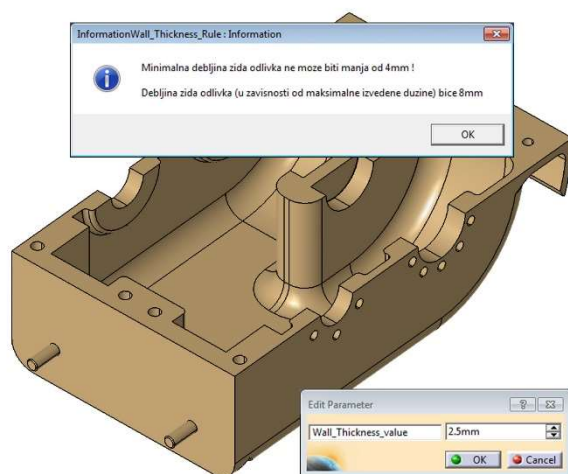


Fig. 4. CATIA Knowledgeware module reaction in the form of a technological advisor to the designer.

6. CONCLUSION

Manufacturability analysis is a comprehensive activity without which it is not possible to imagine the concept of modern design and product development.

The basis of the system is a parametrically designed product based on features. This ensures that product model knowledge is incorporated into a virtual product using certain relationships.

In this paper, a parametrically design model of the power transmitter housing is presented, created by simultaneous approach of experts from different fields. The use of CATIA V5 software and its Knowledgeware enables the introduction of technological constraints during the product design phase, allowing the designer to use the available resources or to clearly define certain design parameters, which ensures that the system acts as a technology advisor.

The proposed concept is successfully verified and further research of this concept will be directed towards the inclusion of other methods of artificial intelligence, such as expert systems.

7. REFERENCES

- [1] V. Miltenović, *Razvoj proizvoda – strategija, metode, primena*. Univerzitet u Nišu – Mašinski fakultet, 2003.
- [2] G. Devedžić, *CAD/CAM tehnologije*. Fakultet inženjerskih nauka u Kragujevcu, 2009.
- [3] Gauseimer J., Frank T., Hahn A., Integrated product development: An Integral Approach to Computer Aided Development of Advanced Mechanical Engineering Products, *Proceedings of International Conference on Engineering Design ICED 95*, pp. 1276-1289., WDK, Heurista, 1995.
- [4] J. Bralla, editor. *Design for manufacturability handbook*, 2nd ed. McGraw-Hill Professional, 1998.
- [5] Schleipen, M. et al., *Production Monitoring and Control Systems within the Digital Factory*. Advances in Intelligent and Soft Computing, 66 (Proceedings of the 6th CIRP-Sponsored International Conference on Digital Enterprise Technology.), pp. 711-724, 2010.
- [6] Manić M., Miltenović V., Stojković M., Banic M., *Feature Models in Virtual Product Development*. Strojišni vestnik, 56 (3). 2010
- [7] V. Mišković, *Sistemi za podršku odlučivanju*. Univerzitet Singidunum, Beograd, 2013.
- [8] Ristić M., *Projektovanje proizvoda sa aspekta tehnološkičnosti*, Magistarski rad, Univerzitet u Nišu – Mašinski fakultet, Niš, 2012.
- [9] Ristić M., Manić M., Cvetanović B., Pavlović M., Kosanović M., *Projektovanje proizvoda sa aspekta tehnološkičnosti: primer zupčastog prenosnika*. Infotech Vol. 15, pp.452-455, Jahorina, 2016.
- [10] M. Trbojević, M. Janković, J. Vugdelija, N. Plavšić, V. Latinović, *Reduktori*, Naučna knjiga, Beograd, 1977

Authors:

Professional Studies Prof. Miloš Ristić¹⁾, Full Prof. Miodrag Manić²⁾, Teach. Assist. Miloš Kosanović¹⁾, Teach. Assist. Milan Pavlović¹⁾

¹⁾ College of Applied Technical Sciences Nis, Aleksandra Medvedeva 20, 18000 Niš, Serbia, Phone: +381.18.588.211, Fax: +381.18.588.210.

²⁾ University of Niš, Faculty of Mechanical Engineering, Aleksandra Medvedeva 14, 18000 Niš, Serbia, Phone: +381.18.588.255, Fax: +381.18.588.244.

E-mail:

milos.ristic@vtsnis.edu.rs,
miodrag.manic@masfak.ni.ac.rs,
milos.kosanovic@vtsnis.edu.rs,
milan.pavlovic@vtsnis.edu.rs

ACKNOWLEDGMENTS:

The paper is a result of the project III 41017, supported by the Ministry of Science and Technological Development of the Republic of Serbia.

Ristovska, B., Papazoska, E., Gecevska, V.

IMPROVING MANUFACTURING PROCESS BY OPTIMIZING TIME PARAMETERS

Abstract: *Lean methodology as one of the most modern ways of working, uses a variety of methods and tools that are aimed at continuous improvement and functioning of a single system. Due to its growing use in the manufacturing and service sector, Lean methodology is the subject of this paper. First, a series of Lean methods and tools will be presented to help analyze the current state of the selected production process, from raw materials to finished product. Then, with the help of the obtained data from the monitoring, it will be determined whether it is possible to improve the production process, by calculating the required number of operators in relation to the number of machines operated by one operator and the required number of operators in relation to the takt time, which in turn is related to the volume. Finally, a comparison of these data will be made to determine the future state of the process.*

Key words: *Lean methodology, production process, takt time*

1. INTRODUCTION

The growing domestic and global competition, the incessant development of new technologies, the constant changes in the consumer demands, the short product life cycle, and the increased costs are the reasons why organizations are focused on product development, response times, demands, budget and performance. For a company to be one step ahead of its competitors, the most important thing to focus on is reducing the time that does not add value, continuously improving all of its processes from within and finding a way to produce products with lower price, better quality and faster delivery [1,2]. In order for companies to survive on the market and be competitive, they need to apply methodologies that achieve positive results across the entire process of production.

2. LEAN METHODOLOGY AND LEAN TOOLS

The lean principles are not created as a result of theoretical consideration; they were originally developed in practice and later adopted by scientists [1]. Lean means less of everything: less energy, less investment, effort and capital. Lean is a production philosophy that by its implementation affects the shortening of time of delivery of the finished product to the client; and it eliminates all sources of waste, that is, the losses in the production process. The basic principle of Lean's management, production is to produce exactly what the client wants, in other words, the quality and quantity of the products are directly dictated by the market i.e. the client. Lean management is a way of thinking and working of the entire system. Such a system uses different models and tools in order to continuously improve the functioning of the system.

It is worth pointing out that Lean is thinking about the best performance in all technological processes. The ultimate goal is human development and the use of the mind of all employees. Therefore, such thinking should be shared by all employees and must also be involved in the implementation. Lean principles as means of testing the business process [2]:

- The first principle defines the values. The product or service must be delivered to the client when the client wants it and at the place where the client wants it. It is necessary to listen to and recognize the needs of the client and to identify well the value that the product has for the customer, how customers see the product.
 - The second principle is the mapping of the flow of values
 - The third principle of the Lean methodology is to create a flow. In order to achieve the best flow in the production process, we need to distance ourselves from traditional thinking and rebuild resources so that the process can take place with continuous flow.
 - The fourth principle of Lean's methodology is the pull principle,
 - The ultimate principle of Lean's methodology perfection, pursuing perfection or aspiration for continuous improvements.
- When it comes to Lean in manufacturing companies, several things must be provided to ensure that Lean will function successfully, and these are:
- Well-established and balanced production,
 - Flexible people and machines,
 - Top-notch quality,
 - Reliable equipment and machinery,
 - Reliable suppliers,
 - Very short tool replacement time
 - A great deal of discipline.

The principles discussed above provide the framework of the Lean philosophy and their application supports the transformation of the organization into Lean enterprise [3]. Next is the presentation of some of the most popular Lean management methods and tools and their use in the production environment.

1) Value Stream Mapping (VSM) corresponds directly to the first Lean principle, that is, to the Value Determination Principle. It includes the process of graphically drafting all the activities needed to move the product through the value stream and to identify and remove the waste thereafter. In doing so, it is necessary to illustrate both the material flow and the flow of information. As an initial step for one Lean

business is creating the current state of the value flow. Afterwards, improvements are made according to the Lean philosophy and the desired state (future) is recorded in a new map of the value stream.

2) Standardized work process

The standardization of the work process establishes the best methods and sequences for optimizing performance and minimizing waste (activities that do not add value). This ensures that the activities will be carried out the same way at any time. With the standards in the performance of its activities, Lean company gets consistency in its production processes.

3) 5S Methodology

The 5S methodology provides a standardized working environment and allows the employees see the flow of the process. The 5S can be seen as a good starting point for implementing the Lean Initiative.

4) Visual Management

Visual management allows workers to be fully informed about the production procedures, the current state and other important things so that the process would take place more efficiently. Large displays in the halls are a far better way of communication than written reports, so more should be used. When it comes to improving the processes, visual management helps the team of workers to better understand the work, facilitates understanding of the order of the complicated activities and their internal and external tasks interactions with the surrounding work units

5) Kanban

Kanban is a method based on the extraction system, which uses visual signals (for example, cards in different colors) to signal production contrary to the course of production. In fact it represents a certain complement system: complementing the required parts in the right amount at the right time and at the right time. It is means of communication in the extraction system. Kanban can be: a card, an empty pallet, a visual display, that is, any element that gives a signal to start producing a particular part.

3. CASE STUDY OF LEAN APPLICATION IN A PRODUCTION COMPANY

Lean production presents optimization of the process, using empirical methods to figure out what adds value to the client, as opposed to the uncritical welcome to all ideas [4][5]. The benefits of implementing Lean manufacturing principles to real productive environment are presented in this case study implemented in Aptiv, Macedonia.

Aptiv is one of the largest suppliers to the automotive industry delivering advanced electrical and electronic, motor and vehicle safety technologies around the world, enabling the manufactures to make vehicles that are safer and better connected.

Aptiv Macedonia in particular produces printed circuit boards. The production area as shown in Figure 1 is separated in two parts SMT (surface mount technology) and FA (final assembly). This project aims at improving the final assembly and determining the optimal number of operators in this part of the production.

In this case almost all of the Lean tools are used, but the predominant one is the Standardized Work process because with the help of the Standardized work process it is easier to analyze the working pattern and/or improve it.

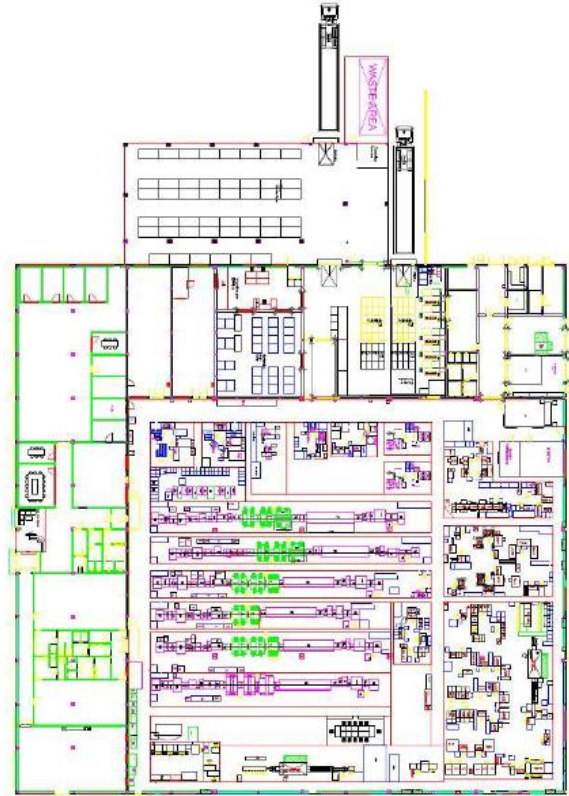


Fig. 1. Company layout

3.1. Definition phase

The analysis of the production process and the standardized work process of every post led to a problem with the operator's utilization after which we decided to analyze the process in terms of two parameters, the number of machines and the takt time to see the optimal number of operators.

3.2. Measurement phase

In this phase we measured each working activity performed by the operators. In this phase both the cycle times and the non-cycle times that are included (for example activity that happens every 3rd or 6th cycle).

The time for one printed board is given in seconds, with 10 measurements done for each cycle (Tab.1& 2).

Line	1	2	3	4	5	6	7	8	9	10	Average
Drilling	6.3	6.05	6.3	6.2	6	6.01	6.4	6.15	6.1	6	6
Pressfit Single	17.4	16	18.7	18.6	19	18.8	18.6	18.5	18.9	19	18
Pressfit Double	13.4	13.5	14	13.05	13.5	13.3	13.6	13.6	13.5	14	13.5
Test	8.9	9	9.25	8.87	9.25	9.25	9.25	9	9	9	9
Coating	8	8.1	8.1	8.1	8.1	8.1	8.1	8.1	8.1	8.1	8
Final assembly	6.8	7	6.5	6.3	6.5	6.6	6.8	6.3	6.6	6.05	7
Test	9	9	8.9	9	8.7	8.8	9	9.2	9.3	9.1	9
Bracket assembly & CMI	9.6	9.3	9	9.15	9.7	9.9	9	9.3	9.4	9.1	9

Table 1. Measured Cycle time

Machine	Time
Singulation	0.65
Pressfit Single	0.3
ICT test	0.5
Coating	0.5
Housing	1
EOL test	2
Bracket assembly & CMI	1.5

Table 2. Measured Non-Cycle time

3.3. Analysis phase

3.3.1 In relation to the number of machines that are operated by one operator

The purpose of this paper is optimization, improving the production process through time parameters. First to calculate is the number of operators required in relation to the number of operated machines, because in some cases there is more than one machine operated by one operator, depending on the times, that is, the manual time and the machine time.

The calculation of the required number of operators also took into account the previously mentioned standardized work process that was created. Also, this calculation takes into consideration the bottlenecks in the production process.

In production, the bottleneck is one process in the process chain that with its limited capacity reduces the capacity of the entire chain. There are short and long-term bottlenecks. Short-term bottlenecks are temporary and are usually not a significant problem. An example of a short-term bottleneck would be a skilled employee who would take several days off work. Long-term bottlenecks occur all the time and can cumulatively slow down production. An example of a long-term bottleneck is when the machine is not efficient enough and as a result there are delays.

The method of calculating the number of operators in relation to the cycle time, the manual time and the machine time will be shown in the following example.

If we have 4 machines, whose machine time is 58 seconds, and the manual operation lasts 22 seconds, in order to get the required number of operators for operating these machines it is necessary to calculate the required number of operators = (manual operation * number of machines) / machine time or in this example

$$(22 * 4) / 58 = 1.5 \text{ operators}$$

Table 3 gives the calculations for the number of operators in relation to the number of machines.

After the calculation and the numbers we can conclude that there is difference of 0.7 and 0.5 operators on the ICT test and EOL test machines.

Machine	Cycle time	Non-Cycle Time	Manual work	NCT + MW	Volume per day	Calculated operators	Number of machines	Current number of operators	Difference
Singulation	6	0.65	4	5	7800	1	1	1	0
Pressfit Single	18	0.3	7	7	7800	0.4	1	1	-0.6
Pressfit Double	13.5	0	13	13	7800	1.0	1	1	0
ICT test	9	0.5	7	8	7800	1.7	2	1	0.7
Coating	8	0.5	6	7	7800	0.8	1	1	-0.2
Housung	7	1	4	5	7800	0.7	1	1	-0.3
EOL test	9	2.0	2.5	5	7800	1.5	3	1	0.5
Bracket assembly & CMI	9	1.5	9	11	7800	1.2	1	1	0

Table 3. Calculated number of operators in relation of the number of machines

3.3.2 In relation to the takt time

Next is the calculation of the required number of operators in relation to takt time, with the help of the collected data and the performed measurements of all processes.

With the takt time, it is shown how often a part or product should be produced, that is, the amount of time the product should come out in terms of volume, the quantity of products that is required by the client.

It is obtained as a ratio between the available working hours per day (in seconds / minutes) and the client's daily demand (in pieces), the quantity of products in number of pieces. This calculation of takt is used to synchronize the pace of production with the pace of sales.

In this particular process, the takt time was calculated by taking the time (in hours) that is used by the company as effective time, together with the foreseen breaks are taken in all of the 3 shifts. It is important to note that the production does not stop during the day, also during the breaks the work continues with less effectiveness and output because fewer operators are working. Here, the takt time for the SMT line and FA is calculated separately (Table 4).

In order to calculate the required number of operators using the takt time which was previously calculated, the same data of the previous calculation will be used.

The calculation of the number of operators with takt time is as follows:

$$\text{Required number of operators} = (\text{manual time} * \text{number of machines}) / \text{time}$$

Takt time		
Work shifts per day	3	Shifts
Hours per Shift	8	Hours
Break time per shift	10	min
Lunch time per shift	20	min
Customer demand per day	7800	units
Available time per shift	480	min
Net working time per shift	460.2	min
Net working time per shift	27612	s
Net working time per day SMT	84960	s
Net working time per day FA	82836	s
Takt time SMT	10.9	s
Takt time FA	10.6	s

Table 4. Calculation of takt time

In this calculation of the required number of operators the volume as a parameter is included in contrast to the

previous calculation.

Table 5. shows the calculations for the number of operators in relation to takt time. If we analyze the Table 6, from the results it can be concluded that this calculation gives similar results, there is a difference in the same processes as before, ICT and Pressfit, but the numbers are smaller than in the previous calculation.

Machine	Cycle time	Non-Cycle Time	Manual work	NCT + MW	Volume per day	Calculated operators	Number of machines	Current number of operators	Difference	Difference	Calculated operators	Takt time
Singulation	6	0.65	4	5	7800	1	1	1	0	-0.6	0.4	10.6
Pressfit Single	18	0.3	7	7	7800	0.4	1	1	-0.6	-0.3	0.7	
Pressfit Double	13.5	0	13	13	7800	1.0	1	1	0	0.2	1.2	
ICT test	9	0.5	7	8	7800	1.7	2	1	0.7	0.4	1.4	
Coating	8	0.5	6	7	7800	0.8	1	1	-0.2	-0.4	0.6	
Housing	7	1	4	5	7800	0.7	1	1	-0.3	-0.5	0.5	
EOL test	9	2.0	2.5	5	7800	1.5	3	1	0.5	0.3	1.3	
Bracket assembly & CMI	9	1.5	9	11	7800	1.2	1	1	0	0.0	1.0	

Table 5. Calculated number of operators in relation to takt time

Machine	Cycle time	Non-Cycle Time	Manual work	NCT + MW	Volume per day	Calculated operators	Number of machines	Current number of operators	Difference	Calculated operators	Takt time
Singulation	6	0.65	4	5	7800	1	1	1	-0.6	0.4	10.6
Pressfit Single	18	0.3	7	7	7800	0.4	1	1	-0.3	0.7	
Pressfit Double	13.5	0	13	13	7800	1.0	1	1	0.2	1.2	
ICT test	9	0.5	7	8	7800	1.7	2	1	0.4	1.4	
Coating	8	0.5	6	7	7800	0.8	1	1	-0.4	0.6	
Housing	7	1	4	5	7800	0.7	1	1	-0.5	0.5	
EOL test	9	2.0	2.5	5	7800	1.5	3	1	0.3	1.3	
Bracket assembly & CMI	9	1.5	9	11	7800	1.2	1	1	0.0	1.0	

Table 6. Calculated number of operators in relation to the takt time and the number of machines (comparison)

4. COMPARATIVE ANALYSIS OF THE IMPROVEMENTS ACHIEVED ON THE ANALYZED PROCESS

If we compare the results of the calculations it can be concluded that in all the processes the optimal number of needed operators obtained with the calculations corresponds to the number of operators currently serving the machines except in the ICT and Pressfit processes, where the operator is missing, both in terms of the number of machines and in relation to time. On these posts more machines are operated by one operator so that the results obtained actually prove that the operator does not manage to operate the machines on time, the operator does not wait for the machines, but the machines wait for the operator and therefore there is a waste of time. Setting up plus one operator on these posts, machines, will result in full capacity and volume and therefore full utilization of the machines.

Additional analysis of the results leads to conclusion that by adding plus one operator on the ICT post, the utilization will reach 70% in comparison to the utilization of the second person of the EOL. By reviewing the remaining results, it can be concluded that the EOL 0.5 operator can be obtained by sharing the operator from the Housing position who is not fully utilized.

5. CONCLUSION

Lean is a production philosophy that, when implemented, shortens the time from order to delivery of the finished product to the client, eliminating all sources of waste, i.e. losses in the process of production. The focus of the Lean philosophy is adding value to the client. This way of thinking reduces the unnecessary steps in the activities that add, but also in the activities that don't add value to the clients.

The benefits of Lean are reflected in the reduction of the production time, increased quality, flexibility and customer satisfaction. The effective implementation of Lean methodology in the organization results in the company strengthening the framework of its organizational and inter-organizational relations. It also

achieves better flexibility and ability to quickly respond to the changes in the customer demand, that is, better involvement of the employees and better financial and non-financial results. Although the Lean system has more advantages than flaws, certain caution is required when implementing Lean, so these flaws can have no negative impact on the company. One of its key disadvantages is that the Lean methodology provides little room for errors and does not create inventory. Lean methodology is applicable in all activities and in all organizational structures, both in the manufacturing sector and in the service sector.

In this paper, on the basis of the obtained results from the calculations and analysis it is concluded that the production process in question in the company Aptiv does not work with the optimal number of operators. With the previously obtained results in relation to the number of machines and the takt time which is connected with the quantity of products to be produced, it is concluded that an ICT operator is needed for full utilization of the machines.

6. REFERENCES

- [1] The Toyota Way: 14 Management Principles from the World's Greatest Manufacturer Jeffrey Liker, 2015.
- [2] Taylor, G. M. "Lean Six Sigma Service Excellence. Fort Lauderdale: J.Ross Publishing, 2009.
- [3] Sunder R., Balaji A., *Review on lean manufacturing implementation techniques*, Procedia Engineering, Vol.97, 2014, p.1875-1885.
- [4] Slack N., Brandon-Jones A., Johnston R., *Operations Management*, Pearson, Edinburgh, 2014.
- [5] Duanmu J., Taaffe K., *Measuring manufacturing through using takt time analysis and simulation*, Proceedings WSC'07, 2007, p.1633-1640.

Authors: Bojana Ristovska, Elena Papazoska, Full Prof.Valentina Gecevska, University „Ss. Cyril and Methodius“ in Skopje, Faculty of Mechanical Engineering, Karpos 2 bb, P.O.Box 464, 1000 Skopje, Republic of Macedonia, tel: +38923099200.

E-mail: ristovskabojana@gmail.com;
elenabacanovska@yahoo.com;
valentina.gecevska@mf.edu.mk

ACKNOWLEDGMENTS: Authors wishing to acknowledge support from company Aptiv Macedonia.

Skenderovska, T., Gecevska, V., Polenakovik, R.

INCREASING PRODUCTION CAPACITIES THROUGH THE DEVELOPMENT AND INTEGRATION OF THE 5 STAGE PROJECT MANAGEMENT METHODOLOGY

Abstract: This paper is based on the discipline that is still in process of continuous development, which is the project management discipline with basic information necessary to run a project. The 5 stage methodology, which is the basic tool for this discipline, has been expanded and integrated into the 7 stage methodology for application in all industries. The application of the improved methodology can be clearly seen where the main goal of the on-going project is to increase project capacities of an existing production plant by introducing a new product for automotive industry as a result of the requirements of the main clients. Finally, an analysis is presented that puts the foundations for further continuous improvement of this methodology.

Key words: Project Management, 5 stage methodology, process group

1. INTRODUCTION

As never before, the application of project management and project development is increasingly being applied especially in the field of industrial aspect, by increasing production capacities, process optimization, and introduction of new production processes, methods of work and continuous improvement of all segments on one plant.

The project is an instant effort that is undertaken in order to make a unique product, service or result [1]. The temporary nature of the projects indicates that each project has its start and end. The end can be seen when the goals are achieved or the project is pre-determined. A project can create:

- A product that is a final part or a component of another part
- Service (a business function that supports production or distribution)
- Improve an existing product or service line (for example a Six Sigma project that is undertaken to reduce defects.
- Document - theoretical research.

2. PROJECT MANAGEMENT METHODOLOGY

Project management uses knowledge, skills, tools and techniques to carry out project activities that need to meet the requirements set by one project [1]. Project management is carried out through the appropriate application Fig.1 and integration of 47 locally grouped processes, which are divided into five process groups:

1.Initiation – these processes are used to define a new project or a new stage of an existing project by providing authorization to start the project or phase.

2.Planning – processes that require introduction of the project scope, defining the objectives, defining the direction of movement of the activities necessary to achieve the objectives of the project.

3.Installation / Construction of the project – these processes are used to perform or complete the defined work activities in the project management plan in order to meet the project specifications.

4.Monitoring and control – these are processes that require monitoring, reviewing and regulating the progress and performance of the project. Also, identification of areas where changes and initiation of appropriate changes will have to be made.

5.Completion of the project – this process or project phase is final and serves to close or complete all activities in all process groups in order to finalize the project or phase.

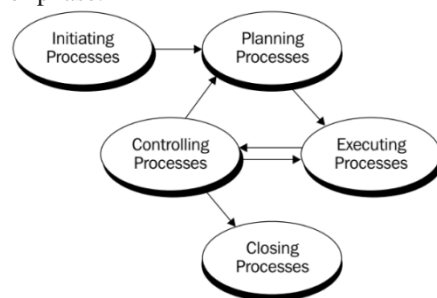


Fig.1. Process groups - 5 stage project methodology

The management of a project actually involves many activities and it is not limited to [1,2]:

- Defining requirements;
- Presentation of needs, care and expectations by stakeholders who are active, effective and collaborative in nature;
- Positioning, maintaining communication with stakeholders who are active, effective and collaborative in nature;
- Getting acquainted with stakeholders through project requirements and defining project tasks and deliveries;
- Balancing the project's intensity which includes but is not limited in terms of: quality, scope, schedule, budget, resources and risk.

3. INTEGRATION OF THE 5 STAGE INTO 7 STAGE METHODOLOGY

The previously presented general methodology of project management with 5 stages has to be adapted for projects where the aim is increasing production capacities and optimization of processes in one production unit [3].

The general five-stage methodology is expanded in 7 stages, thus providing better follow-up of the entire project and its better understanding through a detailed presentation of all activities or tasks to be performed. This methodology allows traceability on the three key performance indicators which present the success on each project stage (Fig.2). The key performance indicators are: Time, Cost and Quality.

The next picture represents the integrated and improved seven stage project methodology with application in all industries:

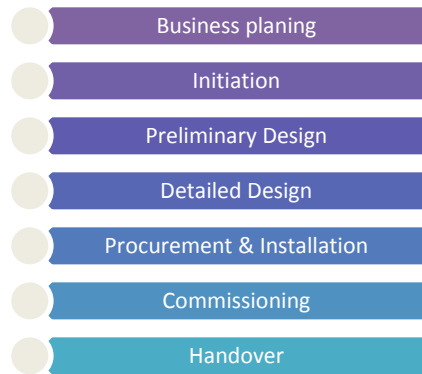


Fig. 2. Process groups - 7 stage project methodology

Running a project according to this methodology must take into account all the stages in their right order, to obtain the desired traceability and information for crossing from one stage to the next. Information is a key and indispensable factor for capital projects, as their lack affects the timeframe for meeting it, and thus causes dissatisfaction with higher-level stakeholders. The good traceability of a project can provide us with an adequate level of sustainability, quality and business continuity, the results of which can be seen with its completion.

Each of the presented stages has a certain time period which depends on the scope of the project itself (Fig.3). The graphic display shows that most of the time is spent in the stages of preliminary and detailed design where the research and analyzes for obtaining an appropriate production process through appropriate equipment is the main objective of the project. Furthermore, business planning and initiating the project are short stages through which the cost-effectiveness of the entire project is realized.

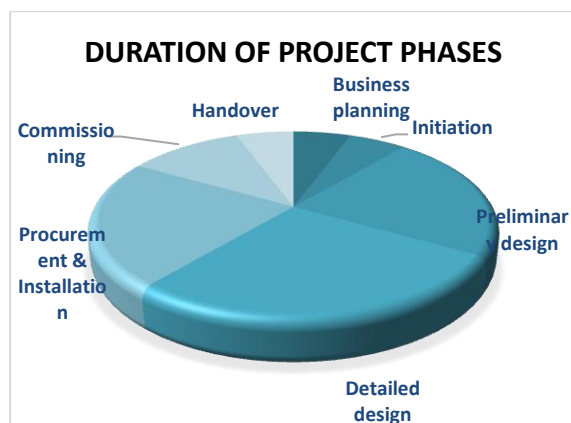


Fig. 3. Duration of the project phases

Procurement and installation is a critical phase of a degree approximately equal to the design phases. The reason for the long period of this phase is the installation of the necessary equipment, which carries additional activities. With the calibration of the new equipment, testing and commissioning is carried out. This is a short-term phase that ensures that the installed equipment is in the proper working condition. Finally, the stage of the project delivery is actually handing over the entire project documentation to one of the main stakeholders and its duration is usually 1 day.

3.1 Difference between stages in both methodologies

The difference between the two methodologies is the number of stages that they are divided in. Main difference in these methodologies can be seen primarily in the business planning phase, preliminary and detailed design. Business planning is an added stage in analyzing the cost-effectiveness of a project and the return of investment. On the other side, the planning phase in the improved methodology is divided into a preliminary and detailed design where the development of production equipment is clearly followed, which is very important for the industrial environment (Fig.4).



Fig.4 Difference between the two methodologies

4. PRACTICAL IMPLEMENTATION OF IMPROVED 7 STAGE METHODOLOGY

The practical use of this methodology can be seen in the following example where the main goal of the project was increasing production capacities by *introducing a new product for automotive industry*, as a demand from the main customer. Production process of the new product is different than the existing one with one main difference, number of production areas where ultimately the final product is obtained.

From the initial information that was known about the new production process and product, it came to the conclusion that many types of new raw materials will be used, which will require additional procurement and installation of production equipment just like the previous one, which will meet the required capacities. By defining this initial information, a delivery project period of 2 years was defined, as this represents the period when the finished product should be delivered to the buyer. The given initial information enables achievement of the main task of the project manager and project team by defining everything that is

necessary for quality delivery of the project and the possibility of obtaining the required products. From the moment of obtaining this top management order, the project is given to the project manager, which is further followed by the integrated methodology as a pilot project after all the steps given for each stage [4].

4.1 Business planning

The stage of business planning is the first and only stage that has not been fully implemented by the project team. It is carried out internally in the company, with each department aiming to carry out a specific work assignment. The activities or steps that cover this stage are:

- ROI
- Traceability matrix
- Feasibility study
- Hazard study 1
- Stage report

Business planning stage gate approval Return of investment analysis is an indispensable step that needs to be taken in order to see if you need to invest in a project and it is calculated according to the following formula (4.1):

$$ROI = (Total\ Revenue - Total\ Cost) / Total\ Cost \quad (4.1)$$

The risk matrix is an important tool used during the start of a project where risk assessment and risk level are defined, taking into account the probability category in terms of the severity of the consequences that can arise in this project.

The Hazard study is a proven method that is used to identify potential hazards and problems associated with occupational health and safety that may arise by installing new equipment or by introducing a new production process.

Stage report and stage approval are one step where general manager approves the activities done for further transition to the next stage.

4.2 Initiation

The second stage of initiation has longer time duration than the previous one, with focus on planning the course of the project and not the feasibility analysis of the project. At this stage, much of the necessary information and details are received, which easily crosses into the third and fourth stages of a detailed and preliminary design. This stage includes:

- Project Structure
- User Requirements Specifications
- Project Scope
- Project Plan
- RACI matrix
- Hazard Study 2
- Stage report & gate approval

Defining the project structure and project scope is made by the project manager where using the given resources, project scope is defined for each team member. Project plan is also closely related to the project scope and that is actually the bottle neck in this methodology that is open for improvements. Satisfying

stakeholders with a good project plan with no delays is very important.

RACI matrix is also defining all human resources which are available for the project. The URS is the basic document listing all the requirements related to the basic parts that cover the equipment as well as the raw materials used for the first production of semi-finished products and ultimately obtaining the final product. This is the most important document for one project that has to be prepared by the main customer of the production equipment.

Last, same as the previous stage a hazard study 2 is made with “What if analysis” where potential risk are being located. Stage report and gate approval are last step of Initiation stage.

4.3 Preliminary Design

The design phase in this integrated methodology is divided into two sub-phases of a preliminary and detailed design. The reason for this division is the need for detailed monitoring of equipment specifications in order not to make a mistake that cannot be easily solved at the installation stage [5]. The preliminary design stage is extremely important because of the changes that need to be made if there are changes of requests in the URS document. This stage includes:

- Defining specifications of all equipment
- Budgetary quotations
- Defining needed budget
- Cost tracking
- Layout of production equipment
- Defining risks
- Hazard study 3 – HAZOP
- Stage report & gate approval

Defining the specifications for the equipment that is going to be procured is an activity that reflects the entire project stage of a preliminary design. Led by the URS document the following equipment was needed: Dosing systems, Preparing units, Extraction system and Filtration system used before the final product is done.

This project activity is simpler in terms of market analysis (research) and the search for suitable vendors. Based on the initial prepared specifications for the equipment, a preliminary offer is required to help create the future budget.

Monitoring costs is an activity carried out by the project manager, it reviews all received budget offers from the vendors. With these offers, a space for making a value analysis is created, with which the appropriate solution can be determined.

Hazard Study 3 (HAZOP) is committed to the equipment that will be procured. From the results obtained from the study of all raw materials that will be used for production, the possibility of igniting one of the raw materials is indicated, and an analysis of all the equipment used for that raw material should be carried out.

Last step is the stage approval.

4.4 Detailed Design

The continuation of the preliminary design stage is the detailed design stage. At this stage, a detailed definition of the specifications of all the equipment to be installed is given in detail, taking into account all the smallest and negligible parts that in the previous phase were not a topic and scope of work. The activities that are going to be undertaken in this phase are few, with the only focus on the production equipment. Other activities included in this phase are [6]:

- P & ID diagrams
- Process flow diagrams of production process
- Hazard study 4
- Stage report & gate approval

P & ID diagrams as well as the process flow diagrams are prepared for all production equipment and processes.

The fourth part of this study concerns the provision of information on the construction of an existing production plant and how its upgrading can affect the overall design. Taking into account are the capacities of existing structures and the load on the floor, electrical and mechanical capacities, existing pipeline capacities.

Last step is the stage approval.

4.5 Procurement & Installation

As the most dynamic stage in the 7 stage methodology is the stage of procurement and installation. Project team starts with procurement and installation of the chosen production equipment. This stage also includes:

- Purchasing orders
- NDA (Non-Disclosure Agreement)
- Hazard study 5
- Induction for installation
- Stage report & gate approval
- NDA will be signed with all chosen vendors.

Induction for installation will be done for all installation contractors.

In parallel with the installation process, the hazard study is carried out where preparations were made for the testing process of the entire installed equipment.

4.6 Commissioning

Testing is the analysis and checking of the installed equipment i.e. machines and electricity whether they work according to the given parameters and meet the requirements.

There are two types of equipment testing:

- FAT (Factory Acceptance Test)
- SAT (Site Acceptance Test)

FAT testing takes place in the production plant of the supplier while Sat testing is performed after the installation and calibration of the equipment in the existing production plant.

4.7 Handover

The final phase of the integrated 7 stage project management methodology applied in this project refers to the preparation of all documentation for maintenance of the purchased equipment that in the end is being delivered to the maintenance department.

5. FINAL REMARKS

From here it is possible to see the purpose of project management and the manner of running projects according to the 5 stage methodology of project management. This methodology according to different needs can be changed, which in the given example was integrated into the 7 stage methodology.

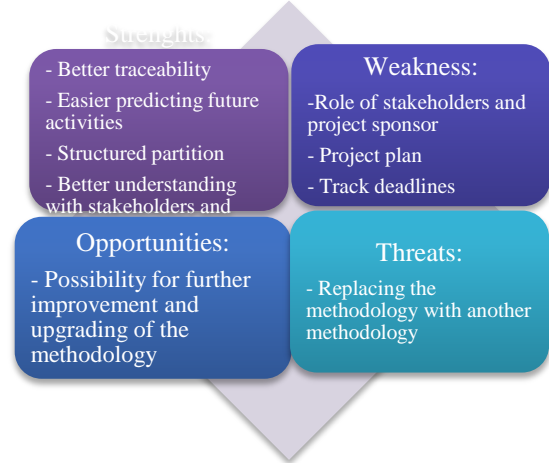


Fig.5 Final remarks for 7 stage methodology

However, although it has improved, this methodology has some disadvantages as well as opportunity for future improvement that can be seen through the following SWOT analysis given at the Fig.5.

6. REFERENCES

- [1] Project Management Institute. *A Guide to the Project Management Body of Knowledge(PMBOK Guide)*, Newtown Square PMI, NY, 2013.
- [2] Turner, J. R. *The handbook of project-based management: improving the processes for achieving strategic objectives*, London: McGraw-Hill, 2016.
- [3] Karlstrom D., Runeson P.: *Combining agile methods with stage-gate project management*, IEEE Software, Vol. 32-3, pp. 43-49, 2015.
- [4] Kerzner H.: *Project Management: A Systems Approach to Planning, Scheduling, and Controlling*, Wiley Pub. 2017.
- [5] Clarke A.: *A practical use of key success factors to improve the effectiveness of project management*, Int. Journal of Project Management, Vol.27-3, pp. 139-145, 2009.
- [6] Chase R., Jacobs F.: *Production and operations management : manufacturing and services*, McGraw-Hill, NY, 2016.

Authors: Tiana Skenderovska BSc, MSc candidate, Full Prof. Valentina Gecevska, Full. Prof. Radmil Polenakovik, University Ss. Cyril and Methodius in Skopje, Faculty of Mechanical Engineering, Karpos 2 bb, P.O.Box 464, Phone.: +3923099200, Fax: +3892 3099298.

E-mail: t.skenderovska18@gmail.com;
valentina.gecevska@mf.edu.mk;
radmil.polenakovikj@mf.edu.mk

Sormaz, D., Gouveia, R., Sarkar, A.

RULE BASED PROCESS SELECTION OF MILLING PROCESSES BASED ON GD&T REQUIREMENTS

Abstract: *The IMPlanner is an ongoing CAPP software project that enables rapid and detailed process selection of manufacturing processes based on specific details of CAD models such as GD&T requirements and feature recognition. A mapping of the different manufacturing routes possible for a given CAD design are outputted by the software, electing the optimal solution. Previously this software focused mainly on hole making operations however, further research has enabled its expansion towards milling operations.*

Key words: *CAPP, Process Planning, Milling Sequence*

1. INTRODUCTION

Process planning is fundamental to ensure an optimize relation between design and manufacturing [1]. By implementing CAPP (Computer Aided Process Planning) tools, the translation of design features and tolerances in to manufacturing processes are no longer dependent of work-force knowledge. A CAPP tool is capable of extracting all of the necessary knowledge from a CAD (Computer Aided Design) design file and allocate the necessary sequence of processes, tools and machines capable of producing such product. The knowledge base and rules with which the CAPP tool functions is the key for an improved result [2]. In this work, the expansion of the IMPlanner CAPP software into the field of milling operations is addressed. Section 2 contains a review of previous work developed, 3 explains modules developed in the software, section 4 presents case studies and section 5 concludes the paper.

2. PREVIOUS WORK

CAPP tools have been a highly researched topic for a few decades now, having been studied through varied methodological approaches as can be seen in [1]. Knowledge based systems are the foundation for the work here developed and a thorough review of these systems can be read in [3]. More recently CAPP systems are being devised to aid as virtual manufacturing tools [4], distributed process planners [5] and integration tools [6]. Process selection is an important task of process planning as it ensures which process and tools are capable of producing a given feature while meeting design specifications. Usually during process selection a series of alternative processes and manufacturing paths are evaluated to determine which are more capable of achieving the desired objectives, such as production speed, cost, accuracy, among others [3]. For a CAPP tool, the process selection segment will verify which equipment/tool set is capable of producing a given feature regarding geometrical and/or dimensional tolerances, or if needed which series of process are

needed to obtain the desired result. Simultaneously, CAPP tools are also able to estimate production time and cost for each manufacturing step.

When performing process selection tasks, regarding a certain process or machine shop, it is necessary to consider three existing levels of knowledge: universal, shop and machine level knowledge [7]. As indicated by the name, universal knowledge does not address the specifics of a process, is usually encountered in handbooks and is only used when details of a process are unknown. Shop level knowledge is drawn upon the specifications of equipment and tools to predict process outcome. Machine level knowledge considers the capabilities of a specific equipment, such as achievable tolerance, based on on-site experience, e.g. on collected data via statistical process control, allowing to quantify the exact capability of an equipment. When equipped with these levels of knowledge in a data base, it is possible to create an accurate and reliable process selection and planning. Even though this paper will only address universal knowledge, the robustness of the model developed can be easily adapted to any type of knowledge base.

Extensive work has been developed regarding process planning of hole making operations by authors in [8], [9] and [10] however, milling operations are still lacking research depth due to higher variation of process equipment, tools and feature geometries.

3. METHODOLOGY

3.1 IMPlanner Software

The IMPlanner CAPP tool is an ongoing software project under development at Ohio University [11] that aims to allow the end user to generate alternate, precise and detailed manufacturing process selection, sequencing and scheduling plans, using CAD design files as a starting point. This is achieved due to the different modules encoded in the IMPlanner software than can convert design features into manufacturing steps and attribute them to specific manufacturing process. A few examples of some important modules in the IMPlanner tool are: the process plan object module

which encompasses all of the information relative to manufacturing processes, their hierarchy and properties of materials, cutting tools, equipment etc.; the rule-based process selection module (RBPS) that detains the knowledge regarding capabilities of a given process, reasoning against GD&T information such as feature dimension, tolerances and their relation; the feature mapping module which captures design information from the CAD model. Process precedence is also evaluated in order to ensure the correct order of manufacturing processes and steps. The overview of the IMPlanner architecture can be seen in Figure 1.

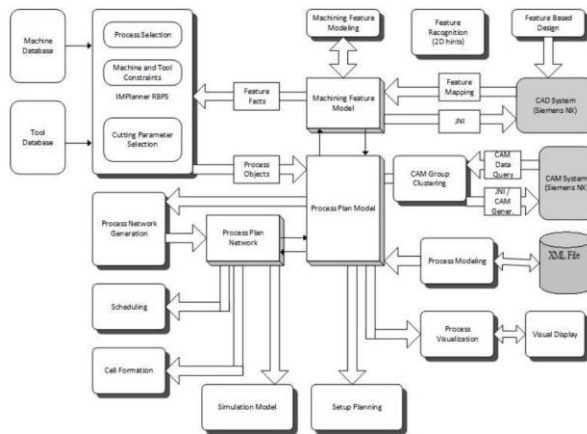


Figure 1. IMPlanner CAPP tool architecture.

3.2 Rule-based Process Selection Module

The RBPS module selects the appropriate manufacturing processes for the feature requirements captured from the CAD file by the feature mapping module, as well as testing for machine and tool availability (rules are essentially If-Then statements coded in Jess (Java Expert System Shell)) [12]. Rules can be grouped into the following areas of action [13]:

1. Process selection rules to decide which processes are compatible with captured features and specifications;
2. Precedence rules for the relation between features, tolerances and quality, returning for instances, the order of processes to manufacture a single or set of features or the machining operations needed;
3. Machine and tool selecting rules;
4. Resting face selection rules for machining operations;

Rules can be separated into two major groups: specific rules and general rules. Specific rules encompass the necessary knowledge for process selection and are reasoned based on a two-way or multi-way relations between design features, manufacturing operations, machines and machine tools. These set of relations can be seen in Figure 2. Following this diagram, features have a two-way relation with manufacturing operations, meaning that reasoning must be done between the shape of the desired feature to produce and the manufacturing operations capable of producing it (e.g. a face mill produces a flat face perpendicular to the rotating axis of the tool). Manufacturing operations has a multi-way relation between process tools and

machines simultaneously, showing that to execute a given operation it is necessary to have the correct tool and machine for the job. Lastly, there is a two-way relation between tools and machines to ensure cross compatibility between these knowledge bases.

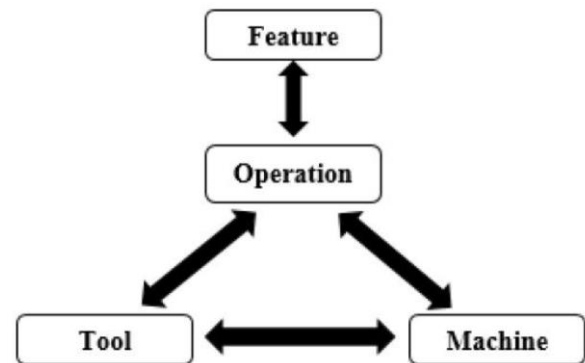


Figure 2. Relation tree between knowledge branches.

Generic rules are used when knowledge base is separated from the inference mechanism, so that the same set of rules may be used with different knowledge bases. The generic set of rules have been implemented in the earlier work on IMPlaner development as reported in [13]. Those generic rules have been used in the developing milling capability knowledge base as described in this paper.

3.3 Milling Capabilities

Milling is a machining process that uses cutting tools to remove material from a raw block or a pre-formed shape to achieve a desired final geometry. Material removal is achieved via the engagement between the surface of the part and a rotating multiple-tooth cutting tool, originating small chips due to the interrupting cutting action of the tool teeth [14]. Milling techniques can be distinguished according to the tool's axis position relative to the work piece. Some examples are:

- Peripheral milling – performs machining via the cutting edges located on the periphery of the cutting tool, in a horizontal position relative to the work piece (tool rotation axis is parallel to work piece plane). Depending on the tool orientation relative to the feed direction, the cutting action can be classified as upward milling or downward milling [15];
- Face milling – has a tool rotation axis perpendicular to the plane of the part being machined. The part is machined by the cutting edges located on the periphery of the cutting tool.
- End milling – is similar to face milling with the same tool orientation however, the tools have cutting edges both on the end and periphery of the tool, being able to generate two machined faces simultaneously (such as a pocket or a shoulder profiles).

Due to the variability that exists in manufacturing, tolerances are set to establish limits/boundaries on the degree of variability [16]. It is somewhat difficult to encounter milling process boundaries beyond the realm of universal knowledge. This is due to high versatility

of milling operations and great dependence on machinist skills, maintenance procedures. Process capabilities are often treated as a proprietary information and knowledge for individual companies and they are seen as competitive advantage of one organization against its competitors. Nevertheless, some authors have been able to compile several specific tolerance values, such as the values in Table 1 and Table 2 adapted from [17] and [16] respectively. The table 1. Show the value in both inches and millimeters.

Boundaries	Milling Approach					
	Face		Peripheral		End	
	Roughing	Finishing	Roughing	Finishing	Roughing	Finishing
Dimensional Tolerance (in/mm)	0.002/0.0508	0.001/0.0254	0.002/0.0508	0.001/0.0254	0.004/0.1016	0.004/0.1016
Flatness (in/mm)	0.001/0.0254	0.001/0.0254	0.001/0.0254	0.001/0.0254	-	-
Angularity (in/mm)	0.001/0.0254	0.001/0.0254	-	-	-	-
Perpendicularity (in/mm)	0.001/0.0254	0.001/0.0254	-	-	-	-
Parallelism (in/mm)	0.001/0.0254	0.001/0.0254	-	-	0.0015/0.0381	0.0015/0.0381
Surface Finish (μm)	50	30	50	30	60	50

Table 1. Process tolerances ranges ([17])

A broader analysis has been done in [15] where the author defines the expected accuracy of a machining processes based on the international tolerance grade defined in the ISO 286 Standard, which defines the given tolerance a process can achieved based on the dimension of the part that it is producing.

Machining operation	Typical Tolerance		Surface Roughness	
	mm	In	μm	$\mu\text{-in}$
Milling			0.4	16
Peripheral	± 0.025	± 0.001		
Face	± 0.025	± 0.001		
End	± 0.05	± 0.002		
Shaping, Slotting	0.025	0.001	1.6	63
Planing	± 0.075	± 0.003	1.6	63
Sawing	± 0.50	± 0.02	6.0	250

Table 2. Process tolerances ranges adapted from ([16]).

Milling approach	ISO 286 Tolerance Grade	Surface roughness R_a (μm)
Peripheral	IT 8	30
Face	IT 6	10
Form	IT 7	20 – 30

Table 3. Achievable accuracies based on part dimensions (from [15])

In addition to presented milling capability knowledge it was also important to define precedence between various milling operations. Usually milling operations are divided into rough and finish operations (sometimes semifinish is included too), in addition to taxonomy of milling operation based on tools used, such as face milling, end milling, side milling, peripheral milling, etc. In this work we have proposed milling operation precedences as shown in Figure 3. The obvious precedence is that rough operations must precede finish operations. In addition to the above-mentioned processes, we have included plunge milling which is required to precede end milling for closed slots and pockets, and rudimentary treatment of planar grinding operations which may follow finish milling if part tolerance requirements are higher than milling capabilities

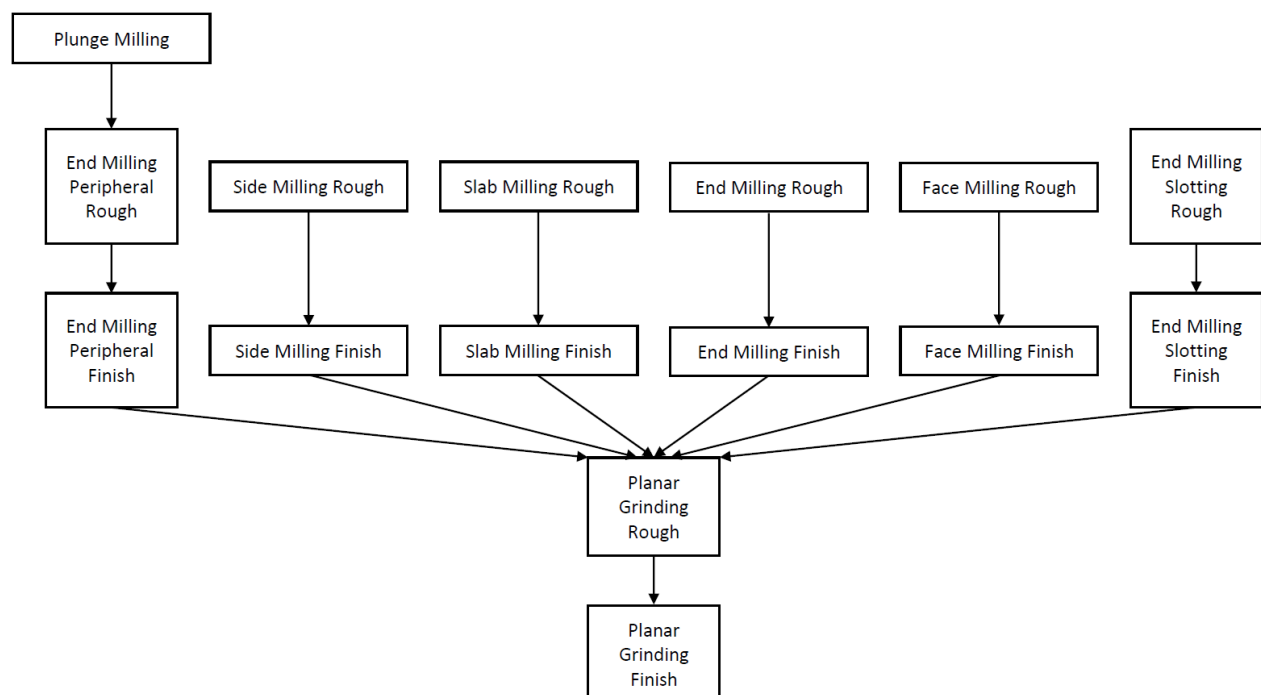


Figure 3. Precedence of milling operations

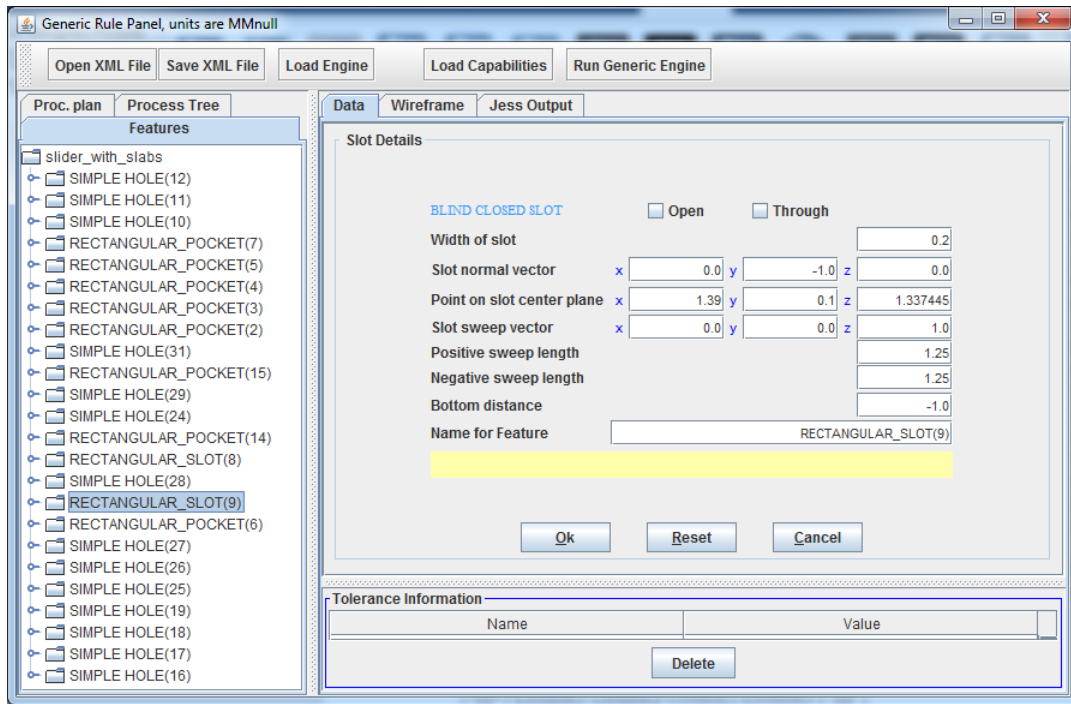


Figure 4 User interface of IMPlanner running milling process selection

4. IMPLEMENTATION

The above-mentioned milling capability knowledge has been implemented as a module in IMPlanner. Implementation consists of three parts:

- Development of process selection rules,
- Milling knowledge representation
- Rules for triggering milling processes for different feature types.

The IMPlanner running an example for milling process selection is shown in Figure 4.

4.1 Process Selection Rules

The process selection rules have been implemented according to the procedure shown in Figure 5. This procedure allows for selection of sequence of multiple processes, when design tolerance requirements can not be satisfied by a single process. The rule details have been explained in [13] and further discussion is beyond the scope of this paper. This also allows for customized selection of planning knowledge, ie. the same set of rules can be used when knowledge base is augmented to increase the manufacturing capability coverage. The method to do that is explained in section 3.2.

The rules for initial trigger of reasoning process have to be implemented for each individual feature type. This is the entry point for reasoning algorithm. Those rules may depend also on feature dimension and subtype. For example, to machine Slab (the feature that represents resulting flat face in the part) it is enough to always start with face milling or slab milling. On the other side, when considering slots and pockets, it is necessary to consider if they are open or closed. For open slots and pockets, we can start with end milling (and side milling for slots), while for closed slots and pockets we do have to start with a plunging operation. Illustration of those rule is shown in Figure 6 for closed slots and pockets. The key information in the figure is bolded and underlines to emphasize the reasoning process.

Similarly, Figure 7 shows the rule for open slots, in which case we start reasoning by considering end milling and side milling processes.

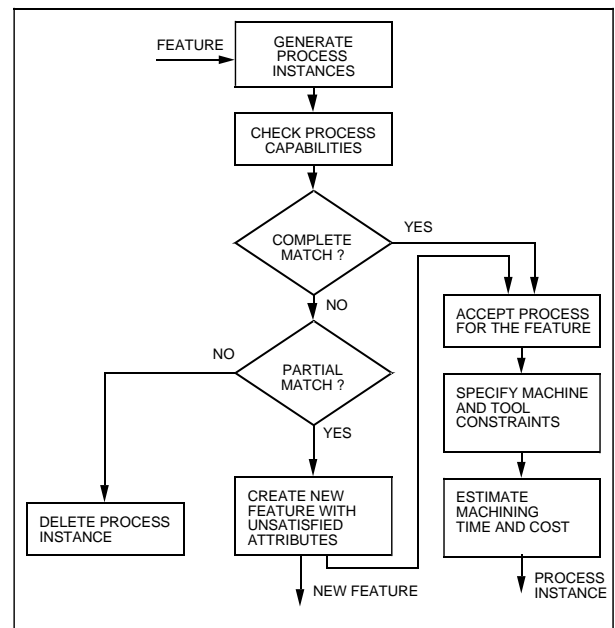


Figure 5 Procedure for process selection

4.2 Milling knowledge representation

Implementation of milling knowledge for IMPlanner consists of the two steps: persistent knowledge storage, and knowledge representation model in the running application. For persistent storage we have adopted the XML format. Figure 8 illustrates data that is stored for each milling process. For each milling process we store two types of data: process capability for each of feasible GD&T tolerances that can be accomplished by milling. This data is based on our discussion section 3. We also provide two alternative data sets, one for ISO units (in millimeters), and another for ANSI units in

```

(defrule AssignPlungeMilling
  ?mf <- (MfgFeature (maybeMachinedBy ?process&:(eq (call
    ?process toArray) (create$ )))
    (processes ?listOfProcesses&:(eq (call ?listOfProcesses
    toArray) (create$ )))
    (OBJECT ?o&:(and (not (?o isHole))(?o isClosed)))
    (mfgPartModelName ?part&:(neq ?part nil)) )
  (not (FeatureRelation (Feature ?mf)))
  =>
  (addToMaybeMachinedBy ?o "edu.ohiou.mfgresearch.
    implanner.processes.PlungeMilling")
  (assert (FeatureRelation (Feature ?mf)
    (status MBMBAssigned) ))
)

```

Figure 6 Rule for closed slots and pockets

inches. In addition, we store required precedence between individual processes, and this serves as information when process selection traverses multiple processes for the same design feature. This is stored under <precedes> tag in the XML file. Once the

external data file is loaded into live IMPlanner application the data in the XML file are converted into the process precedence graph (shown in Figure 9) and table of capabilities (Figure 10).

```

(defrule AssignSlotRoughMilling
  ?mf <- (MfgFeature (maybeMachinedBy ?process&:(eq (call
    ?process toArray) (create$ )))
    (processes ?listOfProcesses&:(eq (call ?listOfProcesses
    toArray) (create$ )))
    (OBJECT ?o&:(?o isSlot)) (mfgPartModelName ?part&:(neq
    ?part nil)) )
  (not (FeatureRelation (Feature ?mf)))
  =>
  (addToMaybeMachinedBy ?o "edu.ohiou.mfgresearch.
    implanner.processes.EndMillingSlottingRough")
  (addToMaybeMachinedBy ?o "edu.ohiou.mfgresearch.
    implanner.processes.SideMillingRough")
  (assert (FeatureRelation (Feature ?mf)
    (status MBMBAssigned) ))
)

```

Figure 7 Rule for open slots

```

<edu.ohiou.mfgresearch.implanner.processes.SideMillingRough>
<precedes>edu.ohiou.mfgresearch.implanner.processes.SideMillingFinish</precedes>
  <Parameter flatness="0.0254"/>
  <Parameter dimensionTolerance="0.0508"/>
  <Parameter sizeTolerance=""/>
  <Parameter surfaceFinish="50"/>
</edu.ohiou.mfgresearch.implanner.processes.SideMillingRough>

<edu.ohiou.mfgresearch.implanner.processes.SideMillingFinish>
<precedes>edu.ohiou.mfgresearch.implanner.processes.PlanarGrindingRough</precedes>
  <Parameter flatness="0.0254"/>
  <Parameter dimensionTolerance="0.0254"/>
  <Parameter sizeTolerance=""/>
  <Parameter surfaceFinish="30"/>
</edu.ohiou.mfgresearch.implanner.processes.SideMillingFinish>

```

Figure 8 Process capabilities in persistent XML format

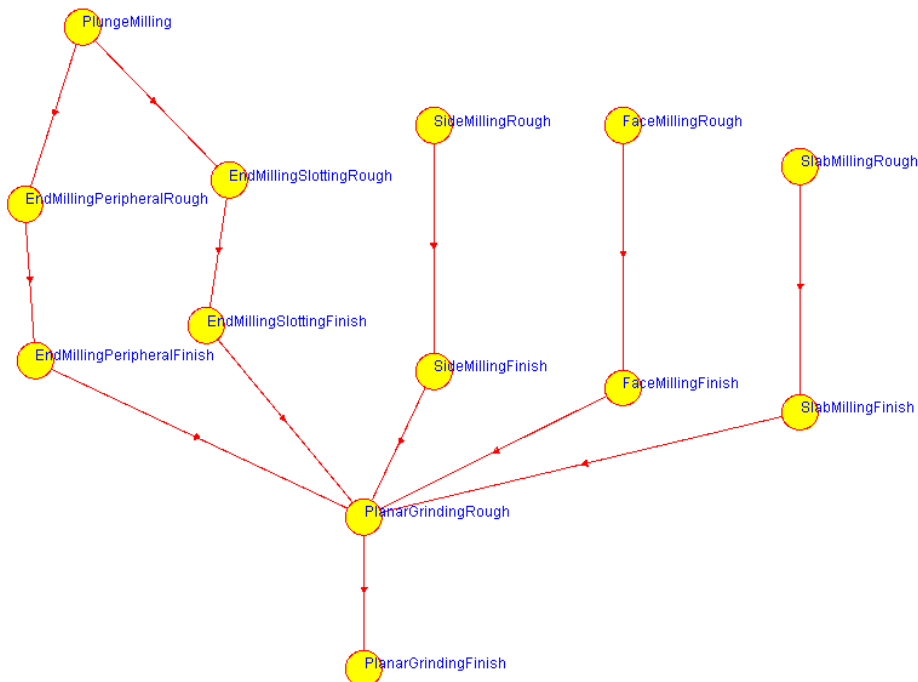


Figure 9 Precedence of the milling operation in the IMPlanner prototype

process capability data							
Name	SlabMillingFinish	EndMillingPeripheralRough	EndMillingPeripheralFinish	EndMillingSlottingRough	FaceMillingRough	PlanarGrindingFinish	FaceMillingFinish
negativeTolerance							
positiveTolerance							
roundness							
largestToolDiameter							
smallestToolDiameter							
straightness							
parallelism				0.0381	0.0254		0.0254
truePosition							
surfaceFinish	30	50	30	60	50		50
perpendicularity					0.0254		0.0254
flatness	0.0254	0.0254	0.0254		0.0254		0.0254
angularity					0.0254		0.0254
dimensionTolerance	0.0254	0.0508	0.0254	0.1016	0.0508		0.0254
sizeTolerance							

Figure 10 Implemented process capability matrix

5. CASE STUDY

To illustrate the developed approach, we have run the process selection procedure on a sample real part called Slider (shown in Figure 11). This is a part design that have served as test design for several research institutions to be able to compare their results.

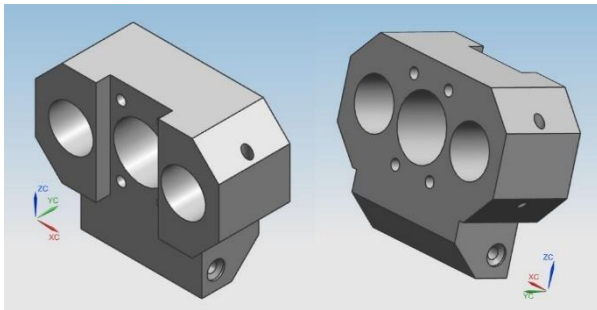


Figure 11 Slider Example

In addition to geometric model (the CAD file) from which we have retrieved feature dimensions and orientations, it was necessary to supply GD&T requirements. From the mechanical drawing for Slider we took tolerance requirements (which also included some datums), but we have added additional tolerance and surface finish requirements in order to be able to test and verify the process selection procedure. Also, since Slider part has several Hole features we have executed the complete procedure for both hoel making and milling. The hole making knowledge base is used from our previous research [13]. The part model is loaded from XML file that contains the part model with the feature dimensions and tolerance requirements. The loaded part with all features before the process selection procedure starts is shown in Figure 12, while an example of feature data is shown earlier in Figure 4. After the part model is loaded the system load process capability data and process selection rules. The process selection is executed in the Jess inference engine and the final results are shown in Figure 13.

The feature/process tree shown in Figure 13 illustrates few results from the process selection procedure:

1. Process selection procedure was successful for all features as shown by change of the icon in the feature tree for all features (compare folder icon in Figure 13 with a terminate node icon in Figure 12, before the process selection is started).
2. For each design feature (shown in black in Figure 13) the selected processes are shown in blue and intermediate features are shown in magenta.

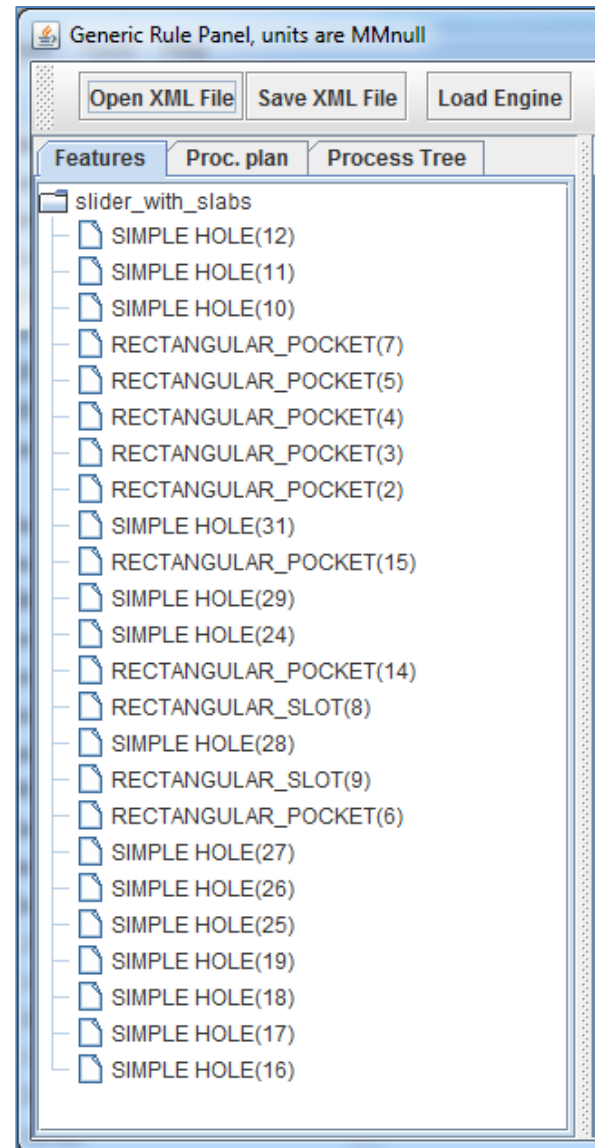


Figure 12 Features of Slider Example

3. For each feature, the procedure considered alternate processes according to the knowledge base, for example *RECTANGULAR SLOT(9)* could be made by *EndMillingRough* or *SideMillingRough*.
4. If a single process satisfies all requirements, there is not further expansion, as shown for *RECTANGULAR SLOT(9)*.
5. If there is a need to consider several processes to obtain the required tolerances, several processes are recommended, see for example *RECTANGULAR*

POCKET(7), for which four different processes in sequence are necessary.

6. If the design required tolerances are such that there is no a set of processes which would satisfy all of them, the last intermediate feature (for which nothing can be selected) is shown in red, as is the case for *SIMPLE HOLE(12)* after *HoleGrinding*. This case would require the change in design or consideration of new resources.

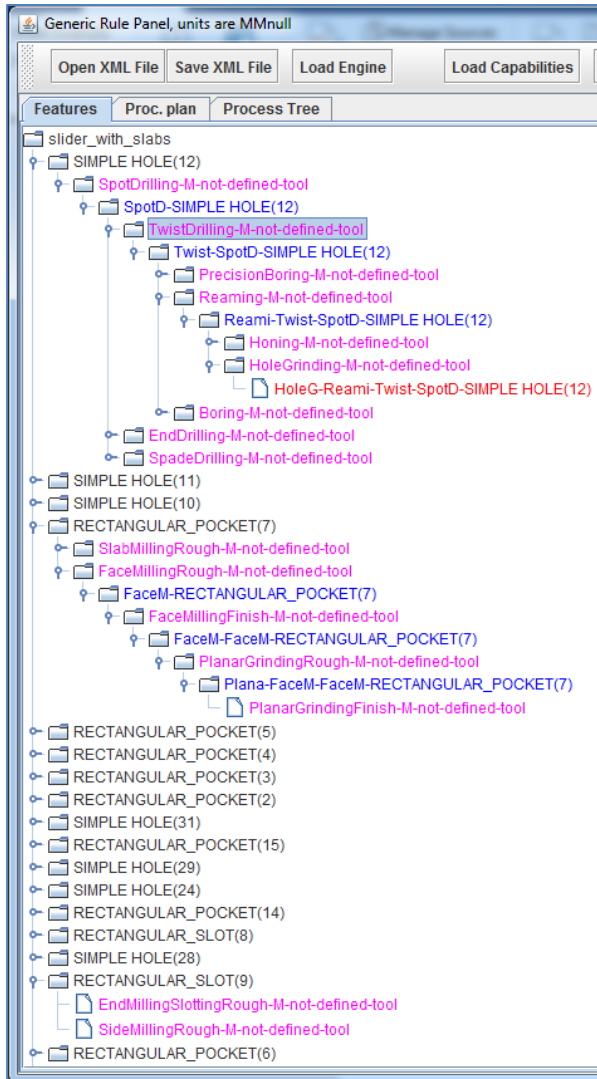


Figure 13 Selected machining processes for several features

The result shown demonstrates the complete consideration of all available processes and their sequence in order to produce each feature in the part design with specified dimensions, tolerance, and surface finish requirements.

The next step is selecting the most efficient set of processes for each feature and sequencing processes of all feature to most optimize production.

6. CONCLUSIONS

This paper has demonstrated a successful development of the knowledge base for milling operations. While the knowledge base may not be complete for all machine shops, it provides a template for development that

could include designed experiments in each shop and real-time monitoring of the machine performance to adjust the process capabilities.

Implementation of the knowledge base as part of the generic rule-based process selection procedure provides a roadmap for incorporating the shop floor knowledge into automated process planning.

Visualization of the process selection results provides a fidelity of the system and increase the trust between engineers and planning software.

While results demonstrate successful approach, there are few other actions that can be taken:

1. consider mil-turn operations by extending the knowledge base to turning processes
2. Extend reasoning to include machine and tool selection by integrating the process selection rule with process/machine/tool compatibilities.
3. Include real-time data collections from running machine (e.g. vibrations, forces, etc) that may have an impact on capabilities and adjust capability knowledge base for dynamic decision making.

11. REFERENCES

- [1] X. Xu, L. Wang, and S. T. Newman, "Computer-aided process planning – A critical review of recent developments and future trends," *International Journal of Computer Integrated Manufacturing*, vol. 24, no. 1, pp. 1-31, 2011/01/01 2011.
- [2] D. Sormaz, M. Wakhare, and N.-U. Arafat, "Rule-Based Process Planning and Setup Planning with Consideration of GD&T Requirements " *International Journal "Advanced Quality"*, vol. 45, no. 1, p. 8, 2017.
- [3] D. Kiritsis, "A review of knowledge-based expert systems for process planning. Methods and problems," *The International Journal of Advanced Manufacturing Technology*, journal article vol. 10, no. 4, pp. 240-262, July 01 1995.
- [4] M. F. Zaeh and H. Rudolf, "Agile Process Planning considering the Continuous Reconfiguration of Factories " in *Preceedings of 3rd International Conference of Reconfigurable Manufacturing Systems*, Ann Arbor, MI, 2005.
- [5] L. Wang and W. Shen, "DPP: An agent-based approach for distributed process planning," *Journal of Intelligent Manufacturing*, journal article vol. 14, no. 5, pp. 429-439, October 01 2003.
- [6] X. W. Xu and Q. He, "Striving for a total integration of CAD, CAPP, CAM and CNC," *Robotics and Computer-Integrated Manufacturing*, vol. 20, no. 2, pp. 101-109, 2004/04/01/ 2004.
- [7] T.-C. Chang, *Expert Process Planning for Manufacturing*. Menlo Park, CA: Addison-Wesley, 1991.
- [8] B. Khoshnevis, W. Tan, and D. N. Sormaz, "A process selection rule base for hole-making," in "Factory Automation Systems Division," Gaithersburg, MD1993.
- [9] D. Sormaz, P. Khurana, and A. Wadtkar, *Rule-Based Process Selection of Hole Making*

- Operations for Integrated Process Planning*. 2005.
- [10] D. Sormaz and M. Wakhare, "Rule Based Process Selection for Hole Feature Considering Tolerance Capabilities," in *Industrial and Systems Engineering Research Conference* Miami, FL, 2016, vol. 2016.
 - [11] D. N. Sormaz *, J. Arumugam, and S. Rajaraman, "Integrative process plan model and representation for intelligent distributed manufacturing planning," *International Journal of Production Research*, vol. 42, no. 17, pp. 3397-3417, 2004.
 - [12] F.-H. Ernest, *Jess in Action*. Manning Publications 2003.
 - [13] D. N. Sormaz, J. Arumugam, and C. Ganduri, "Integration of Rule-based Process Selection with Virtual Machining for Distributed Manufacturing Planning," in *Process Planning and Scheduling for Distributed Manufacturing*, L. Wang and W. Shen, Eds. London: Springer London, 2007, pp. 61-90.
 - [14] A. International, *ASM Metals Handbook - Machining*. 1997.
 - [15] H. Tschätsch and A. Reichelt, "Milling," in *Applied Machining Technology* Berlin, Heidelberg: Springer Berlin Heidelberg, 2009, pp. 173-223.
 - [16] M. P. Groover, Wiley, Ed. *Fundamentals of Modern Manufacturing - Materials, Processes and Systems*, 4th ed. Wiley, 2010, p. 1028.
 - [17] R. A. Wysk. (2008). *Process Engineering Basics for Process Planning for Computer Implementation - IE550 - Manufacturing Systems Fall 2008* [Personal Presentation].

Authors: Dr. Dusan Sormaz, Professor, Ronny Gouveia, BS, Arkopaul Sarkar, MS, Ohio University, Department of Industrial and Systems Engineering, 1 Ohio University, Stocker Center 284, Athens, OH 45701, USA, Phone: +1 740 593 1545, Fax: +1 740 593 0778,
 E-Mail: sormaz@ohio.edu;
rg492318@ohio.edu;
sarkara1@ohio.edu

Vukman, J., Lukic, D., Borojevic, S., Milosevic, M., Kramar, D.

EXPERIMENTAL RESEARCH OF THE INFLUENCE OF HIGH-SPEED MACHINING PARAMETERS ON TIME AND SURFACE ROUGHNESS OF THIN-WALLED PARTS

Abstract: *This paper represents the research of the influence of machining strategies and parameters on machining time and surface roughness of the thin-walled parts made of the aluminum alloy Al 7075. Changes were made to three machining strategies, cutting speeds, feed rates, depths of cut while machining sample parts with the 0,5 and 1,5 mm wall thickness. Experimental research represents the trial studies and thus are conducted on 10 rectangular parts (samples). Three values for the number of revolutions were adopted, 6000, 12000 and 24000 rev./min, while the feed rate was defined as 10% of the cutting speed. The tool made of carbide with the 8 mm in diameter and 2 teeth was used for machining. The main goal of this research is to show whether is it possible to achieve good surface accuracy and surface quality of the thin-walled parts without finishing operations.*

Key words: *Thin-walled parts, aluminum alloy, HSM, machining time, surface roughness.*

1. INTRODUCTION

Due to its homogeneity, corrosion resistance and excellent strength-to-weight ratio, the thin-walled aluminum components are increasingly used as structural parts in aviation, automobile, military and other fields of electro-mechanical industries. A new design of these components is directed towards monolithic parts rather than on a larger number of components that have to be assembled after machining. In this way, a design with good mechanical characteristics, better quality and accuracy, lower weight and with lower manufacturing cost and time is obtained [1]. The forms of machined thin-walled parts which are identified so far can generally be divided into the following forms: triangular type, rectangular type, hexagon type, line type and complex forms [2].

Thin-walled parts are such parts whose wall thickness is considerably smaller compared to the other dimensions on a part. There are several recommendations based on whom the classification of the thin-walled parts is carried out. According to the [3], the basic classification of the thin-walled parts can be carried out in the following way:

- Small height to thickness ratio 15:1
- Moderate height to thickness ratio <30:1
- Very large height to thickness ratio > 30:1.

There are many factors that affect surface accuracy of the thin-walled parts among which the most influential are the following [3, 4, 5]: stresses and deformations, deformations caused by vibrations, wrong direction when removing chips, inadequate machining type and method, i.e. machining strategies and parameters etc.

Narrow tolerances on parts represent a major challenge for manufacturers which is more emphasized while machining the thin-walled parts. Due to the low stiffness of the thin-walled structures there is a high probability of occurrence of deformations during machining which also lead to the occurrence of errors in measures, shapes and positions, as well as deviations

in surface quality [5, 6, 7]. Deformations of the curved thin-walled parts mostly occur under the influence of cutting forces [8, 9, 10, 11]. Cutting forces are directly related to machining parameters which indicates the fact that selecting machining parameters is of key importance for achieving the required surface accuracy and quality. Generally, the stiffness of the thin-walled parts is low, however, for different tool positions during machining, stiffness changes significantly. Besides, if stiffness constantly changes along with the material removal process, different tool paths lead to different inclinations of the thin-walled structure. Therefore, selecting appropriate machining strategies, i.e. the appropriate tool path, is of great significance as well.

In this paper, the trial research studies were performed with the aim of obtaining a good surface quality without finishing as well as defining accuracy parameters. Apart from surface roughness, the following deviations were also measured: wall thickness deviation – Δa , perpendicularity – Δb , flatness – Δc . Also, the measured machining times on the machine tool are compared and times are calculated in the corresponding CAM software system. Also, measured the measured machining times during machining on the machine tool and calculating the time in the corresponding CAM software. Also, compared the measured machining times during machining on the machine tool and calculating the time in the corresponding CAM software.

2. STRUCTURE EXPERIMENTAL PROCEDURES

2.1 Preparation of the experiment

Experimental research studies are conducted on the high-speed CNC vertical turning center - DIGMA HSC 850. Air is used as a cooling agent because machine has only possibility to use air cooling. When machining the thin-walled aluminum parts, the tool from the catalogue [12] is adopted, with the identification

number E5909080, manufactured by YG. The tool material is Carbide with two teeth. Fig. 1 shows the shape of the milling cutter. Characteristics of the cutting tool are given in the Table 1 with all units in mm. The raw piece for producing sample parts is rectangular with 70x40x40 mm in dimensions.

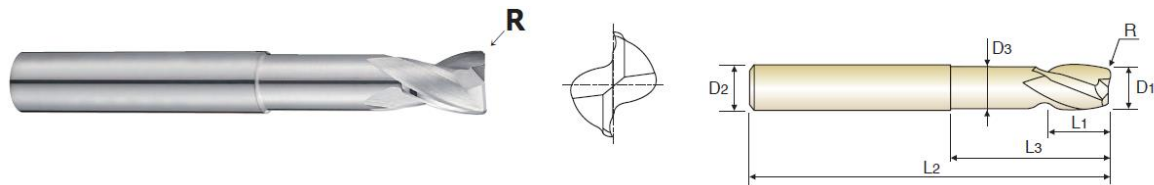


Fig. 1. Cutting tool

No.	Corner Radius (R)	Mill Diameter (D ₁)	Shank Diameter (D ₂)	Length of Cut (L ₁)	Length Below Shank (L ₃)	Overall Length (L ₂)	Neck Diameter (D ₃)
E5909080	R 0.6	8	8	10	30	70	7.2

Table 1. Cutting tool data

2.2 Planining the experiment

Given the fact that these are the trial research studies, the number of experiments is defined with 10 samples). Each of these samples is defined with appropriate tool path and cutting conditions using the Cimatron software. As shown in the Table 2, variations of wall thicknesses, numbers of revolutions, feed rates, depths of cut and machining strategies are defined. Two wall thicknesses are varied, 0.5 mm and 1.5 mm. The adopted machining strategies in the Cimatron software are: climb, convectional and mixed. These strategies are defined in the Table 2 in the following way: climb – Path 1, conventional – Path 2 and mixed – Path 3.

Aluminum alloy AL 7075 (AlZnMgCu1,5) is adopted as the raw piece material. The SolidWorks 2014 software system is selected for defining 3D models, while the Cimatron 10 software is used for generating CNC code.

The alignment of the upper surface is performed on each of these samples. Placing these samples in the clamping tool is performed in the following way: the distance from the upper surface of the raw piece to the clamping tool was 32 mm, Fig. 2. Also, measuring the height deviation value of a raw piece on the clamping device with the comparator clock is performed, Fig. 3a. This deviation ranges are between 0.02 and 0.03 mm. The tool circular runout is measured as well using the dial comparator, Fig. 3b. The cutting tool is placed in the clamp. The tool circular runout recommended by the manufacturer is 0.03 mm while the deviations obtained by measurements using the dial comparator were 0.02 mm.

No.	Wall thickness (mm)	Number of revolutions (rpm)	Feed rate (mm/min)	Depth of cut (mm)	Machining strategies
1.	0.5	6000	600	2	Path 1
2.	0.5	24000	2400	2	Path 1
3.	1.5	6000	600	2	Path 1
4.	1.5	24000	2400	2	Path 1
5.	0.5	6000	2400	4	Path 3
6.	0.5	12000	1200	4	Path 1
7.	0.5	24000	600	4	Path 2
8.	0.5	24000	600	1	Path 2
9.	1.5	6000	2400	3	Path 2
10.	1.5	12000	1200	3	Path 3

Table 2. Experimental data



Fig. 2 Set-up each raw piece – defining 50 mm distance between cutting tool and workpiece



Fig. 3a. Measuring the height deviation value of a raw piece using the comparator clock



Fig. 3b. Measuring circular runout of tool using the dial comparator clock

3. MEASURING RESULTS

The sample parts were measured after the machining. The measurement of the following parameters is planned by the research study, Fig. 4: wall thickness deviation - Δa , perpendicularity deviation - Δb , flatness deviation - Δc , surface roughness - R_a . Machining time T is measured as well and later compared with the machining time T_1 obtained from the CAM software.

The first three values are measured on the coordinate measuring machine Mitutoyo Strato – APEX 9166. Surface roughness was measured using Mitutoyo SJ-301 and the measurement was performed administratively to the direction of the tool. Considering the fact that the linear part was considered, it was dividing into the left and the right side.

Therefore, the roughness was measured on the following sides:

- left side in horizontal direction R_{alh} and left side in vertical direction R_{alv} ;
- right side in horizontal direction R_{adh} and right side in vertical direction R_{adv} .

Machining time, which also has a significant role from in terms of the cost of producing the part and overall production, was based on the calculated time within the Cimatron software and the real measured machining time for the given part. This way of measuring time was performed in order to predict how much the obtained time within the CAM software differs from the time obtained in real manufacturing conditions. Flatness are measured on Cordinate Measuring Machine – Mitutoyo EURO-C-A574 CMM 3D.

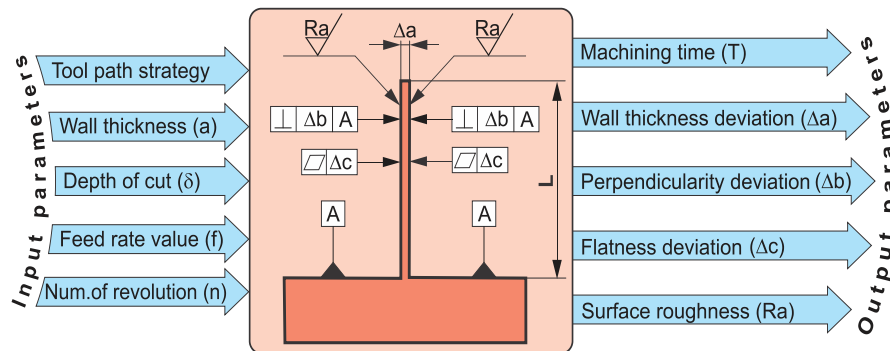


Fig. 4. Measured values on the part

3.1 Analysis of measurement results

The wall thickness was measured in five positions (measuring point, MP). The total length of the thin-walled part is divided into five equal lengths which are marked on each sample. The measurement results are shown in Table 3.

Based on the obtained results it can be concluded that the smallest wall thickness deviation stands for the number 7 with 1 mm in depth, while the second smallest wall thickness deviation is obtained at 2 mm in depth. In cases when the depth of cut was 3 mm or 4 mm experiment could not be conducted until the end

because of tool fractures or damages in the thin-walled part. Tool fractures appeared on the following heights measured from top of raw piece: 11.485, 15.110 and 12.560 mm of the total defined part height. It also must be noted that the tool fractures occurred in the cases 5, 9 and 10, Fig. 5a, when using strategies convencional and mixed. Wall damage occurred in the cases 6 and 7, Fig. 5b. The damage occurred at the very end of the part length or about 5 to 6 mm before tool left the cut. Also, Table 3 gives the wall thickness deviations where negative values represent the cases when tool fractures or wall damages occurred. Taking into account that the experiment was performed in real industrial conditions

and that no equipment for measuring vibrations was used, authors assume that the fractures and damages occurred due to the emergence of self-exciting vibrations.

Figure 6 gives an overview of the parts 1, 2, 3, 4 and 8 which are completely performed the experiment, and then the measured values of all parameters of accuracy and machining quality.

No.	Defined Thickness [mm]	MP 1 [mm]	MP 2 [mm]	MP 3 [mm]	MP 4 [mm]	MP 5 [mm]	Arithmetic mean	Deviation [mm]	Standard deviation (mm)
1.	0.5	0.521	0.523	0.524	0.527	0.524	0.524	0.024	0.00217
2.	0.5	0.515	0.515	0.525	0.515	0.510	0.5160	0.016	0.00548
3.	1.5	1.531	1.526	1.526	1.524	1.522	1.526	0.026	0.00335
4.	1.5	1.509	1.503	1.512	1.507	1.508	1.508	0.008	0.00327
5.	0.5	0.524	0.525	0.520	0.500	0.510	0.516	0.016	0.01064
6.	0.5	0.485	0.495	0.502	0.506	0.495	0.497	- 0.003	0.00802
7.	0.5	0.460	0.470	0.480	0.470	0.500	0.476	- 0.024	0.01517
8.	0.5	0.510	0.508	0.502	0.500	0.500	0.504	0.004	0.00469
9.	1.5	1.492	1.425	1.430	1.432	1.390	1.434	-0.066	0.03675
10.	1.5	1.460	1.500	1.490	1.480	1.490	1.484	-0.016	0.01517

Table 3. Measured values of wall thickness

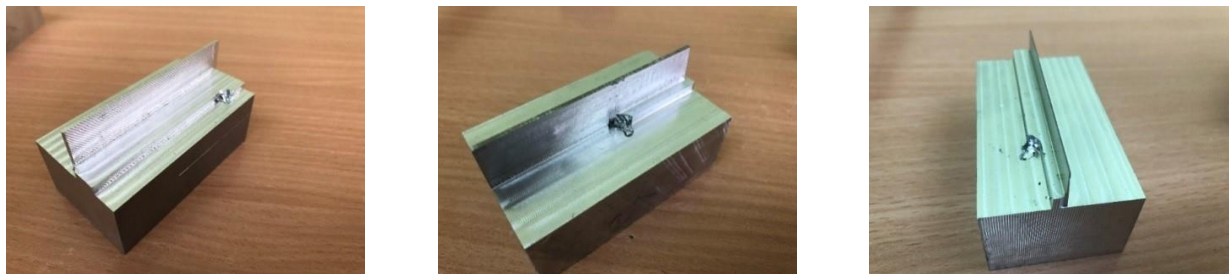


Fig. 5a. Depth at which the tool fractures appeared while machining samples 5,6 and 7 respectively

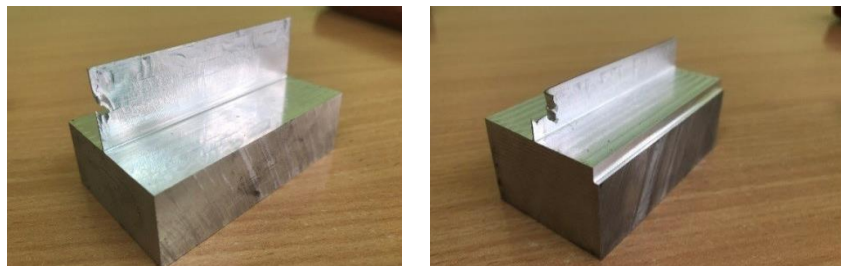


Fig. 5b. Damages in thin-walled parts in experiments 9 and 10 respectively

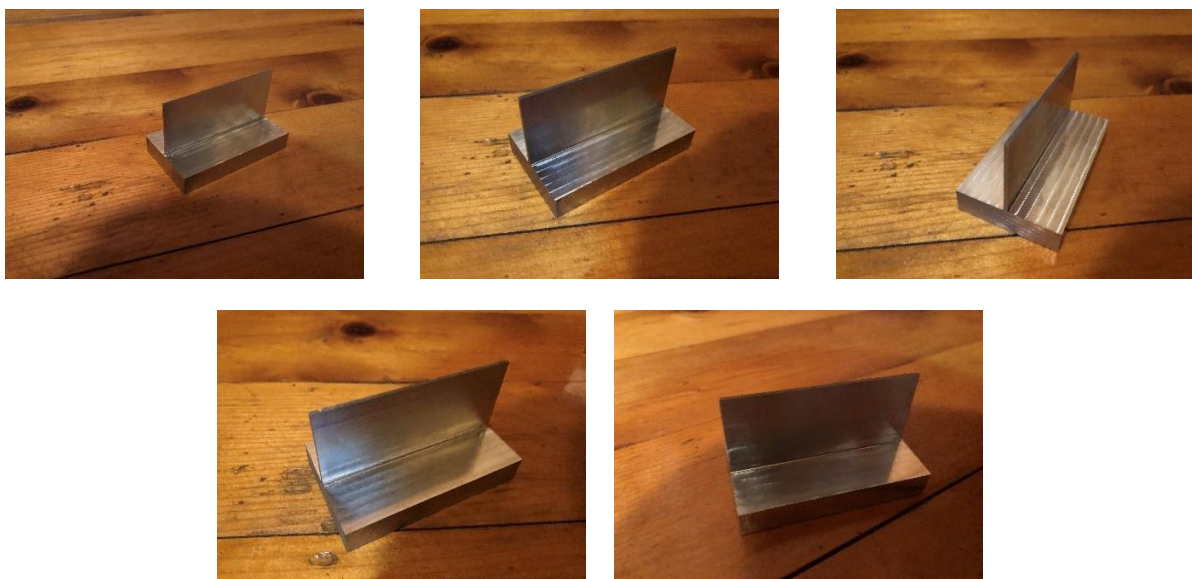


Fig. 6. Displaying the correctly made parts 1, 2, 3, 4 and 8 respectively

By comparing the measured machining times and the same times obtained from the CAM software, the certain differences were acquired and therefore shown in Table 4. Since the samples 5, 6, 7, 9 and 10 showed the fractures of the tool and damages in the wall thickness, the difference between the measured time and the time obtained from the software was not calculated.

Experiments for sample numbers 1-4 and number 8 were done to the very end and were approached by measuring perpendicularity deviation - Δb , flatness deviation - Δc and surface roughness deviation - R_a . Measurement results are shown in Table 5a and 5b. Surface roughness is given in μm . The prescribed value of flatness deviation is 0.050 mm. Flatness was measured for the left and the right side in horizontal and vertical direction. So, we have: Δc_{DV} – right side in vertical direction; Δc_{DH} – right side in horizontal direction; Δc_{LV} – left side in vertical direction and Δc_{LH} – left side in horizontal direction.

Perpendicularity deviation was measured for the left and the right side. So, we have: Δb_{LV} – perpendicularity deviation of the left side in vertical direction and Δb_{DV} – perpendicularity deviation of the right side in vertical direction.

Based on the measured results of surface roughness it can be noted that the machining strategy has the significant influence on surface quality. Also, it can be seen that the quality of machining the left and the right side in the vertical direction is almost the same, but different for the horizontal direction. The obtained results for sample number 2 match with the machining quality which can got with grinding.

In terms of flatness and perpendicularity deviation the satisfactory values are obtained, except for the cases 1 and 4 which shown the bigger value of flatness deviation in the horizontal direction. Machining strategy has the significant influence on the surface flatness as well.

No.	Wall thickness (mm)	Num. of revolutions (rpm)	Feed rate (mm/min)	Software time (min)	Measured time (min)	Time difference
1.	0.5	6000	600	00:33:00	00:36:02	00:00:02
2.	0.5	24000	2400	00:09:00	00:12:50	00:03:50
3.	1.5	6000	600	00:28:55	00:32:57	00:04:02
4.	1.5	24000	2400	00:09:00	00:12:10	00:03:10
5.	0.5	6000	2400	00:04:24	00:01:08	-
6.	0.5	12000	1200	00:09:16	00:04:09	-
7.	0.5	24000	600	00:15:25	00:04:57	-
8.	0.5	24000	600	01:04:02	00:47:16	00:16:46
9.	1.5	6000	2400	00:05:24	00:03:45	-
10.	1.5	12000	1200	00:09:21	00:04:33	-

Table 4. Machining times

No.	Wall thickness (mm)	Num. of revolutions (rpm)	Feed rate (mm/min)	R_{lv} (μm)	R_{lh} (μm)	R_{dv} (μm)	R_{dh} (μm)
1.	0.5	6000	600	0.21	0.19	0.17	0.21
2.	0.5	24000	2400	0.23	0.22	0.18	0.24
3.	1.5	6000	600	0.23	0.22	1.93	0.24
4.	1.5	24000	2400	0.22	0.24	0.23	0.27
5.	0.5	24000	600	0.88	0.22	0.42	0.12

Table 5a. Machining times

No.	Wall thickness (mm)	Num. of revolutions (rev./min)	Feed rate (mm/min)	Δc_{LV} (mm)	Δc_{LH} (mm)	Δc_{DV} (mm)	Δc_{DH} (mm)	Δb_{LV} (mm)	Δb_{DV} (mm)
1.	0.5	6000	600	0.004	0.012	0.010	1.004	0.042	0.252
2.	0.5	24000	2400	0.034	0.016	0.026	0.021	0.047	0.352
3.	1.5	6000	600	0.043	0.029	0.041	0.018	0.081	0.051
4.	1.5	24000	2400	0.009	0.016	0.011	1.032	0.053	0.043
8.	0.5	24000	600	0.048	0.020	0.074	0.025	0.107	0.160

Table 5b. Deviation of perpendicularity and flatness

4. CONCLUSION

In this paper, preliminary research was carried out through 10 experiments, which were realized with the aim of defining the boundary values of input parameters, which will be used in further investigation of treatment of thin-walled linear aluminum structures.

One of the goals was to show that high quality machined surfaces, which can be very high in components used in automotive and aviation industry, tools making, etc., can be obtained using high speeds without finishing pass. Final passes often know a long time to last, and therefore increase the cost of producing the part.

On the basis of the obtained results it can be concluded that the defined conditions are not feasible in industrial practice when the processing depth was 3 and 4 mm. Machining times that are obtained in the CAM software are not adequate but should increase from 20% in order to get the real time of making some work. It turned out that it is not suitable for small number of revolutions /cutting speeds and high feed values, and that the best results with the maximum number of revolution/cutting speed and feed are best.

Analyzing the obtained results, it can be concluded that by choosing the appropriate tool path strategy, shift values, depth and number of revolution/ cutting speed in the process of processing of thin-walled structures, significant savings can be achieved in terms of machining time, while meeting the accuracy of the thickness of the wall, the accuracy of the management and the straightness, roughness of the machined surface. The initial values of the input parameters that are suitable for application in future experimental investigations of the process of processing of thin-walled aluminum structures of the line shape have been determined.

Future research needs to be carried out on the basis of the defining of experimental plan, with the use of additional equipment, such as vibration measurement equipment and cutting forces. The basic expected output results refer to the defined optimal processing parameters through the corresponding mathematical models of the processing process.

Acknowledgements

This paper is part of a research on projects - TR 35025 Ministry of Education, Science and Technological Development of Republic of Serbia. The authors thank the companies Frezal and Unimet from Serbia for the realization of these experimental research.

5. REFERENCES

- [1] Smith, S., Dvorak, D.: *Tool path strategies for high speed milling of aluminum workpieces with thin webs*. Mechatronics, Vol.8, pp.291-300, 1998.
- [2] Pompa, M.: *Computer Aided Process Planning for High-Speed Milling of Thin-Walled Parts - Strategy-Based Support*, PhD Thesis, University of Twente, Netherlands, 2010.
- [3] Shoulder milling of thin deflecting walls. www.sandvik.coromant.com/engb/knowledge/milling/application/overview/shoulder_milling/shoulder_milling_thin_walls. Accessed 21-12 2017
- [4] Zhang, D., Gao, K., Zhou, T.: *Discussion on NC machining process of thin walled parts technical measures*, Applied Mechanics and Materials, Trans Tech Publications, Switzerland, Vol. 701-702, pp. 864-868, 2015.
- [5] Bing, D., Guang-bin, Y., Yan-qi, G., Jun-peng, S., Yan-qi, G., Xue-mei, W., Yu-xin, L.: *Machining Surface Quality Analysis of Aluminum Alloy Thin-Walled Parts*, In Aerospace, International Journal of Security and Its Applications, Vol. 9, pp. 201-208, 2015.
- [6] Izamshah, R.R.A.: *Hybrid Deflection Prediction for Machining Thin-Wall Titanium Alloy Aerospace Component*, PhD. Thesis, School of Aerospace, Mechanical and Manufacturing Engineering RMIT University, 2011.
- [7] Wojciechowski, I.S.: *The estimation of cutting forces and specific force coefficients during finishing ball end milling of inclined surfaces*, International Journal of Machine Tools and Manufacture, Vol.89 pp.110-123, 2015.
- [8] Gao, Y.Y., Ma, J.W., Jia, Z.Y., Wang, F.J., Si, L.K., Song, D.N.: *Tool path planning and machining deformation compensation in high-speed milling for difficult-to-machine material thin-walled parts with curved surface*, The International Journal of Advanced Manufacturing Technology, Vol. 84, pp. 1757-1767, 2016.
- [9] Ramanaiah, B.V., Manikanta, B., Sankar, M.R., Malhotra, M., Gajrani, K.K.: *Experimental Study of Deflection and Surface Roughness in Thin Wall Machining of Aluminum Alloy*, Materials Today: Proceedings, Vol. 5, pp. 3745-3754, 2018.
- [10] Bolar, G., Mekonen, M., Das, A., Joshi, S.N.: *Experimental Investigation on Surface Quality and Dimensional Accuracy during Curvilinear Thin-Wall Machining*, Materials Today: Proceedings, Vol.5, pp. 6461-6469, 2018
- [11] Khairul, A.S., Ab-Kadir, A.R., Mohd Hairizal, O.: *A Comparison of Milling Cutting Path Strategies for Thin-Walled Aluminium Alloys*, International Journal Of Engineering And Science, Vol.2, pp. 1-8, 2013.
- [12] http://www.toolontool.hu/DNNGranTool/PDF/YG-1_Aluminum_E5909.pdf Accessed 25-01-2018.

Authors: MSc. Jovan Vukman, Assoc. Prof. Dejan Lukic, Assoc. Prof. Mijodrag Milosevic, University of Novi Sad, Faculty of Technical Sciences, Department of Production Engineering, Trg Dositeja Obradovica 6, 21000 Novi Sad, Serbia, Phone.: +381 21 450-366, Fax: +381 21 454-495.
E-mail: vukman@uns.ac.rs;
lukicd@uns.ac.rs;
mido@uns.ac.rs;

Assist. Prof. Stevo Borojevic, University of Banja Luka, Faculty of Mechanical Engineering, Stepe Stepanovića 75, 78000 Banja Luka, Bosnia and Herzegovina, Phone.: +387 51 433 000, Fax: +387 51 465 085.
E-mail: stevoborojevic@hotmail.com

Assoc. Prof. Davorin Kramar, University of Ljubljana, Faculty of Mechanical Engineering, Department for Management of Manufacturing Technologies, Askerceva 6, 1000 Ljubljana, Slovenia, Phone.: +386 1 4771-737, Fax: +386 1 477 1 768.
E-mail: davorin.kramar@fs.uni-lj.si



Section E:

**MATERIALS, METAL FORMING,
CASTING AND WELDING**

Cabrilo, A., Geric, K.

CHARPY IMPACT PROPERTIES OF A CRACK IN WELD METAL, HAZ AND BASE METAL OF WELDED ARMOR STEEL

Abstract: *Welding of armored steel is complicated by the high percentage of carbon in the base metal, the presence of faults in the form of cracks and pores that occur in the weld metal and heat affected zone (HAZ) during the welding process. The crack formed in base metal or HAZ, due to dynamic or impact loads, can easily continue to propagate to the fusion line, after which its accelerated growth may occur. Due to the significant interest in quantifying the resistance of material to initiation and propagation of cracks, the impact energy was measured with instrumented pendulum in the zone of base metal, weld metal and HAZ, at temperatures of -40 °C, -20 °C, 0 °C and 20 °C. The impact energy tests showed high energy for initiation as well as crack propagation in weld metal and HAZ zones, while the lowest energy was in the base metal.*

Key words: *GMAW welding, Armor steels, Austenitic stainless steel and Instrumented Charpy tests.*

1. INTRODUCTION

Armor steel belongs to the ultra-high tensile strength and hardness group of steels. Welding of armor steel is complicated due to the high percentage of carbon content in the base metal and the presence of faults in the form of cracks and pores in the weld metal zone, whereby fractures may be initiated in the weld metal [1]. Austenitic filler material is traditionally used for armor steel welding because of hydrogen dilution improved in an austenitic phase [2]. After the welding process, solidification cracking may result from high thermal expansion of the austenitic stainless steel and invisible defects may be created in the weld metal zone. For heavy structural engineering, such as armored military vehicles frequently being under the effects of impact and variable loads, mechanical properties of welded joints and the weld metal zone must be known. Due to variable loads, cracks created in the weld metal may easily propagate towards the sensitive fusion line (FL), followed by their possible rapid growth. The impact load is critical for armored vehicles, so the determination of the impact energy required for crack initiation and growth made by instrumented pendulum with Charpy V specimens, is very significant, [3].

For armored vehicle structures safe and rational dimensioning, it is necessary to know dynamic effects extreme values and time periods. Therefore, there is a significant interest in material resistance related to crack initiation and propagation. For the armored military vehicles reliable operation, it is very important to be able to carry out a good risk assessment of existing crack type faults.

Although austenitic filler material is used the most frequently for welding and has several unusual features including its high manganese content, few articles consider the problem of its mechanical properties. The main goal of this study was to investigate the impact energy by instrumented pendulum in welded joint. Fracture surfaces for the impact energy were also investigated by Scanning Electron Microscope (SEM).

Subsequently, samples in the weld metal region were studied by tensile strength test, hardness measurements, metallography and chemical analysis.

2. MATERIALS AND EXPERIMENTAL PROCEDURE

2.1 Material and welding properties

Gas metal arc welding (GMAW) and AWS ER307 solid wire is used for welding armor steel Protac 500. Welding direction is parallel to the rolling direction. Cold rolled plates 12 mm thick are cut to the required dimensions (250 x 100 mm), while V joint under the angle of 55° is prepared by Water Jet Device. Robot Kuka and Citronix 400A device was used during the welding process testing, [4]. Robotic welding is used for human factor effect elimination, in order to allow a fine adjustment of parameters and results repeatability.

The chemical composition (wt. %) of the base metal, armor steel, was 0.27 C, 1.07 Si, 0.706 Mn, 0.637 Cr, 1.09 Ni, 0.3 Mo, 0.039 V, 0.01 S, and 0.02 P. The chemical composition (wt. %) of the filler material, Mn type stainless steel, was 17.76 Cr, 8.24 Ni, 6.29 Mn, 0.89 Si, and 0.08 C. The chemical composition of the welded joint after the welding process was obtained by an ARL 2460 spectrometer, [4].

2.2 Mechanical property tests

Welded joint tensile strength testing was performed in transverse direction of the weld bead. It should be noted that specimens was cut with Water Jet Device, to eliminate possibilities of thermal effects to high hardness steel. Tensile strength testing was made on servo - hydraulic testing machine Instron 8033. The loading rate was set as 0.125 mm/s until fracture took place.

2.3 Metallography and hardness testing

The microstructural examination was performed using a "Leitz-Orthoplan" metallographic microscope and a scanning electron microscope JEOL JSM 6460LV at 25 kV. The samples were ground using SiC

papers, polished with a diamond paste and finally etched with a mixture HCl and HNO₃ in weld metal region, and 3% HNO₃ reagent to reveal the structure of base metal. Microhardness distribution from top to bottom along the centreline of the weld was measured for the purpose of welded metal characterization. Digital Micro Vickers Hardness Tester HVS 1000, Laizhou Huayin Testing Instrument Co, under the load of 500 g, was used in order to measure microhardness.

2.4 Instrumented Charpy tests

Charpy impact tests in base metal, heat affected zone and weld metal, were performed on specimen's size 10 x 10 x 55 mm, with V notch of 2 mm three time set least for each datum point at: 20 °C, 0 °C, -20 °C and -40 °C. Load-displacement curves were obtained from the instrumented Charpy impact system attached in to the impact tester. After the test, fracture surface were examined by a SEM to observe fracture modes.

3. RESULTS

3.1 Tensile testing results

While tensile characteristics were being tested, a fracture appeared in the weld metal. The tensile strength was 833 MPa, while the yield strength of 552 MPa was within the expected limits. The difference between tensile and yield strength was 311 MPa, indicating a high ductility of the weld.

3.2 Hardness and microstructure results

The weld metal micrograph Fig. 1 a) consist of austenite with delta ferrite. Delta ferrite becomes finer at lower heat input and cooling rate. The content of delta ferrite measured by Feritscope: in the weld root 11.7%, in the center 5.4%, in the upper part 3.2%. The base metal micrograph Fig. 1 b) in quenched and tempered condition consists of tempered and quenched martensite within the range of hardness 480-540 HB which is within accepted criteria of standard, MIL-STD-1185, [5].

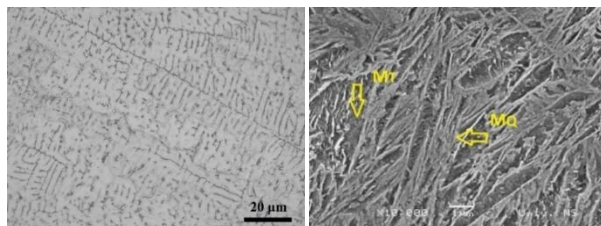


Fig. 1. a) Optical micrograph of AWS ER 307 filler, b) SEM micrograph of base metal. MT - tempered martensite, MQ - quenched martensite.

Hardness rises from the center of the weld metal (WM) (190 HV), to the line of fusion and along the line on WM side has a value of 339 HV. The hardness is growing in the HAZ zone and reaches a maximum value of 521 HV, at a distance of 8 mm from the weld metal axis. After a maximum, the hardness trend is in decline with the achieved minimum hardness of 378 HV, at a distance of 10 mm from the weld metal axis. The hardness then grows and ends at a distance of 14

mm from the weld metal axis with a value of about 509 HV. The distance of 14 mm is also the limit of HAZ and base metal. The BM hardness value is 509 HV. The hardness was measured also longitudinally along the width zone of 0.5 mm following fusion line. Results from Fig. 2 b) show that fusion line hardness does not exceed 442 HV, which is very good for this zone. Hardness falls from the bottom to the upper zone, which can be the result of the heat effect that is higher in zones closest to the last passage than it is in the root passage, which is certainly affected by the already cooled additional and base metal.

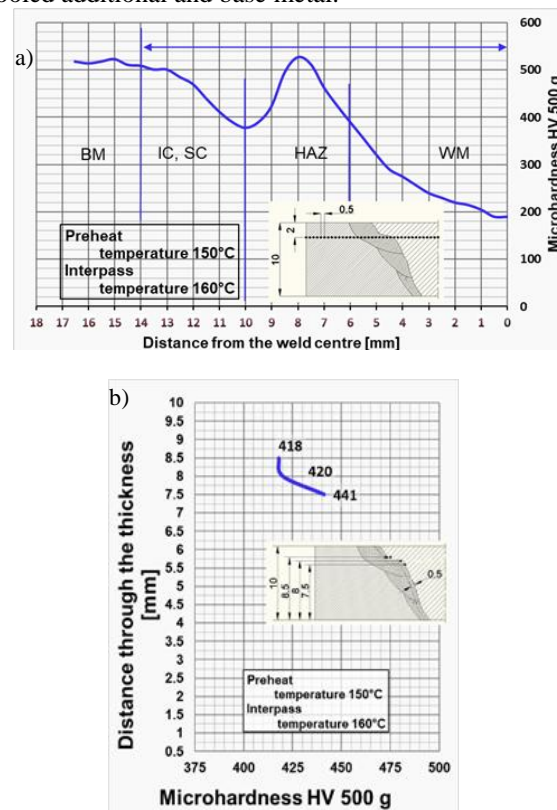


Fig. 2. a) Hardness profile for welded high hardness plate. Note: hardness was measured 2 mm under the upper surface. BM-base metal, IC-inter critical zone, SC-sub critical zone, HAZ-heat affected zone, WM-weld metal, b) close to the fusion line.

3.3 Instrumented Charpy impact energies results

By determining the impact energy for the base metal tested at 20 °C, a diagram was obtained, Fig. 3 a), with a mixed brittle and ductile fracture surface, Fig. 4 a). In order to create a crack in this zone, the measured impact energy is 28.6 J, and 5.6 J is used for propagation. The impact energy diagram for the temperature of -40 °C, Fig. 3 d) shows more pronounced brittle fracture, Fig. 4 d). At this temperature, the largest difference between the energy for creation in relation to the energy for crack propagation is of the highest percentage. The energy to create a crack of 27.8 J slightly decreased compared to the previous temperature tests, while the crack propagation energy was significantly lower and amounted only to 1.0 J.

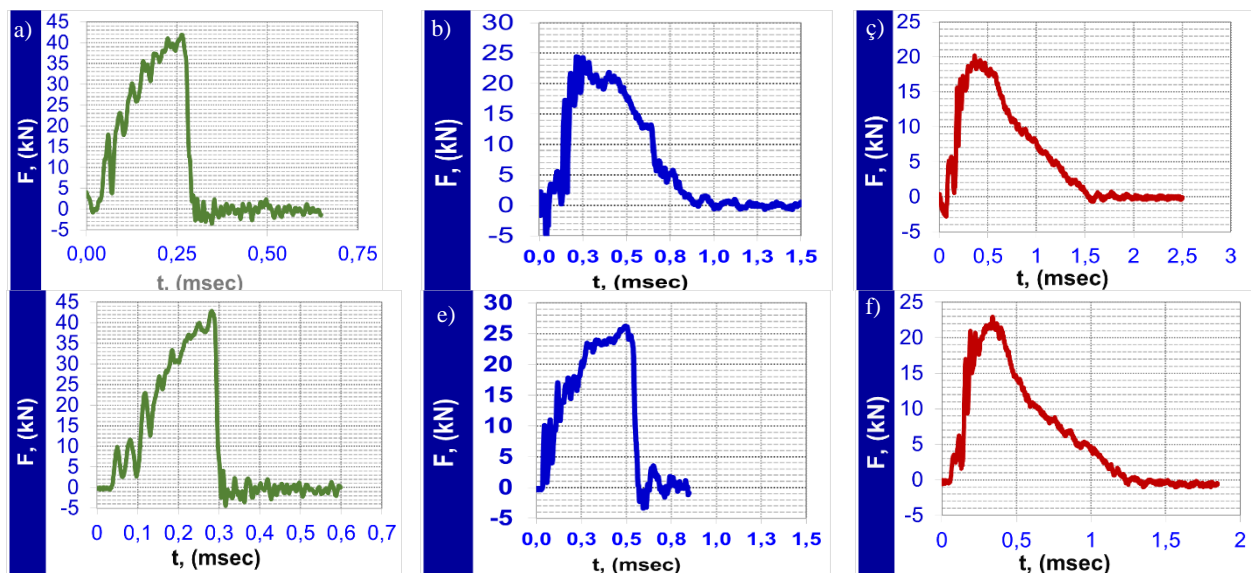


Fig. 3. The load-time (F-t) curve recorded by oscilloscope of Charpy impact specimens fractured at 20 °C a) base metal, b) HAZ and c) weld metal. The load-time (F-t) curve recorded by oscilloscope of Charpy impact specimens fractured at -40 °C d) base metal, e) HAZ and f) weld metal.

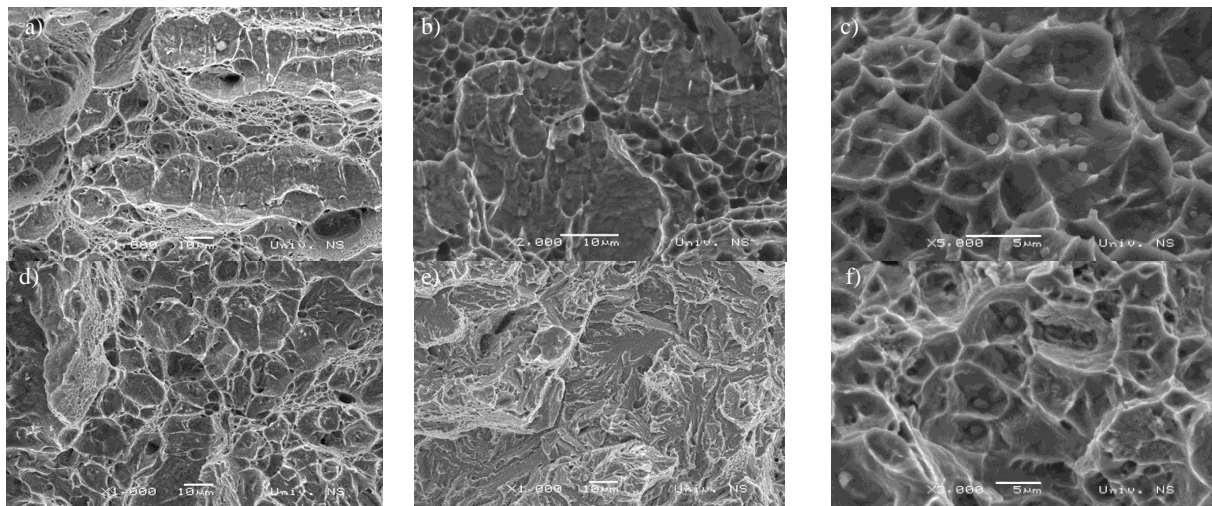


Fig. 4. SEM fractograph of Charpy impact specimens fractured at 20 °C a) base metal, b) HAZ and c) weld metal. SEM fractograph of Charpy impact specimens fractured at -40 °C d) base metal, e) HAZ and f) weld metal.

Determining the fracture energy for fusion line tested at 20°C, the diagram was obtained, Fig. 3 b), with the prevailing ductile fracture surface, Fig. 4 b). For creation of crack in this zone, the measured impact energy is 45.7 J, and 29.6 J is used for growth. Diagram of the impact energy for temperature of -40°C, Fig. 3 e) is a purely brittle fracture, Fig. 4 e). The crack creation energy of 27.7 J slightly decreased compared to tests at previous temperatures, while the crack propagation energy was significantly lower and amounted to 12.3 J. By determining the impact energy for the weld metal

examined at 20 °C, a diagram with a typical ductile fracture surface was obtained, Fig. 3 c) and 4 c). In order to create a crack in this zone, the measured impact energy was 29.0 J, while significantly more energy was used for crack propagation, in the amount of 55.4 J. The diagram of energy impact for the temperature of -40 °C, Fig. 3 f) and 4 f) is a ductile fracture. The energy to create a crack of 24.2 J significantly decreased compared to tests at previous temperatures, while the crack propagation energy was slightly lower and amounted to 37.3 J.

4. DISCUSSION

It is known that welded joints are very heterogeneous, since they include weld metal, heat affected zone and base metal. Hardness is therefore defined by the zone of minimum hardness, which in the case of armor steel welding with austenitic filler material, is the weld metal zone. The tensile strength achieved in this research of 833 MPa is rather high for austenitic filler material and significantly higher than the tensile strength obtained

by low austenite consumable, [6].

The impact energy value at all temperatures indicates that the crack propagation was very difficult. However, it can be concluded that there has been a pronounced drop in the impact energy with a drop in the test temperature. With a decrease in temperature from 20 °C to -40 °C, the energy impact drop is from 75.3 J to 40.0 J. At a temperature of 20 °C, the ratio of energy for initiation and propagation is 70:30. On the energy - time curve, after the initiation energy, a mild drop

occurred, which indicates that more energy was needed for crack propagation. The impact energy data can be linked to the obtained hardness values measured around the fusion line, as the impact energy increases with the decrease in the hardness value. Fracture area fractography at -20 °C and -40 °C shows the prevailing brittle fracture.

Reducing the impact energy in the weld metal from 84.4 J to 64.4 J, obtained at temperatures of 20 °C and -40 °C, is noticeable. A large drop is characteristic of ductile materials, [7] because at lower temperatures, the energy needed to crack propagation is reduced. The SEM tests showed ductile fracture at all test temperatures. On the load - time curve, after the energy for initiation, a very slight drop, characteristic of ductile fracture, occurred. When it comes to temperatures of -40 °C, the ratio of energy for propagation and crack initiation remained the same, 34:66% in favor of propagation energy. After achieving the initiation energy of 20.8 J, there is a slight fall in the curve and the required energy for propagation is 40.7 J. The impact energies at temperatures of -40 °C and 20 °C are achieved due to an optimum hardness of 200 HV and high content of nickel and manganese. At a temperature of -40 °C, the initiation energy decreased considerably, but still remained high. SEM microscopy indicates that the fracture was ductile at all investigated temperatures. In relation to the metallography shown in the study, [8] segregated δ - ferrite is noticeable, while in the results of this work it is evenly distributed, which can be the cause of higher impact energy regarding both tests. Thicker and more uniform arrangement of δ -ferrite was obtained by the REL method compared to the MIG procedure, [9]. The amount of δ - ferrite measured in this test is approximately the same with REL welding in the study with the notion that the arrangement of δ - ferrite in this test is even more uniform.

5. CONCLUSIONS

On the basis of the results presented in this work, the following conclusions may be made:

1. Tensile strength of weld metal in the specimen welded with austenitic filler metal reached 833 MPa, which is greater than results published for the same filler metal in researches of manual welding.
2. Austenitic filler material shows a significant decrease in impact energy, followed by reduction in testing temperature. The results at room temperature showed high energies for crack initiation 56 J and propagation 29 J. The results at -40 °C indicate that significantly less energy is required for crack initiation 41 J, while a small drop was observed for propagation 21 J. During SEM analysis of the fracture surface, small high density dimples were clearly visible. Morphology of the fracture surface at -40 °C indicates a mixed brittle ductile fracture. The results at room temperature showed high energy absorptions for crack initiation (48 J) and propagation (27 J). The results at -40 °C indicated that significantly less energy is required for crack initiation (29 J) and propagation (11 J). The lowest energy for initiation (30 J) and crack

propagation (5 J) at room temperature has a base metal. In this zone, a slight decrease in the energy of the impact between the test temperature of 20 °C and -40 °C.

6. REFERENCES

- [1] Atabaki, M., Ma, J., Yang, G., Kovacevic, R.: *Hybrid laser/arc welding of advanced high strength steel in different butt joint configurations*, Material and Design, pp. 573–587, 2014.
- [2] Kuzmikov, L., Norrish, J., Li, H., Callaghan, M.: *Research to establish a systematic approach to safe welding procedure development using austenitic filler material for fabrication of high strength steel*, 16th International Conference on the Joining of Materials pp. 1-13, 2011.
- [3] Enrico, L.: *Estimating dynamic ultimate tensile strength from instrumented Charpy data*, Material and Design, pp. 437–443, 2016.
- [4] Cabrilo, A., Geric, K., : *Weldability of High hardness armour steel*, in Advance Material Research, pp. 79-84, 2016.
- [5] MIL-STD-1185 :*Department of defense manufacturing process standard: welding, high hardness armor*; [SUPERSEDES MIL-W-62162], 2008.
- [6] Magudeeswaran, G. Balasubramanian, V., R.: *Effect of welding processes and consumables on fatigue crack growth behaviour of armour grade quenched and tempered steel joints*, Defence Technology, pp. 47-59, 2014.
- [7] Hu, J., Du, L. X., Xu, W., Zhai, J. H., Dong, Y., Liu, Y.J., Misra, R., D., K.: *Ensuring combination of strength, ductility and toughness in mediummanganese steel through optimization of nano-scale metastable austenite*, Materials Characterization, pp. 20–28, 2018.
- [8] Magudeeswaran, G. Balasubramanian, V., R.: *Effect of welding processes and consumables on fatigue crack growth behaviour of armour grade quenched and tempered steel joints*, Defence Technology, pp. 47-59, 2014.
- [9] Magudeeswaran, G., Balasubramanian, V., Sathyanarayanan, S., Madhusudhan, G., R.: *Dynamic Fracture Toughness of Armour Grade Quenched and Tempered Steel Joints Fabricated Using Low Hydrogen Ferritic Fillers*, Journal of Iron and Steel Research, International, pp. 51-56, 2010.

Authors: M.Sc. Aleksandar Cabrilo, Full Prof. Katarina Geric, University of Novi Sad, Faculty of Technical Sciences, Department of Production Engineering, Trg Dositeja Obradovica 6, 21000 Novi Sad, Serbia, Phone.: +381 21 450-366, Fax: +381 21 454-495.
E-mail: cabrilo@uns.ac.rs; gerick@uns.ac.rs;

ACKNOWLEDGMENTS:

This study was financially supported by the Ministry of Education, Science and Technological Development of the Republic of Serbia through the Project Nos. ON 174004.

Flegarić, S., Marjanović, D., Štorga, M., Bojčetić, N.

SMART SHEET METAL FORMING TOOLS DESIGN

Abstract: Industry 4.0 changes the practice of manufacturing. Integrating production machines with information technology outlines a trend of “smart product” development which specific segment are smart sheet metal forming tools. Controllable actuators in the direction different from the press opening and sensors that give information about workpieces, tools and process regulate the production process parameters in real time which affects the product design process. Smart product design process models should enable the integrated processing of complex requirements that exist in such a process. This paper presents results of the literature review in the relevant research area which indicate that there are immense needs for research in the field of smart technical systems development and design. It is evident that a methodological approach to the development of smart products/systems in the industry is partially implemented. The same is valid for the smart sheet metal forming tools field.

Keywords: smart sheet metal forming tools, design theory, product development

1. INTRODUCTION

The presented research is concentrated on smart sheet metal forming tools design process as an upgrade of traditional sheet metal forming tools design process. The differences in the design process of smart and classical sheet metal design tools are recognised in the practice and literature, so the goal of the research is to propose and evaluate a new applicable design process model. As the starting point, the literature review is conducted for the better understanding of the existing models, methods and features of the smart components used in sheet metal tools design and the summarised results of that phase are reported in this paper.

2. SMART PRODUCTS DESIGN

Manufacturing has always been adopting according to state of the art in technology. Nowadays it is possible to collect a vast amount of the information about the working process, product, tools and environmental conditions by sensors and send them to the digital twin [1]. Contemporary information infrastructure enables analytical insight into such collected data: from the process of interest, from another process that runs in the same time but not necessarily on the same place, or from processes that ran before. According to the results of complex algorithms, the control unit gives orders to controllable actuators in the real process in real time. This is enabled by “smart components” that embed knowledge about their function, behaviour and structure. “Smart components” are the basic element of “smart products”. Current and future research has to give answers to questions arising out of this new situation. Recently, the researchers from 13 UK universities worked together to define the research roadmap for smart products through lifecycles [2]. They detected that there are significant needs for researches in the field of smart technical systems development and design. Even the newest research reviews in the design and

development process methods area, as is [3], detected that a methodological approach to the development of products is only partially implemented in industry.

2.1 Smart sheet metal forming tools design

The same is valid for the smart sheet metal forming tools field. Smart sheet metal forming tools are a specific segment of smart products. Controllable actuators in the direction different from the press opening direction and sensors that give information about workpieces, tools and processes regulate the production process parameters in real time. In comparison with classical, smart tools enable production without bad products, without tool damage and without production breaks or with significantly less of them. They also allow the production of more complex products.

In another hand, smart tools include more complex components in tools design, which classical tools is not, or include them significantly less and more straightforward kind of them. Common conventional tools have inductive sensors as counting sensors and stop sensors. Smart sheet metal forming tools can have, except counting and stop sensors, many different kinds of sensors for different quality control purposes or process regulating purposes. There are also controllable actuators independent of main press movement which are used for active adjusting tool setup or as the source of active working force in some part of forming process. These elements need to be connected together and with the control unit as with power unit, so there also have to be information processing and power infrastructures. This new kinds of components in tools design and components that support them demand new approaches to some of the design phases, new smart tools design process models. These models should enable the integrated processing of complex requirements that exist in such a process. They should include information processes throughout the tools lifecycles as a source of information for the tools design process in real time.

3. SMART SHEET METAL FORMING TOOLS RESEARCHES

This paper analyses scientific literature on the topic published since 2013. Papers are sorted according to theme and year of publication (Table 1.). Themes chosen by authors represent parts of sheet metal forming process relevant for smart sheet metal forming tools design process. Papers selection criteria were a possibility of using the methods described in the paper in smart sheet metal forming tools or for design processes. Each of the themes is divided into three segments: 1. Analysis (An) - include works that have an accent on analysis of situations (reviews), behaviours or phenomenon relevant for smart sheet metal forming tools design or their design processes but without applicable methods or components, 2. Method (M) - include works that have an accent on methods that can be used in smart sheet metal forming tools design or their design processes but without application useful in real processes, 3. Application (App) - include works that have an accent on methods or components used or can be used in real smart sheet metal forming tools design or their design process application.

3.1 Servo Presses

Presses with actively controllable actuators were the first step to smart sheet metal forming tools and appear before period included in this review. The interesting idea at that time was to upgrade classical mechanical press to the servo powered presses. For the smart sheet metal forming tools, the more imported work is [4] were the new high controllable application for forming small precision parts were presented. This application had four ball connection points on the ram, and four horizontality checking sensors. It was driven by two servo motors and could ensure horizontality of the ram nonmatter on position of the load center in most of the applications. In the case when two controllable actuators were not enough, the four servo motors could be connected with the ram by ball-screws as is described in [5] which enabled the analyses of the servo presses with the accent on the used mechanism.

Except for common press mechanisms that enable parallel movement of ram there were also described flexible mechanisms that allow the angular movement of the ram. With this kind of action, more than one forming process operation can be performed in the single sheet metal design stage which is often in smart sheet metal building tools used as a method of optimisation. Method for modelling energy analysis during forming operation [6] used for efficiency optimisation of one press, can also be used for energy peak load optimisation of the family of servo presses with smart sheet metal forming tools. It is predictable that the next step in servo press development will be integrating control of servo presses with the power of smart sheet metal forming tools in the integrated controlled process instead parallel control as is usual at the moment. There will be further development of the information protocol that will be standard for incoming data in a quick sheet metal forming tool design process.

3.2 Bending

Controlled movements that can be achieved by servo presses can have effects on the results of bending forming process, and several papers is dealing with this phenomenon. Springback effect is known as the main problem during bending. Authors in [7] analyzed springback for different motion modes of servo presses and different workpiece materials. They concluded that reduction of springback can be achieved with right chose of press motion mode. The sensitivity of springback is the leading cause of the variety among the results of the bending process, and tool adjustment has to be done accordingly to the measurement reports. In smart sheet metal forming tools, it can be done automatically in one, or two steps application [8]. The solution is that actively controllable actuators drive adjustment elements, while inline measuring sensors are sending measured data to the control unit which controlled the actuators according to this information. This should be used in an application with adjustment needs as is in production in small series because of every change of the workpiece material can have a different effect on the spring back.

Table 1. Reviewed papers distribution according themes and years of publication

		2013.	2014.	2015.	2016.	2017.
Servo Presses	An	[4]		[6]	[5]	
	M					
	App					
Bending	An				[7]	
	M					
	App					
Deep drawing	An		[9]	[10] [12]	[11]	
	App					
	Blank holder					
	App					
	M					
Draw-bead	M				[15], [16]	[14] [17] [18] [17]
	App					
Quality control	App				[19], [21]	[20]
Design process	An	[22]		[24]	[25]	[23] ???? →
	M					
	App					

3.3 Deep drawing

The deep drawing process is the most demanding sheet metal forming process where the quality of the product highly depends on friction conditions during the process. Because of that, it is essential to analyse the influence of forming speed, surface structure, load pulsation [9], local temperature [10] or nonlinearity [11]. Car industry always pushes technology to produce more complex and higher quality products. There is a different way to ensure the quality of products as is integrating pressure control sensors in depth drawing tools. Authors in [12] describe the usage of the fluid as the source of counter pressure. Such smart sheet metal forming tools are high controllable for application in precise micro size parts production and represent one of the rears, but interesting, ways for deep drawing process quality control.

The most common way to ensure product quality is friction control. There are two commonly used components to do it: blank holder and drawbead. Using FEM it can be determined different blank holder force for different areas [13], or through forming process [14]. In smart sheet metal forming tools pressured fluid can achieve active blank holder force, or piezo-electric actuator [15] or servo motor [16] in the application. The best results can be obtained with use of the active controllable blank holder force and drawbead high as is described in [17]. Theoretically, this kind of smart sheet metal forming tool can control the friction force in any place and any phases of the forming process, but some optimisation has to be done. In a real application, any place has to be converted into characteristic place. There is an optimisation method for blank holder segmentation in [13] and in [18] is a method for optimisation drawbead geometry in both senses: segmentation and cross-sections. Deep drawing of complex parts would be impossible without FEM, but all of the previously mentioned methods are used parallel with the design process. They are too robust to be integrated into the design process. In smart sheet metal, forming tools design process existing FEM should be adapted on the way that can be embedded into the design process and use information from real forming process to predict setup adjustment for the new forming process. It can be expected low accuracy but enormous speed. Applicable accuracy will be achieved in a few steps.

3.4 Quality control

Quality control of the sheet metal forming tools can be done by measuring lateral force or temperature, and load [19] with sensors integrated into sheet metal forming parts. Level of deviation in this data represents the level of decreasing quality of some tool parts. Sheet metal forming production is noise, and method for tool wear monitoring by audio signal analysis [20] represent an example of using state of the art in software in combination with low-cost audio sensors for the optimal solution in place where it looks like impossible. There is another metrological solution as is presented in [21] which combine the camera with laser sensors and according to complex algorithms gives

high accuracy inline measuring reports. Camera control setup in multi-setups tools and measurement of workpieces or design parts position by laser sensors became normal in smart sheet metal forming tools. Many sensors with their infrastructure are normal in smart products. Smart product design process has to pay close attention to the sensor because of it becomes a significant component here and not any more minor one as in traditional products design was.

3.5 Design process

Iteratively interchange the data between sheet metal forming tools design process and FEM analysis is often. In [22] authors present an integrated approach of tools planning and design in a simulation environment as acceptable way to do this. Potential of using surrogate assisted optimization methods in sheet metal forming tools design process is presented in [23]. Methods for automatic: nesting and piloting system design [24] and design flat blank by “un-forming” [25] also represent less requiring FE methods that can be integrated in sheet metal forming tools design process but they cover only separated segments of it. In [26] author presents application that can save time consumed in blanking die design processes. This application is adaptation of CAD software as is some another similar applications commented by author in same paper, but again, blanking is only one phase of sheet metal forming process. Further researches in this area should find out the best way to connect methods from separated segments of design process, integrate FE methods in design process and use data from production in this process.

4. CONCLUSION

It is evident that in the smart sheet metal tools design process area is many more questions than answers. Methods and applications listed here cover only small separated segments in this area, and further researches are necessary. They should give a comprehensive view of the possibility which Industry 4.0 offers to smart sheet metal forming tools and find out the best way to use them in smart sheet metal forming tools design process. For that purpose, observation of real sheet metal tools design processes in tools making company that produce both classical and smart sheet metal forming tools is needed and it is next predicted step in this research.

5. REFERENCES

- [1] Parrott, A., Warshaw, L.: *Industry 4.0 and the digital twin: Manufacturing meets its match*, Deloitte University Press, London, 2017
- [2] Duffy, A., Whitfield, I., Ion, W., Vuletic, T.: *Smart Products Through-Life: Research Roadmap*, University of Strathclyde, Glasgow, 2016.
- [3] Wynn, D.C., Clarkson, P.J.: *Process models in design and development*, Research in Engineering Design, 29(2), pp. 161-202, April 2018.
- [4] Cheng, P. Y., Chen, P. J., Lin, Y. T.: *Small mechanical press with double-axis servo system*

- for forming of small metal products, *International Journal of Advanced Manufacturing Technology*, 68, pp. 2371-2381, 07 March 2013.
- [5] Halicioglu, R., Dulger, L. C., Bozdana, A. T.: *Mechanisms, classifications, and applications of servo presses: A review with comparisons*, Proceedings of the Institution of Mechanical Engineers Part B: Journal of Engineering Manufacture, 7, pp. 1177-1194, 01. July 2016.
 - [6] Tao, J., Li, L., Yu, S. R., Peng, Q. J., Asme: *Modular modeling method for energy analysis of the mechanical servo press*, Proceedings of the ASME 2015 International Design Engineering Technical Conferences & Computers and Information in Engineering Conference IDETC/CIE 2015, pp. V004T05A025, Boston, ASME, New York, 2015.
 - [7] Majidi, O., Barlat, F., Lee, M. G.: *Effect of slide motion on springback in 2-D draw bending for AHSS*, *International Journal of Material Forming*, 9, pp. 313-326, July 2016.
 - [8] Senveter, J.; Balic, J.; Ficko, M.; Klancnik, S.: *Prediction of technological parameters of sheet metal bending in two stages using feed-forward neural network*, *Tehnicki vjesnik-Technical Gazette*, 23(4), pp. 1155-1161, 2016.
 - [9] Maeno, T., Mori, K., Hori, A.: *Application of load pulsation using servo press to plate forging of stainless steel parts*, *J of Materials Processing Technology*, 214(7), pp. 1379-1387, July 2014.
 - [10] Klocke, F., Trauth, D., Shirobokov, A., Mattfeld, P.: *FE-analysis and in situ visualization of pressure-, slip-rate-, and temperature-dependent coefficients of friction for advanced sheet metal forming: development of a novel coupled user subroutine for shell and continuum discretization*, *Int J Adv Manuf Technol*, 81, pp. 397-410, 2015.
 - [11] Tamai, Y., Inazumi, T., Manabe, K.: *FE forming analysis with nonlinear friction coefficient model considering contact pressure, sliding velocity and sliding length*, *Journal of Materials Processing Technology*, 227, pp. 161-168, January 2016.
 - [12] Sato, H., Manabe, K., Ito, K., Wei, D., Jiang, Z.: *Development of servo-type micro-hydronechanical deep-drawing apparatus and micro deep-drawing experiments of circular cups*, *J of Materials Processing Technology*, 224, pp. 233-239, 2015.
 - [13] Volk, M., Nardin, B., Dolšák, B.: *Determining the optimal area-dependent blank holder forces in deep drawing using the response surface method*, *Advances in Production Engineering And Management*, 9(2), pp. 71-82, June 2014.
 - [14] Kitayama, S., Koyama, H., Kawamoto, K., Miyasaka, T., Yamamichi, K., Noda, T.: *Optimization of blank shape and segmented variable blank holder force trajectories in deep drawing using sequential approximate optimization*, *Int J Adv Manuf Technol*, 91(5-8), pp. 1809-1821, July 2017.
 - [15] Baume, T., Zorn, W., Drossel, W. G., Rupp, G.: *Iterative process control and sensor evaluation for deep drawing tools with integrated piezoelectric actuators*, *Manuf. Review*, 3(3), pp.1-8, 2016.
 - [16] Meng, D. A., Zhao, S. D., Li, L., Liu, C.: *A servo-motor driven active blank holder control system for deep drawing process*, *International Journal of Advanced Manufacturing Technology*, 87(9-12), pp. 3185-3193, December 2016.
 - [17] Su, C., Zhang, K., Lou, S., Xu, T., Wang, Q.: *Effects of variable blank holder forces and a controllable drawbead on the springback of shallow-drawn TA2M titanium alloy boxes*, *Int J Adv Manuf Technol*, 93(5-8), pp. 1627-1635, November 2017.
 - [18] Zhang, Q. C., Liu, Y. Q., Zhang, Z. B.: *A new optimization method for drawbead in sheet forming process based on plastic forming principles*, *Int J Adv Manuf Technol*, 92(9-12), pp. 3143-3153, October 2017.
 - [19] Biehl, S., Rumposch, C., Paetsch, N., Braeuer, G., Weise, D., Scholz, P., Landgrebe, D.: *Multifunctional thin film sensor system as monitoring system in production*, *Microsystem Technologies*, 22(7), pp. 1757-1765, July 2016.
 - [20] Ubhayaratne, I., Pereira, M. P., Xiang, Y., Rolfe, B. F.: *Audio signal analysis for tool wear monitoring in sheet metal stamping*, *Mechanical Systems and Signal Processing*, 85, pp. 809-826, February 2017.
 - [21] Matthias, S.; Loderer, A.; Koch, S.; Grone, M.; Kastner, M.; Hubner, S.; Krimm, R.; Reithmeier, E.; Hausotte, T.; Behrens, B. A.: *Metrological solutions for an adapted inspection of parts and tools of a sheet-bulk metal forming process*, *Production Engineering-Research and Development*, 10, pp. 51-61, February 2016.
 - [22] Tisza, M., Lukacs, Z.: *Computer Aided Process Planning and Die Design in Simulation Environment in Sheet Metal Forming*, *AIP Conference Proceedings*, 1567, pp. 1002-1007, December 2013.
 - [23] Wang, H., Ye, F., Chen, L., Li, E.: *Sheet Metal Forming Optimization by Using Surrogate Modeling Techniques*, *Chinese J of mechanical engineering*, 30, pp. 22-36, January 2017.
 - [24] Moghaddam, M. J., Farsi, M. A., Anoushe, M.: *Development of a new method to automatic nesting and piloting system design for progressive die*, *International Journal of Advanced Manufacturing Technology*, 77(9-12), pp. 1557-1569, April 2015.
 - [25] Loukaides, E. G.; Allwood, J. M.: *Automatic design of sheet metal forming processes by "un-forming"*, *International Journal of Mechanical Sciences*, 113, pp. 61-70, July 2016.
 - [26] Hussein, H. M. A.: *Computer Aided Blanking Die Design using CATIA*, *Procedia CIRP*, 18, pp. 96-101, 2014.

Authors: Lecturer Stjepan Flegarić mag.ing.mech, Prof. dr.sc. Dorian Marjanović, Prof. dr.sc. Mario Štorga, Prof. dr.sc. Nenad Bojčetić, University of Zagreb, Faculty of Mechanical Engineering and Naval Architecture, Ivana Lučića 5, 10000 Zagreb, Croatia, Phone: +385 16168432, E-mail: stjepan.flegaric@fsb.hr; dorian.marjanovic@fsb.hr; mario.storga@fsb.hr; nenad.bojetic@fsb.hr

Ghionea, I. G., Opran, C. G., Čuković, S., Pleša, M.

IMPROVEMENTS AND MATERIALS FOR PRODUCTION OF A MAGNETIC DRIVE MICROPUMP: AN OVERVIEW AND RECOMMENDATIONS

Abstract: This paper presents an overview of an improved solution for an existing micropump model and, also, of the materials recommended to be used in the current stage of the prototype research. This micropump is provided with a closed system for driving and pumping the fluid, obtained by a special constructive solution, where the rotation of the motor shaft is provided by induction of a magnetic field. The micropump system is composed by an external driving and an internal driven magnet, connected to a pair of gears that moves the fluid between the inlet and outlet apertures. These magnets are separated by a metal cover, that provides a closed volume for the transported fluid with no need for supplementary sealing, as in the case of classical hydraulic pumps. Due to this constructive solution and to the applicative fields where these magnetic drive micropumps operate, their components are produced from compatible materials to provide a low friction/wear and high efficiency in use.

Key words: micropump, magnetic drive, polymeric composite, polymeric, POM, PEEK

1. INTRODUCTION

The magnetic drive pumps are, subjects of many research, design and manufacturing projects studied in industrial and academic environments due to their large applications in the fields of aerospace, automotive industry, medical systems, energy plants, food supply and refrigerate systems, consumer goods, etc. Industrial customers need special hydraulic pumps, with a complex factor of innovation and variable functional parameters adapted to their requirements [1, 2]. These pumps drive a specific fluid characterized by flow, pressure, viscosity, presence of particles, for various applications like: fuel transfer, injection and/or mixing of additives, dosing of substances in a medical installation, printing on textiles and ceramic tiles, etc. The magnetic drive pumps should be of a good constructive simplicity, reliability, very good sealing, low weight, small size and in a wide range of applicability.

The authors of the paper performed a research in the GEX UPB project 57/2017 for the design and development of an innovative prototype of a magnetic drive micropump.

The project is about to identify and manufacture the best constructive variants of the magnetic drive micropump and to maximize its efficiency. Along with CAD/FEM modeling and simulation, the authors search for a combination of materials to manufacture the micropump's main components to provide these advantages over the classic pumps: high sealing, low wearing, compatibility with various fluids, manufacturing solutions and costs. In the research, we intend to implement and use of polymeric composite materials for gears and suction element to reduce the wear resulted from the micropump operation. Also, for its body and cover some steel and aluminum alloys may be used in accordance with the composite materials of the gears.

The research project raises a number of challenges in all its phases: conception, design of the selected ideas, numerical and technological simulations [3], which will

contribute to generating and expanding new knowledge into industrial environment. The documentation phase of other solutions (constructive and materials) in this field of magnetic drive pumps is very important.

2. SCIENTIFIC AND INDUSTRIAL RELEVANCE

Generally, the magnetic drive pumps have various components made of steel, composite and polymeric materials. They are important for industry because their need for industrial application is growing every year. The innovative development of new prototypes is based on the scientific research, calculus, simulations and tests. There are considered: the conception and development of new models, the improvement of existing ones, the identification of new materials that can be used for their components according to purpose and to the fluids driven in specific hydraulic installations. Thus, a research team should consider: a low number of components, based on a relatively simple configuration, volumetric characteristics [4, 5] calculated and parameterized using CAD software, a very good efficiency, a good wearing resistance of the components, the possibility of cooling the pump under certain stress conditions, possibilities of manufacturing certain components with composite materials adapted to functional requirements, bi-directional transfer, fast response to fluid flow, low maintenance, fast replacement of worn components, etc.

The biggest challenge of the proposed research is to design the pump prototype, optimize the choice of metallic and polymeric composite materials for its components, to apply specific manufacturing and assembly technologies. Due to various constraints imposed by beneficiaries, the materials used for its components should provide perfect operation in harsh environments, at temperatures over 100° C, with corrosive fluids such as sulfuric acid and hydrochloric acid, chlorine or various chemical solutions. Generally, fluid losses during the operation of a hydraulic pump are

an important issue for the hydraulic installation, for the environment, especially for hazardous, expensive fluids or those not to be contaminated from the outside. Of course, despite these constraints, the project's cost should be optimal and the resulted prototype reliable and affordable for mass industrial production.

Conception and development of a new magnetic drive pump rises some risks: the magnetic field creation system required to drive the pump may have a high energy consumption; high costs for experiments and validation of the pump variant; dissipation of the magnetic flux inside the pump without a proper driving effect [1]; certain functional requirements [2] may not be fulfilled by the functional prototype, leading to a decrease of the prescribed pressure and the appearance of certain worn areas; the choice of the metallic and polymeric composite materials may require further laborious researches; difficulties in balancing the resulting forces from pump operation [6], etc.

3. WHY TO USE MAGNETIC DRIVE PUMPS ?

A standard pump requires solution of sealing necessary to stop the driven fluid from leaking out around the pump shaft, especially when it is at high pressure. There are some constructive variants to prevent this leaking, thus: a soft packing material compressed around the pump shaft in the pump's casing; a lip seal or an O-ring that is a rubber or plastic ring fitted around the drive shaft and held in place in a recess in the pump housing; a mechanical seal that consists of two parts: a stationary component attached to the pump housing and a second, rotating component on the pump shaft. The faces of the two components are manufactured to be flat and smooth and are pressed by springs to keep them together. This is the most effective option, but may be expensive and difficult to apply, especially in the case of small pumps or in the transfer of high pressure fluids [7]. Even by using expensive solutions, the leakage cannot be fully eliminated. It is important to maintain a small leakage to lubricate and cool the seal and the pump shaft that exits the pump being connected to a motor [5].

Often, it is necessary to add an external lubricant to avoid wear/overheating and this creates the unwanted chance of contamination of the driven fluid. Also, any pump seal needs to be monitored and maintenance to prevent excessive leakage, particularly when the driven fluid is toxic, medical, flammable or environmentally dangerous. Some of the leaked fluids may have to be isolated, contained and disposed of safely, with important costs and additional constructive solutions.

Leakages are one of the main causes of standard pumps failures or shutdowns of the hydraulic installations. The monitoring and maintenance of standard pumps is expensive and time-consuming.

Environmental concerns pushed the research teams to conceive a cleaner pumping technology and to implement magnetic drive pumps that contains the fluid completely inside the housing. These pumps have a hermetic seal, a stationary gasket or O-ring, that is not in contact with moving parts. This seal is therefore wear-proof and the pump can be used in applications where no leakage is highly required.

4. PROPOSED MODEL OF A MAGNETIC DRIVE MICROPUMP

In this research project we focused on improving an existing hydraulic gear micropump with helical teeth. We made some constructive and functional changes, due to the wear appeared on some of its components. The wear has been observed at the arrival of the micropump (Fig. 1) at our university Composite Products Laboratory provided by the service department of the Axflow Romania. The pump is withdrawn from the service, its type is GB-P25.JF5S.A, by Micropump Inc. [8].



Fig. 1. Disassembly of the magnetic drive micropump

According to the manufacturer specifications, the pump flow rate varies between $Q_p = 1.65 - 3.1$ l/min corresponding to the drive speed variation of $n = 2850 - 5500$ rev/min. This micropump can generate a maximum pressure of 8.6 bar, and it can uphold a maximum pressure of 21 bar. The temperature during its operation may vary in the range of -46° to 177° C. The viscosity of the hydraulic medium may be of 0.5 - 1500 cp [8].

Following the pump's driving under laboratory conditions and testing with a fuel fluid (characteristics in the range prescribed by the manufacturer), it was noted an increase in the drive torque (by 12-18%) and a pressure variation, due to the damaged worn areas.

The areas with the most pronounced wear (Fig. 2) are located on the body's flat surface around the two shafts: under the driving and the driven gears (W1 and W2). There was also observed an increased wear of the pinion's shaft due to the forces in the gear. The worn areas led to an increase of gearing forces and to a deficient contact between the teeth flanks. At the same time, there we remarked vibrations, noise and heating inside the micropump during operation.

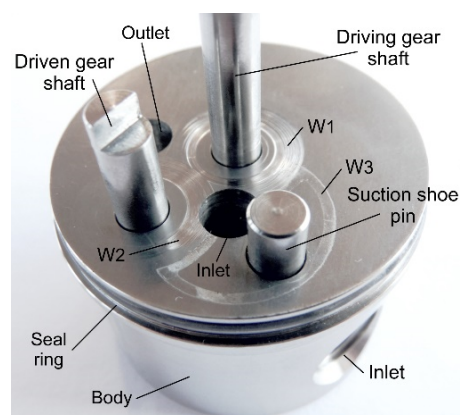


Fig. 2. Fixed parts and different areas of the micropump

The micropump has a suction shoe to guide the fluid into the micropump to be placed in the gaps between the teeth, driven and discharged through the outlet aperture [8]. There is also a wearing zone W3 in the contact area between this suction shoe and the flat surface of the body due to the vibrations resulted from the operation.

In a previous paper [9] we presented 3D modeling phase (Fig. 3) and proposed innovative and constructive solutions to improve the characteristics of this micropump. The most important modification was to replace its pair of gears with the new corrected (displaced) helical gears, but with another module size, offering an increase of the micropump's flow, at the same distance between the shafts and same drive speed.

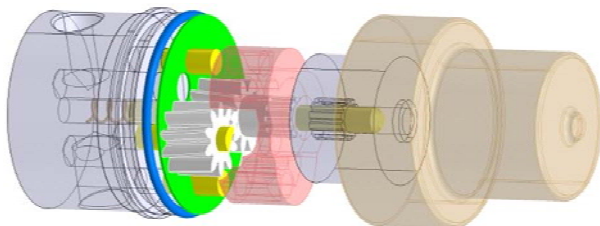


Fig. 3. 3D model of the proposed micropump

Another innovative change on the original micropump assembly is the design of a new suction element to separate the aspiration zone of the fluid by the driving gear through the inlet port to the outlet port. Thus, a significant reduction in torque is required to drive the fluid from the entire cavity under the metal cover. So, the vibrations, noise and wear will be significantly reduced. The fluid inside the micropump's cavity, under the cover, between the inlet and outlet ports, is still trained by the driven gear to ensure the lubrication [10], but at a smaller rate.

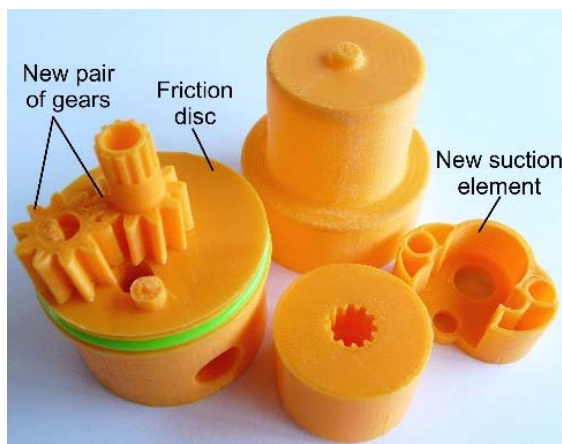


Fig. 4. 3D printed prototype of the modified micropump

The 3D model of the proposed micropump is completed by a friction disc assembled in contact with the flat surface of the body. This variant was conceived and designed [9] in CATIA v5 and 3D printed (Fig. 4) to verify the gearing, positions and compatibility of the new suction element and of the friction disc with the unmodified components of the micropump. The friction disc is provided with holes for mounting the gears shafts, the two pins that support the new suction element and the inlet and outlet holes (Fig. 2). This disc bears the

wear of the micropump body's flat face in the improved version and it is simple to be replaced, if needed, during service and maintenance intervals. Through its flat surface, the disc can also be used with actual micropumps, still in service, that have an acute wear of the body, to increase their lifetime and operation.

5. MATERIALS USED FOR THE MICROPUMP'S COMPONENTS

Our new micropump model needs a confirmation of current materials selected or new ones. The wear observed on the micropump (Fig. 2) in our laboratory resulted from the long contact of the gears and the suction element with the metal components (body and driving gear's shaft).

In the company's documentation for this model, the gears and the suction shoe element are made of PEEK (PolyEther Ether Ketone) because it is a high-performance engineering plastic with great resistance to chemicals, solvents, fuels and additives, with an excellent mechanical strength and dimensional stability. It is neutral to steam, water and salt water. PEEK has also the ability to maintain the parts stiffness at high temperatures up to 170°C. The main benefits of gears made of PEEK over metal gears are: up to 70% weight reduction, up to 50% noise reduction and up to 80% reduced moment of inertia [7]. The reduced weight and moment of inertia are necessary for the operation of this micropump driven by magnets.

According to [11], Victrex PEEK polymers maintain mechanical properties at high temperatures and in adverse chemicals and moisture, making them the material of choice over other gear materials to the industry demands for extended service life in various challenging environments. Victrex has created a new PEEK for use in gears applications improving the already proven properties of Victrex PEEK 450G to achieve better performance. Based on the literature review [2, 9, 12], we recommend this material for the micropump's gears because of a low energy consumption (gears result with an important weight reduction), less vibrations and noise, a reduced moment of inertia leads to improved responsiveness, simplicity in mass production (by injection-molding process) with no other machining and/or finishing operations, easy to be integrated in hybrid technology with composites, metals and other plastics, etc.

We also recommend for gears, the suction shoe element and the friction disc to be produced of the POM (Polyoxymethylene) material. For this micropump we propose the use of Ultraform [13], a co-polymeric POM created by the BASF company with excellent mechanical properties (strength, toughness, fatigue endurance, low tendency to creep), surface hardness, resistance to wear, moisture and chemicals. It can be processed rapidly by extrusion and injection molding, without deposits and are also easy to demold, with a very good surface quality.

For the metal components of the micropump, the 316 or 304 steel types [14] can be retained, as in the current micropump. They are austenitic chromium-nickel stainless steels containing molybdenum, that increases

general corrosion resistance, improves resistance to pitting from chloride ion solutions and provides increased strength at high temperatures. These steels have also an improved corrosion resistance against hydrochloric, sulfuric, acetic, formic and tartaric acids, acid sulfates and alkaline chlorides.

6. CONCLUSIONS

This paper is part of the research project for creating new and/or improving actual magnet drive micropumps to increase their performance, lifetime and optimizing their maintenance. Changes proposed refer to a new constructive solution with a new pair of gears to raise the micropump's flow, but also to the concerns to reduce the wear of its components. Along with dimensional or shape changes of the components, the materials used are very important because of the micropump's role and fluids pumped in the hydraulic installations.

Gears have a very important role in pumping the fluid with good efficiency, they need a low maintenance, so their life can be maximized by selecting a polymeric material suitable to the hydraulic medium. This material should balance friction and wearing properties, flanks surface quality, strength and fatigue resistance at high operating temperatures. The plastic gears are lightweight, easy to manufacture by injection molding at low cost and large production, non-rusting and able to operate without lubrication by mating with proper metal gears and/or other of the pump's components.

However, in certain conditions (viscosity, high flow or pressure, presence of particles etc.), these gears may prove to have low strength, tendency to hold heat, become worn too fast and not functional compared to metal gears [7].

Future research in the field of this type of micropumps will include the redesign of the body and the metal cover to add and ensure the mixing and dosing functions of two compatible fluids to pump them into the hydraulic system. It is also expected a complex study for the parameterized creation of a micropump family to provide a wider range of flows and pressures and the possibility to flow fluids with different viscosities.

7. REFERENCES

- [1] Ghionea, I., Opran, C., Tarbă, I., Tiriplică, P., *Magnetic drive pumps. Current state and overview*, Scientific Bulletin, Serie C, Tribology, Machine Manufacturing Technology, pp. 79 – 82, 2017.
- [2] Rundo, M., *Models for flow rate simulation in gear pumps: A Review*, Journal of Energy Research, Engineering and Policy, 2017.
- [3] Rajeshkumar, S., Manoharan, R., *Design and analysis of composite spur gears using finite element method*, IOP Conference Series: Materials Science and Engineering, no. 263, IOP Publishing, 2017.
- [4] Borghi, M., Zardin, B., Specchia, E., *External gear pump volumetric efficiency: Numerical and experimental analysis*, SAE Technical Paper; SAE International: Warrendale, USA, vol. 2(1), pp. 1285 – 1302, 2009.
- [5] Ghionea I., Ionescu, N., Ghionea, A., Ćuković S.,

Tonoiu, S., Catană, M., *Computer aided parametric design of hydraulic gear pumps*, Acta Technica Napocensis, Applied Mathematics, Mechanics and Engineering, Technical University of Cluj-Napoca, vol. 60, no. I, pp. 113–124, ISSN: 1221-5872, WOS: 000416959000017, Cluj-Napoca, Romania, 2017.

- [6] Opran, C., Ghionea, I., Pricop, M., *Embedded modelling and simulation software system for adaptive engineering of hydraulic gear pumps*, Proceedings of the 26th DAAAM International Symposium, pp. 0311–0319, DAAAM International, ISSN 1726-9679, Vienna, Austria, 2016.
- [7] <https://www.michael-smith-engineers.co.uk/resources/useful-info/magnetic-drive-pumps>
- [8] ***, *Magnetic drive gear pump, GB series, GB EagleDrive*, Micropump Inc, 2018.
- [9] Ghionea, I., Opran, C., G., Ghionea, A., Ćuković, S., Tarbă, C., I., *Adaptive design of a 3D model magnetic drive micropump for an extended life cycle and low maintenance*, Acta Technica Napocensis, vol. 61, issue 2, Applied Mathematics, Mechanics and Engineering, Technical University of Cluj-Napoca, ISSN: 1221-5872, pp. 201-212, WOS: 000437045000008, Cluj-Napoca, Romania, 2018.
- [10] Meng, H., Sui, G., Xie, G., Yang, R., *Friction and wear behavior of carbon nanotubes reinforced polyamide 6 composites under dry sliding and water lubricated condition*, Composites Science and Technology, vol. 69, pp. 606–611, 2009.
- [11] <https://www.victrex.com/en/victrex-peek>
- [12] Pogačnik, A., Kalin, M., *The running in phase of polymer materials for gears*, Centre for Tribology and Technical Diagnostics, University of Ljubljana, Slovenia, 2017.
- [13] ***, *Ultraform® (POM) Product brochure*, BASF company, 2017.
- [14] ***, *316/316L Stainless steel*, SAE grades, 2017.

Authors: Assoc. Prof. Ionuț Gabriel Ghionea¹, Full Prof. Constantin Gheorghe Opran¹, Scientific Associate Saša Ćuković², PhD Student Mihaela Pleșa³, ¹University Politehnica of Bucharest, Faculty of Engineering and Management of Technological Systems, Department of Machine Manufacturing Technology, Bucharest, Romania, Spl. Independenței nr. 313; ²University of Kragujevac, Faculty of Engineering, Kragujevac, Serbia, Sestre Janjic 6, 34000; ³University Politehnica of Bucharest, Doctoral School of Faculty of Engineering and Management of Technological Systems.

E-mail: ionut.ghionea@imst.pub.ro; constantin.opran@ltpc.pub.ro; cukovic@kg.ac.rs; elaplesa@gmail.com

ACKNOWLEDGEMENTS:

This work has been funded by University Politehnica of Bucharest, through the “Excellence Research Grants” Program, UPB – GEX 2017, Ctr. No. 57/2017.

The authors wish to thank AxFlow Romania for providing the micropump and the necessary documentation for this research.

This work is also in the frame of the PhD thesis: Researches on the manufacturing flux of constant flow hydraulic pumps to improve the technical and economical performances, PhD supervisor: Full Prof. Adrian Ghionea.

Kovačević, L., Terek, P., Miletić, A., Kukuruzović, D., Škorić, B.

INFLUENCE OF COMPUTATIONAL GRID DENSITY ON RESULTS OF CASTING SIMULATION

Abstract: Traditionally, foundries develop new gating systems according to empirical rules and volumetric calculations. This process is not perfect and requires a lot of trial-and-error adjustments on the shop-floor. Nowadays, numerical simulations may provide great help in this process. However, although power of computer hardware and software has been significantly increased over the last few decades, it is still insufficient for running detailed simulations in a real production environment where an engineer cannot wait days or even weeks for simulation to finish. Therefore, there exists a widespread use of low grid density meshes that deteriorate simulation accuracy. The purpose of this research is to assess the most commonly used rule of thumb for selecting the grid density at critical sections which states that there should be three cells in the direction of wall thickness. Guidelines are given for cases where time and price constraints prevent the use of large meshes, while small meshes lack accuracy necessary to detect mold filling problems.

Key words: casting simulation, grid density, control volume, mesh quality, mesh size

1. INTRODUCTION

The performance of structural castings is strongly affected by defects formed early in the process, i.e. during pouring of liquid metal into the molds [1]. Therefore, in order to obtain maximum mechanical properties the process engineers need to optimize gating systems and reduce surface turbulence during pouring as much as it is technologically and economically feasible.

Gating system optimization is particularly important in manufacturing aluminum alloy castings. Aluminum has very high affinity towards oxygen and quickly creates insoluble oxides on its surface. Therefore, surface turbulence leaves lasting marks inside casting microstructure even when the entrained bubbles have enough time to leave the metal before solidification traps them. Numerous research done in previous years has been able to show notable correlation between turbulent mold filling and decrease in mechanical properties of castings [3]. Turbulent filling was even correlated to several types of corrosion, such as pitting corrosion, exfoliation corrosion and stress corrosion cracking [4].

Although these problems most notably influence only aluminum alloy casting production, they should not be discarded since aluminum casting will be the main source of foundry industry growth in the foreseeable future. According to census of world casting production, aluminum casting shipments in 2016 totaled 17.9 million metric tons [5]. For comparison, in 2003 the world produced only 9.3 million metric tons of aluminum castings [6]. Large part of this growth comes from automotive industry, which is currently the largest consumer of castings. Average aluminum content in an European produced car in 1990 was 50kg. This figure rose to 140kg per vehicle in 2012, and is expected to rise to 180kg by

2020 [7]. Most of this rise is attributed to castings and is mainly influenced by desire to increase fuel efficiency and reduce air pollution through vehicle weight reduction [8].

Traditionally, foundries develop new gating systems according to empirical rules and volumetric calculations. This process is not perfect and requires a lot of trial-and-error adjustments on the shop-floor. Nowadays, numerical simulations may provide great help in this process. What's more, casting process simulations are considered so vital in achieving requested product quality that automotive industries own internal standards, e.g. AIAG CQI-27, request for all foundry suppliers of OEM automotive castings to implement both solidification and filling casting simulations [9]. All simulations have to be performed by approved software and results must be reviewed with the customer product engineering sector. At any high stress features detected by the finite element analysis (FEA) models, the simulation must show absence of hot spots, air entrapment and convergence of multiple metal fronts [9].

Necessity to conduct casting simulation for large number of parts in many foundries led to another problem. Although power of computer hardware and software has been significantly increased over the last few decades, it is still insufficient for running detailed simulations in a real production environment. In most real world cases, engineer cannot wait days or even weeks for one simulation to finish. Especially considering that process technology is optimized through several design iterations. Therefore, there exists a widespread use of low grid density meshes. This practice can cause significant deterioration of simulation accuracy [10]. In most cases, engineers use meshes where the volumes belonging to castings are meshed with only three layers of elements. Even only two layers are often considered satisfactory.

The purpose of this research is to assess the most commonly used rule of thumb for selecting the grid density at critical sections which states that there should be three cells in the direction of wall thickness.

2. METHODOLOGY

Geometry selected for this investigation is shown in Fig. 1. Casting is ring shaped with 100 mm outside diameter and 5 mm wall thickness. In order to make simulations computationally efficient, the only part of the gating system that was included was the ingate. Ingate is attached to the side of the casting and is shown as hatched in gray color. Similar geometries can often be found in real casting geometries, e.g. when casting automotive pistons, and therefore it can be considered as a suitable representative of real production parts.

The simulations were carried out using MAGMA⁵ v5.2 from MAGMA Giessereitechnologie GmbH, Germany. In all simulations the casting material was AlSi12 alloy, pouring temperature was set to 650°C and the pouring was defined by pouring rate boundary condition. The mold material was silica waterless and the initial mold temperature was set as 20°C. Values of material properties and heat transfer conditions were selected from internal database of the MAGMA⁵ software package.

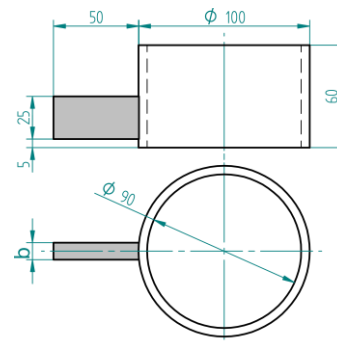


Fig. 1 Drawing of the selected geometry

In this investigation two parameters were varied in two levels. Normal and fine grid density meshes were generated by using equidistant cells that had the same width of 1.67 mm and 0.5 mm, respectively in each direction. Pouring rates, corresponding to ingate widths of 5 mm and 10 mm, were also varied. Volumetric flow rate (Q) used in the simulations was calculated from sprue height ($H = 100$ mm) by using following equation:

$$Q = ab\sqrt{2gH} \quad (1)$$

where a is ingate height, b is ingate width and g is gravitational acceleration.

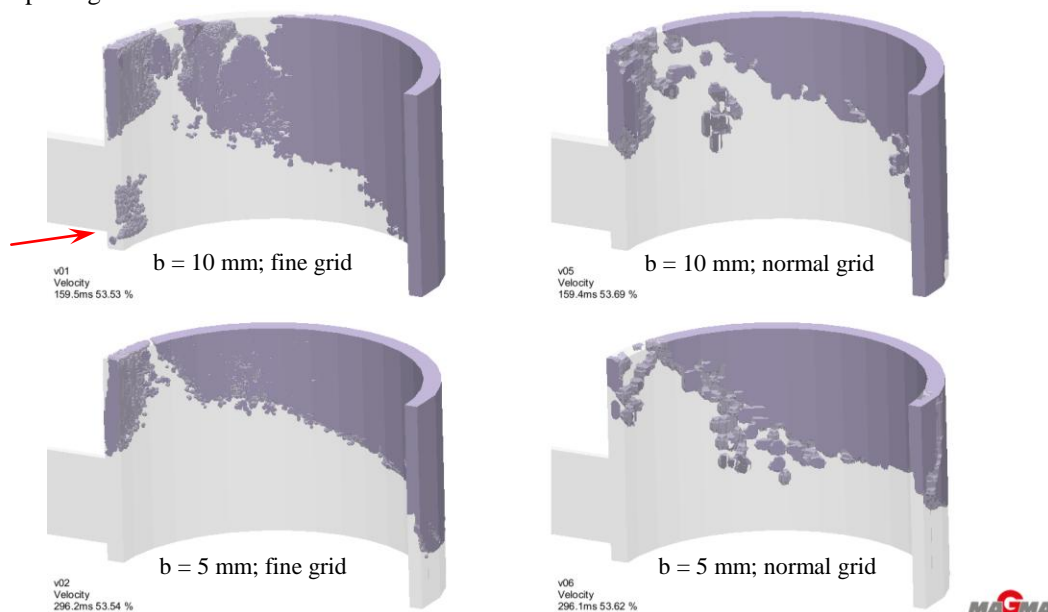


Fig. 2 Filled regions of the mould cavity at the time when 53.54% of the total cavity volume is filled

3. RESULTS AND DISCUSSION

Simulation runs that used normal grid were finished in significantly less time. Average runtime for normal grid simulations was approximately 3 min, while fine grid simulation runs lasted more than 3 hours and 20 minutes. Therefore, time penalties for the use of higher density grids are significant. For typical casting geometries that are orders of magnitude more complex than the one used in this study, the use of higher density grids could prolong process of technology optimization for weeks, or even months. In most cases, this time penalty cannot be justified since filling

patterns obtained by both grids were found similar, Figs. 2 and 3. Normal grid simulation results show obvious lack of fine detail on the melt-gas interface. However, filling patterns are mostly preserved, and based on these results the engineer can design gas vent locations with sufficient degree of confidence.

The absolute velocity fields at the time when approximately half of the mold cavity is filled are shown in Fig. 4. As with the filling pattern, fields obtained with simulations calculated using fine and normal grids are different, but comparable. Although some spatial interpolation in result display is present, larger cells in normal grid simulations lead to averaging

of velocity field and therefore to the loss of precision (see circled areas in Fig. 4).

Temperature field of the castings at the end of the mold filling, i.e. at the start of the solidification process is presented in Fig. 5. As expected, general patterns of the temperature fields are notably different when comparing results with dissimilar flowrates. However, when comparing simulation results for which the flowrate is identical and only grid density is varied, the temperature field variance is notably smaller.

During this analysis, one needs to keep in mind the overall accuracy of casting simulations. In the last few decades, a lot of work has been done in order to accurately predict properties of many commonly used alloys, and CALPHAD techniques extend these possibilities to new alloys with sufficient accuracy. However, there is still a lot of work to be done in this regard and errors induced due to the variance in material properties and by imprecise boundary conditions are larger than detected errors induced by coarse grid density. Therefore, one may conclude that

used rule of the thumb gives satisfactory results. However, this is not the case for aluminum alloy castings when one takes into account the new findings related to existence of bifilms [1]. Although normal grid is able to accurately predict general filling patterns, the mesh density is not sufficiently high to detect turbulence and backflows inside sufficiently thick walls. For selected geometry, melt exiting the ingate impinges the core and is divided into several streams. One stream is pushed downwards where the melt starts circular motion creating the gas pocket (marked by red arrow in Figs 2a and 3a). By comparing presented results, one can notice its absence in normal grid simulations. In simulations performed on fine grids, this expected gas pocket is detected, and is relatively large in size even after 50% of the mold is already filled, Fig 2a. The pocket is filled by existence of metal backpressure only after filling more than 63% of the mold cavity. This is enough time to cause formation of thick oxide layer and consequently deteriorate casting properties. Therefore the use of

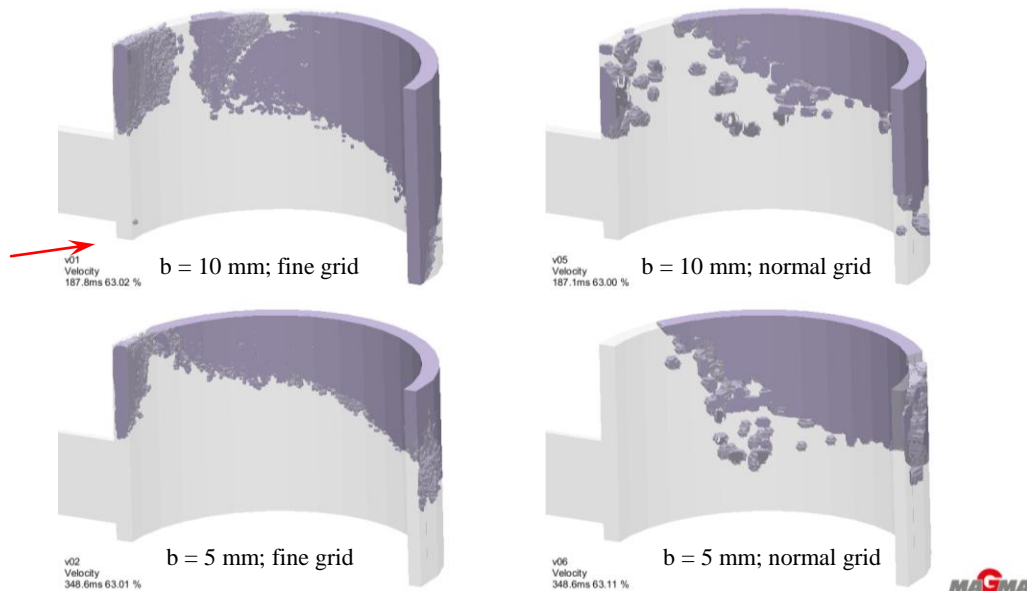


Fig. 3 Filled regions of the mould cavity at the time when 63% of the total cavity volume is filled

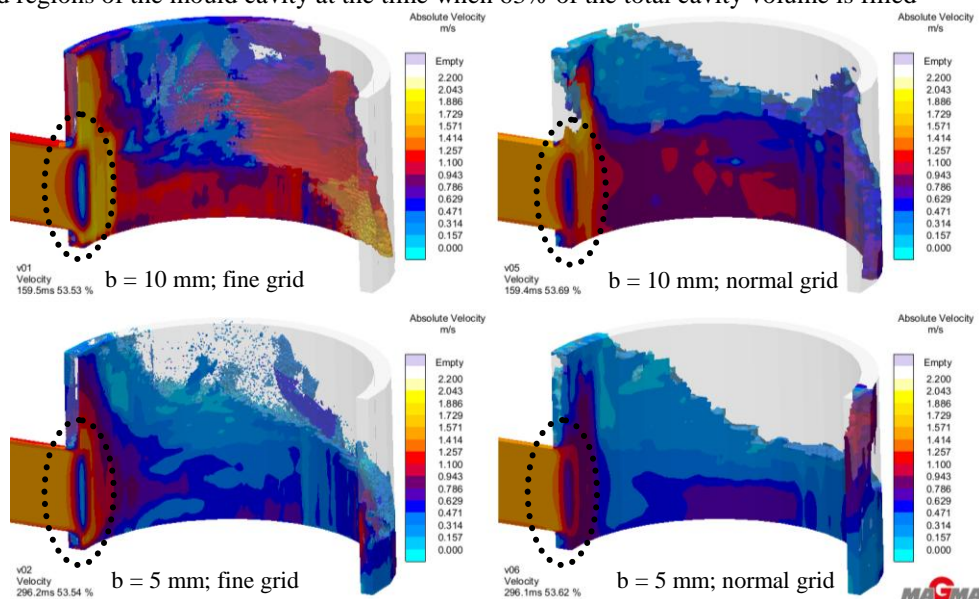


Fig. 4 Velocity field at the time when 53.54% of the total cavity volume is filled

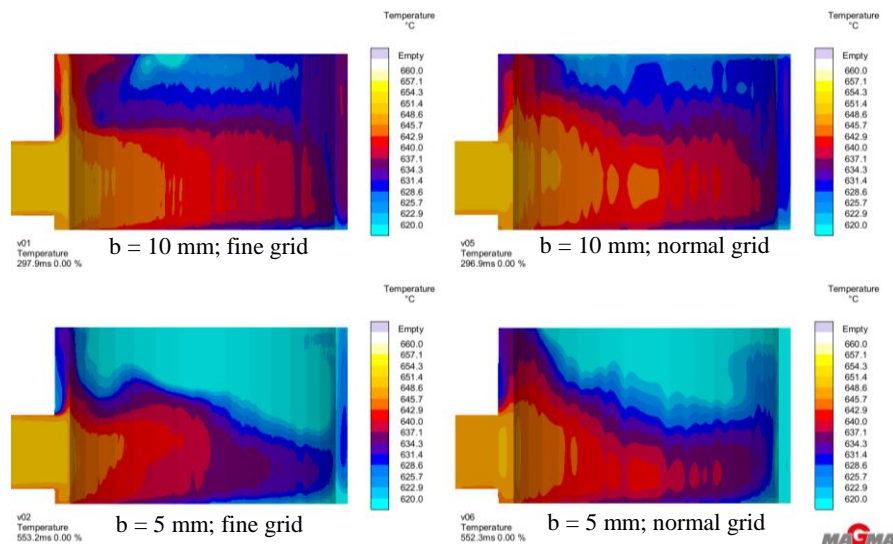


Fig. 5 Temperature field at the end of the mold filling and start of the solidification

normal grid meshes can be considered unsatisfactory for geometries where significant melt impingement exists and the alloy easily reacts with the mold atmosphere. The problem is that most of commercial aluminum alloy castings fall into this category and thus require unreasonably long simulation times in order to achieve adequate result accuracy. Considering the satisfactory accuracy of velocity and temperature fields in normal grid simulations, the solution could be found by running multiple simulations. First, the engineer needs to run one normal grid simulation on the whole geometry. Select critical portions in geometry where severe melt impingement exist, and then run several fine grid simulations that encompass these critical sections. These secondary simulations would, as initial conditions, use velocity and temperature fields calculated in initial simulation.

5. CONCLUSIONS

Presented comparison of mold filling patterns, temperature and velocity fields suggest that the generally accepted rule of thumb for mesh is acceptable for most cases. The filling pattern is sufficiently precise to determine vent locations, solidification patterns and general velocity fields. However, small surface turbulences caused by melt impingement cannot be accurately predicted when using such meshes. Since this phenomena is a significant bifilm generator, it cannot be disregarded when studying critical aluminum components and in those cases a denser grids need to be used in order to accurately predict them.

6. REFERENCES

- [1] Campbell, J.: *Castings Practice: The Ten Rules of Castings*, Elsevier Butterworth-Heinemann, Oxford, 2004.
- [2] Mi, J., Harding, R.A., Campbell, J.: Effects of the entrained surface film on the reliability of castings, *Metallurgical and materials transactions A*, Vol 35A, pp 2893-2902, 2004.
- [3] Uludag, M., Cetin, R., Dispinar, D.: *Freezing*

range, melt quality, and hot tearing in Al-Si alloys, *Metallurgical and materials transactions A*, Vol 49, pp 1948-1961, 2018.

- [4] Campbell, J.: *Consolidation and corrosion of metals: an overview of the role of bi-films in corrosion*, *Innovations in corrosion and materials science*, Vol 6, pp 132-139, 2016.
- [5] A Modern casting staff report: *Census of world casting production. Global casting production growth stalls*, *Modern Casting*, December 2017, pp 24-28, 2017.
- [6] A Modern casting staff report: *38th Census of world casting production – 2003*, *Modern Casting*, December 2004, pp 25-27, 2004.
- [7] EAA – European aluminium association: *Aluminium in cars. Unlocking the light-weighting potential*, EAA, Brussels – Belgium, 2016.
- [8] Modaresi, R.: *Dynamics of aluminum use in the global passenger car system*, PhD thesis, Norwegian University of Science and Technology, 2015.
- [9] Automotive Industry Action Group: *CQI-27 Special process: casting system assessment, 1st edition*, AIAG, Southfield - Michigan, USA, 2015
- [10] Merder, T., Saturnus, M., Warzecha, M., Warzecha, P.: *Validation of numerical model of a liquid flow in a tundish by laboratory measurements*, *Metalurgija*, Vol 53, pp 323-326, 2014.

Authors: Asst. Prof. Lazar Kovačević, Asst. Prof. Pal Terek, Asst. Prof. Aleksandar Miletić, MSc. Dragan Kukuruzović, Prof. Branko Škorić, University of Novi Sad, Faculty of Technical Sciences, Trg Dositeja Obradovica 6, 21000 Novi Sad, Serbia, Phone.: +381 21 485-2330, Fax: +381 21 454-495. E-mail: lazarkov@uns.ac.rs

ACKNOWLEDGMENTS: Authors would like to thank MAGMA Giessereitechnologie GmbH (Aachen, Germany) and their regional representative Exotherm-it d.o.o., (Kranj, Slovenia) for providing licenses for MAGMA⁵ casting process simulation software

Kukuruzović, D., Terek, P., Kovačević, L., Škorić, B., Baloš, S., Panjan, P., Čekada, M., Miletić, A.

ESTIMATION OF SOLDERING TENDENCY OF AL-ALLOY TOWARD CrAlN AS A CANDIDATE COATING FOR HPDC TOOLS

Abstract: High pressure die casting (HPDC) tools exhibit wear during the process of casting. One of the mechanisms of tool wear is soldering. As a result of soldering of the casted alloy to the die surface there is a change in surface quality and die mass. Due to tool wear, there is also an increase in downtime. As a result, there are significant financial losses. In order to reduce those losses, HPDC tool surfaces are subjected to different types of surface enhancements. In this study, CrAlN coatings with different chemical compositions were used. A detachment test was used to evaluate the amount soldering of the casted alloy to the sample surfaces. Contact surfaces of the cast alloy and the samples were evaluated using a scanning electron microscope. It was found that the chemical composition of the coatings didn't show high influence on the soldering resistance of Al-Si-Cu cast alloy.

Keywords: HPDC, die soldering, CrAlN coating.

1. INTRODUCTION

High pressure die casting (HPDC) is a mass production process, where molten metal is injected into a die cavity with high velocity and pressure, and then forcibly cooled. It is one of the most commonly used casting processes for aluminum alloys. The casted aluminum products are mostly used in the automotive industry, and this industry represents the largest market for this type of products. Typical representatives of casted aluminum in the automotive industry are engine blocks and cylinder heads.

During the HPDC process of molten aluminum, the die is exposed to thermal shock, oxidation, erosion, corrosion and soldering processes [1,2]. Soldering or sticking is a casting defect where the molten metal "welds" to the surface of the metallic die during the casting process [3,4]. Soldering is a major issue limiting the productivity of aluminum die casts [5–8]. As a result of soldering there is shortening of die life, it effects casting quality and increases machine downtime due to increased tool maintenance. A liquid lubricant is sprayed on to the die surface before each injection to prevent the soldering of aluminum. High process temperatures cause lubricant to evaporation. Its chemical composition is such that it causes noticeable harmful influence on the environment. Furthermore, since significant amount of lubricant is used during production, there is a rise in the cost of manufacturing.

In order to reduce the use of lubricants and its negative influence on the environment, there have been numerous studies in the field of surface modification to achieve higher die corrosion and erosion resistance towards molten aluminum. Research is mainly directed towards surface modifications in the form of thermochemical processes, such as plasma nitriding, coating deposition via PVD processes or combinations in the form of duplex treatments [9–12].

The aim of this study is to investigate the interaction between the Al-Si-Cu alloy and hot-working tool steel (H11) with duplex treated surfaces by

applying a detachment test and by examining the amount of soldering that occurs on the contact surface. Special attention was given to define the influence of the chemical composition of CrAlN coatings on the soldering that occurs during the process of die casting.

2. EXPERIMENTAL

The detachment test was used for simulating the HPDC process, and schematic of the process is given in figure 1. The casting mold was made from castable heat resistant refractory based on Al₂O₃ ceramic. In order to quickly simulate damage done to the samples over large number of HPDC cycles, the molds were put in a heat treatment furnace and held to 700°C. Two holding periods were varied: 30 min and 60 min. After holding period, the molds were taken out of the furnace and left to cool in still air. The heat inertness of the molds helped to preserve the contact of the sample with the liquid aluminum after pouring by not allowing the melt to cool below solidus temperature. In order to prevent solidification at the melt-sample interface, the pouring temperature of EN AB-46000 alloy was set to approximately 750°C. Before the casting process, the samples were preheated to 300°C, which is the standard temperature of the HPDC tools during production.

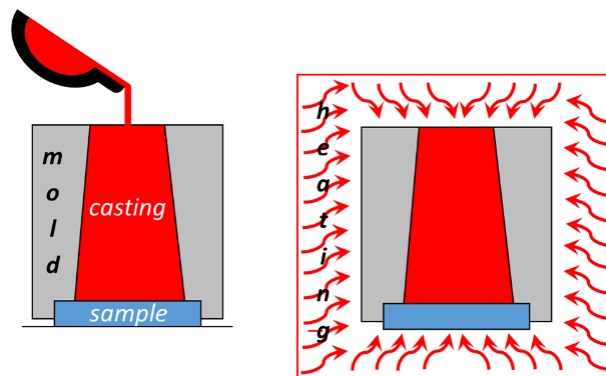


Fig. 1. Casting process

The ceramic molds were preheated to 650°C. The contact surface between the sample and the molten aluminum was set at $\phi 22$ mm.

The dimensions of the samples used for this experiment were $\phi 30 \times 5$ mm quenched and double tempered H11 steel discs. Samples were prepared by grounding with sandpapers to the finest roughness (360, 500, 1000 and 2000). After surface preparation, plasma nitriding was carried out in an industrial nitriding unit ION-25I (IonTech) equipped with a pulsed plasma generator. Nitriding was conducted for 12 h at a temperature of 510°C using a gas ratio of $H_2:N_2=3:1$, and by applying a 0.6 duty cycle. After the plasma nitriding process of the samples, the compound layer that was produced on the surface was removed before deposition of the CrAlN coatings. The removal was done to produce duplex layers with high adhesion and heat resistance. The compound layer was removed by polishing samples using a 3 μ m diamond paste.

A CC800/9 (CemeCon) industrial DC-magnetron sputtering system was used to deposit three CrAlN coatings with different chemical compositions. The first coating had more aluminium (CrAlN-Al), the second one had more chrome (CrAlN-Cr) and the third one had the same amount of aluminium and chrome (CrAlN). The coatings were deposited using a 2-fold rotation. The deposition process was conducted using for targets. Two triangle-like segmental Cr/Al targets, one Cr and one Al target.

Coating thickness measurements were obtained using a ball cratering test, while the sample surface roughness was obtained using a Hommel Tester T2000 profilometer. The characteristics of obtained samples are given in table 1.

Sample	Sq [μ m]	Coating defects density [num/mm ²]	Area of coating defects [μ m ²]	Coating thickness [μ m]
CrAlN	0.15	121	11634	5.7
CrAlN-Al	0.13	85	7893	4.9
CrAlN-Cr	0.24	174	20659	7.1

Table 1. Average measurement results of sample contact surface

In order to define the amount of soldering that occurs on the contact surface of the casted assembly, a detachment between sample and casted aluminum alloy needed to be performed. For this purpose ZGIM 500 tensile tester machine was used.

A TH3030 Hitachi Scanning Electron Microscope (SEM) and a LEITZ-Orthoplan optical microscope were used to analyze the contact surfaces of the samples and the casted alloy.

The ammount of soldering present on contact surfaces, of both the castings and the samples, was determined by image analysis employing the Scanning Probe Image Processing software (SPIP).

3. RESULTS AND DISCUSSION

Appearance of contact surfaces of both the sample and the casting are presented in Fig. 2. Contact surface of the casted alloy (Fig. 2b), represents a mirror image of the contact surface of the samples (Fig. 2a).

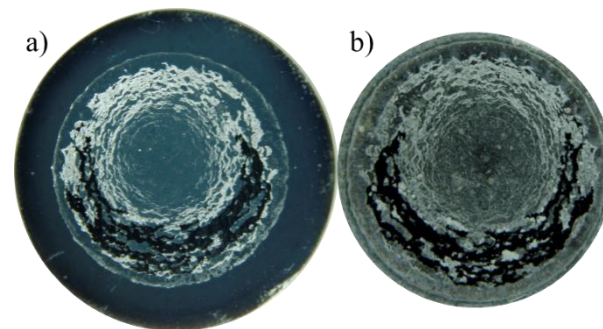


Fig. 2. Contact surfaces of a) the sample and b) the casted aluminum alloy.

Examination of contact surfaces revealed a large amount of coating delamination and soldering present on the contact surface of the sample. It is well known that ceramics don't corrode in contact with molten alloys [13]. The formation of intermetallic compounds between iron and soldered aluminum occur due to the high solubility of iron in aluminum [14–15].

High magnification SEM and EDX analysis of contact surfaces revealed that development of intermetallic compounds between the sample and molten alloy started to form through the droplet defects formed during coating deposition. SEM image of the contact surface on the casting is presented in Fig. 3. The image was obtained using Back-scattered electrons (BSE) and the intensity of the signal is strongly related to the atomic number of the material. Materials with lower atomic number provide weaker signal, and thus have a darker color, and vise versa the element with a higher atomic number will give a brighter image. Therefore, the brighter area in Fig. 3 represents the delaminated coating that remained attached to the casting during detachment test. Darker area is aluminum alloy.

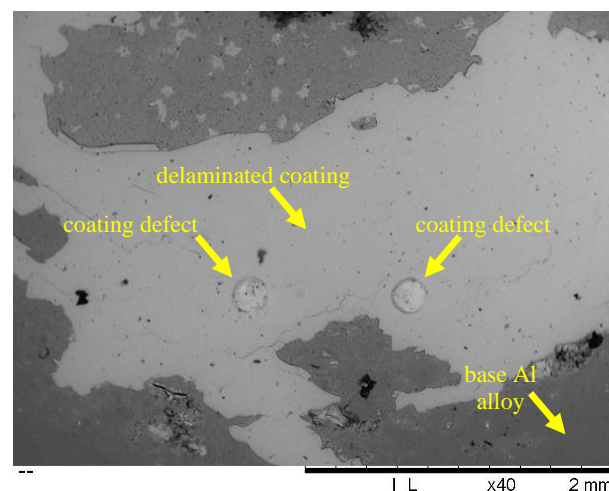


Fig. 3. BSE SEM image of the of the casting contact surface after the detachment test.

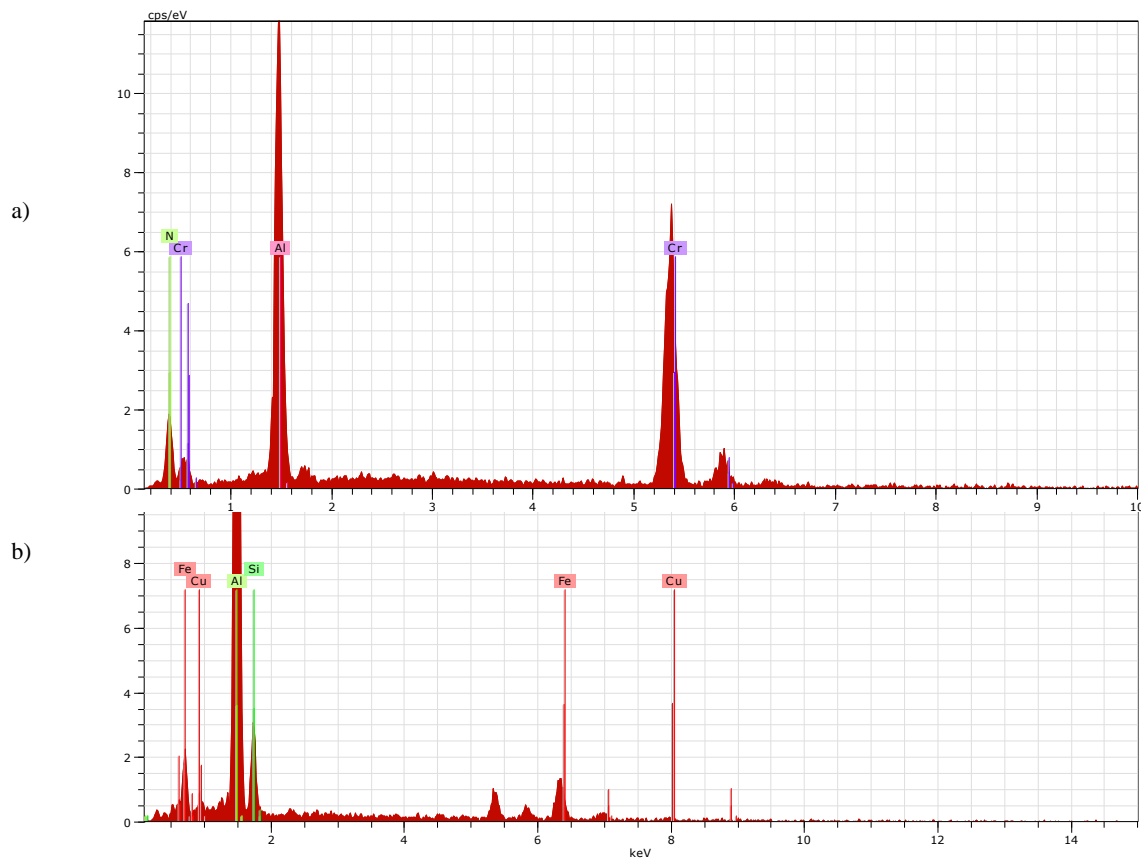


Fig. 4. EDX spectra: a) delaminated coating; b) coating defect.

Two large coating defects are present in the delaminated coating. In order to confirm findings made by visual examinations, EDX analysis was performed and spectrums are given in Fig. 4. Spectrum given in Fig. 4a was made on a bright area of the Fig. 3 next to one of the defects. Spectrum shows large presence of Cr and N and confirms initial assumption that this is most probably a delaminated coating. Spectrum shown in Fig. 4b is made inside the area of one of the coatings defects. Chemical composition corresponds to the base aluminum alloy with the increased presence of iron, which can be correlated to the formation of Fe-rich intermetallics.

Therefore, although the ceramic coatings are chemically inert toward the aluminum alloy melts, effects of soldering are nevertheless visible even on coated samples. The underlying mechanism is probably as follows. During industrial coating process there is a high probability for formation of defects that extend over whole thickness. Through these defects aluminum can get in contact with underlying steel and form intermetallic compounds. These compounds can then mechanically cause coating delamination.

Results of quantitative image analysis of contact surfaces are presented in Figs. 5 and 6. As expected, soldered area has increased by increasing duration of the contact between melt and the sample. For holding times of 60 min, all samples showed similar amount of soldering irrespective of chemical composition of the coating. This is in line with previous findings [5].

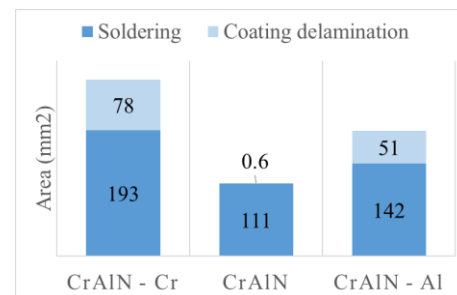


Fig. 5. The obtained amount of soldering and coating delamination for the time of 30 minutes.

For holding times of 30 min the CrAlN-Cr sample exhibited highest soldering tendency, followed by CrAlN-Al and CrAlN, respectively. However, this difference is probably not caused by difference in chemical compositions. Analysis of the surface roughness (Table 1) has shown that the root mean square roughness (S_q) is highest for the CrAlN-Cr coating, followed by CrAlN-Al and CrAlN coatings, respectively. This difference in roughness can be explained by the area covered by coating defects and the number of those defects on the surface of the samples (Table 1). Therefore, soldered area is directly correlated to presence of defects on the surface of PVD coatings. This finding provides new insight and offers new directions of coating technology development. Instead of searching for new ceramics and chemical compositions that are only nominally less wetted by the melt, the development should be directed towards finding technology that offers minimum presence of defects that extend over whole thickness. Future research should be based on finding ways to reduce the

number of critical coating defects, and determining substrate and coating materials properties that influence their formation.

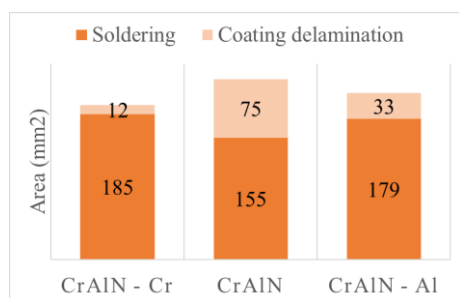


Fig. 6. The obtained amount of soldering and coating delamination for the time of 60 minutes.

5. CONCLUSIONS

Results of this work showed that:

- The detachment test enables evaluation of the interaction of molten aluminum alloy with the die material.
- The number of coating defects on the contact surface between the die tool and the casted aluminum alloy represents the highest influence on die soldering.
- Controlling the number and density of coating defects can affect the bonding of the casting to the coated die surfaces, resistance, and durability of the coating.

6. REFERENCES

- [1] Chen, Z.W., Jahedi, M.Z., *Die erosion and its effect on soldering formation in high pressure die casting of aluminium alloys*, Materials & Design. 20 pp. 303–309 1999.
- [2] Persson, A., Hogmark, S., Bergström, J., *Failure modes in field-tested brass die casting dies*, Journal of Materials Processing Technology. 148 pp. 108–118 2004.
- [3] Gobber, F., Pisa, A., Ugues, D., Lombardo, S., Fracchia, E., Rosso, M., *Study of the Effect of Surface—Roughness of Dies and Tooling for HPDC on Soldering*, in: 2018: pp. 977–981.
- [4] Han, Q.Y., *Mechanism of die soldering during aluminum die casting*, China Foundry. 12 pp. 136–143 2015.
- [5] Terek, P., Kovačević, L., Miletić, A., Panjan, P., Baloš, S., Škorić, B., Kakaš, D., *Effects of die core treatments and surface finishes on the sticking and galling tendency of Al–Si alloy casting during ejection*, Wear. 356–357 pp. 122–134 June 2016.
- [6] Zhu, H., Guo, J., Jia, J., *Experimental study and theoretical analysis on die soldering in aluminum die casting*, Journal of Materials Processing Technology. 123 pp. 229–235 2002.
- [7] Chen, Z.W., *Formation and progression of die soldering during high pressure die casting*, Materials Science and Engineering A. 397 pp. 356–369 2005.
- [8] Han, Q., Viswanathan, S., *Analysis of the mechanism of die soldering in aluminum die casting*, Metallurgical and Materials Transactions A. 34 pp. 139–146 2003.
- [9] Peter, I., Rosso, M., Gobber, F.S., *Study of protective coatings for aluminum die casting molds*, Applied Surface Science. 358 pp. 563–571 Elsevier B.V. 2015.
- [10] Lorusso, M., Ugues, D., Oliva, C., Ghisleni, R., *Failure modes of PVD coatings in molten Al-alloy contact*, Acta Metallurgica Slovaca. 19 pp. 30–42 2013.
- [11] Persson, A., Hogmark, S., Bergström, J., *Thermal fatigue cracking of surface engineered hot work tool steels*, Surface and Coatings Technology. 191 pp. 216–227 2005.
- [12] Joshi, V., Srivastava, A., Shivpuri, R., Rolinski, E., *Investigating ion nitriding for the reduction of dissolution and soldering in die-casting shot sleeves*, Surface and Coatings Technology. 163–164 pp. 668–673 January 2003.
- [13] Salman, A., Gabbitas, B.L., Cao, P., Zhang, D.L., *The performance of thermally sprayed titanium based composite coatings in molten aluminium*, Surface and Coatings Technology. 205 pp. 5000–5008 Elsevier B.V. 2011.
- [14] Rosso, M., Peter, I., Gobber, F.S., *Overview of heat treatment and surface engineering, influences of surface finishing on hot-work tool steel*, International Journal of Microstructure and Materials Properties. 10 pp. 3 2015.
- [15] Nazari, K.A., Shabestari, S.G., *Effect of micro alloying elements on the interfacial reactions between molten aluminum alloy and tool steel*, Journal of Alloys and Compounds. 478 pp. 523–530 2009.

Authors: Teach. Assist. Dragan Kukuruzović, Assist. Prof. Pal Terek, Assist. Prof. Lazar Kovačević, Full Prof. Branko Škorić, Assoc. Prof. Sebastian Baloš, Assist. Prof. Aleksandar Miletić, University of Novi Sad, Faculty of Technical Sciences, Department of Production Engineering, Trg Dositeja Obradovica 6, 21000 Novi Sad, Serbia, Phone.: +381 21 450-2330, Fax: +381 21 454-495.
E-mail: kukuruzovic@uns.ac.rs; palterek@uns.ac.rs; lazarkov@uns.ac.rs; skoricb@uns.ac.rs; sebab@uns.ac.rs; miletic@uns.ac.rs

Res. Cnslr. Peter Panjan, Assist. Prof. Miha Čekada Jožef Stefan Institute, Jamova 39, 1000 Ljubljana, Slovenia, Phone.: +386 01 477-389, Fax: +386 01 251-9385.
E-mail: peter.panjan@ijs.si; miha.cekada@ijs.si

ACKNOWLEDGMENTS: The authors would like to thank the Provincial Secretariat for Higher Education and Scientific Research of Vojvodina, Serbia grant No. 114-451-2192/2016-02. Special thanks to the colleges from Department of Thin films and surfaces, Institute "Jožef Stefan" (Ljubljana, Slovenia) who helped with samples characterization. BioSens Institute (Novi Sad, Serbia), for making their equipment available. We acknowledge GasTeh d.o.o. (Indjia, Serbia) for samples fabrication and Termometal d.o.o. (Ada, Serbia) for heat treatment.

Miletic, A., Panjan, P., Cekada, M., Terek, P., Kovacevic, L., Skoric, B.

MECHANICAL AND TRIBOLOGICAL PROPERTIES OF INDUSTRIALLY PREPARED TiAlN HARD CERAMIC COATINGS

Abstract: Lifetime and efficiency of different tools and mechanical components may be successfully improved by application of hard ceramic coatings. When it comes to tools for machining of hard materials such as hardened steel, TiAlN is one of the most usually applied coatings. This material is of high hardness, high oxidation resistance and high temperature stability. In this research, surface morphology, mechanical and tribological properties of industrially prepared TiAlN coatings were studied. Three different coatings were prepared by selecting different rotational types in a magnetron sputtering deposition chamber. Mechanical properties were characterized by nanoindentation technique and Rockwell indentation test, surface morphology by stylus profilometry and atomic force microscopy, while pin-on-plate test was used to study tribological behavior. It was found that coatings prepared by higher number of rotations are smoother, harder, and more resistant to cracking and wear. These differences are attributed to differences in coating microstructure which refines with increased number of rotations.

Key words: hard coating, TiAlN, magnetron sputtering, hardness, wear

1. INTRODUCTION

In order to meet challenges of a modern industry, i.e. to provide high productivity at low costs, along with meeting the harsh ecology standards, machining tools have to be protected with hard ceramic coatings. Today around 90% of all machining tools are protected by some type of ceramic coating. Mostly nitrides such as TiAlN and CrAlN, oxides such as Al_2O_3 , and carbides such as TiCN are applied on tool surfaces.

TiAlN coatings are widely applied due to their high hardness (≈ 32 GPa), high oxidation resistance (≈ 800 °C), and high temperature stability (≈ 900 °C) [1]. They are especially suitable for machining of hard materials, such as hardened steel, even without lubrication.

Hard coatings are applied on tools in special deposition chambers. When physical vapor deposition techniques are used, tools have to be mounted on special fixation systems which enable complex rotation which is necessary for achieving the uniform deposition on all tool surfaces. Such a fixation system of the industrial deposition unit used in this research is presented in Fig. 1. This system enables three different rotation types named 1-fold, 2-fold, and 3-fold rotation. In 1-fold rotation, samples rotate around the first rotational axis, which is the axis of symmetry of the whole turntable. In 2-fold rotation, samples rotate around the first and the second rotational axis. The second rotational axis is the axis of symmetry of substrate towers. Finally, in 3-fold rotation, samples rotate around three axes, the first, the second, and the third, where the third rotational axis is axis of symmetry of tool holders.

Although during coating deposition different parameters such as partial pressure of active and reactive gases, power on targets, bias voltage, and others are same for all samples, yet the deposition conditions are not same for the samples mounted in different rotation types. Namely, there are differences in the trajectory, and orientation of samples relative to targets [2]. In 1-fold

rotation samples move along circular trajectory, in 2-fold along helical trajectory, while in 3-fold rotation the trajectory is a double helix. Orientation of samples toward targets does not change during deposition in 1-fold rotation, while this is not true for 2-fold and 3-fold rotations. This means that samples mounted in different rotations spend different time in plasma, which is the longest for the 1-fold rotation, and that as a consequence deposition rate is different for different rotations. In reactive physical vapor deposition, changes in deposition rate might lead to changes in chemical composition and coating microstructure [2].

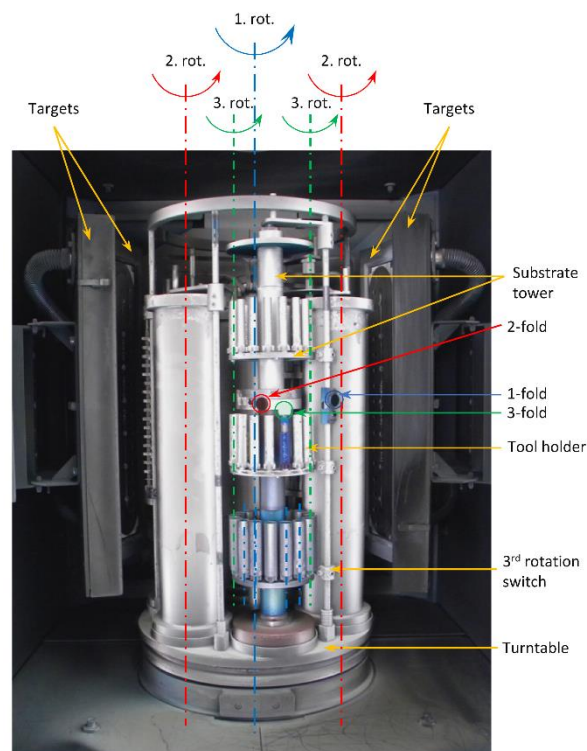


Fig. 1. Interior of CemeCon CC800/9 deposition unit.

The aim of this research is to study the change in surface topography, mechanical properties, and tribological behavior of TiAlN coatings with the change of the rotation type. For that purpose, different TiAlN coatings were produced by mounting the samples in different rotations, as shown in Fig. 1, within the same batch.

2. EXPERIMENTAL DETAILS

2.1 Coating preparation

TiAlN coatings were prepared in an industrial magnetron sputtering unit (CC 800/9). The unit is equipped with four DC powered unbalanced magnetron sources and planetary rotational turntable, as shown in Fig. 1. During deposition only two sources were used, coatings were deposited from TiAl targets. The turntable enables continuous 1-fold and 2-fold rotations, with a gear ratio of 100:37. In the 3-fold rotation, rotation around third axis is not continuous, it is achieved by a switch which rotates the tool holder for around 160°. More details about turntable can be found in [3]. Cold work tool steel EN X160CrMoV121 (AISI D2) was used as a substrate material. Prior to deposition, steel samples were ground, polished by a 3 μm diamond paste, ultrasonically cleaned and dried in hot air. During the deposition following parameters were used: working pressure 0.66 Pa, power on targets 9.5 kW, bias -90 V, N₂ flow 100 ml/min, rotation rate 1 rev/min. Vacuum chamber was heated to 450° prior to coating deposition.

2.2 Coating characterization

Surface topography of coated samples was analyzed by 3D stylus profilometry. For achieving the higher magnification of surface features, atomic force microscopy (AFM) was applied. Cracking resistance and coating adhesion were assessed by a standard HRC test (VDI 3198) [4]. In this test, a Rockwell C diamond prism is indented into a coated sample with a load of 150

kg. Coating quality is then determined by observing the formed indent, number of cracks and areas of delaminated zones around the indent. Nanoindentation technique was utilized to acquire mechanical properties. For that purpose, Fischerscope H100C tester and Vickers diamond indenter were used. Tribological properties were evaluated by a ball-on-plate methodology. Tribological tests were run in dry air, at room temperature. Alumina ball with diameter of 6 mm was used as a counter-body. Linear velocity was kept at 5 cm/s, normal load at 5 N, stroke length at 5 mm, and number of cycles at 2000 for all coatings. Confocal optical microscopy was used to observe samples after tribological test. Generated wear tracks were measured by 2D stylus profilometry.

3. RESULTS AND DISCUSSION

Three-dimensional images of surface topography acquired by stylus profilometry and atomic force microscopy are presented in Fig. 2. Beside each image, surface roughness parameters are provided. Growth defect, which are typical for PVD coatings, are dominating surface features in images obtained by 3D stylus profilometry. It may be seen that size of these defects reduces with increased number of rotations. Accordingly, both average surface roughness (S_a) and root mean square roughness (S_q) decrease with increased number of rotations. Smaller surface features may be seen in AFM images. Protruding features in these images present upper parts of individual columns, which usually constitute microstructure of PVD grown coatings. These images reveal that size of the columns reduces with increased number of rotations, i.e. that coating microstructure becomes finer. Consequently, coatings prepared with 2-fold and 3-fold rotations are of much lower surface roughness than coating prepared with 1-fold rotation.

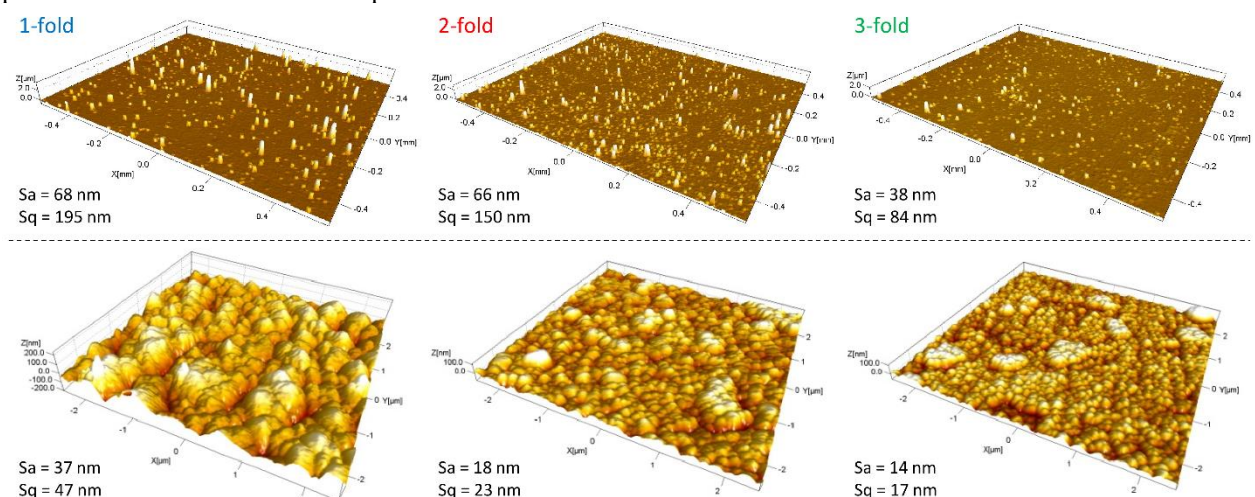


Fig. 2. Surface topography of TiAlN coatings deposited with different rotations obtained by stylus profilometry (upper row) and atomic force microscopy (lower row).

Indents generated by Rockwell C prism are presented in Fig. 3. Higher number of radial cracks was observed around each indent, while there were no circumferential cracks. Large areas of adhesive detachment, as well as

areas of cohesive coating spallation may be seen around indent of 1-fold coating. On the other side, only smaller zones of complete coating detachment are seen around indents in 2-fold and 3-fold coatings. This implies that

both cracking resistance (cohesive strength), and adhesive strength between coating and substrate are higher for coatings prepared with higher number of rotations. According to the VDI 3198 standard, coating quality ranges from HF1 to HF6, where lower number

means higher quality, and where everything from HF1 to HF4 is considered adequate. Coating prepared with 1-fold is of HF4, while the other two coatings are of HF3 quality, which means that all three coatings are of adequate quality for industrial application.

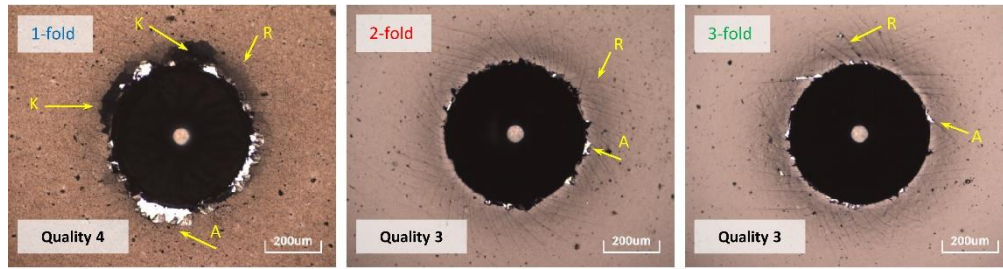


Fig. 3. Indents generated during HRC test with load of 150 kg. Designations "A", "K", and "R" indicate adhesive detachment, cohesive detachment, and radial cracks, respectively.

Thickness and mechanical properties of three coatings are presented in Table 1. Coating thickness decreases with increasing the number of rotations, which is related to change in the deposition rate which is highest for coatings prepared with 1-fold rotation. The deposition rate is the highest for the samples which spend more time in dense plasma [3]. Table 1 shows that coating hardness, elastic recovery, as well as ratio of hardness and modulus of elasticity H^3/E^{*2} are lowest for 1-fold

coating, and highest for 3-fold coating. When it comes to wear resistance, in past the greatest attention was given to hardness. Nowadays, both elastic recovery, and H^3/E^{*2} ratio, which is related to coating cracking resistance, are also recognized as important parameters for tribological behavior. Improvement in mechanical properties is directly related to the improvement in microstructure which becomes finer when number of rotations is increased.

	d (µm)	H (GPa)	E (GPa)	We (%)	H^3/E^{*2} (GPa)
1 - fold	6.9	19 ± 6	352 ± 67	44 ± 4	0.05
2 - fold	3.4	24 ± 2	345 ± 22	52 ± 2	0.10
3 - fold	2.1	27 ± 3	337 ± 33	56 ± 1	0.15

Table 1. Thickness (d), hardness (H), modulus of elasticity (E), elastic recovery (W_e) and H^3/E^{*2} ratio.

Results of tribological test are presented in Fig. 4. Friction curves of all three coatings exhibit two stages, running-in, and transitional stage, while steady-stage was reached only for the 3-fold coating. In the first stage, friction coefficient increases quickly to approximately 0.5 for all coatings. Transitional stage begins after around 50 cycles. First coefficient of friction decreases and after short number of cycles it increases relatively steeply. Considering that steady-state was not reached for all coatings, average values of friction coefficient were calculated for cycles from 1000 to 2000, and are presented in Table 2. It may be seen that friction coefficient is between 0.7 and 0.9, which are values typical for TiAlN coating in contact with alumina [5].

	Coefficient of friction	Wear rate ($\text{mm}^3\text{N}^{-1}\text{m}^{-1}$)
1 - fold	0.71	16.1×10^{-6}
2 - fold	0.77	13.6×10^{-6}
3 - fold	0.86	14.9×10^{-6}

Table 2. Coefficient of friction and wear rate.

2D profiles of wear tracks, presented in the right portion of Fig. 4, were used to calculate wear rate. Table 2 shows that wear is lower for coatings prepared with higher number of rotations, however it is not the lowest for the 3-fold coating. On the other side, there is a direct

relationship between friction coefficient and number of rotations.

In order to better understand wear behavior, wear tracks were analyzed by optical microscopy. Pronounced wear scars may be observed inside the wear track of 1-fold coating, while smooth wear tracks were generated in 2-fold and 3-fold coatings (see also 2D profiles). Wear tracks of all three coatings are relatively clean, wear debris are not seen inside the wear tracks and are mostly agglomerated at the edges and ends of wear tracks. The highest amount of wear debris was observed for 1-fold coating. In our previous research, we showed that wear debris are partly oxides which generate due to heating induced by friction [6]. When TiAlN is in contact with alumina, TiO_2 and Al_2O_3 oxides might form. High coating hardness and presence of hard oxides are main factors leading to a high friction coefficient in the present study. Generally, lower the roughness, lower the friction coefficient. However, although 3-fold coating was of the lowest roughness, the highest friction coefficient was measured for this coating. This may be attributed to its high hardness, i.e. high shear strength in contact with alumina ball. Presented results show that the main wear mechanisms of all coatings are abrasion and tribochemical wear. However, there was difference between three coatings, while pronounced abrasion marks were generated in 1-fold coating, 2-fold and

3-fold coatings were only mildly abraded. This is related to their hardness and cracking resistance. Coating prepared with 1-fold rotation is of the lowest hardness and cracks easier, and is therefore the most abraded. From this point, one might expect the lowest wear for

the 3-fold coating. However, this study shows that the highest mechanical properties and the lowest roughness may not be enough for the best tribological performance. Generation of wear debris and efficiency of their removal from wear track are also of great importance.

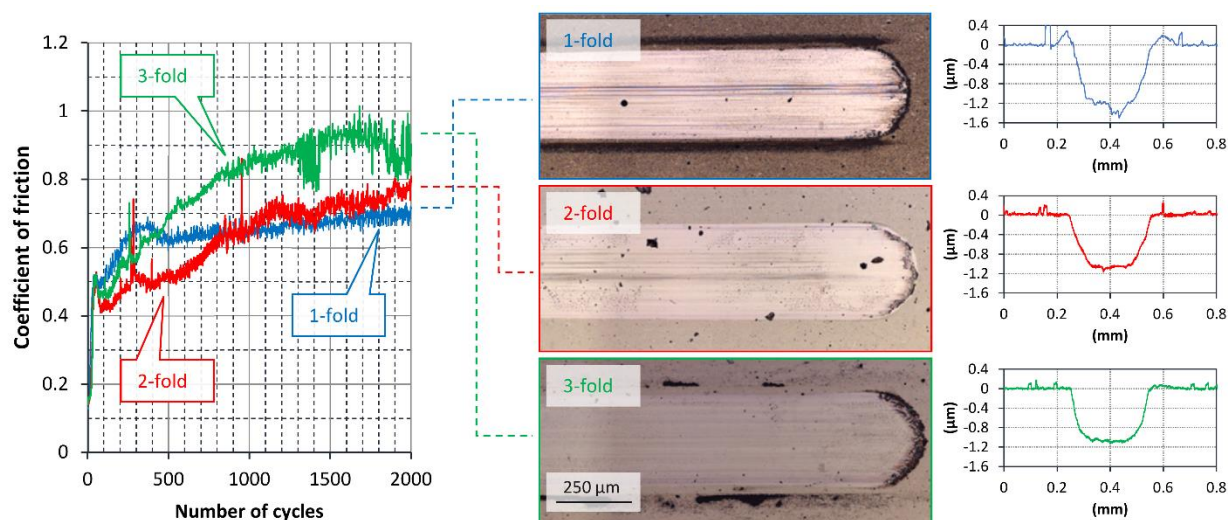


Fig. 4. Evolution of friction coefficient (left), optical images of wear tracks (middle) and wear track profiles (right).

4. CONCLUSION

The presented study shows that the type of rotation used during coating processing inside industrial deposition units has great influence on coating properties. Surface roughness and mechanical properties are improved when switching from one to higher number of rotations. The differences between coatings prepared with one and two rotations are more pronounced than differences between coatings prepared by two and three rotations. Tribological properties are well related to surface topography and mechanical properties of coatings. However, the lowest wear rate was not obtained for the smoothest and the hardest coating, showing the complexity of tribological behavior. It may be concluded that tools requiring different types of rotations should not be placed in the deposition chamber in the same batch. In order to achieve same properties for coatings prepared with different rotations, deposition parameters should be carefully adjusted for each rotation type.

5. REFERENCES

- [1] Chen, L., Paulitsch, J., Du, Y., Mayrhofer, P.H.: *Thermal stability and oxidation resistance of Ti-Al-N coatings*, Surf. Coatings Technol., 206, pp. 2954–2960, 2012.
- [2] Panjan, M.: *Influence of substrate rotation and target arrangement on the periodicity and uniformity of layered coatings*, Surf. Coatings Technol., 235, pp. 32–44,
- [3] Panjan, M., Čekada, M., Panjan, P., Peterman, T.: *Computer Simulation of Multilayer Structure of TiAlN/CrN Coatings*, Plasma Process. Polym., 4, pp. S921–S926, 2007.
- [4] Vidakis, N., Antoniadis, A., Bilalis, N.: *The VDI 3198 indentation test evaluation of a reliable qualitative control for layered compounds*, J. Mater. Process. Technol., 143–144, pp. 481–485, 2003.

- [5] Qi, Z.B., Sun, P., Zhu, F.P., Wu, Z.T., Liu, B., Wang, Z.C., Peng, D.L., Wu, C.H.: *Relationship between tribological properties and oxidation behavior of $Ti_{0.34}Al_{0.66}N$ coatings at elevated temperature up to 900°C*, Surf. Coatings Technol., 231, pp. 267–272, 2013.
- [6] Miletić, A., Panjan, P., Terek, P., Kovačević, L., Kukuruzović, D., Škorić, B.: *Tribological properties of nanocomposite TiSiN and monolayer TiAlN coating*, Proc. 15th Int. Conf. Tribol. - SERBIATRIB '17, pp. 216–220, Kragujevac, Serbia, University of Kragujevac, 2017. pp. 216–220.

Authors: Asst. Prof. Aleksandar Miletić, Asst. Prof. Pal Terek, Asst. Prof. Lazar Kovacevic, Asst. Prof. Branko Skoric, University of Novi Sad, Faculty of Technical Sciences, Department of Production Engineering, Trg Dositeja Obradovica 6, 21000 Novi Sad, Serbia, Phone.: +381 21 485-2354, Fax: +381 21 454-495.

E-mail: miletic@uns.ac.rs; palterek@uns.ac.rs; lazarkov@uns.ac.rs; skoricb@uns.ac.rs

Res. Cnslr. PhD Peter Panjan, Asst. Prof. Miha Čekada, Jozef Stefan Institute, Department of Thin Films and Surfaces, Jamova Cesta 39, 1000 Ljubljana, Slovenia, Phone: +386 1 477-3796, Fax: +386 1 251-9385.

E-mail: peter.panjan@ijs.si; miha.cekada@ijs.si

ACKNOWLEDGMENTS: This research was supported by the Serbian Ministry of Science and Technological Development and by the Slovenian Research Agency (ARRS) which the authors gratefully acknowledge.

Miletic, O., Todric, M.

ANALYTICAL-EXPERIMENTAL DETERMINATION OF INSPECTION AT PROFILIZATION OF V-PROFILE

Abstract: In the process of profiling in cold conditions, the phenomenon of reinforcement of the material occurs. For embedded profiles in a steel construction, it is necessary to know their bearing capacity, which can only be known if the level of reinforcement of the profile material in the profiling process is determined. Particularly important is that reinforcement in the joints of the profile is gained in this process, which does not occur in the classical bending process.

Key words: profiling in cold conditions, strengthening phenomenon, profile bearing capacity

1. INTRODUCTION

This problem relates to the bearing capacity of the construction made of profiles obtained by profiling. Thus, it is necessary to determine the profile reinforcement at profiling. An important analysis of the microfibre distribution on the transverse cross-section of the profile, on the basis of which it is possible to determine the legality of its change that can be expressed by a particular function.

The analytical solution method for this problem is illustrated by the example of corner design in different profiling regimes. Usage is a common engineering measurement method, due to physical understanding by students who need to adopt real engineering practice. An analysis of the possible distribution of microfibre of material on the cross section of the profile was performed, and the course of the change of the boundary of the tensile strength was determined, Figure 1.

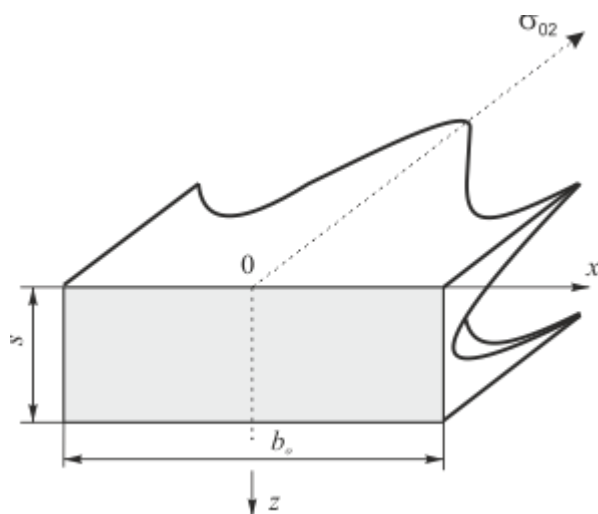


Fig. 1. Graphic representation of possible distribution of plastic deformation on the corner

2. MATERIAL FLOW LIMIT AT PROFILIZATION

Based on the measurement of microhardness on the profiles of the material C 4580 of the chemical derivative, Table 1 obtained the calculation values of the bending limit $\sigma_{0,2}$ for the surface layer profiles, Table 2.

Table 1. Steel Composition X15 CrNiSi 25-21

C %	Si %	Mn %	Cr %	Ni %	Ti %
≤0,12	≤0,18	1,9-2,0	17-19	8-9,5	0,7

Table 2. Change of the flow limit $\sigma_{0,2}$ on the surface of the flat angle 45x45x2.5 mm from stainless steel X15 CrNiSi 25-21 EN (or 314 AISI)

Cut off profile	Cross section x (mm) measured from central or corner	$\sigma_{0,2}$ (daN/mm ²) at the profile in two pairs of rollers	$\sigma_{0,2}$ (daN/mm ²) in profiling in one pair	$\sigma_{0,2}$ (daN/mm ²) when profiling in four pairs of rollers
I	0	61	56	53
II	5	57	54	50
III	10	49,5	47	45
IV	15	38	40,5	40,5
V	20	37,5	35,5	37
VI	25	32,5	34	35,5
VII	30	32,5	34	35,5
VIII	35	33,5	35,5	37
IX	40	35,5	37	39
X	45	39	42,5	44

In Figure 2. An experimental function of surface reinforcement, the material of the corner, was presented.

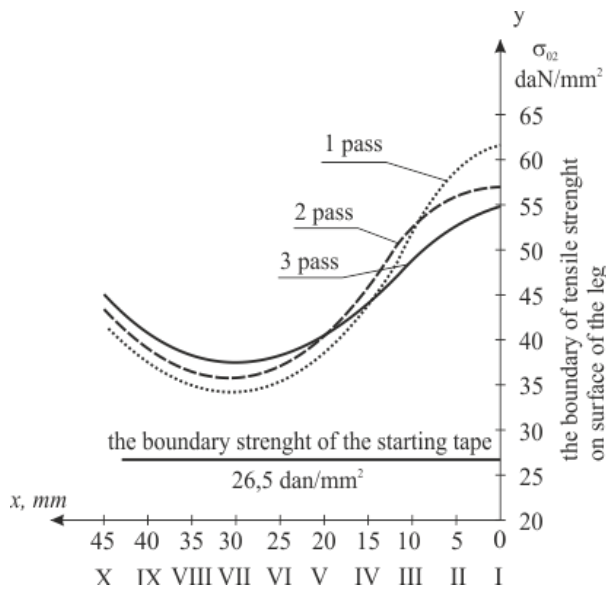


Fig. 2. Experimental function of the surface reinforcement of the upright 45x45x2.5 from X15 CrNiSi 25-21 made from
a- distribution of the stress ,
b- experimental function,
c i d- the deformation distribution on the thickness of the profile wall.

The distribution of plastic deformation on the thickness of the wall of the corner on different cross sectionalities is shown in Figure 3.

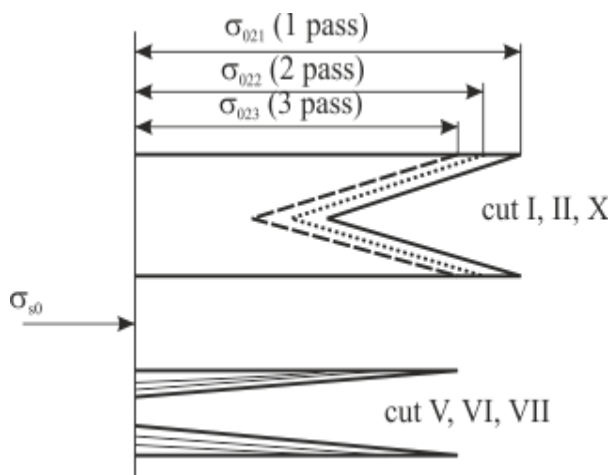


Fig. 3. Distribution of plastic deformation by thickness of corner wall

3. THE REINFORCEMENT FUNCTION IN THE PROFILING PROCESS

Based on the experimental data shown in Table 2, a function has been defined, which represents the distribution of surface reinforcement of the profile material in the profiling groove and the extent of the corner. The function of reinforcing the material in the profiling process is shown in Figure 4 for the corner formed in the four-roller profiling mode.

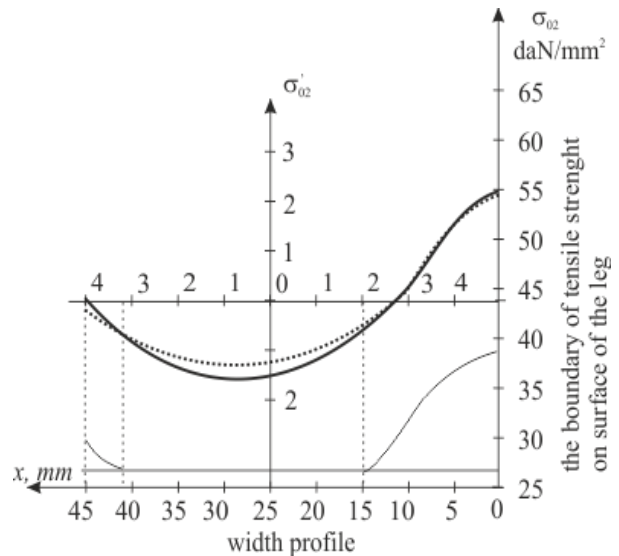


Fig. 4. Diagram of surface strength function by profile extent: x-position of the given section of the profile; $\sigma_{0,2}$ -distribution of the flow limit on the surface of the profile.

4. THE NUMERICAL ANALYSIS OF OPERATION FUNCTIONS

Using the numerical analysis of the reinforcement function, for the minimum sum of squares of deviation of the experimental and computational values for the flow rate of the profile material, a function was obtained:

$$\sigma_{02} = 9,275 - 1,25x + 0,6735x^2 + 0,0415x^3 \quad (1)$$

Figure 5 shows the experimental and calculation functions of the flow rate of the profile material $\sigma_{0,2}$, where their deviations range from 1% to 2%.

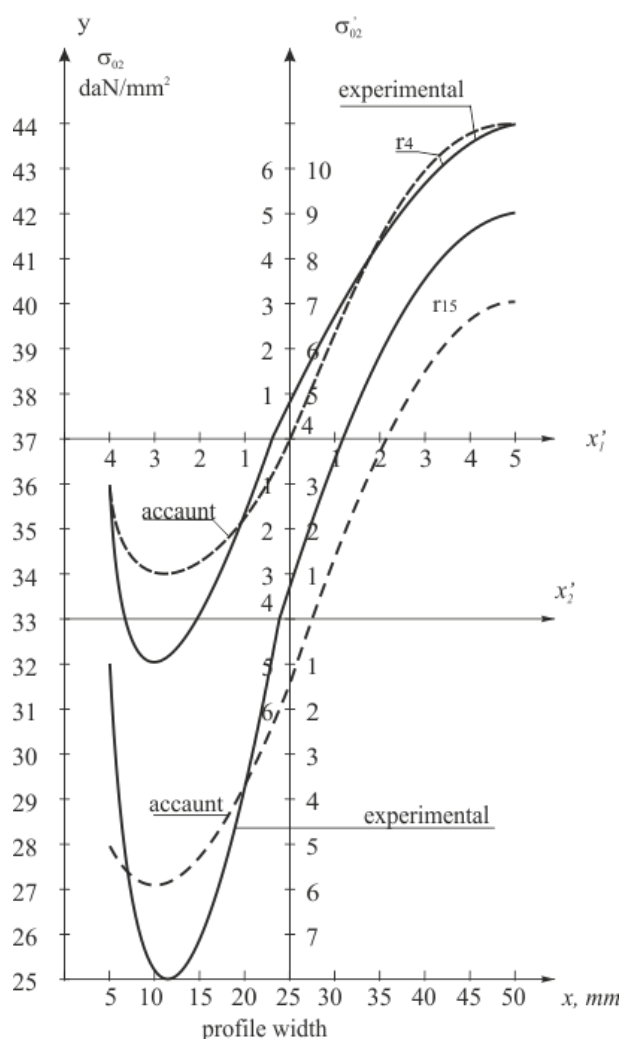


Fig. 5. Weak changes in reinforcement of the material to the profile range obtained in multiple profiling processes:

— experimental curve;
 ---- calculus curve

4. CONSLUSION

The research carried out in determining the reinforcement of the material in profiling enables the qualitative and quantitative characteristics of the profile to be obtained throughout its cross section.

From the reinforcement function it is obvious that the reinforcement of the profile material depends on factors such as: the type of material and its ejection, the bending angle, the bending profiling technology, the thickness of the preparation and the correlation of the dimension profile elements.

The qualitative and quantitative characteristics of the reinforced material of the tested profiles, of different dimensions and materials, made by different profiling regimes, allow to solve the practical problems both in the profiling technology and in the dimensioning of the supporting structure derived from these profiles.

Determined qualitative characteristics between microhardness and other mechanical properties for a whole range of metals depending on the mechanical properties of the entire metal chain depending on the

material history, enabling the correlation between these parameters to be determined. Cross-sectional reinforcement throughout the cross-section is reflected as a cross-bending force, which allows to find the strength value throughout the entire section of the profile.

The analytical-experimental determination of the function of reinforcing the profile material allows for the reinforcement of the material throughout the profile section.

5. REFERENCES

- [1] Miletic O., Todoc M.: Ugao ojacavanja pri savijanju profilisanjem, Medjunarodno savjetovanje o dostignucu elektro i masinske industrije, DEMI 202, str . 65-71, Banja Luka, 2002.
- [2] Miletic O., Todoc M.: Stabilnost elasto-plasticnih sistema, teorijska razmatranja, Univerzitet u Banjoj Luci, Masinski fakultet, 2012.

Authors: Full Prof. Ostoja Miletic, Assoc. Prof. Mladen Todoc, University of Banja Luka, Faculty of Mechanical Engineering, Vojvode Stepe Stepanovica 71, 78000 Banja Luka, Republika Srpska BiH, Phone.: +387 51 433-000, Fax: +387 51 454-495.

E-mail: miletic.ostoja@unbl.rs;
mladentodic@unibl.rs

Milutinović, M., Movrin, D., Skakun, P., Stefanović, Lj., Vilotić, D., Randelović, S.

SOME REMARKS ON PROCESS OF COMBINED FORWARD - BACKWARD EXTRUSION OF STEEL

Abstract: Cold extrusion of metals is one of the most important manufacturing technology that involves different material shaping procedures. Current paper deals with the process of combined forward rod - backward can extrusion. In this process, billet material is forced to flow simultaneously in two opposite directions and therefore divided material flow occurs. Amount of material flows in one or another direction depends on given geometrical relation between tooling elements and on the friction. Therefore, the focus of research is paid on material flow during the investigated process, as well as pressure and forming load. Three different investigation methods are employed: theoretical approach, experiment and FE modeling. Numerical analysis and simulation of the extrusion process is performed using the Finite Element Method (FEM) and the commercial software package Simufact. Forming. Obtained results are compared and discussed.

Key words: forming, cold combined extrusion, load-stroke characteristic, FEM simulation, divided material flow

1. INTRODUCTION

Cold extrusion of billets into final parts of different configurations is a highly effective metal forming technology which is predominantly used for the production of small and middle size components. Main advantages of this technology are improved mechanical properties, high production rates and improved surface quality of the extruded parts. High loading of tooling elements is main disadvantage of cold extrusion.

There exist a number of different variants and sub-variants of this technology. One of the most comprehensive classification of cold extrusion is given in [1]. According to this method all cold extrusion processes are divided into 4 classes which are based upon their geometrical characteristics. Every class consists of a definite number of sub-classes.

In [2] all cold extrusion operations are divided into three basic groups with three sub-groups: forward, backward and side extrusion. Simultaneous performance of two or more basic processes is called "combine extrusion"

Cold extrusion has been a subject of numerous investigations, from different aspects and with different aims. Some of the newer topics in the field of cold extrusion are elaborated in the [3], [4], [5]. Combined micro cold extrusion is presented in [3]. Authors were investigated effects of grain size on the main process parameters. Conclusion is that grain refinement significantly improved product quality and accuracy. Combine radial-backward extrusion is described in [4]. Rigid plastic FE method was applied in the simulation. Total energy consumption is determined, including ideal, frictional and redundant energy. Possibilities to manufacture more complex shapes by cold extrusion are illustrated in [5], [6] and [7].

Radial extrusion was employed to manufacture gear like elements of different geometries [5]. Phenomenon of divided flow, which takes place in this process is elaborated in detail.

In the works [8] and [9] application of upper bound

element technique (UBET) method in the analysis of backward extrusion is illustrated. Theoretically obtained results are verified by experiment. Relevant punch design modification in order to decrease deformation load is suggested.

Current paper is focused at the process of combine forward rod - backward can extrusion. In this process, due to geometrical relations between main tooling elements (punch, die, counter punch) billet material is forced to flow simultaneously in two opposite directions in relation to the movement of punch. Amount of material flows in one or another direction depends on given geometrical relation between tooling elements and on the friction [1].

Present investigation is related to material flow, force – stroke characteristic and the punch pressure. Three different investigation methods are employed: theoretical approach, experiment and FE modeling.

2. THEORETICAL APPROACH

The scheme of the investigated extrusion process, together with the main tooling elements and geometry of the final part, are shown in Fig.1. As it can be seen, under the punch pressure workpiece material is forced to flow both forward through the conical opening in the lower part of the die and backward into the gap between the die wall and punch land. Dimensions of the die opening d_l and the lateral clearance $D_o - d$ together with friction conditions predominately influence the way the material flow i.e. the amount of material that goes into one or the other direction. For a given reduction the die angle α , which may vary within the range 0-90°, affects the level of internal shear deformation of material and it also influences the material flow and the process development.

According to Da Chang et al. [10] the deforming zone in case of combined forward rod - backward can extrusion may be divided into 3 zones (Fig.2). The zone 1 is an area in which material is directly compressed while zones 2 and zone 3, are indirectly

compressed areas. Stress shemes for all three zones are the same and represented by three negative (pressure) components. On the other hand, strain schemes are different in different zones.

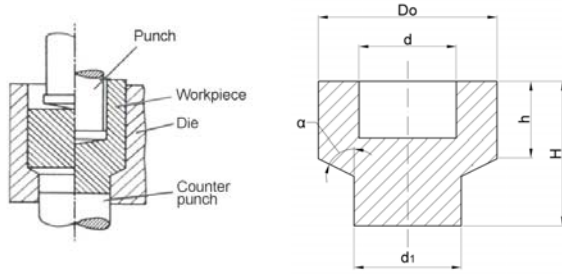


Fig. 1. Scheme of combined forward rod-backward can extrusion and geometry of extruded part

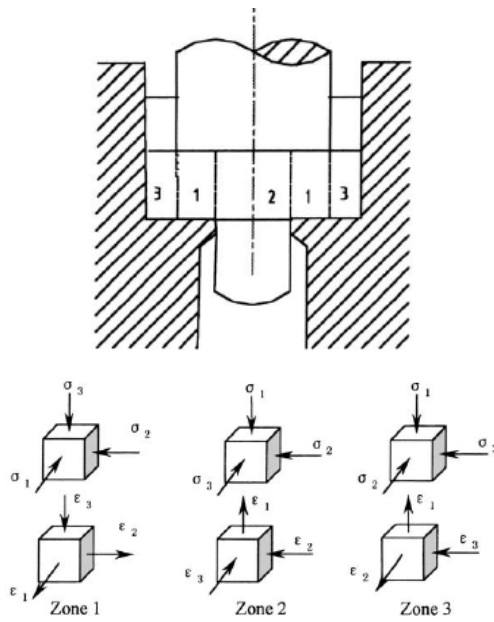


Fig. 2. Deforming zones of the combined extrusion and corresponding stress-strain schemes [10]

In literature there are a number of solutions for predicting the extrusion pressure and forming load for single operations of forward rod and backward can extrusion [11]. Those formulas are mostly derived from the general theory of plasticity using different analytical methods (SLAB, Upper Bound, etc.) and introducing some mathematical approximation and the process simplification or by combining the theory with experimental results. However, in the case of processes of combined extrusions such as forward rod - backward can extrusion the analytical solutions for the extrusion pressure are relatively rare. This could be explained by complex models of the process and uncertainties related to material flow. Furthermore, in practice but in the theoretical analysis too, the process of combined extrusion is very often decomposed and split into basic operations for which an analytical solution for extrusion pressure exists. These single operations are then treated separately. By another words, this solution is based on the assumption that component operations take place one after another while the total extrusion pressure is obtained by summing up partial (component) values [12]. Yet, some experimental results show that the real pressure is generally smaller

than the pressure calculated by this approach [13]. Therefore, this method requires to be additionally checked and validated.

In the following paragraphs the values for the extrusion pressure/forming load for the model given in Fig.1 will be calculated using two different analytical formulas and compared with results obtained experimentally and by numerical simulation.

Solution 1

First analytical solution for extrusion pressure and forming load refers to the case when combined extrusion process is treated (analyzed) as a single process in which material flows simultaneously in two directions – forward and backward. Based upon their experimental investigation, authors [14] derived analytical formula for calculation of the maximal punch pressure in the next form:

$$p_{max} = \frac{k_o + k_l}{2} \left[\frac{D_o^2}{d^2} \ln(m) + \frac{H}{d} \left(1 + \frac{d_1}{d} \right) \cdot m \right] \left[1 + \frac{2}{3} \mu \frac{d^3 - d_1^3}{d^2 H} \right] \quad (1)$$

where are:

$$m = \frac{D_o^2}{D_o^2 - d^2 + d_1^2} \quad (2)$$

k_o – yield stress at the beginning of forming process

k_l – yield stress at the end of forming process

μ - friction coefficient

Extrusion load is then obtained as:

$$F = p \frac{d^2 \pi}{4} \quad (3)$$

Solution 2

In getting the second solution the extrusion process is divided onto two separate operations – forward and backward extrusion. It is important to note that for the process modeling and solution development the sequence of individual operations is not important and it does not influence the values of total pressure. If the punch diameter d is close to die diameter D , assumption is that forward extrusion is dominant process and it is set as the first phase and vice versa.

The extrusion pressure for single operation of forward rod p_{FE} and backward cup extrusion p_{BE} are calculated on the base on the following analytical expressions [1]:

$$p_{FE} = \frac{k_o + k_l}{2} \cdot \varphi_{FE} \cdot \left(1 + \frac{\mu}{\alpha} + \frac{2 \cdot \alpha}{3 \cdot \varphi_{FE}} \right) + 4 \mu \cdot k_o \frac{H}{D_o} \quad (4)$$

$$p_{BE} = k_o \left(1 + \frac{\mu}{3} \cdot \frac{d}{H_o - s} \right) + k_l \left[1 + \frac{2 \cdot (H_o - s)}{D_o - d} \left(0.25 + \frac{\mu}{2} \right) \right] \quad (5)$$

where are:

$$\varphi_{FE} = 2 \ln \frac{D_o}{d} - \text{effective strain in process of forward extrusion}$$

α - cone angle
 H_o – initial height of billet
 s – punch stroke

The last member in the equation 4 which takes into account the load necessary to overcome friction at die surface may be omitted since it is also included in equation 5. Therefore, the final expression for total pressure is given by the following formula:

$$P_{tot} = P_{FE} + P_{BE} = \frac{k_o + k_1}{2} \cdot \varphi_{FE} \cdot \left(1 + \frac{\mu}{\alpha} + \frac{2\alpha}{3\varphi_{FE}} \right) + k_o \left(1 + \frac{\mu}{3} \cdot \frac{d}{H_o - s} \right) + k_1 \left[1 + \frac{2(H_o - s)}{D_o - d} \left(0.25 + \frac{\mu}{2} \right) \right] \quad (6)$$

Forming load for this case is also determined by the expression 3.

3. EXPERIMENT

Cylindrical billets with the diameter $D_o = 28$ mm and height $H_o = 25$ mm are employed in the experimental investigation. Coefficient of friction was determined in ring test $\mu = 0.12$ (phosphated billet surfaces lubricated by mineral oil). Punch diameter was $d = 18.80$ mm and die opening $d_1 = 21.70$ mm. Die cone angle was 30° . In the experiment steel C45 (DIN standard) was used. Experiment was performed on the Sack&Kiesselbach hydraulic press of 6300KN. In Fig.3 billet and extruded component are given and Fig.4 shows the tooling mounted on the press.

In the process die was stationary and punch moved downward. Punch velocity was 0.12 mm/s with total stroke of 18 mm. During extrusion load-stroke diagram was recorded using force transducer KDB – 2 MN (HOTTINGER BALDWIN MESSTECHNIK GmbH – HBM), stroke transducer W100 (HBM), as well as Spider 8 amplifier.

4. FINITE ELEMENT MODELING

Simufact.Forming 11.0 commercial software package were employed for numerical modeling and simulation of the investigated extrusion process. The program uses the two solution methods: the Finite Element Method (FEM) - based on MSC.Software's first class standard solvers for nonlinear applications and the Finite Volume Method (FVM)–based on MSC.Dytran solver and combines axisymmetric and full 3D simulation. It enables detailed analysis of forming processes from many points of view. More details regarding this software can be found in [15].

In simulation an axially-symmetric 2D FEM model were used. Modeling procedure started with creation of

3D model of the tooling and workpiece in CAD software SolidEdge V.18 which is then imported into Simufact.Forming11.0. Workpiece material was modeled as elastic-plastic with flow curve given in analytical form: $k = 289.671 + 597.581 \cdot \varphi^{0.333}$ which was determined experimentally by Rastegaev compression test. On the other hand, the punch and die were treated as rigid bodies. Geometry of the die and workpiece was identical as in the experiment. Starting configuration of billet and tool elements is shown in Fig.5.

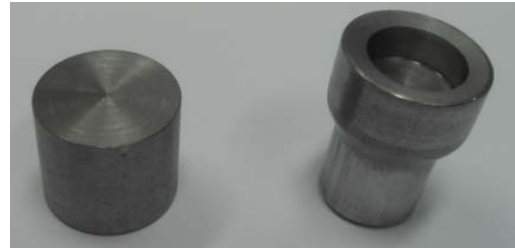


Fig. 3. Initial billet and final component



Fig.4. Extrusion tooling

The meshing procedure was initially performed under different mesher criteria and elements of different size and types with goal of checking the convergence of the numerical solution. Finally, after a few iterations, the advancing front quad mesher and the quad elements in size of 1mm were chosen.

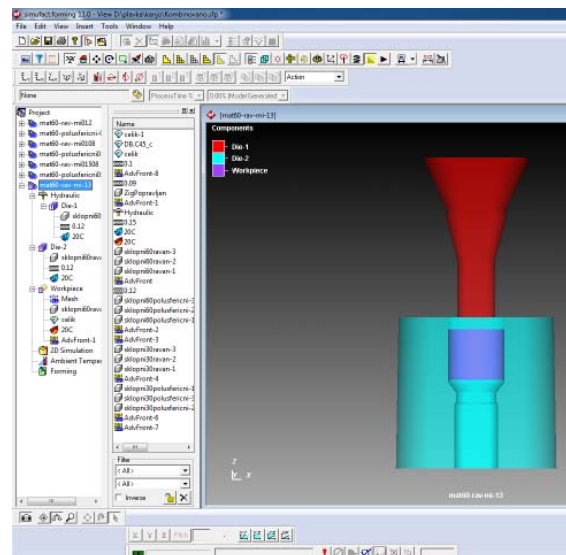


Fig. 5. FEM model in Simufact.Forming software

The remeshing of starting elements was executed in the most highly deformed zones of the workpiece at every five increments in order to minimize the effect of tool penetration through the elements due to large workpiece deformations. Coupled thermo-mechanical FEM analysis is performed under condition of low friction ($\mu=0.12$).

5. RESULTS

Distribution of effective stress and strain within the workpiece volume at the end of the process (punch stroke $s=18\text{mm}$) obtained by FE analysis are shown in Fig. 6. It is obvious that the stress and strain state is heterogeneous. Maximum stress value exists in the narrow transition region between the bottom and the wall of the workpiece (1160 MPa) while strain value in this region reaches the amount of 3.09. In general, highest values of strain and stress are concentrated in the vertical plane at the radius r . This is the plane of divided material flow. In the central part of the workpiece as well as in the wall itself the stresses are significantly lower as deformations are minimal and therefore, these zone are very often called “dead zones”.

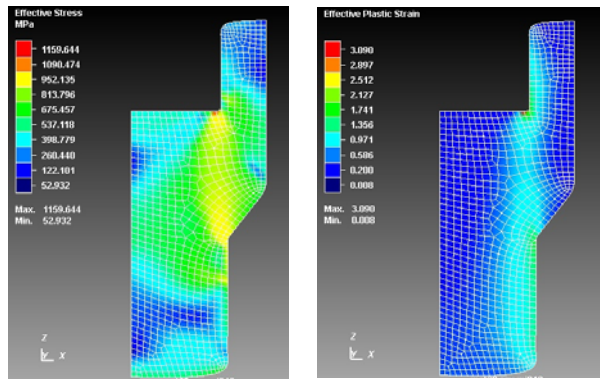


Fig. 6. Effective stress (left) and effective strain (right) at the end of the extrusion process ($s=18\text{mm}$)

Material flow during the process was observed and analyzed using Simufact.forming software package. In Fig.7 geometry of workpiece after every 2.6 mm of the punch strokes is given. As it can be seen, in the initial stage of deformation more intensive material flow occurs through the die opening (forward extrusion) while at later stage wall of the workpiece is formed (backward extrusion). However, it should be noticed that this picture of material flow is developed only for concrete given geometrical relations (D_o , d , d_I). It is noticeable that for the each stage the maximum effective stress appears around the plane of divided material flow.

In Fig.8 numerically, analytically and experimentally obtained extrusion load and punch pressure are shown. The experimental pressure (average value) on the punch head was determined from the next equation:

$$p = \frac{F_{\text{exp.}}}{A_p} \quad (7)$$

where $F_{\text{exp.}}$ is experimentally measured load and A_p is the cross-sectional area of the punch head.

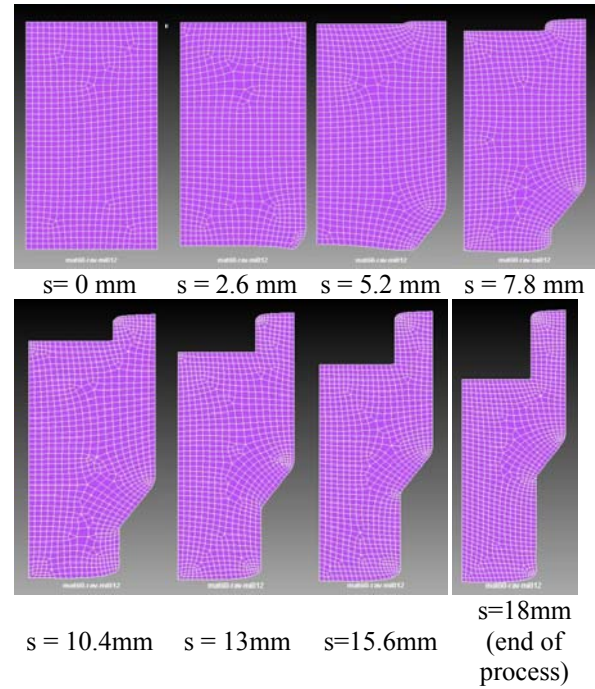


Fig. 7. Geometry of workpiece for different punch strokes

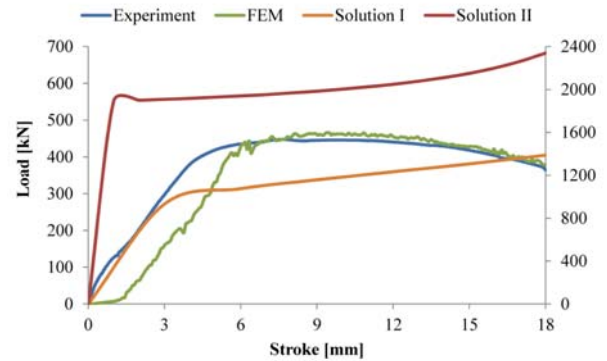


Fig. 8. Load-stroke characteristics and punch pressure obtained by three different methods

Figure 8 suggests that in the beginning of the extrusion process load (and corresponding punch pressure) rises steeply up to 1 mm of punch stroke (Solution II) i.e. up to 4 – 6 mm (Solution I, experiment and FEM). After that theoretically obtained load continue to rises, reaching their maximal value at the end of the process. Contrary to this loads obtained by FEM and by experiment slowly decline after reaching their maximal value. Significant difference between the load obtained by two theoretical solution is obvious. Solution 2 gives the load value which is for app.70% higher than the load obtained by theoretical Solution I. Agreement between FEM, experiment and Solution I is acceptable. Punch pressure at the end of the process is 2350 MPa (according to the theoretical Solution I) i.e.1300 MPa (according to the Solution 1, FE and experiment). Significant differences between Solution II and the other results (FEM, Exp., and Solution I) for the load/punch pressure indicate that the approach used in

the development of Solution 2 is not correct. By another words, combined forward/backward extrusion process cannot be considered modeled as a simply sum of two separate operations (forward and backward extrusion) and so the interaction must be taken into account. Analyzing the equation 6, i.e., equations 4 and 5, and the combined extrusion process itself, it can be concluded that the first member of the equation 5 does not correspond to the process conditions since it originally refers to the free upsetting - first phase of backward extrusion process [1]. In the combined forward/backward extrusion there is no real the free upsetting because material flow through the die opening – lower surface of the billet is partly free. It means that at the very beginning of the process the conditions are similar to the process of free upsetting with flow relief openings. Therefore, the first member of the equation 5 can be considered as the main source of the inaccuracy and might be omitted. For this case, total forming is less for approximately 30-40% compared to the values given in Fig.8.

6. CONCLUDING REMARKS

Current work is focused on the application of different methods (analytical, numerical and experimental) to obtain load – stroke characteristic and punch pressure in cold combine backward can – forward rod extrusion. Furthermore, material flow, obtained by FEM software, was determined and analyzed. Steel material was considered. For the load calculation two theoretical solutions are employed. Both analytical solution suggests that there is a permanent increase of the force during deformation while loads obtained by experiment and by FEM decline after reaching their maximum. Agreement between Solution I, FEM and experiment is rather good while Solution II gives significantly higher load value during whole process. This suggests that approach at which Solution II is based is incorrect and requires correction. Continuation of the research on this subject is planed which would involve the most important influential process parameters: geometry, friction, materials, process conditions. Focus would be not only at the forming load but also on velocity distribution, process optimization etc. Variation of the punch and die geometry would be also included in the research.

7. REFERENCES

- [1] Lange, K.: *Handbook of metal forming*, SME Dearborn, Michigan, USA, 1985.
- [2] Spur, G., Stoferle, Th.: *Handbuch der Fertigungstechnik*, Band 2/2, Umformen, Carl Hansen Verlag, 1984.
- [3] Chao-Cheng Chang, Jian-Chen Lin, Cheng-Ping Siao: *Effect of temperature and grain size on combined micro forward and backward extrusion*, Proceedings of the 14th International conference on Metal Forming - Metal Forming 2012, Krakow, Poland, pp.467-470., AGH University of Science and Technology, Krakow, Poland
- [4] Ho Yong Lee, Beong Bok Hwang, Su Hyen Lee: *Forming load and deformation energy in combined radial backward extrusion*, Proceedings of the 14th International conference on Metal Forming - Metal Forming 2012, Krakow, Poland, pp.539-542., AGH University of Science and Technology, Krakow, Poland.
- [5] Skakun, P. Plančak M., Vilotić D., Lužanin O., Milutinović M., Movrin D.: *Manufacturing of gear like components by metal forming – possibilities and limitations*, MMA Conference, Novi Sad, 2012, pp. 489-492., Faculty of technical sciences, Novi Sad, Serbia.
- [6] Plančak, M., Vilotić D., Skakun P.: *A study of radial gear extrusion*, Int. Journal of Forming Processes, Vol.6, Nr.1, 2003, pp.71-86.
- [7] Huang H.S., Hsia Y.H.: *New design of process for cold forging to improve multi-stage gas fitting*, Advances in Mechanical Engineering 2016, Vol. 8(4), pp. 1–12
- [8] Marinković, V.: *Pressure determination in the backward cup extrusion*, Journal for Technology of Plasticity, Vol.33, 2008, Novi Sad, pp.125-140.
- [9] Marko Vilotić, Vesna Mandić, Miroslav Plančak: *UBET analysis, FE simulation and experimental investigation of backward extrusion*, Journal for Technology of Plasticity, Vol.29, 2004, Novi Sad, pp.85-96.
- [10] Kang Da Chang, Sun Hong Yi, Chen Yu, Yang Hong Liang: *Research on the „ shear - extrusion“ process to form large – scale cut – off valve bodies*, Journal of Materials Processing Technology 117 (2001), pp.15 – 20.
- [11] Altan T., Ngaile G., Shen G.: *Cold and hot forging: fundamentals and applications*, ASM Publication, 2004.
- [12] Marinković, V.: *Metal forming– the book of solved problems (in serbian)*. Mechanical engineering faculty, Niš, 1990.
- [13] Kanjo, Z.: *Theoretical - experimental investigation of bulk metal forming processes with divided material flow (in serbian)*, Master work, Faculty of technical sciences, Novi Sad 2014.
- [14] Golovin V.A., Mitkin A.N., Reznikov A.G.: *Technology of cold forming (in russian)*, Mašinostroenie, Moskva, 1970.
- [15] www.simufact.de. Accessed on 20.05.2016.

Authors: Assist. Prof. Mladomir Milutinović, Assist. Prof. Dejan Movrin, Assist. Prof. Plavka Skakun, MSc Ljiljana Stefanović, Full Prof. Dragiša Vilotić, Full Prof. Saša Randelović.

University of Novi Sad, Faculty of Technical Sciences, Department of Production Engineering, Trg Dositeja Obradovica 6, 21000 Novi Sad, Serbia

Email: mladomil@uns.ac.rs;
movrin@uns.ac.rs;
plavkas@uns.ac.rs;
ljiljanastefanovic@uns.ac.rs;
vilotic@uns.ac.rs

Pecanac, M., Dramicanin, M., Janjatovic, P., Ristic, M., Rajnovic D., Sidjanin, L., Balos, S.

INFLUENCE OF TOOL GEOMETRY ON FRICTION STIR WELDED JOINTS

Abstract: In this paper, Friction Stir Welding (FSW) process is described, with theoretical basics as well as advantages, disadvantages and applications of the process. Special attention was dedicated to geometry of the tool. Tool geometry was analyzed, particularly the shoulder geometry and welding speed. Al5052 H32 alloy was used, which was welded with tools that have different shoulder geometries and the same square pin, at different welding speeds. Tensile, bending and hardness tests were performed, as well as metallographic testing. Most suitable characteristics were achieved by using tool with concentric reservoirs, with slowest welding speed. Optimal welding parameters were identified.

Key words: Friction Stir Welding (FSW), welding parameters, shoulder geometry

1. INTRODUCTION

Friction Stir Welding (FSW) process was patented at the end of 1991 at The Welding Institute (TWI) in United Kingdom [1]. Specific thing about this process is that welding is performed by the special tool which is generating heat necessary for the welding process [1–6]. The biggest advantage of this process is the lack of melting of the base material, which negatively influences the microstructure of the material (growth of the grain) and mechanical properties. There is another advantage of this process, the welding of dissimilar materials (materials that have different melting temperatures) that are usually difficult to weld (e.g. aluminum alloys to steel, aluminium alloys to copper alloys) [6,7]. Schematics of the welding process are shown on fig. 1.

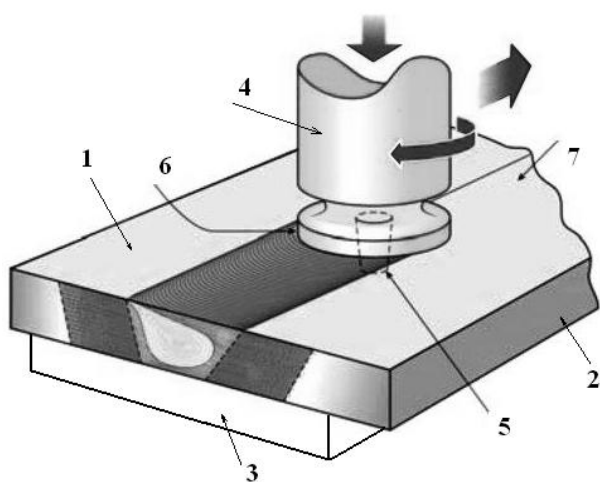


Fig. 1. FSW process schematics.

On fig. 1 is shown: Base material (1 and 2) special mount (3), cylindrical tool (4), pin (5), shoulder (6) and joint line (7). Friction Stir Welding is performed in few steps: Base material is positioned and clamped in the special accessory, then rotating tool is positioned above the joint line, friction between the tool and base material generates heat necessary for the process.

Generated heat softens the base material, turning of the tool actually mixes one plate of the base material into another. Tool follows the joint line and forms the weld [8,9]. Earlier was mentioned that tool consists of two parts: pin and shoulder, and they can have a various geometries and it have significant impact on welding speed and mechanical properties of welded joint. Shoulder geometry can be: flat, concave and convex geometry [2,3]. Mentioned geometries can be profiled (various spirals and shapes) to ease material flow into mixing zone. Tool pin can also have different geometries and profiles (shapes, e.g. square, cylindrical, polygonal shapes etc.) that enables grater welding speeds and material flow [3–6]. Friction stir welding is performed with specialized machines, but it is possible to modify (adjust) existing machines (vertical milling machine) because of the price of the specialized machines [7–9]. Defining parameters of friction stir welding are: Axial force (of tool on base material), rotating speed of the tool, welding speed (tool shifting speed) and tilt angle of the tool. Friction stir welding is process that is gaining more and more importance in the industries like: transportation industry, airplane and aerospace industry, etc.

2. THE EXPERIMENT

In this experiment for the base material was used aluminum plates alloyed with Mg (Al 5052 H32), 5mm thick. Chemical composition of the base material is given in the table 1, mechanical properties are also given in table 2.

Cu	Mn	Mg	Si	Fe	Zn	Ti
0,09	0,09	2,78	0,24	0,38	0,046	0,015

Table 1. Chemical composition (mass %) of the base material (Al 5052 H32), balance Al.

R _{p0,2} [MPa]	R _m [MPa]	A [%]	HV10
123,8	193,4	21,7	60

Table 2. Mechanical properties of Al 5052 H32.

For this experiment, vertical milling machine was

modified for the process ("Prvomajska UHG 200"). Two welding tools with different shoulder geometry were used. One tool had concentric reservoirs, and the second tool had one reservoir (concave geometry). Segments of tool's technical drawings (cross section view) are shown in fig 2.

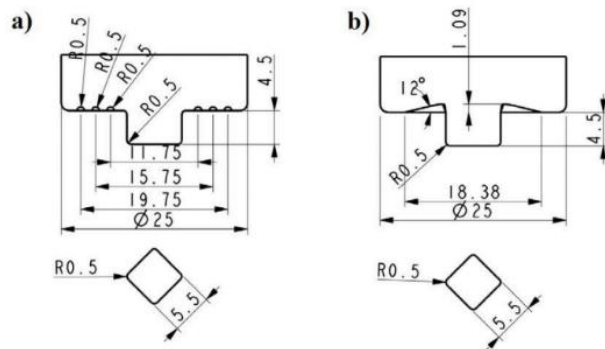


Fig 2. Cross section of welding tools.

Tool was made from hot-work tool steel (X38CrMoV5-1) rod, machined and heat treated. Chemical composition of tool material is shown in table 3.

C	Si	P	S	Cr	Mo	V
0,37	1,01	0,017	0,0005	4,85	1,23	0,32

Table 3. Chemical composition of tool material.

Base material is positioned and clamped in the special tool (dimensions 400x370x35 mm), which is mounted in workbench of the machine. From top side of special tool there is a groove, 130 mm width and 5 mm deep trough whole length of tool so the base material can be positioned and clamped. Welding parameters of the experiment are shown on in table 4.

Tool	Spec. No.	n [min ⁻¹]	s [mm/min]
Tool with one reservoir	1	925	17
	2	925	46
	3	925	91
Tool with concentric reservoirs	4	925	17
	5	925	46
	6	925	91

Table 4. Welding parameters of the experiment.

In the table 4 can be seen that rotation speed of tool is kept at constant value, but moving speed (welding speed) was increasing. During the experiment, visual control was conducted to determine if there is any defects (tunnels) on the surface of welded joints. Afterwards, tension test was performed on mechanical tensile testing machine WPM, ZDM 5/91. Bend testing was performed on the same machine, but with usage of special tool. Hardness testing was performed on the VEB HPO 250 device, with load of 5 kg. Distance between indents was 1.5 mm. Hardness is measured from retreating side of the welt to advancing side of the weld. Macroscopic and microscopic examination is done on the light microscope Leitz Orthoplan with

standard preparation of the samples (cutting, grinding, polishing and aching).

3. RESULTS

3.1. Visual control

After visual control it was seen that there are no defects on the surface of the specimens. On fig 3 is top and bottom side of representative specimen 5.

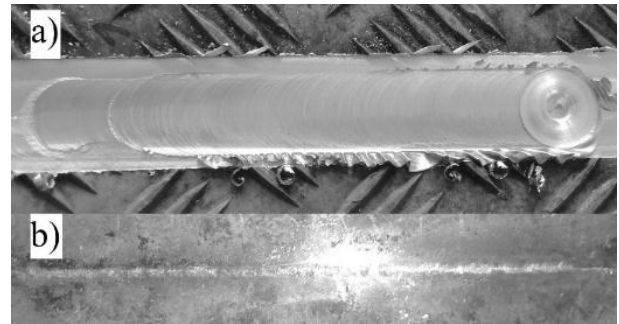


Fig. 3. Top and bottom side of specimen 5.

3.2 Tensile testing

Tensile testing results for welded material are given in the table 5.

Tool	Specimen No.	R _{p0,2} [MPa]	R _m [MPa]
Tool with one reservoir	1	162	198
	2	138	161
	3	109	129
Tool with concentric reservoirs	4	148	181
	5	141	181
	6	111	148

Table 5. Tensile test results.

Based on the testing results it can be seen that specimens 1 and 4 have the highest tensile characteristics in comparison to the other specimens. Specimens 1 and 4 are welded with the lowest welding speed of 17 mm/min.

3.3 Bend test

Bend test is performed by bending welded joints over the face and root of the weld. All specimens bent over the face of the weld are bent to angle of 180° without appearance of the cracks. And in the table 6 is shown bend test results of bending over the root.

Tool	Specimen no.	Crack angle appearance [°]	Fracture angle [180°]
Tool with one reservoir	1	26	No fracture
	2	16	No fracture
	3	12	No fracture
Tool with concentric reservoirs	4	No crack	No fracture
	5	55	No fracture
	6	18	No fracture

Table 6. Bend test results by root.

From the table 6 it can be seen that all specimens are bent to angle of 180° without fracture, but only specimen 4 is bent to 180° without any cracks.

3.4 Hardness test

Results of Vickers hardness test (HV 5) is shown on fig 4 and 5 (representative specimens: 1 and 4).

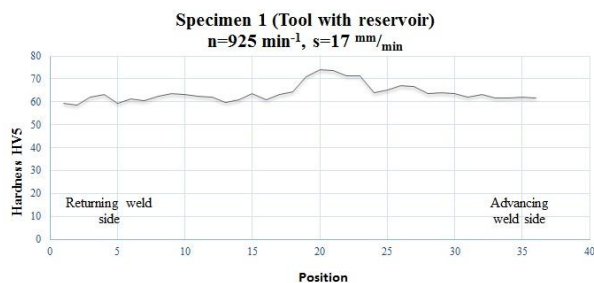


Fig. 4: Hardness distribution for specimen 1. On the

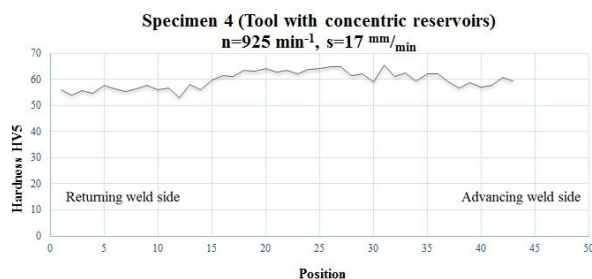


Fig. 5. Hardness distribution for specimen 4.

On the figures 4 and 5 can be seen that highest hardness values are around the middle of specimen. Around the middle of specimen is grain zone.

3.5 Metallography results

Macrostructure of welded material is shown on figures 6 and 7.

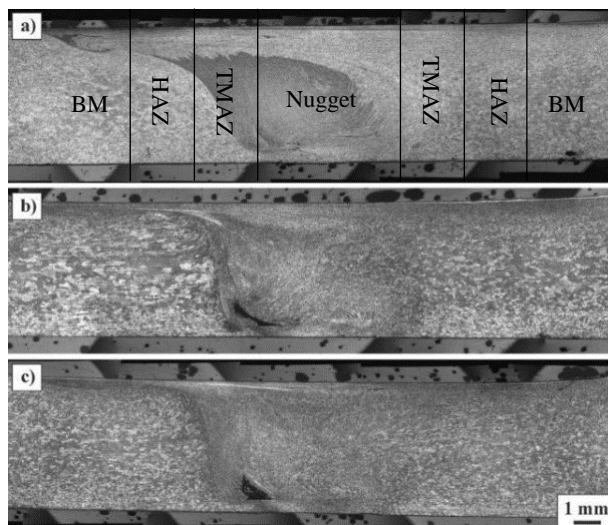


Fig. 6: Macroscopic depiction of welds welded with one reservoir tool; welding speeds: a) 17 mm/min , b) 46 mm/min , c) 91 mm/min .

From fig. 6 it can be seen that specimen b and c have defects (tunnels) in their nugget zone. In fig 7, macrostructures of welds welded with concentric reservoir tool are depicted.

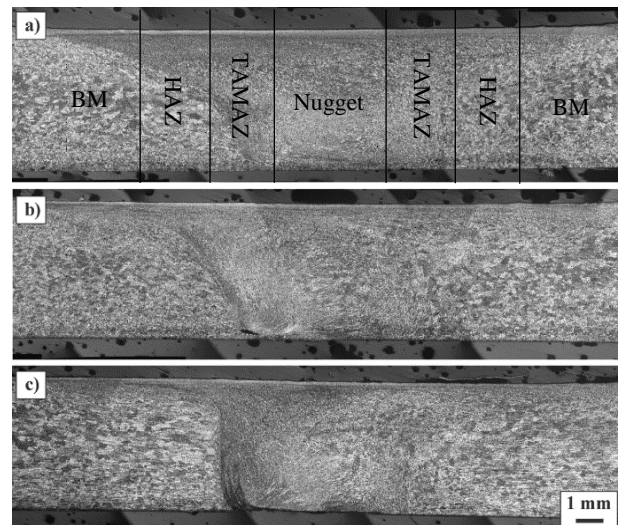


Fig. 7: Macroscopic depiction of welds welded with concentric reservoir tool; welding speeds: a) 17 mm/min , b) 46 mm/min , c) 91 mm/min .

From figure 6 it can be seen that only specimen b have defect (tunnel) in lower left side of nugget zone of the weld.

4. DISCUSSION

In the table 7 is given efficiency of welded joints. From the table 7, it can be seen that specimens 1 and 4 have the highest values of weld efficiency, measured by the yield strength and ultimate strength. Named specimens are welded with lowest welding speeds, and as the result is achieved greater degree of plastic deformation (which manifest as strain hardening) of base material. In the nugget zone is biggest influence of strain hardening, as the result in that zone grains will be smaller and result is another hardening mechanism (grain boundary strengthening). Also is noticed that specimens welded by the toll with concentric reservoirs have grater tensile characteristics in comparison to specimens welded by the toll with one reservoir (concaved shoulder geometry). Also specimens 1 and 4 have no defects in the volume of the weld and they have biggest tensile characteristics of the joint. Defects in weld have negative influence on welded joint, because it works as stress concentrator and cracks are created on sharp parts of tunnels spreading onward trough the material, thus reducing mechanical properties greatly. During bend test all specimens are bent by the bottom of weld to angle 180° without cracks. Same is for the specimens bent by the surface of the weld, but only specimen 4 is bent to angle of 180° without any appearance of cracks. As for hardness, increase of hardness values is noticed around the middle of the welded joint that correspond to nugget zone of the weld. This is confirmed by metallographic examination. Also is noticed peak close

to nugget zone. This is present because that is returning side of the weld, and during welding process its present accumulation of processed material.

Tool	Specimen no.	Re efficiency [%]	Rm efficiency [%]
Tool with one reservoir	1	125	103
	2	111	83
	3	97	76
Tool with concentric reservoirs	4	129	103
	5	125	102
	6	101	80

Table 7: Efficiency of the welded joints

5. CONCLUSIONS

The following conclusions can be drawn from this study:

- Specimens 1 and 4 are the one with best mechanical properties, which are welded with lowest welding speeds of 17 mm/min .
- Lowest welding speed (17 mm/min) is proven to be most adequate because there are no defects in welded joint.
- Greatest tension characteristics are achieved with specimens that are welded with concentric reservoir tool.
- Greatest mechanical properties achieved with specimen 4 is compatibility of welding parameters with tool geometry, which allows optimal flow of material during stirring.

6. REFERENCES

- [1] T. Stotler, J. Bernath, Friction Stir Welding, (2009) 47. www.esab.com.
- [2] R.S. Mishra, M.W. Mahoney, Friction Stir Welding and Processing, ASM International, 2007. doi:10.1361/fswp2007p001.
- [3] R.S. Mishra, Z.Y. Ma, Friction stir welding and processing, Mater. Sci. Eng. R Reports. 50 (2005) 1–78. doi:10.1016/j.mser.2005.07.001.
- [4] D.B.R.G.R. Reddy, B Supraja, Effect of Tool Geometry and Process Parameters on Mechanical Properties and Micro Structure of Various dissimilar Aluminium Alloys Welded by Friction Stir Welding – Review, Int. J. Eng. Technol. Manag. Appl. Sci. 3 (2015) 316–328.

- [5] D. a Burford, B.M. Tweedy, C. a Widener, Influence of Shoulder Configuration and Geometric Features on Fsw Track Properties, : 6th Int. Symp. Frict. Stir Weld., Montréal, Canada, 2006.
- [6] A. Zivkovic, H. Dascau, I. Radisavljevic, M. Perovic, A. Sedmak, The effect of tool geometry on the quality of Al 5052 friction stir welded joint, 1–6.
- [7] M. Mijajlovic, D. Milicic, M. Djurdjanovic, V. Grabulov, A. Zivkovic, M. Perovic, OSNOVNI POJMOVI KOD POSTUPKA ZAVARIVANJA TRENJEM SA MEŠANJEM PREMA AWS D17 . 3 / D17 . 3M : 2010 I ISO 25239-1 : 2011 BASIC TERMS IN FRICTION STIR WELDING ACCORDING TO AWS, Zavar. I ZAVARENE Konstr. 2 (2012) 61–68.
- [8] S. Balos, L. Sidjanin, D. Rajnovic, V. Vucic, Zavarivanje trenjem sa mešanjem friction stir welding, Konf. o međulaboratorijskim Ispit. Mater. XIX (2013).
- [9] A. Meilinger, I. Torok, the Importance of Friction Stir Welding Tool, Prod. Process. Syst. 6 (2013) 25–34.

Authors: **M. Sc. Milan Pecanac**, **M. Sc. Miroslav Dramicanin**, **M. Sc. Petar Janjatovic**, **M Sc. Mirjana Ristic**, **Assoc. Prof. Dragan Rajnovic**, **Emeritus Prof. Leposava Sidjanin**, **Assoc. Prof. Sebastian Balos**, University of Novi Sad, Faculty of Technical Sciences, Department of Production Engineering, Trg Dositeja Obradovica 6, 21000 Novi Sad, Serbia.

E-mail: pecanac.milan@uns.ac.rs; dramicanin@uns.ac.rs; janjatovic@uns.ac.rs; mirjana.ristic@uns.ac.rs; draganr@uns.ac.rs; lepas@uns.ac.rs; sebab@uns.ac.rs

ACKNOWLEDGMENTS: The authors gratefully acknowledge research funding by the project entitled “Development and Application of Advanced Characterization of Materials and Welds in Production Engineering” on the Department of Production Engineering, Faculty of Technical Sciences Novi Sad, Serbia

Radman, M., Jovanović, M., Uran, M., Trivković, Lj.

TRAINING FOR INTERNATIONAL WELDING COORDINATORS

Abstract: Nowadays is industrial welding production unthinkable without the introduced quality system. The responsibility person for QA is the welding coordinator. In most cases, this is IWE - International Welding Engineer or IWT International Welding Technician. The diploma for this knowledge is obtained at international specializations in institutions authorized by the International Institute for Welding - IIW and European Welding Federation - EWF. Due to the challenges of giving up time, these specializations are increasingly being carried out by distance learning - DL.

Key words: welding coordinator, EWE, EWT, QA, DL

1. INTRODUCTION

International quality standards classified welding as a 'special process'. The quality requirements in this process can only be met if care is taken regarding the appropriate usage of equipment, welding procedures, materials and availability of suitably qualified welding personnel [1]. Personnel qualification is one of the main tasks of the European Welding Federation (EWF) and the International Institute of Welding (IIW) [1]. European Federation for Welding, Joining and Cutting (today European Welding Federation – EWF) started working in 1992 when EU member countries who carried out specializations for welding engineers, started a process to harmonise its education content and implementation. EWF developed the comprehensive and harmonised system for training, qualification and certification of welding personnel. By using an uniform syllabus for each level of the training course and a harmonised system for examinations, the same qualification can be awarded in any country and the same knowledge are assured for any person holding diploma, awarded throughout the world [2,3].

2. THE EDUCATION SYSTEM OF EWF AND IIW

EWF licensed its qualification system to IIW in year 2000. A combined EWF/IIW system has been offered in 46 countries worldwide, with 44 Authorized National Bodies (ANB) and 683 Authorised Training Bodies (ATB) [2].

Slovenia became a member of EWF soon after its establishment. The role of ANB is carried out by the Slovensko društvo za varilno tehniko (SDVT), and the role of ATB by the Institut za varilstvo d.o.o. [4]

As already mentioned, an important part of EWF and IIW activities is training of personnel for welding coordination. The welding coordinator is a person who is responsible and competent to carry out coordination of welding works. The tasks and responsibilities of the welding coordinators are defined in the standard EN ISO 14731 and are the basis for quality in welding production according to the standard EN ISO 3834.

The tasks and responsibilities comprise the preparation of welding documentation and specifications, welding control and supervision or presence [5].

The personnel for coordination of welding works is divided into four levels, depending on the nature and/or complexity of the welding production:

- International/European Welding Engineer (I/EWE);
- International/European Welding Technologist (I/EWT);
- International/European Welding Specialist (I/EWS);
- International/European welding practitioner (I/EWP).

Training for international welding coordinators is carried out in accordance with the guidelines and authorization of the EWF and the IIW. Guidelines are prepared by the International Authorization Board (IAB), which represents one of the two branches of the IIW organization. The guidelines for education, examination and qualification are formed to ensure that the requirements are applied uniformly by all countries involved, and that the diplomas granted are mutually recognized. This is done by appointing ANBs, which are responsible for ensuring that the standards of education, examination and qualification are maintained. In this, the objective is that IIW qualified personnel at a certain level will have achieved the same minimum level of knowledge, irrespective of the country in which they had been qualified. Participants successfully completing a course of education and examinations will be expected to be capable of applying the welding technology at a level consistent with the qualification diploma [6].

3. TRAINING FOR INTERNATIONAL WELDING COORDINATORS IN SLOVENIA

Regarding the number of issued diplomas of welding coordinators versus the number of inhabitants, Slovenia has always been one of the first three countries in Europe. Table 1 shows the number of diplomas by

individual levels of competence issued by the Slovenian ANB in cooperation with the Slovenian ATB (situation on 25.7.2018):

	EFW diploma – training	EFW diploma – automatic route*
EWE	169	44
EWT	63	22
EWS	/	3
	IIW diploma – training	IIW diploma – automatic route *
IWE	229	47
IWT	186	19
IWS	85	/

Table 1: Number of diplomas by individual levels of competence issued by the Slovenian ANB in cooperation with the Slovenian ATB

Source: Archive of Institut za varilstvo d.o.o. [7]

* All those who already possess the EFW or IIW diploma of the welding coordinator can automatically obtain a diploma from institution whose diplomas do not already have (EFW or IIW), by virtue of the mutual recognition of both of these institutions in the field of training programs and the qualification of welding coordinators [8].

Slovenia does not implement I/EWP training level because there is insufficient interest in the Slovenian market for this type of qualification.

As already mentioned, there are four levels of personnel for welding coordination: I/EWE, I/EWT, I/EWS, I/EWP. The access conditions to courses for each level of qualification are defined in the current guideline issued by the IAB and vary by country. In Slovenia, the current access conditions are as follows:

- IWE: diploma of the university degree in mechanical, shipbuilding, metallurgical, electrical or civil engineering (minimum three years study - I. bologna level);
- IWT: diploma of higher professional education or diploma of a technical school in mechanical, shipbuilding, electrical, metallurgical or civil engineering (four years schooling);
- IWS: technical diploma from a vocational school of 3 years of schooling, age of at least 20 years and 2 years of work experience [9].

The content of training for international welding coordinators is divided into four modules:

1. Welding processes and equipment
2. Materials and their behaviour during welding
3. Construction and design
4. Fabrication, applications engineering [8]

Each module comprises a certain number of hours of theoretical and practical training.

Qualifications for the international welding coordinator can be obtained through the following routes:

1. the standard route,
2. the alternative route,
3. the distance learning route,
4. the experiential route,
5. the transition route [8].

In the following, the standard route and the distance learning route are presented in more detail, according to which most of the personnel for coordination of welding tasks are educated in Slovenia.

3.1 The standard route

The standard route requires successful completion of IAB approved courses which are designed to meet all the requirements of guideline. As can be seen from Figure 1, two paths are possible, namely Path 1 and Path 2. Path 1 is recommended by IAB as offering the fastest, most comprehensive manner in which the syllabus may be covered. Path 2 is allowed for participants who are approved by ANB to acquire the appropriate knowledge of Part 1 before the course, which is in accordance with the syllabus of the course [8].

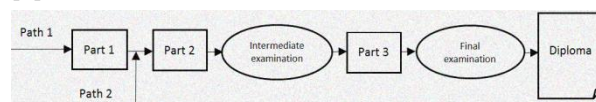


Figure 1: The standard route for obtaining a diploma of the international welding coordinator

Source: IAB-International Authorisation Board (2016). Minimum requirements for the education, training, examination, and qualification. Personnel with qualification for welding coordination. Page 10 [8].

Part 1 and Part 3 represent theoretical education, while Part 2 represents training for acquiring fundamental practical skills [8].

3.2 The distance learning route (DL)

Welding is an industry that constantly strives to adapt and respond to changes in the environment. Thus, in 2004 IIW issued a guideline for the distance learning. The standard route courses are based on conventional classroom teaching approach. The distance learning route is more efficient and takes less time, than the classroom learning. This type of education enables the participant a customized way of learning. In order to consolidate and deepen the knowledge, in the classroom shorter, intensive lectures and exercises are carried out [1].

The aim of the distance learning is to improve access to IAB approved qualifications (diplomas). It is essential that the quality of courses delivered in this way must be equivalent to that of the classroom learning [1].

The basis of the distance learning route is the standard route. The content of theoretical and practical training is followed by a current guideline for the training of personnel for coordination of welding works, with the

exception that certain parts of the content are transferred to the distance learning system [1]. The distance learning route is therefore a blended way of learning, where education in the classroom (theoretically and practically) is combined with the distance learning.

There are several different methods for delivering learning materials on distance. The current guideline for distance learning gives the list of following options:

- video/DVD,
- audio,
- computer based (e.g. installation of the software package),
- internet delivery (e.g. e-mail, on-line program),
- broadcast television/radio [1].

The actual delivery technique chosen is not restricted to those described and may involve a combination of various options as well as an increased proportion of classroom delivery (over and above the minimum levels set out in the guidelines). The resources chosen should be capable of delivering the material required by the syllabus and should enable the student to achieve equivalent learning outcomes as those attained in a conventional classroom situation. A minimum number of hours of practical and laboratory work (as set out in the relevant guidelines) is required to support the distance delivery material. The ANB will ensure that the proposed package is appropriate and meets the requirements of the IIW/EFW guidelines [1].

As for the content, the current guideline for the standard route is also the basis for access conditions, examination, course duration and equipment in the distance learning route.

As already mentioned, the distance learning route has several advantages over the standard route, namely:

- approximately 2/3 of training takes place at a distance,
- the participants determine the pace of a large part of education on their own, according to their obligations,
- participants are less absent from the work process in the organizations in which they are employed,
- participants are offered an interactive study environment and counseling assistance from lecturers,
- an online chat room is possible with other participants,
- for the majority of their education, participants can choose their own study space, since they have their own materials [1].

Despite many advantages, the distance learning route also has disadvantages, which represent important challenges in managing such a training system. Students can lose motivation more easily, then if they have classroom lectures; the identity of the student performing the on-line lessons and quizzes can be

dubious; when delivering content to a participant, technical problems may arise (e.g. Internet connection, computer equipment, etc.) [10].

Slovenian ATB Institut za varilstvo carries out training for international welding coordinators both by the standard route (for the IWS level) as well as by the distance learning route (for IWT and IWE level), for which uses the Moodle on-line platform. It is a learning content management system that allows creating online learning environments, publishing e-materials, collaborating with learners, monitoring progress, conducting tests, etc. Moodle is a learning platform designed to provide educators, administrators and learners with a single robust, secure and integrated system to create personalised learning environments [10].

Moodle is one of the computer-based training methods (CBT). Its' worldwide numbers of more than 65 million users across both academic and enterprise level usage makes it the world's most widely used learning platform. Moodle is trusted by institutions and organisations, including Shell, London School of Economics, State University of New York, Microsoft and the Open University. Moodle is recommended, tested and validated for all Slovene public schools and Universities by Ministry of education^[10].

Approach of Institut za varilstvo for self-paced e-learning is a set of interactive lessons. A lesson is a linear sequence of screens, which can include text, graphics, animations, audio, video and interactivity in the form of questions and feedback. Lessons can also include recommended reading and links to online resources, as well as additional information on specific topics. Most commonly used on-line learning elements in Moodle for Institut za varilstvo are:

- lessons/with interactive elements (treat them as PowerPoint slides, but with the ability of interactive navigation through questions);
- quizzes (quizzes are generated from bases of questionnaires and are very powerful for assessment, grading and report generation);
- resources (documents and links that are not interactive) [10].

The success and progress of participants in on-line learning on Moodle is evaluated by using the built-in functions of this platform. These tools provide a quick, but complete insight into the activity of the students, which areas they find difficult and where improvement is most necessary. Tools and criteria followed by the Institut za varilstvo are:

- completion data (all lessons passed and all quizzes should be completed),
- login data (time spent on each lesson/module should follow the number of hours specified in the current guideline),
- date of first/last login of students (course should be finished within a specified period),
- success statistics evaluated on a question-by-question basis (each question should be completed in specified number of attempts) [10]

4. CURRENT EXPERIENCE

Preparations of the ATB Institut za varilstvo for the implementation of the distance learning lasted for 3 years. During this time, existing material for the standard route had to be processed and made useful for the on-line Moodle platform. It was also necessary to provide personnel for distance learning implementation, such as tutors, IT professionals and administrators, as well as a technical and software background to support this way of material delivery, supervision of the learning process and conduction of exams.

Based on the responses of the first two generations of IWE and IWT participants at the Institut za varilstvo, it was found that the transition to distance learning was a very good decision, as there are obvious savings in time and financial expenses. In the last few years, many participants who were financially able to afford training, were able to meet access requirements and have appropriate knowledge, but they could not be absent from the work process to the extent required by the standard qualification route. Due to their responsible role in companies, participants expect flexibility in the time needed for training, so they give preference to the distance learning route versus the standard route.

In total, both generations of IWE and IWT distance learning were successfully completed by 87 students. The results of on-line surveys show that the students were generally satisfied with the implementation of the training. Despite many advantages of distance learning, lectures in the classroom were selected as the most effective way of knowledge delivery. All lecturers received very good grades from students and students were very satisfied with professional, technical and administrative support too. There were no major (technical) problems with the use of the Moodle on-line platform, which further confirmed the relevance of the choice of distance learning method.

The results of examination were at a similar level as the standard route. This means that the level of knowledge of the participants is comparable to that of the standard route.

5. CONCLUSIONS

The International/European diploma for the welding coordinators in the industry has become a necessary condition for the organization and performance of any work related to welding. This need was recognized decades ago at the Institut za varilstvo and the Slovensko društvo za varilno tehniko. Therefore, when we talk about qualification of welding coordinators, Slovenia is one of the most successful European countries.

Distance learning has been steadily increasing over the past few years. The need for more flexible ways of learning with the support of modern computer technologies has never been greater. The main gear of this kind of change are needs of the industry for as educated as possible personnel, who, on the other hand, are difficult absent from work for longer periods.

The Institut za varilstvo recognized these needs and, following the example of some other countries (Germany, Spain, Italy, Norway, etc.), started qualification for welding coordinators with a distance learning system in 2016. The result is a higher number of candidates on trainings and a much lower absence of welding experts from the workplace. The results of the examinations remained similar to that of the standard way of learning in the classroom.

6. REFERENCES

- [1] IAB-International Authorisation Board (2013): Minimum requirements for the education, training, examination and qualification. Distance learning. EWF/IIW-IAB Secretariat, Portugalska.
- [2] EWF Corporate profile (2018): <https://www.ewf.be/upload/processos/d001336.pdf>
- [3] Website IIW. About IIW: <http://iiwelding.org/about-iiw>
- [4] Website SDVT. Izobraževanje varilnega osebja: <http://drustvo-sdvt.si/izobrazevanje-varilnega-osebja>
- [5] Moder M., Rihar G., Tomc J. (2017): Uvod v zagotavljanje kakovosti pri varjenju. Gradivo za specializacijo IWE/IWT. Institut za varilstvo d.o.o., Ljubljana
- [6] IAB-International Authorisation Board (2016). Rules for the implementation of IIW Guidelines for the education, examination and qualification of welding personnel. EWF/IIW-IAB Secretariat, Portugalska.
- [7] Archive of Institut za varilstvo d.o.o.
- [8] IAB-International Authorisation Board (2016). Minimum requirements for the education, training, examination, and qualification. Personnel with qualification for welding coordination. EWF/IIW-IAB Secretariat, Portugalska.
- [9] IAB-International Authorisation Board (2016). Directory of access conditions to the courses based on the IIW Guidelines for education, examination and qualification.
- [10] Knez S. (2017). Report DLC. ATB: Institut za varilstvo d.o.o., Ljubljana.

Authors: Dr. Miloš Jovanović¹, M.A. Mojca Radman¹, Dr-Ing. Miro Uran¹, MSc. Ljubiša Trivković²

¹ Institut za varilstvo d.o.o., Ljubljana, Ptujška ulica 19, 1000 Ljubljana, Slovenia

² Institut za varilstvo d.o.o., Beograd, Vojislava Ilića 59, 11000 Beograd, Serbia

E-mail: milos.jovanovic@i-var.si
mojca.radman@i-var.si
miro.uran@i-var.si
ljubisa.trivkovic@i-var.si

Randjelovic, S., Milutinovic, M., Mladenovic, S., Blagojevic, V.

FEM ANALYSIS OF DIE PLATE AT PIERCING AND BLANKING TOOL

Abstract: *The piercing and blanking tools are characterized by a standard but also a specific cross-section which is directly determined by the technological arrangement of the finished part on the workpiece in the shape of a strip. While the construction of standard tools is the result of a detailed analysis of the stress - strain state in the material of the tool itself, specific tools always represent a new constructive task that in most cases must be solved very quickly in the most optimal solutions. In such conditions, the FEM analysis of the tool for piercing and blanking is a good method to check the internal stresses and deformations of these tools so that in the most unfavorable technological conditions a constructive tool solution would have an optimal solution for big serial and mass production.*

Key words: *piercing, blanking, FEM analysis, die plate*

1. INTRODUCTION

The modern industry of sheet metal processing is in great expansion today thanks to new technological solutions and methods for sheet metal processing. This is qualified by the most diverse requirements of the market, on the basis of which the finished sheet metal products are complex, but increasingly 3D shapes [1]. A good example is the automotive industry, the home appliance industry, modern construction, the furniture industry, and so on. where the range of products is increasingly and technologically more demanding. Therefore the necessary tools in one such production have to meet the strictest requirements so that the products obtained are competitive in the open global market. The big manufacturers of industrial tool (HASCO, FEINTOOL, OERLIKON Balzers, ...) very well recognize the requirements of large companies that have this type of production and standardize a large number of tools so that they can be available to the potential user at any time [2].

For such a type of technology, where sheet processing is raised to the highest level, standardized housing are primarily designed to unify the workspace, but also provide simple and quick tool change while standard tools for blanking and piercings (punch, die plates) can serve as partial tools wherever possible in order to get an defined hollow or a finished part. In the case of complex contours of smaller and larger dimensions, it is necessary to create an appropriate contour tool in order to obtain the desired geometry in one stroke. In such a case, they are not standard geometry tools, but shapes that correspond completely to the geometry of the finished part. Solutions with the segment tools can often occur in order to obtain the desired complex contour in the concrete case from the simplest forms [3]. The FEM analysis, test and verification of such tools imposes itself in order for the proposed solutions of die plate to have the right choice of materials, a longer lifetime, consistent geometry, the ability to obtain a large number of finished parts in larger series.

2. FEM ANALYSIS OF DIE PLATE

At the very beginning of the software application, it is allowed to parameterize the characteristic dimensions of the finished part (fig. 1), the width (the predetermined range is from 30 to 50mm) and the heights that directly condition the other constructive parameters. At this level of the software solution, the dimensions of the hollows are in predefined dependence with respect to the external dimensions so that they are not inputted already are calculated.

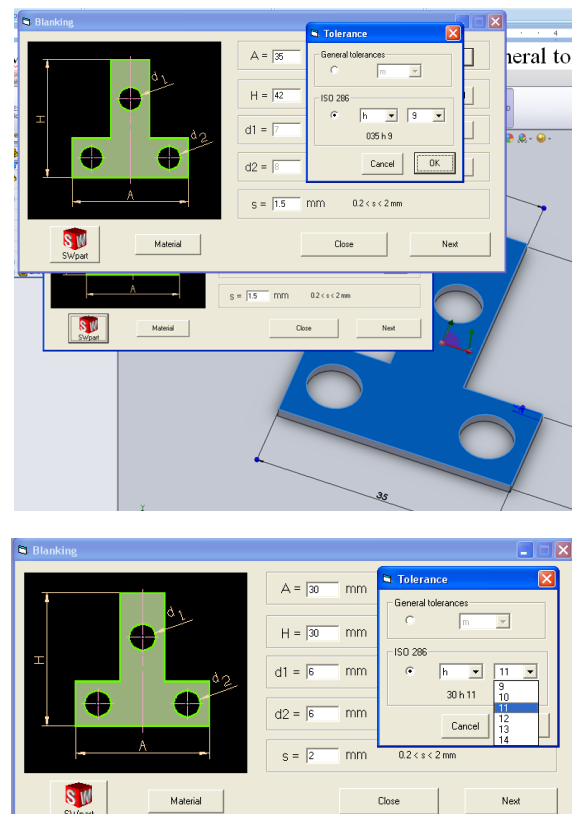


Fig. 1. Parametric input of dimensions of finished part and tolerance of given measures, SolidWorks2015®

Independently of these dimensions, the thickness of the strip material is determined (the range is from 0.2 to 2mm).

After entering the dimensions, you can see the 3D model of the finished part in SolidWorks with the actual dimensions of external or internal counter. By providing the possibility of introducing free tolerances of all dimensions and more precise tolerances according to the ISO 286 standard for each of these dimensions, the finished part can be completely defined, which determines the characteristics of the tool or the die plate.

In the application database lists all the tolerance fields and their corresponding position that can be monitored according to the standard, for a tolerated dimension $A = 30 h11$.

The constructive layout solutions on the strip workpiece directly determine the shape and layout of the holes on the die plate as part of the tool that directly determines the completion of the finished part. For now, only one-line and two-line layout of the finished part on the strip (fig. 2) are offered here, which clearly show how much material savings can be made when choosing a two-line schedule if there is a possibility.

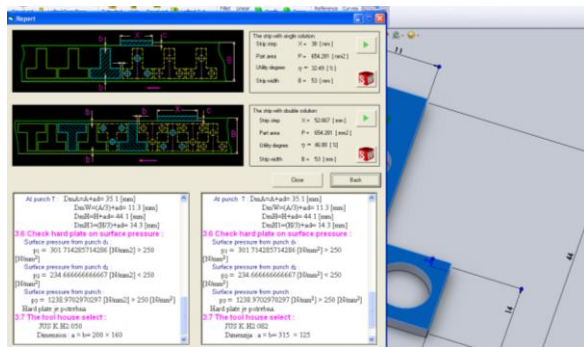


Fig. 2. Some results for the thickness of the die plate for the defined geometry, SolidWorks2015®

Two constructive solutions of the die plate are offered, where one or two finished part in one step are given, represent two special cases of static load. The die plate in a simpler static analysis can be treated as a free beam, with multiple weakened cross sections, loaded with bending moment and big surface pressure on cutting edges. In order to obtain greater stiffness, it receives a much larger thickness to achieve a satisfactory resistance as well as the ability to obtain new cutting edges during the process of exploitation by flat grinding. Reliance conditions, in the case when one or two finished parts are obtained in the step, and the distribution of the already mentioned loads on the cutting edges are given in Fig. 3.

Today, the novel constructive solutions of the die plate are performed with segmented inserts made of hard metal and cutting ceramics that are attached to a more elastic base than a structural steel so that the cutting edge itself is easily removable if there is breakage and its damage in the production conditions. Such constructive solutions require a more detailed FEM

analysis in order to obtain optimum dimensions and field of internal stress and strains in a large number of cyclic loads.

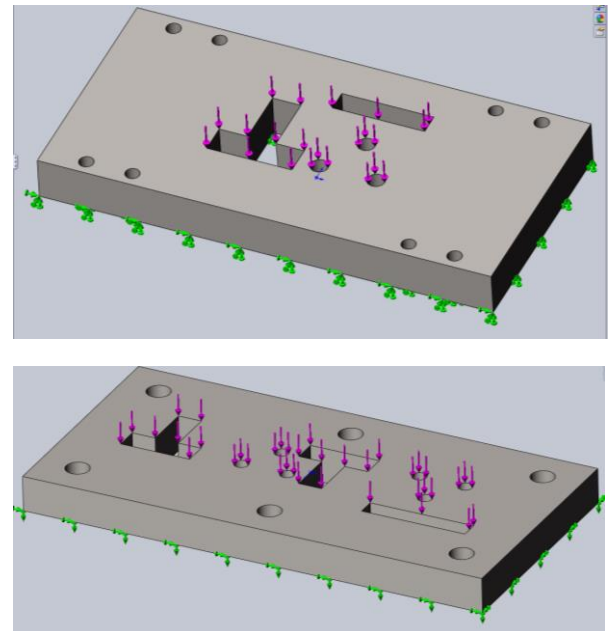


Fig. 3. CAD models of die plates with cutting edges, SolidWorks2015®

The results of the FEM analysis for internal stress and strain along the structure of the die plate indicate large surface loads near the cutting edges that have a decisive influence on the intensive wear of the cutting edges themselves. In this analysis, the h -adaptive method shows good results by adjusting the finite element network and adding nodes in which stress and strain values near the cutting edges are determined in order to get the most accurate results.

Considerable progress has been made on both the a posteriori error analysis of finite element methods for a wide range of partial differential equations of practical interest, and the theoretical and computational assessment of local refinement indicators. We note that once a computable error bound has been established for a particular discretisation of a partial differential equation, the refinement indicator is generally constructed by simply "localising" the a posteriori bound over an element, or patch of elements. On the other hand, the state of development of "optimal" mesh modification strategies which are capable of delivering the greatest reduction in the error for the least amount of computational cost, is far less advanced. Indeed, the majority of adaptive finite element software will simply subdivide elements where the local refinement indicator is large, while keeping the polynomial degree fixed at some low value. Clearly, if the analytical solution to the underlying partial differential equation is smooth, or at least locally smooth, then this may not provide the most efficient adaptive strategy. In this case, an enrichment of the polynomial degree (h -refinement) may be much more effective in reducing the error per unit cost.

The aim of this method is to focus on the design of an

automatic mesh modification strategy that is capable of exploiting both local h- and p-refinement. Such general hp-adaptive finite element methods offer greater flexibility and improved efficiency than mesh refinement methods which only incorporate either local mesh subdivision of the computational domain $\Omega \subset \mathbb{R}^d$, $d \geq 1$, with the degree of the approximating polynomial fixed, or global polynomial degree variation on a fixed coarse mesh. Indeed, in recent years there has been tremendous interest in the development of automatic hp-mesh refinement algorithms.

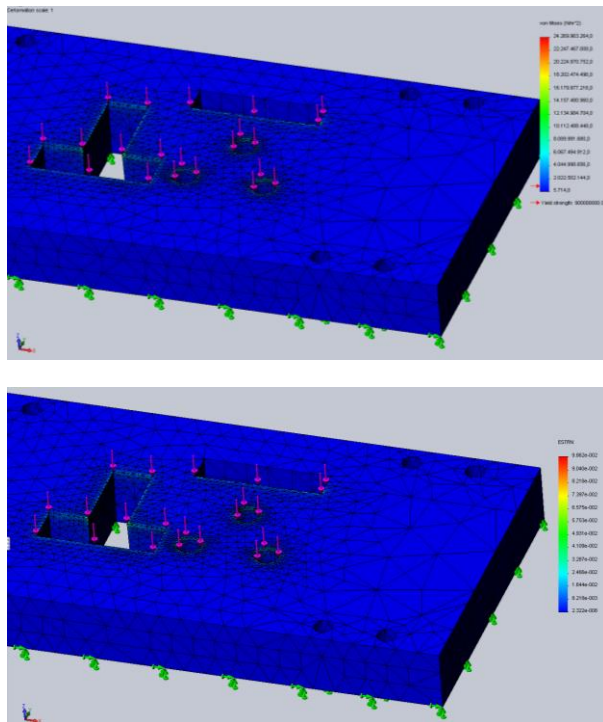


Fig. 4. The field of stress and strain generated by FEM h - adaptive method

In order to gain insight into the results of this FEM analysis, where the h - adaptive method is used, several characteristic cross sections are given indicating the size of individual mechanical parameters according to the structure of the die plate.

3. CONCLUSION

The described approach to the design of blanking and piercing technology points to many advantages of FEM modeling and analysis of the stress deformation state of the body of standard but also special tools. Whenever standard tooling is possible, this should be used as a reliable, proven and tested solution by major tool and equipment manufacturers for this type of sheet metal technology. However, when it comes to special tools, or forms that are specifically designed for the defined geometry of the finished part, this approach is a guarantee to the constructor that the field of stress and strain along the body of the die plate will not exceed the critical permissible stress and lead to permanent deformation and breakage of the tool, or set up the question of the technological stamping process.

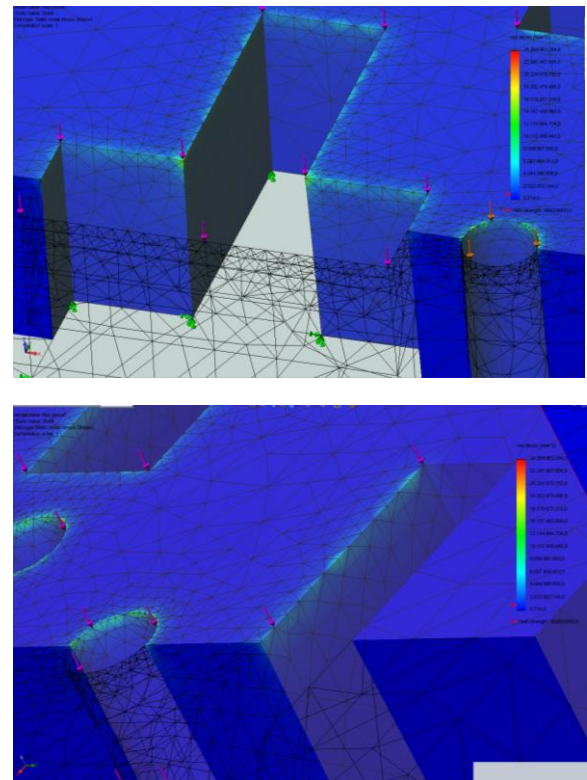


Fig. 5. The field of stress near the hollow of the die plate obtained by the h - adaptive method

4. REFERENCES

- [1] Wang, C. T.: *Advanced Stamping Simulation Technology – State of Business and Industrial Prospect*, NumiSheet Conf., pp. 250-256., Besancon, 13-17. Sept. 1999.
- [2] Oehler, G.: *Schneid und Stanzwerkzeuge*, Springer Verlag, Berlin/Heidelberg, 1995.
- [3] Randelović, S., Marinković V.: *Proizvodne tehnologije, Obrada metala plastičnim deformisanjem*, Mašinski fakultet u Nišu, Niš, 2017.
- [4] Wang, C. T., *Evolutions of Advanced Stamping CAE*, NumiSheet Conf., pp. 78-82., 19-24. May 2005.
- [5] Hu, P., Ying, L., He, B.: *Hot Stamping Advanced Manufacturing Technology of Lightweight Car Body*, Springer Verlag, Singapore, 2017.

Authors: Prof. dr Sasa Randjelovic, Assistant Srdjan Mladenovic, Associate Prof. dr Vladislav Blagojevic University of Nis, Faculty of Mechanical Engineering, Aleksandra Medvedeva 14, 18000 Nis, Serbia, Phone.: +381 18 500627, Associate Prof. dr Mladomir Milutinovic, University of Novi Sad, Institute for Production Engineering, Trg Dositeja Obradovica 6, 21000 Novi Sad, Serbia, Phone.: +381 21 485-2337
E-mail: sassa@masfak.ni.ac.rs; mladomil@uns.ac.rs; maki@masfak.ni.ac.rs; vlada@masfak.ni.rs;

ACKNOWLEDGMENTS: The research is supported by the Ministry of Education, Science and Technology Development of the Republic of Serbia, project number III44004 HUMANISM

Ristic, M., Rajnovic, D., Macas, M., Balos, S., Sidjanin, L., Pecanac, M.

THE STUDY OF THE CONTAMINATED SURFACE LAYER OF HIP TREATED SUPERALLOY IN100

Abstract: In this paper the process of the hot isostatic pressing – HIP, its types and significance for superalloy castings, is described. The study of the thickness and chemical composition of contaminated surface layer for HIP treated superalloy IN100 is presented. It was concluded that the appearance of the contaminated layer is due to the diffusion of carbides from the metal matrix to the surface and their reaction with the impurities in the argon atmosphere, thus causing the formation of a layer of oxides, nitrides and carbides. The carbides diffusion to the surface also results in the formation of a carbide-free zone.

Key words: HIP – hot isostatic pressing, superalloys, contamination layer, carbide-free zone

1. INTRODUCTION

HIP process (Hot Isostatic Pressing) is a thermal-mechanical process that is used to improve strength and density by combining high temperature ($>1000^{\circ}\text{C}$) and pressure ($\sim 180\text{MPa}$). Argon is most often used as a working medium, but beside him, nitrogen is also used [1]. From economical aspect, duration of this process is of great importance, Table 1. Certain materials, as Ti alloys, are processed on lower temperature, so they require more time for process to be completed. Other materials are processed faster, which is more economical.

HIP MATERIALS	TEMPERATURE [$^{\circ}\text{C}$]	PRESSURE [MPa]
HSS powder	1000-1200	~ 100
Superalloys based on Ni	1170-1280	100-150
Ti Alloys (Ti-6Al-4V)	800-960	~ 100
Cr	1200-1300	~ 100
Cu Alloys	500-900	~ 100
Al Alloys	350-500	~ 100
Hardmetal WC-Co	1300-1350	30-100
Ni-Zn-ferrite	1050-1180	~ 100
Mn-Zn-ferrite	1180-1250	~ 100
Al_2O_3	1350-1450	~ 100
SiC	1950-1050	100-200

Table 1. Materials that are subjected to HIP process and temperature and pressure that is used.

HIP process has several advantages over the commonly used processes:

- Powders are compressed to higher densities at lower temperatures,
- Ability to create highly complex parts,
- Parts subjected to HIP process have homogenous density,
- Higher density helps with heat transfer, which results with faster heating and shorter processing times,
- Brittle materials can be processed because of uniform heating.

HIP process is largely used for powder metallurgy, ceramics, casting repair and diffusion bonding [2].

1.1 Superalloys

Superalloys are a kind of advanced materials that are used in extreme conditions. High temperature strength of all superalloys is based on stable face centered cubic structure matrix which is combined with precipitation reinforcement and / or reinforcement with solid phases. Superalloys can be based on Ni-Fe, Ni, and Co and they are used in places where working temperature can be over 560°C . They are most commonly used for parts in aviation industry and also for components in oil industry. Most important is application in airplane engines.

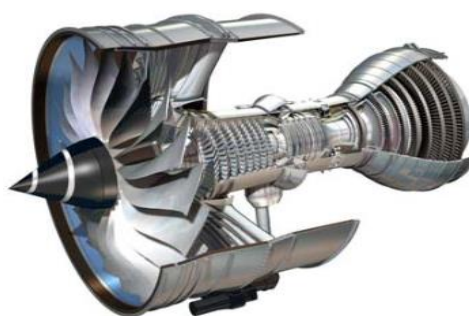


Fig.1. High-pressure turbines [Rolls-Royce]

Application of HIP process increases with development of advanced superalloys based on Ni, and with the introduction of castings with complex geometry where higher degree of porosity is present. These kinds of demands can only be met with HIP process [3].

1.2 Importance of HIP process for superalloys

When castings are hot isostatically pressed, simultaneous application of temperature and pressure almost completely eliminates microporosity by combining plastic deformation, creep and diffusion. Removing internal faults leads to improved results in non-destructive testing, mechanical testing, and it also increases the repeatability of the results.

2. EXPERIMENTAL PROCEDURE

2.1 Problem description

On the surface of workpieces processed by the HIP process, a contaminated layer appears. The thickness of the layer is not constant and is visible in the naked eye in the form of a color change of the pieces. The occurrence of contamination is a multiple problem:

- The size of the castings increases
- Need additional cleaning operation
- Dirt on the surface can be the initiators of corrosion and cracks

2.2 Description of the experiment

Samples are casted from superalloy Inconel 100, oldest of superalloys, based on nickel with precipitates and which has increased creep resistance at temperatures of 1000 °C. This alloy is entirely cast in vacuum due to the reactivity of the alloying elements with oxygen, i.e. air. Nominal chemical composition of the IN100 superalloy with tolerance limits is shown in Table 2.

Elem ent	[mass %]	Elem ent	[mass %]	Elem ent	[mass %]
C	0.15-0.20	Al	5-6	Mn	max 0.2
Cr	8-11	V	0.7-1.2	Si	max 0.2
Co	13-17	Zr	0.03-0.09	S	max 0.015
Mo	2-4	B	0.01-0.02	Ni	base
Ti	4.5-5	Fe	max 1	-	-

Table 2. Nominal chemical composition IN100

It is necessary to examine, the occurrence of contamination, thickness of the contaminated layer on the samples placed in three zones within the HIP furnace:

- 3 samples in upper zone
- 3 samples in middle zone
- 3 samples in bottom zone

After HIP processing is finished, the thickness of the contaminated layer was measured (5 measurements on 5 visible fields, magnification of 1000×).

Aim of experiment is to see how surface preparation effects contaminated layer that appears after the HIP cycle is finished, as well as the character of the contaminated layer. Also, the aim of the test is to determine chemical composition of the contamination by examining the surface area of the sample on SEM (Scanning electronic microscope) using EDX methods (X-ray energy dispersion spectroscopy). Three kinds of samples were used, with different surface quality, coarsely grinded (P 240), finely grinded (P 1000) and polished with cloth and diamond suspension of 1 µm. After HIP process, the mean thickness of the contaminated layer was determined, through 5 measurements on 5 visible fields, at a magnification of 1000 ×. For the examination of surface contamination, samples separate from each mold by way of shell breaking were used. Before the HIP process, samples

are prepared by grinding with grinding paper that has grain grit of P240, P1000, or polished in accordance to the technical requirements for the test procedure. Image of one such sample is shown in Figure 2. The samples are then cut in half and mounted in Bakelite, after that samples are grinded to give a uniformly flat surface.

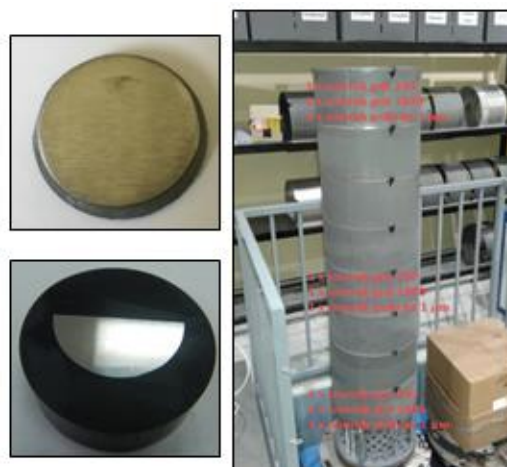


Fig 2. A sample for examining the contaminated layer and distribution of samples by baskets in the HIP process

2.3 HIP process parameters

Samples were processed in the standard HIP cycle prescribed for the IN100 material from which the castings and test samples were produced. The maximum temperature was 1200 ° C for 4 hours, at a pressure of 1379×10^5 Pa (20000 psi), and the whole process lasted 9h.

2.4 Microstructure testing

Light microscope (LM) Leica DM1750M with a magnification of 1000× was used to measure the thickness of the contaminated layer. Layer measurement was performed using the appropriate LAS V4.9 software. In addition, an analysis of the contaminated layer was carried out using the SEM microscope at the University Center for Electronic Microscopy, University of Novi Sad. The microscope model is JEOL JSM-6460LV, equipped with the INCA Oxford Instruments EDS system. The observations were carried out at a working voltage of 20 kV. After the HIP process has finished, samples are taken out of the basket and re-mounted so that the surface visible after the mounting is at a right angle with the surface where the contaminated layer has form. Samples on which the contaminated layer was examined must be further grinded for microscopic observation (grinding papers P240, P600, and P1000) and then polished with cloth and diamond suspension of 3 µm and finally with 1 µm.

3. ANALYSIS OF RESULTS

For each type of sample preparation (P240, P1000 and polished, Figures 3 to 5, respectively), a 5 measurements of the contaminated layer on the LM

microscope are performed. The result of the measuring of the sample with contaminated layer that was grinded with P240 is shown in Figure 3. Figure 4 shows the contaminated layer of the sample grinded with P1000, while Figure 5 shows the result for the contaminated layer of a sample that was polished with cloth and diamond suspension of 1 μm size.

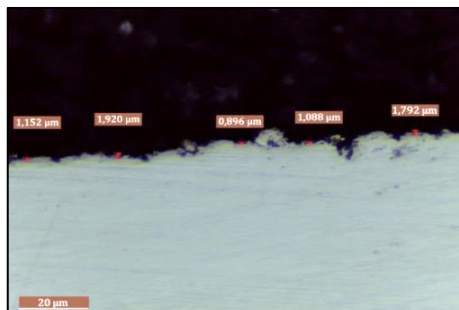


Fig. 3. Contaminated layer of sample from the first basket grinded with P240 (LM)



Fig. 4. The contaminated layer sample from the first basket which was grinded with P1000 (LM)



Fig 5. The contaminated layer sample from the first basket which was polished with cloth and 1 μm diamond (LM)

The mean value of the measured contamination layer thickness and standard deviation is given in Table 3, depending on the sample preparation and the position in the furnace. After looking at all of the measured values, it can be concluded that the highest contamination is in the samples from basket number 4, which were prepared with P240, and is 1.968 μm , while the smallest contamination of 0.832 μm is for the samples prepared by polishing from the basket number 1. The samples from the basket number 8 show that the sample grinded with paper P1000 has the smallest layer. When grinding with grinding paper P1000 or polishing, the mean values of the layer are similar, and therefore additional preparation of the sample by

polishing in order to obtain the smaller layer is not justified.

		Basket No. 1	Basket No. 4	Basket No. 8	Mean value
P240	Mean value	1.536	1.968	1.488	1.728
	St. dev.	0.608	0.624	0.176	
P1000	Mean value	1.056	1.296	0.784	1.040
	St. dev.	0.288	0.336	0.080	
Pol	Mean value	0.832	0.864	0.944	0.888
	St. dev.	0.128	0.128	0.144	

Table 3. Mean values of the measured contaminated layer with standard deviation [μm]

3.1 The SEM microscope and EDS results

For study on the SEM microscope, a sample grinded with P 1000 from the basket number 1 was chosen as a representative because it had most uniform contamination layer. The appearance of the contaminated layer examined by the SEM microscope is shown in Figures 6 and 7.

The upper surface shows the contaminated layer, while the bottom flat surface represents the cross-section of the base material, Figure 6. In the Figure 7 it is showed that the contaminated layer grows stratified in the form of clusters and globules, while linear orientation of the globules suggests that contamination occurs on the grinding marks.

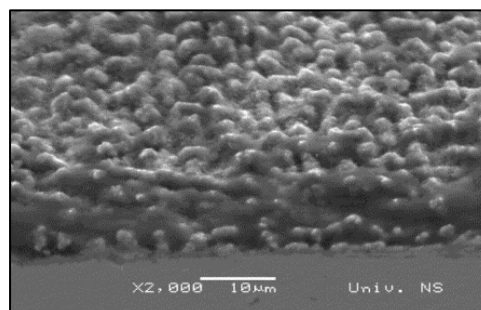


Fig. 6 Contaminated layer (SEM)

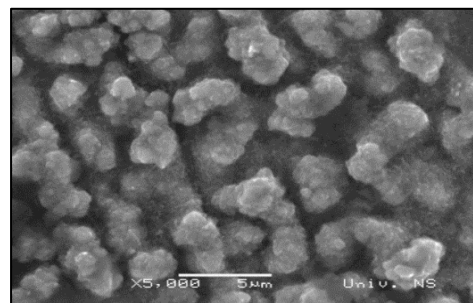


Fig 7. Appearance of a contamination globules (SEM)

With EDS, the chemical composition of the contaminated layer was determined. Figure 8 shows area of EDS analysis measurements, while in table 4 the chemical composition of individual test sites is given.

SPEKTRUM	C	N	O	Al	Ti	V	Cr	Co	Ni	Mo
SPEKTRUM 1	8.15	1.03	19.11	10.17	49.59	0.42	1.32	1.61	6.66	1.95
SPEKTRUM 2	12.16	7.15	13.13	5.47	56.57		0.82	0.61	1.96	2.12
SPEKTRUM 3	10.92	3.79	17.44	6.95	55.12	0.25	0.71	0.53	2.45	1.83

Table 4. Chemical composition of spectrums (mass %)

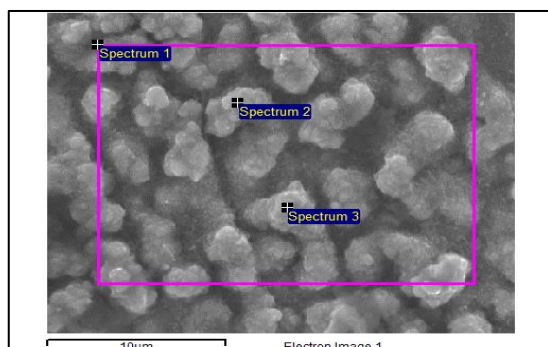


Fig 8. EDS method test sites.

The Table 4 shows that the first spectrum (purple tetragon in Figure 8) contains more C, Al, Ti, O and traces of N, V, Cr, Co, Ni and Mo. The spectrums 2 and 3, which represent the upper part of the globules, show the same concentration of elements. Globules formed on the surface of superalloys are a combination of oxides, nitrides and carbides which are formed when atmospheric impurities (oxygen and nitrogen) react with alloying elements Al, Ti, Cr, Co, V, Mo, which, due to the high temperature of the HIP process diffuse to the surface and react with environment. Furthermore, a part of the contaminated layer is entirely the result of the diffusion of the alloying elements.

The consequence of the HIP process is the so-called free carbide zone, which is the result of the dissolution of the MC carbide and the diffusion of carbide elements from the sub-surface layer of the metal on to the free surface. The depth of the carbide-free zone is up to 100 µm, in samples with P240, 78 µm in samples with P1000, and 48 µm (Figure 9) in samples that were polished. The highest depth of the carbide-free zone coincidence with largest contaminated layer, and vice versa, the smallest depth of the carbide-free zone correspond to smallest contamination. With the EDS analysis of individual zones through depth from the surface of the superalloys has been found that carbide-free zone occurs along the surface, in which the concentration of Al, Ti, V, Mo decreases, because these elements diffuse to the surface of the superalloys, while the Cr and Co elements generally remain dissolved in Ni metal matrix.

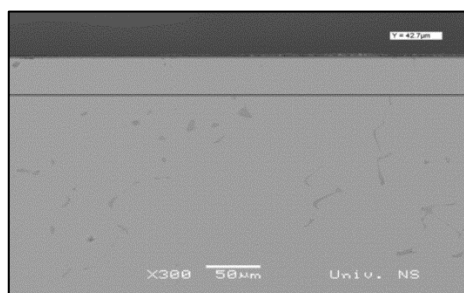


Fig. 9 Carbide free zone

4. CONCLUSION

Based on the results of this study, it was determined that:

- The thickness of the contaminated layer depends on the surface roughness. Samples grind with grinding paper P240 have the highest average layer thickness of 1.728 µm, while the lowest have polished samples, 0.888 µm.
- The contaminated layer is consisted of oxides, nitrides and carbides formed on the surface of the castings produced by the HIP process.
- The contaminated layer is formed by diffusion of carbides and dissolved elements from the metal base to the surface.
- The formation of a contaminated layer during the HIP process causes the formation of zone without carbides beneath the surface. The thickness of the carbide free zone is proportional to the thickness of the contaminated layer.

5. LITERATURE

- [1] N. L. Loh, K. Y. Sia: An overview of hot isostatic pressing, *Journal of Materials Processing Technology*, 30, (1992), 45-65
- [2] M. H. Bocanegra-Bernal: Review Hot Isostatic Pressing (HIP) Technology and its applications to metals and ceramics, *Journal of Materials Science*, 39, (2004), 6399-6420
- [3] Matthew J. Donachie, Stephen J. Donachie, *SUPERALLOYS A technical guide*, ASM International, Materials Park, Ohio, USA, 2nd Edition (2002)
- [4] D. Richter, G. Haour, D. Richon: Hot Isostatic Pressing (HIP), *Materials and Design*, 6, (1985), 303-305

Authors:

M.Sc. Mirjana Ristic, Doc. Dr Dragan Rajnovic, M.Sc. Milan Pecanac, Assoc. Prof. Dr Sebastian Balos, Emeritus Prof. Dr Leposava Sidjanin
University of Novi Sad, Faculty of Technical Sciences, Department of Production Engineering, Trg Dositeja Obradovica 6, 21000 Novi Sad, Serbia.

E-mail: mirjana.ristic@uns.ac.rs; draganr@uns.ac.rs; sebab@uns.ac.rs; lepas@uns.ac.rs; pecanac.milan@uns.ac.rs

M.Sc. Mario Macas

Precise Casting Plant – LPO, Ada, Serbia

Simonović, S.

ON OPTIMIZATION OF ATOMIC FORCE MICROSCOPE CANTILEVER DESIGN WITH RESPECT TO ITS MECHANICAL REQUIREMENTS

Abstract: The performance of an Atomic Force Microscope and the quality of its images greatly depend on the mechanical properties of the cantilevers in use. The paper deals with impact of the cantilever design characteristics on its vibrational and statical properties. The resonances and stiffnesses of the cantilever are determined and preferable design characteristic of the cantilever are enumerated in terms of the cantilever material and geometry.

Key words: Vibrational, Statical, Material, Geometry

1. INTRODUCTION

The Atomic force microscope (AFM) [1] is based on the principle that a very soft cantilever with a tip that is moved to the vicinity of a surface (metallic or insulating) can sense the roughness of the surface and deflect by an amount which is proportional to the proximity of the tip to the surface. The cantilever which probes the surface has an atomically sharp tip which is brought into contact with the surface.

The large scale use of AFM today is because of the application of microfabricated tips of Si or Si₃N₄. The spring constant k of the tip is of the order of 1 N/m and the shortest vertical displacement, d measurable can be obtained from, $\langle 1/2 k d^2 \rangle \sim 1/2 k_B T$. With $k_B T$ of the order of 4×10^{-21} J at 298 K, the smallest vertical displacement observable is 0.5 nm [2,3].

The extent of interaction between the cantilever and the tip is measured by cantilever displacements. The interaction between the tip and the sample is of the order of a nano Newton, which is not directly measured in AFM. The piezoelectric control is used to position the cantilever and tip in x,y, and z with a precision of ~ 0.1 nm. When it is mounted in the microscope, a laser is reflected from the back of the cantilever onto a position-sensitive detector. There is a sufficiently long optical lever effect that cantilever deflections ~ 0.1 nm can be detected. (figure 1) [4].

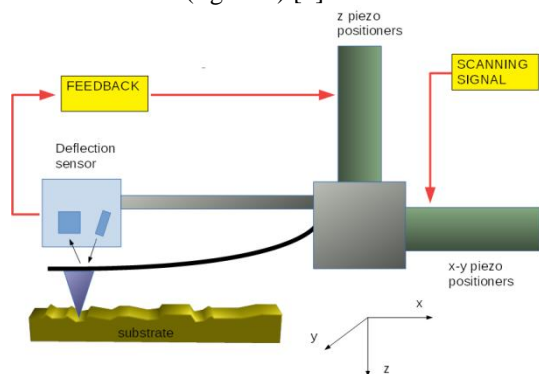


Fig. 1. Funcional model of atomic force microscope

The most important application of the AFM is imaging where it can work in various modes: the

contact mode, tapping mode and the jumping mode. For example, in the tapping mode the tip is made to oscillate close to the sample surface. The amplitude of the oscillation is recorded and controlled by a feedback loop mechanism that keeps such amplitude constant. When passing over a bump the amplitude decreases so the distance between tip and surface is increased to keep the amplitude of oscillation constant. When passing over a depression the tip is moved to the surface. This mode has the advantage that the transverse motion of the tip along the surface is not influenced by shearing and frictional forces, thereby avoiding damage to the sample and noisy interference effects. A map of the distance of the tip from the sample provides an accurate topographic image of the surface [5].

2. CANTILEVER DESIGN REQUIREMENTS

The cantilever stylus used in the AFM should meet the following criteria: (1) low normal spring constant (stiffness); (2) high resonant frequency; (3) high cantilever quality factor Q ; (4) high lateral spring constant (stiffness); (5) short cantilever length; (6) incorporation of components (such as mirror) for deflection sensing; and (7) a sharp protruding tip [5].

In order to register a measurable deflection with small forces, the cantilever must flex with a relatively low force (on the order of few nN), requiring vertical spring constants of 10^{-2} to 10^2 N/m for atomic resolution in the contact profiling mode. The data rate or imaging rate in the AFM is limited by the mechanical resonant frequency of the cantilever. To achieve a large imaging bandwidth, the AFM cantilever should have a resonant frequency of more than about 10 kHz (30–100 kHz is preferable), which makes the cantilever the least sensitive part of the system. Fast imaging rates are not just a matter of convenience, since the effects of thermal drifts are more pronounced with slow scanning speeds. The combined requirements of a low spring constant and a high resonant frequency are met by reducing the mass of the cantilever. The quality factor Q ($= \omega_R / (c/m)$), where ω_R is the resonant frequency of the damped oscillator, c is the damping constant and m is

the mass of the oscillator) should have a high value for some applications. For example, resonance curve detection is a sensitive modulation technique for measuring small force gradients in noncontact imaging. Increasing the Q increases the sensitivity of the measurements. Mechanical Q values of 100–1000 are typical. In contact modes, the Q value is of less importance. A high lateral cantilever spring constant is desirable in order to reduce the effect of lateral forces in the AFM, as frictional forces can cause appreciable lateral bending of the cantilever. Lateral bending results in erroneous topography measurements. For friction measurements, cantilevers with reduced lateral rigidity are preferred [5].

A sharp protruding tip must be present at the end of the cantilever to provide a well-defined interaction with the sample over a small area. The tip radius should be much smaller than the radii of the corrugations in the sample in order for these to be measured accurately. The lateral spring constant depends critically on the tip length. Additionally, the tip should be centered at the free end [5].

Property	Young's modulus (E) (GPa)	Density (ρ) (kg/m ³)	Microhardness (Gpa)	Speed of sound ($\sqrt{E/\rho}$) (m/s)
Diamond	900 – 1050	3515	78.4 – 102	17 000
SisN ₄	310	3180	19.6	9900
Si	130 – 188	2330	9–10	8200
W	350	19310	3.2	4250
Ir	530	–	≈3	5300

Table 1. Properties of materials used for cantilevers [5]

3. AFM AS LUMPED MASS SYSTEM

All of the building blocks of an AFM, including the body of the microscope itself and the force-measuring cantilevers, are mechanical resonators. These resonances can be excited either by the surroundings or by the rapid movement of the tip or the sample. To avoid problems due to building- or air-induced oscillations, it is of paramount importance to optimize the design of the AFM for high resonant frequencies. This usually means decreasing the size of the microscope [6].

By using cube-like or sphere-like structures for the microscope, one can considerably increase the lowest eigenfrequency. The fundamental natural frequency ω_0 of any spring is given by

$$\omega_0 = \frac{1}{2\pi} \sqrt{\frac{k}{m_{eff}}} \quad (1)$$

where k is the spring constant (stiffness) in the normal direction and m_{eff} is the effective mass. The spring constant k of a cantilever beam with uniform cross section (Fig.2) is given by [7]

$$k = \frac{3EI}{L^3} \quad (2)$$

where E is the Young's modulus of the material, L is the length of the beam and I is the moment of inertia of the cross section. For a rectangular cross section with a width B (perpendicular to the deflection) and a height h one obtains the following expression for I [7] :

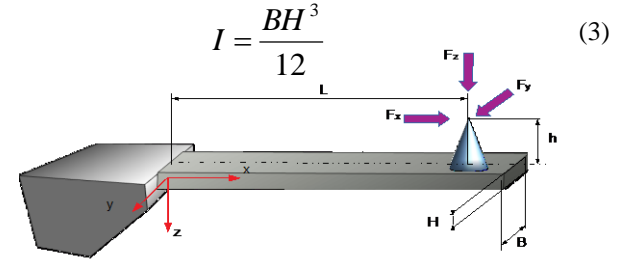
$$I = \frac{BH^3}{12} \quad (3)$$


Fig. 2. Model of an AFM cantilever

Combining (1)–(3), an expression for ω_0 is obtained as

$$\omega_0 = \sqrt{\frac{EBH^3}{4L^3 m_{eff}}} \quad (4)$$

The effective mass can be calculated using Raleigh's method. The general formula using Raleigh's method for the kinetic energy T of a cantilever rod is [8]

$$T = \frac{1}{2} \int_0^L \frac{m}{L} \left(\frac{\partial w(x,t)}{\partial t} \right)^2 dx \quad (5)$$

For the case of a uniform beam with a constant cross section and length L , one obtains for the deflection $w(x,t) = w_{max}(t) [1 - (3x/2L) + (x^3/2L^3)]$. Inserting w into (5) and solving the integral gives

$$\begin{aligned} T &= \frac{1}{2} \int_0^L \frac{m}{L} \left(\frac{dw_{max}(t)}{dt} \left(1 - \frac{3x}{2L} + \frac{x^3}{2L^3} \right) \right)^2 dx \\ &= \frac{1}{2} m_{eff} \left(\frac{dw_{max}}{dt} \right)^2 \end{aligned}$$

which gives

$$m_{eff} = \frac{9}{20} m \quad (6)$$

Substituting (6) into (4) and noting that $m = \rho LBH$, where ρ is the mass density, the following expression is obtained

$$\omega_0 = \left(\frac{\sqrt{5}}{3} \sqrt{\frac{E}{\rho}} \right) \frac{H}{L^2} \quad (7)$$

4. STIFFNESS OF AFM CANTILEVERS

AFM cantilevers are mechanical devices specially shaped to measure tiny forces. To better understand the intricacies of force detection systems, the example of a

cantilever with uniform cross section will be considered (Fig. 2). The bending of a cantilever due to a normal load on the cantilever is governed by the Euler equation [7, 8]

$$M = EI(x) \frac{d^2 w}{dx^2} \quad (8)$$

where M is the bending moment acting on the cantilever cross section. $I(x)$ is the moment of inertia of the cross section with respect to the neutral axis, defined by

$$I(x) = \int \int_z z^2 dz dy \quad (9)$$

For a normal force F_z acting at the tip

$$M(x) = (L-x) F_z \quad (10)$$

Integrating (8) for a normal force F_z acting at the tip and observing that EI is a constant for cantilevers with a uniform cross section, one obtains

$$w(x) = \frac{F_z L^3}{6EI} \left(\frac{x}{L} \right)^2 \left(3 - \frac{x}{L} \right) \quad (11)$$

The slope of the cantilever is

$$w'(x) = \frac{F_z L}{2EI} \left(2 - \frac{x}{L} \right) x \quad (12)$$

From (11) and (12), at the end of the cantilever (for $x=L$), for a rectangular cantilever cross section, and by using the expression for I in (3), one obtains

$$w(L) = \frac{4}{EB} \left(\frac{L}{H} \right)^3 F_z \quad (13)$$

$$w'(L) = \frac{3}{2} \left(\frac{w}{L} \right)^3 \quad (14)$$

Now, the stiffness in z direction k_z is

$$k_z = \frac{F_z}{w(L)} = \frac{EB}{4} \left(\frac{H}{L} \right)^3 \quad (15)$$

and the change in angular orientation of the end of cantilever beam is

$$\alpha = \frac{3}{2} \frac{w(L)}{L} = \frac{6}{EBH} \left(\frac{L}{H} \right)^2 F_z \quad (16)$$

Now, the question is, to a first-order approximation,

what will happen if we apply a lateral force F_y to the end of the cantilever tip (Fig. 2). The cantilever will bend sideways and it will twist. The stiffness in the lateral (y) direction k_y can be calculated with (15) by exchanging B and H

$$k_y = \frac{EH}{4} \left(\frac{B}{L} \right)^3 \quad (17)$$

Therefore, the bending stiffness in the lateral direction is larger than the stiffness for bending in the normal direction by $(B/H)^2$. The twisting or torsion on the other hand is more complicated to handle. For a wide, thin cantilever ($B \geq H$) we obtain torsional stiffness along y -axis k_{yT}

$$k_{yT} = \frac{GBH^3}{3Lh^2} \quad (18)$$

where G is the modulus of rigidity ($=E/2(1+\nu)$; ν is Poisson's ratio). The ratio of the torsional stiffness to the lateral bending stiffness is

$$k_{yT} = \frac{k_{yT}}{k_y} = \frac{1}{2} \left(\frac{hB}{HL} \right)^2 \quad (19)$$

where we assume $\nu=0.333$. Finally, we calculate the ratio between the torsional stiffness and the normal bending stiffness,

$$k_{yT} = \frac{k_{yT}}{k_z} = 2 \left(\frac{L}{h} \right)^2 \quad (20)$$

Equations (18) to (20) hold in the case where the cantilever tip is exactly in the middle axis of the cantilever. Triangular cantilevers and cantilevers with tips which are not on the middle axis can be dealt with by finite element methods.

The third possible deflection mode is the one from the force on the end of the tip along the cantilever axis, F_x (Fig. 2). The bending moment at the free end of the cantilever is equal to $F_x h$. This leads to the following modification of (10) for forces F_z and F_x

$$M(x) = (L-x) F_z + F_x h \quad (21)$$

Integration of (8) now yields

$$w(x) = \frac{1}{2EI} \left[Lx^2 \left(1 - \frac{x}{3L} \right) F_z + hx^2 F_x \right] \quad (22)$$

and

$$w'(x) = \frac{1}{EI} \left[\frac{Lx}{2} \left(2 - \frac{x}{L} \right) F_z + hx F_x \right] \quad (23)$$

Evaluating (22) and (23) at the end of the cantilever, we get the deflection and the tilt

$$w(L) = \frac{L^2}{EI} \left[\frac{L}{3} F_z + \frac{h}{2} F_x \right] \quad (24)$$

$$w'(L) = \frac{L}{EI} \left[\frac{L}{2} F_z + h F_x \right] \quad (25)$$

5. RESONANCES OF AFM CANTILEVERS

A second group of interesting properties of cantilevers is their resonance behavior. For cantilever beams, the resonant frequencies can be calculated as [8,9]

$$\omega_n^{free} = \frac{\lambda_n^2}{2\sqrt{3}} \frac{H}{L^2} \sqrt{\frac{E}{\rho}} \quad (26)$$

with $\lambda_0 = (0.596864\dots)\pi$, $\lambda_1 = (1.494175\dots)\pi$, $\lambda_n \rightarrow (n+1/2)\pi$. The subscript n represents the order of the frequency, such as the fundamental, the second mode, and thenth mode.

A similar equation to (26) holds for cantilevers in rigid contact with the surface. Since there is an additional restriction on the movement of the cantilever, namely the location of its endpoint, the resonant frequency increases. Only the terms of λ_n change, according to [9], as

$$\begin{aligned} \lambda_0' &= (1.2498763\dots)\pi, \\ \lambda_1' &= (2.2499997\dots)\pi, \\ \lambda_n' &\rightarrow (n+1/4)\pi \end{aligned} \quad (27)$$

The ratio of the fundamental resonant frequency during contact to the fundamental resonant frequency when not in contact is 4.3851.

For the torsional mode, the resonant frequencies can be calculated as

$$\omega_0^{tors} = 2\pi \frac{H}{LB} \sqrt{\frac{G}{\rho}} \quad (28)$$

For cantilevers in rigid contact with the surface, the following expression for the fundamental resonant frequency is obtained [9]

$$\omega_0^{tors,contact} = \frac{\omega_0^{tors}}{\sqrt{1 + 3\left(\frac{2L}{B}\right)^2}} \quad (29)$$

The amplitude of the thermally induced vibration can be calculated from the resonant frequency using

$$\Delta z_{therm} = \sqrt{\frac{k_B T}{k}} \quad (30)$$

where k_B is Boltzmann's constant and T is the absolute temperature. Since AFM cantilevers are resonant structures, sometimes with rather high Q values, the thermal noise is not as evenly distributed as (30)

suggests. The spectral noise density below the peak of the response curve is [9]

$$z_0 = \sqrt{\frac{4k_B T}{k\omega_0 Q}} \quad (\text{in m/(Hz}^{0.5}) \quad (31)$$

where Q is the quality factor of the cantilever, described earlier.

6. CONCLUSION

It is evident from (7) and (26) that one way to increase the natural frequency is to choose a material with a high ratio E/ρ ; see Table 1. for typical values of $\sqrt{E/\rho}$ for various commonly used materials.

Another way to increase the lowest eigenfrequency is also evident in (7) and (26). By optimizing the ratio H/L^2 , one can increase the resonant frequency. However, it does not help to make the length of the structure smaller than the width or height. Their roles will just be interchanged. Hence the optimum structure is a cube. This leads to the design rule that long, thin structures like sheet metal should be avoided.

For a given resonant frequency, the quality factor Q should be as low as possible. This means that an inelastic medium such as rubber should be in contact with the structure in order to convert kinetic energy into heat.

From (19) can be seen that thin, wide cantilevers with long tips favor torsion while cantilevers with square cross sections and short tips favor bending.

7. REFERENCES

- [1] Binnig, G., Quate, C. F., Berger, C. H.: *Atomic force microscope*, Phys. Rev. Lett. 56(9), pp. 930–933, 1986
- [2] Pradeep, T.: *Nano - The Essentials*, Tata McGraw-Hill Publishing Company Limited, New Delhi, 2007
- [3] Lindsay, S.M.: *Introduction to Nanoscience*, Oxford University Press Inc., New York, 2010
- [4] Binns, C.: *Introduction to Nanoscience and Nanotechnology*, John Wiley & Sons, Inc., 2010
- [5] Bhushan, B. (Ed): *Springer Handbook of nanotechnology*, Springer-Verlag Berlin Heidelberg, 2010
- [6] Pohl, D.W. : *Some design criteria in STM*, IBM J. Res. Dev. 30, pp. 417,1986
- [7] Mayr, M.: *Technische mechanik*, Carl Hanser Verlag, München, 2012
- [8] Thomson, W.T., Dahleh, M.D.: *Theory of Vibration with Applications*, 5th edn. Prentice Hall, Upper Saddle River, 1998
- [9] Colchero J.: *Reibungskraftmikroskopie*. Ph.D. Thesis, University of Konstanz, Konstanz 1993, in German

Author: Prof. Svetomir Simonović, Technical College, Bulevar Zorana Đinđića 152a, 11070 Belgrade, Serbia
E-mail: svsimonovic@gmail.com

Trajanoska, B., Gavriloski, V., Doncheva, E.

DEVELOPING AND TESTING HYBRID GLASS TO STEEL STRUCTURAL ELEMENTS – FLEXIBLE DESIGN APPROACH

Abstract: *Structural integrity of elements depends on their geometry, function and connections used between them. In this paper new hybrid glass to steel elements are investigated concerning their mechanical behavior and function which directly influences their design and vice versa. Their basic design is tested experimentally and then a flexible design approach including parametrical study is proposed for developing unique structural elements for different application. The concept design takes advantage of the mechanical properties of tempered glass, steel and polymer adhesive and achieves structural geometry which results in high mechanical, structural and architectural potential.*

Key words: *hybrid elements, glass and steel, design, concept, structural integrity*

1. INTRODUCTION

The geometry of structural elements, their function and connections used between them are the main three factors in gaining structural integrity in construction. The appearance and the behavior of a structure depend on the geometry and mechanical characteristics of the used materials.

Structural glass is a brittle isotropic material that is mainly used in construction for its transparency as an infill element in building's facade. However, today glass is known to be vital part of structures even as a bearing element. This comes as result of revolutionary changes in the processes of production, including glass product dimensions and forms as well as larger use of strengthening processes and laminated structures of glass panels. [1] All of these transformations are made with one cause of changing the mechanical behavior of the glass and make it more suitable for a structural element that can accept and transmit loads without compromising its integrity.

This paper presents new approach in designing hybrid structural element consisting of three different materials that acts as layered composite providing changed structural behavior of the element as whole. The concept design takes advantage of the mechanical properties of tempered glass, steel and polymer adhesive and achieves structural geometry which results in high mechanical, structural and architectural potential.

2. DESIGN CONCEPT OF HYBRID ELEMENTS

Glass, under normal temperatures of service behaves as a linear elastic material that will break when tensile stresses exceed a critical value. But the most prominent characteristic of glass as a structural element is its brittleness causing the glass elements to collapse suddenly, without any residual post-failure strength due to the brittle way of fracturing and its propagation through the whole element. [2] On the other hand, good compressive strength of the glass allows for including

connection elements with greater strength and hardness, like steel.

When using point support and bolted connections in connecting glass elements, stress concentrations occur, which demand using additional elements with appropriate mechanical characteristics able to accept and transfer stresses toward bearing structure providing more even stress distribution in the brittle element.

Greatest designers' challenge when working with glass elements is overcoming tensile strength as well as post-breakage behavior deficiency especially when it comes to glass planar elements. Other than known laminated design, other investigated design approach is to reinforce the overall structural capacity by adding a supporting layer or lamination. This can be done by combination of two materials developing a structural composite: individual or doubled glass plate and reinforcing steel layer [3]. The reinforcing layer could be used to enhance the load bearing capacity of the planar element or to introduce more plasticity in the structural behavior of the glass element and to enhance the post-breakage behavior of laminated glass [4]. The metal layer is added to the glass element usually perforated in order to provide certain level of transparency of the structural element. However, the use of standard perforated metal sheets although are adding to the load bearing capacity of the glass element, it is also reducing glass transparency and due to its standard formats of perforation it is limiting the architectural expression.

The presented hybrid elements in this paper consist of a single glass pane adhesively reinforced by a non-standard perforated stainless-steel sheet added in the tension zone of the structural element. This design results in layer composite element which provides added value in structural integrity by overcoming the brittleness of the glass, gaining post-breakage capacity and certain transparency level. All of these characteristics are among other factors (discussed in this paper) dependent on the perforation geometry which allows for free element design potential as well.

3. DEVELOPING AND TESTING THE HYBRID ELEMENTS

The new proposed concept of hybrid elements includes single tempered glass panel and thin perforated sheet (layer) of steel that form a laminated structure where the bond between laminates is made by means of adhesive and not the usual interlayer polymer materials used in producing laminated glass (PVB, EVA etc.).

The perforated metal layer is located at the tensile zone of the glass panel bonded with adhesive along the surface of the glass panel (Fig. 1). In this way, the reinforcement is achieved in the weakest zone of the panel where tensile stresses occur under out of plane bending. The used surface type of bonding allows for laminate effect of the structure and ensures composite action of the element.

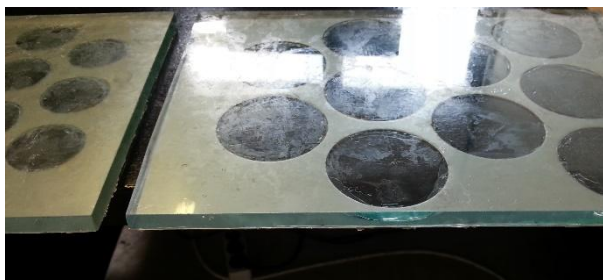


Fig. 1. Small scale models of the hybrid elements representing its structure (glass – adhesive – steel)

With the purpose of defining the mechanical characteristics and the reinforcement capacity, the new element underwent an experimental testing. Under standard four-point bending test, the structure is loaded with out of plane force which is distributed to the elasto-plastic perforated steel sheet that has a capacity of accepting higher stresses than the glass. (Fig. 2)

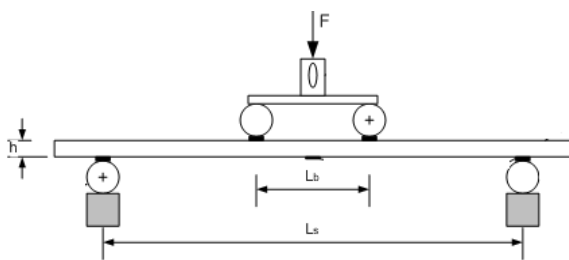


Fig. 2. Experimental setup of four point bending

Unified perforation of parallel grid of circle forms is used for the presented and tested models. The used glass pane in the hybrid models is made of fully tempered glass with experimentally defined bending strength of 200 MPa. The other two glass characteristics relevant for this testing are its Young's modulus of 70 000 MPa, which does not change with the glass thermal treatment, and Poisson's coefficient of 0,22. Steel reinforcement used in the models is made out of stainless steel with tensile strength of a 550 MPa. The surface bond to the metal layer to the glass panel is

made by structural adhesive type DC3145 which is silicon based. [6]

Evaluation of the mechanical properties of the elements is done in two phases. In the first phase, flat glass panes with the defined dimensions were tested, for evaluating the bending stiffness of a single tempered glass pane.

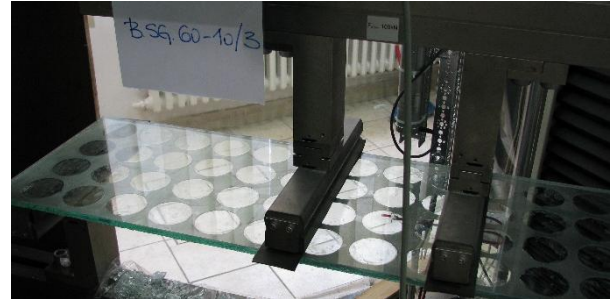


Fig. 3. Experimental setup for hybrid element

Considering probability for surface flaws that can influence the strength of the element, several specimens were tested.[5] In the second phase of the testing, hybrid elements consisting of glass panel with 10mm of thickness and a bonded reinforcement with circle forms of 60mm in diameter were tested. The setup of testing the reinforced elements is shown in figure 3.

In order to identify and define the post-breakage behavior, the testing was done until full element failure (Fig. 4).



Fig. 4. Full hybrid element failure

4. DISCUSSING RESULTS

The goal of the experimental testing was defining the composite action of the structural elements through measurable variables and observe the changes in the mechanical behavior of the new element as result of the included reinforcement. The composite action was defined by measuring the bending strength of the hybrid models. The standard used for the experimental testing defines the bending strength of the tested element by means of the maximal force of failure for the glass elements, and force at first crack for the hybrid elements (crack of glass pane). Thus, as results of this experimental testing a force deflection curves were gained and analyzed for the tested models (Fig.5)

Result force-deflection curves show existent residual strength of the structural element since the force magnitude increases again after the appearance of first crack, failure of the glass panel.

Different parameters influence the results of the testing, including manual technology of applying the

adhesive, thus different thickness of the adhesive along the surface of the elements, production flaws on the surface of the glass elements and edge conditions which is seen through deviation in results for different specimens of the hybrid model.

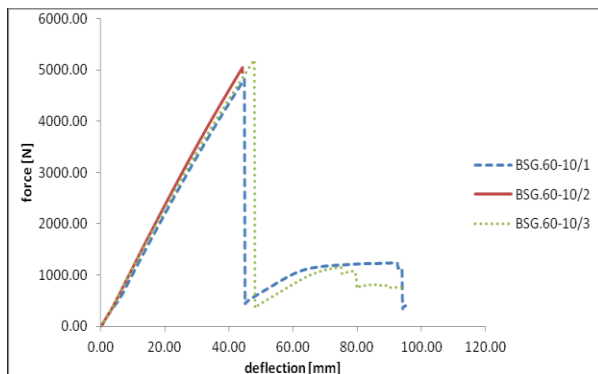


Fig. 5. Force-deflection curves for hybrid models (d=60mm)

The second specimen showed no post-breakage capacity and collapsed fully, quickly after glass panel failure.

Defining the influence of the perforation size was made by testing other set of element specimens with circle forms of 40mm in diameter. Comparative analysis shows different mechanical behavior of the hybrid elements depending on reinforcement layer perforation size (Fig. 6).

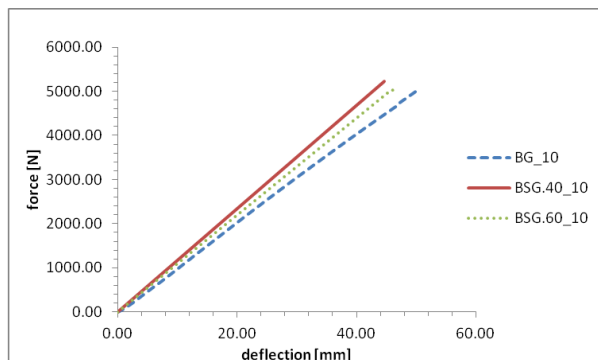


Fig. 6. Comparative force-deflection curves

Reinforced hybrid elements that use uniform perforation with smaller sized forms show greater increase in bending strength of the elements.

5. DIFFERENT DESIGN APPROACH

As stated before, the main factor influencing the mechanical properties of the new model is the perforation forms size. Having this in mind, a different design approach was investigated.

Namely, a parametrical analysis using finite element modeling was performed observing the influence of the perforation size and geometry on stress distribution in the glass panel under different element support conditions (Fig. 7).



Fig. 7. Stress distribution in glass panel – 4 nodes support tension zone

After defining the stress state of a glass pane under specific support and out of plane load, results were used to design perforation geometry and size. Different design concepts were gained using perforation form changer (Fig. 8). At the last stage of the numerical analysis, structural stress analysis was made, this time using the perforation element and the change in glass panel stress distribution was observed, as part of the modeled hybrid element.

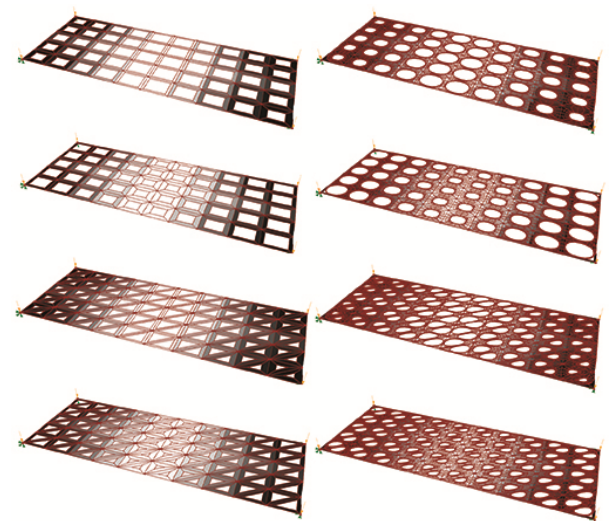


Fig. 8. Different perforation design concepts

Great change in stress distribution can be observed from the graphical preview of the models with four nodes support. The stress concentration near the supports is the biggest problem. As we can see from the results, these concentrations cannot be seen in the tensioned zone of the composite because the distribution of the stresses is more uniform. That is the side where reinforcement is applied with specific perforation forms (Fig. 9).

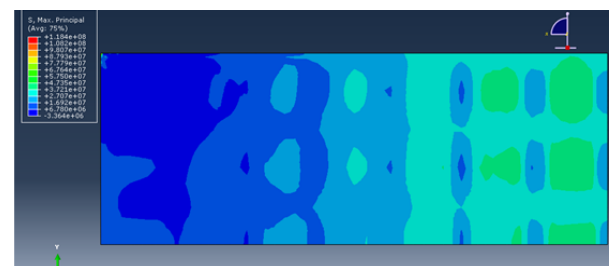


Fig. 9. Stress distribution in glass panel – 4 nodes support tension zone (hybrid element)

6. CONCLUSIONS

Structural integrity of an element is defined by its geometry and material properties. Using tempered glass that has no residual strength provides structural element that will collapse as soon as critical failure strength of glass is reached. Due to tempered glass breakage pattern, laminating this type of glass is one way of dealing with the problem, but usually in more than two glass panes or combination of glass types which increases the total weight of the structural element.

Another possible approach of solving the problem of post breakage behavior is applying reinforcement which has a ductile properties. Steel is this kind of material, which is used for forming hybrid glass elements concepts in form of laminated structures. This form of reinforcement allows for composite action which changes the mechanical behavior of the element and increases its overall mechanical strength.

The resulting hybrid elements are using the material properties advantage of a perforated steel layer with thickness of 1mm to act as reinforcement layer giving residual strength to a tempered glass panel by means of adhesive bonding to the glass elements tension zone and at the same time not compromising the overall transparency of the glass.

The perforation type of the reinforcement layer influences the mechanical characteristics of the hybrid element and thus providing design potential for achieving unique and different element depending on its function in the structure.

The parametrical analysis for defining the perforation shapes and size can be upgraded with additional deciding variables that can influence the design of the concept including light transmittance, transparency capacity, structural element support type etc.

7. REFERENCES

- [1] M. Haldimann, A. Luible, and M. Overend: Structural use of Glass. 2007.
- [2] Belis, J., Van Impe, R., Vanlaere, W., Lagae, G. Buffel, P. and M. De Beule: Glass Structures and Plasticity: Contradiction or Future?, Key Eng. Mater., vol. 274–276, pp. 975–980, 2004.
- [3] Feirabend, S. and Sobek, P. W.: Improved post-breakage behavior of laminated glass due to embedded reinforcement, Glass performance days 2009, pp. 726–729, 2009.
- [4] Nhamoinesu, S.: Steel-Glass Composite Structures (thesis), 2014.
- [5] F. a. Veer: The strength of glass, a nontransparent value, Heron, vol. 52, no. 1–2, pp. 87–104, 2007.
- [6] B. Trajanoska, V. Gavriloski, Z. Bogatinoski, F. Zdraveski: Glass – steel hybrid elements under four point bending test, Journal of Applied Engineering Science iipp, 13(2015)3, 322, 141 – 146, 2017.

Authors: Assist. Prof. Bojana Trajanoska, Full Prof. Viktor Gavriloski, Assist. Prof. Elisaveta Doncheva, "Ss. Cyril and Methodius" University in Skopje, Faculty of Mechanical Engineering, Rugjer Boshkovikj 18, 1000 Skopje, Macedonia, Phone.: +389 2 3099 200, E-mail: bojana.trajanoska@mf.edu.mk; viktor.gavriloski@mf.edu.mk; elisaveta.doncheva@mf.edu.mk



Section F:

**MECHANICAL ENGINEERING AND
ENVIRONMENTAL PROTECTION**

Ašonja, A., Mikić, D.

FACILITIES WITH RES ON PUBLIC BUILDINGS IN THE CITY OF NOVI SAD

Abstract: *In this paper were examined facilities with RES that were installed on public buildings in the City of Novi Sad. The facilities were examined and classified in two groups, namely, those of the City of Novi Sad and those that are not in the authority of the City of Novi Sad (objects under the jurisdiction of the Province and the Republic). Public buildings are selected, in this work, for analysis because the public sector that manages them at the EU level should be the actuator of all energy saving activities using EE, RES and etc. The aim of this paper was to analyze the current level of energy production from the RES on public buildings, to define the estimates of primary energy savings on an annual basis at these facilities.*

Key words: RES, public buildings, primary energy

1. INTRODUCTION

The history of EU energy policy and legislation has evolved much over the last 50 years [1, 2]. Reducing imported energy and energy products dependency is the goal of EU energy policy that promotes energy efficiency measures and renewable energy sources (RES) integration [3, 4].

The total potential of an energy source can be divided into three groups [5]:

- Theoretical potential - is defined as the total potential of an energy source that can be calculated theoretically. The budget is implemented on the basis of natural dispositions in some area. It depends on natural prerequisites and it is almost predictable variable;
- Technically achievable potential - is defined as the total potential that could turn into a useful form of energy with a positive material and energy balance from the standpoint of available technologies. It is slowly changing, and specially depends on the available technologies that can be applied and exploited.
- Economically viable potential - is defined as the total potential that can be financially justifiably exploited under given economic conditions. Observed potential depends of a number of factors, most of the current relationships in the energy market and it is very rapidly changing.

Typically, the technically achievable potential is usually taken into consideration for analyzing the potential of RES at a particular site.

2. THE POTENTIAL OF THE OIE IN THE REPUBLIC OF SERBIA AND THE CITY OF NOVI SAD

Technically usable energy potential of RES in the Republic of Serbia is very significant, and it is estimated to be over 4.3 million toe/year (toe – tones of oil equivalent) [6-9] - of which around 2.7 million toe per year (62.79 %) is produced from biomass exploitation; 0.6 million toe per year (13.95 %) in

unexploited hydro potential; 0.2 million toe per year (4.65 %) from the existing geothermal springs; 0.2 million toe per year (4.65 %) in wind energy and 0.6 million toe per year (13.95 %) in the exploitation of solar radiation [10-13].

The City of Novi Sad, as the center of the AP Vojvodina, is the most developed city in the AP Vojvodina, and the second in terms of development in the Republic of Serbia and it has huge potential for the production of RES, especially biomass, hydropower, solar energy and geothermal energy [14].

Novi Sad is the largest city of the Autonomous Province of Vojvodina. The City of Novi Sad is the administrative, economic, cultural, scientific and tourist center of AP Vojvodina and it is the seat of the provincial authorities and the administrative center of the South Bačka District. The City of Novi Sad has 15 suburban settlements, the municipality of Novi Sad covers an area of 702.7 km². The City of Novi Sad is the second city in Serbia according to the number of inhabitants in the administrative territory of Novi Sad, which has 341,625 inhabitants [15].

Observed from a broader point of view, the City of Novi Sad is located in the center of Europe, located at the intersection of roads between north and south, west and east of the continent. It is located in the Pannonian plain, the granary of Europe. The city of Novi Sad with the wider environment is destined to be an excellent logistic center for biomass - the remains of products from agricultural production. Such centers must not be located more than 15 km from the place of collection of raw materials due to transport costs [16].

Technical potential of RES at the level of the City of Novi Sad or Republic of Serbia is shown in Tab.1. On the territory of the City of Novi Sad, a significant number of family housing facilities use certain types of RES (mainly solar, geothermal and biomass energy), but these facilities are not the subject of research in the work.

The total RES potential for the City of Novi Sad was presented within the Study on Renewable Energy Sources in the City of Novi Sad [17], Tab.1. Estimation of the total potential of RES in the area of the City of

Novi Sad can be considered from two directions; if in accordance with the planning documents it is planned to build a hydroelectric power plant - in that case, hydropower in renewable sources will participate with 57%, and on the other hand, if the plan documents are abandoned and the hydroelectric power plants are not built - in that case the biomass energy in renewable sources will participate with 48%. It is assumed that the total potential of the RES in the area of the City of Novi Sad can cover 18-40% of the total needs of the city of Heat and Electricity. This, of course, depends on whether a large hydroelectric power plant will be built in the city area [17].

RES	City of Novi Sad [17]		Republic of Serbia [10-13]	
	teo*	%	teo	%
Solar energy	20,047	11.22	600,000	13.95
Biomass	35,699	19.98	2,700,000	62.79
Geothermal energy	18,045	10.10	200,000	4.65
Hydro energy	104,920	58.71	600,000	13.95
Wind Energy	0	0.00	200,000	4.65
In total	178,711	100,00	4,300,000	100,00

Table 1. Technical potential of the RES in the City of Novi Sad and the Republic of Serbia

*toe - tonne of oil equivalent (1 toe=41.869 GJ = 11.630 MWh electric energy = 2 t stone coal = 5.586 t raw lignite = 1.4 t soft coal = 1,270 m³ natural gas) [17].

In Tab.2 are shown data of the types of energy sources in use and the number of households using these energy products for the City of Novi Sad.

Types of energy sources	Number of households	Estimated percentage of participation
Remote heating	103,609	70%
Natural gas	32,069	20%
Electricity	No data	5%
Coal, wood	No data	5%

Table 2. Data of types of energy sources and the number of households that using individual energy sources

3. MATERIALS AND METHODS

The aim of this paper was to analyze the current level of energy production from the RES on public buildings, to define which estimates are the primary energy savings and which are CO₂ savings annually.

For the calculation of annual energy consumption, the excel form SEM 02/03 was used. In the paper, the methodology of the OPG "bottom up" will be used to estimate the final energy savings in kWh/yr for the built RES plants (solar collectors and boilers on

biomass). For a solar panel (power plant), a budget-based estimate will be used, generally accepted in practice.

3.1. Facilities with RES on public buildings in the City of Novi Sad (objects in the competition of the City of Novi Sad)

According to AENS data on the objects of the City of Novi Sad there are the following facilities with RES, Tab.2:

- In the "Nikola Tesla" Elementary School in 2014 a solar panel of 500 Wp was installed, the energy is stored in a battery and used for the needs of a classroom (lighting, etc.), Fig.1;
- In the Electrical Engineering School, "Mihajlo Pupin" in 2014 solar panels of 3 kWp power grid were installed, solar collectors (6 collectors TS 300 with total collectors ~ 11 m²) for heating hot water, (Fig.2a). Also, a small mini wind turbine of 500 W, (Fig.2b) and a biomass boiler of 22 kW were installed, but these two facilities will not be recorded in operation, as they are used in the form of teaching aids;
- On the roof of the Health Center in Zmaj Ognjena Vuka, solar collectors were installed in 2016 (32 collectors TS 300 with total collectors ~ 64 m²) for heating hot water in the building, Fig.3;
- In the Secondary Agricultural School in Futog in 2011 it was installed a boiler (200 kW of the manufacturer AD PODVIS TERM) on biomass (baled harvest residues). There is one biomass boiler that heats a separate school building;
- In the Health Center in Kisač in 2016, a boiler (TKAN 100 kW manufacturer Radiator Engineering) was installed on a biomass (pellet) that heats the building of the Health Center. The boiler efficiency is 91%.

RES	Investor	Public object name	Year of installation
Solar panel of-grid 500 Wp	Energy Agency City of Novi Sad, Novi Sad	ES Nikola Tesla, Novi Sad	2014
Solar panel of-grid 3 kWp	EU and City of Novi Sad	EES Mihajlo Pupin, Novi Sad	2014
Solar collectors	EU and City of Novi Sad	EES Mihajlo Pupin, Novi Sad	2014
Solar collectors	AP Vojvodina 79% and City of Novi Sad 21%	Health Center Zmaj Ognjena Vuka, Novi Sad	2016
Biomass boiler 200 kW	AP Vojvodina, Provincial Secretariat for Energy and Mineral Resources	Middle agricultural school with students' home in Futog	2011
Biomass boiler 100 kW	AP Vojvodina 79% and City of Novi Sad 21%	Health Center Kisač	2016

Table 3. Installed facilities with RES at public buildings in the City of Novi Sad - which are under the jurisdiction of the City of Novi Sad



Fig.1. Solar power plant ES „Nikola Tesla”



a)



b)

Fig.2. RES at the objects of Secondary Technical School "Mihajlo Pupin" Novi Sad, a) Solar panels and collectors and b) Wind turbine



a)



b)

Fig.3. Solar collectors - Health Center Zmaj Ognjena Vuka

In Fig.3, solar collectors for heating domestic hot water are shown - Health Center Zmaj Ognjena Vuka, the basic characteristics of the facilities are:

- Investment: 58,374 €,
- Annual savings of final energy 42,386 kWh/yr,
- Annual financial savings 3,226 €,
- Annual less broadcast 8.5 tCO₂/yr.

3.2. Facilities with RES on public buildings in the City of Novi Sad (objects under the jurisdiction of the Province and the Republic)

According to AENS data on public buildings in the City of Novi Sad, which are under the jurisdiction of the Province and the Republic, there are the following RES plants, Tab.4:

- At the objects of Faculty of Technical Sciences in Novi Sad, two solar power plants were installed - total power of about 24 kWp. In the first phase, a photovoltaic power plant of 8 kWp was installed above the amphitheater of the Faculty of Technical Sciences, which was put into operation in 2011 (Fig.4a), and later above the flat roof of the Machine Institute and the 16 kWp power plant that was put into operation in 2015 (Fig.4b);
- On the objects of the "Milorad Pavlović" Children's Home and Youth Center - solar collectors were installed in 2011 (32 collectors TS 300 total area ~57 m²) for heating of hot water. Equivalent energy of the collector is calculated in el. energy and it amounts 44.8 kWh;
- On the student dormitory of the object "Brankovo kolo" - in 2014 solar collectors (30 collectors TS 300, total area ~53 m²) were installed for heating hot water. Equivalent energy of the collector is calculated in el. energy is 42 kWh, Fig.5.

RES	Investor	Public object name	Year of installation
Solar power plants on-grid 24 kWp	Faculty of Technical Sciences, Novi Sad	Faculty of Technical Sciences, Novi Sad	2011 and 2015
Solar collector s, TS 300, (30 pcs)	AP Vojvodina, Provincial Secretariat for Energy and Mineral Resources	Student dormitory of the object "Brankovo kolo", Novi Sad	2011
Solar collector s, TS 300, (32 pcs)	„Termosolar” (Donation of the Slovakian company)	Children's Village „Dr.Milorad Pavlovic” Sremska Kamenica	2014

Table 4. Installed facilities with RES at public objects in the City of Novi Sad, which is under the jurisdiction of the Province and the Republic



a)



b)

Fig. 4. Solar power plants on-grid on Faculty of Technical Sciences a) At the administrative building b) On the building of the institute



Fig. 5. Solar collectors on student dormitory of the object "Brankovo kolo"

In Fig.5, there is shown a facility for heating hot water using solar collectors on the roof of the "Brankovo kolo" school building at Episkop Visarion Street no. 3 in Novi Sad installed in 2011. The basic characteristics of the facility are:

- Investment: od 17,583 €,
- Annual savings of final energy ~34,883 kWh/yr,
- Annual financial savings ~2,655 €/yr,
- Annual less broadcast 7 tCO₂/yr.

A good example of socially responsible behavior is the Coca Cola project, that financed the installation of solar public lighting on the playground at Liman near Štrand, Fig.6.



Fig. 6. Solar public lighting at the playground at Liman near Štrand

4. RESULTS OF RESEARCH

According to the data from Tab.3, the estimated annual primary energy savings for public buildings in the City of Novi Sad owned by the City of Novi Sad amount to 9.3 toe, Tab.5. According to the data from Tab.4, the estimated annual primary energy savings for public buildings in the City of Novi Sad owned by the Province and the Republic are 9.0 toe, Tab.5. The estimated annual primary energy savings for all public buildings in the City of Novi Sad is 18.3 toe, Tab.5.

Energy	Unit	Energy at the entrance	Final energy (toe)	Primary Energy (toe)	Emiss. CO ₂ (tCO ₂)
<i>Estimation of savings for public buildings under the jurisdiction of the City of Novi Sad</i>					
Solar energy	1.000 kWh	51.4	4.4	4.4	0
Biomass energy	t	54.7	4.9	4.9	43.0
<i>Estimation of savings for public buildings outside the jurisdiction of the City of Novi Sad</i>					
Solar energy	1000 kWh	104.2	9.0	9.0	0
In total	-	-	18.3	18.3	43.0

Table 5. Estimated annual primary/final energy savings to all public buildings in the City of Novi Sad

5. CONCLUSION

The current estimate of the primary energy savings from the RES plant at the level of public buildings in the territory of the City of Novi Sad amounts about 18.3 toe, and it grows year after year. This potential of energy produced at public buildings of the City of Novi Sad is currently the largest of all municipalities in the Republic of Serbia, and it is a result of the trend of the energy policy of the City of Novi Sad where renewable energy sources and healthy environment have priority.

From year to year it is growing the number of facilities that produce OIE, which are located on public buildings. Currently, the construction of heat pumps for heating buildings in 5 elementary schools is being completed in Novi Sad (some works are underway in some schools, and some are planned to be built). It is

planned that the new Central Music School that is being built has a built-in heating system with heat pumps. This year, the construction of solar panels in street public lighting starts. Also, there are currently more international IPA projects aimed at the construction of plants that produce RES at public facilities.

6. REFERENCES

- [1] Heffron, R. J.: *Energy Law: An Introduction*, Springer, New York, 2015.
- [2] Franjić, S.: *Legal regulations of European energy policy in Croatia*, Applied Engineering Letters, Vol.1, No.2, pp.39-44, 2016.
- [3] Ivanović, M.: *Contributions for The Establishment of a Regional Energy Policy For Renewables in The Slavonia and Baranja Region*, 24th Scientific Meeting Organisation and Technology of Maintenance, pp.25-33, 17 April, 2015, Donji Miholjac, Croatia.
- [4] Šerman, B., Glavaš, H., Vukobratović, M., Kraus, Z.: *TELOS Feasibility Analysis of Photovoltaic Power Plant*, Applied Engineering Letters, Vol.2, No.3, pp.91-97, 2017.
- [5] Škobalj, D., Đuričić, M., Lukić, S.: *The Sustainable Use of Geothermal Energy in Serbia*, Tractors and Power Machines, Vol.17, No.4, pp.29-42, 2012.
- [6] Komatina, MStupak., I., Perić, M.: *Legal Framework for Sustainable Use of Biomass in Serbia and Denmark*, 7th Symposium „Recycling Technologies and Sustainable Development“ 05-07 septembar 2012, Soko Banja, Serbia.
- [7] Trninić, M., Jankes, G., Stamenić, M., Simonović, T., Tanasić, N.: *Industrial Scale Demonstration Plant with Downdraft Gasifier coupled to Pebble Bed Regenerative Heater for CHP Production*, The 25th International Conference on Efficiency, Cost, Optimization, Simulation and Environmental Impact of Energy Eystems - Proceedings of ECOS 2012, pp.212/1-212/7, Perugia, Italy, 26-29 June, 2012.
- [8] Pucar, M.: *Building and Regulations in the Field of Energy Efficiency and RES in Serbia, Regional Countries and EU*, Network of Spatial Research and Planning in Central, Eastern and South Eastern Europe Network Conference 2012, Kecskemét (Hungary), 24-26 October 2012.
- [9] Pekez, J., Radovanovic, Lj., Desnica, E., Lambic, M.: *The increase of exploitability of renewable energy sources*, Energy Sources, Part B: Economics, Planning, and Policy, Vol. 11, No. 1, pp.51-57, 2016.
- [10] Pucar, M., Nenković-Riznić, M.: *Potencial and Spatial Distribution of Soft Energy Sources in Serbia*, International Conference: “Protection and Restoration of the Environment XI”, pp.1479-1488, Solun, 2012.
- [11] *Serbian Power Sector Current status*, 6th Partnership Activity PA PUCAERS, 25-29 October, 2010 Harrisburg, Pennsylvania.
- [12] Nikolić, R., Furman, T., Samardzija, M., Tomić, M., Simikić, M.: *The Use of Renewable Energy Sources in Serbia*, Tractors and Power Machines. Vol.16, No.3, pp.7-14, 2011.
- [13] Ašonja, A., Pekez, J., Janjić, N., Mikić, D.: *The Validity for the Application of Solar Energy in Irrigation of Perennial Plants in Fruit Growing in the Republic of Serbia*, Applied Engineering Letters, Vol.1, No.3, pp. 85-90, 2016.
- [14] Ašonja, A., Čirilović, R.: *Green Novi Sad*, The Serbian Academic Center, Novi Sad, 2017.
- [15] Ašonja, A., Rajković, J.: *An Energy Consumption Analysis on Public Applications in the City of Novi Sad*, Applied Engineering Letters Vol.2, No.3, pp.115-120, 2017.
- [16] *The Energy Efficiency Program of the City of Novi Sad 2013-2015*, Energy Agency City of Novi Sad, Novi Sad, 2016.
- [17] *Study on Renewable Energy Sources in the City of Novi Sad*, JP "Institute for Urbanism" Novi Sad, 2014
- [18] Ašonja, A., Manojlović, K., Aliđukić, E.: *Green Energy*, Training Center for Education – Energy Agency City of Novi Sad, Novi Sad, 2017.

Authors:

Assoc. Prof Aleksandar Ašonja

Energy Agency City of Novi Sad, Novi Sad, Serbia and Faculty of Economics and Engineering Management in Novi Sad, University Business Academy in Novi Sad, Serbia

E-mail: aleksandar.asonja@aens.rs
asonja.leksandar@fimek.edu.rs

Prof. dr Danilo Mikić

Higher Technical School of Professional Studies Zvečan-Kosovska Mitrovica, Serbia

E-mail: vtsm@open.telekom.rs

Bijelić, Z., Milanović, B., Miletić, D.

DEVELOPMENT OF MATHEMATICAL MODEL FOR OPTIMAL MANAGEMENT OF TECHNOLOGICAL DEVELOPMENT CHANGES

Abstract: *The goal of development management is to design optimal management of development systems and processes whose development is observed. Development is the most complex social activity, as it relates to future times. Today, under conditions of uncertainty before science, it is a challenge to make the future more certain. Mathematical modeling is today the most reliable method of managing development changes. The paper presents the original model for optimal systemic management of technological development. The design of optimal technological development is based on the methodology of reducing the multi-criteria function to the function of one variable by the application of the theory to the stage of sets.*

Key words: *modeling, optimization, system, development, change*

1. INTRODUCTION

Technology is a key factor in the development of all systems and processes. In this paper, the system is viewed from the aspect of the general theory of systems and cybernetics. The subject of observation is technical-technological, biological and organizational systems. Modern technological systems are extremely complex systems, both from the aspect of structures and from the aspect of management. Technological system subsystems are technical, biological and organizational systems. Each complex system is simultaneously an element of a more complex system, and is complex because it has its own structure of elements and the input and output of the system. The logical conclusion is that today's technological systems and processes are extremely intertwined from the aspect of governance and the aspect of the hierarchy of the system. [1]

The subject, or problem of this work, is an exceptional dynamic phenomenon related to future times, and these are the developmental changes.¹ It is known that the management of complex development-related systems leads to decision-making.² The decision-making process must address some of the extremely complex issues related to: what, how, who, when and why³?

¹Development is a change whose effects are expressed numerically and positively increasing. Presented by the mathematical form $Y_t - Y_{t-1} > 0$.

²Decision making is the same management and it is always about the problem that will happen in the future in the near or future time.

³The basic question that must be clearly defined is what is the object of decision. This problem and questions are mostly imposed by themselves and do not require specific knowledge. The second question, how is it, is the most complex as it relates to problem-solving technology. The third question implies that people who make decisions must know who can most effectively and effectively implement the problem that is the subject of decision-making. The fourth question is also very complex and requires multidisciplinary knowledge and a pavilion assessment of the timing of the decision-making process. The last question is to get an answer related to the goals and benefits of executing the subject matter of the decision. The

In this paper a mathematical model for the optimal management of development changes is developed, which brings the problem of multi-dimensional decision making to an integrated single-dimensional system with one input and output in discrete time. The goals of the work are to demonstrate to the scientific public that it is possible to mathematically model development (the most complex phenomenon from the aspect of management, that is decision making). The paper presents a basic and one additional hypothesis. Both hypotheses have been confirmed.

2. GENERAL NOTES RELATED TO DEVELOPMENT CHANGES

2.1 Development systems

Development systems are systems that are created for the purpose of abstract representation of growth and development of the real system (object). The facility can have many different development systems. If the system includes a smaller number of development factors, it is simpler. With the growth of the number of developmental factors in the development system, the complexity of development management systems is growing.⁴ Development systems are by nature dynamic systems, that is, the state of the system is a function of time. This fact greatly complicates the management. The efficiency and effectiveness of development systems and processes is a numerical measure of the ability of the development system to optimally manage the developmental changes. The most widely used measure of ability is the success of the developmental

basic hypothesis reads: Technological development changes can be mathematically modeled for the purpose of optimization.

⁴ Additional hypothesis: The developed model of mathematical optimization is in accordance with the author's doctrine: Optimus economy, optimal technological progress and optimal business. It is known that the complexity of management (SU) systems is approximately equal to the factor of the number of system elements (N), ($SU = N!$). [2]

change. The success of a development change is a function of a number of independently variable.

A possible structure of the set of factors on which the success of development changes depends on: [1]

1. The power (energy) of the change,
2. Knowledge (basic technological and managerial),
3. Resistance to change,
4. Motivation for changes,
5. Influence of infection on changes,
6. The risk of change,
7. Speed of change and
8. Other.

Using the theory of the stage of conferences with the excellent knowledge of the scientific field to which the development system belongs, it is easy to mathematically model the success of developmental changes as a function of the aforementioned factors [3, 5, 6, 7]. Analogously to the modeling of the success of a development change, it is possible to model any problem related to technological development systems of a technical, biological and organizational nature. Successful modeling requires multidisciplinary knowledge.

2.2 Development technology systems

The basic three characteristics of all technological development systems from the perspective of system theory and cybernetics are: dynamics, manageability and openness. [1, 4, 8] Dynamism is a key feature of the technological development system. Technological development systems are the driving force of not only technological progress, but a driver of a series of developmental changes. In literature and practice, technology-development systems are called modern systems. Under the influence of the constant growth of the dynamics of changes in the environment and internal changes in the system, an increasingly complex situation for managing the development is being created. This state of result is paradox. It is logical that with the growth of the complexity of the situation, the time needed to adjust to changes is growing. However, the available time to adapt to the environment is reduced with the increasing complexity of management.

One of the biggest problems in managing the technological development of a certain space is the dual evaluation of technological and developmental changes. The developmental change in the concise situation of managing technological development changes can be viewed as an input or output of the system, and at the same time one and the other. If we consider the development change as the input of the system, then it is a technological mechanism of change, and if we consider it as an output, then we have the result of management that is measured by the effects, or degree is used by some thought projected change.⁵ [1].

⁵Duality means the opposite. However, this is not about the contrast of the black-and-white type, but the type of day-night. In the first case, we have exclusivity because they can either one or the other, and in the other case day and night are part of one whole only with a time shift.

When it comes to technological development systems and technological development changes from the aspect of duality we can have two extreme situations. First, from the aspect of longer time observation, we have the emergence of a technology, to replace this technology with new technology for a certain time interval.⁶ However, one or other technology can be designed from the aspect of use for the needs of an organizational system.⁷

This behavior in practice requires science to explore the possibility of applying in the practice of optimum management from the level of system hierarchy in a complex global system structure. Secondly, the problem that the world is facing today in terms of new technologies is conflict technology with natural systems.⁸ The third problem is in various types of latent interest. The solution of the problem is in optimizing integrated changes (graphic illustration of Fig.1.) [1].

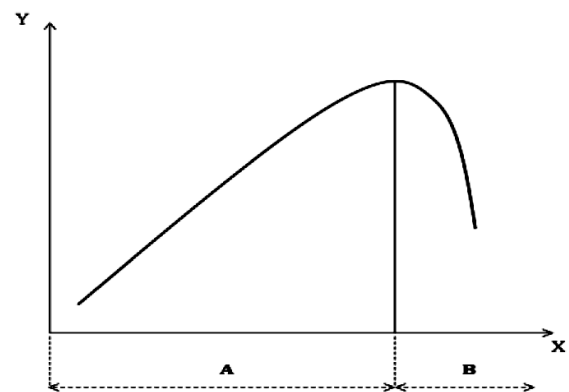


Fig.1. Optimizing integrated

3. MATHEMATICAL MODEL FOR OPTIMAL MANAGEMENT TO TECHNOLOGICAL DEVELOPMENT CHANGES

3.1 System modeling

Technological development changes are an extremely complex problem for optimization. Optimization in itself implies that the efficiency of

⁶In the first case, technology is the output of a system called technological progress, and in the second case, technologies are an entry into a system that is transformed into a product for the market. In the case of a biological system such as a man with his knowledge, in the first case, it is about two types of knowledge that have arisen in two time phases, and in the second, two technologies from which only one can be used (two types of remedies for the treatment of diseases arising in various time phases). With the technical systems, we can implement a construction with one or another type of material.

⁷Developed countries, and above all multinational corporations, many technologies are sold to the poor and underdeveloped as an exclusively right solution without taking into account whether this is the optimal solution for the poor, but educating them from the point of view of their own optimality.

⁸Sometimes the technologies used natural systems as a resource for human needs, without the environmental nature being threatened. Today's modern technologies in the heated number with a certain degree of danger threaten the nature of the environment. This is an additional argument, that underdeveloped countries must find a mechanism for optimization from the point of view of their values and benefits [13].

technological changes is measured numerically. It has already been pointed out that a higher value measure of efficiency technologies does not determine what is of modern character. In many situations it is more efficient to solve a technological problem by applying traditional than modern technologies. The problem must be considered systematically and, depending on the evaluation criteria in the conditions of different constraints, the optimal solution will be different. Depending on the hierarchical level (macro or micro) in the creation of the system, the structure of the important inputs and outputs to the system should be determined (Fig. 2.).

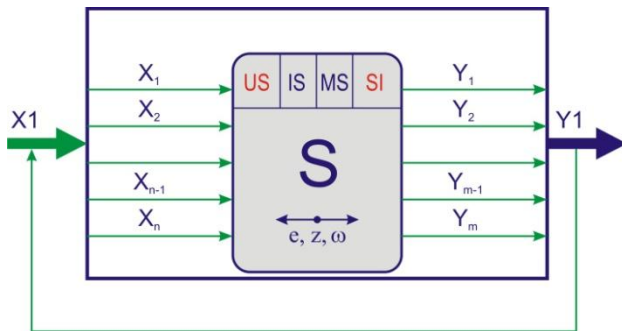


Fig. 2. System structure

In the situation where the subject matter of the observation is the industrial system, the most common evaluation criterion or system exit (Y_m) are: economic, technical, ecological, safety and criteria of degree of reliability, sensitivity, stability and degree of product quality. The input structure (X_n) consists of resources (material, immaterial and informational). The industrial system (S) using technological structures transforms the inputs into outputs based on the projected evaluation criterion.⁹

3.2 Mathematical model for optimization of management technological development changes

Under the conditions of technological progress, the structure of all subsystems of the industrial technological system is extremely complicated, and the complexity of management gets an exponential character in relation to the number of elements in the structure of the system [7, 8]. This situation is not a reason to not mathematically model the developmental changes in order to optimize the structures and dynamics of technological level growth for a specific complex hierarchical system at macro or micro level.

The author developed a general systemic approach to mathematical modeling based on a scientific idea to integrate multidimensional inputs and outputs using the

phase of sets [1, 3, 6, 7, 8]. The mathematical form of integration using the phase of sets, and on the structure of the system input and output (S) (Fig. 2.), would be:

$$X = p_1 X_1 + p_2 X_2 + \dots + p_n X_n \quad (1)$$

$$Y = s_1 Y_1 + s_2 Y_2 + \dots + s_m Y_m \quad (2)$$

Developmental changes by nature are a growing function of time. The time of the observed developmental changes should be divided into a number of time phases, and for each phase determine the value of the integrated input and output. Based on such specific integrated phase inputs and outputs, it is easy to determine in the first step the functions that satisfactorily reflect the dependence of the integrated input and output in the function of time. In the second step, the elimination of time gives the function $Y = F(X)$. Fig. 3. shows a graphic illustration.¹⁰

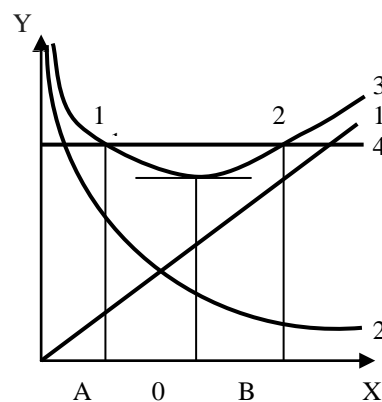


Fig.3. Efficiency of technological changes as a function of the complexity of the technological system

As a measure of the efficiency of developmental changes in the technological character of a real system (entity), it is best to shift from the point of financial investment to developmental changes.¹¹

Total financial margins (Y_3) will be a sum of two functional components Y_1 and Y_2 and limited to level Y_4 . The situation on the graph can be very well represented by the following mathematical function:

$$Y_3 = aX + b/X \quad (3)$$

The form thus acquired is a very simple mathematical function whose optimal solution is the minimum level of financial investment (Y_0). The zone of possible solutions is in the interval A to B .¹²

⁹39 years ago at the time of intensive automation of technological systems, the author advocated the scientific position that automation can not be an objective, but an instrument of efficiency. [5]. Today stands for the view that modern technology can not be the only goal from the point of view of use, but the goal must be the production of technologies in system structures for the needs of the system and environment (market).

¹⁰Models thus created are a logistic mechanism in the function of the decision-making process related to developmental changes. In a concrete situation, the technological change model reflects a reality with a greater or lesser degree of accuracy. However, from the aspect of reliability and benefit, it is better to use mathematical improvisation to manage development projections rather than make decisions based on various descriptive strategic plans for technological warfare. [1]

¹¹Multi-dimensional effects (partial outputs) are most easily integrated with measured financial value.

¹²Financial investment (Y_1) grows with the complexity of technology systems (X). Possible financial loss (Y_2) due to inefficient technology is reduced with the increase in the complexity of technological systems (X).

3.3 Real industrial system

For an example of the real system, an extremely complex technological object is taken from the aspect of decision-making in the design phase and the operational operation stage.

During the war in Bosnia and Herzegovina, the first author of this paper realized a very complex project: explosives foundry for mortar ammunition. From the aspect of the problem of this work, the project has a high level of applied scientific and developmental research.¹³ Fig. 4. shows the technological structure of the foundry [1, 13].

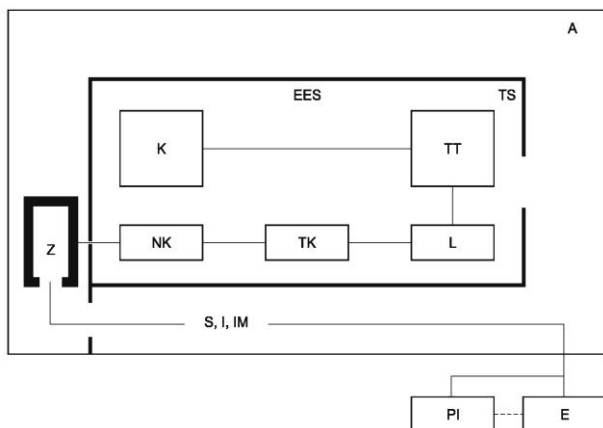


Fig. 4. The technological structure of the explosive foundry

K-Hot water boiler, TT-Solving, L-Casting, TK-Timing, NK-Pouring, Z-Drilling, A- Ambiance, EES-Electroenergy system, S-Stock, I-Examination, IM-Integraton of mines, PI-Polygon testing, E-Exploitaion

The project was implemented in wartime conditions characterized by: lack of financial resources, lack of experience in explosive technologies, lack of adequate space from the aspect of security, lack of adequate heat source and instability of electricity supply. the project had to be implemented within a precisely determined period of three months.

Using the mathematical modeling of the project, an optimal solution to the problem was found.¹⁴

4. RESULTS OF RESEARCH

4.1 Synthesis of research results

The goals of the paper are to demonstrate to the scientific public that it is possible to model technological development changes mathematically. The aim of the work is achieved by the development of the model (3).

The paper presents a basic and one additional hypothesis. The basic hypothesis reads: Technological development changes can be mathematically modeled for the purpose of optimization.

Additional hypothesis: The developed model of mathematical optimization is in line with the author's doctrine: **Optimus economy, optimal technological progress and optimal business.**

Both hypotheses have been confirmed by the development of a mathematical model (3).

4.2. Conclusion

Today, when changes occur extremely quickly and when extremely uncertain, technological developments can be mathematically modeled in order to optimize the structure and dynamics of change. Designed models will enable the development projects to be more reliable. In order for designers to successfully design a development path, they need to have multidisciplinary knowledge.

5. REFERENCES

- [1] Bijelić, Z., Razvoj modela optimizacije upavljanja integrisanim razvojnim promjenama, Postdoktorska disertacija, Univerzitet u Novom Sadu, Fakultet tehničkih nauka.
- [2] Zelenović, D., Inteligentno privređivanje, Prometej, Novi Sad.
- [3] Tadić, D., Teorija fazi skupova, Mašinski fakultet, Kragujevac,
- [4] Sorak, M., Medadžment proizvodnje, Tehnološki fakultet, Banja Luka.
- [5] Bijelić, Z., Ocjena opravdanosti primjene automatizovane proizvodnje, Časopis Direktor broj 10/1982, pp 21.
- [6] Bijelić, Z., Milanović, B., Razvoj integrisanih modela primenom integrisane optimizacije u funkciji integrisanog kvaliteta, ETIKUM 2017, Novi Sad.
- [7] Bijelić, Z., Milanović, B., Bijelić, M., Integrisana nauka i integrisane poslovne studije u funkciji integrisanog razvoja, Konferencija NAUKA I PRAKSA 2017, Zbornik radova, pp 104-117, Banja Luka.
- [8] Bijelić, Z., Milanović, B., Jovišić Simić, M., Industrial systems from crisis to development, IS'17 Novi Sad, pp 430-435.
- [9] Petrović, R., Specijalne metode optimizacije sistema, Tehnička knjiga, Beograd.
- [10] Stanić, J., Uvod u teoriju tehnoekonomske optimizacije, Mašinski fakultet, Beograd.
- [11] Madžar, Lj., Osnovi teorije proizvodnje, Oeconomica, Beograd.
- [12] Bijelić, Z., Cvijić, M., Own production technology as akeyout of powerty, The 3rd Intrnational Scientif Conference CAPITALISM IN TRANSITION, Zbornik radova (pp 181-190), Beograd.
- [13] Bijelić Z. i dr.,Projekat: Livnica eksploziva u ratnim uslovima, Banja Luka.

Authors: Prof. PhD Zdravko Bijelić. M.Sc. Biljana Milanović i PhD Dragan Miletić, Inastitute to be established „LOGOS“ Novi Sad.
E-mail: bijeliczdravko51@gmail.com;
milanovicb82@gmail.com ; dragmil@gmail.com

¹³Due to the limited space in this paper, a brief description of the problem faced by designers is given.

¹⁴The deadline was determined on the basis of a reliable insight into non-residential plans.

Cveticanin, L., Zukovic, M.

PROPERTIES OF MASS-IN-MASS UNITS OF THE ELASTIC METAMATERIAL

Abstract: Recently, significant investigations are done in the so called 'elastic metamaterial'. It is a kind of composites where in the basic material mass-in-mass units are incorporated with the aim to eliminate vibrations at certain frequencies. The units are modeled as two-degree-of-freedom oscillatory systems with strong nonlinear elastic and damping properties. Mathematical description of the unit is a system of two coupled non-homogenous second order differential equations. The aim of the paper is to solve equations and to analyze the influence of the nonlinear properties of the mass-in-mass units on the wideness of the frequency stop-bands. We developed a new analytical solving procedure for treating of equations. The method is based on the perturbation of the exact solution for the truly nonlinear oscillator. To prove the correctness of the computed results, they are compared with numerically obtained ones.

Key words: nonlinear oscillations, two-degree-of-freedom system, primary resonance

1. INTRODUCTION

Elastic metamaterial is a new kind of composites made to eliminate vibrations and mitigate the energy of vibration at certain, mostly low, frequencies [1]. The most widely spread metamaterial has the honey comb structure, obtained by 3D printing, fulfilled with units which act as vibration absorbers [2]. Numerous experiments with the metamaterial are done (see [3-5]). It is concluded that the vibration absorption depends on the mechanical properties of the metamaterial units. Analytically, the units are modeled as forced two-degree-of-freedom oscillatory systems. Mathematical description of the unit is a system of two coupled non-homogenous second order differential equations. Most of investigation is done with linear models [6,7]. Unfortunately, in spite of the fact that the model is very simple, it is shown that the obtained results are far to be satisfactory. It is the reason that the nonlinear property of the mass-in-mass system is added [8]. Equations of motion are more complex due to strong nonlinearity but more close to the real system.

The aim of this paper is to analyze the influence of the nonlinear properties of the mass-in-mass units on the vibration stop-bands. A new analytical solving procedure for treating strong nonlinear equations is introduced. The method is based on the perturbation of the exact solution for the truly nonlinear oscillator. The obtained solutions depend not only on the parameters of excitation but also on the order and coefficient of nonlinearity of the system. To prove the correctness of the analytical results, they are compared with numerically obtained ones.

2. MODEL OF THE MASS-IN-MASS UNIT

In Fig.1 the mass-in-mass unit is plotted. The basic mass m_1 is connected with an additional mass m_2 with elastic properties modeled with a spring with nonlinear elastic property. On the basic mass an external excitation force acts.

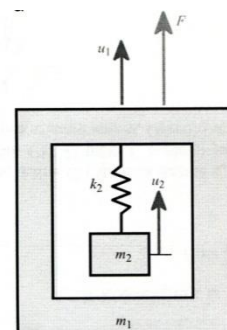


Fig. 1. Mass-in-mass model

Motion of masses is given with u_1 and u_2 , respectively. Mathematical model of the system is

$$m_1 \ddot{u}_1 + c(\dot{u}_1 - \dot{u}_2) + k_2(u_1 - u_2) + k_\alpha(u_1 - u_2)|u_1 - u_2|^{\alpha-1} = F_0 \exp(i\Omega t), \quad (1)$$

$$m_2 \ddot{u}_2 - c(\dot{u}_1 - \dot{u}_2) - k_2(u_1 - u_2) - k_\alpha(u_1 - u_2)|u_1 - u_2|^{\alpha-1} = 0, \quad (2)$$

where $\epsilon \in \mathbb{R}_+$, c_l is the coefficient of damping, k_2 and k_α are coefficients of the linear and nonlinear stiffness, u_1 and u_2 are independent displacement functions, F_0 and ω are amplitude and frequency of excitation. Introducing the new variable $x = u_1 - u_2$, after some transformation, the relative motion of masses is obtained as

$$\ddot{x} + \frac{k_2}{M}x + \frac{k_\alpha}{M}x|x|^{\alpha-1} + \frac{c_l}{M}\dot{x} = \frac{F_0}{m_1}\cos(\Omega t), \quad (3)$$

where $\frac{1}{M} = \frac{1}{m_1} + \frac{1}{m_2}$. The equation (3) is strong nonlinear. To find the closed form solution is impossible. It is the reason that an approximate solving procedure for the problem is developed.

3. SOLVING PROCEDURE

For the case when damping and excitation are small and the linear elastic term is much smaller than the nonlinear term, the equation (3) transforms into

$$\ddot{x} + K_\alpha x|x|^{\alpha-1} = \epsilon F \cos(\Omega t) - \epsilon kx - \epsilon c\dot{x}, \quad (4)$$

where $\epsilon \ll 1$ is a small parameter and

$$K_\alpha = \frac{k_\alpha}{M}, \quad \varepsilon F = \frac{F_0}{m_1}, \quad \varepsilon c = \frac{c_l}{M}, \quad \varepsilon k = \frac{k_2}{M} \quad (5)$$

For $\varepsilon=0$ the equation (5) transforms into a truly nonlinear differential equation

$$\ddot{x} + K_\alpha x|x|^{\alpha-1} = 0 \quad (6)$$

In general the solution of (6) is (see [9])

$$x = Aca(\alpha, 1, \omega t + \theta), \quad (7)$$

where ca is the cosine Ateb function, A and θ are arbitrary constants of integration and Ω is the frequency which satisfies the relation

Substituting (7) and derivatives of Ateb functions [10]

$$\begin{aligned} \dot{x} &= -A\omega \frac{2}{\alpha+1} sa(1, \alpha, \omega t), \\ \ddot{x} &= -A\omega^2 \frac{2}{\alpha+1} ca^\alpha(\alpha, 1, \omega t) \end{aligned} \quad (8)$$

into (6) we obtain

$$\omega^2 = \frac{\alpha+1}{2} K_\alpha A^{\alpha-1} \quad (9)$$

where sa is the sine Ateb function.

Comparing (4) and (6) it can be concluded that (4) is the perturbed version of the relation (6). Then, we can assume that the solution of (4) has to be the perturbed version of the solution of (6), i.e. of (7).

Let us assume the solution of (4) and its first time derivative in the form (7) and (8)

$$x = Aca(\alpha, 1, \psi), \quad \dot{x} = -A \frac{2}{\alpha+1} \omega sa(1, \alpha, \psi), \quad (10)$$

where $A=A(t)$, $\psi=\psi(t)$ and

$$\dot{\psi} = \omega + \dot{\theta} \quad (11)$$

Comparing the expression (10)₂ with the first derivative of (10)₁

$$\begin{aligned} \dot{x} &= -A \frac{2}{\alpha+1} \omega sa(1, \alpha, \psi) + \dot{A} ca(\alpha, 1, \psi) - \\ &A \frac{2}{\alpha+1} \dot{\theta} sa(1, \alpha, \psi), \end{aligned} \quad (12)$$

the constraint follows

$$\dot{A} ca - A \frac{2}{\alpha+1} \dot{\theta} sa = 0, \quad (13)$$

where $ca=ca(\alpha, 1, \psi)$ and $sa(1, \alpha, \psi)$.

Using the time derivative of (10)₂ and also the relations (10) the equation (4) transforms into new variables A and ψ , i.e., θ

$$\begin{aligned} -\frac{2}{\alpha+1} \frac{d}{dt} (A\omega) sa - \frac{2}{\alpha+1} A\omega \dot{\theta} ca^\alpha &= \varepsilon F \cos(\Omega t) - \\ &\varepsilon k Aca + \varepsilon c \frac{2}{\alpha+1} \omega A sa. \end{aligned} \quad (14)$$

Using (9) and the relation [9]

$$sa^2 + ca^{\alpha+1} = 1, \quad (15)$$

equations (13) and (14) transform into

$$-\dot{A}\omega = \varepsilon F \cos(\Omega t) sa - \varepsilon k A sa ca + \varepsilon c \frac{2}{\alpha+1} \omega A sa^2, \quad (16)$$

$$\begin{aligned} -\frac{2}{\alpha+1} A\omega \dot{\theta} &= \varepsilon F \cos(\Omega t) ca - \varepsilon k A ca^2 + \\ &\varepsilon c \frac{2}{\alpha+1} \omega A sa ca. \end{aligned} \quad (17)$$

To solve (16) and (17) is not an easy task. In this paper the special case of primary resonance is considered.

4. PRIMARY RESONANCE

Let us transform the Ateb functions into trigonometric one with period 2π . Namely, using the periodicity of the Ateb function [9]

$$2\pi_\alpha = 2B\left(\frac{1}{2}, \frac{1}{\alpha+1}\right), \quad (18)$$

And equating the periods of vibration of the Ateb function and of the trigonometric one we have

$$T = \frac{2\pi_\alpha}{\omega} = \frac{2\pi}{\omega^*} \quad (19)$$

where B is the complete beta function, i.e., the first order Euler function [11] and Ω^* is the corresponding frequency of the trigonometric function. In Fig.2 the ca Ateb functions with frequency

$$\omega = \frac{B(\frac{1}{2}, \frac{1}{\alpha+1})}{\pi} \omega^* \quad (20)$$

are compared with cosine trigonometric function with frequency $\Omega^*=1$. It is seen that

$$ca(\alpha, 1, \omega t) \approx \cos(\omega^* t). \quad (21)$$

Using the Fourier series expression of the ca function [12] it is

$$ca(\alpha, 1, \omega t) = \sum_{n=1}^{\infty} a_n \cos\left(\frac{n\pi\omega}{\pi_\alpha} t\right) \quad (22)$$

or applying (20) it is

$$ca(\alpha, 1, \omega t) = \sum_{n=1}^{\infty} a_n \cos(n\omega^* t) \quad (23)$$

where

$$a_n = \frac{1}{T} \int_0^T ca(\alpha, 1, \Omega t) \cos(n\omega^* t) dt. \quad (24)$$

It is evident that the first term of series expansion (23) corresponds to the function $\cos(\omega^* t)$.

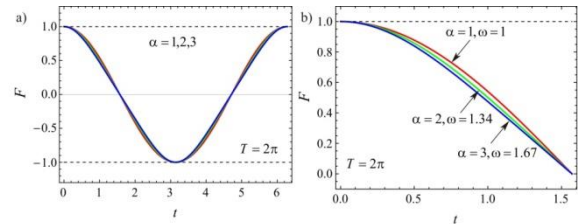


Fig. 2. a) Cosine Ateb functions $F(t)$ with the period $T=2\pi$; b) $F(t)$ functions with variable α and ω and constant period T

Omitting the higher terms of series expansion (23) equations (16) and (17) are rewritten in the form

$$\begin{aligned} -\dot{A}\omega &= \varepsilon F \cos(\Omega t) \sin\psi_1 - \varepsilon k A \sin\psi_1 \cos\psi_1 + \\ &\varepsilon c \frac{2}{\alpha+1} \omega A \sin^2\psi_1, \end{aligned} \quad (25)$$

$$\begin{aligned} -\frac{2}{\alpha+1} A\omega \dot{\theta} &= \varepsilon F \cos(\Omega t) \cos\psi_1 - \varepsilon k A \cos^2\psi_1 + \\ &\varepsilon c \frac{2}{\alpha+1} \omega A \sin\psi_1 \cos\psi_1, \end{aligned} \quad (26)$$

where

$$\psi_1 = \omega^* t + \theta. \quad (27)$$

For the case when the difference between the excitation frequency and the frequency of the system is small we have

$$\Omega = \omega^* + \varepsilon\sigma \quad (28)$$

where $\varepsilon\sigma \ll 1$. For the phase angle (27) we have

$$\Omega t = \psi_1 + \gamma \quad (29)$$

where

$$\gamma = \varepsilon\sigma t - \theta \quad (30)$$

Substituting (29) into (25) and (26) we obtain

$$-A\omega = \varepsilon F \cos(\psi_1 + \gamma) \sin\psi_1 - \varepsilon k A \sin\psi_1 \cos\psi_1 + \varepsilon c \frac{2}{\alpha+1} \omega A \sin^2\psi_1, \quad (31)$$

$$-\frac{2}{\alpha+1} A \omega \dot{\theta} = \varepsilon F \cos(\psi_1 + \gamma) \cos\psi_1 - \varepsilon k A \cos^2\psi_1 + \varepsilon c \frac{2}{\alpha+1} \omega A \sin\psi_1 \cos\psi_1. \quad (32)$$

For simplification the averaging procedure is introduced. Averaging the equations over the period of functions and using the averaged values

$$\frac{1}{2\pi} \int_0^{2\pi} \sin^2\psi_1 d\psi_1 = \frac{1}{2\pi} \int_0^{2\pi} \cos^2\psi_1 d\psi_1 = \frac{1}{2},$$

$$\frac{1}{2\pi} \int_0^{2\pi} \sin\psi_1 \cos\psi_1 d\psi_1 = 0$$

we obtain

$$\dot{A}\omega = \frac{1}{2} \varepsilon F \sin\gamma - \varepsilon c \frac{1}{\alpha+1} \omega A, \quad (33)$$

$$\frac{2}{\alpha+1} A \omega \dot{\theta} = -\frac{1}{2} \varepsilon F \cos\gamma + \frac{1}{2} \varepsilon k A. \quad (34)$$

Finally, using (30) we have

$$\dot{A}\omega = \frac{1}{2} \varepsilon F \sin\gamma - \varepsilon c \frac{1}{\alpha+1} \omega A, \quad (35)$$

$$\frac{2}{\alpha+1} A \omega \dot{\gamma} = \frac{2}{\alpha+1} A \omega \varepsilon\sigma + \frac{1}{2} \varepsilon F \cos\gamma - \frac{1}{2} \varepsilon k A. \quad (36)$$

Equations (35) and (36) are the averaged differential equations of motion.

4. STEADY-STATE SOLUTION

For the steady state motion when $\dot{A} = 0$ and $\dot{\gamma} = 0$ two nonlinear algebraic equations follow

$$\frac{1}{2} \varepsilon F \sin\gamma = \varepsilon c \frac{1}{\alpha+1} \omega A, \quad (37)$$

$$\frac{1}{2} \varepsilon F \cos\gamma = \frac{1}{2} \varepsilon k A - \frac{2}{\alpha+1} A \omega \varepsilon\sigma. \quad (38)$$

Eliminating the parameter γ and using (9) we obtain $F^2 =$

$$4A^2 \left[\left(\frac{c}{\alpha+1} \right)^2 \frac{\alpha+1}{2} K_\alpha A^{\alpha-1} + \left(\frac{1}{2} k - \sigma \sqrt{\frac{2}{\alpha+1} K_\alpha A^{\alpha-1}} \right)^2 \right] \quad (39)$$

Equation (39) is an implicit equation for the amplitude of the response A as a function of the detuning parameter σ (the frequency of excitation), amplitude of excitation F and order of nonlinearity α . The relation (39) represents the frequency-response equation for the resonance case of the strong nonlinear oscillator. After some transformation it is

$$\left(\frac{1}{2} k \pm \sqrt{\frac{F^2}{4A^2} - \left(\frac{c}{\alpha+1} \right)^2 \frac{\alpha+1}{2} K_\alpha A^{\alpha-1}} \right) \sqrt{\frac{\alpha+1}{2K_\alpha A^{\alpha-1}}} = \sigma$$

The equation indicates that the peak amplitude is

$$A_p = \left(\frac{F^2}{2K_\alpha c^2} (\alpha+1) \right)^{1/(\alpha+1)}, \quad (40)$$

for the detuning parameter

$$\sigma_p = \left(\frac{1}{2} k \right) \sqrt{\frac{\alpha+1}{2K_\alpha A^{\alpha-1}}} = \left(\frac{1}{2} k \right) \left(\frac{c}{F} \right)^{\frac{\alpha-1}{\alpha+1}} \left(\frac{\alpha+1}{2K_\alpha} \right)^{\frac{1}{\alpha+1}}. \quad (41)$$

The peak amplitude depends on the excitation amplitude, coefficient and order of nonlinearity. It is obvious that the peak amplitude does not depend on the coefficient of the linear elastic force. The peak amplitude is higher for higher values of excitation, while is smaller for higher value of the damping coefficient. The higher is the coefficient of nonlinearity the amplitude of vibration is smaller. However, the position of maximal amplitude depends not only on the excitation amplitude, damping coefficient, coefficient and order of nonlinearity but also on the coefficient of the linear term. If the coefficient of the linear term is higher the value of σ is also higher.

5. DISCUSSION AND CONCLUSION

Let us consider the unit with cubic nonlinearity. The amplitude-frequency relation is

$$\frac{1}{A} \left(\frac{1}{2} k \pm \sqrt{\frac{F^2}{4A^2} - \frac{1}{8} c^2 K_3 A^2} \right) \sqrt{\frac{2}{K_3}} = \sigma \quad (42)$$

The equation indicates that the peak amplitude is

$$A_p = \left(\frac{2F^2}{K_3 c^2} \right)^{1/4}, \quad (43)$$

for the detuning parameter

$$\sigma_p = \left(\frac{1}{2} k \right) \sqrt{\frac{2}{K_3 A^2}} = \left(\frac{1}{2} k \right) \left(\frac{c}{F} \right)^{\frac{1}{2}} \left(\frac{2}{K_3} \right)^{\frac{1}{4}}. \quad (44)$$

Thus, the expression of the backbone curve in σ - A plane for the system with cubic nonlinearity, which gives the locus of the peak amplitudes, is

$$A_p = \left(\left(\frac{1}{2\sigma} k \right)^2 \frac{2}{K_3} \right)^{\frac{1}{2}} \quad (45)$$

In Fig. 3. A- σ diagram for $F=0.1$, $k=1$, $K_3=0.1$ and $c=0.2$ is plotted.

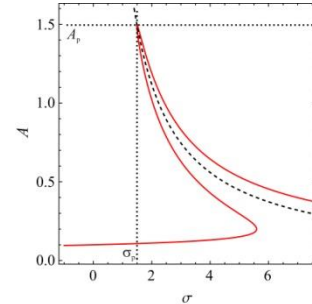


Fig.3. A- σ (red line) and the backbone curve (dotted line) with the peak amplitude A_p and its position σ_p

The backbone curve (47) and the peak amplitude (45) and its position (46) are also shown in figure.

In Fig. 4. A- σ curves for various values of nonlinearity coefficient are plotted. It is seen that for higher coefficient of nonlinearity the peak amplitude is smaller.

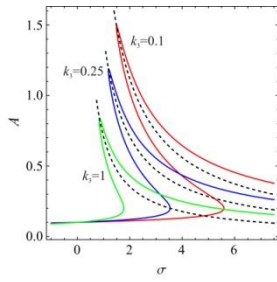


Fig. 4. A-σ curves for various values of K_3

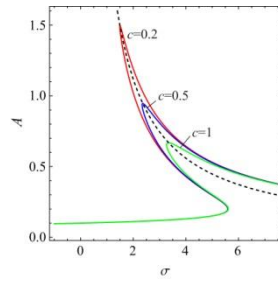


Fig. 5. A-σ curves for various values of c

In Fig. 5. the influence of the damping is analyzed. It is concluded that in the nonlinear oscillator for higher values of damping coefficient the peak amplitude is smaller. The backbone curve (dotted line) is independent on c .

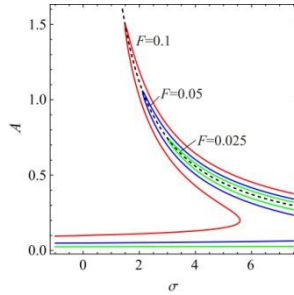


Fig. 6. A-σ curves for various values of F

In Fig. 6. the amplitude-frequency diagrams versus excitation amplitudes are plotted. It is obtained that the backbone curve is independent on the excitation amplitude. However, the amplitude of excitation has a significant influence on the peak amplitude: the higher is the excitation amplitude, the higher is the peak.

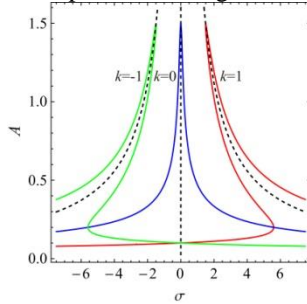


Fig. 7. A-σ diagram for various values of k .

Let us consider the case for various values of the coefficient of linear elasticity. For the case when the linear term is negative the relation transforms into

$$\frac{1}{A} \left(\frac{1}{2}k \pm \sqrt{\frac{F^2}{4A^2} - \frac{1}{8}c^2K_3A^2} \right) \sqrt{\frac{2}{K_3}} = \sigma \quad (48)$$

while, if it is zero we have

$$\frac{1}{A} \left(\pm \sqrt{\frac{F^2}{2A^2K_3} - \frac{1}{4}c^2A^2} \right) = \sigma \quad (49)$$

In Fig. 7. the A-σ diagram for $k = -1, 0, 1$ are plotted. It is seen that for the negative value the curve bends left from the position which corresponds to pure nonlinear oscillator. For the positive value of k the curve bends right.

6. REFERENCES

- [1] Cveticanin, L., Mester, Gy.: *Theory of acoustic metamaterials: an overview*, Acta Polytechnica Hungarica, 13(7), pp. 43-62, 2016.
- [2] Liu, Z., Zhang, X., Mao, Y., Zhu, Y.Y., Yang, Z., Chan, C.T., Sheng, P.: *Locally resonant sonic materials*, Science, 289, pp. 1734-1736, 2000.
- [3] Huang, H.H., Sun, C.T., Huang, G.I.: *On the negative effective mass density in acoustic metamaterials*, International Journal of Engineering Science, 47, pp. 610-617, 2009.
- [4] Zhu, R., Liu, X.N., Hu, G.K., Sun, C.T., Huang, G.I.: *A chiral elastic metamaterial beam for broadband vibration suppression*, Journal of Sound and Vibration, 333, pp. 2759-2773, 2014.
- [5] Li, X., Xue, C., Fau, L., Zhang, S., Chen, Z., Ding, J., Zhang, H.: *Simultaneous realization of negative group velocity, fast and slow acoustic waves in a metamaterial*, Applied Physics Letters, 108, 231904, 2016.
- [6] Sheng, P., Zhang, X.X., Liu, Z., Chan, C.T.: *Locally resonant sonic materials*, Physica B, 338, pp. 201-205, 2003.
- [7] Sheng, P., Mei, J., Liu, Z., Wen, W.: *Dynamic mass density and acoustic metamaterials*, Physica B, 394, pp. 256-261, 2007.
- [8] Cveticanin, L., Zukovic, M.: *Negative effective mass in acoustic metamaterial with nonlinear mass-in-mass subsystems*, Communications in Nonlinear Science and Numerical Simulation, 51, pp. 89-104, 2017.
- [9] Cveticanin, L.: Pure nonlinear oscillator, in *Strong Nonlinear Oscillators*, Mathematical Engineering, Springer, 9783319588254, pp. 17-49, 2018.
- [10] Cveticanin, L.: Free vibrations, in *Strong Nonlinear Oscillators*, Mathematical Engineering, Springer, 9783319588254, pp. 51-117, 2018.
- [11] Gradstein, I.S., Rjizhik, I.M.: *Tablici integralov, summ, rjadov i proizvedenij*, Moscow, Nauka, 1971.
- [12] Cveticanin, L., Zukovic, M., Cveticanin, D.: *On the elastic metamaterial with negative effective mass*, Journal of Sound and Vibration, On-line, 16 Aug 2018.
- [13] Nayfeh, A.H., Mook, D.T.: *Nonlinear Oscillations*, Wiley, New York, 1979.

Authors: Full Prof. Livija Cveticanin, Assoc. Prof. Miodrag Zukovic, University of Novi Sad, Faculty of Technical Sciences, Trg Dositeja Obradovica 6, 21000 Novi Sad, Serbia, Phone.: +381 21 485-2237.
E-mail: cveticanin@uns.ac.rs; zukovic@uns.ac.rs

ACKNOWLEDGMENTS: This investigation was supported by the Department of Mechanics of the Faculty of Technical Sciences in Novi Sad (Proj. No. 054/2018).

Desnica, E., Vulić, M., Pavlović, A., Nikolić, M.

ELV MANAGING THROUGH ANALYSIS OF RESOURCE CAPACITIES OF THE SERBIA: EQUIPMENT, HUMAN RESOURCE AND FINANCIAL SUPPORT

Abstract: *The automotive industry is emerging as a new initiator of the development of national economies and an integrator of modern achievements in technical and technological fields. On the other hand, the automotive industry is a significant consumer of raw and energy resources as well as an important participant in the destruction of our environment. Therefore, managing the entire life cycle of vehicles has become an important issue in the development of today's and future automotive industries. Starting from the state analysis of the end of life vehicles (ELV) in the Republic of Serbia, this paper provides a review of sustainability of the ELV recycling and the technological level of ELV equipment. Also, it covers the state analysis in the field of development and training of human resources for managing the ELV as well as the analysis of financial support through institutional and economic capacities.*

Key words: *ELV, sustainable development, recycling, equipment for ELV, human resources*

1. INTRODUCTION

The treatment of ELVs and the environmental impact of discarding the resulting residues are subjects of worldwide concern [1]. The automotive industry is facing several serious challenges related to the environmental impact of automotive throughout their entire life cycle. Recent initiatives on recovery of end of life vehicle component had a new impact not only to the automotive industry, but also the public at large. End of Life Vehicle (ELV) recovery that includes recycling, reuse or remanufacturing is an initiative by the automotive industry to respond to the global sustainable development [2].

Developing sustainable technologies for recycling of motor vehicles at the End of the Life Vehicle (ELV), achieving multiplier effects, which are related to environmental protection, sustainable use of natural resources, energy conservation, intensive employment of labor, improve economic performance and achievement of significant profits, as realization of sustainable development of the entire automotive industry [3].

2. ELV MANAGING IN REPUBLIC OF SERBIA

The Republic of Serbia is in the beginning of this process. The level of the national conscience about the importance of ELV is also rather low, which presents the initial problem for this process [4].

In the aim to join European Union (EU) one of the tasks is regulation of the problem of waste vehicles. In the mid of 2016 European commission assessed transposition of EU legislation in the legislation of our country as good, but the implementation is on the low level.

Problems occurring at the national level are related to a small number of vehicles for the treatment of waste vehicles, since a large number of waste vehicles end up being separated into parts on the black market. Also a big number of licenses for managing with waste

vehicles has been issued but most just for storage, only a few permits for vehicle treatment are active, so it is necessary to expand this network. For comparison, in the EU, this percentage is now 95%.

Solving these problems should be reflected in determining incentives for the recycling industry. The prerequisite for this is to Customs, Agency for Environmental Protection, Road Traffic Safety Agency and Ministry of Interior of the Republic of Serbia (RS) be connected in monitoring of waste vehicle flows.

The ecological tax per ton of vehicle put on the market of RS is 100 euros. According to the data of Association of importers and distributors annually about 100,000 used vehicles were imported on average, of which 20000-22000 were new. The environmental tax is paid by importers of new vehicles, while those who import used cars through private individuals do not pay, which is a paradox and the problem of the system.

As example, in the Croatia the most important function in the system regulation with waste vehicles has the "Fund". In the Croatia 1,5 million of vehicles per year paying fees due to excellent communication between the "Fund" and Customs. However, the problem persists because 35% of the waste vehicles end up on the black market.

2.1 ELV Management plan

The overall aim of the Waste Management Plan is to establish an effective system for the management of waste vehicles in Serbia, including Legal, Institutional and Technical aspects. To achieve this goal, it was made an assessment of the current situation regarding ELVs and it were identified deficiencies in the legal framework and implementation in practice. The main objective of EU Directive about ELV is synchronization of different national measures about ELV in order to minimize the ELV impact on the environment thereby contributing to the protection, conservation and improvement of environmental quality and conservation of energy.

For 2019 year it is expected 124,000 tons of ELV, and for the period from 2010 to 2019 year it is estimated that around 30 million euros are needed for the ELV management.

Based on the production market factors of vehicles and number of registered passenger vehicles as well as basis data from Agency for Environmental Protection the Republic of Serbia about amount of ELV with combining two methods of assessment, it has been established that the amount of ELV generated annually in Serbia is between 40000 and 42000 tons. Unfortunately, registered amounts of ELV which have treatment in RS are on the very low level, due to the fact that certain entities do not fulfill the obligation to report, as well as due to the informal collection network in order to sell spare parts and metal waste.

According to published data by AZŽS, about 3000 tons of ELV were produced by conducting business activities in the RS in 2014. About 40% of ELV is registered as dangerous waste. An estimate based on the annual number of passenger vehicles registered for the first time and the growth of passenger automobile fleet, according to which between 78,000 and 96,000 passenger vehicles should be excluded from the automobile fleet in RS annually. Provided that about half of the vehicles being excluded from the streets will be ELV, the annual amount of ELV in RS would be between 37500 tons and 45900 tons. Based on this assessment method, the average amount of ELV produced in Serbia would be 40000 tons. Using the estimation method per capita, the average amount of generated waste vehicles per capita, 7 kg, the estimated amount of waste vehicles that occur annually in Serbia would be 50000 tons. Based on the average amount of generated waste materials per passenger car, which is 19 kg, calculated in selected EU Member States, the estimated amount of waste vehicles that occur annually in Serbia would be 34100 tons. Thus, by combining these two methods, the amount of ELVs is between 40000 and 42000 tons.

In order to establish an efficient ELV management system, all actors need to take on a part of their responsibilities, such as: the state - to ensure that the relevant legislation is applied, to conduct a strict inspection control, to continually curb the "gray market"; vehicle manufacturers - when designing and manufacturing take into account disassembly, reuse and recycling, then they must not use hazardous heavy metals and must provide a collection system; operators (treatment centers) - must have a regular license and manage the hazardous components of the waste vehicle in a responsible manner; owners of the ELVs must execute a vehicle deregistration with a previously obtained disassembly certificate from an authorized recycler [5].

3. PROCESSES AND EQUIPMENT IN ELV MANAGING

At the beginning of ELV treatment it is necessary to perform a detoxification. This means a removing of all potential dangerous components from vehicle: batteries, lead balances for wheel balancing, TNG reservoirs,

potentially explosive materials, all types of liquid in the vehicle (fuels, all kinds of oil, cold liquids, antifreeze, windscreen-cleaning liquids), oil filters, live components (eg switches), fluids from the shock absorber or the shock absorbers themselves. The specialized equipment for ELV depollution process has already been available on the market for a while. The widely known producers are Vortex [6] and SEDA [7], while the national metal processing industry and academic institutions try to design competitive equipment [8, 9]. They offer stable and mobile stations for individual detoxification for entire vehicle. Following their technology and adapted by the needs of recyclers in RS, under the projekt TR 35033 it was developed stable station for ELV detoxification.

Next step is separation of valuable components from vehicles, which represent an important economic component of demountable units, ensures their sustainability (catalysts, metal parts containing copper, aluminum and magnesium and other). It is usual to remove parts that can be reused, which defines which parts could not be reused [10]. These are primarily parts that depend on the functionality of the vehicle.

For the easier packaging and transport of scrap metal, ELV baling is required [11]. Considering the extremely high price baling devices, a service of baling must often be applied.

Central process of the ELV treatment is fragmentation using the Shredder after which the metal is separated [12]. Austrian company "SEDA" produce modern Shredders. Depending on applied technologies, dimensions and capacities, different series of Shredders are distinguished.

Due to rigorous environmental standards and higher prices of secondary materials, higher focus is on an inexhaustible remnant after the automobile shredding process (ASR).

4. AN ANALYSIS OF THE STATE IN THE FIELD OF DEVELOPMENT AND EDUCATION OF HUMAN RESOURCES IN ELV MANAGING

Employment – Within the project of technological development, a model of integrated and sustainable recycling of motor vehicles at the end of their life cycle in the Republic of Serbia was defined and developed, thus laying the foundations for intensive employment in the field of recycling. The detailed model is presented in [13].

The employment analysis in terms of ELV recycling encompasses several groups of different jobs, starting from collection, transportation, manipulation and disassembly of ELVs up to recycling of different materials such as metals, plastics, glass, rubber, oil, etc. According to the data given in [13], Table 1 shows the total number of recycling workers working on recycling of motor vehicles at the end of their life cycle using the model of integrated and sustainable recycling of ELVs in Serbia.

Option	Number of ELVs (vehicles/annually)	Number of workers
1	60.000	5.147
2	80.000	6.557
3	160.000	11.262

Table 1. Total number of ELV recycling workers [13]

Also, the table shows the dependency of the number of ELV recycling workers on the number of vehicles available for recycling. However, apart from this dependency, the number of recycling workers on automobile recycling also depends on the level of motor vehicle recycling and the level of component repairs.

Education – Despite the fact that human resources represent the most important potential of the Republic of Serbia, domestic market requirements do not meet the needs of the economy and society. It turns out that, unlike the situation in the EU, the education system of the Republic of Serbia do not address the needs of the economy and society at all. Namely, the domestic education system is not identified as a driver and creator of personnel that would easily find its place in domestic and international division of labor. The education profile is, in fact, determined far from the needs of the economy, while the occurrence of changes in those needs is followed by slow decision making and even slower implementation.

Higher education system in Serbia is faced with many problems and challenges, especially with material and financial constraints, because relatively symbolic funds for science and education are available (due to the problem of financial insecurity). Therefore, the weakest points in the Strategy for Education Development refer to the reality and possibility of achieving the set goals, as well as the possibility of hiring highly educated staff members in Serbia.

The development of human resources for adequate and sustainable management of the ELVs can be divided into three main areas:

Education – Education programs for primary and secondary schools; Continuing education of teachers on sustainable development and recycling; Education programs for the University – education of students (Basic courses in recycling technologies and sustainable development); Project stock exchange – a platform for students and industry; Advanced studies (Master and PhD level);

Professional staff training – Education of industrial workers; Inspirational learning environment – using modern technologies for expert education; Lifelong learning – models and support.

Developing public awareness.

Implementing the Strategy, segments of education on sustainable development are gradually included at all levels of education. At the higher education level in recent years, a series of faculties, departments, courses or study groups in the field of the environment are established for basic, master and PhD programs. School curricula regarding sustainable development are still present at the technical faculties, although there is the rise in interest of social courses [14].

5. FINANCIAL SUPPORT THROUGH INSTITUTIONAL AND ECONOMIC CAPACITIES

In every country, including Serbia, used motor vehicles represent a major environmental issue, both in terms of waste volume and numerous hazardous materials they were made of. That was the main reason for developed countries to adopt and implement adequate legal actions in order to trigger organized recycling of motor vehicles that are at the end of their life cycle. On the other hand, models of waste management are developed on the basis of waste resulted from motor vehicles during their entire life cycle and according to the principles of sustainable development. In that way, waste is minimized while recycling of materials and reuse of components, assemblies and aggregates are maximized. The Republic of Serbia is also faced with the problem of used motor vehicles. For now, their recycling takes place sporadically, in unorganized way and very incidental to the environment. The way to overcome this situation is to adopt legal solutions and apply the model of integrated and sustainable recycling of motor vehicles at the end of their life cycle.

Sources of financing or funds in Serbia that can support activities on establishing the recycling system for motor vehicles at the end of their life cycle are the following ones:

1. national budget,
2. funds for environmental protection,
3. enterprise funds,
4. public sector funds,
5. investment programs,
6. local budgets,
7. foreign investments, loans (The World Bank),
8. Foreign public funds.

It is recommended to make significant changes in terms of project financings in the field of environmental protection in the Republic of Serbia. The financial burden in the field of ecology should be transferred from the national budget to polluters and users (prominent funds, enterprise financings), and by raising funds on the market (using market instruments, favorable loans, full implementation of the „polluter pays“ principle and compensation for ecological damage, etc.), municipal funding and more efficient use of foreign funds.

Government of the Republic of Serbia must legislatively and financially regulate the field of ELV recycling so that the whole system can function optimally. Thereby, the Ministry of Environmental Protection, Ministry of Interior and Ministry of Transport should regulate interrelations (deregistration, ownership, sending for recycling, transportation and transport documentation) that refer to the ELV management. The recycling agency must be in charge of ELV monitoring, until the final recycling of a material. It also has to establish an inspection of company's operations in this area [13].

FIAT – Unfortunately, the impact of our country through incentive measures for recyclers in companies “old for new” was cancelled on July 1, 2016, and “Fiat”

customers do not receive subsidies for recycling their used vehicles. The Republic of Serbia has thus become the only country in the region in which no environmental subsidies are received for recycling of used vehicles. When selling cars across Europe, ecology has an increasingly important role. Donations provided by the EU countries for buying electric or hybrid vehicles range from 4.000 up to 35.000 euros. One who wants to safely destroy his old vehicle and buy a new one, can enjoy donations in 2.000 to 5.000 euros. A few hundred cars were sold in our country in this way with a discount that went up to 2.500 euros.

6. CONCLUSION

Economic profitability of the ELV recycling, increase in the level of energy efficiency, development of the recycling industry for motor vehicles at the end of their life cycle, reinstallation of recycled materials into new vehicles, use of repaired parts, assemblies and aggregates, then, sustainable use of natural resources (ores, energy), direct and foreign investments, healthier environment, ensuring high quality development of domestic automobile industry and export, development of socially sustainable automobiles (new recycled materials, minimizing waste, minimal impact of motor vehicles on the environment) as well as development and implementation of novel ecological technologies represent the techno-economic effects of the integrated and sustainable system for recycling motor vehicles at the end of life cycle in the Republic of Serbia. It is about practicing what our society has assumed as an obligation by signing international and designing national strategies, which, given the new global development goals, will be an imperative in the future.

Besides, education and human resources are an unavoidable factor in the implementation of the above, thus a more efficient and effective integration of sustainability in higher education requires a systematic approach, institutional support and setting a generally favorable atmosphere – both at the level of the University and all relevant instances in society, including the connection with international scientific and research community.

7. REFERENCES

- [1] Simić, V., Dimitrijević, B., *Perspectives for application of RFID on ELV CLCS*, 1st Olympus International Conference on Supply Chains, Katerini, Greece, october 2010.
- [2] Wahab, D.A., Fadzil, Z.F.: *Public Community Knowledge on Reuse of End-of-Life Vehicles: A Case Study in an Automotive Industrial City in Malaysia*, Journal of Applied Sciences, 14: 212-220, 2014.
- [3] Pavlović, M., Vulić, M., Arsovski, S., Tomović, A., *Sustainable technologies in recycling of motor vehicles, ELV*, V International conference Ecology of urban areas 2016, pp. 69-73, Zrenjanin, september 2016.
- [4] Vulić, M., Pavlović, M., Tomović, A., Curčić, S., *The analysis of economy capacities for the support of elv recycling*, VII International conference Industrial engineering and environmental protection IIZS 2017, pp. 123-127, Zrenjanin, october 2017.
- [5] <https://www.energetskiportal.rs/plana-za-upravljanje-otpadnim-vozilima/>.
- [6] <http://www.vortexdepollution.com/>
- [7] <http://www.seda-international.com/en/>
- [8] Pavlović, M., Arsovski, S., Nikolić, M., Tadić, D., Tomović, A., *The Technological Level of Equipment in the ELV recycling Process in Serbia and Region*, 6th International Conference on Solid Waste Management, pp. 573-579, Kolkata, november, 2016.
- [9] Desnica, E., Vulić, M., Nikolić, M.: *AHP method in the function of adequate equipment choice for ELV detoxification in Serbia and EU*, Applied Engineering Letters - Journal of Engineering and Applied Sciences, Vol.1, No.4, pp. 115-121, 2016.
- [10] *Pravilnik o načinu i postupku upravljanja otpadnim vozilima*, „Sl. glasnik RS“ br. 98/2010.
- [11] Tomović, A., Pavlović, M., Manojlović, V., Simić, M., *Prisutna oprema u reciklaži motornih vozila usaglašena sa zakonodavstvom, tendencije promena*, 40. Nacionalna konferencija o kvalitetu, pp. A427-A432 Kragujevac, maj, 2013.
- [12] Vermeulen, I., Caneghem, Van J., Block, C., Baeyens, J., Vandecasteele, C., *Automotive shredder residue (ASR): Reviewing its production from end-of-life vehicles (ELVs) and its recycling, energy or chemicals' valorisation*, Journal of Hazardous Materials 190 (2011), pp. 8-27, 2011.
- [13] Pavlović, A., *Doprinos integrisanog modela upravljanja motornim vozilima na kraju životnog ciklusa razvoju Republike Srbije*, Doktorska disertacija, Tehnički fakultet "Mihajlo Pupin", Zrenjanin, 2016.
- [14] Desnica, E., Popescu, F., Nikolić, M., Vulić, M.: *Education strategy analysis and development of human resources in the field of elv recycling*, VII International Symposium Engineering management and competitiveness – EMC 2017, pp. 124-128, Zrenjanin, june 2017.

Authors: Assoc. Prof. Eleonora Desnica¹, M.Sc. Miroslav Vulić², Assist. Prof. Aleksandar Pavlović², Full. Prof. Milan Nikolić¹, ¹University of Novi Sad, Technical Faculty „Mihajlo Pupin“, Zrenjanin, Department of Mechanical Engineering, Đure Đakovića bb, 23000 Zrenjanin, Serbia, Phone.: +381 21 550-548, Fax: +381 23 550-520. ²University Business Academy in Novi Sad, Faculty of Economics and Engineering Management in Novi Sad, Department of Road traffic and Transport, Cvečarska 2, 21000 Novi Sad, Serbia, Phone.: +381 21 400-484.
E-mail: desnica@tfzr.uns.ac.rs; miroslavvulic@live.com

ACKNOWLEDGMENTS: This paper is a result of the research activities conducted under the project “Sustainable development of technology and equipment for motor vehicles recycling” TR 35033, which is financed by the Ministry of Education, Science and Technological Development of Republic of Serbia.

Dobrotvorskiy, S., Dobrovolska, L., Aleksenko, B.A.

THE USE OF INTERNAL DISSECTORS IN THE PROCESS OF REGENERATION OF ADSORBENTS BY MEANS OF THE MICROWAVE ENERGY

Abstract: Waveguide structure which can be used in the adsorption columns of compressed air dehumidifiers for the purpose of molecular sieve regeneration by using microwave energy in the process of desorption is considered. The presented theoretical experiment which opens the prospect for further practical studies of the effect of microwave radiation on the process of molecular sieve desorption under conditions of the adsorption column operation as part of the adsorption dryer, and the creation of an effective innovative sample of industrial equipment.

Keywords: dryer, dissector, microwave radiation, regeneration

1. INTRODUCTION

Mathematical modeling of physical processes is an actual and rapidly developing field of scientific knowledge. Modern software products can be used to obtain S-parameters [1], create SPICE (Simulation Program with Integrated Circuit Emphasis) models and three-dimensional modeling of the electromagnetic field by the finite element method, which greatly facilitates and accelerates the development of new equipment, which uses microwave energy.

In this paper, the problem of using adsorption in the cavity of adsorption column is considered [2-4].

2. RESEARCH PROBLEM

The main task of the developers [5] is to improve the efficiency of the microwave heater by increasing the uniformity of the distribution of microwave energy inside the heating chamber, increasing the efficiency and stabilizing the heat treatment of the processed materials. The equipment for microwave drying [6] is known in which the regulation of the power of the action of the energy of microwave radiation is carried out by alternately removing or approximating the processed material to the zone of the highest radiation intensity of the microwave energy. In other designs [7], the transmission antennas rotate along the electric axes relative to the normal to the surface of the material on both sides. Similar designs with the number of radiators, that are multiples of the number of microwave generators are characterized by an increase in energy costs, a complex process of uniform distribution of electromagnetic radiation in the material is dried and low operational reliability.

Irradiation of the dried volume of the adsorbent on only from above [8] causes a decrease in the transparency of the upper layers for the electromagnetic field, while the top-laid adsorbent heated to the overheats temperature with uneven drying of the lower layers, which leads to loss of adsorbent useful properties and longer drying times.

The best way to improve the uniformity of heating if the available modes of oscillation or some of them

are switched in turn. As a result, each section of the column volume is alternately subjected to the influence of fields of different configuration and intensity. It is with a large number of combinations that the effect of microwave energy can be fairly uniform [9].

In this article, we consider the problem of creating an adsorption column, which provides drying of KCMG adsorbent using microwave energy.

3. RESEARCH METHODOLOGY

The present study is devoted to the study of the effect of the dissector on the propagation of microwave energy [10-12] in the adsorbent volume. The principle of operation of a dissector consists in disturbing the electromagnetic field's structure. Under the action of the dissector, the excitation conditions for different modes vary, depending on the relative turn of the dissector. Therefore, the spectrum of electromagnetic oscillations, and, accordingly, the structure of the field [13,14] is constantly changing.

The process of regenerating the adsorbent was studied using simulation modeling. The thermodynamic forces due to the electromagnetic field are equal (1)

$$X_3 = (\text{grad}E) \cdot \pi_3; X_M = (\text{grad}E) \cdot \pi_M \quad (1)$$

Thus, in the electromagnetic field the transfer of moisture is due to the action of not only the diffusion forces (∇u) , thermal diffusion (∇T) , but also the action of the forces X_3 and X_M . Thus, the moisture flux will be determined in accordance with the Onsager equation (2)

$$j_n = L_{n1}X_1 + L_{n2}X_2 + L_{n3}X_3 + \dots \quad (2)$$

by the relation (3)

$$j = -u_m p_0 \nabla u - u_m^T p_0 \nabla T - a_m^3 p_0 (\nabla E) \cdot \pi_3 - a_m^M (\nabla B) \pi_M \quad (3)$$

The first term of this formula determines the amount of diffusion of moisture, the second term - the

thermal diffusion of moisture, the third term corresponds to the transfer of moisture under the action of an inhomogeneous electric field, and the fourth - to the transfer under the action of the magnetic field.

The coefficients a_m^3 and a_m^M are the coefficients of electrodiffusion and the magnetodiffusion of moisture in the material [15].

Drying in an alternating magnetic field is fundamentally different in that the transfer of moisture is additionally affected by the thermodynamic force, which is represented as the product of the magnetic field induction gradient by the polarization vector ($\nabla B \cdot \pi_m^*$), and the magnetic field affects the velocity of the liquid in the capillary.

The total moisture flux in this case is expressed by the equation (4):

$$j = -a_m p_0 \nabla u - a_m^T p_0 \nabla T - K_p \nabla p - a_m^M p_0 (\nabla B) \pi_m \quad (4)$$

where a_m^M - coefficient of magnetic diffusion, depending on the moisture content and magnetic field strength [16].

Thus a mathematical model has been constructed that takes into account the additional influence of the electromagnetic field intensity on the rate of moisture movement in the porous structure of the adsorbent.

4. MODEL DEFINITION

The calculation was carried out using the mathematical model of a desiccant adsorption tower (Fig. 1, 2.) with a capacity of 1.5 m³/min.

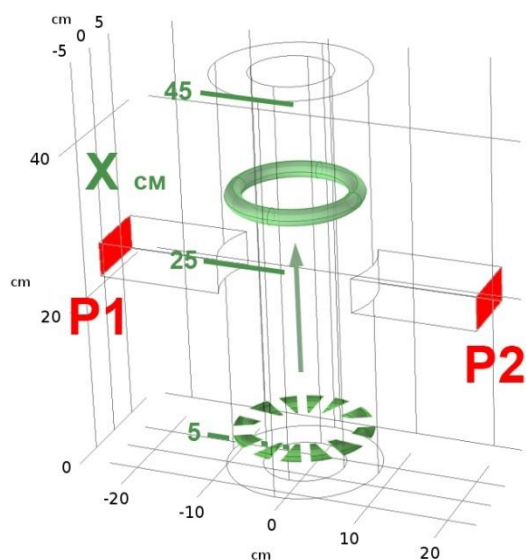


Fig. 1. An annular dissector and its movement in the cavity of the adsorption column. X [cm] – the vertical position.

The adsorption column is a metal cylinder connected to a microwave source through rectangular waveguides operating in the TE₁₀ mode. Effects of 2.45 GHz are made using two opposing ports with a capacity of 500 Wt each, denoted by the letters P1 and

P2. Inside the column there is a radiocarbon enclosure. There is an air gap between the radio-transparent casing and the column wall. The volume of silica gel is inside the radiocarbon case. The 3d model is based on the model used in previous calculations [8], the configuration of which has been previously optimized in terms of minimizing microwave energy losses.

Two waveguide constructions are considered:

I) An annular dissector that is placed between the radio-transparent case and the column wall and moves in a vertical direction (Fig. 1.);

II) A double-pin dissector that is placed between the radio-transparent casing and the column wall and rotates along the vertical axis of the column (Fig. 2.);

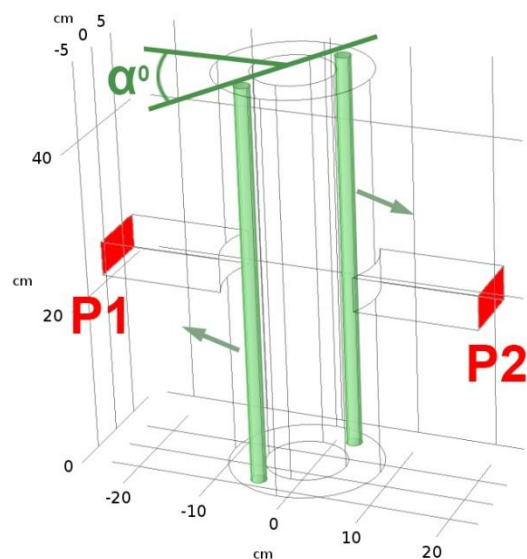


Fig. 2. A double-pin dissector and its rotation in the cavity of the adsorption column. α [°] – the angle of rotation.

As shown above, the most important task of stabilizing the heat treatment regime is to increase the uniformity of the distribution of microwave energy inside the heating chamber, which is achieved by a change in the overall structure of the electric field.

5. RESULTS

We made a step-by-step simulation of the distribution of power in the cavity of the adsorption column, depending on the position of the dissector (Fig. 7, 8.). The Figs show the distribution of the electromagnetic field strength and the temperature after 6 minutes of heating in the investigated models (Fig. 3-6.).

I) It has been established that when an annular dissector moves a significant change in the overall structure of the electric field is observed (Fig. 3.).

Pictures of the electromagnetic field (Fig. 3.) correlates with the temperature distribution in the volume of the adsorbent material (Fig. 4.). In this case, there is a more intensive redistribution of power in the vertical direction, synchronous with the displacement of the dissector (Fig. 7.).

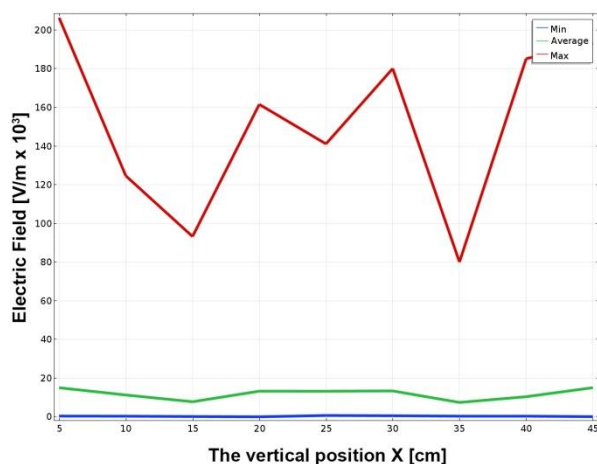


Fig. 3. The graph of the distribution electromagnetic field strength in the adsorption column during the moving of the annular dissector.

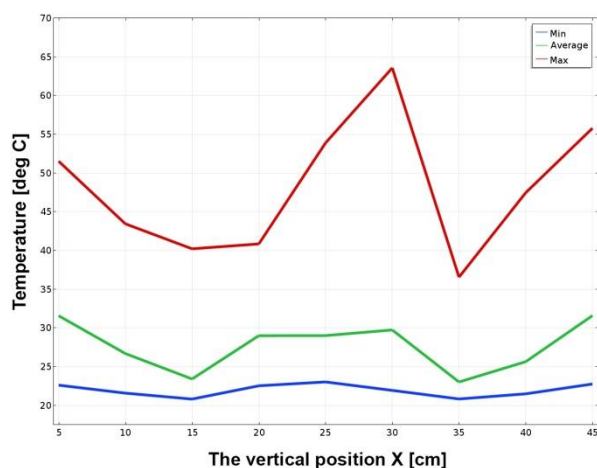


Fig. 4. The graph of the temperature distribution in the volume of the adsorbent material during the moving of the annular dissector.

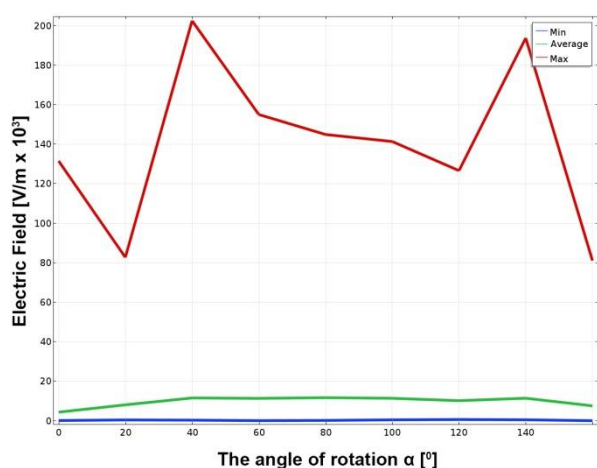


Fig. 5. The graph of the distribution electromagnetic field strength in the adsorption column during the rotation of the double-pin dissector.

II) The model with the double-pin dissector that is placed between the radio-transparent casing and the

column wall and rotates along the vertical axis of the column (Fig. 8.).

The use of a double-pin dissector (Fig. 5.) causes less pronounced changes in the microwave intensity (Fig. 6.). In this case, there is a more intensive redistribution of power in the radial direction, synchronous with the rotation of the dissector (Fig. 8.).

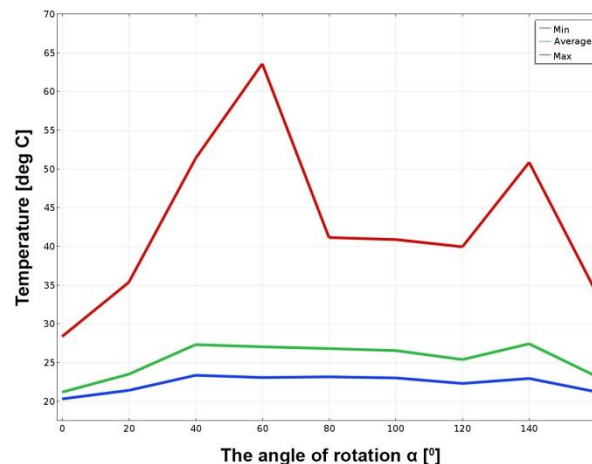


Fig. 6. The graph of the temperature distribution in the volume of the adsorbent material during the rotation of the double-pin dissector.

In both cases, an intensive non-cyclic redistribution of power in the volume of the adsorbent is observed. (Fig. 3,5.).

6. CONCLUSIONS

The study showed the possibility of using dissectors to create a traveling wave in the cavity of the column with a different intensity of microwave radiation in order to increase the uniformity of the influence of microwave energy on the volume of the adsorbent. The experiment shows, that in case of use of additional phase rotation [17], preference should be given to using a annular dissector, otherwise is better to use a double-pin dissector.

The completed theoretical experiment opens the prospect of further practical studies of microwave radiation on the molecular sieve desorption process.

11. REFERENCES

- [1] Sophocles J. Orfanidis.: Electromagnetic Waves and Antennas (2016), <http://www.ece.rutgers.edu/~orfanidi/ewa/ewa-2up.pdf>, last accessed 2017/02/10.
- [2] Jones, S.: Comparing Microwave to Conventional Heating and Drying Systems, http://www.chemicalprocessing.com/assets/wp_downloads/pdf/comparing-microwave-to-conventional-heating-drying-systems-v2.pdf, last accessed 10/05/2017.
- [3] Gao, F.: Comparison of Microwave Drying and Conventional Drying of Coal. Science Queen's University, Canada (2010).

- [4] Tanaka, K., Asakuma, et al., Phan C.: Surface tension profiles of nanofluid containing surfactant during microwave irradiation. In: 29th Symposium of Malaysian Chemical Engineers (SOMChE) 2016, vol. 206, pp. 101-105. Miri, Malaysia (2017).
- [5] Gareev, F.H.: Pat. 2199064 RF. Ustanovka dlya sushki dielektricheskikh materialov svch-energiey. <http://www.freepatent.ru/patents/2199064>, last accessed: 2017/02/20. [in Russian]
- [6] Monolakov V.A., Yudin V.V.: Pat. 2113666 RF. Sposob sushki pilomaterialov. <http://documents.allpatents.com/1/18048118/RU2113666C1>, last accessed: 2017/02/20. [in Russian]
- [7] Valeev G.G.: Pat. 2115073 RF. Sushilnaya ustanovka. <http://www.freepatent.ru/patents/2115073>, last accessed: 2017/02/20. [in Russian]
- [8] Vergasov A.A.: Pat. 2111631 RF. uni-versalnaya sverhvyisokochastotnaya sushilnaya ustanovka (vari-antyi). <http://www.freepatent.ru/patents/2111631>, last accessed: 2017/02/20. [in Russian]
- [9] Dobrotvorskiy S., Dobrovolska L., Aleksenko B.: Computer simulation of the process of regenerating the adsorbent using microwave radiation in compressed air dryers. Lecture Notes in Mechanical Engineering, Springer vol. 11236, 511-519 (2017).
- [10] Berezin A.V., Markov M.B., Plyushchenkov B.D.: Locally one-dimensional finite-difference scheme for the electrodynamic problems with given wavefront. Russian Academy of Science, Moscow (2005).
- [11] Bankov S.E., Kurushin A.A. Razevig V.D.: Analysis and optimization of three-dimensional microwave structures using HFSS™. Solon-Press. Moscow (2004). [in Russian]
- [12] ECE-329 Fields and Waves I. 21. Monochromatic waves and phasor notation. Phasor form of Maxwell's equations and damped waves in conducting media: Lecture Notes. ECE ILLINOIS Department of Electrical and Computer Engineering, <http://jsa.ece.illinois.edu/ece329/notes/329lect21.pdf>, last accessed 2017/02/10.
- [13] Balanis K. A.: Antenna Theory: Analysis and Design, Wiley & Sons, 2 nd edition, (1997).
- [14] Solovyanova I.P., Naymushin M.P., Theory of wave processes. Electromagnetic Waves: A Training Manual. GOU VPO UGTU, Ekaterinburg (2005). [in Russian]
- [15] A.V. Lykov, Yu.A. Mikhailov Theory of energy and matter transfer. Institute of Energy, Minsk. 1959, 328p.
- [16] Lykov, A.W.: Theory of Drying. Moscow: Energia, 1968. [Rus]
- [17] The use of waveguides with internal dissectors in the process of regeneration of industrial adsorbents by means of the energy of ultrahigh-frequency radiation / S.S. Dobrotvorskiy, L.G Dobrovolska, B.A Aleksenko, Ye. V. Basova // Advances in Design, Simulation and Manufacturing. DSMIE 2018. – June 16, 2018. Sumy, Ukraine – P.433-442.

Authors: Full Prof. Dobrotvorskiy Sergey, Assoc. Prof. Dobrovolska Ludmila, Post Grad. St. Aleksenko Borys A., National Technical University «Kharkov Polytechnic Institute», Department of Technology of Mechanical Engineering and Metal-Cutting Machine Tools, 2, Kyrpychova str., 61002, Kharkov, Ukraine,
Phone.: +38057-707-66-00.
E-mail: sdobro50@gmail.com;

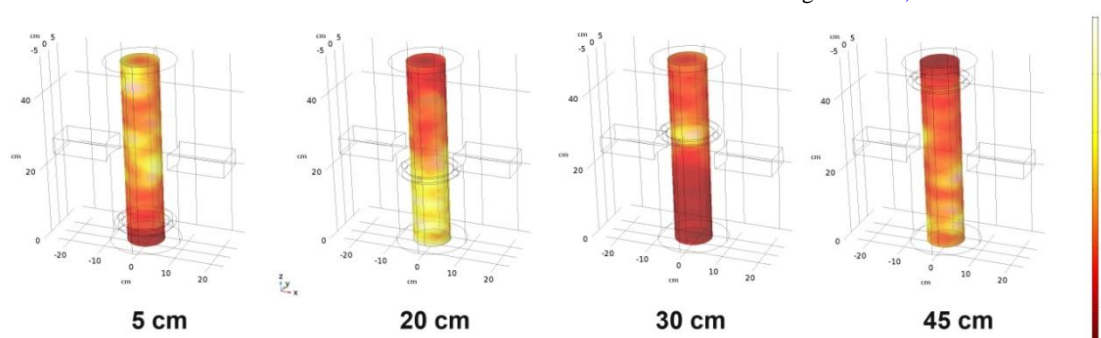


Fig. 7. The pattern of the temperature distribution in the adsorbent during the moving of the annular dissector.

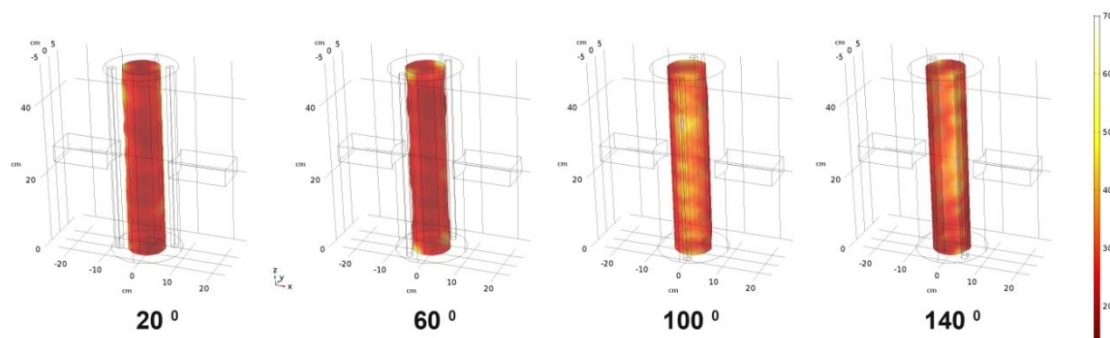


Fig.8. The pattern of the temperature in the adsorbent depending on the rotation of the double-pin dissector.

Djordjic, D., Djuric, S., Hadzistevic, M.

ANALYSIS OF FLOWS AND MANAGEMENT OF HAZARDOUS WASTE IN COMPLEX SYSTEMS

Abstract: A good quality analysis of generated waste flows is the basis for the safe and efficient management of various types of hazardous waste in complex systems, as a set of systematic activities that involves monitoring different types and quantities of waste, development and updating documents, continuous education, collection and temporary storage of waste and the final disposal of waste. The implementation of analyses and activities for the safe management of waste oils, accumulators, toners and other types of hazardous waste, generated in different systems, should be carried out in accordance with applicable legal norms, appropriate standards requirements and environmental objectives. The presented analysis of hazardous waste flows and the management of generated hazardous waste have been carried out in power distribution units of the Republika Srpska - Bosnia and Herzegovina - Power Company /Elektroprivreda/, as a standard example of complex system's model.

Key words: hazardous waste, material flow analysis, power distribution unit, environmental protection, security and health at work

1. INTRODUCTION

In the process of construction, maintenance and reconstruction of facilities and devices, as well as other activities, various types of hazardous waste arise, especially in complex systems, which are obligated to analyse waste flows and to safely manage generated waste in the manner prescribed by the regulations.

All activities undertaken during analysis and management of hazardous waste must be done with minimum impact on human health and the environment, and in a manner to minimize generated waste, reduce the use of natural resources and enable re-use, recycling and safe disposal of waste at the end of the process.

2. MATERIALS AND METHODS

2.1 Definition and sites of temporary disposal of hazardous waste

In complex dynamic systems, such as power distribution systems, various types of hazardous and non-hazardous waste are generated in the process of maintenance, reconstruction, replacement of equipment and other regular and extraordinary activities.

Hazardous waste is waste which, according to its origin, composition or concentration of dangerous substances, can cause environmental and human health hazards and has at least one of the hazardous characteristics defined by special regulations, including packaging in which hazardous waste has been or is packaged. [1]

Table 1 shows the types and sites of temporary disposal of hazardous waste mostly generated in power distribution units, as very complex and demanding systems.

2.2 Types of hazardous waste most commonly generated in complex systems

2.2.1 Waste oils

Waste types	Temporary disposal site	Hazardous waste
Waste motor, hydraulic and gear oil	- main warehouse - warehouses in business units	yes
Waste insulating oil	- main warehouse - warehouses in business units	yes
Waste turbine oil	warehouses in business units (small hydro-power plants)	yes
Waste electrical and electronic equipment	- main warehouse - warehouses in business units	yes
Waste accumulators and batteries	- main warehouse - warehouses in business units	yes

Table 1. Types, classification and sites of temporary waste disposal [2]

Waste motor, hydraulic and gear oil

The use of various types of motor and other oils in motor vehicles and devices of various purposes results in generation of waste oils.

Due to the malfunction of a motor vehicle, an operating machine or other device, in case of a smaller or greater oil leakage in the event of regular and extraordinary circumstances, the oil topping up or oil replacement follow. Also, the use of oil is mostly followed by the use of oil filters. Waste oil filters and wiping cloths are discarded in specially designed cases and / or containers.

Replacement of motor, hydraulic and gear oil in motor vehicles and operating machines is done in power distribution units' workshops or authorised services.

Waste insulating oil (transformer oil and oil switches)

The waste insulating oil is generated after the analysis of transformer and/or other oil samples, when the results show unsatisfactory quality that leads to the oil replacement. The transformer failure leads to the generation of waste oil, as the result of oil spill into the environment or oil collecting pit. [2]

In the case of transformer overhaul by authorised institutions, if the oil replacement takes place, the process of waste oil management is within the competence of that institution. In case this institution does not operate in accordance with the ISO 14001 standard, it is power distribution units' obligation to manage waste oil [2, 3].

Waste turbine oil

During the plant overhaul in small hydro-power plants and the replacement of turbine oil, waste turbine oil is generated.

The waste oil is released into a metal barrel, or if that is unfeasible, first into jerry cans of less volume, and then into the barrels. Replacement and collection of waste turbine oil is carried out by turbine operators in hydro-power plants and placed in a 200-liter barrels.

2.2.2 Waste electrical and electronic equipment

Due to the dangerous substances and heavy metals this waste is classified as hazardous. The following waste is classified to this waste group:

- damaged transformers,
- faulty condensers,
- faulty clutches,
- defective computers and their parts,
- useless video and audio devices,
- useless air conditioners and other waste electrical appliances and equipment.

If an electrical appliance classified as a waste contains oil, the oil is offloaded, and the product is stored as waste iron. Smaller parts are collected into smaller containers or crates to prevent spillage.

2.2.3 Waste accumulators/batteries

Due to heavy metals and dangerous substances (lead, mercury, nickel, cadmium, electrolyte) in accumulators/batteries, waste batteries are classified as hazardous waste.

Once the battery is malfunctioned and/or significantly damaged, the new one is to be procured, while the old one is to be disposed as waste.

Employees in charge of vehicles dispose waste batteries from motor vehicles and operating machines, to temporary storage. Electro mechanics/repairmen replace and check the batteries in electrical power plants and power distribution units, and dispose waste batteries to storage.

2.3 Material Flow Analysis Method (MFA)

The MFA is a method for analyzing waste and other materials flows, which can provide a detailed overview of materials and substances in the flows of the organisations of scale complexity, thus providing an efficient environmental management system. The MFA

method is the basic method for monitoring the flows of materials and generated waste. The MFA is applied in many engineering branches, especially in complex systems, in order to optimize the management system for hazardous and non-hazardous waste.

Under the concept of environmental management, the most important fields are the applications of industrial ecology, resource management, assessment and optimization of key processes and material flows. [4, 5]

In order to be able to choose the most efficient reduction and prevention strategies, the stock & flow diagrams allow the insight into flows relevant for resources and environmental aspects. [6]

The MFA takes into account the mass balance principle based on the law on conservation of matter. Balancing all incoming and outgoing processes enables the calculation and taking into account data from various unknown flows. [7]

The application of the MFA procedure offers the possibility to develop ways to reduce the pollution problem. As a consequence, the MFA reveals potential problems with regard to current and future legal frameworks. The MFA is a systematic approach to display material and inventory flows within the system's spatial and temporal boundaries.

2.3.1 MFA definition procedure

Defining the MFA system requires the following steps: defining spatial and temporal boundaries of the system and defining processes and flows.

Defining spatial boundaries of system

The spatial limit of the system is determined by the scope of this paper, which mainly deals with the distribution of electricity. Accordingly, the boundary is defined as the field of immovable infrastructure, including the environment.

Defining time limit of system

When it comes to defining the time limit of the system, different time periods depending on the system being analyzed and the objectives of the analysis can be adopted. Due to the specific nature of the structure and the business of power distribution units, as well as the way of doing business, for the purposes of this analysis, the adopted time limit is 1 year.

Defining processes and flows

When it comes to defining the process within a complex power distribution system, in order to take a more comprehensive view of the overall situation in the system, the process definition is carried out at the appropriate levels. The appropriate levels involve defining power distribution units within the Power Company/Elektroprivreda as separate processes, or as independent parts of the organisational unit. Spatial boundaries of these power distribution units represent the geographical boundaries of their organisational parts.

The entire system is divided into subsystems that represent power distribution units or business units, as well as the associated branch offices. The model

according to which the grouping was done is the same for all power distribution units - business units, within the complex system of the Republika Srpska Power Company /Elektroprivreda - Bosnia and Herzegovina (BiH). All processes are linked by appropriate flows. Defined flows include flows of different hazardous waste materials.

2.3.2 Modeling of hazardous waste types at the level of power distribution units

When it comes to modeling of potential types of hazardous waste, the very structure of the system is defined in accordance with the possible waste generation site within the enterprise Elektro-Bijeljina a.d., as an important segment of the Power Company/Elektroprivreda RS-BiH. Modeling was done by dividing the system into levels. A level represents the grouping of power distribution units into independent organisational units within the Enterprise.

In order to optimize the hazardous waste management of the entire system at the level of the enterprise Elektro-Bijeljina a.d., with the associated business units (power distribution units Bijeljina, Ugljevik, Zvornik, Bratunac and Vlasenica), analyzed flows of generated hazardous waste material are presented in Figures 1-4, as the flows of:

- waste oils, l / yr,
- waste electrical equipment, kg / yr,
- waste toners, kg / yr,
- waste accumulators and batteries, kg / yr.

3. RESULTS AND DISCUSSION

Analyzing the hazardous waste flows, monitoring and implementing procedures for hazardous and other waste management meet all obligations and requirements regarding environmental protection and waste management activities. Material flow analysis is the basis for hazardous waste management [8]. Analyzes and hazardous waste management must be carried out in an appropriate manner so as not to pollute the environment and endanger human health. Employees who come into contact with hazardous substances and waste must possess personal protective equipment and be adequately trained [1, 9, 10, 11].

Professionals in the field of technics, protection, etc., as well as competent authorities must have open communication, based on an integral principle, and the possibility of efficient cooperation between themselves, as well as with responsible persons and the public [12], which represent the unavoidable links of the system.

3.1 Waste oils

After procurement process is completed, the oil and lubricants are transported to the main warehouse, from where they are distributed to the warehouses of power distribution units. Warehousemen (in the main warehouse and the warehouses of business units) receive oils and lubricants, and then, in accordance with the needs, issue the necessary quantities of oil for use to the competent persons of power distribution unit, based on the appropriate documents and instructions.

The use of motor, transformer and other oils, in the

processes of maintenance, reconstruction, replacement of equipment etc. generates waste oils. Oil leak collected during sampling or spillage is categorised as waste oil [13].

The dynamics of oil sampling of all types of electrical devices is not completely uniform in all system segments, and the record of individual oil top up in transformers and/or other devices is not always up-to-date. The above facts make detailed waste oils flow analysis difficult and limited. The analysis results show that the share of generated quantities in waste oil flows in business units amounts to: 43% in Vlasenica, 33% in Bratunac, 20% in Bijeljina and 4% in Zvornik (Figure 1). The mentioned results of the waste oil flows analysis in the monitored system are logical, since in the analyzed period the overhauls of certain electric power plants belonging to the mentioned business units were performed, and the most intensive ones were in Vlasenica, Bratunac and Bijeljina.

Temporary storage facilities must meet existing needs with their capacity, thus during the design, the calculations are made for double quantity of hazardous waste than the quantity normally generated between the two processing cycles, i.e. transport [14]. All types of waste oil from the power distribution units' warehouses, in which the oils are temporarily stored, are recycled by an authorized waste management company in accordance with the contract.

3.2 Waste electrical equipment

Waste equipment arises as a by-product of the activities related to removing failures, reconstructing low-voltage and medium-voltage grids, as well as power and other facilities. Waste electrical equipment (damaged transformers and other defective electrical appliances and equipment), is collected by electrical fitters engaged in appropriate work activities. After replacing or removing a defective device or part thereof, this electrical equipment shall be returned and temporarily disposed of within warehouse of the relevant power distribution facility, in specially designated site. If the electrical device-equipment contains oil, the oil is offloaded and the equipment is stored as waste iron. In case an external organisation conducts works for the enterprise Elektro-Bijeljina a.d. then all the waste material generated during these works is removed and transported by it (the external organisation), i.e. it further manages waste material, which is regulated by the contract.

The analysis results show that the share of generated quantity in electrical equipment waste flows in power distribution units is 40% in Bijeljina, 22% in Vlasenica, 19% in Ugljevik, 16% in Bratunac and 3% in Zvornik (Figure 2). The above mentioned analysis results of waste electrical equipment flows are directly related to the reconstruction of power plants and parts of the power distribution grid, which was realized within monitored period in all organisational units, i.e. power distribution units, and the most intensive ones are in Bijeljina and Vlasenica.

Waste electrical equipment is periodically handed to authorized organisations, which carry out further waste management in accordance with regulations.

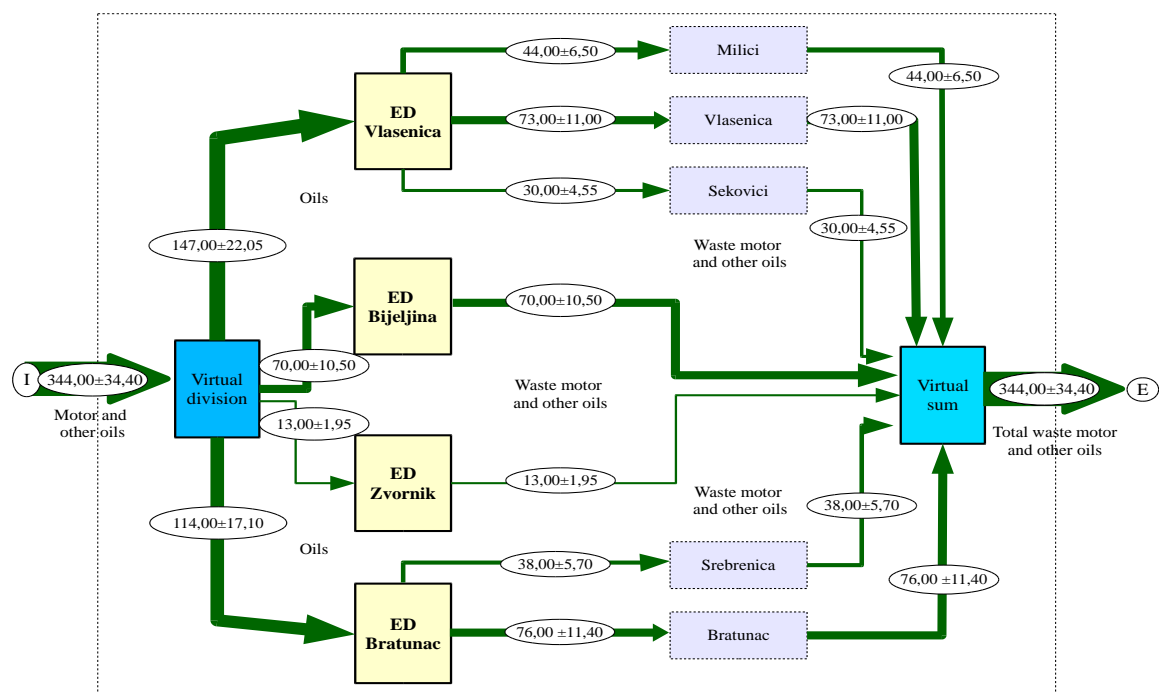


Fig. 1. Oil flows in power distribution units (ED) of Elektro-Bijeljina a.d., RS-BiH, 1/yr.

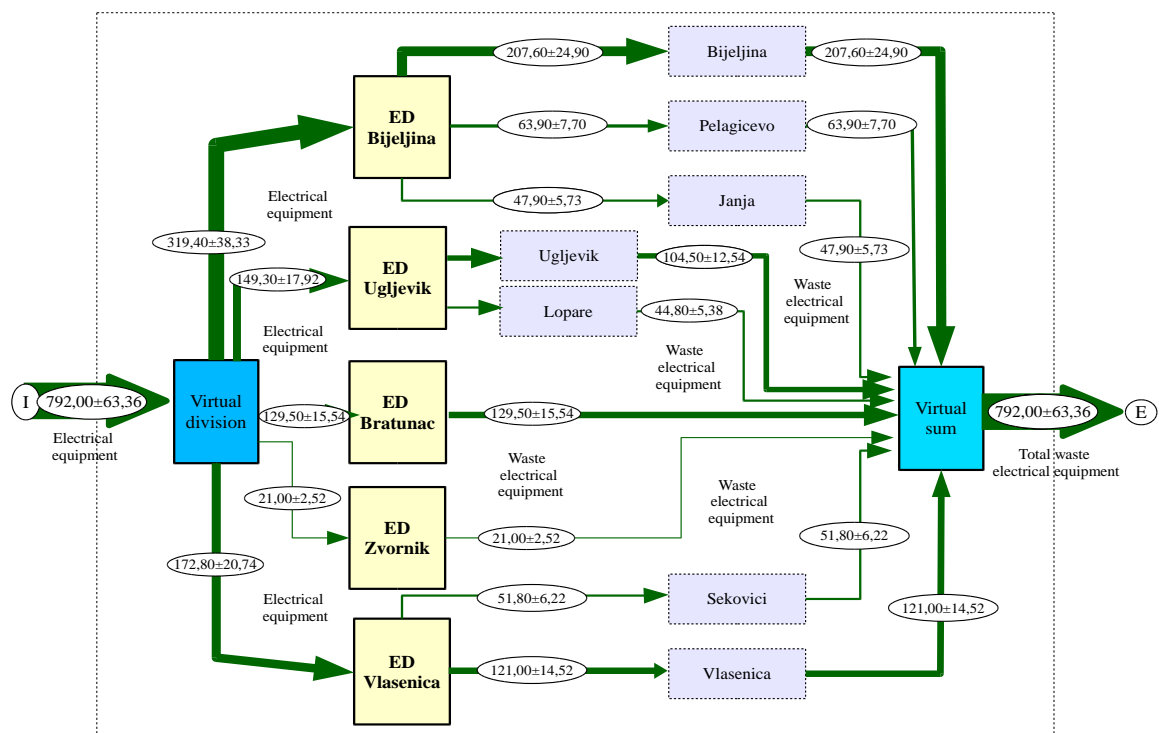


Fig. 2. Flows of electrical equipment in power distribution units (ED) of the Elektro-Bijeljina a.d., RS-BiH, kg/yr.

3.3 Waste toners

After replacing printing toners, this equipment is temporary disposed as hazardous waste in a specially designated site within the warehouse of the appropriate organisational unit of the power distribution system.

The analysis results show that the share of generated quantities in waste toner flows in power distribution units is 62% in Bijeljina, 33% in Bratunac, 3% in Zvornik and 2% in Vlasenica (Figure 3). The

above analysis results of waste toner are in direct relation with repair, elimination of defects and replacement of defective parts of printers and other electronic equipment and devices done within the monitored period in the mentioned organisational units, i.e. business units of the company, primarily in Bijeljina. After temporary storage, toner cartridges are periodically handed to authorised organisations, which further manage this type of hazardous waste.

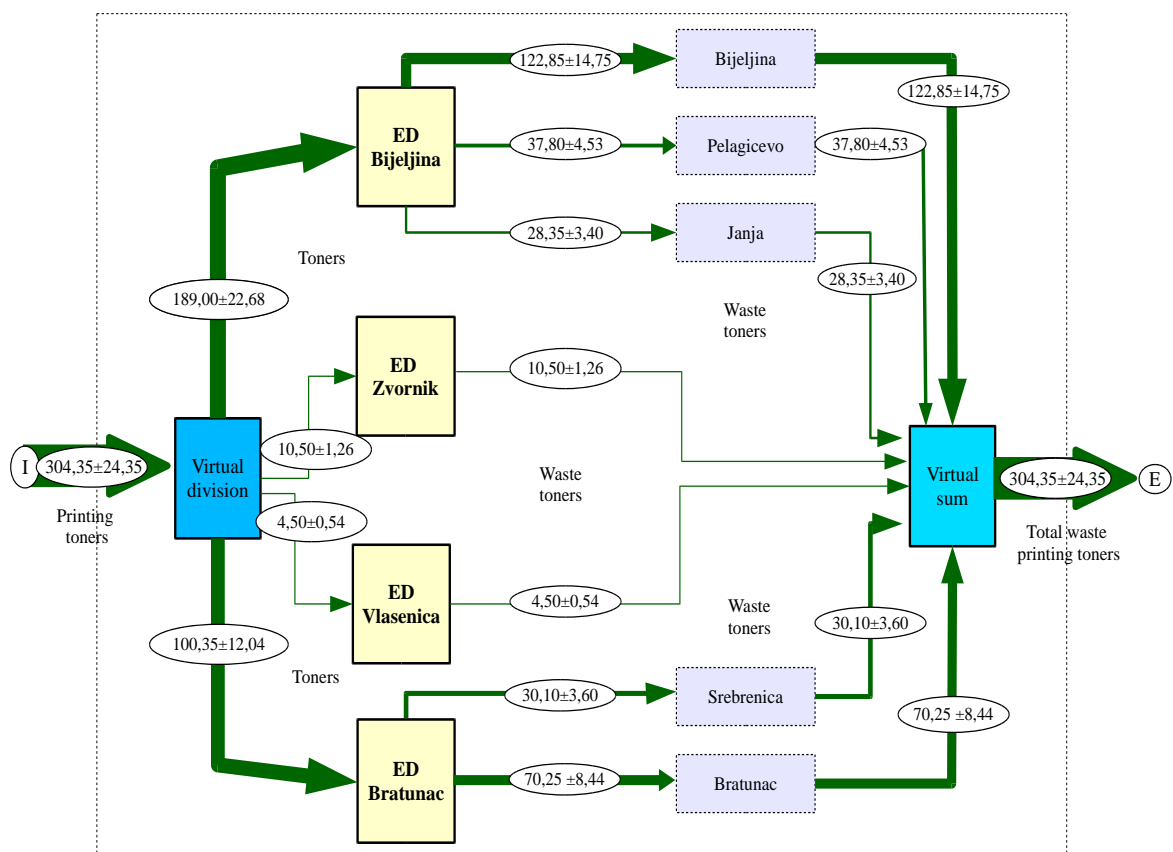


Fig. 3. Printing toner flows in power distribution units (ED) of the Elektro-Bijeljina a.d., RS-BiH, kg/yr.

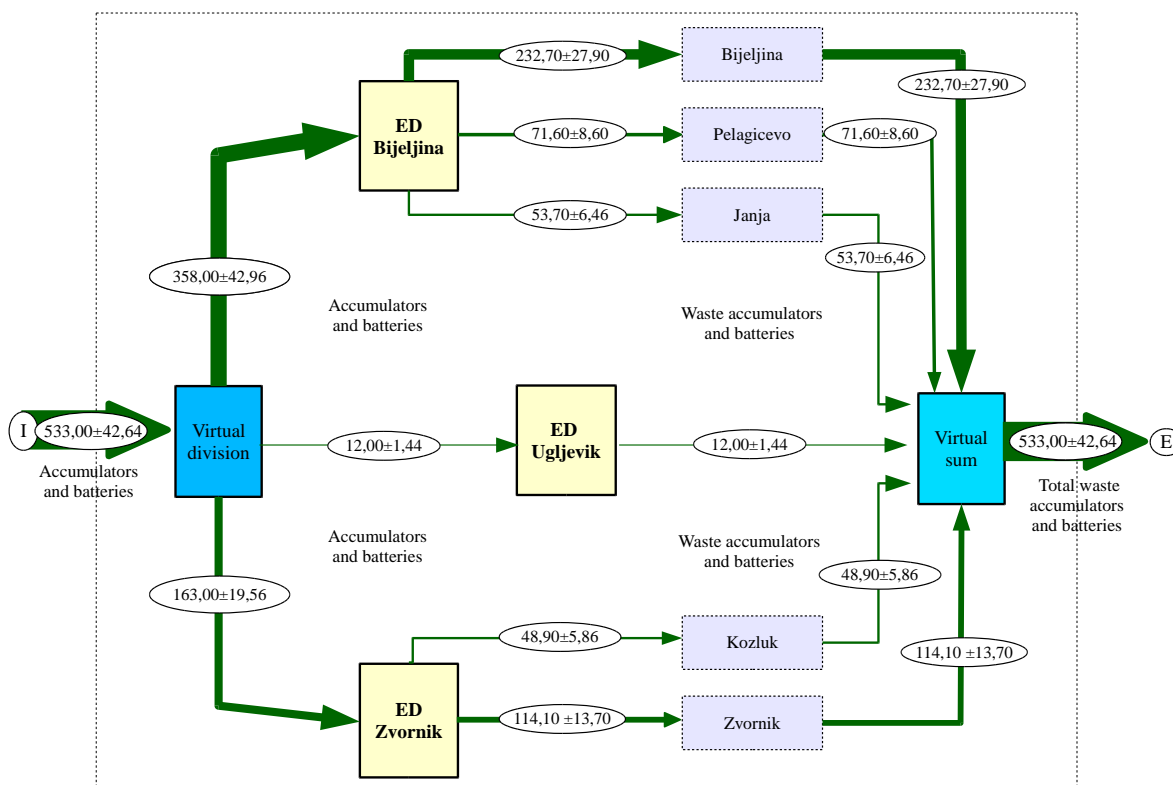


Fig. 4. Flows of accumulators and batteries in power distribution units (ED) of the Elektro-Bijeljina, RS-BiH, kg/yr.

3.4 Waste accumulators and batteries

After accumulator and/or battery becomes dysfunctional or significantly damaged, a new one is procured and the old one is disposed of as waste. Replacement of accumulators and batteries is carried

out in authorised services, and the old ones are returned as waste materials and deposited in designated site within the main warehouse or warehouse of business units. The analysis results show that the share of the generated quantities in the flows of waste accumulators

and batteries varies between: 67% in the business unit Bijeljina, 31% in the business unit Zvornik and 2% in the business unit Ugljevik (Figure 4). The above analysis results of the waste accumulators and batteries flows are in direct relation to the maintenance and replacement of defective and non-functional elements in the power plants and vehicle fleet of power distribution unit, which was realized within the monitored period, in the organisational units of the Elektro-Bijeljina a.d. After being temporary stored, accumulators and batteries are periodically sold and handed over for further treatment to authorized institutions that buy them off and safeguard them as hazardous waste.

4. CONCLUSION

The existing model of analysis, management and treatment of hazardous waste in complex power distribution systems meets certain aspects of a good system of integrated management of analyzed waste flows, but there is a room for certain improvements of existing waste management practice. Analysis and control of waste flows is not always fully functional and adequate, due to the current method of keeping records. Waste materials records in certain parts of the system are not always precise, timely and/or complete, which results in the MFA and other analyses losing quality, which among other things represents one of the deficiencies of the system and an important parameter to be improved.

Teams carrying out operational activities on the ground do not always report which transformers and what oil quantity they have topped up, and/or what oil quantities have been returned while discharging oil for sampling and other possible activities. This treatment prevents the possibility of precise waste quantification and the identification of location of hazardous waste generation, so there is not always a complete record of all generated flows of hazardous and non-hazardous waste.

Information on waste materials is not always available on time to all competent persons, especially those in charge of various activities related to waste management, so it is necessary to provide a better, faster and better quality information flow. The situation in individual power distribution warehouses does not fully meet the storage terms and conditions required for the temporary storage of hazardous waste, so it is necessary to build and/or expend the capacity of warehouse for temporary disposal of hazardous waste at the sites of the organisational units of the system where they are missing, for the purpose of security and environmental protection.

The quality and timely analysis of waste flows, along with the synthesis of all analyzed data, significantly contributes to a more efficient hazardous waste management, risk reduction and better functioning of complex systems.

5. REFERENCES

- [1] *Law on Waste Management*, "Official Gazette of RS", no 111, 2013.
- [2] *Technical and other documentation*, Mixed Holding Power Company/Elektroprivreda of Republika Srpska, ZEDP Elektro-Bijeljina a.d. Bijeljina, 2013.-2018.
- [3] *Technical rules and instructions for maintenance of distribution power plants and devices*, Mixed Holding Power Company/Elektroprivreda of Republika Srpska, Banja Luka, 2008.
- [4] Nakamura, S., Kondo, Y.: *Waste input-output analysis, Concepts and application to industrial ecology*. In Eco-efficiency in industry and science, edited by A. Tukker. Dordrecht, the Netherlands: Springer Science+Business Media B.V., V.26, 2009.
- [5] Nakamura, S., Nakajima, K., Kondo, Y., Nagasaka T.: *The waste input-output approach to materials flow analysis*. Journal of Industrial Ecology 11(4): 50–63., 2007.
- [6] Stanisavljevic, N., Brunner, P.H.: *Combination of material flow analysis and substance flow analysis: A powerful approach for decision support in waste management*. Waste Management & Research, 0734242X14543552, 2014.
- [7] Brunner, P.H., Rechberger, H.: *Practical handbook of material flow analysis*. Boca Raton, FL, USA: CRC Press, 2004.
- [8] Vujic, G., Stanisavljevic, N., Batinic, B., Ubavin, D., Kovacevic, S.: *Material flow analysis as a basis for hazardous waste management in transition economies - power company distribution case study*, Hazardous and Industrial Waste Management, Crete: Technical University of Crete, pp. 55-56, 2010.
- [9] *Law on Environmental Protection*, "Official Gazette of RS", no. 71, 2012.
- [10] *Law on Safety at Work*, "Official Gazette of RS", no. 01, 2008. and no. 13, 2010.
- [11] *Fire Protection Act*, "Official Gazette of RS", no. 71, 2012.
- [12] Todorovic, M., Bakrac S.: *Integration of the environmental risk assessment process into the environmental impact assessment process - methodological approach*; University Singidunum, Ministry of Defense of the Republic of Serbia, Belgrade, 2010.
- [13] Musulin, B.: *Ecological aspects of the use and disposal of transformer oils, Fourth counseling*; Croatian Committee of International Conference on Large Electrical Systems, Koncar - Institute of Electrical Engineering, Zagreb, 1999.
- [14] Panic, M.: *Hazardous waste management, planning, organization, system functioning*, Special editions, Serbian Academy of Sciences and Arts, Belgrade, 2010.

Authors: Dragisa Djordjic, Specialist in Environmental Engineering, Ph. D. Slavko Djuric, Full Prof., Ph. D. Miodrag Hadzistevec, Full Prof., University of Novi Sad, Faculty of Technical Sciences, Department of Environmental and Occupational Safety Engineering, 6, Dositeja Obradovica Square, 21000 Novi Sad, Serbia, Phone:+38765738060. E-mail: zastitad@gmail.com

Ilic, B.

MANUFACTURE OF HEAT AND ELECTRIC ENERGY BY CONSTRUCTION OF MUNICIPAL SOLVENT AND AGRICULTURAL WASTE

Abstract: *In order to stop or at least mitigate negative side effects and to enable sustainable development, the general trend in the world is the tendency to decrease the consumption of non-renewable energy sources (fossil fuels) in three ways: by using renewable energy sources instead of non-renewable ones, by using municipal solid waste energy and by improving energetic efficiency. Bearing in mind the aforementioned, the EU countries, as well as many other countries in the world, have decided to incorporate plans for higher usage of renewable energy sources into their strategies of energetic development and the environment protection, for higher usage of municipal solid waste energy and for improving efficiency of using energy, as well as for establishing a legislative framework within which these plans will be realised. According to Waste Framework Directive 2008/98/EC, one of the methods to manage waste should include the usage of waste energy, which would lead to reduction of fossil fuel consumption. The aim of this paper is to consider the economic benefits of the plant constructed for the combustion of municipal solid and agricultural waste in which both heat and electricity would be simultaneously produced.*

Key words: *municipal solid waste, agricultural waste, cogeneration plant, heat energy, electrical energy, economic analysis.*

1. INTRODUCTION

The construction costs of cogeneration plant for the municipal solid waste are generally high, so that the investments into such plant are hardly economically cost-effective. Therefore, this paper considers the possibility of constructing the cogeneration plant for municipal solid and agricultural waste, having two times higher caloric value than the municipal solid waste itself, in order to enhance the economic cost-effectiveness of such plant construction.

Municipal solid waste usually includes solid waste material from households and municipal facilities, industrial plants, tourist and commercial facilities, waste from public areas (parks, construction and other waste from demolition), as well as agricultural waste material generated due to various agricultural activities in suburban areas. Agricultural waste is the waste from agricultural residues, forestry, food and wood industry, and it is present in significant amounts. Agricultural residues can be classified into three main groups: waste produced during the cultivation of field crops, waste originating from fruit crops and waste resulting from breeding livestock.

Waste incineration is one of the technically most developed options of waste management available today. However, capital and operating costs for a modern incinerator working in accordance with the emission limitations are high, generally much higher than the costs of waste disposal to sanitary landfills.

Based on conducted research, as well as available data in performed studies on the state and prospects of urban waste [1-9], this paper sets forth the techno-economic analysis of the justification of constructing a cogeneration plant for the on the territory of Novi Sad which would concurrently produce thermal and electrical energy.

2. SELECTION OF AN COGENERATION PLANT

2.1. Estimation of waste composition and its quantity

The project for the construction of the cogeneration plant which would concurrently produce thermal and electrical energy is sustainable only if it is economically and technically justified. Economic justification of such a project mostly depends on waste composition and its quantity. Every project like this involves usage of certain components of waste, therefore these components must be present in sufficient quantities in the waste intended for use. The amount of waste is even more important than the composition because without sufficient quantities of waste, the investment costs cannot be reimbursed.

According to the Waste Management Strategy of the Republic of Serbia for the period from 2010 to 2019, every citizen produces approximately 1 kg of waste on a daily basis [1-3]. According to the results of the latest official population census in 2011, the total number of citizens in Novi Sad is 341 625. This means that the amount of waste produced in Novi Sad per year is approximately 125 000 tons ($341\,626 \text{ citizens} \times 1 \text{ kg of waste} / \text{citizen} \times 365 \text{ days} / \text{year} = 124\,693\,490 \text{ kg waste} / \text{year} \approx 125\,000 \text{ tons waste} / \text{year}$).

Based on the recommendations of the World Bank, key conditions for using waste as fuel in cogeneration plants are: average low thermal power of waste must not be smaller than 6 MJ/kg throughout the year and the yearly average low thermal power must not be smaller than 7 MJ/kg. These conditions are met on the territory of Novi Sad, according to the aforementioned Strategy [1-3].

Biomass in agriculture represents very important source of biomass in Serbia, particularly in the region of Vojvodina. When it comes to biomass in agriculture, then, first of all, it refers to the processing of residues from plants, fruits and vineyards. It has been estimated that total of about 12,5 million tons of biomass are produced in Serbia every year, out of which about 9 million tons (72%) in the region of Vojvodina. The region of Vojvodina disposes of relatively large potentials of biomass, which is produced as “surplus” in the primary productivity of agriculture. The potentials of biomass produced from some „more valuable“ energy crops and its thermal potentials are shown in Table 1[1].

Types of biomass	Lower caloric value, MJ/kg
Wheat straw	14.00
Barley straw	14.20
Oat straw	14.50
Soybean straw	15.70
Maize stalks	13.50

Table 1. Potentials of biomass produced from some “more valuable” crops and its thermal potentials [1]

2.2. Selection of the cogeneration plant

Capital costs of the plant for burning waste directly depend on the plant capacity. Generally, the costs of the plant are significantly decreased if the capacity is increased, from 100 000 to 200 000 tons per year, i.e. 400000 tons per year. The optimal plant capacity is hard to determine. It is believed that economically profitable cogeneration plants can burn from 100 000 to 150 000 tons of waste per year; considering the fact that 125 000 tons of waste are produced in Novi Sad per year, the cogeneration plant which can burn around 120 000 tons of waste per year has been chosen [1-3].

Moreover, it is estimated that cogeneration plant would also benefit of the agricultural waste i.e. biomass produced as „surplus“ in the primary productivity of agriculture, namely 60 000 tons of agricultural waste per year. Since the caloric value of agricultural waste is twice higher than the caloric value of municipal solid waste, then from 60 000 tons of agricultural waste approximately the same quantity of heat and electricity would be produced as from 120 000 tons of municipal solid waste per year.

2.3. Selection of the waste burning technology in the cogeneration plant

The technology of burning waste on a grate has been chosen since it is most often used for the incineration of larger quantities of residual waste (above 100 000 tons of waste per year). The combustion grate is a reliable and proven technology, and the various performances provide a relatively high degree of control and efficiency. Lack of combustion on a grate is seen in the waste of different quality and with a high moisture content when achieving even burning is a special problem. Even and complete

combustion increases efficiency and decreases emission of toxic gases.

The actual plant design and plant configuration are considerably different depending on the applied technology. Regardless of the type of technology, the plants for burning waste and obtaining energy consist of the following elements, Figure 1: waste reception and handling, combustion chamber, plant for obtaining energy from waste, treatment of gases produced in the process of combustion and treatment of ash and pollution generated from the air pollution control device.

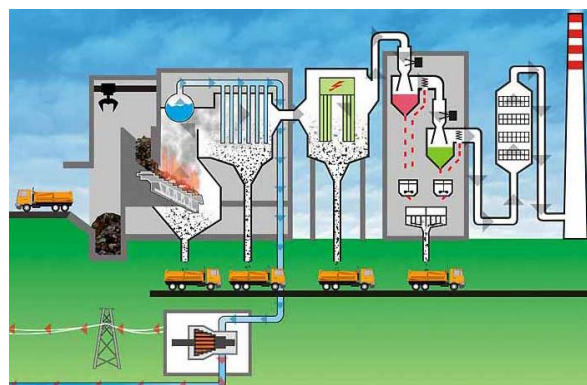


Figure 1. Municipal cogeneration plant [1]

3. ECONOMIC ANALYSIS

Incineration of waste involves high investment costs, as well as high operation and maintenance costs. The net price of treatment costs per ton of waste treated by incineration is higher comparing to other options (usually landfills). Depending on the actual costs (which considerably depend on the size of the plant), as well as the income from the energy sales, the net treatment costs per ton of waste are from 25 € to 100 €, on average 50 €. At the same time, average costs of waste disposal at landfills are from 10 € to 40 € per ton [1, 2].

The costs of constructing an cogeneration plant and the operating costs are high. One of the main problems of implementing incineration is non-homogeneity of waste. The composition of waste is constantly changing over time, therefore it is difficult to achieve a steady work process. The hardest factor is to adjust the quantities of moisture and non-combustible materials in waste to the burning process. Public resistance is also inevitable and it can pose a serious problem due to the air pollution caused by the incineration process. This pollution cannot be completely avoided even in the most advanced plants.

3.1. Total costs of investment in the construction of the plant for cogeneration

It has been estimated that the total costs of investment I in the construction of the plant for cogeneration plant are around 190 000 000 €, which can be seen in Table 2.

Type of cost	Amount of cost, €
Costs of land purchase and the construction of road infrastructure	4 000 000
Costs of building the constructional part of the facility	24 000 000
Costs of building a waste storage	6 000 000
Costs of acquiring and installing an incinerator with a boiler	64 000 000
Costs of acquiring and installing water and steam systems	26 000 000
Costs of acquiring and installing electro-mechanical equipment	16 000 000
Costs of acquiring and installing the equipment for purification of flue gases	12 000 000
Other investment costs	22 000 000
Designing costs	6 000 000
Total costs of investment in the construction of the cogeneration plant <i>I</i>	190 000 000

Table 2. Total costs of investment in the construction of the plant for cogeneration plant

3.2. Total yearly gross income

Total yearly gross income *B* that the cogeneration plant would achieve approximately amounts to 19 106 400 € and it has been calculated as the sum of several incomes, which can be seen in Table 3:

- the income from waste disposal reimbursement, which amounts to around 6 000 000 € per year. It has been estimated that the reimbursement for waste disposal amounts to 50 € per ton of waste (120 000 tons of waste / year \times 50 € / tons of waste = 6 000 000 €).
- the income from the sales of electrical energy to the distribution network, which amounts to around 6 170 400 €. It has been estimated that electrical energy of 0.300 MWh/tons of waste would be sold per year and that the incentive price of electrical energy produced in the waste power plant amounts to 0.0 857 € / kWh (0.300 MWh / tons of waste \times 120 000 tons of waste \times 0.0 857 € / kWh + 0.600 MWh / tons of waste \times 60 000 tons of waste \times 0.0 857 € / kWh = 72 000 MWh \times 0.0 857 € / kWh = 72 000 kWh \times 85.7 € / kWh = 6 170 400 €). In order to encourage the investors and reduce the investment risk, the Government of the Republic of Serbia has prescribed Feed-in tariffs, i.e. the incentive purchase price of electrical energy produced in waste power plants, which is 0.0 857 € / kWh. The price of heat energy is about 0.05 € / kWh.
- the income from the sales of produced heat energy to the adjacent commercial sector (for heating the process steam in the industry, for drying

agricultural products, for heating greenhouses, etc.) which amounts to around 6 936 000 €. It has been estimated that thermal energy of 0.578 MWh / tons of waste would be sold per year and that the price of thermal energy amounts to 0.05 € / kWh (0.578 MWh / tons of waste \times 12 00 00 tons of waste \times 0.05 € / kWh + 1.156 MWh / tons of waste \times 60 000 tons of waste \times 0.05 € / kWh = 138 720 MWh \times 0.05 € / kWh = 138 720 kWh \times 50 € / kWh = 6 936 000 €).

Type of income	Amount of income, €
Income from the fee for the disposal of waste	6 000 000
Income from the sales of produced electrical energy to the distribution network	6 170 400
Income from the sales of produced heat energy to the adjacent commercial sector	693 6000
Total yearly income which the cogeneration plant <i>B</i>	19 106 400

Table 3. Total yearly income which the plant for cogeneration plant

3.3. Total yearly costs

Total yearly costs T_{uk} that would be made by the cogeneration plant amount to around 1 820 000 €, and have been calculated as the sum of:

$$T_{uk} = T_{st} + T_{ekspl} = 1 020 000 + 6 600 000 = 1 820 000 \text{ €}$$

where the following are:

T_{zr} - total yearly costs for paying wages to workers

T_{od} - total yearly maintenance costs.

3.3.1. Total yearly costs for paying gross wages to workers

Total yearly costs for paying gross wages to workers amount to approximately 1020000 €. It has been assumed that the plant will work 24 hours a day in three shifts, seven days a week. It has been estimated that 80 workers will be employed and that their average gross wages will be 1000 € per month (160 \times 1000 \times 12 = 1 020 000 €).

3.3.2. Total yearly maintenance costs

Total yearly maintenance costs amount to around 6 600 000 € since it has been estimated that they make around 3% of the total investment costs (220 000 000 \times 3 / 100 = 6 600 000 €).

3.4. Total yearly net income

Table 4 shows the costs and incomes that the cogeneration plant.

Type of cost or income	Amount of cost or income, €
Total costs of investment in the construction of cogeneration plant I	190 000 000
Total yearly gross income B	19 106 400
Total yearly costs T_{uk}	1 820 000
Total yearly net income $Z = B - T_{uk}$	17 286 400

Table 4. Costs and incomes which the cogeneration plant

Total yearly net income Z that the cogeneration plant is 17 286 400 €, and is calculated when total yearly costs T_{uk} are subtracted from the total yearly gross income B :

$$Z = B - T_{uk} = 19\,106\,400 - 1\,820\,000 = 17\,286\,400 \text{ €}$$

3.5. Repayment period of the investment in the construction of the cogeneration plant

The repayment period of the investment in the construction of the cogeneration plant is a time period which should pass in order to collect the total investments from the future earnings. It is, in fact, the number of years N for which the investment in the construction of the cogeneration plant will be repaid. The repayment period (the return) of the investment N in the construction of the cogeneration plant is calculated if the total costs of investment in the construction of that plant I are divided by the total yearly net income Z which the plant would achieve.

$$N = \frac{I}{Z} = \frac{190\,000\,000}{17\,286\,400} = 11 \text{ years}$$

Based on the completed analysis, it may be deduced that the investment in the construction of the cogeneration plant would be repaid in 11 years. This plant's operation would contribute to the decrease of fossil fuel consumption, provide about 1600 new job openings, contribute to environmental protection, etc.

4. CONCLUSION

Based on the research results can be concluded that the construction of cogeneration plant using the municipal solid and agricultural waste would become cost-effective in about 11 years. The construction of such plant would contribute to the opening of new working places, then to the reduction of greenhouse gas emissions and thus to the reduction of global heat, as well as to the reduction of human environment pollution, since the consumption of fossil fuels would be reduced.

The use of municipal and agricultural waste contribute to the increase of security in energy supply and to the lower import of energy supply products. As already known, fossil fuels will not last for ever and when the world spends all its biomass reserves, the

municipal solid waste will become even more attractive source of energy. In the light of foregoing reasons, municipal solid waste and agricultural waste are gaining more and more significance as energy supply resources.

5. REFERENCES

- [1] Ilić, B., Adamović, Ž., Kenjić, Z., Blaženović, R.: *Obnovljivi izvori energije i energetska efikasnost*, Srpski akademski centar, Novi Sad, 2013.
- [2] EEA, Biodegradable municipal waste management in Europe Part 3: Technology and market issues, EEA Report No. 15/2001, Copenhagen, Denmark. 2002.
- [3] Mihajlović, V.: *Model upravljanja otpadom zasnovan na principima smanjenja negativnog uticaja na životnu sredinu i ekonomske održivosti*, Doktorska disertacija, Fakultet tehničkih nauka, Univerzitet u Novom Sadu, 2015.
- [4] *Strategiju upravljanja otpadom Republike Srbije za period 2010- 2019.*, Vlada Republike Srbije, 2010.
- [5] Fakultet tehničkih nauka, Novi Sad: *Utvrdjivanje sastava otpada i procene količine u cilju definisanja strategije upravljanja sekundarnim sirovinama u sklopu održivog razvoja Republike Srbije*, Ministarstvo životne sredine i prostornog planiranja, 2008.
- [6] Brkić, M., Alimpić, M., Đukić, Đ: *Neke mogućnosti korišćenja nekonvencionalnih izvora energije u poljoprivredi i prehrambenoj industriji*.
- [7] Brkić, M., Janić, T: *Mogućnosti korišćenja biomase u poljoprivredi*, Zbornik radova sa II savetovanja: „Briketiranje i peletiranje biomase u poljoprivredi I šumarstvu”, Regionalna privredna komora iz Sombora i „Dacom” iz Apatina, Sombor, 1998.
- [8] Studija: *Potencijali i mogućnosti briketiranja i peletiranja otpadne biomase na teritoriji pokrajine Vojvodine*, Novi Sad, decembar 2007.
- [9] Vujić G., Ubavin D., Stanisavljačić N., Batinić B.: *Upravljanje otpadom u zemljama u razvoju*, Novi Sad: FTN Izdavaštvo, 2012.

Authors: Prof. Bozo Ilic, The Higher Education Technical School of Professional Studies in Novi Sad, 1 Street, E-mail: ilic@vtsns.edu.rs

Ilic Micunovic, M., Agarski, B., Hadzistevic, M., Kosec, B., Vukelic, D.

COMPARABILITY OF LIFE CYCLE ASSESSMENT RESULTS IN TYPE III ENVIRONMENTAL DECLARATIONS

Abstract: Environmental declarations type III contain quantitative data of product based on life cycle assessment (LCA) also known as life-cycle data declarations. ISO 14025 establishes procedures and principles for validity of type III environmental declarations and ISO 14025 is closely related to ISO 14040 which defines content and format for LCA studies. For comparability of LCA results, different environmental declarations must have the same goal and scope, as well as calculation rules. In order to determine all the specific requirements and achieve the necessary goals, product category rules have been developed. Although the product category rules are a key part of ISO 14025 for the comparability of the environmental declarations scheme, differences still exist. Basic goal of this paper is to present discrepancies in some aspects of LCA results in Type III programs. The representation of LCA results through the number of impact categories and consumption of natural resources have been examined. Research found that there was no consistency within LCA results from environmental declarations of different products.

Key words: Environmental declarations, Type III, LCA, PCR

1. INTRODUCTION

A number of misleading “green” environmental claims have developed the need not only for standardization of environmental information, but also transparency of quantitative information on products and service has become evident [1,2]. Series of standards ISO 1402X has been developed to support and dissemination of such environmental aspects of products. This series of standards defines three type of eco-labelling program (Fig. 1):

- **Type I** - a voluntary, multiple-criteria based, third party program that awards a license that authorizes the use of environmental labels on products indicating overall environmental preferability of a product within a particular product category based on life cycle considerations;
- **Type II** - informative environmental self-declaration claims, and
- **Type III** - voluntary programs that provide quantified environmental data of a product, under pre-set categories of parameters set by a qualified third party and based on life cycle assessment, and verified by that or another qualified third party.

The regulatory framework for Type III environmental declarations (better known as environmental product declarations EPD) are also included in the ISO 14000 series of standards, more precisely ISO 14040 (2006) and ISO 14044 (2006) (Fig. 1) and developed according to a set of pre-defined product category rules (PCR) [3,4].

In recent years the number of Type III programme operator and bodies for administration and verification of Environmental Declaration

Programme (also known as EPD programme or EPD scheme) has increased [4]. Some of the programmes that have published the greatest number of Environmental Product Declarations are Japan Environmental Management Association for Industry, Korean Environmental Industry & Technology Institute, Agency for Environmental and Energy Management in France (ADEME), IBU-EPD in Germany or the International EPD at the European level [5].

Based on LCA, EPDs should enable comparison between products, fulfilling the same function [6]. Increasing number of EDP schemes, on the one hand provides more information and greater credibility and comparability of products from different categories. But on the other hand, because everyone can become a programme operator to develop PCRs and to verify EPDs [7], EPD schemes can also lead to trade barriers on the market because of different requests. All this has resulted in inconsistencies and absence of a systematic coordination of PCRs for the same product categories [8]. Moreover, comparability between the environmental performances of products lacks significance and bears to risk the legitimacy of LCA based claims on the market [6]. Methods for calculation environmental impacts can also lead to confusion among consumers.

Therefore, in order to analyses the current state and practical challenges in the field, the objective of this paper is to examine consistency in LCA results for some product categories. The examination of the results was done from the aspect of the three criteria. The method of research has been tested on fifteen product categories including the International EPD system

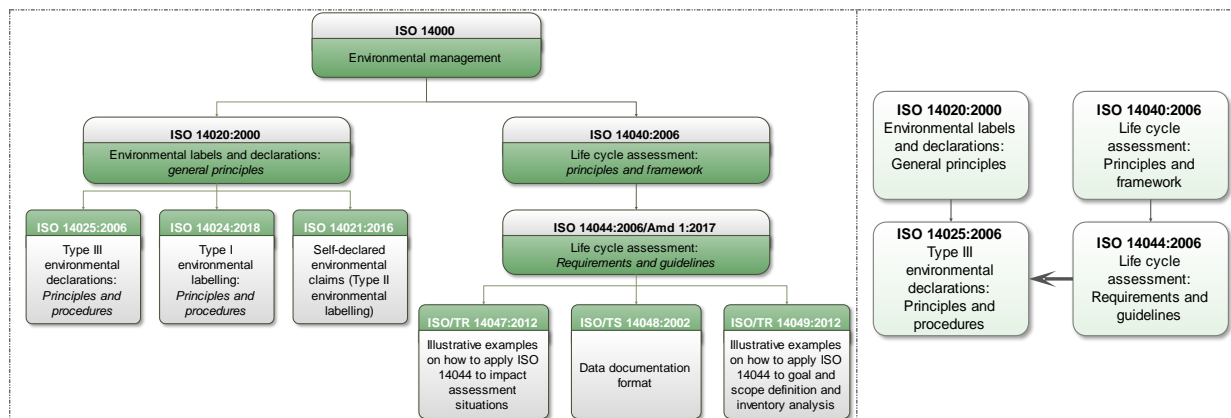


Fig. 1 Regulatory framework for environmental certification

(made in: Spain, Swedish, Italy), Norwegian EPD and EcoLeaf Japan. The basic assumption of the research was that these EPDs based on LCA study have some consistency in the results. The aim of this paper is to explore that assumption on different product.

2. RESEARCH METHOD

General Programme Instructions defined by ISO 14025 is crucial and obligatory for every operative who makes EPD schemes. There are 13 requirements in General Programme Instructions [11]. Also, in the same standard there are procedures for developing PCR. All examined Environmental Declaration Programme in this work are based on this standard. In order to determine the consistency of the results, in this case which are expected. Also, in line with results, we determine the certainty for greater harmonization in process of generating EDP scheme.

The study included a parallel examination of fifteen products from different EPD schemes, and their inclusion of the same parts of the LCA study. The research method here was to discuss the experiences from the practical work with the EPDs and draft text to arrive at consensus guidelines within the framework of relevant standards and norms [12,13].

In previous literature, comparison of Environmental Declaration Programme has been studied from several perspectives based on different approaches and parameters of these eco labels [1,2,3,5,9]. In this study, with in environmental approach we have considered in LCA results: the impact categories and specifications of energy consumption, in the sense of the existence of specially defined renewable/non-renewable energy resources. We also took an interested in the existence of system boundaries that are shown in the results.

The main findings of the programs comparison and analysis are further presented.

3. EVALUATION AND OUTCOMES

Overview of EPD schemes, to examine consistency of LCA results in practices worldwide are shown in Table 1. The table contains five products of International EPD System, EcoLeaf, and five of The Norwegian EPD Foundation.

The results from the investigation show, there is no consistency in the results. System boundaries include Cradle-to-Gate, Cradle-to-Grave or Gate-to-Gate life cycle. There are three LCA studies that include gate-to-gate system boundaries, although it is easiest to collect data from manufacturers, there is still a clear need for more complete data on resource extraction, consumer use and end-of-life. Cradle-to-Grave system boundaries provide more comprehensive information about product impact.

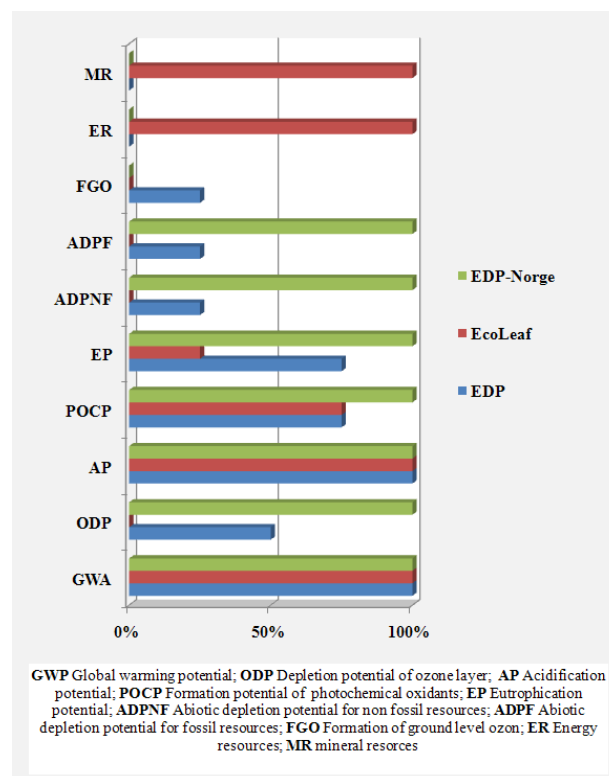


Fig. 2. Representation of impact categories in EDP schemes.

Program name	Country of program origin	Type	Management system	Product	System boundaries	Number impact categories	Specification of renewable/non-renewable energy resources
International EPD System	Sweden	EPD	ISO 9001, OHSAS 18001, ISO 14001	Mooring chain	Cradle-to-Gate	5	Yes
International EPD System	Spain	EPD	ISO 14025	Ceramic tiles. Glazed Stoneware tiles	Cradle-to-Grave	7	No
International EPD System	Italy	EPD	ISO 14040-14044	Beer made from malt	Gate-to-Gate	4	Yes
International EPD System	Europe	EPD	ISO 14025, ISO 14040, ISO 14044, PCR 2007	Electricity, steam and hot/cold water generation and distribution	Cradle-to-Grave	4	Yes
International EPD System	Spain	EDP	ISO 9001, ISO 14001	Uni CPC Corrugated paper and paperboard	Gate-to-Gate	4	Yes
EcoLeaf	Japan	EPD	ISO14001	Data Projector	Cradle-to-Grave	4	Yes
EcoLeaf	Japan	EPD	ISO14001	Paper Beverage Carton	Cradle-to-Gate	7	Yes
EcoLeaf	Japan	EPD	ISO14001	Flat-bed/ Sheet-fed scanner	Cradle-to-Gate	5	Yes
EcoLeaf	Japan	EPD	ISO14001	Network camera	Cradle-to-Gate	5	Yes
EcoLeaf	Japan	EPD	ISO14001	EP and IJ printer	Cradle-to-Grave	4	Yes
The Norwegian EPD Foundation	Denmark	EPD	ISO 14001, ISO 9001, OHSAS 18001	Knauf Danogips Secura Board	Cradle-to-Grave	7	No
The Norwegian EPD Foundation	Norway	EPD	ISO 14001, ISO 9001	Steel structures	Gate-to-Gate	7	No
The Norwegian EPD Foundation	Norway	EPD	ISO 14025, ISO 14044	Permanent Bar Anchor	Gate-to-Gate	7	No
The Norwegian EPD Foundation	Norway	EPD	ISO 14001, ISO 9001	Con II - high backrest	Cradle-to-Grave	7	No
The Norwegian EPD Foundation	Norway	EPD	ISO 14001, ISO 9001	WPC cladding profiles	Cradle-to-Gate	7	No

Table 1. Issues precluding comparison within EPDs

The number of impact category is also uneven. Only results of EDP Norway always considered the same impact categories, which include: global warming potential, depletion potential of the stratospheric ozone layer, formation potential of tropospheric photochemical oxidants; acidification potential of land and water, eutrophication potential, abiotic depletion potential for non fossil resources and abiotic depletion potential for fossil resources. The other two EDP schemes did not take into account neither the same number nor the same impact category within the LCA results (Fig. 2.).

EDP Norwegian labels showed the same system for displaying LCA results of energy consumption from renewable and non-renewable resources. There are summarized, in the sense for example: renewable/non renewable primary energy resources used as energy carrier or use of renewable/non renewable secondary fuels. There are no distinctness which are specific sources of renewable/non renewable energy. Japan EcoLeaf provides a specification of non renewable energy resources (coal, crude oil, LNG, uranium content of an ore), but for renewable resources it only appears in the form of wood and water consumption. In International EPD System the presence of LCA

results of specification of the energy resource varies. But if the specification exists accurately accentuated which are the sources of energy consumption. For renewable resources there is hydroelectric, solar, wind, biomass, geothermal; for non renewable resources there is uranium, fuel oil, coal, lignite, natural gas.

4. CONCLUSIONS

Environmental labels type III that are quantitative and based on life cycle of product or service have a large potential to provide the most concrete and most accurate data of impacts on environment. However, like other environmental claims, they can be subject to wrong management by the operator of LCA study, without transparent rules that ensure their complete accuracy and data content. Ultimately, environmental product declarations made for a product or service need to be comparable in terms of LCA results, so potential buyers or consumers, can make choices based on legitimate, quantifiable information.

This study has contributed to investigation of consistency and comparability of LCA results in EDP scheme and the need for policy improvement.

It is very important to respect the policy in these in this area, like ISO standards and product category rules because they provide the guidance on how life cycle study should be estimated and reported. It can be noticed that, within our results, although the sample is not large, there is a discrepancy in the processing of the LCA study and also in the way the results are published.

Future efforts need to be directed toward aligning of existing policy and developing new one that can permit consistent comparison of product environmental declarations at international level, and will require overcoming the aforementioned challenges in a consensus process that is transparent.

5. REFERENCES

- [1] Ingwersen, W.W, Stevenson, M.J.: *Can we compare the environmental performance of this product to that one? An update on the development of product category rules and future challenges toward alignment*, Journal of Cleaner Production, Vol. 24, pp 102-108, 2012
- [2] Minkov, N., Schneider, L., Lehmann, A., Finkbeiner, M.: *Type III Environmental Declaration Programmes and harmonization of product category rules: status quo and practical challenges*, Journal of Cleaner Production, Vol. 94, pp 235-246, 2015
- [3] Ibanez-Foresa, V., Pacheco-Blanco, B., Capuz-Rizo, S.F., Bovea, M.D.: *Environmental Product Declarations: exploring their evolution and the factors affecting their demand in Europe*, Journal of Cleaner Production, Vol. 116, pp 157-169, 2016
- [4] Bovea, M.D., Ibanez-Foresa, V., Agustí-Juan, I.: *Environmental product declaration (EPD) labelling of construction and building materials*, Eco-efficient Construction and Building Materials, Life Cycle Assessment (LCA), Eco-Labeling and Case Studies, Pages 125-150, 2014
- [5] Zackrisson, M., Rocha, C., Christiansen, K., Jarnehammar, A.: *Stepwise environmental product declarations: ten SME case studies*, Journal of Cleaner Production, Vol. 16, pp 1872-1886, 2008
- [6] Gelowitz, M.D.C., McArthur, J.J.: *Comparison of type III environmental product declarations for construction products: Material sourcing and harmonization evaluation*, Journal of Cleaner Production, Vol. 157, pp 125-133, 2017
- [7] Knauf, M.: *Applying opportunity costs to correctly interpret resource efficiency in LCA studies and environmental product declarations*, European Journal of Wood and Wood Products, Vol. 73, pp 251–257, 2015
- [8] Strazza, C., Del Borghi, A., Blengini, G.A., Gallo, M.: *Definition of the methodology for a Sector EPD (Environmental Product Declaration): case study of the average Italian cement*, The International Journal of Life Cycle Assessment, Vol. 15, pp. 540–548, 2010.
- [9] Lee, K.M., Park, P.: *Application of Life-Cycle Assessment to Type III Environmental Declarations*, Environmental Management, Vol 28, pp. 533-46, 2001.
- [10] Magerholm Fet, A., Skaar, C., Michelsen, O.: *Eco-labeling, Product Category Rules and Certification Procedures Based on ISO 14025 Requirements*, The International Journal of Life Cycle Assessment, Vol. 11, pp 49–54, 2006.
- [11] ISO, 2006a. Environmental Labels and Declarations Type III Environmental Declarations-Principles and Procedures (ISO 14025:2006), International Organization for Standardization.
- [12] ISO, 2006b. Environmental Management Life Cycle Assessment e Principles and Framework (ISO 14040:2006), International Organization for Standardization.
- [13] ISO, 2006c. Environmental Management Life Cycle Assessment e Requirements and Guidelines (ISO 14044:2006). International Organization for Standardization.

Autori: M.sc. Milana Ilic Micunovic, Assis. Prof. Boris Agarski, Full Prof. Miodrag Hadzistevic, Assoc. Prof. Djordje Vukelic, University of Novi Sad, Faculty of Technical Sciences, Department of Production Engineering, Trg Dositeja Obradovica 6, 21000 Novi Sad, Serbia, Phone.: +381 21 485 2350, Fax: +381 21 454 495.
Full Prof. Borut Kosec, University of Ljubljana, Faculty of Natural Sciences and Engineering, Department of Materials and Metallurgy, Askerceva 12, 1000 Ljubljana, Slovenia, Phone.: +386 1 2000410, Fax: +386 1 4704560
 E-mail: milanai@uns.ac.rs; agarski@uns.ac.rs; miodrags@uns.ac.rs; vukelic@uns.ac.rs; borut.kosec@omm.ntf.uni-lj.si.

Karanovic, V., Andric, S., Jocanovic, M., Orosnjak, M., Bugaric, U.

IMPORTANCE OF OFFLINE FILTRATION SYSTEM USE

Abstract: Any machine which uses mineral oil for power transfer or lubrication is dependent on the condition of the oil. Maintaining oil performance and machine components at their best is therefore vital. System filters are primarily the last line of defence, but are not conducive to achieving optimum oil cleanliness, as pressure shocks will result in the release of a large amount of the particles already retained by the filter insert. However, originally installed (suction, pressure, return) filters are still important as last chance inline filters. Secondary oil filtration is ideal for ensuring the lowest possible degree of contamination in the system, e.g. to achieve a specific level of oil cleanliness. Because an secondary filter circuit works independently of the hydraulic or any other oil lubrication system, its level of efficiency remains constant –in any situation of system operation. This paper will present reasons that justify use of an secondary filtration system.

Key words: Contamination control, secondary filtration systems, lubricating oil, maintenance

1. INTRODUCTION

Condition and proper treatment of the hydraulic, engine, gear, turbine or any other type of oil, have a great influence on machine working performances, its service life but also the lifetime of the oil itself [1].

Important oil conditioning techniques are: condition monitoring, solid particles filtration, dewatering, degassing, varnish removal and system temperature control. What kind of conditioning techniques will be applied depends on the conditions of exploitation, environment conditions, machine complexity, etc. It has been proven that significant number of machine failures is related to wear caused oil contamination with solid particles [2-4], which puts particles filtration on the first place as an oil conditioning technique.

Irrespective of where it is applied, filtration could be as primary (screening) and secondary (cleaning). Primary filtration is intended to protect the equipment and it is usually installed by the Original Equipment Manufacturers (OEM). This type of filtration needs to assure full fluid flow with minimal flow resistance and to retain rough solid particles. Therefore, this kind of filtering is called screening. Its purpose is not to maintain the oil clean, but to extract large solid particles or other foreign bodies which can cause great damage to the equipment and instantaneous loss of operating function (movement blockage or breakage of moving elements, blockage of flow channels, increase of friction or energy consumption). In order to fulfill these requirements and to provide pressure drop as small as possible, screening filters have short flowing paths, and filter media is very porous.

On the other hand, secondary filtration systems are designed to extend the equipment service life, by separating finer particles, to the level determined by the most critical component which have clearances from 1 to 10 $\mu\text{m}_{(c)}$ (hydraulic servo and proportional valves, pumps, bearings, etc.). Except causing wear of components, friction and energy consumption increase,

this particles acting as catalysts of lubricant physical and chemical degradation processes [5]. This strongly influences overall machine performances and service life of the machine and components. Original Equipment Manufacturers (OEM) rarely include, secondary filtration systems, which is why they are mainly sold as an accessory.

Controlling the lubricant level of contaminants by filtration, allows significant prolongation of its service life [6,7], which can significantly affect the amount of waste oil produced, the costs of its storage, transport and disposal on an annual basis [7].

2. OFFLINE FILTERING SYSTEM COMPOSITION AND CONSTRUCTION

According to the principle of operation, secondary filtration systems can be compared with the work of kidneys and dialysis devices. The secondary filtration system has its own pump and a separate circulation circuit, so it operates independently of the system whose oil is filtered (Figure 1), which is why it is also called the offline filtration system. This means that it can be stopped at any time for a filter element change without interrupting operations.

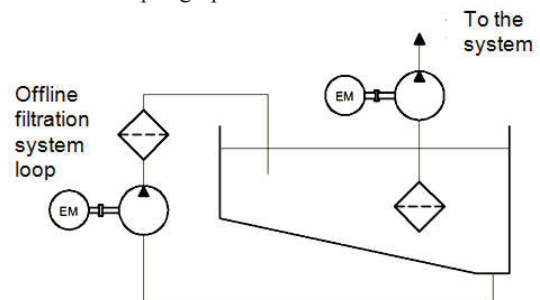


Figure 1. Offline filtering system scheme

Offline filtering systems can be divided into mobile and stationary. Systems are mobile if their task is to

serve multiple machines, regardless of which volume or oil type is filtered, while stationary filtration systems are specifically designed to serve only one machine.

The complexity of the offline filtration system varies depending on the needs, but essentially all consist of basic elements such as: supporting structure (metal frame), electric motor, pump, filter (low-pressure housing and filter insert), saturation indicator and hoses for connection (Figure 2).

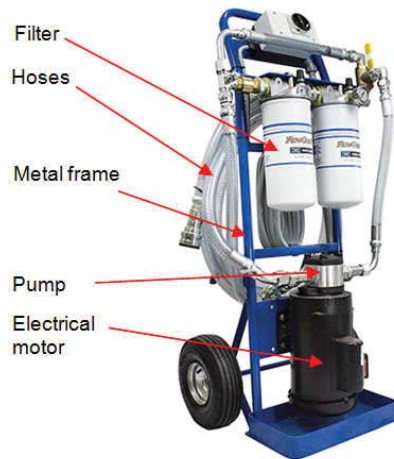


Figure 2. Typical mobile offline filtering system (Des-Case)

In addition to the above mentioned basic elements, the filtering system can be upgraded with filters specifically designed for water extraction, filters for the varnish removal, vacuum system for air extraction or heating and cooling system. Its expansion also includes the installation of systems and sensors for monitoring the level of contamination during filtering.

As filter inserts in offline system, high-capacity filters are used, with small porosity and long flow path with absolute degree of separation of particles smaller than $10 \mu\text{m}_{(c)}$. Secondary filtration beta factor, which stands for particulate removal efficiency (according to multi-pass test procedure - ISO 16889:1999), should not be lower than 200. However, performance of installed filters can vary, and depend on condition of system and the environment.

Pumps used in offline filtration systems are vane or gear pumps, and the choice depends on the operating viscosity of the oil to be filtered. The vane pumps can be used for fluids whose working viscosity is within the range of values from 15 to $\sim 490 \text{ mm}^2/\text{s}$, while gear pumps are used for fluids with viscosity up to $1000 \text{ mm}^2/\text{s}$. Offline filtration system pumps are working with low pressures (up to $p = 10 \text{ bar}$). This eliminates or at least minimize the risk of hydraulic shocks appearance that could damage the filters and reduce its efficiency in retaining impurities. As far as the pump capacity is concerned, it varies depending on the application of the filtration system and moves within the range of values from 5 to 100 l/min for mobile offline systems, and over 100 l/min for stationary filtering systems.

System design varies depending on the needs of the end user. An example of the simplest structure of the offline filtration system is shown in Figure 3.

The complexity of the filtration system construction increases as the higher demands are set, such as the requirement for the existence of a sensor that monitors the level of contamination during the filtration process (Figure 4).

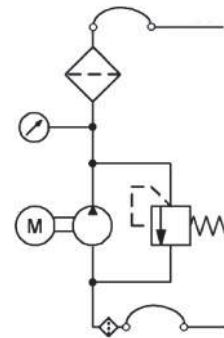


Figure 3. Usual offline filtering system hydraulic circuit

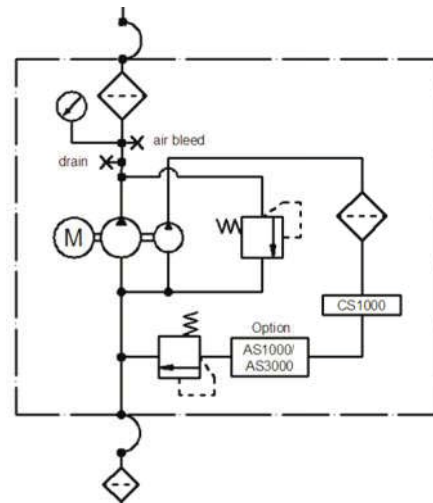


Figure 4. Example of an offline filtration system with APC sensor [8]

Presence of the Automatic Particle Counter (APC) make filtration system efficiency monitoring easier and increases reliability in the offline filtration system results. There are recommendations for specific applications where exist the risk of water contamination and mixing of water and lubricant (marine and offshore applications, turbine machines, etc.) to use offline filtration systems which have dewatering filters. Water separation can be done with coalescence filters, absorbent filters, centrifugal process or vacuum chambers. Figure 5. shows the system which have coalescent filter for water retention.

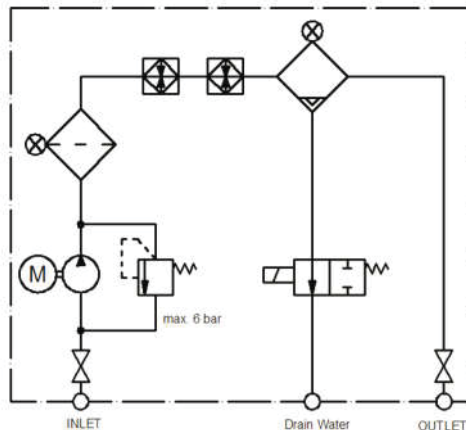


Figure 5. Example of an offline filtration system with coalescing filter for water removal [8]

3. REASONS FOR USE

First of all, offline filtration system should not be purchased before the level of fluid contamination is established. In order to calculate cost-effectiveness of the investment in offline filtration system implementation, one should know parameters such as: contamination level, machine downtime costs, costs of changing the oil and filters with new one, costs of old lubricant and filters disposal, labor costs, etc. Without this, implementation of the offline filtration system, will not do any harm to the machine, but it could be just an unnecessary waste of money (especially when applying filtration treatment on oil which is chemically and physically depleted). Trough the practice, there is a lot of cases where was noted misusing of the offline filtration systems in Serbia. In most cases offline filtration program, where it should be, is not used at all.

One of the reasons for the offline filtration systems utilization, as it was mentioned before, is that filtering systems installed by machine manufacturer (suction and return-line filters), are usually designed to detain rough dirty particles thereby preventing damage to the pumps, or other components that are sensitive to the presence of the same. Those system filters are always a compromise between flow rates, linear velocity, viscosity, contamination, system pressure, pressure drop, dirt-holding capacity, physical size, accessibility and cost [9]. Offline filters are not governed by system requirements as they operate independently from the system. Therefore, operators have many options for filters, their capacity, media and micron ratings.

As for in-line pressure filters, they can be designed to extract particles $\leq 10 \mu m_{(c)}$, but it affects flow restriction to a level that would deny the equipment proper lubrication. In addition, they have low capacity, and as pressure shocks caused by stop/start of the main pump will result in the release of a large amount of the particles already retained by the filter insert.

The biggest reason to filter oil by offline filtration is to maximize the return on the investment in the oil and to extend equipment life.

Filter system selection must follow a thorough analysis of the system constraints and a clear definition of the task objectives. Following questions could be

very helpful when determining elements of the offline filtration system:

- What is the tank volume?
- What will the fluid viscosity be during filtration?
- What is the initial and what is the targeted cleanliness level?

It is highly recommended to use offline filtering systems where the consequences of contaminated oil are high (wind turbines, steam and gas turbines, rolling mills, paper machines, et cetera). Utilization of the offline filtering provides:

- Removal of oil aging products, solid particles and water,
- Continuous maintenance of desired lubrication oil cleanliness level,
- High contamination retention capacity,
- Optimal protection of oil system components,
- Avoiding expenses on flushing and manual cleaning of oil tank and other components,
- Reducing the load on in-line pressure filters,
- Reduce the number of equipment downtimes,
- Increase equipment availability and operational reliability,
- Lowering costs for service and maintenance, etc.

4. OFFLINE FILTERING SYSTEM APPLICATIONS

There are various applications of the offline filtration system usage (Figure 6). Except filtration, offline systems could be used as following: flushing (flushing of the system, pipes, tanks or any other system component), reservoir draining, oil transferring, stored oil cleaning, etc. Power flush involves reducing the oil level in a tank or sump and flowing the oil at a high velocity across the bottom to push out low-lying sediment. Wand flush implies that wand which is attached to one of the cart hoses, is used first to discharge at high pressure (kicking up adherent debris). Then the flow is reversed and the wand vacuums the sediments. Transfer cart is application where oil is transferred from a storage container to the machine's lube compartment or reverse. Another application is the cleaning stored lubricants. The cart multipasses fluid out of and back into the drum to drawdown contamination. Sump and reservoir drains will wash out debris better if the waste oil is pumped out as opposed to simply flowing out by gravity. Line or hose flush is another application where filter cart is used for cleaning.

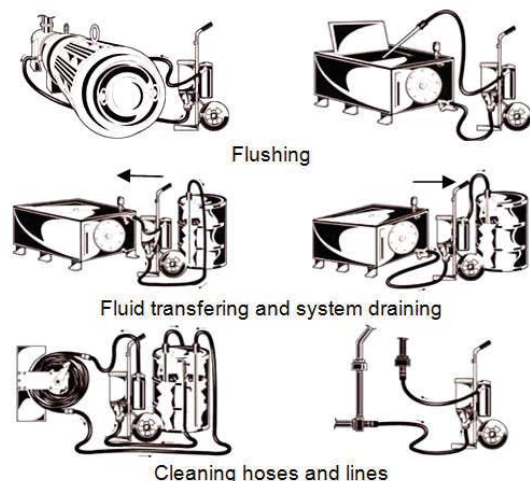


Figure 6. Applications for filter carts [10]

5. CONCLUSION

Primary filtration will help protect the equipment investment whereas secondary filtration helps to maximize the return on the equipment and oil investment. Because it extends useful life of oil and the machinery, filtration helps the environmental protection. With the continued rise in equipment costs, machine downtime costs and oil replacement costs, adding offline filtration to equipment can be very smart decision for the equipment owner.

Offline filtration systems utilizes low-pressure filters that are easily accessible and serviceable. This type of filtration significantly reduces risk of releasing previously retained impurities due to low pressure oscillations in offline filtering circuit. Using of secondary filtration systems guarantees optimum protection of machine components, and provides higher level of reliability.

In order to be economical and rational, before utilization of the offline filtration, oil analysis must be performed. Only then, the technicians will know the right moment when the application of the offline filtration is appropriate, otherwise it could be a waste of money.

6. REFERENCES

- [1] Botly, J.: *Engine filtration: Effective maintenance is the key to optimal performance*, Filtration+Separation, November/December, pp. 22-24, 2010.
- [2] Battat, B., Babcock, W.: *Understanding and reducing the effects of contamination on hydraulic fluids and systems*, The AMPTIAC Quaterly, Vol. 7, No. 1, pp. 11-15, 2003.
- [3] Kumar, M., Mukherjee, P.S., Misra, N.M.: *Advancement and current status of wear debris analysis for machine condition monitoring: a review*, Industrial lubrication and tribology, Vol. 65, No. 1, pp. 3-11, 2013.
- [4] Nash, T.: *Filtration: It's the little things that get you*, Hydraulics and Pneumatics, No. 5, pp. 29-31, 2006.

- [5] Karanović, V., Jocanović, M., Orošnjak, M.: *Condition Monitoring of Hydraulic Machinery by Oil Analysis*, Proceedings of PSU-UNS International Conference on Engineering and Technology - ICET, pp. 1-4, Novi Sad, Serbia, Faculty of Technical Sciences, June, 2017.
- [6] *Hydraulic fluids: Controlling contamination in hydraulic fluids*, Filtration & Separation, Volume 47, Issue 3, May-June 2010, pp. 28-30
- [7] Sutherland, K.: *Filters and Filtration Handbook - Sections 5 D, E*, Elsevier, Oxford, 2008.
- [8] Hydac International, *Filter Systems – Product Catalogue*, Sulzbach/Saar Germany, 2016.
- [9] Khonsari, M., Booser, E.R.: *How to Match Oil Filtration to Machine Requirements*, Machinery lubrication, No. 11, 2006.
- [10] Cooper, D., Perez, R.: *Onsite Portable Filtration Case Study*, Practicing Oil Analysis, No. 5, 2002.

Authors: Assistant Prof. Velibor Karanovic, Mech. Eng. Sladan Andrić, Assoc. Prof. Mitar Jocanovic, Ass. Marko Orosnjak, University of Novi Sad, Faculty of Technical Sciences, Department of Industrial Engineering and Management, Trg Dositeja Obradovica 6, 21000 Novi Sad, Serbia.
E-mail: velja_82@uns.ac.rs.

Prof. Ugljesa Bugaric, University of Belgrade, Faculty of Mechanical Engineering, Department of Industrial Engineering, Kraljice Marije 16, 11120 Belgrade, Serbia

Kecic, V., Prica, M., Kerkez, D., Becelic-Tomin, M., Kulic, A., Leovac Macerak, A., Dalmacija, B.

APPLICATION OF A DEFINITIVE SCREENING DESIGN TO MAGENTA DYE DEGRADATION BY HOMOGENEOUS FENTON PROCESS

Abstract: The homogeneous Fenton process for flexographic Magenta dye removal from synthetic aqueous solution and real printing effluent was optimized with a recently developed design of experiments method, definitive screening design (DSD). The effects of four quantitative parameters on Magenta removal rate were investigated: initial dye concentration, iron concentration, hydrogen peroxide concentration and pH value. The results indicated that decolorization process was influenced by all four investigated parameters, with the most positive effects of iron concentration on decolorization efficiency. After the confirmation of the adopted model, DSD was used to explore the final optimal operating conditions. Model proposed that 97.41% of decolorization efficiency can be obtained under optimal conditions. Treatment of real printing effluent confirmed obtained results, resulting with 95.91% of decolorization efficiency under optimal conditions.

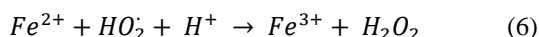
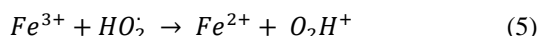
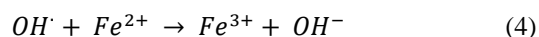
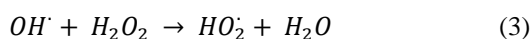
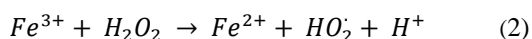
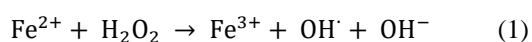
Key words: homogeneous Fenton process, definitive screening design, Magenta, dye removal, optimization

1. INTRODUCTION

Printing industry actualize the major environmental impact through the pollutants discharge, water consumption and energy consumption. A principal source of environmental contamination in printing industry is a discharge process of colored wastewater into the receiving media without pretreatment. These effluents may be considered as highly toxic to the aquatic biota since they affect the photosynthetic activity, aesthetic appearance, makes water inappropriate for drinking and for the use of domestic purposes [1]. Therefore, exists a great need for proper removal and disposal, as well as for the application of the corresponding treatment that is effective in removing dyes from large volumes of effluents.

A widely studied for treatment of different wastewaters, advanced oxidation processes (AOPs) involves the generation of hydroxyl radicals ($\cdot\text{OH}$) in sufficient quantity to affect the removal of refractory and traceable organic contaminants or certain inorganic pollutants [2]. The $\cdot\text{OH}$ radicals are very nonselective and rapidly react with numerous species, transforming them into less and even non-toxic products, thereby increasing wastewater biodegradability and providing an ultimate solution for wastewater treatment [3].

One of the most commonly used AOPs is the Fenton process, where the decomposition of hydrogen peroxide is catalyzed by ferrous ions, and the second strongest oxidants after fluorine, hydroxyl radicals, are generated. The classical Fenton radical mechanisms primarily involve the following reactions (1-7) [4]:



The optimum pH value for the Fenton process is about 2.5 - 3.5 since Fe^{3+} can also react with hydrogen peroxide at lower pH levels, in which the hydroxyl and hydroperoxyl radicals are formed, and the catalyst is regenerated. On the other hand, further precipitation of iron oxyhydroxide is expected at higher pH values. Upon adequate adjustment of operational conditions, taking into account the initial iron and hydrogen peroxide concentration, pH values and the characteristics of the treated wastewater, the Fenton system is relatively easy to monitor and maintain [5].

A recently developed design of experiments method, the definitive screening design (DSD), enables to investigate the effect of process parameters including their interactions or quadratic effects on the process efficiency, therefore optimizing the degradation process. Additionally, the statistical model is able to estimate the model coefficients in the descriptive equation for k parameters with only $2k + 1$ experiments. This strategy leads to a dramatic reduction in the number of experiments to be performed, compared to traditional screening methods, thus enabling a significant saving in time and reagent costs [6].

The aim of this article is to investigate the effect of homogeneous Fenton process conditions, such as initial dye concentration, iron dosage, pH value and hydrogen peroxide concentration on the decolorization efficiency of water-soluble azo dye Magenta aqueous solution and real printing effluent. In addition, the DSD approach was initially applied to identify the significant main and interaction effects involved in the reaction system, as well as to optimize the dye removal process.

2. MATERIALS AND METHODS

2.1 Reagents

The water-soluble azo dye Magenta (C.I.: PR57:1) was selected for this study, since it has been commercially important and commonly used in printing industry. Wastewater sample was obtained from flexographic facility located in Novi Sad, Serbia, as a result of daily discharging of a certain wastewater amount to a recipient, where the effluent amounts and dye concentrations vary daily. Magenta dye was purchased from Flint group. The molecular structure of Magenta dye is illustrated in Figure 1 and corresponds to the chemical formula $C_{18}H_{12}N_2CaO_6S$.

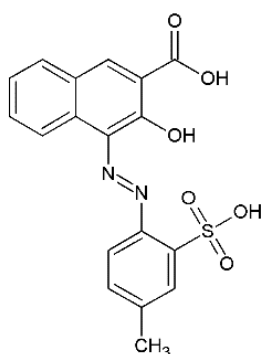


Fig. 1. Chemical structure of Magenta dye

In all experiments, chemicals of analytical grade were used. Ferrous sulfate heptahydrate - $FeSO_4 \cdot 7H_2O$ and sodium hydroxide - NaOH were purchased from POCH, while the sulfuric acid - cH_2SO_4 (>96%) was produced by J.T. Baker. The hydrogen peroxide - H_2O_2 (30%) was obtained from NRK engineering, Serbia. All working solutions were prepared by dilution in deionized water.

2.2 Experimental procedure

The degradation tests were performed on JAR apparatus (FC6S Velp Scientific, Italy) in a glass beaker containing 250 mL of Magenta solution at desired concentration. After the addition of iron in different concentrations and the adjustment of the appropriate pH value with 0.1M H_2SO_4 and 0.1M NaOH solution, the Fenton reaction was initiated by adding the required volume of hydrogen peroxide. The mixture was kept at a constant stirring of 120 rpm at the temperature of 23 °C for 60 min. Prior to the measurement, a calibration curve was obtained by using the standard Magenta solution with known concentrations, and a dye concentration of 53.92 mgL^{-1} was determined in a wastewater sample. The initial, as well as residual dye concentrations in the reaction mixture were determined by measuring the absorbance of the aqueous solutions at 573 nm by using UV/VIS spectrophotometer (UV 1800, Shimadzu, Japan). Decolorization efficiency of aqueous solution was obtained based on the following equation (8):

$$E(\%) = \frac{A_0 - A}{A_0} * 100 \quad (8)$$

where A_0 is initial absorbance of aqueous solution before homogeneous Fenton treatment, whereas A represents absorbance of aqueous solution after treatment.

2.3 Experimental design and statistical analysis

The DSD proposed by Jones and Nachtsheim (2011) was adopted to investigate the effects of four continuous factors ($k = 4$): initial Magenta concentration (20 - 180 mgL^{-1}), iron concentration (0.75 - 60 mgL^{-1}), pH value (2 - 10) and hydrogen peroxide concentration (1 - 11 mM), as potentially important for the homogeneous Fenton process. This implies that 9 experiments are required for the DSD. However, additional runs were included to delineate the model and determine the significance of interactions. For that reason, the number of experiments is double and two additional central points were added. Finally, software JMP 13 (SAS Institute, USA) used for statistical analysis in this study generates tables of experiment with 28 experimental runs. DSD requires 3 levels (minimum, center and maximum) for each factor, to cover a range of values of practical interest, as well as to detect and identify a strong nonlinear effect. Therefore, Table 1, presenting the operating levels of these variables with the corresponding code (-1, 0, +1), is generated.

Variables	Unit	Symbol coded	Levels		
			-1	0	+1
Dye concentration	mgL^{-1}	X_1	20	100	180
Iron concentration	mgL^{-1}	X_2	0.75	30	60
H_2O_2 concentration	mM	X_3	1	6	11
pH	-	X_4	2	6	10

Table 1. Factors with coded and natural levels for the DSD

3. RESULTS AND DISCUSSIONS

The experimental design layout indicates that decolorization efficiency of synthetic dye solution is in interval 4.97 – 98.66%, which implies great efficiency of homogeneous Fenton process, but still largely dependable on the influence of applied experimental conditions. DSD analysis was carried out by forward stepwise regression, as well as by determination of standard criteria: Akaike Information Criterion (AICc), Bayesian Information Criterion (BIC), and Root Mean Square Error (RMSE) to determine the model with the best prediction capability. The coefficient of determination (R^2) was equal to 0.956, R^2_{adj} was 0.934, RMSE was 5.90%, AICc was 205.01, and BIC was 203.17. Although statistical software have chosen model with 9 terms that best fit the experimental data, the adopted regression model contained 10 terms. In that way lack of fit test was insignificant, additionally confirming the validity of the model. Table 2 and 3 present Analysis of variance (ANOVA) results and estimated model coefficients for the main, interaction and quadratic effects of the described model, respectively.

Source	DF	SS	MS	F ratio
Model	9	13632.087	1514.68	43.463
Error	18	627.287	34.85	Prob>F
C. Total	27	14259.374	-	<0.0001
Lack of Fit	16	623.246	38.953	19.279
Pure Error	2	4.041	2.020	Prob>F
Total Error	18	627.287	-	0.0504

Table 2. ANOVA test

Term	Estimate	t ratio	Prob> t
Intercept	84.858	28.92	< 0.0001
Dye conc	-8.648	-6.55	< 0.0001
Fe conc	10.092	7.64	< 0.0001
H ₂ O ₂ conc	-8.855	-6.71	< 0.0001
pH	-14.821	-11.23	< 0.0001
Block	1.371	1.21	0.2429
Fe * Fe	-8.456	-2.24	0.0381
Dye conc * pH	-7.838	-3.54	0.0023
Fe conc * pH	6.566	3.68	0.0017
H ₂ O ₂ conc * pH	-9.429	-4.26	0.0005

Table 3. Estimates of the model coefficients, t-values and p-values

Table 3 indicates that all main effects are statistically significant, where catalyst concentration is the most influential factor and achieve a positive effect on the decolorization efficiency. Moreover, dye concentration, Fe and H₂O₂ concentration are involved in a significant two-way interaction with pH. Specifically, the positive role of pH is easy to understand since the pH value is one of the key factors affecting dye removal efficiency by Fenton process [5].

To achieve the maximum dye removal performance, further statistical analysis was directed towards the optimization of process conditions under the limits of the tested variables: $20 \leq x_1 \leq 180$, $0.75 \leq x_2 \leq 60$, $1 \leq x_3 \leq 11$, $2 \leq x_4 \leq 10$. With the important operational conditions for dye removal efficiency, optimal conditions can be obtained from the prediction profiler shown in Figure 2.

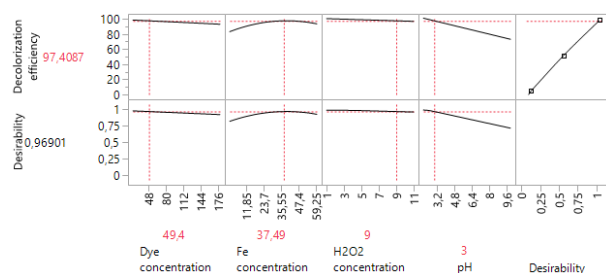


Fig. 2. Optimization plot for significant parameters influencing decolorization efficiency

As illustrated in Figure 2, the maximum decolorization efficiency was obtained with dye concentration of 49.4 mgL⁻¹, iron concentration of 37.5 mgL⁻¹, H₂O₂ concentration of 9 mM and pH value 3, which predicted decolorization efficiency to be 97.41% with a high desirability of 0.96901. This confirms the fact that process is most efficient with the H₂O₂ concentration at its high level and with the pH at its low level. The validity of the optimum levels is then

conducted through the confirmation experiment by manufacturing eight additional runs. Based on eight confirmation runs (%): 97.6; 97.26; 96.64; 96.92; 97.11; 97.08; 96.87 and 96.97 a 95% confidence interval was calculated as CI [96.753 - 97.284]. The decolorization efficiency value of 97.41%, optimized by the adopted model (Figure 2), obviously fits in the confirmatory run confidence interval. Thus, the adopted model successfully passed the confirmation test at the present stage of investigation.

After the experiments conducted on synthetic dye solution, real printing effluent was subjected to homogeneous Fenton process with optimal experimental conditions, and a dye removal of 95.91% was achieved. In that way, homogeneous Fenton process presents a suitable technology to be implemented on the colored printing wastewater before its disposal into the recipient.

4. CONCLUSIONS

The paper describes the application of homogeneous Fenton process in treatment of synthetic aqueous solution and real printing effluent generated after the flexographic printing process with water-soluble Magenta dye. As reliable and predictive tools with excellent accuracy, DSD was applied in order to investigate the influence of operating variables, as well as to predict optimal process conditions for maximum removal efficiency. Optimum degradation of Magenta dye in synthetic aqueous solution was achieved by applying initial dye concentration of 49.4 mgL⁻¹, iron concentration of 37.5 mgL⁻¹, H₂O₂ concentration of 9 mM and pH value of 3, with decolorization efficiency of 97.41%. Under the same conditions real printing effluent was treated, and excellent 95.91% were obtained.

5. REFERENCES

- [1] Kecić, V., Kerkez, Đ., Prica, M., Rapajić, S., Leovac Maćerak, A., Bečelić-Tomin, M., Tomašević Pilipović, D.: *Optimization of Cyan flexo dye removal by nano zero-valent iron using response surface methodology*, Journal of Graphic Engineering and Design, 8, pp. 35-45, 2017
- [2] Deng, Y., Z, R.: *Advanced oxidation processes (AOPs) in wastewater treatment*, Current Pollution Reports, 1, pp. 167-176, 2015
- [3] Punzi, M.: *Treatment of Textile Wastewater by Combining Biological Processes and Advanced Oxidation*, Doctoral Dissertation, Lund University, pp. 1-78, 2015
- [4] Bokare, A., Choi, W.: *Review of iron-free Fenton-like systems for activating H₂O₂ in advanced oxidation processes*, Journal of Hazardous Materials, 275, pp. 121-135, 2014
- [5] Babuponnusami, A., Muthukumar, K.: *Advanced oxidation of phenol: A comparison between Fenton, electro-Fenton, sono-electro-Fenton and photo-electro-Fenton processes*, Chemical Engineering Journal, 183, pp. 1-9, 2012
- [6] Zhang, C., Chen, W., Xian, J., Fu, D. *Application of a novel definitive screening design to in situ chemical oxidation of acid orange-II dye by a Co²⁺/PMS system*, RSC Advances, 8, pp. 3934-3940, 2018

Authors: M.Sc. Vesna Kecic, Assoc. Prof. Miljana Prica University of Novi Sad, Faculty of Technical Sciences, Department of Graphic Engineering and Design, Trg Dositeja Obradovica 6, 21000 Novi Sad, Serbia, Phone.: +381 21 485 2554.

E-mail: kecic@uns.ac.rs; miljana@uns.ac.rs

Assist. Prof. Đurđa Kerkez, Assoc. Prof. Milena Becelic-Tomin, M.Sc. Aleksandra Kulic, PhD Anita Leovac Macerak, Full Prof. Božo Dalmacija

University of Novi Sad, Faculty of Sciences, Department of Chemistry, Biochemistry and Environmental Protection, Trg Dositeja Obradovica 3, 21000 Novi Sad, Serbia, Phone.: +381 21 485 2734.

E-mail: djurdja.kerkez@dh.uns.ac.rs; milena.becelic-tomin@dh.uns.ac.rs; aleksandra.kulic@dh.uns.ac.rs; anita.leovac@dh.uns.ac.rs; bozo.dalmacija@dh.uns.ac.rs

ACKNOWLEDGMENTS: The authors acknowledge the financial support of the Ministry of Education, Science and Technological Development of the Republic of Serbia within the Projects No. TR 34014 and III43005.

Kovács, R., P., V., Keszthelyi-Szabó G., Szendrő P.

ENHANCING BIOGAS PRODUCTION KINETIC OF WASTEWATER BY MICROWAVE PRE-TREATMENT

Abstract: Pretreatment methods play an important role in the improvement of biogas production from the anaerobic digestion of industrial wastewater. The effect of microwave pre-treatment on the anaerobic degradation of industrial wastewater was evaluated through the calculation of performance parameters by using simplified mathematical models. The models were all used with experimental data from the anaerobic biodegradability tests fed with microwave pre-treated wastewater. After treating these samples anaerobic biodegradation was carried out. Experiments indicated that pre-treated samples gave higher yield of biogas compared to Non-pretreated one. In this study microwave method was performed on industrial wastewater to analyze the effect of pretreatment on anaerobic digestion by the calculation of performance parameters using Logistic function, modified Gompertz equation, and transference function.

Key words: wastewater, pre-treatment, biogas, microwave, anaerobic digestion

1. INTRODUCTION

During anaerobic digestion process organic matter is broken down by a consortium of microorganisms in the absence of oxygen. This method is used as an effective technology for converting organic residues into biogas which mainly consist of methane and carbon dioxide. Besides energy recovery, it has several benefits including waste stabilization, reduction of chemical oxygen demand, production of bio fertilizer and soil conditioners, reduction of greenhouse gas emission, decreased levels of deforestation and ease of the technology with no geographical restriction [1], [2], [3]. The principal reaction sequences can be classified into four major groups: hydrolysis, fermentation, acetogenesis, methanogenesis. During biogas production, the rate-determining step for the conversion of complex organic matter is the hydrolysis [4], [5].

Different pretreatment methods aid in facilitating the anaerobic digestion by increasing the rate of organic matter hydrolysis. [6]. By improving the hydrolysis step, organic substrates are more accessible to anaerobic bacteria, accelerating the digestion and increasing the volume of biogas produced.

Many authors were modeled kinetic of biogas production but most of them focused only in the hydrolysis step. Therefore, the establishment of methodologies to evaluate the effectiveness of pre-treatment becomes necessary.

2. MATERIAL AND METHODS

2.1 Wastewater

The wastewater used was obtained from a dairy factory located in Szeged, Hungary producing milk, cream, cheese, butter, butter cream.

Parameter	BOD [mg/L]	COD [mg/L]	TDS [mg/L]	TSS [mg/L]	TS [mg/L]
Value	672.5	1448.75	1222.5	267.5	1487.5

Table 1. Characteristics of wastewater

BOD(Biological Oxygen Demand), COD (Chemical Oxygen Demand),TDS(Total dissolved Solids), TS(Total Solids), TSS(Total suspended Solids)

2.2 Microwave pre-treating system

Continuous flow microwave pre-treating system contains a water-cooled, variable-power magnetron operating at 2450 MHz. High-voltage power supply feeding the magnetron consists of two transformers, one of them produces cathode heating voltage and heating current, the other produces the anode voltage which can be controlled by the primary circuit of an external auto-transformer. With this device the power of the magnetron can be set as well. Electromagnetic energy of the magnetron spread over a resonant slot. Getting through this slot the energy gets in the toroidal resonator [7]. During the operation of toroid resonator energy is given to the treated material. As a result of

energy transmission the temperature of the material rises and the dielectric properties change continuously. The effect of the microwave energy intake, variable power, impedance and dielectric relationships are formed in the microwave resonator. Some of these can be measured (eg. power dissipation, reflected power), some of them can only be determined by calculation, knowledge of the other parameters [8]. Material is transferred in the continues-flow microwave treating system by a peristaltic pump with variable flow.

Treatments were carried out at different powers of magnetron (PM), at different flows (FR), and different treating numbers (NT). Two levels from these parameters were used and combined (Table 2.)

Power of the magnetron (PM) [W]	Flow rate (FR) [Lh ⁻¹]	Number of treatings (NT) [-]
300	6	1
700	25	5

Table 2. Factorial design of the experiment

2.3 Fermentation process, biogas measurement

Anaerobic digestion (AD) tests were carried out under controlled mesophilic temperature range (35±0,2°C). in 12 mini continuously stirred laboratory scale reactors with 250 mL total volume, equipped with Oxitop C. Measuring heads recorded the pressure in the bottle at 2-hour intervals. Measurement data is downloaded from the infrared transmitter unit built into the measuring heads by the device's own software. Pressure charts can be displayed and converted to MS Excel compatible formats by the software. Calculating the volume of the resulting biogas normalized to room temperature and atmospheric pressure:

$$V_{N, biogas} = \frac{p_r \cdot V_r \cdot T_{norm}}{p_{atm} \cdot T_f} \quad (1)$$

where $V_{N, biogas}$ is volume of the resulting biogas normalized to room temperature and atmospheric pressure (Nm³), p_r is pressure recorded in the reactor (Pa), V_r the volume of the reactor space above the sample (m³), p_{atm} is atmospheric pressure (Pa), T_{norm} room temperature (K), T_f fermentation temperature (K).

2.4 Models for data fit

In this study the kinetic model of biogas production was predicted using modified Gompertz equation, Logistic function, and transference function. Originally, Gompertz equation was used to predict bacterial growth rate. This equation describing a sigmoidal growth curve contained mathematical parameters (a, b, c). These mathematical parameters did not have biological meaning. Therefore, Zwietering has rewritten the Gompertz equation to substitute the mathematical parameter (a, b, c) A, λ and k, where A was maximum value of population, λ was maximum specific growth rate, k was lag time [9]. Assuming biogas production rate has correspondence to methanogenic bacteria growth rate many authors use modified Gompertz equation (2) to predict biogas production rate [10], [11], [12].

$$B = P \cdot \exp\left[-\exp\left(\frac{R_m \cdot e}{P}(\lambda - t) + 1\right)\right] \quad (2)$$

Using logistic function (2) assumes that the rate of gas production is proportional to the amount of gas already produced, the maximum production rate and the maximum capacity of biogas production. This model fits the global shape of the biogas production kinetics: an initial exponential increase and a final stabilization at a maximal production level. [13].

$$B = \frac{P}{1 + \exp\left(\frac{4R_m(\lambda - t)}{P} + 2\right)} \quad (3)$$

The transference function (Reaction curve-type model) (4) is used mainly for control purposes, which

considers that any process can be analyzed as a system receiving inputs and generating outputs. This type of model has been implemented in anaerobic digestion in some cases [14].

$$B = P(1 - \exp\left(-\frac{R_m(t - \lambda)}{P}\right)) \quad (4)$$

In (2) (3) (4) equations B is cumulative of biogas production (mL), P is biogas production potential (mL), R_m is maximum biogas production rate (mL/day), λ is lag phase period or minimum time to produce biogas (days), t is cumulative time for biogas production (days) and e is mathematical constant (2,718282). Kinetic constant of P, R_m and λ was determined using non-linear regression with help of IBM SPSS software. Setting parameters for the highest increment were 700W, 25 Lh⁻¹ and 5 treating number.

3. RESULTS AND DISCUSSION

With regard to microwave pretreatment, maximum biogas production rate increased by minimum 37% and maximum 95% compared to the Non-pretreated sample depending on the adjustment parameters, respectively. Setting parameters for the highest increment were 700W, 6 Lh⁻¹ and 5 treating number.

The results of the highest biogas yield and the non-pretreated sample are shown in Figure 1.

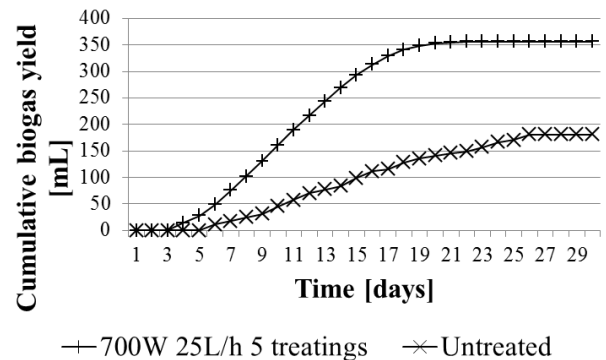
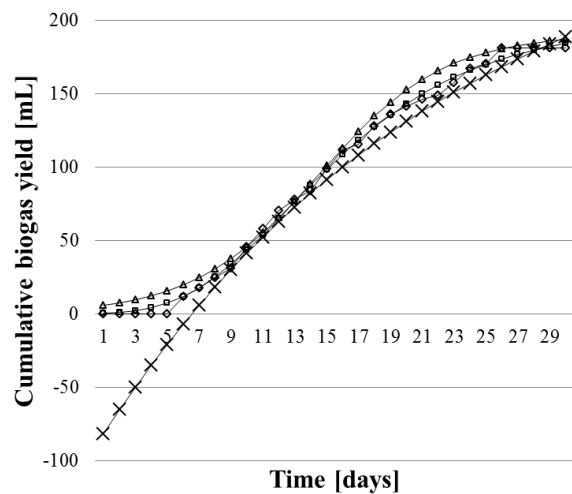


Fig. 1. Cumulative biogas yield of non-pretreated and treated samples

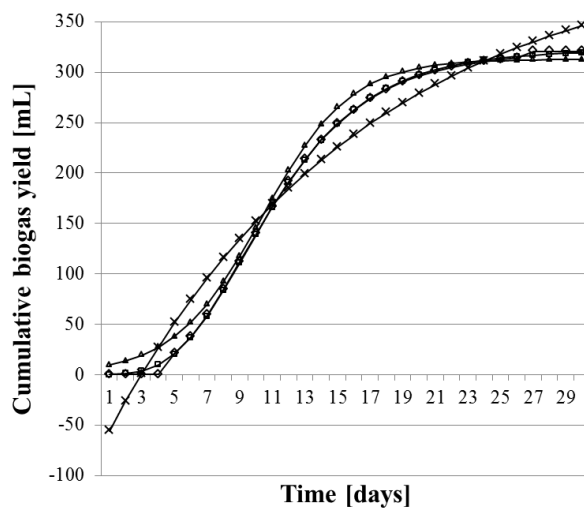
3.1 Models for Biogas Production

Figure 2 (a-i) shows the three models fit the experimental data from the anaerobic digestion of non-pretreated and microwave-treated samples.

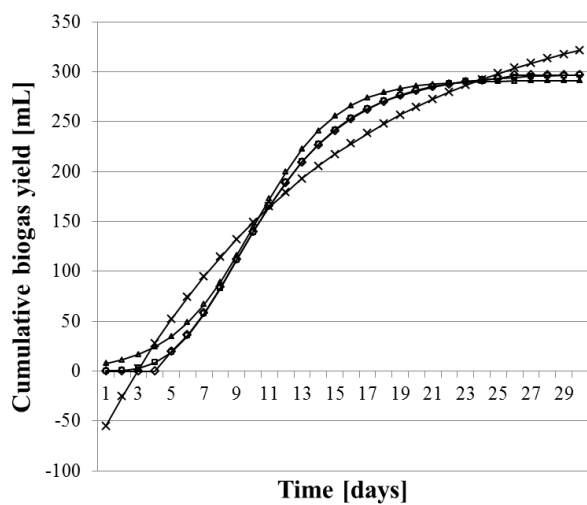
The sample numbers and estimated values of the parameters obtained in the optimization process are summarized in Table 3. All models are fit with experimental data from anaerobic biodegradability tests.



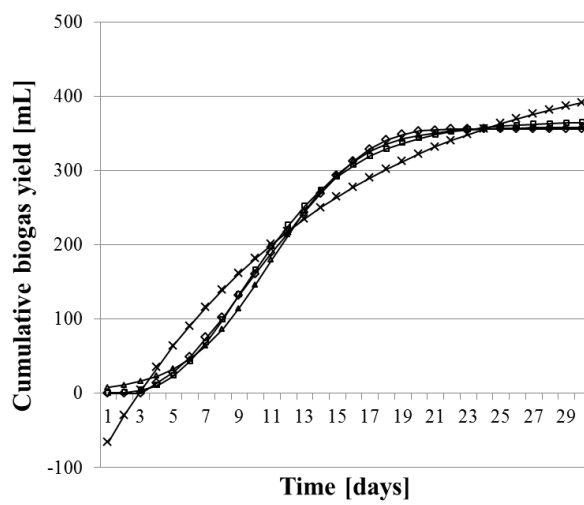
a) Sample No.1.



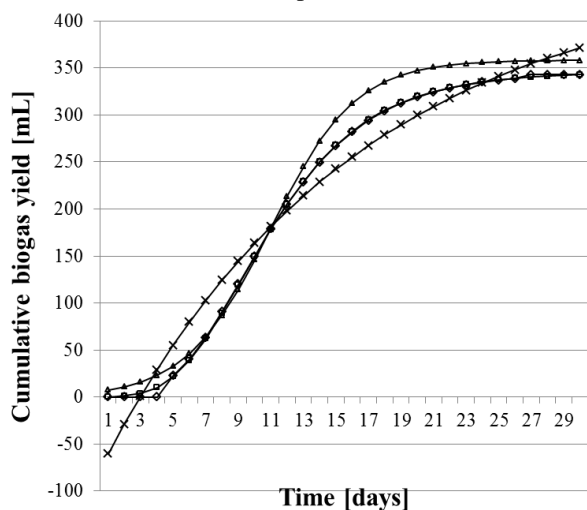
b) Sample No.2.



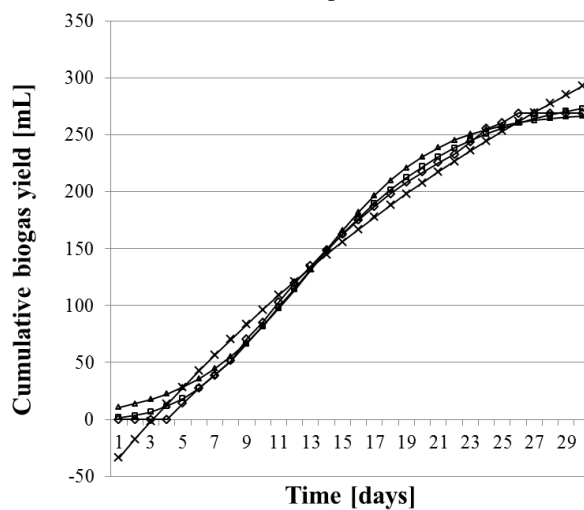
c) Sample No.3.



d) Sample No.4.



e) Sample No.5.



f) Sample No.6.

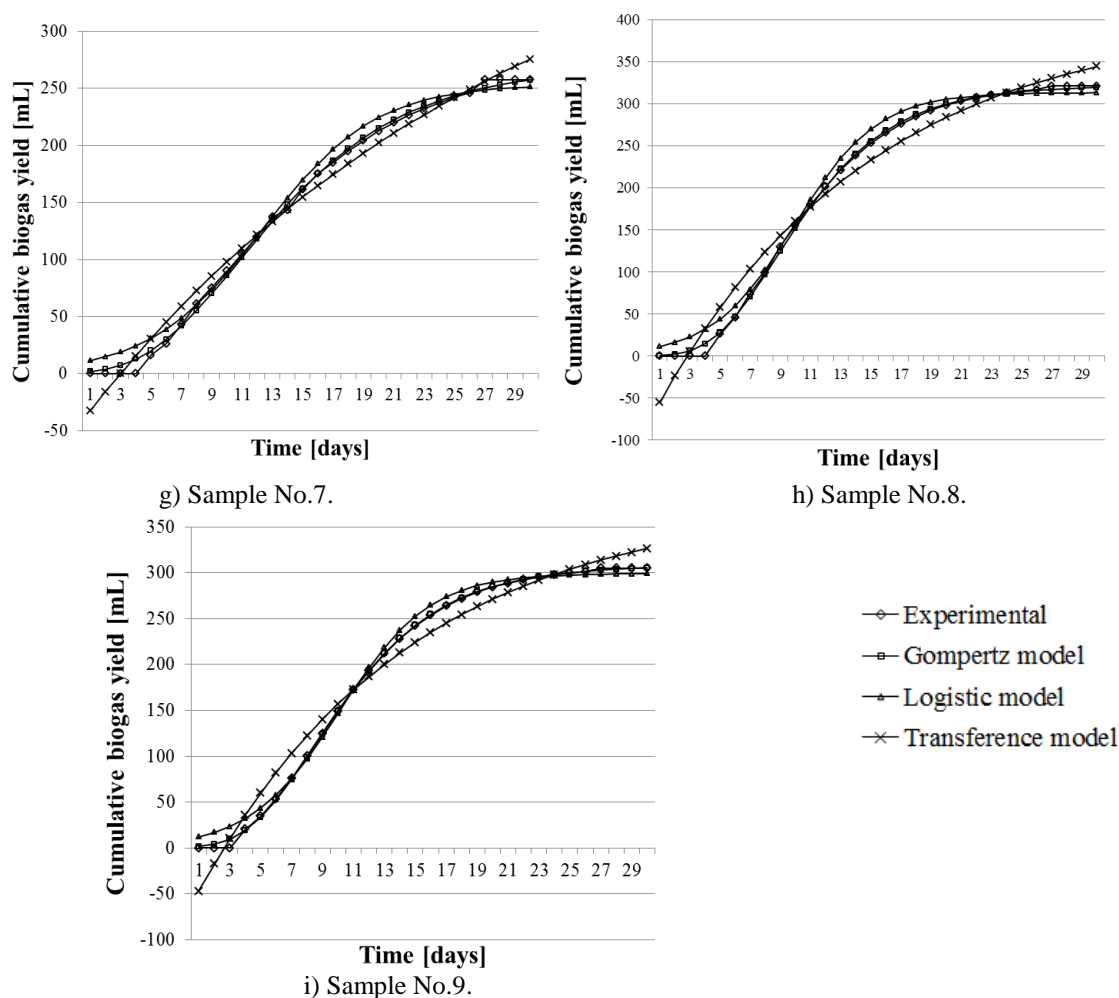


Fig. 2. Models fit with cumulative biogas yield using non-pretreated and microwave-treated samples

No.	MODEL	P [mL]	R_m [mL/day]	λ [days]	R^2
1. Non-pretreated	Gompertz equation	197,023	11,249	6,235	0,998
	Logistic function	190,35	12,106	6,665	0,992
	Transference function	290,9	12,941	6,565	0,981
2. Microwave treated (700W, 25 Lh ⁻¹ 5 treating number)	Gompertz equation	321,583	28,105	5,049	0,999
	Logistic function	312,782	28,938	4,96	0,996
	Transference function	421,686	26,806	2,96	0,964
3. Microwave treated (700W, 25 Lh ⁻¹ 1 treating number)	Gompertz equation	298,177	28,254	5,06	0,999
	Logistic function	291,341	28,936	5,012	0,996
	Transference function	376,389	26,811	2,92	0,96
4. Microwave treated (700W, 6 Lh ⁻¹ 5 treating number)	Gompertz equation	366,268	33,624	5,057	0,998
	Logistic function	358,284	34,301	5,756	0,998
	Transference function	459,2	32,496	2,878	0,955
5. Microwave treated (700W, 6 Lh ⁻¹ 1 treating number)	Gompertz equation	345,251	30,323	5,073	1,000
	Logistic function	358,284	34,301	5,756	0,996
	Transference function	451,546	28,886	2,965	0,964
6. Microwave treated (300W, 25 Lh ⁻¹ 5 treating number)	Gompertz equation	288,253	16,655	5,079	0,998
	Logistic function	269,927	17,604	5,54	0,992
	Transference function	561,939	15,381	3,124	0,983
7. Microwave treated (300W, 25 Lh ⁻¹ 1 treating number)	Gompertz equation	268,65	16,145	4,689	0,998
	Logistic function	253,346	16,979	4,898	0,991
	Transference function	451,445	15,745	2,99	0,984
8. Microwave treated (300W, 6 Lh ⁻¹ 5 treating number)	Gompertz equation	321,614	27,955	4,543	0,999
	Logistic function	313,262	28,551	4,484	0,993
	Transference function	402,991	28,539	2,807	0,969
9. Microwave treated (300W, 6 Lh ⁻¹ 1 treating number)	Gompertz equation	307,957	25,288	4,083	1,000
	Logistic function	299,352	25,925	4,353	0,995
	Transference function	378,408	27,422	2,615	0,974

Table 3. Parameters and goodness fit obtained with the evaluated models

In general, there was an overall agreement between the models and the experimental data. Comparing the performance models, the best fit was obtained using the modified Gompertz model in both curve shape and goodness of fit, which in each case received the highest regression of the coefficients, but the Logistics model showed almost the same fit in most cases. ($R^2 > 0,99$) which means that these models might explain the 99% (and over) of total variation in the data. Transference model showed worse but still appropriate fit ($R^2 > 0,96$)

which made it more useful for prediction.

In order to evaluate the effects of microwave pre-treatment on the biogas production potential (P) and on the maximum biogas production rate (R_m), the increase with respect to the corresponding untreated sample was calculated using Eq. (5). [15]. The results obtained are presented in Fig. 3:

$$\text{Increase}[\%] = \frac{(P \text{ or } R_m)_{\text{pret}} - (P \text{ or } R_m)_{\text{non-pret}}}{(P \text{ or } R_m)_{\text{non-pret}}} \cdot 100 \quad (5)$$

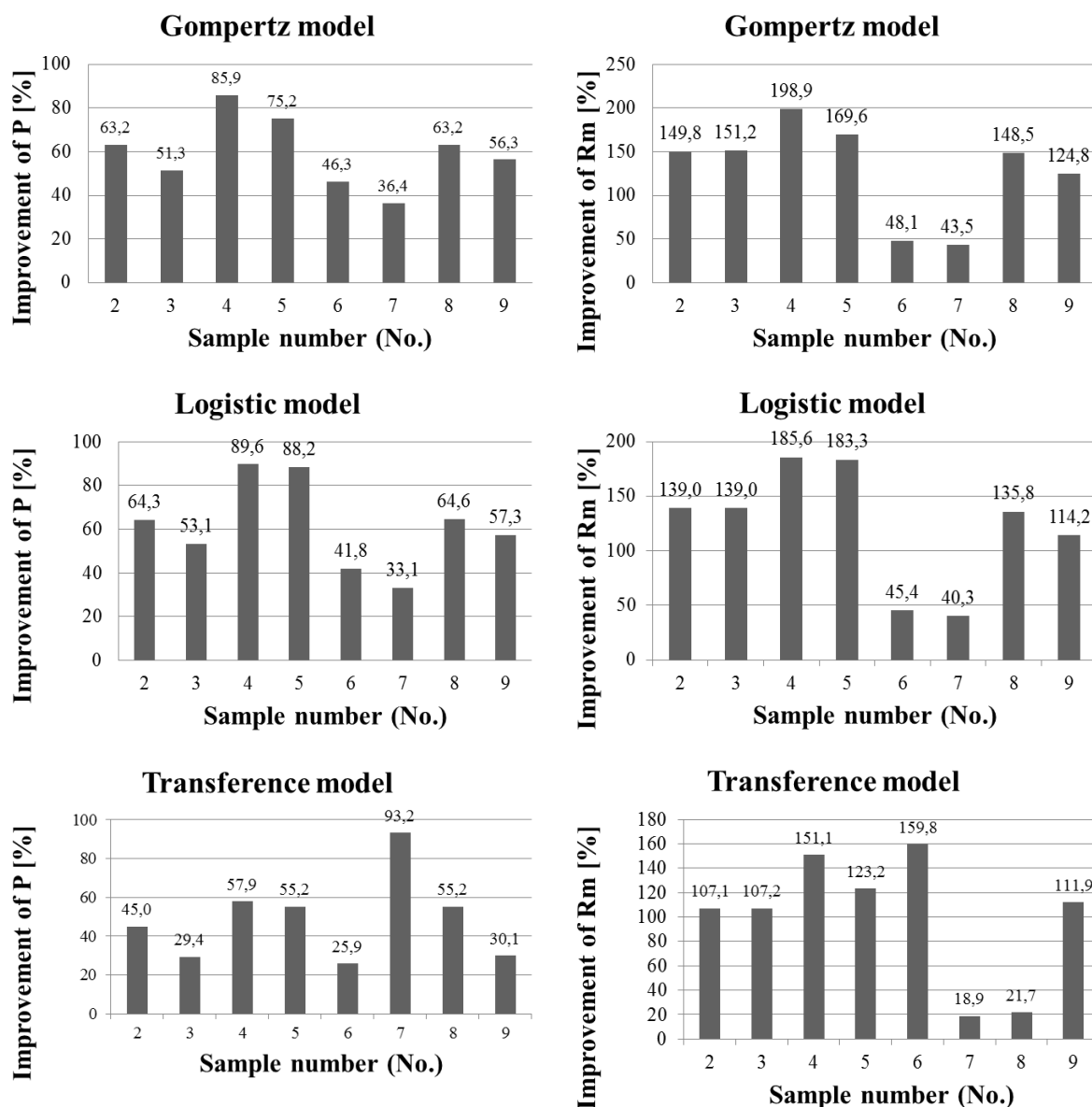


Fig. 3. Increase of the biogas production (P) and increase of the maximum biogas production rate (R_m) according to the models for each type of samples used in the experiment.

It can be noted, from Fig. 3, that there was an increase in both the maximum biogas production (P) and maximum biogas production rate (R_m) using microwave pre-treated wastewater. According to set parameters, microwave pre-treatment had different effect on the wastewater, reaching an increase close to 90%.

Gompertz model and Logistic model agree with the experimental data as it was expected of fitting the

measured data.

4. CONCLUSIONS

The use of three simple models in the anaerobic degradation of non-treated and pre-treated wastewater showed to be a proper tool used to obtain performance parameters, allowing for a more reliable comparison between the non-treated and pre-treated wastewater.

In spite of the proper results obtained, Modified Gompertz and Logistic models showed better agreements with the experimental data than the Reaction curve model. Hence, by using Gompertz or Logistic model, the maximum biogas production and the maximum biogas production rate can be calculated accurately anaerobic digestion of wastewater.

5. REFERENCES

- [1] Surendra, K.C., D. Takara, A.G. Hashimoto and S.K. Khanal: *Biogas as a sustainable energy source for developing countries: Opportunities and challenges*, *Renew. Sustain. Energy Rev.*, 31: 846-859. 2014.
- [2] Parawira, W.: *Biogas technology in sub-Saharan Africa: Status, prospects and constraints*, *Rev. Environ. Sci. Bio/Technol.*, 8: 187-200. 2009.
- [3] Weiland, P.: *Biogas production: Current state and perspectives*, *Applied Microbiol. Biotechnol.*, 85: 849-860. 2010.
- [4] V.A. Vavilin, B. Fernandez, J. Palatsi, X. Flotats: *Hydrolysis kinetics in anaerobic degradation of particulate organic material: an overview*, *Waste Management* 28 939–951. 2008.
- [5] D.J. Batstone, S. Tait, D. Starrenburg: *Estimation of hydrolysis parameters in full-scale anaerobic digesters*, *Biotechnology and Bioengineering* 102 1513–1520. 2009.
- [6] Kim, J., C. Park, T.H. Kim, M. Lee, S. Kim, S.W. Kim and J. Lee, *Effects of various pretreatments for enhanced anaerobic digestion with waste activated sludge*, *J. Biosci. Bioeng.*, 95: 271-275. 2003.
- [7] Kovács P. V. R., Beszédes S., Ludányi L., Hodúr C., Szabó G.: *Development of a continuous flow microwave toroidal cavity resonator*, 11th International Scientific Conference MMA 2012: Advanced Production Technologies, Novi Sad: University of Novi Sad, 2012. pp. 357-360. 2012.
- [8] J. Zhu, A.V. Kuznetsov, K.P. Sandeep: *Mathematical modeling of continuous flow microwave heating of liquids*, *International Journal of Thermal Sciences*, Vol. 46, 328–341. 2007
- [9] Zwietering, M.H., Jongenburger, I., Rombouts, F.M., van't Riet: *Modelling the bacterial growth curve*, *Appl. Environ. Microbiol.* 56 (6), 1875–1881. 1990.
- [10] Budiyono, Widiassa, I.N., Johari, S., Sunarso: *The kinetic of biogas production rate from cattle manure in batch mode*, *Int. J. Chem. Biol. Eng.* 3 (1), 39–44. 2010.
- [11] Patil, J.H., Raj, M.A., Muralidhara, P.L., Desai, S.M., Raju, G.K.M.: *Kinetics of anaerobic digestion of water hyacinth using poultry litter as inoculum*, *Int. J. Environ. Sci. Dev.* 3 (2), 94–98. 2012.
- [12] Adiga, S., Ramya, R., Shankar, B.B., Patil, J.H., Geetha, C.R.: *Kinetics of anaerobic digestion of water hyacinth, poultry litter, cow manure and primary sludge: a comparative study*. *Int. Conf. Biotechnol. Environ. Manag.* 14 (2), 73–78., 2012.
- [13] S. Pommier, D. Chenu, M. Quintard, X. Lefebvre: *A logistic model for the prediction of the influence of water on the solid waste methanization in landfills*, *Biotechnology and Bioengineering* 97 473–482. 2006.
- [14] G. Redzwan, Ch. Banks: *The use of a specific function to estimate maximum methane production in a batch-fed anaerobic reactor*, *Journal of Chemical Technology and Biotechnology* 79 1174–1178. 2004.
- [15] A. Donoso-Bravo, S.I. Pérez-Elvira, F. Fdz-Polanco: *Application of simplified models for anaerobic biodegradability tests. Evaluation of pre-treatment processes*, *Chemical Engineering Journal* 160 pp.607–614, 2010.

Authors: M.Sc. Petra Veszelovszki Róbertné Kovács¹, Full Prof. Gábor Keszthelyi-Szabó², Full Prof. Péter Szendrő³

¹University of Szeged, Faculty of Engineering, Department of Technology, 9. Moszkvai krt. H-6725 Szeged, Hungary;

²University of Szeged, Faculty of Engineering, Department of Process Engineering, 9. Moszkvai krt. H-6725 Szeged, Hungary

³ Szent István University, Faculty of Mechanical Engineering, Institute of Mechanics and Machinery, 1. Páter K. u., H-2100, Gödöllő, Hungary

Phone.: +3662546559

E-mail: veszelov@mk.u-szeged.hu

Krnjetin, S., Šupić, S.

CONSTRUCTION WITH BALED STRAW - FIRE SAFETY

Abstract: *The paper presents new, characteristic trends in the construction of buildings with a baled straw around the globe, which, in different ways, improve the ecological parameters of urban spaces. Some specificity of construction by baled straw and basic fire characteristics of such buildings were analyzed. Based on several laboratory tests, their satisfactory safety in the conditions of fire has been confirmed. Representative straw buildings in Serbia and the world are also shown in this paper.*

Key words: *construction with baled straw, technology, fire characteristics*

1. INTRODUCTION

Researchers all around the world are searching for low-carbon materials used in construction. They are developing new ways of using wood and other natural materials, such as hemp, natural fiber composites and straw. It is estimated that such materials can help achieve long-term goals in reducing carbon dioxide emissions, as the impact of the construction industry on the environment is enormous. It is known that in the world cement production participates in the total industrial carbon dioxide emissions of as much as 10%, hence alternative solutions are necessary. Straw is a material that has been used for many years in the construction industry, and today it is gaining popularity. Although some challenge its qualities, claiming that it is insect litter, easily flammable and not stable enough, previous experiences and tests have shown differently. Baled straw is used not only as insulation, but complete walls are built of it. Baled straw comes in blocks of different sizes, in the form of a prism or roller, depending on the desired final shapes.

2. PROPERTIES OF BALED STRAW AS BUILDING MATERIAL

Straw represents dried grains of stems - natural and healthy material, annually renewable, created by the process of photosynthesis, with solar energy, and treated as waste material. Annually huge quantities of straw or spade in the fields are produced, which is a major environmental problem (for example, 4 million tons in the UK, of which 450,000 houses could be built with floor area of 150m²). Baled straw is pressed and bound straw, rectangular shaped 100cm long, about 45cm wide and about 35cm high. Binding of a bale is performed with a polypropylene rope or hemp. The safety level of humidity, which does not result in the development of fungi and

bacteria, is 15% within the bale, while the relative humidity of the space must not be maintained above 70% over a longer period of time. The use of straw may lead to lower consumption of environmentally harmful materials, and in case that the facility becomes unnecessary, which is unlikely, it can be recycled or used as compost.

Straw provides high insulation at an affordable price. Considering the thickness of the bale of about 45 cm, the value of the coefficient of thermal conductivity of 0.13 W/mK is obtained, which is two to three times lower than in modern materials and much lower than required value by the regulations. The walls built with baled straw are an extraordinary sound insulator (in the USA there are two music studios built with this material). The results of the tests showed that plastered baled straw walls have a lower fire risk from paneled wooden walls using the same wall coverings (ASTM tests confirm their fire resistance with the class F90-F120). The current price of straw in our region is 3 bales per 1 Euro. Considering that with 3 bales we get 1 m² of highly insulated façade wall, comparing it with classic brick construction, which requires additional thermal insulation, the financial justification of baled straw is obvious. Also, due to the specific construction technology, people without or with very little construction experience can participate in the design and construction of the building, and in this way can significantly reduce the costs related to the working staff.

The most significant saving in such facilities is the long-term reduction of heating costs - outstanding thermal insulation properties of straw. Heating costs can be reduced by 75% compared to the cost of commonly used materials. Because of the above, savings occur throughout the life-cycle of the building. In terms of capacity, it can be used for building two-storey buildings.



Figure 1. Forming a wall built of baled straw - possible self-construction [1]

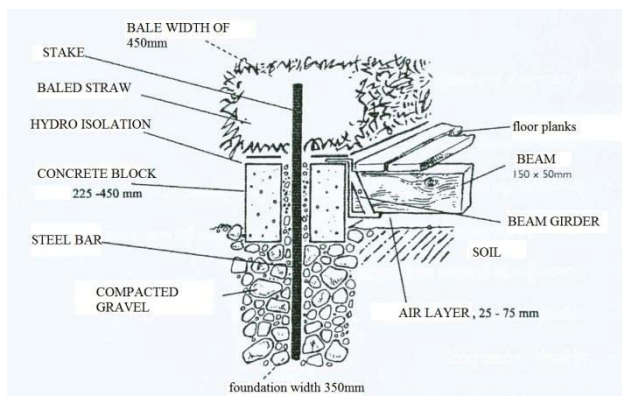


Figure 2. Detail of the foundation with concrete blocks and drainage [1]

Straw does not cause allergies (pollen, etc.) and represents the ideal material from this aspect. In these buildings, the air quality is improved because there is no emission of harmful materials from the walls. Straw is a material that breathes and allows constant, natural filtration and air exchange into the room. Together with the use of non-toxic organic materials

for final work, such as clay, natural pigments and colors, a completely healthy and comfortable atmosphere can be created for life. The ambience inside these buildings is calm, warm and comfortable. The following methods of construction are known:

- Nebraska or a self-sufficient method,
- a light frame and self-esteem,
- load bearing frame and a filler of baled straw,
- Hybrid techniques.

The beginning of using straw as a building material started at the end of the XIX century, when the first baling machine was made. More recently, according to renewed technologies, about 1,000 new buildings are being built around the world (In Great Britain, in the 1970s, 70 buildings were built from baled straw with urban permits. In Russia, many such buildings were built in the village of Majak on Ural. In Belarus at the Academy of Ecology two-storey experimental facility is being built - Figure 3.



Figure 3. Strohpolis – the first multi-storey building of baled straw on three floors in Europe (World habitat award finalist - 2007) [5]

3. FIRE AND SEIZMIC CHARACTERISTICS OF BALED STRAW

Contrary to beliefs, baled straw buildings are superior to wood structures when it comes to fire resistance. This is due to the high straw density, in which there is not enough oxygen to flame progress. In the United States, a series of tests were carried out on the resistance of the walls of straw-baled straw, in which it was concluded that, depending on whether they are unprotected or have a layer of plaster, they represent a barrier against flame lasting for two to three hours. In testing an independent laboratory in Texas in 2000, the unplastered straw-baled wall had a flame spread index 10 (FSI) and a smoke development index (SDI) 350. According to the valid regulations (International Building Code and International Residential Code), a maximum FSI of 25 and maximum 450 SDI for insulation materials was required, indicating that baled straw could easily meet the conditions for use in both business and public buildings. Tests have shown that baled straw houses have very high fire resistance. On the test, the stacked bales without mortar were able to withstand the half-hour effect of the fire, while the plastered wall was resistant for two hours! This is primarily because there are no vertical channels and passages in the wall itself, the wall mass is compact and does not allow the flame to spread easily. When installing a thicker layer of mortar (compared to standard structures), it is clear that straw has better protection. However, it must be ensured that the straws do not penetrate the mortar itself or the joints around the holes, as it practically becomes a fitting. For this reason, if we want to protect all joints with straw, special attention should be paid to the corners around the holes and at the places where the installations come out of the walls - these places must be carefully coated with plaster or fire-resistant coatings.

Baled straw buildings are of particular value in seismic areas. Conventional buildings made of earth, adobe or stone (80% of homes in the world) are hazardous in earthquakes and expensive to reinforce. Compared to the buildings of these materials, baled straw has a good ratio of width and height, and can be easily and effectively reinforced with wood, bamboo or steel reinforcement.



Figure 4. Precast panels built of baled straw - fast, cheap and safe construction [3]

The nature of baled straw, its flexibility and strength are almost ideal from a seismic point of view, as long as the connections between the walls of baled straw, roof structure and foundations are adequate. Straw-baled walls can absorb earthquakes, instead of transferring them to the roof as in case of conventional buildings. The layer of mortar (reinforced with wire) can further strengthen such walls. In 1994, architect Bob Theis designed the first approved load-bearing rice baled straw facility in California, designed to withstand seismic forces.

4. OTHER SAFETY CHARACTERISTICS OF STRAW

Safety of construction sites - ease of construction

The construction of straw-baled walls requires much less physical work compared to other materials, such as concrete blocks, brick, adobe or stone, and require significantly less skills. Many people feel intimidated by the process of constructing a building with conventional materials. The complexity, the skill required, the time needed and the investments may seem too overwhelming and discouraging. The construction of baled straw simplifies the whole process and allows less experienced and skillful people to get involved directly in the process of creating their homes. The great advantage is that this can be done by anyone, including women and

children, and there is also a social aspect of making such walls, which has come to life more than once, joining people from the same communities in such ventures. There are practically no injuries on such sites.

Health safety - comfort and aesthetics

The construction with baled straw does not only imply the use of cereal stems but also hemp, flax and other industrial plants (the construction use of recycled materials from paper, plastic, car tires and other inorganic materials is still in a phase of testing in a constructive, and in terms of human health and environment impact way). Combined with their high insulating properties and breathability, these walls can produce a sense of comfort, which is impossible to find in thin flat walls of modern materials. The straw-baled walls resemble the old stone walls, seen on European country houses as well as Mediterranean villas. Finished with plaster and paints, straw-baled walls can breathe, making the inner air cleaner and fresher than stagnant air with little oxygen that is often encountered in houses. High insulation value also helps to create a stable environment that is easily cooled and heated and provides far superior living conditions than most modern homes. Another advantage of the buildings built from baled straw is excellent sound insulation, from natural sources of noise such as winds, as well as from artificial sources (city noise, traffic, etc.).

Safety of insects and pesticide content

Compared to wood, there are only a few insects that like straw (in the United States, termites are a common danger for objects of organic matter). In any case, it is quite enough to follow the same procedure as when protecting wood. The bales give insects much less room for life and movement than for example bondruksystem, which is normally used in the United States (although there are more and more hollow walls with gypsum-cardboard boards). Unlike hay, straw contains very little nutrients and does not attract insects. Sufficient, but not necessary, standard bale protection, which is normally used in disinfection. Great concern was due to the pesticide in the straw itself, which was sprinkled on rice (as the most common raw material for construction in the United States). However, this level in the straw itself is minimal, and compressed bale provides very little space for their any harmful effect.

Moisture safety and thermal characteristics

Walls of straw bales protected by mortar or clay mud have the capacity to accumulate and transfer

heat: during the day, they will collect heat and then discharge it into the room during the night, while cooling, hence during the day they can give the room a freshness collected during the night. This feature will have great advantages in comfort throughout the longer summer, but the main advantage is the effect on energy consumption. The monolithic composition is of key importance for the extraordinary thermal insulation properties of straw walls. There are special advantages in relation to multilayer and masonry walls: a high degree of friction between the straw bales keeps them in place without any binders, and by correct installation, and thanks to the vertical loading of the roof structure, a very compact connection (intertwining straps) occurs between the horizontal rows, but also between the neighboring bale in one row. In addition, there is a completely absence of horizontal and vertical joints, which in the masonry structures become mini-cold bridges (the thermal conductivity of the coupling is never equal to the thermal conductivity of the coated element, and the protection by the thermal insulation layer will not annul this distinction). One-layer wall ensures proper exchange and regulation of external and internal influences of temperature and water vapor, without risk of condensation inside the wall (steam dam unnecessary).



Figure 5. In the idyllic Swiss valley of Val d'Herens, a new Maya hotel was built from baled straw in a wooden skeleton

Fungi may occur in straw at high humidity (over 20% dry weight, ie relative humidity 70-80%). Serious damage occurs only when the straw is exposed to these conditions for a longer period of

time. Chronic alternate humidity change does not pose any threat. In California, intense rainfalls follow the days of dry winds that dry out the walls perfectly. For this reason, the appearance of moisture on the walls is very rare, such as, for example in Britain (however, this disadvantage applies to all other facade systems). Construction paper, which is often used in the USA for impregnating plywood walls, etc., can reduce the ability of the bale to emit moisture, becoming the surface where concentrated moisture will be maintained over a longer period of time. Therefore, vapor-permeable gaskets and coatings are recommended, which prevents water/humidity from penetrating through the mortar and reach within the wall, but at the same time allows the steam to pass from the inside of the building through a mortar a wall is coated with.

The statistics for the walls of baled straw show the importance of the vapor permeability of the wall covering - the most frequent runoff of such houses occurred where full sealing/impregnating of the wall was carried out with parampent coatings, which allowed the detrimental effect of moisture (this phenomenon is almost exclusively the result of the application of modern building materials) . Without this problem, house can easily be maintained for several decades under very humid climates (over 60 percent). For example, the Oak Place palace in Huntsville, Alabama, maintains high humidity in the US south since 1938. One house near Rockport, Washington, receives an annual rainfall of up to 190cm, and the house at Tonasket in the same country without foundation and any reinforcement in the walls shows no sign of damage to the structure since 1984. More recent buildings built in this system in the north New York (wet winters) and New Scotland (cold wet winters) proved to be very resistant to climatic conditions. Due to the large amount of rain-water collected at the lower parts of the walls, it is recommended to use hydro insulation - but only in this part of the wall. The top of the wall is also sensitive to the moisture due to the evaporation of the internal moisture to the roof structure. Consequently, experienced builders of baled straw recommend that construction paper (waterproofing) should be placed on the top and bottom of such walls (where it is also necessary to place a layer of plain gravel, rather than a waterproofing membrane, which would ensure the correct regulation of moisture in the touch surface of the wall and the base plate .

Durability of material

Straw grain is decomposed after six months, while rice straw lasts twice as long (due to the high

percentage of silicates, which protects it further against rotting). However, straw has been used for centuries as an insulation material, and immediate evidence found at archaeological sites shows that, under optimal conditions, its lifetime may be over several thousand years old. Traces of straw in the Egyptian pyramids confirm this thesis - the straw is placed in a perfectly preserved condition inside the tombs - hence, on dry it does not decompose (positive experiences are our karatavans). Accordingly, baled straw used in the construction of buildings can last from three weeks to nine thousand years, depending on the way it is built in and maintained.

5. CONCLUSION

Based on all the analyzed technical and especially security features of the buildings built of baled straw, as well as the positive experiences in such built houses, it can be concluded that they have significant advantages in relation to the classically built building of other materials. Their ecological, health, sociological, energy and, finally, not less important, overall economic advantages can be emphasized. Faster integration of such types of buildings into our construction is necessary, adoption of incentive standards and appropriate regulations, as well as more intensive work on their promotion in the media and educational institutions.

6. REFERENCES

- [1] Ginder, E.: *Vojvodina village houses built of natural materials*, Small book, Novi Sad, 1996.
- [2] Krnjetin, S.: *Natural materials in construction*, FTN, Novi Sad, ISBN 978-86-7892-770-6, 2015.
- [3] Krnjetin, S.: *Construction and environment*, FTN, Novi Sad, ISBN 978-86-7892-864-2, 2016.
- [4] Nikolić, I.: *Precast house built of straw*, Eco house, Magazine for eco architecture and culture, Beograd, No.26/2018.
- [5] Tetior, A.N.: *Architectural ecology, building structures*, Moscow, 2003. pp. 35.

Authors:

Full Prof. Slobodan Krnjetin, M.Sc. Slobodan Šupić, University of Novi Sad, Faculty of Technical Sciences, Department of Environmental Protection, Trg Dositeja Obradovica 6, 21000 Novi Sad, Serbia, Phone.: +381 21 464/135.

E-mail: krnjetis@ptt.rs; ssupic@uns.ac.rs

Raspudic, V., Mikulic, Z.

OPTIMUM DESIGN OF I-SHAPED CROSS-SECTION USING NONLINEAR PROGRAMMING

Abstract: Built-up welded sections are extensively used as load-bearing structural members due to their high strength-to-weight ratio and the flexibility of cross-sectional shapes and sizes. In the limit state design approach given in the Eurocodes, the procedure for selecting the final design is often an iterative process, which is largely dependent on the constructor's experience. A large number of design possibilities create thereby an important challenge in choosing the most economical design. The objective of the study presented in this paper is to minimize the mass of an I-shaped doubly symmetrical built-up welded section for a laterally unrestrained beam subjected to bending around its major axis. According to design constraints, practical limitations and rules defined in EC3, an algorithm for constrained nonlinear optimization in MATLAB has been developed. The FEA simulation confirmed the suitability of the algorithm as a time-consuming tool for achieving the final design.

Key words: optimization, I-shaped cross-section, EC3, MATLAB, FEA

1. INTRODUCTION

Built-up welded sections are generally used in situations where rolled steel sections of the required sizes are not available to span long distances and carry heavy loads, but also in all other cases where their application is economically justified. They have a number of advantages over rolled profiles, such as lower weight, greater freedom in choice of shape and cross section dimensions and the possibility of making a variable height beam with better adjustment to bending moment diagram. Built-up welded sections have a slightly larger unit price than the rolled ones, which is the consequence of the larger volume of works necessary for their manufacture. Specifically, connecting steel sheets to the whole and forming a single cross section requires additional workshops, and thus costs. In spite of this, considering the lower consumption of steel, as well as the advantages mentioned above, build-up sections are in many cases the most economical solution, and therefore have a very large application in building and bridge construction. In general, structural design is a complex, iterative, trial-and-error and decision-making process. In the design of a new section, the dimensions are usually unknown factors. In the limit state design approach given in the Eurocodes, starting dimensions for built-up profiles are very often chosen by the designer based on his expertise and past experience. Design check is then undertaken to evaluate all the constraints, practical limitations and rules defined in the corresponding design code. If the cross-section does not satisfy them, its dimensions are changed and a new check is performed. Thereby, it is essential that the final design should also represent the most economical solution taking into account the amount of material used or the total cost of the construction. As there are usually a large number of design possibilities, selection of the most favorable dimensions can be improved and accelerated by using the optimum design techniques.

2. STATIC SYSTEM

The most common type of built-up welded cross-section is a doubly symmetrical I-shaped cross-section built up from two flange plates and one web plate, as shown in Fig. 1.

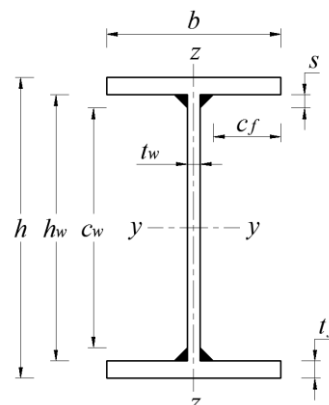


Fig. 1. I-shaped welded cross-section

The objective of the study presented in this paper is to automatize the procedure for obtaining dimensions of the cross-section shown in Fig.1, which minimize the mass of a laterally unrestrained beam subjected to bending around its major axis (Fig.2), satisfying thereby all the practical limitations and constraints according to the European design guidelines for build-up structural members [1,2].

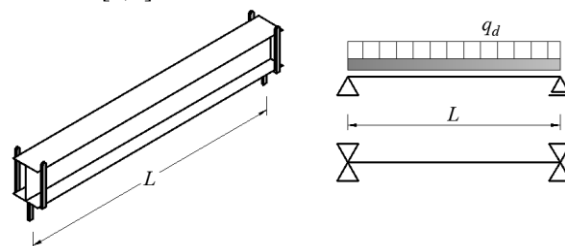


Fig. 2. Static system

3. DESIGN CONSTRAINTS

The structural design is influenced by various design parameters and constraints imposed by the design codes. In Eurocode, the verification of the ultimate limit states consists of the verification of the condition:

$$E_d \leq R_d \quad (1)$$

where E_d is the design value of the effect of actions, such as internal forces and R_d represents the design value of the corresponding resistance. The design value of an action effect, at each cross-section, should not exceed the corresponding design resistance, and if several action effects act simultaneously, the combined effect should not exceed the resistance for that combination. In general, the safety of steel members at ultimate limit state is ensured by applying partial safety factors γ_M to the various characteristic values of resistance. The following three failure modes are considered:

- resistance of cross-sections (γ_{M0});
- resistance of members to instability assessed by member checks (γ_{M1});
- resistance of cross-sections in tension to fracture (γ_{M2}).

3.1 Cross-section classification

The resistance of cross-sections depends on their class. In Eurocode 3, cross-sections are placed into one of four behavioral classes depending upon the material yield strength, the width-to-thickness ratios of webs and flanges, and the loading arrangement.

Class 1 cross-sections are fully effective under pure compression, and are capable of reaching and maintaining their full plastic moment in bending. The optimization algorithm developed in this work includes constraints by which the dimensions of the cross section are determined so that both flanges and web belong to class 1 (Fig.1):

$$c_f/t_f = (b - t_w - 2s)/(2t_f) > 9\varepsilon \quad (2)$$

$$c_w/t_w = (h - 2t_f - 2s)/t_w > 72\varepsilon \quad (3)$$

where ε depends on material yield strength f_y and is defined as:

$$\varepsilon = \sqrt{235/f_y} \quad (4)$$

3.2 Bending resistance of cross-sections

The bending resistance about the principal axis $M_{c,Rd}$ represents the in-plane flexural strength of a beam. For Class 1 cross-sections, it is based upon the full plastic section modulus and is determined as:

$$M_{c,Rd} = \frac{W_{pl} f_y}{\gamma_{M0}} \quad (5)$$

where W_{pl} is the plastic section modulus and γ_{M0} is the partial safety factor, which is equal to 1.0.

The design bending moment M_{Ed} must satisfy the condition:

$$M_{Ed}/M_{c,Rd} \leq 1 \quad (6)$$

3.3 Shear resistance of cross-sections

The resistance of cross-sections to shear is satisfied if:

$$V_{Ed}/V_{pl,Rd} \leq 1 \quad (7)$$

where the plastic shear resistance is defined as:

$$V_{pl,Rd} = \frac{A_v (f_y/\sqrt{3})}{\gamma_{M0}} \quad (8)$$

The shear area A_v is the area of the cross-section that can resist the applied shear force with a moderate allowance for plastic redistribution. For welded I-shaped sections, with load parallel to the web, this is the area of the web:

$$A_v = \eta h_w t_w \quad (9)$$

where the value of coefficient η depends on steel grades. The resistance of the web to shear buckling need not be considered provided:

$$\frac{h_w}{t_w} \leq 72 \frac{\varepsilon}{\eta} \quad (10)$$

3.4 Resistance of cross-sections under combined bending and shear

The effect of shear force on the moment resistance is negligible and may be ignored if the applied shear force is less than half the plastic shear resistance of the cross-section:

$$V_{Ed} > 0.5V_{pl,Rd} \quad (11)$$

3.5 Lateral torsional buckling resistance

If the beam loaded in its stiffer principal plane does not have sufficient lateral stiffness or lateral support, then it may buckle out of the plane of loading, as shown in Figure 3. The load at which this buckling occurs may be substantially less than the beam's in-plane load resistance. For an idealized perfectly straight elastic beam, there are no out-of-plane deformations until the applied moment M_{Ed} reaches the elastic buckling moment M_{cr} , when the beam buckles by deflecting laterally and twisting. Real beams differ from the ideal beams due to the possible impact of many imperfections, such as initial crookedness, twist, eccentricity of load, residual stresses or variations in material properties.

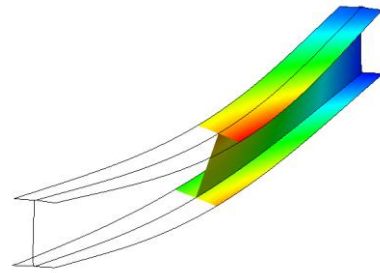


Fig. 3. Lateral torsional buckling of a simply-supported beam

For the EC3 method of designing against lateral torsional buckling, the design bending moment M_{Ed} must be less than the lateral torsional buckling resistance $M_{b,Rd}$ and checks should be carried out on all unrestrained segments of beams:

$$M_{Ed}/M_{b,Rd} \leq 1 \quad (12)$$

The lateral torsional buckling resistance for Class 1

cross-sections is defined as:

$$M_{b,Rd} = \chi_{LT} W_y \frac{f_y}{\gamma_{M1}} \quad (13)$$

where $W_y = W_{pl,y}$ for Class 1 cross-sections, χ_{LT} is a reduction factor and γ_{M1} is the safety factor, which is equal to 1.0.

The reduction factor for lateral-torsional buckling χ_{LT} is described through equation:

$$\chi_{LT} = \frac{1}{\phi_{LT} + \sqrt{\phi_{LT}^2 - \bar{\lambda}_{LT}^2}} \quad (14)$$

but:

$$\chi_{LT} \leq 1.0 \quad (15)$$

where:

$$\phi_{LT} = \left[1 + \alpha_{LT} (\bar{\lambda}_{LT} - 0.2) + \bar{\lambda}_{LT}^2 \right] \quad (16)$$

α_{LT} is the imperfection factor corresponding to the appropriate buckling curve.

Relative slenderness for lateral-torsional buckling is defined as:

$$\bar{\lambda}_{LT} = \sqrt{\frac{W_y f_y}{M_{cr}}} \quad (17)$$

where M_{cr} is the elastic critical moment for lateral torsional buckling based on gross cross-sectional properties and taking into account the load conditions, the real moment distribution and the lateral restraints:

$$M_{cr} = C_1 \frac{\pi^2 EI_z}{(kL)^2} (SR - C_2 z_g) \quad (18)$$

$$SR = \sqrt{\left(\frac{k}{k_w} \right)^2 \frac{I_w}{I_z} + \frac{(kL)^2 GI_T}{\pi^2 EI_z}} + (C_2 z_g)^2 \quad (19)$$

Coefficients C_1 and C_2 depend on the shape of the bending moment diagram and on the support conditions. Terms k_w and k are the effective length factor dealing with warping end restraint and rotation about the y-y axis. z_g is the distance between the level of application of the loading and the shear center. I_T is the torsion constant, I_w is the warping constant, I_z is the second moment of area about the minor axis and L is the length of the beam between points of lateral restraint.

4. FORMULATION OF THE OPTIMIZATION PROBLEM

Optimization can be defined as the process of finding the conditions that give the maximum or minimum value of an objective function. The optimum seeking methods are also known as *mathematical programming techniques* and they are useful in finding the minimum of a function of several variables under a prescribed set of inequality and equality constraints. When either the objective or any constraint function is nonlinear in terms of the variables, it is generally referred as constrained nonlinear optimization or a nonlinear programming (NLP) problem. The optimization problem can be formulated mathematically as follows [3]:

Minimize:

$$f(\mathbf{x}), \quad x_i \in R^n, \quad i = 1, \dots, n \quad (20a)$$

subject to:

$$g_i(\mathbf{x}) \leq 0, \quad i = 1, \dots, m \quad (20b)$$

$$h_j(\mathbf{x}) = 0, \quad j = 1, \dots, p \quad (20c)$$

$$x_k^l \leq x_k \leq x_k^u, \quad k = 1, \dots, n \quad (20d)$$

where $f(\mathbf{x})$ is to be minimized. In this study, the aim is to minimize the mass of the beam, so that the cross-sectional area of the I-shaped profile is taken as the objective function:

$$f(\mathbf{x}) = A = (h - 2t_f)t_w + 2bt_f \quad (21)$$

where:

- \mathbf{x} is the vector of design variables, $\mathbf{x} = [h, b, t_w, t_f]^T$;
- $n=4$ is the total number of design variables;
- x_k^l and x_k^u are the lower and upper bounds of the k th design variable x_k , respectively;
- $g_i(\mathbf{x})$ is the i th inequality constraint and $h_j(\mathbf{x})$ is the j th equality constraint.

In MATLAB, this kind of problem can be solved using the function *fmincon* [4]. It attempts to find a constrained minimum of a scalar function of several variables starting at an initial estimate using derivative-based search methods, also known as gradient-based search methods. In such approaches, we estimate an initial design, which improves iteratively, until optimality conditions are satisfied. The general syntax of this function is:

$$\mathbf{x} = \text{fmincon}(\text{fun}, x0, A, b, Aeq, beq, lb, ub, \text{nonlcon}, \text{opt}) \quad (22)$$

where *fun* is the function to be minimized, and *nonlcon* is the function that computes the nonlinear inequality and equality constraints. The solution process involves selecting a most suitable optimization technique or algorithm to find an optimal solution. The algorithm used in this problem was interior-point algorithm, which handles large, sparse problems, as well as small dense problems. The algorithm satisfies bounds at all iterations and can recover from NaN or Inf results [4]. Both of these functions *fun* and *nonlcon* have been written as separate .m files, where the constraint functions are formulated based on previously described design constraints and EC3 rules presented in paragraph 2.

The required input values for the algorithm are: the yield strength f_y (MPa), Young's modulus E (MPa), Poisson's ratio ν , the beam span L (m), dead load g_k (kN/m), live load p_k (kN/m), limiting value for vertical deflection m (L/m), C_1 and C_2 coefficients (depending on the shape of the bending moment diagram), min. web thickness $t_{w,min}$ (mm), the weld size s (mm) and the max. ratio of the flange width and the section height b/H .

The result of the optimization process is the vector of design variables $\mathbf{x} = [h, b, t_w, t_f]^T$. Based on the obtained optimized values for t_w and t_f , the standard sheet metal thicknesses are adopted and a second cycle of optimization is performed with a new vector of two design variables $\mathbf{x} = [h, b]^T$ and with the same constraints

as defined in the first cycle. The graphical representation of the optimization result has also been created through MATLAB code, as shown on Fig. 4. The iso-contours of the objective function, i.e. the area of the cross section A , are plotted in a two-dimensional design space with the axes that represent the two design variables, flange width b and cross-section height h . The optimized solution is given by point O . The max values of b and h for which the conditions (2) and (3) are fulfilled are represented by vertical and horizontal lines b_{max} and h_{max} . The graph also shows the iso-contour corresponding to the value of the lateral torsional buckling resistance $M_{b,Rd}$, required to fulfill the condition (12), as well as the iso-contours for the bending resistance about the principal axis corresponding to the applied moment M_{Ed} and the bending resistance determined for the optimized cross-section $M_{c,Rd}$.

4.1 Numerical example

An example of an optimization of a laterally unbraced beam with an I-shaped cross-section will be shown for a simple supported beam with end-fork conditions (Fig. 2). In the represented example, the following values were used: $E=210$ MPa, $\nu=0.3$, $L=5$ m, $g_k=4$ kN/m, $p_k=8$ kN/m, $L/m=L/300$, $C1=1.132$, $C2=0.45$, $t_{w,min}=6$ mm, max. $b/H=1$.

The following results were obtained:

Height: $h = 268$ mm

Flange width: $b = 174$ mm

Flange thickness: $t_f = 9$ mm

Web thickness: $t_w = 6$ mm

Surface area of the section: $A = 46.32$ cm²

Elastic critical moment and corresponding critical loads:

$M_{cr} = 90.28$ (kNm), $q_{cr} = 28.89$ (kN/m),

$F_{cr} = q_{cr} \times L = 144.5$ (kN)

Conditions for bending and lateral torsional buckling resistance of the cross-section:

$M_{Ed} / M_{c,Rd}$ (kNm): $54.375 / 117.35 = 0.46$

$M_{Ed} / M_{b,Rd}$ (kNm): $54.375 / 54.375 = 1.00$

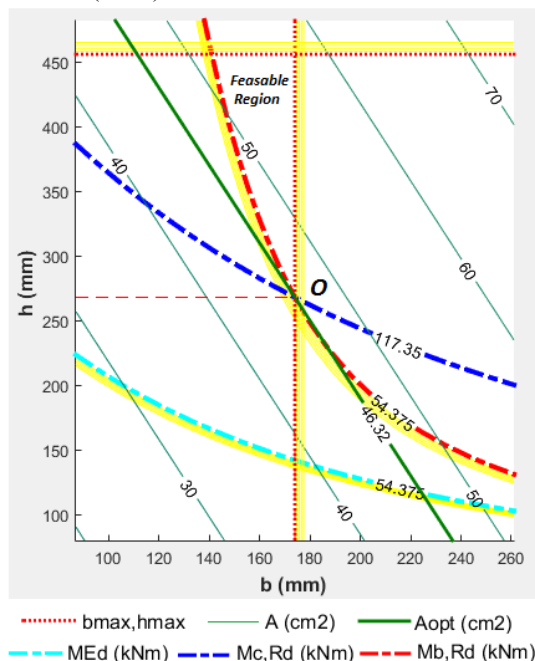


Fig. 4. Graphical representation of the MATLAB optimization solution

4.2 FE simulation

The flexural capacity of the optimized cross-sections in the numerical example was also studied using FE buckling analyses performed with SolidWorks Simulation. The FE model of the beam was developed using shell elements, with a mesh size of 20 mm. The analysis showed that the lowest critical load for the idealized perfectly straight elastic beam with the optimized cross-section is 145 kN, which corresponds to the critical load F_{cr} determined in the Matlab algorithm according to EC3. The lateral torsional buckling mode is illustrated in Fig. 3.

5. CONCLUSION

It is important to notice that design in EC3 is often an iterative process. Initial assumptions about cross-section dimensions are made and after calculations it might be necessary to revise them and start from the beginning. A large number of design possibilities that meet the EC3 design rules create thereby the problem of choosing the most economical design. In this paper, a procedure for optimization of an I-shaped doubly symmetrical built-up welded section for a laterally unrestrained beam subjected to bending around its major axis has been presented. The choice of appropriate cross-sectional dimensions is enabled by the development of MATLAB programs, which implement constrained nonlinear optimization methods. The graphical representation of the optimized values provides thereby a better insight into the bearing capacity on the bending and lateral bending of the cross section. Based on the obtained values, FE analysis was done in SolidWorks Simulation, which confirmed the results defined by the EC3 design rules. The developed algorithm can be used as a time-consuming tool for achieving the final design.

6. REFERENCES

- [1] CEN, Eurocode 3: *Design of Steel Structures. Part 1-1: General Rules and Rules for Buildings*, European Committee for Standardization, Brussels, 2005
- [2] Gardner, L., Nethercot, D.: *Designers' Guide to Eurocode 3: Design of Steel Buildings, EN 1993-1-1, -1-3 and -1-8*, ICE Publishing, London, 2011
- [3] Arora, J.S.: *Introduction to Optimum Design*, Elsevier Inc., 2017
- [4] *MATLAB Documentation*, <https://www.mathworks.com/help/matlab/>

Authors: Assoc. Prof. Vesna Raspudić University of Mostar, Faculty of Mechanical Engineering, Computing and Electrical Engineering, Matice hrvatske bb, 88000 Mostar, Bosnia and Herzegovina, Phone.: +387 36 337-028, Fax: +381 36 337-012, E-mail: vesna.raspudic@fsre.sum.ba
 Assist. Željko Mikulić, B. Sc. Civ. Eng. University of Mostar, Faculty of Civil Engineering, Matice hrvatske bb, 88000 Mostar, Bosnia and Herzegovina, Phone.: +387 36 355-032, Fax: +387 36 355-001, E-mail: zeljko.mikulic@gf.sum.ba

Živanić, D., Gajić, A., Zelić, A., Ilanković, N.

FLAT BELT FEEDER REGULATION POSSIBILITIES

Abstract: In modern industrial production, feeding is an integral part of any process. There are flow, belt, vibration and other feeding devices. In continuous feeding processes for bulk materials, one of the possible solutions is a flat belt feeder. A programmable logic controller (PLC) is used to control flat belt feeder operation, which is located in the Laboratory of Machine Design, Transport Systems and Logistics. The paper describes the operation of the flat belt feeder, are presented and explained the functional components that are responsible for the automation of work, their function and connection diagram.

Key words: flat belt feeder, feeding, regulation

1. INTRODUCTION

Feeding is an integral part of any process in modern industrial production. The name of the device or the machine for feeding is commonly given by the technical solution which is used for transportation during the process. There are flow, belt, vibration and other feeding devices. Flat belt feeder gives the possibility to transport the desired amount of material during the given time period, it provides the desired material flow. The flat belt feeder consists of a short flat belt conveyor with a mechanism for measuring mass (weigh scale) and regulation devices. The flat belt feeder continuously and automatically measures the flow of the bulk material which is transported by the conveyor belt, without the disturbance of the flow [3]. Except mass measurement, it is necessary to simultaneously measure the velocity of the conveyor belt.

2. THE CONSTRUCTION OF THE FLAT BELT FEEDER

Flat belt feeder, figure 1, consists of two pulleys, the driving pulley (1) which transmits pull on the belt by friction, and the take-up pulley (5). The endless belt (7) wrapped around these pulleys is at the same time the drive and the carrying element of the transporter. In order to provide good conditions for the driving pulley to obtain a grip on the belt sufficient to drive the conveyor, a certain amount of initial tension is applied to the belt through pulling screws (8) which are shown on the take-up pulley. The driving pulley receives its rotation from the drive unit (2) through the chain drive. The belt is on the upper side (conveying) supported by idlers (4) which prevent big sag of the belt. The material to be conveyed is loaded onto the belt by the hopper (6) with a slide gate that provides regulation of the amount of the loaded material [1]. The weigh scale is used to measure the transported material on the belt; it consists of an idler which is connected to the beam load cell through a teeter mechanism. The control cabinet (9) is placed next to the frequency converter (10). The control cabinet contains the PLC, wire runs,

control relays, the motor protection circuit breaker and it has buttons and control lights on its door. All of the numbered elements are placed on the frame (3) of the flat belt feeder. The belt of the conveyor has side walls which provide a bigger cross-section area of the transported material, i.e. it provides a bigger capacity of the conveyor.

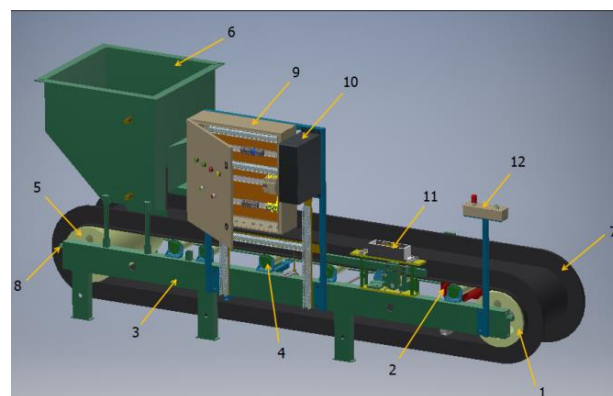


Fig. 1. Construction of the flat belt feeder

3. THE WORKING PRINCIPLE OF THE FLAT BELT FEEDER

Pressing the NO start button activates the drive of the flat belt conveyor whereby the green control light is turned on, figure 2. If the hopper is empty, capacitive sensor of the material level, which is positioned on the bottom of the hopper, detects that there is no material and according to that, the PLC activates the imagined material income. The imagined material income is in the user program and in the practical part of the task presented by the yellow control light (that would be an other machine in real production which would deliver material to the feeder or an another hopper, silo). During the loading of the material, the hopper is being filled and in one moment, material covers the capacitive sensor which is positioned on the top of the hopper. When that happens, the PLC gets a signal to turn off the yellow control light, i.e. the imagined material income. When the hopper is filled up, it is necessary that the flat belt feeder operator presses the

In that moment data SPIDER 8 HBM can be used in order to set the desired material flow. When the material is loaded on the belt, weigh scale, i.e. the beam

SPIDER 8 is also in charge to process signals from other sensors. SPIDER 8 is connected with the contactless inductive sensor which measures rpm of the driving pulley, and with two pulling screws which have strain gauges that detect the dilatation of the screws and on behalf of that they give the information of the tension in the belt. All of that data SPIDER 8 shows on the PC via the HBM software CATMAN.

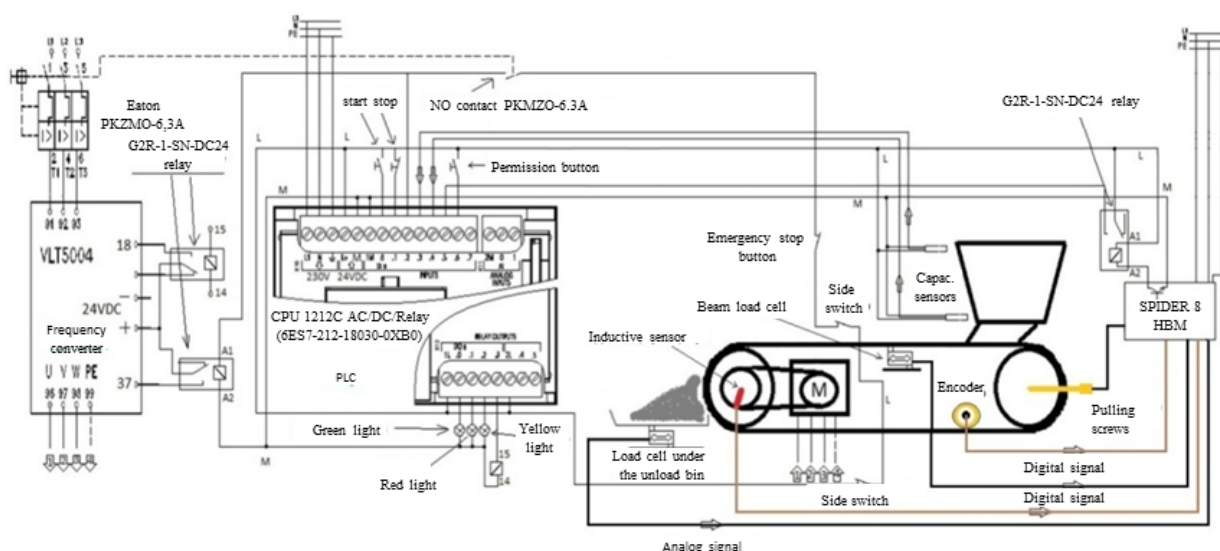


Fig. 2. Schematic representation of the connection of all elements on the flat belt feeder [6]

4.1. Frequency converter

Frequency converters, figure 3, are devices which control the rotation speed of the asynchronous and synchronous electric motors by changing the frequency and voltage in order to achieve the desired rpm. Today in all automated operations usage of 3-phase motors with the frequency converters became standard. Because of that, it is necessary to select the adequate frequency converter. They are selected based on the load in accordance with the function they are operating and based on other techno-economic parameters. In this case, the drive of the flat belt feeder is the low voltage 3-phase cage asynchrony motor (Sever, catalogue number ZK80 B-4) with the nominal power of 0,75 kW. The drive is transmitted from the motor to the driving pulley via the transmission gear reducer and the chain drive. Frequency converter Danfoss VLT 5000 Series-type 5004 nominal power 2,2 kW is used for the regulation of the drive.



Fig. 3. Configuration of the control system

4.2. Programmable logic controller PLC

The PLC is a digital electronic device which uses programmable memory for remembering commands which demand performance of specific functions like logical functions, sequencing, counting, time measurement, calculating in order of controlling different machines and processes [2]. When the drive equipment was defined and described, and the working principles were established, it was possible to select the controller and the type of the automation which will be realized with the help of the SIMATIC S7 PLC family

controller. A simplified model of the project task is given here, figure 4, in order to provide the programmer a full picture about what is connected to the input and output ports of the PLC. On the behalf of that it is easier to understand what has to be defined in the ladder diagram so that the PLC could correctly perform its function and respond to all requirements during managing the mentioned drive.

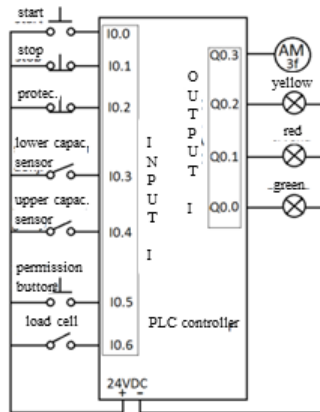


Fig. 4. Simplified model of the project task

4.3. Acquisition data system SPIDER 8 - HBM

Acquisition data system SPIDER 8, figure 5, is a multichannel electronic unit for parallel measurement of dynamic sizes by a computer. It is easy to connect the SPIDER with the computer through the printer port and it takes no time to prepare for measurements. Each channel provides impulse for passive 4 pole converters, filters and its own converter. A small software package, which is installed in the SPIDER 8 system, works under the MS Windows operating system and provides the possibility of data acquisition (continual or periodic) and to save data files. HBM has developed the software package CATMAN which provides arbitrarily defining the way of measurement result presentation, complete (live and post process) analysis of the results, arbitrarily interaction between the user and the software, control and help during measurements.



Fig. 5. SPIDER 8 HBM

4.4. Load cells

The purpose of load cells is to measure mechanical values, e.g. forces, and to transform them to electronic form (voltage). They consist of strain gauges which are strongly bonded with the spring element. There are mostly four strain gauges connected in a full Wheatstone bridge. On the flat belt feeder there are four load cells. One is the part of the weigh scale and measures the weight of the material on the belt, figure

6. The second is positioned under the unload bin and measures the weight of the transported material, figure 7. The third and fourth load cells are the same, they are made by applying strain gauges on the pulling screws of the take-up pulley and they give the information of the tension in the belt, figure 8.

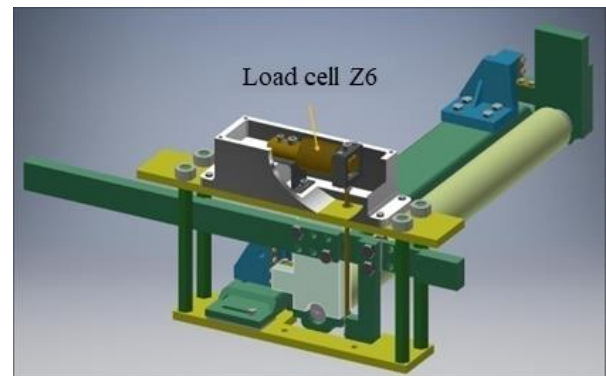


Fig. 6. Beam load cell positioned on the weigh scale



Fig. 7. Load cell positioned under the unload bin



Fig. 8. Load cell on the take-up pulley

4.5. Additional equipment

In order to make the flat belt feeder fully functional and provide the mandatory safety measures, it is necessary to use additional equipment. Here are included buttons for starting and turning off the drive, light signalization, emergency stop button and side switches which detect lateral movement of the belt. If they get activated, they shut down the drive of the flat belt feeder. For the security of the electric motor and the frequency converter from overcurrent, the motor protection circuit breaker PKZM0 is used. There are also capacitive sensors for material level in the hopper and relays for galvanic isolation of communication between the PLC and the SPIDER. The rotation encoder, figure 9, is positioned on the lower (return) strand of the belt. The encoder rotates due the belt movement because it lies on the inner side of the belt [4]. Comparing data of the driving pulley rotation speed and the belt velocity, it is possible to control and eventually detect slipping of the belt on the driving pulley.



Fig. 9. Rotation encoder

5. METHODOLOGY

The aim of the scientific inquiry is to determine the precision of the feeder, i.e. calibration of the feeder. Before the feeder could be put into operation, it is necessary to check all electric connections visually and with adequate equipment. It is important to set the proper tension in the belt in order to ensure that the belt axis matches the feeder axis. Initial starting of the feeder has to be with the minimal rpm of the electric motor along with the control of belt position on pulleys in order to be able to notice if lateral movement of the belt is happening. It is necessary to check the functionality of the safety equipment, the emergency stop button and side switches. When all of the measuring sensors get connected to the SPIDER 8, their calibration has to be done – the weigh scale was calibrated by two different chains and the load cell under the unload bin was calibrated with standardized weights [5]. If it is necessary, the tension in the belt is corrected until both take-up screws get the same load and the belt gets positioned properly. Only then is possible to start with the measurement and in this case for the trial inquiry barley was used. At first, the signal of the weigh scale due to the empty belt was recorded. After that, barley was loaded onto the belt from the hopper and then the signal of the weigh scale due to the barley and belt was also recorded.



Fig. 10. Putting the flat belt feeder into operation

On the other hand, in order to verify the accuracy of the measurement of the weigh scale, the load cell under the unload bin was used. That load cell measured the transported amount of the barley. The weigh scale signal due to the barley alone was got by the subtraction of the weigh scale signal due to the empty belt from the weigh scale signal due to the belt and the

barley on it. That clear weigh scale signal due to barley alone was compared with the signal from the load cell under the unload bin.

6. CONCLUSION

In the paper, especial attention was given to the way of automation and regulation of the work of the flat belt feeder. All of the necessary control equipment for regulated work and measurements with the flat belt feeder was given. Each component of the flat belt feeder in charge of the automation was carefully and functionally described. The necessary components were implemented on the existing flat belt conveyor so they could together form a functional flat belt feeder.

7. REFERENCES

- [1] Vlastic, J.: *Continuously operating and automated transport*, FTN, Novi Sad 1991.
- [2] Marcetic, D.: *Programmable logic controllers and communication protocols in electroenergetics*, FTN, Novi Sad 2014.
- [3] Vasic, V.: *Systematization of packaging machines, conveyor systems and testing of belt feeders*, Master's thesis, FTN, Novi Sad 1999.
- [4] http://www.usas.no/index.php?page=shop.getfile&file_id=25&product_id=38&option=comvirtuemart&Itemid=2 (visited in June 2018.)
- [5] Ilankovic, N.: *Analysis of influential parameters of measurement accuracy with the belt feeder*, Master's thesis, FTN, Novi Sad 2018.
- [6] Kuzmancev, M.: *Design and working regulation of the belt feeder*, Master's thesis FTN, Novi Sad 2018.

Authors: Assist. Prof. Dragan Živanić, Assist. Prof. Anto Gajić², Assist. – Master Atila Zelić, Teaching Assoc. Nikola Ilanković, University of Novi Sad, Faculty of Technical Sciences, Department of Mechanization and Design Engineering, Trg Dositeja Obradovica 6, 21000 Novi Sad, Serbia, Phone.: +381 21 450-366, Fax: +381 21 454-495.

² - Mine and Thermal Power Plant, Ugljevik, Republic of Srpska,

E-mail: zivanic@uns.ac.rs, antogajic@yahoo.com, zelic@uns.ac.rs, ilankovic@uns.ac.rs,



Section **G**:

BIO-MEDICAL ENGINEERING

Bojanić Šejat, M., Todić, V., Mladjenović, C., Beju, L. D., Grujić, J.

TECHNOLOGICAL PREPARATION OF THE ENDOPROSTHESIS PRODUCTION

Abstract: In the metal processing industry the basic goal of manufacturing is a product. In the design and production process, reduction of product life and frequent changes in the production program lead to the need for a faster and more efficient transfer of information between engineers and other participants. For insertion of the implant into the human organism, modern medicine requires faster progress in finding of the new solutions. The correct selection and proper installation of endoprosthesis ensures the normal functioning of the hip joint itself and, consequently, of the entire locomotor system. Using computers ensure better conditions for the development of new implants, their testing and production. Modern computer systems can modeling implants and prosthetic elements, calculating performing and checking, functionality simulation and preparing of the programs for their producing on CNC machine tools. In the world these systems are unified under the name CAD/CAM systems. In the paper a modular endoprosthesis of the hip joint which is produced in small and individual production is presented.

Key words: endoprosthesis, product, CAD/CAM

1. INTRODUCTION

In the design and production process, reduction of product life and frequent changes in the production program lead to the need for a faster and more efficient transfer of information between engineers and other participants.

The mutually opposing requirements have never been more prominent, since the product developing team has to design and manufacture a product that has the lowest cost in the lifetime as soon as possible, while having quality and other attributes that are maximally adapted to the changing demands and needs of customers.

Contemporary production of machines, equipment, devices and parts within industrial metal processing is characterized by continuous expansion of assortments and increasing volume, raising the technical level of the product and reducing the deadlines for their production [1].

For insertion of the implant into the human organism, modern medicine requires faster progress in finding of the new solutions. The use of implants and prosthetic components is very widespread in medicine. Most of the insertion of the implant into the human organism have become routine, thanks to decades of research. In this way, it is possible to replace the diseased and damaged part of the human body completely, which contributes to the functionality and / or aesthetics of the same [2].

The correct selection and proper installation of endoprosthesis ensures the normal functioning of the hip joint itself and, consequently, of the entire locomotor system. In clinical practice, endoprostheses with different body shapes (which take part in the function of the femur) are used. They are, according to their application and form, divided into: primary, revision and tumor endoprosthesis. In addition, in the case of revision and tumor endoprosthesis geometry endoprosthesis body is determined only by the disease,

and they are made according to the measures of the patient ("custom-made") [3].

Using computers has created better conditions for the development of new implants, their testing and development. Modern computer systems can model implants and prosthetic elements, perform calculations and checks, simulate functionality, and prepare programs for their creation on computer-controlled machine tools. In the world, these systems are unified under the name CAD / CAM systems.

In the paper a modular endoprosthesis of the hip joint which is produced in small and individual production is presented.

2. PRODUCT DEVELOPMENT TECHNOLOGY

Preparation of production in metal processing is based on technical and operational preparation. Technical preparation of production consists of two functions of the production system, one refers to the design of the product, and the other to the design of the technological process of manufacturing products, Figure 1.

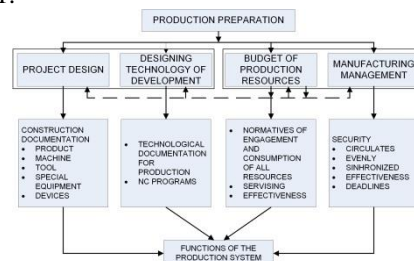


Fig. 1. The basic structure of the production preparation function [4,5]

As can be seen from the picture, the product design function includes all the calculations and designs, that is, the production of technical documentation for the product, special machine tools, accessories, tools, devices and equipment for the realization of the product manufacturing process.

The function of technological preparation includes

all the tasks of selecting the most favorable product technology, specifying the content of the technological process and product manufacturing operations, including the precision and selection of accessories, tools, measuring equipment, processing regimen as well as determining the norms of the processing and technological cycle times.

Technical preparation of production must be based on the application of computers and program systems suitable for the calculation and design of products, as well as systems suitable for designing technological processes for the production of products.

The modern approach in the development of technical preparation is characterized by a high degree of automation, both in the part of product design and in the design of technological processes for the production and assembly of products.

3. ENDOPROTEX DEVELOPMENT TECHNOLOGY

3.1 Introductory remarks

Modern medicine requires ever faster progress in finding new solutions when implanting in the human organism. Due to the human body's ability to reject foreign bodies from the body, this method of treatment requires a great deal of time and resources, as well as the cooperation of experts in various fields such as medicine, engineering, design, and others.

There are still a number of questions to be considered during the construction of an implant. Experts around the world are working to find optimal answers to the same. Although a large number of such operations have become routine, scientists still strive for even more practical and better solutions. Over the years, the study of the human body and its defects has resulted in a number of different implants in all areas of medicine such as: dentistry, orthopedics, plastic surgery, cardiology, and others. Figure 2 shows some of the most commonly implanted implants.

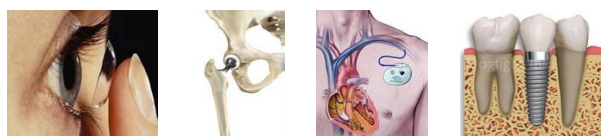


Fig.2. Examples of implants: a) Lens b) Artificial hip c) Pacemaker d) Bioceramic implants[6,7]

Using computers has created significantly better conditions for the development of new implants, their testing and development. Modern computer systems can model implants and prosthetic elements, perform calculations and checks, simulate functionality, and prepare programs for their production on numerically controlled machine tools. In the world, these systems are unified under the name CAD / CAM systems [2]. All this is in the function of enabling normal life and work of users of implants and prosthetic elements.

3.2. The technological process of making modular endoprosthesis of the hip joint

Endoprosthesis of the hip joint is produced by cutting, forging and precise casting. They are made in

small-sized and individual production, based on special geometric requirements. Since endoprosthesis are special parts, the most economical treatment is cutting, so within this work, the processing of modular endoprosthesis will be performed on the CNC turning.

Figure 3 gives the content of the technological process for the processing of the body, the central and neck part of the endoprosthesis. Since this is a modular endoprosthesis, the procedure for producing a body that begins with the setting and clamping of the rod on CNC turning is described below. The first operation is cutting off the testers. After cutting, the second operation is roughly scraping and then finishing scraping. The third operation is spot drilling and the fourth drilling. With the completion of the drilling, the processing of the right side of the endoprosthesis body was completed.

№	OPERATION	CONTENT OF THE TECHNOLOGICAL PROCEDURE	UNIT OF MEASURE	QUANTITY	TIME
1	CUTTING OFF	CUTTING OFF THE TESTERS	mm	1	0.1
2	ROUGH SCRAPING	ROUGH SCRAPING OF THE BODY	mm	1	0.5
3	FINISHING SCRAPING	FINISHING SCRAPING OF THE BODY	mm	1	0.5
4	SPOT DRILLING	SPOT DRILLING OF THE BODY	mm	1	0.1
5	DRILLING	DRILLING OF THE BODY	mm	1	0.5
6	DRILLING	DRILLING OF THE BODY	mm	1	0.5
7	DRILLING	DRILLING OF THE BODY	mm	1	0.5
8	DRILLING	DRILLING OF THE BODY	mm	1	0.5
9	DRILLING	DRILLING OF THE BODY	mm	1	0.5
10	DRILLING	DRILLING OF THE BODY	mm	1	0.5
11	DRILLING	DRILLING OF THE BODY	mm	1	0.5
12	DRILLING	DRILLING OF THE BODY	mm	1	0.5
13	DRILLING	DRILLING OF THE BODY	mm	1	0.5
14	DRILLING	DRILLING OF THE BODY	mm	1	0.5
15	DRILLING	DRILLING OF THE BODY	mm	1	0.5
16	DRILLING	DRILLING OF THE BODY	mm	1	0.5
17	DRILLING	DRILLING OF THE BODY	mm	1	0.5
18	DRILLING	DRILLING OF THE BODY	mm	1	0.5
19	DRILLING	DRILLING OF THE BODY	mm	1	0.5
20	DRILLING	DRILLING OF THE BODY	mm	1	0.5
21	DRILLING	DRILLING OF THE BODY	mm	1	0.5
22	DRILLING	DRILLING OF THE BODY	mm	1	0.5
23	DRILLING	DRILLING OF THE BODY	mm	1	0.5
24	DRILLING	DRILLING OF THE BODY	mm	1	0.5
25	DRILLING	DRILLING OF THE BODY	mm	1	0.5
26	DRILLING	DRILLING OF THE BODY	mm	1	0.5
27	DRILLING	DRILLING OF THE BODY	mm	1	0.5
28	DRILLING	DRILLING OF THE BODY	mm	1	0.5
29	DRILLING	DRILLING OF THE BODY	mm	1	0.5
30	DRILLING	DRILLING OF THE BODY	mm	1	0.5
31	DRILLING	DRILLING OF THE BODY	mm	1	0.5
32	DRILLING	DRILLING OF THE BODY	mm	1	0.5
33	DRILLING	DRILLING OF THE BODY	mm	1	0.5
34	DRILLING	DRILLING OF THE BODY	mm	1	0.5
35	DRILLING	DRILLING OF THE BODY	mm	1	0.5
36	DRILLING	DRILLING OF THE BODY	mm	1	0.5
37	DRILLING	DRILLING OF THE BODY	mm	1	0.5
38	DRILLING	DRILLING OF THE BODY	mm	1	0.5
39	DRILLING	DRILLING OF THE BODY	mm	1	0.5
40	DRILLING	DRILLING OF THE BODY	mm	1	0.5
41	DRILLING	DRILLING OF THE BODY	mm	1	0.5
42	DRILLING	DRILLING OF THE BODY	mm	1	0.5
43	DRILLING	DRILLING OF THE BODY	mm	1	0.5
44	DRILLING	DRILLING OF THE BODY	mm	1	0.5
45	DRILLING	DRILLING OF THE BODY	mm	1	0.5
46	DRILLING	DRILLING OF THE BODY	mm	1	0.5
47	DRILLING	DRILLING OF THE BODY	mm	1	0.5
48	DRILLING	DRILLING OF THE BODY	mm	1	0.5
49	DRILLING	DRILLING OF THE BODY	mm	1	0.5
50	DRILLING	DRILLING OF THE BODY	mm	1	0.5
51	DRILLING	DRILLING OF THE BODY	mm	1	0.5
52	DRILLING	DRILLING OF THE BODY	mm	1	0.5
53	DRILLING	DRILLING OF THE BODY	mm	1	0.5
54	DRILLING	DRILLING OF THE BODY	mm	1	0.5
55	DRILLING	DRILLING OF THE BODY	mm	1	0.5
56	DRILLING	DRILLING OF THE BODY	mm	1	0.5
57	DRILLING	DRILLING OF THE BODY	mm	1	0.5
58	DRILLING	DRILLING OF THE BODY	mm	1	0.5
59	DRILLING	DRILLING OF THE BODY	mm	1	0.5
60	DRILLING	DRILLING OF THE BODY	mm	1	0.5
61	DRILLING	DRILLING OF THE BODY	mm	1	0.5
62	DRILLING	DRILLING OF THE BODY	mm	1	0.5
63	DRILLING	DRILLING OF THE BODY	mm	1	0.5
64	DRILLING	DRILLING OF THE BODY	mm	1	0.5
65	DRILLING	DRILLING OF THE BODY	mm	1	0.5
66	DRILLING	DRILLING OF THE BODY	mm	1	0.5
67	DRILLING	DRILLING OF THE BODY	mm	1	0.5
68	DRILLING	DRILLING OF THE BODY	mm	1	0.5
69	DRILLING	DRILLING OF THE BODY	mm	1	0.5
70	DRILLING	DRILLING OF THE BODY	mm	1	0.5
71	DRILLING	DRILLING OF THE BODY	mm	1	0.5
72	DRILLING	DRILLING OF THE BODY	mm	1	0.5
73	DRILLING	DRILLING OF THE BODY	mm	1	0.5
74	DRILLING	DRILLING OF THE BODY	mm	1	0.5
75	DRILLING	DRILLING OF THE BODY	mm	1	0.5
76	DRILLING	DRILLING OF THE BODY	mm	1	0.5
77	DRILLING	DRILLING OF THE BODY	mm	1	0.5
78	DRILLING	DRILLING OF THE BODY	mm	1	0.5
79	DRILLING	DRILLING OF THE BODY	mm	1	0.5
80	DRILLING	DRILLING OF THE BODY	mm	1	0.5
81	DRILLING	DRILLING OF THE BODY	mm	1	0.5
82	DRILLING	DRILLING OF THE BODY	mm	1	0.5
83	DRILLING	DRILLING OF THE BODY	mm	1	0.5
84	DRILLING	DRILLING OF THE BODY	mm	1	0.5
85	DRILLING	DRILLING OF THE BODY	mm	1	0.5
86	DRILLING	DRILLING OF THE BODY	mm	1	0.5
87	DRILLING	DRILLING OF THE BODY	mm	1	0.5
88	DRILLING	DRILLING OF THE BODY	mm	1	0.5
89	DRILLING	DRILLING OF THE BODY	mm	1	0.5
90	DRILLING	DRILLING OF THE BODY	mm	1	0.5
91	DRILLING	DRILLING OF THE BODY	mm	1	0.5
92	DRILLING	DRILLING OF THE BODY	mm	1	0.5
93	DRILLING	DRILLING OF THE BODY	mm	1	0.5
94	DRILLING	DRILLING OF THE BODY	mm	1	0.5
95	DRILLING	DRILLING OF THE BODY	mm	1	0.5
96	DRILLING	DRILLING OF THE BODY	mm	1	0.5
97	DRILLING	DRILLING OF THE BODY	mm	1	0.5
98	DRILLING	DRILLING OF THE BODY	mm	1	0.5
99	DRILLING	DRILLING OF THE BODY	mm	1	0.5
100	DRILLING	DRILLING OF THE BODY	mm	1	0.5

Fig.3. The content of the technological procedure for the processing of the body, the central and neck part of the endoprosthesis

Before the fifth operation, the release and re-clamping of the workpiece are carried out, this time in soft packs for processing on the left side. The fifth operation is rough, and then the final scraping. In the next six operations in the content of the technological process, final endoprotection, visual inspection, laser marking is performed, where each prosthesis receives a unique identification number, cleaning in special plants, packaging in sterile rooms and finally sterilization by gamma ray radiation.

As the complex endoprotection body, the most convenient way of generating the NC code for its development is by applying one of the CAM software, based on the previously developed endoprosthesis model. In this paper we will show the process of generating the NC code for the scraping operation of the body as well as the simulation of its processing.

3.3 Simulation of hip joint endoprosthesis production

It takes a lot of time and effort to create technical documentation, modeling and simulating work processing. The emergence of a computer and its massive use significantly reduces time and serves as a place to archive all phases of product design, from drawings to simulation processing, and to generating a control program. Nowadays, when designing and constructing, such analysis and synthesis are made possible by highly sophisticated software tools.

For the simulation of turning the modular prosthesis of the hip joint is over used prosthesis CAD model

created in previous research. The CAD model consists of several components (modules). Individual modules are: body, central part longer, central part shorter and neck. As for the preparation, it is defined for each part separately.

From the previously defined technological processes, a turning operation of the modular endoprosthesis body was selected. This operation was performed in the Machining module, and for some processing operation to be credibly simulated, it is necessary to define the following data in detail:

- Preparation and processing models
- The type of processing operation
- Machine tool for processing, optional and accessories
- Required processing operations
- Required tools for defined processing tasks
- Processing modes

The preparation for the turning operation is defined in the *Assembly* module, as a block of each individual part of the modular endoprosthesis (Figure 4) and the preparation model. After defining the model of endoprosthesis and preparation models, it moves to the *Machining* module, choosing the type of processing operation, in this case, *Lathe Machining*, which represents a turning operation, in which a large number of different processing operations are given.



Fig.4. Model of modular endoprosthesis of hip joint

Due to credible processing simulation, the machine header and packs are also made, which are also implemented in the virtual machine tool space. Figure 5a shows the virtual machine tool area with a set of preparation and modification of the body of modular endoprosthesis for the right hand side. In Figure 5b, a set of preparation and processing in the chuck head is shown, for processing the left, after the processing of the right side.

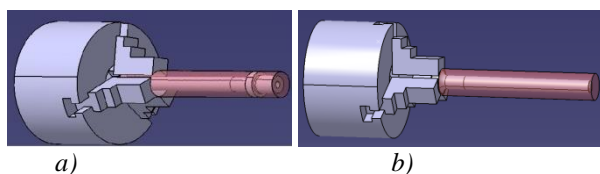


Fig. 5. Processing of the a) right side b) left side

3.3.1. Defining operations, tools, and processing modes

The turning of the right side of the endoprosthesis is performed in four interventions with three different tools. The first processing operation is a rough turning of the workpiece and is performed with a knife. For this procedure, it is necessary to define the depth of turning, the tool, the contour which defines tool movement and

cutting regimes (Figure 6). In addition, it is also possible to define in detail the tool gestures before and after the cutting, ie the path of the tool's access to the workpiece and the path of its return to the tool change point. Also, it is necessary to note that one defined tool is automatically stored in the tool list, and can be reused by simple calling.

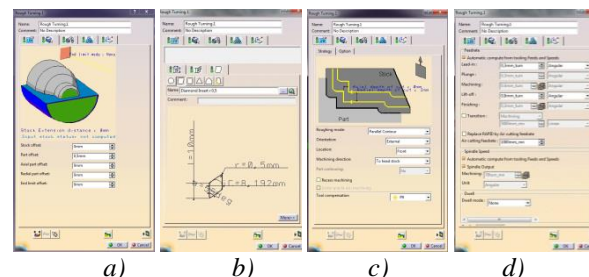


Fig. 6. a) surface and depth of turning b) dimension and name of the tool c) information on the tool path d) cutting modes

The second step is a fine turning. The tools used for this operation are a turning knife. In addition to the finishing tool, it is necessary to select the processing and preparation, define the starting point of the processing and the finishing additive. Also, it is necessary to define the tool itself, as well as data on tool paths and processing modes. The definition of the finishing operation is performed in the same way, the only difference is in the add-on that remains after processing, in the used tool and in the processing modes. After finishing turning, spot drilling then working on a drilling.

After fully defined all the procedures for turning the endoprosthesis of the hip joint, it is simple to perform a simulation of the scraping process. However, as the process of simulation can not be displayed in the work, Figure 7 shows the appearance of the workpiece after all the processing steps.

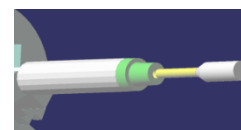


Fig 7. Appearance of the right side of the preparation of the body after drilling

3.3.2. Generating a program

Software allow you to generate a control NC code for a CNC machine tool based on simulated processing (Fig.8). In order to use the NC code in practice, you need to know the type of control unit installed on the selected machine tool. By selecting the appropriate control unit, by clicking the Execute button, a text file is generated automatically in which the NC code for the selected machine is written, which is stored in a predefined place. As the hip joint endoprotection body is a very complex part, the NC code for its development on the NC lathe is very extensive, and therefore will not be shown in this paper.

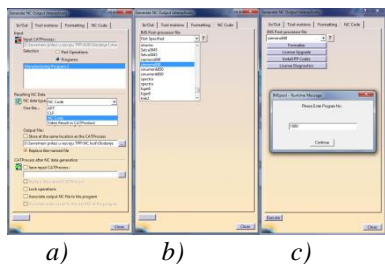


Fig. 8. a) selecting the type of NC data and defining the code storage location; b) selection of the control unit of the machine; c) entering the regular program number

4. FINAL REMARKS

The complex requirements that are placed in front of production systems are to a considerable extent realized within the development of products and preparation of production, which is an integral part and function of technological preparation, which is the connection between the design process and the production of products. In order to accomplish the set tasks, the application of modern engineering methods and information technologies is necessary.

In this paper a technological preparation of the production of modular endoprosthesis of the hip joint as a complex product was carried out. Due to its characteristic, both in terms of shape and in terms of the method of installation, the development of endoprosthesis of the hip joint requires a close cooperation between the surgeon who installs the endoprosthesis and the engineer who projects it. In this work, the method of turning of modular endoprostheses on the CNC lathe is selected, that is, the simulation of the processing of the modeling endoprosthesis in the selected software package, which also enables the development of the NC code, which can be applied to the real machine.

In order to be able to talk about endoprosthesis modeling, modern diagnostic imaging, such as magnetic resonance imaging (MRI) and computed tomography (CT), are required. Contemporary diagnostic imaging of the diseased extremity, in addition to high reliability in the diagnosis of the disease, enables the reconstruction of spatial computational models of both femur and medullary canal. Depending on the acquired computer models, the design of orthopedic implants requires an increasing accuracy, due to the production of better implants that fit into the anatomy of the patient. This is reflected in both the design and the production of type implants, as well as implants made to the extent of the patient. In the case of prostheses, a large number of parameters are determined by the outer and inner surface of the femur.

The obtained computational models make it easy to create endoprostheses, because using a computer and the corresponding software packages it is possible to perform a simulation processing and see any problems before the production itself. In addition to the possibility of simulating and removing possible errors, modern technologies allow, as already mentioned, the creation of a NC code, which can be easily used on CNC machines in production facilities.

The current development of endoprostheses is in the

direction of their modular construction, because in this case the endoprotection elements would be produced serially as type elements, and with their appropriate combinations there would be special endoprostheses, which would significantly save time needed for their design, and the price itself production would drop significantly. In this case, it would be ideal to design typical technological processes for modular endoprotection elements, which would reduce the volume and complexity of tasks that are set before the technological preparation of the production of complex products such as hip joint endoprosthesis.

5. REFERENCES

- [1] Todić, V.: *Varijantni automatizovani sistemi tehnoeconomске optimizacije tehnoloških procesa obrade*, Doktorska disertacija, Fakultet tehničkih nauka, Novi Sad, 1987.
- [2] Grujić, J.: *Računarsko modeliranje i eksperimentalno ispitivanje proteze zgloba kuka*, magistarska teza, Fakultet tehničkih nauka, Novi Sad, 2008.
- [3] Tabaković, S., Grujić, J., Bojanić, M., Zeljković, M., Sekulić, J.: *Modeliranje medularnog kanala femura na osnovu digitalnog signala sa CT ili MRI u cilju dimenzionisanja stema tumorske endoproteze zgloba kuka*, Zbornik radova, Naučno-stručni simpozijum informacione tehnologije-Infoteh, Jahorina, ISBN 99938-624-2-8, 2012.
- [4] Todić, V.: *Projektovanje tehnoloških procesa*, Fakultet tehničkih nauka, Novi Sad, 2004, ISBN 86-80249-93-9.
- [5] Warnecke, H. J.: *Produktionsbetrieb*, IPA, Stuttgart, 1977.
- [6] <http://croatiahipandkneeclinic.co.uk/hr/bol-u-kuku/>, 03.07.2012.
- [7] <http://sr.scribd.com/doc/28724342/Anatomija-donjih-extremiteta>, 03.07.2012
- [8] Bojanić, M.: *Savremeni prilazi u razvoju tehnološke pripreme proizvodnje*, ispitni rad, Fakultet tehničkih nauka, Novi Sad, 2015.

Authors: M.Sc. Mirjana Bojanić Šejat, Full Prof. in retired Velimir Todić, M. Sc. Cvijetin Mladenović, University of Novi Sad, Faculty of Technical Sciences, Department of Production Engineering, Trg Dositeja Obradovica 6, 21000 Novi Sad, Serbia, Phone.: +381 21 450-366, Fax: +381 21 454-495. Full Prof. Livia Dana Beju, University „Lucian Blaga“ of Sibiu, Department of Industrial Engineering and Management, 10, Victoriei Bd., Sibiu, 550024, România, Phone.: +40 269 21 60 62, Fax: +40 269 21 04 92, Jovan Grujić, DOO „Grujić i Grujić“, Bulevar Vojvode Stepe 6, Novi Sad, Serbia, Phone.: +381 21 518 381
E-mail: bojanicm@uns.ac.rs; lukicd@uns.ac.rs; mladja@uns.ac.rs; liviadana_beju@yahoo.com;

ACKNOWLEDGMENTS: The work is part of research project on "Modern approaches in the development of special bearings in mechanical engineering and medical prosthetics," TR 35025, supported by the Ministry of Education, Science and Technological Development, Republic of Serbia.

Kosec, B., Karpe, B., Vodlan, M., Kopac, I., Budak, I., Pavlic, A., Puskar, T.,
Zupancic, K., Fir, B., Gojic, M., Nagode, A.

THERMAL PROPERTIES OF TITANIUM ALLOYS USED IN DENTAL MEDICINE

Abstract: *Titanium and its alloys are used in dental medicine because of their resistance to electrochemical decomposition, excellent compatibility with live tissues, easily combine with bone, are relatively light, and have high tensile and yield strength. Today almost all manufacturers of dental materials in their certificates of quality of material give its chemical composition, mechanical properties, process ability in aesthetic characteristics while information about thermal properties are not available. Within the presented work measurements of the thermal properties of two selected titanium dental alloys have been carried out. Measurements were carried out modern and high-quality instrument Hot Disk TPS 2200 in accordance with the international standard ISO 22007-2, at ambient temperature, and in a temperature range between 0 °C and 45 °C.*

Key words: *Dental materials, Thermal properties, Measurement.*

1. INTRODUCTION

The thermal properties of dentine and tooth enamel affects the rate of response of the tooth nervous system to the temperature changes to which the tooth is exposed on a daily basis. In addition to strength and aesthetic requirements, artificial dental materials must also provide a similar thermal protection for the tooth pulp. Likewise, implants and artificial tooth crowns must transfer similar heat flow to the bone as is transferred by a natural tooth, which has a strong influence on the patient's general acceptance of the foreign body (Figure 1).

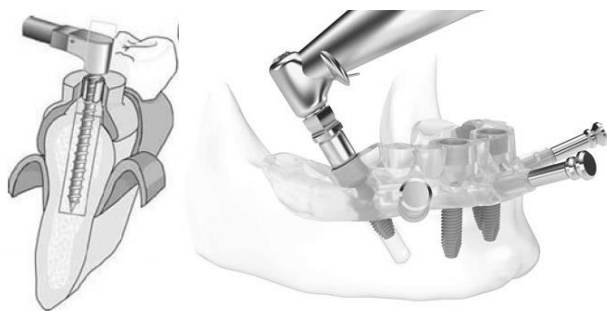


Fig 1. An example of insertion of the dental implant into the jawbone.

Manufacturers of dental materials in their certificates of material quality describe chemical composition, mechanical properties, machinability and aesthetic characteristics, while thermal properties of the material are rarely given.

The reported values of human teeth thermal properties show significant discrepancies, with data for thermal conductivity of dentine between 0.11 to 0.98 Wm⁻¹ K⁻¹, and 0.7 to 0.8 Wm⁻¹ K⁻¹ for tooth enamel, while thermal diffusivity varies between 0.058 to 0.269 mm²/s and 0.092 to 0.42 mm²/s for dentin and enamel

respectively. The significant discrepancy between the reported results may be attributed to several challenges associated with the measurements, like tooth heterogeneous microstructure and associative anisotropic thermal properties, difficulties at establishing perfect thermal contact or lack of precise emissivity data when axial heat flow or laser flash measuring methods are applied. Thermal conductivity, specific heat and thermal diffusivity are basic thermal properties of material that determine the heat transfer in the system under consideration. Despite the remarkable progress of measuring methods and techniques, it is still difficult to determine them with an error of less than ±2 %, even for bulk materials.

In our research, we used one of the most advanced instruments for determining the thermal properties, Hot Disk TPS 2200, a product of Hot Disk AB company, Gothenburg, Sweden. The instrument can be used for determining thermal properties of various materials including pure metals, alloys, minerals, ceramics, plastics, glasses, powders and viscous liquids with thermal conductivity in the range from 0.01 to 500 W/mK, thermal diffusivity from 0.01 to 300 mm²/s and heat capacity up to 5 MJ/m³K. Measurements can be perform in a temperature interval between -50 up to 750 °C.

Hot disk measuring method is a transient plane source technique (TPS). Based on the theory of TPS, instrument utilizes a sensor element in the shape of 10 µm thick double spiral (Figure 2), made by etching from pure nickel foil. Spiral is mechanically strengthen and electrically insulated on both sides by thin polyimide foil (Kapton ®Du Pont) for measurements up to 300 °C or mica foil for measurements up to 750 °C. Sensor acts both as a precise heat source and resistance thermometer for recording the time dependent temperature increase. During measurement of solids, encapsulated Ni-sensor is sandwiched between two halves of the sample and constant precise pre-set heating power is released by the sensor,

followed by 200 resistance recording in a pre-set measuring time, from which the relation between time and temperature change is established. Based on time dependent temperature increase of the sensor, thermal properties of the tested material are calculated.

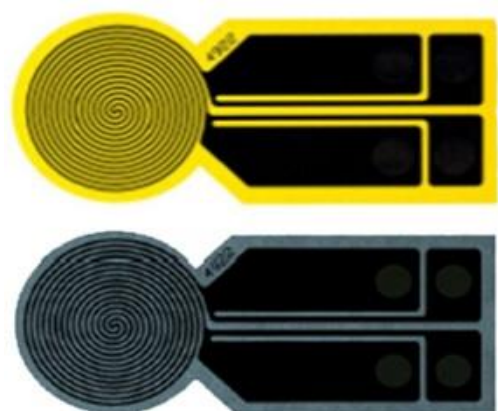


Fig 2. Sensor element (yellow - Kapton, gray - Mica) (above), sensor sandwiched between two halves of a sample during measurement (below).

In our study, we measured thermal properties of five important dental materials, used at the Department of Dental Prosthesis of the Medical Faculty, University of Ljubljana. Tested materials were 99 % pure titanium and titanium alloy TiAl6V4 alloy. Thermal properties were measured in the temperature interval that teeth are most frequently exposed, between 7 °C and 45 °C.

2. EXPERIMENTAL WORK

Measurements and analysis of thermal properties of selected dental materials were performed in accordance with ISO 22007-2 standard in the Laboratory for measurements, Chair of Thermal Engineering, Faculty of Natural Sciences and Engineering, University of Ljubljana (Figure 3).

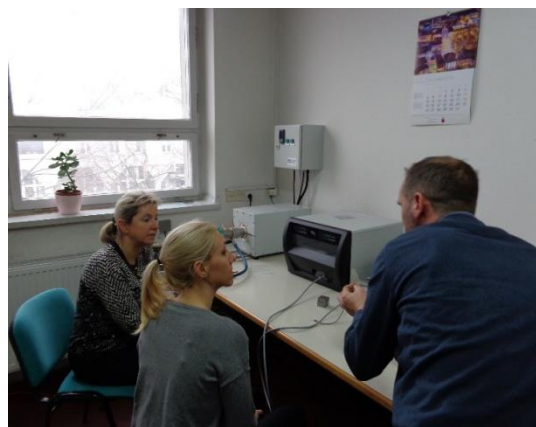


Fig 3. Measurements in the Laboratory for measurements, Chair of Thermal Engineering, Faculty of Natural Sciences and Engineering, University of Ljubljana.

Titanium and its alloys are used in dentistry because of their resistance to electrochemical decomposition, excellent compatibility with live tissues, easily combine with bone (osseointegration), are relatively light (4.61 g/cm^3) and have high tensile (450 MPa) and yield (275 MPa) strength. Titanium forms a very persistent oxide layer on the surface, formed in a few nanoseconds. Because of this oxide layer, it is corrosion-resistant and biocompatible. It is used for manufacturing of dental implants, crowns, braces, bridges, partial prostheses and orthodontic wires. Commercially pure titanium (impurities < 1%) disks were measured in the temperature interval between 0 °C and 45 °C, and as expected, changes of thermal properties were negligible.

Table 1. Thermal properties of pure Ti disks (impurities < 1%, temperature interval from 0 °C to 45 °C)

Measurement	Thermal conductivity [$\text{Wm}^{-1}\text{K}^{-1}$]	Thermal diffusivity [mm^2s^{-1}]	Specific heat [$\text{MJm}^{-2}\text{K}^{-1}$]
Average	22.546	6.7196	3.36
SD	0.356573	0.265174	0.123366

Table 2. Thermal properties of pure Ti disks (impurities < 1%) at ambient temperature (22 °C)

Measurement	Thermal conductivity [Wm ⁻¹ K ⁻¹]	Thermal diffusivity [mm ² s ⁻¹]	Specific heat [MJm ⁻² K ⁻¹]
1	22.21	6.371	3.486
2	22.16	6.889	3.218
3	22.53	6.448	3.494
Average	22.30	6.569	3.569

Table 3. Thermal properties of pure Ti disks (impurities < 1%) at temperature 3 °C

Measurement	Thermal conductivity [Wm ⁻¹ K ⁻¹]	Thermal diffusivity [mm ² s ⁻¹]	Specific heat [MJm ⁻² K ⁻¹]
1	22.49	8.507	2.644
2	22.14	6.831	3.388
3	22.69	7.059	3.214
Average	22.41	7.466	3.082

TiAl6V4 (Grade 5: 6% Al, 4% V, 0.25% > Fe and 0,2% > O (bal. Titanium)) is the most commonly used titanium alloy in dentistry. It is significantly stronger ($R_m > 895$ MPa, $R_{p0.2} > 828$ MPa) than commercially pure titanium while having the same stiffness. This grade is an excellent combination of strength, corrosion resistance, weldability and machinability, and has good osseointegration properties.



Fig 4. Testing disk from TiAl6V4 alloy.

Alloying elements reduce thermal conductivity and diffusivity considerably compared to commercially pure titanium. In the temperature interval between 0 and 45 °C thermal properties can be considered as constant.

Table 4. Thermal properties of TiAl6V4 disks (temperature interval from 0 °C to 45 °C)

Measurement	Thermal conductivity [Wm ⁻¹ K ⁻¹]	Thermal diffusivity [mm ² s ⁻¹]	Specific heat [MJm ⁻² K ⁻¹]
Average	6.668286	2.809286	2.375857
SD	0.051146	0.083763	0.073172

Table 5. Thermal properties of pure TiAl6V4 (disks (impurities < 1%) at ambient temperature (22 °C)

Measurement	Thermal conductivity [Wm ⁻¹ K ⁻¹]	Thermal diffusivity [mm ² s ⁻¹]	Specific heat [MJm ⁻² K ⁻¹]
1	6.615	2.857	2.315
2	6.687	2.709	2.469
3	6.644	2.899	2.292
4	6.774	2.808	2.412
5	6.684	2.880	2.320
Average	6.681	2.861	2.362

Table 6. Thermal properties of TiAl6V4 (disks (impurities < 1%) at temperature 3 °C

Measurement	Thermal conductivity [Wm ⁻¹ K ⁻¹]	Thermal diffusivity [mm ² s ⁻¹]	Specific heat [MJm ⁻² K ⁻¹]
1	6.661	2.851	2.337
2	6.613	2.661	2.486
Average	6.637	2.756	2.412

3. CONCLUSIONS

Measurements and analysis of the thermal properties of selected characteristic dental materials were performed using the Hot Disk method on the Hot Disk TPS 2200 in accordance with ISO 22007-2 in the Laboratory for measurement of the Chair of Thermal Engineering, Department of Materials and Metallurgy, Faculty of Natural Sciences and Engineering, University of Ljubljana.

The teeth and dental supplements are most often exposed to temperatures at an interval between 0 °C and 50 °C, which was the reason why we selected this temperature interval to perform our measurements. We found that for both dental materials there is no significant difference in thermal properties in this temperature interval and can be considered as constant.

With the performed measurements, we have completed the existing material quality certificates of dental materials with their thermal properties.

4. REFERENCES

- [1] F. H. Froes, Titanium: A Historic and Current Perspective, Part II, Advanced Materials and Processes, 176 (2018) 3, 18 – 23.
- [2] B. Kosec, B. Karpe, Instrument for thermal properties analysis Hot Disk TPS 2200, IRT3000, 70 (2017), 67.
- [3] Internal script Hot Disk AB; Hot Disk Thermal Constants Analyser, Instruction Manual, Revision date 2014-03-27.
- [4] A. B. Auklend Kroh, Measurement of conductivity of intumescent materials (Degree of Master of Science). University of Bergen, Faculty of Mathematics and Natural Sciences, Bergen, 2009.
- [5] I. Budak, B. Kosec, M. Sokovic, Application of contemporary engineering techniques and technologies in the field of dental prosthetics, Journal of Achievements in Materials and Manufacturing Engineering, 54 (2012) 2, 233-241.
- [6] C. Scheller-Sheridan, Basic Guide to Dental Materials, Wiley-Blackwell, Dublin, 2010.
- [7] J. J. Manappallil, Basic Dental Materials, Jaypee Brothers, New Delhi, 2003
- [8] Certificate CC DISK Ti2, Interdent d.o.o., Celje, 2014.
- [9] Certificate CC DISK Ti5, Interdent d.o.o., Celje, 2014.
- [10] B. Karpe, M. Vodlan, I. Kopač, A. Nagode, T. Puškar, A. Pavlič, H. Taubmann, M. Gojić, M. Bizjak, B. Kosec. Thermal properties of dental materials, ETIKUM 2017, Novi Sad, 2017, 117-120.
- [11] B. Kosec, M. Vodlan, B. Karpe, A. Nagode, M. Bizjak, I. Kopač, A. Pavlič, I. Budak, T. Puškar, H. Taubmann, M. Gojić, Thermal properties of selected dental materials. MNM 2018, Zenica, 2018, 1-6.

Authors: Prof. Dr. Borut Kosec, Ass. Prof. Dr. Blaž Karpe, Katja Zupančič, Brina Fir, Asocc. Prof. Dr. Aleš Nagode, University of Ljubljana, Faculty of Natural Sciences and Engineering, Aškerčeva 12, 1000 Ljubljana, Slovenia, Phone: +386 1 2000413, Fax: +386 1 4704560. E-mail: borut.kosec@omm.ntf.uni-lj.si; blaz.karpe@omm.ntf.uni-lj.si; zupancic.kaatja@gmail.com; firbrina@gmail.com; ales.nagode@omm.ntf.uni-lj.si

Mateja Vodlan, LEK d.d., Verovskova 57, 1526 Ljubljana, Phone: +386 1 5802111, Fax: +386 1 5683517. E-mail: vodlan@gmail.com

Asocc. Prof. Dr. Igor Kopač, Assoc. Prof. Dr. Alenka Pavlič, University of Ljubljana, Faculty of Medicine, Korytkova 2, 1000 Ljubljana, Slovenia, Phone: +386 1 5224268, Fax: +386 1 5222504. E-mail: igor.kopac@mf.uni-lj.si; alenka.pavlic@mf.uni-lj.si

Assoc. Prof. Dr. Igor Budak, University of Novi Sad, Faculty Technical Sciences, Trg D. Obradovića 6, 21000 Novi Sad, Serbia, Phone.: +381 21 4852255, Fax: +381 21 4852313. E-mail: budaki@uns.ac.rs

Assoc. Prof. Dr. Tatjana Puškar, University of Novi Sad, Faculty of Medicine, Hajduk Veljkova 6, 21000 Novi Sad, Serbia, Phone: +381 21 526120, Fax: +381 21 6613262. E-mail: tpuskar@uns.ac.rs

Prof. Dr. Mirko Gojić, University of Zagreb, Faculty of Metallurgy, Aškerčeva 6, 1000 Sisak, Croatia, Phone: +385 43 533 381, Fax: +385 43 533 381. E-mail: gojic@simet.hr

Puškar, T., Budak I., Jakimov, D., Djurović Koprivica, D., Kojić, V., Ilić Mićunović, M.

TESTING BIOCOMPATIBILITY OF BONE SUBSTITUTE BY FLUORESCENT MICROSCOPY

Abstract: *Biocompatibility is the most important property of materials for regenerative dentistry. Any material intended to be incorporated into the human body must be tested and the safety of the application must be confirmed. The use of bone substitutes does not mean unconditionally successful bone regeneration. The impact of two bone implantation material (Bio-Oss, Geistlich; and SmartBone, Ibi) on cell metabolism and proliferation was examined by cytological testing methods and with fluorescent staining. Results showed the absence of cytotoxicity and the adhesion of fibroblast to tested implant materials was confirmed by fluorescent staining. Examining the biocompatibility of implantation materials in vitro using continuous cell lines and fluorescent microscopy, it is possible to determine the adhesion of cells to the implanting material and predict the success of reconstruction and remodeling of bone defects.*

Key words: *biocompatibility, cytotoxicity, fluorescence microscopy*

1. INTRODUCTION

In oral surgical interventions based on the reconstruction of bone defects, the use of autologous bone substitutes is considered a gold standard because of the absence of immune response and its structural, osteoinductive, osteoconductive and osteogenic properties. When reconstruction of large bone defects is necessary, taking a large amount of autologous bone from the patient can lead to complications. Because of this, homologous bone substitutes have become a routine alternative. Biomaterials are designed to replace parts of the living system after implantation in human body and fulfill the appropriate biological function. However, they require a number of tests to ensure the reliability of their application. One of the basic tasks of biological evaluation of biomaterials is testing their biocompatibility.

Biocompatibility is the ability of material to perform a certain function after application in the body, without causing adverse response to the host tissue. Biocompatibility implies the harmony of interaction between the host tissue, the applied material, and the function it performs [1,2].

For successful application of dental materials to patients, it is necessary to get acquainted with their physical, chemical, mechanical and biological properties. These properties depend on chemical structure of the material and its behavior under changing conditions in the oral cavity [3,4,5]. The acceptable response of the host to the application of biocompatible material, in most cases means that the reaction of the living system to the presence of biomaterials is either tolerable or absent.

Any material intended to be incorporated into the human body must be tested. Which tests will be carried out for various types of material is determined by the ISO standard (ISO 10993 and ISO 7405 for dentistry tests).

The first step in assessing biocompatibility is laboratory *in vitro* cytotoxic and genotoxic testing and

assays on cell cultures. *In vitro* estimation is simpler, cheaper and can provide faster data on biological interactions compared to clinical trials. *In vitro* tests are designed to simulate the biological response of the tissue that comes in contact with the test material. If these experiments give promising results, then more complex experiments are carried out on experimental animals and finally human usage tests [6]. Artificial bone must fulfill biological criteria such as biocompatibility, controlled biodegradability, osteoconductive and osteogenic potential.

The aim of this paper is to present the method of cytological analysis *in vitro* - examining the impact of bone implants Bio-Oss® (Geistlich) and SmartBone® (Ibi).

2. MATERIALS AND METHODS

The study was conducted on MRC-5 (ATCC CCL 171, American Type Culture Collection) human lung fibroblasts cell line. We performed three tests to investigate the cytotoxicity of tested materials. The successful adhesion of the cells to the material was tested with fluorescence microscopy.

Dye exclusion test (DET). After the 24 hours incubation with tested substances, the cells were reseeded into the fresh medium and incubated for 48h, 72h and 96h. Cells were counted using inverted microscope (REICHERT) [7].

Colorimetric test with tetrazolium salts (MTT test). After incubation with the test materials (24h), the viable cells were seeded into 96-well microplates and left for the next 48, 72, 96 hours. Absorbance was obtained on spectrophotometer and cell survival is expressed as a percentage of control [8].

Agar diffusion test. Neutral-red color was added to the tested material. The colorless zones around the tested material and the controls were evaluated using an inverted microscope with a calibrated barrier. Agar diffusion test, as the least sensitive, provides information on the cell membrane preservation [9,10].

Fluorescent imaging. After incubation of cells with tested material, 100 μ L solution of fluorescent stain etidium bromide was added to the medium of each culture and incubated 15 min. Cultures were then washed with PBS and immediately observed under a fluorescence microscope. Cells adhered to the material were detected by the signal of incorporated fluorescent dye. Microphotographs of cells on the material are obtained by overlapping double exposures: the inverted bright field exposure with the material and the fluorescent cell signal. Images were processed in the ImageJ computer program (NIH Image, <http://imagej.nih.gov>).

3. RESULTS AND DISCUSSION

Our study of biocompatibility of the bone substitutes used for bone reconstruction in the orofacial region has shown complete absence of a cytotoxic effect of tested materials on cell cultures.

Detection of cell death is identified by a Trypan blue dye exclusion test, DET [9]. Mosmann's colorimetric MTT test has a wide application in the assessment and measurement of the cytotoxic, antiproliferative effect (especially of potential antitumor agents) [10]. It provides information on the mitochondrial function preservation. The MTT test measured the antiproliferative effect of bone

implantation materials and the rate of cell recovery after incubation. The results of both tests are given in **Table 1**.

Time [h]	DET [%]		MTT [%]	
	1	2	1	2
24+48	90.23	82.46	101.58	81.79
24+72	96.22	91.43	110.21	93.62
24+96	105.34	97.78	125.98	101.34

Table 1. The results of DET and MTT tests of tested materials on MRC-5 cell line. 1 – Bio-Oss, 2 – SmartBone.

The results of agar diffusion test are negative. No red color was observed in experimental cultures.

Microscopic photographs of the MRC-5 cells stained with etidium bromide fluorescent dye reveal good contact between cells and both applied materials Bio-Oss and SmartBone, which also indicate that the materials are not cytotoxic. The fibroblasts growing on the surface of tested bone substitutes are shown on **Figures 1, 2 and 3**.

The testing of bone implants *in vitro* provides important information on the use of these materials *in vivo*. The results of *in vitro* tests are used to evaluate the biosecurity of the material.

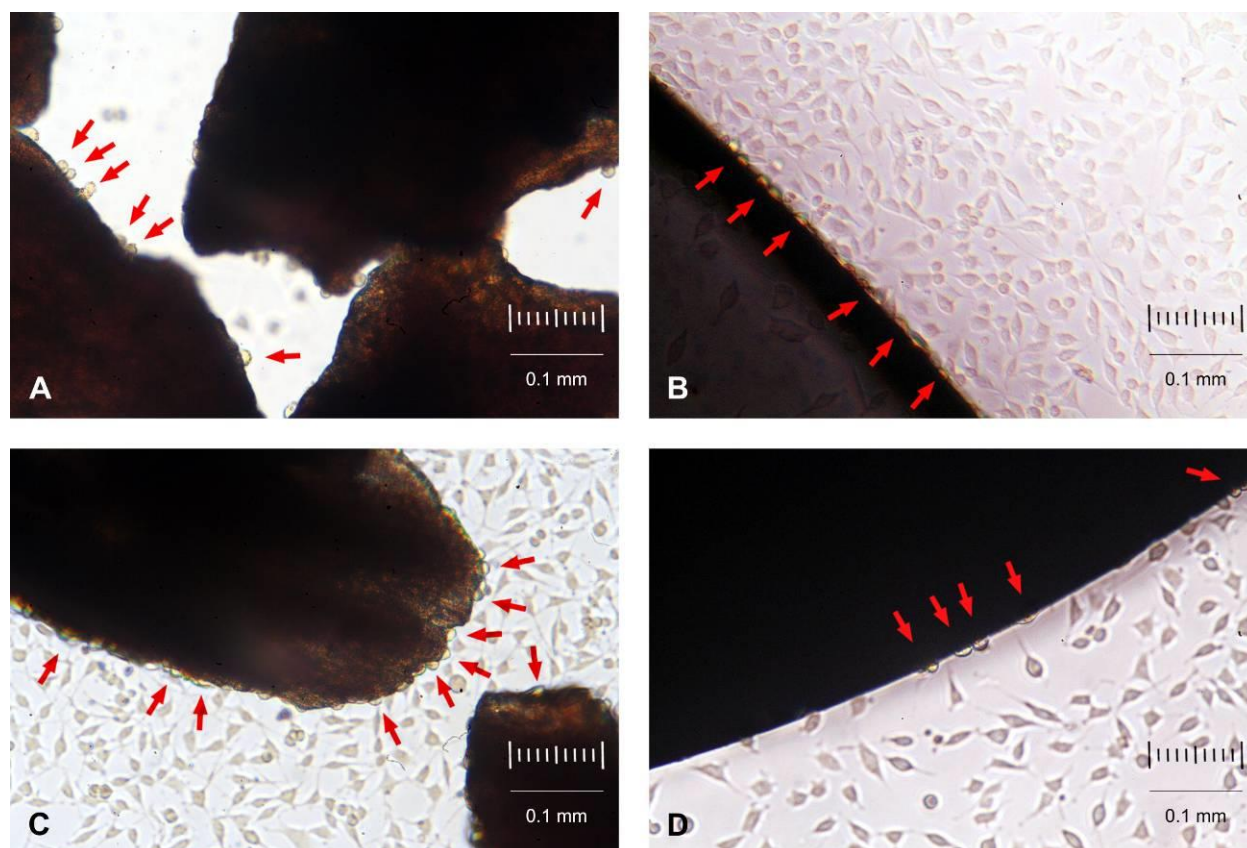


Fig. 1. Microphotographs of native fibroblasts of the MRC-5 cell line in direct contact with tested material (20 \times 10 magnification). Both materials were tested in form of particles and as solid tablets. Arrows indicate the cells attached to the tested material. A and B – Bio-Oss. C and D – SmartBone.

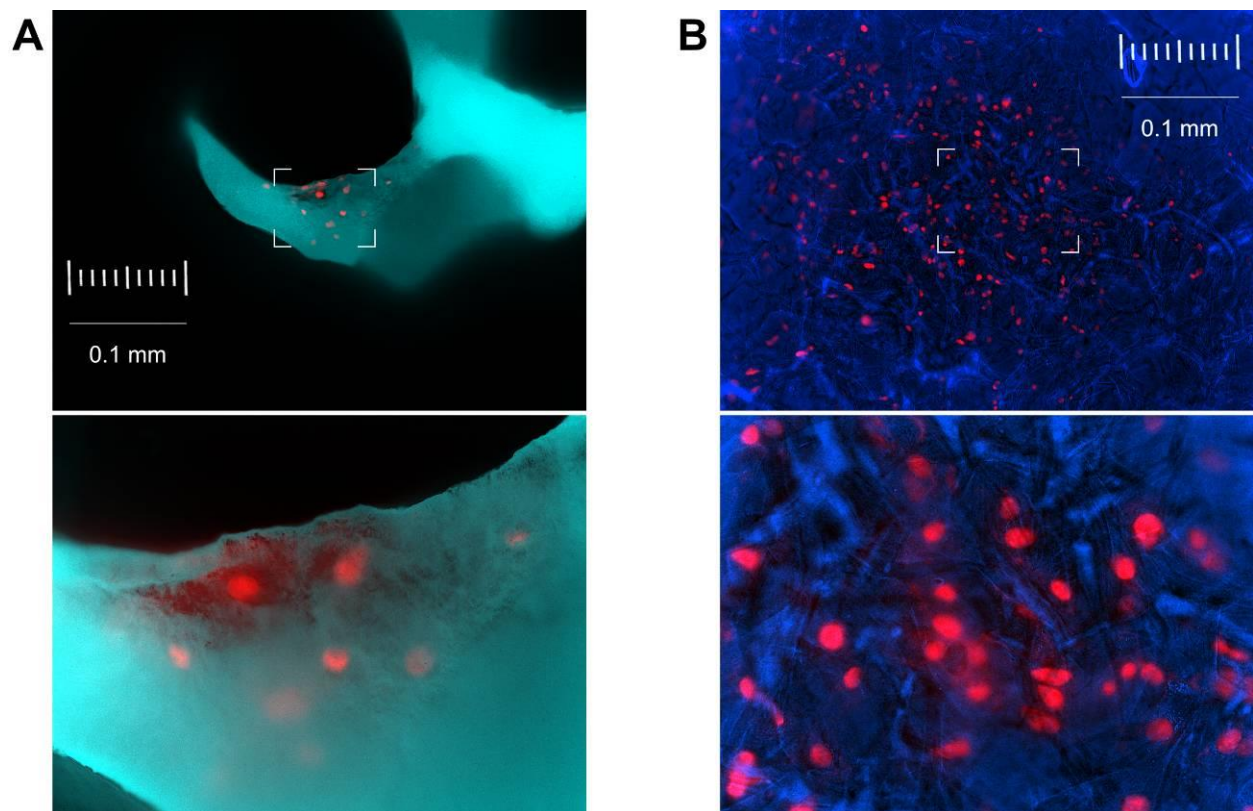


Fig. 2. Fluorescence microscopy of MRC-5 cells of human fibroblasts stained with etidium bromide (red color), bound to the Bio-Oss material. A – Material in form of particles. B – Material in form solid tablet. Magnification is 10×10 for upper and 40×10 for lower images.

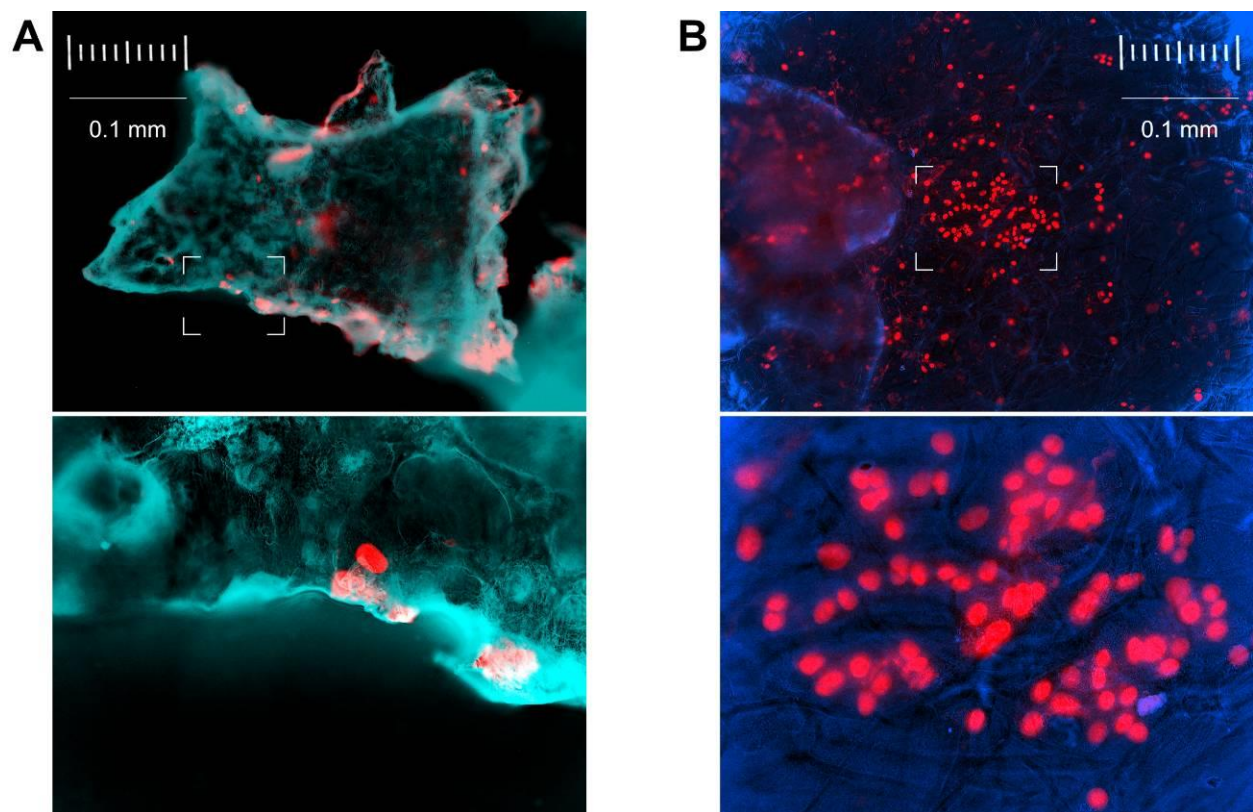


Fig. 3. Fluorescence microscopy of MRC-5 cells of human fibroblasts stained with etidium bromide (red color), bound to the SmartBone material. A – Material in form of particles. B – Material in form solid tablet. Magnification is 10×10 for upper and 40×10 for lower images.

With these tests we have the ability to control and observe the cell-material system in controlled environment and this gives us insight into how the tested materials influences the biological system.

The cytotoxic effects of Bio-Oss and SmartBone materials were tested on the continuous cell line of human fibroblasts (MRC-5) as prescribed by the ISO standard [11].

For evaluation of cytotoxic effect, it is necessary to use several different *in vitro* methods, which examine the integrity of different parts of the cells, i.e. different cell functions. Usage of only one method does not provide sufficient information on the tested dental material for a valid conclusion [12]. For this reason, the cytotoxic effects of the two tested materials were examined using three tests. The DET test and the agar diffusion test gave us data that support the preservation of the cell membrane and in this way the preserved viability of the cells, while the MTT test showed that the mitochondrial function in the examined cell line remained preserved, which, at the same time, gives us information on the preserved metabolic activity of cells.

In contemporary research, possible harmful effects of dental alloys and materials are determined by a large number of *in vitro* and *in vivo* tests. *In vivo* tests are performed on animals, which are certainly more difficult and less humane. Clinical trials have the advantage of valuable data, but they can last long and ethical problems can always take place.

The advantage of the tests with cell cultures is that each agent can be tested on the basis of its effect on cell growth and division [13]. However, after obtaining good results for the cytotoxicity of the material *in vitro*, the research must continue with animal studies, and the final response to biocompatibility should be obtained after clinical testing and long-term administration.

4. CONCLUSION

The results of the biocompatibility testing showed the absence of cytotoxic effects of the tested materials on fibroblast cell culture. The adhesion of human fibroblast cells to implant materials was confirmed by fluorescent staining.

5. REFERENCES

- [1] Williams, D.F.: *Definitions in biomaterials*, Elsevier, Oxford, UK, 1987.
- [2] Watacha, J.C.: *Principles of biocompatibility for dental practitioners*, J Prosthet Dental, 86, 203-209, 2001.
- [3] Bhola, R., Bhola, M. S., Liang, H., Mishram, B.: *Biocompatible Denture Polymers*, Trends Biomater Artif Organs, 23, 129-136, 2010.
- [4] Ivković, N., Božović, Đ., Ristić, S., Mirjanić, V., Janković, O.: *The Residual Monomer in Dental Acrylic Resin and its Adverse Effects*, Contemporary materials, 4, 84-91, 2013
- [5] Bettencourt, A.F., Neves, C.B., De Almeida, M.S., Pinheiro, L.M., Oliveira, S.A., Lopes, L.P., Castro, M.F.: *Biodegradation of acrylic based resins: A review*, Dental Materials., 26, 171-180, 2010
- [6] Watacha, C.J.: *Predicting clinical biological responses to dental materials*, Dental Materials, 28, 23-40, 2012.
- [7] Phillips, H.J.: *Tissue culture*, Elsevier 1973, p. 406
- [8] Mosmann, T.: *Rapid Colorimetric Assay for Cellular Growth and Survival: Application to Proliferation and Cytotoxicity Assays*, Journal of Immunological Methods, 65 55-65, 1983.
- [9] International Standard ISO 10993-5 . *Biological Evaluation of Medical Devices – Part 5: Tests for in vitro Cytotoxicity*, Geneva: International Organisation for Standardisation, 1999.
- [10] International Standard ISO 7405 . *Preclinical Evaluation of Biocompatibility of Medical Devices Used in Dentistry – Test Methods for Dental Materials*, Geneva: International Organisation for Standardisation, 1997.
- [11] International standard 405 dentistry- *preclinical evaluation of biocompatibility of medical devices used in dentistry test methods for dental materials*.
- [12] Al, R.H., Dahl, J.E., Morisbak, E., Polyzois, G.L.: *Irritation and cytotoxic potential of denture adhesives*, Gerodontology, 22 177-183, 2005.
- [13] Wallin, R.F., Arscott, E.F.: *A Practical Guide to ISO 10993-5: Cytotoxicity*, An MD&DI 1998.

Authors: Assoc. Prof. Tatjana Puškar, Assist. Prof. Daniela Djurović Koprivica, University of Novi Sad, Faculty of Medicine, Department of dentistry, Hajduk Veljkova 3, 21000 Novi Sad, Serbia, **Assoc. Prof. Igor Budak**, Assistant **Milana Ilić Mićunović** University of Novi Sad, Faculty of Technical Sciences, Trg Dositeja Obradovića 4, 21000 Novi Sad, Serbia; **PhD Research Associate Dimitar Jakimov**, **PhD Research Associate Vesna Kojić**, University of Novi Sad, Faculty of Medicine, Oncology Institute of Vojvodina, Put Doktora Goldmana 4, 21204 Sremska Kamenica, Serbia, Phone.: +381 21 526 120, mob: +381 60 585 7170. E-mail: tpuskar@uns.ac.rs, budaki@uns.ac.rs; jakimov.dimitar@onk.ns.ac.rs; daniela.djurovic-koprivica@mf.uns.ac.rs kojic.vesna@onk.ns.ac.rs; milanai@uns.ac.rs

ACKNOWLEDGMENTS: The study was financially supported by the Provincial Secretariat for Science and Technological Development of the Autonomous Province of Vojvodina (Grant No. 142-451-3619/2017-01/02).

Sekulic, J., Grujic, J., Maric, D., Zeljković, M., Tabakovic, S., Balos, S.

TESTING BIOCOMPATIBILITY OF MATERIAL FOR IMPLANTS

Abstract: After the implant insertion many complications may occur, caused by using inappropriate material or technological process for production. With the aim to provide biocompatibility of material, before production must be defined protocol for material testing. Testing protocol should contain testing the chemical composition on a quantimeter, structure testing, shape and grain size on electronic microscope, as well as stress state. After that, verification of biocompatibility and technological process for manufacturing should be conducted producing appropriate specimen, and inserting them in experimental animals.

This paper presents results of biocompatibility testing of material for production of a modular hip endoprosthesis in "Grujić i Grujić" company from Novi Sad. Chemical composition is comparable and identical with chemical composition, for this kind of material, which is provided producer of semi-finished products as well with ISO standard. Experimental animals behaviors, after implant insertion, specimen, as well as histological-pathological analysis of bone and surrounded soft tissue, and implant after extraction indicates reliable biocompatibility according to the standards set forth for it.

Using an appropriate method for testing a material biocompatibility reduces risk of occurs unwanted complications during the insertion.

Key words: biocompatibility, hip endoprosthesis, implant materials

1. INTRODUCTION

Production of implants of biocompatible materials, represents market with significant potential for metal industry. Value on global market of orthopedically implants is estimated more than 40 billion dollars (2016 market analysis), with potential to be doubled in upcoming decade [2]. For that reason significant researches are conducted with aim to upgrade development and producing process of implants and material. This particularly refers to implants of which is expected a long period of exploitation (joint endoprostheses, internal fixators, etc.) [6].

Implant development and production is complex engineering process which includes:

- Choosing appropriate material,
- Defining the conception of implant from aspect of functionality,
- Construction in accordance with engineering and medical criteria,
- Defining the optimal technological process of production,
- Immediate production,
- Cleaning and disinfecting implants,
- Packaging according to standards,
- Transport to customer.

In doing so, it must be ensured that the implant as a product that is installed and exploited in the body of living beings meets the appropriate requirements:

- That is not harmful to the body,
- That is indifferent to liquids in the environment where it is exploited,

- It is resistant to the electromagnetic field (that it can be exposed to computerized tomography, CT, MRI and radiotherapy devices without harmful consequences for the patient and the implant)
- Not to change the physico-chemical characteristics during exploitation unless it is one of the design goals (there are bioresorptive materials)
- To ensure the normal functioning of the organism part in which one or more elements are replaced

The problems of testing materials biocompatibility which are used in certain areas of orthopedic surgery are the basis for selecting the appropriate material for the specific purpose. Biocompatible materials used in the implants production are purchased as semi-finished products and correspond to chemical composition according to the standards for the production of implants. In the production process implants are exposed to various technological processes (casting, forging, cutting), which may cause structural and composition changes in material. In addition, there is a risk of contamination during the technological process, using inappropriate equipment and tools or the hygienic conditions of the workspace and workers. This may cause implant with different biomedical characteristics than desired, as well as risk of complications after implanting in form of metallosis (Figure 1), of mechanical damage (Figure 2). For that reason during the implant development material characteristic testing is necessary.



Figure 1 Complication after implant insertion - metallosis



Figure 2 Complication after implant insertion - mechanical damage

In this paper has been presented part of researches, conducted with aim to determinate optimal technological production process of modular hip endoprosthesis with aim to provide biocompatibility of implants. Specific part of research refers to the establishment a protocol for the analysis of implants biocompatibility.

2. MATERIALS AND METHODS

2.1 Material biocompatibility

Application an appropriate materials is of key importance for the expected exploitation characteristic [1]. In biomedical engineering, especially in the production of implants, the material must, in addition to its basic mechanical properties, also satisfy a set of requirements that ensure that the implanted implant does not cause any unwanted local or global effects in the organism, which makes it a group of biocompatible. Biocompatibility testing of the materials for implants is regulated by set of standards that regulate areas of biological evaluation of medical devices (ISO 10993), risk analysis (ISO 14971), and similar.

In the area of implant research, the implication is the implementation of samples in experimental animals and

the assessment of potential changes in the three time frames (near, delayed, and permanent). Thereby are evaluated changes in the tissue and bones, as well as the blood of experimental animals [5].

2.2 Experimental research

Taking into account that the research was carried out in order to improve the endoprosthesis of the locomotor system, the research included the tests of biocompatibility "In Vivo" by producing appropriate specimens, implants and incorporation into experimental animals. Implants were made in form of specimen suitable for implantation in the bone [4]. Figure 3 shows the sketch of testing specimen.

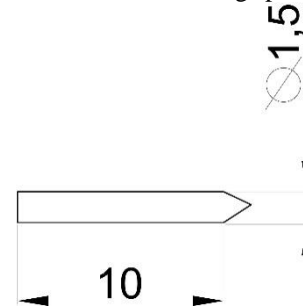


Figure 3. Implant sketch, testing specimen for adjusted for implantation into the thigh bone of the rabbit

Experimental research included the biocompatibility analysis of three, most commonly used, materials for making implants in orthopedic surgery. Those are:

1. Superalloys steel 316 LVM (Figure 4a)
2. Superalloys Cobalt CoCrMo (Figure 4b)
3. Superalloys titanium Ti6AL4V "eli" (Figure 4c)

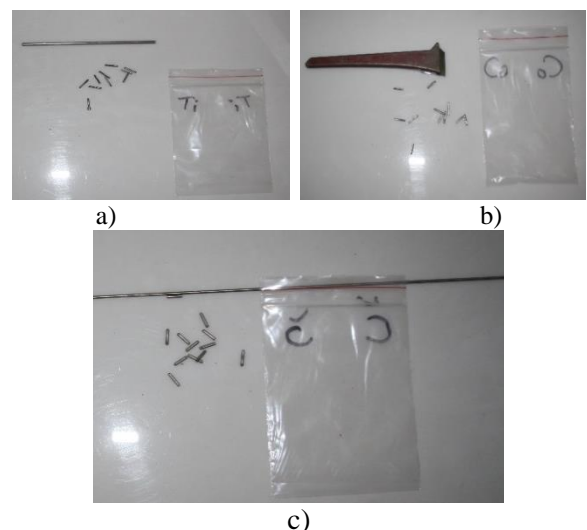


Figure 4 Implants and test specimens prepared for implantation into experimental animals: a) Superalloys steel 316 LVM, b) Superalloys of CoCrMo, c) Superalloys titanium Ti6Al4V "eli"

Testing specimens are after production but before implantation washed, packed and sterilized in clinical condition Figure 5.



Figure 5. Sterilized implants, tubes and tools designed for incorporation into the butt bone of the rabbit

Testing was carried out on a group of ten rabbits from one litter (Figure 6), where three groups of three rabbits and one control without implants were used to test the characteristics of each type of material.



a)



b)

Figure 6 a) Stationary where cages are located with rabbits, b) cages for transport

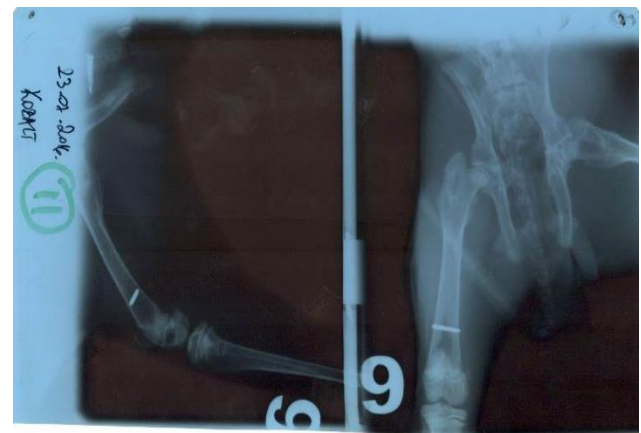
After insertion of the implants (Figure 7a), the control Rtg images were shown in figure. 7b

Testing was carried out in two phases: by sacrificing the first group of three rabbits after 30 days of implantation and by sacrificing the remaining rabbits after 70 days, as well as analyzing implants and

surrounding soft tissue for irritation.



a)



b)

Fig. 6 a) Implantation, b) Control Rtg imaging after implantation

3. RESULTS

During the postoperative period, groups of samples, i.e. their behavior, the increase in the body weight of rabbit, were monitored.

Table 1 shows the key data on experimental animals: physical characteristics (color, mass when is implanted), implant material and mass at the moment of implant extraction.

After 30 days of insertion of the implant by the random sample method, the first group of three rabbits with different materials was selected and extraction of the implants was performed, while this procedure was performed for the remaining rabbit group after 70 days of implementation.

Implant extraction involved the removal of the implant tube with surrounding bone and soft tissue. After the extraction, control samples were taken on all samples (Figure 8a and 8) indicating the successful osteointegration of implants, tubes, and the histological-pathological findings of implants and surrounding bone and soft tissue were also neat.

No. rabbits	Color	Material	Date	Mass	Date of extraction	Mass	Growth	Date of extraction II phase	Mass	Growth
1.	red	Č316LVM	23.07.2016.	1750	08.10.2017			08.10.2017.		
2.				1700		2585	885			
3.				1700					3400	1700
4.	green	CoCrMo		1620		2350	730			
5.				1630					3360	1730
6.				1750	died 10.08.2016.					
7.	blue	Ti6Al4V		1400		2020	620			
8.				1720						
9.				2000					4000	2000
10.					1780		3050		1700	

Tabele 1 Plan and results of measurement experimental rabbit

4. DISCUSSION

Experimental animals, rabbits, used to test the biocompatibility of the material, behaved normally in the postoperative period, without complications, caused by surgery or any other cause. Veterinary control was carried out weekly, and during the entire observation period the results were regular.

Control Rtg images indicate a satisficing condition of implants as well as surrounding bone and soft tissue with present osteointegration without infection.

Observing the increasing the body weight of the control rabbit no.10, and the rabbit with implanted implant No.2, No.4, No.7, it appears that after 30 days, occurred a slower progression of the rabbit with the implant. In the second group of rabbits No.3, No.5, No.9, and control rabbit no. 10, there is no significant difference in weight gain after 70 days. This suggests that trauma after implantation of implants, early postoperative recovery, influenced the slow growth of the rabbit, but after successful osteointegration of the implant and bone in the later period, the increase in body weight of the control and rabbit with the implant implanted is identical as can be seen from Table 1

5. FINAL REMARKS

Laboratory tests performed with the aim of testing the biocompatibility of hip joint endoprosthesis materials showed that during the investigated period, which was determined according to ISO 10993, there was no appearance of collision on implants made of 316LVM alloys, CoCrMo cobalt and titanium Ti6Al4V "eli". There is also no metallosis or ions of metal in the surrounding bone and soft tissue. There was no infection.

On the basis of the obtained results, it can be concluded that the biocompatibility and implantability of the material, the technological process of production and implantation of the implants included in the research, are satisfactory.

6. REFERENCES

- [1] Boddy, R.: *Biomaterials science*, Academic press, 1996
- [2] Chandra G., Srivastava, D.: *Orthopedic Implants Market by Product - Global Opportunity Analysis and Industry Forecast, 2017-2023*, Allied Market Research, 2017

- [3] Grujić, J., Sovilj, B., Krklec, V., Vukelić, B.: *Analiza triboloških procesa veštačkog zgloba kuka*, Savetovanje tribologije, Kragujevac, 1992.
- [4] Grujić, J.: *Tumorska modularna endoproteza zgloba kuka, doktorska disertacija*, Fakultet tehničkih nauka, Novi Sad, 2018.
- [5] Marković D, Radovanović A, Kovačević-Filipović M, Francuski J, Todorović V. *Histološke karakteristike mekih tkiva posle implantacije biokeramičkih materijala i procena biokompatibilnosti*. Veterinarski glasnik 2012;66(3-4):285-297.
- [6] Raković, D., Uskoković, D.: *Biomaterijali*, Institut tehničkih nauka, Srpska akademija nauka, Beograd, 2010

Authors: Jovan Sekulic¹, Jovan Grujić², Dušan Marić³, Milan Zeljković⁴, Slobodan Tabaković⁴, Sebastian Baloš⁴

¹ Health center Zrenjanin, Serbia

² DOO "Grujić i Grujić" Novi Sad, Serbia

³ University of Novi Sad, Faculty of medicine, Hajduk Veljkova 3, 21000 Novi Sad, Serbia, Phone: +381 21 420 102, Fax: +381 21 662 4153

⁴ University of Novi Sad, Faculty of Technical Sciences, Department of Production Engineering, Trg Dositeja Obradovica 6, 21000 Novi Sad, Serbia, Phone.: +381 21 450-366, Fax: +381 21 454-495.

E-mail: grujicgrujicns@gmail.com; ducamaric@gmail.com; milanz@uns.ac.rs; tabak@uns.ac.rs; sebab@uns.ac.rs;

ACKNOWLEDGMENTS: The work is part of research project on "Modern approaches in the development of special bearings in mechanical engineering and medical prosthetics," TR 35025, supported by the Ministry of Education, Science and Technological Development, Republic of Serbia.

Trajanovic, M., Tufegdzcic, M.

TRENDS IN PRODUCING PERSONALIZED BONE IMPLANTS USING ADDITIVE MANUFACTURING

Abstract: Additive Manufacturing (AM), formerly known as Rapid Prototyping (RP), enables quick production of personalized bone implants using different techniques and materials. Therefore, there is a need to examine the possibilities for AM application in the field of orthopedics and prosthetics and to provide an overview of current state. Progress done in the area of biomaterials is presented from the perspective of different AM technologies used. Patient specific implants and prostheses in different branches of surgery and implantology, as well as some examples in tissue engineering are shown. The results are presented in the form of systematic review, bearing in mind challenges and future trends related to bone healing and regeneration.

Key words: bone implants, biocompatible materials, AM

1. INTRODUCTION

AM application in medical context is well documented and described. It is the subject of a large number of research, especially in orthopedics and prosthetics [1,2,3,4]. Research status of AM application and literature review are presented in [5].

Personalized implants production from titan and shape memory alloys, as well as from biodegradable metals and some other porous metals using AM technologies are examined [6,7]. Technology optimization approach was used for implant design [8]. Challenges and issues in producing implants for bone reconstruction as a subset of personalized medical products are presented [9]. Use of AM for production of patient-specific implants is described [10]. The possibilities of 3D printing technique in patient specific orthopedic are shown [11].

This paper presents systematic review of current issues and trends in producing personalized bone implants from two different aspects such as biomaterial types (their mechanical properties and biocompatibility), and AM technologies used in accordance to selected material. Concepts for selection of appropriate materials and design are considered in order to satisfy implant requirements and allow refinement of different methods used for obtaining patient specific models. Biomaterial characteristics and the process of obtaining the physical model of personalized implants are presented together with AM technologies in conjunction with commonly used biomaterials.

2. PERSONALIZED IMPLANT DEVELOPMENT

With the development of Computer Aided Design (CAD), Computer Aided Engineering (CAE), Computer Aided Design/Computer Aided Manufacturing (CAD/CAM), new trends in medical technology are emerging and lead to a personalized approach which allows the construction and production of personalized implants at an affordable price, within a reasonable time span [6]. Such systems are based on advanced visualization tools and 3D modeling, but obtaining an accurate implant model is a complex

process, conditioned by the patient's disease and degree of bone damage [12].

Personalized implants are constructed, designed, and produced to fit the anatomy of a given patient perfectly and with high accuracy. They are considered as the best solution for bone reconstruction, especially in cases of major damage and trauma, as well as large bone cancers, serious deformities, genetics, complex implants revisions, arthrosis, infectious disease, some metabolic conditions and clinical problems when the geometry and bone size do not allow embedding a standard implant [9,11,13,14,15].

The main advantages of using personalized implants are in reducing the time of surgery, and in decreasing the amount of the resected tissue [6,11,15]. In addition, the patient's quality of life is improved, the operational flow is facilitated and the success rate of interventions increases. The design and development of personalized medical products is based on data of a particular patient in the form of 3D models of anatomical structures in order to meet clinical and technical constraints, using medical imaging, simulation and 3D modeling [9].

In any case, there are always problems in creating an implant of the appropriate shape from the selected material. For an example, in orthopedics, the geometry of the personalized implant was manually drawn, and such implants may have errors in geometry [16]. To avoid such errors and make improvements in the field of prosthetics and implantation, AM is introduced as a new approach. It is possible to design and manufacture patient specific implants with high accuracy from medical image data using AM technology in a very short time [1,15]. In order to achieve this goal, it is necessary to implement the following steps: data acquisition and processing, formatting the data for AM, model creation and evaluation, production and validation [1,3].

The most common modes for data acquisition are CT - Computed Tomography and MRI - Magnetic Resonance Imaging. Also, some other imaging modalities, such as PET - Positron Emission Tomography, SPECT - Single Photon Emission Computed Tomography and US - Ultrasonography can be used [2,15,17,18]. Images are written in a common

medical file format - DICOM (Digital Imaging and Communications in Medicine) and 3D segmentation and visualization are performed [15]. During these processes a virtual 3D model is created as an approximate representation of the real model in STL (Stereolithography) format¹, which is generally accepted as AM file format [19]. Virtual model is imported into AM commercial software, specific for each AM system, and physical model is obtained using some of the AM technologies [20, 21].

The procedures for obtaining and personalized implant development are illustrated at the Figure 1.

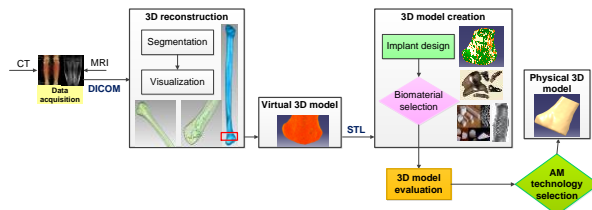


Figure 1. Workflow in the process of personalized implant production

3. AM TECHNOLOGIES

AM technologies, in general, include techniques based on deposition processes or layer-by-layer manufacturing processes without using tools (so called additive manufacturing) [2]. The main difference between these techniques arises from the material which is used [21, 22]. So far the following procedures have been identified: stereolithography (STL), where photosensitive resins are used (e.g. photosensitive polymers), selective laser sintering (SLS), where plastic, metal or ceramic powders are used (e.g. nylon or ceramic powder), laminated object manufacturing (LOM), where paper or plastic films are used, fused deposition modeling (FDM) where thermoplastics or eutectic metals are used, electron beam melting (EBM), where metal powders are used and 3D printing (3DP) where fine powders are used [2, 15, 19, 21, 22].

Using AM enables designing, visualization and evaluation of 3D complex models, but also facilitates fast fabrication and direct manufacturing of biocompatible and bioactive implants [6]. The choice of the appropriate material depends on implant's shape, purpose, type and properties. Depending on the type of material, a proper manufacturing process should be also selected.

SLS is usually used for obtaining metal or ceramic implants. STL is used for producing 3D structures of photocurable resin [3]. Some advantages of FDM are reflected in the application of a large number of different materials, but producing permanent implants is restricted to anatomical models made out of white acrylonitrile-butadiene-styrene. These models are used as templates for personalized implants [1,3,14]. FDM also could be used for creating polymer-ceramic composites [3]. Titanium root-form implants (Ti-6Al-

4VELI), femur hip implants, dental implants and knee replacement implants are some examples of implants obtained by EBM process [14].

Cell and scaffold printing and patterning is possible using ordinary ink-jet and laser printing technology [3,14]. Because of the fact that the scaffolds will be implanted in the human body materials used for producing, scaffolds must be biocompatible² and must have adequate macro- and micro-structural properties (e.g. pore size and shape, mechanical strength) [14,17].

3.1 Materials and utilization

The development of biomaterials is the reason why utilization of AM for bone implants is growing exponentially. Biomaterials are divided based on different criteria, aligned in three generations. Examples of the first generation are: metals (stainless steel and cobalt-chrome-based alloys, Ti and Ti alloys), ceramics (Alumina Al_2O_3 and Zirconia ZrO_2) and polymers (silicone rubber, acrylic resins). The representatives of the second generation are bioactive metals (metal surface is coated with bioactive ceramics or chemically modified), ceramics (bioactive glass, glass-ceramics and calcium phosphates (CaPs)) and natural or synthetic biodegradable polymers (polyglycolide (PGA), polylactide (PLA)). In the third generation bioactivity and biodegradability are combined [23]. According to [24], metals, polymers, ceramics and composites are the main categories of biomaterials. This categorization is expanded with biodegradable polymeric biomaterials [25]. Bhat and Kumar [26] divide biomaterials in three major classes: polymers, metals and ceramics. Based on the physicochemical nature biomaterials could be classified as metallic, ceramic, polymeric, composite and biodegradable polymers [27]. Single crystals, polycrystals, glass, glass-ceramics, polymers and composites are considered as different groups of biomaterials [28]. Classification based on the interaction between a biomaterial and surrounding tissue reports three kinds of biomaterials: biotolerant, bioactive and bioinert materials [29].

A variety of different materials (liquid based, solid based and powder based) are used in medical AM: a) ceramics (aluminium, zirconia, calcium phosphate based bioceramics and porous ceramics); b) polymers, such as biodegradable (e.g. polyvinyl chloride (PVC), polyethylene (PE), polypropylene (PP), polymethyl methacrylate (PMMA), polystyrene (PS), polytetrafluoroethylene (PTFE), polyesters, polyamides (PA-nylon), polyurethanes (PUR), and polysiloxanes (silicone)), hydrogels and shape memory polymers; c) polymer-based composite materials (polypropylene-tetracalcium phosphate (PP-TCP)); d) metals and alloys (stainless steel, titanium alloys, cobalt-chromium alloys, shape memory alloys, such as nitinol - consist of about 50% nickel and 50% titanium, copper based shape memory alloys); e) bone cement and many others [2,14,20].

Ceramics (e.g. alumina, zirconia) are often used for

¹ There is a possibility to use another data formats such as Initial Graphic Exchange Specification (IGES), Standard for the Exchange of product Model Data (STEP), Virtual Reality Modeling Language (VRML), etc., depending on the AM system [15,17].

² Biodegradability and bioactivity are required in some cases.

joint implants which are exposed to loads, but also for mold making in metal alloy implants production. Problems may occur with bone ingrowth and implant anchoring, due to the fact that alumina ceramics are not bioactive. In such cases bioactive coating made from hydroxyapatite is used. Ceramic scaffolds are directly fabricated and applied in bone tissue engineering, hydrogels are usually used as scaffolds for cell culture, porous composites are used for bone tissue regeneration, nano-hydroxyapatite is used in prosthetic applications for bone and teeth enamel [3]. Due to its mechanical properties, polymethyl methacrylate is the most frequently applied non-metallic implant material in orthopedics [6, 21]. Bioceramics, hydroxyapatite and titanium are often used for bone reconstruction. In the cases when it is necessary to treat bone fracture, temporary implants from stainless steels and titanium alloys are commonly used [6].

In the cases where the great value of specific strength, as well as corrosion and fatigue resistance are of primary importance, titan and its alloys are used (e.g. Ti-6Al-4V). Stainless steel, cobalt-chromium alloys (Co-26Cr-6Mo), aluminum and aluminum alloy foams have a certain share in metal implants production [30].

Synthetic bone graft substitutes from biocompatible materials such as zirconia/hydroxyapatite compositions are capable of replacing human bones, but some problems related to osteoconduction, osteoinduction and osteogenesis which are necessary for bone healing and regeneration may occur [13].

Mechanical or biological fixation of the personalized implants to the host bone, is an important issue to deal with. It is closely related to the disparity between the values of the elastic modulus (Young's modulus) of the bone and implant material [31].

Due to the ability to quickly manufacture complex 3D models and structures from various raw materials with great precision (from few micrometers to hundreds of nanometers), AM has a great impact on the biomedical engineering and industry [14,15,17,18]. There are numerous examples of using AM for production of patient specific medical prostheses and implants in craniofacial, oral and maxillofacial surgery, dental implantology, neurosurgery (including spine surgery), oncology, orthopedic and trauma surgery (e.g. pelvic surgery), as well as cardiovascular and visceral surgery [3,14,15,32].

AM technology is used for fabrication of skull and mandible implants, designed using CAD software [12]. Facial prosthetics, cranioplasty plates, osteointegrated titanium implants - titanium screws for cranioplasty, dental implants, 3D-printed titanium mandibular prosthesis, individual auricular prostheses, vascular prostheses, joint implants (e.g. hip and knee implant), orthopedic jigs for arthroplasty of the knee are the examples of patient specific implants, fabricated by AM technologies [1,2,14,15,19, 32].

In some case studies the stainless steel implant of the hip joint made in carbon-dioxide casting process with pattern from acrylonitrile butadiene styrene plastic [33], 3D-printed trabecular titanium personalized implant for the purpose of revision hip arthroplasty with serious acetabular bone loss [11], and the

personalized 3D-printed implant in the case of bone defect after pelvic tumor resection are presented [34].

4. CONCLUSION

AM covers a broad variety of areas in biomedical engineering and the number of applications is increasing, driven by material development. It has a great potential for patient specific implant manufacturing. The accuracy of obtained products depends to a large extent on the accuracy of input data and quality of volumetric image, obtained by some of the common modes for data acquisition. The second influencing factor is AM technology involved. The standard procedures involve integration of Computer Aided Design (CAD) and 3D medical imaging. But, there are still some challenges to set up an environment for producing personalized bone implants with high accuracy from the materials which can overcome the problems related to bone healing and regeneration.

5. REFERENCES

- [1] Bibb, R., Dominic, E., Abby P: *Medical Modelling*, 2nd ed. Elsevier Science, 2014.
- [2] Brennan, J.: *Production of Anatomical Models from CT Scan Data*, Master dissertation, De Montfort University, Leicester, United Kingdom, 2010.
- [3] Hoque, M.: *Advanced applications of rapid prototyping technology in modern engineering*, InTech, Rijeka, Croatia, 2011.
- [4] Vehviläinen, J.: *Process and Web Application Development of Medical Applications of Additive Manufacturing*, Master thesis, School of Science, Aalto University, 2011.
- [5] Javaid, M., Haleem, A.: *Additive manufacturing applications in medical cases: A literature based review*, Alexandria Journal of Medicine, <https://doi.org/10.1016/j.ajme.2017.09.003> (article in press), 2017.
- [6] Parthasarathy, J.: *3D modeling, custom implants and its future perspectives in craniofacial surgery*, Annals of Maxillofacial Surgery, 4(1), pp.9-18, 2014.
- [7] Pfeiffer, R., Müller, C., Christof Hurschler, C., Kaierle, S., Wesling, V., Haferkamp, H.: *Adaptable Orthopedic Shape Memory Implants*, Procedia CIRP 5, pp. 253 – 258, 2013.
- [8] Wang, X., Xu, S., Zhou, S., Xu, W., Leary, M., Choong, P., Qian, M., Brandt, M., Xie Y.: *Topological design and additive manufacturing of porous metals for bone scaffolds and orthopedic implants: A review*, Biomaterials, 83, pp. 127-141, 2016.
- [9] Le, C., Okereke, M., Dao, V., Shwe, S., Zlatov, N., Le, T.: *Personalised medical product development: methods, challenges and opportunities*, Romanian Review Precision Mechanics, Optics & Mechatronics, 40, pp.11-20, 2011.
- [10] Cronskar M.: *The use of additive manufacturing in the custom design of orthopedic implants*, Thesis, Östersund: Mid Sweden University, 2011.

- [11] Wong, K.: *3D-printed patient-specific applications in orthopedics*, Orthopedic Research and Reviews, 2016:8, pp.57-66, 2016.
- [12] Guoqing, Z., Yongqiang, Y., Hui, L., Changhui, S., Ran, X., Jiakuo, Y.: *Modeling and Manufacturing Technology for Personalized Biological Fixed Implants*, Journal of Medical and Biological Engineering, 37(2), pp.191-200, 2017.
- [13] Ahlhelm, M., Schwarzer, E., Scheithauer, U., Moritz, T., Michaelis, A.: *Novel Ceramic Composites for Personalized 3D Structures*, Journal of Ceramic Science and Technology, 8(1), pp.91-100, 2017.
- [14] Bartolo, P., Kruth, J., Silva, J., Levy, G., Malshe, A., Rajurkar, K., Mitsuishi, M., Ciurana, J., Leu, M.: *Biomedical production of implants by additive electro-chemical and physical processes*, CIRP Annals, 61(2), pp. 635-655, 2012.
- [15] Rengier, F., Tengg-Kobligh, H., Zechmann, C., Kauczor, H., Giesel, N.: *Beyond the Eye – Medical Applications of 3D Rapid Prototyping Objects*, European medical imaging review, pp.76-80, 2008.
- [16] Mukund, J.A.: *Process planning for the rapid machining of custom bone implants*, Master thesis, Ames: Iowa State University, 2011.
- [17] Geng, L., Wong, Y., Huttmacher, D., Fenga, W., Loha, H., Fuha, J.: *Rapid Prototyping of 3D Scaffolds for Tissue Engineering Using a Four-Axis Multiple-Dispenser Robotic System*, The Fourteenth Solid Freeform Fabrication (SFF) Symposium, Austin, The University of Texas, pp.423-432, 2003.
- [18] Lantada, A., Morgado, P.: *Rapid Prototyping for Biomedical Engineering: Current Capabilities and Challenges*, Annual Review of Biomedical Engineering, 14(1), pp.73-96, 2012.
- [19] Mallepree, T.: *An advanced prototyping process for highly accurate models in biomedical applications*, PhD Thesis, Universität Duisburg-Essen, 2011.
- [20] Milovanović, J., Trajanović, M.: *Medical applications of rapid prototyping*, Facta Universitatis, Series: Mechanical Engineering, 5(1), pp.79 - 85, 2007.
- [21] Berce, P., Chezan, H., Balci, N.: *The application of Rapid Prototyping Technologies for manufacturing the custom implants*, ESAFORM 2005 Conference, Cluj-Napoca, Romania, 2005.
- [22] Joshi, A.: *Process planning for the rapid machining of custom bone implants*, Master thesis, Iowa State University, 2011.
- [23] Biomaterials generations, available at: http://www.uobabylon.edu.iq/eprints/publication_12_1581_1707.pdf
- [24] *Handbook of materials for medical devices*, Ed. Davis, J.R., ASM International, 2003.
- [25] Parida, P., Behera, A., Mishra, S.: *Classification of Biomaterials used in Medicine*, International Journal of Advances in Applied Sciences, 1(3), pp. 125-129, 2012.
- [26] Bhat, S., Kumar, A.: *Biomaterials in regenerative medicine*, Journal of Postgraduate Medicine, Education and Research, 46(2), pp. 81 - 89, 2012.
- [27] Ferraro, A.: *Biomaterials and therapeutic applications*, IOP Conf. Series: Materials Science and Engineering, Volume 108, Conference 1, 2016.
- [28] Prakasam, M., Locs, J., Kristine Salma-Ancane, K., Loca, D., Largeteau, A., Berzina-Cimdina, L.: *Biodegradable Materials and Metallic Implants - A Review*, Journal of Functional Biomaterials, 8 (44), 2017.
- [29] Bergmann, C. P., Stumpf, A.: *Dental Ceramics, Topics in Mining, Metallurgy and Materials Engineering*, Springer-Verlag Berlin Heidelberg, 2013.
- [30] Murr, L., Gaytan, S., Medina, F., Lopez, H., Martinez, E., Machado, B., Hernandez, D., Martinez, L., Lopez, M., Wicker, R., Bracke, J.: *Next-generation biomedical implants using additive manufacturing of complex, cellular and functional mesh arrays*, Philosophical Transactions of the Royal Society A: Mathematical, Physical and Engineering Sciences, 368(1917), pp.1999-2032, 2010.
- [31] Ryan, G., Pandit, A., Apatsidis, D.: *Fabrication methods of porous metals for use in orthopaedic applications*, Biomaterials, 27(13), pp.2651-2670, 2006.
- [32] Frame, M., Huntley, J.: *Rapid Prototyping in Orthopaedic Surgery: A User's Guide*, The Scientific World Journal, pp.1-7, 2012.
- [33] Kannan, V., Yogasundar, S., Singh, S., Tamilarasu, S., Kumar, B.: *Rapid Prototyping of Human Implants with Case Study*, International Journal of Innovative Research in Science, Engineering and Technology, 3(Special Issue 2), pp.319-324, 2014.
- [34] Wong, K., Kumta, S., Geel, N., Demol, J.: *One-step reconstruction with a 3D-printed, biomechanically evaluated custom implant after complex pelvic tumor resection*, Computer Aided Surgery, 20(1), pp.14-23, 2015.

Authors:

Full Prof. Miroslav Trajanovic¹, PhD Milica Tufegdžić², Lecturer

¹ University of Nis, Faculty of Mechanical Engineering, Department for Production and IT, Aleksandra Medvedeva 14, 1800 Nis, Serbia, Phone: +381 18 500-662, ² College of Applied Mechanical Engineering Trstenik, Department for IT, Radoja Krstića 19, 37240 Trstenik, Serbia, Phone: +381 37 714-121,
E-mail:miroslav.trajanovic@masfak.ni.ac.rs;
miltufegdžić@gmail.com

ACKNOWLEDGMENT

The paper is part of the project III41017 - Virtual human osteoarticular system and its application in preclinical and clinical practice, sponsored by the Ministry of Education, Science and Technology development of the Republic of Serbia for the period 2011- 2018.

Zigic, M., Grahovac, N.

ESTIMATION OF HUMAN BODY PARTS ORIENTATION USING DATA FROM IMU SENSORS

Abstract: Inertial measurement unit (IMU) sensor consisting of three axis gyroscopes and accelerometers is becoming increasingly popular in various domains, including biomedical engineering and robotics. This paper presents an application of an earlier developed numerical algorithm for rigid body attitude estimation to the problems of the human body motion. The algorithm uses a quaternion representation of orientation to describe the coupled nature of orientations in three dimensional space. This avoids singularities associated with an Euler angle representation. In the end, one numerical example is presented to show efficiency of the algorithm.

Key words: attitude estimation, kinematics, Euler angles, inertial measurement unit (IMU)

1. INTRODUCTION

The problem of accurate tracking of the attitude of rigid bodies is very important in different fields including aerospace, marine and automotive engineering, robotics and human movement analysis, see [1,2,3]. Several technologies are available to produce motion tracking systems, which derive orientation estimates from electrical measurements of different types of sensors (inertial, magnetic, optical, mechanical). In recent years, inertial and magnetic sensors are often used in biomedical applications, see [4,5,6]. An IMU (inertial measurement unit) is device consists of gyroscopes and accelerometers enabling the tracking of rotational (angular velocity of a body) and translational (acceleration of its point) motions. The measured attributes of motion are expressed in the body reference frame. Some of the devices enable measuring the Earth's magnetic field as well, see [7]. From these data the body attitude needs to be determined.

The algorithm for rigid body position estimation using the Lagrange-d'Alembert principle from variational mechanics is analyzed in [8]. For the same purpose it is possible to use quaternion representation which is an excellent tool for describing arbitrary rotations in space, without singularities. The name of quaternion denotes a quadrinomial expression, where one term stands for the real part, while the other terms together represents the imaginary part. The algorithms for the body attitude estimation based on quaternion representation are presented in [7,9]. In this paper quaternions are used in rigid body kinematics, i.e. for determination of a rotation matrix. We show how to apply the numerical algorithm for estimation of both a rigid body orientation and the linear acceleration of an arbitrary point of the body, based on the quaternion approach, presented in [9], to the problem of human body motion.

Input data for the numerical algorithm can be obtained from IMU sensor measurement or data obtained on the basis of solution of differential equation of motion, like in [9]. Some experimental data

obtained by use of IMU sensor, for human arm motion, are given in [5].

2. DESCRIPTION OF PROBLEM

Biomechanical model of the human body proposed in [3] is shown in Figure 1. The body consists of 23 segments and IMU sensor is mounted on each of the 17 segments indicate with bold text.

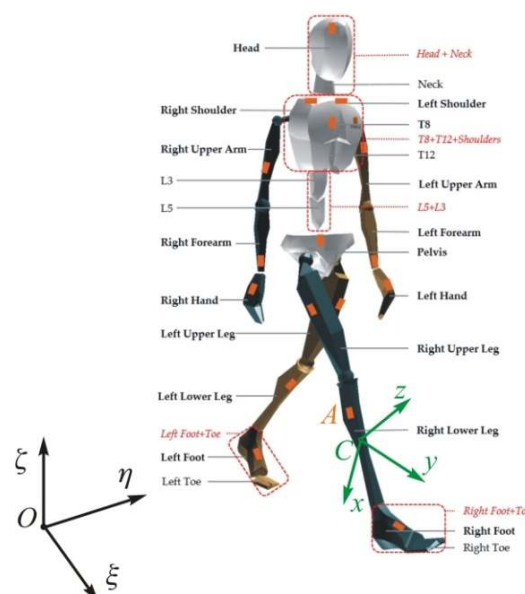


Fig. 1. Biomechanical model of the human body, inertial reference frame $O\xi\eta\zeta$ and moving reference frame $Cxyz$.

In this paper the movement of only one part of the human body will be considered. An IMU sensor is located at an arbitrary point A , see Figure 1. Two coordinate systems are introduced: an inertial reference frame $O\xi\eta\zeta$ and a moving frame $Cxyz$ which is fixed to the part of the human body and moves together with it. The task is to calculate the attitude of the human body part and the acceleration of the center of mass C expressed in the inertial reference frame. Input data are

the projections of the angular velocity $\boldsymbol{\omega}$ onto moving axes x , y and z together with the projections of acceleration of an arbitrary point A onto moving axes. These attributes of motion are measured by IMU sensor. Position vectors of points A and C , in the inertial reference frame, read

$$\begin{aligned} \mathbf{r}_C &= \xi_C \boldsymbol{\lambda} + \eta_C \boldsymbol{\mu} + \zeta_C \boldsymbol{\nu}, \\ \mathbf{r}_A &= \xi_A \boldsymbol{\lambda} + \eta_A \boldsymbol{\mu} + \zeta_A \boldsymbol{\nu}. \end{aligned} \quad (1)$$

On the basis of considerations of a rigid body kinematics following relationship (Rivals theorem) between accelerations of points A and C can be written

$$\mathbf{a}_A = \mathbf{a}_C + \mathbf{a}_A^C = \mathbf{a}_C + \dot{\boldsymbol{\omega}} \times \mathbf{r}_A^C + \boldsymbol{\omega} \times (\boldsymbol{\omega} \times \mathbf{r}_A^C), \quad (2)$$

where \mathbf{r}_A^C stands for the position vector of point A relative to the mass center C , while $\boldsymbol{\omega}$ and $\dot{\boldsymbol{\omega}}$ represent the angular velocity vector and angular acceleration vector. All three vectors are expressed in moving reference frame $Cxyz$.

The acceleration of mass center C expressed in the inertial coordinate system, marked with $\mathbf{a}_C^{(I)}$, can be determined by multiplying the acceleration expressed in the moving frame $\mathbf{a}_C^{(M)}$ (see Equation (8) in paper [9]) with rotation matrix R

$$\mathbf{a}_C^{(I)} = R \cdot \mathbf{a}_C^{(M)}, \quad (3)$$

where the elements of R stand for the cosines of the angles between corresponding moving and non moving axes. Determination of the rotation matrix R between the moving reference frame and inertial reference frame together with one example are presented in the next section.

3. SOLUTION AND RESULTS

In order to determine the acceleration of mass center C in the inertial coordinate system it is necessary to find the orientation of the moving reference frame relative to the inertial one. Using the theory of quaternions represents an efficient way to determine the rotation matrix R

$$R = \begin{bmatrix} c_{11} & c_{12} & c_{13} \\ c_{21} & c_{22} & c_{23} \\ c_{31} & c_{32} & c_{33} \end{bmatrix}, \quad (4)$$

where coefficients c_{ij} , $i, j \in \{1, 2, 3\}$ read

$$\begin{aligned} c_{11} &= \cos \angle(\boldsymbol{\lambda}, \mathbf{i}), \quad c_{12} = \cos \angle(\boldsymbol{\lambda}, \mathbf{j}), \\ c_{13} &= \cos \angle(\boldsymbol{\lambda}, \mathbf{k}), \quad c_{21} = \cos \angle(\boldsymbol{\mu}, \mathbf{i}), \\ c_{22} &= \cos \angle(\boldsymbol{\mu}, \mathbf{j}), \quad c_{23} = \cos \angle(\boldsymbol{\mu}, \mathbf{k}), \\ c_{31} &= \cos \angle(\boldsymbol{\nu}, \mathbf{i}), \quad c_{32} = \cos \angle(\boldsymbol{\nu}, \mathbf{j}), \\ c_{33} &= \cos \angle(\boldsymbol{\nu}, \mathbf{k}). \end{aligned} \quad (5)$$

These coefficients can be calculated using the

quaternion approach in the following way

$$\begin{aligned} c_{11} &= q_0^2 + q_1^2 - q_2^2 - q_3^2, \\ c_{12} &= 2(q_1 q_2 - q_0 q_3), \\ c_{13} &= 2(q_0 q_2 + q_1 q_3), \\ c_{21} &= 2(q_1 q_2 + q_0 q_3), \\ c_{22} &= q_0^2 - q_1^2 + q_2^2 - q_3^2, \\ c_{23} &= 2(q_2 q_3 - q_0 q_1), \\ c_{31} &= 2(-q_0 q_2 + q_1 q_3), \\ c_{32} &= 2(q_2 q_3 + q_0 q_1), \\ c_{33} &= q_0^2 - q_1^2 - q_2^2 + q_3^2, \end{aligned} \quad (6)$$

where q_0, q_1, q_2, q_3 are parameters often called as the Euler parameters, which are used in the theory of quaternions, for more details see [10]. The time derivative of the Euler parameters read

$$\begin{aligned} \dot{q}_0 &= -\frac{1}{2}(q_1 \omega_x + q_2 \omega_y + q_3 \omega_z) + \lambda q_0, \\ \dot{q}_1 &= \frac{1}{2}(q_0 \omega_x + q_2 \omega_z - q_3 \omega_y) + \lambda q_1, \\ \dot{q}_2 &= \frac{1}{2}(q_0 \omega_y + q_3 \omega_x - q_1 \omega_z) + \lambda q_2, \\ \dot{q}_3 &= \frac{1}{2}(q_0 \omega_z + q_1 \omega_y - q_2 \omega_x) + \lambda q_3, \end{aligned} \quad (7)$$

where ω_x, ω_y and ω_z are projections of angular velocity to the axis of the body frame, while λ stands for the correction factor $\lambda = 1 - (q_0^2 + q_1^2 + q_2^2 + q_3^2)$.

Projections ω_x, ω_y and ω_z represent sensor data. If the inertial and the body reference frames coincide at the initial time instant $t=0$ the initial values of the Euler parameters read

$$q_0(0) = 1, \quad q_1(0) = q_2(0) = q_3(0) = 0. \quad (8)$$

For practical applications of the presented theory it is useful to perform a time discretization $t_n = nh$, ($n=0, 1, 2, \dots$), where h stands for the time step. In this way the numerical algorithm for deriving the acceleration of the center of mass C and the attitude of a rigid body can be developed, see equations (32) - (37) in [9].

Numerical example includes analysis of spherical motion of extended arm. The extended arm will be modelled by a simplified model consisting homogeneous rectangular cuboid of mass m and dimensions l_1, l_2 and l_3 . The arm is connected to a spherical joint, representing the shoulder, at the center O of the base of the cuboid, with edges l_1 and l_2 . Some experimental data obtained by IMU sensor are given in paper [5]. Roll, pitch and yaw angles are presented but there are no data about acceleration of any point during motion of a human arm. For this reason, we are not able to use experimental data from [5] as an input data in numerical procedure presented in [9]. Instead of

using data from [5], the input data will be obtained by solving the differential equations of motion as in the numerical example presented in [9].

Point A , representing the position of the sensor is defined in the moving frame by coordinates $(l_1/2, l_2/2, l_3)$, while the center of mass C is determined by coordinates $(0, 0, l_3/2)$. For the following values describing the arm, $m=7$ kg, $l_1=l_2=0.1$ m, $l_3=0.4$ m, and $g=9.81$ m/s², and for initial conditions $\psi(0)=\theta(0)=\varphi(0)=0$, $\dot{\psi}(0)=\dot{\theta}(0)=\dot{\varphi}(0)=0.1$ s⁻¹, by solving Lagrange's equations of second kind, the Euler angles $\psi(t)$, $\theta(t)$ and $\varphi(t)$ can be obtained. Now, using the Rivals theorem the acceleration of point C in the body reference frame can be determined. By using equations (47) and (48) from [9] the acceleration of point C in the inertial reference frame can be calculated. The projections of this acceleration are shown in Figures 2,3 and 4 by solid lines.

In order to calculate the same acceleration $\mathbf{a}_C^{(I)}$ using the algorithm based on quaternion method we use the acceleration $\mathbf{a}_A^{(M)}$ and the angular velocity $\boldsymbol{\omega}$, as input data. These input data are obtained using equations (44) and (46), by use of Euler angles $\psi(t)$, $\theta(t)$ and $\varphi(t)$, which are previously calculated.

Results for the acceleration $\mathbf{a}_C^{(I)}$ obtained using the quaternion approach, with the time step $h=0.005$ s, are shown in Figures 2,3 and 4 by dots.

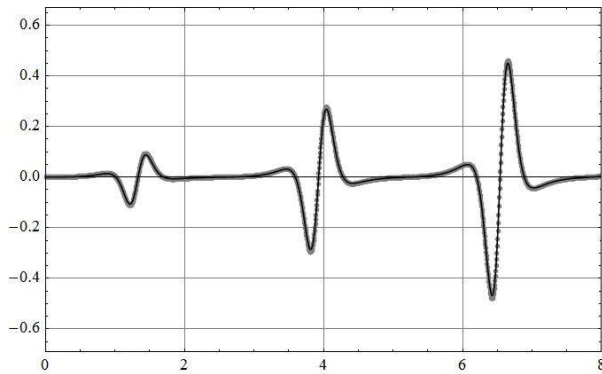


Fig. 2. Projection of acceleration of point C onto ξ axis, dots present results of the numerical algorithm while solid line presents results obtained by solving equations of motion.

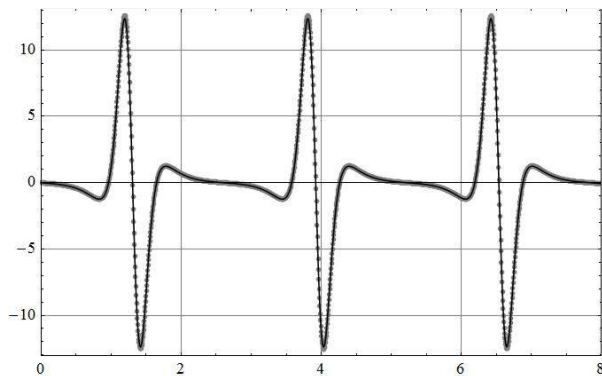


Fig. 3. Projection of acceleration of point C onto η axis, dots present results of the numerical algorithm while solid line presents results obtained by solving equations of motion

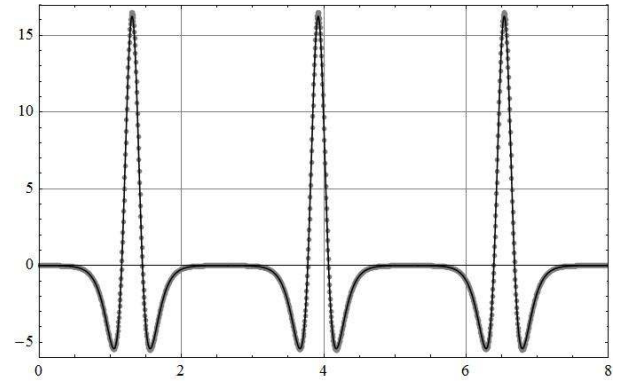


Fig. 4. Projection of acceleration of point C onto ζ axis, dots present results of the numerical algorithm while solid line presents results obtained by solving equations of motion.

Figures 2, 3 and 4 show good agreement between the results of the quaternion approach and the results obtained by solving the system of differential equations of motion for spherical motion of extended arm.

4. FINAL REMARKS

In this paper a motion of human body parts is analyzed in order to determine its attitude and the acceleration of an arbitrary point of the body part. We apply the numerical procedure for calculation of the acceleration of the center of mass, which is proposed in [9]. The procedure is applied to the problem of motion of an extended arm. The acceleration of the center of mass in an inertial coordinate system is calculated. Instead of using IMU, input data are obtained from the solution of the differential equations of motion. The results for the acceleration of the center of mass are compared with the ones obtained by the application of general theory (differential equation of motion and Rivals theorem), where satisfactory agreement is achieved.

5. REFERENCES

- [1] Grauer, J.A., Hubbard, J.E.Jr., *Flight Dynamics and System Identification for Modern Feedback Control*, Woodhead Publishing, Philadelphia, USA, 2013.
- [2] Barshan, B., Durrant-Whyte, H.F., *Inertial navigation systems for mobile robots*, IEEE Transactions on Robotics and Automation, 11 (3), pp. 328–342, 1995.
- [3] Karatsidis, A., Bellusci, G., Schepers, H., De Zee, M., Andersen, M., Veltink, P., *Estimation of Ground Reaction Forces and Moments During Gait Using Only Inertial Motion Capture*, Sensors, 17, 75, pp. 1–22, 2017.
- [4] Sabatini, A.M., *Estimating three-dimensional orientation of human body parts by inertial/magnetic sensing*, Sensors, 11, pp. 1489–1525, 2011.
- [5] Prayudi, I., Kim, D., *Design and Implementation of IMU-based Human Arm Motion Capture System*, Proceedings of IEEE International Conference on Mechatronics and Automation, pp. 670–675, Chengdu, China, 2012.

- [6] Filippeschi, A., Schmitz, N., Miezal, M., Bleser, G., Ruffaldi, E., Stricker, D., *Survey of Motion Tracking Methods Based on Inertial Sensors: A Focus on Upper Limb Human Motion*, Sensors, 17, 1257, pp. 1-40, 2017.
- [7] Madgwick, S.O.H., Harrison, A.J.L., Vaidyanathan, R., *Estimation of IMU and MARG orientation using a gradient descent algorithm*, Proceedings of 2011 IEEE International Conference on Rehabilitation Robotics, pp. 179-184, Zurich, Switzerland, 2011.
- [8] Izadi, M., Sanyal, A.K., *Rigid body pose estimation based on the Lagrange-d'Alembert principle*, Automatica, 71, pp. 78-88, 2016.
- [9] Zigic, M., Grahovac, N., *Numerical algorithm for rigid body position estimation using the quaternion approach*, Acta Mechanica Sinica, 34, pp. 400-408, 2018.
- [10] Goldstein, H., *Classical mechanics*, Addison/Wesley Publishing Company, 1980.

Authors: Assist. Prof. Miodrag Zigic, Assist. Prof. Nenad Grahovac, University of Novi Sad, Faculty of Technical Sciences, Department of Mechanics, Trg Dositeja Obradovica 6, 21000 Novi Sad, Serbia, Phone.: +381 21 485-2240.
E-mail: mzigic@uns.ac.rs; ngraho@uns.ac.rs

ACKNOWLEDGMENTS: Funding for this work was partially provided by the Faculty of Technical Sciences of the University of Novi Sad, Project No2018-054.



AUTHOR INDEX

Author Index

A

Ačko Bojan	157
Agarski Boris	323
Aleksenko Borys A.	309
Aleksić Anđelko	37
Andrić Slađan	327
Anić Jelica	117
Antić Aco	53
Ašonja Aleksandar	291

B

Baloš Sebastian	249, 267, 279, 367
Bavec Boštjan	131
Bečelić-Tomin Milena	331
Bećirović Denis	29
Begić-Hajdarević Đerzija	45
Beju Livia Dana	355
Berus Lucijano	57
Bijelić Zdravko	297
Biševac Sonja	157
Bizjak Milan	131
Blagojević Vladislav	275
Blanuša Vladimir	61
Bojanić Šejat Mirjana	355
Bojčetić Nenad	237
Bojić Savo	141
Borojević Stevo	15, 75, 127, 169, 179, 227
Bugarić Uglješa	327
Budak Igor	153, 359, 363

C

Cakó Szabolcs	141
Cerjaković Edin	65
Cogo Zlatan	45
Crnokić Boris	71
Cvetičanin Livija	301
Cvetković Nela	187, 199

Č

Čabrilo Aleksandar	233
Čavić Maja	141
Čekada Miha	249, 253
Čerče Luka	15
Čiča Đorđe	75, 179

Ć

Ćuković Saša	241
--------------------	-----

D

Dalmacija Božo	331
Delić Milan	157
Desnica Eleonora	183, 305
Dimić Zoran	195
Dobrotvorskiy Sergey	309
Dobrovolska Ludmila	309
Doncheva Elisaveta	287
Dramićanin Miroslav	267
Durakbasa M. Numan	103

Đ

Đorđić Dragiša	313
Đurđev Mića	183
Đurić Slavko	313
Đurović Koprivica Daniela	363

F

Fajsi Angela	187, 199
Ferčak Žan	131
Ficko Mirko	57
Fir Brina	359
Flegarić Stjepan	237

G

Gajić Anto	351
Gavriloski Viktor	287
Gečevska Valentina	215
Gerić Katarina	233
Ghionea Ionuț Gabriel	241
Gojić Mirko	131, 359
Gostimirović Marin	21, 33, 37
Gotlih Janez	57
Gouveia Ronny	219
Gračanin Danijela	199
Grahovac Nenad	375
Grubišić Miroslav	71
Grujić Jovan	355, 367
Grujović Nenad	149

H

Hadžistević Miodrag	87, 127, 145, 157, 313, 323
Halilović Jasmin	29
Herić Muhamed	65
Hozdić Elvis	79

I

Ilanković Nikola	351
Ilić Božo	319
Ilić Jovica	117
Ilić Mićunović Milana	153, 323, 363

J

Jakimov Dimitar	363
Jakovljević Živana	195
Janković Predrag	11
Janjatović Petar	267
Janjić Nenad	121
Jeleč Ajdin	203
Jocanović Mitar	327
Jokanović Simo	169
Jokić Aleksandar	175
Jotić Goran	117, 127
Jovanović Miloš	271
Jovišević Vid	179

K

Karanović Velibor	327
Karpe Blaž	131, 359
Kecić Vesna	331
Kerkez Đurđa	331
Keszthelyi-Szabó Gábor	335

Klančnik Simon	57
Klimenko Sergii	137
Klobučar Rok	157
Knežev Miloš	83, 95
Knežević Ivan	141
Kojić Vesna	363
Kokotović Branko	25, 99
Kolundžić Nenad	37
Kopač Igor	359
Kopeykina Marina	137
Kosanović Miloš	207
Kosec Borut	131, 323, 359
Košarac Aleksandar	95
Kovács Róbertné Petra Veszelo	335
Kovač Pavel	21, 33
Kovačević Lazar	245, 249, 253
Kožuh Stjepan	131
Kraišnik Milija	117
Kramar Davorin	15, 227
Krnjetin Slobodan	341
Krstanović Lidija	53
Kukuruzović Dragan	245, 249
Kulić Aleksandra	331
Kuric Ivan	183
Kuzinovski Mikolaj	161, 165

L

Lanc Zorana	87
Leovac Maćerak Anita	331
Lovrić Slađan	29, 65
Lukić Dejan	141, 145, 183, 227

Lj

Ljubičić Aleksandar	187
---------------------------	-----

M

Macas Mario	279
Madić Miloš	11
Majstorović Vidosav	103
Manić Miodrag	5, 207
Manokhin Andry	137
Marić Dušan	367
Marjanović Dorian	237
Matijašević Lazar	91
Matin Ivan	145
Mikić Danilo	121, 291
Mikulić Željko	347
Milanović Biljana	297

Miletić Aleksandar	245, 249, 253
Miletić Dragan	291
Miletić Ostoja	257
Milisavljević Branko	61
Milivojević Miloš	91
Miljković Zoran	175
Milošević Mijodrag	183, 227
Milutinović Mladimir	261, 275
Mircheski Ile	191
Mišić Dragan	5
Mitrović Slobodan	149
Mitrović Stefan	195
Mladenović Srđan	11, 275
Mladenović Cvijetin	83, 95, 355
Morača Slobodan	187, 199
Movrin Dejan	261
Mustafić Adnan	29

N

Nagode Aleš	131, 359
Nasić Edis	29
Nikolić Milan	305

O

Opran Constantin Gheorghe	241
Orošnjak Marko	327
Osmić Midhat	29

P

Palić Nikola	149
Panjan Petar	249, 253
Pavlič Alenka	359
Pavlović Aleksandar	305
Pavlović Milan	207
Pećanac Milan	267, 279
Pejić Vlastimir	169
Penčić Marko	141
Petković Darko	203
Petković Dušan	11
Petrović Dragan	121
Petrović Milica	175
Petrović B. Petar	91
Pleša Mihaela	241
Polenakovik Radmil	215
Prica Miljana	331
Pucovsky Vladimir	21
Puškar Tatjana	359, 363

R

Rackov Milan	141
Radman Mojca	271
Radovanović Miroslav	11
Rajnović Dragan	267, 279
Ranđelović Saša	261, 275
Raspudić Vesna	347
Ristić Miloš	207
Ristić Mirjana	267, 279
Ristovska Bojana	211
Rodić Dragan	21, 33

S

Sarkar Arkopaul	219
Santoši Željko	145, 153
Savić Branko	61, 121
Savković Borislav	33
Sekulić Jovan	367
Sekulić Milenko	21, 33, 37
Sharma Varun	149
Svetomir Simonović	283
Skakun Plavka	261
Skenderovska Tiana	215
Slavković Nikola	49
Smolej Samo	131
Soković Mirko	131
Sovilj Bogdan	107
Sovilj-Nikić Sandra	61, 107
Sredanović Branislav	75, 179
Stanković Nenad	121
Stefanović Ljiljana	261
Stojadinović Slavenko	103
Stojković Miloš	5
Suzić Nikola	199
Szendrő Péter	335

Š

Šiđanin Lepasava	267, 279
Šimunović Goran	153
Škorić Branko	245, 249, 253
Šogorović Danijel	41
Šokac Mario	153
Šormaz Dušan	3, 219
Štorga Mario	237
Štrbac Branko	83, 87, 127, 145, 157
Šupić Slobodan	341

T

Tabaković Slobodan	83, 367
Tadić Branko	153
Tanović Ljubodrag	137
Terek Pal	245, 249, 253
Tešić Saša	75
Todić Mladen	257
Todić Velimir	183, 355
Tomov Mite	161, 165
Topčić Alan	65
Trajanoska Bojana	287
Trajanović Miroslav	5, 371
Trivković Ljubiša	271
Tufegdžić Milica	371

U

Ungureanu Nicolae	53
Uran Miro	271

V

Vekić Aleksandar	187
Velkoska Cvetanka	161, 165
Vilotić Dragiša	261
Vitković Nikola	5
Vodlan Mateja	359
Vorkapić Nikola	25, 99
Vračević Isabella	41
Vukelić Đorđe	145, 153, 323
Vukman Jovan	127, 227
Vulić Miroslav	305

W

Wang Lihui	1
------------------	---

Z

Zelić Atila	351
Zeljković Milan	53, 61, 83, 87, 95, 367
Zuković Miodrag	301
Zupančič Katja	359

Ž

Žiga Alma	45
Žigić Miodrag	375
Živanić Dragan	351
Živanović Saša	49
Živić Fatima	149
Živković Aleksandar	61, 87

IN MEMORIAM

IN MEMORIAM

Mr DRAGAN BANJAC (1935–2015)



Suddenly and early, our distinguished M.Sc. Dragan Banjac, a colleague, associate and lecturer at the Faculty of Mechanical Engineering and the Faculty of Technical Sciences in Novi Sad passed away in September 2015 after a short illness.

M.Sc. Dragan Banjac was born on March 6, 1935, in Bara near Bosanski Petrovac. He had attended elementary school in his native place after he moved to Čelarevo with his parents in 1946 where he finished lower gymnasium. With excellent grades, he graduated from mechanical technical school in Novi Sad in 1954. As a mechanical technician, he worked for a year in the companies „Jugodent“ and „Novkabel“ in Novi Sad. He enrolled on studies at the Faculty of Mechanical Engineering in Belgrade in 1955/56 and graduated from manufacturing engineering in early 1961. Afterwards, he enrolled on postgraduate studies in 1968/69 at the Faculty of Mechanical Engineering in Belgrade. In 1977, he defended his master's thesis entitled „Investigating drilling process of polygonal holes,, at the same Faculty.

After finishing his studies, he was employed in the company „Majevica“ in Bačka Palanka where he was a scholarship holder. In this company, he was employed on a number of responsible functions. He was a chief of construction bureau, chief of technical control, technical director and acting director of the company. At the same time, he lectured at the Mechanical technical school in Bačka Palanka. In the autumn of 1962, he joined the military service, after which he became a captain's reserve. In September 1963, he started working in the „Institute for improving production and productivity,, in Novi Sad where he participated as a designer in design and realization of a number of design and technological projects. Then, he worked as an expert associate in the „Insitute for machine tools and tools“ in the sector for machine tools and was employed on the delopment of several projects and research subjects funded by the Provincial Fund for Scientific Research. From 1963 until becoming a permanent teaching assistant at the Faculty of Mechanical Engineering in Novi Sad in 1966, he was a honorary assistant for the courses Manufacturing processes and Manufacturing systems. In 1969 he was reelected for a teaching assistant for the course Manufacturing processes planning and cutting tools. In July 1971, he was elected as a lecturer for the course Manufacturing processes planning and cutting tools. He spent two months in the Federal Republic of Germany on improving his German language skills.

Working at the Faculty of Mechanical Engineering in Novi Sad, or at the Faculty of Technical Sciences, in the period from 1963 until his retirement, Dragan achieved very notable results in all segments of his engagement, among which the most significant are teaching on academic and master studies, scientific research, personnel development, cooperation with the economy, social engagement and so on. He invested all his energy, knowledge and desire in the teaching process in order to share as much knowledge and information with students as possible. He followed the most recent inovations in technics and technology with much skill and shared them with students. In addition to course Manufacturing processes planning and cutting tools, he developed and presented the following courses in the teaching process of basic academic studies: Process planning, Machining tools and Technoeconomic optimization. Also, he developed and introduced the courses Basics of technoeconomic optimization and Automation of process planning in the teaching process of master studies. Due to his popularity among students, fairness and principledness, as well as lavish knowledge, students in manufacturing engineering programs, around a hundred of them, chose Dragan Banjac as the mentor on their bachelor theses. He was mentoring theses conscientiously and responsibly and always had time and satisfaction to timely point out certain omissions and corrections. Most of graduate and master theses he was mentoring were related to tasks from the economy which he, considering his clear research talent, easily recognized and later determined the frameworks and research directions.

Dragan was a mentor on five master theses which were demanding in terms of experimental research in manufacturing practice. He was a member of defence committees for a large number of graduate and master theses.

He wrote two textbooks for courses on regular studies and was a coauthor of two university textbooks. In scientific research, as an excellent analyst and researcher, he participated in the development of more than seventy scientific research projects and was a leader of a large number of them, including the most significant: Technoeconomic optimization, Rationalization of technological preparation of production on the principles of type and group technologies, Automation of group manufacturing lines. He published over 150 scientific-expert paper in conference proceedings and journals in the country and abroad. Also, he achieved remarkable results in the development of personnel potentials for the need of the narrower scientific area, because under his mentorship, three teaching assistants earned master's degrees and later completed their PhDs and became lecturers.

Dragan Banjac's character was characterized by numerous human and moral values, among which the most significant ones are honest and principledness, cultural behaviour, willingness to listen and appreciate different opinions, dignity and justice. He was a witty man, with high general culture, an excellent connoisseur of sports and music. At work, among colleagues and associates he was adorned by constructiveness and readiness for cooperation, team work, exchange of information and literature. He was well known, recognized and respected in economic organizations and institutions. At the Department, University and public, he belonged to the group of people who are a symbol of production engineering. In the marriage with his wife Vera, the son Milan and daughter Dragana were born.

IN MEMORIAM

Prof. Dr JANKO HODOLIČ (1950–2015)



Prof. dr Janko Hodolič was born on 09. August 1950 in Pivnice, Republic of Serbia. He graduated at Mechanical faculty in Novi Sad, while he obtained his master and doctor of science diploma on Faculty of Technical Sciences in Novi Sad. After he graduated he started to work as assistant in scientific field of machine tools, and later assistant for subjects automatic machine handling at Faculty of Technical Sciences in Novi Sad. 21st June 1989 he becomes assistant professor in scientific field of machine tools, flexible technological systems and automation of design processes at Faculty of Technical Sciences in Novi Sad. In the same scientific field and for flexible technological systems and machine tools subjects he became associate professor on 27th June 1994. On 06th June 1997 he became full professor in scientific field of metrology and fixtures for measurement and control and fixtures subjects. His scientific-research activity is mostly oriented on application of computer in various engineering fields (FTS, CAD, CAM, CAQ). Since 2000 year he intensively works with aspects of measurement and quality in field of environmental engineering, and from 2008 in field of biomedical engineering.

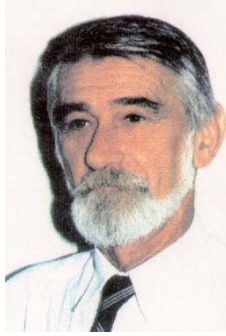
For a great contribution to scientific development in 2006 he was promoted to honorary doctor of science at the Technical University in Kosice (Dr.h.c.). In the same period he was elected for a visiting professor at the Slovak Technical University in Bratislava and the Central European College in Skalica, Slovakia. He performed lectures on a number of subjects, among of which should be noted: machine tools, automated management of machine tools, FTS, fixtures, fixture design accessories and measuring machines, measurement and quality, computer integrated manufacturing - CIM, information technologies in plastic design, environmental technologies and systems, ecodesign, measurement and control of pollution, and mechanical engineering in environmental protection. Most of these subjects, he conceived and developed with his closest associates.

He published over 450 scientific papers as author and co-author, of which about half were published at the international level, in monographs, journals and at conferences. He reviewed a number of books and numerous scientific papers in his scientific field. He participated in the realization of more than 50 scientific-research national and international projects, including projects of technological development of Republic of Serbia, projects of importance for the technological development of AP Vojvodina, CEEPUS, TEMPUS, bilateral, multilateral, etc. For more than 20 projects he was the manager or coordinator. As a mentor and a member of the commission he participated in committees for the defence of a large number of a graduate works, master's theses and doctoral dissertations at universities in Serbia, Slovenia and Slovakia. At the same universities he also participated in a number of commissions for elections in a collaborative and teaching positions. Even as a student he showed an affinity for social engagement. He was President of the International Cooperation Student Association of Mechanical Engineering and Vice President of Student Association. After the employment, he served as a President of the Council OOUR, director of the Institute for Production Engineering, vice dean for finances and vice dean for science and international cooperation at the Faculty of Technical Sciences. He was also the head of the study program environmental management at doctoral studies at the Central European College in Skalica, Slovakia, where he held the position of vice-rector for research. On the Slovak Technical University in Bratislava he was elected as a member of the Scientific and Academic Council.

He was a member of several national and international scientific professional associations (JUSK, DAAAM, SETAC, etc.), editorial boards of national and international journals, as well as organizational, programme, and scientific committees of national and international conferences. He is the founder of scientific conferences ETIKUM and CASE LCA network of scientific LCA centres of Central and Eastern Europe. He won the charter "Prof. Dr. Pavle Stanković" for outstanding contribution to the field of production engineering.

IN MEMORIAM

Prof. Dr LJUBOMIR BOROJEV (1945–2016)



Our esteemed Dr Ljubomir Borojev, retired full professor of the Faculty of Technical Sciences in Novi Sad, suddenly died on Sunday, 4th of September 2016.

Ljubomir Borojev was born on 11th of June 1945 in Pancevo. He finished his Primary and Secondary School education in Novi Sad. He graduated from the Faculty of Mechanical Engineering in Novi Sad in 1970. and completed postgraduate studies for the degree of Master of Science from the Faculty of Technical Sciences in Novi Sad. His Master's thesis entitled "Hydrostatic support of the machine tools elements for finishing machining," was completed in 1980, and doctoral thesis entitled "Contribution to the development of design methodology of modern machine tools on the basis of experimental and computer modeling of the hydrostatic bearings for the high-precision spindles " was done at the same Faculty in 1994.

After graduation in 1970, he joined the Mechanical Engineering Department of the Faculty of Technical Sciences as an assistant at the Department of metal cutting machining. He became Assistant Professor in 1994, Associate Professor in 2000 and a Full Professor for the scientific field "Machine tools, flexible manufacturing systems and automation of process designing" in July 2005.

He has achieved a remarkable and enviable academic career during 40 years of working at the Faculty. In the course of his career at the Faculty of Technical Sciences, he conducted a large number of practical classes and lectures within the courses of Machine tools, Exploitation of machine tools, Processing and Technological Systems and Automatic flexible technological systems, which are remembered by his students for an interesting way of presenting as well as inspiration they were performed with. He also performed lectures for postgraduate courses, including Modern Machining Systems and Selected Chapters in Automatic Flexible Manufacturing Systems. During all those years he actively worked on improving the teaching process, gained a significant experience as a teacher and became extremely appreciated lecturer by both his colleagues and students. According to many, he was and will always remain one of the best lecturers of the Faculty of Technical Sciences.

Prof. Borojev gave a great contribution to the development of young scientists. Under his primarily teaching methods as well as his professional and scientific leadership, dozens of students gained their professional qualification of mechanical engineer. He also participated in management and in the committees for the defense of master's and doctoral theses at the Faculty of Technical Sciences. It can be said that Prof. Borojev dedicated his whole life to his work commitment at the Faculty, Institute, Department, Laboratory and his work with students.

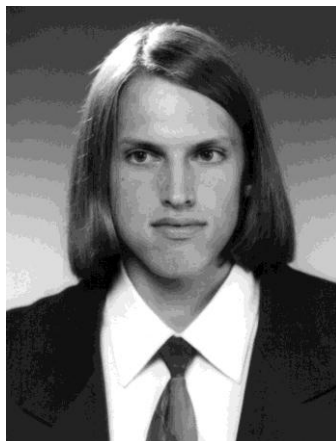
It can be considered that Professor Borojev was one of the pioneers, and one of the few researchers in the world dealing with the problems of hydrostatic and aerostatic bearing of main spindles for grinding machine tools. His scientific and technical work is included in over 100 scientific papers published in journals and conference papers in the country and abroad, over 40 research projects studies, several monographic scientific publications, textbooks, scripts, and more than 50 technical papers in the form of projects, feasibility studies and specialized publications. In many companies of the metal complex Vojvodina he was always very welcomed as a product development consultant, especially in the field of experimental testing of processing systems.

During his professional career at the Faculty, he performed a large number of social functions, including: Director of the Institute for Production Engineering, President of the Council of the Institute for Production Engineering, Member of the Council of the Faculty of Technical Sciences, Head of the Laboratory for Machine Tools, Flexible Technological Systems and Automation of Process Design. He was repeatedly commended and rewarded for his work.

We, his friends and associates, colleagues, former students, will always remember Professor Ljubomir Borojev with utmost respect.

IN MEMORIAM

Teach. Ass. IVAN SOVILJ-NIKIĆ, MSc. Eng. (1981 – 2017)



On Sunday, July 2, 2017, high-minded heart of Ivan Sovilj-Nikić at the age of 37 stopped working. Ivan Sovilj-Nikić was assistant-master at the Faculty of Technical Sciences in Novi Sad. He abandoned his colleagues and associates prematurely, without experiencing the realization of many ideas and goals for which he constantly advocated. By ethnicity Serb, Ivan Sovilj-Nikić was born on 17.05.1981. in Novi Sad from mother Ljiljana Nikić, a native of Fruška Gora, and father Bogdan Sovilj, a native of Lika. After finishing elementary school “Ivo Lola Ribar” and Gymnasium “Isidora Sekulić” in Novi Sad with an average grade of 5.00 and received the Vuk's diploma, he enrolled at the Faculty of Technical Sciences in Novi Sad at the Department of Production Engineering. Graduated-master thesis titled “Application of the genetic algorithm in optimizing the geometrical parameters of the hob milling tool” was defended on July 10, 2007. He was one of the best students since the founding of the Faculty of Mechanical Engineering in 1960 and the best student in the promotion of graduate engineers with an average grade of 10.00 (ten) in December 2007 at the Faculty of Technical Sciences in Novi Sad. In April, 2015, he planned to start the procedure for defense of his doctoral dissertation, but on April 6, he started a great battle for his health and life, which prevented him from defending his doctoral dissertation.

From early childhood he had the gift for making different models of various materials. The title of his dissertation also begins with the word Modeling. He imagined the last model on the Easter holiday on April 16, 2017. He designed a carriage and made its model from baked bread dough. You can see the photo of this model with this text.

In the final years of the Gymnasium, Ivan showed affinity for scientific research. His final examination in physics that was highly rated contained elements of research work and indicated that he was a young and promising researcher. In October 1999 he presented his first scientific paper as a co-author in Timisoara at a conference of young researchers. In the autumn of 2000, Ivan was a participant at the First Mediterranean Conference on Tribology in Jerusalem where he presented his work as a co-author, too. Ivan then picked up the applause of the attendees at the conference for a witty approach to the presentation of scientific research. As one of the top 100 students of all universities in Serbia, Ivan was a participant in the trip to Europe organized by the European Movement in 2005.

Along with the steps in education, Ivan cleared his way into the sport. He won a large number of medals in all ages and in all racing disciplines. He was the champion of the state and the representative of Vojvodina and the state in the most difficult technical discipline-steeplechase.

In professional work, Ivan has been a research scholar of the Ministry of Science and Technological Development since 2007 on the project Development of progressive technology for the back machining of profile tools on CNC machines at the Faculty of Technical Sciences in Novi Sad. During his doctoral studies, he gained his first pedagogical experience by engaging in exercises on Cutting tools, Tribology, Tribology and tools for CIM systems. Ivan was elected in the title assistant-master in 2012 for the narrow scientific field Tribology, maintenance and cutting tools. Ivan participated in the preparation and teaching in the following subjects: Tribology, Tribology and Maintenance, Cutting tools, Biotribology, Evolutionary Methods, Tribology and modern tools for CIM systems, Measurement and tools in precision engineering, Modern tools for CIM systems. Among the students he enjoyed high reputation, popularity and respect both as an expert and as a human being. He participated in the organization of several professional excursions for the students of Production Engineering, from which excursions to Prague, Ljubljana and Boljevac are set out.

Ivan was a young scientific researcher of great potential, which unfortunately did not fully develop. Despite his academic career premature stopped, Ivan achieved an outstanding number of scientific papers for his young age.

During his work at the Faculty of Technical Sciences within the Department of Production Engineering at the Chair of Metrology, quality, ecological-engineering aspect, tools and fixtures he participated in several scientific and research projects of international and national significance where he achieved significant results. During his scientific and pedagogical career he has published over 70 scientific papers, from which four monographs of international importance can be distinguished, 5 original scientific papers in international journals on the SCI list, more than 50 papers published and presented at international and national congresses, symposiums and conferences, more than 10 papers published in national journals. In the framework of doctoral studies and engagement at CEEPUS international projects, he stayed at technical faculties and institutes in Poland, Slovakia, Romania, Hungary, Bulgaria, Moldova, Macedonia, Croatia, Bosnia and Herzegovina.

Ivan Sovilj-Nikič's personality was characterized by numerous human and moral values, among which the most important honesty, the culture of behavior and behavior, the tendency to listen and appreciate a different opinion. Ivan was a well-educated, witty young man, an intellectual, a fan of sports and music. In everyday life he liked socializing, honest and friendly conversations. He had nice manners and spread positive energy. He was cheerful and well-off. He was a cordial and attentive colleague. Whenever he traveled somewhere, he traveled a lot, thought about others, and especially liked to treat friends and colleagues with gifts and small signs of attention.

At work among his colleagues at the Chair, Department, Faculty and University he was decorated by constructiveness and readiness for cooperation, that is, teamwork. His giftedness, intellectual and research capacity have put him in a group of highly capable and creative researchers. In a mountain called scientific research, Ivan did not stray, but he deliberately cleared his way to clearly defined goals.

Ivan has contributed immensely to the education and encouragement of young scientists in his country and abroad. Ivan was an energetic and active expert in the field of tribology. The originality and importance of his work, the success in applying the results of the research in practice and the promotion of tribology had a great significance at the national and international level. He constantly encouraged and influenced the scientific research work of students. As a creative engineer and scientist, he designed, constructed and executed several devices for testing the tribological characteristics of hob milling tools and gears.

Ivan successfully built a solid bridge between university researchers and engineers in industry. As an assistant, he significantly contributed to the graduation of engineers in tribology, tribodiagnostics, maintenance and cutting tools that they are now working in key positions in the Serbian and Republic of Srpska industries. As an author, Ivan prepared material for two patents that did not succeed to be formalized. Ivan was the first to have the idea of forming Tribological Society of Vojvodina, but he was not able to carry it out. His influence on the development of tribology in Vojvodina was significant. Also, Ivan's tireless work on obtaining support for research projects of national importance and his efforts for the benefit of engineers have a lasting significance in the field of tribology.

Ivan loved history, theater and literature. He was able to express himself orally and in writing. He wrote and published novels. In his desk there were more notes and sketches for new novels, and in one of them he pointed out that he shared his Christian goodness with others without leaving anything to him.

The family, Chair, Department, Faculty and University have lost their valuables and wealth that cannot be compensated with anything. Ivan was a young man for an example that by his goodness, honesty, work, responsibility and, above all, high moral, labor and human qualities can never be forgotten and erased from the memory of parents, sister, colleagues, associates and friends.

A patient, thoughtful and just man, a strong person, a creative and curious intellectual, an outstanding pedagogue and a scientific researcher left us. His contribution to the education of engineers and the formation of scientific disciplines is irreplaceable. We will all remember Ivan for a long time.





INFORMATION ABOUT SPONSORS AND DONATORS

MINISTRY OF EDUCATION, SCIENCE AND TECHNOLOGICAL DEVELOPMENT



Nemanjina 22-26
11000 Beograd

www.mpn.gov.rs

REPUBLIC OF SERBIA

PROVINCIAL SECRETARIAT FOR HIGHER EDUCATION AND SCIENTIFIC RESEARCH



Bulevar Mihajla Pupina 16
21108 Novi Sad

Tel: (021) 487 4641
Fax: (021) 456 044
E-mail: secretary@apv-nauka.ns.ac.rs

<http://apv-nauka.ns.ac.rs/vece/index.jsp>

UNIVERSITY OF NOVI SAD



Dr Zorana Đinđića 1
21001 Novi Sad
Republic of Serbia
Switchboard: +381 21 485-2000
E-mail: rektorat@uns.ac.rs
www.uns.ac.rs

University of Novi Sad
Faculty of Technical Sciences
Trg Dositeja Obradovića 6
21000 Novi Sad
Republic of Serbia

FACULTY OF TECHNICAL SCIENCES



FTN marketing service:

Tel: (021) 485 20 61

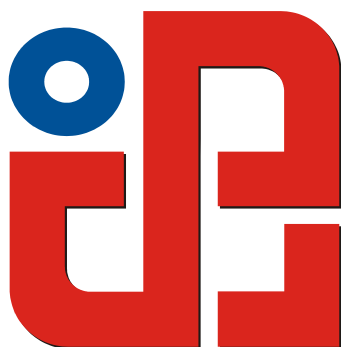
Fax: (021) 458 133

E-mail: agak@uns.ac.rs

www.ftn.uns.ac.rs

University of Novi Sad
Faculty of Technical Sciences
Vladimira Perića-Valtera 2
21000 Novi Sad
Republic of Serbia

DEPARTMENT OF PRODUCTION ENGINEERING



Secretariat of the Department:
Tel: (021) 450-366, 485-23-20
Fax: (021) 454-495
E-mail: ipm@uns.ac.rs
www.dpm.ftn.uns.ac.rs



Factory of Rolling Bearings
and Cardan Shafts



Industrijska zona bb
21235 Temerin
SERBIA

Head of Sales +381 21 6841 222
Foreign Markets +381 21 6841 190
+381 21 6841 205
+381 21 6841 201

www.fkl-serbia.com

sales@fkl-serbia.com

marketing@fkl-serbia.com

**FANUC**

Highest Quality - shortest processing time **100% FANUC - Technology**



No.1 in the world

FANUC is a leading global of factory automation, with more than 55 years' experience in the development of computer numerical control equipment.

It has 3 million CNC controls and 20,000 laser systems installed worldwide, 65% market share in the global CNC sector, and satisfied customers in every corner of the globe.



WWW.FANUC.EU

FANUC Adria d.o.o.

Ipavčeva 21, 3000, Celje, Slovenija

Tel: +386 8 205 64 97; Fax: +386 8 205 64 98;

Mob: +381 62 800 13 05 / +386 40 570 575;

info@fanuc.si

ATB SEVER

Technology in Motion



Our electric motors and generators are optimized in accordance with our client's technical and economical requests. Our clients will receive from us, within a very short notice, most advanced and high quality technical solutions of electric motors, generators, electric drives and complete technical solutions of small and middle sized hydroelectric power plants, along with economically most favourable conditions.

We are constantly moving your ideas. We are not just manufacturing motors and generators, we turn ambitious concepts of our clients into advanced, innovative and reliable products, which are unique and future oriented. Our reliability, creativity and flexibility will assist our clients in achieving their goals.

Keeping track with newest technological and technical solutions, our products are being constantly developed and therefore we are improving all our activities aimed to fulfil our client's requests. Our view of the future is oriented towards development of high power and big sized electric motors, hydrogenerators for small and middle sized hydroelectric power plants, as well as



ATB SEVER DOO SUBOTICA

Magnetna polja 6

24 000 Subotica

Srbija

<http://www.sever.rs>

<http://www.atb-motors.com>

Prodaja / Sales department:

Tel./Phone: +381 24 665 124

Fax: +381 24 665 125

Servis / Service department:

Tel./Phone: +381 24 665 161

Fax: +381 24 665 125





VOS_{system}

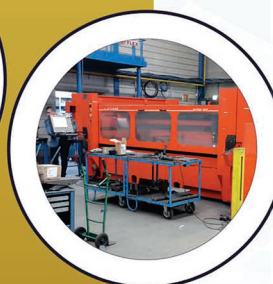
Sa ponosom možemo reći da je „VOS-SYSTEM“ već sada postao lider na našem tržištu u proizvodnji opreme za stočarstvo.

MONTAŽA



42.000 m²
Ukupne površine

CNC
LASERSKO
SEČENJE
MATERIJALA



24h NON-STOP
Servis

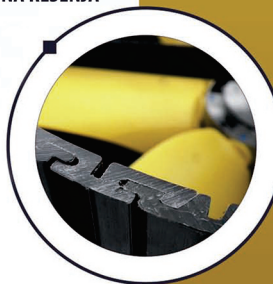


VARENJE



INOVATIVNA REŠENJA

CNC
REZANJE
PLAZMOM



MODERNA TEHNOLOGIJA



CNC
SAVIJANJE

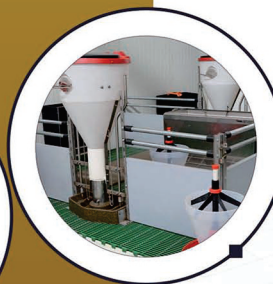


KVALITET
prva kompanija u sektoru koja
je ostvarila ISO 9001 standard

CNC
WATER-JET
REZANJE



PROIZVODNJA
10.000 m² Proizvodnog pogona



AAA
Creditworthiness Rating



VOS-SYSTEM d.o.o

Čuruška 3,
21230 Žabalj, Srbija

Tel: (381) 21 831 283

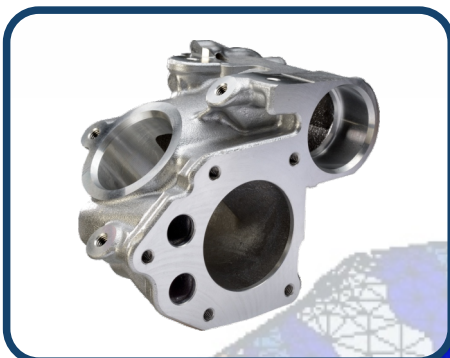
Fax: (381) 21 831 261

office@vos-system.com

www.vos-system.com



Development
Engineering
Manufacturing



STREIT NOVA
Evropska 11
22300 STARA PAZOVA
SERBIA
+381 22 32 12 99
Latitude = 44°59'27.75"N
Longitude = 20°11'43.03"E



FLEXIBLE SOLUTIONS BY **TEHNOEXPORT**



FLEXIBLE SOLUTIONS BY **TEHNOEXPORT**

ADRESA: Jovana Popovića 43, 22320 Indija

TEL: +381(0) 22 553 453

FAX: +381(0) 22 561 417

E-MAIL: office@tehnoexport.co.rs

WEB: www.texo.rs, www.tehnoexport.rs



INSTITUT ZA BEZBEDNOST
I HUMANIZACIJU RADA
NOVI SAD



- PREGLED I ISPITIVANJE OPREME ZA RAD
- ISPITIVANJE USLOVA RADNE OKOLINE
- PREGLED I ISPITIVANJE INSTALACIJA
- OBRAZOVANJE
- IZRADA ELABORATA, STUDIJA, AKATA, PRAVILNIKA
- ZAŠTITA OD POŽARA
- ZAŠTITA ŽIVOTNE SREDINE



Matični broj: 08803978

Šifra delatnosti: 73109

Broj tekućeg računa: 160-923939-34 BANCA INTESA A.D. Beograd

PIB : 103183591

Bul. Oslobođenja 30, 21000 Novi Sad, Telefon - Telefax: +381 (0)21 / 468 – 636, E-mail: hib@NSpoint.net

GM-CNC d.o.o.

PREDUZEĆE ZA PROIZVODNJU TRGOVINU I USLUGE
Nikole Bursaća 22
INĐIJA



ČELIK

ČELIK d.o.o. Bački Jarak

COMPANY ČELIK D.O.O. IS QUALIFIED AND FITTED FOR CONSTRUCTION OF BUILDING AND CRAFT WORKS, SPECIALIZED FOR THE MANUFACTURING AND INSTALLATION OF STEEL STRUCTURES.



ANALYSIS AND TECHNICAL SUPPORT

We analyze your project in order to rationalize and achieve maximum efficiency. We provide technical and advisory support to ensure that we fully understand your needs and the goal you want to achieve.



PROJECT

Our design office, which consists of experienced licensed engineers, has full capacity to create the most complex projects related to the production and installation of steel structures.



MANUFACTURE

We produce the most complex and demanding steel components based on the drawings and calculation.



MONTAGE

With the help of special machinery, our own equipment, as well as specially trained installers, we perform all kinds of construction and assembly works in the field of steel structures and supporting works.

QUALITY AND CERTIFICATION

Our company is trying to achieve maximum customer satisfaction. We apply a quality management system to monitor the quality of final production and create better conditions for our employees.

ISO 9001

The quality management system has been standard for several decades in the civilized world, which is a synonym for quality and confirms that the company strictly respects and meets the requirements of the International Organization for Standardization. This certificate serves as the main criterion for selecting the company and for guaranteeing the quality of the offered services.

EN ISO 3834 (ISO 3834) is a European (international) standard created by welding professionals. Standard EN ISO 3834 is not a comprehensive quality management system, but provides a definite list of special elements and the organization of controls that is needed in places where welding is used. It was developed to identify all factors that could affect the quality of the welded product and require control at all stages before, during and after welding.



ČELIK DOO

METAL CONSTRUCTIONS – DESIGN,
PRODUCTION AND MONTAGE
Novosadska bb, 21234 Bački Jarak ,
Srbija



www.celikdoo.rs

Tel: +381(0)21/847-606

E-mail: office@celikdoo.rs

KATALOG PROIZVODA

www.merniinstrumenti.com

1. Instrumenti za merenje električnih veličina

Gossen Metrawatt, Nemačka (www.gossenmetrawatt.com)



- 1.1. Multimetri
- 1.2. Miliometri
- 1.3. Procesni kalibratori
- 1.4. Analizatori snage i energije
- 1.5. Analizatori kvaliteta napona
- 1.6. Instrumenti za ispitivanje električnih instalacija
- 1.7. Merila otpora izolacije
- 1.8. Merila otpora uzemljenja
- 1.9. Detektori napona
- 1.10. Ispitivanje medicinskih elektr. uređaja
- 1.11. Strujna klešta
- 1.12. Izvori napajanja

2. Instrumenti za merenje osvetljaja i luminanse

Gossen, Nemačka (www.gossen-photo.de)



- 2.1. Luksmetri
- 2.2. Luminansmetri
- 2.3. Spektrometri
- 2.4. Flešmetri za fotografije

3. Instrumenti za merenje buke

Cesva, Španija (www.cesva.com)



- 3.1. Merila buke - fonometri
- 3.2. Dozimetri buke
- 3.3. Merila vibracija zgrada

4. Instrumenti za termovizijsku dijagnostiku

Guide Infrared, Kina (www.guide-infrared.com)



- 4.1. Termovizijske kamere
- 4.2. Termovizijske kamere za dronove

5. Instrumenti za merenje nedestruktivnim metodama

Sonatest, Velika Britanija (www.sonatest.com)



- 5.1. Ispitivanje bez razaranja (IBR)
- 5.2. Ispitivači korozije, EDDY Current-instrumenti, ispitivanje metala analizator metalnih legura, kamera za vizuelnu inspekciju

6. Instrumenti za prevođenje mernih veličina

Camille Bauer, Švajcarska (www.camillebauer.com)



- 6.1. Merni pretvarači (transmiteri) električnih veličina, ugaone pozicije, konverzije signala, izolatora signala, temperature, inklinometri
- 6.2. Industrijski pisaci
- 6.3. Industrijski termometri

7. Analizatori dimnih gasova (emisija)

IMR, SAD (www.imrusa.com)



- 7.1. Prenosni analizatori
- 7.2. Stacionarni analizatori

8. Instrumenti za merenje vibracija

MMF, Nemačka (www.mmf.de)



- 8.1. Merila humanih vibracija, ruka-šaka i celog tela
- 8.2. Merila mašinskih vibracija
- 8.3. Analizatori vibracija

9. Instrumenti za merenje parametara mikroklimе

Kimo, Francuska (www.kimo.fr)



- 9.1. Instrumenti za merenje parametara mikroklimе (temperature, vlage, vlage drveta, brzine strujanja i protoka vazduha kvaliteta vazduha CO/CO₂, pritiska i atmosferskog pritiska)
- 9.2. Data logeri (žični i bežični) za temperaturu, vlagu, osvetljaj, struju, napon, impulse i pritisak
- 9.3. Merni pretvarači (transmiteri) pritiska i atmosferskog pritiska, temperature, vlage, strujanja i protoka vazduha, osvetljaja, CO, CO₂, solarni

10. Instrumenti za merenje i kalibraciju

AOIP, Francuska (www.aqip.fr)



- 10.1. Kalibratori: procesni, temperature, pritiska, vlage i frekvencije
- 10.2. Testeri kablova za LAN i TELEKOM mreže
- 10.3. Starteri asinhronih motora

11. Instrumenti za merenje elektromagnetnog polja

Maschek, Nemačka (www.maschek.de)



- 11.1. Merenje elektromagnetnog polja
- 11.2. SAR metri
- 11.3. Dozimetri zračenja mobilnih telefona

12. Instrumenti za merenje čestica prašine-aerosoli

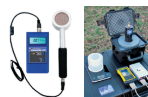
Met One, SAD (www.metone.com)



- 12.1. Merenje čestica prašine na otvorenom
- 12.2. Merenje čestica prašine u zatvorenom
- 12.3. Meteorologija

13. Instrumenti za merenje radiološkog zračenja

Seintl, SAD (www.seintl.com)



- 13.1. Merenje alfa, beta, γ, x -zračenja
- 13.2. Dozimetri radiološkog zračenja

14. Instrumenti za detektovanje cevi i kablova

Ridgid, SAD (www.ridgid.com)



- 14.1. Lokatori cevi i kablova pod zemljom

15. Instrumenti za ispitivanje VN-transformatora

RAYTECH, Švajcarska (www.raytech.ch)



- 15.1. Prenosni odnos
- 15.2. Merenje otpora namotaja transformatora
- 15.3. Mikroammometri
- 15.4. Softver za merenje transformatora
- 15.5. Tester strujnih transformatora
- 15.6. Tester kapacitivnosti i faktora snage, tangensa δ



Unimet provides its customers with CNC turned and machined parts, sheet metal parts, assembling and testing of parts and instruments. We employ more than 230 people. Our head office is situated in Kać, next to Novi Sad in north part of Serbia. We have two manufacturing locations, one in Kać and the other in Rudnik, 80 km south of Belgrade. In Kać we have five production facilities covering 6500 m2 workspace and in Rudnik approximately 2000 m2.

Our highly productive CNC machines are capable of executing complex and precise demands. Our machines are of renowned Japanese, American and European brands. We currently have about 50 CNC machines at our disposal. Apart from the CNC machines, we have a large number of universal machines with accompanying equipment.

Materials that we machine are: Aluminium, Steel, Stainless steel, Brass and bronze, Titanium, Super alloys like Inconel and cobalt. Services that we offer: Turning from diameter 1 mm up to diameter 400mm, Milling, Sheet metal punching on CNC press and tool design for our mechanical presses, Grinding, Welding, Laser engraving.

Industries that we deliver our services to are process industries, automotive and aerospace.

Certificates that we hold are ISO9001, OHSAS18001, ISO14001 and AS9100.

We export all our goods and our main customers are Brovex Precision Engineering in Sweden, Trox in Germany, Knorr-Bremse Germany, Pratt and Whitney Canada and Telsonic Ultrasonic in Switzerland.

Unimet d.o.o

Delfe Ivanić 51, 21241 Kać

Telephone: +381 21 6211 194

+381 21 6211 410

+381 21 6211 404

Fax: +381 21 6211 061

www.unimet.rs

Email: info@unimet.rs

primar tehno

FILLING & PACKAGING

"PRIMAR TEHNO", company with limited liability has been engaged in design of manufacturing processes and production of process equipment and machines for the food industry since 1993. We have focused on engineering, manufacture and installation of machines for filling and packaging of all types of fluids and other foodstuff products.

DOO PRIMAR TEHNO

Ćirpanova 25 a

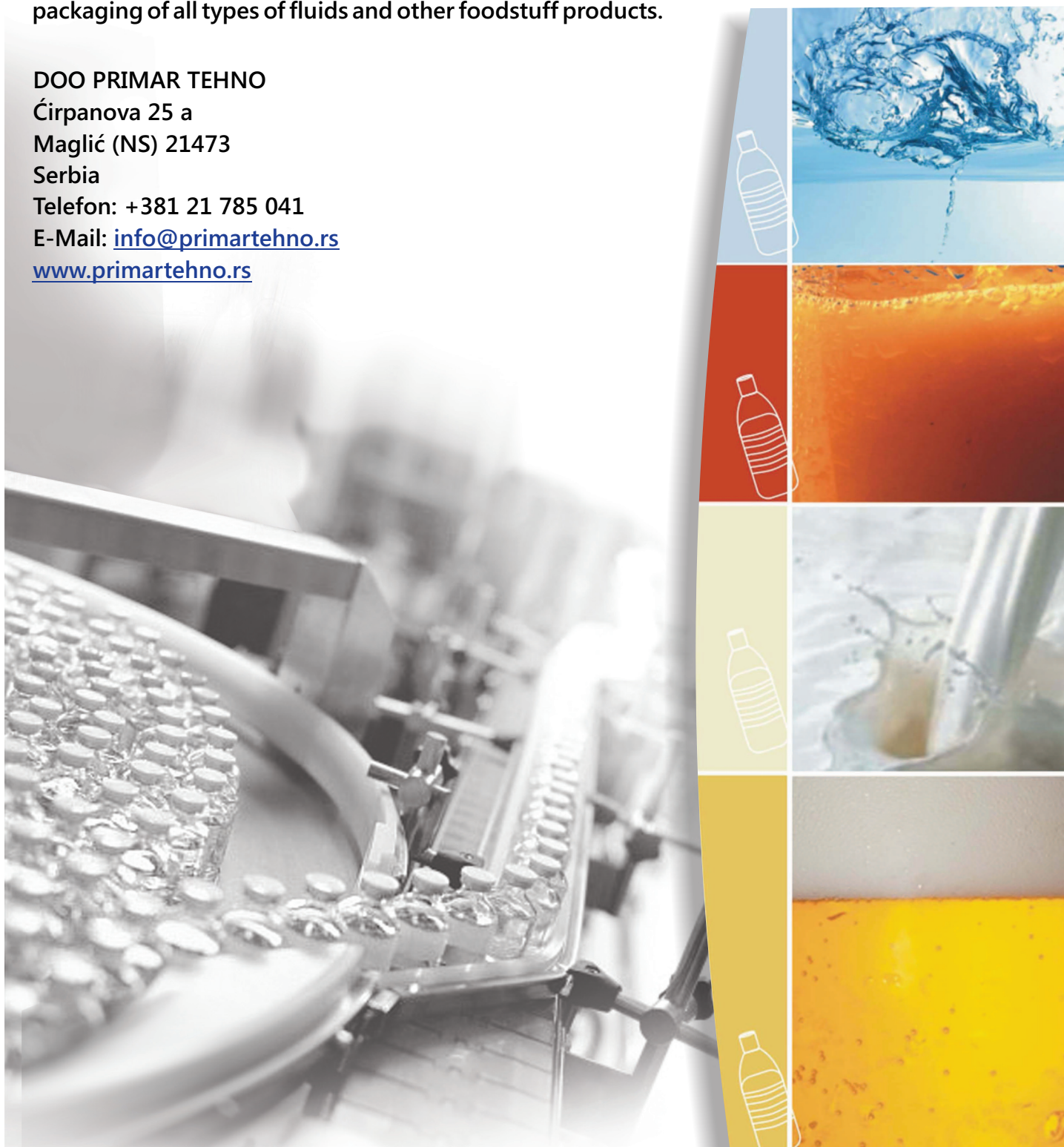
Maglić (NS) 21473

Serbia

Telefon: +381 21 785 041

E-Mail: info@primartehno.rs

www.primartehno.rs







ULJARICE BAČKA



StarBev Group Company



DOO "GRUJIĆ I GRUJIĆ"

Bul. Vojvode Stepe 6, NOVI SAD, SRBIJA, Tel/fax: 021/518 381, 021/6403 091
Mob. 063/865 78 79, e-mail:grujicgrujicns@gmail.com

Endoproteza ramena



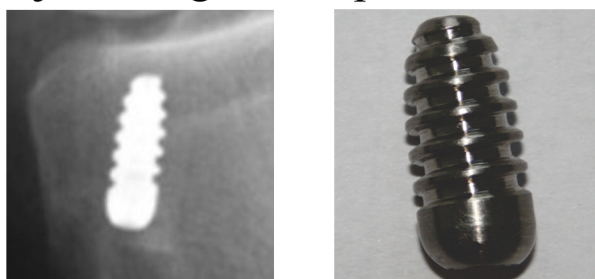
Modularna proteza zgloba kuka



Modularna proteza zgloba kuka i kolena – „total femur”



Vijak za ligamentoplastiku kolena



TPS d.o.o. preduzeće je ćerka Tvornice poljoprivrednih strojeva **Labinprogres-TPS d.o.o.**, priznatog proizvođača poljoprivredne mehanizacije.

Proizvodni program preduzeća čine:

- traktori,
- motokultivatori,
- motokopačice,
- motokosačice,
- prikolice,
- razni priključci.



TPS d.o.o. / Nemanjina 102 / 23330 Novi Kneževac / Srbija / Tel.: + 381 230 81 203 / Fax : + 381 230 83 333 / e-mail: info.tps@timos.eu



DESIGN | MOLD MAKING | INJECTION MOLDING

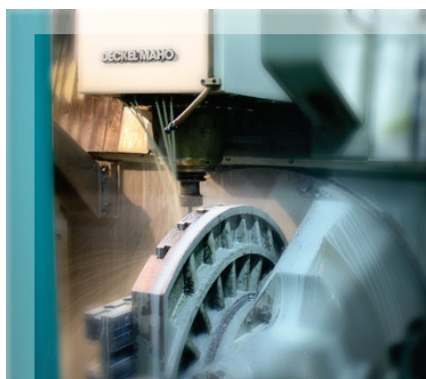


Photo: Frezal 5 axis machining centre

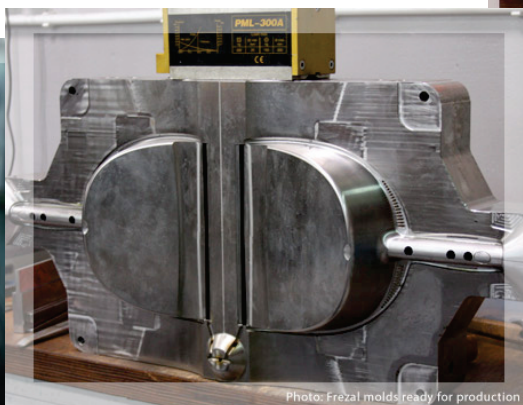


Photo: Frezal molds ready for production



FREZAL company, a family run mold making workshop, was established in 2005. in Ruma, Serbia. During all these years of continuous growth and development, FREZAL has grown to be a reliable partner in this part of Europe's moldmaking market. FREZAL is specialised for the production of termoplast injection molds, duroplast compression molds and molds for the lost wax process.

Constant searching for new challenges and the customers growing needs, had an impact on the company's fast development. FREZAL has established a complete process, necessary for the production of high quality molds.

Frezal can offer mold design service, mold manufacturing, mold testing, maintenance and repair tools and plastic parts production to the customers.

FREZAL DOO

Adress: Marka Oreskovica 42, 22400 Ruma, Srbija

tel: +381(0)22 49 00 57

cell: +381(0)64 590 18 18

e-mail: office@frezal.co.rs

www.frezal.co.rs



YOUR LEADER IN MANUFACTURING

D.O.O. Vuves Commerce

Svetosavska 75, Kač

Telephone number: **+381216213472**

Mobile number: **+381691116891** – Aleksandar.

e-mail:

Office: **office@vuves.co.rs**

Financial sector: **finansije@vuves.co.rs**

Engineering team: **inzenjering@vuves.co.rs**



MK-Holding d.o.o. Beograd - Ogranak Pobeda Petrovaradin

Address:

Rade Končara 1, 21131 Petrovaradin, Srbija

Management:

tel. +381 21 6431 386, fax. +38121 6433 955,

Sales/Supply Dept.:

tel. +381 21 6433 870, +381 21 6432 717, fax. +38121 6433 144

Financial Dept.:

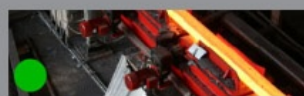
tel. +381 21 431 301.

GROUP



GROUP

We are industrial group of companies involved in mining, metallurgy, energy and trading



STEEL

Metalfer steel mill owns and operates EAF based steel mill producing construction steel products



MINING

Metalfer mining owns and operates a number of mining projects in the balkan region



ENERGY

Metalfer Invest is responsible for development of new projects concentrating on energy generation, environmental projects and new technologies

WE ARE INDUSTRIAL GROUP OF COMPANIES INVOLVED IN MINING,
METALLURGY, ENERGY AND TRADING

Metalfer Steel Mill d.o.o.
Rumski Put 27
SRB - 22000 Sremska Mitrovica





FABRIKA REZNOG ALATA JSC Čačak



General Information

Full legal name	JOINT STOCK COMPANY FABRIKA REZNOG ALATA ČAKAK
Address	No 37 Hajduk Veljkova Street, 32000 Čačak
Identification Number	07181965
Core activity	Production of tools
Foundation Year	1953
Number of Employees	80 (total 596 at 7 associated legal entities)



Capital structure (in%)

Shareholders' fund	47.86
Pension and Disability Fund	9.79
Others	42.35

Company has 7 associated legal entities with 100% of share in total capital.

Keynote Speakers

LIHUI WANG

Chair Professor at KTH Royal Institute of Technology, Stockholm, Sweden



Lihui Wang is a Professor and Chair of Sustainable Manufacturing at KTH Royal Institute of Technology, Sweden. His research interests are focused on cyber-physical systems, cloud manufacturing, predictive maintenance, real-time monitoring and control, human-robot collaborations, adaptive and sustainable manufacturing systems. Professor Wang is actively engaged in various professional activities. He is the Editor-in-Chief of International Journal of Manufacturing Research, Editor-in-Chief of Robotics and Computer-Integrated Manufacturing, and Editor of Journal of Intelligent Manufacturing. He has published 8 books and authored in excess of 450 scientific publications. Professor Wang is a Fellow of CIRP, SME and ASME, and a Board Director of North American Manufacturing Research Institution of SME.

DUŠAN ŠORMAZ

Professor at Department of Industrial and Systems Engineering, Athens, Ohio, USA

Dušan N. Šormaz is a Professor at Ohio University, Department of Industrial and System Engineering, United States. His principal research interests are in process planning, cost modeling and estimation, Computer Integrated Manufacturing (CIM), concurrent engineering, group technology and application of knowledge based systems in engineering. He has been working on applying AI techniques in engineering problem areas such as cost estimation and oil corrosion prediction. Šormaz has organized several international conferences, he is a member of the editorial board of International Journal of Industrial Engineering and Management (IJIEM), he edited a special issue of International Journal of Production Research, and he serves as regular reviewer for several research journals in his area of expertise.



MIODRAG MANIĆ

Professor at Faculty of Mechanical Engineering, Niš, Serbia



Miodrag T. Manić is a Professor at University of Niš, Faculty of Mechanical Engineering, Serbia. The numerous research projects and papers he conducted are mainly focused on the scientific field of production mechanical engineering, specifically the following areas: Technology processes designing, CNC technologies, Biomedical engineering, Experiment planning and conducting. He published more than 280 scientific papers in national and international scientific magazines, and in conference proceedings of both national and international scientific conferences. On several occasions, he has been the member of the scientific and program defining board for national and international conferences. His career also included review of several papers for scientific magazines.

